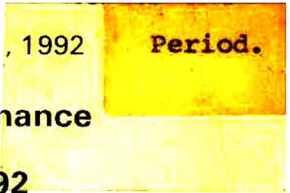


VOL. **608** NOS. **1 + 2** SEPTEMBER 11, 1992  
COMPLETE IN ONE ISSUE

Period.

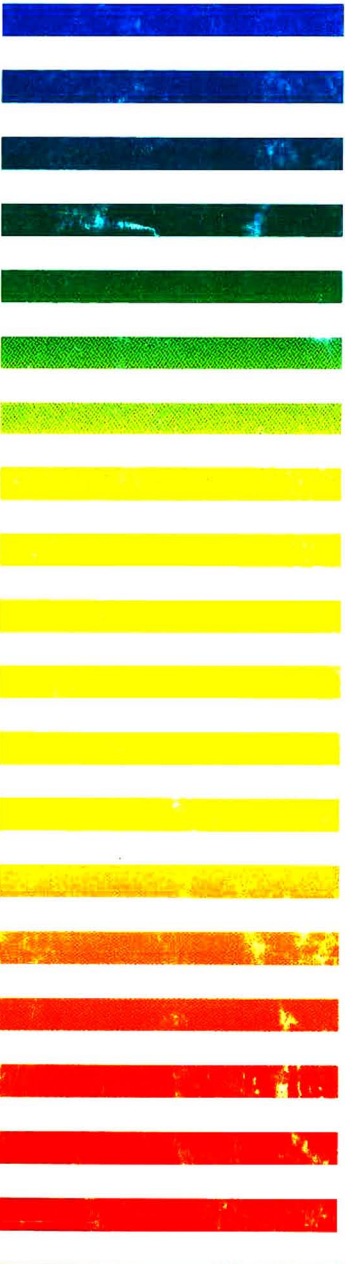
**4th Int. Symp. on High Performance  
Capillary Electrophoresis  
Amsterdam, February 9-13, 1992**



JOURNAL OF

# CHROMATOGRAPHY

INCLUDING ELECTROPHORESIS AND OTHER SEPARATION METHODS



## SYMPOSIUM VOLUMES

### EDITORS

E. Heftmann (Orinda, CA)  
Z. Deyl (Prague)

### EDITORIAL BOARD

E. Bayer (Tübingen)  
S. R. Binder (Hercules, CA)  
S. C. Churms (Rondebosch)  
J. C. Fetzer (Richmond, CA)  
E. Gelpi (Barcelona)  
K. M. Gooding (Lafayette, IN)  
S. Hara (Tokyo)  
P. Helboe (Brønshøj)  
W. Lindner (Graz)  
T. M. Phillips (Washington, DC)  
S. Terabe (Hyogo)  
H. F. Walton (Boulder, CO)  
M. Wilchek (Rehovot)

ELSEVIER



# JOURNAL OF CHROMATOGRAPHY

INCLUDING ELECTROPHORESIS AND OTHER SEPARATION METHODS

**Scope.** The *Journal of Chromatography* publishes papers on all aspects of chromatography, electrophoresis and related methods. Contributions consist mainly of research papers dealing with chromatographic theory, instrumental development and their applications. The section *Biomedical Applications*, which is under separate editorship, deals with the following aspects: developments in and applications of chromatographic and electrophoretic techniques related to clinical diagnosis or alterations during medical treatment; screening and profiling of body fluids or tissues with special reference to metabolic disorders; results from basic medical research with direct consequences in clinical practice; drug level monitoring and pharmacokinetic studies; clinical toxicology; analytical studies in occupational medicine.

**Submission of Papers.** Manuscripts (in English; four copies are required) should be submitted to: Editorial Office of *Journal of Chromatography*, P.O. Box 681, 1000 AR Amsterdam, Netherlands, Telefax (+31-20) 5862 304, or to: The Editor of *Journal of Chromatography, Biomedical Applications*, P.O. Box 681, 1000 AR Amsterdam, Netherlands. Review articles are invited or proposed by letter to the Editors. An outline of the proposed review should first be forwarded to the Editors for preliminary discussion prior to preparation. Submission of an article is understood to imply that the article is original and unpublished and is not being considered for publication elsewhere. For copyright regulations, see below.

**Publication.** The *Journal of Chromatography* (incl. *Biomedical Applications*) has 39 volumes in 1992. The subscription prices for 1992 are:

*J. Chromatogr.* (incl. *Cum. Indexes, Vols. 551-600*) + *Biomed. Appl.* (Vols. 573-611):

Dfl. 7722.00 plus Dfl. 1209.00 (p.p.h.) (total ca. US\$ 4880.25)

*J. Chromatogr.* (incl. *Cum. Indexes, Vols. 551-600*) only (Vols. 585-611):

Dfl. 6210.00 plus Dfl. 837.00 (p.p.h.) (total ca. US\$ 3850.75)

*Biomed. Appl.* only (Vols. 573-584):

Dfl. 2760.00 plus Dfl. 372.00 (p.p.h.) (total ca. US\$ 1711.50)

**Subscription Orders.** The Dutch guilder price is definitive. The US\$ price is subject to exchange-rate fluctuations and is given as a guide. Subscriptions are accepted on a prepaid basis only, unless different terms have been previously agreed upon. Subscriptions orders can be entered only by calendar year (Jan.-Dec.) and should be sent to Elsevier Science Publishers, Journal Department, P.O. Box 211, 1000 AE Amsterdam, Netherlands, Tel. (+31-20) 5803 642, Telefax (+31-20) 5803 598, or to your usual subscription agent. Postage and handling charges include surface delivery except to the following countries where air delivery via SAL (Surface Air Lift) mail is ensured: Argentina, Australia, Brazil, Canada, China, Hong Kong, India, Israel, Japan\*, Malaysia, Mexico, New Zealand, Pakistan, Singapore, South Africa, South Korea, Taiwan, Thailand, USA. \*For Japan air delivery (SAL) requires 25% additional charge of the normal postage and handling charge. For all other countries airmail rates are available upon request. Claims for missing issues must be made within three months of our publication (mailing) date, otherwise such claims cannot be honoured free of charge. Back volumes of the *Journal of Chromatography* (Vols. 1-572) are available at Dfl. 217.00 (plus postage). Customers in the USA and Canada wishing information on this and other Elsevier journals, please contact Journal Information Center, Elsevier Science Publishing Co. Inc., 655 Avenue of the Americas, New York, NY 10010, USA, Tel. (+1-212) 633 3750, Telefax (+1-212) 633 3990.

**Abstracts/Contents Lists** published in Analytical Abstracts, Biochemical Abstracts, Biological Abstracts, Chemical Abstracts, Chemical Titles, Chromatography Abstracts, Clinical Chemistry Lookout, Current Awareness in Biological Sciences (CABS), Current Contents/Life Sciences, Current Contents/Physical, Chemical & Earth Sciences, Deep-Sea Research/Part B: Oceanographic Literature Review, Excerpta Medica, Index Medicus, Mass Spectrometry Bulletin, PASCAL-CNRS, Pharmaceutical Abstracts, Referativnyi Zhurnal, Research Alert, Science Citation Index and Trends in Biotechnology.

**US Mailing Notice.** *Journal of Chromatography* (main section ISSN 0021-9673, *Biomedical Applications* section ISSN 0378-4347) is published (78 issues/year) by Elsevier Science Publishers (Sara Burgerhartstraat 25, P.O. Box 211, 1000 AE Amsterdam, Netherlands). Annual subscription price in the USA US\$ 4880.25 (subject to change), including air speed delivery. Application to mail at second class postage rate is pending at Jamaica, NY 11431. **USA POSTMASTERS:** Send address changes to *Journal of Chromatography*, Publications Expediting, Inc., 200 Meacham Avenue, Elmont, NY 11003. Airfreight and mailing in the USA by Publication Expediting.

**See inside back cover** for Publication Schedule, Information for Authors and information on Advertisements.

© 1992 ELSEVIER SCIENCE PUBLISHERS B.V. All rights reserved.

0021-9673/92/\$05.00

No part of this publication may be reproduced, stored in a retrieval system or transmitted in any form or by any means, electronic, mechanical, photocopying, recording or otherwise, without the prior written permission of the publisher, Elsevier Science Publishers B.V., Copyright and Permissions Department, P.O. Box 521, 1000 AM Amsterdam, Netherlands.

Upon acceptance of an article by the journal, the author(s) will be asked to transfer copyright of the article to the publisher. The transfer will ensure the widest possible dissemination of information.

**Special regulations for readers in the USA.** This journal has been registered with the Copyright Clearance Center, Inc. Consent is given for copying of articles for personal or internal use, or for the personal use of specific clients. This consent is given on the condition that the copier pays through the Center the per-copy fee stated in the code on the first page of each article for copying beyond that permitted by Sections 107 or 108 of the US Copyright Law. The appropriate fee should be forwarded with a copy of the first page of the article to the Copyright Clearance Center, Inc., 27 Congress Street, Salem, MA 01970, USA. If no code appears in an article, the author has not given broad consent to copy and permission to copy must be obtained directly from the author. All articles published prior to 1980 may be copied for a per-copy fee of US\$ 2.25, also payable through the Center. This consent does not extend to other kinds of copying, such as for general distribution, resale, advertising and promotion purposes, or for creating new collective works. Special written permission must be obtained from the publisher for such copying.

No responsibility is assumed by the Publisher for any injury and/or damage to persons or property as a matter of products liability, negligence or otherwise, or from any use or operation of any methods, products, instructions or ideas contained in the materials herein. Because of rapid advances in the medical sciences, the Publisher recommends that independent verification of diagnoses and drug dosages should be made.

Although all advertising material is expected to conform to ethical (medical) standards, inclusion in this publication does not constitute a guarantee or endorsement of the quality or value of such product or of the claims made of it by its manufacturer.

This issue is printed on acid-free paper.

Printed in the Netherlands

For Contents, see p. VII.

JOURNAL OF CHROMATOGRAPHY

VOL. 608 (1992)





# JOURNAL of CHROMATOGRAPHY

INCLUDING ELECTROPHORESIS AND OTHER SEPARATION METHODS

## SYMPOSIUM VOLUMES

### EDITORS

E. HEFTMANN (Orinda, CA), Z. DEYL (Prague)

### EDITORIAL BOARD

E. Bayer (Tübingen), S. R. Binder (Hercules, CA), S. C. Churms (Rondebosch), J. C. Fetzer (Richmond, CA), E. Gelpí (Barcelona), K. M. Gooding (Lafayette, IN), S. Hara (Tokyo), P. Helboe (Brønshøj), W. Lindner (Graz), T. M. Phillips (Washington, DC), S. Terabe (Hyogo), H. F. Walton (Boulder, CO), M. Wilchek (Rehovot)



ELSEVIER  
AMSTERDAM — LONDON — NEW YORK — TOKYO

---

*J. Chromatogr.*, Vol. 608 (1992)

*Amsterdam, River Amstel*

© 1992 ELSEVIER SCIENCE PUBLISHERS B.V. All rights reserved.

0021-9673/92/\$05.00

No part of this publication may be reproduced, stored in a retrieval system or transmitted in any form or by any means, electronic, mechanical, photocopying, recording or otherwise, without the prior written permission of the publisher, Elsevier Science Publishers B.V., Copyright and Permissions Department, P.O. Box 521, 1000 AM Amsterdam, Netherlands.

Upon acceptance of an article by the journal, the author(s) will be asked to transfer copyright of the article to the publisher. The transfer will ensure the widest possible dissemination of information.

**Special regulations for readers in the USA.** This journal has been registered with the Copyright Clearance Center, Inc. Consent is given for copying of articles for personal or internal use, or for the personal use of specific clients. This consent is given on the condition that the copier pays through the Center the per-copy fee stated in the code on the first page of each article for copying beyond that permitted by Sections 107 or 108 of the US Copyright Law. The appropriate fee should be forwarded with a copy of the first page of the article to the Copyright Clearance Center, Inc., 27 Congress Street, Salem, MA 01970, USA. If no code appears in an article, the author has not given broad consent to copy and permission to copy must be obtained directly from the author. All articles published prior to 1980 may be copied for a per-copy fee of US\$ 2.25, also payable through the Center. This consent does not extend to other kinds of copying, such as for general distribution, resale, advertising and promotion purposes, or for creating new collective works. Special written permission must be obtained from the publisher for such copying.

No responsibility is assumed by the Publisher for any injury and/or damage to persons or property as a matter of products liability, negligence or otherwise, or from any use or operation of any methods, products, instructions or ideas contained in the materials herein. Because of rapid advances in the medical sciences, the Publisher recommends that independent verification of diagnoses and drug dosages should be made.

Although all advertising material is expected to conform to ethical (medical) standards, inclusion in this publication does not constitute a guarantee or endorsement of the quality or value of such product or of the claims made of it by its manufacturer.

This issue is printed on acid-free paper.

Printed in the Netherlands

SYMPOSIUM ISSUE



**FOURTH INTERNATIONAL SYMPOSIUM ON  
HIGH PERFORMANCE CAPILLARY ELECTROPHORESIS**

*Amsterdam (Netherlands), February 9–13, 1992*

*Guest Editors*

**F. M. EVERAERTS**  
(Eindhoven)

**Th. P. E. M. VERHEGGEN**  
(Eindhoven)





## CONTENTS

## 4TH INTERNATIONAL SYMPOSIUM ON HIGH PERFORMANCE CAPILLARY ELECTROPHORESIS, AMSTERDAM, FEBRUARY 9-13, 1992

Foreword	
by Th. P. E. M. Verheggen . . . . .	1
On-column transient and coupled column isotachophoretic preconcentration of protein samples in capillary zone electrophoresis	
by F. Foret, E. Szoko and B. L. Karger (Boston, MA, USA) . . . . .	3
Conversion of capillary zone electrophoresis to free-flow zone electrophoresis using a simple model of their correlation. Application to synthetic enkephalin-type peptide analysis and preparation	
by V. Kašička, Z. Prusík and J. Pospíšek (Prague, Czechoslovakia) . . . . .	13
Microemulsion electrokinetic chromatography: comparison with micellar electrokinetic chromatography	
by S. Terabe and N. Matsubara (Hyogo, Japan) and Y. Ishihama and Y. Okada (Kyoto, Japan) . . . . .	23
Micellar electrokinetic capillary chromatography of neutral solutes with micelles of adjustable surface charge density	
by J. Cai and Z. El Rassi (Stillwater, OK, USA) . . . . .	31
Sample self-stacking in zone electrophoresis. Theoretical description of the zone electrophoretic separation of minor compounds in the presence of bulk amounts of a sample component with high mobility and like charge	
by P. Gebauer (Brno, Czechoslovakia), W. Thormann (Berne, Switzerland) and P. Boček (Brno, Czechoslovakia) . . . . .	47
Effects of carrier electrolyte composition on separation selectivity in capillary zone electrophoresis of low-molecular-mass anions	
by W. Buchberger (Linz, Austria) and P. R. Haddad (Kensington, Australia) . . . . .	59
Optimization of selectivity in capillary zone electrophoresis via dynamic pH gradient and dynamic flow gradient	
by H.-T. Chang and E. S. Yeung (Ames, IA, USA) . . . . .	65
Laser fluorescence detector for capillary electrophoresis	
by E. S. Yeung (Ames, IA, USA) and P. Wang, W. Li and R. W. Giese (Boston, MA, USA) . . . . .	73
Dynamic light-scattering studies of hydroxyethyl cellulose solutions used as sieving media for electrophoretic separations	
by P. D. Grossman, T. Hino and D. S. Soane (Berkeley, CA, USA) . . . . .	79
Indirect time-resolved luminescence detection in capillary zone electrophoresis	
by M. W. F. Nielen (Arnhem, Netherlands) . . . . .	85
Indirect photometric detection of polyamines in biological samples separated by high-performance capillary electrophoresis	
by Y. Ma, R. Zhang and C. L. Cooper (Kirksville, MO, USA) . . . . .	93
Theoretical and experimental aspects of indirect detection in capillary electrophoresis	
by G. J. M. Bruin, A. C. van Asten, X. Xu and H. Poppe (Amsterdam, Netherlands) . . . . .	97
Membrane fraction collection for capillary electrophoresis	
by Y.-F. Cheng, M. Fuchs, D. Andrews and W. Carson (Milford, MA, USA) . . . . .	109
Low-cost laser-induced fluorescence detector for micellar capillary zone electrophoresis. Detection at the zeptomol level of tetramethylrhodamine thiocarbonyl amino acid derivatives	
by J.-Y. Zhao, D.-Y. Chen and N. J. Dovichi (Edmonton, Canada) . . . . .	117
Application of capillary isoelectric focusing with universal concentration gradient detector to the analysis of protein samples	
by J. Wu and J. Pawliszyn (Waterloo, Canada) . . . . .	121
Analogy between micelles and polymers of ionic surfactants. A capillary isotachophoretic study of small ionic aggregates in water-organic solutions	
by C. Tribet, R. Gaboriaud and P. Gareil (Paris, France) . . . . .	131
Effect of total percent polyacrylamide in capillary gel electrophoresis for DNA sequencing of short fragments. A phenomenological model	
by H. R. Harke, S. Bay, J. Z. Zhang, M. J. Rocheleau and N. J. Dovichi (Edmonton, Canada) . . . . .	143
Switching valve with internal micro precolumn for on-line sample enrichment in capillary zone electrophoresis	
by A. J. J. Debets, M. Mazereeuw, W. H. Voogt, D. J. van Iperen, H. Lingeman, K.-P. Hupe and U. A. Th. Brinkman (Amsterdam, Netherlands) . . . . .	151
Capillary electrophoresis washing technique (Short Communication)	
by S. Abdel-Baky and R. W. Giese (Boston, MA, USA) . . . . .	159

Adjustment of resolution and analysis time in capillary zone electrophoresis by varying the pH of the buffer by E. Kenndler and W. Friedl (Vienna, Austria) . . . . .	161
Capillary electrophoresis of fluorescein-ethylenediamine-5'-deoxynucleotides by W. Li, A. Moussa and R. W. Giese (Boston, MA, USA) . . . . .	171
Influence of pH on the migration properties of oligonucleotides in capillary gel electrophoresis by A. Guttman (Budapest, Hungary), A. Arai (Kyoto, Japan) and K. Magyar (Budapest, Hungary) . . . . .	175
Determination of vasoactive intestinal peptide in rat brain by high-performance capillary electrophoresis by J. Soucheleau (Lyon, France) and L. Denoroy (Vernaison, France) . . . . .	181
Monitoring excitatory amino acid release <i>in vivo</i> by microdialysis with capillary electrophoresis-electrochemistry by T. J. O'Shea, P. L. Weber, B. P. Bammel, C. E. Lunte and S. M. Lunte (Lawrence, KS, USA) and M. R. Smyth (Dublin, Ireland) . . . . .	189
Effect of buffer constituents on the determination of therapeutic proteins by capillary electrophoresis by N. A. Guzman, J. Moschera, K. Iqbal and A. W. Malick (Nutley, NJ, USA) . . . . .	197
Capillary electrophoretic determination of the protease Savinase in cultivation broth by A. Vinther (Bagsvaerd, Denmark), J. Petersen (Gentofte, Denmark) and H. Søeberg (Lyngby, Denmark) . . . . .	205
Separation of phosphorylated histone H1 variants by high-performance capillary electrophoresis by H. Lindner, W. Helliger, A. Dirschlmaier, H. Talasz, M. Wurm and B. Sarg (Innsbruck, Austria), M. Jaquemar (Klosterneuburg, Austria) and B. Puschenclorf (Innsbruck, Austria) . . . . .	211
Ultramicro enzyme assays in a capillary electrophoretic system by J. Bao and F. E. Regnier (West Lafayette, IN, USA) . . . . .	217
Capillary electrophoresis of hemoglobins and globin chains by M. Zhu, R. Rodriguez, T. Wehr and C. Siebert (Hercules, CA, USA) . . . . .	225
Attachment of a single fluorescent label to peptides for determination by capillary zone electrophoresis by J. Y. Zhao, K. C. Waldron, J. Miller, J. Z. Zhang, H. Harke and N. J. Dovichi (Edmonton, Canada) . . . . .	239
Analysis of antiepileptic drugs in human plasma using micellar electrokinetic capillary chromatography by K.-J. Lee and G. S. Heo (Daeduk Science Town, South Korea) and N. J. Kim and D. C. Moon (Cheongju, South Korea) . . . . .	243
Confirmation testing of 11-nor- $\Delta^9$ -tetrahydrocannabinol-9-carboxylic acid in urine with micellar electrokinetic capillary chroma- tography by P. Wernly and W. Thormann (Berne, Switzerland) . . . . .	251
Study of protein-drug binding using capillary zone electrophoresis by J. C. Kraak, S. Busch and H. Poppe (Amsterdam, Netherlands) . . . . .	257
Chiral separations of basic drugs and quantitation of bupivacaine enantiomers in serum by capillary electrophoresis with mod- ified cyclodextrin buffers by H. Soini (Bloomington, IN, USA), M.-L. Riekkola (Helsinki, Finland) and M. V. Novotny (Bloomington, IN, USA) . . . . .	265
Chiral separation by capillary electrophoresis with oligosaccharides by A. D'Hulst and N. Verbeke (Leuven, Belgium) . . . . .	275
High-performance capillary electrophoresis of unsaturated oligosaccharides derived from glycosaminoglycans by digestion with chondroitinase ABC as 1-phenyl-3-methyl-5-pyrazolone derivatives by S. Honda, T. Ueno and K. Takechi (Higashi-Osaka, Japan) . . . . .	289
Separation of natural and synthetic heparin fragments by high-performance capillary electrophoresis by J. B. L. Damm, G. T. Overkluft, B. W. M. Vermeulen, C. F. Fluitsma and G. W. K. van Dedem (Oss, Netherlands) . . . . .	297
Identification of vitamin B <sub>12</sub> and analogues by high-performance capillary electrophoresis and comparison with high-perform- ance liquid chromatography by D. Lambert, C. Adjalla, F. Felden, S. Benhayoun, J. P. Nicolas and J. L. Guéant (Vandoeuvre, France) . . . . .	311
Effect of the buffer solution on the elution order and separation of bis(amidinohydrazones) by micellar electrokinetic capillary chromatography by P. Lukkari, J. Jumppanen, T. Holma and H. Sirén (Helsinki, Finland), K. Jinno (Toyohashi, Japan) and H. Elo and M.-L. Riekkola (Helsinki, Finland) . . . . .	317



Determination of quaternary ammonium compounds by capillary electrophoresis using direct and indirect UV detection by C. S. Weiss, J. S. Hazlett, M. H. Datta and M. H. Danzer (Racine, WI, USA) . . . . .	325
Investigation of the properties of novel acrylamido monomers by capillary zone electrophoresis by C. Gelfi, P. de Besi, A. Alloni and P. G. Righetti (Milan, Italy) . . . . .	333
Investigation of the properties of acrylamide bifunctional monomers (cross-linkers) by capillary zone electrophoresis by C. Gelfi, A. Alloni, P. de Besi and P. G. Righetti (Milan, Italy) . . . . .	343
Sodium dodecyl sulfate-capillary gel electrophoresis of proteins using non-cross-linked polyacrylamide by D. Wu and F. E. Regnier (West Lafayette, IN, USA) . . . . .	349
Assessment of the capabilities of capillary zone electrophoresis for the determination of hippuric and orotic acid in whey by P. A. Tienstra, J. A. M. van Riel, M. D. Mingorance and C. Olieman (Ede, Netherlands) . . . . .	357
Factors influencing the separation and quantitation of intact glucosinolates and desulphoglucosinolates by micellar electrokinetic capillary chromatography by S. Michaelsen, P. Møller and H. Sørensen (Frederiksberg, Denmark) . . . . .	363
Analysis of alkylaromatic sulphonates by high-performance capillary electrophoresis by P. L. Desbène (Evreux, France), C. Rony (Paris, France) and B. Desmazières and J. C. Jacquier (Rouen, France) . . . . .	375
Various approaches to analysis of difficult sample matrices of anions using capillary ion electrophoresis by W. R. Jones and P. Jandik (Milford, MA, USA) . . . . .	385
Optimization of detection sensitivity in the analysis of inorganic cations by capillary ion electrophoresis using indirect photo- metric detection by A. Weston and P. R. Brown (Kingston, RI, USA) and P. Jandik, A. L. Heckenberg and W. R. Jones (Milford, MA, USA) . . . . .	395
Determination of phenolic carboxylic acids by micellar electrokinetic capillary chromatography and evaluation of factors affect- ing the method by C. Bjerregaard, S. Michaelsen and H. Sørensen (Frederiksberg, Denmark) . . . . .	403
Separation of inositol phosphates by capillary electrophoresis by A. Henshall, M. P. Harrold and J. M. Y. Tso (Sunnyvale, CA, USA) . . . . .	413
Chiral separations by capillary electrophoresis using cyclodextrin-containing gels by I. D. Cruzado and Gy. Vigh (College Station, TX, USA) . . . . .	421
<i>Author Index</i> . . . . .	427





















## Foreword

The *4th International Symposium on High Performance Capillary Electrophoresis (HPCE '92)* was held in Amsterdam, February 9–13, 1992. It was the first in the successful series of HPCE symposia to be held outside the USA. The meeting was extended from three to four days, in order to accommodate more adequately the greatly increased number of oral and poster presentations.

Progress in the development of the theory, instrumentation and applications is still growing and this fact was testified by the papers in this volume. Approximately 450 participants were present from all over the world; 180 presentations were given and exhibits of instruments and supplies were shown by 13 companies.

We would like to express our gratitude to the research workers who contributed to the success of the symposium. The efforts of the Scientific Committee formed by Frans Everaerts, Stellan Hjertén,

James Jorgenson, Barry Karger and Shigeru Terabe is gratefully acknowledged. We also like to thank Shirley Schlessinger (symposium manager) and Tom Gilbert for their excellent cooperation; without them the symposium would have been difficult to realize. Zdenek Deyl is thanked for his editorial efforts in organizing this volume. Finally, the San Francisco Bay Area Chromatography Colloquium is acknowledged for its assistance in providing travel grants for students to enable them to attend this meeting.

We look forward to HPCE '93, the 5th meeting in the rapidly expanding field of capillary electrophoresis, which will be held in Orlando, Florida, USA from January 25–28, 1993, under the chairmanship of Barry Karger.

Th. P. E. M. Verheggen  
*Eindhoven (Netherlands)*





# On-column transient and coupled column isotachophoretic preconcentration of protein samples in capillary zone electrophoresis

Frantisek Foret<sup>☆</sup>, Eva Szoko and Barry L. Karger

Northeastern University, Barnett Institute, Boston, MA 02115 (USA)

---

## ABSTRACT

Two strategies for the isotachophoretic preconcentration of samples were evaluated using a standard protein mixture as an example. In the first, on-column transient isotachophoretic migration permits the injection of relatively large volumes of sample into a commercial instrument. Depending on the composition, 30–50% of the column length can be filled with the sample while maintaining good resolution of the sample components. When proper electrolyte compositions are selected, the conventional single-column instrument can be used for an isotachophoretic sample preconcentration of 50-fold or more without any modification. In the second strategy, a coupled-column system was examined which, in principle, provides a higher degree of freedom in the selection of capillary zone electrophoretic running conditions and the possibility of injection of higher sample volumes. The gain in detection level is at least a factor of 1000 in the coupled-column arrangement; however, the instrumentation is more complicated.

---

## INTRODUCTION

A main limitation of the current methodology for capillary electrophoresis is the relatively low sample detection level, *i.e.*, the minimum concentration of an analyte in a sample that can be detected. Especially when UV detection is used, the low detection level may exclude the use of capillary zone electrophoresis (CZE) for analyses of sample components in low concentrations. Several strategies to improve the detection limit in CZE have been described, including injection from low-conductivity sample matrices where the diluted sample components are preconcentrated during the stacking across the stationary concentration boundary between the sample and the background electrolyte [1–3], the use of an

on-line packed precolumn [4], the variation of pH and the use of sample-induced stacking [5–7], and the use of on-line coupled column isotachophoresis (ITP)–CZE [8–13].

The use of ITP preconcentration would appear to be very promising especially when the sample is not dissolved in pure water or diluted buffer but also contains other ions which increase its conductivity. Moreover, at very dilute buffer concentrations, biopolymers may not be stable and such low-conductivity media also generate excess heat within the injected sample which can degrade thermally unstable species [14]. During the ITP step, the concentrations of all ionic components of the sample are rearranged according to the concentration and electrophoretic mobility of the leading electrolyte [15], *i.e.*, the highly concentrated components are diluted and trace components concentrated. Generally, the resulting concentration of the preconcentrated zone is in the millimolar range. From the instrumental point of view, on-line ITP preconcentration can be performed either on-column or in a coupled-column arrangement. Because in the on-column proce-

---

Correspondence to: Professor B. L. Karger, Barnett Institute, Northeastern University, Boston, MA 02115, USA.

<sup>☆</sup> On leave from the Institute of Analytical Chemistry, Veveri 97, Brno, Czechoslovakia.

ture the migration mode gradually changes from isotachopheresis to zone electrophoresis, we suggest the term on-column transient ITP preconcentration.

There are several basic arrangements of electrolytes for both on-column transient and coupled-column ITP–CZE for the preconcentration of species. The classification can be based on the relationship between the effective electrophoretic mobilities of the co-ion of the background electrolyte C, the sample constituents S, the leading ion L and the terminating ion T, where the co-ion represents the constituents of the background electrolyte with the same charge sign as the species to be separated.

In this paper, the feasibility of the ITP preconcentration method is demonstrated with protein samples; however, this approach is general and can be applied to the analysis of most ions. The basic instrumental approaches and electrolyte arrangements are described in the following section.

#### CLASSIFICATION OF ITP PRECONCENTRATION METHODS

##### *On-column transient arrangement*

In this method, the analysis is conducted such that both ITP preconcentration and CZE separation proceed in the same capillary. Two basic electrolyte systems can be envisioned (see Fig. 1), as follows.

**Method A1.** If the background electrolyte (BGE) is selected with the co-ion having a higher effective mobility than the sample ions, *i.e.*,  $u_C > u_S$ , ITP migration is achieved by using a suitable terminating electrolyte behind the sample zone ( $u_S > u_T$ ) (see Fig. 1A). The sample is injected by pressure or gravity at time  $t_0$  and, after adding the terminating electrolyte, ITP stacking of the sample takes place during time  $t_1$ . After on-column ITP preconcentration, the terminating electrolyte in the electrode vessel is replaced with the background electrolyte, and separation in the zone electrophoretic mode during time  $t_2$ , including the migration of a zone of terminating ions behind the sample zones, results.

**Method A2.** If, on the other hand, the capillary contains a background electrolyte with a lower effective mobility co-ion C, *i.e.*,  $u_S > u_C$ , the sample itself must be supplemented by a leading ion (such

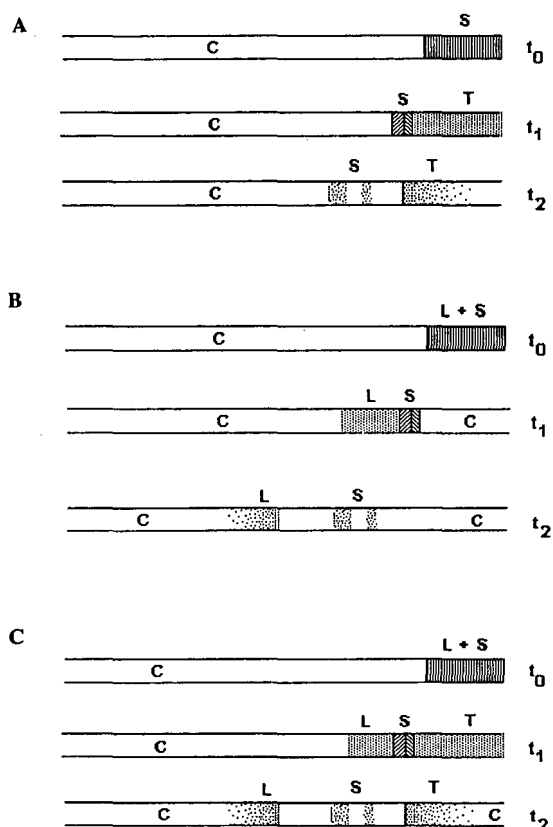


Fig. 1. Illustration of transient ITP preconcentration in a single-column arrangement. (A) The co-ion of the background electrolyte C has a mobility higher than those of the sample components S and can thus serve as the leading ion. The analysis starts with the sample injection at time  $t_0$ . When a suitable terminating electrolyte T is used, the sample can be isotachophoretically preconcentrated during the time  $t_1$ . Next, the terminating electrolyte is replaced with the background electrolyte C, and separation proceeds in the zone electrophoretic mode from time  $t_2$ . (B) When the mobility of the co-ion of the background electrolyte C is lower than that of the sample ions, a suitable leading ion L must be added to the sample. The separation starts in the isotachopheretic mode during  $t_1$ . As the concentration of the leading zone gradually decreases owing to its electromigration dispersion [14], the migration mode converts into zone electrophoresis. After the transient ITP preconcentration, the bands continue to move in a zone electrophoretic mode,  $t_2$ . (C) Both previous modes can be combined and this situation will always occur when method A is applied to a sample containing salts of highly mobile ions.

as  $\text{NH}_4^+$ ,  $\text{K}^+$  or  $\text{Na}^+$  for cationic solutes) to maintain transient ITP migration (Fig. 1B). The co-ion, C, of the BGE then serves as a terminating ion. This option was recently confirmed by mathematical

modeling [16,17]. Real samples often contain such high-mobility ions in sufficient amounts to permit ITP pre-concentration. Alternatively, appropriate amounts of salt can be added, and this may additionally aid in the stabilization of protein sample components. Of course, both basic arrangements can be combined, as depicted in Fig. 1C, and this situation will always occur when method 1A is applied to a sample containing salts of highly mobile ions.

#### Method B: coupled column arrangement

In this instance the sample migrates isotachophoretically in the pre-concentration capillary between the leading L and terminating T ions. The analytical

capillary is connected on-line at the end of the pre-concentration capillary, as described previously [11]. The overall instrument is shown in Fig. 2 and is described in the Experimental section. The expanded view of the interface of the coupled capillary columns shown schematically in Fig. 2 depicts the moment when the ITP pre-separated zones arrive at the conductivity detector located in front of the entrance to the analytical capillary. This latter capillary is filled with a background electrolyte whose actual composition (concentration, pH) influences the effective electrophoretic mobilities of both the separating species and the terminating ion. After the sample zones have entered the analytical capillary, the separation continues in either the ITP or

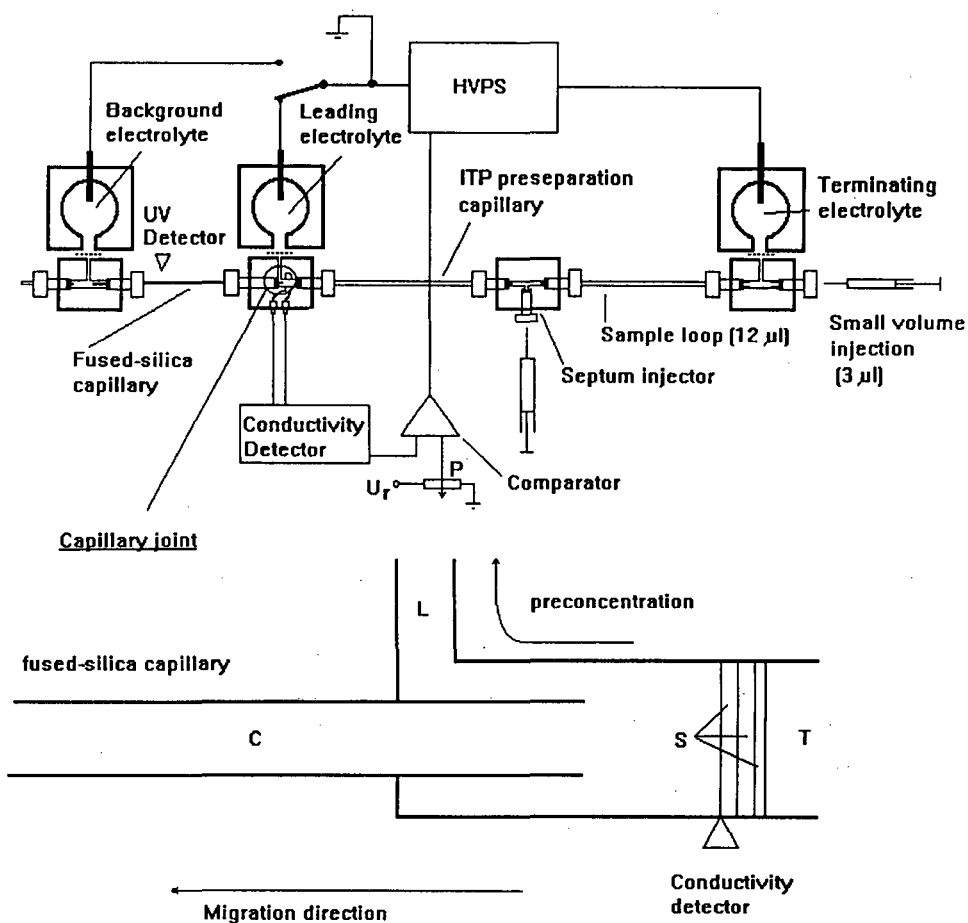


Fig. 2. Schematic diagram of the coupled column system with an expanded view of the capillary column connection.  $U_r$  = Reference voltage; P = potentiometer; C = co-ion of the background electrolyte; L = leading ion; S = sample bands; T = terminating electrolyte. Specific components are detailed in the Experimental section.

TABLE I

RELATIONSHIP BETWEEN THE MOBILITIES OF IONS IN THE COUPLED-COLUMN SYSTEM WITH ITP PRECONCENTRATION (METHOD 2) AND RESULTING MODES OF MIGRATION IN THE ANALYTICAL CAPILLARY

Co-ion C		Sample S		Terminator T	Mode of migration
$u_C$	>	$u_S$	>	$u_T$	ITP
$u_C$	>	$u_S$	<	$u_T$	CZE in T
$u_C$	<	$u_S$	<	$u_T$	CZE in C
$u_C$	<	$u_S$	>	$u_T$	CZE in C

CZE mode. The most important cases are depicted in the Table I. In addition, the terminating electrolyte in the preconcentration capillary can be replaced after ITP and migration continued in the analytical capillary without restriction on the electrophoretic mobilities [11].

## EXPERIMENTAL

### Instrumentation

A P/ACE 2100 capillary electrophoresis instrument controlled by System Gold software (Beckman, Fullerton, CA, USA) was used for experiments in the on-column transient ITP arrangement. Fused-silica capillaries, 27 cm (20 cm to the detector)  $\times$  75  $\mu$ m I.D. and 47 cm (40 cm to detector)  $\times$  75  $\mu$ m I.D., with the inner wall coated with linear polyacrylamide [18], were used as analytical separation columns.

For the ITP preconcentration approach of method B, a laboratory-made coupled column system, shown schematically in Fig. 2, was used. The ITP system consisted of 20 cm  $\times$  0.4 mm I.D. PTFE tubing as a preconcentration capillary connected to a 39 cm (30 cm to detector)  $\times$  75  $\mu$ m fused-silica analytical capillary with the inside wall coated with linear polyacrylamide. All connection blocks and electrode chambers were made from Plexiglas. The electrode chambers were separated from the connection blocks by a semipermeable Cellophane membrane in order to prevent any liquid flow. As the apparatus was designed for the future coupling to a mass spectrometer, the capillaries were opened at both ends. When necessary, the system can be closed at both the injection and detector ends. A laboratory-made conductivity detector [19], equipped with a conductivity detection cell [20] molded from an acrylic resin (Castolite-AP; Casto-

lite, Woodstock, IL, USA), was used to identify the front of the ITP migrating zone and to control the high-voltage power supply. The output voltage of the conductivity detector (proportional to the resistance of the isotachophoretic zones) was compared with a reference voltage  $U_r$  by means of an operational amplifier connected as an electronic comparator, and the resulting signal was used for the remote control of the high-voltage power supply. The actual level of the reference voltage could be set by a potentiometer P. Thus, the high-voltage power supply was automatically turned off exactly at the moment of the arrival of a selected ITP zone to the detection cell. At this point the high driving current (85  $\mu$ A) used to speed up the ITP step was decreased to 12  $\mu$ A, and the grounded electrode of the high-voltage power supply was connected to the electrode vessel close to the UV detector. The separation then proceeded in the fused-silica analytical capillary. A similar system was described for use in column switching isotachopheresis [21].

The sample was injected into a variable-volume sample loop. In the present experiments, the loop was formed by a piece of PTFE capillary (10 cm  $\times$  0.4 mm I.D.) which corresponds to a sample volume of *ca.* 12  $\mu$ l. A Spectra 100 spectrophotometer (Spectra Physics, San Jose, CA, USA) was used for UV detection at 214 nm, and the driving current was supplied by a Series EH high-voltage power supply (Glassman High Voltage, Whitehouse Station, NJ, USA).

### Chemicals

All chemicals used for the preparation of running buffers were of analytical-reagent grade and were supplied by Sigma (St. Louis, MO, USA). Lysozyme (chicken egg white), cytochrome *c* (bovine heart), ribonuclease A (bovine pancreas), trypsin

(bovine pancreas) and trypsinogen (bovine pancreas), also supplied by Sigma, were used as received. Doubly distilled water was employed for the preparation of all solutions. The running buffers were prepared by dissolving the appropriate amount of triethylamine or  $\epsilon$ -aminocaproic acid in distilled water with the pH being set by the addition of the glacial acetic acid. When refrigerated, the electrolytes could be used for several weeks.

## RESULTS AND DISCUSSION

### Method A: on-column transient ITP preconcentration

As described in the introduction, samples dissolved in water can be effectively preconcentrated during migration across the stationary concentration boundary between the sample and background electrolyte [1,2]. In such cases no sample pretreatment is necessary and, owing to the initial sharpening of the sample zone, relatively high sample volumes can be injected. An example of such a separation is shown in Fig. 3, where 38 nl of a model

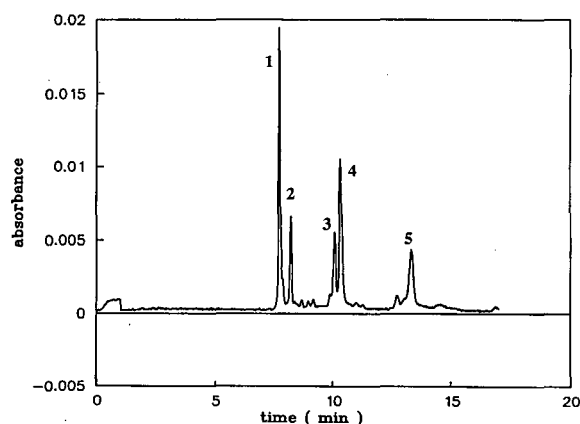


Fig. 3. CZE separation of proteins in the single capillary column system. The sample was dissolved in water. Background electrolyte 0.02 M triethylamine–acetic acid (pH = 4.4). Injection: pressure 3 s, 38 nl. The estimate of this volume is based on the measured time of the sample flow from the injection to detection end of the capillary when applying a constant sampling pressure difference ( $\Delta p = 50$  kPa). Capillary: 27 cm (20 cm to detector)  $\times$  75  $\mu$ m I.D. Current: 22  $\mu$ A, 8.2 kV; UV detection at 214 nm. Concentration of the sample: 1 = lysozyme, 72  $\mu$ g/ml ( $5 \cdot 10^{-6}$  M); 2 = cytochrome c, 40  $\mu$ g/ml ( $3.3 \cdot 10^{-6}$  M); 3 = trypsin, 56  $\mu$ g/ml ( $2.3 \cdot 10^{-6}$  M); 4 = ribonuclease A, 54  $\mu$ g/ml ( $4 \cdot 10^{-6}$  M); 5 =  $\alpha$ -chymotrypsinogen A, 56  $\mu$ g/ml ( $2.4 \cdot 10^{-6}$  M).

mixture of basic proteins dissolved in water were electrophoresed in capillary free zone electrophoresis. However, as the conductivity of the sample plug is much lower than that of the background electrolyte, the initial voltage distribution along the capillary will not be uniform but will be mainly spread over the sample plug. This can result in excessive Joule heating of the injected sample and, as was shown recently, degradation of thermally labile sample components may occur.

When the above sample was diluted fourfold with the background electrolyte, the focusing effect was lost, and neither pressure nor electrokinetic injection permitted satisfactory separation (see Fig. 4). This situation always occurs when the sample is not dissolved in distilled water ions but also contains other or dilute electrolyte in sufficient amount. In these realistic cases, ITP may represent an optimum on-line preconcentration technique.

In the above example, triethylamine, the co-ion

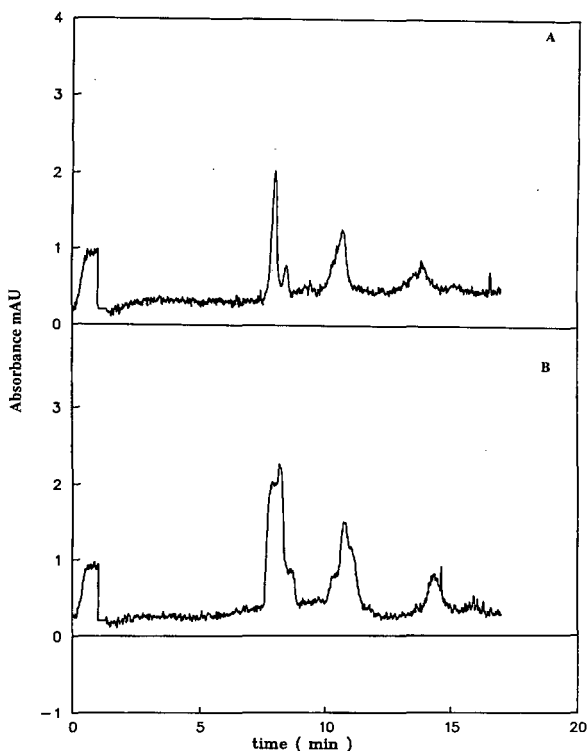


Fig. 4. CZE separation of the protein mixture used in Fig. 3 diluted fourfold with the running buffer. Injection: (A) pressure; (B) electrokinetic, 8 kV, 20 s. Other conditions as in Fig. 3.

in the background electrolyte, had an electrophoretic mobility of  $33 \cdot 10^{-5} \text{ cm}^2/\text{V} \cdot \text{s}$  [22]. Measured mobilities of separated proteins were in the range  $18 \cdot 10^{-5}$ – $25 \cdot 10^{-5} \text{ cm}^2/\text{V} \cdot \text{s}$ . Hence in this instance triethylamine can act as a leading ion for ITP migration. At the same time, for stable ITP migration, a terminating ion must be selected with an effective electrophoretic mobility lower than that of any sample component. When the counter ion of the leading electrolyte is a weak acid, the migrating front of hydrogen ions can be always used as a universal terminator for the ITP separation of cations [15]. In such a case, the extremely high electrophoretic mobility of  $\text{H}^+$  ions ( $360 \cdot 10^{-5} \text{ cm}^2/\text{V} \cdot \text{s}$ ) is slowed by a recombination reaction with the counter ion, and therefore a solution of any weak acid can be used as the terminating electrolyte. The mobility of terminating  $\text{H}^+$  ions can be influenced by the concentration of the counter ion, its pK value and the pH of the leading electrolyte.

An example of the ITP separation of protein zones with UV detection is shown in Fig. 5. Here the proteins from an identical sample as in Fig. 4 migrate between the leading electrolyte (triethylamine) and the  $\text{H}^+$  front forming the terminator. As all the proteins are focused into a very narrow zone, they could not be resolved by ITP. However,

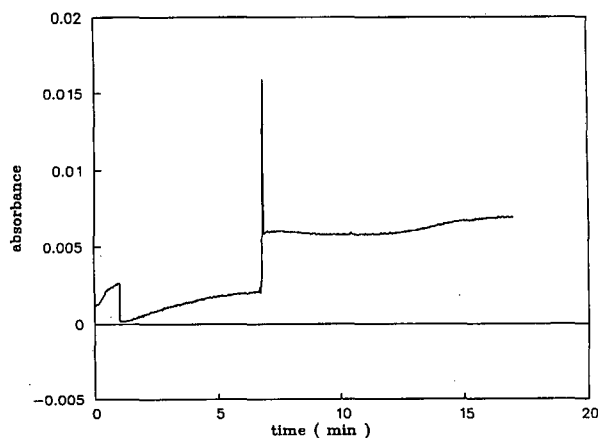


Fig. 5. ITP migration of the protein mixture diluted with the background electrolyte. Leading electrolyte, 0.02 M triethylamine–acetic acid (pH 4.4); terminating electrolyte, 0.01 M acetic acid. Injection: pressure, 30 s, 380 nl, i.e., 42% of the volume of the separation capillary (injection–detection). Other conditions as in Fig. 3.

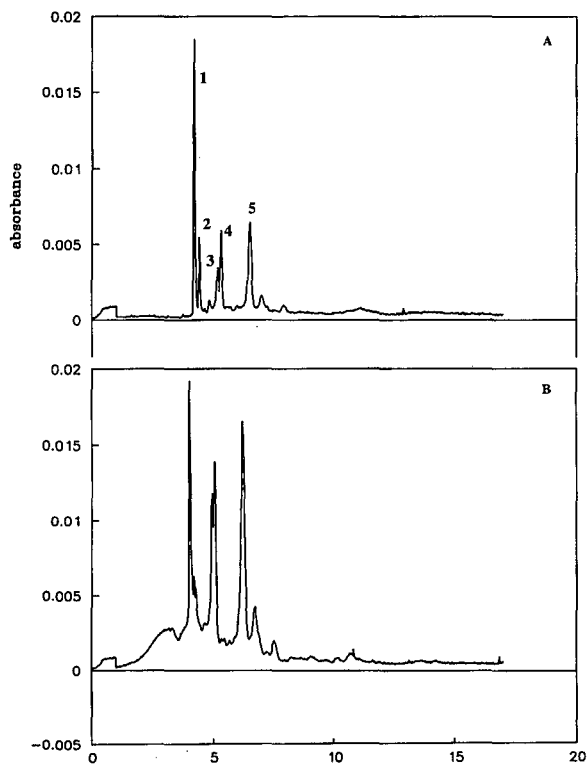


Fig. 6. CZE separation with transient ITP sample preconcentration in the column. After 90 s of ITP preconcentration in the electrolyte system from Fig. 5, the terminating electrolyte (acetic acid) was replaced with the leading electrolyte, serving now as the background electrolyte for CZE migration. Injected volume: (A) 127 nl; (B) 380 nl. Other conditions as in Fig. 3.

such a narrow zone represents an ideal starting point for the CZE analysis.

The use of an on-column transient ITP sample preconcentration step with CZE separation is shown in Fig. 6. In this example, the starting conditions were the same as in Fig. 5; however, after 90 s of the ITP migration, the terminating electrolyte in the electrode vessel was automatically replaced by the background electrolyte, and the separation was continued in the zone electrophoretic mode (see Fig. 1A). In Fig. 6A, the sample volume injected was 127 nl, i.e. 15% (3 cm) of the capillary was filled with the sample, and good resolution of protein zones was obtained. The separation is slightly compressed relative to that shown in Fig. 3 because a shorter length of the capillary was available for CZE, following the ITP step. When the injected

sample occupied 42% of the length of the capillary, as shown in Fig. 6B, the migration distance remaining after preconcentration was too short to complete the separation.

In order to increase the injection volume beyond that in Fig. 6 without a decrease in resolution, it is necessary to increase column length. This is demonstrated in Fig. 7 where the effective capillary length (length from injection to detection point) was doubled. The volume of the sample injected is now 1  $\mu\text{l}$ , which represents 57% of the total effective volume of the capillary; however, the remaining migration distance is still sufficient for good resolution of protein zones. Although the migration distance left for the CZE separation after the transient ITP preconcentration was shorter than that without the ITP step, the resolution was still better as the proteins were focused into a very sharp zone during the ITP step. The reproducibilities of migration times when the separation column was thermostated at room temperature was better than 0.5% (relative standard deviation).

It is interesting to compare Figs. 7 with Fig. 3, where a typical CZE analysis was performed using a

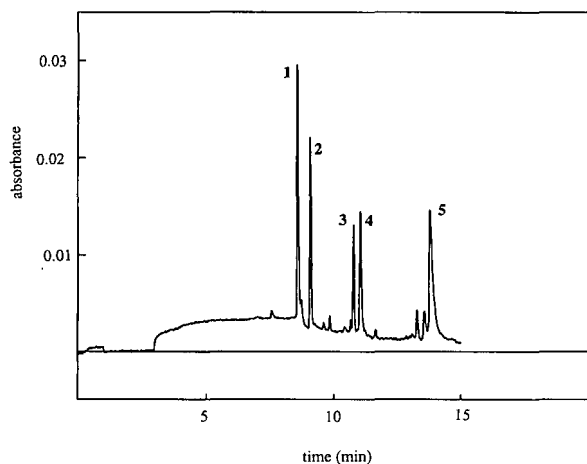


Fig. 7. CZE separation with transient ITP preconcentration in the column. Leading electrolyte, 0.02 *M* triethylamine–acetic acid (pH 4.4); terminating electrolyte, 0.01 *M* acetic acid. Capillary: 47 cm (40 cm to detector)  $\times$  75  $\mu\text{m}$ . Concentration of the sample: 1 = lysozyme, 13.5  $\mu\text{g}/\text{ml}$  ( $1 \cdot 10^{-6}$  *M*); 2 = cytochrome *c*, 15  $\mu\text{g}/\text{ml}$  ( $1.2 \cdot 10^{-6}$  *M*); 3 = trypsin, 7  $\mu\text{g}/\text{ml}$  ( $3 \cdot 10^{-7}$  *M*); 4 = ribonuclease A, 7  $\mu\text{g}/\text{ml}$  ( $5.2 \cdot 10^{-7}$  *M*); 5 =  $\alpha$ -chymotrypsinogen A, 7  $\mu\text{g}/\text{ml}$  ( $3 \cdot 10^{-7}$  *M*); dissolved in the leading electrolyte. Injection: 1  $\mu\text{l}$  (57% of the effective length of the separation capillary). Current: 22  $\mu\text{A}$ , 20 kV.

dilute buffer sample matrix. The injection volume in Fig. 3 was 38 nl, which is relatively high for this type of injection. As 1  $\mu\text{l}$  was used in Fig. 7, the increase is 30-fold in volume with on-column ITP preconcentration. Further, the average signal-to-noise ratio for peaks 3–5 in Fig. 7 is *ca.* 30, which suggests that the concentration of proteins (*ca.*  $3 \cdot 10^{-7}$  *M*) can in principle be further reduced by a factor of 10. Also, it can be noted that the separation time, *i.e.*, the time from the point at which the leading electrolyte enters the injection side of the capillary) for the longer column in Fig. 7 is similar to that in Fig. 3. The additional ITP focusing time of 2.5 min does not significantly increase this analysis time. This result means that in principle even higher volumes of the sample can be injected using longer capillaries with good resolution.

As has already been noted, if the co-ion of the background electrolyte possesses a lower electrophoretic mobility than the sample components, the co-ion can then serve as a terminating electrolyte during the transient ITP separation with leading electrolyte ions added to the sample itself. Fig. 8A shows a separation of the protein mixture in the background electrolyte containing  $\epsilon$ -aminocaproic acid as the co-ion, with the effective mobility at this pH of *ca.*  $15 \cdot 10^{-5}$   $\text{cm}^2/\text{V} \cdot \text{s}$  [22]. As the sample was dissolved in the background electrolyte, no sample preconcentration is evident. When the sample was dissolved in ammonium acetate, ammonium served as a leading ion (effective mobility *ca.*  $79 \cdot 10^{-5}$   $\text{cm}^2/\text{V} \cdot \text{s}$ ) during the transient ITP migration, and the separation dramatically improved, as shown in Fig. 8B.

From the above examples, it is clear that on-column transient ITP migration can greatly improve concentration detection limits in the typical column system. The extent of enhancement is limited mainly by the volume of the sample which can be injected into the separation capillary. Depending on the length of the capillary, up to several microliters can in principle be injected with corresponding concentration detection limits in the nanomolar region.

#### Method B: coupled-column ITP preconcentration

The sample concentration detection level can be further increased with the aid of the coupled-column system where sample volumes in the 10- $\mu\text{l}$  range or higher can effectively be preconcentrated



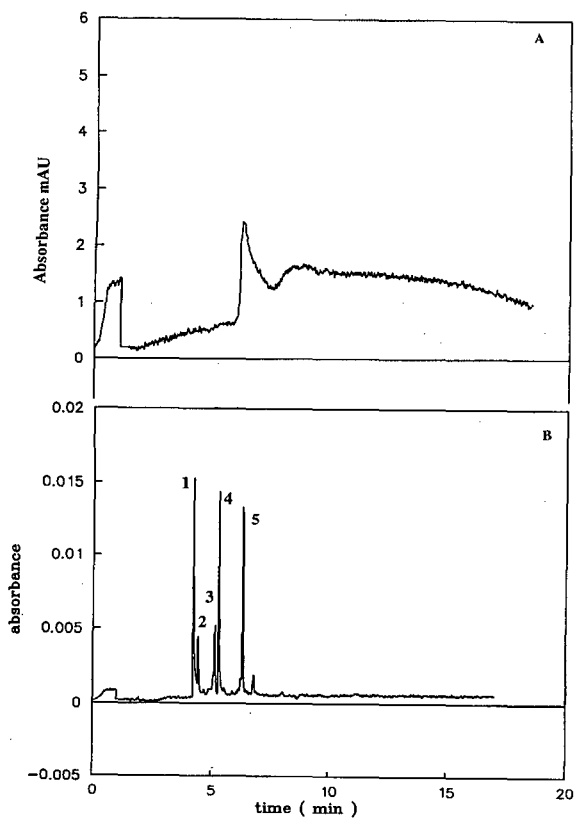


Fig. 8. CZE separation of the protein mixture in the background electrolyte with the co-ion possessing a low electrophoretic mobility. Background electrolyte:  $0.02\text{ M}$   $\epsilon$ -aminocaproic acid-acetic acid (pH 4.4). (A) Without ITP pre-concentration. Pressure injection, 10 s, 127 nl. Current:  $22\ \mu\text{A}$ , 13.9 kV. Sample: lysozyme,  $22\ \mu\text{g/ml}$  ( $1.6 \cdot 10^{-6}\text{ M}$ ); cytochrome *c*,  $12.5\ \mu\text{g/ml}$  ( $1 \cdot 10^{-6}\text{ M}$ ); trypsin,  $16.7\ \mu\text{g/ml}$  ( $0.7 \cdot 10^{-6}\text{ M}$ ); ribonuclease A,  $16.7\ \mu\text{g/ml}$  ( $1.2 \cdot 10^{-6}\text{ M}$ );  $\alpha$ -chymotrypsinogen A,  $16.7\ \mu\text{g/ml}$  ( $0.7 \cdot 10^{-6}\text{ M}$ ); dissolved in  $0.0075\text{ M}$   $\epsilon$ -aminocaproic acid-acetic acid (pH 4.4). (B) With on-column transient ITP sample pre-concentration. Conditions as in Fig. 6A except that sample was dissolved in  $0.003\text{ M}$  ammonium acetate. Ammonium served as the leading ion in the transient ITP migration.

in the ITP step. Moreover, the bulk amounts of ions present in the sample can be pre-separated and, when desired, automatically directed out from the system prior to the subsequent CZE analysis, *i.e.*, column switching [9]. An example of the analysis performed with the coupled-column system is shown in Fig. 9. Here the concentrations of individual proteins were at the level of  $10^{-8}\text{ M}$  dissolved in the background electrolyte. Although the concentration of the background electrolyte in the sam-

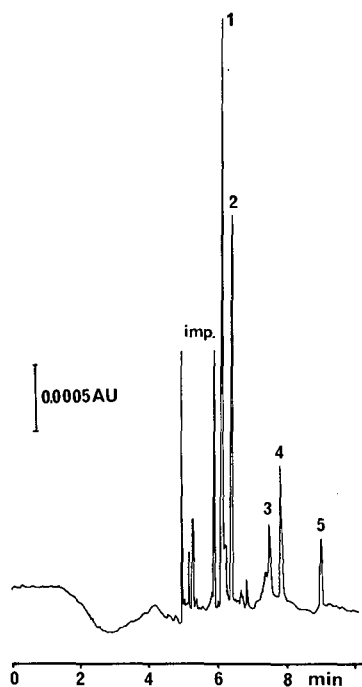


Fig. 9. CZE, separation of the protein mixture with ITP pre-concentration in the coupled column apparatus. Electrolytes: (A) pre-separation capillary,  $L=0.01\text{ M}$  ammonium acetate-acetic acid (pH 4.8) containing 1% Triton X-100,  $T=0.02\text{ M}$   $\epsilon$ -aminocaproic acid-acetic acid (pH 4.4); (B) analytical capillary,  $0.02\text{ M}$   $\epsilon$ -aminocaproic acid-acetic acid (pH 4.4). Sample: 1=lysozyme,  $0.4\ \mu\text{g/ml}$  ( $2.9 \cdot 10^{-8}\text{ M}$ ); 2=cytochrome *c*,  $0.5\ \mu\text{g/ml}$  ( $4 \cdot 10^{-8}\text{ M}$ ); 3=trypsin,  $1\ \mu\text{g/ml}$  ( $4.2 \cdot 10^{-8}\text{ M}$ ); 4=ribonuclease A,  $0.6\ \mu\text{g/ml}$  ( $4.4 \cdot 10^{-8}\text{ M}$ ); 5= $\alpha$ -chymotrypsinogen A,  $1.0\ \mu\text{g/ml}$  ( $4.2 \cdot 10^{-8}\text{ M}$ ); dissolved in BGE. Volume:  $12\ \mu\text{l}$ . Current: ITP,  $85\ \mu\text{A}$ , 3-10 kV; CZE,  $12\ \mu\text{A}$ , 15 kV. Imp. = impurities accumulated from the terminating electrolyte during the ITP step.

ple is  $10^6$  higher than the concentration of the sample proteins, the ITP pre-concentration step permits the detection of sample proteins with a signal-to-noise ratio of  $> 50$ . A main advantage of the coupled-column system stems from the possibility of injecting extremely large sample volumes which exceed the volume of the analytical separation capillary itself. The corresponding detection limit is then in the subnanomolar region. In the present case the injected volume was nine times higher than the effective volume of the analytical separation capillary itself.

The actual concentration of proteins in their ITP zones can be determined by calibration of the detector response with standard protein solutions. As

confirmed by separate experiments (data not shown), the sample proteins were preconcentrated from the level of 1  $\mu\text{g}/\text{ml}$  to ca. 20  $\text{mg}/\text{ml}$  during the ITP step. At this concentration the possibility of precipitation of proteins must be kept in mind. In our experiments we did not observe precipitation, probably due in part to the high positive charge of basic proteins which were separated at a pH well below their isoelectric points. This high charge can minimize aggregation due to coulombic repulsion. In cases where precipitation is an issue, the use of additives to the running buffer electrolytes, such as non-ionic detergents or carrier ampholytes, may reduce the problem [19]. In the present example, Triton X-100 at a level of 1% was added to the leading electrolyte, and this detergent may have helped reduce precipitation. The addition of a non-ionic detergent usually also suppresses the sorption of proteins on the wall of the Teflon preconcentration capillary, in addition to minimizing electroosmotic flow.

## CONCLUSIONS

The use of ITP sample preconcentration is a useful approach to improve the detection of proteins in CZE analysis. This method will work well not only for small molecules but also, as shown in this work, for proteins. In the single-column arrangement, 1–2 orders of magnitude higher sample volumes can be injected than in the normal mode of CZE with little if any preconcentration. Furthermore, the sample need not to be dissolved in distilled water or dilute buffer and may contain an excess of other ions which may be useful for stabilization. The main prerequisite for successful ITP preconcentration is a knowledge of the range of solute mobilities in the sample. This can be estimated by a preliminary CZE run of the sample mixture. The appropriate leading L, terminating T and running C buffer ions can be chosen with the aid of tabulated data [22].

Method A1, which involves the change of the terminating electrolyte in the electrode vessel to the leading electrolyte after ITP preconcentration, is the most universal approach, as no sample pretreatment is necessary. Disadvantages from electrolyte change are minor when an automated instrument is used, where the change can easily be programmed. The duration of the ITP step depends on the sample

composition and usually ITP will be completed within 1–5 min.

Method A2, where the background electrolyte itself serves as the terminating electrolyte for the transient ITP preconcentration, is useful mainly for samples containing salts of highly mobile ions which can serve as a source of leading ions. Moreover, the addition of a salt can be also expected to narrow the differences in conductivity and ionic strength between various samples. The optimum concentration of the leading electrolyte in the sample should generally be around 0.01  $M$ .

The coupled-column approach (method 2) has several advantages, including the possibility of injecting large volumes of the sample, effective sample clean-up, and, with controlled current switching, selected ion analysis. Detection levels in the subnanomolar range can easily be achieved, and quantitative trace analysis is feasible, providing that possible sample losses during the preconcentration step are minimized [23]. Here especially, the sorption of the separating species on the wall of the ITP preconcentration capillary must be eliminated, because at protein concentrations below  $10^{-7} M$  even residual adsorption can cause a significant loss of material during migration.

The electrolyte systems used here are suitable for cationic analyses; however, the basic rules for electrolyte selection are applicable also for the analysis of anions. Compositions of many suitable electrolytes for ITP separation can be found in the literature [15,19,22].

## ACKNOWLEDGEMENT

The authors thank Beckman Instruments for supporting this work. This paper is contribution No. 523 from the Barnett Institute.

## REFERENCES

- 1 F. E. P. Mikkers, F. M. Everaerts and T. P. E. M. Verheggen, *J. Chromatogr.*, 169 (1979) 1–10.
- 2 R. L. Chien and D. S. Burgi, *J. Chromatogr.*, 559 (1991) 141–152.
- 3 P. Jandik and W. R. Jones, *J. Chromatogr.*, 546 (1991) 431–443.
- 4 N. A. Guzman, M. A. Trebilock and J. P. Advis, *J. Liq. Chromatogr.*, 14 (1991) 997–1015.
- 5 R. Aebersold and H. D. Morrison, *J. Chromatogr.*, 516 (1990) 79–88.

- 6 S. Hjertén, K. Elenbring, F. Kilar, J. Liao, A. J. C. Chen, C. J. Siebert and M. Zhu, *J. Chromatogr.*, 403 (1987) 47–61.
- 7 E. Kenndler and K. Schmidt-Beiwil, *J. Chromatogr.*, 545 (1991) 397–402.
- 8 F. E. P. Mikkers, *Thesis*, Eindhoven University, Eindhoven, 1980.
- 9 D. Kaniansky and J. Marák, *J. Chromatogr.*, 498 (1990) 191–204.
- 10 V. Dolník, K. A. Cobb and M. V. Novotny, *J. Microcol. Sep.*, 2 (1990) 127–131.
- 11 F. Foret, V. Šustáček, and B. Boček, *J. Microcol. Sep.*, 2 (1990) 299–303.
- 12 D. S. Stegehuis, H. Irth, U. R. Tjaden and J. van der Greef, *J. Chromatogr.*, 538 (1991) 393–402.
- 13 L. Křivánková, F. Foret and P. Boček, *J. Chromatogr.*, 545 (1991) 307–313.
- 14 A. Vinther, H. Soeberg, L. Nielsen, J. Pedersen and K. Biedermann, *Anal. Chem.*, 64 (1992) 187–191.
- 15 P. Boček, M. Deml, P. Gebauer and V. Dolník, *Analytical Isotachophoresis*, VCH, Weinheim, 1988.
- 16 P. Gebauer, W. Thormann and P. Boček, *J. Chromatogr.*, 608 (1992) 47.
- 17 J. L. Beckers and F. M. Everaerts, *J. Chromatogr.*, 508 (1990) 19–26.
- 18 S. Hjertén, *J. Chromatogr.*, 347 (1985) 191–197.
- 19 F. M. Everaerts, J. L. Beckers and T. P. E. M. Verheggen, *Isotachophoresis: Theory, Instrumentation and Practice*, Elsevier, Amsterdam, 1976.
- 20 F. Foret, M. Deml, V. Kahle and P. Boček, *Electrophoresis*, 7 (1986) 430–432.
- 21 D. Kaniansky, *Thesis*, Komenský University, Bratislava, 1981.
- 22 J. Pospichal, P. Gebauer and P. Boček, *Chem. Rev.*, 89 (1989) 419–430.
- 23 D. S. Stegehuis, U. R. Tjaden and J. van der Greef, *J. Chromatogr.*, 591 (1992) 341–349.

# Conversion of capillary zone electrophoresis to free-flow zone electrophoresis using a simple model of their correlation

## Application to synthetic enkephalin-type peptide analysis and preparation

Václav Kašička, Zdeněk Prusík and Jan Pospíšek

*Institute of Organic Chemistry and Biochemistry, Czechoslovak Academy of Sciences, Flemingovo 2, 166 10 Prague 6 (Czechoslovakia)*

---

### ABSTRACT

A simple mathematical model of the correlation between capillary zone electrophoresis (CZE) and continuous free-flow zone electrophoresis (FFZE) was developed. The model results from the fact that both methods are based on the same separation principle (zone electrophoresis) and both are performed in a free solution of the same composition. Based on this model, a procedure for the conversion of an analytical microscale CZE separation into a preparative FFZE separation was developed. The applicability of this procedure is demonstrated by CZE analysis at the picomole level and FFZE preparative fractionation (60 mg/h throughput) of crude synthetic biologically active peptide [D-Tle<sup>2,5</sup>]-dalargin. The combination of CZE and FFZE provides an efficient and economical tool for synthetic peptide analysis and preparation.

---

### INTRODUCTION

Capillary electromigration methods, generally called high-performance capillary electrophoresis (HPCE), have undergone a period of rapid development [1–5] and they are becoming a powerful tool for the separation of both low- and high-molecular-mass charged and, in the case of electrokinetic chromatography, also uncharged substances and particles. Nowadays HPCE is mostly used for analytical purposes. However, attempts to use HPCE in a micropreparative mode have been reported and this trend will probably become more pronounced in the future especially in cases where

separation problems are better solved by HPCE than by other, *e.g.*, chromatographic, methods.

The reason for the less frequent application of the micropreparative mode of HPCE is not only an inevitable compromise between capacity and separability but also the more complicated conversion from an analytical HPCE mode to a micropreparative mode than in chromatography. This is due to the fact that in HPCE both ends of the capillary are dipped into the electrode vessels and an electric field is applied for the whole duration of the experiment. Although several devices have been developed [6–9] and some micropreparations were successfully achieved, one substantial disadvantage remains: because of the miniature dimensions of the capillary separation compartment, the capacity of the preparation is very low, in the range of nanograms to micrograms depending on the capillary dimensions

---

*Correspondence to:* Dr. Z. Prusík, Institute of Organic Chemistry and Biochemistry, Czechoslovak Academy of Sciences, Flemingovo 2, 166 10 Prague 6, Czechoslovakia.

and initial sample concentration. The possibilities of increasing the capacity by increasing the capillary diameter are limited owing to Joule heat problems in capillaries of larger diameter, especially under non-steady-state conditions as in capillary zone electrophoresis (CZE).

A different way to increase the capacity of a preparation is to convert the capillary separation into a continuous thin-layer free-flow system in a flow-through electrophoretic chamber [10,11]. In such a type of separation the capacity can be increased by several orders of magnitude up to several hundred milligrams per hour.

The principle of free-flow zone electrophoresis (FFZE) [10–13] is that an electric field is oriented perpendicularly to the laminar flow of the carrier electrolyte and of the sample solution. Different sample components are deflected from the direction of the laminar flow depending on their electrophoretic mobilities at the different angles and at the outlet side of the chamber they are collected in the fraction collector. Provided that both types of separation, *i.e.*, capillary and free-flow, are performed in the same separation mode (zone electrophoresis in our case), a direct correlation can be found between these two methods [14,15]. Based on this correlation, CZE can be used for the development of suitable separation conditions, especially with regard to pH and carrier electrolyte composition, which can then be used directly in preparative FFZE. However, the different migration times of various components in CZE must then be converted into optimized deflection angles in FFZE.

The aim of this work was to develop a simple mathematical model of the correlation between CZE and FFZE, to develop a procedure for the conversion of analytical CZE separation into the preparative FFZE process and to demonstrate the application of the procedure to the analysis and preparation of the synthetic peptide [D-Tle<sup>2,5</sup>]-dalargin.

## THEORY

In this section a simple mathematical model of the electrophoretic and electroosmotic movements in the capillary and in the flow-through chamber is presented and their correlation is shown.

The resulting velocity,  $v_r$ , of the movement of a charged substance in a d.c. electric field in the

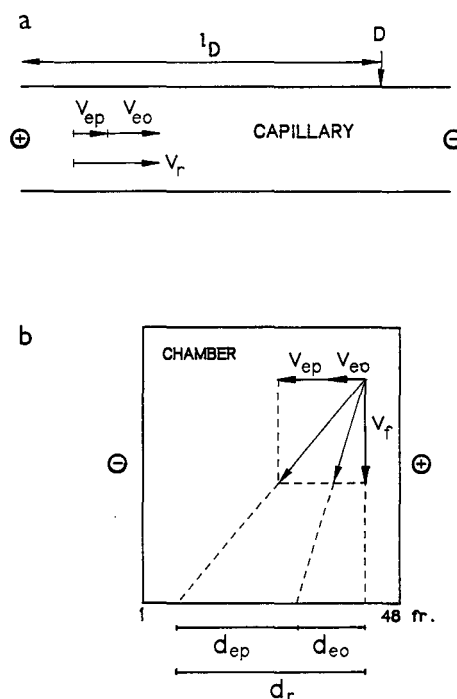


Fig. 1. Vector sum of velocities in (a) CZE and (b) FFZE.  $v_{ep}$  = Electrophoretic velocity;  $v_{eo}$  = electroosmotic velocity;  $v_r$  = resulting migration velocity;  $l_D$  = effective length of the capillary;  $D$  = detector position on the capillary;  $d_{ep}$  = electrophoretically migrated distance;  $d_{eo}$  = electroosmotically migrated distance;  $d_r$  = resulting migrated distance.

capillary (see Fig. 1a) is given by the sum of the electrophoretic velocity,  $v_{ep}$ , and the electroosmotic flow velocity,  $v_{eo}$ :

$$v_r = v_{ep} + v_{eo} \quad (1)$$

In CZE performed in a capillary with an effective length  $l_D$  ( $l_D$  is a capillary length from the sample injection end to the detector), from eqn. 1 it follows that

$$\frac{l_D}{t_r} = \frac{l_D}{t_{ep}} + \frac{l_D}{t_{eo}} \quad (2)$$

where  $t_r$ ,  $t_{ep}$  and  $t_{eo}$  are the resulting, electrophoretic and electroosmotic migration times, respectively.

By combination of eqns. 1 and 2, the following relationship is obtained for the electrophoretic velocity,  $v_{ep,c}$ , in the capillary:

$$v_{ep,c} = \frac{l_D}{t_{ep}} = \frac{l_D(t_{eo} - t_r)}{t_{eo}t_r} \quad (3)$$

From this relationship,  $v_{ep,c}$  can be calculated from the experimentally available data:  $t_r$  is the resulting measurable migration time of a charged substance which is moved in the capillary by both electrophoretic movement and electroosmotic flow and  $t_{eo}$  is measured as the migration time of an uncharged substance which is moved by the electroosmotic flow only.

The electroosmotic velocity in the capillary,  $v_{eo,c}$ , is given as the ratio of  $l_D$  and  $t_{eo}$ :

$$v_{eo,c} = l_D/t_{eo} \quad (4)$$

The superposition of velocities in the flow-through electrophoretic chamber and the distances migrated by both charged and uncharged substances are shown in Fig. 1b.

In FFZE the resulting migrated distance,  $d_r$ , is given as the sum of the electrophoretically migrated distance,  $d_{ep}$ , and the electroosmotically moved distance,  $d_{eo}$ :

$$d_r = d_{ep} + d_{eo} \quad (5)$$

The distance  $d_{ep}$  is given as the product of electroosmotic velocity in the flow-through chamber,  $v_{ep,f}$ , and the mean flow-through time,  $t_f$ :

$$d_{ep} = v_{ep,f}t_f \quad (6)$$

Substituting eqn. 6 into eqn. 5, the following relationship can be derived:

$$v_{ep,f} = (d_r - d_{eo})/t_f \quad (7)$$

Eqn. 7 makes it possible to calculate the electrophoretic velocity from the experimentally available data, *i.e.*, from the resulting deviation distance,  $d_r$ , of a charged substance, from the deviation distance,  $d_{eo}$ , of an uncharged substance and from the known mean flow-through time,  $t_f$ . The electroosmotic velocity in the flow-through chamber,  $v_{eo,f}$ , is obtained as the ratio of the electroosmotically moved distance,  $d_{eo}$ , and the flow-through time,  $t_{eo}$ :

$$v_{eo,f} = d_{eo}/t_f \quad (8)$$

From eqns. 3 and 7, the ratio,  $p$ , of electrophoretic velocities in the flow-through chamber and in the capillary can be expressed as

$$p = \frac{v_{ep,f}}{v_{ep,c}} = \frac{(d_r - d_{eo})t_r t_{eo}}{t_f l_D (t_{eo} - t_r)} \quad (9)$$

In most instances the ratio  $p$  will be  $< 1$  because the electrophoretic velocity in the flow-through chamber is usually lower than that in the capillary because of the lower electric field intensity and lower temperature in the efficiently cooled flow-through chamber, with a usual gap width of 0.5–0.3 mm, than in the capillary with a typical I.D. one order of magnitude lower (0.025–0.075 mm). It is reasonable to assume that  $p$  is approximately constant for different charged components separated by CZE and FFZE under the same separation conditions. In other words, this assumption means that if the electrophoretic velocity of the substance 1 is  $p$  times lower in FFZE than in CZE, then the electrophoretic velocity of substance 2 will also be  $p$  times lower in FFZE than in CZE. This is a realistic assumption if we realize that the deviations of  $p$  may be caused by (a) the differences in the temperature dependences of the electrophoretic mobilities of different substances and (b) adsorption of the sample components on the inner surface of the separation compartments.

As the coefficients of the temperature dependence of electrophoretic mobilities for most substances are approximately the same (2.5–2.8%/°C), the deviations caused by (a) will be negligible in most instances. More critical may be case (b), because adsorption of some sample components on the different wall materials of the separation compartments (fused-silica capillary and glass–glass or glass–plastic flow-through chamber) with different volume/surface ratios sometimes occurs. This phenomenon may be more pronounced for very small I.D. fused-silica capillaries without an inner coating. However, the symptoms of adsorption (*e.g.*, peak tailing) can be recognized and the separation conditions can be changed in order to suppress the adsorption. Henceforth in this paper the adsorption of the sample components on the inner surface of the separation compartments is neglected. Provided that  $p$  can be assumed to be constant for different sample components,  $p$  determined for standard component 1 can be used also for other substances (*e.g.*, components 2,3,...) that are separated under the same conditions as component 1 in CZE and FFZE. Based on the above-mentioned relationships and assumptions, the procedure for the conversion of an analytical CZE separation into a preparative FFZE separation can be formulated.

Let us consider a peptide sample for which suitable conditions for CZE separation have been developed. From the analysis of this sample, which we may call CZE<sub>2</sub>, the resulting migration times,  $t_{r2}$ , of a charged sample component and the electroosmotic time,  $t_{eo2}$ , of an uncharged sample component can be obtained. Substituting these values into eqn. 3, the electrophoretic velocity of the components in the capillary,  $v_{ep,c2}$ , can be calculated.

Then the CZE analysis of a mixture of standard charged components and of an uncharged electroosmotic flow marker is performed under the same separation conditions as in CZE<sub>2</sub>. From this analysis, which we may call CZE<sub>1</sub>, the resulting migration time of a charged standard component,  $t_{r1}$ , and the electroosmotic time of a zero-charged component,  $t_{eo1}$ , are obtained. Substituting them into eqn. 3, the electrophoretic velocity of the standard components in the capillary,  $v_{ep,c1}$ , can be calculated.

The standard mixture is then separated in the free-flow zone electrophoresis regimen (FFZE<sub>1</sub>) under estimated non-optimized conditions, *i.e.*, usually at a lower than optimum deflection angle. From this experiment the magnitudes of the resulting migrated distance of charged components,  $d_{r1}$ , and the migrated distance of an uncharged component,  $d_{eo1}$ , are obtained. The electrophoretic velocity of the charged standard components in the flow-through chamber,  $v_{ep,f1}$ , is then calculated according to eqn. 7.

From these experiments, the ratio  $p$  of electrophoretic velocities of the standard components in the free-flow chamber and in the capillary can be determined:

$$p = v_{ep,f1}/v_{ep,c1} \quad (10)$$

and the electrophoretic velocity of the sample components in FFZE,  $v_{ep,f2}$ , can be calculated:

$$v_{ep,f2} = v_{ep,c2}p \quad (11)$$

The resulting distance,  $d_{r2}$ , of the sample components in the chamber can be predicted:

$$d_{r2} = d_{eo1} + v_{ep,f2}t_f \quad (13)$$

Based on these predicted resulting migration distances of different sample components, their separability by FFZE can be estimated.

In addition to the prediction of separability, the prediction of the resulting migrating distance of the

fastest sample is important for practical conversion of CZE into FFZE, as this distance should be shorter than the maximum safety distance,  $d_{max}$ . Such a prediction allows the prevention of the migration of the fastest sample component in the close vicinity of ion-exchange or other membranes separating electrode vessels from the separation chamber. At the lateral sides of the FFZE chamber in homogeneities of electric field and carrier electrolyte composition, pH and conductivity changes often occur and fast sample components can be damaged or even lost on reaching this region. Also, electric breakthrough of membranes in contact with the precipitating protein zone may thus be avoided.

Based on the predicted values of the migration distances of the sample components, the separation conditions of FFZE can be optimized, *i.e.*, the clamp voltage and/or flow-through time can be either increased if the migrated distances are too small and the separation capability of the FFZE chamber is not exploited effectively, or these parameters have to be decreased if the predicted distances indicate that sample components might migrate outside the collector region of the FFZE chamber.

## EXPERIMENTAL

### *Instrumentation and methods*

CZE was carried out in an apparatus developed in our laboratory [14]. It consists of a fused-silica capillary (I.D. 0.050 mm, O.D. 0.150 mm, with an outer polyimide coating, total length 310 mm, effective length to the detector 200 mm), supplied by the Institute of Chemistry of Glass and Ceramic Materials, Czechoslovak Academy of Sciences (Prague, Czechoslovakia), a single-wavelength on-column UV detector set at 206 nm and a 20-kV high-voltage power supply, with a current or voltage stabilization regimen. The sample was introduced manually by hydrostatic pressure formed by a height difference of 50 mm between the sample solution and electrode vessel solution level for 5–15 s. All experiments were performed under the following conditions: carrier electrolyte, 0.5 mol/l acetic acid; constant current, 10.0  $\mu$ A; voltage, 9.2–9.5 kV; and temperature, ambient (22–23°C).

FFZE experiments were carried out in an apparatus developed in our Institute [12,16]. Separation was realized in a glass flow-through chamber

(500 × 500 × 0.5 mm, with an effective length from sample inlet to fraction collector outlets, *i.e.*, sample hydrodynamic flow trajectory, of 440 mm), cooled on both sides, under the following conditions: carrier electrolyte, 0.5 mol/l acetic acid (pH 2.6); electrode electrolyte, 1.0 mol/l acetic acid; mean flow-through time, 31 min; number of collected fractions, 48; temperature of outer cooling media at the chamber outlet, -3°C; constant voltage, 3000 V; current, 118–121 mA; and off-line fraction evaluation (absorbance at 280 nm). Sample solution was introduced continuously at a flow-rate of 1.5 ml/h.

**Chemicals**

All chemicals were of analytical-reagent grade. Diglycine and triglycine were purchased by Reanal (Budapest, Hungary) and phenol and acetic acid from Lachema (Brno, Czechoslovakia); the acetic acid was distilled before use. [D-Tle<sup>2,5</sup>]-Dalargin was synthesized in our Institute (for more details, see Results and Discussion).

**RESULTS AND DISCUSSION**

From the above theory, it follows that for practical utilization of the correlation between CZE and FFZE, *i.e.*, for conversion of analytical CZE into preparative FFZE, the ratio *p* of the electrophoretic velocities of standard components in the flow-

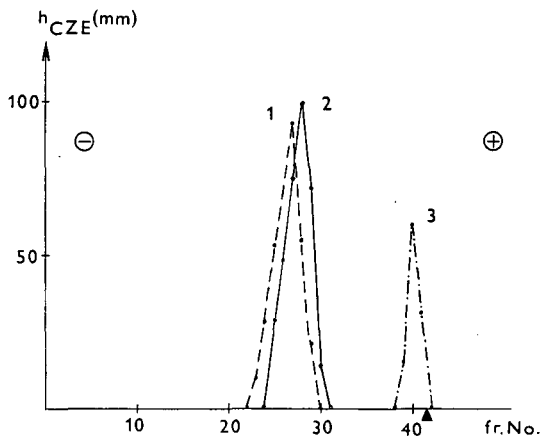


Fig. 3. FFZE separation of standard mixture evaluated by CZE analysis of individual FFZE fractions. 1 = Diglycine (15 mg/ml); 2 = triglycine (15 mg/ml); 3 = phenol (5 mg/ml).  $h_{CZE}$  = Peak height of the sample component present in the FFZE fractions; ▲ = coordinate of the sample inlet in the chamber; fr. No. = fraction number.

through chamber and in the capillary must be known. Its value was determined from the CZE and FFZE separations of a standard mixture containing diglycine, triglycine and phenol (see Figs. 2 and 3). Both separations were performed in the same medium (0.5 mol/l acetic acid, pH 2.6) which was earlier found suitable for the CZE analysis of the crude synthetic peptide [D-Tle<sup>2,5</sup>]-dalargin. The peptides diglycine and triglycine were used as standards of

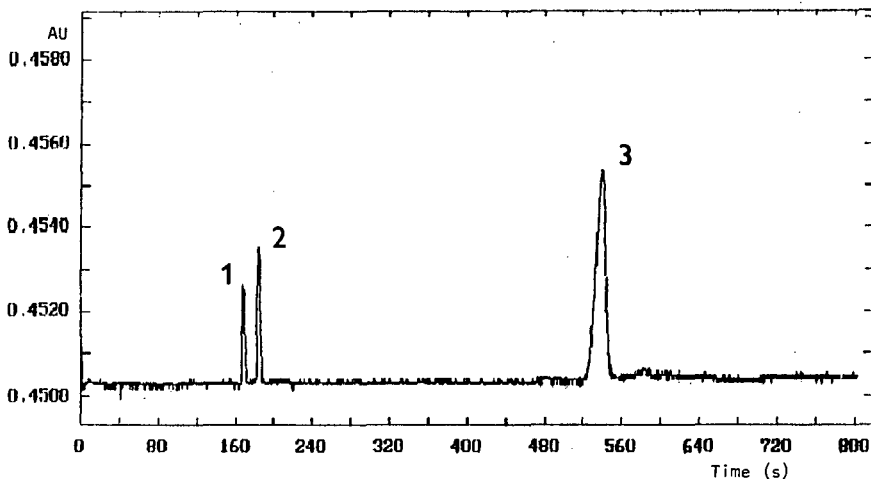


Fig. 2. CZE analysis of standard mixture. 1 = Diglycine (0.3 mg/ml); 2 = triglycine (0.3 mg/ml); 3 = phenol (0.1 mg/ml). Absorbance at 206 nm; AU = absorbance.



TABLE I  
EXPERIMENTAL DATA FOR CZE AND FFZE SEPARATIONS OF STANDARD COMPONENT MIXTURE

$t_r$  = Resulting migration time;  $t_{eo}$  = migration time of electroosmotic marker;  $d_r$  = resulting migration distance;  $d_{eo}$  = distance migrated by electroosmotic flow. Details of experimental conditions are given in the text.

Standard component	CZE		FFZE	
	$t_r$ (s)	$t_{eo}$ (s)	$d_r$ (mm)	$d_{eo}$ (mm)
Diglycine	168	—	145	—
Triglycine	184	—	135	—
Phenol	515	510	15	15

charged substances and phenol, non-dissociated in the low-pH medium, served as an uncharged electroosmotic flow marker.

The experimental data, namely migration times and the migration distances of standard mixture components obtained from their CZE and FFZE separations, are given in Table I.

From these data, the electrophoretic and electroosmotic velocities,  $v_{ep}$  and  $v_{eo}$ , both in the capillary and in the flow-through chamber were calculated using eqns. 3 and 4 for CZE data and eqns. 7 and 8 for the FFZE data. The ratio  $p$  was determined from the calculated velocities using eqn. 10. The results are summarized in Table II.

The value of  $p$ , determined for standard components, can be used for the prediction of the migration distances of other sample components. This fact was utilized in the analysis and preparation

of [D-Tle<sup>2,5</sup>]-dalargin. First CZE analysis of the crude synthetic peptide was performed (see Fig. 4) and the migration times of the fastest component A, of the main synthetic product M, of the slow component S and of the uncharged component N were determined from this analysis (see  $t_r$  in Table III).

Substituting these data and the average value of  $p$  from Table II into eqns. 3 and 11 sequentially, the electrophoretic velocities of these components,  $v_{ep,c}$  in the capillary and  $v_{ep,f}$  in the flow-through chamber, were calculated (see Table III). Using these calculated values and eqn. 12, the predicted migration distances of the selected sample components were obtained (see Table III). These predicted values of migration distances (15–221 mm) indicated a relatively suitable distribution of the sample components at the fraction outlet side of the FFZE chamber. For this reason, the same separation conditions of FFZE that were used for the standard mixture (clamp voltage 3000 V, flow-through time 31 min) were applied also for the separation of [D-Tle<sup>2,5</sup>]-dalargin.

[D-Tle<sup>2,5</sup>]-Dalargin, a synthetic hexapeptide with the sequence H-Tyr-D-Tle-Gly-Phe-D-Tle-Arg-OH, represents an analogue of dalargin (H-Tyr-D-Ala-Gly-Phe-Leu-Arg-OH), an enkephalin-type peptide with opiate activity. The abbreviation D-Tle indicates an amino acid residue of tertiary leucine D-configuration; the other amino acid residues are present in the L-configuration.

The crude product of this peptide was synthesized by the usual Merrifield solid-phase method. With the exception of D-Tle, all amino acids were added to

TABLE II  
CALCULATED ELECTROPHORETIC AND ELECTROOSMOTIC VELOCITIES OF STANDARD COMPONENTS IN CZE AND FFZE

$v_{ep}$  = Electrophoretic velocity;  $v_{eo}$  = electroosmotic velocity;  $p$  = ratio of electrophoretic velocities in FFZE and CZE. For further details, see text.

Standard component	CZE		FFZE		$p$ (FFZE/CZE)
	$v_{ep}$ (mm/s)	$v_{eo}$ (mm/s)	$v_{ep}$ (mm/s)	$v_{eo}$ (mm/s)	
Diglycine	0.805	—	0.0699	—	0.087
Triglycine	0.707	—	0.0645	—	0.091
Phenol	0	0.396	0	0.0081	—

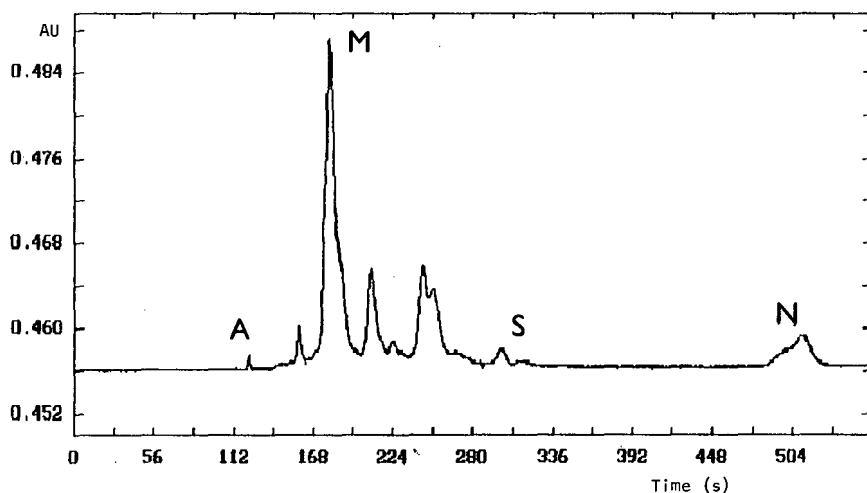


Fig. 4. CZE analysis of the crude synthetic product of [D-Tle<sup>2,5</sup>]-dalargin. 0.6 mg of the lyophilizate dissolved in 0.4 ml of 0.5 mol/l acetic acid. A = Fastest component; M = main component of the synthetic product; S = slow component; N = uncharged component(s). Absorbance at 206 nm; AU = absorbance.

the reaction in the form of hydroxybenzotriazole esters; D-Tle was condensed directly in the reaction mixture in the presence of N,N'-dicyclohexylcarbodiimide and hydroxybenzotriazole. Coupling of all amino acids was checked by the Kaiser test (to the loss of blue colour). The peptide was cleaved from the resin (simultaneously with the cleavage of the protective group) by liquid hydrogen fluoride (10 ml per gram of resin) containing 5% of ethanedithiol and 20% of anisole. After hydrogen fluoride distillation the peptide was eluted from the resin with 50% acetic acid. The solution was diluted with water to

15% (v/v) concentration of acetic acid and lyophilized. The lyophilizate of the crude synthetic product (190 mg) was dissolved in 5 ml of 0.5 mol/l acetic acid, centrifuged and applied to the FFZW separation. The pattern of UV absorbance at 280 nm of FFZE fractions is shown in Fig. 5.

Comparing Figs. 4 and 5, the qualitative similarity of the CZE and FFZE separation patterns can be observed. The differences in relative peak heights are caused by the different wavelengths used for detection in CZE (206 nm) and FFZE (280 nm). It is naturally evident that the separation power of FFZE

TABLE III

MIGRATION TIMES, ELECTROPHORETIC VELOCITIES AND PREDICTED AND EXPERIMENTAL MIGRATION DISTANCES OF SELECTED COMPONENTS OF CRUDE PRODUCT OF [D-Tle<sup>2,5</sup>]-DALARGIN

$t_r$  = Resulting migration time obtained from CZE analysis in Fig. 4;  $v_{ep,c}$  = electrophoretic velocity in the capillary;  $v_{ep,f}$  = electrophoretic velocity in the chamber;  $d_{r,pred}$  = predicted migration distance;  $d_{r,real}$  = experimental migration distance obtained from FFZE separation in Fig. 5. Details of experimental conditions are given in the text.

Sample component <sup>a</sup>	CZE		FFZE		
	$t_r$ (s)	$v_{ep,c}$ (mm/s)	$v_{ep,f}$ (mm/s)	$d_{r,pred}$ (mm)	$d_{r,real}$ (mm)
A	123	1.234	0.1111	221	235
M	175	0.747	0.0665	139	155
S	310	0.250	0.022	56	55
N	510	0	0	15	15

<sup>a</sup> A = Fastest component; M = main component of the synthetic product; S = slow component; N = uncharged component(s).

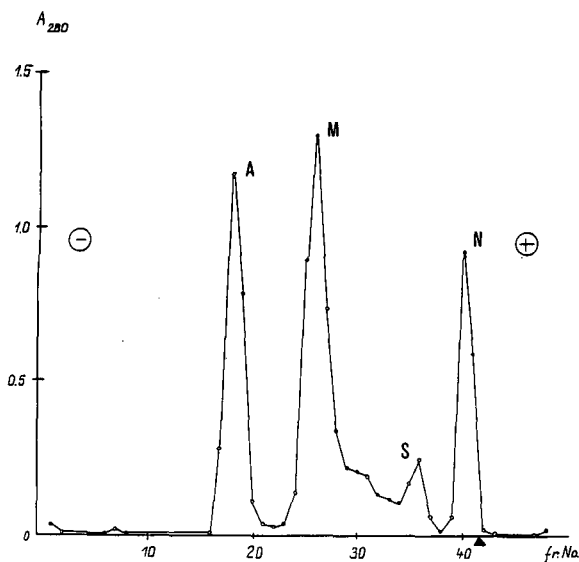


Fig. 5. FFZE separation of crude preparation of [D-Tle<sup>2,5</sup>]-dalargin. A = Fastest component; M = main synthetic product ([D-Tle<sup>2,5</sup>]-dalargin); S = slow component; N = uncharged component(s). Experimental conditions are given in the text.  $A_{280}$  = absorbance at 280 nm; fr. No. = fraction number;  $\blacktriangle$  = coordinate of the sample inlet in the chamber.

is lower than that of CZE. This is understandable when one considers all the differences in these two experimental arrangements of the same zone electrophoresis principle: better anticonvective stabilisation and Joule heat dissipation in the 0.05 mm I.D. capillary than in the 0.5-mm gap flow-through chamber, about one order of magnitude lower migration time in CZE for the main product, one order of magnitude lower sample concentration in CZE than in FFZE, absence of hydrodynamic flow in the capillary and the relatively large width of the collected fraction (10.4 mm) in FFZE. However, although the FFZE separation is not complete, its usefulness for peptide purification is obvious from Fig. 5. The purification effect of FFZE was quantitatively evaluated by CZE analysis of individual FFZE fractions. Examples of these analyses for FFZE fractions 18, 26, 31 and 36 are shown in Fig. 6.

Fig. 6a and b represent examples of fractions containing electrophoretically homogeneous material; single peaks were obtained in CZE analyses. Fig. 6c and d show CZE analyses of FFZE fractions 31 and 36 containing mixtures of several sample components that remained unresolved after FFZE.

Nevertheless, these side-product components of peptide synthesis were not the subject of further interest and their further separation was not pursued. The main product of the solid-phase peptide synthesis, [D-Tle<sup>2,5</sup>]-dalargin, is completely free from the fastest component and relatively well separated also from the slower components. Some fractions of the main product were obtained in a pure form, that can be isolated as an acetate and/or acetic acid adduct after lyophilization, *i.e.*, directly applicable in a physiologically tolerable form for biological tests.

The high degree of purity of the main peak component was checked also by high-performance liquid chromatographic analysis and its sequence was confirmed by amino acid analysis: Tyr (0.93), D-Tle (1.80), Gly (0.98), Phe (0.96), Arg (1.02). The opiate activity of [D-Tle<sup>2,5</sup>]-dalargin is substantially decreased in comparison with dalargin, probably because of the great changes in configuration and conformation of peptide chain caused by the presence of two voluminous D-Tle residues, which results in weaker interaction with the receptor [17].

Comparison of the experimentally determined migration distances of selected components with the predicted migration distances (see Fig. 5 and Table III) shows relatively good agreement. The relatively small discrepancy between the predicted and experimental distances of the fastest sample component (*ca.* 6%) confirms the quantitative correlation between CZE and FFZE. The larger discrepancy with the main peak component (*ca.* 10%) is probably caused by its relatively high concentration in the FFZE experiment. The accuracy of the prediction is also unfavourably influenced by the relatively large fraction width in our apparatus (10.4 mm).

## CONCLUSIONS

The procedure developed, involving consecutive utilization of CZE, FFZE and CZE methods in peptide analysis and preparation, represents a rapid and economical approach to the decision as to whether and how to use effectively a carrier-free and almost loss-free continuous electrophoretic mode of preparation and what the optimized separation conditions are.

First CZE is used for microanalyses of the synthetic peptide at the nanogram level. Suitable separa-

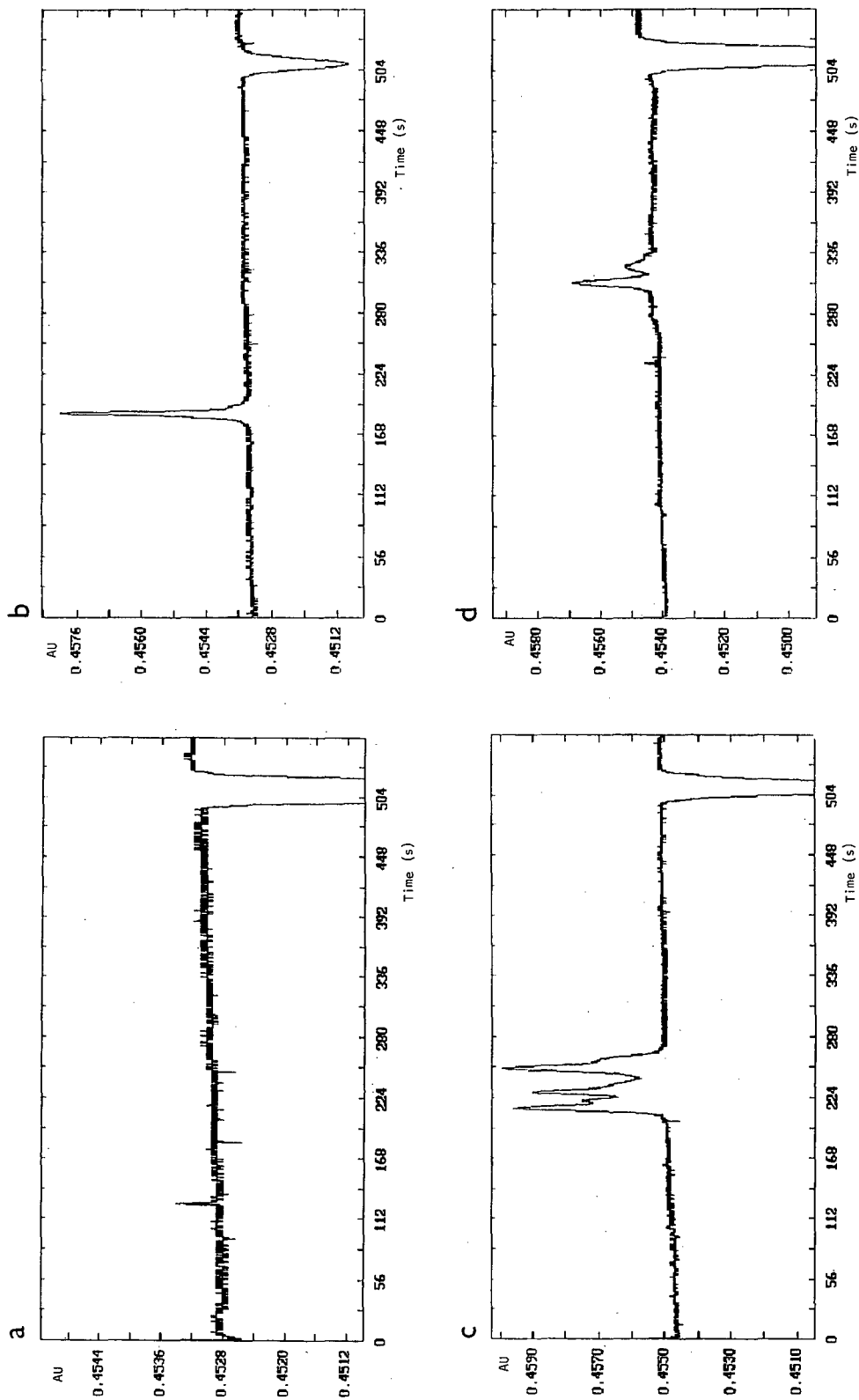


Fig. 6. CZE analyses of selected FFZE fractions: (a) fraction 18; (b) fraction 26; (c) fraction 31; (d) fraction 36. Aliquots of these fractions were analysed directly as obtained by FFZE. For experimental details, see text. Absorbance at 206 nm; AU = absorbance.

tion conditions are developed with minimum sample and electrolyte consumption. These data obtained by optimized CZE are used for conversion into preparative FFZE without loss of the sample material for FFZE tests. The purity of FFZE fractions is then examined by CZE and the purification effect of FFZE can thus be quantitatively evaluated.

#### ACKNOWLEDGEMENTS

P. Mudra, J. Štěpánek, J. Weisgerber, K. Danhelka and K. Ženíšek are thanked for their help in the development and the construction of the experimental devices used in this work. The skilful assistance of V. Lišková in the FFZE experiments is appreciated.

#### REFERENCES

- 1 B. L. Karger (Guest Editor), *1st International Symposium on High Performance Capillary Electrophoresis, Boston, MA, April 10–12, 1989*; *J. Chromatogr.*, 480 (1989).
- 2 B. L. Karger (Guest Editor), *2nd International Symposium on High Performance Capillary Electrophoresis, San Francisco, CA, January 29–31, 1990*; *J. Chromatogr.*, 516, No. 1 (1990).
- 3 J. W. Jorgenson (Guest Editor), *3rd International Symposium on High Performance Capillary Electrophoresis, San Diego, CA, February 3–6, 1991*; *J. Chromatogr.*, 559 (1991).
- 4 W. G. Kuhr, *Anal. Chem.*, 62 (1990) 403R.
- 5 Z. Deyl and R. Stružinský, *J. Chromatogr.*, 569 (1991) 63.
- 6 S. Hjertén and M. D. Zhu, *J. Chromatogr.*, 327 (1985) 157.
- 7 D. J. Rose and J. W. Jorgenson, *J. Chromatogr.*, 438 (1988) 23.
- 8 X. Huang and R. N. Zare, *J. Chromatogr.*, 516 (1990) 185.
- 9 N. Banke, K. Hansen and I. Diers, *J. Chromatogr.*, 559 (1991) 325.
- 10 Z. Prusík, in Z. Deyl (Editor), *Electrophoresis. Part A: Techniques*, Elsevier, Amsterdam, 1979, p. 229.
- 11 H. Wagner, V. Mang, R. Kessler and W. Speer, in C. J. Holloway (Editor), *Analytical and Preparative Isotachopheresis*, Walter de Gruyter, Berlin, 1984, p. 347.
- 12 Z. Prusík, *J. Chromatogr.*, 91 (1974) 867.
- 13 H. Wagner and J. Heinrich, in H. Tschesche (Editor), *Modern Methods in Protein and Nucleic Acid Research*, Walter de Gruyter, Berlin, 1990, p. 69.
- 14 Z. Prusík, V. Kašička, P. Mudra, J. Štěpánek, O. Smékal and J. Hlaváček, *Electrophoresis*, 11 (1990) 932.
- 15 Z. Prusík, V. Kašička, G. Weber and J. Pospíšek, in B. J. Radola (Editor), *Electrophoresis Forum '91*, Technische Universität München, Munich, 1991, p. 201.
- 16 Z. Prusík, J. Štěpánek and V. Kašička, in B. J. Radola (Editor), *Electrophoresis '79*, Walter de Gruyter, Berlin, 1980, p. 287.
- 17 J. Pospíšek, T. Barth, Z. D. Běspalova, M. I. Titov, H. P. Mašková, A. S. Molokoedov and N. F. Septov, *Collect. Czech. Chem. Commun.*, 54 (1989) 22.

# Microemulsion electrokinetic chromatography: comparison with micellar electrokinetic chromatography

Shigeru Terabe and Norio Matsubara

*Faculty of Science, Himeji Institute of Technology, Kamigori, Hyogo 678-12 (Japan)*

Yasushi Ishihama and Yukihiro Okada

*Department of Industrial Chemistry, Faculty of Engineering, Kyoto University, Sakyo-ku, Kyoto 606 (Japan)*

---

## ABSTRACT

The fundamental characteristics of microemulsion electrokinetic chromatography (MEEKC) were studied in comparison with micellar electrokinetic chromatography (MEKC). A microemulsion consisting of heptane–sodium dodecyl sulphate–butanol–buffer (pH 7.0) (0.81:1.66:6.61:90.92) was mainly employed. The separation selectivity of MEEKC was compared with that of MEKC with SDS micelles by using three different test mixtures. The microemulsion showed a stronger affinity to non-polar compounds than the SDS micelle. The migration-time window in MEEKC was easily extended owing to an increase in the electrophoretic mobility of the microemulsion by increasing the SDS fraction in the microemulsion. The efficiency in MEEKC was also compared with that in MEKC. The plate heights in MEEKC were higher than, but less than double, those in MEKC. The effect of microheterogeneity was not significant but the effect of sorption–desorption kinetics seemed more serious in MEEKC than in MEKC.

---

## INTRODUCTION

Electrokinetic chromatography (EKC) [1] requires two phases, between which analytes are distributed. One phase, which is named separation carrier, must have an electrophoretic mobility to migrate at a velocity different from that of the surrounding medium; the other phase is generally an aqueous phase which is the solvent of the separation carrier. The carrier must interact with the analyte, and the aqueous phase must be electrically conductive and preferably transparent to UV radiation.

Ionic micelles are the most widely accepted carriers and the technique is named micellar EKC (MEKC) [2,3]. An advantage of MEKC is the easy availability of various surfactants, because different micelles show different selectivity. For example, bile salt micelles give significantly different selectivity

from the sodium dodecyl sulphate (SDS) micelle [4,5]. Bile salts are also useful for enantiomeric separation owing to their chirality [6–8]. The other advantage of MEKC is easy modification of the aqueous phase, which is effective for selectivity manipulation.

Cyclodextrin (CD) derivatives having ionic groups and polymer ions have also been successfully employed in CDEKC [9] and ion-exchange EKC [10], respectively. CDEKC is useful for the separation of isomers of aromatic compounds and enantiomers [1,9]. A disadvantage of CDEKC is the difficulty of the preparation of CD derivatives useful for CDEKC. CD-modified MEKC (CD–MEKC), which employs a micellar solution containing a neutral CD, is easier to perform than CDEKC, because various CDs or CD derivatives are commercially available, but CD–MEKC provides a similar selectivity to CDEKC [11,12]. Ion-exchange EKC has limited applications.

Recently, Watarai [13,14] reported the use of an

---

*Correspondence to:* Dr. S. Terabe, Faculty of Science, Himeji Institute of Technology, Kamigori, Hyogo 678-12, Japan.

oil-in-water (o/w) microemulsion as a separation carrier in EKC. He showed that the microemulsion works similarly to the ionic micelle for the separation of neutral analytes and that the migration-time window is easily extended by changing the composition of the microemulsion. The migration-time window is defined as the possible range of the migration time of neutral analytes and is limited between the migration time of the bulk solution ( $t_0$ ) and that of the micelle or of the microemulsion ( $t_m$ ). A wider migration-time window leads to better resolution, although the total separation time becomes longer. Watarai [13,14] also observed no serious band broadening in spite of the larger size of the microemulsion compared with the micelle.

Microemulsions (o/w) prepared by mixing oil, water, a surfactant and a cosurfactant such as a medium alkyl-chain alcohol are transparent and thermodynamically stable if the composition is properly chosen. The structure of the o/w microemulsion is similar to that of the micelle, except that the microemulsion has a core of a minute droplet of an oil. The surfactant and the cosurfactant are located on the surface of the oil droplet to stabilize the droplet, as shown in Fig. 1.

This study was performed to evaluate the fundamental characteristics of microemulsion EKC (MEEKC) compared with MEKC, especially from the viewpoint of selectivity and efficiency. In this paper, preliminary results are outlined.

## EXPERIMENTAL

EKC was performed with a P/ACE System 2000 (Beckman, Palo Alto, CA, USA) or a laboratory-

built capillary electrophoresis (CE) instrument. The latter instrument was essentially the same as described previously [2] and consisted of a high-voltage d.c. power supply of a Matsusada Precision Devices HCZE30PN0.25-LDSW (Kusatsu, Shiga, Japan) or a Bertan High Voltage Series 230-30R (Hicksville, NY, USA) and a Jasco (Tokyo, Japan) UVIDEC-100-V spectrophotometric detector modified to accommodate a capillary for on-column detection. For detection, absorption was measured at 214 nm with the P/ACE System 2000 and at 210 nm with the Jasco detector. Chromatograms were recorded with a Shimadzu (Kyoto, Japan) Chromatopac C-R3A or C-R6A data processor. Plate numbers were calculated from peak area, migration time and peak height as described previously [15].

A fused-silica capillary of 50  $\mu\text{m}$  I.D. and effective length 30 or 50 cm was used without any special wall treatment. Sample solutions were injected into an end of the capillary by the pressure injection (0.5 p.s.i., 1 s) method (P/ACE System 2000) or by the siphoning method (laboratory-built instrument). The temperature of the capillary was controlled at 35°C in the P/ACE System 2000, and the capillary was cooled with a small fan at ambient temperature in the laboratory-built instrument.

All the reagents and samples were of analytical-reagent grade. A microemulsion was prepared by mixing heptane (0.81%), SDS (3.31%), butanol (6.61%) and 100 mM borate–50 mM phosphate buffer (pH 7.0) (89.28%), according to the method reported by Watarai [13], although Watarai used water instead of the buffer solution and adjusted the pH with a carbonate–hydrogencarbonate buffer. In most instances a microemulsion consisting of a half fraction of SDS (60 mM) was used. SDS solutions were prepared with the same borate–phosphate buffer (pH 7.0) as were employed to prepare the microemulsion or 100 mM N,N-bis(2-hydroxyethyl)-2-aminoethanesulphonic acid (BES)–100 mM sodium hydroxide buffer (pH 7.0). The borate–phosphate buffer was prepared by mixing 25 mM sodium tetraborate and 50 mM sodium dihydrogenphosphate solutions in the appropriate ratio to give the desired pH, as described previously [2]. The BES buffer was similarly prepared from 100 mM BES and 100 mM sodium hydroxide solutions.

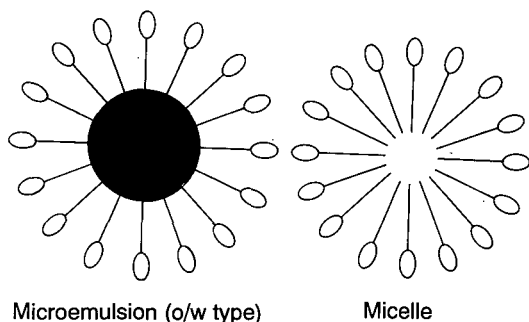


Fig. 1. Schematic illustration of the o/w microemulsion and micelle.

## RESULTS AND DISCUSSION

## Separation selectivity

Three examples of MEEKC separations of some test mixtures are given in Figs. 2–4 together with MEKC separations with the SDS micelle. All the sample zones migrated from the positive to the negative electrode. Both the microemulsion and the micelle had negative charge and hence migrated toward the positive electrode by electrophoresis. Therefore, the results indicate that the electroosmotic flow was stronger than the electrophoretic migration of either the microemulsion or the micelle. Although timepidium bromide was conveniently used as a tracer of the SDS micelle [16], it did not seem to be a correct tracer of the microemulsion, because phenanthrene and *p*-amylphenol migrated more slowly than timepidium bromide. Phenanthrene and *p*-amylphenol, which migrated at the same velocity, are electrically neutral, and therefore the slower velocity means that they are incorporated more into the microemulsion.

The capacity factor,  $k'$ , defined as the ratio of the

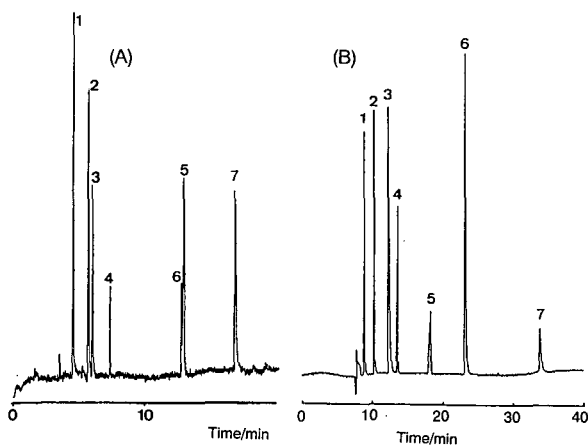


Fig. 2. (A) Microemulsion electrokinetic chromatogram and (B) micellar electrokinetic chromatogram of a test mixture. 1 = Resorcinol; 2 = phenol; 3 = *p*-nitroaniline; 4 = nitrobenzene; 5 = toluene; 6 = 2-naphthol; 7 = timepidium bromide. (A) Capillary, 50 cm  $\times$  52  $\mu$ m I.D. (30 cm to the detector); separation solution, heptane–SDS–butanol–borate–phosphate buffer (pH 7.0) (0.81:1.66:6.61:90.92); applied voltage, 15 kV; current, 48  $\mu$ A; temperature, ambient. (B) Capillary, 57 cm  $\times$  52  $\mu$ m I.D. (50 cm to the detector); separation solution, 50 mM SDS in borate–phosphate buffer (pH 7.0); applied voltage, 10 kV; current, 24  $\mu$ A; temperature, 35°C.

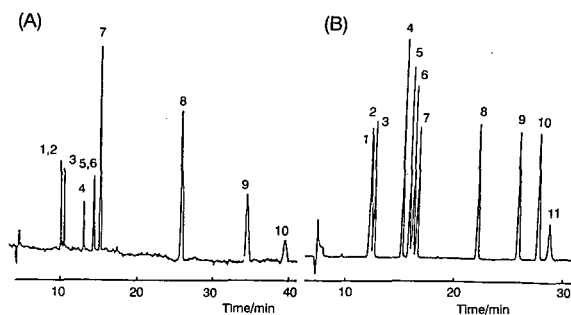


Fig. 3. Comparison between (A) MEEKC and (B) MEKC. 1 = *o*-Cresol; 2 = *m*-cresol; 3 = *p*-cresol; 4 = 2,6-xyleneol; 5 = 2,3-xyleneol; 6 = 3,4-xyleneol; 7 = 2,4-xyleneol; 8 = *p*-propylphenol; 9 = *p*-butylphenol; 10 = *p*-amylphenol; 11 = timepidium bromide. (A) Capillary, 48.2 cm  $\times$  52  $\mu$ m I.D. (28.2 cm to the detector); separation solution, 79 mM heptane–60 mM SDS–874 mM butanol in borate–phosphate buffer (pH 7.0); applied voltage, 13 kV; current, 33  $\mu$ A; temperature, ambient. (B) Current, 29  $\mu$ A; other conditions as in Fig. 2B.

total moles of an analyte in the microemulsion or micelle to those in the surrounding aqueous phase, can be calculated according to [3]

$$k' = \frac{t_R - t_0}{t_0(1 - t_R/t_m)} \quad (1)$$

where  $t_R$ ,  $t_0$  and  $t_m$  are the migration times of the analyte, aqueous phase and microemulsion or micelle, respectively. The migration time of the aqueous phase was assumed to be equal to that of methanol. Timepidium bromide was used as a tracer of the micelle and phenanthrene was assumed to be a tracer of the microemulsion, as mentioned above, although the mixtures shown in Figs. 2–4 did not contain phenanthrene.

The capacity factor values are given in Tables I and II for the solutes shown in Figs. 2 and 4. It should be noted that the conditions employed to obtain the capacity factors in MEEKC were slightly different, mainly in the ambient temperature, from those in Figs. 2A–4A. Therefore, some discrepancies were observed between Fig. 2A and Table I and Fig. 4A and Table II. As can be seen in Table I, MEEKC gave substantially higher  $k'$  values than MEKC, except for toluene. The elution orders of toluene and 2-naphthol were reversed between MEEKC and MEKC, as shown in Fig. 2. The higher  $k'$  value of toluene in MEEKC suggests that the microemulsion has a stronger affinity for non-polar



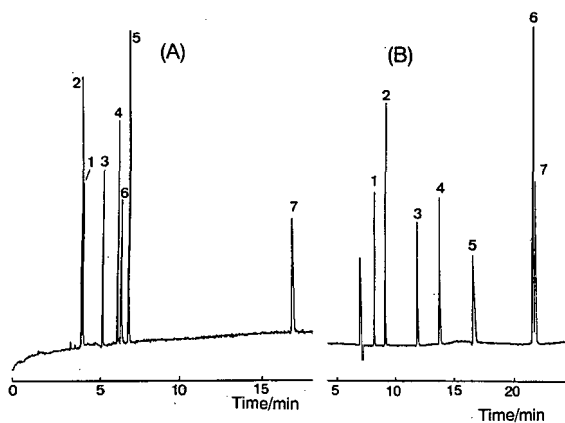


Fig. 4. Separation of cold medicine ingredients by (A) MEEKC and (B) MEKC. 1 = Acetaminophen; 2 = caffeine; 3 = guaiphenesin; 4 = ethenzamide; 5 = isopropylantipyrine; 6 = trimetoquinol; 7 = timepidium bromide. (A) Conditions as in Fig. 2A. (B) Separation solution, 50 mM SDS in BES buffer (pH 7.0); current, 19  $\mu$ A; other conditions as in Fig. 2B.

compounds than the SDS micelle. For a strict comparison, the capacity factor or preferably the distribution coefficient at the same temperature should be employed as described below, because both the capacity factor and distribution coefficient are temperature dependent. However, the capacity factors in Tables I and II are still helpful for the purpose of qualitative comparison.

TABLE I  
COMPARISON OF CAPACITY FACTORS OF TEST SAMPLES

Solute	$k'$	
	Microemulsion (MEEKC) <sup>a</sup>	Micelle (MEKC) <sup>b</sup>
Resorcinol	0.36	0.18
Phenol	0.76	0.44
<i>p</i> -Nitroaniline	0.94	0.87
Nitrobenzene	1.38	1.22
Toluene	6.19	2.89
2-Naphthol	6.19	6.10

<sup>a</sup> Separation solution, buffer (pH 7.0)–butanol–SDS–heptane (90.92:6.61:1.66:0.81, w/w); applied voltage, 15 kV; current, 37  $\mu$ A. Other conditions as in Fig. 2.

<sup>b</sup> Separation solution, 50 mM SDS in borate–phosphate buffer (pH 7.0). Conditions as in Fig. 2.

TABLE II  
COMPARISON OF CAPACITY FACTORS OF COLD MEDICINES

Solute	$k'$	
	Microemulsion (MEEKC) <sup>a</sup>	Micelle (MEKC) <sup>b</sup>
Acetaminophen	0.20	0.28
Caffeine	0.20	0.52
Guaiphenesin	0.62	1.52
Ethenzamide	1.00	2.59
Trimetoquinol	1.38	194
Isopropylantipyrine	1.68	5.66

<sup>a,b</sup> See Table I.

The capacity factor is also described by

$$k' = K(V_m/V_{aq}) \quad (2)$$

where  $K$  is the distribution coefficient and  $V_m$  and  $V_{aq}$  are the volumes of the microemulsion or the micelle and of the aqueous phase, respectively. The ratio  $V_m/V_{aq}$  is called the phase ratio. Therefore, it is more reasonable to discuss the relative affinity of the analyte between the microemulsion and micelle in terms of the distribution coefficient  $K$  rather than the capacity factor  $k'$ , because  $K$  does not depend on the phase ratio. The volume of the micelle is easily calculated from the concentration of the micelle, which is equal to the difference between the surfactant concentration and the critical micelle concentration, and the partial specific volume, but the volume of the microemulsion is difficult to calculate precisely. In this study, the volume of the microemulsion is evidently larger than that of the SDS micelle by a factor of more than at least three. Therefore, the distribution coefficients of the analytes given in Table I are probably smaller for the microemulsion than for the SDS micelle.

It is apparent from Fig. 3 that selectivity is higher in MEKC than in MEEKC for isomeric cresols and xylenols. This may be due to the difference in surface structures between the microemulsion and micelle and also the core structures. The surface of the micelle will be more rigid than that of the microemulsion, because the surfactant molecules aggregate tightly to form the micelle, whereas the surfac-

tant will be on the surface of the oil droplet of heptane together with butanol in the microemulsion. The rigid surface structure will be capable of recognizing differences in the molecular structures of the isomers. On the other hand, it will be easier for the solute to penetrate into the core oil in the case of microemulsions.

The difference in selectivity between MEEKC and MEKC is also evident in Fig. 4. The capacity factors of the cold medicines are lower than those in MEKC, as given in Table II. This is also explained in terms of the polarity of the analytes. Because the core of the microemulsion is heptane and hence non-polar, the relatively polar cold medicines are not incorporated strongly by the microemulsion. In other words, the analytes do not adsorb on the surface of the microemulsion but are rather incorporated into the core of the droplet, because the capacity factors are much smaller than those of MEKC. This explanation is consistent with a lower selectivity among isomeric cresols or xylenols in MEEKC compared with MEKC, as mentioned above. Different elution orders are also observed between MEEKC and MEKC as shown in Fig. 4. The highest  $k'$  value of isopropylantipyrine is probably due to its non-polar character compared with trimetoquinol, although the latter shows a stronger affinity than isopropylantipyrine to the SDS micelle.

#### Migration-time window

The resolution equation in EKC is [3]

$$R_s = \frac{\sqrt{N}}{4} \left( \frac{\alpha - 1}{\alpha} \right) \left( \frac{k'_2}{1 + k'_2} \right) \left[ \frac{1 - t_0/t_{mc}}{1 + (t_0/t_m)k'_1} \right] \quad (3)$$

where  $R_s$  is the resolution,  $N$  is the plate number and  $\alpha$  is the separation factor, which is equal to  $k'_2/k'_1$ . The last term on the right-hand side originates from the contribution of the limited migration-time window between  $t_0$  and  $t_m$ . The smaller the migration time ratio,  $t_0/t_m$ , the higher is the resolution. To decrease  $t_0/t_m$ , it is necessary either to reduce the electroosmotic velocity or to increase the electrophoretic mobility of the micelle or microemulsion, as is easily predicted from the equation

$$\frac{t_0}{t_m} = \frac{v_m}{v_{eo}} = \left[ 1 + \frac{\mu_{ep}(m)}{\mu_{eo}} \right] E \quad (4)$$

where  $v_m$  is the migration velocity of the microemulsion or micelle,  $v_{eo}$  is the electroosmotic velocity,

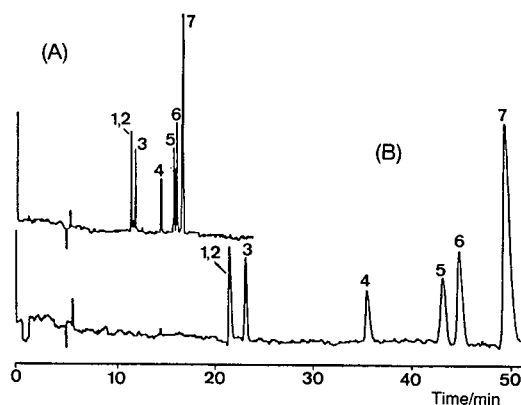


Fig. 5. Effect of the SDS fraction of the microemulsion on resolution. Peak numbers as in Fig. 3. (A) Conditions as in Fig. 3A. (B) Separation solution, 70 mM heptane–120 mM SDS–874 mM butanol in borate–phosphate buffer (pH 7.0); other conditions as in (A).

$\mu_{ep}(m)$  and  $\mu_{eo}$  are electrophoretic mobilities of the microemulsion or micelle and the electroosmotic mobility, respectively, and  $E$  is the electric field strength. It should be noted that the ratio  $\mu_{ep}(m)/\mu_{eo}$  is usually less than zero and greater than  $-1$  in MEEKC and MEKC. Under the conditions of this study,  $\mu_{ep}(m)$  is negative and  $\mu_{eo}$  is positive. In MEKC, it is generally difficult to change  $\mu_{ep}(m)$  freely over a wide range. Only when a high concentration of urea was added to micellar solutions has a decrease in  $t_0/t_m$  due to an increase in  $\mu_{ep}(m)$  been reported [17]. Therefore, to extend the migration-time window in MEKC, the electroosmotic velocity must be reduced by adding an organic solvent [18,19] or by using a coated capillary [20].

Watarai [13] mentioned that  $t_0/t_m$  is easily decreased in MEEKC by increasing the volume fraction of the organic components. Fig. 5 demonstrates the effect of the SDS fraction on the migration times of analytes. The electroosmotic velocities were almost identical between the two chromatograms in Fig. 5, although they were slightly different between Figs. 3A and 5A even under the same experimental conditions. Fig. 5 clearly shows that doubling the SDS fraction increased dramatically the migration times of all the analytes or increased the electrophoretic mobility of the microemulsion without affecting the electroosmotic velocity. The enhanced resolution in Fig. 5B compared with Fig. 5A is apparent. This suggests that the migration-time

window can possibly be manipulated by changing the SDS fraction of the microemulsion without affecting the selectivity significantly. This is an obvious advantage of MEEKC over MEKC.

#### Band broadening

Band broadening in MEKC has been discussed in detail by Sepaniak and Cole [21] and Terabe *et al.* [15]. The total band broadening in the capillary is described as the sum of plate heights generated by five factors:

$$H_{\text{tot}} = H_1 + H_m + H_{\text{aq}} + H_T + H_{\text{ep}} \quad (5)$$

where  $H_{\text{tot}}$  is overall plate height, and  $H_1$ ,  $H_m$ ,  $H_T$  and  $H_{\text{ep}}$  are plate heights generated by longitudinal diffusion, sorption–desorption kinetics in micellar solubilization, intermicelle mass transfer in the aqueous phase, radial temperature gradient effect on the electrophoretic velocity of the micelles and dispersion of electrophoretic mobilities of the micelles, respectively. Among these five factors,  $H_1$ ,  $H_m$  and  $H_{\text{ep}}$  were found to contribute significantly to band broadening [15]. The same discussion will also be applicable to MEEKC.

The longitudinal diffusion decreases with an increase in the migration velocity or applied voltage, whereas  $H_m$  and  $H_{\text{ep}}$  increase linearly with increase in migration velocity [15]. The relative significance of each contribution depends on the capacity factor and  $v_{\text{eo}}$ ;  $H_1$  is the most significant factor when both  $k'$  and  $v_{\text{eo}}$  are low;  $H_{\text{ep}}$  becomes serious when  $k'$  is large

and  $v_{\text{eo}}$  is high;  $H_m$  contributes considerably when  $k'$  is medium and  $v_{\text{eo}}$  is high. The plate height  $H_{\text{ep}}$  is due to the microheterogeneity of the micellar size or, more correctly, to the difference in mobilities of the micelles [15].

The dependence of plate height on the applied voltage is illustrated in Fig. 6 for the compounds shown in Fig. 2. The band broadening in MEKC is also shown in Fig. 6 for comparison. The most interesting point of band broadening in MEEKC is the contribution of the  $H_{\text{ep}}$  term compared with MEKC. The total plate heights in MEEKC were roughly twice those in MEKC, as shown in Fig. 6. The plate heights in MEKC shown in Fig. 6B can be explained by the major contribution of  $H_1$ . However, the results shown in Fig. 6A for MEEKC are not easily explained. In the region below 10 kV  $H_1$  was the main contributor and above 10 kV sorption–desorption kinetics seemed to be the major cause of band broadening. The microheterogeneity did not seem very significant, because 2-naphthol, which had a higher capacity factor, showed the lowest plate height among the solutes. The results in Fig. 6A are preliminary, and temperature was not controlled. To clarify the mechanism of band broadening in MEEKC, a more detailed study is necessary.

#### CONCLUSIONS

Although only preliminary results on MEEKC are given in this paper, MEEKC seems to be of comparable utility to MEKC. The efficiency of MEEKC is slightly lower than that of MEKC, but the migration-time window is easily manipulated to enhance the resolution. The separation selectivity of MEEKC may be affected by the character of the core oil of the microemulsion. The stability of the microemulsion and the reproducibility of migration times were not extensively studied in this work. The composition of the microemulsion containing 1.66% SDS, which was mostly used in this work, was not very stable and hence the reproducibility was probably worse than in MEKC with SDS.

#### ACKNOWLEDGEMENTS

The authors thank Dr. H. Watarai for helpful comments on the microemulsion. S.T. is grateful to Yokogawa Electric, Hitachi and Sumitomo Chemi-

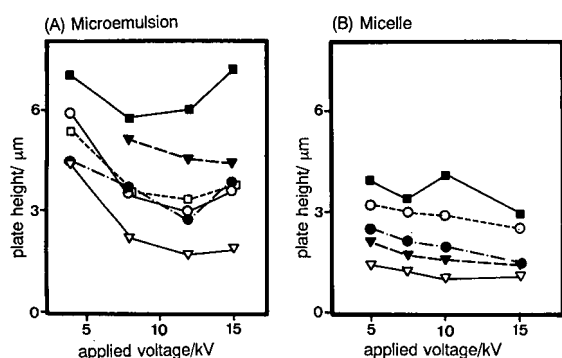


Fig. 6. Dependence of plate heights on the applied voltage in (A) MEEKC and (B) MEKC.  $\square$  = Resorcinol;  $\blacksquare$  = phenol;  $\circ$  = *p*-nitroaniline;  $\bullet$  = nitrobenzene;  $\blacktriangledown$  = toluene;  $\nabla$  = 2-naphthol. (A) Conditions as in Fig. 2A except for applied voltages. (B) Conditions as in Fig. 4B except for applied voltages.

cal for research funds and also to Beckman Instruments for the loan of the CE instrument.

## REFERENCES

- 1 S. Terabe, *Trends Anal. Chem.*, 8 (1989) 129.
- 2 S. Terabe, K. Otsuka, K. Ichikawa, A. Tsuchiya and T. Ando, *Anal. Chem.*, 56 (1984) 111.
- 3 S. Terabe, K. Otsuka and T. Ando, *Anal. Chem.*, 57 (1985) 834.
- 4 H. Nishi, T. Fukuyama, M. Matsuo and S. Terabe, *J. Chromatogr.*, 513 (1990) 279.
- 5 R. O. Cole, M. J. Sepaniak, W. L. Hinze, J. Gorse and K. Oldiges, *J. Chromatogr.*, 557 (1991) 113.
- 6 S. Terabe, M. Shibata and Y. Miyashita, *J. Chromatogr.*, 480 (1989) 403.
- 7 H. Nishi, T. Fukuyama, M. Matsuo and S. Terabe, *J. Microcol. Sep.*, 1 (1989) 234.
- 8 R. O. Cole, M. J. Sepaniak and W. L. Hinze, *J. High Resolut. Chromatogr.*, 13 (1990) 579.
- 9 S. Terabe, H. Ozaki, K. Otsuka and T. Ando, *J. Chromatogr.*, 332 (1985) 211.
- 10 S. Terabe and T. Isemura, *Anal. Chem.*, 62 (1990) 650.
- 11 S. Terabe, Y. Miyashita, O. Shibata, E. R. Barnhart, L. R. Alexander, D. G. Patterson, B. L. Karger, K. Hosoya and N. Tanaka, *J. Chromatogr.*, 516 (1990) 23.
- 12 H. Nishi, T. Fukuyama and S. Terabe, *J. Chromatogr.*, 553 (1991) 503.
- 13 H. Watarai, *Chem. Lett.*, (1991) 391.
- 14 H. Watarai, *Anal. Sci.*, 7, Suppl. (1991) 245.
- 15 S. Terabe, K. Otsuka and T. Ando, *Anal. Chem.*, 61 (1989) 251.
- 16 H. Nishi, N. Tsumagari and S. Terabe, *Anal. Chem.*, 61 (1989) 2434.
- 17 S. Terabe, Y. Ishihama, H. Nishi, T. Fukuyama and K. Otsuka, *J. Chromatogr.*, 545 (1991) 359.
- 18 K. Otsuka, S. Terabe and T. Ando, *Nippon Kagaku Kaishi*, (1986) 950.
- 19 A. T. Balchunas and M. J. Sepaniak, *Anal. Chem.*, 59 (1987) 1466.
- 20 S. Terabe, H. Utsumi, K. Otsuka, T. Ando, T. Inomata, S. Kuze and Y. Hanaoka, *J. High Resolut. Chromatogr. Chromatogr. Commun.*, 9 (1986) 666.
- 21 M. J. Sepaniak and R. O. Cole, *Anal. Chem.*, 59 (1987) 472.



# Micellar electrokinetic capillary chromatography of neutral solutes with micelles of adjustable surface charge density

Jianyi Cai and Ziad El Rassi

*Department of Chemistry, Oklahoma State University, Stillwater, OK 74078-0447 (USA)*

---

## ABSTRACT

Novel micelles with adjustable surface charge density were introduced for micellar electrokinetic capillary chromatography. These micelles are based on the complexation between octylglucoside surfactant and alkaline borate. The surface charge density of the octylglucoside–borate micelles can be conveniently varied by changing the operating parameters such as borate concentration and/or pH of the running electrolyte. This feature permitted the tuning of the elution range, a parameter that largely influences the peak capacity and resolution in micellar electrokinetic capillary chromatography. Furthermore, with its balanced hydrophile–lipophile character, the octylglucoside–borate micellar system allowed the separation of hydrophobic species including herbicides, *e.g.*, prometon, prometryne, propazine and butachlor, and some polyaromatic hydrocarbons. High separation efficiencies were obtained over a wide range of elution conditions, and consequently the detection limit for the herbicides was in the range of 18–52 fmol using UV detection.

---

## INTRODUCTION

Micellar electrokinetic capillary chromatography (MECC), first reported in 1984 by Terabe *et al.* [1], is increasingly used for the separation of neutral and charged species [1–7]. In MECC, the separation medium consists of an electrolyte containing an ionic surfactant in an amount above its critical micellar concentration. Thus, there are two phases inside the capillary tube, an aqueous mobile phase and a micellar pseudo-stationary phase. Whereas the aqueous mobile phase moves at the velocity of electroosmosis, the micelles migrate much slower due to opposing electrophoretic forces. This creates a retention window that extends from the retention time of an unretained solute,  $t_0$ , to the retention time of another solute completely solubilized by the micelles,  $t_{mc}$ . Neutral solutes are eluted within the

retention window and are separated through their differential distribution between the two phases.

Thus far, most MECC applications have utilized aqueous sodium dodecyl sulphate (SDS) as the micellar phase. Although other surfactants can be used, their potentials have been briefly explored [3,7–10]. This may be due to the fact that these ionic surfactants (*e.g.*, cetyltrimethylammonium bromide, sodium tetradecyl sulphate, etc.) showed little or no improvements over SDS as far as the quality of separation is concerned. Due to the pronounced unbalance in the hydrophile–lipophile character of SDS and similar ionic surfactants, hydrophobic solutes of low water solubility are almost totally incorporated in such micelles and are not separated. Few attempts have been made to alleviate this problem. In one approach, a cyclodextrin (CD)-modified SDS micellar phase was introduced for the separation of hydrophobic compounds [11]. In this system, the water-insoluble compound is partitioned between the CD cavity, which is moving at the velocity of the aqueous phase,

---

*Correspondence to:* Dr. Z. El Rassi, Department of Chemistry, Oklahoma State University, Stillwater, OK 74078-0447, USA.

and the interior of the SDS micelle which is migrating at a slower velocity. Therefore, a more equitable distribution of the solutes can be obtained and consequently improved separation. In another approach, bile salt surfactants in the presence of relatively high methanol content were described for the separation of hydrophobic compounds including polyaromatic hydrocarbons [12].

MECC is characterized by an elution range or retention window that strongly influences peak capacity and resolution. With SDS and other ionic surfactants that have been evaluated thus far [3,7–9], the elution range is rather predetermined and can not be varied systematically. The retention window of MECC can be somewhat elongated by using surfactants having shorter alkyl chains (*e.g.*, sodium decyl sulphate) [13], but its width is still predetermined. Another approach through which the breadth of the retention window can be enlarged has been the surface modification of fused-silica capillaries [13–15]. Under these conditions, both  $t_{mc}$  and  $t_0$  increased, which yielded longer analysis time (see Theory section). The only approach through which the retention window can be systematically manipulated seems to be the inclusion of methanol in the micellar system [16,17]. Under these circumstances, however, both  $t_{mc}$  and  $t_0$  increased. Such method led to long analysis time, and because methanol induced polydispersity in the micelles, the separation efficiency was significantly reduced.

This paper is concerned with the investigation of the potentials of micelles of adjustable surface charge density. The new micelles are based on the complexation between octylglucoside surfactant and alkaline borate. These micelles provided several advantages over traditionally used surfactants. First, octylglucoside has a relatively short non-polar chain and a large polar head moiety. This balance in the hydrophile–lipophile character of the octylglucoside surfactant is advantageous for the separations of both polar and highly non-polar species. Furthermore, with the octylglucoside–borate micelles, the surface charge density can be varied conveniently by changing the borate concentration and/or the pH of the running electrolyte, and consequently the retention window of the micellar system can be varied systematically over a wider range. These readily tuned features provided a means to manipulate the separation efficiencies, peak capacity and

resolution. Other alkylglucoside surfactants are being investigated in our laboratory with a broader range of neutral and charged species. These studies are planned for future papers.

## THEORY

Many of the fundamental characteristics of MECC are well understood and have been described by Terabe and co-workers [1,2]. In MECC, retention and resolution are related to the electrokinetic velocities of the aqueous phase (*i.e.*, the electroosmotic velocity) and the micellar pseudo-stationary phase. The net velocity of the micelle,  $v_{mc}$ , is the sum of the electroosmotic velocity of the aqueous phase,  $v_{eo}$ , and the electrophoretic velocity of the micelle,  $v_{ep}$  [14,18]:

$$v_{mc} = v_{eo} + v_{ep} = -\frac{\varepsilon E \zeta_c}{\eta} + \frac{2\varepsilon E \zeta_{mc}}{3\eta} f(\kappa a) \\ = -\frac{\varepsilon E}{\eta} \left[ \zeta_c - \frac{2\zeta_{mc}}{3} f(\kappa a) \right] \quad (1)$$

where  $\zeta_c$  and  $\zeta_{mc}$  are the  $\zeta$  potentials of the inner surface of the capillary and of the outer surface of the micelle, respectively,  $\varepsilon$  and  $\eta$  are the dielectric constant and the viscosity of the electrolyte, respectively,  $f(\kappa a)$  depends on the shape of the micelle [18],  $a$  is the radius of the micelle,  $\kappa$  is the familiar Debye–Hückel constant and  $E$  is the electric field strength. The value of  $f(\kappa a)$  varies between 1.0 and 1.50 depending on the dimensions of  $\kappa a$ . The negative sign in eqn. 1 is to indicate that when the  $\zeta$  potential of the capillary is negative the electroosmotic flow is toward the negative electrode [18].

With negatively charged micelles and untreated fused-silica capillaries  $\zeta_{mc}$  is smaller than  $\zeta_c$  and both have the same sign [1,2]. Neutral solutes are eluted between  $t_0$  and  $t_{mc}$ , which are the retention times of unsolubilized and completely solubilized solute by the micelle, respectively. This is referred to as the elution range or the retention window.

An important variable in MECC is the elution range parameter defined by the ratio [14]:

$$\frac{t_0}{t_{mc}} = \frac{v_{mc}}{v_{eo}} = 1 - \frac{2\zeta_{mc}}{3\zeta_c} f(\kappa a) \quad (2)$$

The  $\zeta$  potentials can be expressed by the following relationship [19]

$$\zeta = \frac{4\pi\delta\rho}{\epsilon} \quad (3)$$

where  $\rho$  is the surface charge density of either the capillary surface ( $\rho_c$ ) or the micelle ( $\rho_{mc}$ ), and  $\delta$  is the thickness of the diffuse double layer adjacent to either the capillary wall ( $\delta_c$ ) or the micelle surface ( $\delta_{mc}$ ). Modern theory equates  $\delta$  to  $1/\kappa$ . Thus, by a rearrangement of eqn. 3

$$\zeta = \frac{4\pi\rho}{\kappa\epsilon} \propto \frac{1}{\sqrt{I}} \quad (4)$$

It follows then, from eqns. 1 and 4, that the electroosmotic flow of the aqueous phase and the electrophoretic velocity of the micelle will be inversely proportional to the square root of the ionic strength,  $I$ .

As the elution range parameter decreases the retention window increases. An elution range parameter of 1 means that the micelle is uncharged and all neutral solutes coelute and migrate at the velocity of the electroosmotic flow. An elution range parameter of zero means an infinite retention window. This corresponds to a situation where the electrophoretic velocity of the micelle is of the same magnitude and opposite in direction to the electroosmotic flow. Since  $\zeta_c$  and  $\zeta_{mc}$  are directly proportional to the surface charge density (or the amount of charge per unit surface area, see eqn. 3) of the capillary,  $\rho_c$ , and that of the micelle,  $\rho_{mc}$ , respectively, the elution

range parameter can be varied conveniently by changing the charge density of the micelles and/or that of the capillary inner surface (see eqn. 2). One of the characteristics of the new micellar system under investigation is that while the surface charge density of the capillary can be kept almost constant, the surface charge density of the micelle can be readily adjusted through several operational parameters, see below.

The adjustment of the surface charge density of the surfactant under investigation, and consequently the elution range parameter is based on varying the extent of complexation between the octylglucoside surfactant and borate ions. Fig. 1 is a schematic illustration of the novel MECC system developed and evaluated in this work. It shows the mechanism of retention of neutral solutes and the control of the surface charge density of the micelle through complexation with borate.

It has been known for a long time that polyhydroxy compounds can reversibly form cyclic boronate esters with borate ions in alkaline pH, and the formation of these complexes is dependent on pH, ionic strength, temperature and the nature of the hydroxylated compound [20–22]. Octylglucoside, which is a non-ionic sugar-containing surfactant, can acquire a negative charge upon complexing with borate ions. The following reaction scheme illustrates the complexation of borate across the C-4 and C-6 of the glucose moiety [23] of octylglucoside surfactant:

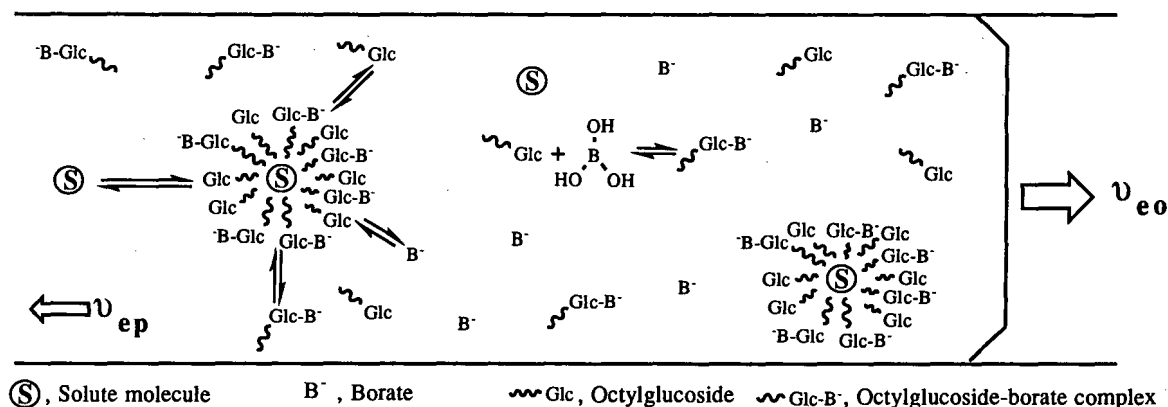
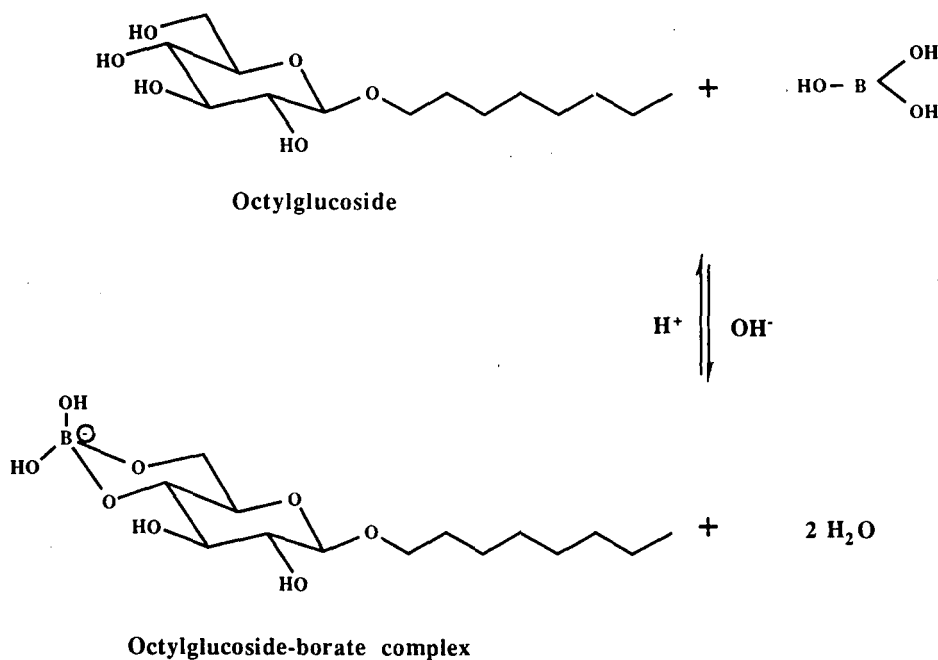


Fig. 1. Schematic illustration of the separation principle in MECC with octylglucoside-borate micellar system.





The alkylglucoside–borate complexation is a reversible reaction, and has an equilibrium constant,  $K_{\text{eq}}$ , given by

$$K_{\text{eq}} = \frac{[\text{OG-Borate}]}{[\text{OG}][\text{Borate}][\text{OH}^-]} \quad (5)$$

where  $[\text{OG}]$  and  $[\text{OG-Borate}]$  stand for the total concentrations of the uncomplexed octylglucoside surfactant and octylglucoside–borate surfactant, respectively, and  $[\text{Borate}]$  and  $[\text{OH}^-]$  are the borate and hydroxide ions concentrations, respectively. Presumably, it is the negatively charged OG-Borate which migrate in zone electrophoresis. The concentration of OG-Borate in aqueous boric acid is low, and an increase in pH would be expected to raise their concentration and, concomitantly, to result in an increased electrophoretic mobility of the micelle.

As a result of the complexation, the overall surface charge density of the micelle,  $\rho_{\text{mc}}$ , can be expressed as

$$\begin{aligned} \rho_{\text{mc}} &= \frac{[\text{OG-Borate}]}{[\text{OG-Borate}] + [\text{OG}]} \rho_{\text{mc-c}} \\ &= \frac{\rho_{\text{mc-c}}}{1 + \frac{[\text{OG}]}{[\text{OG-Borate}]}} \end{aligned} \quad (6)$$

where  $\rho_{\text{mc-c}}$  is the limiting charge density of the octylglucoside–borate micelle. The higher the charge density the more negative the micelle. There are several operational parameters that can alter  $\rho_{\text{mc}}$ . These are the concentrations of the surfactant and borate, and pH of the running electrolyte. According to eqn. 5, at constant surfactant concentration, any increase in the borate concentration or pH will result in a decrease in the ratio  $[\text{OG}]/[\text{OG-Borate}]$ , and therefore a larger  $\rho_{\text{mc}}$  (see eqn. 6). At constant pH and borate concentration, an increase in the surfactant concentration will yield an increase in the ratio  $[\text{OG}]/[\text{OG-Borate}]$ , and as a result,  $\rho_{\text{mc}}$  will decrease (see eqns. 5 and 6). According to eqn. 2 these readily tuned features of the micelles would allow the tailoring of the elution range for a given separation problem.

As mentioned above, with alkylglucoside surfactants in alkaline borate, the surface charge density of the micelle can be conveniently manipulated through pH, borate concentration or surfactant concentration without drastically affecting the surface charge density of the fused-silica capillary. In fact, since at alkaline pH (*i.e.*, above pH 8.0) the surface silanols are fully ionized,  $\rho_c$  will remain constant. However, increasing the pH or borate

concentration is accompanied by an increase in the ionic strength of the electrolyte, which will decrease the thickness of the electric double layer near the capillary surface,  $\delta_c$ , and that near the surface of the micelle,  $\delta_{mc}$ . Furthermore, increasing the surfactant concentration will increase the viscosity of the medium and the amount of surfactant accumulated on the capillary wall. Since  $\rho_c$  remains constant, the changes in the ionic strength and viscosity of the medium as well as the variation in the amount of surfactant adsorbed on the capillary wall will be accompanied by some changes in the electroosmotic flow. On the other hand, the magnitude of  $\rho_{mc}$  will be largely affected by the operation conditions, which in addition to changes in  $\delta_{mc}$  and the viscosity of the medium will cause the electrophoretic velocity of the micelle to change considerably. Under these conditions, while the electroosmotic flow velocity will vary over a narrow range, the electrophoretic velocity of the micelle will change over a wider range. According to the following equation (where  $l$  is the separation distance):

$$t_{mc} = \frac{l}{v_{eo} + v_{ep}} \quad (7)$$

these processes will lead to large changes in  $t_{mc}$ . This is particularly important in manipulating the retention window and the separation behavior of MECC. Stating it differently, in alkaline borate while  $\zeta_c$  of the capillary will undergo small changes,  $\zeta_{mc}$  of the micelle will be affected to a much larger extent through borate and surfactant concentrations and the pH of the running electrolyte. According to eqn. 2, this corresponds to tailoring the breadth of the retention window and consequently the magnitude of peak capacity and resolution.

In fact, in MECC both peak capacity,  $n$ , and resolution,  $R_s$ , are influenced, among other things, by the retention window through the following equations [2]:

$$n = 1 + \frac{\sqrt{N}}{4} \ln \frac{t_{mc}}{t_0} \quad (8)$$

$$R_s = \frac{\sqrt{N}}{4} \cdot \frac{\alpha - 1}{\alpha} \cdot \frac{k'_2}{k'_2 + 1} \cdot \frac{1 - \frac{t_0}{t_{mc}}}{1 + \frac{t_0}{t_{mc}} \cdot k'_1} \quad (9)$$

where  $N$  is the number of theoretical plates,  $\alpha$  is the selectivity factor and  $k'$  is the retention factor which is calculated by the following equation [2]:

$$k' = \frac{t_r - t_0}{t_0 \left(1 - \frac{t_r}{t_{mc}}\right)} \quad (10)$$

where  $t_r$  is the retention time of the solute. For two adjacent peaks, *i.e.*,  $k'_1 = k'_2 = k'$ , a convenient approximation to eqn. 9 is

$$R_s = \frac{\sqrt{N}}{4} \cdot \frac{\alpha - 1}{\alpha} f(k') \quad (11)$$

where

$$f(k') = \frac{k'}{k' + 1} \cdot \frac{1 - \frac{t_0}{t_{mc}}}{1 + \frac{t_0}{t_{mc}} \cdot k'} \quad (12)$$

For a given surfactant and with neutral solutes,  $\alpha$  is virtually independent of  $k'$  [6,24,25] (*i.e.*, the surfactant concentration), while  $N$  can be approximated as constant since it is slightly dependent on  $k'$  in the useful range of surfactant concentration [26-29]. From eqn. 7, it follows that peak capacity,  $n$ , is governed by the ratio  $t_{mc}/t_0$ , and from eqn. 12, it is clear that resolution is controlled by the retention term,  $f(k')$ , which encompasses the elution range parameter,  $t_0/t_{mc}$ .

A particular feature of the surfactant under consideration is that the elution range can be manipulated through  $t_{mc}$  while keeping  $k'$  constant. This is readily achieved by varying the pH or the borate concentration at fixed surfactant concentration. In these situations, the peak capacity  $n$ , which is another measure of the efficacy of the system [30], can be tailored to accommodate a given separation problem (see later for more details).

It has been shown by Terabe *et al.* [2] that when  $f(k')$  is evaluated as a function of  $k'$ , bell-shaped curves are obtained, each one is valid for a particular value of  $t_0/t_{mc}$ . By differentiating eqn. 12 with respect to  $k'$  and setting the resulting expression equal to zero, the optimum  $k'$  (*i.e.*, optimum surfactant concentration) value for maximum resolution is given by [31,32]

$$k'_{opt} = (t_{mc}/t_0)^{\frac{1}{2}} \quad (13)$$

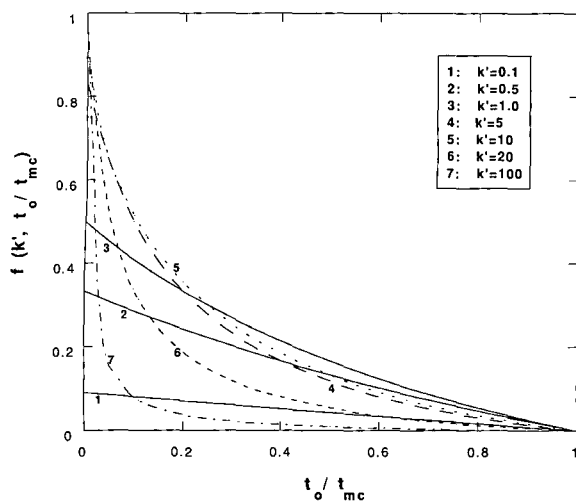


Fig. 2. Plots of  $f(k', t_0/t_{mc})$  versus  $t_0/t_{mc}$  at various  $k'$  values.

The retention factor,  $k'$ , of neutral solutes is determined by the concentration of the surfactant and is independent of the pH. With the traditionally used surfactants  $t_{mc}/t_0$  is largely independent of the pH and the surfactant concentration [2,14]. This means that the retention window is predetermined and cannot be varied systematically. According to eqn. 13, this limits the MECC system to a narrow  $k'$  range as far as resolution is concerned.

As mentioned above, the optimum value of  $f(k')$  for maximum resolution is influenced by the ratio  $t_0/t_{mc}$ . On the other hand, for a given value of  $k'$ , the higher the retention window (*i.e.*, the smaller the ratio  $t_0/t_{mc}$ ), the larger the value for the function  $f(k')$  will be, and the more satisfactory the resolution. The dependence of  $f(k')$  on the ratio  $t_0/t_{mc}$  for various values of  $k'$  is depicted in Fig. 2. This figure shows that at low values of the retention window (*i.e.*, at high  $t_0/t_{mc}$ ), a pair of solutes for which  $k'$  is in the range 0.5–1.0 has a higher  $f(k')$  value (*i.e.*, a better resolution), than those pairs that are 10 times more retained, *e.g.*,  $k' = 5.0$ –10. Early eluting peaks as well as strongly retained ones are better resolved at relatively high retention window. It takes an infinite retention window (*i.e.*,  $t_0/t_{mc} \rightarrow 0$ ) to affect a good resolution for species that are almost completely dissolved by the micelle.

The above discussion underlines the need for surfactants that are less retentive than the existing

ones. This article addresses this need by introducing surfactants with balanced hydrophile–lipophile character, the alkylglucoside–borate surfactants. In addition, with the new micellar systems the retention window can be increased by increasing  $t_{mc}$  while keeping  $k'$  constant. This is readily achieved by increasing the pH or the borate concentration at fixed surfactant concentration. This corresponds to moving up along the bell-shaped curve (*i.e.*,  $f(k')$  vs.  $k'$ ) and so increasing the contribution of  $f(k')$  to resolution. Thus, with the micellar systems under consideration, it is possible to affect simultaneously a double optimization of resolution through  $k'$  and  $t_{mc}$ . With SDS and other ionic surfactants, window optimization is most often achieved through an increase in both  $t_0$  and  $t_{mc}$  by adding an organic solvent to the running electrolyte [17]. But increasing the organic modifier lead to a drastic increase in the analysis time. In addition, SDS micellar system can not tolerate a large amount of organic solvent without disrupting the micelle shape and producing polydispersity that leads to band broadening [28].

## EXPERIMENTAL

### Instrument and capillaries

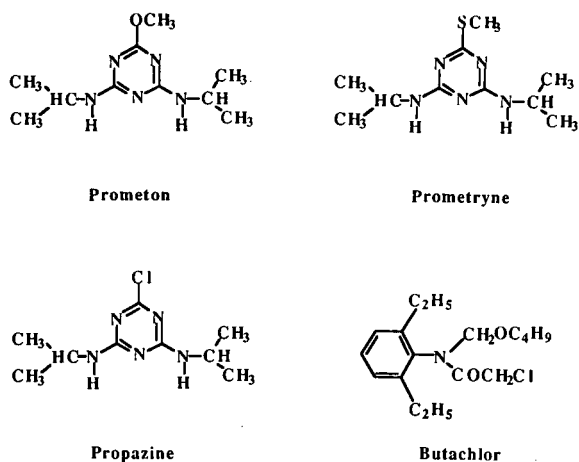
The capillary electrophoresis instrument used in this study is the same as that described previously [33]. It consisted of a 30-kV d.c. power supply Model EH30P03 of positive polarity from Glassman High Voltage (Whitehouse Station, NJ, USA) and a UV–Vis variable-wavelength detector Model 200 from Linear Instrument (Reno, NV, USA) equipped with a cell for on-column detection. The detection wavelength was set at 210 nm. In all the experiments the running voltage was 15 kV. The electropherograms were recorded with a computing integrator Model CR601 from Shimadzu (Columbia MD, USA).

Fused-silica capillaries having an inner diameter of 50  $\mu\text{m}$  and an outer diameter of 375  $\mu\text{m}$  were obtained from Polymicro Technology (Phoenix, AZ, USA). In all experiments, the total length of the capillary was 80 cm with 50 cm separation distance, *i.e.*, from the injection end to the detection point.

### Reagents and materials

Octyl- $\beta$ -D-glucopyranoside (OG) was obtained from Sigma (St. Louis, MO, USA). Triphenylmeth-

anol, *o*-terphenyl and four herbicides, *i.e.*, prometon, prometryne, butachlor and propazine, were purchased from Chem Service (West Chester, PA, USA). The structures of the four herbicides are shown below:



Sudan III, which was used for the determination of the migration time of the micelles,  $t_{mc}$ , was obtained from Aldrich (Milwaukee, WI, USA). All chemicals for the preparation of electrolyte were from Fisher Scientific (Pittsburgh, PA, USA). Methanol was purchased from EM Science (Cherry Hill, NJ, USA). Naphthylamine and naphthalene were from Eastman Kodak (Rochester, NY, USA). All solutions were prepared with deionized water and filtered with 0.2- $\mu$ m Uniprep Syringeless filters from Fisher Scientific to avoid capillary plugging.

#### Procedures

The running electrolyte was prepared by dissolving proper amount of boric acid and octylglucoside, and adjusting the pH to the desired value with sodium hydroxide. Sample solutions were made by dissolving pure compounds in the running electrolyte (*i.e.*, micellar solution). Due to the limited solubility of the herbicides in aqueous solvent, the concentrations of the sample solutions were determined from calibration curves that were established with standard solutions prepared by dissolving the pure compounds in water-acetonitrile solvents. The calibration curves were obtained by capillary zone electrophoresis using 10 mM phosphate buffer, pH 6.0.

Hydrodynamic sample injection mode, *i.e.*, gravity-driven flow, was used in this study. The sample reservoir was raised to a height of 20 cm above the outlet reservoir for a certain period of time. The following equation was used for the determination of the injected quantities,  $Q$ :

$$Q = \frac{\pi r^2 l C t_i}{t_r} \quad (14)$$

where  $t_i$  is the injection time,  $r$  is the inner radius of the capillary,  $C$  is the concentration of the sample,  $l$  is the length of the capillary from the injection point to the detection point and  $t_r$  is the time it takes for the sample zone to migrate from the injection end to the detection point under the gravity force.

#### RESULTS AND DISCUSSION

The novel micellar system was characterized with neutral solutes over a wide range of elution conditions including pH of the running electrolyte, borate concentration and surfactant concentration. Various electrokinetic parameters were measured, and the results are discussed in light of the theoretical treatment given above.

##### Tunable retention window

As demonstrated in the theory section, the reten-

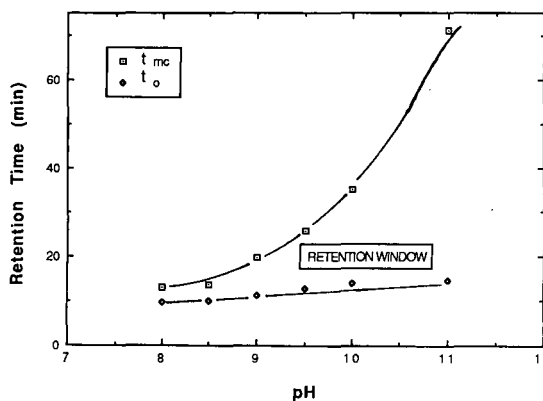


Fig. 3. Effect of pH on the magnitude of retention window. Separation capillary, untreated fused-silica, 50 cm (to the detection point), 80 cm (total length)  $\times$  50  $\mu$ m I.D.; running electrolytes, 50 mM octylglucoside, 400 mM borate at various pH; sample injection, hydrodynamic, 5 s; running voltage, 15 kV; tracers, Sudan III (for  $t_{mc}$ ) and methanol (for  $t_o$ ); detection, 210 nm.

tion window of the micellar system depends on borate concentration, pH of the running electrolyte and the concentration of the surfactant.

*pH of the running electrolyte.* To evaluate the relationship between retention window and the pH of the running electrolyte, the electrophoretic experiments were carried out with electrolyte solutions containing 50 mM OG and 400 mM borate at various pH. Fig. 3 portrays the results in terms of  $t_0$  and  $t_{mc}$  versus the pH of the running electrolyte. As can be seen in Fig. 3,  $t_{mc}$  increased much more than did  $t_0$  over the pH range studied. The larger increase in  $t_{mc}$  arises primarily from increasing the extent of complexation of the surfactant with borate at higher pH. Stating it differently, as the pH rises the surface charge density of the micelle increases and consequently the electrophoretic velocity of the micelle in the opposite direction to the electroosmotic flow increases (see Theory section). The slight increase in  $t_0$  or in another word the shallow decrease in the electroosmotic flow is primarily due to increasing the ionic strength with pH, since higher pH values were obtained by adding larger amount of sodium hydroxide to the solution of boric acid. At pH above 8, the charge density of the capillary inner surface is virtually constant since the silanol groups of the siliceous wall are fully ionized in the pH domain investigated. However, as the ionic strength of the running electrolyte increases with increasing pH, the

viscosity of the medium would increase and the  $\zeta$  potential of the capillary wall would decrease. Consequently, the electroosmotic flow is reduced since it is directly proportional to the  $\zeta$  potential and inversely proportional to viscosity, see eqns. 1, 3 and 4. On the other hand, the decrease in the thickness of the double layer (*i.e.*, the ion atmosphere) surrounding the micelle,  $\delta_{mc}$ , with increasing pH is outweighed by the larger increase in its surface charge density,  $\rho_{mc}$ ; reason for which  $t_{mc}$  increases. An additional factor that would also contribute to the increase in  $t_{mc}$ , is the fact that the electroosmotic flow decreased. According to eqn. 7, the slight decrease in the electroosmotic velocity can result in a dramatic increase in the  $t_{mc}$  as the magnitudes of  $v_{eo}$  and  $v_{ep}$  approach the same value because they are of opposite sign. This phenomenon can explain the continuous and steep rising in  $t_{mc}$  at pH values higher than 10. In fact, the electrophoretic mobility of glucose in alkaline borate has been found to level off at pH above 9 in paper-free zone electrophoresis [34], a pH which is above the  $pK_a$  value of borate ( $pK_a = 9.23$ ).

Fig. 4 displays typical electropherograms of three triazine herbicides (*i.e.*, prometon, prometryne and propazine) and butachlor, an acetamide herbicide, obtained at three different pH, *i.e.*, three different retention windows. This figure shows the significance of being able to systematically vary the

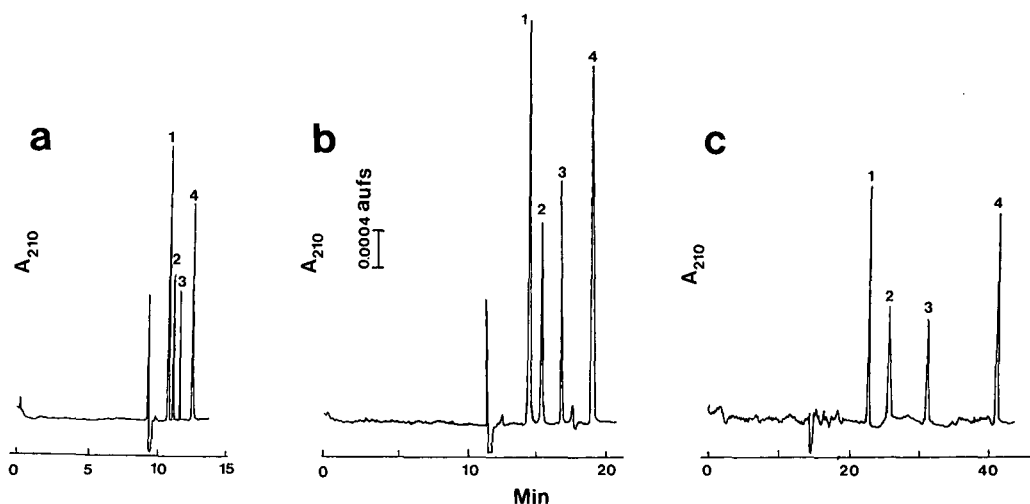


Fig. 4. Typical electropherograms of herbicides at various pH: (a) pH 8; (b) pH 9; (c) pH 10. Electrolytes, 400 mM borate containing 50 mM OG. Peaks: 1 = prometon; 2 = prometryne; 3 = propazine; 4 = butachlor. Other experimental conditions as in Fig. 3.

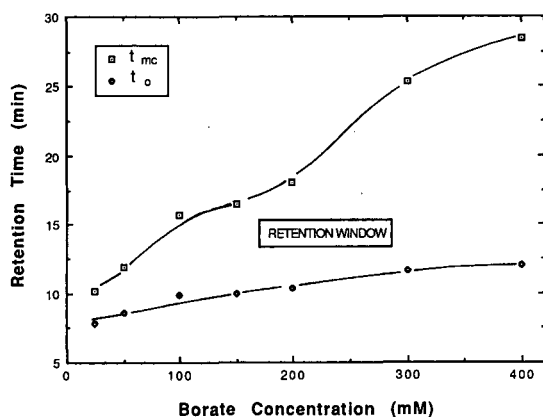


Fig. 5. Effect of borate concentration on the magnitude of the retention window. Running electrolytes, 50 mM octylglucoside, pH 10, at various borate concentrations. Other experimental conditions as in Fig. 3.

retention window. In fact, when the separation is satisfactory (Fig. 4a) there is no point to work at high retention window whereby the analysis time is increased. It is therefore important that the retention window stays a freely adjustable parameter. Unlike previously described micellar phases whose retention window is predetermined, octylglucoside-borate micelles offer the advantage of tunable retention window, which can be adjusted to suit a given separation problem, see also below.

**Borate concentration.** To examine the dependence of retention window on borate concentration, the electrophoretic measurements were performed with running electrolytes of 50 mM OG, pH 10, at various borate concentration. Fig. 5 illustrates typical plots of  $t_o$  and  $t_{mc}$  versus the borate concentration in the running electrolyte. As expected, the retention window increased with borate concentration. The retention time of the micelles,  $t_{mc}$ , increased substantially with increasing borate concentration from 25 to 400 mM while the retention time of the inert tracer,  $t_o$ , increased only slightly in the concentration range studied. The increase in  $t_{mc}$  with borate concentration is primarily due to an increase in the charge density of the micelles upon complexation with borate (see eqns. 3, 5 and 6). The slight increase in  $t_o$ , which corresponds to a shallow decrease in the electroosmotic flow velocity, may be the result of increasing the ionic strength of the running electrolyte with increasing borate concentration (see eqns. 1,

3 and 4). As discussed in the preceding section, the larger increase in  $t_{mc}$  at relatively high borate concentration may be due in part to the slight decrease in  $v_{eo}$ .

**Surfactant concentration.** The effect of alkylglucoside concentration on the electrokinetic behavior of the MECC system was investigated with electrolytes containing 200 or 400 mM borate, pH 10 at various concentration of OG. Fig. 6a and b shows the dependence of  $t_{mc}$  and  $t_o$  on surfactant concentration. In general, the retention window decreased slightly with increasing surfactant concentration. At constant pH and borate concentration, increasing surfactant concentration will increase the ratio  $[OG]/[OG\text{-Borate}]$ , which then lead to a monotonic decrease in the surface charge density of the micelle

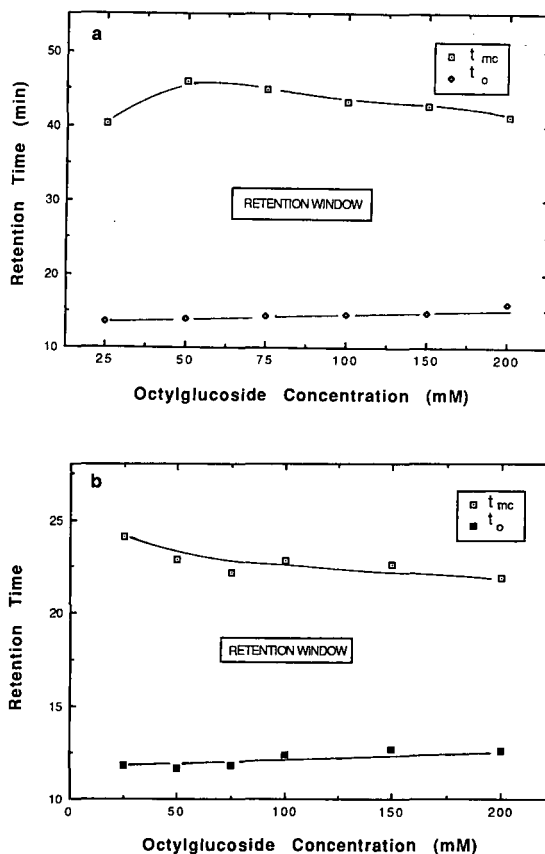


Fig. 6. Effect of octylglucoside concentration on the magnitude of retention window. Running electrolytes, 400 mM borate in (a), 200 mM in (b), pH 10 at various concentration of OG. Other experimental conditions as in Fig. 3.

TABLE I  
COMPARISON OF THE RETENTION FACTORS,  $k'$ , OF NITROBENZENE AND HERBICIDES OBTAINED WITH SDS AND OG-BORATE MICELLAR PHASES

Conditions: 25 mM SDS in 25 mM phosphate, pH 9.0; 50 mM OG in 400 mM borate, pH 9.0; running voltage, 15 kV.

Analyte	$k'$	
	SDS	OG
Nitrobenzene	0.53	0.88
Prometon	6.49	1.38
Prometryne	7.45	2.73
Propazine	14.79	12.73
Butachlor	192.30	59.00

TABLE II  
CMC VALUES OF OCTYLGLUCOSIDE

Conditions as in Fig. 6.

Surfactant	CMC values [mM]		
	Pure water	200 mM borate, pH 10	400 mM borate, pH 10
Octylglucoside	25 <sup>a</sup>	23	20

<sup>a</sup> From ref. 38.

and consequently in  $t_{mc}$  (see eqns. 5 and 6). The electroosmotic velocity decreased slightly, which was probably due to the increase in the viscosity of the running electrolyte as a result of high concentration of the surfactant, and perhaps to the adsorption of the surfactant to the capillary walls. This shallow decrease in  $v_{eo}$  (i.e., increase in  $t_0$ ) may be responsible for the slight decrease in  $t_{mc}$  despite the fact that the surface charge density of the micelle decreased.

The above studies show that the retention window of the micellar system can be readily tuned by borate concentration and pH of the running electrolyte, and to a lesser extent, by varying the concentration of the surfactant.

#### Retention factor

To further characterize the new micellar system under investigation, the retention factors,  $k'$ , of

neutral model solutes were measured using eqn. 10 under various elution conditions with OG-borate micelles. Also, the OG-borate micellar phase was compared to SDS.

**Comparison with SDS.** Table I presents the  $k'$  values of five model solutes obtained with SDS and OG-borate micelles. Due to the more balanced hydrophile-lipophile character of OG-borate micelles, the  $k'$  values obtained with the alkylglucoside micellar phase were lower than those obtained with SDS. As expected, nitrobenzene, which is a relatively more polar species than the other model solutes, exhibited higher partitioning in the OG-borate micelles, whereas butachlor the more hydrophobic solute in the test mixture was almost completely solubilized by SDS. These results demonstrate that OG-borate micellar system allows more equitable distribution of polar and non-polar solutes between the micelles and the aqueous phase containing the monomers.

To further illustrate the utility of OG-borate micelles, some polyaromatic hydrocarbons were analyzed with the new micellar phase as illustrated in Fig. 7. The OG-borate micellar system permitted

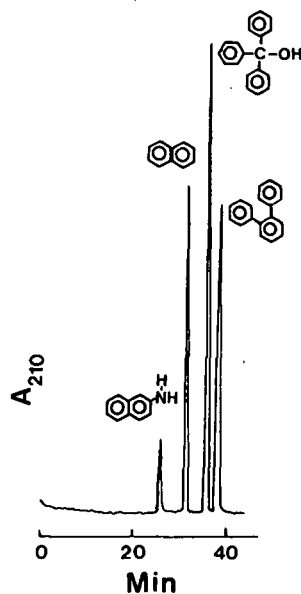


Fig. 7. Typical electropherogram of polyaromatic hydrocarbons. Electrolyte, 200 mM borate, containing 50 mM OG, pH 10. Samples from left to right: 2-naphthylamine, naphthalene, triphenylmethanol and *o*-terphenyl. Other experimental conditions as in Fig. 3.

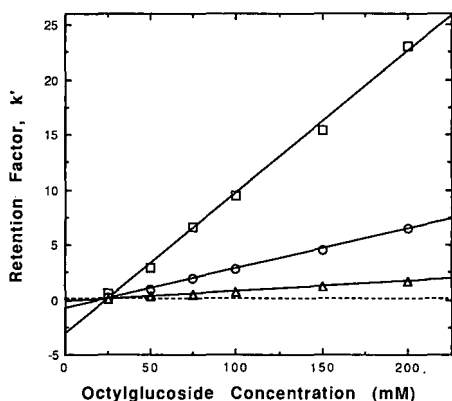


Fig. 8. Retention factor,  $k'$ , versus octylglucoside concentration in the running electrolyte, 200 mM borate, pH 10, at various OG concentrations. Other experimental conditions as in Fig. 3.  $\square$  = Prometryne;  $\circ$  = prometon;  $\triangle$  = nitrobenzene.

the baseline resolution of these water-insoluble compounds without the addition of organic solvent to the running electrolyte.

**Concentration of surfactants.** Fig. 8 portrays typical plots of the retention factor,  $k'$ , versus octylglucoside concentration in the running electrolyte. The results were obtained with electrolytes containing 200 mM borate, pH 10, at various OG concentrations. As expected, the retention factors of the model solutes increased linearly with the surfactant concentration in the range studied. Increasing the octylglucoside concentration in the running electrolyte corresponds to increasing the phase ratio

$\phi$ , i.e., ratio of the volume of the micellar pseudo-stationary phase to that of the aqueous phase. According to the following equation the retention factor is a linear function of the surfactant concentration [2]:

$$k' = \phi K \approx K\nu([S] - \text{CMC}) \quad (15)$$

where  $K$  is the distribution coefficient of solute between micellar and aqueous phases,  $\nu$  is partial specific volume of the micelle,  $[S]$  is the concentration of the surfactant and CMC is the critical micellar concentration.

The octylglucoside-borate surfactant can be considered as an anionic surfactant. This surfactant will associate at monomer concentration different than the uncomplexed octylglucoside, and the value of its CMC should be different. The CMC values of the alkylglycoside-borate surfactant were determined from the MECC measurements at two borate concentration using the linear plots of  $k'$  versus the surfactant concentration, i.e., eqn. 15. The results are summarized in Table II. The CMC of OG-borate surfactant decreased by a factor of ca. 0.9 and 0.8 at 200 and 400 mM borate, respectively, with respect to the CMC of OG in pure water. Due to electrostatic repulsion between their charged polar head groups, anionic surfactants are characterized by a higher CMC than neutral surfactants having the same length of the alkyl tail [35]. But in the case of OG-borate surfactant, at relatively high ionic strength, the concentration of counter ions becomes

TABLE III  
LIMITS OF DETECTION

Electrolyte, 40 mM OG in 200 mM borate, pH 10. Other conditions as in Fig. 3. The injected quantities were determined by eqn. 14.

Sample solute	Limit of detection		
	Concentration ( $\mu\text{M}$ )	Injected quantity	
		(pg)	(fmol)
Prometon	4.4	6.0	26.5
Prometryne	8.3	12	49.9
Propazine	3.0	4.2	18.0
Butachlor	8.7	16	52.3

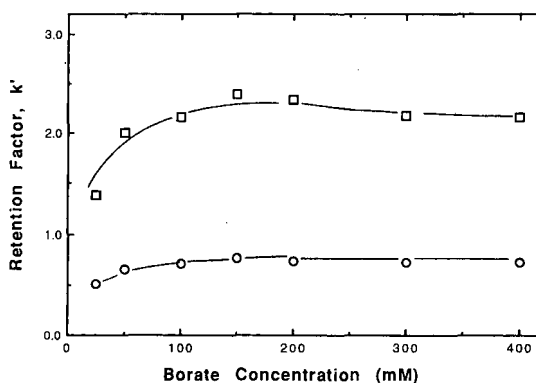


Fig. 9. Retention factor,  $k'$ , versus borate concentration in the running electrolyte. Electrolytes, 50 mM OG, at various borate concentration, pH 9.0. Samples, prometon ( $\circ$ ) and prometryne ( $\square$ ). Other experimental conditions as in Fig. 3.



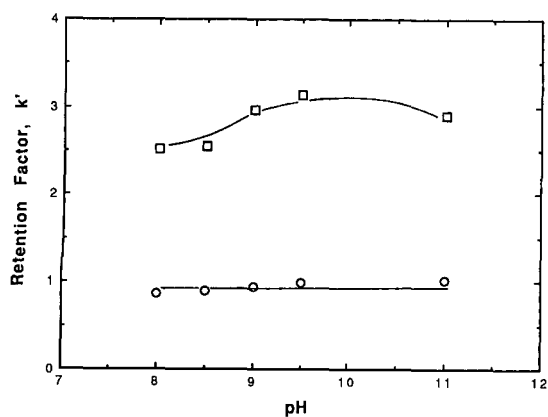


Fig. 10. Retention factor,  $k'$ , versus pH of the running electrolyte. Electrolytes, 200 mM borate containing 50 mM OG, at various pH. Samples, prometon (○) and prometryne (□). Other experimental conditions as in Fig. 3.

high, thus reducing the electrostatic repulsion between the charged head groups (*i.e.*, borate-sugar moieties) and consequently allowing the association of the OG–borate surfactant at lower monomer concentration. This corroborate earlier findings with ionic surfactants [36].

**Borate concentration.** Fig. 9 shows the change in  $k'$  values of the neutral model solutes with borate concentration at constant pH and OG concentration. Although, the surfactant concentration was kept the same and the solute are neutral at the pH of the experiments ( $pK_a$  values of prometon, prometryne and propazine are 4.20, 4.05 and 1.85, respectively [37]), the  $k'$  values first increased at low borate concentration (*ca.* 25–100 mM) and then leveled off at high borate concentration. This may be explained by a salting-out effect in the sense that increasing the ionic strength of the running electrolyte would increase the extent of solubilization of neutral solute in the inner core of the micelle [35]. The effect of increasing the ionic strength with increasing borate concentration is to decrease the repulsion between the similarly charged ionic head groups of the OG–borate surfactant, thereby decreasing the CMC and increasing the aggregation number and volume of the micelles. The increase in the aggregation number of the micelles presumably results in an increase in the solubilization of neutral solutes in the inner core of the micelle [35]. On the other hand, at relatively high borate concentration, the micelle

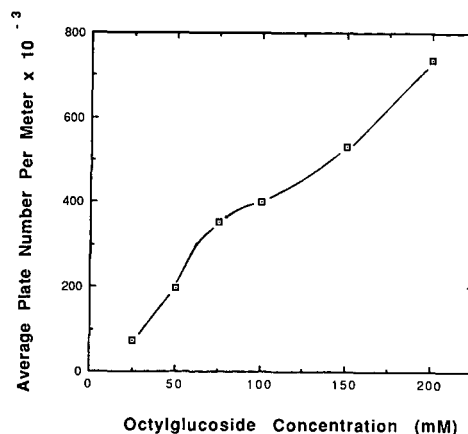


Fig. 11. Average plate number per meter versus octylglucoside concentration in the running electrolyte. Electrolytes, 200 mM borate, pH 10, at various OG concentrations. The average plate number was measured from the peaks of nitrobenzene, prometon and prometryne. Other experimental conditions as in Fig. 3.

configuration would stabilize and the  $k'$  value too.

**pH of the running electrolyte.** Fig. 10 shows the dependence of the retention factor on pH. As expected, since the borate and surfactant concentrations were kept constant, the  $k'$  values of prometon and prometryne did not change in the pH domain studied. The slight fluctuations in the  $k'$  values of prometryne are within the range of experimental errors.

#### Efficiency and peak capacity

Fig. 11 presents typical data on separation efficiencies in terms of average plate number per meter versus the surfactant concentration. As can be seen in Fig. 11,  $N$  increased sharply with increasing OG concentration in the running electrolyte. In MECC, the micelles are so small that the mass transfer resistance in the pseudo-stationary phase is insignificant [26,27]. In the absence of excessive joule heating longitudinal molecular diffusion is the ultimate limitation [26,27]. Under these conditions, increasing the surfactant concentration would lead to more densely packed capillary with micelles so that the intermicellar diffusion distances become shorter which would give rise to faster mass transfer in the mobile phase and concomitantly higher separation efficiencies [26]. In most cases high separation efficiencies were obtained with the new

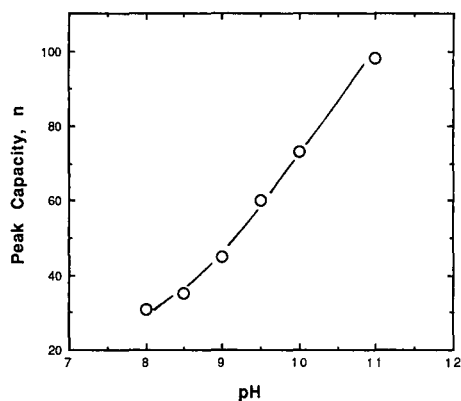


Fig. 12. Peak capacity,  $n$ , versus the pH of the running electrolyte. Electrolytes, 400 mM borate containing 50 mM OG, at various pH. Other experimental conditions as in Fig. 3.

micellar system, and the average theoretical plate number per meter was normally above 150 000 plates. As can be seen in Fig. 11, as high as 700 000 theoretical plates per meter was achieved.

At constant surfactant concentration, the separation efficiency was practically independent of borate concentration and pH in the range studied. On the other hand, peak capacity, which is another measure of the efficacy of the system, almost always increased with borate concentration and pH of the

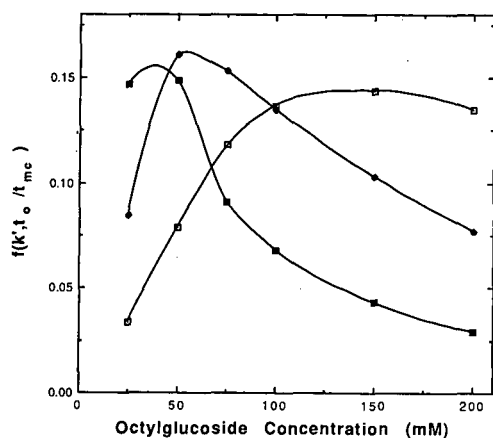


Fig. 13. Dependence of  $f(k', t_0/t_{mc})$  versus octylglucoside concentration in the running electrolyte. Electrolytes, 200 mM borate containing various OG concentration, pH 10. Samples, nitrobenzene ( $\square$ ), prometon ( $\blacklozenge$ ) and prometryne ( $\blacksquare$ ). Other experimental conditions as in Fig. 3.

running electrolyte. Typical results are shown in Fig. 12, whereby peak capacity increased from 30 to 100 when pH changed from 8 to 11. This is because of the large increase in the retention window.

### Resolution

As in chromatography, the resolution in MECC is a function of retention [*i.e.*,  $f(k')$ ], selectivity and separation efficiencies (see eqn. 11). With OG-borate surfactant, the selectivity for the neutral solutes under investigation did not vary to any significant extent by changing the surfactant concentration, borate concentration or pH of the running electrolyte. Although, separation efficiencies can be increased with increasing OG concentration (see above), which in turn would increase resolution, there is a limit beyond which increasing the amount of surfactant would cause the contribution of  $f(k')$  for resolution to decline. Fig. 13 displays the dependence of  $f(k')$  on surfactant concentration under conditions of relatively constant retention window, *i.e.*, constant  $t_0/t_{mc}$ . The optimum surfactant concentrations at which maximum  $f(k')$  values are obtained decreased with increasing  $k'$ . For a pair of solutes having an average retention as high as that of prometryne, the optimum surfactant concentration is low, whereas, for a pair of solutes whose average  $k'$  is similar to that of nitrobenzene, the optimum surfactant concentration corresponding to the maximum  $f(k')$  is located at higher values. This means that for a multicomponent mixture, the optimization of resolution for the various pairs of solutes cannot be effectively achieved through  $k'$ , *i.e.*, surfactant concentration. High surfactant concentrations are unfavorable for good resolution, because  $f(k')$  will drop considerably.

However, one of the unique characteristics of the OG-borate micelles is that the retention window can be adjusted over a certain range to any desired level without affecting  $k'$ , by keeping the surfactant concentration constant while varying borate concentration or pH of the running electrolyte. Under these conditions, the contribution of  $f(k')$  to resolution can be increased through increasing the retention window. To illustrate the dependence of  $f(k')$  on the elution range parameter at constant  $k'$ ,  $f(k')$  of a pair of solute having similar retention behavior to the model solute prometon was plotted against the ratio  $t_0/t_{mc}$ , for several different studies of borate

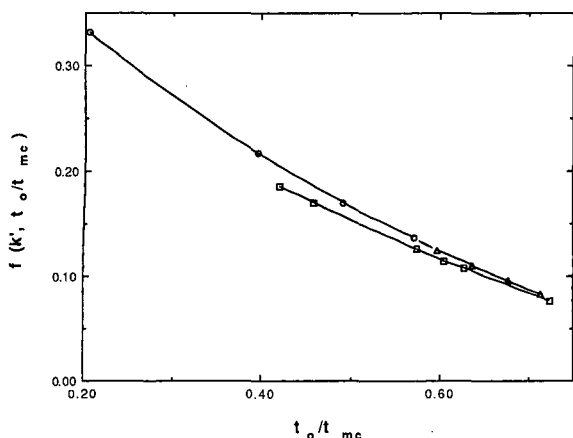


Fig. 14. Dependence of  $f(k', t_0/t_{mc})$  versus the elution range parameter,  $t_0/t_{mc}$ . Solute, prometon. Values were obtained at different borate concentration and pH but at constant OG concentration (50 mM). □ = Various borate concentrations, pH 10; Δ = various borate concentrations, pH 9.0; ○ = 400 mM borate at various pH.

concentration and pH of the running electrolyte, see Fig. 14. In all cases, average  $k'$  values were used for the calculation of  $f(k')$  over the range in which the retention factors of the solutes were almost constant regardless of the change in borate concentration or pH. As the retention window increased, *i.e.*,  $t_0/t_{mc}$  decreased, the  $f(k')$  contribution to resolution increased (see Fig. 14). Thus, with OG–borate micelles a suitable compromise between analysis time and resolution can be readily reached by first selecting a moderate surfactant concentration and subsequently either increase or decrease  $t_{mc}$  by varying the pH or the borate concentration of the running electrolyte while  $k'$  remains practically unchanged.

#### Limit of detection

The limits of detection of herbicides obtained in this study are listed in Table III. The data were determined by injecting several dilutions of a relatively concentrated standard mixture using an electrolyte of 200 mM borate containing 40 mM OG, pH 10. The concentration limits correspond to a signal-to-noise ratio of 3. The detection limits show that as low as few micromolar in terms of concentration or a few picograms in terms of absolute mass of solute injected can be determined. The amounts injected were calculated using eqn. 14.

## CONCLUSIONS

MECC with octylglucoside–borate micellar phases has shown promise for the determination of neutral organics at low level. The new MECC method with micelles of adjustable surface charge density offered tunable retention window by simply altering some of the operational parameters, and thus allowed the manipulation of peak capacity and resolution of the system. Very high theoretical plate numbers were obtained, and consequently the detection limits were quite promising with a UV detector. In addition, due to the balanced hydrophile–lipophile character of the surfactant, the OG–borate micellar phase exhibited decreased retention toward hydrophobic solute and promoted more equitable distribution of relatively polar compounds, *e.g.*, nitrobenzene.

## ACKNOWLEDGEMENTS

The financial support from the Oklahoma Water Resources Research Institute and in part from the Dean Incentive Grant Program, College of Arts and Sciences, at Oklahoma State University are gratefully acknowledged.

## REFERENCES

- 1 S. Terabe, K. Otsuka, K. Ichikama, A. Tsuchiya and T. Ando, *Anal. Chem.*, 56 (1984) 111.
- 2 S. Terabe, K. Otsuka and T. Ando, *Anal. Chem.*, 57 (1985) 834.
- 3 K. Otsuka, S. Terabe and T. Ando, *J. Chromatogr.*, 332 (1985) 219.
- 4 D. E. Burton, M. J. Sepaniak and M. P. Maskarinec, *J. Chromatogr. Sci.*, 24 (1986) 347.
- 5 A. S. Cohen, S. Terabe, J. A. Smith and B. L. Karger, *Anal. Chem.*, 59 (1987) 1031.
- 6 S. Fujiwara, S. Iwase and S. Honda, *J. Chromatogr.*, 447 (1988) 133.
- 7 J. Liu, K. A. Cobb and M. Novotny, *J. Chromatogr.*, 519 (1990) 189.
- 8 H. Nishi, N. Tsumagari, T. Kakimoto and S. Terabe, *J. Chromatogr.*, 477 (1989) 259.
- 9 P. Gozel, E. Gassmann, H. Michelsen and R. N. Zare, *Anal. Chem.*, 59 (1987) 44.
- 10 D. E. Burton and M. J. Sepaniak, *Anal. Chem.*, 59 (1987) 1466.
- 11 S. Terabe, Y. Miyashita, O. Shibata, E. R. Barnhart, L. R. Alexander, D. G. Patterson, B. L. Karger, K. Hosoya and N. Tanaka, *J. Chromatogr.*, 516 (1990) 23.
- 12 R. O. Cole, M. J. Sepaniak, W. L. Hinze, J. Gorse and H. Oldiges, *J. Chromatogr.*, 557 (1991) 113.

- 13 A. T. Balchunas and M. J. Sepaniak, *Anal. Chem.*, 59 (1987) 1466.
- 14 S. Terabe, H. Utsumi, K. Otsuka, T. Ando, T. Inomata, S. Kuze and Y. Hanaoka, *J. High Resolut. Chromatogr. Chromatogr. Commun.*, 9 (1986) 667.
- 15 J. A. Lux, H. Yin and G. Schomburg, *J. High Resolut. Chromatogr.*, 13 (1990) 145.
- 16 J. Gorse, A. T. Balchunas, D. F. Swaile and M. J. Sepaniak, *J. High Resolut. Chromatogr. Chromatogr. Commun.*, 11 (1988) 554.
- 17 A. T. Balchunas, D. F. Swaile, A. C. Powell and M. J. Sepaniak, *Sep. Sci. Technol.*, 23 (1988) 1891.
- 18 R. J. Hunter, *Zeta Potential in Colloid Science*, Academic Press, London, 1981, Ch. 3.
- 19 C. J. O. R. Morris and P. Morris, in *Separation Methods in Biochemistry*, Wiley, New York, 2nd ed., 1976, p. 719.
- 20 I. Boeseken, *Adv. Carbohydr. Chem.*, 4 (1949) 189.
- 21 W. L. Weith, J. L. Wiebers and P. T. Gilham, *Biochemistry*, 9 (1970) 4396.
- 22 T. F. McGutchan, P. T. Gilham and D. Soll, *Nucleic Acids Res.*, 2 (1975) 853.
- 23 A. B. Foster and M. Stacey, *J. Chem. Soc.*, (1955) 1778.
- 24 K. H. Row, W. H. Griest and M. P. Maskarinec, *J. Chromatogr.*, 409 (1987) 193.
- 25 S. Fujiwara and S. Honda, *Anal. Chem.*, 59 (1987) 2773.
- 26 M. J. Sepaniak and R. O. Cole, *Anal. Chem.*, 59 (1987) 472.
- 27 S. Terabe, K. Otsuka and T. Ando, *Anal. Chem.*, 61 (1989) 251.
- 28 A. T. Balchunas and M. J. Sepaniak, *Anal. Chem.*, 60 (1988) 671.
- 29 J. M. Davis, *Anal. Chem.*, 61 (1990) 2455.
- 30 J. C. Giddings, *Anal. Chem.*, 39 (1967) 1027.
- 31 J. P. Foley, *Anal. Chem.*, 62 (1990) 1302.
- 32 H. Nishi, T. Fukuyama, M. Matsuo and S. Terabe, *J. Microcol. Sep.*, 1 (1989) 234.
- 33 J. Cai and Z. El Rassi, *J. Liq. Chromatogr.*, 15 (1992) 1193.
- 34 R. Consden and W. M. Stanier, *Nature (London)*, 169 (1952) 783.
- 35 M. J. Rosen, *Surfactants and Interfacial Phenomena*, Wiley, New York, 2nd ed., 1988.
- 36 A. Helenius and K. Simons, *Biochim. Biophys. Acta*, 415 (1975) 29.
- 37 E. Smolkova and V. Pacakova, *Chromatographia*, 11 (1978) 698.
- 38 L. Hjelmeland and A. Crambach, *Methods Enzymol.*, 104 (1984) 305.



## Sample self-stacking in zone electrophoresis

# Theoretical description of the zone electrophoretic separation of minor compounds in the presence of bulk amounts of a sample component with high mobility and like charge

Petr Gebauer

*Institute of Analytical Chemistry, Czechoslovak Academy of Sciences, Veveří 97, CS-611 42 Brno (Czechoslovakia)*

Wolfgang Thormann

*Institute of Clinical Pharmacology, University of Berne, Murtenstrasse 35, CH-3010 Berne (Switzerland)*

Petr Boček

*Institute of Analytical Chemistry, Czechoslovak Academy of Sciences, Veveří 97, CS-611 42 Brno (Czechoslovakia)*

---

### ABSTRACT

A theoretical description of the sample self-stacking effect in zone electrophoresis is given. This effect applies to samples that contain a high concentration of an ionic component with high mobility and like charge. After current application, the sample components are stacked at the rear of the zone of the major component by an isotachophoretic mechanism. Later, the sample substances gradually destack in order of increasing mobility and continue to migrate and separate by the normal mechanism of zone electrophoresis. Simple relationships are derived for model systems allowing an explicit description of the properties of such systems and the zone parameters such as detection time, variance and resolution. The reliability of the model presented is verified and illustrated by computer simulation of selected examples. It is shown that the described sample self-stacking effect provides at least the same concentrating power as is obtained with conventional zone electrophoretic sample stacking.

---

### INTRODUCTION

In principle, zone electrophoresis is a dispersive technique. Once introduced into the column and migrating in the background electrolyte (BGE), the sample zone broadens by diffusion and other dis-

persive effects. One of the most important problems with this technique is therefore the question of how to make the starting sample peak as sharp as possible to get narrow and well separated peaks into the detector. There are various approaches that are employed to achieve this aim. In the sample stacking technique [1,2], a large zone of diluted sample (sample dissolved in water or diluted BGE) is introduced into the column by hydrodynamic flow. During the electrophoresis run, the sample compo-

---

*Correspondence to:* Dr. P. Gebauer, Institute of Analytical Chemistry, Czechoslovak Academy of Sciences, Veveří 97, CS-611 42 Brno, Czechoslovakia.

nents are concentrated when passing the sample/BGE interface and the size of the sample zone is thus considerably reduced. The field amplification technique [3] is based on the same principle, the difference being that the diluted sample solution is applied by the effect of an electric field. When a suitable slow ion is added to the sample, its stacking by an isotachophoretic mechanism temporally proceeds [4]. A very effective tool is the on-line combination of isotachopheresis and capillary zone electrophoresis [5–8]. In the first (isotachophoretic) step, concentration of the sample components into narrow, consecutive zones is achieved. These zones are introduced in the second step into a zone electrophoretic system where they are separated. This technique, however, requires special instrumentation and cannot be run on commercial instruments for capillary zone electrophoresis.

An important factor affecting zone electrophoretic separation is the composition of the sample solution; this was demonstrated by computer simulation [9,10]. Problems may occur when analysing samples that contain one component in large excess. A typical example is body fluid involving large amounts of sodium and chloride ions. When looking for components that are present in minor concentrations only, further dilution of the sample for using the above-mentioned techniques may not be advantageous and will not bring an improvement. Fortunately, the ion that is in excess usually has a high mobility. As was shown previously [11–13], this causes a temporal stacking of the minor sample components at the rear of the sample zone, thus permitting their separation as narrow zones. It is the aim of this paper to present a simple theoretical description of this type of system. The reliability of the model presented is verified and illustrated by computer simulation.

#### THEORETICAL

For the theoretical treatment of the present problem, a very simple zone electrophoretic system had to be selected as a model to be able to provide a sufficiently explicit description. The background electrolyte consists of a solution of anion  $B^-$  of a strong acid  $HB$  and of cation  $RH^+$  of a weak base  $R$ . The BGE is considered to be in the buffering optimum of the weak base where  $C_R = 2c_{RH} = 2c_B$

( $C$  is the total and  $c$  the ionic concentration). The investigated sample contains a major concentration of a fast anion  $A^-$  of a strong acid  $HA$  and minor concentrations of anions  $X^-$  and  $Y^-$  of strong acids  $HX$  and  $HY$ , respectively, which are negligible when compared with the concentration of the major component. The concentrations of the minor sample components are assumed to be negligible even when being concentrated and stacked during the electrophoretic separation process. The sample solution is assumed to have the same pH as the background electrolyte (although this changes during the electrophoresis, the maximum pH deviation will not be greater than 0.2 pH units). As all investigated sample components are strong anions, the influence of small pH differences on their migration behaviour can be neglected. By this approach the changes in the concentrations of both  $H^+$  and  $R$  along the column are neglected. Moreover, the pH is assumed to lie within the neutral region where the contribution of  $H^+$  to conductivity can also be neglected.

We further assume that we have a hydrodynamically closed capillary system with absence of hydrodynamic and electroosmotic flow, and are operating with constant electric current. The amount of sample substance  $A$  introduced is so high that, under the given operating conditions, electromigration is the major dispersion effect and other than diffusional dispersions can be neglected anywhere except the regions of self-sharpening boundaries. The mobilities of the anionic species are selected so that  $u_A > u_X > u_Y > u_B$ . This is an important prerequisite for proper functioning of the discussed type of systems: the major sample component must have the highest mobility to act as the stacking leader and the background co-ion must have the lowest mobility to act as the stacking terminator.

#### *Migration of the major sample component*

Before discussing the behaviour of the minor sample components in the given system, the characteristics of the evolution of the concentration profile of the major sample substance  $A$  must be briefly given. We assume that the sample is introduced hydrodynamically into the (one-dimensional) column as a rectangular concentration pulse (see Fig. 1a). The BGE and the sample are denoted zones 1 and 3, respectively. Let us put the origin of the  $x$ -axis ( $x = 0$ ) into the right boundary between

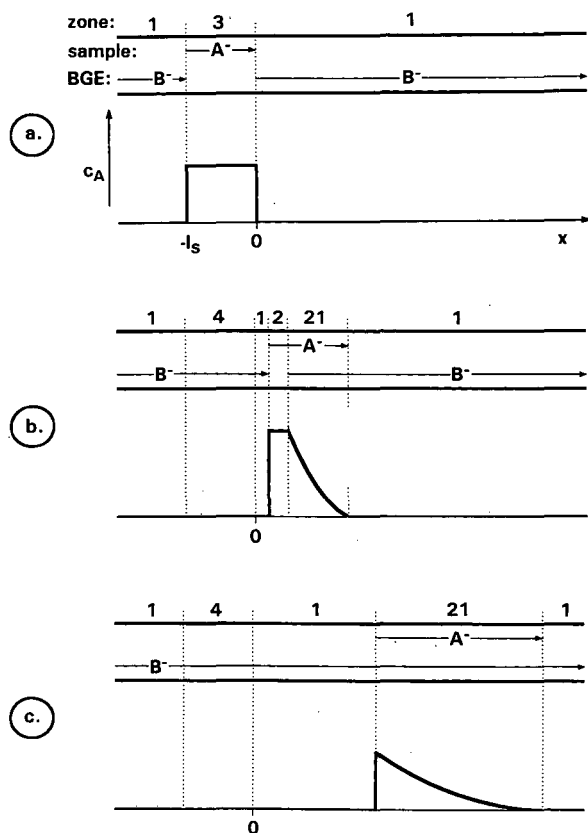


Fig. 1. Scheme of migration of a zone of anion A<sup>-</sup> in the background electrolyte R<sup>+</sup>A<sup>-</sup> at three different values of electrophoresis time. (a) Initial state showing the position and designation of the zones (above) and concentration profile of the zone of A<sup>-</sup>, being here a rectangular pulse of length  $l_s$ . (b) Situation after the entire zone of A<sup>-</sup> has migrated through the point  $x = 0$ ; the concentration profile consists of two distinguished parts, viz., a rectangular (isotachophoretic) one and a descending (transition or diffuse) one. (c) Situation where the zone of A<sup>-</sup> is represented only by the diffuse descending concentration profile.

the sample zone and the background electrolyte (boundary 3-1), i.e., at the beginning of the separation compartment. Let  $l_s$  be the length of the original sample zone (length of the sampling compartment, see Fig. 1a).

When now passing electric current through the system so that anions move to the right, the zone of substance A migrates through the boundary 3-1 and readjusts its concentration isotachophoretically [14] to the conditions of zone 1. The so-formed zone of

substance A is denoted zone 2 (see Fig. 1b) and its readjusted concentration is given by

$$c_{A,2} = c_{B,1} m_B/m_A \quad (1)$$

where  $c_{i,j}$  is the concentration of ion  $i$  in zone  $j$ ,  $m_i = (u_i + u_R)/u_i$  and  $u_i$  is the electrophoretic mobility of ion  $i$ .

The content of the sampling compartment is displaced by the BGE adjusted to the parameters of zone 3 (zone 4) and at the positions of the original sample boundaries (1-3 and 3-1), the stationary concentration boundaries 1-4 and 4-1 are found. During the process when the sample zone migrates out of the sampling compartment, its rear boundary remains sharp (boundary 4-3 between the sample zone 3 and the BGE zone 4 adjusted to its parameters); it moves with the velocity

$$v_{4-3} = i u_A/\kappa_3 = i u_B/\kappa_4 \quad (2)$$

where  $i$  is the electric current density and  $\kappa_3$ , e.g., is the specific conductivity of the sample solution given by

$$\kappa_3 = F c_{A,3}(u_A + u_R) \quad (3)$$

where  $F$  is the Faraday constant. The rear boundary of the sample zone reaches the point  $x = 0$  at the time

$$t_0 = l_s/v_{4-3} = l_s \kappa_3/i u_A \quad (4)$$

It then continues to migrate as a sharp boundary but now between zones 1 and 2 (boundary 1:2, see Fig. 1b) with the velocity

$$v_{1-2} = i u_A/\kappa_2 = i u_B/\kappa_1 \quad (5)$$

Whereas the rear boundary of zone 2 migrates as an isotachophoretic (sharp) boundary, no self-sharpening effect will apply at its front. Here the originally rectangular concentration profile spreads into a more and more diffuse transition zone (zone 2:1, see Fig. 1b). The velocities of its front and rear edges correspond to velocities of single ions A<sup>-</sup> and B<sup>-</sup> in zones 1 and 2, respectively:

$$v_{A,1} = i u_A/\kappa_1 \quad (6)$$

$$v_{B,2} = i u_B/\kappa_2 \quad (7)$$

The time- and coordinate-dependent parameters of the transition zone 2:1 can be obtained by solving the set of partial differential equations (continuity equations valid for the three substances A, B and R).



The solution of such a system for three fully ionized species was given by Weber [15] (see also ref. 16). The present system brings a new aspect in that the counter-substance is a weak base. Fortunately, we may take advantage of the rule [17] that the total concentration of neutral particles remains constant with time; for the present system it holds in the form  $\partial c_R / \partial t = 0$ . Therefore, the continuity equation for the counter-substance can be written in the same form as for a fully ionized species and the set of continuity equations may be solved in the same way as referred to above.

For the descending concentration profile of substance A in zone 21 (see Fig. 1b), e.g., it holds that

$$c_{A,21} = \frac{u_B c_{B,1} m_B}{m_A (u_A - u_B)} \left[ \left( v_{A,1} \cdot \frac{t}{x} \right)^{\frac{1}{2}} - 1 \right] \quad (8)$$

and for the conductivity we obtain

$$\kappa_{21} = F [c_{A,21} (u_A + u_R) + c_{B,21} (u_B + u_R)] = \kappa_1 (v_{A,1} t/x)^{\frac{1}{2}} \quad (9)$$

The velocity of the rear boundary of zone 2 is higher than that of the rear edge of the transition zone 21,  $v_{1-2} > v_{B,2}$ ; the boundary 1–2 and the edge 2–21 meet at the point  $x_d$ . The following balance holds:

$$x_d/v_{B,2} = t_0 + x_d/v_{1-2} \quad (10)$$

from which we obtain

$$x_d = l_s \cdot \frac{\kappa_3}{\kappa_1} \cdot \frac{u_B}{u_A} \cdot \frac{u_B}{u_A - u_B} \quad (11)$$

Note that all the time of its existence zone 2 has kept its isotachophoretic character and did not contain any amount of the background substance B (see Fig. 1b). The respective time of disappearance of zone 2 is then

$$t_d = x_d/v_{B,2} = l_s \kappa_3/i (u_A - u_B) \quad (12)$$

Starting at this time point, the sample zone (zone of anion  $A^-$ ) is formed only by the descending concentration profile as shown in Fig. 1c. Note that now the sample zone is completely mixed, i.e., substance A migrates completely on the background of anion  $B^-$ . Whereas the front edge of this zone 21 migrates still with constant velocity given by eqn. 6, its rear edge now consists of the sharp boundary 1–

21. The migration velocity of this boundary is a function of time [16] and may be written as

$$v_z = dx_z/dt = i u_A/\kappa_z \quad (13)$$

where the subscript z relates to the parameters of zone 21 at its rear boundary 1–21. By expressing  $\kappa_z$  from eqn. 9, we obtain the differential equation

$$dx_z/dt = (v_{A,1} x_z/t)^{\frac{1}{2}} \quad (14)$$

Integration (starting at  $x_d$  and  $t_d$ ) provides the position of boundary 1–21 at any time  $t > t_d$ :

$$x_z^{\frac{3}{2}} = (v_{A,1} t)^{\frac{3}{2}} - x_d^{\frac{3}{2}} \cdot \frac{u_A - u_B}{u_B} \quad (15)$$

### Migration of a minor component

Let us now consider the same situation and system as described in the previous section with the one exception that the sample zone (zone 3) contains additionally a minor amount of the substance X (Fig. 2a). After application of electric current, both anions  $A^-$  and  $B^-$  behave in the same way as described in the previous section and only the presence of anion  $X^-$  makes a difference. An own (isotachophoretic) zone of  $X^-$  starts to be formed between the zones of  $A^-$  (zone 3 or 2 from Fig. 1, now including the minor content of  $X^-$ ) and of  $B^-$  (zone 4 or 1 from Fig. 1). Let us describe the situation at a time point corresponding to Fig. 1b where the whole sample has left the sampling compartment. As is depicted in Fig. 2b, the ions of  $X^-$  leave zone 2 of the major sample substance A both via its rear boundary (to be stacked here, as it holds that both  $v_{X,2} < v_{A,2}$  and  $v_{X,1} > v_{B,1}$ ) and via its front edge (to penetrate into the diffuse part of the  $A^-$  zone, as it holds that  $v_{X,2} > v_{B,2}$ ).

The stacking process proceeds by the isotachophoretic mechanism. As the isotachophoretic steady-state concentration of  $X^-$  in its own zone is independent of its concentration in the sample zone, it may be higher than the latter by many orders of magnitude [14]. This indicates an effective concentrating potential that applies even in our case when the substance X is present in such a minor amount that the sample zone does not reach the adjusted concentration plateau and, instead, forms only a small concentration peak behind the zone of A (Fig. 2b).

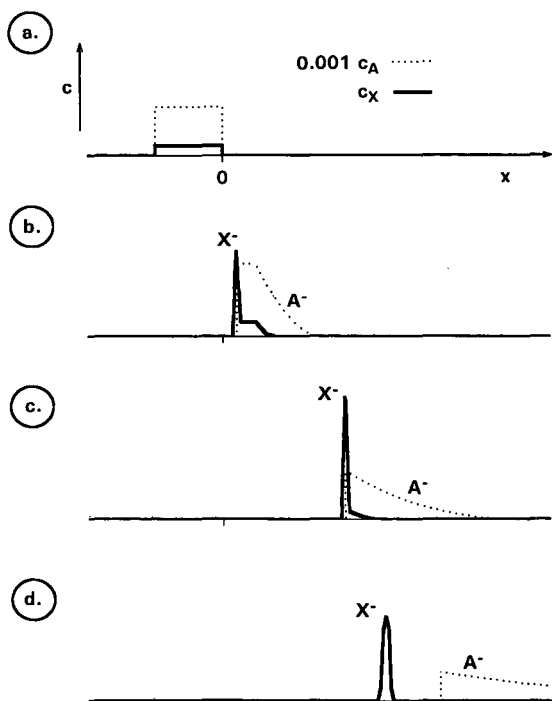


Fig. 2. Scheme of migration of a sample zone containing a major amount of a fast anion  $A^-$  and a minor amount of a slower anion  $X^-$ . (a) Initial state. (b) Starting phase of separation of both anions; in addition to the rectangular (isotachophoretic) part of the pattern where the concentration ratio still corresponds to the initial state, concentration (stacking) proceeds at the rear of the zone of  $A^-$  and, additionally, some penetration of  $X^-$  into the diffuse part of the zone of  $A^-$  is seen. (c) Situation where the stacking of  $X^-$  at the rear boundary of the  $A^-$  zone is almost complete; the amount of residual  $X^-$  in the diffuse  $A^-$  zone is already very small. (d) Complete separation and start of diffusional broadening of zone  $X^-$ .

The concentration of  $X^-$  having migrated forward into zone 21 is negligible in comparison with those of  $A^-$  and  $B^-$ ; its migration behaviour is thus controlled by the parameters of zone 21 only as described in the previous section. Obviously  $X^-$  cannot reach the front edge of zone 21 as  $u_X < u_A$ ; instead, it forms its own descending concentration profile with its own edge. As each point of zone 21 migrates with a constant velocity (in the present instance directly equal to  $x/t$ ) [15,16], the migration velocity of the front edge of the  $X^-$  profile,  $v_{X,m}$ , must also be constant. The  $x/t$  point of zone 21 that corresponds to this velocity can be found from the equality

$$v_{X,m} = i u_X / \kappa_{21}(x/t) = x/t \tag{16}$$

By expressing  $\kappa_{21}$  by analogy with, e.g., eqn. 9, we obtain after rearrangement

$$v_{X,m} = \frac{i u_X u_X}{\kappa_1 u_A} \tag{17}$$

After zone 2 has disappeared from the system (i.e., at time points  $t > t_d$ , see eqn. 12), the process of separation of  $X$  from  $A$  continues but  $X^-$  now migrates out of zone 21 and is stacked at the 1–21 boundary (Fig. 2c). Note that the zone system still migrates in stack as both the 1–21 boundary keeps its self-sharpening properties and the migration velocity of  $X^-$  in (the rear) zone 1 given by

$$v_{X,1} = i u_X / \kappa_1 \tag{18}$$

is still higher than the migration velocity of the boundary itself ( $v_{X,1} > v_z$ ). Of course, this boundary stack continuously speeds up with time as  $v_z$  increases (see eqn. 13).

The time point is now of interest when the sample zone leaves the stack. As is shown below, at this time point the migration velocity of  $X^-$  in zone 1 ( $v_{X,1}$ , eqn. 18) reaches the value of the migration velocity of the boundary itself ( $v_z$ , eqn. 13) and, simultaneously, the last traces of  $X^-$  migrate out of the transition zone 21. The time  $t_{X,e}$  of equal migration velocities,  $v_{X,1} = v_z$ , can be obtained from eqn. 18 and 14 after substitution using eqns. 5–7, 12 and 15 and rearrangement:

$$t_{X,e} = t_d \cdot \frac{(u_A - u_B)^2}{(u_A - u_X)^2} \tag{19}$$

At that time, the rear boundary of zone 21 is at the point  $x_{X,e}$  that is determined by eqn. 15 (with  $x_z = x_{X,e}$  and  $t = t_{X,e}$ ):

$$x_{X,e}^{\frac{1}{2}} = (v_{A,1} t_{X,e})^{\frac{1}{2}} - x_d^{\frac{1}{2}} \cdot \frac{u_A - u_B}{u_B} \tag{20}$$

By substitution and rearrangement using eqns. 19, 12, 5–7 and 17, we obtain the expression

$$x_{X,e} = t_d v_{A,1} \cdot \frac{(u_A - u_B)^2}{(u_A - u_X)^2} \cdot \frac{u_X^2}{u_A^2} = t_{X,e} v_{X,m} \tag{21}$$

which shows that the values of  $x_{X,e}$  and  $t_{X,e}$  also express the position of the front edge of  $X^-$  in zone 21 (see eqn. 12). In other words, the last ions of

substance X leave zone 21 just at the moment when the zones of X<sup>-</sup> and A<sup>-</sup> lose their immediate contact, *i.e.*, the zone of substance X<sup>-</sup> starts to migrate out of the stack.

After the zone of substance X leaves the stack, it migrates in a normal zone electrophoretic mode in the BGE (in zone 1) (see Fig. 2d). Its position at a time point  $t > t_{X,e}$  is given by the balance

$$x_{X,t} = x_{X,e} + (t - t_{X,e})v_{X,1} \quad (22)$$

Rearrangement using eqns. 18, 19 and 21 results in

$$x_{X,t} = v_{X,1} \left[ t - t_d \cdot \frac{(u_A - u_B)^2}{(u_A - u_X)u_A} \right] \quad (23)$$

#### Detection time and variance of the zone of a minor component

On the basis of the above considerations, we are able to give explicit expressions of the zone parameters that are important for analytical practice. We assume that the detection of the zone of the minor sample component X proceeds after it has left the stack, *i.e.*, at times  $t > t_{X,e}$ . As will be shown below (see Results and Discussion), this approximation is justified.

For a detector placed at point  $x_r$ , we obtain for the detection (elution) time of zone X from eqn. 23 directly

$$\begin{aligned} t_{X,r} &= \frac{x_r}{v_{X,1}} + t_d \cdot \frac{(u_A - u_B)^2}{(u_A - u_X)u_A} \\ &= \frac{x_r}{v_{X,1}} + t_{X,e} \cdot \frac{u_A - u_X}{u_A} \end{aligned} \quad (24)$$

The first term in this equation represents the expression for the normal zone electrophoretic mode of migration. The second term expresses the delay of zone X in the present system (when compared with normal zone electrophoresis) caused by the fact that the zone of substance X migrates a certain time in stack, *i.e.*, slower than corresponds to its zone electrophoretic velocity,  $v_{X,1}$ . Note that both  $t_d$  and  $t_{X,e}$  are directly proportional to  $c_{A,3}$  (see eqns. 12, 3 and 19).

For expressing the zone variance we assume that diffusion is the only dispersion effect that applies. While migrating in stack, the zone of X is very sharp

and diffusional broadening is effectively suppressed by electromigrational (isotachophoretic) sharpening. After leaving the stack, *i.e.*, at times  $t > t_{X,e}$ , normal diffusional broadening of zone X proceeds. The total variance of this zone at the detection time  $t_r$  is then

$$\sigma_{X,r}^2 = \sigma_{X,e}^2 + 2D_X (t_{X,r} - t_{X,e}) \quad (25)$$

where  $\sigma_{X,e}^2$  is the zone variance at time  $t_{X,e}$ . Substitution from eqn. 24 and rearrangement give

$$\sigma_{X,r}^2 = 2D_X \cdot \frac{x_r}{v_{X,1}} + \sigma_{X,e}^2 - 2D_X t_{X,e} \cdot \frac{u_X}{u_A} \quad (26)$$

This equation consists of three terms of which the first,  $2D_X x_r / v_{X,1}$ , expresses the variance the zone would have when undergoing normal zone electrophoresis. The variance in the present instance is lower because the diffusional peak broadening does not proceed as long; this is expressed by the third term. On the other hand, some variance is contributed by the concentration peak not being infinitely sharp when migrating out of the stack (second term in eqn. 26). We may expect that  $\sigma_{X,e}^2$  is much smaller than  $\sigma_{X,r}^2$ , *i.e.*, that the minor sample component undergoes efficient concentrating/stacking at the rear boundary of the zone of the major sample component. In such a case the resulting peak variance is smaller than in normal zone electrophoresis. Eqn. 26 also implies one important fact, *viz.*, owing to the mentioned stacking effect, the resulting variance of a sample zone is independent of the injection conditions.

#### Separation and resolution of a pair of minor sample components

The above considerations may now be used to describe the case that is of analytical interest, *viz.*, the separation and resolution of a pair of minor sample components, say substances X and Y. If we assume that the separation from the major component (component A) and the zone migration of each minor sample component proceed independently of each other, we can directly use the results in the previous section.

The resulting distance of two separated sample peaks can be expressed as the difference in detection times; from eqn. 24 we obtain directly

$$\Delta t_{X,Y,r} = \frac{x_r}{v_{X,1}} \cdot p_{X,Y} - t_d \cdot \frac{(u_A - u_B)^2}{u_A} \cdot \frac{u_X - u_Y}{(u_A - u_X)(u_A - u_Y)} \quad (27)$$

where  $p_{X,Y} = (u_X - u_Y)/u_Y$  is the selectivity between X and Y. The first term corresponds to the case of normal zone electrophoresis. The second term represents the decrease in the detection times difference of the present case when compared with simple zone electrophoresis; the reason is the same as for the increase in detection time in eqn. 24.

The time-based variance of the peak of component  $i$  passing through the detector may be approximated by

$${}^t\sigma_{i,r} = \sigma_{i,r}/v_{i,1} \quad (28)$$

The resolution is thus

$$R_{X,Y} = \frac{\Delta t_{X,Y,r}}{2({}^t\sigma_{X,r} + {}^t\sigma_{Y,r})} \quad (29)$$

When compared with normal zone electrophoresis, the resolution here is decreased by the nominator and increased by the denominator (see the comments on eqns. 27 and 26, respectively).

## EXPERIMENTAL

Computer simulations were performed using the model by Bier *et al.* [18] and Mosher *et al.* [10] in the form of a PC-adapted software package. The software was run on a Mandax AT 286 computer (Panasonic, Zürich, Switzerland) featuring a mathematical coprocessor, a 40 Mbyte hard disk and 1 Mbyte of RAM memory. The simulation results were imported into SigmaPlot Scientific Graphing Software version 4.01 (Jandel Scientific, Corte Madera, CA, USA) and the plots were printed on an HP Laserjet IIIP printer (Hewlett-Packard, Widen, Switzerland).

For all simulations, the same model system was taken with the ionic mobility values  $u_A = 8 \cdot 10^{-8} \text{ m}^2 \text{ V}^{-1} \text{ s}^{-1}$ ,  $u_B = 3 \cdot 10^{-8} \text{ m}^2 \text{ V}^{-1} \text{ s}^{-1}$  and  $u_{RH} = 4 \cdot 10^{-8} \text{ m}^2 \text{ V}^{-1} \text{ s}^{-1}$ . The dissociation constant of the counter-species was taken as  $\text{p}K_a = 6$ . The concentration of the background electrolyte of like charge was  $c_{B,1} = 0.1 \text{ M}$  and the concentration of the major sample ion in the sample zone was

$c_{A,3} = 0.1 \text{ M}$ ; the concentrations of all minor sample components in the sample zone were  $1 \cdot 10^{-4} \text{ M}$  and the concentration of the counter component was  $0.2 \text{ M}$ . The electric current density was kept constant at  $2000 \text{ A m}^{-2}$  in all simulations.

## RESULTS AND DISCUSSION

To illustrate the theoretical considerations presented, computer simulations of model systems were performed. Although the conclusions in the Theoretical section are valid for the separations of both anions and cations, all the simulations performed

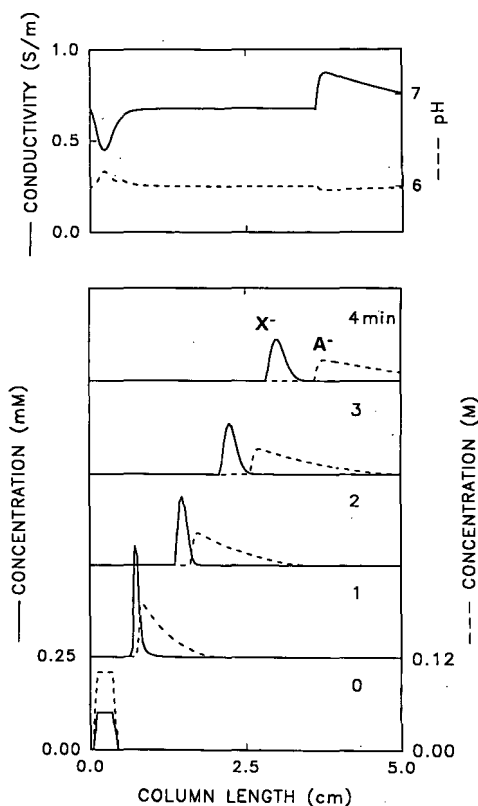


Fig. 3. Computer simulation of zone electrophoretic migration of a minor amount of strong anion  $X^-$  ( $u_X = 45 \cdot 10^{-9} \text{ m}^2 \text{ V}^{-1} \text{ s}^{-2}$ ) in the presence of a major amount of a strong and fast anion  $A^-$ . The lower panel shows the simulated concentration profiles of both components after 0, 1, 2, 3 and 4 min of electrophoresis time (see the numbers on the right; the concentration scale of each following time point is shifted upwards using an offset of  $0.25 \text{ mM}$ ). The upper panel shows pH and conductivity profiles along the column for the last time point (4 min). Simulation was performed for an 8-cm long column with 200 segments; the initial sample pulse length was 0.32 cm.

are related to anionic separations. Fig. 3 shows typical simulation data of a simple model system with the major sample anion and one minor sample component. The depicted evolution of the concentration profiles clearly shows both the concentration and stacking of the minor component at the rear boundary of the zone of the major component (see profile at 1-min electrophoresis time) and the subsequent migration of the minor component zone out of the stack and its gradual broadening. For this example, the time of the beginning of destacking calculated from eqn. 19 is 1.3 min. This result compares favourably with that obtained by computer simulation. The pH and conductivity data presented in the top panel of Fig. 3 (last time point only) depict that the major component strongly influences the local conductivity and pH. This is not the case for the minor component. These findings are in complete agreement with previous computer simulations [10,19]. Nevertheless, the pH deviation does not exceed *ca.* 0.2 units, showing that the presumption made in the Theoretical section were justified.

Fig. 4 makes use of a similar simulation run with one minor sample component and gives details on the process of zone broadening. After sharpening (first 30 s) the zone variance is very low and remains almost constant. It starts to increase shortly before the electrophoresis time approaches the value of  $t_{X,e}$

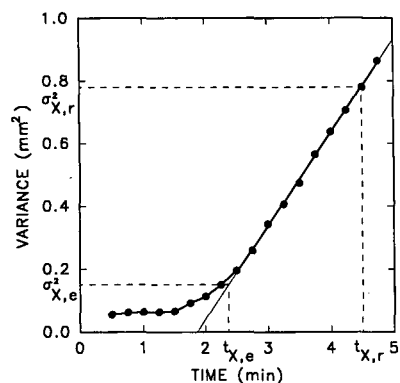


Fig. 4. Simulated dependence of the variance of the concentration profile of zone X ( $u_X = 55 \cdot 10^{-9} \text{ m}^2 \text{ V}^{-1} \text{ s}^{-2}$ ) on time. Simulation was performed for a 10-cm long column with 400 segments; the initial sample pulse length was 0.3 cm. The variance was evaluated from the peak width at half-height ( $W$ ) of the plotted simulation results using the equation  $\sigma^2 = W^2/5.545$ . For explanation, see text.

(2.4 min, calculated from eqn. 19). As expected, the zone variance shows a perfect linear dependence on time at times higher than 2.4 min (see eqn. 25 and the marked values of  $\sigma_{X,r}^2$ ,  $\sigma_{X,e}^2$ ,  $t_{X,r}$  and  $t_{X,e}$ ).

In order to obtain a better insight into the discussed type of systems, some numerical calculations were performed for the given model system and for a pair of minor sample components. For a 0.3-cm long sample pulse with the concentration of the major component being  $c_{A,3} = 100 \text{ mol m}^{-3}$ , we obtain the parameters of the system, *viz.*, the time when the sample completely leaves the sampling compartment  $t_0 = 22.5 \text{ s}$  (eqn. 4), the isotachophoretic velocity of the self-sharpening boundary stack,  $v_{1-2} = 0.86 \cdot 10^{-4} \text{ m s}^{-1}$  (eqn. 5), the velocities of the front and rear edges of the transient zone 21,  $v_{A,1} = 2.29 \cdot 10^{-4} \text{ m s}^{-1}$  (eqn. 6) and  $v_{B,2} = 0.32 \cdot 10^{-4} \text{ m s}^{-1}$  (eqn. 6), respectively, and the specific conductivity of the background electrolyte,  $\kappa_1 = 0.7 \text{ S m}^{-1}$  (see eqn. 3). Note the great difference between the velocities of both edges of

TABLE I

NUMERICAL VALUES OF ZONE PARAMETERS OF SEPARATION OF A PAIR OF MINOR SAMPLE COMPONENTS  $X^-$  AND  $Y^-$  ( $u_X = 45 \cdot 10^{-9} \text{ m}^2 \text{ V}^{-1} \text{ s}^{-2}$ ,  $u_Y = 40 \cdot 10^{-9} \text{ m}^2 \text{ V}^{-1} \text{ s}^{-2}$ ) AND THEIR DEPENDENCE ON THE CONCENTRATION OF THE MAJOR SAMPLE COMPONENT

The sample pulse length was 0.3 cm and the detector was positioned at  $x = 10 \text{ cm}$ . The current density was  $2000 \text{ A m}^{-1}$ .

Parameter	$c_{A,3} \text{ (mol m}^{-3}\text{)}$			
	0	50	100	200
$\kappa_3 \text{ (S m}^{-1}\text{)}$	0.00165	0.6	1.2	2.4
$t_d \text{ (eqn. 12) (s)}$		18.1	36.2	72.3
$x_{X,e} \text{ (eqn. 21) (cm)}$		0.27	0.53	1.07
$x_{Y,e} \text{ (eqn. 21) (cm)}$		0.16	0.32	0.65
$t_{X,e} \text{ (eqn. 19) (s)}$		36.9	73.8	147.6
$t_{Y,e} \text{ (eqn. 19) (s)}$		28.3	56.5	113.0
$t_{X,r} \text{ (eqn. 24) (s)}$	778	794	810	842
$t_{Y,r} \text{ (eqn. 24) (s)}$	875	889	903	932
$\Delta t_{X,Y,r} \text{ (eqn. 27) (s)}$	97	95	93	90
$\sigma_{X,r}^2 \text{ (eqn. 26)}^a \text{ (mm}^2\text{)}$	1.70	1.71	1.67	1.59
$\sigma_{Y,r}^2 \text{ (eqn. 26)}^a \text{ (mm}^2\text{)}$	1.70	1.73	1.70	1.65
$t_{X,r}^* \text{ (eqn. 28) (s)}$	10.14	10.17	10.05	9.81
$t_{Y,r}^* \text{ (eqn. 28) (s)}$	11.44	11.51	11.41	11.24
$R_{X,Y} \text{ (eqn. 29)}$	2.25	2.19	2.17	2.14

<sup>a</sup>  $D_i = RTu_i/F$ ;  $\sigma_{X,e}^2 = \sigma_{Y,e}^2 = 0.05 \text{ mm}^2$ .

zone 21, which indicates the fast growing and flattening of the concentration profile of  $A^-$ . Further numerical data including those calculated for the minor sample components  $X^-$  and  $Y^-$  ( $u_X = 45 \cdot 10^{-9} \text{ m}^2 \text{ V}^{-1} \text{ s}^{-2}$ ,  $u_Y = 40 \cdot 10^{-9} \text{ m}^2 \text{ V}^{-1} \text{ s}^{-2}$ ) are given in Table I. As can be seen, the time points of leaving the stack,  $t_{i,e}$ , are low for both components when compared with the final detection times  $t_{i,r}$  for the present length of the sample pulse. Nevertheless, they differ substantially (see the dependence on mobility,  $u_X$  or  $u_Y$ , in eqn. 19). For  $t_{i,e} > t_{i,r}$ , the sample zone would pass through the detector still in the stack. However, only very high concentrations of  $A^-$  in the sample would lead to such an increase in the  $t_{i,e}$  values, e.g., for  $X^-$  in Table I, the critical value of  $c_{A,3}$  is as high as 1.88 M.

Interesting conclusions may be drawn from Table I by comparing the data for various concentrations of the major sample anion and especially for the case with  $c_{A,3} = 0$  (the sample solution contains only the

minor sample components). It is seen that the presence of  $A^-$  in the sample substantially changes (increases) the detection times of both components; this is given by the dependence of  $t_{i,e}$  on  $t_d$  (see eqn. 19). The difference in the detection times of  $X^-$  and  $Y^-$ , however, remains nearly constant, decreasing only slightly with increasing  $c_{A,3}$ . As far as zone broadening is concerned, Table I shows that for the case presented there is no substantial difference in zone variance between the case with and without  $A^-$  in the sample. The final resolution decreases slightly with increasing concentration of the major sample component.

It can be concluded from the data presented in Table I that the systems with sample self-stacking provide a similar separation power for minor sample components compared with the samples containing only these minor sample components. The analysis times are slightly increased in the presence of a major compound of like charge. This is illustrated with the

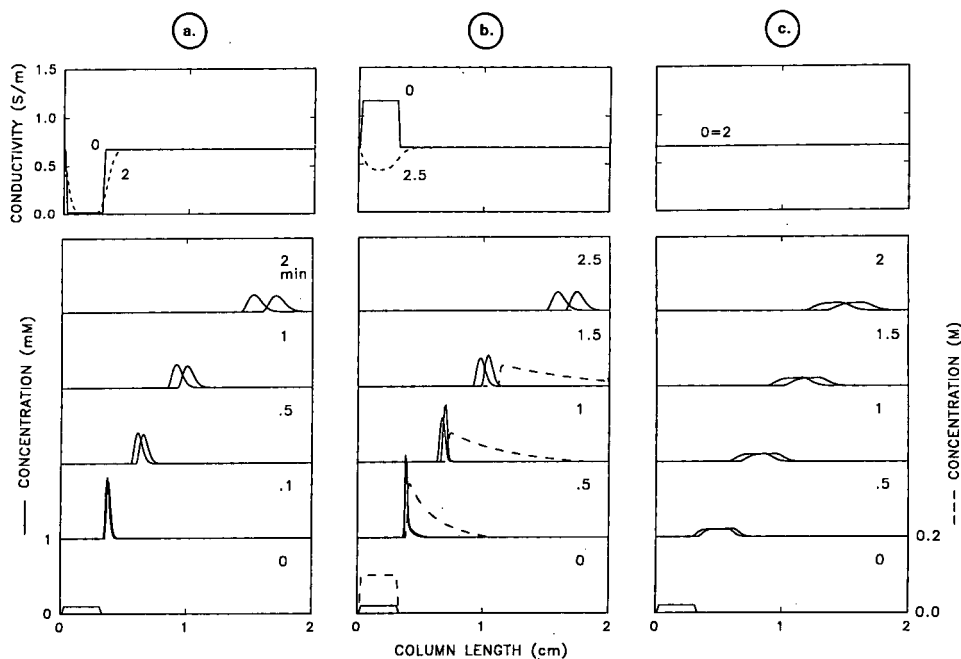


Fig. 5. Computer-simulated dynamics of the concentration profiles during the separation of two strong anions  $X^-$  and  $Y^-$  ( $u_X = 40 \cdot 10^{-9} \text{ m}^2 \text{ V}^{-1} \text{ s}^{-2}$ ,  $u_Y = 35 \cdot 10^{-9} \text{ m}^2 \text{ V}^{-1} \text{ s}^{-2}$ ). The sample contained  $X^-$  and  $Y^-$  ( $1 \cdot 10^{-4} \text{ M}$  each) with (a) addition of a 0.002 M concentration of the background electrolyte anion  $B^-$ , (b) addition of a 0.1 M concentration of anion  $A^-$  (the profile of  $A^-$  is shown by the dashed line) and (c) addition of a 0.1 M concentration of the background electrolyte anion  $B^-$ . The electrophoresis time in minutes of each profile is shown by the numbers on the right. The three upper panels show the conductivity profiles along the separation column at the first (solid line) and last (broken line) time point of each simulation; the numbers indicate the respective electrophoresis time in minutes. Simulation was performed for a 2-cm long column with 200 segments; the initial sample pulse length was 0.3 cm.

simulation data depicted in Fig. 5. Fig. 5a shows the situation with the sample solution containing the two minor components accompanied by a minute concentration of background electrolyte. Here, the sample stacking effect applies (see Introduction) owing to the very low conductivity of the sample solution (see top panel of Fig. 5a). Effective sharpening of the sample zones is seen at the beginning of the analysis. Fig. 5b illustrates the case where the sample shows the self-stacking effect produced by the presence of  $A^-$ . Although the conductivity of the sample solution is even higher than that of the BGE (see top panel of Fig. 5b), effective sharpening of both zones of the separated components is seen at the rear of the zone of the major component. Comparison of Fig. 5a and b reveals that the sample self-stacking mechanism has approximately the same effect as normal sample stacking. For comparison, Fig. 5c shows the case when the sample is dissolved in the background electrolyte. The conductivities of the sample solution and of the BGE are the same and there is no

mechanism to sharpen the zones. Flat zone patterns and poor resolution are the result.

Fig. 6 illustrates the self-sharpening effect in multi-component samples by showing the simulation result for a sample with four minor substances and one major component of like charge. As can be seen, the very narrow zone stack spreads gradually into four individual peaks. The time point at which the sample components begin to migrate out of stack is given by the mobility of the respective substance; for the anions with mobilities  $35 \cdot 10^{-9}$ ,  $45 \cdot 10^{-9}$ ,  $55 \cdot 10^{-9}$  and  $65 \cdot 10^{-9} \text{ m}^2 \text{ V}^{-1} \text{ s}^{-2}$ , eqn. 19 provides destacking times of 0.7, 1.2, 2.4 and 6.7 min, respectively. At  $t = 5$  min, for example, three of the four zones are already destacked and broadening; only the fastest component with the highest mobility remains in the stack, as is demonstrated by its narrower shape.

#### CONCLUSION

The sample self-stacking effect belongs to the sampling techniques which provide electromigrative concentration of minor sample components into narrow zones. The concentration power of this technique is about the same as with, e.g., normal sample stacking, but the application range is different. The sample self-stacking applies to minor components in samples containing a bulk amount of a high-mobility ion of like charge. A necessary condition is that the mobility of the background co-ion is lower than the mobilities of all the sample components so that it can act as a terminator of the stacking process. The process of sample self-stacking can be described by simple relationships describing the timing of the particular steps of the process, viz., readjustment of the sample concentrations to the parameters of the background electrolyte, isotachophoretic stacking of the minor sample components at the rear boundary of the major component zone and destacking followed by normal zone electrophoretic migration. The numerical values compare well with data obtained by computer simulation. Interestingly, the final resolution does not show a pronounced dependence on either electric current density or initial concentration of the major component in the sample. This concentration, however, significantly affects the conductivity of the sample solution and thus the Joule heating in the

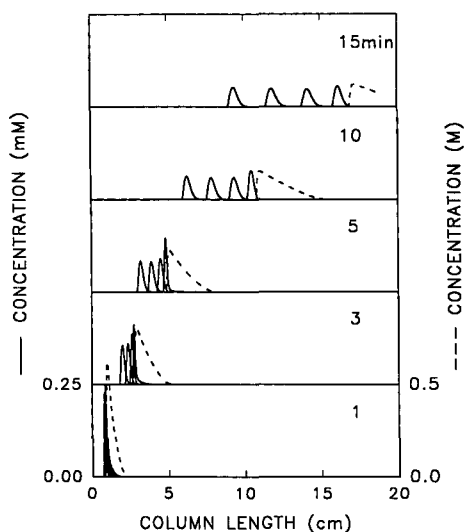


Fig. 6. Computer-simulated dynamics of the zone electrophoretic separation of four strong anions with mobilities  $35 \cdot 10^{-9}$ ,  $45 \cdot 10^{-9}$ ,  $55 \cdot 10^{-9}$  and  $65 \cdot 10^{-9} \text{ m}^2 \text{ V}^{-1} \text{ s}^{-2}$  in the presence of a major amount of a strong and fast anion  $A^-$ . The initial concentration of all minor sample components was  $1 \cdot 10^{-4} \text{ M}$ . The concentration profiles of all four components and of anion  $A^-$  (dashed line) are shown at 1, 3, 5, 10 and 15 min of electrophoresis time (see the numbers on the right). Simulation was performed for a 20-cm long column with 400 segments; the initial sample pulse length was 0.3 cm.

sampling compartment. Addition of a fast anion to dilute solutions of thermolabile samples may therefore prevent their thermal degradation, which is a real problem when using normal sample stacking [20]. The concentration of the major component in the sample significantly affects the elution times of the individual minor components. As these differences represent typically tens of percent, qualitative evaluations of electropherograms must be performed with great care in all instances where sample self-stacking may apply. The equations presented may be easily modified to describe cationic separations and systems with electroosmotic flow.

#### ACKNOWLEDGEMENT

This work was supported in part by the Swiss National Science Foundation.

#### REFERENCES

- 1 F. E. P. Mikkers, F. M. Everaerts and Th. P. E. M. Verheggen, *J. Chromatogr.*, 169 (1979) 11.
- 2 S. E. Moring, J. C. Colburn, P. D. Grossman and H. H. Lauer, *LC · GC*, 8 (1989) 34.
- 3 R. L. Chien and D. S. Burgi, *J. Chromatogr.*, 559 (1991) 141.
- 4 P. Jandik and W. R. Jones, *J. Chromatogr.*, 546 (1991) 431.
- 5 D. Kaniansky and J. Marák, *J. Chromatogr.*, 498 (1990) 191.
- 6 V. Dolnik, K. A. Cobb and M. Novotny, *J. Microcol. Sep.*, 2 (1990) 127.
- 7 F. Foret, V. Šustáček and P. Boček, *J. Microcol. Sep.*, 2 (1990) 229.
- 8 F. Foret, E. Szoko and B. L. Karger, *J. Chromatogr.*, 608 (1992) 3.
- 9 R. A. Mosher and W. Thormann, *Pittsburgh Conference and Exposition, New Orleans, February 22-26, 1988*, Abstract No. 646.
- 10 R. A. Mosher, D. A. Saville and W. Thormann, *The Dynamics of Electrophoresis*, VCH, Weinheim, 1992.
- 11 Th. P. E. M. Verheggen, A. C. Schoots and F. M. Everaerts, *J. Chromatogr.*, 503 (1990) 245.
- 12 A. C. Schoots, Th. P. E. M. Verheggen, P. M. J. M. De Vries and F. M. Everaerts, *Clin. Chem.*, 36 (1990) 435.
- 13 J. L. Beckers and F. M. Everaerts, *J. Chromatogr.*, 508 (1990) 19.
- 14 P. Boček, M. Deml, P. Gebauer and V. Dolnik, *Analytical Isotachophoresis*, VCH, Weinheim, 1988.
- 15 H. Weber, *Die Partiellen Differential-Gleichungen der Mathematik und Physik*, Vol. I, Friedrich Vieweg u. Sohn, Braunschweig, 1910, p. 503.
- 16 P. Gebauer, M. Deml, J. Pospichal and P. Boček, *Electrophoresis*, 11 (1990) 724.
- 17 L. M. Hjelmeland and A. Chrambach, *Electrophoresis*, 3 (1982) 9.
- 18 M. Bier, O. A. Palusinski, R. A. Mosher and D. A. Saville, *Science (Washington, D.C.)*, 219 (1983) 1281.
- 19 W. Thormann, J. P. Michaud and R. A. Mosher, in M. J. Dunn (Editor), *Electrophoresis '86*, VCH, Weinheim, 1986, p. 267.
- 20 A. Vinther and H. Soeberg, *J. Chromatogr.*, 559 (1991) 27.





# Effects of carrier electrolyte composition on separation selectivity in capillary zone electrophoresis of low-molecular-mass anions

W. Buchberger

*Department of Analytical Chemistry, Johannes-Kepler-University, A-4040 Linz (Austria)*

P. R. Haddad

*Department of Analytical Chemistry, University of New South Wales, P.O. Box 1, Kensington, N.S.W. 2033 (Australia)*

---

## ABSTRACT

A systematic investigation was carried out on the influence of carrier electrolyte composition on separation selectivity in capillary zone electrophoresis of inorganic anions. Chromate, chloride, sulphate or nitrate was used as the carrier electrolyte, each containing a quaternary ammonium salt to reverse the electro-osmotic flow. The concentration and nature of the carrier electrolyte salt affected the separation order only to a minor degree. Much more pronounced effects could be achieved by adding organic solvents to the carrier electrolyte or by using different quaternary ammonium salts. Chemical modification of the inner wall of the fused-silica capillary did not affect the migration order significantly. There is no indication of retention by effects similar to ion-interaction chromatography as long as capillaries with an inner diameter of 75  $\mu\text{m}$  are used. Nevertheless, such effects might play an important role for capillaries with diameters of 10  $\mu\text{m}$  or less.

---

## INTRODUCTION

Recently, capillary zone electrophoresis (CZE) has been demonstrated to be a useful technique for high-efficiency separations of inorganic anions [1–4]. A typical carrier electrolyte consists of sodium chromate containing a reagent to reverse the electro-osmotic flow (EOF). Anions are separated according to their mobility under the influence of an applied potential of 10–30 kV. Detection can be achieved by indirect UV absorption. Under these conditions, high-efficiency separations of anions are possible with plate numbers greater than 300 000 per metre. For certain samples CZE might be a better technique than ion chromatography (IC), which

is now well established for the analysis of ionic species.

Unlike IC, little information is available on the parameters affecting separation selectivity in CZE of low-molecular-mass anions. Jones and Jandik [3] have reported small selectivity changes by varying the concentration of chromate or of the EOF modifier. Further data would make the optimization of CZE separations much easier, but unfortunately these data are still awaited. This paper reports a more systematic investigation into separation selectivity in CZE. Different EOF modifiers as well as different carrier electrolytes were tested. Totally aqueous electrolytes, but also mixtures with organic solvents, including methanol, acetonitrile, acetone, tetrahydrofuran and ethylene glycol, were used. Furthermore, the applicability of capillaries with hydrophobic phases bonded to fused silica was investigated.

---

*Correspondence to:* Dr. W. Buchberger, Department of Analytical Chemistry, Johannes-Kepler-University, A-4040 Linz, Austria.

## EXPERIMENTAL

The CZE instrument employed was a Quanta 4000 (Waters, Milford, MA, USA) interfaced to a Maxima 820 data station (Waters). Separations were carried out using an AccuSep fused-silica capillary (60 cm  $\times$  75  $\mu$ m I.D., Waters) or a CElect-H2 capillary (70 cm  $\times$  75  $\mu$ m I.D., Supelco, Bellefonte, PA, USA). The effective length of the capillaries (from the point of sample introduction to the point of detection) was 8 cm shorter than the total length. Injection was performed hydrostatically by elevating the sample at 10 cm for 20 s at the cathodic side of the capillary. Direct or indirect UV detection at 214 nm or indirect UV detection at 254 nm was used.

The carrier electrolytes were prepared from sodium chromate tetrahydrate, potassium nitrate, potassium chloride or sodium sulphate and an EOF modifier such as dodecyltrimethylammonium bromide, tetradecyltrimethylammonium bromide, hexadecyltrimethylammonium bromide (all obtained from Fluka, Buchs, Switzerland) or tetradecyltrimethylammonium chloride (prepared by passing a 5 mM solution of the corresponding bromide salt through a column filled with a strong anion-exchange resin). The electrolytes were prepared either in Milli-Q water or in water–organic solvent mixtures. Analytical-grade ethylene glycol and high-performance liquid chromatography (HPLC)-grade methanol, acetonitrile, tetrahydrofuran and acetone were obtained from Merck (Darmstadt, Germany). Samples were prepared in Milli-Q water.

All migration times were normalized to that of nitrate in order to obtain reproducible results. A normalization to a neutral electro-osmotic marker was less feasible because in some cases the electro-osmotic flow was very small, which resulted in excessively long migration times for the marker.

## RESULTS AND DISCUSSION

*Concentration effects*

For investigating selectivity effects in CZE, a test mixture containing ten anions (thiosulphate, bromide, chloride, iodide, sulphate, nitrite, nitrate, chlorate, thiocyanate and fluoride) was used throughout this work. The separation of several of these anions has been reported in the literature [3]

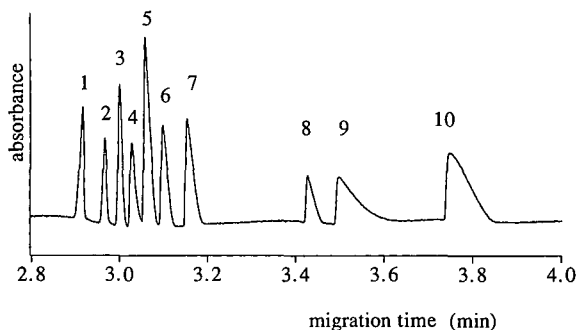


Fig. 1. Separation of a standard mixture of inorganic anions using standard conditions (see text). Peaks: 1 = thiosulphate; 2 = bromide; 3 = chloride; 4 = iodide; 5 = sulphate; 6 = nitrite; 7 = nitrate; 8 = chlorate; 9 = thiocyanate; 10 = fluoride. Indirect UV detection at 254 nm.

and was carried out with chromate as the carrier electrolyte and a proprietary EOF modifier. Our own experiments started with a carrier electrolyte of 5 mM chromate and 0.5 mM tetradecyltrimethylammonium bromide. This quaternary ammonium salt was introduced by Altria and Simpson [5,6] for reversing the EOF in the capillary. The separation was carried out at a voltage of 20 kV, resulting in an electric current of approximately 20  $\mu$ A. Throughout this paper these conditions will be referred to as standard conditions. A typical electropherogram obtained under standard conditions is given in Fig. 1.

Varying the chromate concentration within a range from 1 to 7 mM influenced the separation only to a minor degree since the migration order of only iodide, sulphate and nitrite was affected. By decreasing the chromate concentration, the order gradually changed to sulphate/nitrite/iodide, whereas by increasing the concentration the migration order became iodide/sulphate + nitrite (co-migrating).

When the EOF modifier concentration was varied over the range 0.2–0.8 mM, the separation was affected only with respect to the migration order of iodide, sulphate and nitrite. Decreasing the concentration resulted in a migration order iodide/sulphate + nitrite (co-migrating), whilst increasing the concentration led to a migration order sulphate/nitrite/iodide. More pronounced effects have been reported by Jones and Jandik [3] by varying their proprietary EOF modifier up to 5 mM. This concentration range was not investigated in this work.

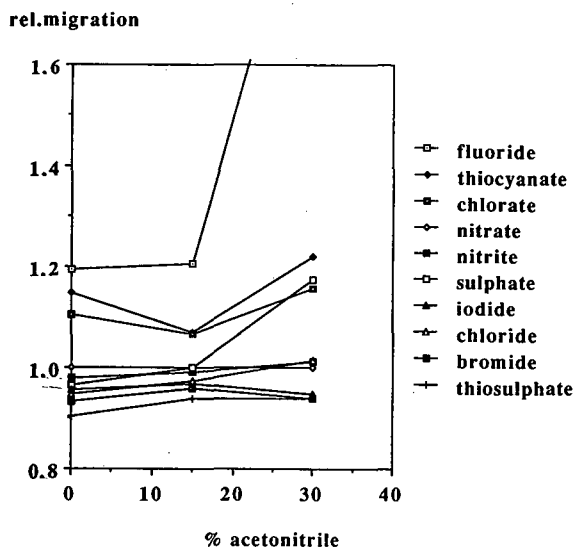


Fig. 2. Effect of acetonitrile in the carrier electrolyte on migration order.

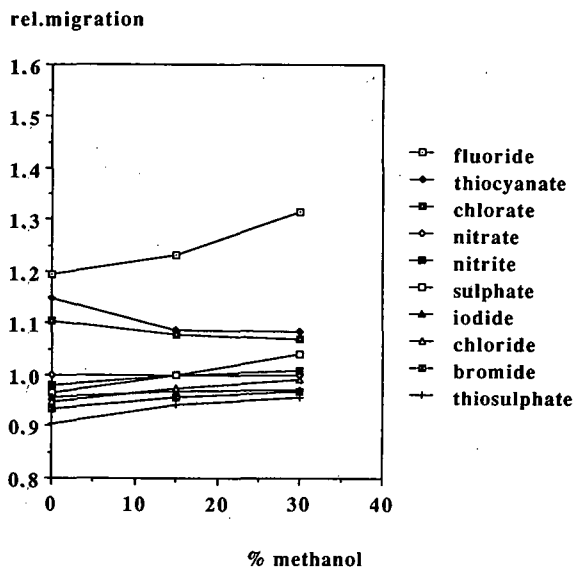


Fig. 3. Effect of methanol in the carrier electrolyte on migration order.

*Organic modifier effects*

In a series of experiments the influence of organic solvents in the carrier electrolyte was investigated. Up to 30% methanol, acetonitrile, tetrahydrofuran, acetone or ethylene glycol was used. As can be seen from the results given in Figs. 2-6, migration order is strongly influenced by the content of organic solvent in the carrier electrolyte. Obviously, there are some general trends for all organic modifiers (at 30% modifier the migration order sulphate/nitrate is reversed; the resolution between at least two peaks of the triplet thiosulphate/bromide/chloride decreases; the relative migration time of nitrite tends to increase, thereby eventually reversing the migration order nitrite/nitrate), but the data obtained so far do not allow the establishment of a relationship between the nature of the organic solvent and its influence on the electrophoretic mobility of different ions. Furthermore, organic solvents caused a general increase in the migration times of all ions, which can be attributed to two facts: on the one hand, the organic solvent decreases the electrical conductivity, thereby decreasing the current (a carrier electrolyte prepared in 30% organic solvent decreased the current to 10-14  $\mu$ A, depending on the solvent); on the other hand, the organic solvent possibly decreases the amount of EOF modifier ad-

sorbed onto the inner wall of the fused-silica capillary, which results in a lower EOF to the anode. The following numbers are the factors by which the migration time of nitrate is increased in a carrier electrolyte with 15 and 30% organic solvent: 1.4 and 1.9 (methanol), 1.2 and 3.0 (acetonitrile), 1.5 and 3.3

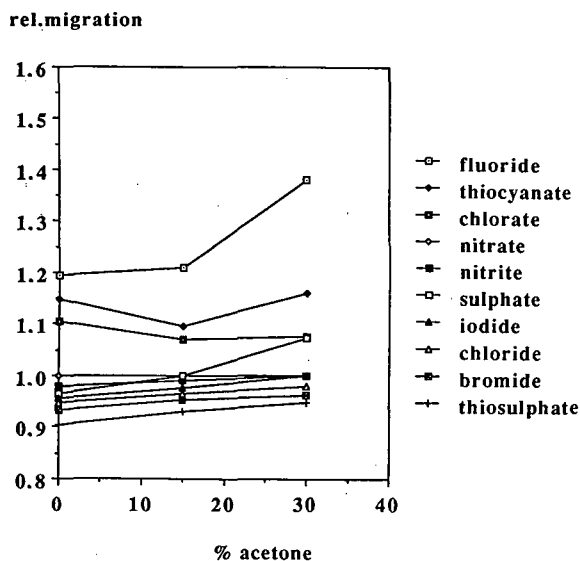


Fig. 4. Effect of acetone in the carrier electrolyte on migration order.

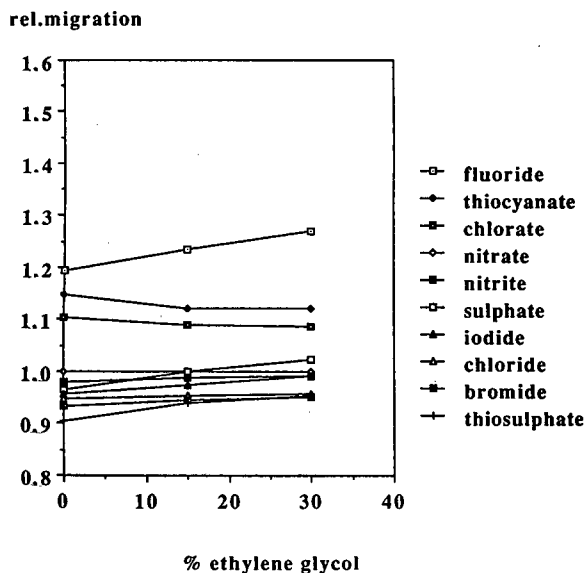


Fig. 5. Effect of ethylene glycol in the carrier electrolyte on migration order.

(tetrahydrofuran), 1.4 and 2.2 (acetone), 1.6 and 2.4 (ethylene glycol).

A typical electropherogram obtained with a carrier electrolyte containing 30% methanol is given in Fig. 7.

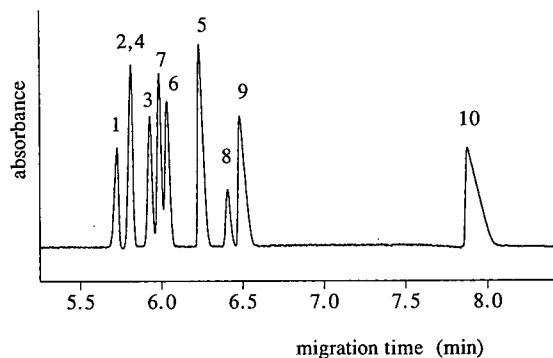


Fig. 7. Separation of a standard mixture of inorganic anions using a carrier electrolyte containing 30% methanol. All other conditions and peaks as for Fig. 1.

#### Nature of the carrier electrolyte

Next, several other salts were used instead of chromate in the carrier electrolyte. These included potassium chloride, potassium sulphate and potassium nitrate. All other conditions remained the same as the standard conditions, except the detection, which was carried out at 214 nm either in the direct mode or in the indirect mode. This low wavelength necessitated the use of the EOF modifier as the chloride salt form instead of the bromide salt.

The potassium chloride electrolyte yielded a migration order and migration times similar to those obtained under standard conditions. Direct UV detection was employed for the separation of bromide, iodide, nitrite, nitrate and thiocyanate. The migration times (relative to nitrate) were 0.943 (bromide), 0.964 (iodide), 0.996 (nitrite) and 1.104 (thiocyanate). The use of a potassium sulphate electrolyte instead of potassium chloride resulted in a similar separation with migration times (relative to nitrate) of 0.928 (bromide), 0.951 (iodide), 0.984 (nitrite) and 1.118 (thiocyanate). The only advantage of a chloride or sulphate carrier electrolyte with direct UV detection at 214 nm might be the increased detection selectivity if UV-absorbing anions must be determined in a matrix which does not absorb at 214 nm but would interfere with indirect detection modes.

The situation is somewhat more complicated if potassium nitrate is used as the carrier electrolyte. There can be positive as well as negative peaks depending on the UV absorption ratio of the sample anion and the carrier electrolyte anion. Nitrate in

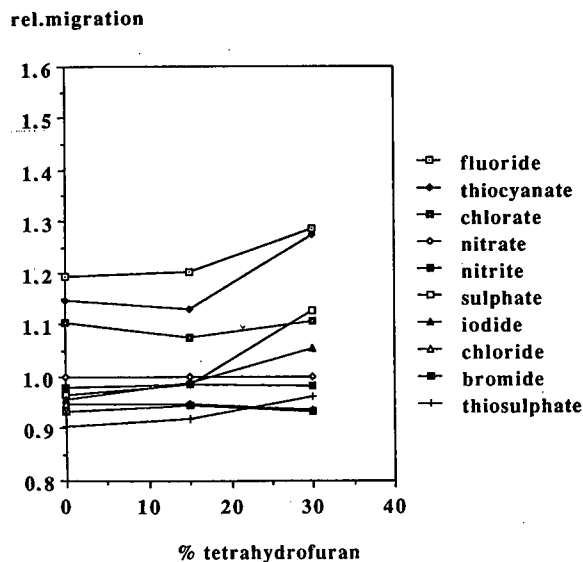


Fig. 6. Effect of tetrahydrofuran in the carrier electrolyte on migration order.

the sample should give no signal. In our experiments the injection of nitrate resulted in a positive peak at the migration time of chloride. The reason for this peak is not clear at the moment. The elution order for the other anions was the same as for standard conditions, but peak shape was worse. Therefore, nitrate as a carrier electrolyte does not offer any advantages and was not investigated further.

#### EOF modifier effects

An important component of the carrier electrolytes investigated is the EOF modifier, a quaternary ammonium salt which reverses the EOF to the anode. The influence of the nature of the EOF modifier on separation selectivity was studied by using three alkyltrimethylammonium bromides with different chain lengths of the alkyl group. The results are given in Fig. 8. Again, several pronounced changes in the migration order could be observed, especially with respect to the ions thiosulphate, iodide and thiocyanate. A further effect that was noted was that the average migration times were roughly doubled when using the EOF modifier with the shorter alkyl group, whereas the use of the EOF modifier with the longer alkyl group did not change the migration times significantly.

Huang *et al.* [4] have reported that hydrophobic quaternary ammonium salts, such as tetradecyltrimethylammonium bromide, attach to the inner surface of fused-silica capillaries, thereby shielding the negative charge of the silica and influencing the electro-osmotic flow in an opposite direction. On the other hand, the adsorbed quaternary ammonium salt might also act as an anion exchanger. Such phenomena are well known from ion-pair (or ion-interaction) liquid chromatographic analysis of anions using a reversed-phase material as the stationary phase and an eluent containing a quaternary ammonium salt. Recently, Pfeffer and Yeung [7] have demonstrated the use of ion-pairing effects for CZE separation of the anions of isomeric aminonaphthalenesulphonic acids. These anions were separated by differences in retention rather than by differences in electrophoretic mobility. The separation was therefore described as electrochromatography. Analogous to this, additional ion-exchange effects might be expected to occur for the CZE separations of inorganic anions described in this paper. Any modification of the inner fused-silica wall of

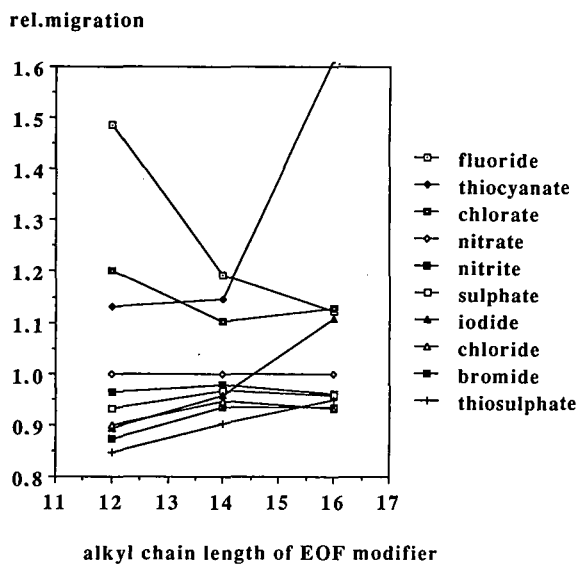


Fig. 8. Effect of alkyl chain length of the EOF modifier on migration order.

the capillary can influence the amount of adsorbed EOF modifier, thereby influencing the EOF as well as any ion-exchange mechanism. These effects were studied by using a commercially available capillary (CElect-H2), which is modified by C<sub>18</sub> on the inner wall (unfortunately, data on the extent of the modification, such as carbon loading, are not available).

#### Capillary effects

A C<sub>18</sub>-modified CElect-H2 capillary was tested using the chromate electrolyte as described for the standard conditions as well as using this electrolyte in 30% ethylene glycol. It was necessary to increase the voltage to 30 kV in order to obtain reasonable migration times. The separations obtained were exactly the same as those obtained with the bare fused-silica capillary. One might expect that the more hydrophobic wall would adsorb a larger amount of the EOF modifier, thereby eventually increasing the EOF to the anode. Contrary to this, the voltage had to be increased by 50% to achieve the same migration times. There is no simple explanation at hand for this fact. The separation order remained the same, which would mean that anion-exchange effects are either non-existent or exactly the same for both capillaries. Another argument against an anion-exchange mechanism is the fact that the use of organic solvents in the carrier elec-

trolyte influenced the migration order in a way quite different from the effects that would be expected from ion-interaction chromatography.

Nevertheless, a closer look at the electropherograms obtained for unmodified and modified capillaries revealed some interesting details. The peak shapes obtained for iodide and thiocyanate were more asymmetrical than can be explained by the mismatch of electric mobility of sample anion and carrier electrolyte anion. In ion-interaction chromatography, iodide and thiocyanate would be strongly retained if tetradecyltrimethylammonium bromide was used as the ion-interaction reagent. Therefore, it can be concluded that in CZE there is some interaction between the adsorbed reagent and iodide as well as thiocyanate, leading to peak tailing. On the other hand, this effect could not be used to manipulate the retention of these solutes, because the inner diameter of the capillaries used in this work is too large to allow efficient mass transfer between the solution and the wall of the capillary. In the experiments of Pfeffer and Yeung [7] mentioned above, this problem was overcome by the use of capillaries with only 10  $\mu\text{m}$  inner diameter, which allows an efficient mass transfer and chromatographic retention. The fact that some interactions between inorganic anions and the adsorbed EOF modifier are evident from our electropherograms suggests that further experiments with 10- $\mu\text{m}$  capillaries would be interesting. In this case, a careful choice of the carrier electrolyte will be necessary. Chromate will not necessarily be the best carrier

electrolyte, since it acts as a strong eluent in IC chromatography, thereby reducing the ion-exchange effects of the EOF modifier. Electrolytes acting as weak eluents in ion chromatography could be preferable.

The results presented in this paper indicate that the use of organic solvents in the carrier electrolyte is one of the most efficient ways to change the retention order and to optimize the separation selectivity, as long as capillaries with an inner diameter much larger than 10  $\mu\text{m}$  are used. This concept has been found useful for the analysis of anions in samples containing small amounts of iodide in the presence of a large excess of sulphate. Under standard conditions, the large sulphate peak makes the accurate evaluation of the iodide peak area difficult. Organic solvents such as ethylene glycol can improve the resolution of these two peaks dramatically. Details of these applications will be reported in another paper.

#### REFERENCES

- 1 J. Romano, P. Jandik, W. R. Jones and P. E. Jackson, *J. Chromatogr.*, 546 (1991) 411.
- 2 P. Jandik and W. R. Jones, *J. Chromatogr.*, 546 (1991) 431.
- 3 W. R. Jones and P. Jandik, *J. Chromatogr.*, 546 (1991) 445.
- 4 X. Huang, J. A. Luckey, M. J. Gordon and R. N. Zare, *Anal. Chem.*, 61 (1989) 766.
- 5 K. D. Altria and C. F. Simpson, *Anal. Proc.*, 23 (1986) 453.
- 6 K. D. Altria and C. F. Simpson, *Chromatographia*, 24 (1987) 527.
- 7 W. D. Pfeffer and E. S. Yeung, *J. Chromatogr.*, 557 (1991) 125.

# Optimization of selectivity in capillary zone electrophoresis via dynamic pH gradient and dynamic flow gradient

Huan-Tsung Chang and Edward S. Yeung

Ames Laboratory—US Department of Energy and Department of Chemistry, Iowa State University, Ames, IA 50011 (USA)

---

## ABSTRACT

Two different techniques, dynamic pH gradient and electroosmotic flow gradient, were introduced to control selectivity in capillary zone electrophoresis. These two types of gradients showed dramatic effects on the resolution of organic acids. Dynamic pH gradient from pH 3.0 to 5.2 is readily generated by a high-performance liquid chromatography gradient pump. Electroosmotic flow gradient is produced by changing the reservoirs containing different concentrations of cetylammmonium bromide for injection and running. The two gradient techniques are applied to the separation of model anions which are not resolved at constant pH or at constant flow conditions.

---

## INTRODUCTION

Capillary zone electrophoresis (CZE) has played an important role in separation science because of its high efficiency [1–3]. In CZE, the separation performance depends on the electrophoretic mobilities of the analytes and the electroosmotic flow when high voltage is applied. Conventionally, the same electrolyte is used in the capillary tube, the inlet reservoir and the outlet reservoir. In such cases, it is often difficult or impossible to separate a broad range of analytes which have very similar electrophoretic mobilities. Many approaches have been reported to improve the resolution in CZE. Control of the factors governing the electrophoretic mobilities of analytes and the electroosmotic flow are typically used to improve the separation resolution in CZE.

In principle and in practice, changing the pH of the buffer electrolyte seems to be the easiest way to control the electrophoretic mobilities of analytes.

For the separation of ionic species such as weak acids or bases, the selection of pH near their dissociation constants ( $pK_a$  or  $pK_b$ ) can generally provide good results. For complex mixtures, however, complete separation may not be possible at any one pH since the components may span a large range of pK values. In such cases, the use of a pH gradient can be advantageous. So far, several approaches for generating pH gradients in CZE have been reported. Boček and co-workers [4,5] used a three-pole, two-buffer system to force the migration of varying ratios of two ions into the capillary during separation. Šustáček *et al.* [6] dynamically modified the pH of the electrolyte at the inlet of the capillary by a steady addition of a modifying electrolyte. A step change in pH can also be used by switching the buffer electrolyte at the column inlet, with  $[H^+]$  controlled either directly [7] or by the use of different co-ions [8]. It is also possible to simply introduce a transient pulse of electrolyte at a different pH to enhance separation [9].

There are some subtle considerations relevant to the implementation of a pH gradient. It is necessary for the changing pH zone to actually interact with the analytes.  $H^+$  (and  $OH^-$ ) is a special case be-

---

Correspondence to: Dr. E. S. Yeung, Ames Laboratory—US Department of Energy and Department of Chemistry, Iowa State University, Ames, IA 50011, USA.



cause of its very high electrophoretic mobility, allowing it to overtake any positively charged analyte within a reasonable distance into the column, even with a high electroosmotic flow-rate. Still, to guarantee that the final pH of the buffer at the inlet end actually contributes to the selectivity, the pH change must be completed well before the elution of the components that are to be manipulated. Direct control of  $[H^+]$  is practical only at low pH, where the concentration is high enough to overcome other ionic equilibria. Even for unbuffered electrolytes [4,5], dissolved  $CO_2$ , surface silanol groups, and most importantly the analyte, will have to be titrated to alter the mobilities significantly even at neutral pH conditions. To overcome this problem, co-ions have been utilized [8], such as the carbonate–oxalate system. Since the co-ions are at much higher concentrations, the pH is easily altered. Naturally, the co-ions must migrate past the analyte ions to produce any effect. So far, only a step gradient has been generated, although one should be able to alter the ratio of the co-ions to generate a continuous gradient.

To guarantee that each analyte species actually experiences the pH step or gradient, a pH gradient derived from temperature changes has been reported [10]. It is also possible to introduce the pH change from the exit (detector) end of the capillary [11]. Regardless of the signs of the electrophoretic mobilities and the electroosmotic flow coefficient, the net travel of the analytes is then opposite in direction to that of the pH front. One can therefore influence the migration of the early eluting components as well as the late-eluting components. So far, only a step change in an unbuffered system has been demonstrated [11]. To provide accurate and reproducible changes over a wide range of pH, it is best to use a polybasic acid (or base) rather than a monobasic acid (or base) for the buffer electrolyte. The pH of a solution of an acid can be controlled by changing the concentration of a counter ion (e.g.  $Na^+$ ) for a fixed analytical concentration  $[A]_0$  of the acid, *i.e.* the fraction ionized. For a monobasic acid the ratio goes from 0 to 1 with the two extremes providing unbuffered conditions. It is also difficult to introduce very low concentrations of any counter ion since trace contaminants can dominate the equilibria. For polybasic ( $H_nA$ ) acids in between  $pK$  val-

ues *e.g.*  $pK_1 < pH < pK_2$ , the ratio goes from 1 to  $n - 1$  and external control is easy over a wide, well-buffered range. The direction of the pH change is also important. For a change from high to low pH, one can introduce  $H^+$  and decrease the counter ion concentration and expect the front to catch up with the analytes. For a change from low to high pH, one must increase the counter ion concentration and decrease  $H^+$  in the column. The mobility of the counter ion rather than the mobility of  $H^+$  becomes important in establishing the gradient. This further restricts the magnitudes and directions of the electrophoretic mobilities and the electroosmotic flow coefficient if the gradient is generated at the inlet end of the capillary. No such restrictions exist if the pH change is introduced from the outlet end, provided there is a net flow of the counter ion into the capillary.

The factors controlling electroosmotic flow, which is governed by the  $\zeta$  potential on the inner wall of the capillary, include the nature, concentration and pH of the background electrolyte, origin of the capillary and the applied voltage. Adding surfactant [12,13] to the background electrolyte is one simple way to enhance selectivity in CZE since the surfactant can effectively suppress or change the direction of the electroosmotic flow. Organic solvents [14] such as methanol, which can be used to change electroosmotic flow, are also useful to enhance the separation resolution. External electric field [15], which can change the direction and the rate of electroosmotic flow by external voltage, is another approach to improve the separation ability in CZE. Coating the inner walls of the capillary with silylated organic compounds [16] and adding salts [17] like NaCl are other options to affect the separation resolution. Field-amplified CZE [18,19], where two different concentrations of buffer electrolytes are used for injection and running, is another powerful method to control the electroosmotic flow.

In this paper, two methods, altering the electrophoretic mobilities of anions by using a dynamic pH gradient and changing the electroosmotic flow-rate by running CZE in two different concentrations of cetylammmonium bromide (CTAB), were described to demonstrate their utility in the separation of organic weak acids at acidic conditions.

## EXPERIMENTAL

A commercial electrophoresis instrument (Model 3850 Isco; Lincoln, NE, USA) was used for all electrophoretic experiments. High voltages applied in the experiment of dynamic pH gradient and dynamic flow gradient were 10 and 12 kV, respectively. The wavelength was set at 218 nm to detect anions and minimize the background absorption. The fused-silica capillary (Polymicro Technologies, Phoenix, AZ, USA) was 60 cm  $\times$  75  $\mu$ m I.D. At 40 cm from the injection end the polyimide coating was burned off to form the detection window. An integrator (SP Model 4600; Spectra-Physics, San Jose, CA, USA) was used to record all of the data. A high-performance liquid chromatographic (HPLC) gradient pump (two 2150 HPLC pumps and a 2152 HPLC controller; LKB, Gaithersburg, MD, USA) was used to introduce the dynamic pH gradient. The setup is shown in Fig. 1. Coupling is accomplished through a PTFE tube (1.6 mm I.D.  $\times$  3.0 mm O.D.) with the buffer at the exit end of the capillary constantly modified by the HPLC pump.

All chemicals were of reagent grade and were obtained from Aldrich (Milwaukee, WI, USA), except that phosphoric acid, sodium phosphate and sodium hydroxide were from Fisher (Fair Lawn, NJ, USA). Buffer solutions of phosphate were prepared from  $\text{NaH}_2\text{PO}_4$  by adding NaOH or  $\text{H}_3\text{PO}_4$  to adjust its pH to 5.2, or 4.1 and 3.0, respectively. Acetate buffer solution (pH 6.5) was made by adding NaOH to acetic acid. CTAB was added to buffer

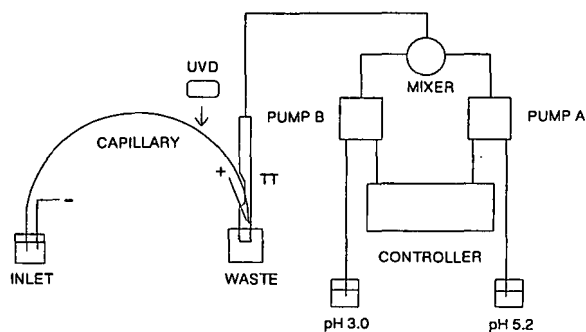


Fig. 1. Schematic of the electrophoresis equipment for generating a dynamic pH gradient. UVD = Ultraviolet detector; TT = PTFE tube, in which a small groove was cut in the middle to insert the electrode and the capillary.

solutions to suppress electroosmotic flow.  $\alpha$ -Naphthol (a neutral molecule at these pH values) was used to measure the electroosmotic flow. The sample solutions were injected hydrostatically. The buffer vial at the cathodic end of the capillary was raised to 20 cm high for 4 s to introduce samples into the capillary tube.

The capillary was equilibrated for 20 min between each run. Before injecting sample solutions, the capillary was flushed with 0.05 ml of 0.01 M NaOH solution, then 0.5 ml of buffer solution to improve reproducibility. A step change in CTAB was created by injecting sample solutions into the capillary containing a low concentration of CTAB, then running with buffer electrolyte containing a high concentration of CTAB at the exit (anodic) end. The capillary was treated as above before each run.

## RESULTS AND DISCUSSION

In CZE, the resolution between a pair of adjacent analytes can be calculated from the following equation [20]:

$$R = 0.177 (m_{\text{eff}1} - m_{\text{eff}2}) [V/D (m_{\text{av}} + m_{\text{eo}})]^{1/2} \quad (1)$$

where  $R$  is the resolution,  $V$  is the applied voltage,  $D$  is the diffusion coefficient,  $m_{\text{av}}$  is the average mobility of the two analytes and  $m_{\text{eff}1}$ ,  $m_{\text{eff}2}$  and  $m_{\text{eo}}$  are the effective mobilities of the two analytes and the electroosmotic flow coefficient, respectively. As eqn. 1 shows, the resolution can be enhanced by increasing the difference between the effective electrophoretic mobilities of the analytes and (or) decreasing the sum of electroosmotic flow and the average electrophoretic mobilities of two analytes.

#### Control of effective electrophoretic mobilities with dynamic pH gradient

Effective electrophoretic mobilities of ions are proportional to the fraction of free ions according to the Tiselius equation (see ref. 21):

$$m_{\text{eff}} = \sum a_i m_i \quad (2)$$

where  $a_i$  is the degree of dissociation and  $m_i$  is the absolute mobility of the  $i$ th ionic form of a molecule. The degree of dissociation again can be calculated from the following equations:

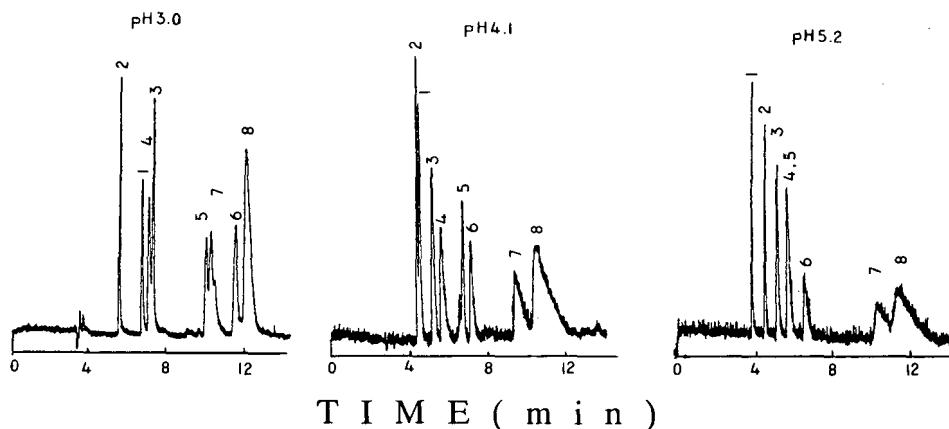


Fig. 2. Effect of change in pH on the migration rates of different anions. Capillary, 60 cm total length (40 cm to detector)  $\times$  75  $\mu$ m I.D.; applied voltage, 10 kV; wavelength, 218 nm; CTAB concentration, 0.35 mM; phosphate concentration, 10 mM; concentration of other anions, 0.2 mM. Peaks: 1 = citraconate; 2 = maleate; 3 = fumarate; 4 = *o*-nitrobenzoate; 5 = *o*-toluate; 6 = benzoate; 7 = *m*-nitrobenzoate; 8 = *m*-toluate.

For divalent anions:

$$a_1 = K_{a1} [H^+] / ([H^+]^2 + K_{a1} [H^+] + K_{a1} K_{a2}) \quad (3)$$

$$a_2 = K_{a1} K_{a2} / ([H^+]^2 + K_{a1} [H^+] + K_{a1} K_{a2}) \quad (4)$$

For monovalent anions:

$$a = K_a / ([H^+] + K_a) \quad (5)$$

where  $K_{ai}$  is the  $i$ th dissociation constant of the acid.

The amount of negative charge on the inner wall of the capillary and the analyte ions should be a function of pH of the buffer electrolyte as indicated by eqns. 3-5. For a bare silica column at these pH, electroosmotic flow is generally towards the cathode (injection end). For separation of these anions by migration towards the anode, we need to reverse the electroosmotic flow by adding a cationic surfactant, CTAB. At 0.35 mM CTAB, the amount of the positive charge on the inner wall of the capillary caused by the adsorption of CTAB increases as pH decreases since the degree of dissociation of the SiOH groups decreases as pH decreases. That is, electroosmotic flow toward the anodic direction increases when pH decreases. Our results show that  $m_{eo} = -3.15 \cdot 10^{-4}$ ,  $-1.8 \cdot 10^{-4}$  and  $-1.31 \cdot 10^{-4}$   $\text{cm}^2 \text{V}^{-1} \text{s}^{-1}$  at pH 3.0, 4.1 and 5.2, respectively. The experiments here thus take advantage of the combined results of the changes in electrophoretic mobilities and in electroosmotic flow. However, since  $m_{eo}$  is negative (same direction as  $m_{eff}$ ), the

numerator in eqn. 1 dominates in determining the resolution. We note that  $m_{eo}$  is smaller than  $m_{eff}$  for  $\text{Na}^+$  ( $= 5.0 \cdot 10^{-4} \text{cm}^2 \text{V}^{-1} \text{s}^{-1}$ ) so that the pH change can be introduced from the outlet end.

Fig. 2 shows the separation of the model anions at pH 3.0, 4.1 and 5.2. The calculated electrophoretic mobilities are listed in Table I. The separations of *o*-nitrobenzoate from fumarate, and *o*-toluate from *m*-nitrobenzoate are impossible at pH 3.0. At pH 4.1, there is overlap between the peaks of citraconate

TABLE I  
OBSERVED ELECTROPHORETIC MOBILITIES ( $m_{ep}$ ) OF ANIONS

Electroosmotic flow coefficient ( $m_{eo}$ ;  $\times 10^{-4} \text{cm}^2 \text{V}^{-1} \text{s}^{-1}$ ) is negative as electroosmotic flow is toward the anode.  $m_{eo} = -3.15$  at pH 3.0,  $-1.80$  at pH 4.1 and  $-1.31$  at pH 5.2. [Anions] = 0.2 mM.

Anions	$-m_{ep} (\times 10^{-4} \text{cm}^2 \text{V}^{-1} \text{s}^{-1})$		
	pH 3.0	pH 4.1	pH 5.2
Citraconate	3.1	7.0	8.2
Maleate	4.1	7.1	7.4
Fumarate	2.7	5.7	6.0
<i>o</i> -Nitrobenzoate	2.8	5.0	5.3
<i>o</i> -Toluate	0.8	4.1	5.3
Benzoate	0.3	3.6	4.4
<i>m</i> -Nitrobenzoate	0.7	2.3	2.4
<i>m</i> -Toluate	0.1	1.9	2.3

onate and maleate. Serious tailing on the late eluting peaks and the separation of *o*-toluate from *o*-nitrobenzoate are problems at pH 5.2. It is worth noting that the electrophoretic mobilities of *m*-isomers are lower than those of *o*-isomers. A likely reason is steric effects in the *o*-isomers which decrease the interaction between the anions and CTAB. The tailing problem is more serious for later eluting peaks at higher pH. Two factors that contribute to this are the stronger interaction between anions and CTAB due to increased dissociations of anions at higher pH and the larger difference of mobilities between the buffer ions and the anions at higher pH [22,23]. Based on literature values [24,25] of dissociation constants and mobilities we have calculated the effective mobilities of this set of anions at these pH. The trends are comparable to those in Table I but the absolute magnitudes are different. In all cases except for fumarate, the calculated values are larger than the experimental values. We note that the literature values are for systems at infinite dilution and for 20 or 25°C. Differences are expected in the presence of the buffer ions and CTAB. Further, since our column temperature is higher than ambient during electrophoresis, the viscosity of water decreases and the effective mobilities should be higher as observed.

As Fig. 2 shows, it is impossible to separate all of the model anions with an isocratic buffer electrolyte. The problem can be overcome by introducing a

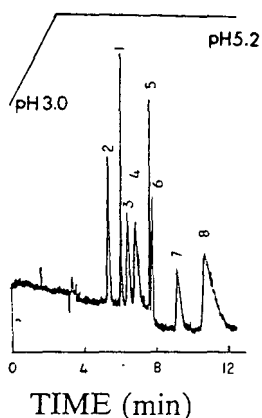


Fig. 3. Influence of a pH gradient on the separation of organic anions. Conditions as in Fig. 2 except a pH gradient is introduced through the outlet end of the capillary as indicated by the top plot in this figure.

TABLE II

ELECTROOSMOTIC FLOW COEFFICIENT ( $m_{eo}$ ) AT DIFFERENT CONCENTRATIONS OF CTAB

$m_{eo}$  is negative for electroosmotic flow toward the anode.

[CTAB] ( $\mu M$ )	$m_{eo}$ ( $\times 10^{-4} \text{ cm}^2 \text{ V}^{-1} \text{ s}^{-1}$ )
4.0	5.7
6.0	2.9
10.0	0.4
14.0	0.03
40.0	-0.8

dynamic pH gradient from pH 3.0 to 5.2 as Fig. 3 shows. The resolution was enhanced, the separation took less than 11 min, and the tailing problem was also reduced by this method. Even though the gradient starts immediately after injection, the components do not meet the moving front until they migrate further down the column. However, every component is guaranteed to meet the moving front in this mode of operation.

#### Control of the electroosmotic flow by step change in CTAB

To reduce the problem of tailing caused by the difference of mobilities between the buffer ion and the model anions, acetate buffer was used instead of phosphate buffer. The use of pH 6.5 was based on the following two reasons. First, to minimize the effect of variations in pH on electrophoretic mobilities the pH of the buffer solution is chosen to be much higher than most of the  $pK_a$ . Second, the effect of the surfactant on the electroosmotic flow is larger at higher pH since the dissociation of SiOH on the inner wall of capillary increases as pH increases.

Table II shows that CTAB not only can suppress electroosmotic flow, it can also change its direction at higher concentrations of CTAB, consistent with published reports [12,13]. Table III shows that the electrophoretic mobilities of the model anions are almost constant when the concentration of CTAB changes. Slight variations on electrophoretic mobilities of the anions may be due to the formation of an ion-pair between the anions and CTAB at higher concentration of CTAB. This is evident for the larger anions, naphtholate and coumarate. So, the

TABLE III  
ELECTROPHORETIC MOBILITIES ( $m_{ep}$ ) OF ANIONS AT DIFFERENT CONCENTRATIONS OF CTAB

[Anion] = 0.2 mM, except [pyruvate] = 0.5 mM and [ $\alpha$ -naphtholate] = 50  $\mu$ M.

Anion	$-m_{ep}$ ( $\times 10^{-4}$ cm <sup>2</sup> V <sup>-1</sup> s <sup>-1</sup> )			
	6 $\mu$ M CTAB	10 $\mu$ M CTAB	14 $\mu$ M CTAB	40 $\mu$ M CTAB
Citraconate	7.6	7.4	7.4	7.4
Maleate	7.0	6.8	6.7	6.9
Phthalate	7.0	6.8	6.7	6.8
Pyruvate	6.2	6.1	5.8	5.9
<i>o</i> -Nitrobenzoate	5.3	5.1	5.0	4.9
Benzoate	5.1	4.9	4.8	4.8
$\alpha$ -Naphtholate	4.8	4.3	4.2	3.6
Coumarate	4.7	4.3	4.0	4.1

dominant term in eqn. 1 is the denominator when the CTAB concentration is varied. Fig. 4 shows all anions except phthalate and maleate can be separated in less than 18 min at 6  $\mu$ M CTAB buffer electrolyte. As the CTAB concentration increased to 10

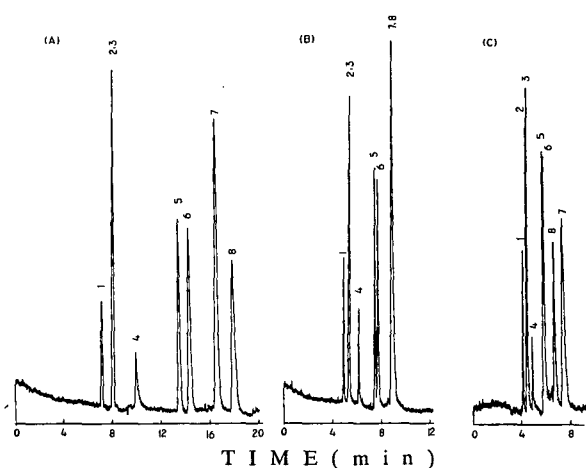


Fig. 4. Effect of changes in concentration of CTAB on the migration rates of different organic anions. CTAB concentration: (A) 6  $\mu$ M, (B) 10  $\mu$ M, (C) 40  $\mu$ M; capillary, 60 cm total length (40 cm to detector)  $\times$  75  $\mu$ m I.D.; applied voltage, 12 kV; wavelength, 218 nm; acetate concentration, 5 mM; concentration of other anions, 0.2 mM except pyruvate concentration, 0.5 mM and  $\alpha$ -naphtholate concentration, 50  $\mu$ M. Peaks: 1 = citraconate; 2 = maleate; 3 = phthalate; 4 = pyruvate; 5 = *o*-nitrobenzoate; 6 = benzoate; 7 =  $\alpha$ -naphtholate; 8 = coumarate.

$\mu$ M,  $\alpha$ -naphtholate and coumarate cannot be separated and there is little separation between the peaks of phthalate and maleate. The resolution between *o*-nitrobenzoate and benzoate decreases dramatically as the CTAB concentration changed to 40  $\mu$ M where electroosmotic flow is in the same direction as the electrophoretic mobilities of anions. The increase in  $m_{ep} + m_{co}$  results in the poor resolution of these two anions because the difference between their electrophoretic mobilities is very small. However, the resolution between coumarate and  $\alpha$ -naphtholate increases and the elution order changes. This may have resulted from the complexation of CTAB with  $\alpha$ -naphtholate and with coumarate. So, Fig. 4 shows it is impossible to separate all the model anions under isocratic condition.

Helmer and Chien [18] mentioned that the relationship between the bulk velocity,  $m_b$ , and the local electroosmotic velocity,  $m_l$ , in the two buffer regions can be expressed by the following equation:

$$m_b = x m_{l1} + (1 - x) m_{l2} \quad (6)$$

where  $x$  is the fraction of length filled with buffer 1 and  $m_{l1}$  and  $m_{l2}$  are the local electroosmotic flow rates when buffer 1 and 2 are used individually, respectively. This means that if we create a step change of two buffers containing different concentrations of CTAB it is possible to monotonically change the electroosmotic flow. Fig. 5 shows a computer simulation of the electroosmotic flow rate resulting from a step change in CTAB concentration, in agreement with the above discussion. The change is indeed monotonic, but not linear. The rate of change can be controlled by the magnitude of the buffer step. It is interesting to note that the electroosmotic flow can never be reversed in this mode. It is also irrelevant which direction the analytes are moving relative to the flow, since there is only one flow-rate to consider [18]. All analytes experience the same flow gradient regardless of where the front is. Fig. 6 shows the effect on the enhancement of the separation of model anions by a step change in the concentration of CTAB. Comparing the results of Fig. 6A and B, it is obvious that the bulk electroosmotic flow gradient can be controlled by stepping to different concentrations of CTAB. Improvements in resolution and reduction in separation time are simultaneously achieved by the method of step change in CTAB concentration.

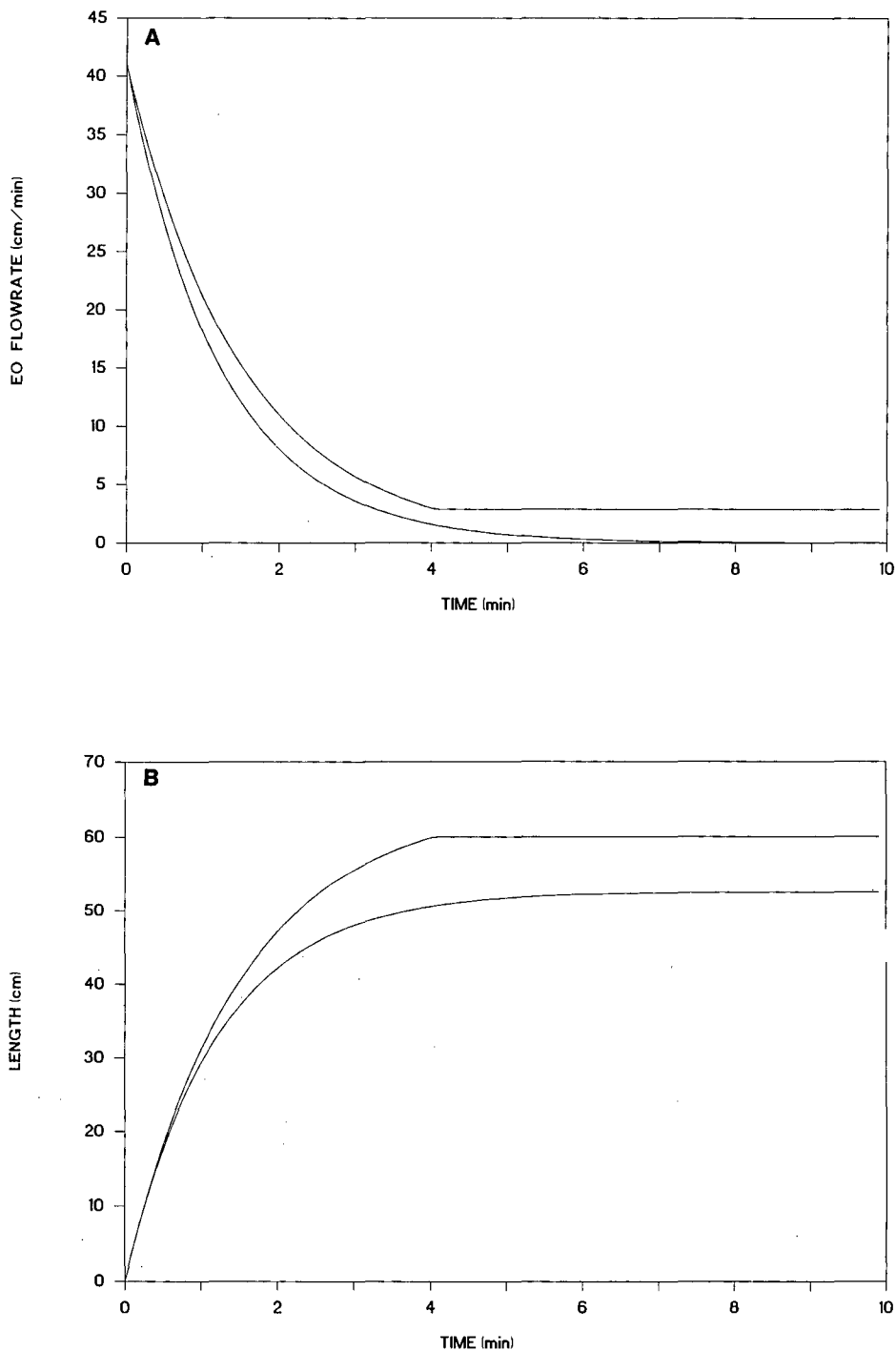


Fig. 5. Computer simulation of electroosmotic flow gradient for a step change in CTAB concentration. The data in Table II were used. Initial CTAB concentration is  $4 \mu M$ ; final CTAB concentration is  $10 \mu M$  for top trace and  $40 \mu M$  for bottom trace. (A) Flow-rate as a function of time; (B) location of moving boundary from the exit end of a 60-cm capillary as a function of time. Applied voltage, 12 kV; column length, 60 cm (40 cm to detector).

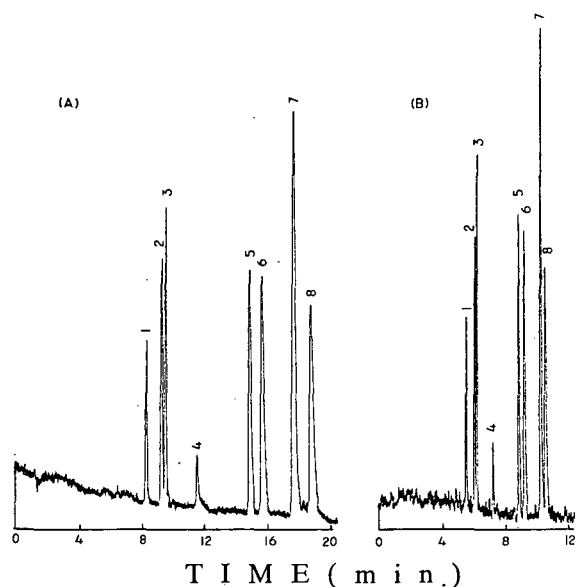


Fig. 6. Influence of a step change in CTAB concentration on the separation of organic anions. Before injection, the concentration of CTAB is  $4 \mu\text{M}$  while the running concentrations are  $10 \mu\text{M}$  (A) and  $40 \mu\text{M}$  (B). Conditions as in Fig. 4.

The control of electroosmotic flow rate and electrophoretic mobilities of analytes are important to improve the resolution and reduce the separation time in CZE. Many approaches have already been used to control the electroosmotic mobilities of analytes in order to enhance the separation resolution. In this work, we demonstrated the effect of a dynamic gradient in pH on the effective electrophoretic mobilities of several model anions by introducing the change at the outlet end of the capillary. Altering the electroosmotic flow is another known method for increasing the resolution. In this paper, a simple gradient approach, which is based on the combination of the effect of a surfactant on electroosmotic flow and the idea of field-amplified electroosmosis, is outlined. Eight organic acids are successfully separated by this method in less than 11 min.

#### ACKNOWLEDGEMENTS

Ames Laboratory is operated for the US Department of Energy by Iowa State University under contract No. W-7405-Eng-82. This work was supported by the Director of Energy Research, Office of Basic Energy Sciences and Office of Health and Environmental Research.

#### REFERENCES

- 1 J. W. Jorgenson and K. D. Lukacs, *Science (Washington D.C.)*, 222 (1983) 266.
- 2 R. A. Wallingford and A. G. Ewing, *Adv. Chromatogr.*, 29 (1989) 1.
- 3 W. G. Kuhr, *Anal. Chem.*, 62 (1990) 403R.
- 4 P. Boček, M. Deml, J. Pospichal and J. Sudor, *J. Chromatogr.*, 470 (1989) 309.
- 5 J. Pospichal, M. Deml, P. Gebauer and P. Boček, *J. Chromatogr.*, 470 (1989) 43.
- 6 V. Šustáček, F. Foret and P. Boček, *J. Chromatogr.*, 480 (1989) 271.
- 7 F. Foret, S. Fanali and P. Boček, *J. Chromatogr.*, 516 (1990) 219.
- 8 J. Sudor, J. Pospichal, M. Deml and P. Boček, *J. Chromatogr.*, 545 (1991) 331.
- 9 P. Boček, M. Deml and J. Pospichal, *J. Chromatogr.*, 500 (1990) 673.
- 10 C. W. Whang and E. S. Yeung, *Anal. Chem.*, 64 (1992) 502.
- 11 J. Sudor, Z. Stránský, J. Pospichal, M. Deml and P. Boček, *Electrophoresis*, 10 (1989) 802.
- 12 T. Kaneta, S. Tanaka and H. Yoshida, *J. Chromatogr.*, 538 (1991) 385.
- 13 X. Huang, J. A. Luckey, M. J. Gordon and R. N. Zare, *Anal. Chem.*, 61 (1989) 766.
- 14 C. Schwer and E. Kenndler, *Anal. Chem.*, 63 (1991) 1801.
- 15 C. S. Lee, D. McManigill, C. T. Wu and B. Patel, *Anal. Chem.*, 63 (1991) 1519.
- 16 W. G. Kuhr and E. S. Yeung, *Anal. Chem.*, 60 (1988) 2642.
- 17 S. Fujiwara and S. Honda, *Anal. Chem.*, 58 (1986) 1811.
- 18 J. C. Helmer and R. L. Chien, *Anal. Chem.*, 63 (1991) 1354.
- 19 J. I. Ohms and X. Huang, *J. Chromatogr.*, 516 (1990) 233.
- 20 J. W. Jorgenson and K. D. Lukacs, *Anal. Chem.*, 53 (1981) 1298.
- 21 F. M. Everaerts, J. L. Beckers and Th. P. E. M. Verheggen, *Isotachopheresis—Theory, Instrumentation and Applications*, Elsevier, Amsterdam, New York, 1976, pp. 27-40.
- 22 G. D. Roberts, P. H. Rhodes and R. S. Snyder, *J. Chromatogr.*, 480 (1989) 35.
- 23 S. Hjertén, *Electrophoresis*, 11 (1990) 665.
- 24 M. J. Astle, W. H. Beyer and R. C. Weast (Editors), *CRC Handbook of Chemistry and Physics*, CRC Press, FL, 56th ed., 1984, pp. D165-166.
- 25 T. Hirokawa, M. Nishino, N. Aoki, Y. Kiso, Y. Sawamoto, T. Yagi and J. Akiyama, *J. Chromatogr.*, 271 (1983) D1.

# Laser fluorescence detector for capillary electrophoresis

Edward S. Yeung

*Department of Chemistry and Ames Laboratory—US Department of Energy, Iowa State University, Ames, IA 50011 (USA)*

Poguang Wang, Wenni Li<sup>☆</sup> and Roger W. Giese

*Department of Pharmaceutical Sciences, College of Pharmacy and Allied Health Professions, and Barnett Institute of Chemical Analysis and Materials Science, Northeastern University, Boston, MA 02115 (USA)*

---

## ABSTRACT

A simple, rugged, and relatively inexpensive laser-based fluorometer for detection in capillary electrophoresis is described. This is assembled from commercially available components and requires minimal experience for operation. Yet, the detection performance is comparable to those achieved in laser laboratories with sophisticated layouts. As an example, detection of a 3 pM solution of fluorescein is demonstrated. The design principles of laser fluorometric detection are critically examined, and the special adaptation for the present detection arrangement is discussed.

---

## INTRODUCTION

Laser-induced fluorescence (LIF) detection has shown tremendous promise for applications in capillary electrophoresis (CE) [1–4]. Its acceptance naturally depends on having simple, inexpensive and reliable instrumentation for the routine user. Most laboratory systems are mounted on optical tables in partially darkened rooms for flexibility and ready access to the individual components. Certain optimization steps are also easier to perform in an open system. The need remains for a compact instrument that can be interfaced to any CE setup and which can provide close to state-of-the-art detection performance.

The requirements for good performance in fluorescence detection are (i) a stable light source, since

it is the fluctuations in the residual background signal that determine the limit of detection (LOD); (ii) a rugged but adjustable mounting technique for the capillary column, since mechanical movements lead to misalignment and flicker noise; (iii) low stray light levels, which include room light plus scattering and fluorescence from the capillary walls.

In this paper we describe a compact laser fluorometer for CE that achieves high performance. It can be assembled from commercially available components with a minimum of additional engineering. The design addresses the main requirements outlined above. Operation and alignment are simplified to allow use by non-experts. The major part of the cost of the system is the laser source, which can range from several hundred dollars upwards.

## EXPERIMENTAL

### *Chemicals and reagents*

Trizma base [tris(hydroxymethyl)aminomethane, or Tris] was purchased from Sigma (St. Louis, MO, USA). Boric acid, HPLC-grade acetonitrile and 0.22- $\mu\text{m}$  MSI Cameo filters were from Fisher Scien-

---

*Correspondence to:* Dr. E. S. Yeung, Department of Chemistry and Ames Laboratory—US Department of Energy, Iowa State University, Ames, IA 50011, USA.

<sup>☆</sup> Present address: American Cyanamid Company, Agriculture Research Division, Princeton, NJ 08540, USA.



tific (Bedford, MA, USA). Fluorescein, water soluble, dye content *ca.* 70%, was obtained from Aldrich (Milwaukee, WI, USA). Buffer (pH 8.7) was prepared by combining 0.8 ml of stock buffer (0.5 M Tris, 0.5 M boric acid, stored at room temperature), 35 ml of water and 4 ml of acetonitrile, giving pH 8.7. This buffer (10 mM Tris–borate, 10% acetonitrile) was filtered (0.22  $\mu\text{m}$ ) and degassed (bubbling with helium for 15 min) prior to use as a diluent to prepare solutions for injection using polypropylene tubes and pipetting tips.

### Instrumentation

As depicted in Fig. 1, the device represents a simple and rugged design for LIF detection. It consists of 8 main components: a quartz 1-cm focal length lens (L), capillary holder (CH), 20 $\times$  microscope objective (MO), microscope objective holder (MOH), mirror (M) and mirror mount (MM), photomultiplier tube (PMT) with filter (F), Plexiglass box (PB) and 2 light shields (LS). The laser beam enters the otherwise light-tight box PB through a 3-mm hole. L is rigidly mounted to PB so that the focal point of the excitation beam is uniquely defined and used as the reference point for all the other components. The capillary with a small section of its coating removed is mounted on a two-dimen-

sional stage CH capable of 10  $\mu\text{m}$  resolution. Two short pieces of quartz capillary 350  $\mu\text{m}$  O.D.  $\times$  250  $\mu\text{m}$  I.D. glued to CH serve to guide the separation capillary through the optical region. This can hold the common 150  $\mu\text{m}$  O.D. capillary tubing. Alternatively, 350  $\mu\text{m}$  O.D. separation capillaries can be inserted directly into CH. The mounted capillary is at about 20° with respect to the incident laser beam to minimize scattering off the capillary walls. We find that this configuration is rigid enough with regard to noise from mechanical vibrations. With this design, capillary change can be accomplished in less than 5 min.

### Instrumental conditions

The photomultiplier was operated at 820 V and the laser at 5 mW. CE was performed in a fused-silica capillary (60 cm  $\times$  75  $\mu\text{m}$  I.D.  $\times$  145  $\mu\text{m}$  O.D.; PolyMicro Technologies, Phoenix, AZ, USA). The polyimide coating of the capillary was burned off to form a window 30 cm from the injection end (grounded anode end) of the capillary. The capillary was cleaned by vacuum siphoning the following sequence of solutions (5 drops each) over a 1.5 h period: (a) methanol–water (1:1, v/v); (b) 0.1 M NaOH; (c) methanol–water as before, and buffer. The data were collected at 20 Hz and processed by a Dynamax HPLC Manager utilizing software version 1.2 (Rainin, Woburn, MA, USA) interfaced to a Macintosh Classic computer.

### RESULTS AND DISCUSSION

#### Equipment

The choice of the laser naturally depends on the application on hand. The 488-nm line of the Ar ion laser however does have an overall edge as a general purpose light source. Many fluorescence derivatization procedures have already been worked out for blue-green excitation for important biological molecules. Most notable are fluorescein and rhodamine derivatives of amino acids and nucleotides, including commercial chemistry kits for DNA sequencing. A continuous wave laser is a better choice than a pulsed laser, because the former usually have superior intensity stability, can be focused to smaller spots, and are less likely to damage the capillary column for a given number of excitation photons. Diode lasers are the most rugged devices, but pres-

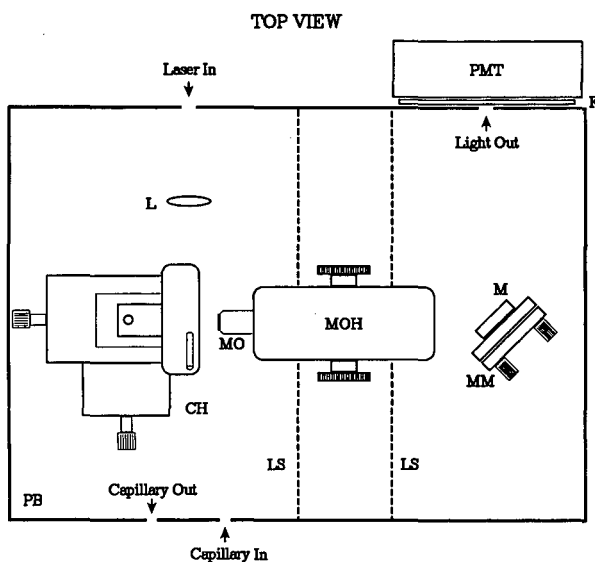


Fig. 1. Experimental arrangement for laser fluorometric detection. Abbreviations are explained in the text.

ently are only available at 670 nm or higher, where few fluorescent tagging schemes have been developed [5]. They also produce output that can be collimated to around 100  $\mu\text{m}$ , which is marginal for clean excitation in CE. The HeCd laser at either 442 nm or 325 nm is often used in the research laboratory because of the availability of good derivatization reagents. However, the HeCd laser tube has a significantly shorter lifetime and the output is sensitive to the temperature of the room, leading to larger intensity fluctuations. The UV lines of an argon ion laser and krypton ion laser lines are useful for exciting a broad range of chromophores, including protein native fluorescence [6] at 275 nm, but these systems are too large and too expensive for a routine instrument. Many commercial sources are available for small air-cooled Ar ion lasers with output of a few mW. We favor one with hard-sealed mirrors and a stable power supply, which is internally stabilized to  $\pm 0.1\%$ . The lack of tunability among the various visible Ar ion laser lines is not a serious limitation regarding the selection of fluorophores. On the other hand, mechanical and optical ruggedness is significantly improved. There is a less expensive source of 543 nm light, *viz.* the HeNe “green” laser. The intensity is less stable and the derivatization chemistry is less well established. With time, this may become a good alternative to the Ar ion laser.

For efficient excitation and reduced stray light, the laser beam should be focused tightly to pass through the center of the capillary tube. A simple biconvex lens with around 1 cm focal length can produce a beam waist of 5  $\mu\text{m}$ , which fits just about any capillary size commonly used. This lens can be mounted rigidly relative to the laser and never needs adjustment. To place the capillary column at exactly the laser beam waist, a holder with guides for the column is mounted on a microscope *x-y* stage. The latter is readily available and even the simplest models have sufficiently fine movement and minimal mechanical backlash. Translation is needed in line with the laser beam (focusing) and in a horizontal plane perpendicular to it (crossing). The capillary column with a liquid core is equivalent to a cylindrical lens. If the laser beam crosses that at exact center, its direction of propagation will not be altered. If the capillary column is placed symmetrically at the focal point of the lens, then the beam

shape and size at far field should not deviate from those with the capillary removed. These criteria can be used to initially align the excitation beam. The holder for the capillary column consists of clearances drilled out to fit the 350- $\mu\text{m}$  O.D. tubes, which are widely used in CE. With 1 cm or so between these clearances, the capillary column is held with almost no play. To replace columns, one simply threads the new one through the same clearances.

To collect fluorescence originating from the liquid core, a microscope objective is used. This need not be achromatic or of special flat-field design. For 50- $\mu\text{m}$  columns, a 10 $\times$  standard objective is adequate both in terms of magnification and numerical aperture. For columns 20  $\mu\text{m}$  or narrower, a 20 $\times$  objective can be used. This can be mounted on a commercial microscope focusing tube, without the eyepiece or its holder. That provides adequate movement for exact imaging of the fluorescence onto the spatial aperture. It is well known that specular reflections from the cylindrical tube can be a problem. This is confined to a plane perpendicular to the capillary tube. So, the capillary holder is designed to impose a 20° angle between this plane and the microscope objective. The region of the mount behind the capillary tube in direct view of the microscope objective is also cleared out to avoid reflections. The focusing tube can be set once and for all to coincide with the fixed beam waist of the laser beam to minimize alignment. For convenience, a mirror on a small integral mount is used to direct the collected fluorescence image onto the spatial aperture. Alignment is performed in a darkened room with a solution of 5  $\mu\text{M}$  fluorescein running through the capillary by pressure flow. It is essential to obtain a sharp image of the fluorescence, which appears as a line, so that reflections, scattering, and fluorescence from the capillary walls can be rejected by the aperture. With practice, one can look for the scattering centers corresponding to the entrance and exit of the laser beam at the column to define the fluorescence image, without the use of a dye stream.

To shield the optical system from room light, the entire set of components is enclosed in a black Plexiglass box. This also serves as protection against high voltage applied to the capillary tube. The cover of the box can be interlocked to the laser

power supply to allow operation as a Class I laser. The base of the Plexiglass box is extended for mounting the laser head and the phototube. The defocused laser beam after hitting the lens and the capillary column continues to the back wall of the box and is effectively stopped. Two cardboard light shield (LS in Fig. 1) basically divide the box into three compartments. This is extremely effective in eliminating stray light in the excitation region and the residual laser light not absorbed by the back wall. Two 1-mm holes are present in the plexiglass box to allow entrance and exit of the capillary column. These holes do not pass sufficient room light into the optical region to change the background level. The other two openings in the box are 3 mm and 5 mm for the laser input and the fluorescence output, respectively. At the inside of these openings, interference filters for the laser line and for the fluorescence wavelength are taped on to seal off almost all room light. The excitation filter is necessary also to eliminate plasma emission from the laser, which can be at the detection wavelength.

Almost any photomultiplier tube can be used to monitor the emission. A red-sensitive phototube is needed in this case. It is fairly straightforward to assemble this from an integral high-voltage power supply and a base with voltage divider. The output can be sent to a compact current-to-voltage converter (about  $10^6$  V/A) with switchable gain levels and time constants. The photomultiplier tube and all associated electronics can be placed inside a  $10 \times 15 \times 15$  cm metal box. It is important to also block room light from entering the phototube compartment. This can be accomplished by taping another emission filter onto the photomultiplier tube itself, exposing only a small region of the photocathode, combined with cardboard light shields inside the box. The opening to the photomultiplier tube can then be matched and sealed against the exit aperture of the optical isolation box. Typically, room light only results in a doubling of the dark-current output of the photomultiplier tube, so that maximum gain can be used in the detection electronics.

#### Fluorescein detection

Fluorescein standard solutions were prepared in buffer based on weight and assuming that the compound, as listed by the supplier, was 70% pure. Cal-

ibration curves were linear for both peak heights and areas (data not shown) from the lowest concentration injected ( $3.2 \cdot 10^{-12}$  M) up to at least  $10^{-8}$  M. For these curves, average values for duplicate injections were calculated, and the correlation coefficient was 0.999 in each case. This shows the high stability of the system. Shown in Fig. 2 is an electropherogram for the lowest concentration injected, in which the signal-to-noise ratio is about 3. The presence of acetonitrile in the running buffer contributed to band sharpness.

It can be difficult to compare different laser fluorescence detectors for capillary electrophoresis because several factors beyond the inherent performance of the detector can influence the detection limits that are reported: analyte tested, frontal (continuous) or plug injection of analyte, capillary dimensions, running buffer, type of injection technique (including any mechanism for analyte enrichment), condition of capillary tip, use of zone *vs.* a gel separation technique, how the signal-to-noise is calculated, whether the detection limit is observed or extrapolated, and whether a linear calibration curve is constructed. While there are some variables, it nevertheless appears that the sensitivity of our detector is comparable to what others have achieved for state-of-the-art laser fluorescence detection in a capillary electrophoresis system. For example, in terms of the concentration of the solution injected, Sweedler *et al.* [7] detected 6 pM fluorescein isothiocyanate (signal-to-noise ratio *ca.* 10), Zhang *et al.*

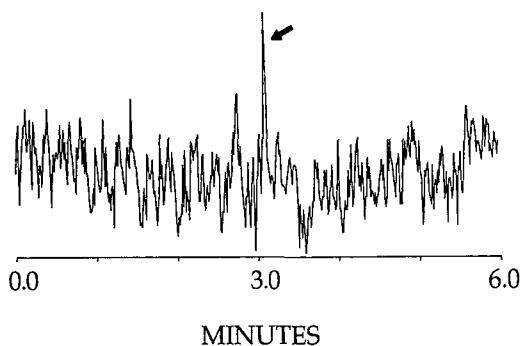


Fig. 2. Detection of  $3.2 \cdot 10^{-12}$  M fluorescein (concentration of solution injected) by capillary electrophoresis with laser fluorescence detection. Injection and running buffer: 10 mM Tris-borate, pH 8.7, 10% acetonitrile. Injection technique: hydrodynamic, with anode end 5 cm higher for 20 s. Applied voltage: 30 kV.

[8] reported a detection limit of 20 pM for a fluorescein labeled deoxynucleotide triphosphate and 5 pM for a fluorescein-labeled 100-mer oligonucleotide [8], and Cheng and Dovichi [9] reported that the detection limit for a fluorescein-arginine conjugate was less than 5 pM. For tetramethylrhodamine isothiocyanate, a related analyte, Chen *et al.* [10] reported a linear calibration curve down to 64 pM ( $r = 0.986$ ).

## CONCLUSIONS

We have outlined here the design and performance of a home-built laser-based fluorometric detector for CE that has state-of-the-art performance. Commercial detectors of this type have just appeared on the market, but the present system is more flexible and much less expensive. In contrast to a commercial design using optical fibers to deliver laser light to the capillary column, the present system offers better focusing properties and thus better rejection of stray light for working with small diameter capillaries. Light collection here is based on imaging and spatial filtering. This is similar to one commercial scheme which uses a fluorescence microscope, but is much easier to implement. The system here is also ready for UV excitation, *e.g.* at 275 nm [6], requiring only substitution of the optical filters.

## ACKNOWLEDGEMENTS

This work was funded by the Office of Health and Environmental Research Division, Department of Energy, as Grant DE-FG-02-90ER60964. Publication number 543 from the Barnett Institute. The Ames Laboratory is operated by Iowa State University for the US Department of Energy under contract No. W-7405-Eng-82. This work was supported by the Director of Energy Research, Office of Basic Energy Sciences and Office of Health and Environmental Research.

## REFERENCES

- 1 P. Gozel, E. Gassmann, H. Michelsen and R. N. Zare, *Anal. Chem.*, 59 (1987) 44.
- 2 C. A. Monnig and J. W. Jorgenson, *Anal. Chem.*, 63 (1991) 802.
- 3 E. S. Yeung and W. G. Kuhr, *Anal. Chem.*, 63 (1991) 275A.
- 4 H. Swerdlow, S. Wu, H. Harke and N. J. Dovichi, *J. Chromatogr.*, 516 (1990) 61.
- 5 G. Patonay and M. D. Antoine, *Anal. Chem.*, 63 (1991) 321A.
- 6 T. T. Lee and E. S. Yeung, *J. Chromatogr.*, 595 (1992) 319.
- 7 J. V. Sweedler, J. B. Shear, H. A. Fishman, R. N. Zare and R. H. Scheller, *Anal. Chem.*, 64 (1991) 496.
- 8 J. Z. Zhang, D. Y. Chen, S. Wu, H. R. Harke and N. J. Dovichi, *Clin. Chem.*, 37 (1991) 1492.
- 9 Y. F. Cheng and N. J. Dovichi, *Science (Washington, D.C.)*, 242 (1988) 562.
- 10 D. Y. Chen, H. P. Swerdlow, H. R. Harke, J. Z. Zhang and N. J. Dovichi, *J. Chromatogr.*, 559 (1991) 237.



# Dynamic light-scattering studies of hydroxyethyl cellulose solutions used as sieving media for electrophoretic separations

Paul D. Grossman, Toshiaki Hino and David S. Soane

*Department of Chemical Engineering, University of California at Berkeley, Berkeley, CA 94720 (USA)*

---

## ABSTRACT

Dynamic light-scattering experiments are performed on semi-dilute solutions of hydroxyethyl cellulose which have been shown to be suitable as molecular sieving media for electrophoretic separations in a capillary format. The multi-exponential data analysis program CONTIN is used to determine the various relaxation processes present. The relationship between polymer concentration,  $C$  (g/ml), and the mesh-size of the entangled network,  $\xi$ , is found to be  $\xi(\text{\AA}) = 6.0 C^{-0.68}$ , which is in good agreement with predictions based on the scaling theory of De Gennes and intrinsic viscosity measurements.

---

## INTRODUCTION

Recently it has been demonstrated that low-viscosity ( $< 2$  cP) semi-dilute polymer solutions can be used as molecular sieving media for electrophoretic separations performed in micro-capillary tubes [1–7]. These systems promise significant practical advantages over traditional rigid-gel electrophoresis media in that no gel preparation step is required. Furthermore, because of their low viscosity, these solutions are well suited for use in automated capillary electrophoresis instrumentation. In essence, the use of semi-dilute polymer solutions in a capillary electrophoresis format decouples the two roles of a traditional electrophoresis gel: that of an anti-convective support and of a molecular sieve.

In our previous report [3] the scaling theory of De Gennes [8] and traditional theories of electrophoretic migration were used to relate the properties of the mesh-forming polymer to the mesh size of the polymer network and to the resulting electrophoretic

ic migration behavior of a series of DNA restriction fragments. It was shown that the mesh size of the entangled polymer solution was similar to that of traditional agarose gels and that the migration mechanism of the DNA fragments was the same as that found in traditional rigid-gel matrices. Furthermore, a relationship was proposed which could be used to design optimal entangled polymer systems for different electrophoresis applications.

Since the first successful application of scaling theory to polymer solutions by De Gennes [8], dynamic light scattering (also known as photon correlation spectroscopy or quasielastic light scattering) has played an important role in the study of the dynamics of semi-dilute polymer solutions. Here we apply the technique of dynamic light scattering to measure the mesh size of the hydroxyethyl cellulose (HEC) solutions which were shown to be useful as sieving media in electrophoretic separations of DNA restriction fragments. In particular, we confirm the predictions for the mesh size based on scaling theory and intrinsic viscosity measurements for aqueous HEC solutions used in our previous electrophoresis study.

---

*Correspondence to:* Dr. P. D. Grossman, Applied Biosystems, Inc., 850 Lincoln Center Drive, Foster City, CA 94404, USA (present address).

## THEORY

*Physical basis*

Dynamic light-scattering measurements yield directly the mutual diffusion coefficient of a scattering species undergoing Brownian motion. The time dependence of the intensity fluctuations of the scattered light,  $I(t)$ , can be related to the transport properties of the scattering species.

A simple picture of a light-scattering photometer is given in Fig. 1. A monochromatic laser light is used to illuminate a region of the sample solution. The sample scatters light in all directions and a record of the intensity fluctuations of the light scattered through a small range of angles is collected using a photodetector. These intensity fluctuations are then related to the Brownian motion of the scattering species.

In the case of semi-dilute polymer solutions, light scattering is caused by fluctuations in the concentration of the sample polymer induced by its thermal motion within the illuminated volume. The relaxation rate of these concentration fluctuations can be determined using the scattered intensity autocorrelation function,  $G(2)(\tau)$ , where

$$G(2)(\tau) = \langle I(t)I(t + \tau) \rangle = \lim_{T \rightarrow \infty} \frac{1}{T} \int_0^T I(t)I(t + \tau) dt \quad (1)$$

where  $I(t)$  is the time dependent intensity of the scattered light,  $\tau$  is the delay time of the fluctuations,  $T$  is total time for the measurements and the angle brackets denote a statistical average. The relaxation rate of the intensity fluctuations,  $\Gamma$ , is calculated by fitting experimental data to a theoretical formulation of  $G(2)(\tau)$ .

The diffusive nature of the relaxation process responsible for the decay in  $G(2)(\tau)$  indicates that the scattered intensity autocorrelation function is characterized by an exponentially decaying function, with the time constant given by  $\Gamma^{-1}$ , where

$$\Gamma = D|q|^2 \quad (2)$$

where  $\Gamma$  is the relaxation rate of the process,  $D$  is the diffusion constant and  $q$  is the scattering vector. The scattering vector is a measure of the characteristic length associated with the diffusive fluctuations

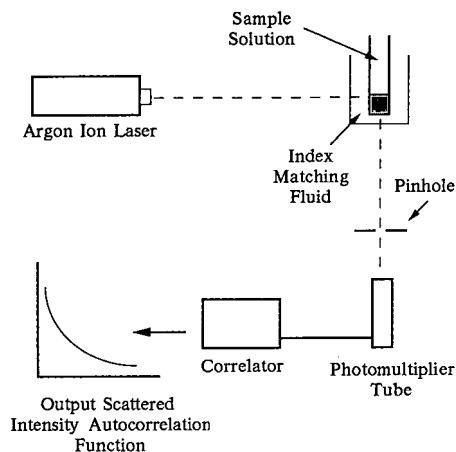


Fig. 1. Schematic diagram of light scattering apparatus.

which can be measured at a given scattering angle with a given incident radiation. The magnitude of  $q$  is given by the relation

$$q \cong \frac{4\pi n}{\lambda} \sin\left(\frac{\theta}{2}\right) \quad (3)$$

where  $\theta$  is the angle between the incident and scattered light,  $n$  is the refractive index of the scattering medium, and  $\lambda$  is the wavelength of the incident light *in vacuo*. Thus, knowing  $\Gamma$ , one can determine the value for  $D$ .

In the limit of infinite dilution, the self diffusion coefficient,  $D_0$ , of a spherical particle is given by the Stokes-Einstein relation as

$$D_0 = \frac{kT}{6\pi\eta R} \quad (4)$$

where  $k$  is Boltzmann's constant,  $T$  is the absolute temperature,  $\eta$  is the viscosity of the pure solvent and  $R$  is the particle radius. According to the scaling theory of De Gennes [8], in semi-dilute polymer solutions, the cooperative diffusion coefficient of the polymer,  $D_c$ , is given by

$$D_c = \frac{kT}{6\pi\eta\xi_d} \quad (5)$$

where  $\xi_d$  is the dynamic correlation length of the polymer, which can be interpreted as a measure of the mesh size of the polymer network. De Gennes

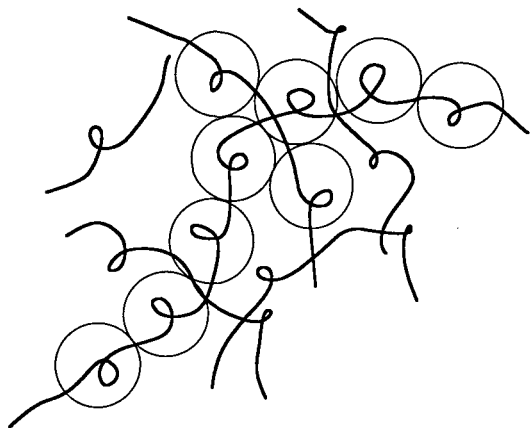


Fig. 2. Schematic illustration of a semi-dilute polymer solution according to the scaling theory of De Gennes [8].

theory assumes that semi-dilute polymer solutions can be modeled as a group of spherical polymer "blobs" having a characteristic size  $\xi_d$  whose motion is uncorrelated (see Fig. 2). Thus, given an experimentally measured value of  $\Gamma$ , in a semi-dilute solution, using eqns. 2 and 5, one can obtain an estimate of the value  $\xi_d$ . The value of  $\Gamma$  is calculated from the measured autocorrelation function of  $I(t)$ . This procedure will be discussed in the following section.

#### The autocorrelation function

In general, correlation functions provide a method for expressing the degree to which dynamic properties are correlated over time. As mentioned earlier, dynamic light-scattering experiments measure the intensity autocorrelation function through the recorded time dependent intensity of the scattered light,  $I(t)$ . However, because the dielectric constant fluctuations which are responsible for light scattering are proportional to the *electric field* of the scattered light rather than the *intensity*, it is necessary to know the relationship between the *scattered intensity* and the *scattered electric field* autocorrelation functions. (The structural information is contained in the behavior of the scattered electric field, but all we can measure directly is the scattered intensity.) The scattered electric field autocorrelation function,  $g(1)(\tau)$  is defined as

$$g(1)(\tau) = \langle E^*(t)E(t+\tau) \rangle = \lim_{T \rightarrow \infty} \frac{1}{T} \int_0^T E^*(t)E(t+\tau) d\tau \quad (6)$$

where  $E(t)$  is the time dependent electric field of the scattered light, and  $E^*(t)$  is the complex conjugate of  $E(t)$ .  $E(t)$  is related to the intensity of the scattered light by

$$I(t) = E^*(t)E(t) \quad (7)$$

For the case of semi-dilute polymer solutions, the relationship between  $G(2)(\tau)$  and  $g(1)(\tau)$  is given by the homodyne autocorrelation function [9], thus

$$G(2)(\tau) = B[1 + \beta|g(1)(\tau)|^2] \quad (8)$$

where  $B$  is the baseline and the pre-exponential factor  $\beta$  is an instrumental correction factor having a value between 0 and 1. A typical plot of the scattered electric field autocorrelation function is shown in Fig. 3.

The analysis of the measured autocorrelation function,  $G(2)(\tau)$ , is a critical step in a dynamic light-scattering experiment. In the simplest case, that of a monodisperse suspension of nearly spherical particles, *e.g.* polystyrene latex spheres, the autocorrelation function can be fitted to a single exponential function. In this case,

$$g(1)(\tau) = A \exp(-\Gamma\tau) + B \quad (9)$$

where  $A$  is the spectral amplitude and  $B$  is the baseline.

In the case of semi-dilute polymer solutions, a number of relaxation processes occur simultaneously, and a single exponential approach is not satisfactory. These processes include center-of-mass motion of a single chain, center-of-mass motion of groups of chains and changes in the conformation of individual chains. Therefore, one is forced to use a multi-exponential approach to resolve the different relaxation modes present. In this study we will use the CONTIN method [10,11]. CONTIN fits the electric field autocorrelation function to a series of exponential functions,

$$g(1)(\tau) = \int_{j=1}^{N_j} G(\Gamma_j) \exp(-\Gamma_j\tau) + 1 \quad (10)$$



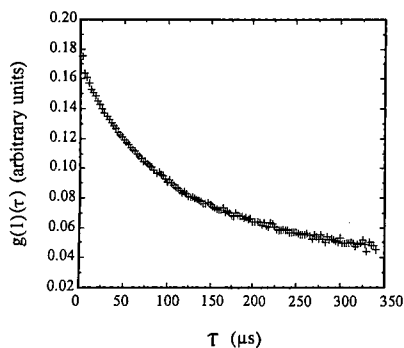


Fig. 3. Representative plot of the scattered electric field auto-correlation function,  $g(1)(\tau)$ . Data are from a solution of 0.006 g/ml HEC in TBE buffer at 30°C. The scattering angle is 90°.

where  $G(\Gamma)$  is the normalized rate distribution, 1 is a constant and  $N_j$  is the number of exponentials used in the sum. Note that if  $N_j = 1$ , eqn. 10 reduces to eqn. 9. In this study 31 exponentials were used to extract values for  $\Gamma_j$  from measurements of  $g(1)(\tau)$ .

#### MATERIALS AND METHODS

The light-scattering instrument used in these studies was purchased from Brookhaven Instruments Corporation (Holtville, NY, USA). The light source is a Loxel Model 95-2 argon ion laser (Palo Alto, CA, USA) whose incident polarization is perpendicular to the scattering plane. The sample cell is immersed in an index matching liquid (toluene) in order to reduce the reflection of the incident beam from the surface of the sample cell. All measurements were made at a scattering angle of 90° and the sample time was 2.5  $\mu$ s. Data for each measurement were accumulated over a period of 5 min. The temperature was controlled at 30.0  $\pm$  0.1°C using a Lauda Model RM6 circulating water bath (Westbury, NY, USA). The correlator is a Brookhaven BI-2030 real-time 136-channel digital correlator.

As mentioned before, the measured autocorrelation functions were analyzed using the LaPlace inversion program CONTIN [10,11].

The buffer used in all experiments was 89 mM tris(hydroxymethyl)aminomethane, 89 mM boric acid and 5 mM ethylenediaminetetraacetic acid (TBE buffer) at pH 8.1. Varying amounts of (hydroxyethyl) cellulose was added to the TBE buffer to make up the polymer solutions. All the solutions

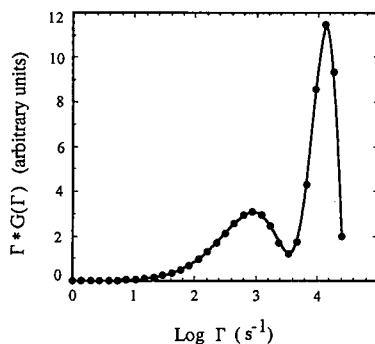


Fig. 4. Representative plot of the distribution of relaxation times. Data are from a solution of 0.01 g/ml HEC in TBE buffer at 30°C. The scattering angle is 90°.

were filtered through a 0.2- $\mu$ m nylon filter (Fisher Scientific, Pittsburgh, PA, USA) to remove any dust particles and were allowed to sit for between 18 and 24 h to insure complete dissolution of the polymer.

#### RESULTS AND DISCUSSION

A plot of the distribution of relaxation times of an HEC solution having a concentration of 0.006 g/ml is shown in Fig. 4. This plot is typical of these seen at other polymer concentrations above the overlap concentration. The origin of the modes has been determined in a previous report from this laboratory using solutions of polyacrylamide [9]. The slow mode (small  $\Gamma$ ) was attributed to the center-of-mass motion of unentangled single polymer chains, while the fast mode (large  $\Gamma$ ) was attributed to the dynamics of the entangled polymer network (co-

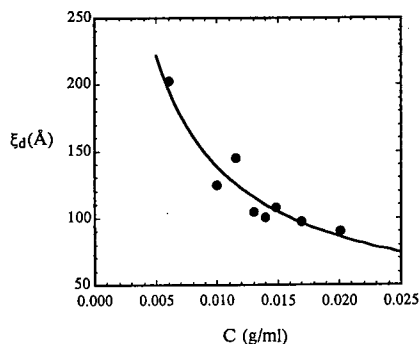


Fig. 5. Plot of the measured dynamic correlation length,  $\xi_d$ , as a function of HEC concentration. The solid curve is a plot of eqn. 11 where  $a = 4.22 \text{ \AA}$  and  $\nu = 0.75$ .

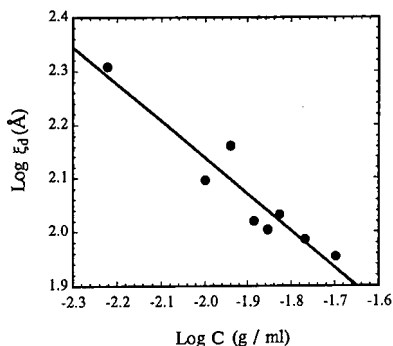


Fig. 6. Concentration dependence of the dynamic correlation length for HEC solutions at 30°C (0.006–0.02 g/ml). The straight line is a linear least-squares fit where  $\xi_d(\text{Å}) = 6.0C^{-0.68}$ .

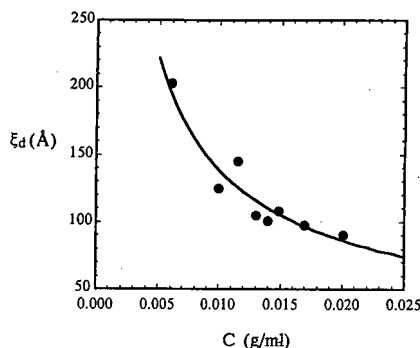


Fig. 7. Plot of the measured dynamic correlation length,  $\xi_d$ , as a function of HEC concentration. The solid curve is a plot of eqn. 12.

operative diffusion). In this work, because we are concerned with the polymer network and not individual polymer chains, we are interested exclusively in the cooperative diffusion (fast) component of the relaxation spectrum.

Fig. 5 shows plot of the measured correlation length,  $\xi_d$ , as a function of polymer concentration. The solid curve is the predicted value of  $\xi_d$  based on the scaling theory,

$$\xi_d = aC^{-\nu} \quad (11)$$

where  $a$  is the polymer segment length and  $C$  is the polymer concentration (in this case the volume fraction and the concentration are assumed to be equivalent) and  $\nu$  is a constant whose value depends on the solvent quality. For a good solvent,  $\nu = 0.75$ . The value of  $a$  used in constructing the curve in Fig. 5 is 4.22 Å. This value was determined using intrinsic viscosity measurements [3] in the TBE buffer. All the points in Fig. 5 are above the experimentally measured value of the overlap threshold of approximately 0.4%.

In order to determine the experimentally measured value of the exponent in eq. (11) and the polymer segment length,  $a$ , a plot of  $\log \xi_d$  vs.  $\log C$  was constructed (Fig. 6). The slope of the solid line is  $-0.68$ , indicating that  $\nu = 0.68$  in this system, in good agreement with the value of 0.75 predicted from theory. The zero intercept of the curve is 0.775,

indicating a segment length of 6.00 Å. This value is higher than the value measured by intrinsic viscosity, 4.22 Å, but well within the margin of error for these measurements. Based on these measurements, for the polymer–solvent system considered here,

$$\xi(\text{Å}) = 6.0C^{-0.68} \quad (12)$$

Fig. 7 compares the experimental data with the curve described by eqn. 12. Thus, comparing Figs. 5 and 7, it can be seen that these data are in close agreement with the predictions of scaling theory.

## REFERENCES

- 1 A. M. Chin and J. C. Colburn, *Am. Biotech. Lab./News Edition*, 7 (1989) 10A.
- 2 M. Zhu, D. L. Hansen, S. Burd and F. Gannon, *J. Chromatogr.*, 480 (1989) 311–319.
- 3 P. D. Grossman and D. S. Soane, *Biopolymers*, 31 (1991) 1221–1228.
- 4 A. Widhalm, C. Schwer, D. Blaas and E. Kenndler, *J. Chromatogr.*, 549 (1991) 446–451.
- 5 J. A. Burroughs and A. Crambach, *Biochem. Biophys. Res. Commun.*, 180(2) (1991) 1070–1074.
- 6 T. Guszczynski and A. Crambach, *Biochem. Biophys. Res. Commun.*, 179 (1991) 482–486.
- 7 H. E. Schwartz, K. Ulfelder, F. J. Sunzeri, M. P. Busch and R. G. Brownlee, *J. Chromatogr.*, 559 (1991) 267–283.
- 8 P. G. de Gennes, *Scaling Concepts in Polymer Physics*, Cornell University Press, Ithaca, NY, 1979.
- 9 T. Hino and D. S. Soane, *J. Appl. Phys.*, 70 (1991) 7295.
- 10 S. W. Provencher, *Comput. Phys. Commun.*, 27 (1982) 213.
- 11 S. W. Provencher, *Comput. Phys. Commun.*, 27 (1982) 229.



# Indirect time-resolved luminescence detection in capillary zone electrophoresis

M. W. F. Nielen

Chemical and Structure Analysis Department, Corporate Research, Akzo Research Laboratories Arnhem, P.O. 9300, 6800 SB Arnhem (Netherlands)

---

## ABSTRACT

Time-resolved luminescence of the terbium(III)-acetylacetonate chelate has been used as an indirect detection method for capillary zone electrophoresis. Three different modes were investigated: dynamic quenching of the background signal by selected anions; ligand displacement of acetylacetonate by other complexing agents; and electrophoretic displacement of acetylacetonate by anions in general. The latter two modes required the use of a post-capillary reactor; in this study, a coaxial flow-type reactor was used for this purpose. The results of dynamic quenching were good for the determination of nitrite, yielding detection limits of  $3 \cdot 10^{-9} M$  (0.2 ppb). In addition, the feasibility of ligand and electrophoretic displacement was demonstrated. However, improvement of the post-capillary reactor and substitution of the xenon lamp by a focused laser beam is required to exploit fully the potential of the ligand and electrophoretic displacement options.

---

## INTRODUCTION

Capillary zone electrophoresis (CZE) gives a fast and efficient separation of ionic compounds. Indirect detection methods [1] can be applied for those compounds without a suitable chromophore. Among the different approaches described so far are indirect UV absorbance [2-5], indirect laser-induced fluorescence [6-8] and indirect amperometric methods [9]. According to Yeung and Kuhr [1], the attainable detection limit,  $C_{lim}$  (in concentration units), is given by the following equation

$$C_{lim} = \frac{C_b}{DR \cdot TR} \quad (1)$$

where  $C_b$  represents the concentration of the buffer ion which generates the background signal,  $DR$  is the dynamic reserve and  $TR$  the transfer ratio. From eqn. 1 it can be seen that  $C_b$  should be as low as

possible while still generating a sufficient background signal. The transfer ratio will depend on the mobilities of the analyte and the background ion and might deviate significantly from unity [5]. The dynamic reserve should be as high as possible. Some representative data are summarized in Table I.

The UV detector gives a good performance with respect to  $DR$ ; its limited sensitivity, however, demands high concentrations of the background ion. Both conventional and laser-induced fluorescence methods yield relatively low  $DR$  values due to instability of the source and scattered light. Only after extensive modifications [7] can the situation be improved.

As an alternative, indirect time-resolved luminescence methods using pulsed sources and gated photomultipliers can be considered. The absence of scattered excitation light will be beneficial, especially at cylindrical flow cells such as CZE capillaries.

Relatively inexpensive luminescence detectors, designed for high-performance liquid chromatography (HPLC), allow time-resolved measurements in the microsecond domain. Thus fluorophores or phosphorophores having relatively long lifetimes

---

Correspondence to: Dr. M. W. F. Nielen, Chemical and Structure Analysis Department, Corporate Research, Akzo Research Laboratories Arnhem, P.O. Box 9300, 6800 SB Arnhem, Netherlands.

TABLE I

## DYNAMIC RESERVE AND DETECTION LIMITS FOR INDIRECT DETECTION MODES IN CZE

Limits of detection (LOD) at a signal-to-noise ratio of 2.

Detection mode <sup>a</sup>	Background ion	C <sub>b</sub> (mM)	DR	LOD (mol/l)	Ref.
UV	Veronal	6	1100	1.5 · 10 <sup>-5</sup>	5
Flu	Quinine	0.1	170	1.0 · 10 <sup>-6</sup>	<sup>b</sup>
Flu	Salicylate	0.25	180	3.0 · 10 <sup>-6</sup>	<sup>b</sup>
LIFlu	Quinine	0.4	380	2.0 · 10 <sup>-6</sup>	8
LIFlu	Salicylate	0.25	270	2.0 · 10 <sup>-6</sup>	6
LIFlu	Salicylate	0.05	>1000	1.0 · 10 <sup>-7</sup>	7

<sup>a</sup> Flu = fluorescence; LI = laser-induced.<sup>b</sup> Using the detector as described in this paper.

are required. Europium chelates fulfill this requirement and are widely used as labels in time-resolved fluorescence immunoassays [10]. Terbiumchelates have been used in spectrofluorimetric determinations of trace amounts of protein [11] and of salicylate in biological samples [12]. Baumann *et al.* [13] proposed dynamic quenching of europium(III) and terbium(III) luminescence as a detection method for ion chromatography. A decrease in background signal is observed for those analytes able to reduce the luminescence quantum yield, *i.e.* the detection limit is not restricted by the concentration of the background ion and does not follow eqn. 1. The method can be improved by excitation of the lanthanide acetylacetonate chelates (instead of direct excitation of the lanthanide ions) [14]. Only a few anions [nitrite, chromate, hexacyanoferrate(II) and hexacyanoferrate(III)] respond, thus the dynamic quenching mode offers both sensitivity and selectivity in ion chromatography.

In this study, the time-resolved luminescence of the terbium(III)-acetylacetonate (Tb-acac) chelate was used as a background signal for indirect detection in CZE. Three different modes have been investigated: dynamic quenching of the signal (selective mode); ligand displacement (less selective mode); and electrophoretic displacement (universal mode). Only the latter mode is comparable with the other systems in Table I and follows eqn. 1.

Both ligand and electrophoretic displacement required the use of a post-capillary reactor [15].

## EXPERIMENTAL

*Apparatus*

Experiments were carried out using a laboratory-made CZE system consisting of an F.u.G. (Rosenheim, Germany) Model HCN 35-35000 power supply operated at +25 or -25 kV, a Plexiglas cabinet equipped with safety interlocks and a Perkin-Elmer (Beaconsfield, UK) Model LS-40 luminescence detector. Unless stated otherwise, the detector was operated at an excitation wavelength of 295 nm. The emission monochromator was replaced by the total emission mirror accessory combined with the 430 nm cutoff filter. Time-resolved luminescence was obtained using a delay time of 0.1 ms and a gating time of 0.5 ms. The original flow cuvette of the detector was removed and replaced by the CZE capillary, without additional optimization or focusing of the optical system. The detection window on the CZE capillary was about 4 mm long. CZE capillaries were either fused silica (Polymicro Technologies, Phoenix, AZ, USA), 120 cm × 50 μm I.D./180 μm O.D., or a synthetic hollow fibre [16], 88 cm × 50 μm I.D./350 μm O.D. Samples were injected either hydrodynamically by raising the injection end and the sample at a specific height and time, or electrokinetically by applying a voltage of -10 kV for a specific time.

Some preliminary experiments were carried out using an Applied Biosystems (San Jose, USA) Model 270A capillary electrophoresis system [17] coupled with the detector described above.

### Post-capillary reactor

Ligand and electrophoretic displacement required the use of a post-capillary reactor. The reactor was of the coaxial flow type and was constructed according to Rose and Jorgenson [15]. The CZE capillary, 50  $\mu\text{m}$  I.D./180  $\mu\text{m}$  O.D., was inserted into a 200  $\mu\text{m}$  I.D./350  $\mu\text{m}$  O.D. reaction capillary. In this work, the reaction is actually a displacement only, thus hardly any reaction time is required. To allow mixing, the CZE capillary was inserted to 1 mm before the beginning of the detection window in the reaction capillary. The reagent was delivered via a stainless-steel tee using an Applied Biosystems Model 140B syringe pump, equipped with an Acurate (LC-Packings, Amsterdam, Netherlands) Model 100 flow splitter and a restriction capillary of 5 m  $\times$  50  $\mu\text{m}$  I.D.

The post-capillary reactor was not optimized in this work. Optimization can be carried out by etching the outer diameter of the CZE capillary and by improved matching with the inner diameter of the reaction capillary [15], or by the use of a focused laser beam [18].

### Chemicals

Terbium(III) chloride hexahydrate and acac were obtained from Aldrich (Steinheim, Germany). All other chemicals were obtained from Merck (Darmstadt, Germany). Distilled water was purified in a Milli-Q apparatus (Millipore, Bedford, MA, USA).

### Methods

Buffers were prepared in Milli-Q water and adjusted to a specific pH with 0.1 M sodium hydroxide solution using a Philips (Cambridge, UK) Model PW 9409 pH meter. Stock solutions of the analytes under investigation were prepared in Milli-Q water at  $1 \cdot 10^{-3}$  M. Samples were freshly diluted or their pH was adjusted in accordance with the buffer system under investigation, or both. Buffers and samples were filtered through 0.45  $\mu\text{m}$  Spartan 30/B filters (Schleicher & Schuell, Dassel, Germany) before use.

## RESULTS AND DISCUSSION

### Dynamic quenching mode

Initial experiments were performed using direct excitation of Tb(III), *i.e.* without acac ligands, at 225

nm in an electrolyte system consisting of 5 mM TbCl<sub>3</sub> in water.

Not surprisingly, the performance was poor. The maximum *DR* value obtained was 70 due to the noisy baseline and the low background signal obtained. The output of the xenon lamp and the molar extinction coefficient of Tb(III) are both low at this wavelength. Indirect excitation of Tb(III) via its acac chelate was expected to yield better results. The excitation and emission maxima were determined and found to be 295 and 545 nm, respectively. The optimum detector settings as described under Experimental, combined with a buffer system consisting of 0.35 mM TbCl<sub>3</sub>, 0.8 mM acac, 6 mM NaCl at pH 8.3 yielded a *DR* value of 360. Compared with the (conventional) fluorescence data in Table I, the *DR* value has increased significantly as a result of the time-resolved measurement. An even bigger increase might have been expected. However, it should be noted that the optics of the detector used were not designed nor optimized for the CZE capillary.

In addition, the chemistry involved might significantly contribute to the baseline noise (chemical noise). Tb ions tend to adsorb onto the capillary wall, complex with acetylacetonate and migrate, free or complexed, in the electric field.

A mixture of nitrite, chromate and hexacyanoferrate(III),  $3 \cdot 10^{-5}$  M each, was separated by CZE at  $-25$  kV and detected using the dynamic quenching mode. A typical electropherogram is shown in Fig. 1. The negative peaks obtained cannot be attributed to electrophoretic displacement of acac because of the excess of chloride ions in the buffer and the complexation of acac with the Tb(III) ions. The results for nitrite were promising but the other two ions, especially chromate, showed a lot of tailing. Tailing has also been observed in HPLC systems for the analysis and detection of these compounds by dynamic quenching of Tb–acac [14,19]. Contrary to the suggestion in these papers, interaction with metal parts cannot be responsible for tailing observed in this fused-silica capillary. The behaviour of these two ions in this CZE system resembles an adsorption mechanism: the respective electrophoretic mobilities are much lower than the theoretical values and a typical concentration dependency occurs on dilution of the mixture in Fig. 1.

In contrast to nitrite, chromate and hexacyanoferrate(III) tend to disappear completely at  $1 \cdot 10^{-6}$

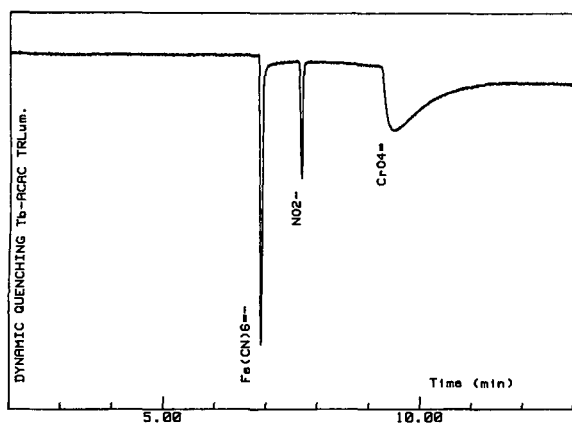


Fig. 1. Electropherogram of  $3 \cdot 10^{-5} M$  nitrite, chromate and hexacyanoferrate(III) using dynamic quenching of Tb-acac luminescence. Conditions: Applied Biosystems Model 270A apparatus equipped with a fused-silica capillary, 120 cm  $\times$  50  $\mu$ m I.D., coupled with the luminescence detector; CZE at  $-25$  kV in 0.8 mM acac, 0.35 mM TbCl<sub>3</sub>, 6 mM NaCl, pH 8.3 (in water); other conditions as given under Experimental.

*M.* These observations might be explained by one or more of the following mechanisms: adsorption onto wall-adsorbed Tb(III) ions; precipitation after complexation with Tb-acac; unintended electrochemical reactions in the CZE system. In this study, aimed at determining the general principles and feasibility of indirect detection in CZE using Tb-acac, chromate and hexacyanoferrate(III) were simply excluded from the test mixture and experiments in the dynamic quenching mode were continued with nitrite alone.

The performance of this system was investigated using a CZE capillary of 113 cm length (71 cm to detector) and a buffer system consisting of 6 mM NaCl, 1 mM acac, 0.2 mM TbCl<sub>3</sub> at pH 7.4. Nitrite samples ( $3 \cdot 10^{-5} M$  in water) were injected hydrodynamically (14 cm, 20 s). The nitrite peaks obtained showed a plate number of 130 000. The repeatabilities of the migration time and the peak height were  $\pm 1\%$  relative standard deviation (R.S.D.) ( $n = 6$ ) and  $\pm 3.8\%$  R.S.D. ( $n = 6$ ), respectively. The lower limit of detection (signal-to-noise ratio-2) was  $2 \cdot 10^{-7} M$ , which is fairly good for a capillary separation technique (*cf.* Table I) and comparable with the results obtained with high-performance liquid chromatographic (HPLC) instruments [13, 14]. It should be noted that the theoretical detection limit for 1% dynamic quenching of the Tb(III)-acac

signal by nitrite is  $1 \cdot 10^{-7} M$  [14], so the results presented here are in good agreement. The lower limit of detection can be simply improved in CZE by using focusing techniques.

We have successfully applied field amplified sample injection [20]. A tapwater sample spiked with  $1 \cdot 10^{-7} M$  nitrite was injected electrokinetically at  $-10$  kV for 15 s. The electropherogram obtained (Fig. 2) shows a good selectivity towards other ionic species normally present in this matrix. The lower limit of detection can be calculated using the Stern-Volmer equation [13] and was found to be  $3 \cdot 10^{-9} M$  or 0.2 ppb, which is, as far as is known, superior to any other separation technique for the selective determination of nitrite in aqueous samples. In addition, the method presented here will cost much less than a comparable ion chromatographic system. An interesting application would be the determination of nitrite (often used as a food preservative and a known precursor of carcinogenic N-nitrosamines) in aqueous extracts of processed meats [21].

#### Ligand-exchange mode

The second indirect detection option using Tb(III)-acac time-resolved luminescence is based on ligand-exchange principles. Any analyte which is able to form a complex or a mixed complex, *i.e.* any analyte having a complexation constant with Tb(III) which is higher than (or comparable with) Tb(III)-acac and which is unable (or less able) to provide indirect excitation of Tb(III) ions at 295 nm, will cause a negative peak on the background signal. A polycarboxylic acid, known as a complexing agent, showed good sensitivity in both batch and flow injection experiments [22].

In this CZE experiment, it was preferred to separate the complexing agents EDTA and nitrilotriacetic acid (NTA) as such, *i.e.* in their uncomplexed form. Consequently, TbCl<sub>3</sub> had to be excluded from the CZE separation system and added after the capillary using the coaxial flow reactor (see under Experimental). The performance of the post-capillary reactor was tested using hydrodynamic injections of nitrite ( $3 \cdot 10^{-5} M$ ). At a reagent flow-rate of 0.0  $\mu$ l/min the plate number was 1600, which is in good agreement with published data for a 200  $\mu$ m I.D. reaction capillary at low flow-rates [15]. The plate number increased towards 7000 at the reagent flow-rate of 0.55  $\mu$ l/min used in this study.

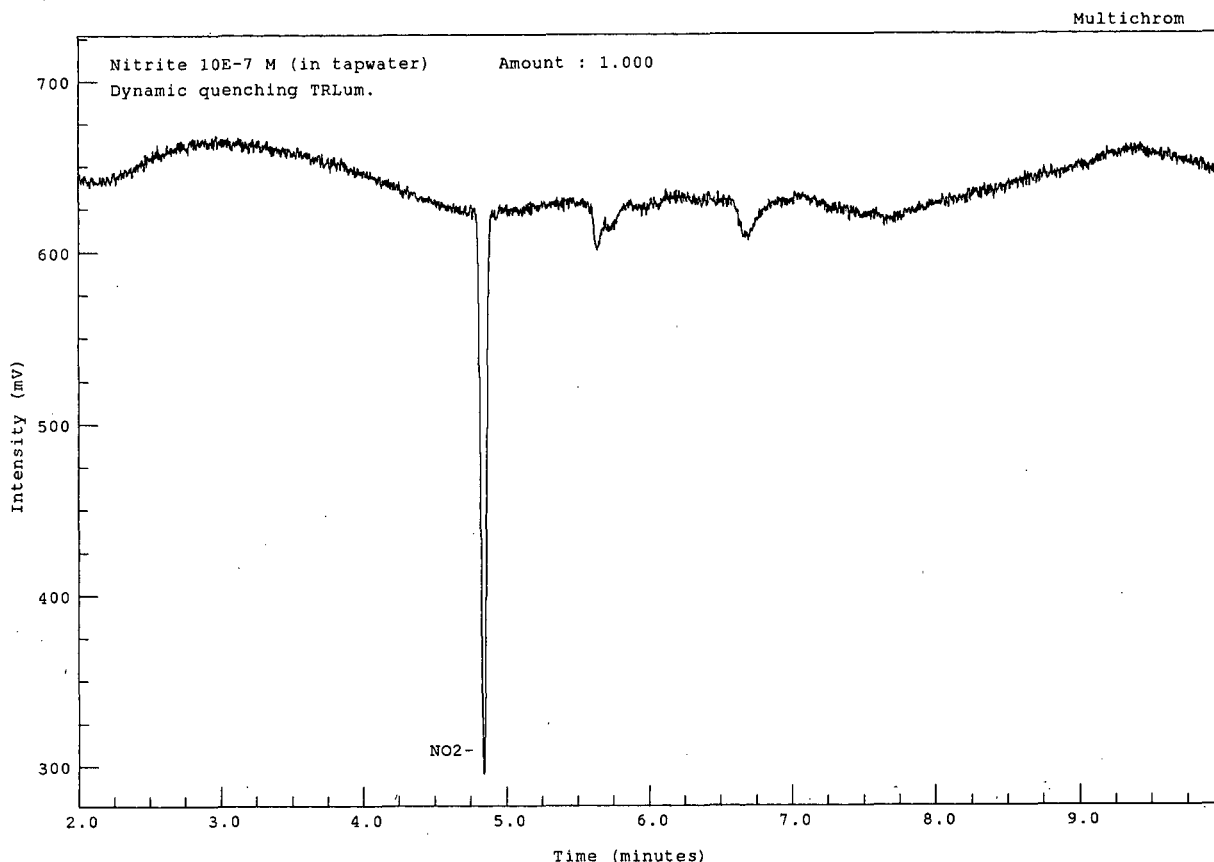


Fig. 2. Electropherogram of tapwater spiked with  $1 \cdot 10^{-7}$  M nitrite using dynamic quenching of Tb-acac luminescence. Conditions: CZE at  $-25$  kV in  $1$  mM acac,  $0.5$  mM  $\text{TbCl}_3$ ,  $10$  mM NaCl, pH 7.1 (in water-methanol, 75:25); capillary, synthetic hollow fibre,  $88$  cm  $\times$   $50$   $\mu\text{m}$  I.D. Apparatus and other conditions as given under Experimental.

The efficiency of the coaxial flow reactor can be significantly improved (plate numbers up to 50 000–600 000) by etching the outer diameter of the CZE capillary and decreasing the inner diameter of the reaction capillary, or using a focused laser beam as an excitation source, or both [15,16]. However, this plate number was considered to be sufficient for the purpose of demonstrating the ligand-exchange option using Tb-acac luminescence.

Complexing agents ( $5 \cdot 10^{-4}$  M) were injected hydrodynamically into a CZE electrolyte system consisting of  $10$  mM NaCl and  $1.4$  mM acac at pH 7.1.  $\text{TbCl}_3$  ( $0.5$  mM, pH 7) was added coaxially at a flow-rate of  $0.55$   $\mu\text{l}/\text{min}$ . Matching the pH of the CZE electrolyte and the reagent was a prerequisite for adequate mixing and a stable background signal. The results obtained are shown by the electro-

pherograms in Fig. 3. In contrast with Figs. 1 and 2, a strong electro-osmotic flow in the direction of the cathode is induced due to the absence of  $\text{Tb}^{3+}$  ions in the CZE capillary. The complexing agents EDTA (Fig. 3A), NTA (Fig. 3B) and the commercially available technical mixture (Fig. 3C) show relatively large responses (peak area/time), demonstrating the potential of this ligand-exchange detection mode. The negative peaks are not caused by electrophoretic displacement of acac because of the excess of chloride ions present in the electrolyte system. The plate numbers and peak shapes are poor compared with Fig. 2. These discrepancies can be explained by the poor performance of the coaxial flow reactor in general and electromigration dispersion caused by differences in effective mobilities between analytes and buffer ions [23].



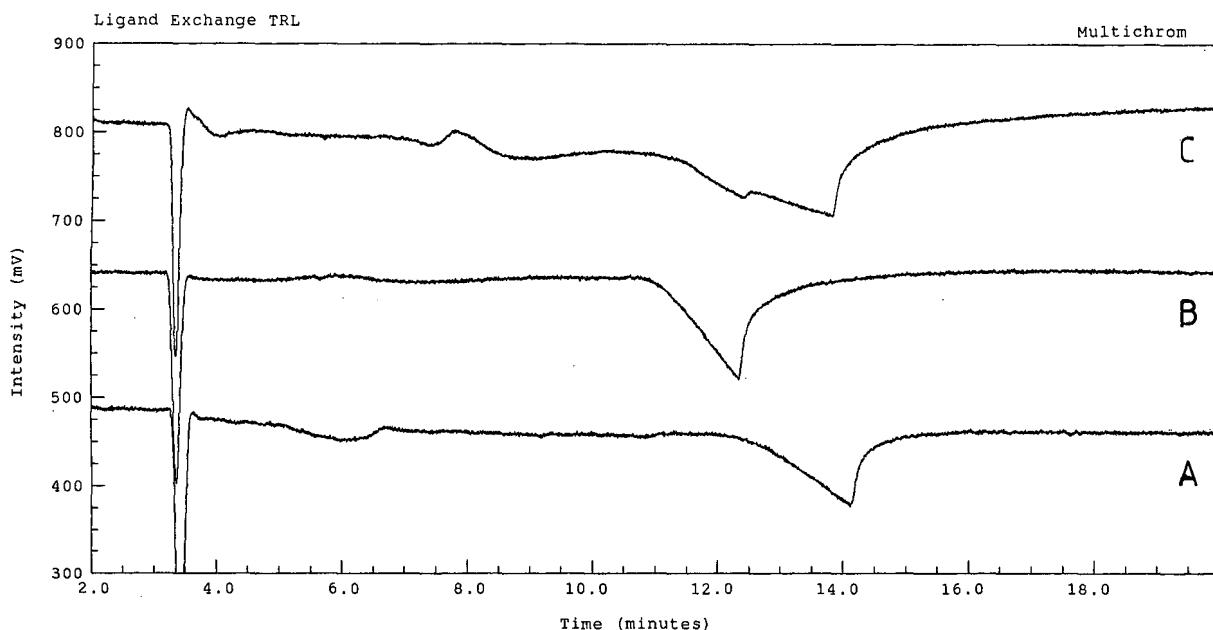


Fig. 3. Electropherogram of (A)  $5 \cdot 10^{-4}$  M EDTA, (B) NTA and (C) a technical mixture using ligand-exchange Tb-acac luminescence. Conditions: CZE at +25 kV in 1.4 mM acac, 10 mM NaCl, pH 7.1 (in water); post-capillary addition of 0.5 mM TbCl<sub>3</sub> at 0.55  $\mu$ l/min; total length of capillaries, 108 cm, CZE fused-silica capillary 63 cm  $\times$  50  $\mu$ m I.D., reaction capillary 200  $\mu$ m I.D. Apparatus and other conditions as given under Experimental.

#### Electrophoretic displacement mode

The third option for indirect detection using the Tb-acac luminescence is electrophoretic or charge displacement. The principles of this mode are the same as for the indirect UV or fluorescence methods (see Table I). In this instance only acac should be present as background electrolyte in the CZE system, so TbCl<sub>3</sub> should be added after the capillary (*cf.* ligand-exchange mode).

The  $pK_a$  value of acac was determined by recording a titration curve and was found to be 8.76. This value is attractive for CZE separation using electroosmotic flow and, in addition, the buffering capability will provide a stable system.

C<sub>9</sub> and C<sub>12</sub> linear alkylsulphates ( $1 \cdot 10^{-3}$  M in water) were injected hydrodynamically in a CZE electrolyte consisting of 10 mM acac buffer at pH 8.5. TbCl<sub>3</sub> (0.25 mM) was added after the capillary at a flow-rate of 3.0  $\mu$ l/min.

CZE was performed at +25 kV and indirect detection was easily obtained (Fig. 4). The plate number increased to 12 000 as a result of the increased reagent flow-rate. It can be seen that these

linear alkylsulphates are partly separated in this system. This unoptimized post-capillary reaction system cannot compete with the indirect UV detection system [5] in which baseline resolution and 400 000 theoretical plates were obtained. Nevertheless, the present indirect detection option might become a serious alternative when the post-capillary reactor [15,18] has been improved or the indirect UV system [5] cannot be used because of interfering compounds with a chromophore, or both.

#### CONCLUSIONS

Indirect time-resolved luminescence detection using the Tb(III)-acac chelate has been applied to CZE using a conventional HPLC luminescence detector. Three different indirect detection modes have been demonstrated: dynamic quenching of the background signal; ligand displacement by complexing agents; and electrophoretic or charge displacement. The dynamic quenching mode offers unequalled sensitivity (less than pbb levels can be detected) and selectivity for nitrite in aqueous

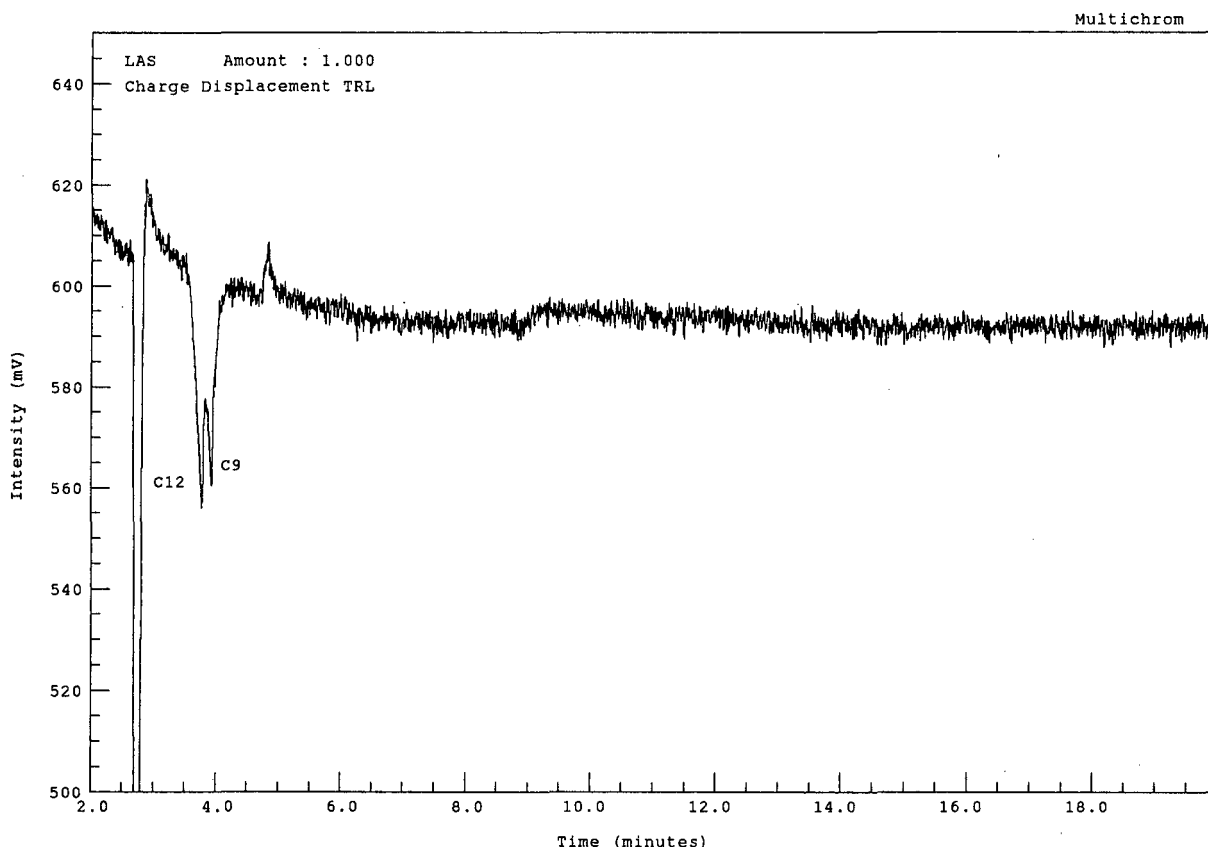


Fig. 4. Electropherogram of a mixture of  $1 \cdot 10^{-3} M$  nonyl- and dodecylsulphate using electrophoretic displacement of acac. Conditions: CZE at +25 kV in 10 mM acac, pH 8.5 (in water); post-capillary addition of 0.25 mM  $TbCl_3$  at 3.0  $\mu$ l/min. Other conditions as in Fig. 3.

samples. The feasibilities of the ligand and electrophoretic displacement options have been preliminarily shown, but were adversely affected by the low plate numbers caused by the unoptimized coaxial flow reactor. Further improvement of the post-capillary reactor following the guidelines of Jorgenson and co-workers [15,18] will be required to exploit fully the potential of the ligand and electrophoretic displacement modes.

#### ACKNOWLEDGEMENTS

M. Schreurs, C. Gooijer and N. H. Velthorst (Free University, Amsterdam, Netherlands) are acknowledged for stimulating discussions.

#### REFERENCES

- 1 E. S. Yeung and W. G. Kuhr, *Anal. Chem.*, 63 (1991) 275A.
- 2 S. Hjertén, K. Elenbring, F. Kilar, J-L. Liao, A. J. C. Chen, C. J. Siebert and M. D. Zhu, *J. Chromatogr.*, 403 (1987) 47.
- 3 F. Foret, S. Fanali, L. Ossicini and P. Bocek, *J. Chromatogr.*, 470 (1989) 299.
- 4 G. J. Bruin, A. C. van Asten, J. C. Kraak and H. Poppe, presented at the 3rd International Symposium on HPCE, San Diego, CA, 1991.
- 5 M. W. F. Nielsen, *J. Chromatogr.*, 588 (1991) 321.
- 6 W. G. Kuhr and E. S. Yeung, *Anal. Chem.*, 60 (1988) 1832.
- 7 W. G. Kuhr and E. S. Yeung, *Anal. Chem.*, 60 (1988) 2642.
- 8 L. Gross and E. S. Yeung, *J. Chromatogr.*, 480 (1989) 169.
- 9 T. M. Olefirowicz and A. G. Ewing, *J. Chromatogr.*, 499 (1990) 713.
- 10 E. P. Diamandis and T. K. Christopoulos, *Anal. Chem.*, 62 (1990) 1149A.

- 11 J. Siepak, *Anal. Chim. Acta*, 218 (1989) 143.
- 12 M. P. Bailey and B. F. Rocks, *Anal. Chim. Acta*, 201 (1987) 335.
- 13 R. A. Baumann, D. A. Kamminga, H. Derlagen, C. Gooijer, N. H. Velthorst and R. W. Frei, *J. Chromatogr.*, 439 (1988) 165.
- 14 M. Schreurs, G. W. Somsen, C. Gooijer, N. H. Velthorst and R. W. Frei, *J. Chromatogr.*, 482 (1989) 351.
- 15 D. J. Rose, Jr. and J. W. Jorgenson, *J. Chromatogr.*, 447 (1988) 117.
- 16 M. W. F. Nielen, in preparation.
- 17 S. E. Moring, J. C. Colburn, P. D. Grossman and H. H. Lauer, *LC · GC Int.*, 3 (1990) 46.
- 18 B. Nickerson and J. W. Jorgenson, *J. Chromatogr.*, 480 (1989) 157.
- 19 R. A. Baumann, *Thesis*, Free University, Amsterdam, 1987.
- 20 R. L. Chien and D. S. Burgi, *J. Chromatogr.*, 559 (1991) 141.
- 21 C. Gooijer, P. R. Markies, J. J. Donkerbroek, N. H. Velthorst and R. W. Frei, *J. Chromatogr.*, 289 (1984) 347.
- 22 M. Schreurs, Free University, Amsterdam, unpublished results.
- 23 F. E. P. Mikkers, F. M. Everaerts and Th. P. E. M. Verheggen, *J. Chromatogr.*, 169 (1979) 11.

# Indirect photometric detection of polyamines in biological samples separated by high-performance capillary electrophoresis

Yinfa Ma, Rulin Zhang and Cynthia L. Cooper

*Division of Science, Northeast Missouri State University, Kirksville, MO 63501 (USA)*

---

## ABSTRACT

A rapid separation of polyamines and some related amino acids in cultured tumor cells by high-performance capillary zone electrophoresis with indirect photometric detection is demonstrated. 60 cm  $\times$  75  $\mu$ m I.D. fused-silica capillary was used for the separation and quinine sulfate was used as a background electrolyte (BGE). Several polyamines (putrescine, spermidine and spermine), amino acids (lysine, arginine, histidine) and simple cations ( $K^+$ ,  $Na^+$ ) were easily separated in less than 10 min. Using the indirect photometric detection method, femtomole amounts of polyamines extracted from the tumor cells were detected from nanoliter injection volumes, and the signal response was linear over two orders of magnitude.

---

## INTRODUCTION

Polyamines such as putrescine, spermidine and spermine are small polycations that are essential for cell viability and are present in sub-millimolar concentrations in many tissues [1,2]. It is widely accepted that they have been implicated in a variety of cell functions involving DNA replication, gene expression, protein synthesis and cell surface receptor function [3,4]. Over-production of polyamines is toxic to cells and facilitates cell death by oxidative mechanisms [2]. Although many studies have been conducted on polyamines, methods for separation are largely confined to high-performance liquid chromatography [5–7] and thin-layer chromatography [8]. Both of these methods require that the polyamines be derivatized or labelled before detection [7,8]. Although several reports have demonstrated that the derivatization of amino acids and peptides with fluorescamine or dansyl chloride can be easy

and fast (nanoseconds) [9–11], the derivatization and labelling procedures for polyamines are often tedious and time consuming [7,8].

High-performance capillary zone electrophoresis (HPCZE) has proved to be a powerful technique in the separation of charged biomolecules with very high resolution [12–14]. Indirect detection techniques have become sensitive and simple to use [15,16]. However, the separation of polyamines in biological samples by HPCZE has not yet been assessed. This paper presents a rapid method to separate and detect extracted polyamines from an established tumor cell line of the rat pheochromocytoma, PC12, using HPCZE and indirect photometric detection.

## EXPERIMENTAL

### *Reagents*

All chemicals were of analytical-reagent grade unless stated otherwise. Deionized water was prepared with a Milli-Q system (Millipore, Bedford, MA, USA).

Quinine sulfate monohydrate was purchased

---

*Correspondence to:* Dr. Y. Ma, Division of Science, Northeast Missouri State University, Kirksville, MO 63501, USA.

from Fisher Scientific (Fairlawn, NJ, USA). Putrescine dihydrochloride, spermidine triphosphate, spermine diphosphate, L-arginine hydrochloride, L-histidine hydrochloride (monohydrate) and L-lysine monohydrochloride and cell culture materials were obtained from Sigma (St. Louis, MO, USA). HPLC-grade ethanol, hydroxypropylmethyl cellulose (HMC) (4000 cP at 25°C for a 2% solution) and all other inorganic chemicals were purchased from Aldrich (Milwaukee, WI, USA).

#### Equipment

The (Model 3850) HPCZE system with a UV detector was purchased from ISCO (Lincoln, NE, USA). A positive high voltage was applied to the capillary by maintaining the injection end at a positive high potential while the cathodic end was held at ground potential. Data were collected with a Datajet computing integrator (Spectra-Physics, Mountain View, CA, USA). The capillary columns (Polymicro Technologies, Phoenix, AZ, USA) were 60 cm (35 cm to the detection system)  $\times$  150  $\mu$ m O.D.  $\times$  50 or 75  $\mu$ m I.D. The polymer coating was burned off 25 cm from the cathodic end of the capillary to form the detection window.

#### Pretreatment of the capillary column

All new capillary columns were filled with 0.1 M sodium hydroxide solution for about 30 min to clean the column. The column was then washed with deionized water and background electrolyte (BGE). The capillary was ready for use thereafter.

#### Preparation of background electrolyte (BGE)

**BGE 1.** Quinine sulfate (313 mg) was dissolved in 20 ml of 95% ethanol with stirring for several minutes. About 70 ml of deionized water were added with stirring until all the quinine sulfate was dissolved (about 5 min). The concentration of quinine sulfate was 8 mM (20% ethanol) after bringing the volume to 100 ml in a volumetric flask, and the pH was 5.9. The BGE was vacuum degassed before use.

**BGE 2.** HMC was added to BGE 1 to a concentration of 0.5% (w/v) and stirred for 40 min until dissolved. The solution was vacuum degassed before use.

#### Growth of PC12 tumor cells

Rat pheochromocytoma (PC12) tumor cells were

purchased from the American Type Culture Collection (Rockville, MD, USA) and were cultivated on RPMI medium supplemented with 5% fetal bovine serum, 10% heat-inactivated horse serum (30 min at 56°C), 100 units/ml of penicillin G and 100  $\mu$ g/ml of streptomycin, and buffered with 0.2% (w/v) sodium hydrogencarbonate (pH 7.4). Cultures were propagated in a humidified growth chamber (Queue Systems, Parkersburg, WV, USA) with 10% carbon dioxide gassing at 37°C in 75-cm<sup>2</sup> flasks.

#### Preparation of tumor cell extract

PC12 cells ( $4.7 \cdot 10^7$ ) were harvested by centrifugation at 1000 g for 15 min. The pellet was washed with 0.3 M sucrose. Deionized water (3 ml) was added to the pellet and the sample was held at 0–4°C for 2.5 h. Insoluble and membranous materials were removed by centrifugation at 60 000 g at 0°C for 30 min. The supernatant was analyzed by HPCZE to determine cytosolic polyamines. For total cellular polyamine analysis, the pellet was resuspended with the supernatant.

#### Electrophoresis

Samples were injected electrokinetically at 30 kV for 3 s, and the separation was carried out at 30 kV for 15 min. The wavelength of detection was set at 236 nm owing to the maximum absorption coefficient of quinine sulfate at this wavelength ( $\epsilon = 34\,900$  l/mol  $\cdot$  cm) [17]. Data were collected and processed by the Datajet integrator. For the convenience of integration, the polarity of the integrator was reversed, so that the sample peaks shown in the following electropherograms appear as if they are absorption peaks.

## RESULTS AND DISCUSSION

Fig. 1 shows the separation of three polyamines and other commonly existing cations in the cell culture media and other biological samples, such as K<sup>+</sup>, Na<sup>+</sup>, L-lysine, L-arginine and L-histidine, with BGE 2. All these components were completely separated in less than 10 min. The effect of HMC in the BGE was twofold: it blocked the evaporation of ethanol and maintained a reproducible migration time for the sample peaks, and an improved resolution was obtained owing to the elimination of electroosmotic flow by the linear HMC polymers. L-

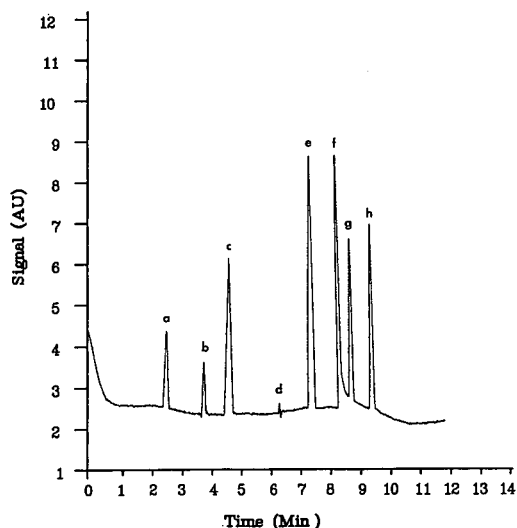


Fig. 1. Separation of three polyamine standards and other commonly co-existing cations in the cell culture media in BGE 2 by HPCZE with indirect photometric detection. A 3-s, 30-kV injection of  $100 \mu\text{M}$  each was followed by electrophoresis at 30 kV on a  $60 \text{ cm} \times 75 \mu\text{m}$  I.D. Pretreated column. Injection volume, 26.1 nl; detection wavelength, 236 nm. Peaks: a =  $\text{K}^+$ ; b =  $\text{Na}^+$ ; c = putrescine; d = L-histidine; e = spermidine; f = spermine; g = L-lysine; h = L-arginine.

Histidine gave a very small signal in BGE 2, as shown in Fig. 1. This is due to its absorption at 236 nm, which almost compensates for the displacement signal.

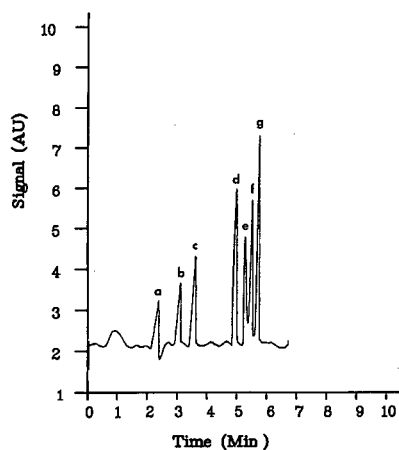


Fig. 2. Separation of polyamines and other cations using BGE 1 by HPCZE with indirect photometric detection. Peaks: a =  $\text{K}^+$ ; b =  $\text{Na}^+$ ; c = putrescine; d = spermidine; e = L-lysine; f = L-arginine; g = spermine. Electrophoresis conditions as in Fig. 1.

We also investigated the separation of the same components shown in Fig. 1 with BGE 1, and the results are shown in Fig. 2. It can be seen that the separation with BGE 1 is not as good as with BGE 2, the elution order of L-lysine and L-arginine changed from BGE 1 to BGE 2 and the L-histidine peak was missing. BGE 1 had another drawback in that the quinine sulfate crystallized very quickly in the open buffer reservoir. This was due to the evaporation of ethanol, which changed the BGE composition and decreased the solubility of quinine sulfate.

Fig. 3 shows the results of using BGE 2 to separate polyamines extracted from tumor cells. It is shown that femtomole amounts of polyamines can be easily detected with the indirect photometric detection technique. The amounts of polyamines extracted and injected on to the column are summarized in Table I. The unidentified peaks may be proteins in the cells, although this was not confirmed.

The linearity of polyamine detection was also investigated, an a linear response over two orders of magnitude ( $1.0 \cdot 10^{-3} - 3 \cdot 10^{-6}$ ) for each poly-

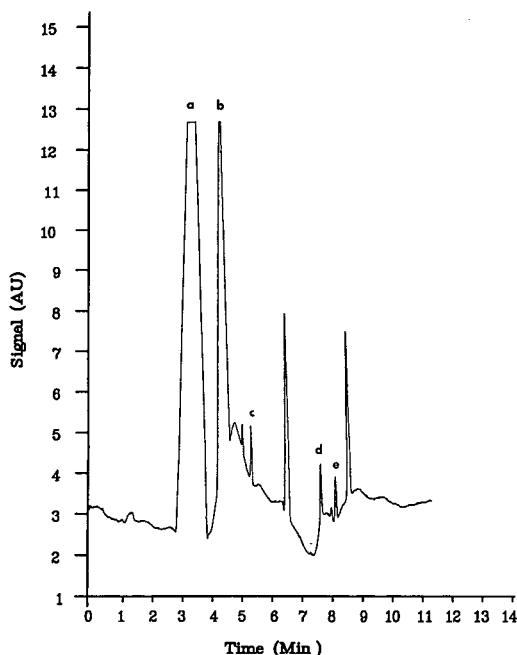


Fig. 3. Separation of polyamines in the tumor cell culture in BGE 2 by HPCZE with indirect photometric detection. Peaks: a =  $\text{K}^+$ ; b =  $\text{Na}^+$ ; c = putrescine; d = spermidine; e = spermine. Electrophoresis conditions as in Fig. 1.

TABLE I  
POLYAMINE MEASUREMENTS IN PC12 CELL EXTRACTS

The injection volume per run was 37.7 nl and the aqueous extract was made from  $35 \cdot 10^6$  cells.

Polyamine	Polyamine extracted (fmol/nl)	Total polyamine injected per run (fmol)	Amount per $10^6$ cells (nmol)
Putrescine	13.6	513	0.39
Spermidine	25.2	952	0.72
Spermine	20.8	786	0.59

amine was obtained, which would be difficult using direct UV detection.

#### CONCLUSION

Indirect photometric detection of polyamines in tumor cells separated by HPCZE has been demonstrated. The method is rapid, simple to use and femtomole amounts of polyamines and other biological cations can be separated and detected. The method should be highly suitable for the separation and determination of polyamines from animals, plants, microorganisms and biological fluids from tumor-bearing patients or animals. Importantly, a simple aqueous extract was injected directly into the capillary column. A preliminary trichloroacetic acid (TCA) extraction of polyamines was found not to be necessary. Indeed, the supernatants of TCA extractions were found to reduce the polyamine signals in both biological samples and standards (data not shown).

#### ACKNOWLEDGEMENTS

This work was supported by Faculty Research Grants awarded to Y. Ma and C. L. Cooper from Northeast Missouri State University.

#### NOTE ADDED IN PROOF

The polyamine measurements given in Table I do not account for polyamines bound tightly to macromolecules such as DNA.

#### REFERENCES

- 1 J. D. Walters and J. D. Johnson, *Biochim. Biophys. Acta*, 957 (1988) 138.
- 2 D. M. L. Morgan, *Biochem. Soc. Trans.*, 18 (1990) 1080.
- 3 U. Bachrack and Y. M. Heimer, *The Physiology of Polyamines*, Vols. 1 and 2, CRC Press, Boca Raton, FL, 1989.
- 4 A. E. Pegg and P. P. McCann, *Am. J. Physiol.*, 243 (1982) C212.
- 5 S. C. Minocha, R. Minocha and C. A. Robie, *J. Chromatogr.*, 511 (1990) 177.
- 6 N. Seiler, *Methods Enzymol.*, 94 (1983) 10.
- 7 T. Matsumoto and T. Tsuda, *Trends Anal. Chem.*, 9 (1990) 292.
- 8 N. Seiler, *Methods Enzymol.*, 94 (1983) 1.
- 9 R. A. Wallingford and A. G. Ewing, *Anal. Chem.*, 59 (1987) 678.
- 10 B. W. Wright, G. A. Ross and R. D. Smith, *J. Microcol. Sep.*, 1 (1989) 85.
- 11 A. Cohen, A. Paulus and B. L. Karger, *Chromatographia*, 24 (1987) 15.
- 12 J. E. Wiktorowicz and J. C. Colburn, *Electrophoresis*, 11 (1990) 769.
- 13 M. V. Novotny, K. A. Cobb and J. Liu, *Electrophoresis*, 11 (1990) 735.
- 14 D. N. Heiger, A. S. Cohen and B. L. Karger, *J. Chromatogr.*, 516 (1990) 33.
- 15 W. G. Kuhr and E. S. Yeung, *Anal. Chem.*, 60 (1988) 2642.
- 16 E. S. Yeung, *Acc. Chem. Res.*, 22 (1989) 125.
- 17 J. G. Grasselli, *Atlas of Spectral Data and Physical Constants For Organic Compounds*, CRC Press, Boca Raton, FL, 1973.

# Theoretical and experimental aspects of indirect detection in capillary electrophoresis

Gerard J. M. Bruin, Arian C. van Asten, Xiaoma Xu and Hans Poppe

*Laboratory for Analytical Chemistry, University of Amsterdam, Nieuwe Achtergracht 166, 1018 WV Amsterdam (Netherlands)*

---

## ABSTRACT

Theoretical and experimental aspects of indirect UV detection are considered. Based on a mathematical treatment of the transport of ions through the capillary, resulting in an eigenvector–eigenvalue problem, some guidelines are formulated about how to increase efficiency and sensitivity in an indirect (UV) detection system. Also, the existence of system peaks can be explained properly. An experimental system consisting of seven amino acids as sample ions and salicylate at pH 11.0 as the UV-absorbing ion was chosen in order to compare theoretical and experimental results. Constructed electropherograms, produced with a computer program based on the above-mentioned mathematical treatment, are also presented and compared with experimental electropherograms.

---

## INTRODUCTION

Most capillary electrophoretic separations are performed using UV detection. Although on-column UV detection requires some degree of miniaturization, it is easy to carry out and is inexpensive. Another important advantage of UV detection is its more or less universal character: peptides, proteins and oligonucleotides can all be detected. However, important classes of compounds such as inorganic ions, amino acids and sugars cannot be detected with UV methods. Indirect detection can be used as a universal detection scheme, without the need for time-consuming precolumn derivatization or experimentally complicated postcolumn derivatization procedures.

The possibilities for indirect laser-induced fluorescence detection have been studied by Yeung and co-workers. They reported successful separations of amino acids [1], proteins, nucleotides [2], tryptic digests [3], sugars [4] and inorganic ions [5]. Detection of aliphatic alcohols and some phenolic com-

pounds separated by micellar electrokinetic capillary chromatography (MECC) in combination with indirect fluorescence detection has been accomplished by Amankwa and Kuhr [6]. The detection mechanism involves a combination of displacement of the fluorescent background ion from the micelle by the sample ion and a net reduction of the quantum efficiency of the fluorophore in the sample zone. Another mode of indirect detection, indirect amperometric detection, has been demonstrated by Olefirowicz and Ewing [7] for the detection of several amino acids and dipeptides.

Indirect UV detection in CZE has been applied for the detection of homologous organic acids and inorganic ions [8–10] and alkylsulphate surfactants [11]. The possibilities for indirect UV detection in MECC systems have been shown recently by Szűcs *et al.* [12]. They added sodium dodecylbenzenesulphonate to the buffer, which allowed the detection of neutral, aliphatic alcohols.

Foret *et al.* [10] argued that the highest sensitivity can be achieved for sample ions having a mobility close to that of the UV-absorbing ion. They also gave some calculations on one of the disadvantages of indirect UV detection, the limited linear range (only two orders of magnitude) under favourable

---

*Correspondence to:* Professor H. Poppe, Laboratory for Analytical Chemistry, University of Amsterdam, Nieuwe Achtergracht 166, 1018 WV Amsterdam, Netherlands.



conditions. The upper limit is badly influenced by concentration overload. This effect can be diminished by choosing conditions such that the effective mobilities of the background electrolyte (BGE) and sample ions do not differ too much.

In this paper we treat the theoretical background of the electrophoretic transport in analytical separations in detail by using a mathematical analysis of the transport equation. This treatment consists of a vector-matrix approach which allows the assignment of the various sample and buffer constituents into a set of eigenvectors with corresponding eigenvalues, representing mobilities.

Also, results of the use of a computer program are presented. It predicts the number and position of system peaks with associated mobilities, the peak widths of sample ions, effective mobilities of sample ions at various pH values and the disturbances of the concentrations of the (UV-absorbing) background ions after injection. The results of the computational calculations are compared with experimental results.

The applicability of indirect UV detection in high-performance capillary electrophoresis (HPCE) is demonstrated with a system, consisting of salicylate as the UV-absorbing anion and seven amino acids as sample constituents.

## THEORY

In indirect detection, a detectable ion is chosen as one of the components of the background electrolyte (BGE), thus creating a large background signal. When a non-detectable analyte ion passes the detection window, there will be an increase or decrease in concentration of the detectable ion in the analyte zone, resulting in either an increase or decrease in the background signal. For a good description of such systems, one has to start with the fundamental transport equations as has been done for high-performance liquid chromatography (HPLC) by Crommen *et al.* [13]. Poppe [14] showed that the mathematical approaches for the description of indirect detection in HPLC and HPCE are analogous. However, in HPCE the model is simpler. In HPLC the simultaneous distribution of analytes towards the stationary phase has to be characterized empirically in order to arrive at predictions of indirect responses. In HPCE, the system consists of only one

phase, while the laws governing coupled transport are unambiguous and well known.

In this mathematical treatment, the following assumptions are made: the injection plug is infinitely sharp; diffusion is neglected, which omits the mass flux, caused by diffusion; no distribution phenomena are involved; and the electro-osmotic flow is zero. These restrictions can be relaxed later on in the model.

We start with Fick's law:

$$\frac{\partial c_i}{\partial t} = - \frac{\partial}{\partial z} \cdot J_i \quad (1)$$

where  $J_i$  and  $c_i$  are the mass flux and concentration of component  $i$ , respectively, and  $z$  the coordinate along the axis of the capillary.

The mass flux can be written as

$$J_i = v_i c_i = \mu_i E_z c_i = \frac{j \mu_i c_i}{\gamma} \quad (2)$$

where  $v_i$  and  $\mu_i$  are the linear velocity and the effective mobility, respectively, of compound  $i$ ,  $j$  the current density and  $\gamma$  the specific conductivity;  $\mu_i$  is a signed quantity and  $E_z$  is the local electric field ( $= j/\gamma$ ). The specific conductivity at position  $z$  in the capillary can be expressed as

$$\gamma = \mathcal{F} \sum_i z_i \mu_i c_i \quad (3)$$

where  $\mathcal{F}$  is the Faraday constant and  $z_i$  the charge of the ion.

Combining eqns. 1 and 2 gives

$$\frac{\partial c_i}{\partial t} = -j \cdot \frac{\partial}{\partial z} \left( \frac{\mu_i c_i}{\gamma} \right) \quad (4)$$

From this, it follows that the transport of one ion depends on the concentration of other ions present in the system. For a set of  $N$  components,  $N - 1$  such equations can be found. We need only  $N - 1$  equations because the concentration of the  $N$ th ion is determined by the electroneutrality.

The set of  $N - 1$  coupled non-linear equations is too complex to solve; only in a limited number of simple systems is it possible to find solutions. If the disturbance of the concentration of the ions in the background electrolyte is relatively small, then it is allowed to create a set of linear equations. The right-hand side of eqn. 4 can be written as

$$\frac{\partial}{\partial z} \cdot \frac{\mu_i c_i}{\gamma} = \frac{\mu_i}{\gamma} \cdot \frac{\partial c_i}{\partial z} + \mu_i c_i \cdot \frac{\partial}{\partial z} \cdot \frac{1}{\gamma} + \frac{c_i}{\gamma} \cdot \frac{\partial \mu_i}{\partial z} \quad (5)$$

The current density  $j$  can be omitted, because it is a constant for a uniform capillary. Both the conductivity,  $\gamma$ , and the mobilities of the ions,  $\mu_i$ , are functions of the  $N - 1$  components in the system:

$$\frac{1}{\gamma} = F_1(c_1, c_2, \dots, c_{N-1}) = \frac{1}{\left( \sum_{i=1}^{N-1} z_i \mu_i c_i \right)} \quad (6)$$

$$\mu_i = F_2(c_1, c_2, \dots, c_{N-1}) \quad (7)$$

The dependence of the  $\mu_i$ s on the electrolyte concentration is a result of ionic strength effects and varying extents of dissociation of acids and bases. Although the latter effects can be handled [15], in this paper we shall treat the  $\mu_i$ s as constants, which means that eqn. 7 needs no further consideration. The partial derivative of eqn. 5 can be expanded as

$$\frac{\partial F}{\partial z} = \frac{\partial F}{\partial c_1} \cdot \frac{\partial c_1}{\partial z} + \frac{\partial F}{\partial c_2} \cdot \frac{\partial c_2}{\partial z} + \dots + \frac{\partial F}{\partial c_{N-1}} \cdot \frac{\partial c_{N-1}}{\partial z} \quad (8)$$

If eqn. 8 is used to calculate the partial derivative of eqn. 5, the following expression will be obtained:

$$\frac{\partial}{\partial z} \cdot \frac{\mu_i c_i}{\gamma} = \sum_{k=1}^{N-1} A_{i,k} \cdot \frac{\partial c_k}{\partial z} \quad (9)$$

where

$$A_{i,k} = \frac{\partial}{\partial c_k} \left( \frac{\mu_i c_i}{\gamma} \right) \quad (10)$$

This means that eqn. 4 can be rewritten as

$$\frac{\partial c_i}{\partial t} = - \sum_{k=1}^{N-1} A_{i,k} \frac{\partial c_k}{\partial z} \quad (11)$$

for ions  $i = 1, \dots, N - 1$ .

In vector-matrix notation, eqn. 11 is

$$\frac{\partial}{\partial t} \cdot \vec{c} = |A| \cdot \frac{\partial}{\partial z} \cdot \vec{c} \quad (12)$$

If there is only one compound in the system, there is also only one differential equation and then the solution is easy to find:

$$c = G(z - \lambda t) \quad (13)$$

where  $\lambda$  is a constant (with the units of velocity) and  $G'(x)$  a function, e.g., the injection profile. This

solution means that the injection pulse occurring in the capillary at  $t = 0$  is transported through it with velocity  $\lambda$  without deformation. A representation of this can be found in Fig. 1A. In reality there is always more than one component in the system, which results in a set of coupled linear equations. This more-dimensional problem can be solved if it is possible to find a set of simultaneously occurring, concerted disturbances in all concentrations, which remain unchanged during transport along the capillary. An example of the situation for a three-ion system at  $t = 0$  and  $t = t$  is depicted in Fig. 1B. The system consists of a sample ion  $A^+$ , which is electrophoresed in a BGE  $B^+C^-$ . For a more-ions system, this can be represented mathematically as

$$c_1 = e_1 G(z - \lambda t) \quad (14)$$

$$c_{N-1} = e_{N-1} G(z - \lambda t)$$

where  $e_1$  to  $e_{N-1}$  indicate the relative intensity of the disturbance of the concentration. If the changes in

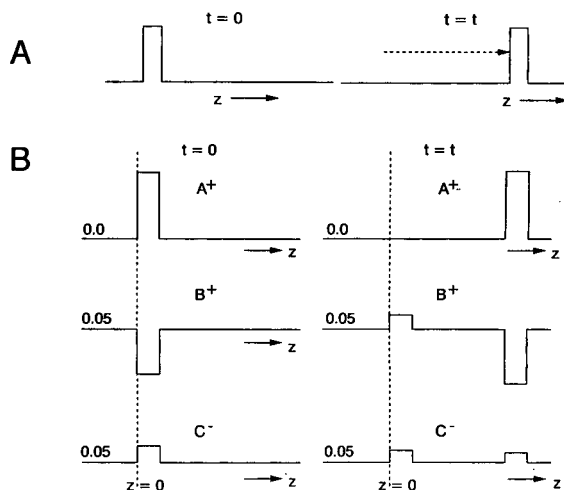


Fig. 1. Schematic representation of disturbances of the concentrations of the components after injection. The zones with the concerted concentration disturbances travel with a fixed velocity  $\lambda$  through the capillary. (A) One-dimensional system; (B) more-dimensional system. Sample ion  $A^+$  is electrophoresed in  $B^+C^-$ . The numbers on the  $z$ -axis indicate the ion concentration. Note also the stagnant zone at  $z = 0$  in case of  $t = t$ . This zone is nearly always visible in indirect detection measurements as a system peak at the position of an electroosmotic flow marker.

the concentrations as described above are substituted in the set of coupled linear equations, the result is

$$e_i \cdot \frac{\partial G}{\partial t} = - \sum_{k=1}^{N-1} [A_{i,k} e_k] \frac{\partial G}{\partial z} \quad (i = 1, \dots, N-1) \quad (15)$$

The term in between brackets does not depend on time and position in the capillary.

The set can only be solved if the concerted disturbances of the various concentrations in the zone migrate at the same velocity. These disturbances can be indicated as eigenpeaks with an associated eigenvalue  $\lambda$ , representing the velocity. The terms in brackets in eqn. 15 can be expressed as

$$- \sum_{k=1}^{N-1} [A_{i,k} e_k] = - \lambda e_i \quad (i = 1, \dots, N-1) \quad (16)$$

This gives rise to the following eigenvalue problem in matrix notation:

$$|A| \bar{e} = \lambda \bar{e} \quad (17)$$

To demonstrate the theoretical treatment above, we use a simple example of the electrophoresis of an amino acid, glycine (gly), in a BGE of sodium salicylate (referred to in the equations as Na and sal). This example was chosen because it shows a resemblance with the experimental part as described in this paper.

It will be assumed here that the ions are not subject to acid–base equilibria. This assumption leads to a fixed effective mobility. In this paper mobilities are always indicated as “overall” when they include the electroosmotic migration and as effective when the effects of acid–base reactions have been taken into account. The  $A$  term is now

$$A_{i,k} = \mu_i \cdot \frac{\partial}{\partial c_k} \left[ \frac{c_i}{\gamma} \right] = \mu_i \left[ c_i \cdot \frac{\partial}{\partial c_k} \left( \frac{1}{\gamma} \right) + \frac{1}{\gamma} \cdot \frac{\partial c_i}{\partial c_k} \right] \quad (18)$$

The  $\text{Na}^+$  ion is selected here as the dependent ion; the concentration is not explicitly given, but can be calculated easily from the rules of electroneutrality in the zone;  $c_{\text{gly}}$  and  $c_{\text{sal}}$  are taken as the independent variables. The conductivity in this electrophoretic system is

$$\gamma = c_{\text{gly}} [\mu_{\text{Na}} - \mu_{\text{gly}}] + c_{\text{sal}} [\mu_{\text{Na}} - \mu_{\text{sal}}] \quad (19)$$

Combining eqns. 18 and 19 results in

$$A_{\text{gly,gly}} = \frac{\mu_{\text{gly}}}{\gamma} - \frac{\mu_{\text{gly}} c_{\text{gly}} [\mu_{\text{Na}} - \mu_{\text{gly}}]}{\gamma^2} \approx \frac{\mu_{\text{gly}}}{\gamma} \quad (c_{\text{gly}} \approx 0) \quad (20)$$

$$A_{\text{gly,sal}} = - \frac{\mu_{\text{gly}} c_{\text{gly}} [\mu_{\text{Na}} - \mu_{\text{sal}}]}{\gamma^2} \approx 0 \quad (c_{\text{gly}} \approx 0) \quad (21)$$

$$A_{\text{sal,gly}} = - \frac{\mu_{\text{sal}} c_{\text{sal}} [\mu_{\text{Na}} - \mu_{\text{gly}}]}{\gamma^2} \quad (22)$$

$$A_{\text{sal,sal}} = \frac{\mu_{\text{sal}}}{\gamma} - \frac{\mu_{\text{sal}} c_{\text{sal}} [\mu_{\text{Na}} - \mu_{\text{sal}}]}{\gamma^2} \approx 0 \quad (c_{\text{sal}} [\mu_{\text{Na}} - \mu_{\text{sal}}] \approx \gamma) \quad (23)$$

The matrix equation is therefore

$$\begin{pmatrix} \frac{\mu_{\text{gly}}}{\gamma} & 0 \\ - \frac{\mu_{\text{sal}} c_{\text{sal}} [\mu_{\text{Na}} - \mu_{\text{gly}}]}{\gamma^2} & 0 \end{pmatrix} \begin{pmatrix} c_{\text{gly}} \\ c_{\text{sal}} \end{pmatrix} = \lambda \begin{pmatrix} e_{\text{gly}} \\ e_{\text{sal}} \end{pmatrix} \quad (24)$$

There are two solutions,

$$\lambda_1 = \frac{\mu_{\text{gly}}}{\gamma} \Rightarrow \frac{e_{\text{sal}}}{e_{\text{gly}}} = - \frac{\mu_{\text{sal}}}{\mu_{\text{gly}}} \cdot \frac{(\mu_{\text{Na}} - \mu_{\text{gly}})}{(\mu_{\text{Na}} - \mu_{\text{sal}})} \quad (25)$$

$$\lambda_2 = 0 \Rightarrow e_{\text{gly}} = 0 \quad (26)$$

The first solution corresponds to the electrophoresis of glycine with the associated disturbance in the salicylate concentration, expressed as  $e_{\text{sal}}/e_{\text{gly}}$ , in the sample zone;  $e_{\text{sal}}/e_{\text{gly}}$  is defined here as the response factor. Salicylate now allows us to monitor the passing non-UV-absorbing ion, glycine, by its change in concentration as a consequence of the presence of this glycine in the zone. It is noteworthy that the disturbance is not a direct consequence of electroneutrality rules; this would give  $e_{\text{gly}} = -e_{\text{sal}}$ , which is only true when  $\mu_{\text{gly}} = \mu_{\text{sal}}$ . In that particular situation, there will be a one-to-one displacement.

The second solution has velocity  $\lambda = 0$ , which will be visualized as a system peak, because it will be transported by the electroosmotic flow (if present). (The existence of such a stagnant concentration disturbance was discussed already in 1967 by Hjertén [16].) This stagnant zone serves as a very effective electroosmotic flow marker in this way. In Fig. 1B, this zone is depicted at  $z = 0$  and  $t = t$ .

The Kohlrausch regulating function (KRF),

which cannot change with time, should be fulfilled at all times for the moving sample zone. This can be checked by applying the KRF to the disturbances in the zone. The change in concentration of  $\text{Na}^+$ ,  $e_{\text{Na}}/e_{\text{gly}}$ , can be calculated from electroneutrality:

$$\frac{e_{\text{sal}}}{e_{\text{gly}}} - \frac{e_{\text{Na}}}{e_{\text{gly}}} + 1 = 0 \Rightarrow \frac{e_{\text{Na}}}{e_{\text{gly}}} = 1 + \frac{e_{\text{sal}}}{e_{\text{gly}}} \quad (27)$$

The term in the KRF caused by the disturbance is

$$\begin{aligned} \Delta\text{KRF} &= \sum_i \left[ \frac{(\Delta c_i) z_i}{\mu_i} \right] \\ &= -\frac{1}{\mu_{\text{gly}}} - \frac{e_{\text{sal}}/e_{\text{gly}}}{\mu_{\text{sal}}} + \frac{(1 + e_{\text{sal}}/e_{\text{gly}})}{\mu_{\text{Na}}} \end{aligned} \quad (28)$$

Combining eqn. 27 and the expression for  $e_{\text{sal}}/e_{\text{gly}}$  (eqn. 25) results in  $\Delta\text{KRF} = 0$ , so that the zone is indeed allowed to move through the capillary.

For the description of this simple three-component system, it is not absolutely necessary to use the eigenvector–eigenvalue treatment; the same results can be obtained by applying the Kohlrausch function and the rules for electroneutrality. However, when more than two components are involved in the BGE and/or the ions possess dissociation constants, one has to use the eigenzone treatment with suitable refinement, in which also  $d\mu/d\text{pH}$  is allowed for [15].

## EXPERIMENTAL

### Instrumentation

The experimental apparatus used was laboratory built and essentially the same as described previously [17]. All the indirect UV detection measurements were done at 234 nm. For this wavelength also a calibration graph for salicylate was measured in the same way as previously described [18]. The capillary detection cell was laboratory made and has an adjustable slit. In all experiments, capillaries of I.D. 50  $\mu\text{m}$  and O.D. 350  $\mu\text{m}$  were used (Polymicro Technologies, Phoenix, AZ, USA). The slit in front of the detection window was adjusted to an aperture width of 50  $\mu\text{m}$ , which gives an optimum signal-to-noise ratio for this type of detection cell [18]. Separations in which potassium chloride was added to the buffer were carried out on a prototype PRINCE (programmable injector for capillary electrophoresis) from Lauer Labs. (Emmen, Nether-

lands) in combination with a FUG (Rosenheim, Germany) high-voltage power supply and a Spectra-Physics (Eindhoven, Netherlands) UV detector. This equipment allowed both accurate electrokinetic and pressure injection.

Separations were performed in 5 and 10 mmol/l salicylate solutions in a capillary with a total length of 59.0 cm and a length from the injection to detection point of 36.0 cm. Injection was done by electromigration at 6 kV for 5 s. The separation voltage was 15 kV with recorded currents between 5.0 and 5.2  $\mu\text{A}$ . The temperature in the air-thermostated safety box was  $24.0 \pm 0.2^\circ\text{C}$  (unless stated otherwise). In some experiments, KCl or 3-cyclohexylamino-1-propanesulphonic acid (CAPS) was added to the background electrolyte to study the influence of the ionic strength on plate number, sensitivity and concentration overload.

UV spectra of  $1 \cdot 10^{-4}$  mol/l sodium salicylate were measured with a Philips PU 8720 UV–VIS scanning spectrophotometer, using quartz cuvettes with an optical path length of 1 cm.

### Chemicals

Sodium salicylate and CAPS were obtained from Aldrich, valine and serine from Nutritional Biochemical, lysine, glutamic acid and sodium chloride from Merck, proline from Janssen Chimica and alanine from P-L Biochemicals.

## RESULTS

The application of indirect UV detection has been demonstrated with the separation of seven amino acids (listed in Table I) at pH 11, ranging in concentration from  $5 \cdot 10^{-3}$  to  $1 \cdot 10^{-3}$  mol/l and dissolved in the BGE. Working at this high pH was necessary to give the amino acids a net negative charge and different electrophoretic mobilities. From Table I, it can be seen that the majority of the amino acids (except proline) are nearly 100% dissociated at pH 11.0. Glutamic acid is doubly negatively charged as a result of the second carboxyl group in the molecule.

In Fig. 2A and B some typical electropherograms obtained with this system are depicted. In Fig. 2A, the salicylate concentration in the background electrolyte (BGE) was 5 mmol/l and in Fig. 2B 10 mmol/l. The sample concentration of each amino

TABLE I

DISSOCIATION CONSTANTS, MEASURED ELECTROPHORETIC MOBILITIES AND RELATIVE STANDARD DEVIATIONS AND RESPONSE FACTORS FOR THE AMINO ACIDS

For experimental conditions, see text.

Amino acid	$pK_a$	$\mu_{\text{eff}}^a$		Response factor <sup>b</sup>
		Value ( $10^{-5} \text{ cm}^2/\text{V} \cdot \text{s}$ )	R.S.D. (%)	
Proline	10.64	-16.8	1.2	1.044
Leucine	9.74	-23.0	0.6	1.191
Valine	9.74	-24.6	0.8	1.144
Alanine	9.92	-28.0	0.7	1.029
Serine	9.26	-29.5	0.5	1.073
Glycine	9.96	-32.6	0.4	0.937
Glutamic acid	9.96	-44.3	0.5	1.738
Salicylic acid <sup>c</sup>	3.11	-35.4		

<sup>a</sup> The mobilities are the mean values of six analyses.

<sup>b</sup> The response factors are calculated by the computer program, based on the theory as described.

<sup>c</sup> Values taken from ref. 19.

acid was 1 mmol/l in both instances. These electropherograms show again that indirect detection offers good possibilities for the detection of non-absorbing ions, in agreement with earlier papers by others [8–11]. The concentration detection limits are close to  $10^{-5}$  mol/l for this separation and detection system, which is in the same range as for normal HPCE with UV detection systems.

As discussed in the theoretical section, a large system peak can be observed in the electropherogram, which migrates with the electroosmotic velocity. The last eluting peak with the lowest overall mobility is glutamic acid, because it is double negatively charged and thus travels with the highest effective mobility, against the electroosmotic flow. The first appearing peak corresponds to proline. Proline, having a high  $pK_a$  value (see Table I), is only partly dissociated at pH 11.0, which causes the effective, electrophoretic mobility to be the smallest. This amino acid is very sensitive to small pH changes; for instance, a pH change from 11.0 to 10.8 gives a 15% reduction in electrophoretic mobility, whereas the reduction for the other amino acids is only between 1 and 3%. This is also an explanation for the observed higher relative standard deviation

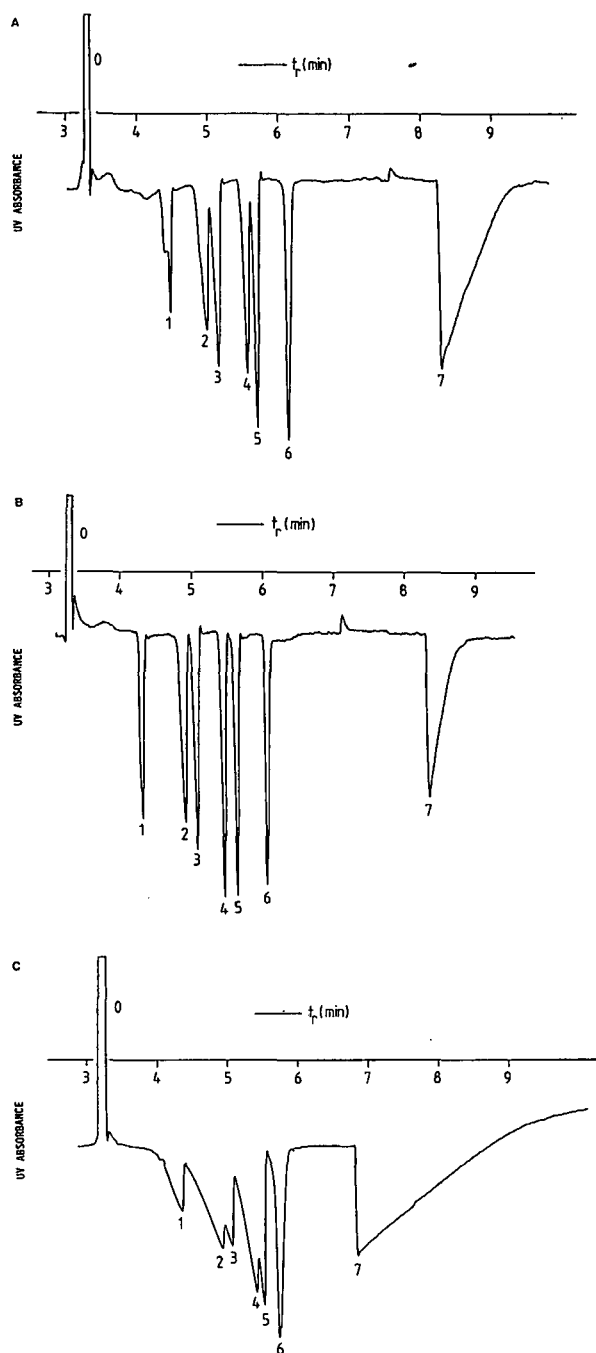


Fig. 2. Electropherograms of the separation of (1) proline, (2) leucine, (3) valine, (4) alanine, (5) serine, (6) glycine and (7) glutamic acid. Background electrolyte: sodium salicylate, pH 11.0. (A) 5 and (B) 10 mmol/l. Injection: 1 mmol/l of each amino acid. (C) Injection of 5 mmol/l of each amino acid, BGE = 5 mmol/l salicylate. For further experimental conditions, see text.

of the measurements of the electrophoretic mobility for this amino acid (Table I).

Overload can be very severe in indirect detection systems [16]. The peak deformation increases at higher sample concentrations and results in a loss of efficiency. This effect depends strongly on the sample/buffer concentration ratio, as can be seen in Fig. 2A and B. In Fig. 2A, the concentration overload, as witnessed by the triangular shape, is much stronger than in Fig. 2B, where 10 mmol/l was used. The experimentally determined effective mobilities of proline, leucine, valine, alanine and serine are smaller than the effective mobility of salicylate (see Table I). This results in fronting peaks, which is more pronounced when the sample/BGE concentration ratio increases. The electrophoretic mobility of glutamate is larger (more negative), resulting in badly tailing peaks [20]. The electrophoretic mobility of glycine nearly equals that of salicylate, which is why the conductivity of the glycine zone will not differ much from the BGE conductivity and peak deformation can be avoided. This is clearly illustrated in Fig. 2C, where 5 mmol/l of each amino acid was injected in a 5 mmol/l salicylate carrier. With this extreme example of concentration overload,

only glycine still has a more or less Gaussian peak shape. In Table I, the effective mobilities of the amino acids and their relative standard deviations (R.S.D.s) are given. Except for proline, all the R.S.D.s are below 1%.

In Fig. 3, a graph of the plate number  $N$  versus the electrophoretic mobilities of the amino acids is shown. It clearly demonstrates the above-mentioned effects with higher plate numbers for peaks having a mobility close to that of the background ion. It is noteworthy that the difference in plate number for 1 and 0.1 mmol/l glycine injection is smaller than for the other amino acids. This can be attributed to the smaller zone deformation for glycine, as explained earlier. The same trends as in Fig. 3 can be found for the situation with 10 mmol/l salicylate in the BGE. The plate numbers are higher, between 70 000 and 120 000 for injection of  $10^{-4}$  mol/l of each amino acid, because the effect of concentration overload is less pronounced.

To obtain an even better performance in this respect, one approach could be to increase the salicylate concentration further. Provided that the tube diameter is not too large and excessive heat dissipation can be avoided, this would certainly

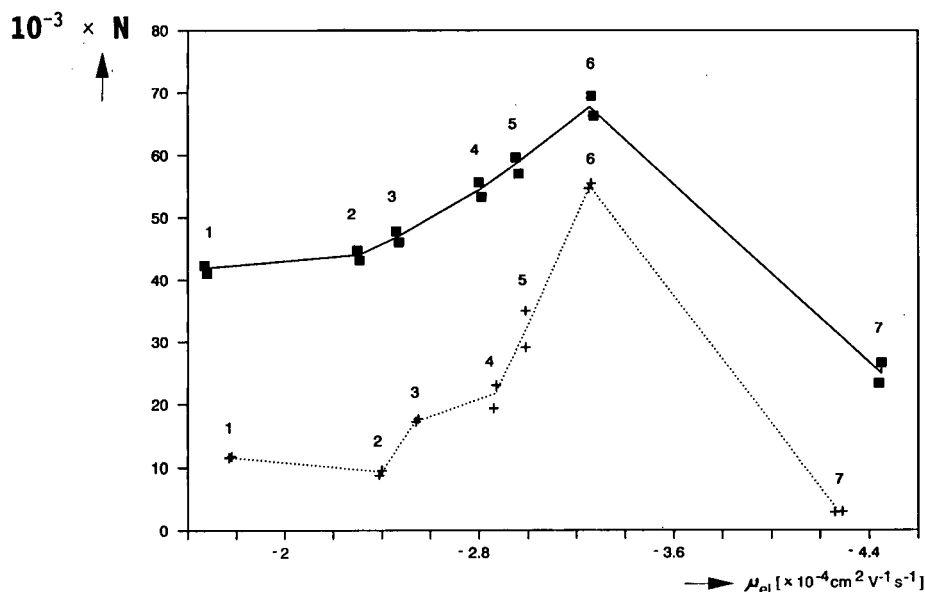


Fig. 3. Plate number versus electrophoretic mobility of the amino acids for two sample concentrations: solid line,  $10^{-4}$  mol/l amino acid; dotted line,  $10^{-3}$  mol/l amino acid. Numbers on the graphs correspond to those in Fig. 2.

improve the separation performance. However, indirect detection is likely to be adversely affected under such conditions, for two reasons. First, the UV absorbance signal turns out to be severely non-linear at salicylate concentrations above 0.01 mol/l, a result of optical non-idealities such as non-uniform path length and stray light. Hence, although the replacement ratio salicylate/sample ion will be virtually the same, the response in experimental absorbance units decreases, leading to a poorer signal-to-noise ratio. The above-mentioned effect is illustrated in Fig. 4, where peak area is plotted *versus* alanine concentration. Smaller peak areas are found for a BGE concentration of 10 mmol/l. It must be noted that as a result of manual electrokinetic injection and manual triangulation of peak areas to determine the area, the accuracy is less than that with an automated injection device.

Second, this degradation of the signal-to-noise ratio is amplified by the increase in noise at the high absorbance values occurring in most photometers. For instance, assuming a constant noise level,  $\sigma_I$ , in the intensity ( $I$ ) measurement, the conversion to absorbance units,  $A$ , would give a noise level,  $\sigma_A$ , of

$$\sigma_A = 0.4343 \frac{\sigma_I}{(I/I_0)} = 0.4343\sigma_I \cdot 10^A \quad (29)$$

which would predict a tenfold higher noise level at  $A = 1$ . Most UV detectors do not have a constant  $\sigma_I$  value; the  $\sigma_I$  value rather increases with  $I$ , with an exponent between 0.5 (shot noise-limited case) and

1.0 (source instability-limited case). For shot noise limitation one would obtain  $\sigma_A = \text{constant} \cdot 10^{0.5A}$  instead of eqn. 29. As indeed (partial) shot noise limitation (*i.e.*, source intensity limitation) is most common, an increase in  $\sigma_A$  with  $A$  can still be expected, although less severe than predicted by eqn. 29.

Preliminary experiments confirmed these expectations, so that the approach of higher salicylate concentration was abandoned.

Another approach would be to increase the ionic strength of the BGE by adding a buffer or a salt. This was tested by adding various concentrations of KCl to the sodium salicylate solution in both the BGE and the sample. In Fig. 5, the peak area of alanine is plotted *versus* KCl concentration. The salicylate concentration was kept constant at 5 mmol/l. Increasing the KCl concentration to 25 mmol/l resulted in a decrease in sensitivity by a factor of 2 (the peak area for alanine with 50 mmol/l in the BGE could not be determined properly, because of increasing thermal noise with increasing KCl concentration). The smaller sensitivity can be attributed to the decrease in the ratio  $e_{\text{sal}}/e_{\text{ala}}$  (eqn. 25) (see the next section). As can be seen in Fig. 5, there is no large difference between pressure injection and electrokinetic injection. For the electrokinetic injection the integrated peak area is larger because of the longer injection plug in this instance. When pressure injection was applied the integrated area had to be

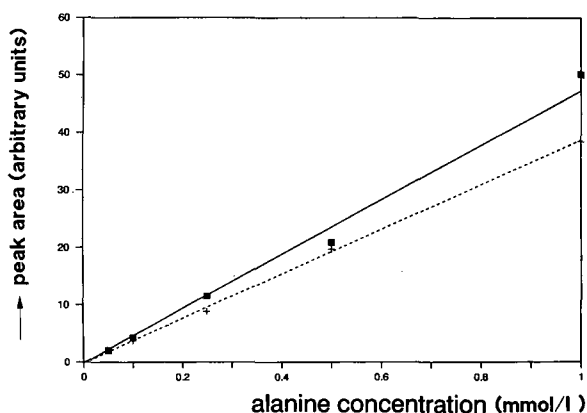


Fig. 4. Peak area *versus* alanine concentration. For experimental conditions, see text. Salicylate concentration: solid line, 5 mmol/l; dashed line, 10 mmol/l.

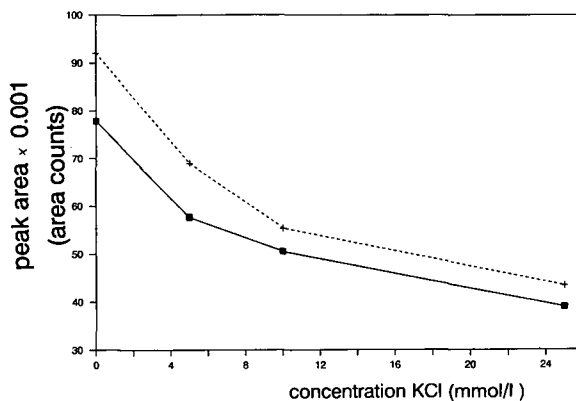


Fig. 5. Peak area of alanine *versus* KCl concentration. Injection of 0.1 mmol/l alanine dissolved in BGE (5 mmol/l salicylate, pH 11.0). Solid line, pressure injection,  $\Delta P = 80$  mbar,  $t_{\text{inj}} = 1.8$  s; dashed line, electrokinetic injection, 6 s, 6000 V.  $L = 59.0$  cm;  $l_{\text{inj-det}} = 41.5$  cm; voltage, 15 000 V;  $T = 30.0^\circ\text{C}$ .

TABLE II

CALCULATED RESPONSE FACTOR OF THE ALANINE PEAK AND MEASURED ELECTROOSMOTIC MOBILITY AS A FUNCTION OF KCl CONCENTRATION

Conditions used as input for the computer program: BGE, 5 mmol/l sodium salicylate, adjusted to pH 11.0 with sodium hydroxide. Absolute mobilities ( $10^{-5} \text{ cm}^2/\text{V} \cdot \text{s}$ ) for the cations and anions:  $\mu(\text{K}^+) = 76.2$ ,  $\mu(\text{Na}^+) = 51.9$ ,  $\mu(\text{Cl}^-) = 78.83$  (all taken from ref. 21),  $\mu(\text{salicylate}) = -35.4$ ,  $\text{p}K_a = 3.1$  (ref. 19);  $\mu(\text{alanine}) = -30.33$  (experimentally determined),  $\text{p}K_a = 9.92$ .

[KCl] (mmol/l)	Response factor	$10^5 \mu_{\text{eo}}$ ( $\text{cm}^2/\text{V} \cdot \text{s}$ )
0	1.029	86.6
5	0.863	77.4
10	0.742	72.2
25	0.523	64.9
50	0.351	59.8

corrected by a factor  $t_{\text{ala}}(\text{BGE1})/t_{\text{ala}}(\text{BGE2})$ , where  $t_{\text{ala}}$  is the migration time of the alanine zone. This correction has to be made in order to compensate for the decreased electroosmotic flow (see Table II) at higher ionic strength, which should give too high a peak area compared with the situation without KCl in the BGE. The correction can be omitted with electrokinetic injection, because one also injects less at higher ionic strength; the injection volume is smaller by the same correction factor. Here, the reduced injection volume and larger integrated area cancel. In Fig. 6, the observed plate numbers are

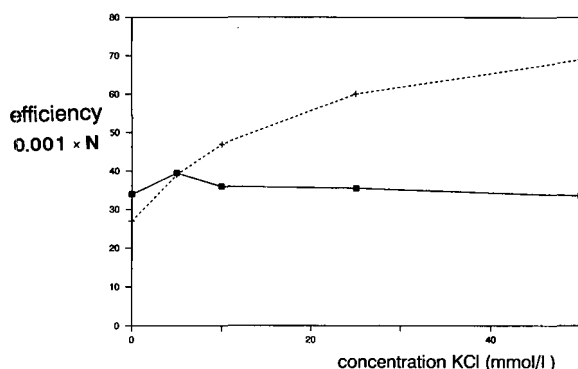


Fig. 6. Effect of KCl concentration on the efficiency of the alanine peak. Injection of 0.1 mmol/l alanine. Salicylate concentration = 5 mmol/l. Dashed line, electrokinetic injection; solid line, pressure injection. Experimental conditions as in Fig. 5.

plotted as a function of the KCl concentration. The efficiency increases from 27 000 plates at zero KCl content to 69 000 plates at 50 mmol/l KCl for an electrokinetic injection of  $1 \cdot 10^{-4}$  mol/l alanine. This gain in efficiency can be attributed to a combined effect of a smaller contribution from concentration overload and injection volume. In pressure injection, the efficiency is constant, because here the injection volume is the predominant source of zone broadening.

Buffering with CAPS, a zwitterion with a low mobility and buffering capacity at high pH, will contribute little to the conductivity of the BGE. This is expected to have a small negative effect on the sensitivity, whereas the stability of the indirect detection system will be increased. However, measurements showed that adding CAPS resulted in a threefold decrease in sensitivity (depending on the CAPS concentration). Also, an extra system peak with  $\mu_{\text{el}} = -18 \cdot 10^{-5} \text{ cm}^2/\text{V} \cdot \text{s}$  appeared in the electropherogram, which partly overlapped the proline peak.

#### Computer simulation of indirect detection

The theory described has been implemented in a computer program. The program itself and the possibilities are treated more into detail elsewhere [15]. The computer program can be a valuable tool to gain some insight into the ionic strength and conductivity of BGEs, the degree of peak deformation due to concentration overload, the response when indirect detection is used and the position and number of system peaks in the electropherogram.

The details of peak construction are also explained in detail elsewhere [15]. Usually, only two points of a peak are evaluated, one at zero sample concentration and the other at  $10^{-6}$  mol/l concentration. The difference in mobility represents the dependence of migration time on concentration. This is forced into a linear equation. By applying the mass balance, one can construct a triangle which would be the peak without other dispersive sources. The dispersion term caused by diffusion and injection is added to the width obtained from the non-linearity equation.

Here, some results from calculations on the response for the seven amino acids and some simulated electropherograms are presented in order to compare them with experimentally obtained



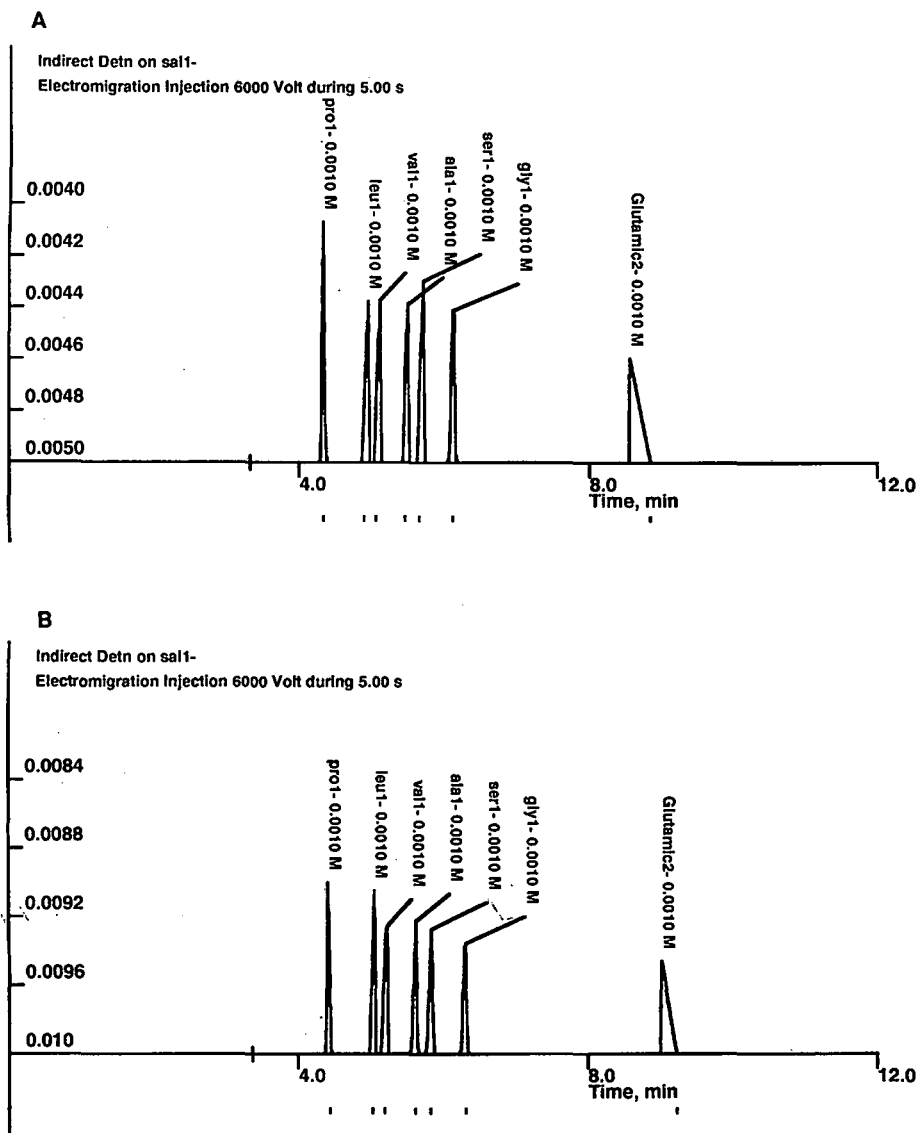


Fig. 7. Constructed electropherograms for two different BGEs at pH 11.0: (A) 5 and (B) 10 mmol/l salicylate. Injection of  $10^{-3}$  mol/l of each amino acid (5 s, 6 kV).  $\mu_{eo} = 71.1 \cdot 10^{-5}$  cm<sup>2</sup>/V · s;  $L = 59.0$  cm;  $l_{inj-det} = 36.0$  cm; voltage = 15 000 V. The small vertical line through the time axis corresponds to the position of the system peak.

results. As can be seen in Table I, for the glutamic acid peak the response factor is much larger than for the other amino acids, because of the double charge of this ion. Fig. 7A and B show simulated electropherograms with 5 and 10 mmol/l salicylate (pH 11.0) as the BGE. The fronting and tailing of the peaks, depending on the electrophoretic mobilities

relative to the salicylate mobility, are well predicted: fronting for the first five peaks, glycine with a reasonable gaussian shape and glutamic acid eluting with a tailing peak shape. The small vertical line through the time axis corresponds to the position of the system peak.

Also, the dependence of the response factor on the

composition of the BGE was calculated. In Table II the dependence of the response factor of alanine is given as a function of KCl concentration, the salicylate concentration being kept at 5 mmol/l. As can be seen, there is a decrease (by a factor of three) in sensitivity on going to 50 mmol/l KCl. The same trend was found in the experiment, as can be seen in Fig. 5. A decrease in sensitivity by a factor of 2 was observed at 25 mmol/l KCl, whereas the computer simulation gave a decrease in the response factor (replacement ratio) from 1.029 to 0.523.

## CONCLUSIONS

The separation and detection of amino acids is a good demonstration of the applicability of indirect UV detection in HPCE, in which detection limits of the order of  $10^{-5}$  mol/l can be obtained without difficulty. For 5 mmol/l salicylate in the background electrolyte, the sensitivity of the detection system was higher than for 10 mmol/l, because of the non-linearity of the calibration graph of salicylate at higher concentrations in this concentration range. However, a low BGE concentration results in lower efficiencies as a result of the stronger influence of concentration overload at higher sample concentrations. Adding KCl to the BGE diminishes the sensitivity, but increases the separation efficiency.

Adjusting the effective mobility to a value close to that of the background ion is one way to increase both the sensitivity and the efficiency. A problem, occurring regularly, was the instability of this indirect detection system. This could be seen as drift and/or large disturbances of the baseline. Indirect detection is a universal method; all ionic compounds that are present in the sample can be detected in principle, which is why the system is sensitive to impurities.

The simple background electrolyte used throughout this study, sodium salicylate at pH 11.0, has some disadvantages. The BGE has to be refreshed after a few hours of electrophoresis, because the pH shifts to lower values as a result of ion depletion and diffusion of carbon dioxide in the solution.

## ACKNOWLEDGEMENT

We thank Dr. Henk Lauer of Lauer Labs. for the loan of a prototype of the programmable injector for CE.

## REFERENCES

- 1 W. G. Kuhr and E. S. Yeung, *Anal. Chem.*, 60 (1988) 2642.
- 2 W. G. Kuhr and E. S. Yeung, *Anal. Chem.*, 60 (1988) 1832.
- 3 B. L. Hogan and E. S. Yeung *J. Chromatogr. Sci.*, 28 (1990) 15.
- 4 T. W. Garner and E. S. Yeung, *J. Chromatogr.*, 515 (1990) 639.
- 5 L. Gross and E. S. Yeung, *J. Chromatogr.*, 480 (1989) 169.
- 6 L. N. Amankwa and W. G. Kuhr, *Anal. Chem.*, 63 (1991) 1733.
- 7 T. M. Olefirowicz and A. G. Ewing, *J. Chromatogr.*, 499 (1990) 713.
- 8 S. Hjertén, K. Elenbring, F. Kilár, J. Liao, A. J. Chen, C. J. Siebert and M. Zhu, *J. Chromatogr.*, 403 (1987) 47.
- 9 M. T. Ackermans, F. M. Everaerts and J. L. Beckers, *J. Chromatogr.*, 549 (1991) 345.
- 10 F. Foret, S. Fanali, L. Ossicini and P. Boček, *J. Chromatogr.*, 470 (1989) 299.
- 11 M. W. F. Nielen, *J. Chromatogr.*, 588 (1991) 321.
- 12 R. Szücs, J. Vindevogel and P. Sandra, *J. High Resolut. Chromatogr.*, 14 (1991) 692.
- 13 J. Crommen, G. Schill, D. Westerlund and L. Hackzell, *Chromatographia*, 14 (1987) 252.
- 14 H. Poppe, *J. Chromatogr.*, 506 (1990) 45.
- 15 H. Poppe, *Anal. Chem.*, in press.
- 16 S. Hjertén, *Chromatogr. Rev.*, 9 (1967) 122.
- 17 G. J. M. Bruin, R. H. Huisden, J. C. Kraak and H. Poppe, *J. Chromatogr.*, 480 (1989) 339.
- 18 G. J. M. Bruin, G. Stegeman, A. C. van Asten, X. Xu, J. C. Kraak and H. Poppe, *J. Chromatogr.*, 559 (1991) 163.
- 19 T. Hirokawa, M. Nishino, N. Aoki, Y. Kiso, Y. Samamoto, T. Yagi and J. Akiyama, *J. Chromatogr.*, 271 (1983) D1–D106.
- 20 F. E. P. Mikkers, F. M. Everaerts and Th. P. E. M. Verheggen, *J. Chromatogr.*, 169 (1979) 1.
- 21 J. L. Beckers, Th. P. E. M. Verheggen and F. M. Everaerts, *J. Chromatogr.*, 452 (1988) 591.



# Membrane fraction collection for capillary electrophoresis

Yung-Fong Cheng, Martin Fuchs, David Andrews and William Carson

*Millipore Corporation, Waters Chromatography Division, 34 Maple Street, Milford, MA 01757 (USA)*

---

## ABSTRACT

A simple instrument system combining high-performance capillary electrophoresis (CE) and membrane technology is described. CE fraction collection is successfully implemented using a membrane assembly at the exit end of a capillary to complete the electrical circuit for electrophoretic separation. This membrane assembly consists of a poly(vinylidene difluoride) membrane, a buffer reservoir (two layers of 3 MM Chrom filter-paper) and a stainless-steel plate as the ground electrode. Two model proteins are separated and collected on the membrane. Direct protein sequencing is demonstrated from this membrane after CE fraction collection.

---

## INTRODUCTION

Membrane technology has found application in electrophoretic separations for some time, principally as a blotting medium on to which separated analytes (proteins or DNA) can be transferred after denaturing or non-denaturing one- or two-dimensional gel electrophoresis [1–4]. Following blotting, a wide variety of staining, immunoassay and chemical analysis techniques can be applied. With the rapid growth of powerful bioanalytical methods such as protein sequencing, membrane transfer media have found increased importance as substrates in such systems. Membrane materials such as poly(vinylidene difluoride) (PVDF) have been developed and their physical structures engineered to produce membranes with properties optimized for these kinds of applications [4,5]. Beck [6] demonstrated the direct blotting of analytes from a slab gel on to a moving membrane belt submerged in buffer solution.

In this paper, we demonstrate the feasibility of membrane fraction collection for capillary electrophoresis (CE). CE has developed into a powerful tool for the separation of ions and also neutral ana-

lytes because of its remarkable separation efficiency [7–11]. In CE, separation occurs in a capillary tube filled with an electrolyte and with the ends immersed in electrolyte reservoirs. Typically, the elution of the analytes is detected near one end of the capillary, and the separated species are discharged into the outlet reservoir. Previous attempts at fraction collection for CE have used small vials for sequential capture of eluted species. A high degree of dilution results. In addition, it is difficult to preserve the spatial resolution of closely spaced sample bands even when the capillary outlet is moved from one fraction vial to another using a programmable timer [12,13]. Hjertén and Zhu [14] used a variant of this technique in which analytes eluting from the electrophoresis capillary emerged into a flowing buffer stream and were carried to the test-tubes of a fraction collector.

Another approach for CE fraction collection, reported by Huang and Zare [15], utilizes a glass frit to create an electrical connection on-column. A porous frit is made near the exit end of a separation capillary. This frit is then immersed in a reservoir filled with electrolyte to complete the electric circuit for CE separation. This method reduces the dilution effect but it is difficult and time consuming to construct the fritted hole. In addition, a portion of the sample can be lost from the capillary through the frit and into the reservoir.

---

*Correspondence to:* Dr. Y.-F. Cheng, Millipore Corporation, Waters Chromatography Division, 34 Maple Street, Milford, MA 01757, USA.

We recently reported a simple and rugged means for recovering separated samples from a CE process without significant sample loss or dilution that still maintains good spatial resolution [16]. This paper describes further work with this simple instrument system combining CE separation and membrane technology. To demonstrate the utility of a membrane interface, direct protein sequencing of the recovered, separated proteins is described.

## EXPERIMENTAL

### Construction of the CE membrane fraction collector

The experimental configuration is illustrated in Fig. 1. A high-voltage d.c. power supply (Spellman High Voltage Electronics, Plainview, NY, USA) was used to provide a 20-kV potential for electrophoretic separation. The positive terminal of this power supply was applied to the sample or buffer vial and then across an untreated fused-silica capillary (Polymicro Technologies, Phoenix, AZ, USA) (70 cm  $\times$  75  $\mu$ m I.D.  $\times$  365  $\mu$ m O.D.). On-column detection was carried out at 58.5 cm from the injection end. UV absorbance was monitored at 210 nm (Model 206 PHD spectrophotometer; Linear Instruments, Reno, NV, USA). The ground terminal of the power supply was connected to the stainless-steel plate of the membrane assembly.

The membrane assembly consisted of an Immobilon-P transfer membrane (Millipore, Bedford, MA, USA), an electrolyte reservoir consisting of two layers of Whatman 3MM Chrom filter-paper (Whatman, Maidstone, UK) and a stainless-steel ground electrode connected to the ground end of

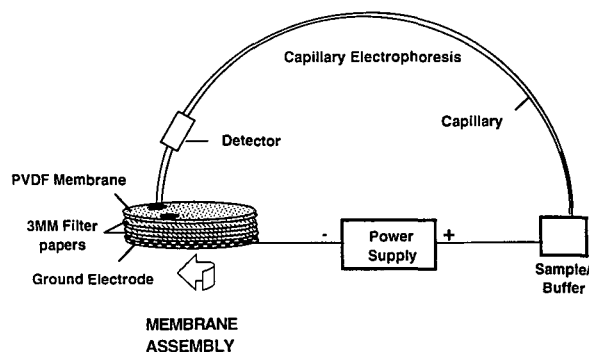


Fig. 1. Schematic diagram of membrane fraction collection for capillary electrophoresis.

the power supply. This membrane assembly was rotated by a stepping motor during electrophoretic separation at *ca.* 2.2 revolutions per hour.

### Sample and reagents

Myoglobin (horse heart, *pI* 6.76 and 7.16) and  $\beta$ -lactoglobulin (bovine milk, *pI* 5.13) were purchased from Sigma (St. Louis, MO, USA). A mixed myoglobin (8 mg/ml) and  $\beta$ -lactoglobulin (8 mg/ml) solution was prepared in 25 mM phosphate buffer (pH 7); 1 M zwitterion solution (AccuPure Z1-Methyl; Waters, Milford, MA, USA) was prepared in phosphate buffer (pH 7) to a final phosphate concentration of 20 mM.

Membrane staining reagent was prepared from 1.25 g of Brilliant Blue R250 (Coomassie Brilliant Blue R; Sigma) in 500 ml of a fixative solution (200 ml of methanol, 35 ml of glacial acetic acid and 265 ml of water). The destaining solution was methanol-water (90:10, v/v).

### Procedure

The procedure for membrane fraction collection for capillary electrophoresis is outlined as follows:

(1) An electrolyte reservoir consisting of two layers of 3MM Chrom filter-paper saturated with phosphate buffer was laid on top of a stainless-steel ground electrode.

(2) A PVDF membrane was prewetted with methanol for 5 s and then laid on top of the electrolyte reservoir (taking care to remove any air bubbles trapped in between).

(3) The membrane assembly was raised to provide good contact with the exit end of the capillary.

(4) The sample solution was injected via electromigration at 6 kV for 10 s. Electrophoretic separation was run at 20 kV using a phosphate buffer with or without added zwitterions.

(5) Rotation of the membrane assembly was started at the beginning of the run; the voltage was turned off after the 20-min CE separation and the membrane was removed from the assembly.

(6) The membrane was stained with Coomassie Brilliant Blue solution for *ca.* 10 min and destained three times.

### Direct protein sequencing

The protein bands were excised with a clean razor blade and then subjected to automated Edman deg-

radiation in a Waters Model 6600 ProSequencer. The whole  $\beta$ -lactoglobulin band was subjected to sequencing, and only a portion of the myoglobin band was sequenced. No precycling of solvent or reagents was performed and degradations were done using the ADS100 (adsorptive) protocol with automatic on-line high-performance liquid chromatographic (HPLC) identification of PTH-amino acids. PTH-amino acids were measured at 269 nm, with dehydro derivatives of serine and threonine residues confirmed by detection at 313 nm.

The PTH-Maxima chromatography analysis software package (Waters) provides a data analysis in which successive HPLC traces are first optimally aligned and then subtracted to give difference traces for adjacent residues. Difference peak-area data were reduced to a semilog arithmetic plot of  $\log(\text{PTH yield})$  versus cycle number and a line fitted by least-squares regression analysis. The average repetitive sequencing yield was derived from the slope of a least-squares regression linear fit to the data.

## RESULTS AND DISCUSSION

### Membrane fraction collection

The two-component mixture containing myoglobin and  $\beta$ -lactoglobulin in phosphate buffer (pH 7) was injected into the capillary of the system shown in Fig. 1. The grounding of the capillary was through the PVDF membrane laid on top of the filter-paper electrolyte reservoir containing sorbed buffer solution. The current during the separation is shown in the upper trace in Fig. 2. The current fluctuated between 100 and 125  $\mu\text{A}$ . This fluctuation is due to Joule heating in the capillary and the fact that the capillary was operated in open air. It was also found that the current fluctuated between 100 and 125  $\mu\text{A}$  for the next four consecutive electrophoretic separations which used the same applied voltage and buffer. We have previously reported that the presence of the membrane assembly does not significantly affect the current observed during the separation, indicating that the membrane does not introduce significant additional resistance to current flow [16].

The separation of these two model proteins is shown in the lower trace in Fig. 2. Peaks A<sub>1</sub> and A<sub>2</sub> are myoglobin (pI 7.16 and 6.76, respectively) and peak B is  $\beta$ -lactoglobulin (pI 5.13).

CE fraction collection onto a continuously rotating PVDF membrane is demonstrated in Fig. 3. This figure, representing a membrane after staining and destaining with Coomassie Brilliant Blue, illustrates the resulting collection from five consecutive injections of a two-component mixture of the above sample solution. The membrane assembly was rotated to the same position prior to each run. Many blue spots are clearly visible in this picture and the reproducibility of the analysis is unacceptable. This phenomenon is due to migration time shifts during successive CE separations. The relative standard deviation (R.S.D.) was found to be 7.7% and 11.6% for the migration time of myoglobin (peak A<sub>1</sub> in Fig. 2) and  $\beta$ -lactoglobulin (peak B in Fig. 2), respectively. This observation suggests that the capillary inner surface was progressively modified by

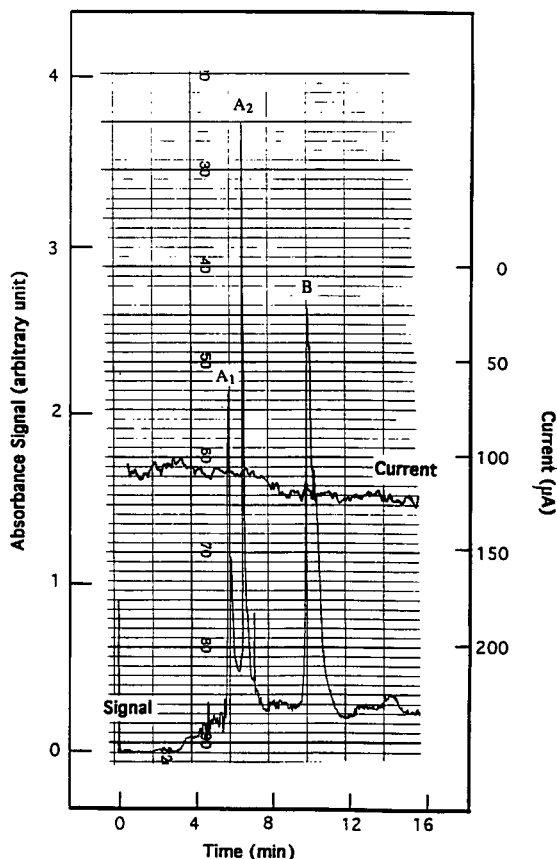


Fig. 2. Electropherogram (lower trace) and current (upper trace) for the separation of a mixture of myoglobin and  $\beta$ -lactoglobulin in a pure running buffer system.

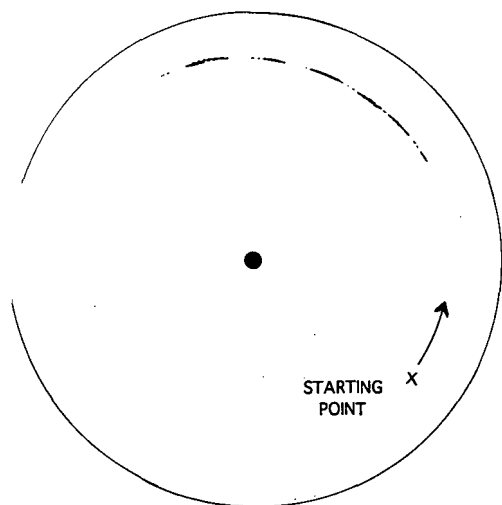


Fig. 3. Photocopy of membrane after staining and destaining with Coomassie Brilliant Blue from five consecutive CE membrane fraction collections in a pure running buffer system.

irreversible adsorption of protein. Similar results have been observed in other protein separations [17–20].

#### *Effect of zwitterion solution of CE membrane fraction collection*

Some of the methods that have been used to counteract adsorption include electrophoresis in buffers with a pH higher than the isoelectric point of the sample proteins [17], electrophoresis in buffers with a very low pH [18] and capillary surface treatments [19,20]. To improve the migration time reproducibility in the present experiments, a zwitterionic compound (AccuPure Z1-Methyl) was added to the buffer solution. This particular compound has a high dipole moment, a zwitterionic character over a broad pH range, good solubility in aqueous buffers and low UV absorbance (0.2 absorbance for a 1-M aqueous solution at 214 nm, 1-cm path length).

The lower trace in Fig. 4 shows the electropherogram from one of the four consecutive injections of the previous two-component mixture containing myoglobin and  $\beta$ -lactoglobulin using 1 M zwitterion in phosphate buffer. The current fluctuated between 52 and 56  $\mu$ A, as shown in the upper trace in Fig. 4. Running the experiment with the AccuPure Z1-Methyl additive greatly improved the reproduc-

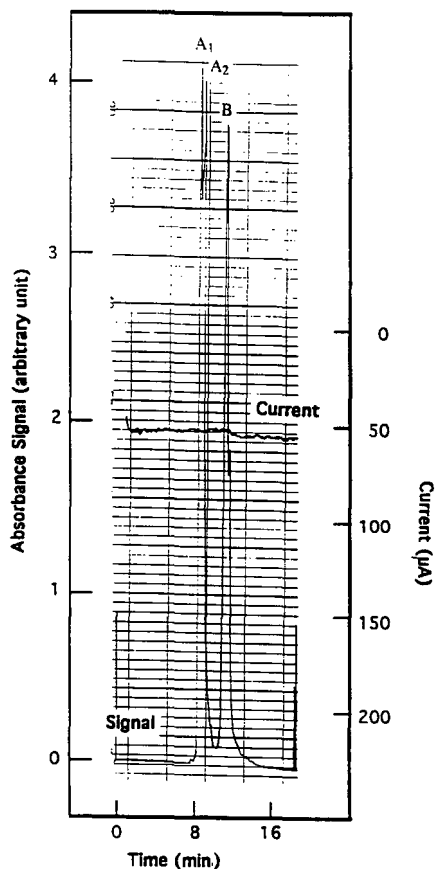


Fig. 4. Electropherogram (lower trace) and current (upper trace) for the separation of a mixture of myoglobin and  $\beta$ -lactoglobulin in a phosphate buffer-1 M zwitterion additive system.

ibility and peak shape, also yielding a better signal-to-noise ratio. The R.S.D. was found to be 0.6% and 1.1% for the migration time of myoglobin (peak A<sub>1</sub>) and  $\beta$ -lactoglobulin (peak B), respectively. Average migration times and R.S.D.s for the separation of these two proteins with and without zwitterion modifier are given in Table I. A longer migration time was observed when the zwitterions was added to pure running buffer solution, owing to the increased viscosity. The resolution between peaks A<sub>1</sub> and A<sub>2</sub> in a pure running buffer system (as shown in the lower trace in Fig. 2) is better than in the 1-M zwitterion additive buffer system (as shown in the lower trace in Fig. 4). Perhaps the zwitterions interact with the protein analytes.

The improved migration time reproducibility of

TABLE I

COMPARISON OF AVERAGE MIGRATION TIMES AND RELATIVE STANDARD DEVIATIONS FOR THE SEPARATION OF PROTEIN WITH AND WITHOUT ZWITTERION MODIFIER (1 M) IN THE RUNNING BUFFER

Component	Migration time (min)			
	Without zwitterion		With zwitterion	
	Mean (n = 5)	R.S.D. (%)	Mean (n = 4)	R.S.D. (%)
Myoglobin	5.90	7.7	8.68	0.6
$\beta$ -Lactoglobulin	9.12	11.6	10.90	1.1

CE separation when zwitterions were added to the running buffer solution generated better fraction collection onto a membrane. Fig. 5 shows, after staining and destaining with Coomassie Brilliant Blue, the resulting fraction collection from four consecutive fraction collections using 1 M zwitterion additive in the buffer. Only two elongated blue spots are clearly visible. Spot A is myoglobin and spot B is  $\beta$ -lactoglobulin. The amount of each solute introduced into the capillary is determined by

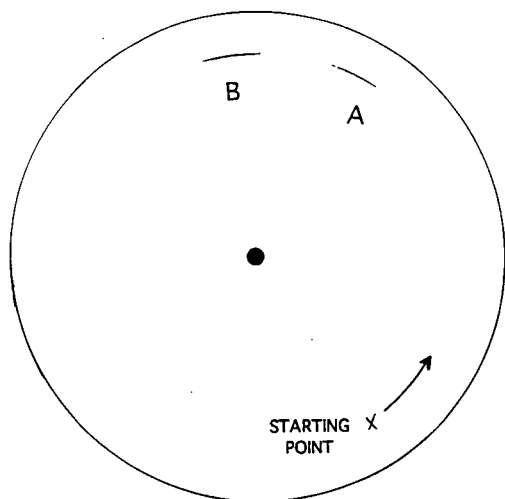


Fig. 5. Photocopy of membrane after staining and destaining with Coomassie Brilliant Blue from four consecutive CE membrane fraction collections in a phosphate buffer–1 M zwitterion additive system.

the mobility of the solute. On this basis, we calculate the total amounts introduced into the capillary from a total four replicate injections to be 28 pmol of myoglobin and 10.8 pmol of  $\beta$ -lactoglobulin.

The spatial resolution of the CE separation is preserved in the pattern on the membrane. It is possible to reduce the length of the spots along the writing track and to increase the distance between separated species on the track, as one can adjust the speed of the motorized fraction collection carousel. From the distance between the on-line detector and the exit end of the capillary, the calculated mobility of each analyte and the width of each peak, the times at which the carousel speed should be reduced or increased can be calculated.

#### Direct protein sequencing from the immobilon-P transfer membrane after CE fraction collection

Coomassie Brilliant Blue-stained bands from the above four replicate CE membrane fraction collection were excised from PVDF membrane and subjected to sequence analysis. A representative sequence of the amino terminal fragment is shown in Figs. 6 and 7 for myoglobin and  $\beta$ -lactoglobulin, respectively.

The repetitive yield was 97.8% and 97.6% for myoglobin and  $\beta$ -lactoglobulin, as shown in Figs. 8 and 9, respectively. The initial yields were 1.9 and 6.8 pmol for myoglobin and  $\beta$ -lactoglobulin. Initial yield is defined as the amount of each protein band loaded on to the sequencer holder (not the total amount of each protein injected onto the capillary for CE separation) that gives a phenylthiohydantoin (PTH) signal in the first sequencing cycle; therefore, the recoverd yield for  $\beta$ -lactoglobulin is 63% (as calculated by 6.8/10.8 picomoles), as the entire  $\beta$ -lactoglobulin band was subjected to protein sequencing.

#### CONCLUSIONS

The feasibility of membrane fraction collection for CE has been demonstrated. The system is simple, cost-effective, rugged and efficient. The advantage of the system is that it enables one to collect separated sample species from high performance capillary electrophoresis continuously while preserving the spatial resolution and preventing dilution. Sample species collected on a membrane after



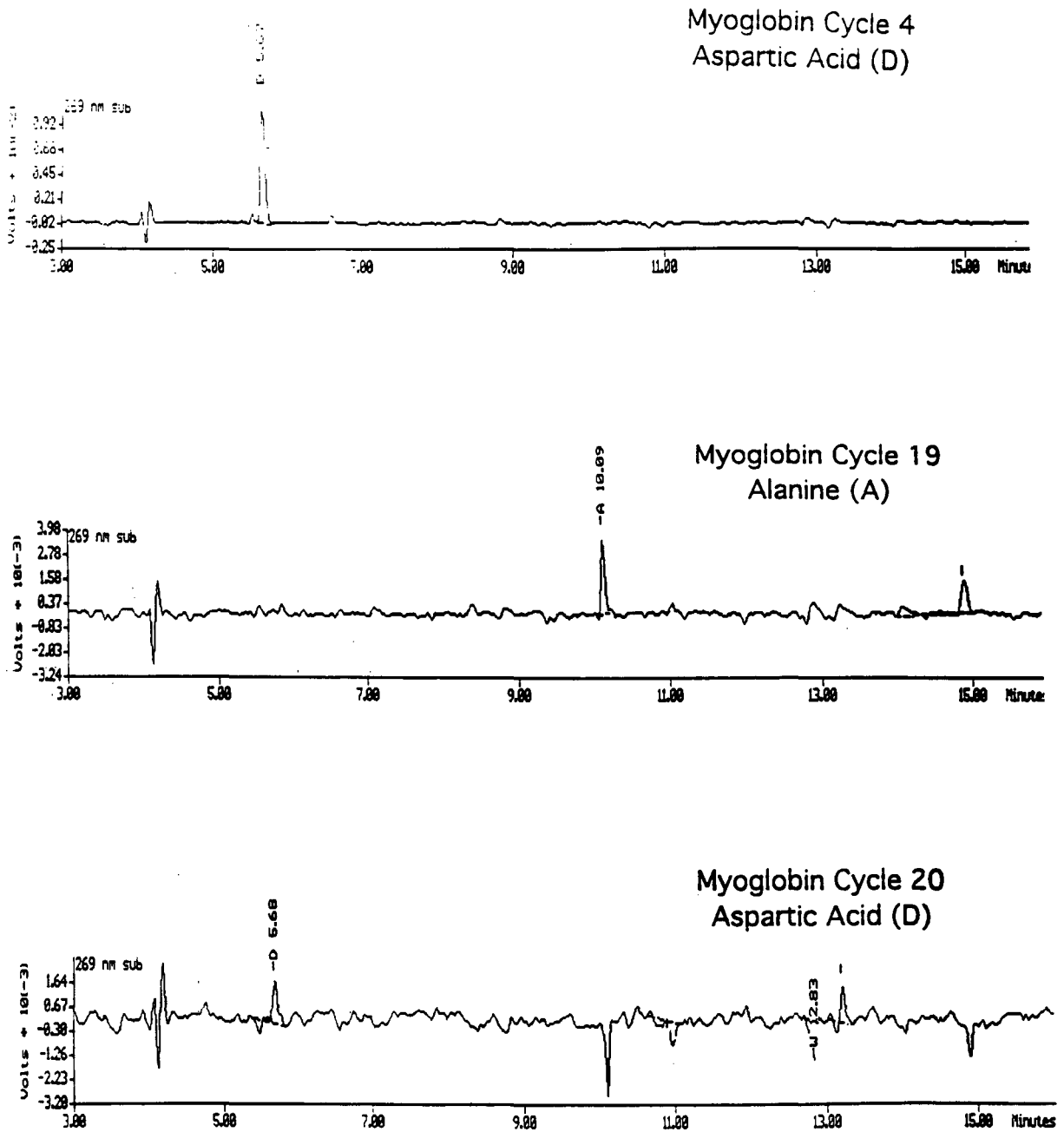


Fig. 6. Representative sequencer cycles from direct sequence analysis of myoglobin after CE membrane fraction collection on to an underivatized PVDF membrane.

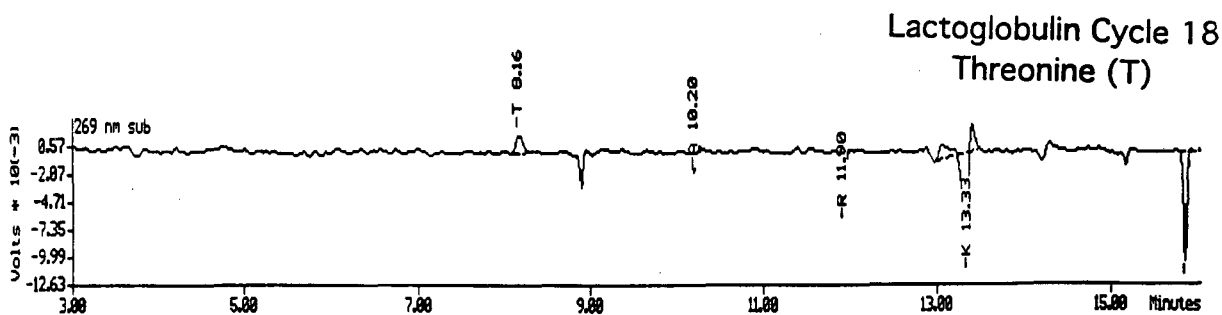
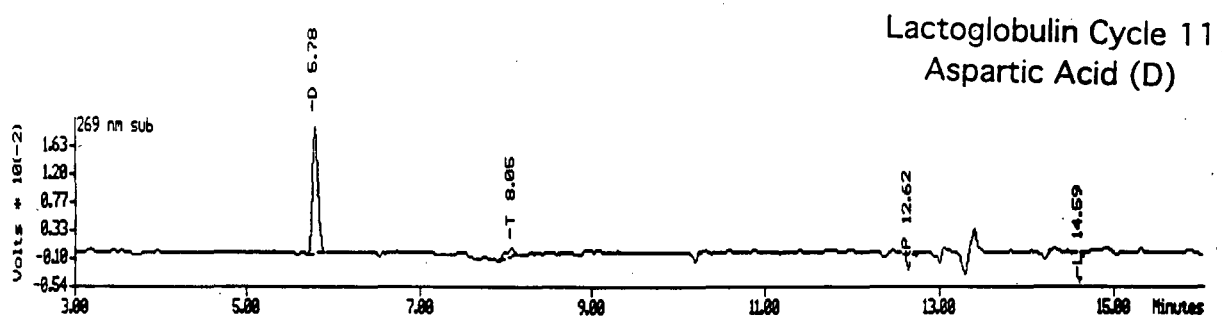
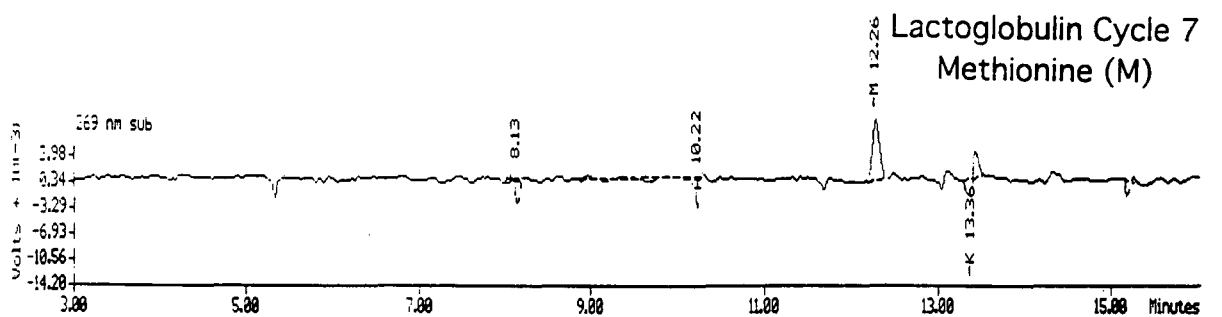


Fig. 7. Representative sequencer cycles from direct sequence analysis of  $\beta$ -lactoglobulin after CE membrane fraction collection on to an underivatized PVDF membrane.

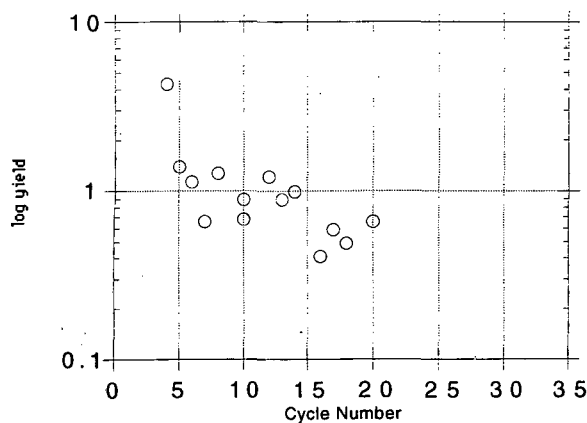


Fig. 8. Yield (O, pm) plot from the direct sequence analysis of myoglobin after CE membrane fraction collection.

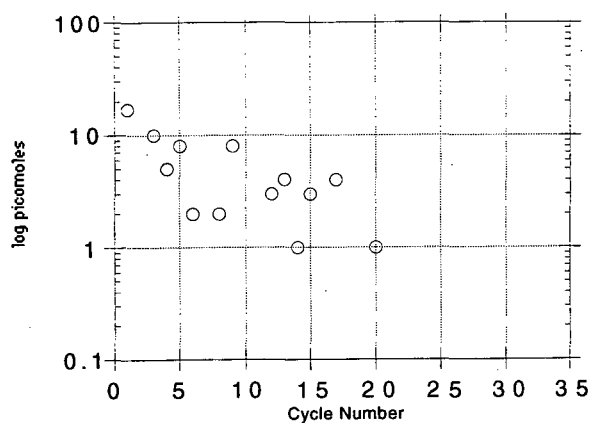


Fig. 9. Yield (O, pm) plot from the direct sequence analysis of  $\beta$ -lactoglobulin after CE membrane fraction collection.

CE separation have been successfully sequenced through direct protein sequence analysis. The combination of high-efficiency CE separation and membrane technology will provide a powerful tool for bioanalysis.

#### ACKNOWLEDGEMENT

We thank Dr. Malcolm Pluskal for helpful discussions on PVDF membrane technology.

#### REFERENCES

- H. Gultekin and K. Heermann, *Anal. Biochem.*, 172 (1988) 320.
- D. Hicks and C. Vecoli, *Biotechniques*, 5 (1987) 206.
- N. LeGendre and P. Matsudaira, *Biotechniques*, 6 (1988) 154.
- G. P. Malcolm, M. B. Przekop, M. R. Kavonian, C. Vecoli and D. Hicks, *Biotechniques*, 4 (1986) 272.
- R. H. Aebersold, D. B. Teplow, L. E. Hood and S. B. H Kent, *J. Biol. Chem.*, 261 (1986) 4229.
- S. Beck, in M. J. Dunn (Editor), *Electrophoresis '86*, VCH, Weinheim, 1986, p. 173.
- J. W. Jorgenson and K. D. Lukacs, *Anal. Chem.*, 53 (1981) 1298.
- J. W. Jorgenson and K. D. Lukacs, *Science*, 222 (1983) 266.
- H. Swerdlow, J. Z. Zhong, D. Y. Chen, H. R. Hark, R. Grey, S. Wu and N. J. Dovichi, *Anal. Chem.*, 63 (1991) 2835.
- Y. F. Cheng and N. J. Dovichi, *Science*, 242 (1988) 562.
- W. R. Jones and P. Jandik, *Am. Lab.*, 22 (1990) 51.
- D. Rose and J. W. Jorgenson, *J. Chromatogr.*, 438 (1988) 23.
- A. S. Cohen, D. R. Najarian, A. Paulus, A. Guttman, J. A. Smith and B. L. Karger, *Proc. Natl. Acad. Sci. U.S.A.*, 85 (1988) 9660.
- S. Hjertén and M.-D. Zhu, *J. Chromatogr.*, 327 (1985) 157.
- X. Huang and R. Zare, *Anal. Chem.*, 62 (1990) 443.
- Y. F. Cheng, M. Fuchs and W. Carson, *Biotechniques*, in press.
- H. Lauer and D. McManigill, *Anal. Chem.*, 58 (1986) 166.
- R. M. McCormick, *Anal. Chem.*, 60 (1988) 2322.
- S. Hjertén, *J. Chromatogr.*, 347 (1985) 191.
- K. Cobb, V. Dolnik and M. Novotny, *Anal. Chem.*, 62 (1990) 2478.

# Low-cost laser-induced fluorescence detector for micellar capillary zone electrophoresis

## Detection at the zeptomol level of tetramethylrhodamine thiocarbamyl amino acid derivatives

Jian-Ying Zhao, Da-Yong Chen and Norman J. Dovichi

*Department of Chemistry, University of Alberta, Edmonton, Alberta T6G 2G2 (Canada)*

---

### ABSTRACT

Tetramethylrhodamine thiocarbamyl (TRTC) amino acid derivatives are determined by micellar capillary zone electrophoresis with laser-induced fluorescence detection. A post-column fluorescence cell, based on a sheath-flow cuvette, is used as the detection chamber. A low-cost and low-power helium–neon laser, operating in the green at 543.5 nm, is used to excite the TRTC-amino acids. The relatively long excitation wavelength, the low-light scatter of the sheath-flow cuvette and the low excitation power result in a very low background signal, which is dominated at room temperature by detector dark current. To minimize the dark current, a cooled photomultiplier tube was used for photodetection. Detection limits ( $3\sigma$ ) are  $1 \cdot 10^{-21}$  mol (600 molecules) injected onto the capillary.

---

### INTRODUCTION

Isothiocyanate derivatives of amino acids are of interest in Edman degradation sequence determination of proteins. The classic Edman reagent, phenyl isothiocyanate (PITC), is universally used in commercial protein sequencers [1]. The products of the sequencing reaction, phenyl thiohydantoin (PTH) derivatives of amino acids, have been separated by capillary electrophoresis and detected by ultraviolet absorbance [2]. Detection limits are about 100 fmol of the PTH derivatives with UV transmission detection. Other isothiocyanates may be used in the sequencing reaction. For example, dimethylaminoazobenzene isothiocyanate is used to produce the non-fluorescent dimethylaminoazobenzene thiohydantoin (DABTH) derivative that absorbs in the

blue portion of the spectrum, with detection limits of *ca.* 100 fmol with liquid chromatographic separation and transmission detection. Sub-femtomole detection limits are produced for the PTH and DABTH derivatives with capillary electrophoretic separation and thermo-optical absorbance detection [3,4].

Fluorescent isothiocyanates can produce excellent detection limits for amino acids, roughly eight orders of magnitude superior to classic absorbance detection limits. This research group has described high-sensitivity detection of fluorescein isothiocyanate (FITC) derivatives of amino acid [3,5,6]. Fluorescein has strong absorbance at the argon ion laser emission wavelength of 488 nm, has high fluorescent quantum efficiency (*ca.* 0.5), but suffers from mediocre photobleaching properties [7]. The best detection limits reported by this laboratory for fluorescein thiohydantoin and thiocarbamyl derivatives of amino acids range from 1 to 2 zepto ( $10^{-21}$ ) mol of derivative injected onto the capillary. Recently,

---

*Correspondence to:* Professor N. J. Dovichi, Department of Chemistry, University of Alberta, Edmonton, Alberta T6G 2G2, Canada.

other laboratories have reported detection limits of 10–20 zeptomol for fluorescein thiocarbamyl amino acid derivatives [8,9].

Tetramethylrhodamine isothiocyanate (TRITC) is an interesting modified Edman degradation reagent. The molecule has similar structure to FITC and should have similar reaction characteristics. TRITC absorbs strongly in the green portion of the spectrum and emits in the red. TRITC has been used to label immunological reagents for histological applications [10]; the red emission of TRITC contrasts nicely with the green emission of FITC in double-labeling experiments. The same chromophore is used by Applied Biosystems as their TAMRA-labeled primer for DNA sequencing.

TRITC offers useful spectroscopic properties for ultra-sensitive detection. The maximum absorbance is greater than  $100\,000\text{ l mol}^{-1}\text{ cm}^{-1}$  at 540 nm while the emission maximum is 567 nm [10]. Soper *et al.* [11] have reported a fluorescence quantum yield of 15% and a photodestruction rate of  $5 \cdot 10^{-6}$  in aqueous solutions. From a practical standpoint, the most important property of the dye is that is conveniently excited by the recently commercialized green helium–neon laser, which produces a 0.75-mW beam at 543.5 nm. The longer-wavelength excitation, compared with 488 nm excitation of fluorescein, produces a decrease in background signal due to the  $\nu^4$  property of light scatter. This green helium–neon laser is similar in construction to the conventional red helium–neon laser and should have similar lifetime, cost and power.

In this paper, we describe the use of TRITC to label amino acids for separation by capillary zone electrophoresis. While this research group has produced zeptomole detection limits for TAMRA-labeled DNA fragments separated by capillary gel electrophoresis [12,13], we know of no applications of the fluorophore for determination of small molecules by electrophoresis. The excitation of TRITC-labeled analyte with the green helium–neon laser results in a low-cost fluorescence detector with detection limits of 1 zeptomol.

## EXPERIMENTAL

Separation was carried out with a  $92\text{ cm} \times 50\text{ }\mu\text{m}$  I.D. fused-silica capillary. The separation buffer was 5 mM pH 9.0 boric acid buffer with 10 mM

sodium dodecyl sulphate. Electrophoresis was driven at 30 kV; the high-voltage (injection) end of the capillary was placed in a safety interlock-equipped Plexiglass box. Sample was injected electrokinetically at 1 kV for 10 s. The detector was locally constructed and is described below.

The beam from a 0.75-mW, 543.5-nm-wavelength, helium–neon laser (Melles Griot, Canada) was focused with a  $4\times$  microscope objective about  $200\text{ }\mu\text{m}$  below the exit of the capillary in a post-column fluorescence flow chamber. The fluorescence detector is based on a sheath-flow cuvette and is similar to that used in FITC detection. The locally assembled cuvette has a  $200\text{-}\mu\text{m}^2$  flow chamber (NSG-Precision Cells, Farmingdale, NY, USA) and 2-mm-thick windows. Fluorescence is collected at right angles with an  $18\times$ , 0.45 numerical aperture objective (Melles Griot) and imaged onto a 0.8-mm-diameter pinhole. A single interference filter (590 nm center, 40 nm band pass, Model 590DF35, Omega Optical, Vermont, NE, USA) blocks scattered laser light while passing much of the fluorescence. Fluorescence was detected with a Hamamatsu (CA, USA) R1477 photomultiplier tube, operated at 1000 V and cooled to  $-25^\circ\text{C}$  with a Products for Research (MA, USA) photomultiplier tube cooler. The photomultiplier tube output was passed through a 0.1-s resistor-capacitor (RC) low-pass filter and displayed on a strip-chart recorder.

Stock amino acid solutions were prepared in 0.2 M pH 8.6 boric acid buffer. Tetramethylrhodamine thiocarbamyl (TRTC) amino acid derivatives were produced by reacting  $800\text{ }\mu\text{l}$  of  $7 \cdot 10^{-5}\text{ M}$  TRITC (Molecular Probes, Eugene, OR, USA) with  $500\text{ }\mu\text{l}$  of 1–3 mM amino acid solution which was allowed to react at room temperature for 20 h in the dark. The TRTC-amino acids were diluted to the desired concentration with the separation buffer.

## RESULTS AND DISCUSSION

The reaction of TRITC with amino acids is rather sluggish at room temperature. Samples of TRTC-glycine were allowed to react over a 10-h period. Small samples were removed from the reaction mixture and analyzed electrophoretically. The average of two or three determinations of the TRTC-amino acid peak height is plotted in Fig. 1; the data are connected by lines as a visual aid. The

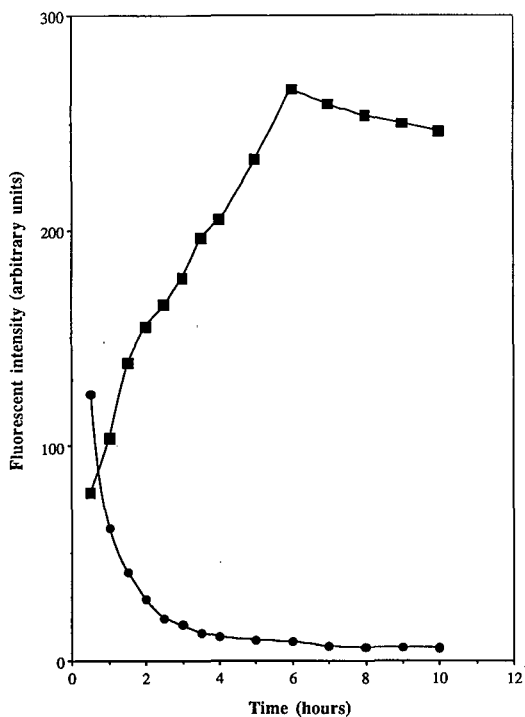


Fig. 1. Reaction efficiency of tetramethylrhodamine isothiocyanate with glycine. ■ = TRTC-glycine; ● = TRITC.

squares correspond to the production of TRTC-glycine while the circles correspond to unreacted TRITC. In this reaction, the amino acid was present in nearly eighteen-fold excess, so that consumption of TRITC and production of TRTC-amino acid are expected to follow first-order kinetics with the same rate constant. Instead, TRITC disappears more rapidly than TRTC-glycine is produced. It appears that TRITC undergoes both reaction with the amino acid and decomposition. Similar behavior has been observed in this laboratory for FITC reaction with amino acids. The isothiocyanates are not particularly stable in protic solvents, presumably undergoing hydrolysis to generate non-fluorescent products. At room temperature, TRITC disappears after about 6–8 h. Analyte concentrations are calculated based on TRITC as the limiting reagent and the assumption that the reaction goes to completion. As a result, the instrumental detection limits quoted below must be interpreted as being upper bounds to the actual detection limit.

Fig. 2 presents the electropherogram of twenty

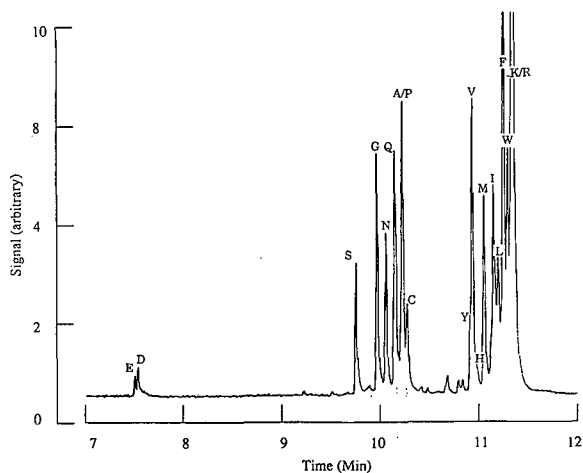


Fig. 2. Electropherogram of twenty TRTC-amino acids. The symbols for each amino acid correspond to the standard one-letter abbreviation.

amino acids. As is typical for zone electrophoretic separation of other thiocarbamyl derivatives of amino acids, separation is not complete; alanine and proline co-elute as do lysine, arginine and TRITC. However, the separation of the remaining amino acids is good and the total separation time is 12 min. On the other hand, the theoretical plate count for the separation is on the order of  $2 \cdot 10^6$  plates. This separation demonstrates that high plate counts do not automatically translate into high resolution. The large size of the derivatizing reagent dwarfs small differences in the size of the amino acids. The size-to-charge ratio of the amino acid derivatives is quite similar and baseline separation is not achieved.

Detection limits are calculated by the method of Knoll [14]; the baseline is inspected over a time period given by 50 times the peak width. The maximum deviation from the average of the baseline is used to estimate the  $3\sigma$  detection limit. This technique, based on the Tchebycheff inequality [14], relies on robust statistics. Very weak assumptions are made on the underlying noise distribution in the data. More importantly, correlation introduced between adjacent datum due to filtering does not artificially underestimate the standard deviation of the baseline. Relatively precise estimates of the detection limit are produced by inspecting baseline over a large number of samples. The  $3\sigma$  detection limit for TRTC-glycine was  $1 \cdot 10^{-12}$  M labeled amino acid

injected onto the capillary. Injection volume was estimated to be 1 nl for this amino acid, so that detection limits correspond to 1 zeptomol of amino acid injected onto the capillary. A 1-zeptomol amount of analyte corresponds to 600 analyte molecules. The detection volume, defined by the intersection of the laser beam and sample stream, was estimated to be 10 pl. There are 5 analyte molecules present on average in the detection volume at the detection limit.

Isothiocyanate derivatives are of interest for protein sequencing. However, given the sluggish nature of the isothiocyanate reaction, other derivatizing reagents are of interest for general amino acid analysis. The most interesting reagents are those that absorb strongly at the excitation wavelength of readily available lasers [15]. Derivatizing reagents that have been coupled with laser-induced fluorescence detection include *o*-phthalaldehyde excited by an argon ion laser operating in the ultraviolet region at 351 and 363 nm [16], Dansyl excited by a helium–cadmium laser at 325 nm [17], naphthalenedialdehyde (NDA) excited by the 457.9-nm line of an argon ion laser [18], fluorescamine-labeled amino acids excited at 325 nm with a mercury lamp [19] and 3-(4-carboxybenzoyl)-2-quinolinecarboxaldehyde excited at 442 nm with a helium–cadmium laser [20]. It will be interesting to see if zeptomole amino acid analysis is possible with these derivatives.

## CONCLUSIONS

TRITC may be used to label amino acids, producing the thiocarbonyl derivatives. These derivatives may be separated by capillary electrophoresis and detected with high sensitivity by a low-cost laser-induced fluorescence system. Detection limits are 1 zeptomole of TRITC-glycine injected onto the capillary.

Tetramethylrhodamine isothiocyanate reacts relatively slowly with amino acids; the reaction rate is far too sluggish for routine use in protein sequencing. The classic Edman reagent, PITC, will react in less than 30 min. An equal-concentration mixture of PITC and TRITC can be used in a double-coupling sequencing reaction. The reaction with both reagents will yield a large excess of the PTH and a small amount of tetramethylrhodamine thiohydantoin after each step in the Edman cycle. The PITC is not detected but instead used to scavenge any unreacted *n*-terminal amino acids. The tetramethylrho-

damine-labeled amino acids can be detected with exquisite sensitivity. Even if the tetramethylrhodamine reaction efficiency is 0.1% of the reaction efficiency of PITC, proteins may be sequenced with attomol sensitivity.

## ACKNOWLEDGEMENTS

This work was funded by the Natural Sciences and Engineering Research Council of Canada, Millipore/Waters and Pharmacia/LKB. J.-Y.Z. acknowledges a fellowship from the Alberta Heritage Foundation for Medical Research. N.J.D. acknowledges a Steacie fellowship from the Natural Sciences and Engineering Research Council.

## REFERENCES

- 1 P. Edman, *Acta Chem. Scand.*, 4 (1950) 277–283.
- 2 K. Otsuka, S. Terabe and T. Ando, *J. Chromatogr.*, 332 (1985) 219.
- 3 K. C. Waldron, S. Wu, C. W. Earle, H. R. Harke and N. J. Dovichi, *Electrophoresis*, 11 (1990) 777–780.
- 4 K. C. Waldron and N. J. Dovichi, *Anal. Chem.*, in press.
- 5 Y. F. Cheng and N. J. Dovichi, *Science (Washington, D.C.)*, 242 (1988) 562–564.
- 6 Y. F. Cheng, S. Wu, D. Y. Chen and N. J. Dovichi, *Anal. Chem.*, 62 (1990) 496–503.
- 7 S. Wu and N. J. Dovichi, *J. Chromatogr.*, 480 (1989) 141–155.
- 8 J. V. Sweedler, J. B. Shear, H.A. Fishman and R. N. Zare, *Anal. Chem.*, 63 (1991) 496–502.
- 9 C.A. Monnig and J. W. Jorgenson, *Anal. Chem.*, 63 (1991) 802–807.
- 10 R. P. Haugland, *Handbook of Fluorescent Probes and Research Chemicals*, Molecular Probes, Eugene, OR, 1989, p. 32.
- 11 S. A. Soper, L. M. Davis, F. R. Fairfield, M. L. Hammond, C. A. Harger, J. H. Jett, R. A. Keller, B. L. Marrone, J. C. Martin, H. L. Nutter, E. B. Shera and D. J. Simpson, *Proc. SPIE*, 1435 (1991) 168.
- 12 H. Swerdlow, J. Z. Zhang, D. Y. Chen, H. R. Harke, R. Grey, S. Wu, C. Fuller and N. J. Dovichi, *Anal. Chem.*, 63 (1991) 2835–2841.
- 13 D. Y. Chen, H. P. Swerdlow, H. R. Harke, J. Z. Zhang and N. J. Dovichi, *J. Chromatogr.*, 559 (1991) 237–246.
- 14 J. E. Knoll, *J. Chromatogr. Sci.*, 23 (1986) 422–425.
- 15 J. Gluckman, D. Shelly and M. Novotny, *J. Chromatogr.*, 317 (1984) 443–453.
- 16 H. Todoriki, T. Hayashi and H. Naruse, *J. Chromatogr.*, 276 (1983) 45–54.
- 17 E. Gassman, J. E. Kuo and R. N. Zare, *Science (Washington, D.C.)*, 230 (1985) 813–814.
- 18 M. C. Roach and M. D. Harmony, *Anal. Chem.*, 59 (1987) 411–415.
- 19 R. A. Wallingford and A. G. Ewing, *Anal. Chem.*, 59 (1987) 678.
- 20 J. Liu, Y.Z. Hsieh, D. Wiesler and M. Novotny, *Anal. Chem.*, 63 (1991) 408–412.

# Application of capillary isoelectric focusing with universal concentration gradient detector to the analysis of protein samples

Jiaqi Wu and Janusz Pawliszyn

*Department of Chemistry, University of Waterloo, Waterloo, Ontario N2L 3G1 (Canada)*

---

## ABSTRACT

The design of a new capillary isoelectric focusing (cIEF) instrument, composed of a rugged cartridge holding a short piece of capillary and a universal, inexpensive concentration gradient detector, was optimized and applied to the analysis of various protein samples. High-efficiency cIEF separations with sub-femtomole detection limits for absolute amounts were obtained using 10  $\mu\text{m}$  I.D. capillaries with large O.D.-to-I.D. ratios. An electric field strength of 1 kV/cm applied in the focusing step resulted in a  $10^{-8}$  M on-column concentration detection limit, which corresponded to  $10^2$  amol absolute amount of proteins. The detection volume was estimated to be 2 pl, which is among the smallest values reported to date for any optical or spectroscopic detector. When a 6-cm long capillary was used, proteins with isoelectric points ranging from 4.7 to 8.8 could be analyzed in about 5 min, the shortest analysis time ever reported for cIEF. Compared with commercial cIEF instruments with UV-visible absorbance detectors, the instrument is easier to use and has lower detection limits and better resolution. Several protein mixtures and real samples were separated with this instrument.

---

## INTRODUCTION

Capillary isoelectric focusing (cIEF) is a newly developed, powerful capillary electrophoretic technique for separations of complex protein samples based on isoelectric point (pI) differences [1,2]. Because the microbore capillaries (25–200  $\mu\text{m}$  I.D.) used in the cIEF offer efficient dissipation of Joule heat, and therefore, eliminate convection effects, a high separation voltage can be employed. This permits highly efficient separations as the zone width of a focused protein decreases with increasing separation voltage [3]. The technique is able to resolve proteins which differ in isoelectric point by less than 0.02 pH unit, and the separation can be completed in about 15–20 min [2,4]. The narrow capillaries also require only small amounts of sample, which is desirable for the analysis of biochemical

materials, such as proteins. cIEF has great potential as an analytical tool for protein analysis.

Since 1985, there have been many reports on the applications of cIEF for the separation of protein samples, most of which were performed on commercial capillary electrophoresis (CE) instruments [2,4, 5]. However, there are three main problems with commercial CE instruments performing in the isoelectric focusing mode. First, although a narrower capillary offers a higher separation efficiency, most commercial CE instruments still use 50–75  $\mu\text{m}$  I.D. capillaries, because of difficulties in performing on-column detection with narrow capillaries. For commercial CE instruments, UV-visible absorbance is the most commonly used detection method. Its performance deteriorates when used with capillaries of less than 25  $\mu\text{m}$  I.D. because it is difficult to send sufficient radiation from an incoherent source across the narrow capillaries. Second, because of the presence of the UV-absorbing carrier ampholytes in cIEF, which usually have 100–1000 times higher concentrations than those of protein samples, a

---

*Correspondence to:* Dr. J. Pawliszyn, Department of Chemistry, University of Waterloo, Waterloo, Ontario N2L 3G1, Canada.



wavelength of 280 nm has to be used for the UV–visible absorbance detector instead of the wavelengths for optical absorption peaks of proteins (180–240 nm [2]). The sensitivity of the UV–visible detector for cIEF is much lower than that for other CE techniques, such as capillary zone electrophoresis. Finally, the designs of most commercial CE instruments are not suited to hold short capillaries. The best isoelectric focusing separations are reportedly achieved on short capillaries (12–14 cm) [2,4], but much longer capillaries have to be used in most commercial CE instruments because the physical size of the UV–visible absorbance detector and the design of the capillary cartridge of those instruments restrict the use of short capillaries.

To address these limitations of the current cIEF instrumentation, we proposed a new cIEF apparatus that consists of a specially designed cartridge accommodating a short piece of capillary and an inexpensive, universal concentration gradient detector [6]. We have shown the unique compatibility of the concentration gradient detector and isoelectric focusing performed on 20–100  $\mu\text{m}$  I.D. capillaries [7]. The detector shows high sensitivity for cIEF owing to the high concentration gradients produced by the narrow protein zones focused inside the capillary by the isoelectric focusing process [7]. The derivative nature of the detector eliminates the high background signal generated by wide zones of the carrier ampholytes [7]. All zones can be detected during mobilization without any derivatization or decrease in resolution because of the universal nature and the small detection volume of the detector [7].

In this work, we investigated further the capability of the cIEF–concentration gradient detector method by optimizing the optical geometry of the detector so that it can be applied to narrow capillaries, and using short capillaries for fast separation of proteins with wide  $pI$  ranges. The potential of this technique was demonstrated by applying it to the analysis of a wide range of biological samples.

## EXPERIMENTAL

### *Instrumental*

The cIEF–concentration gradient detector system used was described in detail previously [7]. A 10 or 20  $\mu\text{m}$  I.D., 350  $\mu\text{m}$  O.D., 12 or 6 cm long capillary

(Polymicro Technologies, Tucson, AZ, USA) was used for separation. The capillary inner wall was coated with non-cross-linked acrylamide to eliminate electroosmosis [8]. As the viscosity of the acrylamide solution used for coating the capillary increased with time, and the solution became difficult to withdraw from the narrow capillaries, the coating time for the 10  $\mu\text{m}$  I.D. capillaries was only 7 min instead of 14–20 min [8] for 20  $\mu\text{m}$  I.D. capillaries. The lifetime of the coating for the 10  $\mu\text{m}$  I.D. capillaries is much shorter than that of 20  $\mu\text{m}$  I.D. capillaries. The laser beam intensity profile after the beam had passed through the capillary was measured by a scanning photodiode with a 0.1 mm slit placed before it.

### *Reagents*

All chemicals were of analytical-reagent grade, and solutions were prepared using deionized water and filtered through 0.2- $\mu\text{m}$  pore size cellulose acetate filters (Sartorius, Gottingen, Germany) prior to use. The anolyte and catholyte were 10 mM  $\text{H}_3\text{PO}_4$  and 20 mM NaOH, respectively [4]. All proteins were purchased from Sigma. Proteins used include carbonic anhydrase (bovine erythrocytes), carbonic anhydrase (human erythrocytes), myoglobin (horse skeletal muscle), phosphorylase *b* (rabbit muscle),  $\alpha$ -chymotrypsin (bovine pancreas), ovalbumin (grade V), hemoglobin (human, 75% methemoglobin, balance primarily oxyhemoglobin),  $\beta$ -lactoglobulin B (bovine milk) and albumin (human, fraction V). Human blood serum samples were obtained from a local clinical laboratory. Monoclonal antibody to fluorescein and transferrin (bovine) were donated by HyClone Laboratories (Logan, UT, USA). Samples were mixed with carrier ampholyte (Pharmalyte, pH 3–10; Sigma) solution for a final concentration of 2% ampholyte [4]. The protein concentrations introduced into the capillary ranged from 0.1 to 0.5 mg/ml. Protein samples were desalted, if necessary, by using dialysis membranes (molecular mass cut-off 5000) purchased from Baxter (Mississauga, Ontario, Canada).

### *The cIEF process*

First, the sample solution was introduced into the capillary by pressure, then a high d.c. voltage was applied to the two ends of the capillary. The voltage applied for focusing performed on the 20  $\mu\text{m}$  I.D.

capillaries was 8 kV and on the 10  $\mu\text{m}$  I.D. capillaries it was 12 kV. The current passing through the capillary was monitored to follow the focusing process. For 12 cm  $\times$  20  $\mu\text{m}$  I.D. capillaries, typically, the current dropped from 1 to about 0.1  $\mu\text{A}$  in 4 min. The final step was mobilization. In the present experiment, cathodic mobilization was employed, which required exchanging the catholyte with a solution containing 20 mM NaOH and 80 mM NaCl [4]. The voltages for mobilization were 10 kV for 20  $\mu\text{m}$  I.D. capillaries and 12 kV for 10  $\mu\text{m}$  I.D. capillaries. During the cathodic mobilization process, the proteins moved through the detector in order of decreasing  $pI$ . All experiments were done in triplicate to control the reproducibility.

## RESULTS AND DISCUSSION

For a sample zone focused in a capillary by the isoelectric focusing process, its concentration distribution along the capillary direction,  $x$ , is assumed to be a Gaussian function [3] with a standard deviation,  $\sigma_x$ , which can be expressed as [7]

$$\sigma_x = \sqrt{\frac{D}{pE}} \quad (1)$$

where  $E = V/l$ ,  $V$  is the d.c. voltage applied to two ends of the capillary,  $l$  is the overall length of the capillary,  $D$  is the diffusion coefficient of the protein sample and  $p$  is given by

$$p = \frac{du}{d(\text{pH})} \cdot \frac{d(\text{pH})}{dx} \quad (2)$$

where  $du/d(\text{pH})$  is the change in the mobility of the sample with respect to change in pH. As predicted by eqn. 1, better resolution is expected when a high voltage is applied. The upper limit of the applied voltage is largely decided by the capillary I.D. Narrower capillaries facilitate the application of higher voltage because of enhanced heat dissipation caused by higher surface-to-sample volume ratios [9]. Hence, narrower capillaries offer higher separation efficiency. On the other hand, the use of narrow capillaries increases the difficulties for the application of the concentration gradient detector to cIEF.

In the concentration gradient detector, a collimated laser beam is focused directly into the separation capillary. The direction of the beam is deflected

when it encounters a refractive index gradient produced by a migrating sample zone [6]. This beam deflection can be created by any sample zone which has a refractive index different from that of the buffer inside the capillary. When the detector is used for cIEF, the maximum value of the deflection angle can be written as [7]

$$\theta_{\max} = \pm 0.24 \cdot \frac{L}{n} \cdot \frac{dn}{dC} \cdot \frac{C_0 l}{\sigma_x^2} = \pm 0.24 \cdot \frac{dn}{dC} \cdot \frac{du}{d(\text{pH})} \cdot \frac{d(\text{pH})}{dx} \cdot \frac{LC_0 V}{nD} \quad (3)$$

where  $n$  is the refractive index of the solution in the capillary,  $L$  is the I.D. of the capillary,  $C_0$  is the concentration of the introduced sample and  $C$  is the concentration distribution of the sample zone along the capillary direction after focusing. As  $dn/dC$  is approximately a constant for a given solute [6], the maximum angle is proportional to the concentration of the introduced sample,  $C_0$ . The angle of deflection can be detected by a light beam position sensor which consists of two photodiodes. The photocurrent,  $\Delta i_{\max}$ , created on the position sensor associated with the deflection angle,  $\theta_{\max}$ , can be written as [6]

$$\Delta i_{\max} = \frac{8KiF}{\pi Z} \cdot \theta_{\max} \quad (4)$$

where  $i$  is the laser beam light intensity,  $F$  is the focal length of the laser beam focusing lens,  $Z$  is the beam diameter before focusing and  $K$  is the efficiency of the conversion of light intensity into current by the light beam position sensor [6].  $\Delta i_{\max}$  represents the sensitivity of the whole detection system for cIEF.

As described by eqn. 3, the sensitivity of the detector decreases linearly with decreasing capillary I.D.,  $L$ . For example, the sensitivity of the detector for a 10  $\mu\text{m}$  I.D. capillary is only half of that for a 20  $\mu\text{m}$  I.D. capillary. A linear relationship between the sensitivity of the detector and the applied voltage is also shown in eqn. 3. This means that the decrease in sensitivity due to decreasing capillary I.D. can be partly compensated for by increasing the separation voltage. As discussed earlier, high voltage can be successfully applied to narrow capillaries.

Another difficulty in applying the detector to a narrow capillary is associated with focusing the probe beam into the capillary. The use of a narrower

capillary requires a smaller laser beam spot. A shorter focal length lens should be used for focusing the laser beam into the narrower capillary, as the focused laser beam spot diameter,  $A$ , is given by

$$A = \frac{4\lambda F}{\pi Z} \quad (5)$$

where  $\lambda$  is the wavelength of the laser beam. In previous work [7], good results were obtained with a 30 mm focal length lens and 20–100  $\mu\text{m}$  I.D. capillaries. By using this lens, the beam spot after focusing is calculated to be 24  $\mu\text{m}$  by eqn. 5 from the 0.6  $\mu\text{m}$  wavelength and 1 mm beam diameter of the He–Ne laser. For a 10  $\mu\text{m}$  I.D. capillary, a smaller beam spot is needed. However, the use of a short focal lens will decrease the sensitivity of the detector as it is proportional to the  $F/Z$  ratio as described in eqn. 4. For example, a 13 mm focal length lens is required to focus the beam into a 10  $\mu\text{m}$  I.D. capillary. This decreases the sensitivity by about 60% compared with that when a 30 mm focal length lens is used. Therefore, trade-off exists between the focal length and the capillary I.D. for obtaining good sensitivity.

Because the 30 mm focal length lens gave good sensitivity when it was used for 20–100  $\mu\text{m}$  I.D. capillaries, and a longer focal length also made optical alignment adjustment easier, we decided to use this lens for 10  $\mu\text{m}$  I.D. capillaries. When the 30 mm focal length lens is used to focus the laser beam for side illumination of a 20 or 10  $\mu\text{m}$  I.D. capillary, the beam will be scattered over 360° in the plane perpendicular to the capillary axis since the capillary I.D. is smaller than the beam diameter [10]. The resulting fringe pattern depends on the refractive index of the capillary, the sample in the capillary and the beam polarization. There are four kinds of beam rays in the probe beam, as shown in Fig. 1: ray 1, which passes through the center of the capillary inner bore without any refraction; ray 2, which propagates through the capillary and emerges without intercepting the inner bore with two refractions at two interfaces; ray 3, which is reflected at the interface between the capillary and sample inside its inner bore; and ray 4, which propagates through both the capillary wall and the inner bore with four refractions at the interfaces. The fringe pattern is produced by the interference of all these four scattered rays, and the pattern becomes complicated

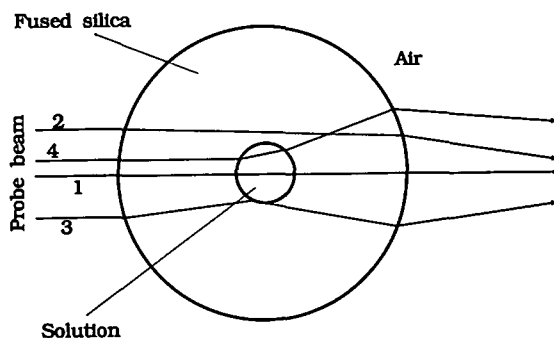


Fig. 1. Capillary cross-section and laser beam ray tracing diagram for four kinds of rays.

when narrow capillaries are used as shown in Figs. 2a and 3a, which illustrate the probe beam intensity profiles after the beam has passed through a 20 or 10  $\mu\text{m}$  I.D.  $\times$  140  $\mu\text{m}$  O.D. capillary. A complicated interference pattern is observed in the center of the beam. This effect is particularly noticeable for the 10  $\mu\text{m}$  I.D. capillary, where only the center part of the beam passes through the inner bore of the capillary. The interference in the beam center is mainly due to the beam rays 1 and 4, which are refracted by the interface between capillary and air and interfere with each other in far field, as shown in Fig. 1. This interference pattern also changes or shifts irregularly as a consequence of changes in the refractive index of the solution inside the capillary, which can be induced by temperature inhomogeneity or a migrating sample zone. For the concentration gradient

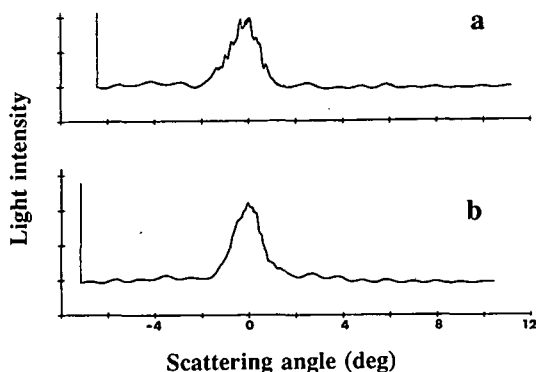


Fig. 2. Laser beam intensity profiles after the beam has passed through (a) a 20  $\mu\text{m}$  I.D., 140  $\mu\text{m}$  O.D. capillary and (b) a 20  $\mu\text{m}$  I.D., 360  $\mu\text{m}$  O.D. capillary.

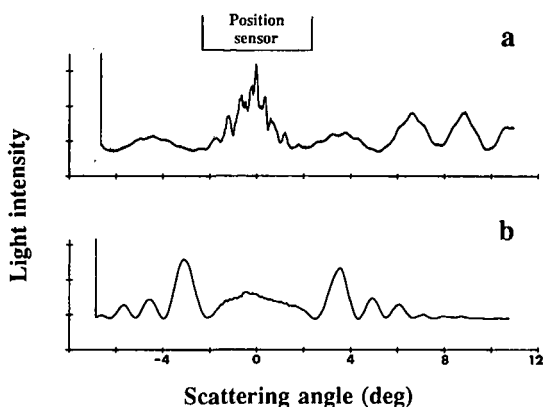


Fig. 3. Laser beam intensity profiles after the beam has passed through (a) a 10  $\mu\text{m}$  I.D., 140  $\mu\text{m}$  O.D. capillary and (b) a 10  $\mu\text{m}$  I.D., 360  $\mu\text{m}$  O.D. capillary. The light intensity coordinate in (a) is expanded twice that in (b).

detector, in which the beam deflection along the capillary axis is monitored, the shifts of the pattern along the capillary axis can cause noise, baseline fluctuation or irregular signal peak shape. This presents a major difficulty when applying the detect or to narrow capillaries.

This interference pattern can be significantly simplified by immersing the capillary in a transparent liquid having the same refractive index as that of the capillary [10]. In this way, the refraction of the beam at the interface between the capillary and air (now the liquid) is eliminated. However, in this method, the temperature should be carefully controlled, as the refractive index of the liquid and the capillary wall change with temperature, and the temperature may be different in the liquid and capillary wall owing to their different heat capacities. In our experiment, the interference pattern is simplified by using larger O.D.-to-I.D. ratio capillaries. In Fig. 4, such a capillary is used (*e.g.*, a 360  $\mu\text{m}$  O.D., 10  $\mu\text{m}$  I.D. capillary). As the laser beam is focused into the center of the capillary, and the focal area of the beam is large compared with the capillary O.D., all light rays can be considered to be emitted from approximately the center of the capillary. The propagation directions of these beam rays are approximately perpendicular to the interface between the capillary and the air. After rays 1 and 4 have passed through the capillary, they will not be refracted at the capillary–air interface, and travel along their original directions. The interference

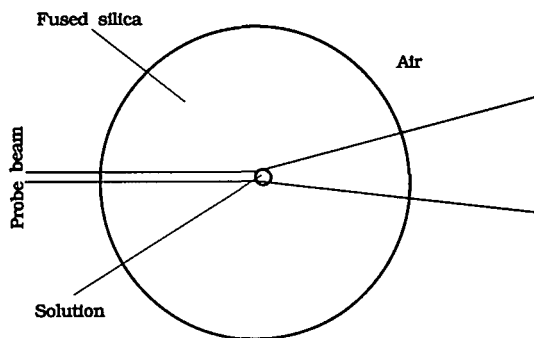


Fig. 4. Propagation directions of the light beam emitted from the center of the capillary.

between rays 1 and 4 is reduced by using larger O.D.-to-I.D. ratio capillaries as shown in Figs. 2b and 3b. As expected, the intensity profile in the beam center is of good quality, and the interference pattern is simplified even for the 10  $\mu\text{m}$  I.D. capillary. In our experiment, only this part of the beam is intercepted by the photodiode light beam position sensor as shown in Fig. 3 when a 10  $\mu\text{m}$  I.D. capillary is used. The above discussion suggests that it is possible to apply the concentration gradient detector to narrow capillaries without loss of sensitivity. It should be mentioned that by intercepting part of the laser beam by the light beam position sensor, we should expect a decrease in sensitivity from eqn. 4 which shows a linear relationship between the beam intensity and the sensitivity. However, for the high-intensity laser beam, the principal noise source of the measurement in the concentration gradient detector is the pointing noise [6]. The noise in signals detected by the position sensor due to the pointing noise is proportional to the beam light intensity, which means that the relative noise level due to pointing noise is a constant. This property allows the interception of part of the laser beam by the light beam position sensor for the narrow capillaries without deterioration of the signal-to-noise ratio and, therefore, the sensitivity of the detector.

Fig. 5 shows the electropherograms of two focused proteins, phosphorylase *b* (peak 1) and ovalbumin (peak 2), in a 20 and a 10  $\mu\text{m}$  I.D. capillary, which are plotted in such a way that the noise levels of the two electropherograms are the same so that their sensitivities can be compared by their peak

heights. Although the capillary I.D. ( $L$ ) decreases by half from 20 to 10  $\mu\text{m}$ , the sensitivity loss due to this decrease is partly compensated for by an increase in the applied voltage ( $V$ ) which increases from 8 to 12 kV. From eqn. 3, under these conditions, the sensitivity in concentration for the 10  $\mu\text{m}$  I.D. capillary is predicted to be 75% of that for the 20  $\mu\text{m}$  I.D. capillary. As expected, the peak heights in Fig. 5b are about 75% of those in Fig. 5a. Other peaks are also observed in Fig. 5, which are attributed to minor components or impurities in the sample. This result confirms that the signal-to-noise ratio does not decrease when only the center part of the laser beam is detected in the optical alignment used in the concentration gradient detector. The on-column mass detection limit for the 10  $\mu\text{m}$  I.D. capillary is much lower than that for the 20  $\mu\text{m}$  I.D. capillary, as the sample volume needed decreases from 38 nl for the 20  $\mu\text{m}$  I.D. capillary to 9 nl for the 10  $\mu\text{m}$  I.D. capillary. The detection limits in concentration are calculated from three times the baseline noise and are  $3.4 \cdot 10^{-8} M$  for phosphorylase *b* and  $6.3 \cdot 10^{-8} M$  for ovalbumin. These values correspond to 270 and 460 amol on-column mass detection limits for phosphorylase *b* and ovalbumin, respectively. This is the first report in which isoelectric focusing has been performed on a 10  $\mu\text{m}$

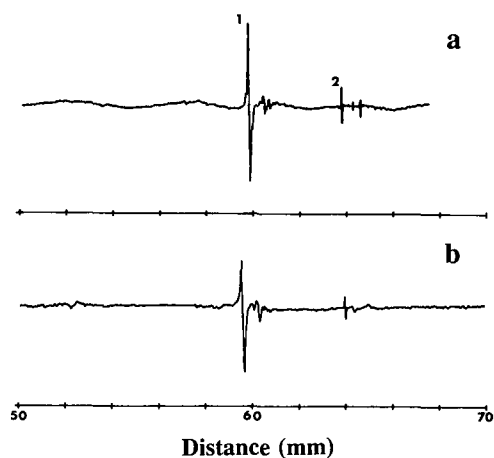


Fig. 5. Mobilization electropherograms of phosphorylase *b* (peak 1) and ovalbumin (peak 2) focused (a) in a 12 cm  $\times$  20  $\mu\text{m}$  I.D. capillary and (b) in a 12 cm  $\times$  10  $\mu\text{m}$  I.D. capillary. Concentrations of the introduced samples are 0.5 mg/ml for phosphorylase *b* and 0.1 mg/ml for ovalbumin, respectively, which correspond to 40 and 17 fmol, respectively, for absolute amounts of samples in the 10  $\mu\text{m}$  I.D. capillary.

I.D. capillary and attomole levels of proteins have been detected by a universal detector.

These experimental results confirm the feasibility of performing isoelectric focusing on a 10  $\mu\text{m}$  I.D. capillary and detection in cIEF with narrow capillaries by a concentration gradient detector. Fig. 6 shows a mobilization electropherogram of five proteins focused in a 10  $\mu\text{m}$  I.D. capillary, and detected by the concentration gradient detector. The concentrations of these proteins range from  $1.6 \cdot 10^{-6}$  to  $5.4 \cdot 10^{-6} M$ , which correspond to 15–50 fmol in absolute amount of proteins introduced into the 12 cm  $\times$  10  $\mu\text{m}$  I.D. capillary. From the signal-to-noise ratio in Fig. 6, the on-column mass detection limit for each protein is again shown to be in the range of  $10^2$  amol.

The detection limit of the concentration gradient detector for absolute amount is lower than that of a UV-visible absorbance detector for cIEF. Although a laser-induced fluorescence detector is the most sensitive detector for CE, it is difficult to apply for many real protein samples as the detector requires derivatization for proteins, which is impossible to perform in pre- or postcolumn modes for ultramicro amounts of samples at low concentrations. Also, the reaction between protein samples and labeling reagents may be not specific, and many unwanted products will be created, increasing the difficulty in identifying and quantifying sample peaks after they are separated. However, attomole level proteins at  $10^{-7} M$  concentrations can be separated and detected by our cIEF instrument with

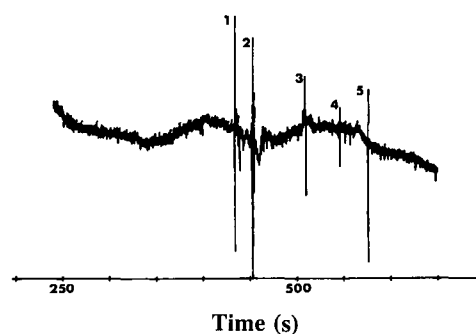


Fig. 6. Mobilization electropherogram of five proteins focused in a 12 cm  $\times$  10  $\mu\text{m}$  I.D. coated capillary. 1, 2 = Human hemoglobin (absolute amount in the capillary 14 fmol) and myoglobin; 3 = human carbonic anhydrase (32 fmol); 4 = bovine carbonic anhydrase (29 fmol); 5 =  $\beta$ -lactoglobulin B (50 fmol). Protein concentrations, 0.1 mg/ml each.

the universal detector without any derivatization.

Although the 10  $\mu\text{m}$  I.D. capillary is applicable to cIEF, its inner wall is difficult to coat by the coating method used in the experiment where a high-viscosity solution must be introduced into the capillary [8]. This problem prevents the practical use of narrow capillaries in cIEF. In our analysis of protein samples, we prefer to use a 20  $\mu\text{m}$  I.D. capillary as it is easier to coat. However, it is still possible to use a 10  $\mu\text{m}$  I.D. capillary or even narrower capillaries in practical cIEF analyses of protein samples because the possibility of performing isoelectric focusing on uncoated capillaries has been demonstrated recently [5].

In the mobilization process, adding salt to one of the capillary ends causes movement of sodium or chloride ions into the capillary at that end. A pH change occurs at this end, and then gradually progresses deeper into the capillary, causing sample zones to move toward the end of the capillary [4]. A long capillary prolongs the mobilization process and also causes pH gradient distortion along the capillary and, therefore, shape distortion of the sample zones, during the mobilization. Long capillaries have to be employed in the commercial instruments. Because of the size of the UV-visible absorbance detector and the design of the capillary cartridge, the detection point of the capillary has to be positioned at some distance from one capillary end toward which the focused sample zones move during the mobilization. This arrangement prevents the detection of the proteins that are focused between the detection point and the capillary end during the mobilization process. The distance ranges from 3 to 20 cm depending on the type of instrument [4,5]. For the commercial CE instruments, the pH range of the carrier ampholytes cannot be fully utilized. To recover those lost proteins between the detection point and the capillary end, two methods can be used: lengthening the separation capillary while keeping the distance from the detection point to the capillary end constant, or mixing certain reagents in the carrier ampholytes to extend the pH range in the capillary end. For example, with  $\text{N,N,N',N'}$ -tetramethylethylenediamine the pH range can be extended from 10 to 12 at the cathode end of the capillary [4,5]. The pH range of the carrier ampholytes is still not fully utilized by the second method, and the first method increases the mobili-

zation time and makes it difficult to mobilize proteins focused near the capillary anode end to the cathode end when cathodic mobilization is employed. We tested the application of short capillaries in the cIEF-concentration gradient detector instrument. Because of the unique design of the cartridge, theoretically there should be no minimum limitation on the distance from the detection point to the capillary end, therefore making it possible to apply short capillaries in the cIEF-concentration gradient detector instrument [7]. Fig. 7 shows a mobilization electropherogram of three proteins focused in a 6 cm  $\times$  20  $\mu\text{m}$  I.D. capillary. All proteins having  $pI$  values ranging from 4.7 to 8.8 [11] can be analyzed in about 5 min, which includes 3 min for focusing and 2 min for mobilization. This rate is much faster than those of commercial CE instruments, and the highest ever reported for cIEF analysis. The use of a short capillary also increases the sensitivity of the detector as its sensitivity is proportional to  $d(\text{pH})/dx$ , as described by eqn. 3. Owing to the small detection volume of the detector, the short capillary did not affect the resolution for the 6 cm long capillary. As shown in Fig. 7, the Gaussian derivatives generated by the concentration gradient detector can be easily converted into peaks associated with electropherograms produced by conventional concentration detection methods. The integration should be performed only on the portion of the trace around the analyte band of interest to re-

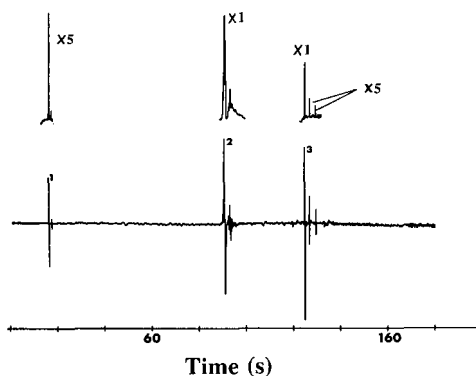


Fig. 7. Rapid analysis of proteins in wide pH range using a 6 cm  $\times$  20  $\mu\text{m}$  I.D. capillary. Samples: 1 =  $\alpha$ -chymotrypsin (major component,  $pI$  = 8.76; one minor component,  $pI$  = 8.38); 2 = phosphorylase *b* (major component,  $pI$  = 6.35; minor components,  $pI$  = 5.50–6.25); 3 = ovalbumin (major component,  $pI$  = 4.70). Above: integrals of portions of the electropherogram. Protein concentrations, 0.5 mg/ml each.

duce the effects of drift associated with the broad band of the carrier ampholytes present in the capillary [7]. The results confirm the feasibility of employing short capillaries in cIEF, and also suggest that the cIEF-concentration gradient detector instrument with a short capillary is suitable for the rapid screening of proteins in a wide  $pI$  range.

The resolution and reproducibility of the instrument were evaluated. Fig. 8 shows the mobilization electropherogram of human hemoglobin when carrier ampholytes of pH 3-10 were used, in which two main peaks are observed. The highest peak (peak 1) corresponds to methemoglobin ( $pI = 7.20$ ) [12] which comprises about 75% of the sample, and peak 2 corresponds to oxyhemoglobin ( $pI = 7.00$ ) [12] which is less than 25% in the sample. Another small peak is also observed before these two peaks, which probably corresponds to the  $A_2$  form ( $pI = 7.40$ ) of human hemoglobin [12]. The resolution can be estimated from the peak width in Fig. 8 to be 0.02 pH unit for the 12 cm long separation capillary; which is in the same order of magnitude as the best results obtained by commercial CE instruments in which longer capillaries are employed [4,5]. This high resolution is considered to be due to the small detection volume and the derivative nature of the detector [7]. Fig. 8 also shows good reproducibility of the peak shape.

The above results and discussion demonstrate the high sensitivity and reliability of the instrument. Be-

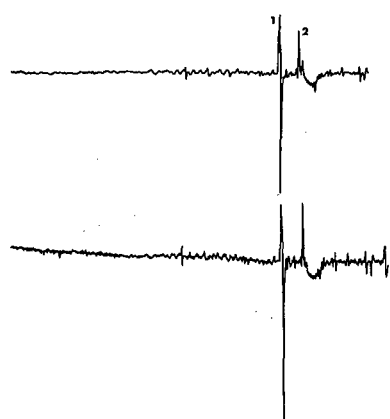


Fig. 8. Replicate separations of human hemoglobin. 1 = Methemoglobin; 2 = oxyhemoglobin. Capillary, 12 cm  $\times$  20  $\mu$ m I.D.; protein concentration, 0.3 mg/ml.

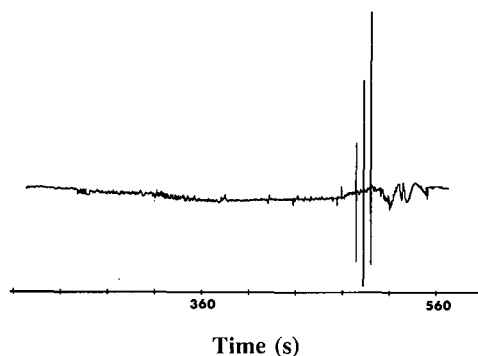


Fig. 9. Mobilization electropherogram of bovine transferrin. Capillary, 12 cm  $\times$  20  $\mu$ m I.D.; protein concentrations, ca. 0.4 mg/ml.

low, some examples of applying the instrument to analyses of proteins are given.

Serum transferrin is an iron-transport protein with different iron-complexed or iron-free isoforms, which can be separated by isoelectric focusing. cIEF offers a fast and high-resolution separation method for studying the protein [8]. Fig. 9 shows the mobilization electropherogram of the bovine serum transferrin, which demonstrates the high resolution of the method. Each peak in Fig. 9 should represent a single isoform [8]. Because of the high resolution of the instrument, transferrin with different iron contents may be characterized by the method.

Monoclonal antibodies manufactured for clinical diagnosis and treatment may exhibit micro-heterogeneity even when they are demonstrated to be pure on the basis of their amino acid content. This mi-

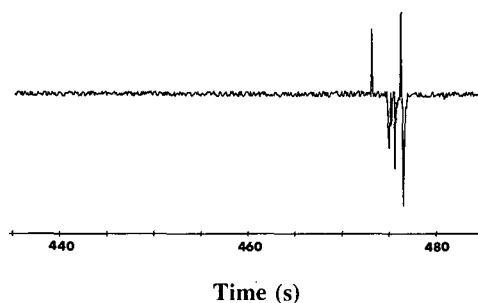


Fig. 10. Mobilization electropherogram of monoclonal antibody to fluorescein. Capillary, 12 cm  $\times$  20  $\mu$ m I.D.; protein concentration, ca. 0.5 mg/ml.

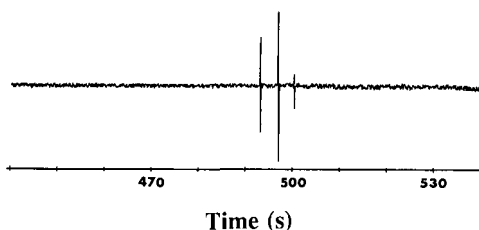


Fig. 11. Mobilization electropherogram of human serum albumin (fraction V). Capillary, 12 cm  $\times$  20  $\mu$ m I.D.; protein concentration, 0.3 mg/ml.

cro-heterogeneity is usually characterized by conventional gel isoelectric focusing. cIEF also offers a high-resolution method for this purpose [2]. Fig. 10 is a high-resolution mobilization electropherogram of the monoclonal antibody to fluorescein, in which several narrow peaks can be observed, showing the micro-heterogeneity of the sample.

Human serum albumin is another important protein, which is often measured and correlated with various disease states. cIEF allows the rapid analysis of isoforms of the protein. Fig. 11 shows a mobilization electropherogram of the human serum albumin, fraction V, in which three peaks are observed around pH 5.8 [11]. Human blood serum obtained from a local medical laboratory was also analyzed by the cIEF instrument, and the results are shown in Fig. 12. Globulins and albumin are contained in the sample, which correspond to peaks around pI 4–6 [4]. Because of its high speed and resolution, the cIEF electropherogram pattern of the serum is possibly employed more efficiently than gel isoelectric focusing to correlate with various disease states. The analysis time for such an applica-

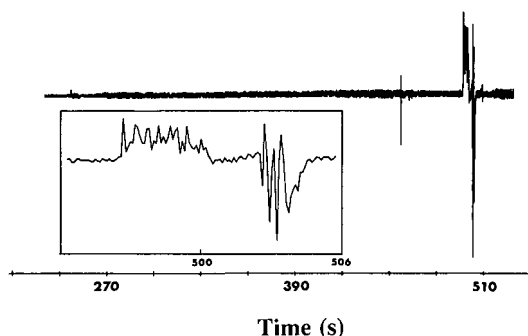


Fig. 12. Separation of human blood serum.

tion can even decrease considerably if the electropherogram of the focused proteins inside the capillary is detected by an imaging system without the mobilization process [13].

## CONCLUSIONS

There are many advantages of the cIEF–concentration gradient detector instrument over commercial instruments. The sensitivity of the instrument is higher than those of commercial instruments. The UV–visible absorbance detector used in commercial CE instruments usually uses 280 nm as the detection wavelength instead of 180–240 nm because of the high background of the high-concentration carrier ampholytes [2,14]. At this wavelength, the sensitivity of the detector for proteins is much lower than that at 180–240 nm. For example, the absorption of bovine carbonic anhydrase at 280 nm is less than one tenth of that at 200 nm [14]. The derivative nature of the concentration gradient detector eliminates the high background generated by the wide band of carrier ampholytes, and high signal peaks are created only by narrow protein zones [7]. The detector has proved to be suitable for narrow capillaries and, because of the use of a narrow capillary which can accommodate high voltages, sharp protein zones are focused inside the capillary, resulting in high sensitivity for the concentration gradient detector. The concentration gradient detector also has a much smaller detection volume than a UV–visible absorbance detector. The detection volume of the detector can be calculated from the capillary I.D., 10  $\mu$ m, and the laser beam diameter of 24  $\mu$ m. It is calculated to be 2 pl, which is among the smallest values ever reported for an optical and spectroscopic detector. Because of the narrow capillary used, the instrument allows the analysis of the microenvironment of biochemical systems. Short capillaries can be used in the instrument, which facilitate the rapid analysis of protein samples. The instrument is also inexpensive and small-sized because the whole detection system consists only of a low-power He–Ne laser and a photodiode light beam position sensor, and a short capillary is used. The sample introduction and change of the buffer solution during the mobilization process can be easily performed by just operating a syringe [7]. The cost of the instrument is less than US\$1000, which is much lower



than those of commercial CE instruments with a UV–visible absorbance detector that requires an expensive monochromator and photomultiplier tube. The cost and size of the instrument are expected to decrease even further if a diode laser is used in the detector. A future avenue of development of the CE instruments will be the construction of a complete CE instrument on a single silicon wafer, which includes a diode laser and a photodiode light beam position sensor as both are silicon devices.

#### ACKNOWLEDGEMENTS

This work was supported by the Natural Sciences and Engineering Research Council of Canada. The donations of protein samples by A. R. Torres of HyClone Laboratories and James Herron of the University of Utah are appreciated.

#### REFERENCES

- 1 S. Hjerten and M. Zhu, *J. Chromatogr.*, 346 (1985) 265.
- 2 T. Wehr, M. Zhu, R. Rodriguez, D. Burke and K. Duncan, *Am. Biotechnol. Lab.*, 8 (1990) 22.
- 3 P. G. Righetti, *Isoelectric Focusing: Theory, Methodology and Applications*, Elsevier, Amsterdam, 1983.
- 4 M. Zhu, R. Rodriguez and T. Wehr, *J. Chromatogr.*, 559 (1991) 479.
- 5 J. R. Mazzeo and I. S. Krull, *Anal. Chem.*, 63 (1991) 2852.
- 6 J. Pawliszyn, *Spectrochim. Acta Rev.*, 13 (1990) 311.
- 7 J. Wu and J. Pawliszyn, *Anal. Chem.*, 64 (1992) 219.
- 8 F. Kilar and S. Hjerten, *Electrophoresis*, 10 (1989) 23.
- 9 C. A. Monnig and J. W. Jorgenson, *Anal. Chem.*, 63 (1991) 802.
- 10 A. E. Bruno, B. Krattiger, F. Maystre and H. M. Widmer, *Anal. Chem.*, 63 (1991) 2689.
- 11 P. G. Righetti and T. Caravaggio, *J. Chromatogr.*, 127 (1976) 1.
- 12 J. W. Drysdale, P. G. Righetti and H. F. Bunn, *Biochim. Biophys. Acta*, 229 (1971) 42.
- 13 J. Wu and J. Pawliszyn, *Anal. Chem.*, 64 (1992) 224.
- 14 W. Thormann, J. Caslavská, S. Molteni and J. Chmelik, *J. Chromatogr.*, 589 (1992) 321.

# Analogy between micelles and polymers of ionic surfactants

## A capillary isotachopheretic study of small ionic aggregates in water–organic solutions

C. Tribet and R. Gaboriaud

*Laboratoire d'Énergétique et Réactivité aux Interfaces, Université Paris VI, 4 Place Jussieu, 75231 Paris Cedex 05 (France)*

P. Gareil

*Laboratoire de Chimie Analytique de l'École Supérieure de Physique et Chimie Industrielles de la Ville de Paris, 10 Rue Vauquelin, 75231 Paris Cedex 05 (France)*

---

### ABSTRACT

Capillary isotachopheresis (ITP) was applied to monitoring the synthesis of cationic polymers by  $\gamma$ -irradiation of various dodecyl- and hexadecylallyldimethylammonium and dodecylvinylimidazolium salts in aqueous solutions at concentrations considerably exceeding their respective critical micellar concentrations (CMC). The isotachopherograms obtained under both acidic and basic water–methanol electrolyte conditions showed distinctive steps for polymer and monomer surfactants, and also for amine (oxide) degradation products. This enables one to determine the amount of remaining monomer as a function of irradiation time, surfactant counter ion and initial monomer concentration. It was found, as far as the polymerization yield was concerned, that halide counter ions played a special (favourable or unfavourable) part in the polymerization reaction, and that bromide was the most suitable ion associated with allylic surfactants. An optimum irradiation time of *ca.* 25 h was determined for these allylic species, above which the ratio of degradation products was observed to increase markedly. Likewise, the initial monomer concentration should not exceed a second critical concentration, beyond which the polymerization yield would fall drastically. In addition, it was ascertained that when the reaction was allowed to take place in an isotropic medium (*i.e.*, at a concentration below the CMC), only low-mobility degradation products were obtained. ITP also appeared to be well adapted to the physico-chemical characterization of these ionic polymerized surfactants. This method enables polymers to be compared with dynamic micelles. The mobility of the polymers was found to be much greater than that of the starting monomer and close to that of a classical dynamic micelle. The analysis of fractions obtained from ultrafiltration assays revealed that their molecular weight was higher than 5000 g/mol. Hence it can be expected to be of the same order of magnitude than that of dynamic micelles. However, unlike the latter, the polymers remain stable in methanolic solutions and for monomer equivalent concentrations less than the CMC. Lastly, the degree of counter-ion binding, also determinable from isotachopherograms, is much higher for the polymers than for the ionic micelles. Nevertheless, these properties overall justify the term polymerized micelles currently applied to these polymers.

---

### INTRODUCTION

During the last decade, the use of surfactants has shown impressive development and, whereas initially it was confined to applications as detergents and for emulsion stabilization, it has recently gained

diversity. The application area of surfactants has even entered the field of fine reagents for analytical

---

*Correspondence to:* Dr. C. Tribet, Laboratoire d'Énergétique et Réactivité aux Interfaces, Université Paris VI, 4 Place Jussieu, 75231 Paris Cedex 05, France.

or preparative chemistry in techniques such as micellar liquid chromatography [1], sodium dodecyl sulphate–polyacrylamide gel electrophoresis (SDS-PAGE) [2], micellar electrokinetic capillary chromatography (MECC) [3], liquid–liquid extraction [4], ultrafiltration [5] and micellar catalysis [6].

Of special interest are the permanently ionic or ionizable surfactants because the aggregates they form in solution (micelles, vesicles) are less disperse than those given by their neutral counterparts. In addition, they are generally commercially available in great purity. Nevertheless, these supramolecular structures have a dynamic character and are chemically fragile, as they must be inevitably in equilibrium with a fixed concentration of the free form of the surfactant. For the case of micelles, this concentration, commonly called the critical micellar concentration (CMC), is typically much higher in organic (or even water–organic) media than in water, so that most of the time the micelle structure can neither be observed nor exploited in those media. Further, non-aggregated species can cross ultrafiltration membranes and hence contaminate ultrafiltrates.

This has been an incentive to investigate ways for stabilizing these aggregates and, among others, the idea of polymerizing surfactants while they are

entangled in a supramolecular structure seemed appealing [7,8]. In this direction, the synthesis of surfactants containing one unsaturated bond was soon realized, leading, for instance, to products such as polyallyldimethyldodecylammonium (poly-ADMDA<sup>+</sup>) bromide [9] and polydodecylvinylimidazolium (polyDVI<sup>+</sup>) iodide [10], as depicted in Fig. 1.

The analytical characterization of the polymers produced is not easy and most often so far, general non-separative techniques have been preferred (<sup>1</sup>H NMR, fluorescence decay, light scattering, etc.). However, capillary isotachoresis (ITP) was recently shown to be an appropriate separation technique for characterizing high-molecular-weight ionogenic polymers and copolymers of various types (with respect to their charge and irrespective of their molecular weight) [11,12]. On the other hand, the lack of a versatile high-performance separation and detection technique allowing the discrimination between surfactant homologues or compounds of the same group recently prompted us to develop closely related ITP methods which are suitable for most groups of monomeric ionic surfactants [13]. In addition, ITP was shown to provide an easy means of estimating the physico-chemical parameters per-

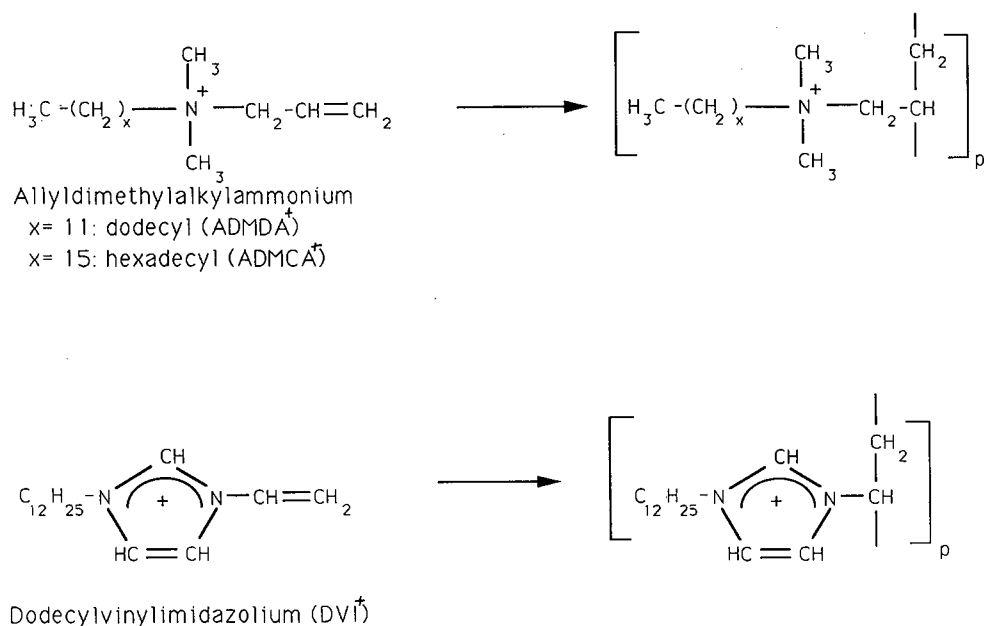


Fig. 1. Monomeric unsaturated surfactants and the corresponding polymers studied.

taining to micellar aggregates [14] and we have recently described a simple model enabling these parameters to be derived from a well chosen set of ITP experiments [15].

The purpose of this work was to show that ITP is also a useful technique for analytical studies of polysurfactants in water–organic media. More precisely, our goal is to illustrate two complementary facets of ITP through the study of a few polymerization reactions of surfactants (Fig. 1): ITP will serve first as an analytical method for the quantitative monitoring of compounds taking part in such polymerization reactions and second for physico-chemical purposes for the comparison of polysurfactants with monomeric micelles from the viewpoint of charge and mobility.

## EXPERIMENTAL

### *Monomer and polymer synthesis*

Allyldimethyldodecylammonium (ADMDA<sup>+</sup>) bromide and dodecylvinylimidazolium (DVI<sup>+</sup>) iodide were synthesized as described [9,10] by allowing *n*-dodecyldimethylamine or 1-vinylimidazole to react with allyl bromide or *n*-dodecyl iodide, respectively. Allyldimethylcetylammmonium (ADMCA<sup>+</sup>) bromide was obtained in the same way as ADMDA<sup>+</sup> bromide, using *n*-hexadecylamine in place of *n*-dodecylamine. The monomers were triply recrystallized in ethyl acetate. Their purities were confirmed by <sup>1</sup>H NMR.

Ion permutation on an anionic resin (Amberlite IRA 400AG; Rohm and Haas, Philadelphia, PA, USA) in its hydroxide form was carried out to obtain ADMDA<sup>+</sup> hydroxide. Apart from ADMDA<sup>+</sup> iodide, which was formed from ADMDA<sup>+</sup> hydroxide by a second ion-exchange process, the other salts result from the neutralization of ADMDA<sup>+</sup> hydroxide with the stoichiometric amount of the appropriate acid solution (hydrochloric, acetic or benzoic acid).

The polymerization reactions were performed in aqueous solutions of surfactant monomers at various concentrations, all well above the CMCs. The solutions were carefully degassed by submitting them to four freeze–pump–thaw cycles. The flasks were sealed and then submitted to  $\gamma$ -irradiation at a constant intensity of 2.4 krad/min for 4–30 hours. With ADMDA<sup>+</sup> ions, reactions were conducted

with various counter ions: hydroxide, acetate, chloride, bromide, benzoate and iodide.

### *Isotachophoresis*

ITP was performed with an LKB (Bromma, Sweden) 2127 Tachophor apparatus and a laboratory-made pilot unit allowing step changes in current intensity and external control of the strip-chart recorder. More details of the experimental set-up were given in a previous paper [13]. The composition of the operating electrolytes and the current intensities used for separation and detection are given in Table I.

### *CMC determinations*

The CMCs were determined from electrical conductivity measurements of aqueous monomer surfactant solutions at various concentrations, using a Tacussel (Villeurbanne, France) CD 60 numerical resistivimeter. The CMC is the concentration at which the plot of conductivity *versus* concentration changes its slope. The results are given in Table II.

### *Ultrafiltration*

Filtron Novacell 150 devices (Pharmacia, Les Ulis, France) with a 5000 g/mol molecular weight cut-off were used to perform the batch ultrafiltrations. Volumes of 20 ml of the sample solution were introduced into the cell and submitted to ultrafiltration under a pressure of  $0.5 \cdot 10^5$  Pa.

## RESULTS AND DISCUSSION

### *ITP analysis of crude irradiated reaction mixtures*

In previous work on the ITP determination of ionic surfactant mixtures, the influence of the composition of the leading electrolyte was studied in detail [13]. It was shown that the three parameters playing a prominent part were the methanol content in water, the leading ion concentration and the leading electrolyte pH.

Methanol was used as an organic modifier in order mainly to suppress the micellization phenomenon. This solvent was selected among other water-miscible solvents as the one maintaining the best resolution between surfactant homologues, although an increased tendency for drifting was generally observed for analyte conductivity steps with contents above 50%. The minimum methanol content

TABLE I  
TYPICAL COMPOSITIONS OF OPERATING ELECTROLYTE SYSTEMS

All solutions were prepared in water–methanol (80:20).

Parameter	Operating electrolyte system			
	L <sub>1</sub>	L <sub>2</sub>	L <sub>3</sub>	L <sub>4</sub>
Leading electrolyte:				
Leading ion	K <sup>+</sup> , 10 mM	K <sup>+</sup> , 10 mM	K <sup>+</sup> , 2 mM	K <sup>+</sup> , 2 mM
Buffer	Acetate, 13.2 mM	β-Alaninate, 12 mM	Acetate, 2.64 mM	β-Alaninate, 2.4 mM
pH <sup>a</sup>	5.5	10.6	5.5	10.6
Additive	TEG <sup>b</sup> , 2% (v/v)	TEG, 2% (v/v)	–	–
Terminating electrolyte	β-Alanine, 10 mM	Ethanolamine, 10 mM	β-Alanine, 2 mM	Ethanolamine, 2 mM
Current (μA): separation/detection	130/30	130/30	70/20	70/20

<sup>a</sup> pH values obtained with electrodes filled with aqueous electrolytes.

<sup>b</sup> TEG = tetraethylene glycol.

required for suppressing polymer aggregation should therefore be employed. As the concentration in any analyte zone remains proportional to that of the leading ion in the leading electrolyte, the latter concentration is another key parameter to be set in keeping with aggregation suppression. The leading ion concentration should therefore be kept below the CMC values in the solvent mixtures considered. Most of the following experiments reported here were performed with 10 mM leading electrolytes, but analysis of long-chain surfactants (*e.g.*, more than sixteen carbon atoms in the main chain) are favoured by lower concentrations. However, in practice, the range of accessible concentrations will be limited if both the correct buffering capacity and

low H<sup>+</sup> and OH<sup>−</sup> contributions to the total zone conductivity are to be maintained. Therefore, no attempt was made to work with leading electrolytes below 2 mM concentration. The pH of the leading electrolyte also remains a major parameter in such separations, even if the main constituents to be determined are strong electrolytes. As will be shown later, a proper choice of pH enables one to either detect or ignore degradation products such as fatty amines. Eventually, four different electrolyte systems were employed, the compositions of which are given in Table I.

Fig. 2 shows an isotachopherogram of a crude polyADMDA<sup>+</sup> sample, obtained with a water–methanol (50:50, v/v) acidic leading electrolyte. By enrichment of the crude polymer sample with known amounts of monomer, the monomer step was first identified as the lowest conductivity step produced by the sample components, while it can reasonably be accepted that the drifting sample step of highest conductivity corresponds to the polymer. Hence, a large separation between the polymer and the monomer was obtained. Figs. 2 and 3A allow the influence of the methanol content in the operating electrolytes to be evaluated and a careful examination of the isotachopherograms shows that a higher methanol content results in more step drifting, probably owing to poorer heat dissipation. It should

TABLE II  
CMC VALUES OF ADMDA<sup>+</sup> IN WATER ASSOCIATED WITH VARIOUS COUNTER-IONS

Determination: see Experimental.

Counter ion	CMC (mmol/l)	Counter ion	CMC (mmol/l)
OH <sup>−</sup>	29	Br <sup>−</sup>	13
CH <sub>3</sub> COO <sup>−</sup>	20	I <sup>−</sup>	5
Cl <sup>−</sup>	16	C <sub>6</sub> H <sub>5</sub> COO <sup>−</sup>	7

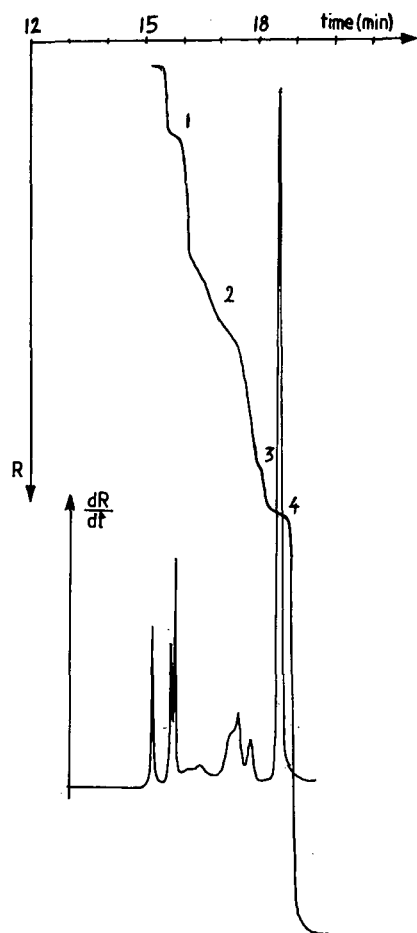


Fig. 2. Isotachopherogram of a 25-h-irradiated 100 mM solution of ADMDA<sup>+</sup> bromide. Operating electrolytes: L<sub>1</sub> (see Table I) except for the water-methanol composition (50:50, v/v). Numerals on the steps: 1 = electrolyte impurity; 2 = polymer; 3 = fatty amine (oxide) degradation product; 4 = monomer. Sample injected: 5  $\mu$ l of the 10 mM diluted solution. *R* axis, electrical resistance; *dR/dt* axis, electrical resistance derivative.

be noted that the leading electrolyte L<sub>1</sub> employed in Fig. 3A sets the analyte concentrations in all zones below the CMC of the monomer in water (20 mM for ADMDA<sup>+</sup> acetate; Table II). Hence, monomer aggregation cannot be observed. The separation conditions in Fig. 3A are good enough to distinguish clearly several species (especially from the differential trace) between the polymer and monomer steps. By submitting the same solution to basic electrolyte conditions (leading electrolyte L<sub>2</sub>, Table I), most of

these intermediate steps disappear (Fig. 3B). The corresponding species could be tentatively recognized as amine or amino oxide degradation products. Moreover, the lack of intermediate steps between those of the polymer and the monomer, under basic conditions, suggests that no, if any, oligomer was obtained. In addition, the flatness of the polymer step suggests that a fairly monodisperse polymer was also obtained in this manner.

The polymerizations of the other two surfactants studied (ADMCA<sup>+</sup> bromide and DVI<sup>+</sup> iodide) were followed isotachophoretically in a similar fashion. However, satisfactory separations between monomer and polymer can only be obtained if the leading ion concentration is lowered to 2 mM. With ADMCA<sup>+</sup>, the longer hexadecyl chain results in a very low CMC value (0.8 mM in its bromide form) and it can be inferred that the monomer micellizes at a 10 mM concentration level, even with a leading electrolyte containing 20% methanol. As for DVI<sup>+</sup>, it was mentioned in a previous paper [16] that an interaction between the monomer and the polymer is likely to occur with concentrations in excess of 2–4 mM in aqueous medium.

In an attempt to establish the best polymerization conditions, the amounts of unreacted monomer and degradation products were studied more systematically in terms of several adjustable parameters.

#### Assessment of the best polymerization conditions

A major interest of the ITP technique is that it enables one to follow quantitatively the remaining monomer and degradation products according to reaction time, counter-ion nature and initial monomer concentration. To this end, a mere standardization of the step lengths by injections of pure monomer is needed, as the response coefficients, *k*, defined as the ratio of the step length on the isotachopherogram (*l*) to the molecular amount injected (*n*) do not vary significantly for analytes of close mobilities bearing the same charge. Accordingly, it can be assumed that the response coefficients for a monomer and its major degradation product, whose conductivity step is close (Fig. 3A), are not basically different from each other.

The polymerization kinetics were first monitored for 100 mM ADMDA<sup>+</sup> bromide solution (CMC 13 mM, Table II). Fig. 4 shows that the reaction is almost completed after *ca.* 20–25 h of irradiation. By

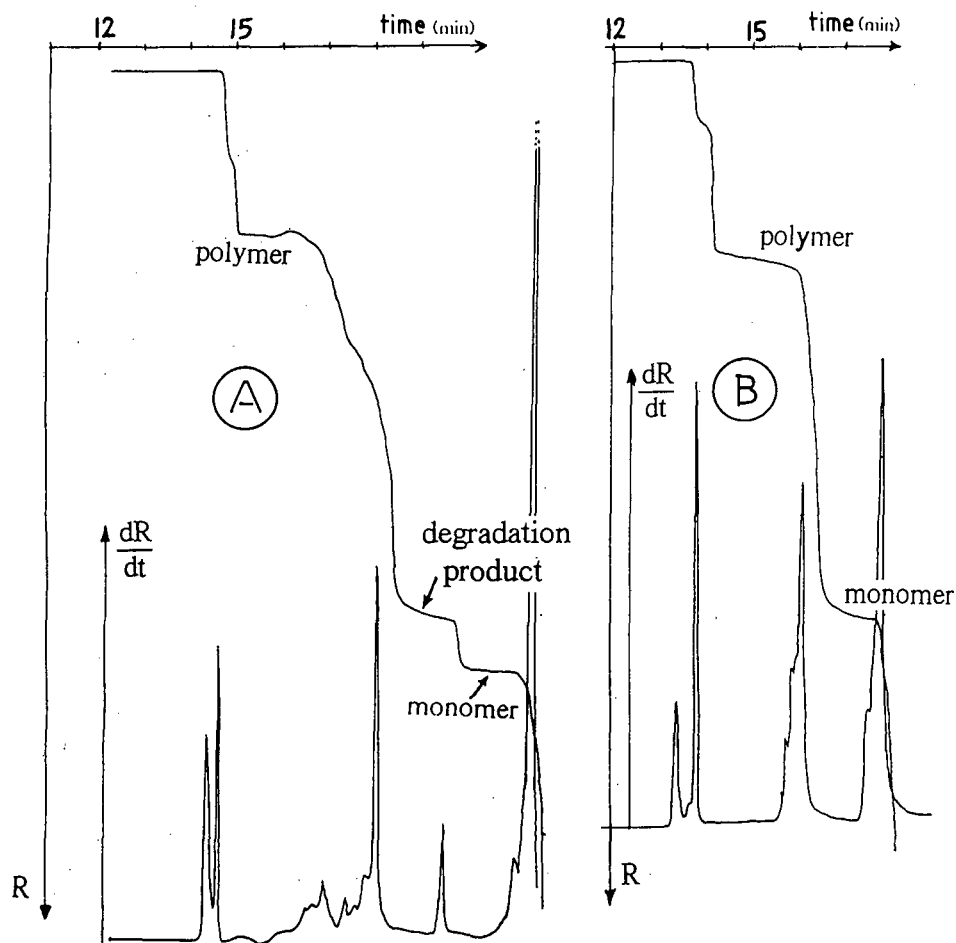


Fig. 3. Isotachopherograms of a crude polyADMDA<sup>+</sup> solution (badly degassed in order to enhance the amount of impurities) obtained under (A) acidic and (B) basic electrolyte conditions. Operating electrolytes: (A) L<sub>1</sub>; (B) L<sub>2</sub> (see Table I). *R* axis, electrical resistance; *dR/dt* axis, electrical resistance derivative.

this time, about 90% of the initial monomer has reacted and *ca.* 10% has been converted into the amine degradation product. Longer irradiation times (> 30 h) or the presence of small amounts of oxygen in the flask cause the amount of degradation products to increase drastically. Thus, a 25-h irradiation time seems optimum with respect to yield for flasks previously submitted to four freeze-pump-thaw cycles.

The polymerization yield was also investigated for ADMCA<sup>+</sup> bromide and DVI<sup>+</sup> iodide with the electrolyte conditions discussed above. It was observed that the monomer step had totally disappeared from

the isotachopherograms of 50 nmol of equivalent monomer amount after irradiation times of 4 h for a 45 mM DVI<sup>+</sup> iodide solution (CMC 4.3 mM) and of 25 h for a 10 mM ADMCA<sup>+</sup> bromide solution (CMC 0.8 mM). This result clearly indicates that the polymerization of ADMDA<sup>+</sup> bromide is not as fast as those of ADMCA<sup>+</sup> bromide or DVI<sup>+</sup> iodide, as a determinable amount of ADMDA<sup>+</sup> monomer is still visible on the isotachopherogram in Fig. 3 after a 25-h irradiation time. Further, a comparison between isotachopherograms obtained under acidic and basic conditions (electrolytes L<sub>3</sub> and L<sub>4</sub>, Table I) enabled us to evaluate the amine degradation prod-

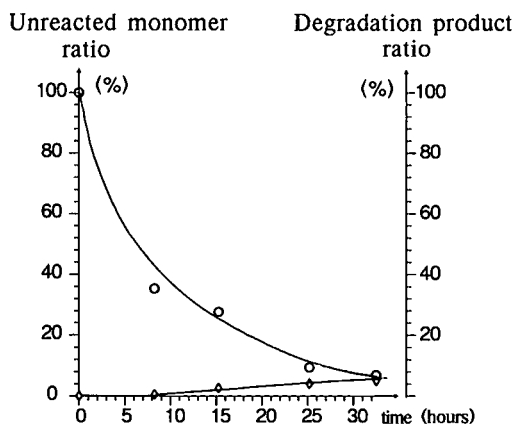


Fig. 4. Effect of irradiation time of a 100 mM ADMDA<sup>+</sup> bromide solution on (○) the unreacted monomer ratio and (◇) the degradation product ratio as determined by ITP. Operating electrolyte: L<sub>1</sub> (see Table I).

uct that had formed on completion of ADMCA<sup>+</sup> bromide polymerization as less than 10%.

In order to optimize the polymerization yield, irradiations were performed with various ADMDA<sup>+</sup> salts, keeping their concentration at 100 mM. The results are shown in Fig. 5, where these salts are arranged in increasing order of the counter-ion binding to micelles. Naturally, these differences in interaction between the micelle and its counter ion are also associated with variation of the CMC values (Table II), but the monomer concentration chosen, in all instances, remains far above these values. Apart from a secondary influence of the degree of counter-ion binding, it clearly appears that halide

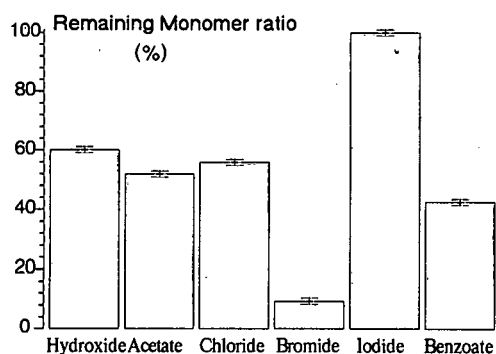


Fig. 5. Effect of counter ion associated with ADMDA<sup>+</sup> during the polymerization reaction (25 h of irradiation) of a 100 mM solution of this surfactant on the remaining monomer ratio, as determined by ITP. Operating electrolyte: L<sub>1</sub>.

counter ions play a special role in the polymerization yield. It is likely that bromide ions generate free radicals in the vicinity of the reactive double bonds, which are taking part in the polymerization reaction, hence leading to the best yield. Conversely, iodide ions might act as a shield impeding the reaction and thus leading to the poorest yield.

The last parameter studied was the initial monomer concentration. ADMCA<sup>+</sup> bromide was chosen for this series of experiments because of its low CMC value (0.8 mM) and its high solubility in water, which enabled us to vary the initial concentration over a wide range, between 8 and 100 mM, while keeping all monomers in the form of a micelle structure. Such experiments would be less easy to perform with ADMDA<sup>+</sup> halides, owing to their higher CMC values (Table II) and with DVI<sup>+</sup> iodide, which is too poorly soluble. It was ascertained (Fig. 6) that after a 25-h irradiation time the monomer conversion ratio is of the order of 90% (taking the degradation products into the account) for initial concentrations (8–10 mM) *ca.* ten times the CMC value, whereas it falls to only 30% for a 100 mM concentration. Undoubtedly, the initial monomer concentration plays a key role in the polymerization reactions and it turns out that it does not suffice to select any concentration above the CMC value to obtain a high yield of micelle

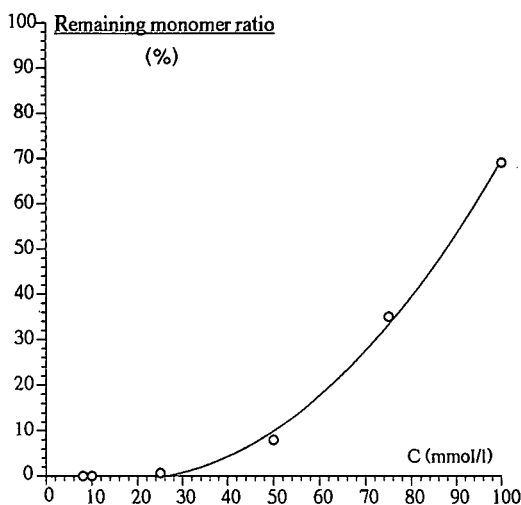


Fig. 6. Variation of the relative amount of ADMCA<sup>+</sup> remaining after a 25-h irradiation time in its bromide form as a function of the initial concentration of this surfactant. ITP operating electrolyte: L<sub>3</sub>.



polymerization. At present, the understanding of this concentration effect suffers from the lack of a kinetic model relevant to this specific reaction, so that we only set forth two putative explanations. First, it can be considered that the fixed intensity of  $\gamma$ -radiation can no longer produce the number of free radicals required with high monomer concentrations. However, this assumption does not seem consistent with the fact that, for the same radiation intensity and the same initial concentration (100 mM), 80% of the initial ADMDA<sup>+</sup> bromide amount was polymerized while an additional 10% was degraded. In addition, the sudden variation in reaction yield observed in Fig. 6 after 25 h of irradiation may originate from a change in the aggregate structure above a second critical concentration of the monomer, as recently suggested by Egorov [17] for a surfactant of similar chain length. However, this second assumption also seems questionable, as a great change in the rate of radical propagation would be related to a corresponding reduction in the fluidity of the micellar surface that has never been observed, to our knowledge. Hence, we consider that this point has not received a sound explanation.

Anyway, the preceding ITP results enable one to choose the optimum counter ion (bromide), the optimum initial concentration of the monomer and the optimum irradiation time, to yield 80–100% polymer, depending on the monomer. We shall now concentrate on comparing these polymers with classical micelles from a physico-chemical point of view.

#### *Analogy between ionic polymers and micelles*

In this study, ITP turned out to be more than an effective and flexible technique for the determination of surfactant monomers. Owing to the absence of a stationary phase and the existence of a steady state, the ITP process is amenable to quantitative modelling, which conversely can give access to the evaluation of physico-chemical parameters, such as absolute mobilities and acidity or complex formation constants. The classical ITP equations can be easily extended to account for the migration of ionic micelles in equilibrium with their monomers, as shown previously [15]. In short, the micelle mobility can be derived from the measurement of the conductivity step height of the micelle zone using usual

procedures, while the degree of counter-ion binding is related to the corresponding step length. Defining  $\beta$  as the ratio of bound counter ion per micelle to the aggregation number and  $\alpha$  as the fraction of free counter ion, we obtained, for the case where the CMC value is negligibly small compared with the total surfactant concentration [15]:

$$\alpha = 1 - \beta = \frac{m_{\text{mic}}}{m_{\text{mic}} - m_{\text{c}}} \cdot \frac{I}{Fv} \cdot \frac{l}{n} \quad (1)$$

where  $m_{\text{mic}}$  and  $m_{\text{c}}$  are the effective mobilities of the micelle and counter ion, respectively,  $I$  is the current intensity,  $F$  the Faraday constant,  $v$  the recorder chartspeed,  $l$ , the step length and  $n$  the amount of monomer injected. The ITP behaviour of poly-surfactants can be modelled in a simpler and more usual way than that of micelles as no equilibrium between monomer and polymer need be considered. Eqn. 1 remains valid with  $n$  representing injected amounts expressed in number of moles of monomer units. On that basis, the analogy between polymers and micelles can be highlighted on isotachopherograms in comparing the step lengths and heights produced by equal amounts of a polymer and a micelle (expressed as monomer units) injected successively. The experiment was conducted with polyADMDA<sup>+</sup> as a test polymer. However, a direct comparison between polyADMDA<sup>+</sup> and micelles of ADMDA<sup>+</sup> was not tempted because the CMCs of ADMDA<sup>+</sup> are too high, even in purely aqueous media (Table II). In effect, a leading electrolyte concentration greater than ten times the CMC value should be employed so that the amount of free monomer in the micelle zone would be negligible (*i.e.*, the CMC value be negligible compared with the surfactant zone concentration). This is why a more common surfactant, *n*-hexadecyltrimethylammonium ion, C<sub>16</sub>H<sub>33</sub>Me<sub>3</sub>N<sup>+</sup> (CMC 1.6 mM), was finally chosen.

As shown in Fig. 7, the steps heights and hence the mobilities of C<sub>16</sub>H<sub>33</sub>Me<sub>3</sub>N<sup>+</sup> micelles and polyADMDA<sup>+</sup> are very close to each other. At this point, it is worth noting that the initial counter ion of the analytes (*i.e.*, bromide here) is rapidly eliminated towards the terminating electrode vessel and replaced in all the zones by the counter ion of the leading electrolyte (*i.e.*, acetate here) migrating in the opposite direction. This aspect is of prime importance for comparing the degrees of counter-

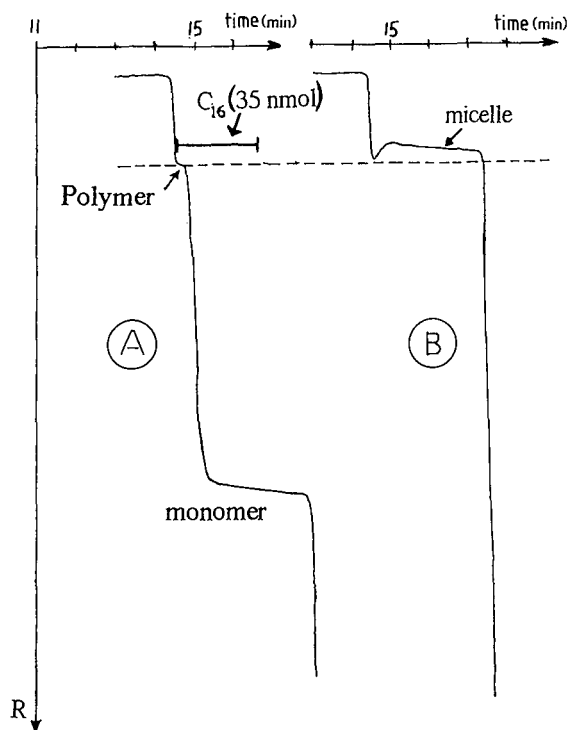


Fig. 7. Comparison of the ITP behaviours of (A) polyADMDA<sup>+</sup> as obtained after a 15-h irradiation of a 100 mM solution of ADMDA<sup>+</sup> bromide, and (B) C<sub>16</sub>H<sub>33</sub>Me<sub>3</sub>N<sup>+</sup> micelles. Operating electrolytes: L<sub>1</sub>, except for the solvent, which was water. Samples injected: 50 nmol of equivalent monomers or C<sub>16</sub>H<sub>33</sub>Me<sub>3</sub>N<sup>+</sup>. R axis, electrical resistance.

ion binding,  $\beta$ , to micelles and polymers. It is well known that  $\beta$  varies markedly with the nature of the counter ion bound, going typically from *ca.* 0.4 to 0.8 on substituting benzoate for OH<sup>-</sup>. The present operating electrolyte enabled us to determine  $\beta$  values for micelles and polymers with acetate as counter ion. The  $\beta$  values with other counter ions could be obtained very simply by changing the counter ion of the leading electrolyte. Hence ITP suppresses the need to perform a tedious counter-ion permutation of the analyte samples on a resin bed on which polymer adsorption can occur.

Measuring the respective step lengths for the C<sub>16</sub>H<sub>33</sub>Me<sub>3</sub>N<sup>+</sup> micelle and polyADMDA<sup>+</sup> from Fig. 7 and using eqn. 1,  $\beta$  values of 0.56 and 0.93 were calculated for the micelle and the polymer, respectively. This result indicates that acetate ions are much more strongly bound to the polymer than

to the micelle. It can be estimated, at a glance, by comparing the length of the polymer step with the length given by an equal amount of C<sub>16</sub>H<sub>33</sub>Me<sub>3</sub>N<sup>+</sup> micellized surfactants. The amount of polymer in Fig. 7A corresponds to 35 nmol of monomer units. Clearly, the much larger zone length of the 35-nmol C<sub>16</sub>H<sub>33</sub>Me<sub>3</sub>N<sup>+</sup> step drawn just above indicates a higher degree of counter-ion binding to the polymer. Similar results were obtained with polyDVI<sup>+</sup> and polyADMCA<sup>+</sup>. Hence the polymers resulting from  $\gamma$ -irradiation of cationic unsaturated surfactants behave like dynamic micelles as far as electrical mobility is concerned, but they seem to interact with their counter ions more strongly. Moreover, as shown in Figs. 2 and 3, these physico-chemical properties are hardly modified when methanol is added to the electrolyte up to at least 50%.

In an attempt to confirm that, as illustrated in Fig. 3B, very few oligomers are formed using this synthesis procedure, and in order to provide further insight into the molecular weight of the polymers obtained, ultrafiltration experiments were performed and the resulting two phases (retentate and ultrafiltrate) were analysed by ITP. The ultrafiltration of dynamic micellar solutions is well controlled at present. In particular, it has been established that the surfactant concentration in the ultrafiltrates will remain near to the CMC if the concentration of the initial sample is higher than the CMC [5]. This means that only free surfactant monomers are allowed to pass through the ultrafiltration membrane and that the size of a micelle is larger than the pore size of the membrane, corresponding to a molecular weight cut-off of *ca.* 5000 g/mol.

In this respect, we decided to ultrafilter a polyADMDA<sup>+</sup> bromide sample resulting from irradiation of a 100 mM monomer solution for 25 h. In order to suppress the micellization of the remaining monomers (CMC 13 mM, Table II), the sample was diluted to a 10 mM monomer equivalent concentration prior to ultrafiltration. Two solvents were tested successively to make the dilution: pure water and water-methanol (40:60, v/v). The ITP analysis of the ultrafiltrates revealed that no polymer is able to cross the membrane when ultrafiltration is carried out with purely aqueous samples (Fig. 8A). This behaviour suggests that the synthesized units do have a permanent structure, independent of the monomer concentration. However, in water, some

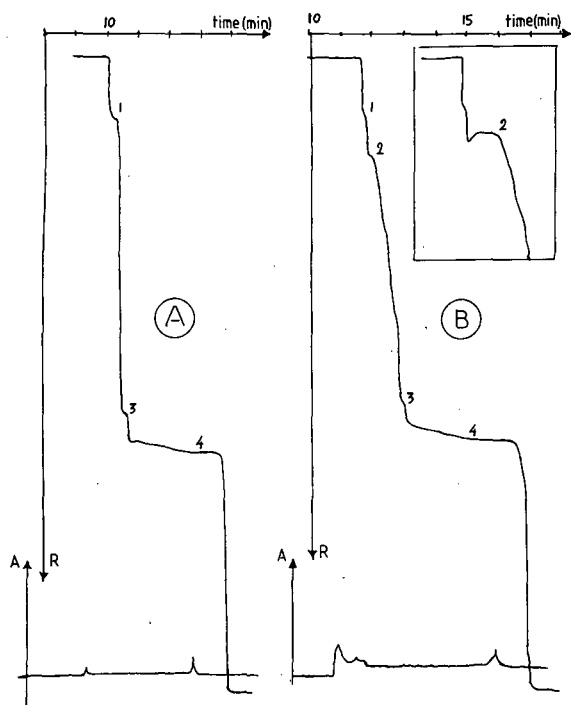


Fig. 8. Comparison of ultrafiltrates of polyADMDA<sup>+</sup> bromide solutions diluted to a 10 mM equivalent monomer concentration with (A) water and (B) water-methanol (40:60, v/v). Inset: part of the retentate isotachopherogram with the same electrolyte conditions. Numerals on the steps: 1 = electrolyte impurity; 2 = polymer; 3 = fatty amine (oxide) degradation product; 4 = monomer. Ultrafiltration membrane: Filtron Novacell 150, molecular weight cut-off 5000 g/mol. Operating electrolyte: L<sub>3</sub>. R axis, electrical resistance; A axis, UV absorbance (254 nm).

aggregates of oligomers might form, hence impeding their passage through the membrane. This is why the influence of methanol on the ultrafiltration separation was also examined. Figure 8B shows that in this instance, a small amount of products having mobilities close to that of the polymer and also some UV-absorbing degradation products are found in ultrafiltrates (the absence of these species in Fig. 8A proves that they were probably solubilized within the polymer aggregates in water). In comparing Fig. 8B with the inset retentate isotachopherogram, it clearly appears that most of the polymer remains in the retentate even in water-methanol (40:60) solution. At this stage, it can be concluded that the molecular weight of the polymer itself is higher than 5000 g/mol.

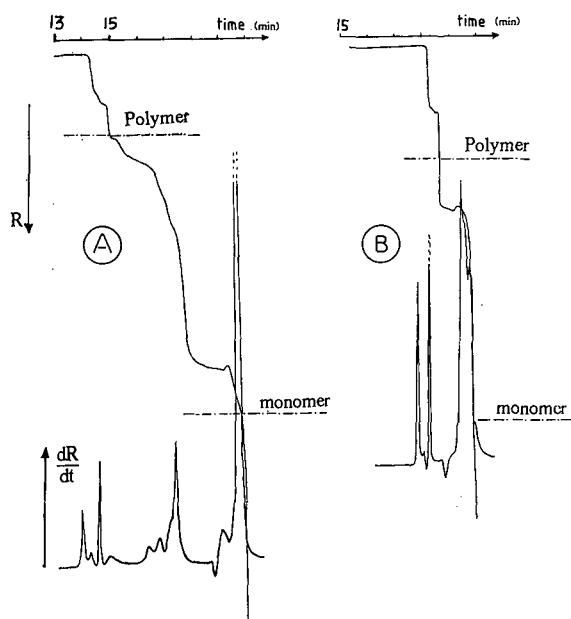


Fig. 9. Isotachopherograms of a 10 mM ADMDA<sup>+</sup> bromide solution after a 25-h irradiation time. (A) Acidic electrolyte conditions (L<sub>1</sub>); (B) basic electrolyte conditions (L<sub>2</sub>). Volume injected, 5  $\mu$ l. R axis, electrical resistance; dR/dt axis, electrical resistance derivative.

In order to stress further the analogy between dynamic micelles and those of ionic polymers, a 10 mM solution of ADMDA<sup>+</sup> bromide, *i.e.*, at a concentration below the CMC value, was irradiated for 25 h. The ITP analysis of the resulting reaction mixture showed that, under these conditions, the high-mobility polymer described previously was not formed at all (Fig. 9A and B). Instead, a large amount of degradation compounds is produced. This last experiment indicates that polymerization only progresses in the core of the micelle and is likely to stop rapidly in a purely aqueous medium. This can also be seen as a hint that the polymers and the micelles are close in size.

## CONCLUSIONS

The ITP monitoring of reaction mixtures of ionic surfactants submitted to  $\gamma$ -irradiation has been shown to be an efficient means for the optimization of operational parameters such as the initial surfactant concentration, the nature of its associated

counter ion and the time of irradiation. Once optimized, these reactions lead to polymeric surfactants with yields in excess of 80%, and it has been shown that these ionic polymers behave like polymerized micelles. In effect, their mobility was determined to be close to that of a classical dynamic micelle and it can be expected from ultrafiltration experiments that their degree of polymerization is of the same order of magnitude as the aggregation number of the corresponding dynamic micelles. Further, ITP provides an original means of evaluating the degree of counter-ion binding to the surfactant aggregates that will be more systematically used in our laboratory in the future.

ITP has turned to be an invaluable method allowing the identification and determination of the major ionic or ionizable compounds present in reaction mixtures. Among other advantages are the absence of a background electrolyte and stationary phase, the control of the analyte concentration in its own zone by the leading ion concentration, the relative ease of modelling, the versatility of conductivity detection and the overall simplicity of implementation and result interpretation.

## REFERENCES

- 1 J. G. Dorsey, *Adv. Chromatogr.*, 27 (1987) 167.
- 2 K. Weber and M. Osborne, *J. Biol. Chem.*, 244 (1969) 4406.
- 3 S. Terabe, K. Otsuka, K. Ichikawa and T. Ando, *Anal. Chem.*, 56 (1984) 111.
- 4 K. Osseo Asare and M. E. Keeney, *Proceedings of International Solvent Extraction Conference, ISEC '80, Vol. 1*, Association des Ingenieurs de l'Université de Liège, Liège, 1980, paper 80-121.
- 5 I. W. Osborne-Lee, R. S. Schechter and W. H. Wade, *J. Colloid Interface Sci.*, 94 (1983) 179.
- 6 J. Fendler and E. Fendler, *Catalysis in Micellar and Macromolecular Systems*, Academic Press, New York, 1975.
- 7 J.-H. Frendler and P. Tundo, *Acc. Chem. Res.*, 17 (1984) 3.
- 8 C. M. Paleos, *Chem. Soc. Rev.*, 14 (1985) 45.
- 9 C. M. Paleos, P. Dais and A. Milliaris, *J. Polym. Sci.*, 22 (1984) 3383.
- 10 J. C. Salamone, S. C. Israel, P. Taylor and B. Swider, *Polymer*, 14 (1973) 639.
- 11 L. R. Whitlock, *J. Chromatogr.*, 363 (1986) 267.
- 12 L. R. Whitlock, *J. Chromatogr.*, 368 (1986) 125.
- 13 C. Tribet, R. Gaboriaud and P. Gareil, *J. Chromatogr.*, 609 (1992) in press.
- 14 K. Ogino, T. Kakihara and M. Abe, *Colloid Polym. Sci.*, 265 (1987) 604.
- 15 C. Tribet, R. Gaboriaud and P. Gareil, *Electrochim. Acta*, 37 (1992) in press.
- 16 C. Tribet, R. Gaboriaud and J. Lelievre, *Polym. Int.*, 29 (1992) in press.
- 17 V. Egorov, *Makromol. Chem., Macromol. Symp.*, 31 (1990) 157.



# Effect of total percent polyacrylamide in capillary gel electrophoresis for DNA sequencing of short fragments

## A phenomenological model

Heather R. Harke, Sue Bay, Jian Zhong Zhang, Marie Josée Rocheleau and Norman J. Dovichi

*Department of Chemistry, University of Alberta, Edmonton, Alberta T6G 2G2 (Canada)*

---

### ABSTRACT

Polyacrylamide capillary gels were prepared with constant (5% C) cross-linker concentration and with total acrylamide concentration ranging from 2.5 to 6% T. At each acrylamide concentration, peak spacing was constant for DNA sequencing fragments ranging from 25 to 250 nucleotides in length. Peak spacing increased linearly with the total acrylamide concentration. The intercept of the retention time vs. fragment length plot was independent of %T. Ferguson plots were constructed for short DNA fragments; the polyacrylamide pore size falls in the 2.5 to 3.5 nm range for the gels studied. Theoretical plate count is independent of total acrylamide concentration; longitudinal diffusion, and not thermal gradients, limit the plate count. A phenomenological model is presented that predicts retention time, plate count, and resolution for sequencing fragments ranging in size from 25 to 250 bases and gels that range from 2.5 to 6% total acrylamide.

---

### INTRODUCTION

DNA sequencing requires separation of labeled DNA fragments by denaturing gel electrophoresis. The separation rate of these fragments is proportional to the electric field strength; high electric fields lead to fast separations. However, Joule heating generates a temperature gradient that limits the maximum electric field strength. Because of the strong dependence of mobility on temperature, 2.3% per degree, thermal gradients can produce band-broadening and degradation of the separation at high electric field strengths in slab gels [1].

Conventional DNA sequencing slab gels are *ca.* 0.5 mm thick. Thinner gels, *ca.* 0.1 mm, generate fast and efficient separations [2–4]. Difficulties in automation, in maintaining a uniform gel thickness

across the slab, and in detection have retarded widespread applications of this technology. On the other hand, capillary gel electrophoresis offers highly uniform chambers and high sensitivity detection technology. Typical fused-silica capillaries of 50  $\mu\text{m}$  I.D. produce outstanding thermal properties. Finally, the highly flexible nature of the capillaries simplifies automation.

Several groups have developed DNA sequencers based on capillary gel electrophoresis and laser-induced fluorescence detection [4–11]. In these systems, the capillaries are filled with denaturing polyacrylamide gels. The sequencing rate observed in these gels depends on the details of the gel composition. In this paper, we describe and model the sequencing rate, resolution, and separation efficiency in DNA sequencing by capillary gel electrophoresis.

---

*Correspondence to:* Dr. N. J. Dovichi, Department of Chemistry, University of Alberta, Edmonton, Alberta T6G 2G2, Canada.

## EXPERIMENTAL

The two-spectral channel DNA sequencing capillary electrophoresis system has been described before [11]. The polyimide coated, fused-silica capillary (Polymicro, AZ, USA) is typically 35 cm long  $\times$  190  $\mu\text{m}$  O.D.  $\times$  50  $\mu\text{m}$  I.D. The gel formulae are described below. The injection end of the capillary is held in a Plexiglass box equipped with a safety interlock. The other end of the capillary is inserted into the flow chamber of a locally constructed sheath flow cuvette. Fluorescence is excited with a low-power argon ion laser (Uniphase, CA, USA) operating in the blue at 488 nm; fluorescence is collected at right angles with a microscope objective (Leitz/Wild, Calgary, Canada), imaged onto a pin-hole, passed through a 525 nm center wavelength spectral filter (Omega, VT, USA), and detected with a photomultiplier tube (Hamamtsu, CA, USA). The current from the photomultiplier tube is dropped across a resistor, digitized, and recorded with a Macintosh IIsi computer.

The sample was prepared from a Genesis 2000 (DuPont, DE, USA) protocol using 3  $\mu\text{g}$  M13mp18 single-stranded DNA, 15 ng–21 17-mer M13 primer, and 2  $\mu\text{l}$  Sequenase 2.0 (US Biochemicals, OH, USA) in a standard ddA terminating reaction mix. The sample was ethanol precipitated and washed and then resuspended in 4  $\mu\text{l}$  of a mixture of formamide–0.5 M EDTA (49:1) at pH 8.0.

Gels are prepared in 5-ml aliquots from carefully degassed mixtures of acrylamide and N,N'-methylenebisacrylamide (Bis) 5% C, 2.5–6% T<sup>a</sup>; Bio-Rad, Toronto, Canada), 1X TBE, and 7 M urea (ICN, Montreal, Canada). Polymerization is initiated by addition of 2  $\mu\text{l}$  of N,N,N',N'-tetramethylethylenediamine (TEMED) and 20  $\mu\text{l}$  of 10% ammonium persulfate. The solution is injected into the capillary by use of a syringe. To prevent deformation of the gel into the detection cuvette, the gel was covalently bound to the last ca. 5 cm of the capillary wall through use of  $\gamma$ -methacryloxypropyltrimethoxysilane [6]. Although polymerization appears complete in 30 min, the capillaries are typically stored overnight before use. With use of high purity reagents and careful degassing, more than 95% of

the gel-filled capillaries are bubble free and generated useful data. Two or three replicates were taken with each capillary.

The sample was injected at 150 V  $\text{cm}^{-1}$  for 30 s; after injection, the sample was replaced with a fresh vial of 1  $\times$  TBE. The electrophoresis continued at 150 V  $\text{cm}^{-1}$ . The sheath stream was 1  $\times$  TBE at a flow-rate of 0.10 ml/h. Time is measured from the application of the separation potential.

## RESULTS AND DISCUSSION

*Sequencing rate and retention time*

Analysis was limited to 250 bases by the signal-to-noise ratio produced by this DNA sample. In all cases, a plot of retention time vs. fragment length (in bases) was linear ( $r > 0.998$ ) for fragments ranging in size from the primer to at least 250 bases; that is, retention time =  $T_0 + M \cdot \text{spacing}$  (1)

where  $T_0$  is intercept, spacing is the peak spacing in s/base, and  $M$  is the fragment length in bases. Fig. 1 presents typical data for a 4% T gel; for these data,  $T_0$  is 21.0 min and the peak spacing is 8.0 s/base.

The peak spacing increased linearly with %T for all fragments (Fig. 2). The data are shown at the 95% confidence interval; the line is the result of an unweighted least-squares fit. Only two runs were made with the 3% gel, resulting in a large confidence interval. The slope of this line, 5.0 s/base per %T, implies that the peak spacing increases by 5 s for every 1% increase in total acrylamide concentration. The intercept,  $-9.9$  s/base, should be related to the

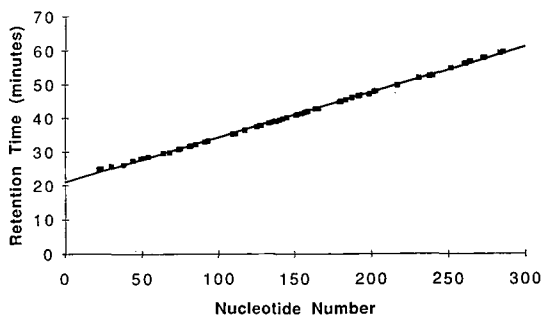


Fig. 1. Retention time as a function of fragment length for single-stranded DNA sequencing fragments separated in a 4% T, 5% C gel at an electric field strength of 150 V  $\text{cm}^{-1}$  in a 35 cm  $\times$  50  $\mu\text{m}$  I.D. fused-silica capillary. The separation was at room temperature.

<sup>a</sup> C = g Bis/%T; T = (g acrylamide + g Bis)/100 ml solution.

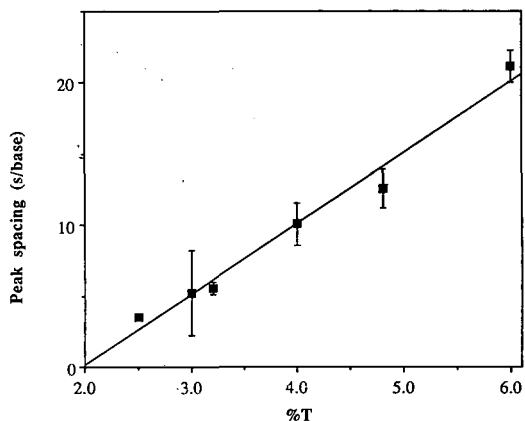


Fig. 2. Peak spacing of DNA fragments for denaturing polyacrylamide gels with constant 5°C, room temperature operation, an electric field strength of 150 V cm<sup>-1</sup>, and a 35 cm × 50 μm I.D. capillary. The data are shown at the 95% confidence interval and the line is the unweighted least-squares fit with a linear function.

free solution mobility of the DNA fragments; presumably, the negative sign implies that longer fragments will have a higher mobility than shorter fragments. The data of Kambara *et al.* [12] data show a quadratic dependence of peak spacing on %T from 2 to 12%T; from 2 to 6%T, their data are similar to ours.

The inverse of peak spacing is sequencing rate (Fig. 3); the data in bases/h are shown at the 95% confidence interval. The sequencing rate observed

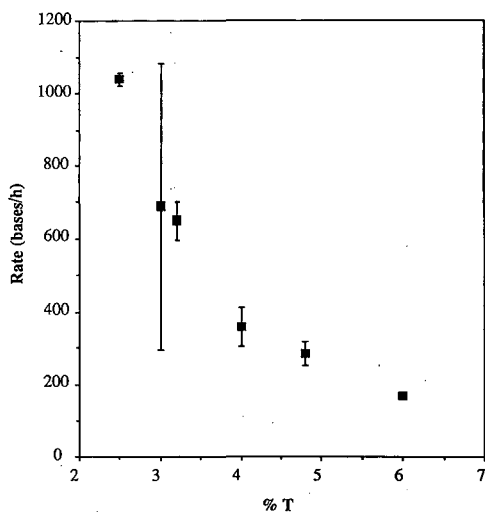


Fig. 3. Sequencing rate for the data of Fig. 1. Data shown at the 95% confidence interval.

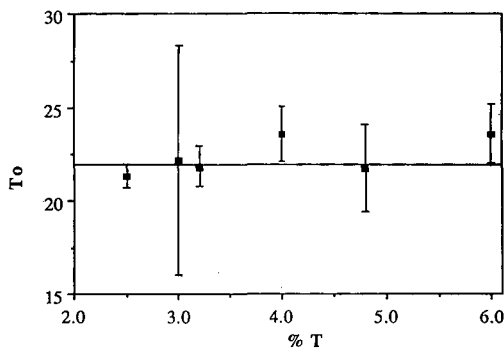


Fig. 4. Retention time for a vanishingly small DNA fragment as a function of total acrylamide concentration. Data shown at the 95% confidence interval.

for the 2.5% gel was 1,040 ± 10 bases/h, which is equal to the highest speed DNA sequencing rates reported in the literature for both capillary and slab gel electrophoresis [2,11].

Stegemann *et al.* [2] reported sequencing rate of 1000 bases/h for a slab gel separation at an electric field strength of 80 V cm<sup>-1</sup>. Their data appears to have been generated at 50°C while our data were taken at room temperature, 20°C. The difference in electric field strength necessary to obtain this sequencing rate is due to the 2.3% °C<sup>-1</sup> change in mobility with temperature [12].

T<sub>0</sub>, the retention time for a vanishingly small DNA fragment, is independent of %T (Fig. 4); that is, the retention time of a hypothetical 0-base fragment does not change with %T. This independence of migration rate is not surprising because the 0-base fragment would experience no retardation by the gel; similar data are reported by Kambara *et al.* [12] for separations of single-strand DNA performed on slab gels at an electric field of 50 V cm<sup>-1</sup>. The weighted average T<sub>0</sub> is 21.9 ± 0.2 min, shown as the horizontal line in the figure. Again, the data are shown at the 95% confidence interval. One datum was Q-tested at the 90% confidence level from the 6% gel data set.

Combining the results from Figs. 2 and 4, the retention time for a DNA fragment in a 5°C gel at 150 V cm<sup>-1</sup> in a 35-cm long capillary at room temperature can be written as

$$\begin{aligned} \text{retention time} &= \\ &= 21.9 \text{ min} + M \cdot \%T \cdot 0.083 \text{ min/base}/\%T \end{aligned} \quad (2)$$



for fragments ranging from 25 to 250 bases in length, gels ranging from 2.5 to 6%T, and room temperature operation. This formula was generated from over 35 electropherograms and represents over 80 h of instrument time.

#### Electrophoretic mobility

The relationship presented in eqn. 2 is quite robust in our laboratory. The equation is used to predict the electrophoretic mobility of a DNA sequencing fragment as a function of gel composition and nucleotide size.

$$\mu(M) = \frac{L/E}{\text{retention time}} \quad (3)$$

where  $L$  is the length of the capillary and  $E$  is the electric field; the ratio  $L/E = 0.233 \text{ cm}^2 \text{ V}^{-1}$  for our experimental conditions. The retention time relationship of eqn. 2 is substituted into eqn. 3 to predict the electrophoretic mobility of DNA fragments ranging in size from 25 to 250 bases and for gels ranging from 2.5 to 6%T.

$$\mu(M) = \frac{0.233 \text{ cm}^2 \text{ V}^{-1}}{1300 \text{ s} + M \cdot (-9.8 \text{ s/base} + 5.0 \text{ s/base} \cdot \%T)} \quad (4)$$

Eqn. 4 is a fundamental description of the electrophoretic behavior of nucleotides in 5%C polyacrylamide gels. This behavior must be described accurately for any successful theoretical description of DNA sequencing by gel electrophoresis.

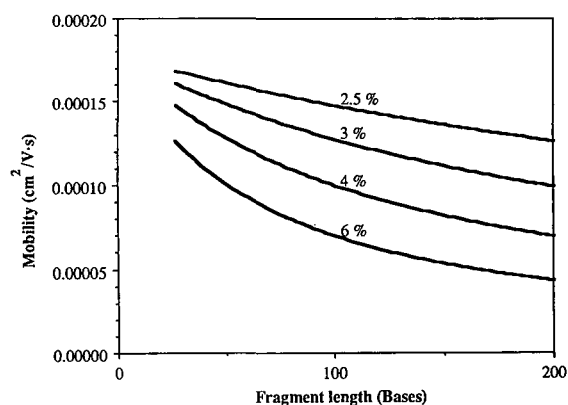


Fig. 5. Mobility of fluorescently labeled DNA fragments. Total percent acrylamide in the sequencing gel is noted above each curve.

Fig. 5 presents the predicted mobility for DNA fragments ranging from 25 to 200 bases in length and gels ranging from 2.5 to 6%T. The data extrapolate to a mobility of  $1.8 \cdot 10^{-4} \text{ cm}^2 \text{ V}^{-1} \text{ s}^{-1}$  for a fragment of zero bases, independent of percentage acrylamide. The mobilities that we obtain are approximately a factor of two smaller than that reported by Holmes and Stellwagen [13] for double-strand DNA separated at an electric field strength of 3.3 V/cm and at room temperature. Our results are about 75% of the values reported by Kambara *et al.* [12] for separation of single-strand DNA in a slab gel at 48°C. The thermal coefficient of mobility,  $2.3\% \text{ } ^\circ\text{C}^{-1}$ , exactly accounts for the observed difference between the data of Kambara *et al.* [12] and our data.

According to the Ogston model [13], mobility may be written as

$$\ln \mu(M) = \ln \mu(0) - K_R(M) \cdot \%T \quad (5)$$

Using eqn. 4 to calculate mobility, Ferguson plots [13] were generated in the range of 2.5 to 6%T for fragments ranging in size from 25 to 100 bases. The Ogston model is fit to the data. The curves extrapolate to a common intercept,  $\ln \mu(0) = -8.41 \pm 0.06$ , corresponding to a mobility in free solution of  $2.2 \pm 0.1 \cdot 10^{-4} \text{ cm}^2 \text{ V}^{-1} \text{ s}^{-1}$ . This result is 25% higher than that estimated above from the peak spacing data and one half the value reported for double stranded DNA [13].

According to the Ogston theory, the retardation of fragments is related to the fractional volume of spaces in the matrix that are accessible to the analyte [13]. To find the %T that produces the same pore size as a particular DNA fragment, the gel composition is found that produces a mobility that is one-half that estimated for free solution. Taking the free solution mobility as  $2.2 \cdot 10^{-4} \text{ cm}^2 \text{ V}^{-1} \text{ s}^{-1}$ , the mobility of interest is  $1.1 \cdot 10^{-4} \text{ cm}^2 \text{ V}^{-1} \text{ s}^{-1}$ , or  $\ln \mu = -9.12$ . A 3.5%T gel is estimated to have a pore size of 3.5 nm, equal to the radius of a 100-mer single stranded fragment; a 4.1%T gel has a pore size of 3.2 nm, equal to the radius of a 75-mer, and a 5.2% T gel has a pore size of 2.8 nm, equal to the radius of a 50-mer. The DNA fragment size is estimated from the formula

$$\text{radius} = 0.755 (\text{bases})^{1/3} \quad (6)$$

and is based on the geometric mean radius for

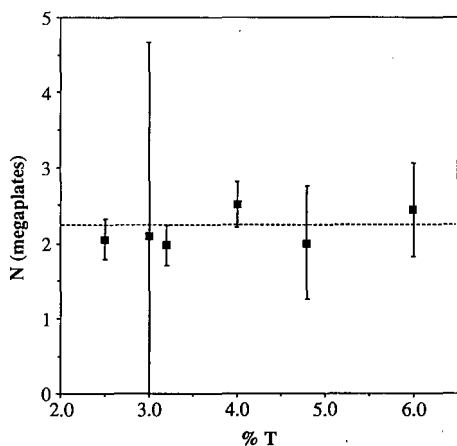


Fig. 6. Plate count for an 85-base DNA sequencing fragments as a function of total acrylamide concentration. Data are shown at the 95% confidence interval; the dotted line is the weighted average plate count.

double strand DNA [13]. A plot of log pore size vs. %T is linear ( $r = 1.000$ ) over the range studied, with slope  $-0.56$ . These data are consistent with those observed for Ferguson plots produced on slab gels with double-stranded DNA [13].

#### Theoretical plates

The theoretical plate count for base 85 was independent of %T over the range studied, with a weighted average of  $2.2 \pm 0.2 \cdot 10^6$  plates (Fig. 6). The data are shown at the 95% confidence interval and the dashed line is the weighted average plate count. Fragments 231 bases in length had separation efficiency,  $N = 2.2 \pm 0.4 \cdot 10^6$  plates, that also was independent of %T. Plate counts were estimated from the second moment calculation. Slab gel data shows a similar independence of plate count on gel composition [12], although plate counts appear to increase slightly with fragment length.

#### Band broadening —injection, detection and thermal gradient

It is interesting to speculate on the origin of the constant plate count. The product of injection voltage and time was varied by several orders of magnitude to determine the effect of column overloading; no improvement in plate count was noted for the smallest sample loadings. Detection time constant and volume do not seem to be important;

the system response time would limit plate counts to *ca.* 100 million.

Thermal band broadening could contribute to plate count. Joule heating will produce a parabolic temperature profile in the capillary. For all the gels studied, the electric current was constant,  $1.61 \pm 0.01 \mu\text{A}$ , and independent of gel composition. The heat generated per unit volume in a capillary of radius  $r$  is

$$Q = \frac{EI}{r^2} = \frac{\lambda CV^2}{L^2} = \frac{150 \text{ V cm}^{-1} \cdot 1.6 \cdot 10^{-6} \text{ A}}{\pi(2.5 \cdot 10^{-3} \text{ cm})^2} = 1.22 \cdot 10^1 \text{ W cm}^{-3} \quad (7)$$

Note that the heat dissipated in the capillary scales with voltage squared, at constant molar conductance,  $\lambda$ , and ionic strength,  $C$ . Knox [14] has stated that the temperature difference between the axis of the capillary and the inner wall,  $\theta$ , is given by

$$\theta = \frac{Qr^2}{4\kappa} = \frac{1.22 \times 10^1 \text{ W cm}^{-3} \times (2.5 \times 10^{-3} \text{ cm})^2}{4 \times (4 \times 10^{-3} \text{ W/cm/K})} = 0.005 \text{ K} \quad (8)$$

where  $\kappa$  is the thermal conductivity of the solution, rather arbitrarily estimated as  $4 \text{ mW cm}^{-1} \text{ K}^{-1}$  for the  $7 \text{ M}$  urea,  $1 \times \text{TBE}$ , polyacrylamide solution. The temperature difference across the capillary is very small for  $50 \mu\text{m}$  I.D. capillaries at  $200 \text{ V cm}^{-1}$  electric fields.

The parabolic temperature profile is translated to a velocity profile by the relative thermal coefficient of mobility,  $(d\mu/dT)/\mu = 0.023 \text{ K}^{-1}$  [12] (where  $T = \text{temperature}$ ). In our gels, the relative mobility of a fragment at the center of the capillary will be  $0.00012$  ( $0.012\%$ ) higher than the mobility of a fragment at the capillary wall. The maximum theoretical plate count in the presence of this thermally induced velocity profile is related to the diffusion coefficient of the DNA fragment; from the Stokes-Einstein formula, the diffusion coefficient of a molecule is given by [15]

$$D = \frac{kT}{6\pi\eta r_{\text{molecular}}} \quad (9)$$

where  $k$  is the Boltzmann constant. The data of Nishikawa and Kambara [1] suggest that the diffusion coefficient of a 100-mer fragment is about  $1.0 \cdot 10^{-7} \text{ cm}^2 \text{ s}^{-1}$  at  $50^\circ\text{C}$ . Converting to  $20^\circ\text{C}$ , the

diffusion coefficient is expected to be about  $9 \cdot 10^{-8} \text{ cm}^2 \text{ s}^{-1}$ . Substituting the diffusion coefficient, capillary length, fraction velocity difference, capillary radius, electrophoretic mobility, and electric field strength into Knox's equation

$$N_{\text{thermal}} = \frac{24D_m L}{\left(\frac{d\mu/dT}{\mu} \theta\right)^2 r^2 \mu E} = \frac{24 \cdot 9 \cdot 10^{-8} \text{ cm}^2 \text{ s}^{-1} \cdot 35 \text{ cm}}{\left[\frac{(0.00012)^2 (2.5 \cdot 10^{-3} \text{ cm})^2}{(1.0 \cdot 10^{-4} \text{ cm}^2 \text{ V}^{-1} \text{ s}^{-1} \cdot 150 \text{ V cm}^{-1})}\right]} = 5.6 \cdot 10^{10} \quad (10)$$

yields  $N_{\text{thermal}} = 56$  billion theoretical plates for an 86-mer fragment! Thermally induced band broadening does not appear to be significant in this capillary system.

$N_{\text{thermal}}$  scales inversely with the fifth power of electric field and thermally induced band-broadening is insignificant except at very high electric fields in capillaries. For example, an electric field strength of  $800 \text{ V cm}^{-1}$  will produce a temperature difference of  $0.2^\circ\text{C}$  across the  $50 \mu\text{m}$  I.D. capillary, corresponding to  $N_{\text{thermal}} = 5 \cdot 10^6$  plates. On the other hand, the thermal plate count scales inversely with the sixth power of radius. A 0.5-mm diameter capillary (with similar thermal characteristics as a 0.5-mm thick slab) will have a limiting plate count of 56 000 when operated at  $150 \text{ V cm}^{-1}$ . Thermal gradients dominate the performance of conventional slab gels at high electric fields.

#### Band broadening —longitudinal diffusion

Longitudinal diffusion appears to dominate band broadening in gel filled capillaries. Using the electrophoretic mobility of 85-mer fragments in 4% T gels, the plate count due to longitudinal diffusion is given by

$$N_{\text{longitudinal}} = \frac{\mu V}{2D_m} = \frac{1.0 \cdot 10^{-4} \text{ cm}^2 \text{ V}^{-1} \text{ s}^{-1} \cdot 5250 \text{ V}}{2 \cdot 9 \cdot 10^{-8} \text{ cm}^2 \text{ s}^{-1}} = 2.9 \cdot 10^6 \quad (11)$$

which, given the assumptions in the estimation of diffusion coefficient, is in remarkable agreement with the data. The dependence of plate count on

fragment size can be estimated from the mobility formula of eqn. 4, the size dependence of DNA from eqn. 6, and the longitudinal diffusion equation above

$$N_{\text{longitudinal}} = \frac{\mu V}{2D_m} = \frac{0.233 \text{ V}}{\frac{1300 \text{ s} + M \cdot (-9.8 \text{ s/base} + 5.0 \text{ s/base} \cdot \%T)}{\frac{2kT}{6\pi\eta \cdot 0.755M^{1/3}}}} = \frac{AM^{1/3} V}{1300 \text{ s} + M \cdot (-9.8 \text{ s/base} + 5.0 \text{ s/base} \cdot \%T)} \quad (12)$$

where  $A$  is a constant related to temperature and cross-linker concentration. For an 85-mer in a 4% T gel at a voltage of  $5250 \text{ V}$ ,  $A \approx 2.7 \cdot 10^5 \text{ s V}^{-1}$ . A plot of expected plate count vs. fragment length is shown in Fig. 7. Plate count maximizes for short fragments, *ca.* 85-mer, but varies by only 25% for fragments ranging in size from 25 to 250 bases. Within experimental error, plate count is independent of fragment length.

Plate count should increase linearly with applied potential. Potential can be increased either by increasing the electric field strength, for a constant length capillary, or by increasing the length of the capillary, at constant applied potential. The electric field strength cannot be increased without bounds. Polyacrylamide gels are unstable at electric field strengths greater than about  $500 \text{ V cm}^{-1}$  in our

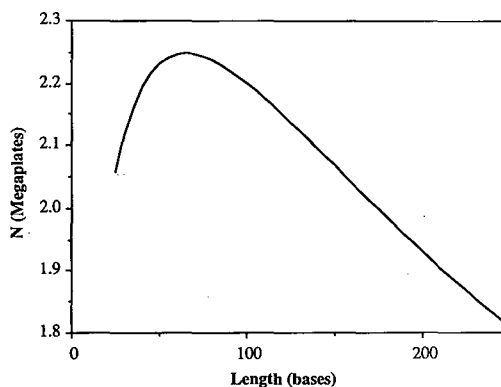


Fig. 7. Predicted plate count in a 4% total acrylamide gel.

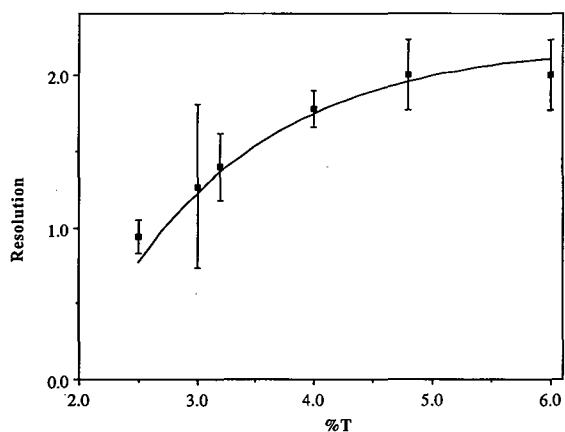


Fig. 8. Resolution of bases 85–86. Data are shown at the 95% confidence interval. The smooth curve is the prediction of eqn. 14; no parameters were adjusted.

laboratory. Large bubbles form in the capillary at high fields, destroying the separation. However, microbubbles may form at intermediate potentials, creating eddy diffusion and degrading the separation efficiency. It appears that longer capillaries are required to produce very high separation efficiency, albeit at the expense of longer analysis time.

### Resolution

Resolution was determined graphically for peaks 85–86 at different %T. The data are shown at the

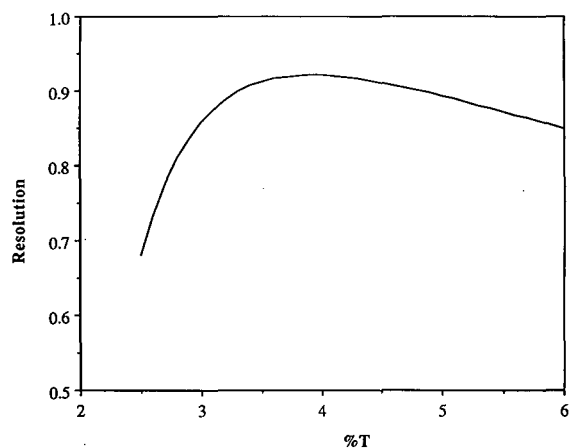


Fig. 9. Predicted resolution for adjacent DNA fragments as a function of total acrylamide concentration for fragments 250–251 bases in length.

95% confidence interval in Fig. 8. The range of resolution observed for the data, from 1 to 2, is quite similar to results from slab gel data [12]. Resolution degraded with increased length of sequencing fragments, for all %T studied; a similar phenomenon is present in the data of Kambara *et al.* [12] for fragments ranging in size from 100 to 400 bases.

Resolution of adjacent peaks is related to the theoretical plate count and the relative peak spacing [16,17]

$$\text{resolution} = \frac{\sqrt{N}}{4} \cdot \frac{\text{spacing}}{t_r} \quad (13)$$

substituting expressions for plate count, peak spacing, and retention time, the resolution is predicted to be

$$\text{resolution} = \frac{\sqrt{AM^{1/3}} \cdot V \cdot \frac{1}{4} \cdot (-9.84 \text{ s/base} + 4.99 \text{ s/base} \cdot \%T)}{[1310 \text{ s} + M \cdot (-9.84 \text{ s/base} + 4.99 \text{ s/base} \cdot \%T)]^{3/2}} \quad (14)$$

The smooth curve in Fig. 8 is a plot of predicted resolution for a fragment 82 bases in length and a potential of 5250 V. Recalling that there are no adjustable parameters in the theory, the agreement with the data is outstanding.

Resolution decreases as *ca.*  $M^{-3/2}$  for larger fragments at constant gel composition. For any given length fragment, resolution is maximized for a particular gel composition. Fig. 9 presents a plot of resolution *vs.* % T for a fragment 250 bases in length. Under the conditions at which our gels are run, the optimum resolution for a 250-mer is produced with a 4%T gel. To analyze long DNA fragments, it is appropriate to use low %T gels.

### CONCLUSIONS

We have presented a phenomenological model of DNA sequencing in polyacrylamide gels with 5% cross-linker concentration. The mobility model has three parameters: fragment length, %T, and the retention time of a vanishingly small DNA fragment. The plate count and resolution model contains one additional parameter, the diffusion coefficient.

cient of a DNA fragment of known size in a gel of known concentration.

This model is limited to 5%C polyacrylamide gels ranging from 2.5 to 6%T and operating at 150 V  $\text{cm}^{-1}$  at room temperature. Based on slab-gel data, eqn. 1 requires a quadratic term to describe sequencing data for gel compositions extending to 10%T. Because mobility increases by 2.3% per degree temperature rise, faster separations are expected at higher temperatures. Similarly, different cross-linker concentration or composition will lead to different sequencing rates.

The phenomenological model presented in this paper is limited to short fragments at an electric field strength of 150 V  $\text{cm}^{-1}$ . Our model is expected to fail for longer fragments and higher electric fields. Theory for double stranded DNA states that short fragments at low electric field exist in a random coil configuration [18]; the mobility of these fragments scale inversely with size. At higher electric fields, or for longer fragments, there is a transition to a stretched or linear configuration; these fragments migrate independently of size. Of course, it is not possible to obtain sequence information from fragments in the linear configuration. For double stranded DNA, the transition from random coil to stretched rod configuration scales as  $M/E^2$  [18]. Extrapolation of our model to fragments longer than 250 bases or for electric fields higher than 150 V  $\text{cm}^{-1}$  is not warranted.

#### ACKNOWLEDGEMENTS

This work was supported in part by the Department of Energy (DOE)–Human Genome Initiative (USA) grant number DE-FGO2-91ER61123. Support by DOE does not constitute an endorsement of the views expressed in this article. This work was also supported by the Natural Sciences and Engi-

neering Research Council of Canada, the Department of Chemistry of the University of Alberta, Pharmacia Inc. and Waters Division of Millipore Inc. H.R.H. acknowledges a predoctoral fellowship from the Alberta Heritage Foundation for Medical Research. N.J.D. acknowledges a Steacie fellowship from the Natural Sciences and Engineering Research Council of Canada.

#### REFERENCES

- 1 T. Nishikawa and H. Kambara, *Electrophoresis*, 12 (1991) 623.
- 2 J. Stegemann, C. Schwager, H. Erfle, N. Hewitt, H. Voss, J. Zimmermann and W. Ansorge, *Nucleic Acids Res.*, 19 (1991) 675.
- 3 A. J. Kostichka, M. K. Marchbanks, R. L. Brumley, H. Drossman and L. M. Smith, *Bio/Technology*, 10 (1992) 78.
- 4 H. Swerdlow and R. Gesteland, *Nucleic Acids Res.*, 18 (1990) 1415.
- 5 H. Drossman, J. A. Luckey, A. J. Kostichka, J. D'Cunha and L. M. Smith, *Anal. Chem.*, 62 (1990) 900.
- 6 A. S. Cohen, D. R. Najarian and B. L. Karger, *J. Chromatogr.*, 516 (1990) 49.
- 7 H. Swerdlow, S. Wu, H. Harke and N. J. Dovichi, *J. Chromatogr.*, 516 (1990) 61.
- 8 J. A. Luckey, H. Drossman, A. J. Kostichka, D. A. Mead, J. D'Cunha, T. B. Norris and L. M. Smith, *Nucleic Acid Res.*, 18 (1990) 4417.
- 9 D. Y. Chen, H. P. Swerdlow, H. R. Harke, J. Z. Zhang and N. J. Dovichi, *J. Chromatogr.*, 557 (1991) 237.
- 10 A. E. Karger, J. M. Harris and R. F. Gesteland, *Nucleic Acids Res.*, 19 (1991) 4955.
- 11 H. Swerdlow, J. Z. Zhang, D. Y. Chen, H. R. Harke, R. Grey, S. Wu, N. J. Dovichi and C. Fuller, *Anal. Chem.*, 63 (1991) 2835.
- 12 H. Kambara, T. Nishikawa, Y. Katayama and T. Yamaguchi, *Bio/Technology*, 6 (1988) 816.
- 13 D. L. Holmes and N. C. Stellwagen, *Electrophoresis*, 12 (1991) 253.
- 14 J. H. Knox, *Chromatographia*, 26 (1989) 329.
- 15 R. A. Mosher, D. Dewey, W. Thormann, D. A. Saville, M. Bier, *Anal. Chem.*, 61 (1989) 362.
- 16 J. W. Jorgenson, K. D. Lukacs, *Anal. Chem.*, 53 (1981) 1298.
- 17 J. C. Giddings, *Sep. Sci.*, 4 (1969) 181.
- 18 J. Noolandi, *Can. J. Phys.*, 68 (1990) 1055.

# Switching valve with internal micro precolumn for on-line sample enrichment in capillary zone electrophoresis

A. J. J. Debets, M. Mazereeuw, W. H. Voogt, D. J. van Iperen, H. Lingeman, K.-P. Hupe and U. A. Th. Brinkman

*Department of Analytical Chemistry, Free University, De Boelelaan 1083, 1081 HV Amsterdam (Netherlands)*

---

## ABSTRACT

The design of a switching valve containing a micro precolumn for on-line sample enrichment in capillary electrophoresis is described. Samples are loaded on to the precolumn with a micro liquid chromatographic pump, while desorption is performed by means of the electroosmotic flow. The influence of the precolumn on the capillary zone electrophoretic separation process was investigated. A zone-cutting procedure was introduced, by means of valve switching, to prevent excessive band broadening and shifting of the migration times. Using papaverine as a model compound, it was shown that sample volumes of up to 100  $\mu\text{l}$  can be enriched on the precolumn. Calibration plots are linear over a concentration range of two orders of magnitude. The detection limit of papaverine is  $5 \cdot 10^{-8}$  M (5 pmol injected; UV detection at 254 nm). The potential of the sample-enrichment valve for on-line coupling to micro liquid chromatography is discussed.

---

## INTRODUCTION

Recent developments in micro separation systems have significantly improved their applicability. Especially in the field of capillary electrophoresis (CE), the combination of high separation efficiency, sensitive detection modes (*e.g.*, amperometric, laser-induced fluorescence, mass spectrometry) and special injection techniques provide low absolute detection limits [1]. Nevertheless, the analysis of complex samples still requires the development of sample treatment methods suitable for micro separations. Apart from the removal of components that can clog the analytical separation system, reduction of the large number of interfering compounds in complex samples is necessary. In addition, the limited injection volumes commonly used in CE (< 10 nl) restrict the detectability of analytes. In addition to off-line liquid-liquid extraction and precipitation methods,

on-line coupled techniques such as liquid chromatography (LC)-capillary zone electrophoresis (CZE) [2] and isotachopheresis (ITP)-CZE [3] can be used for sample clean-up. Coupling of ITP to CZE has also been used to achieve analyte enrichment. Electrodesorption in combination with zone electrophoresis, isoelectric focusing and ITP can also be used for the desorption of protein ligates [4–7].

Recently, off-line solid-phase cartridges have been used to achieve trace enrichment in CZE [8]. In another study, capillaries with interactive walls, *i.e.*, coated capillaries which are frequently used in gas chromatography (GC), have been used for on-line preconcentration in CZE [9]. Using these techniques one order of magnitude analyte enrichment was achieved. However, so far the off-line techniques have not been very successful because they are time consuming and laborious, while the on-line techniques lack sample capacity or result in severe band broadening and, consequently, in loss of resolution. As the use of precolumns to increase sensitivity in GC is a well known technique, as an alternative to

---

Correspondence to: Professor U. A. Th. Brinkman, Department of Analytical Chemistry, Free University, De Boelelaan 1083, 1081 HV Amsterdam, Netherlands.

overcome the mentioned limitations, in this work a laboratory-made rotary-type switching valve was developed that contains a micro precolumn in order to obtain on-line sample enrichment in CZE. Sorption on to the precolumn is performed using an LC pump and desorption is achieved by using electroosmotic flow.

## EXPERIMENTAL

### Chemicals and solutions

Phosphoric acid, sodium dihydrogenphosphate, sodium hydroxide, concentrated hydrochloric acid, glacial acetic acid, tetrabutylammonium bromide, octanesulphonic acid and phenol were purchased from J. T. Baker (Deventer, Netherlands). Acetonitrile (HPLC grade) was obtained from Westburg (Leusden, Netherlands). Codeine, noscapine and papaverine hydrochloride were a gift from P. de Goede (Academic Hospital, Free University, Amsterdam, Netherlands); they were stored as concentrated 10 mM aqueous solutions in distilled, demineralized water at 5°C. All diluted samples (1  $\mu$ M–0.1 mM) were prepared daily in demineralized, distilled water. Unless mentioned otherwise, electrophoresis was performed in an aqueous 7.5 mM phosphate buffer (pH 4.5) containing 25% (v/v) acetonitrile. In order to reduce gas bubble formation, sample solutions contained 5% (v/v) acetonitrile and were degassed with helium before use.

### Instrumentation

CZE was performed using a modified Brandenburg (Thornton Heath, UK) Alpha Series II high-voltage power supply which was operated in the constant-current mode (30  $\mu$ A, voltage *ca.* 16 kV). All instruments were placed in a Plexiglas safety box. A 200  $\mu$ m I.D. (340  $\mu$ m O.D.) fused-silica capillary obtained from Polymicro Technologies (Phoenix, AZ, USA) with a total length of 60 cm was used for the electrophoretic separation. After installation of the capillary and after every ten experiments the capillary was washed with 0.1 M hydrochloric acid and 0.1 M potassium hydroxide in order to clean and activate the capillary wall. Glass vials containing platinum electrodes were used as electrode vessels. A fan was used to cool the outer wall of the electrophoresis capillary. Detection was performed at 250 nm with an Applied Biosystems (Ramsey, NJ,

USA) Model 757 UV absorbance detector, modified for on-column capillary detection.

A laboratory-made six-port injection valve equipped with a 1.0-ml loop was used to load the sample. The sample was flushed on to the precolumn in the switching valve (see below) by means of an LDC/Milton Roy (Riviera Beach, FL, USA) Micro-metric 5-ml syringe pump.

For the LC separation a slurry-packed 14 cm  $\times$  320  $\mu$ m I.D. microcolumn containing 5- $\mu$ m RoSil C<sub>8</sub> (RSL, Eke, Belgium), was used. An LKB (Bromma, Sweden) Model 2150 pump was used for mobile

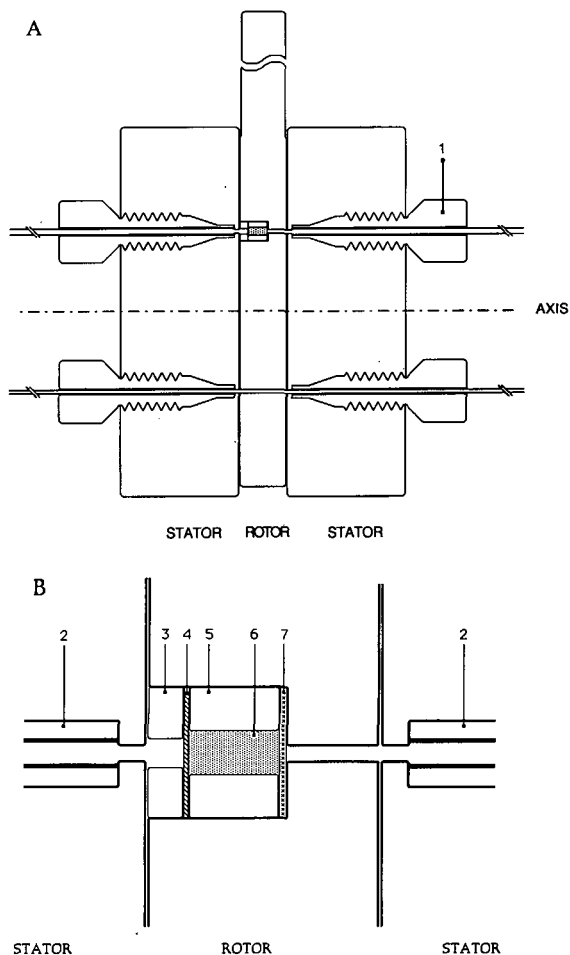


Fig. 1. (A) Cross-sectional view of the switching valve with (B) the precolumn. 1 = Finger-tight connections; 2 = capillary inlet/outlet; 3 = 1.5 mm  $\times$  0.3 mm I.D. PTFE tubing; 4 = metal screen; 5 = 1.5 mm  $\times$  0.5 mm I.D. PEEK tubing; 6 = PLRP-S packing material; 7 = PTFE screen.

phase delivery. Noscapine, codeine and papaverine were separated using methanol–water (40:60, v/v), containing 1% (v/v) glacial acetic acid, 10 mM tetrabutylammonium bromide and 2.5 mM octanesulphonic acid, as the mobile phase. The separation was performed at ambient temperature.

#### *Switching valve with internal precolumn*

The switching valve containing the micro precolumn was a rotary-type injection valve [10], modified for small sample volumes and containing a laboratory-made precolumn. Fig. 1A shows a cross-sectional view of the valve. The polyethylene rotor (6 mm thick) contains the precolumn and a 200  $\mu\text{m}$  I.D. channel parallel to the precolumn. The precolumn (Fig. 1B) consisted of 1.5 mm  $\times$  500  $\mu\text{m}$  I.D. (volume 0.2–0.3  $\mu\text{l}$ ) poly(ether ether ketone) (PEEK) tubing (Alltech, Zwijndrecht, Netherlands) slurry packed with 8- $\mu\text{m}$  PLRP-S divinylbenzene–styrene polymer (Polymer Laboratories, Church Stretton, UK). The inlet of the column was closed with a metal screen (Metaalgaasweverij Dinxperlo, Dinxperlo, Netherlands) and the outlet with a PTFE screen (Alltech). The metal screen was needed for mechanical support during the sample loading procedure and to prevent clogging of the column inlet. A piece of 1.5 mm  $\times$  300  $\mu\text{m}$  I.D. PTFE tubing was used to position the microcolumn in the rotor. The rotor was mounted between two poly(ethylene terephthalate) stators; it can be used at pressures up to 150 bar without leakage. Capillaries were connected to the valve with laboratory-made finger-tight connections.

## RESULTS AND DISCUSSION

#### *Performance of the switching valve*

In order to study the performance of the precolumn, the rotary type switching valve was coupled to an LC set-up (Fig. 2A). For this study the analytical column in the set-up was replaced with a 25 cm  $\times$  200  $\mu\text{m}$  I.D. fused-silica capillary. Via the six-port valve, sample solution was flushed directly on to the micro precolumn in the switching valve by means of a micro LC pump (pump 1). An LC pump (pump 2) was used to pump the eluent through the switching valve, *i.e.*, the precolumn, via the capillary, to the UV detector.

Papaverine ( $\text{p}K_{\text{a}} = 6.6$ ) was chosen as model

compound. This analyte is hardly ionized in demineralized water so that trace enrichment on the polymer-packed precolumn will present no problems. To obtain information on the breakthrough characteristics of papaverine,  $10^{-4}$  M sample solutions were loaded on to the micro precolumn (1.5 mm  $\times$  0.5 mm I.D.) until analyte breakthrough was observed. Breakthrough volumes larger than 1 ml were obtained when papaverine was dissolved in demineralized water. The addition of organic modifier to the sample solution resulted in lower breakthrough volumes: a breakthrough volume of 320  $\mu\text{l}$  was obtained with a water–acetonitrile (95:5, v/v) sample solution, whereas almost immediate breakthrough (breakthrough volume 2  $\mu\text{l}$ ) occurred in the presence of 25% acetonitrile.

Because micro separation systems, and particularly CE, are sensitive to gas bubbles formed in the buffers used for the analytical separation, the addition of 5% of acetonitrile was found necessary in order to obtain efficient degassing. In all further experiments sample solutions in water–acetonitrile (95:5, v/v) were used. Furthermore, sample volumes loaded on the precolumn were 100  $\mu\text{l}$  or less in order to prevent breakthrough.

Loading of the sample on to the precolumn involves three steps. First, the precolumn is washed with 10  $\mu\text{l}$  of aqueous 7.5 mM phosphate buffer (pH 2.2)–acetonitrile (75:25, v/v) to remove contaminants from the precolumn. Next, the precolumn is conditioned with 10  $\mu\text{l}$  of water–acetonitrile (95:5, v/v) at a flow-rate of 5  $\mu\text{l}/\text{min}$ , after which the sample is loaded in the forward flush mode. Finally, the analyte is desorbed by the mobile phase and flushed to the detector via the fused-silica capillary. The sample is loaded on to the precolumn using a flow-rate of 5  $\mu\text{l}/\text{min}$ . Using this flow-rate the peak width of the desorbed analyte is 30 s and the peak height is 0.56 absorbance units. If higher flow-rates (*e.g.*, 10  $\mu\text{l}/\text{min}$ ) are used the accuracy for small sample volumes will decrease [relative standard deviation (R.S.D.)  $> 10\%$ ] whereas for lower flow-rates the peak width increases and the peak height decreases.

The loading procedure was found to be linear over a range of 1–100  $\mu\text{l}$  of sample solution loaded on to the precolumn. The plot of peak height (UV absorbance) versus sample volume was given by the equation  $y = 0.40 (\pm 0.01)x + 1.54 (\pm 0.39)$  ( $r^2 = 0.994$ ,



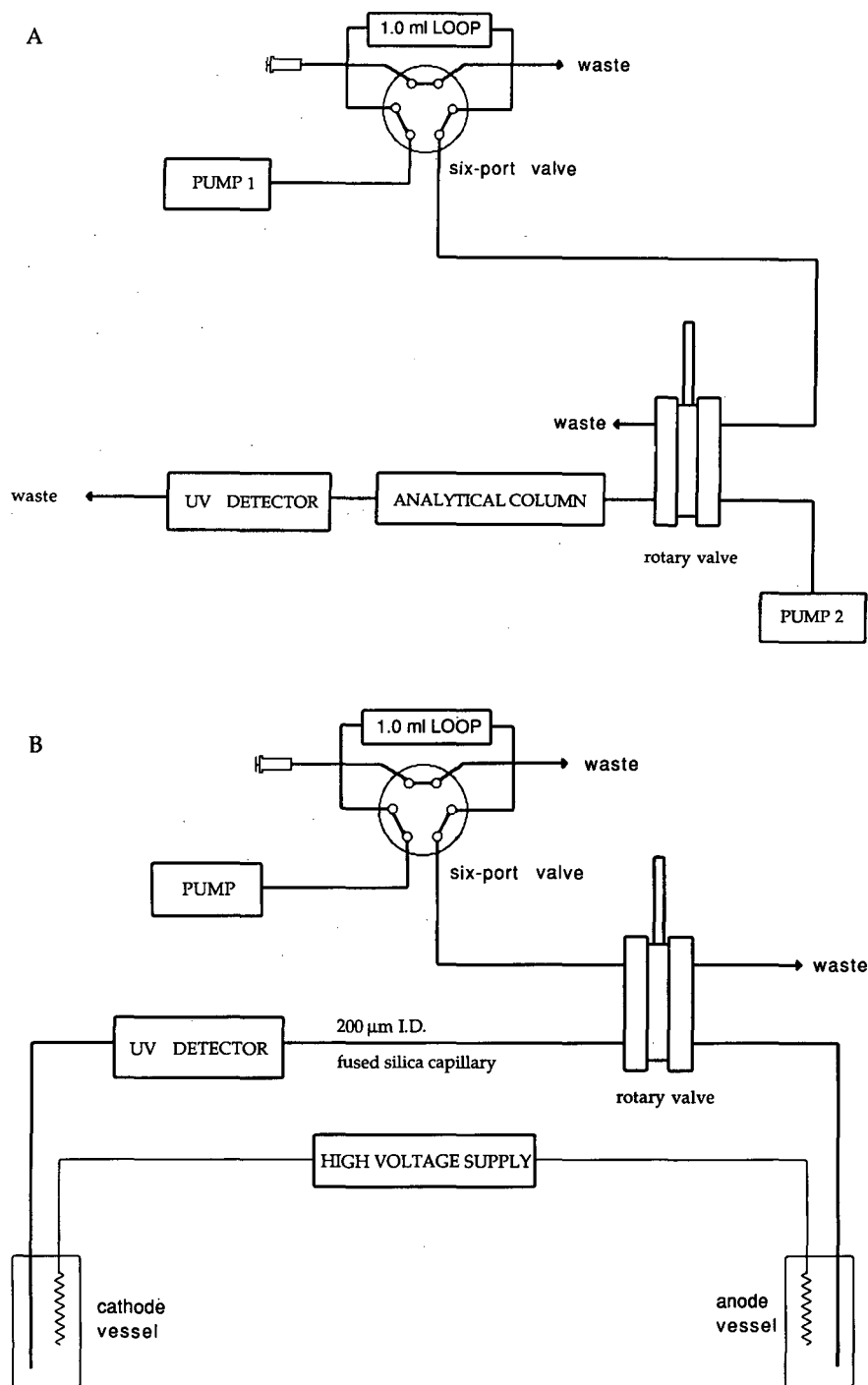


Fig. 2. Set-up of the switching valve coupled to micro separation systems. (A) Switching valve coupled to micro LC system. Pump 1 is used to flush the sample solution into the switching valve and pump 2 for eluent delivery. (B) Switching valve coupled to CZE system.

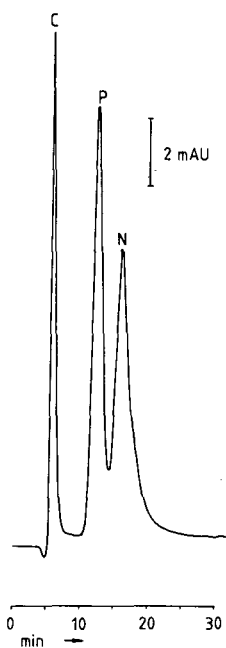


Fig. 3. LC-UV of a mixture of codeine (C) ( $10^{-5}$  M), noscapine (N) ( $10^{-5}$  M) and papaverine (P) ( $10^{-6}$  M) in water after enrichment of 100  $\mu$ l of sample. The 1.5 mm  $\times$  500  $\mu$ m I.D. precolumn was packed with 8- $\mu$ m PLRP-S. UV detection at 250 nm. Eluent flow-rate, 3  $\mu$ l/min.

$n = 6$ ,  $10^{-6}$  M papaverine), where  $y$  and  $x$  are in milliabsorbance units and  $\mu$ l, respectively. As an example, Fig. 3 shows the reversed-phase ion-pair LC separation of a mixture of codeine, papaverine and noscapine with on-line trace enrichment.

#### Rotary switching valve coupled to CZE

The switching valve is made of synthetic material which allows the direct coupling to a high-voltage CZE system. The set-up for the CZE experiments is shown in Fig. 2B. The injection valve was placed in-line between two electrode vessels. The CZE separation was performed in a 60 cm  $\times$  200  $\mu$ m I.D. fused-silica capillary. The high-voltage power supply was operated in the constant-current mode. In this mode temperature changes will have less influence on the electrophoretic separation than when using the constant-potential mode. In this study currents of up to 30  $\mu$ A (electric field 180–250 V/cm) were used. The use of higher currents frequently caused the formation of gas bubbles, which led to breakdown of the electrophoretic separation process.

Instead of a hydrodynamic flow delivered by an LC pump, an electroosmotic (EO) flow, produced by means of the high voltage, was used for eluent delivery. If an electric field is applied over a fused-silica capillary having a negatively charged wall

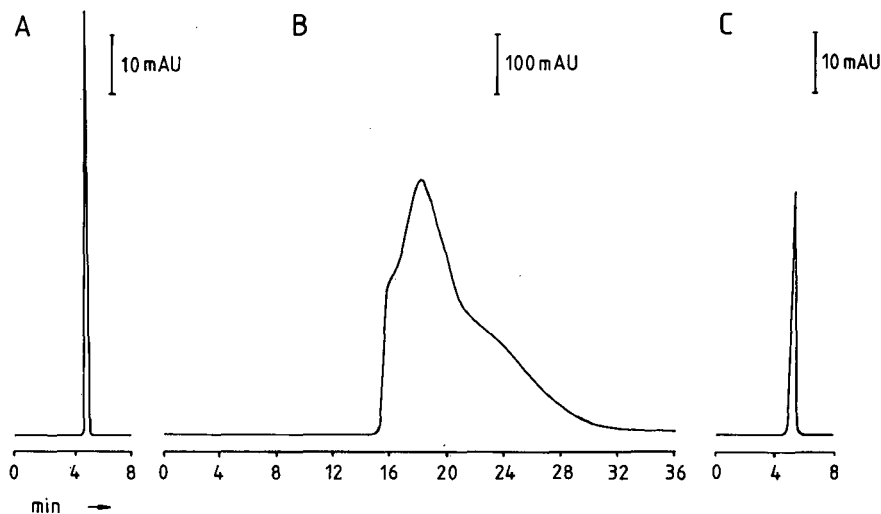


Fig. 4. (A) Electropherogram of 0.2  $\mu$ l of papaverine ( $10^{-4}$  M) in water-acetonitrile (95:5, v/v) after direct injection. (B) Electropherogram of 5  $\mu$ l of papaverine ( $10^{-4}$  M) in water-acetonitrile (95:5, v/v) with precolumn on-line during electrophoresis (current, 20  $\mu$ A). (C) Electropherogram of 5  $\mu$ l of papaverine ( $10^{-5}$  M) in water-acetonitrile (95:5, v/v) after electrodesorption procedure; desorption time, 45 s; current, 30  $\mu$ A. For detailed conditions, see text.

surface, movement of the ion double layer will cause an EO flow. The EO flow-rate depends on parameters such as ionic strength, pH and viscosity of the buffer solutions and the electric field strength. In this study the EO flow and the analyte migration were both towards the negative electrode, which means that detection should take place at the cathode side of the capillary (Fig. 2B).

**Sample enrichment and desorption.** Enrichment of the papaverine-containing sample solution on the precolumn in the rotary switching valve was performed as described above. The precolumn was washed with *ca.* 10  $\mu\text{l}$  of aqueous 7.5 mM phosphate buffer (pH 4.5)–acetonitrile (25:75, v/v) and conditioned with 10  $\mu\text{l}$  of water–acetonitrile (95:5, v/v). Next, it was loaded with papaverine, dissolved in water–acetonitrile (95:5, v/v) at a flow-rate of 5  $\mu\text{l}/\text{min}$  and washed with 0.2  $\mu\text{l}$  of water–acetonitrile (95:5, v/v) to flush the valve dead volume. After washing, the precolumn was switched on-line with the CZE capillary. Next, a constant current of 30  $\mu\text{A}$  was applied and the precolumn was desorbed using the EO flow. During desorption the analyte becomes charged due to the pH shift (7  $\rightarrow$  4.5) and electrophoresis will take place.

When papaverine was desorbed in the forward-flush mode, significant band broadening occurred (compare Fig. 4A and B). This band broadening is probably caused by a combination of several effects; apart from the slow desorption, which was also observed with packed capillaries in other studies [4–7], the relatively large precolumn volume, the dead volume of the injection valve and the disturbance of the EO flow profile caused by the back-pressure of the precolumn are important factors. In addition, the migration time was considerably higher, *i.e.*, 13 min, in the presence (Fig. 4B) than in the absence (Fig. 4A) of the precolumn. The increase in migration time is the result of a *ca.* 70% decrease in the EO flow that occurs on switching the precolumn on-line with the electrophoresis capillary. The EO flow will decrease because of the mechanical resistance of the precolumn and, as the inner diameter of the precolumn (500  $\mu\text{m}$ ) is significantly larger than that of the electrophoresis capillary (200  $\mu\text{m}$ ), the electric field strength will be smaller. An increase in migration time was also observed in experiments with phenol ( $\text{p}K_{\text{a}} = 10$ ), instead of papaverine used as test compound. Under the test

TABLE I

## DEPENDENCE OF ANALYTE RECOVERY ON ELECTRODESORPTION TIME

Conditions: loading of 5  $\mu\text{l}$  of  $10^{-5}$  M papaverine solution; 1.5 mm  $\times$  0.5 mm I.D. precolumn; current, 30  $\mu\text{A}$ ;  $n = 2$ , R.S.D. < 5%.

Electrodesorption time (s)	Peak height (milliabsorbance units)	$w_{0.5}^a$ (s)
30	13	<30
40	34	30
45	44	30
60	42	50

<sup>a</sup> Peak width at half-height.

conditions phenol is neutral and will therefore have a migration velocity equal to the EO flow. For currents of both 25 and 35  $\mu\text{A}$  it was found that the EO flow-rate decreased by 60–75%, *i.e.*, from 27 and 35 mm/min to 7 and 14 mm/min, respectively, when the precolumn was switched on-line.

To prevent excessive band broadening and increased migration times, desorption of the sample was carried out in the backflush mode and a zone-cutting procedure by means of valve switching was used. After loading of the sample on the precolumn the rotor was switched and backflush desorption of the analyte was performed by applying the current (30  $\mu\text{A}$ ) for a limited period of time (30–60 s). After (part of) the analyte had been transferred into the capillary, the power supply was switched off and the rotor was switched back to its initial (load) position. Finally, the high voltage was switched on again and electrophoresis was continued (current 30  $\mu\text{A}$ ). For the time used for electrodesorption in the backflush mode, a compromise between sensitivity and separation efficiency had to be found. Large desorption times will cause an increase in the amount of analyte transferred into the separation capillary, leading to an increased peak height but, unfortunately, also an increased peak width (*cf.*, Table I). Using an electrodesorption time of 45 s (current 30  $\mu\text{A}$ ), the band broadening was dramatically reduced compared with results obtained with forward flush desorption (compare Fig. 4C and B). Further, the migration time now was approximately the same as that obtained with direct injection of the sample (Fig. 4A).

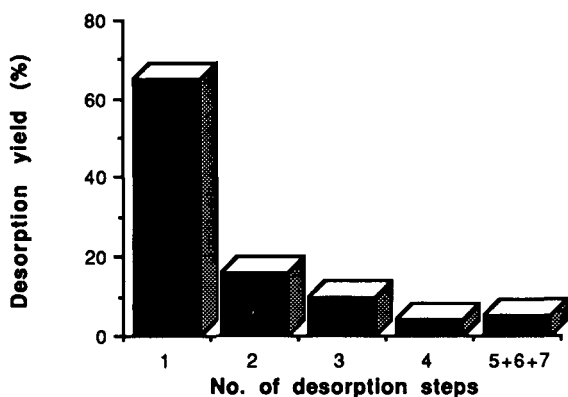


Fig. 5. Yield of the electrodesorption of papaverine for seven repeated desorption steps by means of valve switching, after a single sample loading. Backflush time, 45 s; current, 30  $\mu\text{A}$ . For detailed conditions, see text.

To determine the amount of analyte desorbed during the 45-s desorption step, the valve switching procedure was repeated seven times (*i.e.*,  $7 \times 45$  s with a current of 30  $\mu\text{A}$ ) after a single loading of 10  $\mu\text{l}$  of a papaverine solution, without flushing of the precolumn in between. After the seventh cycle desorption of papaverine was complete. Fig. 5 shows the yield of papaverine after each desorption step, expressed as a percentage of the total yield. The yield after the first injection was 65%. In all further experiments an electrodesorption time of 45 s was used. However, it will be obvious that the desorption time used is optimized for papaverine, and that it should be modified when other analytes are to be determined.

The on-line enrichment procedure for CZE was

investigated for sample volumes of up to 100  $\mu\text{l}$ , using water–acetonitrile (95:5, v/v) containing  $10^{-5}$  M papaverine. The plot of UV absorbance versus sample volume in Fig. 6A shows satisfactory linearity ( $r^2 = 0.992$ ). A linear calibration graph was also obtained when analysing 1- $\mu\text{l}$  samples containing  $10^{-5}$ – $10^{-3}$  M papaverine ( $r^2 = 0.998$ ) (Fig. 6B). The R.S.D. for four consecutive injections (5  $\mu\text{l}$  of sample,  $10^{-5}$  M papaverine) was 6%. With the described enrichment–desorption and CZE–UV procedure a limit of detection of  $5 \cdot 10^{-8}$  M papaverine (signal-to-noise ratio = 3; UV detection at 254 nm) was achieved; using a 100- $\mu\text{l}$  sample an absolute limit of detection of 5 pmol can be obtained.

## CONCLUSIONS

The rotary switching valve with an internal precolumn has promising features for on-line analyte enrichment in capillary separation systems. The high pressure resistance (up to 150 bar) of the valve allows coupling to micro LC, as demonstrated by the analysis of the opiate mixture. As the valve is constructed from synthetic material it can be coupled to CE systems, which is an advantage over micro precolumn-containing switching valves described previously [11]. In comparison with published sample treatment methods for CZE, the main advantage of the present system is that it allows (i) on-line sample pretreatment and, thus, automation, (ii) the next injection to be carried out while the CZE separation is still running and (iii) selective sample pretreatment by using suitable stationary phases. In addition, the system is easy to operate.

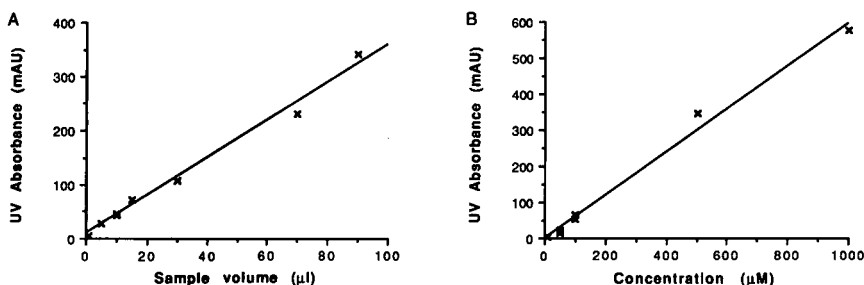


Fig. 6. (A) Plot of peak height (milliabsorbance units) versus loaded sample volume ( $\mu\text{l}$ ) ( $10^{-6}$  M papaverine). The equation is  $y = 3.5 (\pm 0.1)x + 9.7 (\pm 5.7)$ , where  $x$  represents the sample volume and  $y$  the UV absorption signal. (B) Plot of peak height (milliabsorbance units) versus papaverine concentration ( $\mu\text{M}$ ) in 1  $\mu\text{l}$  of a water–acetonitrile (95:5, v/v) sample solution. The equation is  $y = 6.0 (\pm 0.2)x + 2.3 (\pm 8.5)$ , where  $x$  represents the sample concentration and  $y$  the UV absorption signal.

Keeping the precolumn on-line with the separation capillary during the electrophoretic run caused excessive band broadening and increased migration times. The introduction of a rapid zone cutting-desorption procedure essentially solved this problem. As regards the analytical performance of the set-up, sample enrichment was linear over a large range of volumes (1–100  $\mu\text{l}$ ). This corresponds to an increase in the sensitivity of 2–3 orders of magnitude compared with a 0.2- $\mu\text{l}$  direct injection. Furthermore, enrichment was linear over a concentration range of at least two orders of magnitude.

The present switching valve can also be coupled to other micro separation systems. For example, coupling to ITP has the advantage that zone sharpening will occur during the ITP run. This zone sharpening effect, which depends on the concentration and mobility of analytes and leading electrolyte, will suppress the zone broadening owing to slow analyte desorption. This means that ITP can be performed with the precolumn in-line, that is, quantitative desorption of the analyte from the precolumn can now be achieved.

Further investigations are to be made in order to study the influence of real samples on the recovery, selectivity and linearity of the desorption procedure.

#### ACKNOWLEDGEMENT

We thank the mechanical and electronic workshops of the Free University for the construction of the rotary switching valve and the modification of the power supply.

#### REFERENCES

- 1 R. A. Wallingford and A. G. Ewing, *Adv. Chromatogr.*, 29 (1989) 1.
- 2 M. M. Bushey and J. W. Jorgenson, *Anal. Chem.*, 62 (1990) 978.
- 3 D. Kaniansky and J. Marak, *J. Chromatogr.*, 498 (1990) 191.
- 4 V. Kasicka and Z. Prusik, *J. Chromatogr.*, 273 (1983) 117.
- 5 V. Kasicka and Z. Prusik, *J. Chromatogr.*, 320 (1985) 75.
- 6 Z. Prusik and V. Kasicka, *J. Chromatogr.*, 320 (1985) 81.
- 7 Z. Prusik and V. Kasicka, *J. Chromatogr.*, 390 (1987) 39.
- 8 H. Soini, T. Tsuda and M. Novotny, *J. Chromatogr.*, 559 (1991) 547.
- 9 Z. El Rassi and J. Cai, presented at the *3rd Symposium on High-Performance Capillary Electrophoresis, San Diego, CA, February 3–6, 1991*.
- 10 T. Tsuda, *Anal. Chem.*, 59 (1987) 799.
- 11 M. W. F. Nielen, R. C. A. Coordes, R. W. Frei and U. A. Th. Brinkman, *J. Chromatogr.*, 330 (1985) 113.

## Short Communication

# Capillary electrophoresis washing technique

Samy Abdel-Baky and Roger W. Giese

Department of Pharmaceutical Sciences in the College of Pharmacy and Allied Health Professions, and Barnett Institute, Northeastern University, 360 Huntington Avenue, Boston, MA 02115 (USA)

### ABSTRACT

A technique is described for washing a capillary electrophoresis column.

This note presents a convenient technique for introducing or changing the solvent in a capillary electrophoresis column in a manually operated system. We find it useful for both the washing solutions and running buffers. The technique is illustrated in Fig. 1. It relies on the use of two easily available components: (1) a steel syringe needle (e.g. 1.5 in., 24 Gauge); and (2) a side-arm vial fitted with an open-top, screw cap containing a septum (e.g. fabricated by attaching a side-arm to a 5.0 ml, screw-thread vial).

The basic idea of the technique is to use a syringe needle to facilitate insertion of the capillary column through the septum in the vial cap. Thus the overall procedure consists of the following steps: (1) insert the syringe needle through the septum; (2) insert the capillary column through the syringe needle until some of it protrudes (the step illustrated in Fig. 1); (3) while holding the capillary column above the syringe needle to fix its position relative to the vial, pull the syringe needle out of the septum, thereby achieving a tight seal of the capillary column

*Correspondence to:* Dr. S. Abdel-Baky, Department of Pharmaceutical Sciences in the College of Pharmacy and Allied Health Professions, and Barnett Institute, Northeastern University, 360 Huntington Avenue, Boston, MA 02115, USA.

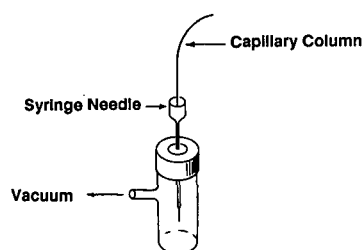


Fig. 1. Device for washing a capillary column.

through the septum (this step may sound awkward but is easily accomplished without breaking the capillary column); and (4) conduct the washing by using a low vacuum to pull solvent through the capillary from the other end.

This technique should be useful not only for the routine solvents that are frequently employed in capillary electrophoresis, but also for the more caustic solvents that are sometimes used. Other techniques for capillary washing have also been presented (e.g. ref. 1).

### ACKNOWLEDGEMENT

This work was funded by the Office of Health and Environmental Research Division, Department of Energy, as Grant DE-FG02-90ER60964. Publication number 525 from the Barnett Institute.

### REFERENCE

- 1 V. Rohlizek and Z. Deyl, *J. Chromatogr.*, 480 (1989) 289–291.



# Adjustment of resolution and analysis time in capillary zone electrophoresis by varying the pH of the buffer

Ernst Kenndler and Werner Friedl

Institute for Analytical Chemistry, University of Vienna, Währingerstrasse 38, A-1090 Vienna (Austria)

## ABSTRACT

An expression for resolution in capillary zone electrophoresis is derived which is a function of the pH of the buffer. It is based on the conventional definitions of resolution, but takes into account the dependence of the efficiency term on the effective mobilities, or the charge numbers, of the separands (monovalent ions). The different shapes of the  $R$  vs. pH curves, as derived from the resolution equation, are discussed and found to agree with the experimental results. An approach for the selection of that single pH where a given resolution can be achieved within the shortest time of analysis is introduced.

## INTRODUCTION

In zone electrophoresis, the degree of separation of two components,  $i$  and  $j$ , is described as in elution chromatography by a dimensionless number, the resolution,  $R_{ji}$ . It is defined by the distance of the centres of the peaks, measured not in absolute but in relative units. The definition introduced by Giddings [1] takes the sum of the twofold of the standard deviations,  $\sigma$ , of the peaks of components  $i$  and  $j$  as the scale unit. Because in capillary zone electrophoresis (CZE) (as in column chromatography) the peaks are represented in the time domain, the migration times,  $t$ , and the standard deviations based on time,  $\sigma_t$ , are applied for the definition of the resolution, which is expressed as

$$R_{ji} = \frac{t_j - t_i}{2 \sigma_{t,i} + 2 \sigma_{t,j}} \quad (1)$$

Using an averaged standard deviation,  $\bar{\sigma}_t$ , of the two peaks, eqn. 1 can be rewritten as  $R_{ji} = (t_j - t_i)/4 \bar{\sigma}_t$ . Based on this definition, baseline separation is

established for two peaks with equal areas at a resolution of 1.5.

Huber [2] introduced a simpler definition of the resolution for elution chromatography, taking into account the standard deviation of only one of the two peaks as the scale unit for expressing the distance between the two peaks, according to

$$R_{ji} = \frac{t_j - t_i}{\sigma_{t,i}} \quad (2)$$

This definition, which is also applicable to zone electrophoresis, is nearly equivalent to that given in eqn. 1 for peaks with very similar widths, but it can be converted into an expression that consists of operating parameters, as discussed below, without using averaged parameters. Baseline separation for peaks with equal areas is established at a resolution of 6; it can be seen that the conversion factor between these two resolution expressions is 4. Both equations are rearranged by substituting  $t$  and  $\sigma$  to obtain expressions with a larger optimization potential. Restricting the following discussion to CZE without electroosmotic flow, the resolution as defined by eqn. 1 then results in [1,3–5]

$$R_{ji} = \frac{1}{4} \cdot \frac{\Delta v}{\bar{v}} \sqrt{N} = \frac{1}{4} \cdot \frac{u_i - u_j}{\bar{u}} \sqrt{N} \quad (3)$$

Correspondence to: Prof. E. Kenndler, Institute for Analytical Chemistry, University of Vienna, Währingerstrasse 38, A-1090 Vienna, Austria.



where  $\Delta v$  is the velocity difference of the separands,  $\bar{v}$  is their average velocity,  $u(\bar{u})$  is the (average) ionic mobility and  $\bar{N}$  is the average plate number, given by

$$\bar{N} = \frac{\bar{u} U}{2 \bar{D}} \quad (4)$$

In this equation  $U$  is the effective voltage applied across the effective length,  $L$ , of the capillary, resulting in a field strength  $E$  and  $\bar{D}$  is the average diffusion coefficient. Eqn. 4 was derived for the case where only longitudinal diffusion causes peak broadening. All other effects are neglected, namely convective mixing (in the case of hydrodynamic or electroosmotic flow), Joule heat (occurring especially at high electrical current), electromigration dispersion (when conductivity gradients are formed between the sample zone and buffer), adsorption and extra-column effects. The influence of these effects on the plate height,  $H$ , was extensively discussed by Hjertén [6]. In the same paper it was also pointed out that under certain circumstances the latter effects are negligible compared with longitudinal diffusion, which is the aspect focused upon in this paper. For simplicity, the discussion will also be restricted to monovalent separands. The more complicated expressions for multivalent or amphoteric electrolytes will be discussed in a subsequent paper.

It was mentioned above that no averaged parameters occur in the expression for the resolution derived from the definition given in eqn. 2, leading to [7]

$$R_{ji} = \frac{u_{\text{eff},i} - u_{\text{eff},j}}{u_{\text{eff},j}} \sqrt{N_i} = \left( \frac{u_{\text{eff},i}}{u_{\text{eff},j}} - 1 \right) \sqrt{\frac{u_{\text{eff},i} U}{2 D_i}} = \left( \frac{u_{\text{eff},i}}{u_{\text{eff},j}} - 1 \right) \sqrt{z_i} \sqrt{\frac{u_{\text{act},i} U}{2 D_i}} \quad (5)$$

where  $u_{\text{eff},i}$  is the effective mobility and  $D_i$  is the diffusion coefficient of separand  $i$ . The effective mobility,  $u_{\text{eff},i}$ , is related by the (effective) charge number,  $z_i$ , to the actual mobility,  $u_{\text{act},i}$ , which is equivalent to the normalized mobility for monovalent analytes, the mobility of the separand with unit charge:  $u_{\text{eff},i} = z_i u_{\text{act},i}$ . It should be mentioned that in contrast to the mobility,  $z_i$  always has a positive sign. It will be discussed below that the actual (or normalized) mobility can be linearly related under the conditions discussed [7–11] to the

diffusion coefficient as given by the Nernst–Einstein equation,  $D = u k T/z e_0$ , where  $e_0$  is the electric charge,  $k$  is the Boltzmann constant and  $T$  is the absolute temperature.

It can clearly be seen from eqn. 5 that the resolution consists of two terms, the selectivity term (with the ratio of the effective mobilities), and the efficiency term (the square root of the plate number). The latter also includes the effective mobility.

It was discussed in previous papers [7–11] that the last term in eqn. 5 ( $u_{\text{act},i} U/2 D_i$ ) is constant for all separands at a given voltage for not too high electrolyte concentrations, where the Nernst–Einstein equation for the (normalized) mobility and the diffusion coefficient is still valid.

Applying the Nernst–Einstein equation, the plate number can be expressed by

$$N_i = \frac{z_i e_0 U}{2 k T} \quad (6)$$

It can be seen that the plate number depends on the charge number of the separand and on the voltage. The validity of this equation was demonstrated experimentally (at least for diluted solutions) for small ions in previous work [7,10], but this equation must also be valid for large molecules such as biopolymers, taking into account that  $z_i$  is the effective and not a nominal charge number. For such molecules this effective charge number must be related to their zeta potential rather than to their nominal charge. For polynucleotides, for example, the effective charge number may then differ from the nominal charge number as calculated from the base number [11].

Combining eqns. 5 and 6 leads to the following expression for the resolution:

$$R_{ji} = \left( \frac{u_{\text{eff},i}}{u_{\text{eff},j}} - 1 \right) \sqrt{z_i} \sqrt{\frac{e_0 U}{2 k T}} \quad (7)$$

For weak electrolytes the charge number and thus the effective mobility are determined, according to the degree of dissociation, by the pH of the buffer in the separation unit. Hence not only the selectivity can be adjusted by the appropriate choice of the electrolyte system, but also the efficiency, and consequently the resolution. An optimization of the resolution was presented by Terabe *et al.* [12] for components with very similar  $pK$  values and equal

actual mobilities. In this paper here a concept for the adjustment of the separation of any pair of analytes is introduced and an expression for the resolution is derived and discussed for monovalent ions. It depends on the pH (and voltage and temperature) as experimental variable. From the pH range where all pairs of components can be separated with a given resolution, a single pH is selected that results in the minimum time of analysis. A more general approach for the adjustment of the resolution of multivalent separands by varying the pH and voltage is the topic of a subsequent paper.

## EXPERIMENTAL

### *Chemicals*

Chemicals used for the preparation of the buffer solutions were orthophosphoric acid, acetic acid, malonic acid and lactic acid (all of analytical-reagent grade from E. Merck, Darmstadt, Germany). The following compounds were used as test substances: 2,4-dinitrophenol ( $\alpha$ -nitrophenol, moistened with 20% water, >97%; Fluka, Buchs, Switzerland), 2,6-dinitrophenol (moistened with 20% water, purum, >98%; Fluka), 2,3-dimethoxybenzoic acid, 3,5-dimethoxybenzoic acid, 3,4-dimethoxybenzoic acid (veratric acid) and 2,4-dimethoxybenzoic acid (all minimum 99%; EGA, Steinheim, Germany). For the coating procedure, methylcellulose (Methocel MC, 3000–5000 mPa s; Fluka) was cross-linked using formic acid and formaldehyde (both of analytical-reagent grade; Merck) as described below. Water was distilled twice from a quartz apparatus.

### *Apparatus*

The measurements were carried out with an instrument which was equipped with a UV absorbance detector (P/ACE System 2100, using System Gold 6.01; Beckman, Palo Alto, CA, USA). The absorbance was measured at 214 nm. The separation capillary was made from fused silica (Scientific Glass Engineering, Ringwood, Australia) of 75  $\mu\text{m}$  I.D. and with a total length of 0.269 m. The effective length (the distance from the injector to the detector) was 0.201 m. The capillary was thermostated at 25.0°C.

Electrophoresis was carried out without electroosmotic flow at a total voltage of 5000 V (field strength 18 600 V/m), leading to an effective poten-

tial drop of 3740 V along the migration distance.

Injection of the sample was carried out from aqueous solution (without buffer) by pressure for 1 s.

The calculations were carried out with a personal computer using MathCAD 2.08 from MathSoft.

### *Procedures*

The pH of the buffers was adjusted by adding sodium hydroxide solution to the solutions of the respective acids (total buffer concentration 0.01 mol/l) using a glass-calomel electrode. The buffers were used in a pH range of  $\pm 1$  unit around the  $\text{p}K_{\text{a}}$  of the respective acid (described under *Chemicals*).

The following procedure was applied to eliminate electroosmosis by coating the inner capillary surface with methylcellulose as described by Hjertén [13]: 400 mg of methylcellulose were dissolved in 100 ml of water and 7 ml of formic acid and 35 ml of formaldehyde were added with stirring. This solution can be used repeatedly for at least 6 months if stored in a refrigerator. The tube was rinsed thoroughly with distilled water for 10 min. The methylcellulose solution was drawn into the dried, clean tube by suction for *ca.* 15 min, then the capillary was sucked dry for 5 min, leaving a thin film of uniform thickness on the wall. Finally, the tube was placed in an oven at 120°C for 40 min. Throughout the coating procedure it is important that air bubbles do not adhere to the capillary wall and that the quartz tube is kept in a vertical position. A second treatment with methylcellulose is recommended. The film was found to be stable for several weeks under the given conditions. The absence of an electroosmotic flow was controlled by measuring the mobility of a reference ion from the migration distance and its migration time.

The ionic mobilities were measured in the usual way as mentioned before. The  $\text{p}K_{\text{a}}$  values were determined from the inflection points of the mobility vs. pH curves.

## RESULTS AND DISCUSSION

It was pointed out in the Introduction that all definitions of the resolution of two compounds include two effects: the difference in migration and the broadening of the peaks. In CZE the difference

in migration is normally expressed by the difference in the residence times caused by the different effective mobilities,  $u_{\text{eff}}$ , of the separands, and is related to the selectivity of the separation system. It can be influenced by solvation, ionic strength, etc., but the most pronounced effect is from the degree of protolysis (or complexation). As the analytes behave as acids or bases in most instances, the degree of protolysis or dissociation,  $\alpha$ , for a given  $\text{p}K_{\text{a}}$  is determined by the pH of the buffer, which is therefore the most effective tool for adjusting the selectivity.

The second effect mentioned above, decisive for the resolution, is the dispersion of the peaks, coun-

teracting the separation, and described by the efficiency term,  $\sqrt{N}$ , in the expression for  $R$ . The plate count, or the plate height,  $H$ , depends on a number of effects as mentioned in the Introduction, but most of them can be reduced or even eliminated under the appropriate conditions, except longitudinal diffusion.

It follows from eqn. 5 that not only the selectivity but also the efficiency depends on the effective mobility via the charge number. For a charge number of 1 the plate number calculated from eqn. 6 is 74 800 under the given conditions (3.74 kV, 25°C). Experimentally a value of *ca.* 54 000 was found, about 25% lower than the theoretical value, which is

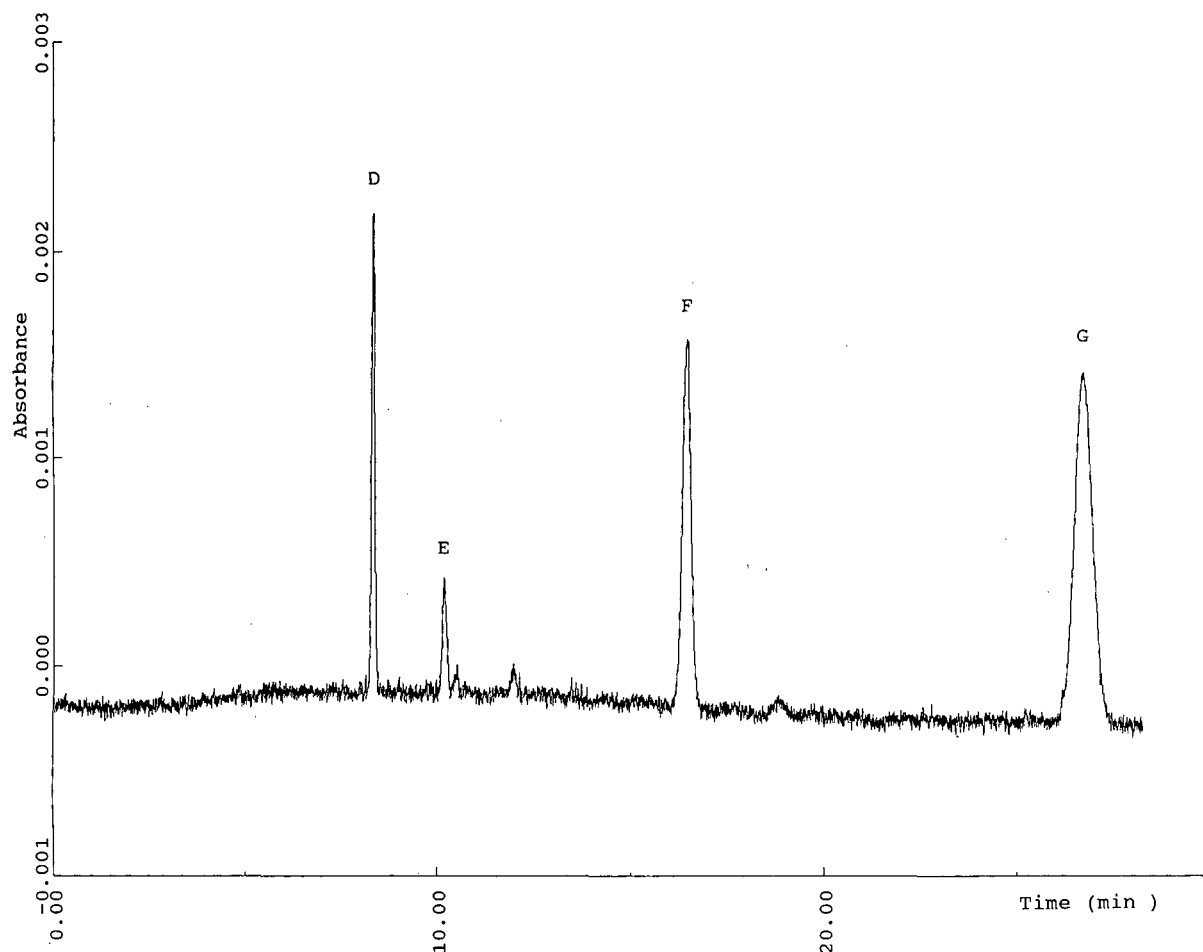


Fig. 1. Electropherogram showing the dependence of the plate number on the effective charge number, according to the degree of dissociation. The degree of dissociation of the separands decreases from D to G. Plate numbers determined from electropherogram at pH 4.17: D = 46 400, E = 35 600, F = 24 800, G = 16 200. For conditions, see Experimental. The symbols of the separands are given in Table I.

in agreement with previous investigations [7,10,11], the reason being discussed there. A voltage of 3.74 kV (5.00 kV total) was selected because it was observed that under this condition the effect of Joule heat is negligible.

The charge number of simple weak electrolytes, considered here and in previous work [7,10], is equivalent to their degree of protolysis,  $\alpha$ . Both efficiency and selectivity are influenced by the pH of the buffer, which determines the degree of dissociation by the well known relationship  $\text{pH} = \text{p}K_a \pm \log(1 - 1/\alpha)$ , where the sign before the logarithm is positive for anions and negative for cations.

#### Effect of pH on efficiency

In Fig. 1 the electropherogram of four dimethoxybenzoic acids with very similar ionic mobilities (D, E, F and G in Table I) is shown. For this type of compound, the limiting mobilities are only slightly higher than the actual mobilities (that is, the mobility of the fully dissociated species at the given ionic strength), namely about 2–3%. The Nernst–Einstein equation should be applicable under these conditions, and the plate number must therefore depend on the charge number of the separands, which is directly related to the degree of dissociation at the given pH.

Based on the  $\text{p}K_a$  values of the analytes given in Table I, the following values for  $\alpha$  are calculated for pH 4.17, where the electropherogram was developed: D 0.807, E 0.661, F 0.448 and G 0.304. As  $\alpha$  decreases in this order, an analogous decrease in the plate number can be expected, according to eqn. 6

TABLE I

ACTUAL MOBILITIES,  $u_{\text{act},i}$  AND  $\text{p}K_a$  VALUES OF THE TEST SUBSTANCES ( $T = 25^\circ\text{C}$ )

Symbol	Compound	$u_{\text{act},i}$ ( $10^{-5} \text{ cm}^2/\text{V} \cdot \text{s}$ )	$\text{p}K_a$
A	Benzoic acid	32.09	4.16 <sup>a</sup>
B	2,4-Dinitrophenol	31.09	4.04 <sup>a</sup>
C	2,6-Dinitrophenol	32.96	3.73 <sup>a</sup>
D	2,3-Dimethoxybenzoic acid	26.33	3.58
E	3,5-Dimethoxybenzoic acid	26.55	3.91
F	3,4-Dimethoxybenzoic acid	25.72	4.29
G	2,4-Dimethoxybenzoic acid	25.74	4.56

<sup>a</sup> Values taken from the literature [14].

( $z_i = \alpha_i$ ). Indeed, it can be seen that  $N$  decreases from 46 400 for separand D to 15 000 for G, the component with the lowest degree of dissociation. If these plate counts are weighted with  $1/\alpha$ , the values found are 57 000, 53 900, 55 300 and 53 200. This result agrees with the predicted value of 54 000 for  $N/\alpha$  (eqn. 6).

#### Resolution

As both selectivity and efficiency depend on the charge number, and therefore on the pH for weak electrolytes, an appropriate expression for the resolution must reflect this dependence. Based on the definitions of the resolution, given in eqns. 1 and 2, replacement of  $t$  by  $L/u_{\text{eff}}$ ,  $E$  and  $\sigma$  by  $t/\sqrt{N}$  consequently leads to the following equations for the resolution  $R_{ji}$  for components  $i$  and  $j$ :

$$R_{ji} = \frac{(r_{ij} - 1) + (r_{ij} \Delta_j - \Delta_i)}{(1 + \Delta_i)^{3/2} + r_{ij}(1 + \Delta_j)^{3/2}} \sqrt{\frac{e_0 U}{32 k T}} \quad (8)$$

according to eqn. 1 and

$$R_{ji} = \frac{(r_{ij} - 1) + (r_{ij} \Delta_j - \Delta_i)}{(1 + \Delta_i)^{3/2}} \sqrt{\frac{e_0 U}{2 k T}} \quad (9)$$

according to eqn. 2, where  $r_{ij} = u_{\text{act},i}/u_{\text{act},j}$  is the ratio of the actual mobilities (of the ions with unit charge),  $\Delta_i = 10^{\text{p}K_{a,i} - \text{pH}}$  and  $\Delta_j = 10^{\text{p}K_{a,j} - \text{pH}}$  for anions.

It can be seen from eqns. 8 and 9 that the resolution depends on the sample properties, namely the constants  $u_{\text{act},i}$ ,  $u_{\text{act},j}$ ,  $\text{p}K_{a,i}$  and  $\text{p}K_{a,j}$ , and the experimental parameters pH,  $U$  and  $T$ . Whereas the former properties are determined by the analytes and cannot be influenced in a simple way (they can be affected, e.g., by using organic solvents), the latter conditions can be varied much more easily (whereby a change in the temperature will lead to the least effect). It is well described in the literature that an increase in the applied voltage can cause an increase in  $N$ , but the voltage raises the resolution by the square root only, and the resulting increase in the electrical current (and therefore of Joule heat) limits the enhancement of the resolution concerning the voltage. The extent of this effect depends on instrumental conditions such as current and capillary inner diameter. This aspect is not discussed further here.

It can be concluded from eqns. 8 and 9 that the most powerful parameter in achieving an appropri-

ate resolution is the pH of the buffer which determines  $\Delta_i$  and  $\Delta_j$ . Its influence is demonstrated using seven test substances given in Table I.

It should be mentioned that both equations give nearly the same results for low values of the resolution (for the case of very similar peak widths for  $i$  and  $j$ ). As our investigations cover a wide range of resolution values, eqn. 8 seems to have some advantage over eqn. 9, and is thus used further.

The resolution of all pairs of separands can be calculated as a function of pH from the  $pK_a$  values and the mobilities. Instead of 1.12 for the constant factor  $e_0/32kT$  with the square root, a value of 0.950 is taken, considering the deviation from the theoretically reachable value of 74 800 for  $N$  as discussed above (the measured plate count was 54 000).

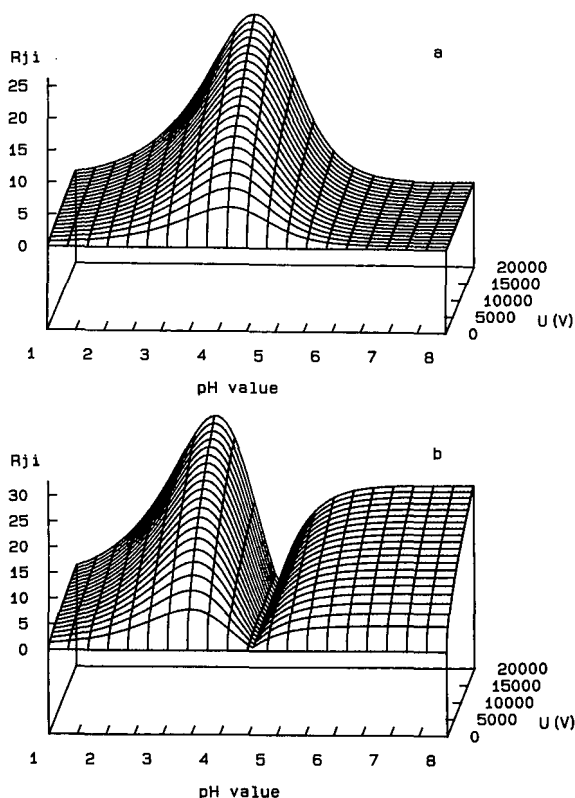


Fig. 2. Dependence of the resolution,  $R_{ji}$ , on pH and voltage  $U$  according to eqn. 8. (a)  $u_{act,i} > u_{act,j}$ ,  $pK_{a,i} < pK_{a,j}$ ; (b)  $u_{act,i} > u_{act,j}$ ,  $pK_{a,i} > pK_{a,j}$ .  $u_{act,i}$  and  $u_{act,j}$  are the actual mobilities of the separands. For monovalent species, they are identical with the normalized mobilities. The curves are calculated based on the data for (a) components F and G and (b) components B and D given in Table I. For discussion, see text.

Typical examples of the resulting  $R$  vs. pH vs.  $U$  curves are shown in Fig. 2. In principle two cases can be distinguished. In Fig. 2a the case is shown where one separand has a higher actual mobility (which is reached at high pH) and a lower  $pK_a$  value than the second separand. The first separand will then always have the higher effective mobility, independent of the pH of the buffer. The  $R$  vs. pH curves (considered at a distinct voltage) have one maximum. These curves have a similar shape to that derived by Terabe *et al.* [12]. This derivation was limited, however, to the case where the separands have very similar  $pK$  values and identical actual mobilities.

The second case arises if the separand with the higher actual mobility is the weaker acid, having the higher  $pK_a$  of the pair considered. When varying the pH, the values of the effective mobilities will approach each other and become equal at a certain pH. Consequently, the resolution is zero at this pH. Beyond this pH the migration order of the two

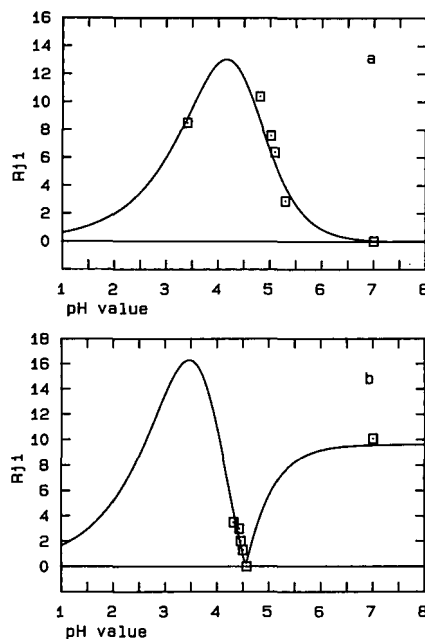


Fig. 3. Theoretical curves and experimental results of the dependence of the resolution,  $R_{ji}$ , on the pH at constant voltage. The curves were calculated for the pairs of components from Fig. 2 by eqn. 8 for an effective voltage of 3.74 kV. The correction for  $N$  was included (see text). (a) According to Fig. 2a; (b) according to Fig. 2b.  $\square$  = Experimentally determined values of  $R_{ji}$  at different pH of the buffer.

components will be reversed (and the indices in the resolution equation change).

The corresponding  $R$  vs. pH vs.  $U$  curves are shown in Fig. 2b. The resolution increases with increasing pH (at a distinct voltage), reaches a maximum, falls off to the resolution zero, increases at higher pH and reaches a plateau with a constant value of the resolution (as in Fig. 2a), because the analytes reach constant actual mobilities in this pH range, as they are fully dissociated. For both cases at constant pH the resolution increases with  $\sqrt{U}$ .

In Fig. 3, two typical examples are given to demonstrate the accordance of the experimental data with the curves derived from eqn. 8. The resolution is shown for the two pairs F-G and B-D (Table I) from Fig. 2a and b, as a function of the pH of the buffer for a constant voltage of 3.74 kV. The experimentally determined values for the resolution indeed follow the theoretical curves within a reasonable deviation. Similar results were obtained for all pairs of separands under investigation.

Based on graphs such as those shown in Figs. 2 and 3, the pH at which a certain resolution is established can be determined. For the case in Fig. 3b, for example, the resolution of 2.00 is obtained at pH 1.16, 4.43 and 4.68. In the pH range 1.16-4.43, and at pH > 4.48, the resolution is larger than 2.00 for this pair of separands. The case shown in Fig. 3a leads to a resolution of 2.00 at pH 1.42 and 6.46. Between these pH values the resolution exceeds 2. In this way the corresponding pH values or ranges can be calculated and determined for each pair of separands. A resolution of 2.00 is chosen (rather than 1.5), because the peak areas in the examples given below are not equal.

The pH ranges where the pairs of components are separated at least with a resolution of 2.00 are shown for all possible cases in Fig. 4. Within the overlapping pH ranges all analytes are separated with that chosen, minimum resolution. This range is represented in Fig. 4 by a single vertical line, because in this example for 21 pairs (given by the combination of the seven test components in Table I) the highest and the lowest pH value of the range are equal by chance, namely 4.43. It follows that for this given set of test components no further selection of the pH can be carried out to vary the time of analysis. For that purpose another example will be given below.

It can be seen from Fig. 5 that the accurate

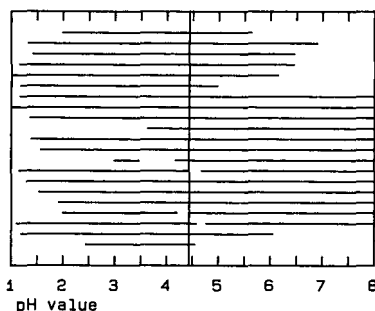


Fig. 4. Plot of the pH ranges within a resolution  $\geq 2.00$  is obtained for different pairs of the seven test compounds. Test components (A-G) according to Table I. The vertical line shows the pH value where the pH ranges of all 21 possible pairs overlap. Sequence of pairs from bottom to top: A-B, A-C, A-D, A-E, A-F, A-G, B-C, B-D, B-E, B-F, B-G, C-D, C-E, C-F, C-G, D-E, D-F, D-G, E-F, E-G, F-G.

selection of the appropriate pH can be very critical, because the resolution changes very rapidly with even small changes in the pH in critical regions. The slope of the  $R$  vs. pH curve is very steep; e.g., for the pair A-E it has a value of 14 in this example, which means that the variation of the pH by only 0.01 unit causes a change in resolution of 0.14. This effect is clearly demonstrated by the electropherogram in Fig. 6, obtained at pH 4.40, only 0.03 pH unit lower than the pH 4.43 given above for a resolution of 2.00. It can be seen from Fig. 6 that this minute deviation from the optimum pH causes a total loss in the resolution of components A and E, with E appearing only as a shoulder on the peak.

The electropherogram obtained at the appropriate pH 4.43 is shown in Fig. 7. As expected from the

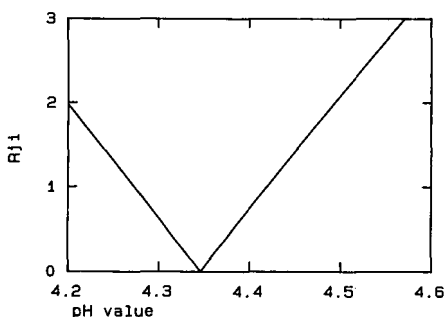


Fig. 5. Expanded graph of the dependence of the resolution,  $R_{ji}$ , on the pH around the critical pH where  $R_{ji} = 0$ . The curve is a section of Fig. 3b for the pair B-D at 3.74 kV.

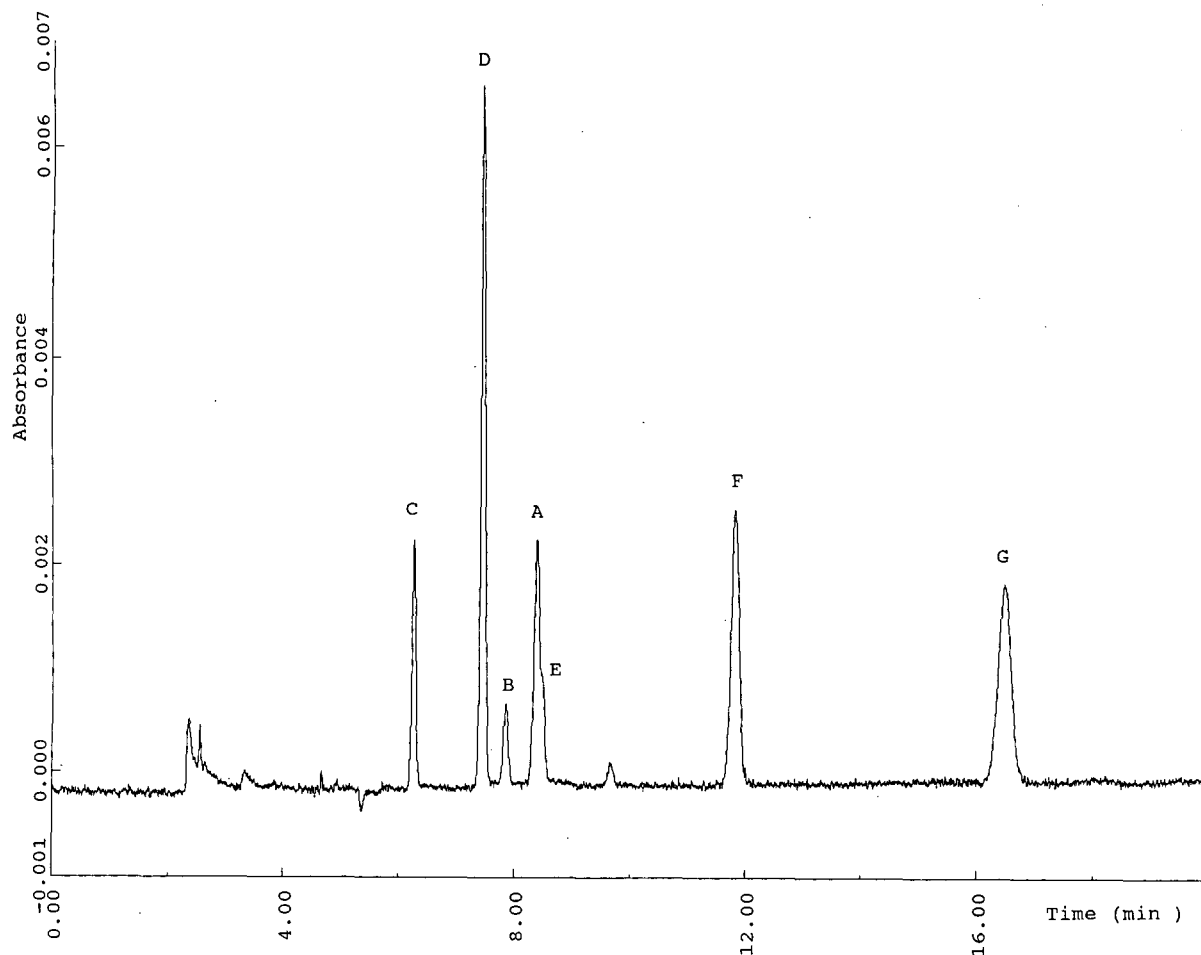


Fig. 6. Electropherogram of seven test components at pH 4.40. The test components are given in Table I. For details, see text.

calculation based on the equation for the resolution (eqn. 8), all components are separated, the most critical pair A and E with a resolution of 1.98, in agreement with the theoretically predicted value of 2.00.

#### *Time of analysis*

It must be taken into account, however, that at a given voltage not all pH values are equivalent within the calculated overlapping range, because in addition to the resolution the time of analysis is a decisive parameter. It is not favourable to select too high a resolution owing to the increase in analysis time. This time of analysis is given by the residence time of

the slowest migrating component, the component with the lowest effective mobility of all separands. Generally for anions this shortest time is always established at the highest pH of the overlapping range calculated, where the selected minimum resolution is reached.

As an example, the pH ranges for a resolution of 2.00 were calculated based on eqn. 8 for four test substances (D-G in Table I). These ranges are plotted in the same way as above and are shown in Fig. 8. Here the overlapping pH ranges can be recognized within the vertical lines: between pH 1.99 and 4.99 the resolution of all components must be 2.00 or higher. For a minimum time of analysis, as a

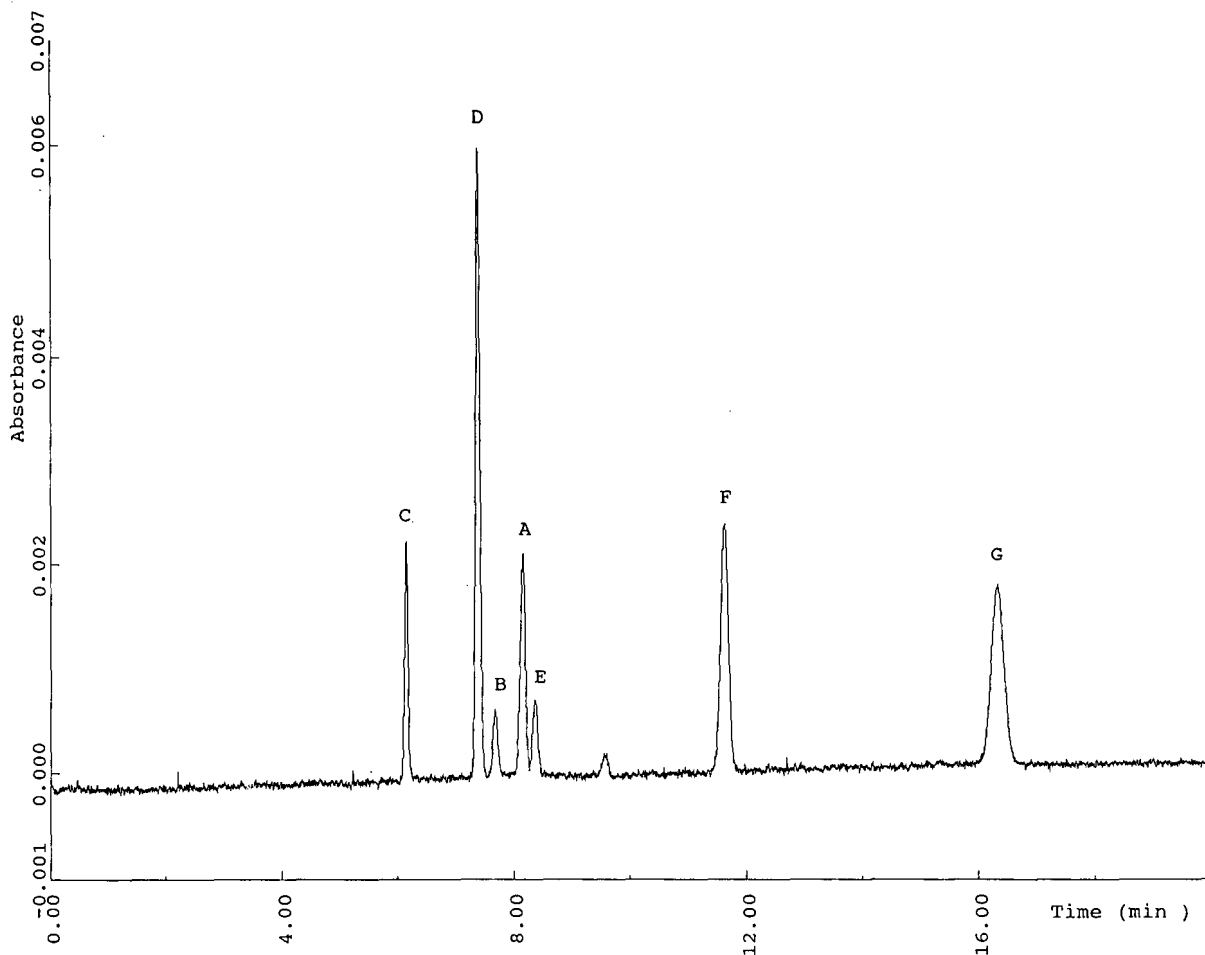


Fig. 7. Electropherogram of seven test components at pH 4.43, as calculated from eqn. 8 for a resolution of 2.00. The test components are given in Table I. The resolution determined for A and E is 1.98. For details, see text.

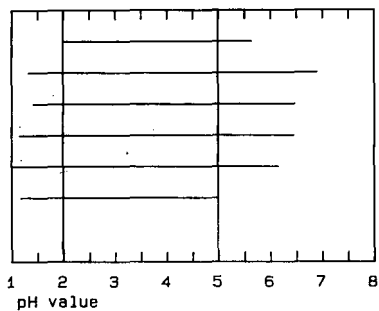


Fig. 8. Plot of the pH ranges with a resolution  $R_{ji} \geq 2.00$  for four test components. As test components, D, E, F and G from Table I were used. The area within the vertical lines represents the pH range where this resolution is obtained or exceeded. Sequence of pairs from bottom to top: D-E, D-F, D-G, E-F, E-G, F-G.

general approach, the highest pH of this range is selected, namely pH 4.99. The electropherogram obtained under these conditions is shown in Fig. 9. The minimum resolution, namely for the pair D-E, is 1.98, again close to that theoretically predicted, and the time of analysis is about 10 min.



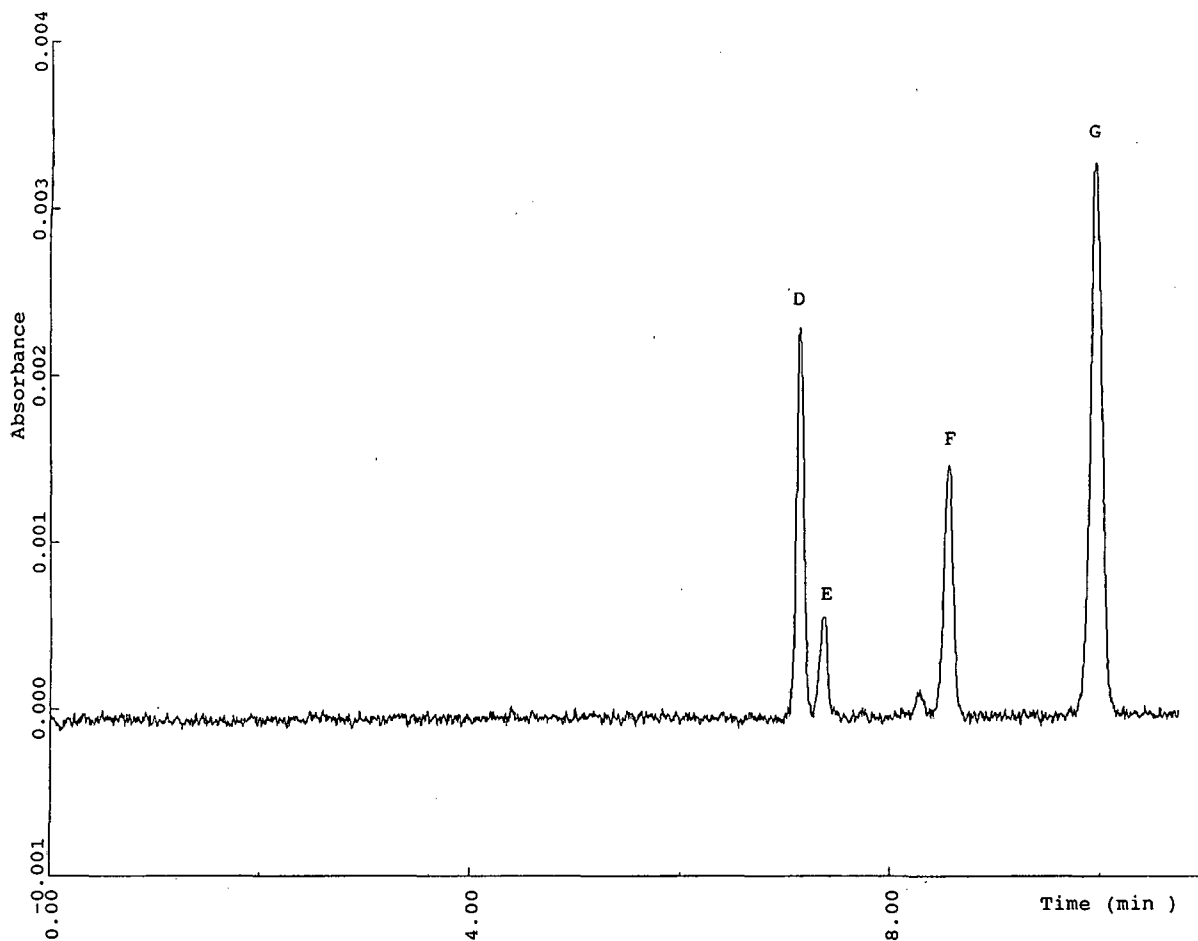


Fig. 9. Electropherogram of four test components at pH 4.99, as adjusted for a resolution of 2.00 and minimum time of analysis. The test components are given in Table I. The resolution determined for D and E is 1.98. For details, see text.

#### REFERENCES

- 1 J. C. Giddings, *Sep. Sci.*, 4 (1969) 181.
- 2 J. F. K. Huber, *Fresenius' Z. Anal. Chem.*, 277 (1975) 341.
- 3 J. C. Giddings, in I. M. Kolthoff and P. J. Elving (Editors), *Treatise on Analytical Chemistry, Part I*, Vol. 5, Wiley, New York, 1981, Ch. 3, p. 63.
- 4 J. C. Giddings, *J. Chromatogr.*, 480 (1989) 21.
- 5 J. W. Jorgenson and K. D. Lukacs, *Anal. Chem.*, 53 (1981) 1298.
- 6 S. Hjertén, *Electrophoresis*, 11 (1990) 665.
- 7 C. Schwer and E. Kenndler, *Chromatographia*, 33 (1992) 331.
- 8 E. Kenndler, *Österr. Chem.-Ztg.*, 12 (1988) 353.
- 9 E. Kenndler, *Chromatographia*, 30 (1990) 713.
- 10 E. Kenndler and C. Schwer, *Anal. Chem.*, 63 (1991) 2499.
- 11 E. Kenndler and C. Schwer, *J. Chromatogr.*, 595 (1992) 313.
- 12 S. Terabe, T. Yashima, Y. Tanaka and M. Araki, *Anal. Chem.*, 60 (1988) 1673.
- 13 S. Hjertén, *Chem. Rev.*, 9 (1967) 122.
- 14 J. L. Beckers, F. M. Everaerts and M. T. Ackermans, *J. Chromatogr.*, 537 (1991) 407.

# Capillary electrophoresis of fluorescein–ethylenediamine–5′-deoxynucleotides

Wenni Li<sup>☆</sup>, Adel Moussa<sup>☆☆</sup> and Roger W. Giese

*Department of Pharmaceutical Sciences in the College of Pharmacy and Allied Health Professions, and Barnett Institute of Chemical Analysis and Materials Science, Northeastern University, 360 Huntington Avenue, Boston, MA 02115 (USA)*

---

## ABSTRACT

Fluorescein–ethylenediamine conjugates of the four major deoxynucleoside-5′-monophosphates were subjected to capillary electrophoresis with laser fluorescence detection. Control of pH was an important parameter controlling resolution, as anticipated. For example, the four conjugates were resolved at pH 10.4, but negligibly at pH 8.7. Apparently secondary effects on solute migration such as conformation or solvation play a role, since the larger conjugate of adenine migrated faster than that of cytosine at pH 10.4, where each has the same charge. Further, the guanine and thymine conjugates, in spite of their different size, co-migrated at pH 11.5. The method promises to be useful for the detection of DNA adducts.

---

## INTRODUCTION

Previously we reported the separation of fluorescein-labeled deoxynucleotides by high-performance liquid chromatography (HPLC) [1]. The purpose of achieving the separation is to facilitate the detection of covalent damage to DNA, termed DNA adducts, by environmental or endogenous chemicals. The overall analytical scheme that we are pursuing is to sequentially purify the DNA from a biological sample, isolate the DNA adducts as damaged deoxynucleotides, label the latter with fluorescein, and then achieve sensitive detection of the resulting fluorescein-labeled deoxynucleotide DNA adducts. This basic strategy is being pursued also by others [2,3]. Potentially the measurement of DNA adducts can help define how much of the human burden of can-

cer and genetic disease results from exposure to toxic chemicals and radiation.

Here we extend our prior HPLC work by examining the separation of these types of compounds by capillary electrophoresis (CE). Because of its speed, resolution, ease of column cleaning, formation of sharp peaks to enhance detection, and tiny injection volumes to conserve precious samples, capillary electrophoresis should be useful for the detection of DNA adducts.

## EXPERIMENTAL

### *Chemicals and reagents*

Trizma base [tris(hydroxymethyl)aminomethane, or Tris] was purchased from Sigma (St. Louis, MO, USA). Boric acid, HPLC-grade acetonitrile and 0.22- $\mu\text{m}$  MSI Cameo filters were from Fisher Scientific (Bedford, MA, USA). The fluorescein–ethylenediamine–deoxynucleoside-5′-phosphates (F-ED-dNMPs) were prepared as described [1] using Isomer II FITC (fluorescein-6-isothiocyanate) from Molecular Probes (Eugene, OR, USA). All solution compositions were v/v unless indicated otherwise.

---

*Correspondence to:* Dr. R. W. Giese, Mugar Building, Room 122, Northeastern University, 360 Huntington Avenue, Boston, MA 02115, USA.

<sup>☆</sup> Present address: American Cyanamide Co., Agriculture Research Division, Princeton, NJ 08540-0400, USA.

<sup>☆☆</sup> Present address: Covalent Associates, Inc., Woburn, MA 01801, USA.

### Capillary electrophoresis with laser fluorescence detection

A laboratory-built apparatus was used for CE. The laser-fluorescence detector was designed and built by Dr. Edward S. Yeung at Iowa State University. It utilized an argon ion laser (Model 2211-30SL; Cyonics, CA, USA) to give excitation at 488 nm. A Model PS/EH60R01.5 regulated high-voltage d.c. power supply (Glassman High Voltage, NJ, USA) was used. CE was performed in a 95-cm long fused-silica capillary (75  $\mu\text{m}$  I.D.; PolyMicro Technologies, Phoenix, AZ, USA). The polyimide coating of the capillary was burned off to form a flow cell 50 cm from the injection end (grounded anode end) of the capillary. All separations were performed at 15 kV and samples were injected hydrodynamically: anode end 5 cm higher for 20 s.

New capillary columns were cleaned initially by syringe-filling (until 4 drops emerged, which was done for all syringe steps) with methanol–water (1:1), followed by 0.1 M NaOH, with standing for 30 min each. After washing with water and then buffer, the buffer of interest was then subjected to 30 min of electrophoresis followed by standing overnight. Periodically (about once per week) the capillary was cleaned by syringe injection of 0.1 M NaOH, standing for 30 min, similarly injecting buffer, and then operating the electrophoresis for 1 h before samples were injected.

### Solutions

**pH 8.7 Buffer.** This was prepared by combining 0.8 ml of stock buffer (0.5 M Tris, 0.5 M boric acid, stored at room temperature), 35 ml of water, and 4 ml of acetonitrile, giving pH 8.7. This buffer (10 mM Tris–borate, 10% acetonitrile) was filtered (0.22  $\mu\text{m}$ ) and degassed (bubbling with helium for 15 min) prior to use as a diluent to prepare solutions for injection. The other buffers were prepared by titrating the 10 mM, pH 8.7 solution to the desired pH with 2 M NaOH.

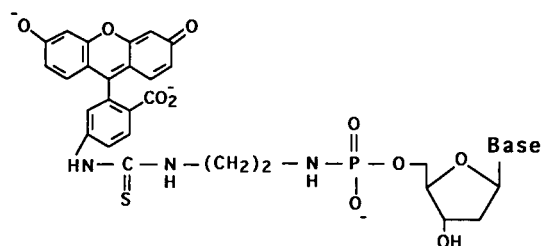
### F-ED-dNMP Stock

The stock solution of each F-ED-dNMP was obtained as an HPLC peak from a C<sub>18</sub>-silica column in a mobile phase of 5 mM acetic acid with an acetonitrile gradient. Immediately after collection, the pH was adjusted to 8.7 by the addition of 0.5 M Tris–borate. This solution was kept in a polypropy-

lene tube, and all dilutions, unless indicated otherwise, were made in polypropylene tubes, and Fisher Brand 1.5-ml polypropylene snap cap tubes. All dilutions were made using polypropylene tips. The stock solutions were stored in the dark at  $-20^{\circ}\text{C}$ .

### RESULTS AND DISCUSSION

The four common deoxynucleotides (dCyd-5'-P, dAdo-5'-P, Thd-5'-P and dGuo-5'-P) were first conjugated to ethylenediamine via the phosphate moiety, and then reacted with fluorescein-isothiocyanate. The resulting F-ED-dNMPs were purified by HPLC, and then subjected, both individually and as a mixture, to capillary electrophoresis with laser fluorescence detection. Shown here is a generalized structure of our analytes.



The first pH that we investigated for the electrophoretic separation was 8.7. The fluorescence of fluorescein reaches a maximum around pH 8.0; pH 8.6 has been recommended for the detection of fluorescein conjugates [4]. A Tris–borate buffer was selected primarily because of the double dose of buffering available from the  $pK_a$  values of 8.3 for Tris and 9.2 for borate ( $25^{\circ}\text{C}$ ). Thus the alkaline pH of 8.7 is half-way between these two  $pK_a$  values and close to the recommended pH of 8.6. We included 10% acetonitrile in the buffer since fluorescein, as a preliminary test solute, gave a narrower peak when this was done (data not shown).

At pH 8.7 the four F-ED-dNMPs essentially co-elute by capillary electrophoresis, as shown in Fig. 1A. This observation is not surprising since the effective mobilities of uridine, cytidine and adenosine 5'-monophosphates were found to be very similar previously in this pH zone by isotachopheresis [5]. Further, the extra structural bulk contributed by the fluorescein-ethylenediamine moiety in our compounds probably reduces the degree to which the

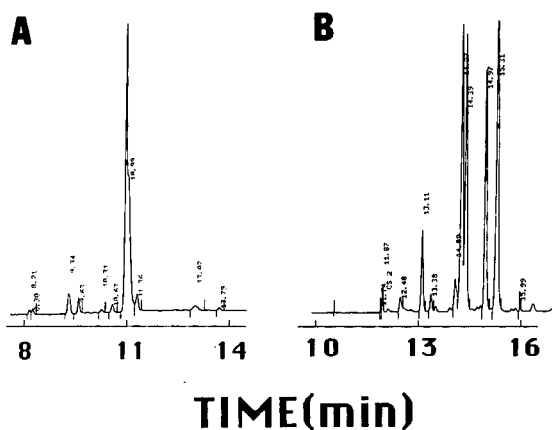


Fig. 1. Electropherograms of a mixture of fluorescein-ethylene-diamine conjugates of dCyd-5'-P, dAdo-5'-P, Thd-5'-P and dGuo-5'-P at pH 8.7 (A) and 10.4 (B). The elution order of the compounds in (B) (4 major peaks) is C > A > T > G, the opposite order of their electrophoretic mobilities. In (B), the impurity at 13.11 min (contributed by the F-ED-dGMP sample), and the other background peaks, are unknowns.

structural differences among the four bases influence the frictional profiles of the compounds. Further, at pH 8.7 the four bases are essentially uncharged, since the nearest  $pK_a$  for any of them is the one at 9.7 for dGua-5'-P [6]. Next is that at 10.0 for Thy-5'-P [6]. No acidic  $pK_a$  values have been reported for the bases in dAdo-5'-P and dCyd-5'-P. The constant effective mobilities of cytidine- and adenosine-5'-monophosphate from pH 9 to 12 [5] indicates that neither has an acidic  $pK_a$  in or near this range.

Mononucleotides can be resolved by capillary electrophoresis under mildly acidic conditions [7–10], largely due to  $pK_a$  differences among the bases in the pH range of 2–4 [5]. A separation of some of them was also reported near neutral pH [11]. However, as pointed out above, we need to detect our compounds at an alkaline pH to maintain the intense fluorescence of fluorescein. Thus we next tested pH values above 8.7 for the running buffer.

As shown in Fig. 1B, all four compounds can be resolved at pH 10.4. The elution order fits the  $pK_a$  values, to the extent they are known (see above). However, it is not clear how F-ED-dAMP achieves a higher mobility than F-ED-dCMP, since neither base is ionized at this pH, and adenine is larger than cytosine. Secondary effects on mobility such as con-

formation or solvation apparently are playing a role. Perhaps the fact that the calculated dipole moments for cytosine and adenine are 7.6 and 2.9, respectively [12], is relevant.

The resolution degrades at pH values above 10.4 (data not shown). For example, at pH 11.5, the highest pH tested, essentially two peaks are observed when a sample containing the four compounds is injected: one at 12.2 min for the cytosine and adenine conjugates, and one at 14.4 min for those of guanine and thymine. The latter co-migration is another surprise, given the different sizes of the guanine and thymine bases, and their active role in the electrophoretic migration of the compounds at this pH, where each base is fully ionized.

Greater understanding is needed of the factors which determine the separation, or lack thereof, of small molecules possessing the same charge and type of charge in electrophoresis. Clearly small size differences can be important, *e.g.* the resolution of alkyl sulfates up to  $C_{12}$  by CE [13]. However, as an example that is more similar to one of our observations, Nielsen *et al.* [14] observed three peptides (5-, 6- and 8-mer) to co-elute at a pH where each possesses the same charge.

## CONCLUSIONS

CE promises to be useful for the detection of fluorescein-labeled DNA adducts, particularly because of the broad pH range that it can utilize to take advantage of distinctive  $pK_a$  values that many adducts possess [6,15].

Given the marginal differences in electrophoretic mobilities for the compounds tested under certain conditions, we plan to investigate more complex conditions involving secondary retention mechanisms for more control over resolution.

CE has certainly rejuvenated interest in the electrophoretic separation of small molecules. This calls for further study of the factors which determine the frictional profiles of such compounds.

## ACKNOWLEDGEMENT

This work was funded by the Office of Health and Environmental Research Division, Department of Energy, as Grant DE-FG02-90ER60964. Publication number 541 from the Barnett Institute.

## REFERENCES

- 1 A. N. Al-Deen, D. C. Cecchini, S. Abdel-Baky, N. M. Abdel Moneam and R. W. Giese, *J. Chromatogr.*, 512 (1990) 409.
- 2 M. Sharma, R. Jain and T. V. Isac, *Bioconjugate Chem.*, 2 (1991) 403.
- 3 O. J. Kelman, K. T. Lilga and M. Sharma, *Chem.-Biol. Interactions*, 66 (1988) 85.
- 4 R. C. Nairn, *Fluorescent Protein Tracing*, Williams & Wilkins, Baltimore, MD, 1969.
- 5 T. Hirokawa, S. Kobayashi and Y. Kiso, *J. Chromatogr.*, 318 (1985) 195.
- 6 G. D. Fasman (Editor), *Handbook of Biochemistry and Molecular Biology*, CRC Press, Boca Raton, FL, 3rd ed., 1975.
- 7 W. G. Kuhr and E. S. Yeung, *Anal. Chem.*, 60 (1988) 2642.
- 8 L. Gross and E. S. Yeung, *J. Chromatogr.*, 480 (1989) 169.
- 9 R. Takigiku and R. E. Schneider, *J. Chromatogr.*, 559 (1991) 247.
- 10 V. Dolnik, J. Liu, J. F. Banks and M. V. Novotny, *J. Chromatogr.*, 480 (1989) 321.
- 11 T. Tsuda, K. Takagi, T. Watanabe and T. Satake, *J. High Resolut. Chromatogr. Chromatogr. Commun.*, 11 (1988) 721.
- 12 W. Saenger, *Principles of Nucleic Acid Structure*, Springer, New York, 1984, p. 107.
- 13 M. W. F. Nielsen, *J. Chromatogr.*, 588 (1991) 321.
- 14 R. G. Nielsen, R. M. Riggan and E. C. Rickard, *J. Chromatogr.*, 480 (1989) 393.
- 15 B. Singer and D. Grunberger, *Molecular Biology of Mutagens and Carcinogens*, Plenum Press, New York, 1983.

# Influence of pH on the migration properties of oligonucleotides in capillary gel electrophoresis

András Guttman

*Central Isotope Laboratory, Semmelweis University of Medicine, Budapest (Hungary)*

Akihiro Arai

*Shimadzu Corp., Kyoto (Japan)*

Kálmán Magyar

*Central Isotope Laboratory, Semmelweis University of Medicine, Budapest (Hungary)*

---

## ABSTRACT

The effect of pH on the electrophoretic migration properties of single-stranded oligodeoxyribonucleotides in capillary gel electrophoresis was investigated. Different homooligodeoxyribonucleotides of equal chain length showed significant differences in relative migration when the pH of the gel buffer was varied from pH 6 to 8, parallel with the running buffer. A similar variation in migration order was observed during the electrophoretic equilibration of a pH 8 gel-filled capillary column with a pH 6 running buffer. In the latter instance, the current reached the new level after 20 min of electrophoretic equilibration with the pH 6 running buffer. However, it was observed that the migration order characteristic of the pH 6 gel was achieved only after 4 h of electrophoretic equilibration. To avoid this time-consuming equilibration process, these results suggest that gel-filled capillary columns should be prepared with the same buffer (composition and pH) that will be used as the running buffer during the separations.

---

## INTRODUCTION

An instrumental approach to electrophoresis, capillary electrophoresis, is currently being developed with the potential for automation and increasing importance as a separation tool in analytical biochemistry [1–4]. Using narrow-bore fused-silica capillaries filled with polyacrylamide gels, separations of biologically important molecules are possible with high performance [5–7]. At present, there is a great deal of interest in the separation and characterization of DNA molecules. We have previously demonstrated the high resolving power of gel-filled

capillaries for the separation of oligonucleotides [8]. In continuation of previous work [9], a mixture of homodecamers was electrophoresed using running buffer systems with the same and different pH as the buffer used to prepare the gel, in order to determine its effect on the migration properties and the electrophoretic equilibration time.

## EXPERIMENTAL

### *Apparatus*

High-performance capillary gel electrophoresis was performed in fused-silica capillary tubing (Polymicro Technologies, Phoenix, AZ, USA) of 75  $\mu\text{m}$  I.D. and 375  $\mu\text{m}$  O.D. with column lengths of 650 mm. The polyimide coating was carefully peeled off by means of a razor blade under a micro-

---

*Correspondence to:* Dr. A. Guttman, Beckman Instruments, Inc., Fullerton, CA 92634, USA (present address).

scope along a 2 mm length at 150 mm from one end of the capillary. A 60-kV high-voltage d.c. power supply (Model PS/MK 60P00.5 × 66, Glassman, Whitehouse Station, NJ, USA) was used to produce the potential across the gel-filled capillary column. A UV detector (V-4, ISCO, Lincoln NE, USA) modified as described previously [7] was used at a wavelength of 260 nm. The detector slit was  $0.1 \times 0.1$  mm. The tubing and the detector were cooled with ambient air using a fan. Each end of the capillary was connected to a separate 3-ml vial filled with the appropriate running buffer. Platinum wire electrodes were inserted in the two vials for connection to the electrical circuit. The electrophoretic data were acquired and stored on an IBM PC/AT computer.

### Materials

The homodecamers polydeoxyadenylic [ $p(dA)_{10}$ ], polydeoxycytidilic [ $p(dC)_{10}$ ] and polydeoxythymidilic [ $p(dT)_{10}$ ] acids were purchased from Pharmacia (Piscataway, NJ, USA). The samples were diluted to  $20 \mu\text{g/ml}$  with water before injection and were stored at  $-20^\circ\text{C}$  when not in use. Ultrapure, electrophoresis-grade acrylamide,  $N,N'$ -methylenebisacrylamide, Tris, boric acid, urea, ammonium peroxydisulfate and tetramethylethylenediamine (TEMED) were employed (Schwartz Mann Biotech, Cambridge, MA, USA). Methacryloxypropyltrimethoxysilane reagent was purchased from Petrarch Systems (Bristol, PA, USA). The buffer solutions were filtered through a Nylon GC filter unit of  $0.2\text{-}\mu\text{m}$  pore size (Schleicher and Schuell, Keene, NH, USA) and carefully vacuum degassed.

### Preparation of capillary gel columns

The fused-silica capillary column was filled with polyacrylamide gel of 3% monomer (acrylamide +  $N,N'$ -methylenebisacrylamide) and 0.15% cross-linker ( $N,N'$ -methylenebisacrylamide) in  $0.1 M$  Tris–boric acid– $7 M$  urea buffer adjusted to the appropriate pH between 6.0 and 8.0 by varying the concentration of boric acid. The polymerization reaction was driven to completion in 25–30 min in all instances in order to achieve a similar polymerization rate, *i.e.*, gel structure. This was accomplished by using increasing amounts of ammonium peroxydisulfate initiator and TEMED catalyst as the pH

of the gel buffer was decreased. For stabilization, the polyacrylamide gel was covalently bound to the wall of the fused-silica capillary column by using a bifunctional reagent (methacryloxypropyltrimethoxysilane). An electric field of  $300 \text{ V/cm}$  was applied to the gel-filled capillary columns in all the experiments. In order to remove impurities from the polyacrylamide gel, the capillary column was pre-electrophoresed with the appropriate running buffer at 100, 200 and  $300 \text{ V/cm}$  for ten min each. The samples were injected electrokinetically on to the column by applying *ca.*  $0.1 \text{ W s}$  of power.

## RESULTS AND DISCUSSION

### Varying the pH of the gel buffer parallel to the running buffer

The effect of the pH of the gel buffer on the sep-

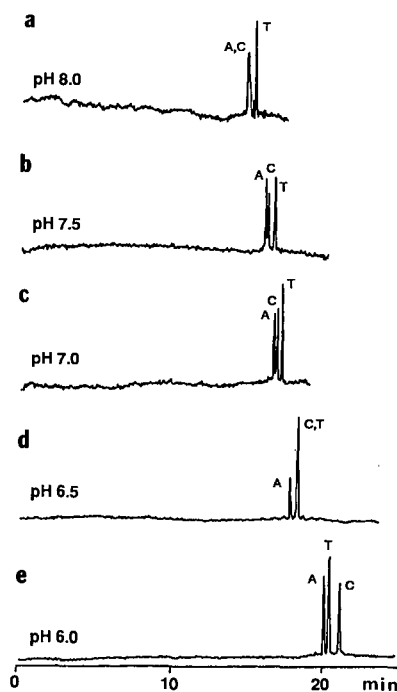


Fig. 1. Separations of the homodecamer test mixture by capillary gel electrophoresis at different pH values. All the gels were prepared at the same pH as the running buffer: (a) pH 8.0; (b) pH 7.5; (c) pH 7.0; (d) pH 6.5; (e) pH 6.0. Peaks: A =  $p(dA)_{10}$ ; C =  $p(dC)_{10}$ ; T =  $p(dT)_{10}$ . Conditions: isoelectrostatic,  $300 \text{ V/cm}$ ; polyacrylamide gel, 3% monomer, 0.15% cross-linker, total column length, 650 mm (effective length from the injection point to the detector point, 500 mm); buffer,  $0.1 M$  Tris– $7 M$  urea, adjusted to the final pH with boric acid.

aration of the homodecamer mixture of  $p(\text{dA})_{10}$ ,  $p(\text{dC})_{10}$  and  $p(\text{dT})_{10}$  was examined first. The omission of the  $p(\text{dG})_{10}$  from the test mixture was done on purpose in order to avoid possible self-association problems [10,11]. Fig. 1a–e compare the separations obtained when the pH of both the gel buffer and the running buffer were varied over the range 8.0–6.0. The peak-height differences observed at different pH values are caused by the pH-dependent UV absorbance of the nucleotide bases [12]. The identification of the homooligomers was accomplished by spiking with the individual compounds.

Fig. 1a shows the separation of the homodecamer test mixture [ $p(\text{dA})_{10}$ ,  $p(\text{dC})_{10}$  and  $p(\text{dT})_{10}$ ] when both the gel preparation buffer and the running buffer were pH 8.0. At this pH, the  $p(\text{dA})_{10}$  and  $p(\text{dC})_{10}$  migrated together, preceding the  $p(\text{dT})_{10}$ , which migrate more slowly. When the pH of both buffers was reduced to 7.5 by increasing the concentration of boric acid in the buffer, almost complete separation of the three components was achieved, as shown in Fig. 1b [migration order  $p(\text{dA})_{10}$ ,  $p(\text{dC})_{10}$  and  $p(\text{dT})_{10}$ ]. The separation was even better when the pH of both buffers was reduced to 7.0, as shown in Fig. 1c [migration order  $p(\text{dA})_{10}$ ,  $p(\text{dC})_{10}$  and  $p(\text{dT})_{10}$ ]. A further decrease in the pH of both buffers to 6.5 led to incomplete separation of the components. Fig. 1d shows that the  $p(\text{dC})_{10}$  and  $p(\text{dT})_{10}$  migrated together, preceded by the  $p(\text{dA})_{10}$ . At pH 6.0, all three homodecamers were baseline separated again, with a different migration

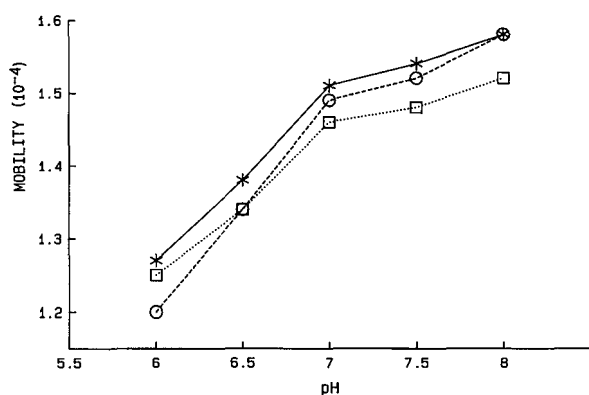


Fig. 2. Relationship between the pH of the gel–running buffer system and the electrophoretic mobility of the homodecamers. Conditions as in Fig. 1. \* =  $p(\text{dA})_{10}$ ; ○ =  $p(\text{dC})_{10}$ ; □ =  $p(\text{dT})_{10}$ .

order of  $p(\text{dA})_{10}$ ,  $p(\text{dT})_{10}$  and  $p(\text{dC})_{10}$ , as shown in Fig. 1e. As mentioned under Experimental, the polymerization rate of the gels prepared at different pH values was maintained at the same level; hence the porosity of the gel (sieving matrix) may be considered to be similar in the pH range examined [13]. Therefore, the migration inversion effect is assumed to be due mainly to the pH changes.

The effect of pH on the mobilities of the components is plotted in Fig. 2; the change in relative migration order of the three homodecamers can be clearly followed. The plots for  $p(\text{dA})_{10}$  and  $p(\text{dT})_{10}$  are almost parallel to each other, whereas the mobility of the  $p(\text{dC})_{10}$  changes differently with pH.

As the pH of both the gel and running buffers was reduced, the migration times of the components became higher. This phenomenon can be explained by the fact that with a decrease in pH the overall charge of a deoxyribonucleotide polyion decreases so the electrophoretic mobility also decreases. However, this migration time shift is different for the three homodecamers because each homooligomer is protonated differently at different pH values [12]. A major pH shift effect can be observed in the migration behavior of  $p(\text{dC})_{10}$ , which migrates together with the  $p(\text{dA})_{10}$  at pH 8.0, preceding the  $p(\text{dT})_{10}$ , but moves behind both of them at pH 6.0.

#### *Electrophoretic equilibration of a gel-filled capillary column by varying the pH of the running buffer*

It is possible to manipulate the pH of a given gel by varying the composition of the running buffer as described by Chrambach [14] in the use of multiphasic buffer systems in slab or rod gel electrophoresis. A major difference is that in capillary electrophoresis, the gel-filled tubing can be used for up to hundreds of runs, not only once as for the slab or rod gels. Hence it was important to examine the possibility of changing the buffer system in a gel-filled capillary column after preparation or even after use.

A capillary gel column, prepared with pH 8.0 buffer, was connected to buffer reservoirs filled with running buffer of pH 6.0, then the electrophoretic equilibration was started by applying a 300 V/cm electric field to the capillary. After 20 min, the current stabilized at a new, higher level that was typical of a pH 6.0 buffer system. Based on this observation, the entire buffer system appears to have



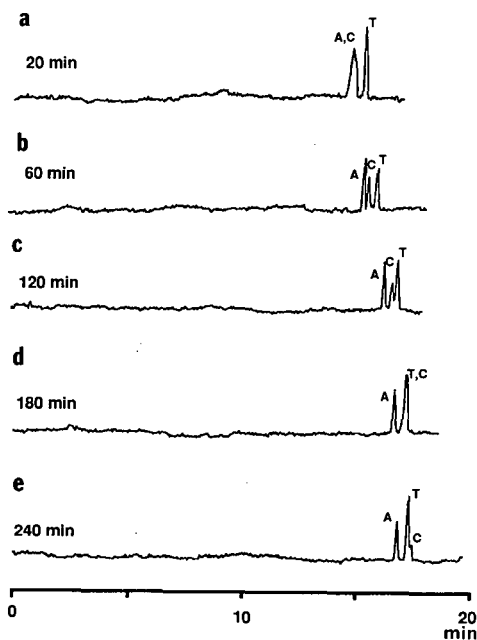


Fig. 3. Capillary electrophoretic separations of the homodecamer test mixture using a pH 8.0 capillary gel column after different equilibration times with the pH 6.0 running buffer: (a) 20; (b) 60; (c) 120; (d) 180; (e) 240 min. Peaks: A =  $p(dA)_{10}$ ; C =  $p(dC)_{10}$ ; T =  $p(dT)_{10}$ . Conditions: gel buffer and running buffer, 0.1 M Tris-boric acid-7 M urea at pH 8.0 and 6.0, respectively, adjusted with boric acid in both instances. Other conditions as in Fig. 1.

changed throughout the gel within 20 min. However, when the separation performance of the gel was checked, almost the same electrophoretic separation and migration order were obtained as with pH 8.0 gel with pH 8.0 running buffer (Fig. 3a). Only after 4 h of electrophoretic equilibration did a retention pattern appear that was characteristic of a gel prepared and run at pH 6.0. After 60 min of electrophoretic equilibration, the migration pattern of the test mixture was similar to that of a column prepared with a pH 7.5 buffer [Fig. 3b, migration order  $p(dA)_{10}$ ,  $p(dC)_{10}$  and  $p(dT)_{10}$ ]. After 120 min of equilibration the gel had a performance similar to a pH 7.0 gel [Fig. 3c, migration order  $p(dA)_{10}$ ,  $p(dC)_{10}$  and  $p(dT)_{10}$ ]. When the homooligomer test mixture was injected after 180 min of equilibration (Fig. 3d), the  $p(dC)_{10}$  and  $p(dT)_{10}$  migrated together, preceded by the  $p(dA)_{10}$ , as was observed on a pH 6.5 gel-filled capillary. The separation

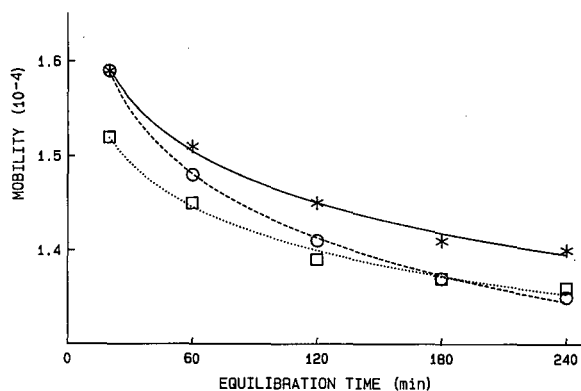


Fig. 4. Relationship between the equilibration time and the electrophoretic mobility of the homodecamers in the pH 8.0 gel-filled capillary column running with a pH 6.0 buffer. Conditions as in Fig. 3. \* =  $p(dA)_{10}$ ;  $\circ$  =  $p(dC)_{10}$ ;  $\square$  =  $p(dT)_{10}$ .

shown in Fig. 3e was the result of a 300 V/cm electric field applied to a pH 8.0 gel-filled capillary column using a pH 6.0 running buffer for 4 h. The  $p(dA)_{10}$  and  $p(dT)_{10}$  preceded the  $p(dC)_{10}$ , as is characteristic of the pH 6.0 gel column.

In conclusion, it is important to note that the current does not seem to be a sufficient indication for determining buffer equilibration in capillary gel electrophoresis. However, the rapid change in current indicates that the small buffer ions in the running buffer have replaced the buffer ions in the gel column, so some other phenomena must occur during the electrophoretic equilibration of the polyacrylamide gel-filled capillaries. However, the reason for this behavior is not clear, and requires more investigation into the physical properties of the gel structure during the electrophoretic equilibration.

Fig. 4 shows plots of the mobilities of the three homodecamers as a function of the equilibration time of the pH 8.0 gel-filled capillary column using a pH 6.0 running buffer. In this instance, as with the data shown in Fig. 2, the mobility of  $p(dC)_{10}$  again shifts faster than that of the other two components. The shape of the curves suggest that equilibration is still not complete after 4 h.

## CONCLUSIONS

The pH of the buffer system used in capillary gel electrophoresis has a marked effect on the migration properties of the different homooligomers. A

mixture of homooligodecamers was co-electrophoresed using buffer systems of different pH values between 6.0 and 8.0 in order to determine its effect on the separation. Gel-filled capillaries, prepared at pH 8.0, were equilibrated with a running buffer of pH 6.0 for various times to determine when full equilibration had taken place, as judged by separation performance. Although it was found to be possible to re-equilibrate the buffer system in a gel-filled capillary, it was found to be extremely time consuming. For example, the electrophoretic equilibration time required for changing the buffer system from pH 8.0 to 6.0 takes more than 4 h for a 650 mm  $\times$  0.075 mm I.D. capillary column filled with 3% polyacrylamide gel. Unfortunately, the time required for completion of this equilibration appears to be much longer than would be appropriate for the capillary gel electrophoretic analysis of oligonucleotides (the average separation time is up to 20-30 min). However, in some instances it is difficult to prepare polyacrylamide gels at the desired pH, e.g., highly acidic gels, special additives. In these instances, after the gel has completely polymerized, equilibration with a suitable running buffer is necessary. Based on these results, it is suggested that for capillary gel electrophoresis of oligonucleotides, the gel should be prepared using buffer of the same pH as the running buffer in order to avoid time-consuming equilibration procedures.

## ACKNOWLEDGEMENTS

The authors thank Professor B. L. Karger and Dr. A. Cohen for stimulating discussions. The help of Phyllis Browning in the preparation of the manuscript is greatly appreciated.

## REFERENCES

- 1 J. W. Jorgenson and K. D. Lukacs, *Science*, 222 (1983) 266.
- 2 S. Hjerten and M. D. Zhu, *J. Chromatogr.*, 347 (1985) 191.
- 3 R. A. Wallingford and A. G. Ewing, *Anal. Chem.*, 58 (1958) 258.
- 4 M. J. Gordon, X. Huang, S. L. Pentoney and R. N. Zare, *Science*, 242 (1988) 224.
- 5 B. L. Karger, *Nature (London)*, 339 (1989) 641.
- 6 J. A. Lux, H.F. Yin and G. Shomburg, *J. High Resolut. Chromatogr.*, 13 (1990) 436.
- 7 B. L. Karger, A. S. Cohen and A. Guttman, *J. Chromatogr.*, 492 (1989) 585.
- 8 A. Guttman, A. S. Cohen, D. N. Heiger and B. L. Karger, *Anal. Chem.*, 62 (1990) 137.
- 9 A. Guttman, A. Akihiro, A. S. Cohen, E. Uhlmann and B. L. Karger, presented at the 14th International Symposium on Column Liquid Chromatography, Boston, MA, May 20-25, 1990, paper P417.
- 10 A. Guttman, R. J. Nelson and N. Cooke, *J. Chromatogr.*, 593 (1992) 297.
- 11 T. Maniatis, E. F. Fritsch and J. Sambrook, *Molecular Cloning: a Laboratory Manual*, Cold Spring Harbor Laboratory, Cold Spring Harbor, NY, 1982.
- 12 G. D. Fasman, *Handbook of Biochemistry and Molecular Biology: Nucleic Acids*, CRC Press, Cleveland, OH, 3rd ed., 1975.
- 13 A. T. Andrews, *Electrophoresis*, Clarendon Press, Oxford, 2nd ed., 1986.
- 14 A. Chrambach, *The Practice of Quantitative Gel Electrophoresis*, VCH, Deerfield Beach, FL, 1985.



# Determination of vasoactive intestinal peptide in rat brain by high-performance capillary electrophoresis

Jérôme Soucheleau

*Département de Médecine Expérimentale, INSERM U52–CNRS URA 1195, Université Claude Bernard, 8 Avenue Rockefeller, 69373 Lyon Cedex 08 (France)*

Luc Denoroy

*Département de Médecine Expérimentale, INSERM U52–CNRS URA 1195, Université Claude Bernard, 8 Avenue Rockefeller, 69373 Lyon Cedex 08, and CNRS, Service Central d'Analyse, 69390 Vernaison (France)*

---

## ABSTRACT

A high-performance capillary electrophoresis (HPCE) method for determining vasoactive intestinal peptide (VIP) in rat brain was developed. Cerebral cortex was first extracted by solid-phase extraction and purified by reversed-phase high-performance liquid chromatography. The VIP-rich fraction was further analysed by capillary zone electrophoresis (CZE) and micellar electrokinetic chromatography using a commercial HPCE instrument with UV detection. The identity of the peak of endogenous VIP was confirmed by performing multiple CZE analyses at different pH values. This HPCE method allows VIP to be detected and measured with good molecular specificity and could represent a reference method to validate data obtained by radioimmunoassay.

---

## INTRODUCTION

Vasoactive intestinal peptide (VIP) is a 28-amino acid polypeptide which was first isolated from porcine small intestine [1]. VIP was later shown also to be present in the central and peripheral nervous system where it may act as a neurotransmitter or neuromodulator [2]. Brain VIP appears to have important biological actions, being involved in cortical energy metabolism [3], the regulation of hormone secretions [4,5], the control of circadian rhythms [6] and the induction of sleep [7].

The determination of VIP in nervous tissue is mainly performed by radioimmunoassay (RIA), a highly sensitive technique that allows the quantification of neuropeptides contained in a complex bi-

ological matrix. Nevertheless, RIA has limited molecular specificity as it is based on the interaction of the peptide with an antibody and therefore monitors a secondary structural parameter and not the amino acid sequence of the peptide [8]. Furthermore, interferences with divalent cations, and also with macromolecules and structural analogues of the peptide of interest, are difficult to evaluate and can hamper the selectivity of any RIA [9,10]. High-performance liquid chromatography (HPLC) followed by RIA improves the selectivity of the analysis, but such an approach is tedious and does not eliminate the ambiguity due to the detection by binding to an antibody. Consequently, it appears that more specific analytical methods in which primary structural parameters (amino acid composition and sequence) are monitored are needed in order to determine neuropeptides in biological samples. Recently, multi-dimensional HPLC followed by mass spectrometry (MS) was used to measure endogenous opioid peptides in animal and human

---

*Correspondence to:* Dr. Luc Denoroy, Département de Médecine Expérimentale, INSERM U52–CNRS URA 1195, Université Claude Bernard, 8 Avenue Rockefeller, 69373 Lyon Cedex 08, France.

tissues [8,11,12]. Although such an approach has a high level of molecular specificity and can give unambiguous data, the MS analysis needs expensive instrumentation and therefore can only be carried out in a few laboratories.

High-performance capillary electrophoresis (HPCE) is a very powerful method for the analysis of biological samples [13–16]. This technique can be performed in most biochemistry laboratories, as commercial HPCE instruments are now available. Two modes of separation can be used to analyse the polypeptides by HPCE, namely capillary zone electrophoresis (CZE) and micellar electrokinetic chromatography (MECC). In both of these modes, peptides are resolved according to their charge to mass ratio, while their hydrophobicity is also involved in MECC separations [13–17]. As these two parameters depend on the amino acid composition and sequence of the peptides, HPCE can be considered to monitor indirectly primary structural characteristics and therefore should allow the specific determination of peptides in biological samples.

HPCE is commonly used for the analysis of peptide maps and for the quality control of synthetic or recombinant polypeptides [18–20], but to our knowledge it has never been used to detect neuro-peptides in brain tissue. The purpose of this study was to develop an HPCE method to detect VIP in rat cerebral regions with good molecular specificity. As a crude brain homogenate is too complex to be analysed directly by HPCE, a multi-dimensional approach including solid-phase extraction, reversed-phase HPLC (RP-HPLC) and finally HPCE was developed.

## EXPERIMENTAL

### Chemicals

Synthetic VIP was purchased from Sigma (St. Louis, MO, USA) and was used without further purification. Trifluoroacetic acid (TFA) was obtained from Pierce and HPLC-grade acetonitrile from Carlo Erba (Milan, Italy). Citric acid and trisodium citrate (Merck, Darmstadt, Germany), monobasic and dibasic sodium phosphate (Sigma) and sodium dodecyl sulphate (SDS) (Sigma) were used to prepare the electrolyte for HPCE. HPLC-grade water obtained with a Milli-Q (Millipore, Bedford, MA, USA) or a Spectrum (Elga, High

Wycombe, UK) purification system was used for making all the solutions.

### Tissue acquisition and homogenization

Male rats (OFA strain) were killed by decapitation and the brain was rapidly removed and dissected over crushed ice. The cerebral cortex, hippocampus and cerebellum were weighed, placed in 10 volumes of cold 0.1 M hydrochloric acid and homogenized in a Potter-Elvehjem glass homogenizer. The homogenates were centrifuged (4000 g for 5 min at 4°C) and the supernatants were collected.

### Solid-phase extraction

The supernatant was applied to an octadecylsilyl (ODS) disposable cartridge (Sep-Pak; Waters, Milford, MA, USA) that had been activated by eluting in sequence with methanol (2 ml), HPLC-grade water (5 ml) and 0.1% (w/v) TFA (10 ml). The supernatant was passed through the cartridge several times. Thereafter the cartridge was washed with 2 ml of a 0.1% TFA solution containing 24% of acetonitrile and the VIP-rich fraction was eluted with 1.6 ml of a 0.1% TFA solution containing 48% of acetonitrile. The collected effluent was evaporated to dryness (Vacuum Speed Vac, Savant). The residue was reconstituted in 1 ml of 0.1% TFA, filtered through a 0.45- $\mu$ m Durapore filter (Millipore) and injected into the HPLC system.

### Reversed-phase high-performance liquid chromatography

Gradient RP-HPLC separation was performed using the following instrument: two Waters Model 510 pumps controlled by a Waters Model 680 automated gradient controller (Millipore), a Waters static mixer, a six-port injection valve with a 1-ml sample loop (Rheodyne, Cotati, CA, USA), an SPD-6A spectrophotometric detector (Shimadzu, Kyoto, Japan) and a Model 330 recorder (Scientific Instruments, Basle, Switzerland). Separations were made at ambient temperature on a Brownlee Aquapore RP 300 C<sub>8</sub> column (220 × 4.6 mm I.D., particle size 7  $\mu$ m, pore size 300 Å), which was protected by a Brownlee Aquapore RP 300 C<sub>8</sub> precolumn (30 × 4.6 mm I.D.) (both from Applied Biosystems, Foster City, CA, USA). The mobile phase for gradient elution was composed of 0.1% TFA (phase A) and 0.09% TFA–80% acetonitrile (phase B). The

monitoring wavelength was 214 nm and the flow-rate was 1.0 ml/min.

The column was equilibrated with a mixture of 95% A-5% B mobile phase, and the sample was then injected. The gradient was started when the absorbance returned to the baseline; this gradient was 5% phase B at 0 min, 65% at 60 min and 80% at 70 min. The elution time of synthetic VIP was determined in a separate experiment, after which the HPLC column was washed to avoid any memory effect. The VIP fraction was collected manually and evaporated to dryness. The residue was reconstituted in 10  $\mu$ l of HPLC-grade water and analysed by HPCE.

#### High-performance capillary electrophoresis

HPCE separations were performed with a Model 270A capillary electrophoresis system (Applied Biosystems) and the electropherograms were recorded on a Chromjet integrator (Spectra-Physics, San Jose, CA, USA). Separations were carried out with an uncoated fused-silica capillary (72 cm  $\times$  50  $\mu$ m I.D.) (Applied Biosystem) and on-column UV detection at 200 nm was carried out. The capillary was flushed with 0.1 M sodium hydroxide solution (2

min) and buffer (5 min) before each electrophoretic run. Injections were made by vacuum for a fixed period of time. HPCE analyses were carried out with two modes of separation *viz.*, CZE and MECC.

The electrolyte used for CZE was 20 mM sodium citrate buffer (pH ranging from 2.5 to 5.0). The capillary was maintained at 30°C and the running voltage was 25 kV. A low-pH mobility marker (Applied Biosystems) was simultaneously injected with the sample. The electrophoretic mobility ( $\mu$ ) was determined according to the equation  $\mu = (L_d L_t / V) (1/t - 1/t_m) + \mu_m$  [17], where  $L_d$  is the length of the capillary from the injection end to the detector,  $L_t$  is the total length of the capillary,  $V$  is the voltage across the capillary,  $t$  and  $t_m$  are the migration times of the sample and of the mobility marker, respectively, and  $\mu_m$  is the electrophoretic mobility of the mobility marker [ $\mu_m = 3.95 \cdot 10^{-4}$  cm<sup>2</sup>/V  $\cdot$  s in 20 mM sodium citrate buffer (pH 2.5) at 30°C]. If  $\mu_m$  was unknown, a relative electrophoretic mobility ( $\mu_r$ ) was determined according to the equation  $\mu_r = (L_d L_t / V) (1/t - 1/t_m)$ .

The MECC separations were made with a 10 mM sodium phosphate buffer (pH 7.0) containing 20

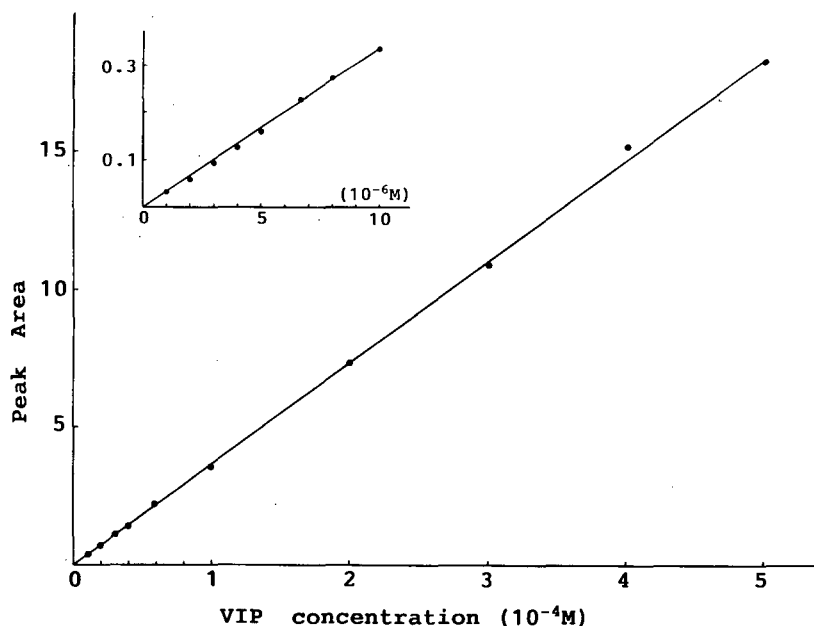


Fig. 1. Plot of the peak area of synthetic VIP vs. the concentration of the standard solutions. Conditions: 20 mM sodium citrate buffer (pH 2.5); 30°C; 25 kV; vacuum injection for 1 s. The inset shows the plot for VIP concentrations between 10<sup>-6</sup> and 10<sup>-5</sup> M.

mM sodium dodecyl sulphate (SDS). A 0.2% mesityl oxide solution (used as a marker of electroosmotic flow) was injected simultaneously with the sample. The capillary was maintained at 35°C and the running voltage was 25 kV. As a marker of micelles migration was not injected, the capacity factor ( $k'$ ) [21] was not determined and only the migration time was expressed.

## RESULTS

### CZE analysis of synthetic VIP

In the first phase of this work, the characteristics of the electrophoretic migration of synthetic VIP were studied using 20 mM sodium citrate buffer (pH 2.5) as electrolyte. The electrophoretic mobility of VIP was found to be  $2.42 \pm 0.05 \text{ cm}^2/\text{V} \cdot \text{s}$  (mean  $\pm$  standard deviation) and the limit of detection was about  $10^{-6} \text{ M}$  (for a 1-s injection). The peak

area varied linearly with synthetic VIP concentration between  $1 \cdot 10^{-6}$  and  $5 \cdot 10^{-4} \text{ M}$  ( $r = 0.99975$ ) (Fig. 1). The relative standard deviation was 1.8% for the migration time, 1.6% for the electrophoretic mobility and 4.6% for the peak area.

### Detection of VIP in rat brain regions

A sample of cerebral cortex (2.97 g of wet tissue dissection from three rats) was homogenized and extracted and the VIP-rich extract was fractionated by RP-HPLC (Fig. 2). A 0.5-ml fraction was collected at the retention time of synthetic VIP and analysed by CZE. A peak exhibiting the same electrophoretic mobility ( $\mu = 2.44 \text{ cm}^2/\text{V} \cdot \text{s}$ ) as synthetic VIP was present on the electropherogram (Fig. 3B). The height of this peak increased when synthetic VIP was co-injected with this sample, whereas no additional peak appeared (Fig. 3C). Consequently, this peak of interest may correspond to endogenous VIP.

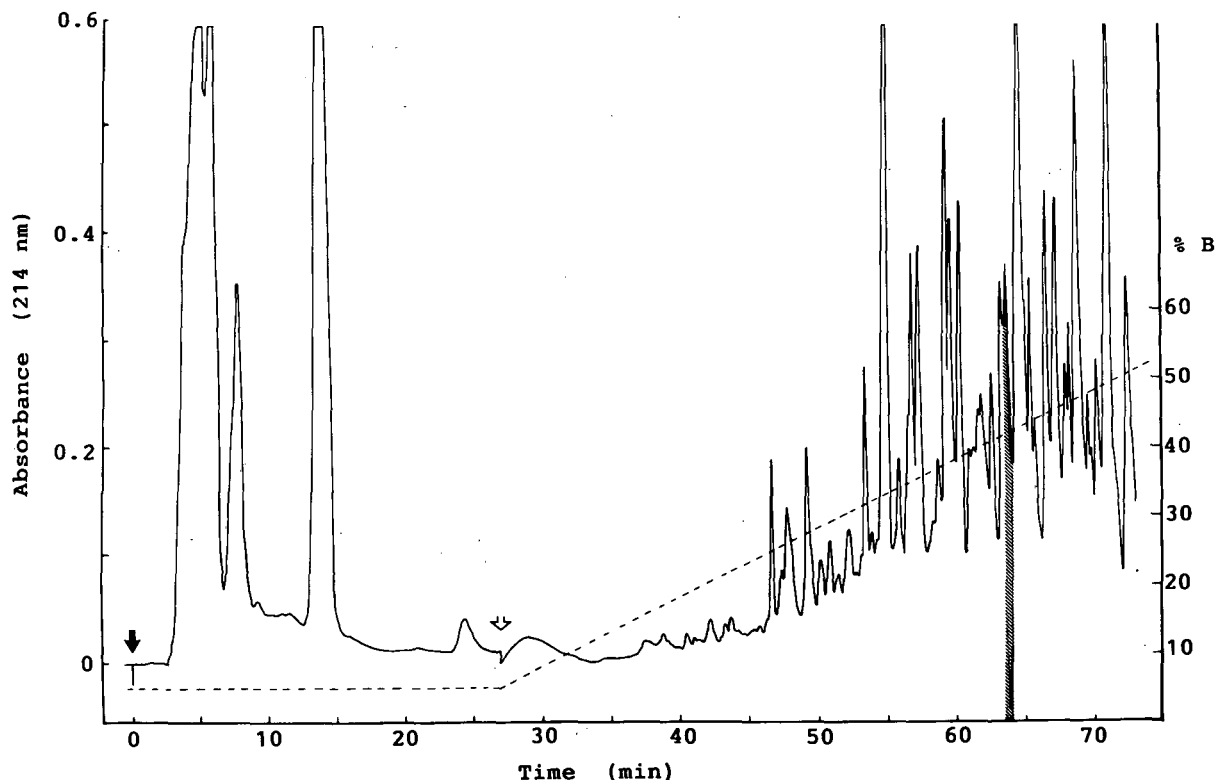


Fig. 2. Reversed-phase HPLC profile of the VIP-rich fraction obtained from the extraction of a cerebral cortex sample. The gradient profile is shown by the dotted line (expressed as % of mobile phase B). Closed arrow, injection; open arrow, beginning of the gradient. The fraction indicated by the shaded area was collected and analysed by HPCE. For chromatographic conditions, see text.

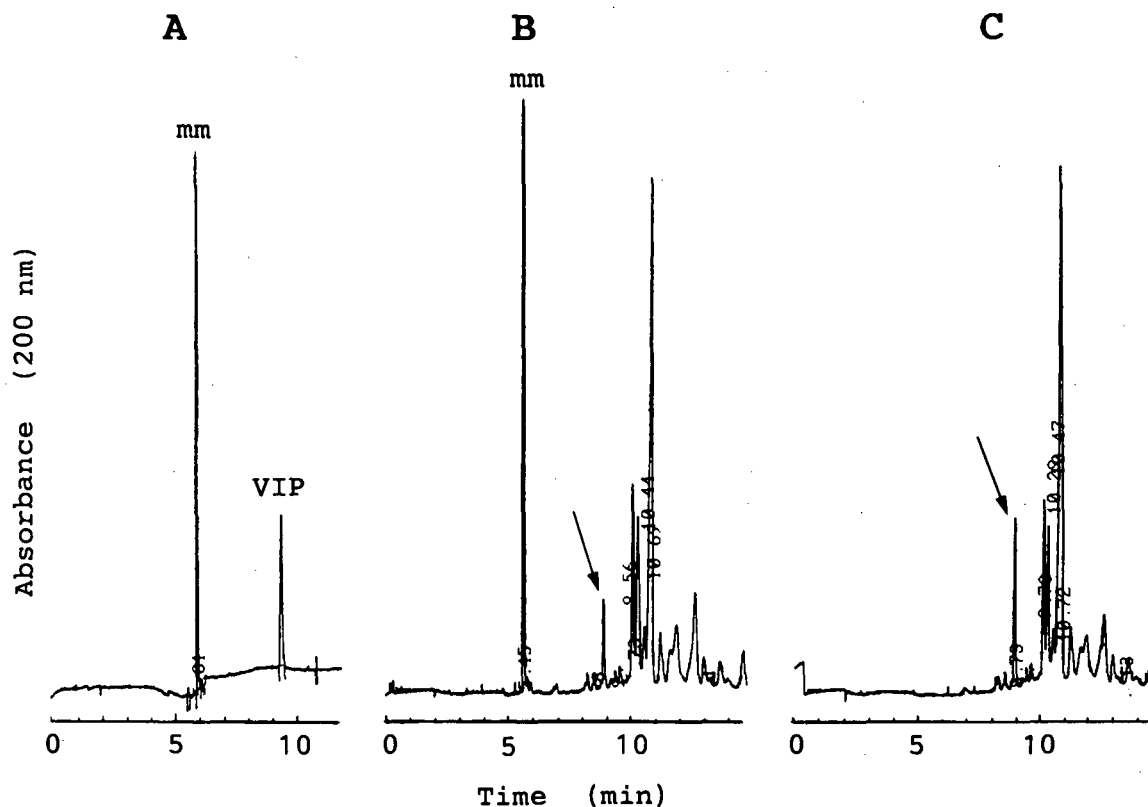


Fig. 3. CZE analysis of the sample of cerebral cortex. Conditions: 20 mM sodium citrate buffer (pH 2.5); 30°C; 25 kV. (A) Injection of  $5 \cdot 10^{-6}$  M synthetic VIP and of mobility marker (mm). Each solution was injected for 2 s. (B) Injection of cerebral cortex sample (4 s) and of mobility marker (2 s). The arrow shows a peak with the same electrophoretic mobility as synthetic VIP ( $2.44 \text{ cm}^2/\text{V} \cdot \text{s}$ ). Sample corresponding to the RP-HPLC fraction indicated on Fig. 2. (C) Injection of the same sample (4 s) and of  $5 \cdot 10^{-6}$  M synthetic VIP (2 s). The height of the peak shown by the arrow is increased as compared with (B).

A sample of hippocampus (0.99 g of wet tissue dissected from five rats) was analysed by the same protocol. The electropherogram showed a small peak with an electrophoretic mobility equal to  $2.44 \text{ cm}^2/\text{V} \cdot \text{s}$ . When synthetic VIP was co-injected with the sample, the height of this peak increased, suggesting that it may be due to endogenous VIP present in the hippocampus.

Finally, a sample of cerebellum (1.0 g of wet tissue) was analysed by the same protocol, but no peak with the same electrophoretic mobility as synthetic VIP was present on the electropherogram.

*HPCE characterization of brain VIP*

A sample of cerebral cortex was analysed by HPCE using different electrolytes in order to characterize better the peak which was detected as VIP.

TABLE I  
ELECTROPHORETIC MOBILITY OF SYNTHETIC AND BRAIN VIP AT DIFFERENT pH VALUES

The mobility is expressed as  $\mu_r$  (see text). Electrophoretic conditions: CZE, 20 mM sodium citrate buffer; 30°C; 25 kV. Sample: cerebral cortex.

pH of electrolyte	$\mu_r$ ( $10^{-4} \text{ cm}^2/\text{V} \cdot \text{s}$ )	
	Synthetic VIP	Brain VIP
2.5	-1.56	-1.61
3.0	-1.22	-1.24
4.0	-0.72	-0.75
4.5	-0.48	-0.48
5.0	-0.29	-0.31



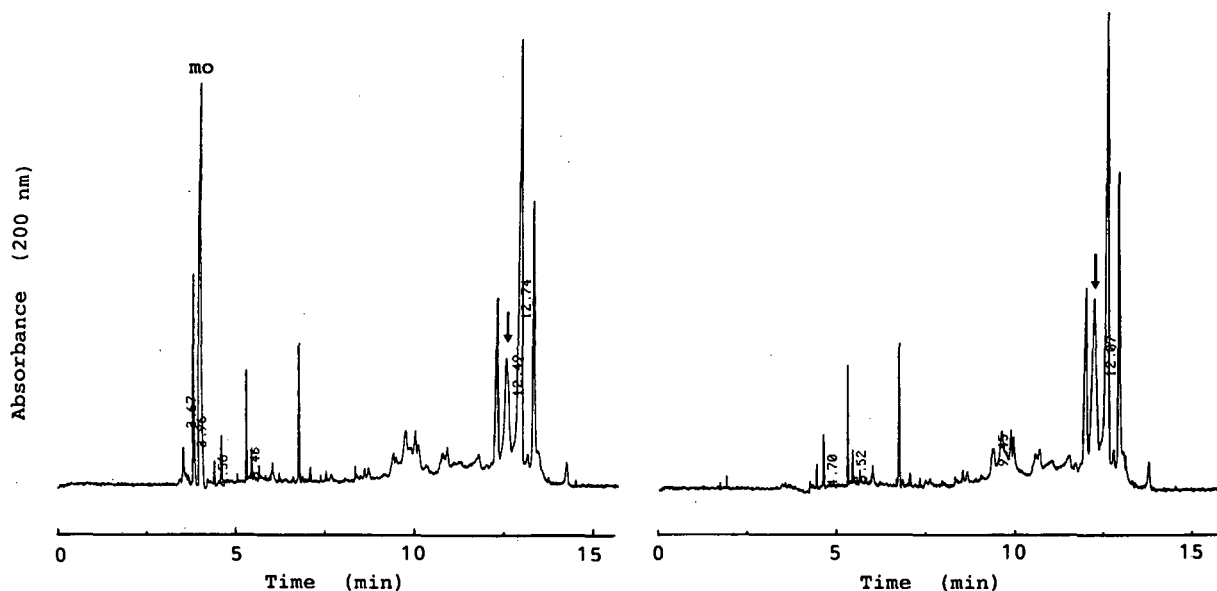


Fig. 4. MECC analysis of the sample of cerebral cortex. Conditions: 10 mM sodium phosphate buffer (pH 7.0) containing 20 mM SDS; 35°C; 25 kV. Left: injection of cerebral cortex sample (2 s) and of 0.2% mesityl oxide (mo; 1 s). Right: injection of the same sample (2 s) and of  $10^{-5}$  M VIP (1 s). The height of the peak shown by the arrow is increased.

Multiple CZE analyses of the cortex sample and of the synthetic VIP were made at various pH values. The values of the relative electrophoretic mobility ( $\mu_r$ ) of the peak from the brain extract and of the synthetic VIP were determined. As shown in Table I, these mobilities exhibited similar changes when the pH of the electrolyte was increased from 2.5 to 5.0.

Attempts were made to perform CZE separations at higher pH, but such conditions appeared unsuitable for analyses for VIP. Synthetic VIP did not migrate when the electrolyte was 10 mM sodium phosphate buffer (pH 7.0) or 20 mM borate buffer (pH 8.25) containing 20 mM sodium chloride. It was detected as a very broad peak when CZE was carried out with 20 mM CAPS buffer (pH 11.0).

Conversely, the cortex sample was analysed by MECC, as VIP migrates in this mode. The electropherogram showed a peak with the same migration time as synthetic VIP. The height of this peak increased when synthetic VIP was co-injected, whereas no additional peak appeared on the electropherogram (Fig. 4).

#### Determinations of VIP in cerebral cortex

Homogenates of cerebral cortex were divided in-

to two equal parts and 500 pmol of synthetic VIP were added to one part as an internal standard. The samples were subjected to the entire protocol and the areas of the peaks corresponding to VIP were measured during the CZE analysis. The concentration of VIP in rat cerebral cortex was found to be  $25.5 \pm 7.5$  pmol per gram of tissue.

#### DISCUSSION

To our knowledge, this is the first work in which a commercial HPCE instrument with UV detection has been used to determine a neuropeptide in mammalian brain. The results presented in this paper illustrate the molecular specificity of the method. VIP was identified on the electropherograms as a peak which was well resolved from other endogenous compounds. Such a result was possible owing to the high separation power of HPCE and the orthogonal approach which has been developed, *i.e.*, gradient RP-HPLC separation followed by HPCE analysis.

The electropherograms of the CZE analysis of rat cerebral cortex showed a peak that seems to correspond to true endogenous VIP for several reasons. First, this peak was present in a fraction that was

collected at the retention time of synthetic VIP during the RP-HPLC step. Second, this peak had the same electrophoretic mobility as synthetic VIP under different conditions of CZE analysis, *i.e.*, with five sodium citrate buffers with pH values between 2.5 and 5.0. These data demonstrated that this peak corresponds to a compound that has the same charge to mass ratio as authentic VIP in this pH range. Third, a peak that has the same migration time as synthetic VIP was found during the MECC analysis of the same samples. These data show that the sample contains a compound that has both the same hydrophobicity and the same charge to mass ratio as synthetic VIP. Finally, this peak was found in samples from cerebral cortex and hippocampus, two brain regions known to contain VIP neurons, whereas it was absent from cerebellum, a part of the brain that is devoid of VIP innervation [22,23].

The marked specificity of the present method arises from the possibility of performing multiple HPCE analyses under various conditions of separation. Indeed, as only a small amount of material is injected into the HPCE instrument, the same sample can be used for many electrophoretic runs. In addition, most of these HPCE analyses can be performed within a day, as the run times are short and because the equilibration of the capillary seems to be rapid after each change of electrolyte. Although the selectivity of the present method seems good, it may be improved by including more HPCE analyses under different conditions of separations, such as CZE with an electrolyte other than citrate buffer, CZE at neutral or basic pH in a coated capillary and MECC in the presence of surfactants other than SDS. During this work, attempts to perform CZE analysis in an uncoated capillary at neutral or basic pH were unsuccessful. Under such conditions, synthetic VIP did not migrate or was eluted as a very broad peak, indicating strong interactions between the peptide and the capillary wall. VIP is a 28-amino acid polypeptide that contains two arginine and three lysine residues and therefore has a basic character. Consequently, VIP is still in a cationic form at pH 7.0–8.5 and interacts with the capillary wall, which is negatively charged owing to the dissociation of silanol groups. Such a phenomenon has been well described for basic proteins and peptides [18,24].

The present method seems to be quantitative, al-

though this aspect has not been fully investigated. In CZE, the peak area, migration time and electrophoretic mobility were reproducible. Moreover, a plot of the peak area of synthetic VIP *vs.* sample concentration gave excellent linearity. The HPCE measurement of VIP in cerebral cortex gave values that are of the same order of magnitude as the concentrations determined by RIA in rats of the same strain [6].

One drawback of the present method is its lack of sensitivity, mainly due to the low sensitivity of the UV detection used in the HPCE analysis. More sensitive means of detection, such as laser-induced fluorescence [19,25], should decrease the limit of detection by several orders of magnitude. In addition, further studies are needed to improve the extraction and the RP-HPLC fractionation, in order to decrease the loss of material that occurs in these two steps.

In comparison with RIA, the present method has a higher molecular specificity, as HPCE separations monitor indirectly primary structural parameters. Nevertheless, it only allows the determination of VIP that is contained in grossly dissected brain regions and cannot determine the low level of VIP present in discrete brain areas dissected as “punches” [6], a measurement that can still only be made by RIA. Hence, the two techniques appear to be complementary, RIA allowing highly sensitive measurements but with a limited molecular specificity, whereas the proposed HPCE method can be either a reference method to validate results obtained by RIA, or can be used to study neuropeptides with good molecular selectivity when the amount of biological material is not as limited.

#### ACKNOWLEDGEMENTS

This work was supported by CNRS (URA 1195 and USR 59) and INSERM (U 52). The authors thank Dr. J. Vialle and M. M. Schmidt for help in preparing the manuscript.

#### REFERENCES

- 1 S. I. Said and V. Mutt, *Science*, 169 (1970) 1217.
- 2 W. Rostene, *Prog. Neurobiol.*, 22 (1984) 103.
- 3 P. J. Magistretti, J. H. Morrison, W. J. Shoemaker, V. Sapin and F. E. Bloom, *Proc. Natl. Acad. Sci. U.S.A.*, 78 (1981) 6535.

- 4 R. A. Pryor-Jones and J. S. Jenkins, *Clin. Endocrinol.*, 29 (1988) 677.
- 5 K. S. L. Lam, *Neuroendocrinology*, 53 (1991) 45.
- 6 A. Morin, L. Denoroy and M. Jouvot, *Brain Res.*, 538 (1991) 136.
- 7 F. Riou, R. Cespuglio and M. Jouvot, *Neuropeptides*, 2 (1982) 265.
- 8 J. L. Lovelace, J. J. Kusmierz and D. M. Desiderio, *J. Chromatogr.*, 562 (1991) 573.
- 9 H. Morris, A. Etienne, A. Dell and R. Albuquerque, *J. Neurochem.*, 34 (1980) 574.
- 10 T. Chard, *An Introduction to Radioimmunoassay and Related Techniques*, Elsevier, Amsterdam, 1987.
- 11 D. O. Desiderio, M. A. Kau, F. R. Tanzer, J. O. Trimble and C. L. Wakelyn, *J. Chromatogr.*, 342 (1984) 245.
- 12 J. O. Kusmierz, R. Sumrada and D. O. Desiderio, *Anal. Chem.*, 62 (1990) 2395.
- 13 B. L. Karger, A. S. Cohen and A. Guttman, *J. Chromatogr.*, 492 (1989) 585.
- 14 A. G. Ewing, R. A. Wallingford and T. M. Olefirowicz, *Anal. Chem.*, 61 (1989) 292.
- 15 W. G. Kuhr, *Anal. Chem.*, 62 (1990) 403.
- 16 F. Robert, J. P. Bouilloux and L. Denoroy, *Ann. Biol. Clin.*, 49 (1991) 137.
- 17 P. D. Grossman, J. C. Colburn and H. H. Lauer, *Anal. Biochem.*, 179 (1989) 28.
- 18 P. Grossman, J. C. Colburn, H. H. Lauer, R. G. Nielsen, R. M. Riggan, G. S. Sittampalan and E. C. Rickard, *Anal. Chem.*, 61 (1989) 1186.
- 19 H. Lüdi, E. Gassmann, H. Grossenbacher and W. Märki, *Anal. Chim. Acta*, 213 (1988) 215.
- 20 T. M. Chen, R. C. George and M. H. Payne, *J. High Resolut. Chromatogr.*, 13 (1990) 782.
- 21 S. Terabe, K. Otsuka and T. Ando, *Anal. Chem.*, 57 (1985) 834.
- 22 K. B. Sims, D. L. Hoffman, S. I. Said and E. A. Zimmerman, *Brain Res.*, 186 (1980) 165.
- 23 I. Loren, P. C. Emson, J. Fahrenkrug, A. Björklund, J. Al-umets, R. Hakanson and F. Sundler, *Neuroscience*, 4 (1979) 1983.
- 24 M. M. Bushey and J. W. Jorgenson, *J. Chromatogr.*, 480 (1989) 301.
- 25 Y. F. Cheng and N. J. Dovichi, *Science (Washington, D.C.)*, 242 (1988) 562.

# Monitoring excitatory amino acid release *in vivo* by microdialysis with capillary electrophoresis–electrochemistry

Thomas J. O'Shea, Paul L. Weber<sup>☆</sup>, Brad P. Bammel<sup>☆☆</sup>, Craig E. Lunte and Susan M. Lunte

*Center for Bioanalytical Research and Department of Chemistry, University of Kansas, Lawrence, KS 66047 (USA)*

Malcolm R. Smyth

*School of Chemical Sciences, Dublin City University, Dublin (Ireland)*

---

## ABSTRACT

Capillary electrophoresis (CE) with electrochemical detection (ED) was used to determine extracellular levels of aspartate, glutamate and alanine in samples from the frontoparietal cortex of the rat which were obtained by microdialysis. The method was used to monitor the effect on the overflow of the excitatory amino acids aspartate and glutamate of an influx of high concentrations of potassium ion. Samples were derivatized with naphthalenedialdehyde–cyanide prior to analysis. Detection limits for aspartate and glutamate were 80 and 100 nM, respectively. CE–ED is extremely useful for the analysis of microdialysis samples because of the very small sample volumes required by this analytical technique. The use of ED provides the requisite sensitivity and allows verification of peak purity by voltammetry.

---

## INTRODUCTION

Electrochemical detection (ED) has been shown to be a sensitive method for use with capillary electrophoresis (CE) [1–3]. The combination of an extremely high-resolution separation technique with a high-sensitivity detector results in a powerful analytical tool. The small sample volume requirement of CE is an added advantage when coupled to microdialysis sampling, in which collected volumes are typically a few microliters. Such volume-limited samples and the ability to easily reduce the volume

to achieve greater temporal resolution using CE should prove to be an ideal combination of both techniques.

Microdialysis, which has recently been reviewed [4,5], is accomplished by implantation of a small probe into the tissue of interest. The probe, composed of a short length of dialysis tubing, is perfused with an isotonic saline solution. The use of a precisely controlled flow-rate allows chemicals to be predictably removed from or introduced into the extracellular space by establishment of a steady-state flux across the membrane wall. This type of sampling is advantageous over conventional methods for several reasons. First, continuous sampling can be achieved without fluid loss. Second, samples collected are relatively clean, and thus amenable to direct injection without the necessity of sample cleanup procedures prior to analysis. Furthermore,

---

*Correspondence to:* Dr. S. M. Lunte, Center for Bioanalytical Research, University of Kansas, Lawrence, KS 66047, USA

<sup>☆</sup> Present address: Briar Cliff College, Sioux City, IA, USA.

<sup>☆☆</sup> Present address: Boise State University, Boise, ID, USA.

post-sampling enzymatic reactions are eliminated since enzymes are prevented from crossing the dialysis membrane.

Many analytes of biological interest, such as amino acids, lack properties for direct determination at physiologically relevant levels. To circumvent this limitation, chemical derivatization is generally employed to enhance detection sensitivity. Naphthalene-2,3-carboxaldehyde (NDA) reacts with primary amines in the presence of cyanide to produce cyanof[*l*]benzoisindole (CBI) derivatives which are both fluorescent and electroactive [6,7]. The analysis of NDA-labeled amino acids by liquid chromatography (LC) with ED has been reported previously [7,8]. We have recently developed a procedure for the determination of the major NDA-labeled amino acids involved in neurotransmission using CE with UV detection [9]. The detection limits obtained with this technique were sufficient for the analysis of a brain homogenate; however, a more sensitive technique is required for the detection of the levels of amino acids found in brain tissue.

In this study, the combination of microdialysis sampling and CE-ED is demonstrated for the continuous monitoring of amino acids in the brain. The ability of the probe to sample a tissue as well as to deliver a test compound to the tissue is shown by the  $K^+$ -induced stimulation of excitatory amino acid release.

## EXPERIMENTAL

### Reagents

All amino acids were purchased from Sigma (St. Louis, MO, USA) and used as received. NDA was supplied by Oread Labs. (Lawrence, KS, USA). Sodium cyanide and sodium borate were obtained from Fisher Scientific (Fair Lawn, NJ, USA). Solutions were prepared in Nanopure water (Sybron-Barnstead, Boston, MA, USA) and passed through a membrane filter (0.2  $\mu\text{m}$  pore size) before use.

### Stock solutions

A 10 mM sodium borate solution, amino acid stock solutions (5 mM) and potassium cyanide (10 mM) were all prepared in Nanopure water. Stock solutions of NDA (5 mM) were prepared in acetonitrile. The Ringer's solution consisted of 147 mM NaCl, 4.0 mM KCl and 2.3 mM  $\text{CaCl}_2$ . For potas-

sium-evoked overflow, the perfusate was changed to 51 mM NaCl, 2.3 mM  $\text{CaCl}_2$  and 100 mM KCl.

### Capillary electrophoresis system

The CE-ED system has been described previously [1]. Briefly, the electrochemical detector is isolated from the applied electrical field using a Nafion joint on the capillary column. This joint is positioned in the cathodic buffer reservoir and permits ion movement but not bulk electrolyte flow. This allows ED to be achieved without adverse effects from the electrical field. Detection was performed in the amperometric mode using a 33- $\mu\text{m}$ -diameter carbon fiber microelectrode with an exposed length of 200-250  $\mu\text{m}$  which was inserted into the end of the capillary column. A three-electrode cell configuration was used with the electrode connections made to a BAS LC-4C amperometric detector (Bioanalytical Systems, West Lafayette, IN, USA). The low currents generated at the microelectrode necessitated the use of a Faraday cage to shield the electrochemical cell from external electrical noise. Electrochemical pretreatment of the microelectrode was accomplished using a function generator (Exact Electronics, Hillsboro, OR, USA) connected to the external input of the BAS LC-4C. An oscilloscope was used to monitor the applied waveform, which involved the application of a 50-Hz square-wave of 2 V amplitude to the microelectrode for 1 min. The pretreatment was performed while the microelectrode was inserted in the capillary column and buffer was flowing past its surface.

A separation voltage of 30 kV and a column length of 1 m were used for all separations. The capillary columns (50  $\mu\text{m}$  I.D., 360  $\mu\text{m}$  O.D.) were obtained from Polymicro Technologies. The operating buffer was 0.02 M borate (pH 9.0). The detection potential was operated at +800 mV vs. Ag/AgCl.

### Cyclic voltammetry

Cyclic voltammetry experiments were conducted in a three-electrode cell configuration using a Model CySy-1 computerized electrochemical analyzer (Cypress Systems, Lawrence, KS, USA). For these studies, excess amino acid was employed in the derivatization step to prevent interference from any impurities or side-reactions.

#### Microdialysis system: apparatus

Microdialysis sampling was performed using a CMA/100 syringe pump coupled to a BAS/Carnege Medicine CMA-12 4-mm dialysis probe (Bio-analytical Systems) with a MW cut-off of 20 000. Perfusion was carried out with Ringer's solution at 1  $\mu\text{l}/\text{min}$  for all experiments.

#### Derivatization procedure

A 1.8- $\mu\text{l}$  volume of sodium borate and 0.9  $\mu\text{l}$  of potassium cyanide were added to 3  $\mu\text{l}$  of dialysate sample containing 1.5  $\mu\text{l}$  of the  $\alpha$ -amino acid (internal standard, varying between 2.5 and 22.5  $\mu\text{M}$  final concentration, depending on the anticipated concentration of aspartate and glutamate) followed by 1.8  $\mu\text{l}$  of NDA. The reaction was allowed to proceed for 30 min.

#### Microdialysis probe characterization

In order to determine the *in vivo* concentration of amino acids giving rise to the concentrations detected in the perfusion medium, it was necessary to calculate the recovery of the dialysis probe. Determination of the recovery was performed by placing the dialysis probes in standard concentrations of amino acids. The probes were perfused at 1  $\mu\text{l}/\text{min}$  and samples of the perfusate were collected and analyzed. Recovery is then expressed as the ratio of the concentration of amino acid in the perfusate to the concentration of the standard. The average recovery of alanine, glutamine and aspartate was  $24.3 \pm 3.7$ ,  $20.8 \pm 4.3$  and  $21.1 \pm 3.7\%$ , respectively ( $n = 3$ ). The recovery was independent of concentration and was determined both before and after implantation. This never differed by more than 6%.

#### *In vivo* experiments

Male Sprague–Dawley rats six months or older (400–700 g) were used. Rats were initially anesthetized with the inhalation anesthetic isoflurane to simplify weighing and administration of chloral hydrate C-IV. Between 0.5 and 1.0 ml of 400 mg/ml chloral hydrate in isotonic saline was administered intraperitoneally to anesthetize rats for surgery. Anesthesia was maintained during the experiment by infusion of 1  $\mu\text{l}$  of 200 or 400 mg/ml chloral hydrate in saline per min via a catheter in the right jugular vein. In some cases, boosts of isoflurane were needed during surgery. Caution must be exer-

cised when using this combination of anesthetics, as it can cause respiratory depression.

The rat was positioned in the stereotaxic apparatus, its scalp was shaved and a sagittal incision was made from just in front of the ears to just behind the eyes. The scalp and underlying soft tissues were scraped back to expose the skull. A hole less than 0.5 mm in diameter and 2.5 mm forward and 2.5 mm to the right of bregma was drilled just through the skull. A 25-gauge hypodermic needle in the probe carrier of the stereotaxic device was lowered until it just touched the membrane covering the brain. The hole for the dialysis probe (2.5 mm deep) was created with the needle since this causes minimal damage to the tissue. The needle was then withdrawn and the dialysis probe inserted, thus centering it in the frontoparietal cortex [10]. The scalp was then closed with tissue staples and the wound covered with paper soaked with isotonic saline to prevent drying.

Experiments were performed by perfusing the implanted probe with a normal Ringer's solution at a perfusion rate of 1  $\mu\text{l}/\text{min}$ . Samples were continuously collected over 5-min intervals. Initial samples were collected for at least 1 h following insertion of the microdialysis probe and discarded. Subsequent dialysis samples were derivatized as described above and analyzed by CE–ED to establish basal extracellular amino acid concentrations. The perfusion fluid was then switched to the hyperpotassium Ringer's solution using the liquid switch. Dialysis samples were collected for an additional hour during continuous perfusion with hyperpotassium Ringer's solution. These samples were also derivatized and analyzed by CE–ED.

## RESULTS AND DISCUSSION

#### Electrochemistry

Initial studies concerned the investigation of the electrochemical behavior of NDA-labeled amino acids. Fig. 1A shows the voltammetric response for glutamate at an untreated microelectrode. A broad peak response was obtained with an  $E_p$  of ca. +680 mV. It has been recognized that the pretreatment of carbon fiber microelectrodes has a pronounced effect on the electron transfer properties of many solution species, in particular, enhancement of the electrochemical response [11–13]. Following elec-

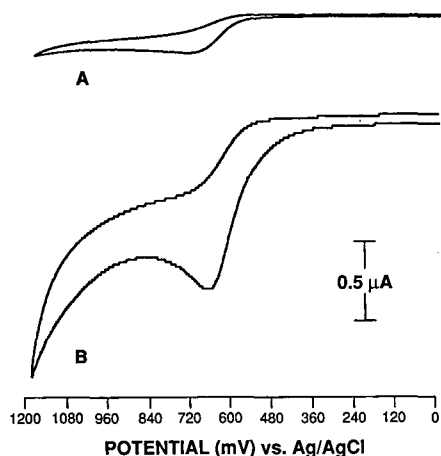


Fig. 1. Cyclic voltammograms of  $5 \cdot 10^{-4} M$  NDA-labeled glutamate (excess glutamate was used in the derivatization procedure) in  $0.1 M$  borate buffer (pH 9.0). Scan-rate,  $100 \text{ mV/s}$ . (A) Response at untreated microelectrode. (B) Response at electrochemically pretreated microelectrode.

trochemical pretreatment (described in the Experimental section), a better-defined peak shape and nearly five-fold increase in peak current were obtained with a cathodic shift in the  $E_p$  value to  $+650 \text{ mV}$  (Fig. 1B). The other NDA-labeled amino acids studied exhibited similar voltammetric behaviors.

Electrochemical pretreatment was found to be necessary between each CE run, as the amino acid derivatives appeared to foul the microelectrode surface. A diminution of *ca.* 10–20% in peak height between successive injections was observed. A similar effect was reported by Oates and Jorgenson [8], who employed carbon fiber microelectrodes for the detection of NDA-labeled amino acids following open tubular chromatography. However, using the electrochemical pretreatment regime between each injection, a reproducible response was obtained with a relative standard deviation of 1.2% ( $n = 7$ ). Hydrodynamic voltammetry was then investigated, and  $E_{1/2}$  values for several NDA-labeled amino acids, including  $\gamma$ -aminobutyric acid (GABA), alanine, glycine, glutamine, aspartate and glutamate, were found to be 600, 610, 626, 635, 640 and 650 mV, respectively. These values are in agreement with those given in a report by Nussbaum *et al.* [14], which indicated that acidic derivatives were more difficult to oxidize than the basic derivatives. On the basis of these studies, an applied potential of  $+800 \text{ mV}$  was selected for subsequent investigations.

#### Detection limit

Fig. 2 shows the separation of alanine, glutamate, aspartate and the internal standard,  $\alpha$ -aminoadipic acid. Quantitation was achieved using response factors which were based on peak areas and were obtained in the range  $2 \cdot 10^{-7}$  to  $1 \cdot 10^{-4} M$ . The limit of detection (signal-to-noise ratio = 3) for all the NDA-labeled amino acids was extrapolated from the electropherograms at  $2 \cdot 10^{-7} M$  levels. For alanine, glutamate and aspartate, the limits of detection calculated were  $4.9 \cdot 10^{-8}$ ,  $1.1 \cdot 10^{-7}$  and  $7.9 \cdot 10^{-8} M$ , respectively. Using  $8.0 \text{ nl}$  as the injection volume, the corresponding mass detection limits were 0.4, 1 and  $0.8 \text{ fmol}$ , respectively. These detection limits were based on derivatizing the actual dilute solution, resulting in apparent detection limits which are higher than those previously reported, where high concentrations of amino acids were derivatized and then diluted [15]. In the latter case, many of the interferences resulting from reagent impurities and side-reactions are diluted along with the analyte.

Based on the recoveries of the amino acids with the dialysis probe, the limits of detection *in vivo* for alanine, glutamate and aspartate were  $8.2 \cdot 10^{-8}$ .

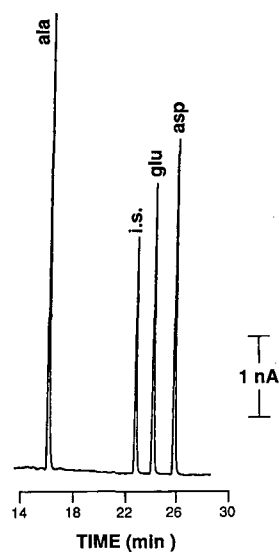


Fig. 2. Capillary electrophoretic separation of  $1 \cdot 10^{-4} M$  standards of alanine,  $\alpha$ -aminoadipic acid (internal standard, i.s.), glutamate and aspartate. Separation conditions:  $0.02 M$  borate buffer (pH 9.0); voltage,  $30 \text{ kV}$ ; column length,  $1 \text{ m}$ ; detection potential,  $+800 \text{ mV vs. Ag/AgCl}$ .

$4.8 \cdot 10^{-7}$  and  $3.7 \cdot 10^{-7}$  M, respectively. Standards of the amino acid derivatives were analyzed periodically between dialysate samples to ensure that the detector response remained reproducible over the course of the study.

#### Voltammetric analysis

A typical electropherogram of a derivatized brain dialysate obtained by *in vivo* microdialysis sampling is shown in Fig. 3A. In addition to co-migration, the identity and purity of the amino acids were confirmed by voltammetric characterization. This identification is based on the  $E_{1/2}$  value and the shape of the current–voltage curve, which together give a characteristic unique to each compound. It has been demonstrated previously that the entire voltammogram is not required; the comparison of current response in the region where most change occurs is sufficient [16]. The use of current ratios for compound identification has been previously reported [14,17,18].

The current ratios were calculated by measurement of the responses in the region where the current is most dependent on potential (450 and 650 mV) and ratioed to the response where the current is no longer dependent on potential, *i.e.*, the mass transport-limited value (800 mV). The current ratios recorded are given in Table I. The ratios for standards of alanine, glutamate and aspartate agreed well with those of the dialysate components

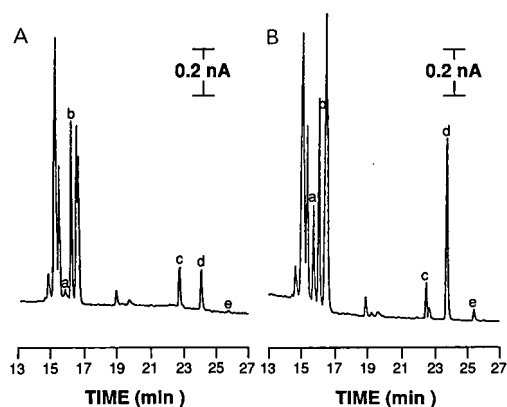


Fig. 3. Derivatized brain dialysate samples obtained by perfusion with (A) normal Ringer's solution and (B) high- $K^+$  Ringer's solution. Peaks: a = GABA; b = alanine; c = internal standard; d = glutamate; e = aspartate. Separation conditions as outlined in Fig. 2.

TABLE I  
VOLTAMMETRIC CHARACTERIZATION

Component	Retention time (min)	Current response	
		+0.45 V/0.80 V	+0.65 V/0.80 V
Peak a	15.9	0.21	0.72
GABA	15.7	0.12	0.65
Peak b	16.2	0.12	0.64
Alanine	16.0	0.10	0.62
Peak d	24.4	0.04	0.55
Glutamate	24.1	0.03	0.55
Peak e	25.7	0.03	0.54
Aspartate	25.9	0.03	0.56

eluting at the same time, confirming peak identification and purity. However, peak a, tentatively identified as GABA based on its migration time, differed significantly from the voltammetric behavior of the GABA standard.

#### Potassium-evoked amino acid overflow analysis

High  $K^+$  stimulus of brain tissue is known to increase the overflow of several amino acids [19,20]. Fig. 3A shows the electropherogram obtained from a typical NDA-labeled brain dialysate sample using normal Ringer's solution. Upon increasing the level of KCl from 4.0 to 100 mM (while still retaining the correct osmolality), the electropherogram (Fig. 3B) showed a substantial increase in the impure GABA (peak a), glutamate (peak d) and aspartate (peak e). These increased levels are indicative of their roles as neurotransmitters. The levels of alanine (peak b) remained unaffected by the  $K^+$  stimulus, which was expected as it is thought only to have a role in metabolic functions. These results are in agreement with the findings of Tossman *et al.* [19].

Fig. 4 shows the concentration–time curves obtained for alanine, glutamate and aspartate. After 30 min of collecting dialysate samples of the basal amino acid concentration levels, the  $K^+$  stimulus was applied. For both glutamate and aspartate, a maximum increase over the basal concentration levels of nearly four-fold was observed. After an initial sharp increase, the levels of both amino acids decreased to a steady-state level approximately 30 min after the stimulus was introduced. The curve ob-



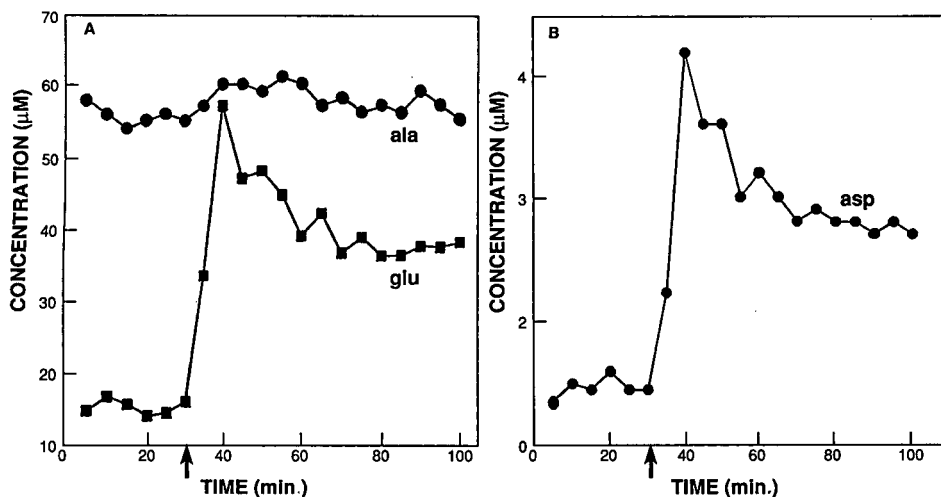


Fig. 4. Concentration–time curves of (A) alanine and glutamate and (B) aspartate in rat brain. Arrow indicates application of potassium stimulation.

tained for alanine fluctuated between  $5.5 \cdot 10^{-5}$  and  $6.2 \cdot 10^{-5}$  M and did not show any response to the  $K^+$  stimulus. The previous studies of  $K^+$ -invoked overflow of amino acids in the brain [19,20] did not present a concentration–time curve; they reported only two concentration levels, a basal level and the level obtained after a 10-min stimulation.

## CONCLUSIONS

One of the main advantages of CE as an analytical tool for microdialysis sample analysis over the more commonly used LC is that it is more amenable to small sample volumes. In this study, 3- $\mu$ l samples were derivatized; however, if microderivatization procedures [21] were employed, much greater temporal resolution could be achieved. Additionally, because of the small injection volumes (typically of the order of a few nanoliters), multiple analyses can be performed on a single sample.

Another purpose of this study was to demonstrate the high sensitivity of ED for CE and the possibility of analyzing a wider range of analytes using derivatization chemistry. Curry *et al.* [3] have reported the high sensitivity obtainable using CE–ED for the determination of several electroactive neurotransmitters. Microdialysis sampling combined with CE–ED should prove to be a very powerful tool for future *in vivo* neurochemical studies.

## ACKNOWLEDGEMENTS

This work was supported by the Kansas Technology Enterprise Corporation. The authors thank Bioanalytical Systems for technical support. T.J.O'S. gratefully acknowledges an Eolas scholarship. The authors thank Nancy Harmony for help in the preparation of the manuscript.

## REFERENCES

- 1 T. J. O'Shea, R. D. Greenhagen, S. M. Lunte, C. E. Lunte, M. R. Smith, D. M. Radzik and N. J. Watanabe, *J. Chromatogr.*, 593 (1992) 305.
- 2 R. A. Wallingford and A. G. Ewing, *Anal. Chem.*, 61 (1989) 98.
- 3 P. D. Curry, C. E. Engstrom-Silverman and A. E. Ewing, *Electroanalysis*, 3 (1991) 587.
- 4 C. E. Lunte, D. O. Scott and P. T. Kissinger, *Anal. Chem.*, 63 (1991) 773A.
- 5 T. E. Robinson and J. B. Justice (Editors), *Microdialysis in the Neurosciences*, Elsevier, Amsterdam, 1992.
- 6 P. deMontigny, J. F. Stobaugh, R. S. Givens, R. G. Carlson, K. Srinivasachar, L. A. Sternson and T. Higuchi, *Anal. Chem.*, 59 (1987) 1096.
- 7 S. M. Lunte, T. Mohabbat, O. S. Wong and T. Kuwana, *Anal. Biochem.*, 178 (1989) 202.
- 8 M. D. Oates and J. W. Jorgenson, *Anal. Chem.*, 61 (1989) 432.
- 9 P. L. Weber, Center for Bioanalytical Research, University of Kansas, Lawrence, KS, unpublished results.
- 10 G. Gaxinos and C. Watson, *The Rat Brain in Stereotaxic Coordinates*, Academic Press, New York, 1982.

- 11 F. G. Gonon, C. M. Fombarlet, M. J. Buda and J.-F. Pujol, *Anal. Chem.*, 53 (1981) 1386.
- 12 T. J. O'Shea, A. Costa Garcia, P. Tunon Blanco and M. R. Smyth, *J. Electroanal. Chem.*, 307 (1991) 63.
- 13 T. J. O'Shea, M. R. Smith, M. Telting-Diaz, S. M. Lunte and C. E. Lunte, *Electroanalysis*, 4 (1992) 463.
- 14 M. Nussbaum, J. E. Przedwiecki, D. U. Staerk, S. M. Lunte and C. M. Riley, *Anal. Chem.*, in press.
- 15 S. M. Lunte and O. S. Wong, *Curr. Sep.*, 10 (1990) 19.
- 16 D. A. Roston and P. T. Kissinger, *Anal. Chem.*, 53 (1981) 1695.
- 17 D. A. Roston, R. E. Shoup and P. T. Kissinger, *Anal. Chem.*, 54 (1982) 1417A.
- 18 C. E. Lunte and P. T. Kissinger, *Anal. Chem.*, 55 (1983) 1458.
- 19 U. Tossmann, G. Jonsson and U. Ungerstedt, *Acta Physiol. Scand.*, 127 (1986) 533.
- 20 U. Tossman, J. Segovia and U. Ungerstedt, *Acta Physiol. Scand.*, 127 (1986) 547.
- 21 M. D. Oates and J. W. Jorgenson, *Anal. Chem.*, 62 (1990) 1577.



# Effect of buffer constituents on the determination of therapeutic proteins by capillary electrophoresis

Norberto A. Guzman, John Moschera, Khurshid Iqbal and A. Waseem Malick

*Pharmaceutical Research and Development, Hoffmann-La Roche, Nutley, NJ 07110 (USA)*

---

## ABSTRACT

Capillary electrophoresis has proved to be a versatile method for the determination of proteins, peptides and amino acids in pharmaceutical formulations. For quantification of the capillary electrophoresis data, however, significant errors may result if the analysis is performed using improper separation conditions. The peak area response for protein analytes, which is generally low in conventional UV detection, may also vary dramatically depending on the nature of the buffer used in the separation. This paper describes the effects of various buffer constituents and analytical conditions on the capillary electrophoretic separation and quantification of a humanized monoclonal antibody in bulk form and in a typical therapeutic formulation. For optimum peak area response and reproducibility, protein derivatization with an appropriate chromophore (*e.g.*, fluorescamine) and separation in the presence of a moderate ionic strength buffer containing lithium chloride, tetramethylammonium chloride or trimethylammonium propylsulfonate is recommended. General guidelines for the determination of proteins by capillary electrophoresis and a rationale for the use of internal standards to improve the quantification of data are also discussed.

---

## INTRODUCTION

Capillary electrophoresis (CE) is an analytical technique capable of yielding remarkable information in a variety of applications, especially in the analysis of proteins and peptides [1–5]. Nevertheless, the technique, in general, has not yet achieved the same degree of acceptance as more conventional procedures, such as high-performance liquid chromatography and conventional gel electrophoresis. This is partly due to the fact that despite the enormous resolving power of CE, quantification of data has encountered numerous problems (especially in the separation of protein macromolecules). These include the potential adsorption of the protein analyte to the capillary walls (which often gives rise to band broadening and low recovery of the separated protein analyte), and the necessity to optimize the

running conditions to maximize the yield and degree of separation.

Numerous efforts have been made to separate proteins by free-solution CE. Some of these separation optimization methods include coating of the capillary surface, changing the pH of the separation buffer and the addition of additives to the separation buffer [6–23]. However, most efforts have been directed to improving the separation profile and very little attention has been placed on the quantitative aspects of the separation.

In a previous paper [24], we demonstrated the importance of temperature in the separation and determination of protein drug substances present in a solution mixture. As little as a 5°C variation in temperature was found to have a critical effect on the separation profile and stability of the drug substance (recombinant interleukin-1 $\alpha$ ). In turn, the quantitative profile was also affected by chemical changes produced in the protein (*i.e.*, deamidation).

In this work, we have tried to develop a better understanding of how chemical factors, such as the presence of certain salts or zwitterions in the run-

---

*Correspondence to:* Dr. N. A. Guzman, The R. W. Johnson Pharmaceutical Research Institute, OPC Administration Building 3021, Route 202, P.O. Box 300, Raritan, NJ 08869, USA (present address).

ning buffer, influence the performance of CE in the determination of a protein drug substance. We have selected the humanized monoclonal antibody<sup>a</sup> anti-TAC [25] as a model protein and have developed the conditions for CE analysis by approaches similar to those previously described for proteins not specifically targeted for therapeutic use [12–14]. In addition, internal standards were used in the CE separation of the monoclonal antibody to monitor changes affecting the quantitative profile. In order to enhance the detection sensitivity, and also to improve analyte resolution, samples were derivatized with the chromophore fluorescamine prior to CE analysis. The proposed reaction scheme of fluorescamine with primary and secondary amines has been discussed previously [26,27] and is shown in Fig. 1.

## EXPERIMENTAL

### Reagents and samples

All chemicals were obtained at the highest purity available from the manufacturer, and were used without additional purification. Sodium hydroxide, sodium tetraborate ( $\text{Na}_2\text{B}_4\text{O}_7 \cdot 10\text{H}_2\text{O}$ ), lithium chloride, N-acetyltryptophan and fluorescamine were purchased from Sigma (St. Louis, MO, USA), tetramethylammonium chloride and L-arginine from Fluka (Ronkonkoma, NY, USA), trimethylammonium propylsulfonate from Waters–Millipore (Milford, MA, USA), acetone (HPLC grade), pyridine (Fisher Certified) and hydrochloric acid solution (12 M) from Fisher Scientific (Fair Lawn, NJ, USA), and purified bulk drug substance (humanized anti-TAC monoclonal antibody) from Hoffmann-La Roche (Nutley, NJ, USA). Reagent solutions and buffers were prepared using triply distilled, deionized water, and routinely degassed and sonicated under vacuum after filtration.

Millex disposable filter units (0.22  $\mu\text{m}$ ) were purchased from Millipore (Bedford, MA, USA) and fused-silica capillary columns from Scientific Glass

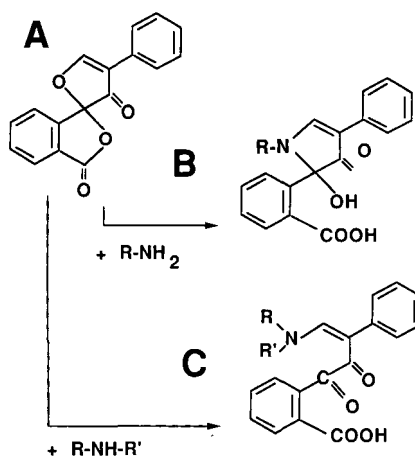


Fig. 1. Schematic representation of the molecular structure of (A) fluorescamine, (B) the derivatized reaction product involving a reacting primary amine functional group-containing analyte and (C) the derivatized reaction product involving a reacting secondary amine functional group-containing analyte.

Engineering (Austin, TX, USA) and Polymicro Technologies (Phoenix, AZ, USA).

### Instrumentation

A commercially available CE instrument (P/ACE System 2000, Beckman Instruments, Palo Alto, CA, USA) was used. The instrument, containing Beckman system software, was controlled by an IBM PS/2 Model 50-Z computer. Samples were stored in a microapplication vessel assembly, consisting of a 150- $\mu\text{l}$  conical microvial inserted into a standard 4-ml glass reservoir and held in position for injection by an adjustable spring. In order to minimize evaporation of the sample volume (100  $\mu\text{l}$ ), about 1–2 ml of cool water was added to the microapplication vessel housing the microvial. The external water serves as a cooling bath for the sample in the microvial and as a source of humidity to prevent sample evaporation and concentration. After insertion of the microvial, the microapplication vessel assembly was covered with a rubber injection septum and placed in the sample compartment of the CE instrument. Samples were injected by pressure and the data acquisition and analysis were carried out using System Gold chromatography software (Beckman Instruments, San Ramon, CA, USA). Data integration was also carried out with a Model D-2500

<sup>a</sup> Humanized monoclonal antibody anti-TAC is an IgG-class genetically engineered hybrid antibody, containing approximately 90% human sequence and 10% murine sequence. The antibody is directed against, and is specifically recognized by, the human receptor for interleukin-2, which is a well characterized lymphokine involved in the complex network of cellular communications [25].

Chromato-integrator (Hitachi Instruments, Danbury, CT, USA)

#### Sample preparation

Stock solutions were individually prepared by dissolving L-arginine (50 mg/ml) and N-acetyltryptophan (1 mg/ml) in 0.1 M sodium tetraborate buffer (pH 9.0). Purified bulk drug anti-TAC (6.7 mg/ml) was prepared in phosphate buffer (pH 7.0) and a typical liquid formulation dosage of anti-TAC (6.0 mg/ml) was prepared in the same buffer. Concentrated solutions were diluted to their specified working strengths with the same sodium tetraborate buffer.

#### Sample derivatization

For CE analysis without fluorescamine derivatization, assay samples were diluted to the desired concentrations with sample dilution buffer [0.1 M sodium tetraborate buffer (pH 9.0)] to a total reaction mixture of 100  $\mu$ l, and directly transferred into the conical vial and then inserted in the microapplication vessel assembly on the CE instrument.

For CE analysis of fluorescamine derivatives, solutions of the respective analyte samples (*i.e.*, humanized anti-TAC monoclonal antibody concentration ranging from 33.5 to 335  $\mu$ g or from 0.22 to 2.23 pmol per 100  $\mu$ l of reaction mixture) were transferred into a 500- $\mu$ l microcentrifuge tube and their total volume was adjusted to 70  $\mu$ l by addition of sample dilution buffer. Derivatization was performed by the addition of 30  $\mu$ l of fluorescamine solution (3 mg/ml of fluorescamine in acetone containing 20  $\mu$ l of pyridine) to the sample while continuously and vigorously vortex mixing. After *ca.* 2 min, the contents of the microcentrifuge were transferred into the conical microvial and then inserted in the microapplication vessel assembly for analysis.

#### Operating conditions

Sample solutions for analysis in microapplication vessels were placed in the sample holder of the analyzer. The analysis program was initiated and the first sample automatically injected into the capillary by a positive nitrogen pressure of 0.5 p.s.i. (3500 Pa) for 5 s. At the completion of each run, the capillary column was sequentially washed by injection of 2.0 M sodium hydroxide solution, 0.1 M sodium hy-

droxide solution and distilled, deionized water, and then regenerated with running buffer.

The CE separations reported were performed using four different buffers: (1) 0.05 M sodium tetraborate buffer (pH 8.3) containing 0.025 M lithium chloride; (2) 0.05 M sodium tetraborate buffer (pH 8.3) containing 0.025 M tetramethylammonium chloride; (3) 0.05 M sodium tetraborate buffer (pH 8.3) containing 0.025 M trimethylammonium propylsulfonate; and (4) 0.05 M sodium tetraborate buffer (pH 8.3) containing 0.50 M trimethylammonium propylsulfonate. The CE instrument was equipped with a 70 cm (63 cm to the detector)  $\times$  75  $\mu$ m I.D. capillary column. The CE separation was performed at 29 kV. The capillary temperature for all experiments was maintained at 25°C during the run. Under these conditions, *ca.* 30 nl (6 nl/s) were injected into the capillary column [28]. Monitoring of the analytes was performed at 214 nm.

#### RESULTS

Fig. 2 depicts the electropherograms of underivatized and derivatized humanized anti-TAC monoclonal antibody. The therapeutic antibody was analyzed in the presence of the commonly used parenteral excipients L-arginine and N-acetyltryptophan. As shown in Fig. 2A, the underivatized analytes were well separated from each other. L-Arginine (peak 1) migrated very fast, followed by anti-TAC (peak 2) and N-acetyltryptophan (peak 3). The fluorescamine-derivatized analytes (Fig. 2B), L-arginine (peak 2), N-acetyltryptophan (peak 4) and anti-TAC (peak 5), were also separated well from each other and from the peaks corresponding to the constituents of the derivatization reagent, fluorescamine (peak 6) and the organic solvents acetone and pyridine (comigrating at peak 1). Derivatization with fluorescamine was observed to have a marked effect on analyte mobility and peak area in CE analysis. As shown in Fig. 2B and Table I, derivatized L-arginine and anti-TAC migrated slower than their underivatized counterparts. For N-acetyltryptophan, however, the mobility and peak area were unchanged after fluorescamine derivatization. This suggests that the potentially reactive amine group was blocked, possibly by steric hindrance, and was unable to react with the reagent.

The linearity of the anti-TAC peak area as a

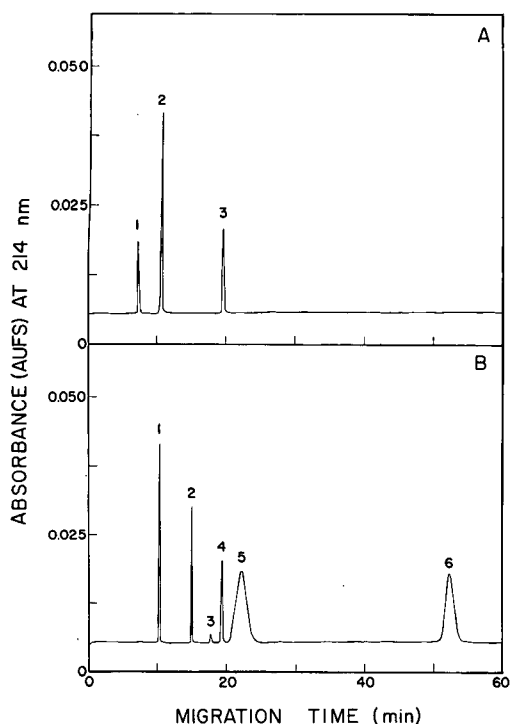


Fig. 2. Capillary electrophoresis profile of underivatized and fluorescamine-derivatized analytes. (A) Electropherogram of underivatized L-arginine (peak 1), anti-TAC (peak 2) and N-acetyltryptophan (peak 3). (B) Electropherogram of fluorescamine-derivatized analytes. Peaks: 1, acetone; 2, L-arginine; 3, unknown; 4, N-acetyltryptophan; 5, anti-TAC; 6, fluorescamine reagent. The separation buffer was 0.05 M sodium tetraborate buffer (pH 8.3) containing 0.025 M LiCl. The concentrations of analytes, per 100  $\mu$ l of reaction mixture, used in this experiment were as follows: (1) underivatized analytes, L-arginine 1000  $\mu$ g (5.74 nmol), bulk anti-TAC monoclonal antibody 201  $\mu$ g (1.34 pmol) and N-acetyltryptophan 10  $\mu$ g (40.6 pmol); (2) derivatized analytes, L-arginine 10  $\mu$ g (57.0 pmol), bulk anti-TAC monoclonal antibody 201  $\mu$ g (1.34 pmol) and N-acetyltryptophan 10  $\mu$ g (40.6 pmol).

TABLE I

EFFECT OF FLUORESCAMINE ON THE MIGRATION TIME AND PEAK AREA OF HUMANIZED ANTI-TAC MONOCLONAL ANTIBODY AND INTERNAL STANDARDS

For this experiment, the data were obtained by using the following concentrations of the various analytes (in 100  $\mu$ l of reaction mixture): (1) native (underivatized), L-arginine 20  $\mu$ l (50 mg/ml); bulk anti-TAC 30  $\mu$ l (6.7 mg/ml), N-acetyltryptophan 10  $\mu$ l (1 mg/ml); (2) fluorescamine-derivatized analytes, L-arginine 10  $\mu$ l (1 mg/ml), bulk anti-TAC 30  $\mu$ l (6.7 mg/ml), N-acetyltryptophan 10  $\mu$ l (1 mg/ml). Values obtained for derivatized samples were corrected for the same concentration of values obtained for underivatized samples. The separation buffer was 0.05 M sodium tetraborate buffer (pH 8.3) containing 0.025 M LiCl.

Sample	Migration time (min)		Peak area (arbitrary units)	
	Native	Derivatized	Native	Derivatized
L-Arginine	7.48	15.09	1 184 351	106 059 100
Anti-TAC	10.93	23.37	3 192 314	7 041 242
N-Acetyltryptophan	19.58	19.51	1 548 623	1 518 171

function of concentration was investigated with and without fluorescamine derivatization. The reaction was carried out in the presence of fixed concentrations of internal standards and increasing concentrations of anti-TAC. As shown in Fig. 3, the peak area for the derivatized anti-TAC monoclonal antibody increased linearly with increasing concentration over the range 0.22–2.23 pmol per 100  $\mu$ l of reaction mixture. The response curve was slightly sigmoidal in shape. For underivatized anti-TAC, the peak area also increased linearly with increasing concentration up to about 1.79 pmol per 100  $\mu$ l of reaction mixture, but then reached a response plateau above which no further increase was observed. The plateau in the peak area suggests that the solubility of the underivatized anti-TAC is decreased in the running buffer, possibly owing to the presence of LiCl, and at concentrations above 1.79 pmol per 100  $\mu$ l of reaction mixture (2.68 mg/ml) the analyte may be precipitating from solution.

The effects of the running buffer additives tetramethylammonium chloride (TMAC), trimethylammonium propylsulfonate (TMAPS) and lithium chloride (LiCl) on the separation and quantification of the anti-TAC monoclonal antibody were investigated. The molecular structures of TMAC and TMAPS are shown in Fig. 4. TMAC, a quaternary salt, has been demonstrated to be an effective agent in preventing adsorption of macromolecules to glass [29,30]. Similarly, TMAPS, a zwitterion, has been used to prevent the binding of proteins to fused-silica capillary columns [31]. Neutral salts, e.g., LiCl, have also been found to stabilize tertiary structures of some proteins in solution [30,32]. As shown in Table II, TMAC, TMAPS and LiCl were

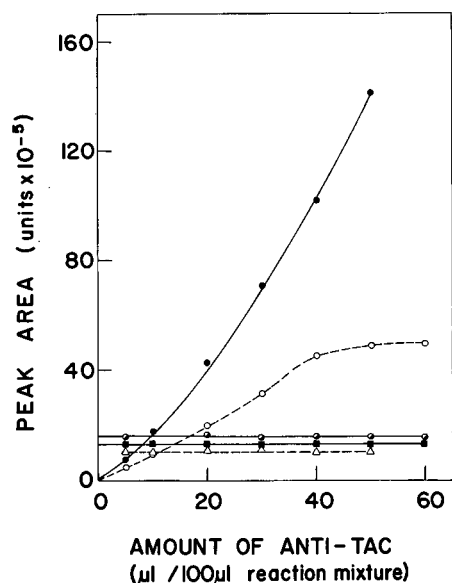
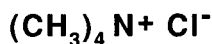
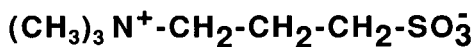


Fig. 3. Calibration graph for anti-TAC monoclonal antibody. The reaction was carried out in the presence of fixed concentrations of internal standards and increasing concentrations of bulk anti-TAC. Typical response curves of (○) native (underivatized) anti-TAC monoclonal antibody, (●) fluorescamine-derivatized anti-TAC, (●) derivatized and underivatized N-acetyltryptophan, (■) underivatized L-arginine and (△) derivatized L-arginine. The concentrations of analytes used, per 100  $\mu\text{l}$  of reaction mixture, were as in Fig. 2.

each found to have an effect on the separation and quantification of the anti-TAC monoclonal antibody. Under conditions of constant voltage (29 kV), constant temperature (25°C) and constant current (less than 2% drop from the starting current), excellent reproducibility was obtained for peak areas (Table II). The running buffer containing the addi-



TETRAMETHYLAMMONIUM CHLORIDE



TRIMETHYLAMMONIUM PROPYLSULFONATE

Fig. 4. Schematic representation of the molecular structures of tetramethylammonium chloride and trimethylammonium propylsulfonate.

tive TMAPS, however, seems to yield results with better reproducibility than buffers containing LiCl or TMAC. In addition, significantly less current was produced with the TMAPS buffer than with the buffers containing either of the salt additives. Apparently, the lower operating current with the TMAPS buffer results in the generation of less internal column heat and as a result a slightly higher degree of reproducibility.

As with the LiCl-containing buffer (Fig. 2), a linear response curve for the fluorescamine-derivatized anti-TAC as a function of concentration was observed with the TMAC and TMAPS buffer systems (Fig. 5). In contrast to the behavior with the LiCl-containing buffer, however, the underivatized analyte did not reach an absorption plateau at higher concentrations, further supporting the hypothesis that the LiCl is adversely affecting analyte solubility.

Optimization of the buffer constituent concentrations seems to be critical for the analysis of quantitative data. Anti-TAC was separated to completion when using 0.05 M sodium tetraborate (pH 8.3) (Fig. 6A), but the peak area was slightly lower than when using the same buffer in the presence of 0.025 M TMAPS (Fig. 6B). Further, if the concentration of TMAPS was increased to 0.5 M, all analytes migrated faster, to a point at which both resolution and quantification were poorer, e.g. when 1.0 M TMAPS was used as additive to the sodium tetraborate buffer (results not shown).

The presence of internal standards was useful in monitoring the performance of the CE system. Disturbances in the electroosmotic flow, which might result in changes in observed peak areas and lead to errors in quantification, would be reflected in changes in the internal standard controls.

An interesting observation was made with regard to the migration and detection of analytes in a mixture of substances. As shown in Fig. 6, the anti-TAC monoclonal antibody (peak 5) migrated much faster than the fluorescamine reagent (peak 6). Nevertheless, the width of the anti-TAC peak was much greater than that of the fluorescamine reagent. Hence, in addition to mobility, and the corresponding residence time in the optical path of the detector, analyte peak width must also be a function of other factors. With anti-TAC, for example, such factors might include capillary wall interaction, shape of the molecule and solubility.



TABLE II

## EFFECT OF BUFFER CONSTITUENTS ON THE DETERMINATION (PEAK AREA) OF FLUORESCAMINE-DERIVATIZED HUMANIZED ANTI-TAC MONOCLONAL ANTIBODY AND INTERNAL STANDARDS

The composition of the buffers was as follows: 0.05 M sodium tetraborate (pH 8.3), (A) containing no additives; (B) containing 0.025 M LiCl; (C) containing 0.025 M TMAC; and (D) containing 0.025 M TMAPS. For L-arginine and N-acetyltryptophan experiments, the mixture consisted of fixed concentrations of L-arginine (10  $\mu$ l of a 1 mg/ml solution) and N-acetyltryptophan (10  $\mu$ l of a 1 mg/ml solution) and increasing concentrations of bulk anti-TAC (5, 10, 20, 30, 40 and 50  $\mu$ l of a 6.7 mg/ml solution). For the anti-TAC experiment, a fixed concentration of all three analytes was used: anti-TAC (40  $\mu$ l of a 6.7 mg/ml solution), L-arginine (10  $\mu$ l of a 1 mg/ml solution) and N-acetyltryptophan (10  $\mu$ l of a 1 mg/ml solution). For the three experiments, sample volumes were adjusted to 70  $\mu$ l with 0.1 M sodium tetraborate buffer (pH 9.0) and then 30  $\mu$ l of fluorescamine reagent were added to the sample as described under Experimental.

Buffer	Parameter <sup>a</sup>	Anti-TAC	L-Arginine	N-Acetyltryptophan
A	<i>n</i>	6	6	6
	$\bar{x}$	10 854 734	1 026 934	1 491 201
	S.D.	398 723	25 865	38 976
	R.S.D. (%)	3.67	2.52	2.61
B	<i>n</i>	6	6	6
	$\bar{x}$	10 972 325	1 043 421	1 501 511
	S.D.	364 719	25 635	38 688
	R.S.D. (%)	3.32	2.46	2.58
C	<i>n</i>	6	6	6
	$\bar{x}$	13 324 256	1 218 024	1 585 017
	S.D.	362 654	28 001	31 820
	R.S.D. (%)	2.72	2.30	2.00
D	<i>n</i>	6	6	6
	$\bar{x}$	13 009 167	1 024 243	1 369 606
	S.D.	328 116	22 419	26 566
	R.S.D. (%)	2.52	2.19	1.94

<sup>a</sup>  $\bar{x}$  = Mean peak area (arbitrary units); S.D. = standard deviation; R.S.D. = relative standard deviation.

## DISCUSSION

Therapeutic monoclonal antibodies and recombinant proteins in general are gaining great importance in the new generation of drugs targeted for human and animal consumption [33]. The non-human origin of these materials, however, and the rigorous purification procedure to which they may be subjected, make proper quality control of the final product and the demonstration of an extremely high degree of purity essential. Many analytical techniques are routinely required for the monitoring of the purity and stability of antibodies. CE is growing continuously in the scope of its applications and holds the promise of becoming a routine method for the analysis of proteins. However, in order for any analytical technique to be useful, the results

obtained must be reproducible. For CE, reproducibility of separation (migration time) is commonly obtained with a relative standard deviation (R.S.D.) of less than 1% for most tested substances. Nevertheless, quantification of the analytes (peak area) varies, for macromolecules such as proteins, from 1 to 5% (R.S.D.).

As therapeutic monoclonal antibodies are routinely produced by methods involving extensive purification schemes, many factors must be evaluated in order to guarantee a product of consistent quality. These laboratory-made proteins are designed to be similar to, if not identical with, their endogenous counterparts. Therefore, not only must the protein be chemically pure, it must also maintain a structural integrity, *i.e.*, conformation necessary for biological activity and the maintenance of the native state.

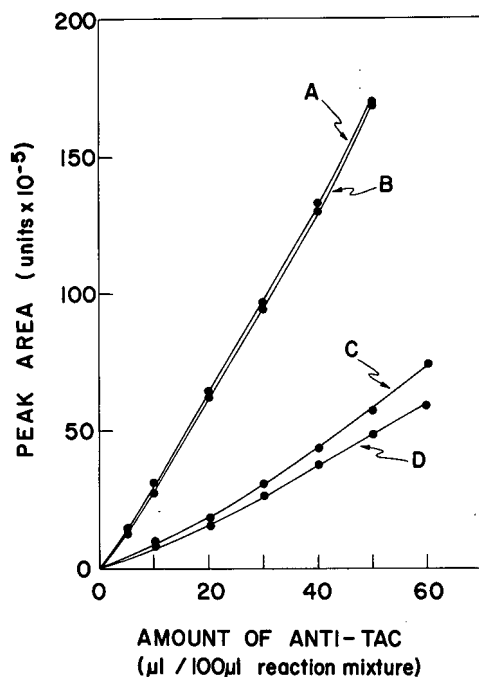


Fig. 5. Comparative calibration graphs for anti-TAC monoclonal antibody using 0.05 M sodium tetraborate (pH 8.3) as the separation buffer containing either TMAC or TMAPS. The reaction was carried out in the presence of fixed concentrations of internal standards and increasing concentrations of bulk anti-TAC solution. Typical response curves of (A) fluorescamine-derivatized anti-TAC in the presence of 0.025 M TMAC; (B) fluorescamine-derivatized anti-TAC in the presence of TMAPS; (C) native (underivatized) anti-TAC in the presence of TMAC; and (D) underivatized anti-TAC in the presence of TMAPS.

The proper interpretation of data necessitates that precautions be taken in designing the technical aspects of the analysis. CE has many operational factors that must be considered in order to obtain consistent reproducibility values for migration time and peak area. At  $\text{pH} > 3.0$ , the surface of the fused-silica capillary column is negatively charged and proteins with a strong positive charge (basic proteins) have a greater tendency to adhere to the walls of the capillary column. As a consequence, separation and recovery are poor and often the adsorption is irreversible.

The experiments described here demonstrate the importance of blocking the negative charges in order to improve separation and quantification. Lithium chloride, tetramethylammonium chloride and trimethylammonium propylsulfonate as running

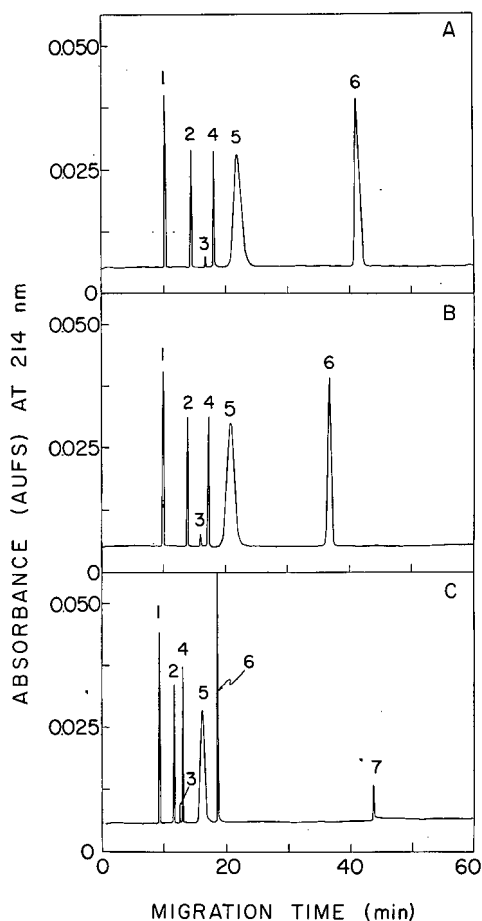


Fig. 6. Capillary electrophoresis profile of fluorescamine-derivatized anti-TAC separated under three different buffer conditions: (A) 0.05 M sodium tetraborate buffer, (pH 8.3); (B) 0.05 M sodium tetraborate buffer (pH 8.3) containing 0.025 M TMAPS; and (C) 0.05 M sodium tetraborate buffer (pH 8.3) containing 0.5 M TMAPS. The humanized anti-TAC monoclonal antibody used in this experiment was present in a simple liquid formulation dosage form at a concentration of 40  $\mu\text{l}$  (240  $\mu\text{g}$  or 1.60 pmol) per 100  $\mu\text{l}$  of reaction mixture, containing 0.2 mg/ml of Tween-80. Peaks as in Fig. 2, except that peak 7 represents an unknown substance.

buffer constituents proved to be effective substances, when used in combination with moderate ionic strength buffers, for preventing adsorption of the monoclonal antibody to the capillary wall.

Apparently, both hydrophobic and electrostatic forces are involved in the adsorption of proteins to glass surfaces. There is a significant coulombic attraction of positively charged regions of the protein to the capillary surface. Some proteins have more

affinity to silicic acid groups than others because of the nature and structural conformation of the molecule. The protein-adsorption blocking power of some buffer constituents (e.g., tetraalkylamines) can be attributed to their dual character as hydrophobic electrolytes as the molecules have both apolar and polar properties. Zwitterions, having both a positive and a negative charge in the molecule, can also compete for the groups which attract proteins to their surfaces and, in turn, prevent adsorption of the proteins to the capillary walls. Adsorption is only one of the factors that may affect the quantitative precision and accuracy of open-tubular free-resolution CE [34]. It is possible that alternative approaches, such as the use of gel-filled capillaries, will minimize some sources of CE variability (e.g., diffusion) that may lead to quantification errors. Many practical problems, however, remain to be solved.

## CONCLUSIONS

Resolution, recovery and reproducibility for proteins separated by CE are strongly compromised when adsorption of proteins to fused-silica capillaries occurs. Addition of alkylamines and/or zwitterions improves the performance of separation and enhances the efficiency, resolution and reproducibility for protein analytes. In addition, the formation of fluorescamine derivatives significantly affects the separation and enhances the sensitivity for therapeutic proteins.

## REFERENCES

- 1 B. L. Karger, A. S. Cohen and A. Guttman, *J. Chromatogr.*, 492 (1989) 585–614.
- 2 N. A. Guzman, L. Hernandez and S. Terabe, in Cs. Horváth and J. Nikelly (Editors), *Analytical Biotechnology — Capillary Electrophoresis and Chromatography (ACS Symposium Series, No. 434)*, American Chemical Society, Washington, DC, 1990, Ch. 1, pp. 1–35.
- 3 R. A. Wallingford and A. G. Ewing, *Adv. Chromatogr.*, 29 (1990) 1–76.
- 4 M. Novotny, K. A. Cobb and J. Liu, *Electrophoresis*, 11 (1990) 735–749.
- 5 Z. Deyl and R. Struzinsky, *J. Chromatogr.*, 569 (1991) 63–122.
- 6 J. W. Jorgenson, *Trends Anal. Chem.*, 3 (1984) 51–54.
- 7 S. Hjertén, *J. Chromatogr.*, 347 (1985) 191–198.
- 8 H. H. Lauer and D. McManigill, *Anal. Chem.*, 58 (1986) 166–170.
- 9 R. M. McCormick, *Anal. Chem.*, 60 (1988) 2322–2328.
- 10 G. J. M. Bruin, J. P. Chang, R. M. Kuhlman, K. Zegers, J. C. Kraak and H. Poppe, *J. Chromatogr.*, 471 (1989) 429–436.
- 11 G. J. M. Bruin, R. Huisden, J. C. Kraak and H. Poppe, *J. Chromatogr.*, 480 (1989) 339–349.
- 12 J. S. Green and J. W. Jorgenson, *J. Chromatogr.*, 478 (1989) 63–71.
- 13 M. M. Bushey and J. W. Jorgenson, *J. Chromatogr.*, 480 (1989) 301–310.
- 14 Y. Walbroehl and J. W. Jorgenson, *J. Microcol. Sep.*, 1 (1989) 41–45.
- 15 S. A. Swedberg, *Anal. Biochem.*, 185 (1990) 51–56.
- 16 J. K. Towns and F. E. Regnier, *J. Chromatogr.*, 516 (1990) 69–78.
- 17 K. A. Cobb, V. Dolnick and M. Novotny, *Anal. Chem.*, 62 (1990) 2478–2483.
- 18 J. E. Wiktorowicz and J. C. Colburn, *Electrophoresis*, 11 (1990) 769–773.
- 19 W. Nashabeh and Z. El Rassi, *J. Chromatogr.*, 559 (1991) 367–383.
- 20 J. R. Florance, Z. D. Konteatis, M. J. Macielag, R. A. Lessor and A. Galdes, *J. Chromatogr.*, 559 (1991) 391–399.
- 21 R. L. Cunico, V. Gruhn, L. Kresin, D. E. Nitecki and J. E. Wiktorowicz, *J. Chromatogr.*, 559 (1991) 467–477.
- 22 I. Z. Atamma, H. J. Issaq, G. M. Muschik and G. M. Janini, *J. Chromatogr.*, 588 (1991) 315–320.
- 23 N. A. Guzman, W. Q. Ascari, K. R. Cutroneo and R. J. Desnick, *J. Cell. Biochem.*, 48 (1992) 172–189.
- 24 N. A. Guzman, H. Ali, J. Moschera, K. Iqbal and A. W. Malick, *J. Chromatogr.*, 559 (1991) 307–315.
- 25 M. A. Costello, C. Woititz, J. De Feo, D. Stremlo, L.-F. L. Wen, D. J. Palling, K. Iqbal and N. A. Guzman, *J. Liq. Chromatogr.*, 15 (1992) 1081–1097.
- 26 N. A. Guzman, J. Moschera, K. Iqbal and A. W. Malick, *J. Liq. Chromatogr.*, 15 (1992) 1163–1177.
- 27 N. A. Guzman, J. Moschera, C. A. Bailey, K. Iqbal and A. W. Malick, *J. Chromatogr.*, 598 (1992) 123–131.
- 28 J. Harbaugh, M. Collette and H. E. Schwartz, *Beckman Instruments Technical Information Bulletin*, No. TIBC-103 (4SP-890-10B), 1990.
- 29 V. M. Papermaster and S. Baron, *Tex. Rep. Biol. Med.*, 41 (1981) 672–680.
- 30 K. C. Chadha and E. Sulkowski, *J. Interferon Res.*, 2 (1982) 229–234.
- 31 M. Merion, N. Astephen and J. Peterson, *3rd International Symposium on High Performance Capillary Electrophoresis, San Diego, CA, February 3–6, 1991*, abstract No. PT-25.
- 32 P. H. von Hippel and K.-Y. Wong, *Science*, 145 (1964) 577–580.
- 33 J. W. Larrick, *Pharmacol. Rev.*, 41 (1989) 539–557.
- 34 E. V. Dose and G. Guiochon, *Anal. Chem.*, 64 (1992) 123–128.

# Capillary electrophoretic determination of the protease Savinase in cultivation broth

Anders Vinther

*Receptor Chemistry, Novo Nordisk A/S, Novo Allé, DK-2880 Bagsvaerd (Denmark)*

Jørgen Petersen

*Department of Fermentation Physiology, Novo Nordisk A/S, Hagedornsvej 1, DK-2820 Gentofte (Denmark)*

Henrik Sørenberg

*Department of Chemical Engineering, Building 229, Technical University of Denmark, DK-2800 Lyngby (Denmark)*

---

## ABSTRACT

The highly basic washing enzyme Savinase and various analogues were analysed by micellar electrokinetic chromatography (MEKC) and electrophoresis. Broth samples were withdrawn during the cultivation of Savinase by recombinant microorganisms. Savinase peak areas obtained by MEKC–electrophoretic analysis were normalized with respect to migration time and compared with traditional enzyme activity measurements. The electropherograms indicated thermal degradation of the Savinase molecule at high field strengths. Baseline separation of Savinase and two analogues was achieved.

---

## INTRODUCTION

Analytical developments are essential in order to achieve a more detailed knowledge of each of the phases present during the production of a protein by recombinant microorganisms. This includes all the steps from the cultivation process via downstream processing to the final product. During the cultivation period, analysis should be performed at frequencies that make it possible to follow the time-varying concentrations of the protein product and key metabolites. For control purposes on-line measurements are preferred.

Whereas, *e.g.*, pH, temperature and  $pO_2$  are measured on-line on a routine basis, the concentrations of the protein product and key metabolites are most

often measured off-line with a time lag which makes concentration-based control impossible. In some instances the analytical results are obtained even days after the cultivation process has been finished.

During the last 2–4 years, capillary electrophoresis (CE) has evolved into a highly efficient separation technique for the analysis of, *e.g.*, peptides and proteins [1–5]. With its simple automated instrumentation and analysis times of the order of 5–15 min, CE is an obvious choice as a potential on-line technique for the analysis of species where changes are not too significant in that time range. Furthermore, sample preparation prior to analysis can normally be reduced to centrifugation and subsequent dilution of the cultivation broth. The dilution step is used to avoid reversed sample stacking conditions (which lead to excessive peak broadening [6,7]) when high ionic strength samples (often the case with cultivation broths) are analysed.

---

*Correspondence to:* Dr. A. Vinther, Receptor Chemistry, Novo Nordisk A/S, Novo Allé, DK-2880 Bagsvaerd, Denmark.

Generally, in CE the elution order of the analytes is manipulated by changing the running buffer composition rather than changing a column. As an example, one might determine the concentration of the protein product in one running buffer, flush the capillary with another buffer, introduce a new sample plug from the sample vial and then determine the concentration of various carboxylates and inorganic anions [8–10].

So far only a few groups have reported on the use of CE during the cultivation and downstream processing of recombinantly produced protein. Paulus and Gassmann [11] used CE to control the purity of recombinantly produced hirudin at different stages during the purification process. The full-length hirudin molecule (hirudin-65) was separated from two major degradation products, hirudin-64 and -63 (missing one and two amino acids at the C-terminus, respectively). Hurni and Miller [12] applied CE analysis to samples from each of the individual purification steps during the production of a recombinant hepatitis B vaccine expressed in *Saccharomyces cerevisiae*. Banke et al. [13] used a commercial CE instrument for the fraction collection of analyte bands in electropherograms of *Aspergillus* cultivation broth samples. The fractions were analysed for alkaline protease activity.

When cultivation broths are subjected to CE analysis, the electropherograms are “fingerprints” of the cultivation process at the specific time of sampling. Hence, in addition to being used to determine the actual concentrations of various identified species, the electropherograms might be used in neural nets for control purposes. In that way a knowledge-based correlation between the fingerprints and successful cultivations might be developed.

Savinase is a protease that is used as an ingredient of washing powder. It consists of 269 amino acid residues and the relative molecular mass is approximately 27 000. The isoelectric point is above 10.5 [14]. Here we report the CE analysis of cultivation broth during the production of Savinase by a recombinant *Bacillus* strain.

## EXPERIMENTAL

### Materials

Samples of Savinase cultivation broth and standards of Savinase and various analogues were ob-

tained from Novo Nordisk A/S (Gentofte, Denmark). Sodium dodecyl sulphate (SDS), disodium hydrogen- and sodium dihydrogenphosphate were purchased from Merck (Darmstadt, Germany), hydroxypropylmethylcellulose (HPMC) from Sigma (St. Louis, MO, USA) and 3-(cyclohexylamino)-1-propanesulphonic acid (CAPS) from Fluka (Buchs, Switzerland). The fused-silica capillaries were obtained from Polymicro Technologies (Phoenix, AZ, USA). The pH of all buffers was adjusted with either 1 M HCl or 1 M NaOH.

### Methods

All the CE experiments were performed on an Applied Biosystems ABI Model 270A CE instrument. The fused-silica capillaries were total length 45 cm × 50 μm I.D. × 192 μm O.D. The distance from the introduction end to the point of detection (effective length) was 25 cm. Sample was introduced by means of a 16.8-kPa vacuum at the detector end of the capillary. An air-bath thermostated the capillary at 30°C. The electropherograms were obtained by UV absorbance detection at 200 nm. Hence, the ordinate of the electropherograms shows the absorbance and the abscissa the analysis time in minutes. Sample preparation of the Savinase cultivation broth samples prior to CE analysis consisted of centrifugation and dilution with distilled water.

The traditional determination of Savinase in culture broth is based on the hydrolysis of dimethylcasein (DMC). The primary amino groups in the peptides formed in this process react with trinitrobenzenesulphonic acid (TNBS) to form a coloured complex, which is continuously detected in order to calculate the change in absorbance per unit time [15].

## RESULTS AND DISCUSSION

At neutral pH the surface of an uncoated fused-silica capillary is negatively charged. Hence, owing to its high isoelectric point, positively charged Savinase molecules adsorb on the capillary surface when CE analysis is performed in the free solution mode (FSCE) at neutral pH. One way to reduce the coulombic attraction between the Savinase molecules and the capillary surface is to titrate most of the negative surface charge off the capillary wall by lowering the buffer pH [5]. However, even in a 25

mM phosphate buffer of pH 1.6, tailing of the Savinase peak indicated adsorption on the capillary wall.

Another approach is to perform the analysis at a pH above the Savinase isoelectric point where it is net negatively charged. FSCE analysis was performed in a 100 mM CAPS buffer (pH 11.0). Concerning the sample solution, dilution of the cultivation broth with the running buffer was superior to dilution with distilled water or dilute acid with respect to resolution between the Savinase and neutral species peaks. A highly alkaline pH of the sample zone results in net negatively charged Savinase molecules migrating electrophoretically in the opposite direction of the detector and away from the neutral zone. In general, however, separation of the Savinase and neutral peaks was not satisfactory.

Addition of the anionic detergent SDS to the buffer at a sub-micellar concentration did not improve the separation.

The next approach was to perform the CE analysis in the micellar electrokinetic chromatographic (MEKC) mode [16,17]. In MEKC a detergent is added to the buffer at a concentration above its critical micellar concentration. Separation of the analytes is based on a combination of differences in electrophoretic mobilities (if the analytes are charged) and different degrees of partitioning with the charged detergent micelles. The detergent of choice was the anionic SDS. Addition of SDS improved the separation of the Savinase and neutral peaks. When a high concentration of anionic detergent molecules is added to the buffer at a pH below the protein isoelectric point, the negatively charged detergent molecule is attracted by the positively charged protein. Further, the hydrophobic tail of the detergent molecules can interact either with other detergent molecules or with the hydrophobic moieties of the protein. In this way the positively charged protein has acquired a net negative charge, thus no longer being attracted by the capillary wall. Hence, separations are based on MEKC in addition to electrophoresis. This means of dynamically coating the protein was performed at various pH values below the isoelectric point of Savinase. Figs. 1 and 2 are electropherograms of two Savinase cultivation broth samples obtained by MEKC–electrophoresis analysis in pH 7.2 (Fig. 1) and pH 9.5 (Fig. 2) SDS–phosphate buffers. Fur-

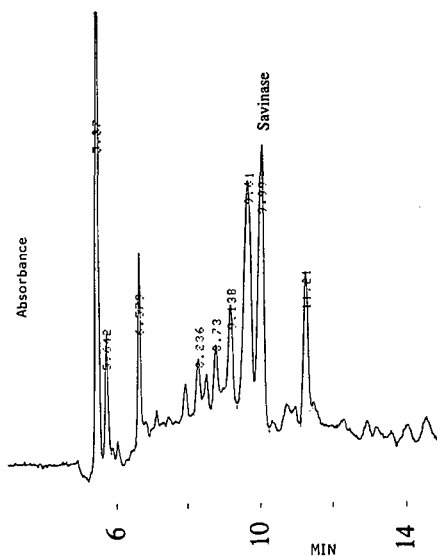


Fig. 1. MEKC–electrophoresis of Savinase cultivation broth sample I. The pH 7.2 running buffer consisted of 25 mM phosphate and 50 mM SDS. 9 kV was applied during analysis.

ther resolution was not achieved by addition of the viscosity-increasing hydroxypropylmethylcellulose (HPMC) at a 0.05% concentration.

Covalently coated capillaries have recently become commercially available. In these capillaries the electroosmotic flow is eliminated, thus greatly reducing coulombic interactions between the ana-

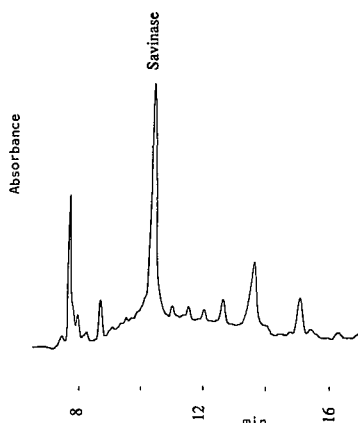


Fig. 2. MEKC–electrophoresis analysis of Savinase cultivation broth sample II. The pH 9.5 running buffer consisted of 30 mM phosphate and 50 mM SDS. 6 kV was applied during analysis.

lytes and the capillary surface. No attempts were made, however, to perform the analysis in the FSCE mode at neutral pH either in covalently or dynamically [5] coated capillaries.

### *Thermal degradation of Savinase at high field strengths*

Fig. 3a–e show electropherograms of one Savinase cultivation broth sample obtained at 3, 9, 15,

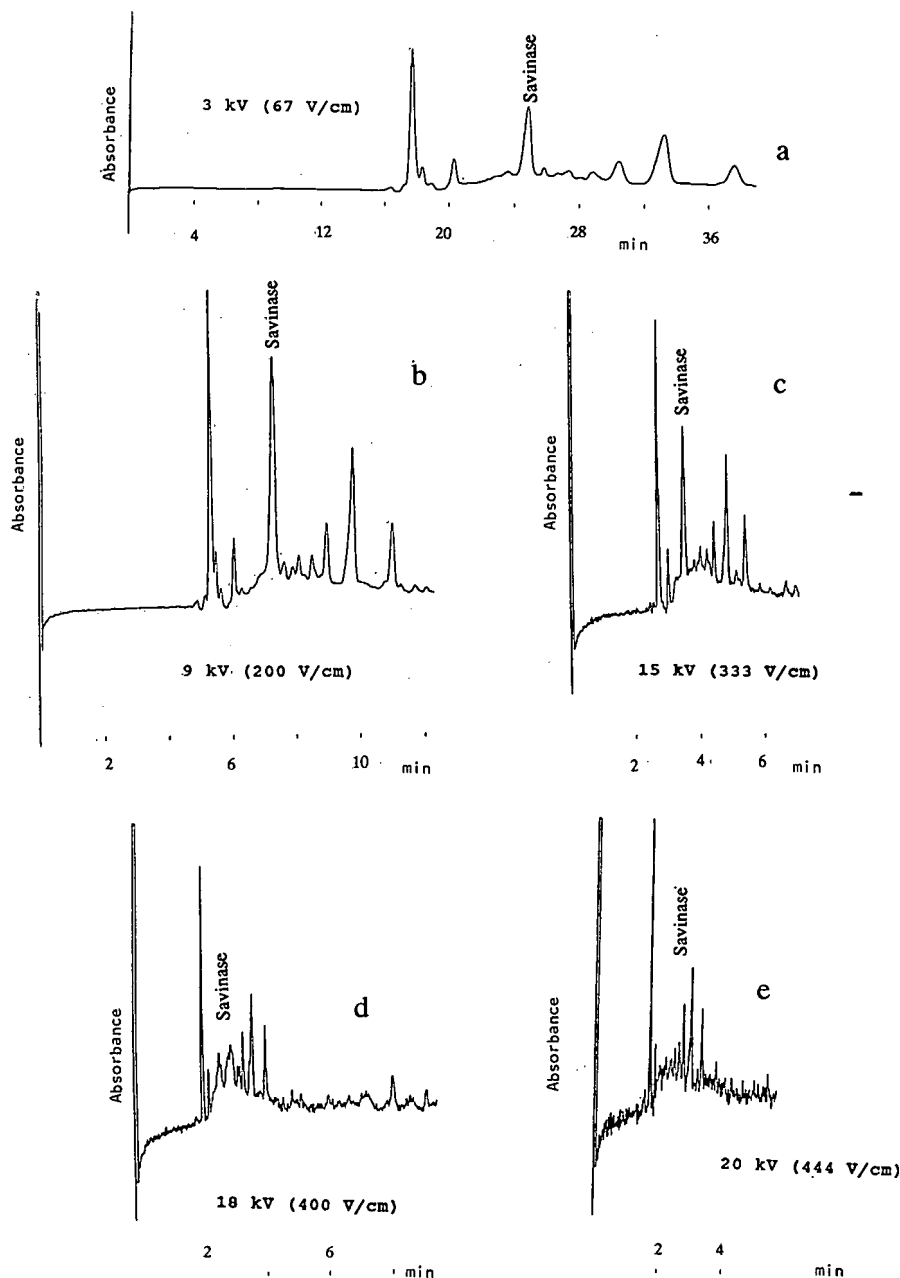


Fig. 3. Thermal degradation of Savinase at high field strengths. At high applied voltages the electropherograms indicate thermal degradation of the Savinase molecules during CE analysis. Applied potential: (a) 3; (b) 9; (c) 15; (d) 18; (e) 20 kV. The pH 9.5 running buffer consisted of 30 mM phosphate and 50 mM SDS.

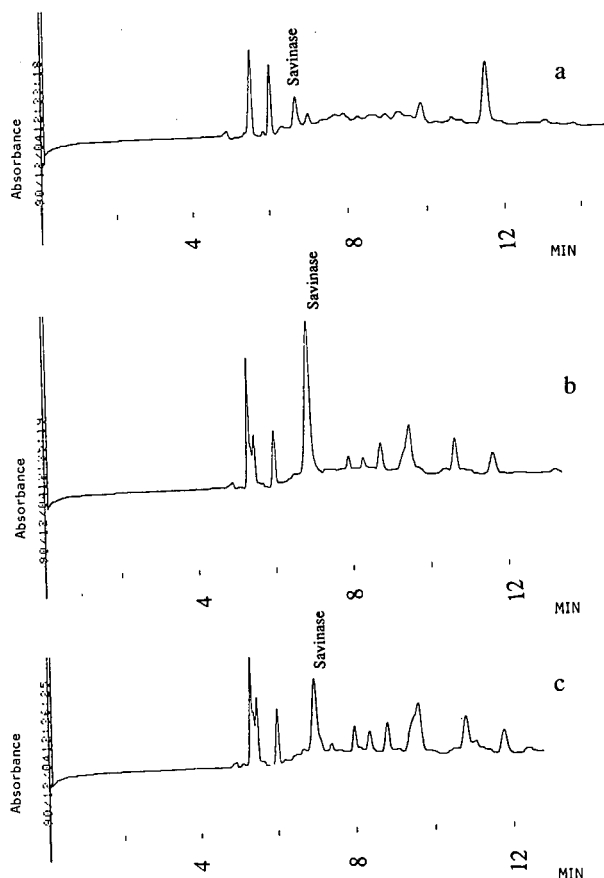


Fig. 4. MEKC-electrophoresis of Savinase cultivation broth. Relative cultivation time: (a) 7.5%; (b) 48%; (c) 100%. The pH 9.5 running buffer consisted of 30 mM phosphate and 50 mM SDS. 9 kV was applied during analysis.

18 and 20 kV, respectively, (field strength 65–450 V/cm). Stacking conditions prevailed [6,7]. The lower is the applied field strength, the larger are the peak areas owing to decreasing velocities of the analyte bands.

At potentials above 15 kV the electropherograms indicate degradation of the Savinase molecule during analysis. At 20 kV it is almost totally degraded owing to elevated temperatures in the capillary tube. At 20 kV the current was 94  $\mu$ A and the power induction *ca.* 4.2 W/m. The corresponding values at 18 kV were 79  $\mu$ A and 3.2 W/m. Conversion of the power values to temperature elevations of the running buffer by the use of the thermal model as described by Vinther and Sørensen [7] yielded temperatures of 50 and 45°C, respectively. As stacking conditions prevailed, the Savinase analyte zone reaches even higher temperatures while still in the originally introduced sample zone. Owing to the thermolability of Savinase, high applied voltages should therefore not be used in order to speed up analysis.

#### Savinase concentration vs. cultivation time

Cultivation broth was sampled six times during an extended Savinase cultivation and analysed by HPCE in the MEKC-electrophoresis mode at pH 9.5. Three of the electropherograms are shown as Fig. 4. Savinase elutes at *ca.* 7 min. In the initial phase of the cultivation period Savinase is being produced rapidly by the recombinant microorganisms. At later stages the Savinase peak area levels

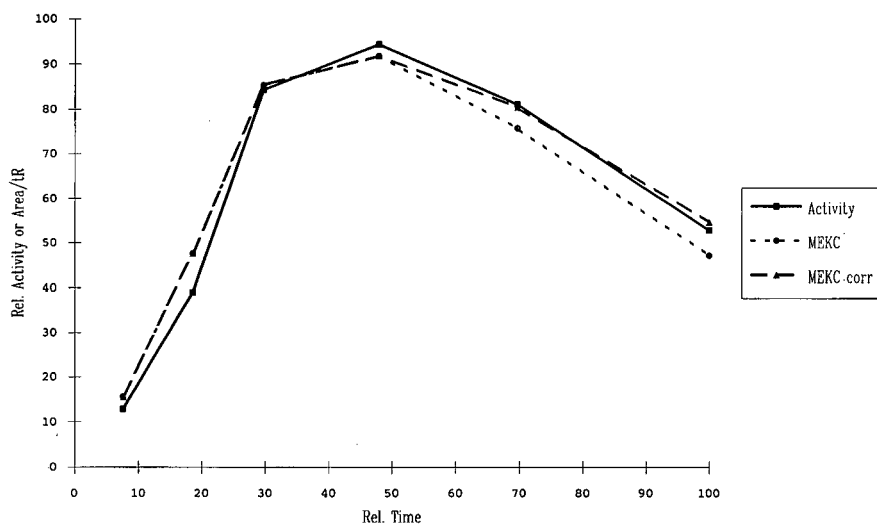


Fig. 5. Relative Savinase activity or peak area/migration time ( $t_R$ ) vs. the relative cultivation time. See text for details.



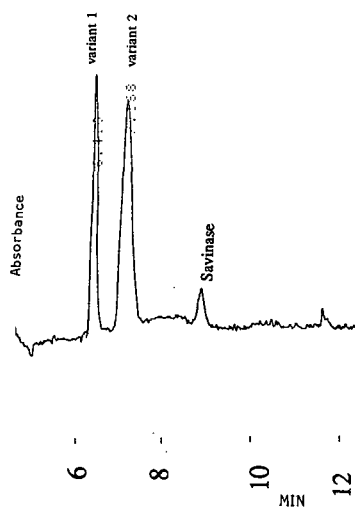


Fig. 6. Separation of Savinase and two of its variants by MEKC-electrophoresis using a 25 mM phosphate–50 mM SDS buffer pH 7.2. 8 kV was applied.

off and during the final part of the cultivation period the peak area even decreases. The reason for the decreasing peak area is probably autoproteolysis of Savinase.

The six broth samples were also analysed with respect to protease activity. Plots of relative enzyme activity and integrated Savinase peak areas (normalized with respect to migration time) are shown versus the relative cultivation period in Fig. 5. The Savinase peak areas were multiplied by an arbitrarily chosen constant in order to relate them to enzyme activity (at the time of analysis the Savinase standard was partly degraded). In the autoproteolysis part of the cultivation period two peaks ascended in the proximity of the Savinase peak, one on each side. If these peak areas are added to the Savinase peak area, the curve labelled MEKC corr curve in Fig. 5 is obtained; this curve agrees well with the enzyme activity curve. The integrated Savinase

peak areas therefore seem to be a simple and rapidly obtained measure of Savinase activity.

#### Separation of Savinase variants

A sample containing Savinase and two variants of Savinase were baseline separated by MEKC-electrophoresis at pH 7.2 (Fig. 6). Variant 2 = M222A + G195E, variant 1 = G195E + H120D + K235L + \*36D + N76D (amino acids numbering according to the sequence of BPN' [18]).

#### REFERENCES

- 1 B. L. Karger, A. S. Cohen and A. Guttman, *J. Chromatogr.*, 492 (1989) 585.
- 2 M. V. Novotny, K. A. Cobb and J. Liu, *Electrophoresis*, 11 (1990) 735.
- 3 P. D. Grossman, J. C. Colburn, H. H. Lauer, R. G. Nielsen, R. M. Riggan, G. S. Sittampalam and E. C. Rickard, *Anal. Chem.*, 61 (1989) 1186.
- 4 A. Vinther, H. Sørensen, H. H. Sørensen and A. M. Jespersen, *Talanta*, 38 (1991) 1369.
- 5 A. Vinther, S. E. Bjørn, H. H. Sørensen and H. Sørensen, *J. Chromatogr.*, 516 (1990) 175.
- 6 A. Vinther and H. Sørensen, *J. Chromatogr.*, 559 (1991) 3.
- 7 A. Vinther and H. Sørensen, *J. Chromatogr.*, 559 (1991) 27.
- 8 A. Vinther, N. Banke, J. Petersen and H. Sørensen, *J. Chromatogr.*, in preparation.
- 9 W. R. Jones and P. Jandik, *Int. Lab.*, May (1991) 61.
- 10 W. R. Jones and P. Jandik, *J. Chromatogr.*, 546 (1991) 445.
- 11 A. Paulus and E. Gassmann, *Beckman Applications Data*, DS-752, Beckman Instruments, Fullerton, CA, 1991.
- 12 W. H. Hurni and W. J. Miller, *J. Chromatogr.*, 559 (1991) 337.
- 13 N. Banke, K. Hansen and I. Diers, *J. Chromatogr.*, 559 (1991) 325.
- 14 C. Betzel, S. Klupsch, G. Papendorf, S. Hastrup, S. Branner and K. S. Wilson, *J. Mol. Biol.*, 223 (1992) 427.
- 15 *Analytical Method AF220/1-GB*, Novo Industri, Bagsvaerd, 1986.
- 16 S. Terabe, K. Otsuka, K. Ichikawa, A. Tsuchiya and T. Ando, *Anal. Chem.*, 56 (1984) 111.
- 17 S. Terabe, K. Otsuka and T. Ando, *Anal. Chem.*, 57 (1985) 834.
- 18 C. von der Osten, S. Branner, S. Hastrup, L. Hedegaard, M. D. Rasmussen, H. Bisgård-Frantzen, S. Carlsen and J. M. Mikkelsen, *J. Biotechnol.*, in press.

# Separation of phosphorylated histone H1 variants by high-performance capillary electrophoresis

Herbert Lindner, Wilfried Helliger, Arnold Dirschlmaier, Heribert Talasz, Martin Wurm and Bettina Sarg

*Institute of Medical Chemistry and Biochemistry, Fritz-Preglstrasse 3, A-6020 Innsbruck (Austria)*

Markus Jaquemar

*Beckman Instruments, A-3400 Klosterneuburg (Austria)*

Bernd Puschendorf

*Institute of Medical Chemistry and Biochemistry, Fritz-Preglstrasse 3, A-6020 Innsbruck (Austria)*

---

## ABSTRACT

High-performance capillary electrophoresis (HPCE) was used to separate successfully distinct phosphorylated derivatives of individual histone H1 variants. With an untreated capillary (50 cm × 75 μm I.D.) the electrophoresis was performed in about 15 min. Inconvenient interactions of these highly basic proteins with the capillary wall were eliminated by using 0.1 M sodium phosphate buffer (pH 2.0) containing 0.03% hydroxypropylmethylcellulose. Under these experimental conditions the histone H1 variants H1b and H1c obtained from mitotic enriched NIH 3T3 fibroblasts and isolated by reversed-phase high-performance liquid chromatography were clearly separated in their non-phosphorylated and different phosphorylated forms. This result was confirmed by acid-urea gel electrophoresis, comparison with non-phosphorylated histones H1b and H1c, isolated from quiescent NIH 3T3 cells, and incubation of multi-phosphorylated histone H1b with alkaline phosphatase and subsequent acid-urea and capillary electrophoresis. The results illustrate that the application of HPCE to the analysis of histone modifications provides a new alternative to traditional gel electrophoresis.

---

## INTRODUCTION

One of the most widely utilized electrophoretic methods for the study of histones and histone modifications has been polyacrylamide gel electrophoresis [1–4]. All methods of gel electrophoresis, however, have shortcomings, *e.g.*, the preparation and the staining and destaining of gels is labour intensive and time consuming. In addition, with low sample concentrations, specialized staining proce-

dures are often required. Finally, gel electrophoretic methods are unsatisfactory for precise quantification.

High-performance capillary electrophoresis (HPCE), combining the substantial advantages of conventional gel electrophoresis and high-performance liquid chromatography, was introduced by Jorgenson and Lukacs [5] and has opened up new prospects for the separation of biomolecules. In HPCE, compounds are resolved according to their ability to migrate in an electric field inside a fused-silica capillary. Nanolitre volumes or less of sample can be separated and, in contrast to common gel electrophoresis, rapid, quantitative, fully automat-

---

*Correspondence to:* Dr. H. Lindner, Institute of Medical Chemistry and Biochemistry, Fritz-Preglstrasse 3, A-6020 Innsbruck, Austria.

ed and highly efficient analyses can be achieved. Although HPCE is still in its infancy, we have previously shown the application of this technique to the separation of core histones and their acetylated modifications [6].

In this paper, we describe an efficient and rapid method for analysing phosphorylated histone H1 variants by HPCE using untreated fused-silica capillaries.

## EXPERIMENTAL

### Chemicals

Hydroxypropylmethylcellulose (HPMC) (4000 cP) and trifluoroacetic acid (TFA) were obtained from Sigma (Munich, Germany), ethylene glycol monomethyl ether (EGME) from Aldrich (Steinheim, Germany), Triton X-100, Tris and phenylmethanesulphonyl fluoride (PMSF) from Serva (Heidelberg, Germany) and colcemid, foetal calf serum (FCS), Dulbecco's minimum essential medium (DMEM), phosphate-buffered saline (PBS) and HAM's medium F12 from Boehringer (Mannheim, Germany). All other chemicals were purchased from Merck (Darmstadt, Germany).

### Cell line and culture conditions

Mouse NIH 3T3 fibroblasts were grown in monolayer cultures and cultivated in DMEM supplemented with 10% FCS, penicillin (60 µg/ml) and streptomycin (100 µg/ml) in the presence of 5% CO<sub>2</sub>. For synchronization, cells were seeded at a density of 4 · 10<sup>5</sup> cells per dish (48 cm<sup>2</sup>) and grown for 12 h in normal supplemented DMEM. The cells were then washed once with prewarmed PBS and then incubated in starvation medium (a 1:1 mixture of HAMs medium F12 and DMEM) supplemented with 0.1% FCS for 72 h to accumulate the cells in G0/G1 phase. To release the cells from the G0/G1 phase arrest, fresh medium supplemented with 10% FCS was added. After 18 h of stimulation, colcemid (0.06 µg/ml) was added to the cultures for 6 h, then the cells were harvested.

### Isolation of whole histones

G0/G1 phase- and colcemid-treated cells were washed twice with ice-cold PBS and incubated in ice-cold lysis buffer [0.05 M Tris-HCl (pH 7.5)–0.025 M KCl–0.01 M CaCl<sub>2</sub>–0.01 M MgCl<sub>2</sub>–0.25

M sucrose–0.01 M 2-mercaptoethanol–0.001 M phenylmethanesulphonyl fluoride–0.1% Triton X-100] for 5 min and were removed from the dish with a "rubber policeman". Nuclei were pelleted at 2500 g for 15 min at 4°C and washed with lysis buffer without Triton X-100. Whole histones were isolated from the resulting nuclear preparation by extraction with 0.2 M H<sub>2</sub>SO<sub>4</sub> at 4°C for 1 h. After centrifugation at 10 000 g in a microfuge for 20 min, the supernatant was mixed with five volumes of chilled acetone–HCl (98:2). After 12 h, the precipitated histones were centrifuged at 10 000 g for 20 min, washed twice with pure acetone, dissolved in water containing 0.01 M 2-mercaptoethanol and lyophilized.

### High-performance liquid chromatography

The equipment used consisted of two Model 114M pumps, a Model 421A system controller and a Model 165 variable-wavelength UV–VIS detector (Beckman Instruments, Palo Alto, CA, USA). The effluent was monitored at 210 nm and the peaks were recorded using Beckman System Gold software. The protein separations were performed on a column (125 mm × 8 mm I.D.) filled with Nucleosil 300-5 C<sub>4</sub> (Machery–Nagel, Düren, Germany). The lyophilized proteins were dissolved in water containing 0.1% of trifluoroacetic acid and samples of 100 µg of histones were injected on to the column. At a constant flow-rate of 1 ml/min the H1 histones were eluted within 35 min using a linear gradient from 41 to 61% B (solvent A = water containing 10% of EGME and 0.1% of TFA, solvent B = 10% EGME–70% acetonitrile–0.1% TFA).

### Polyacrylamide gel electrophoresis

Histone fractions from HPLC runs were collected, lyophilized and stored at –20°C. Histones H1 were analysed by SDS polyacrylamide gel electrophoresis (PAGE) (15% polyacrylamide, 0.1% SDS) as described by Laemmli [1], and by acid-urea (AU) PAGE (15% polyacrylamide, 0.9 M acetic acid, 2.5 M urea) according to Lennox *et al.* [4]. The gels were stained with 0.1% Serva Blue R in 40% ethanol–5% acetic acid and destained overnight in 20% ethanol–5% acetic acid.

### Incubation of histones H1 with alkaline phosphatase

To prevent the appearance of phosphorylated

bands in AU-PAGE and in HPCE, the isolated histones were incubated with alkaline phosphatase. About 100 µg of whole histones in 0.25 ml of 0.01 M Tris–HCl (pH 8.0) and 0.001 M phenylmethylsulphonyl fluoride were mixed with 210 µg of *Escherichia coli* alkaline phosphatase (60 units/mg; Sigma) for 12 h at 37°C according to Sherod *et al.* [7].

*Capillary electrophoresis*

HPCE was performed on a Beckman system P/ACE 2100 controlled by an AT386 computer. Data collection and post-run data analysis were carried out using P/ACE and System Gold software (Beckman Instruments). The capillary cartridge used was fitted with 75 µm I.D. fused silica of 58.8 cm total length (50 cm to the detector). Protein samples (concentration 0.5 mg/ml) were injected by pressure for 5 s and on-column detection was performed by measuring UV absorption at 200 nm. An untreated capillary was used in all experiments, but after every 5–10 injections the capillary was rinsed with water, 0.1 M NaOH, water, 0.5 M H<sub>2</sub>SO<sub>4</sub>, water and finally with the running buffer. Washing with each solvent was applied for 2 min. Runs were carried out in 0.1 M phosphate buffer (pH 2.0) containing 0.03% HPMC at constant voltage (16 kV) and a capillary temperature of 20°C.

RESULTS AND DISCUSSION

The utility of HPCE for the separation of small molecules has been demonstrated [8–10]. However, the application of this new technique to the analysis of proteins can be problematic as they often tend to interact with the negatively charged silanol groups of the capillary wall. These interactions result in band broadening and tailing with significantly reduced separation efficiency and a non-linear relationship between measured absorption values and analyte concentration. Such non-specific adsorption effects may be overcome by the use of buffer pH values higher than the pI of proteins [11], the use of low-pH buffer systems [12], the application of dynamic coating agents, which interact weakly with the capillary surface and are generally added to the separation buffer [13], and chemical derivatization of the silanol groups [5,14,15]. Combinations of these systems have also been described [16].

For the analysis of core histones and their acetyl-

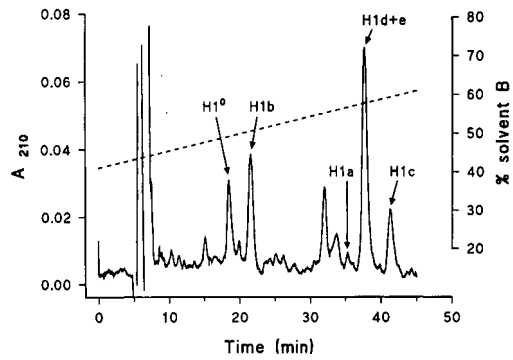


Fig. 1. Separation of H1 histones by RP-HPLC. Amounts of 100 µg of protein samples isolated from mitotic enriched NIH 3T3 fibroblasts were injected on to a Nucleosil 300-5 C<sub>4</sub> column. Flow-rate, 1 ml/min. A linear acetonitrile gradient was used with an increase in solvent B (70% acetonitrile) from 43 to 63% within 45 min. Absorbance was monitored at 210 nm. The purified H1 subtypes were lyophilized and analysed by HPCE and PAGE.

ated modifications, we have recently described an efficient HPCE method [6]. In this work, we have investigated the potential utility of HPCE for the separation of distinct phosphorylated linker histone variants. For this purpose, whole histones were extracted from mitotic enriched mouse NIH 3T3 fibroblasts containing highly phosphorylated H1 his-

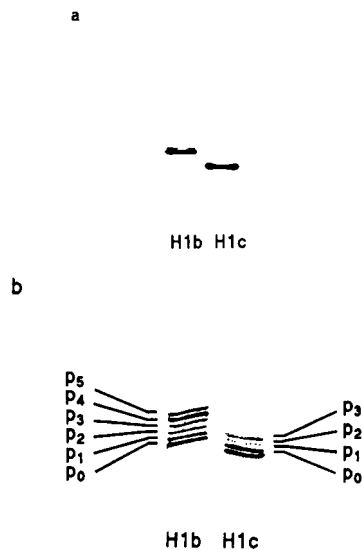


Fig. 2. Gel electrophoresis of multi-phosphorylated histone H1 variants separated by the HPLC system used in Fig. 1. (a) SDS gel electropherogram; (b) AU gel electropherogram.

tone variants. In order to obtain these H1 subtypes we used reversed-phase (RP) HPLC, which has been demonstrated to be an excellent technique for the separation of the very lysine-rich histones [17–19]. As shown in Fig. 1, five H1 subfractions were clearly separated from each other: histone H1<sup>0</sup>, H1b, H1a, a mixture of H1d and H1e and finally H1c. For our investigations we used the subtypes H1b and H1c, which are known to be phosphorylated in interphase and mitotic cells to a larger extent [20]. The purity of the histone samples was checked by SDS-PAGE (Fig. 2a). Neither fraction H1b nor H1c is contaminated with any other proteins, but they consist of a mixture of non-phosphorylated and different phosphorylated forms which are resolved in acid-urea gels (Fig. 2b). These modified protein variants, however, cannot be separated by RP-HPLC. It should be mentioned that the mi-

nor band migrating just above the main component in Fig. 2a represents phosphorylated histone H1b, whose shift is caused by a conformational change of the modified histone [4]. The histone fractions H1b and H1c obtained by HPLC (Fig. 1) were subjected to capillary electrophoresis.

Fig. 3a and b show the HPCE runs of the histone fractions H1b and H1c, respectively, obtained by HPLC (Fig. 1). The parent histone variants and the different phosphorylated derivatives were clearly separated in 0.1 M phosphate buffer (pH 2.0) containing 0.03% HPMC within about 15 min. The histone fraction H1b (Fig. 3a) was baseline separated into six peaks: H1b-p<sub>0</sub>, the fastest migrating component representing the non-phosphorylated H1b variant, followed by five different phosphorylated forms designated H1b-p<sub>1</sub> to H1b-p<sub>5</sub>. The number of peaks in the electropherogram (Fig. 3a) corresponds to the number of bands in the acid-urea gel (Fig. 2b, left) In addition, the relative amounts

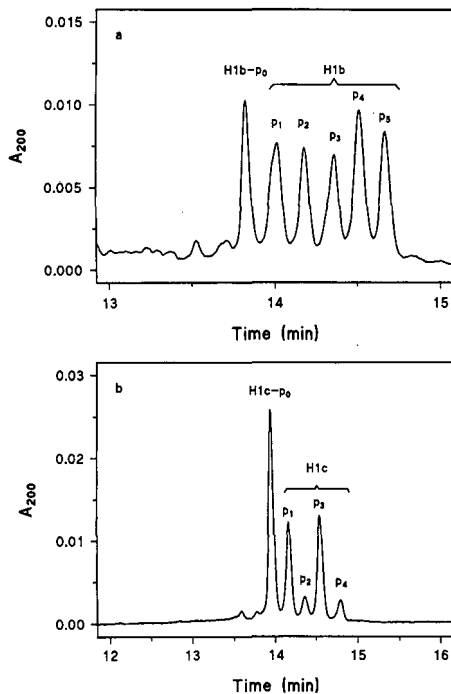


Fig. 3. HPCE of multi-phosphorylated histone H1 variants in a 50 cm × 75 μm I.D. untreated capillary. Samples were injected for 5 s by pressure. Electrophoresis was performed at 16 kV in 0.1 M phosphate buffer (pH 2.0) containing 0.03% HPMC. (a) HPCE of non-phosphorylated histone H1b (H1b-p<sub>0</sub>) and distinct phosphorylated forms of H1b (H1b-p<sub>1</sub> to H1b-p<sub>5</sub>); (b) HPCE of non-phosphorylated histone H1c (H1c-p<sub>0</sub>) and distinct phosphorylated forms of H1c (H1c-p<sub>1</sub> to H1c-p<sub>4</sub>).

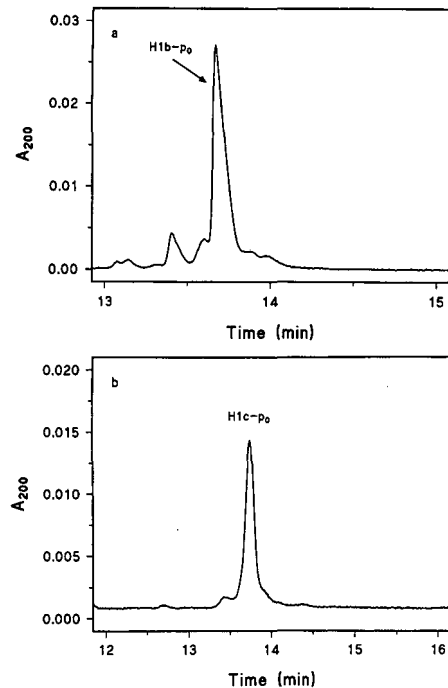


Fig. 4. HPCE of non-phosphorylated histone H1 variants in a 50 cm × 75 μm I.D. untreated capillary. Electrophoretic conditions as in Fig. 3. (a) HPCE of non-phosphorylated histone H1b (H1b-p<sub>0</sub>); (b) HPCE of non-phosphorylated histone H1c (H1c-p<sub>0</sub>).

## H1b H1c

Fig. 5. AU gel electrophoresis of non-phosphorylated histone H1 variants. Non-phosphorylated histone variants H1b and H1c were isolated from quiescent NIH 3T3 fibroblasts by RP-HPLC as in Fig. 1 and subjected to AU gel electrophoresis.

of the individual peaks coincide with those of the bands. The histone fraction H1c consisting of four bands in the AU gel (Fig. 2b, right) was separated by HPCE (Fig. 3b) into five peaks, a non-phosphorylated (H1c-p<sub>0</sub>) and four phosphorylated H1 derivatives (H1c-p<sub>1</sub> to H1c-p<sub>4</sub>).

In order to prove the existence of multi-phosphorylated forms of histones H1b (Fig. 3a) and H1c (Fig. 3b), we analysed these two histone H1 variants obtained from quiescent NIH 3T3 fibroblasts by HPLC (data not shown) and subsequently by HPCE. As slowly or non-dividing cells contain H1 histones primarily in their non-phosphorylated form [7], we expected only a single peak in the corresponding electropherogram. In fact, we found that both histone fractions H1b and H1c consist of a single peak each, designated H1b-p<sub>0</sub> (Fig. 4a) and H1c-p<sub>0</sub> (Fig. 4b), respectively. The purity of these

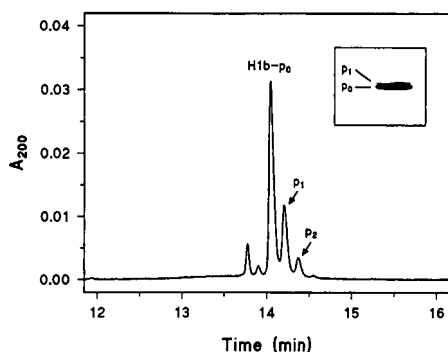


Fig. 6. Removal of phosphate from histone H1b by alkaline phosphatase. Multi-phosphorylated histone variant H1b was isolated from mitotic enriched NIH 3T3 fibroblasts RP-HPLC as in Fig. 1, digested with alkaline phosphatase as described by Sherod *et al.* [7] and subjected to HPCE. Electrophoretic conditions as in Fig. 3. The inset shows the corresponding analysis by AU gel electrophoresis. H1b-p<sub>0</sub> = Non-phosphorylated histone H1b; H1b-p<sub>1</sub> and H1b-p<sub>2</sub> = distinct phosphorylated forms of histone H1b.

histone variants was checked by AU-PAGE (Fig. 5).

In a further experiment, the same material as used for the HPCE analysis shown in Fig. 3a was digested with alkaline phosphatase. After treatment with the enzyme, the sample was chromatographed (data not shown) and subjected to HPCE (Fig. 6). In contrast to Fig. 3a, only three peaks of histone H1b were detectable: one prominent peak consisting of non-phosphorylated histone H1b (designated H1b-p<sub>0</sub>) and two minor peaks of different phosphorylated histones H1b (p<sub>1</sub> and p<sub>2</sub>). Therefore, the total loss of the highly phosphorylated forms of H1b-p<sub>3</sub> to H1b-p<sub>5</sub> and the dramatic decrease in H1b-p<sub>2</sub> and H1b-p<sub>1</sub> confirm our assignment in Fig. 3.

## CONCLUSION

The first application of HPCE to the analysis of phosphorylated H1 histones has been described. With an untreated capillary and a phosphate buffer system (pH 2.0) containing the dynamic coating agent hydroxymethylpropylcellulose, remarkable results were obtained. This new technique permits an excellent resolution of non-phosphorylated and different phosphorylated H1 histone variants within about 15 min and therefore provides an important alternative to the traditional gel electrophoresis.

## ACKNOWLEDGEMENTS

We are grateful to A. Devich and Dr. M. Ritteringer for excellent technical assistance.

## REFERENCES

- 1 V. K. Laemmli, *Nature (London)*, 227 (1970) 680.
- 2 S. Panyim and R. Chalkley, *Arch. Biochem. Biophys.*, 130 (1969) 337.
- 3 A. Zweidler, *Methods Cell Biol.*, 17 (1978) 223.
- 4 R. W. Lennox, R. G. Oshima and L. H. Cohen, *J. Biol. Chem.*, 257 (1982) 5183.
- 5 J. W. Jorgenson and K. D. Lukacs, *Science (Washington, D.C.)*, 222 (1983) 266.
- 6 H. Lindner, W. Helliger, A. Dirschlmyer, M. Jaquemar and B. Puschendorf, *Biochem. J.*, 283 (1992) 467.
- 7 D. Sherod, G. Johnson and R. Chalkley, *Biochemistry*, 9 (1970) 4611.
- 8 T. Tsuda, K. Nomura and G. Nakagawa, *J. Chromatogr.*, 248 (1982) 241.

- 9 E. Gassmann, J. E. Kuo and R. N. Zare, *Science*, 230 (1985) 813.
- 10 T. Tsuda, K. Nomura and G. Nakagawa, *J. Chromatogr.*, 264 (1983) 385.
- 11 H. H. Lauer and D. McManigill, *Anal. Chem.*, 58 (1986) 166.
- 12 P. D. Grossman, J. C. Colburn, H. H. Lauer, R. G. Nielsen, R. M. Giggin, G. S. Sittampalam and E. C. Rickard, *Anal. Chem.*, 61 (1989) 1186.
- 13 S. Hjertén, L. Valtcheva, K. Elenbring and D. Eaker, *J. Liq. Chromatogr.*, 12 (1989) 2471.
- 14 S. A. Swedberg, *Anal. Biochem.*, 185 (1990) 51.
- 15 S. Hjertén, *J. Chromatogr.*, 347 (1985) 191.
- 16 R. M. McCormick, *Anal. Chem.*, 60 (1988) 2322.
- 17 H. Lindner, W. Helliger and B. Puschendorf, *J. Chromatogr.*, 450 (1988) 309.
- 18 H. Lindner, W. Helliger and B. Puschendorf, *Biochem. J.*, 269 (1990) 359.
- 19 H. Lindner and W. Helliger, *Chromatographia*, 30 (1990) 518.
- 20 R. W. Lennox and L. H. Cohen, *J. Biol. Chem.*, 258 (1983) 262.

# Ultramicro enzyme assays in a capillary electrophoretic system

Jianmin Bao and Fred E. Regnier

Department of Chemistry, Purdue University, West Lafayette, IN 47907 (USA)

---

## ABSTRACT

This paper describes an ultramicro method for achieving enzyme assays. Enzyme saturating concentrations of substrate, coenzyme when appropriate, and running buffer were mixed and used to fill a deactivated fused-silica capillary in a capillary zone electrophoresis apparatus. The enzyme glucose-6-phosphate dehydrogenase was injected by either electrophoresis or siphoning and mixed with the reagents in the capillary by electrophoretic mixing. Enzyme activity was assayed by electrophoresing the product, reduced nicotinamide adenine dinucleotide phosphate, to the detector where it was detected at 340 nm. Under constant potential, the transport velocity of enzyme and the product was generally different. This caused product to be separated from the enzyme after it was formed. Because product formation was much faster than the rate of enzyme-product separation, product accumulated. The amount of accumulated product was inversely related to operating potential. In the extreme case, the operating potential was zero. Zero potential assays were generally carried out by electrophoresing the enzyme partially through the capillary and then switching to zero potential. This capillary was left at zero potential for several minutes to allow additional product to accumulate. After this additional amplification step, potential was again applied and the product transported to the detector. Product formed under constant potential appears as a broad peak with a flat plateau. When the voltage is switched to zero at intermediate migration distance, a peak will be observed on top of this plateau. Either the height of the plateau or the area of the peak may be used to determine enzyme concentration. The lower limit of detection was  $4.6 \cdot 10^{-17}$  mol of glucose-6-phosphate dehydrogenase.

---

## INTRODUCTION

Enzymes are often identified and quantitated by measuring their biological activity, *i.e.* their catalytic behavior. The Michaelis-Menten equation

$$v = (V_{\max}[S]) / (K_m + [S]) \quad (1)$$

shows that the initial reaction rate of a single substrate with an enzyme is related to three variables; the maximum velocity ( $V_{\max}$ ) of the enzyme at substrate saturation, substrate concentration [S], and a rate constant ( $K_m$ ) unique to each enzyme. At high concentrations of substrate,  $v$  will approach  $V_{\max}$  and remain constant until either (i) substrate depletion begins to occur or (ii) sufficient product accumulates to cause product inhibition. Short reaction times circumvent both of these problems. This

equation shows that an enzyme may be assayed in two ways by measuring either the rate of product formation or the amount of product formed in a fixed time. To assay an enzyme by either of these techniques requires three steps: initiation of the reaction by rapid mixing of the reactants, a period of incubation during which product accumulates, and a method for measuring the amount of product formed.

There are several problems associated with assaying enzymes in very small volumes of liquid, particularly in the case of enzymes that have been separated in a capillary electrophoretic system. The first is to mix the reactants rapidly without perturbing the separation. One technique is to attach a post-column reaction detector to the capillary [1] as has been done in liquid chromatography [2-4]. Substrate is added to the system through a mixing-tee at the end of the electrophoresis column and the reaction mixture is pumped into a second capillary.

---

Correspondence to: Dr. F. E. Regnier, Department of Chemistry, Purdue University, West Lafayette, IN 47907, USA.



Product detection is achieved at the end of the second capillary with a conventional capillary electrophoresis detector. Because the transit time between the mixing-tee and detector is constant, this system approximates a fixed time assay.

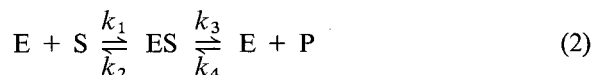
A second problem is to minimize band spreading during the mixing and incubation phases of the reaction. The challenge in post-column reaction detectors attached to a capillary separation system is to blend nanoliter streams of eluent and substrate within a few seconds and transport the reactants through a laminar flow system to the detector with minimal band spreading.

Still another problem is how to deal with enzymes that are dilute or have a low turn-over number. Longer incubation times are required to accumulate sufficient product for detection. It is very difficult to achieve incubation times of more than a few minutes in post-column reaction detectors [5]. To do so requires either very long reactors or stopped-flow.

This paper reports a new technique for achieving enzyme assays in a capillary electrophoretic systems using glucose-6-phosphate dehydrogenase (G-6-PDH, EC 1.1.1.49) as a model enzyme. G-6-PDH has been found in almost all animal tissues and microorganisms in which it catalyzes the first reaction in the hexose monophosphate shunt pathway. Since the erythrocyte lacks the citric acid cycle, it depends on the pentose phosphate pathway for its only supply of NADPH, which is required to maintain the intracellular concentration of reduced glutathione. Deficiency of G-6-PDH is an inherited trait, for which more than 80 variants of the enzyme have been described. The clinic biochemistry of G-6-PDH deficiency is of great importance and has been extensively reviewed [6].

## THEORY

Enzymatic catalysis may be portrayed as the reaction of an enzyme (E) with a substrate (S) to form an enzyme-substrate complex (ES) which then decomposes to a product (P) and regenerates the enzyme.



Depending on the charge characteristics of these substances, they may have different electrophoretic mobilities. This simple fact could be of great use when carrying out ultramicro enzyme assays. Assuming that an enzyme has a net charge of +10, the substrate a net charge of -2, and the product a net charge of -1, the electrophoretic mobility of the enzyme would be much greater than that of the substrate or product and in the opposite direction. A band of enzyme could be made to rapidly overtake a band of substrate by applying potential across the system. The use of electrophoretic transport to merge reagents is a form of mixing. This electrophoretic mixing has several advantages. First, there is little or no dilution when two zones are electrophoretically mixed. Simple diffusion is the only force working to spread and dilute bands in electrophoretic systems [7]. The second advantage of this approach is that turbulence is not required for mixing and band spreading will be minimal. The only exception would be in systems that are dominated by electro-osmotically driven turbulent flow. A third positive feature of electrophoretic mixing is that mixing may be achieved in seconds when the bands or zones are small.

Following mixing, most of an enzyme will be sequestered in the enzyme-substrate (ES) complex. In the example given above, the charge of ES would be the net of  $E + S$ , *i.e.*  $10 - 2 = 8$ . The fact that the electrophoretic mobility of the ES complex can be different than either E or S is well known in affinity electrophoresis [8,9]. Techniques have even been developed to determine binding constants based on the differential electrophoretic mobility of the reactants [10]. Because enzyme assays are carried out under substrate saturating conditions, we will assume in the remainder of this discussion that the electrophoretic mobility of the enzyme is that of ES.

Subsequent to the mixing of reactants, incubation in an electrophoretic system could be carried out in two ways. One would be in the zero potential or stopped-flow mode. At zero potential, neither electrokinetic nor electrophoretic transport occurs and the reactants would stay mixed in a single zone where product would accumulate. This corresponds to a fixed time reaction in conventional enzyme assays. A second method would be to carry the assay out under constant potential. In this model, the reactants would be mixed and separated from prod-

uct continuously. Product accumulation and the possibility of an assay would seem to be precluded by continuously separating the enzyme from product. However, enzyme catalysis occurs orders of magnitude faster than the rate of separation. In essence, enzyme assays carried out under constant potential correspond to short, fixed time assays. Product formation on a molar basis could be  $10^2$ – $10^4$  times greater than the amount of enzyme, depending on the turn-over-number of the enzyme and the potential applied across the zone.

Product detection in the electrophoretic systems described above could be achieved in several ways. In the first, the incubation chamber and optical part of the detector could be juxtapositioned in a manner that would allow absorbance measurements to be made on the incubation mixture. This would be technically difficult and would probably introduce large measurement errors in microsystems. Detection systems that image the whole capillary would probably be the only way detection could be achieved in this manner [11]. A second method would be to transport the product to a fixed detector by some combination of electrophoretic and electrokinetic transport. This approach would adapt readily to capillary electrophoretic (CE) systems. The negative feature of this product transport solution is that some band spreading would occur during transport. Because CE systems produce more than  $10^5$  theoretical plates, this will probably be a small problem.

An enzyme assay could be carried out in the following way. A surface-deactivated capillary would be filled with an enzyme saturating concentration of substrate, buffer, and all the ingredients necessary for the enzyme assay. Enzyme would be introduced as in any CE system; either by suction or by electrokinetic injection. Subsequent application of potential to the capillary would mix the reactants and allow the reaction to start. As noted above, product and enzyme-substrate complex would be transported through the capillary at different velocities in all but rare cases. Product formation would continue until the enzyme exits the system. In all of the systems discussed below it is assumed that (i) there will be some small negative charge on the walls of the fused-silica capillary, (ii) this negative charge would produce electro-osmotic flow that transports liquid from the anodic to the cathodic end of the capillary,

(iii) capillaries would have been sufficiently deactivated that adsorption of enzymes to the capillary walls does not occur, (iv) the enzyme does not absorb at the wavelength chosen for product detection, and (v) assays will be carried out in a conventional capillary zone electrophoresis system.

The theoretical elution profile of an ES–P system in which the transport velocity of ES > P would be as shown in Fig. 1A. Because the ES complex migrates at a higher velocity than the product, the first product detected at point A in the electropherogram will be that which was formed as the enzyme migrated past the detector. In contrast, product detected at point B is that which was formed when the enzyme was introduced at the inlet of the capillary. The peak or spike at B is an artifact that is the result of product formed between the time that enzyme was introduced into the capillary and potential was applied. During this time the capillary was at zero potential and product accumulated. The electropherogram for an ES–P system in which the transport velocity of P > ES would be the opposite (Fig.

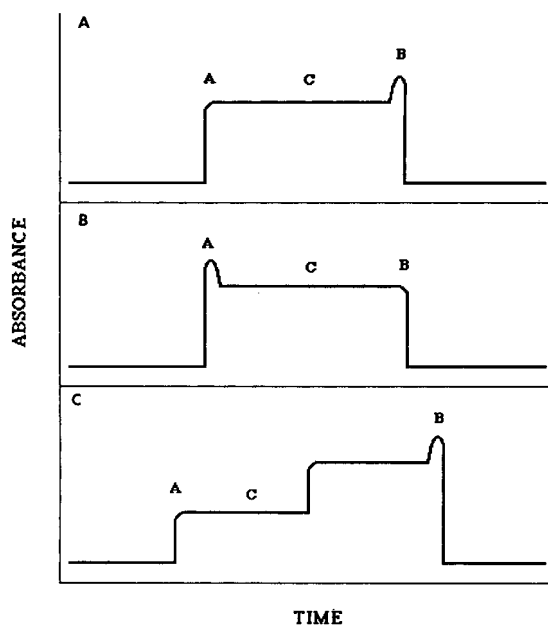


Fig. 1. Predicted models showing various electropherograms in capillary electrophoretic enzyme assay. The moving velocities are (A) ES > P and (B) P > ES. A multiple isoenzyme form is shown in (C) with the moving velocity of their common product smaller than those of these isoenzymes.

1B). The first product to reach the detector at point A would be that which was formed at the capillary inlet. The last product arriving at point B would be that which was formed as the enzyme passes the detector. The transport time of the enzyme and relative transport velocities of ES and P are easily recognized in the electropherograms. When the artifact peak elutes last at point B, the transport velocity of  $ES > P$  and point A is the transit time of the enzyme. The opposite is true in the case where the transport velocity of  $P > ES$ . In the case of isoenzymes it is expected that one would see multiple peaks similar to the illustration in Fig. 1C.

The height of the plateau above the baseline indicated by C in Fig. 1 will be directly proportional to enzyme concentration at constant potential. Sensitivity will be inversely related to potential, highest sensitivity being obtained at low potential where the greatest amount of product can accumulate before the separation of ES and P. The extreme case would be at zero potential. Switching to zero potential for a fixed time intermediate in the transit of enzyme through the system enables more product to be accumulated and sensitivity to be enhanced. The idea is to stop the power supply before the enzyme passes the detection window and let the enzyme catalyze the reaction to accumulate NADPH in its position. When the power is turned on again the enzyme will be separated from the formed NADPH and a peak will be seen on the plateau and indicate the amount of NADPH formed during the accumula-

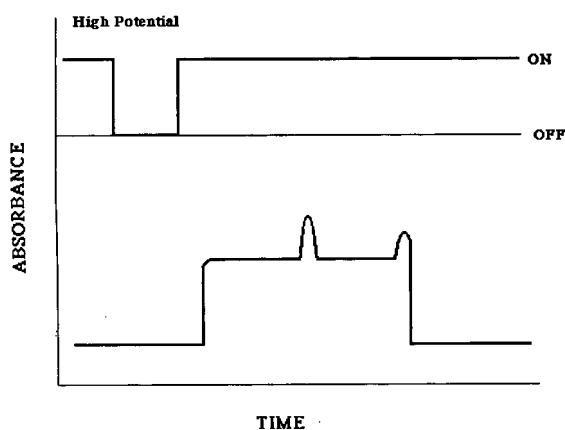


Fig. 2. Proposed potential program and the corresponding electropherogram.

tion period. An illustration of the use of this programmed potential during the course of an assay to enhance sensitivity is shown in Fig. 2. Either peak height or area above the constant potential plateau can be used in quantitation.

## EXPERIMENTAL

### Instrumentation

Assays were carried out on two systems. The first was an ISCO 3850 CE system (Instrument Specialties, Lincoln, NE, USA) which was interfaced to a personal computer using Inject software to collect and process data. This software was obtained from Bioanalytical Systems (Lafayette, IN, USA). The second CE system was in-house design [14]. Polyamine-coated, fused-silica capillaries (Polymicro Technologies, Phoenix, AZ, USA) of and  $35\text{--}60\text{ cm} \times 50\text{ }\mu\text{m I.D.} \times 360\text{ }\mu\text{m O.D.}$  were used to prepare the columns. The separation lengths were varied from 15–40 cm. Detection was achieved with a variable-wavelength UV absorbance detector (Model V4, Instrument Specialties). Protein elution was monitored at 200 nm and the product NADPH at 340 nm. The neutral marker mesityl oxide was detected at 254 nm. Strip chart recordings were obtained with a Linear 2000 (Linear, Reno, NV, USA) recorder.

### Materials

G-6PDH, G-6-PDH reagent and G-6-PDH substrate solutions were purchased from Sigma (St. Louis, MO, USA). Reagents were prepared and the assay carried out according to the literature [12]. Ethyleneglycol diglycidylether (EGDE), 3-glycidoxypropyltrimethoxysilane (GOX), 1,4-Diazabicyclo[2.2.2]octane (DABCO), mesityl oxide, solvents and buffers were obtained from Aldrich (Milwaukee, WI, USA). Buffers were prepared with deionized, doubly distilled water.

### Capillary Coating

An epoxy based coating was applied to the fused-silica capillaries used in this study [13,14]. Fused-silica capillaries were activated with 1.0 M NaOH prior to derivatization with GOX. The GOX-bonded phase was further crosslinked with EGDE using DABCO as the catalyst. Non-bound monomer and oligomers were forced out of the column with pres-

surized nitrogen and the column was washed with methanol.

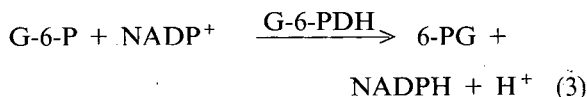
#### Electrophoresis procedures

Protein samples were injected by siphoning. The inlet end of the capillary was inserted into the protein sample and raised about 5 cm for 5 s. Neutral marker was introduced into the capillary in the same way. The running buffer contained all the reagents necessary to assay G-6-PDH. Assay reagents were reconstituted according to the reagent supplier (Sigma). The buffer solution contained 0.7 mmol/l glucose-6-phosphate (G-6-P), 0.5 mmol/l of the coenzyme nicotinamide dinucleotide diphosphate (NADP) and 4 mmol/l maleimide, in addition to a stabilizer and lysing agent. Operating current was controlled within the range 35–50  $\mu\text{A}$  by limiting the applied potential. In no case was a capillary operated above 60  $\mu\text{A}$ . All assays were carried out at ambient temperature without temperature control. Capillaries were cleaned by flushing with 0.01 M sodium hydroxide, doubly distilled water, and then the working buffer solution.

#### RESULTS AND DISCUSSION

##### Assay system

G-6-PDH, also referred to as D-glucose-6-phosphate:NADP oxidoreductase, was chosen to examine ultramicro enzymes assays because this enzyme may be readily assayed spectrophotometrically [15]. G-6-PDH oxidizes G-6-P to 6-phosphogluconate (6-PG) while reducing NADP to its reduced form NADPH in the presence of G-6-P.



The absorbance spectrum of the product NADPH is uniquely different than that of either the assay reagents or the enzyme (Figs. 3 and 4) and may be used to monitor the reaction [15]. It is seen that NADPH has an adsorption maximum at 340 nm ( $\epsilon = 6.22 \cdot 10^6 \text{ cm}^2/\text{mol}$ ). The enzyme 6-phosphogluconate dehydrogenase (6-PGDH) can interfere, such as in serum samples contaminated with 6-PGDH from erythrocytes. In the presence of 6-PGDH, 6-phosphogluconic acid may be further ox-

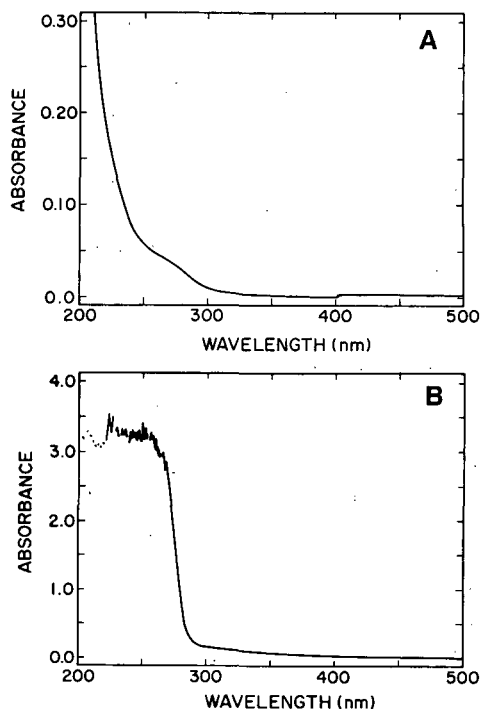


Fig. 3. The absorbance as a function of wavelength, in (A) G-6-PDH, (B) running buffer.

idized to produce a second mole of NADPH. Addition of maleimide to the incubation mixture will inhibit 6-PGDH.

It is necessary to eliminate protein adsorption in fused-silica capillaries used for enzyme assays. Enzyme immobilized by adsorption at the capillary

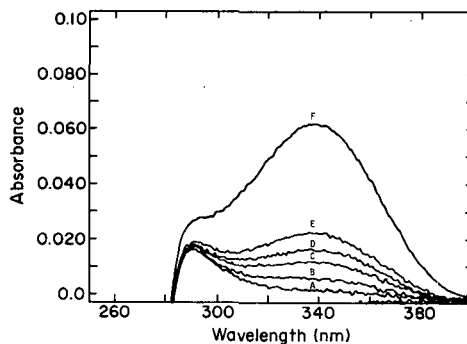


Fig. 4. The absorbance of the reaction system around 340 nm increases as a function of time. (A) 2, (B) 4, (C) 6, (D) 8, (E) 10 and (F) 28 min.

wall causes a series of problems including (i) mixed homogeneous and heterogeneous catalysis, (ii) errors in quantitation from a reduction in product yield, and (iii) increased signal background in subsequent assays. Deactivation was achieved by using a covalently bonded epoxy polymer layer [13,14]. This coating has been shown to give more than 95% recovery of proteins in capillary zone electrophoresis (CZE). Electro-osmotic flow in these deactivated capillaries is substantially reduced and negatively charged species, such as NADPH, can require 20–30 min pass to through 30-cm capillaries. Because G-6-PDH has a relatively high  $pI$  value, it is transported more quickly. The electrophoretic mobilities of G-6-PDH and NADPH were found to be 5 and 18 min, respectively (data not shown).

#### Assay protocol

A CZE system was used in which the buffer tanks

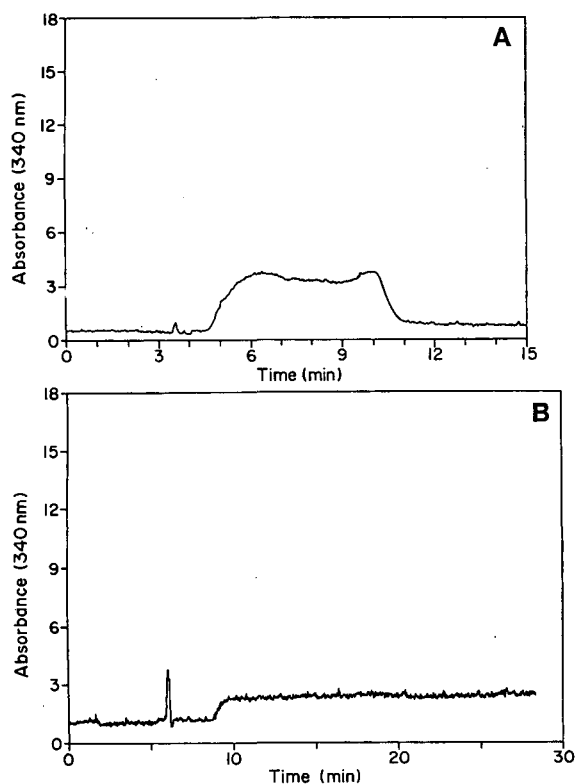


Fig. 5. Typical electropherograms showing the formation of NADPH during the process of G-6-PDH migration through the capillary. (A) Short separation length or high potential situation, (B) long separation length or low potential situation.

and capillary had been filled with running buffer containing all the reagents necessary for an assay except the enzyme. Sample enzyme was introduced into the capillary by injection as in CZE and potential applied to mix the reactants. Product formation was measured with a UV detector at 340 nm. Assays were carried out in two ways: (i) a constant potential mode in which the reactants remained under constant potential throughout the course of the assay and (ii) a zero potential mode in which the separation of reactants is stopped during part of the assay.

*Constant potential assays.* The electropherogram in Fig. 5a of a G-6-PDH assay obtained under constant potential has the general shape predicted in the Theory (Fig. 1) for an enzyme having a greater transport velocity than the product of the reaction

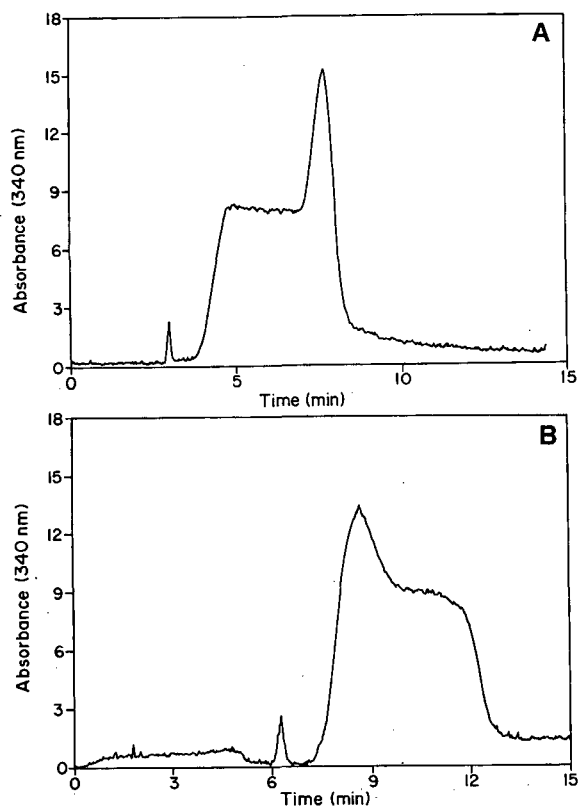


Fig. 6. Electropherograms showing the accumulated peak resulting from the packed reaction at different running times. (A) NADPH accumulated at the beginning before the electrophoresis started, (B) NADPH accumulated just before G-6-PDH passed the detection window.

it catalyzes. This is interpreted to mean that the theory proposed to describe enzyme assays in a capillary electrophoretic system is generally correct. The total time required for the assay in this case is slightly less than 12 min. When a longer capillary was used with a more dilute solution of enzyme it is seen (Fig. 5b) that plateau height is lower and the elution time of the enzyme is longer. Data collection was terminated in this case before the trailing injection artifact peak eluted. The height of the injection artifact peak was variable and of no analytical value. The size of the injection artifact peak was found to be related to the volume and degree of mixing during the injection, enzyme concentration in the sample, and the time elapsed between injection and the start of electrophoresis. An example of allowing several minutes to elapse between injection and the start of electrophoresis is shown in Fig. 6a. For comparison, the sample was injected quickly and the potential dropped to zero for several minutes before the enzyme passed the detector (Fig. 6b). The large peak at approximately 8 min is the result of an interruption of several minutes in the potential, 5 min into the run.

Analysis time could also have been decreased below 12 min without loss in sensitivity by shortening the capillary. The optimum length in terms of minimizing analysis time would be the length required for the product elution curve to plateau. Increasing the potential to shorten analysis time was found to be counter-productive. As predicted, increasing the potential diminishes product accumulation and sensitivity.

The small peak eluting at 3.5 and 6.0 min in Figs. 5a and 5b was not predicted in the Theory. This peak adsorbed at 200 and 340 nm and is thought to be a protein in the sample that either adsorbs at 340 nm or binds NADPH but does not play a role in catalysis.

*Zero potential assays.* Switching the potential to zero before the enzyme elutes from the capillary allows one to increase the incubation time and concomitantly sensitivity. Zero potential assays were carried out in a 41-cm segment of capillary with the detector set 17.8 cm from the inlet. At 8700 V G-6-PDH reached the detector in approximately 6 min. The potential was interrupted after 3 min and held at zero potential for 5 min after which the potential was returned to 8700 V for product elution. An

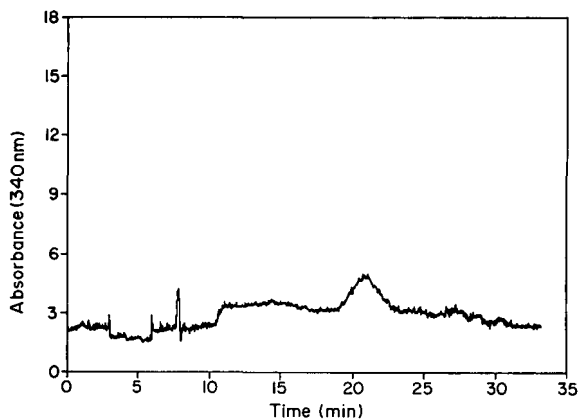


Fig. 7. The accumulation of NADPH by switching to zero potential results in a distinct peak on the plateau. The area of this typical peak may be integrated to give information on enzyme activity.

electropherogram of a sample estimated to contain  $4.6 \cdot 10^{-17}$  mol of G-6-PDH is shown in Fig. 7. This estimate is based on the assumption of a 2-nl injection volume. Note the peak at 20 min which resulted from the 5-min zero potential incubation. The dose response curve for G-6-PDH using this assay procedure is shown in Fig. 8. Data for this figure were obtained from Table I. Quantitation is based on determinations of the peak area above the constant potential product plateau in the electropherogram. A solution containing one unit/ml of G-6-PDH is approximately  $3 \cdot 10^{-8}$  M. No attempt

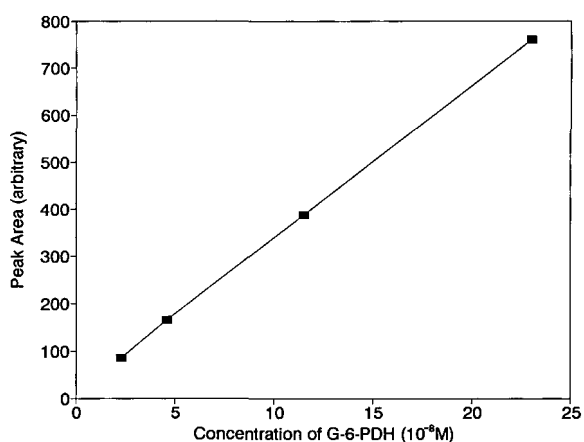


Fig. 8. The relationship between the accumulated NADPH peak area and the concentration of enzyme.

TABLE I

## G-6-PDH ACTIVITIES OBTAINED BY CAPILLARY ELECTROPHORESIS ASSAY

Experimental conditions: column, 41 cm GOX-EGDE coated capillary with a separation length of 17.8 cm (50  $\mu\text{m}$  I.D.); power supply, 8700 V, 50  $\mu\text{A}$ ; detection, 340 nm; sensitivity, 0.02 a.u.; injection, 10 s.

Assay number	G-6-PDH activity (EU) <sup>a</sup>	G-6-PDH concentration (M)	G-6-PDH quantity (mol)	Peak area (arbitrary)
1	0.75	$2.3 \cdot 10^{-8}$	$4.6 \cdot 10^{-17}$	85 241
2	1.50	$4.6 \cdot 10^{-8}$	$9.2 \cdot 10^{-17}$	164 554
3	3.75	$1.15 \cdot 10^{-7}$	$2.3 \cdot 10^{-16}$	386 763
4	7.50	$2.3 \cdot 10^{-7}$	$4.6 \cdot 10^{-16}$	760 207

<sup>a</sup> EU represents enzyme unit as defined in ref. 15.

was made to determine the linear dynamic range of the assay. Based on macroscopic assays it could be two orders of magnitude [15].

## CONCLUSIONS

It may be concluded that small quantities of enzyme may be detected in a CZE system by carrying out the assay in the capillary. Assays are based on the fact that transport velocities of the enzyme, reagents, and product(s) are different under applied potential and may be used both to mix the reactants and separate the enzyme from product(s) after catalysis. Product is transported to the CZE detector where product concentration is determined and related to enzyme concentration. The detection limit by this method appears to be three orders of magnitude lower than by conventional methods.

## ACKNOWLEDGEMENT

The authors thank Dr. Jeffery Seyler for his kind help in running the UV-Vis spectrum. This work was supported by NIH grant number GM 35421.

## REFERENCES

- 1 B. Nickerson and J. W. Jorgenson, *J. Chromatogr.*, 480 (1989) 157.
- 2 T. D. Schlabach, A. J. Alpert and F. E. Regnier, *Clin. Chem.*, 24 (1978) 1351.
- 3 L. R. Snyder, *J. Chromatogr.*, 125 (1976) 287.
- 4 R. S. Deelder, M. J. F. Kroll and J. H. M. van den Berg, *J. Chromatogr.*, 125 (1976) 287.
- 5 T. D. Schlabach, S. H. Chang, K. M. Gooding and F. E. Regnier, *J. Chromatogr.*, 134 (1977) 91.
- 6 A. Yoshida, *Science (Washington, D.C.)*, 179 (1973) 532.
- 7 J. W. Jorgenson and K. D. Lukas, *Anal. Chem.*, 53 (1981) 1298.
- 8 N. H. H. Heegaard and T. C. Bog-Hansen, *Appl. Theor. Electrophor.*, 1 (1990) 249.
- 9 A. Guttman and N. Cooke, *Anal. Chem.*, 63 (1991) 2038.
- 10 P. Borneleit, B. Blechschmidt and H. P. Kleber, *Electrophoresis (Weinheim, Fed. Repub. Ger.)*, 10 (1989) 848.
- 11 J. Wu and J. Pawliszyn, *Anal. Chem.*, 64 (1992) 219.
- 12 G. W. Lohr and H. D. Waller, in H. U. Bergmeyer (Editor), *Methods of Enzymatic Analysis*, Verlag Chemie, Weinheim and Academic Press, New York, 2nd English ed., 1974, pp. 636.
- 13 J. Bao and F. E. Regnier, *J. Chromatogr.*, in preparation.
- 14 J. K. Towns, J. Bao and F. E. Regnier, *J. Chromatogr.*, 595 (1992) 227.
- 15 *Diagnostics Procedure No. 345-UV*, Sigma, St. Louis, MO, 1990.

# Capillary electrophoresis of hemoglobins and globin chains

Mingde Zhu, Roberto Rodriguez, Tim Wehr and Chris Siebert

*Analytical Systems Division, Life Science Group, Bio-Rad Laboratories, 2000 Alfred Nobel Drive, Hercules, CA 94547 (USA)*

---

## ABSTRACT

Capillary isoelectric focusing (cIEF) and free zone capillary electrophoresis were evaluated for separation of native hemoglobins and globin chains. High-resolution separations of adult human hemoglobin A, fetal human hemoglobin F, and hemoglobin variants S and C were obtained using cIEF with cathodic mobilization. Absorbance detection in the UV and visible regions were compared, and on-line fast UV or visible-wavelength scanning detection was used to obtain spectral information on separated components. Globin chain analysis was performed on the same hemoglobin species by free zone capillary electrophoresis following precipitation of the protein with acidic acetone. Free zone separations were carried out at low pH in the presence of 7 M urea.

---

## INTRODUCTION

Analysis of the hemoglobin composition of human blood is of major clinical interest because of the number of disorders associated with abnormal blood hemoglobin content [1,2]. These diseases are grouped into anemias arising from the presence of deleterious genes coding for defective sequence variants of hemoglobins, and thalassemias characterized by abnormal levels of globin chains. Because of the prevalence of genetically-derived anemias in many populations, routine clinical screening for defective hemoglobins has been implemented in many areas of the world. For example, the state of California in the USA has mandated screening of all newborns for the presence of defective hemoglobins in blood samples collected at birth. A second major interest in clinical hemoglobin analysis is the determination of glycosylated hemoglobins as a means of monitoring long-term blood glucose levels in diabetic patients.

A variety of analytical methods have been em-

ployed for hemoglobin determination including immunoassay, gel electrophoresis, and gel isoelectric focusing. More recently, high-performance cation-exchange chromatography has been applied to routine screening of blood hemoglobins [3]. This method has the advantages of rapid analysis times, automated processing of large numbers of samples, and quantitative analysis. High-sensitivity detection is possible by the use of on-line absorbance detection of native hemoglobins at visible wavelengths where non-heme proteins do not interfere.

We are interested in the use of capillary electrophoresis (CE) as an alternative technique for hemoglobins analysis. CE shares with high-performance liquid chromatography (HPLC) the advantages of automation and on-line detection, and offers separation modes which would be complementary to chromatography. In addition, CE is truly a microscale analytical method, consuming minute amounts of sample per analysis compared to HPLC. We have evaluated capillary isoelectric focusing as a method for separation of intact hemoglobins, and investigated the use of UV and visible scanning detection to identify and differentiate hemoglobin species. In addition, we have used free zone electrophoresis under denaturing conditions

---

*Correspondence to:* Dr. T. Wehr, Analytical Systems Division, Life Science Group, Bio-Rad Laboratories, 2000 Alfred Nobel Drive, Hercules, CA 94547, USA.



to separate the globin chains derived from hemoglobins.

## EXPERIMENTAL

### Materials

Hemoglobins A, F, S and C were obtained from Isolab (Akron, OH, USA). Bio-Lyte pH 3–10 ampholytes and AG 501-X8 resin were obtained from Bio-Rad Labs. (Richmond, CA, USA). Triton X-100 reduced was obtained from Aldrich (Milwaukee, WI, USA). Reference standards of hemoglobin A, hemoglobins A + S, hemoglobins A + F, and hemoglobins A + C were the generous gift of Dr. Ken Dobra of the Bio-Rad Diagnostic Group.

### Preparation of globin chains

One volume of hemoglobin sample was mixed with 20–40 volumes of acidic acetone [2% concentrated hydrochloric acid (36%) in acetone] and stirred briefly. The mixture was held at 4°C for 30 min, then centrifuged for 2 min in a microcentrifuge. After drawing off the supernatant, the precipitate was washed twice with acetone and dissolved in 10 mM sodium phosphate buffer (pH 3.2) + 7 M urea + 0.1% reduced Triton X-100. Prior to use, the buffer and urea solution was stirred with AG 501-X8 resin to remove urea impurities.

### Capillary electrophoresis

All separations were performed with the BioFocus 3000 automated capillary electrophoresis system (Bio-Rad Labs, Richmond, CA, USA). All capillaries used in this study were coated internally with a covalently-attached hydrophilic linear polymer [4]. Capillaries were enclosed in a cartridge format and thermostated at 20°C by liquid cooling. The distance from the monitor point to the capillary outlet was 4.5 cm.

Isoelectric focusing of hemoglobins was carried out using 17 cm × 25 μm I.D. coated capillaries. Capillaries were purged with water and 10 mM phosphoric acid between separations. Hemoglobin samples were mixed with pH 3–10 ampholytes to a final ampholyte concentration of 2% and total hemoglobin concentration of about 1 mg/ml. The sample + ampholyte mixtures were pressure-injected into the capillary at 100 p.s.i. (689 476 Pa) for 60 s. Focusing was carried out at 7 kV constant voltage

for 5 min using 40 mM sodium hydroxide as catholyte and 20 mM phosphoric acid as anolyte. Cathodic mobilization was performed by replacing the catholyte with a proprietary zwitterionic solution (Bio-Rad Labs.). Mobilization voltage was 8 kV. Single wavelength mode detection was at 280 nm; in scanning mode, spectra were acquired at 5-nm intervals.

Free zone electrophoresis of globin chains was carried out using 35 cm × 25 μm I.D. coated capillaries. The electrophoresis buffer was 100 mM sodium phosphate (pH 3.2) + 7 M urea + 1% reduced Triton X-100. Samples were loaded electrophoretically at 8 kV for 8 s and separated at 8 kV constant voltage. Detection was at 210 nm.

## RESULTS AND DISCUSSION

Human hemoglobin is a tetramer consisting of two  $\alpha$ -globin and two  $\beta$ -,  $\delta$ - or  $\gamma$ -globin chains, to each of which is bound a heme group. The  $\beta$  chain contains 141 amino acid residues while the other chains contain 146 residues. Normal adult human blood contains hemoglobin A ( $\alpha_2\beta_2$ ) and hemoglobin A<sub>2</sub> ( $\alpha_2\delta_2$ ). Fetal blood contains hemoglobin F ( $\alpha_2\gamma_2$ ) as the predominant species, and during the sixth months following birth hemoglobin F is replaced by hemoglobin A. Several hundred genetic variants of the hemoglobin molecule are known, many of which are associated with blood disorders. Since there are only two copies of the  $\beta$ -globin gene in the human genome, most of the known hemoglobinopathies are associated with mutations in the  $\beta$ -globin molecule. For example, sickle cell disease arises from a glutamic acid to valine transition at position 6 in the  $\beta$ -globin gene. In the homozygous state, this results in the production of the mutant hemoglobin S ( $\alpha_2\beta_{S_2}$  which causes a characteristic sickling morphology of erythrocytes. A glutamic acid to lysine transition at the  $\beta^6$  position results in production of hemoglobin C. Although benign in the heterozygous state, the  $\beta_C$  allele in the homozygous state or in the  $\beta_C\beta_S$  heterozygote causes moderate to severe sickling.

### Capillary isoelectric focusing (cIEF) of hemoglobin variants

Hemoglobin variants are excellent candidates for analysis by cIEF. This technique can resolve pro-

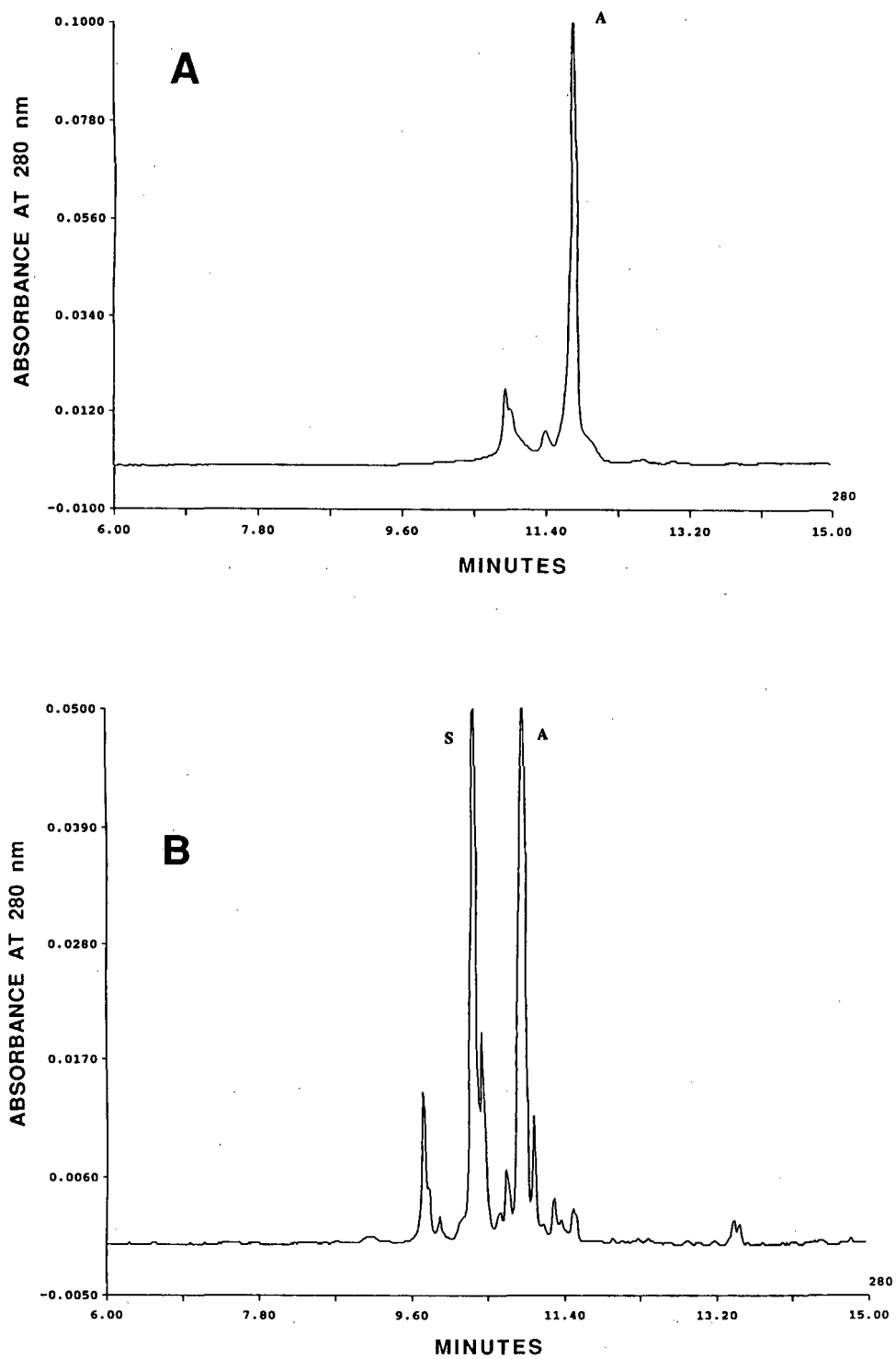


Fig. 1.

(Continued on p. 228)

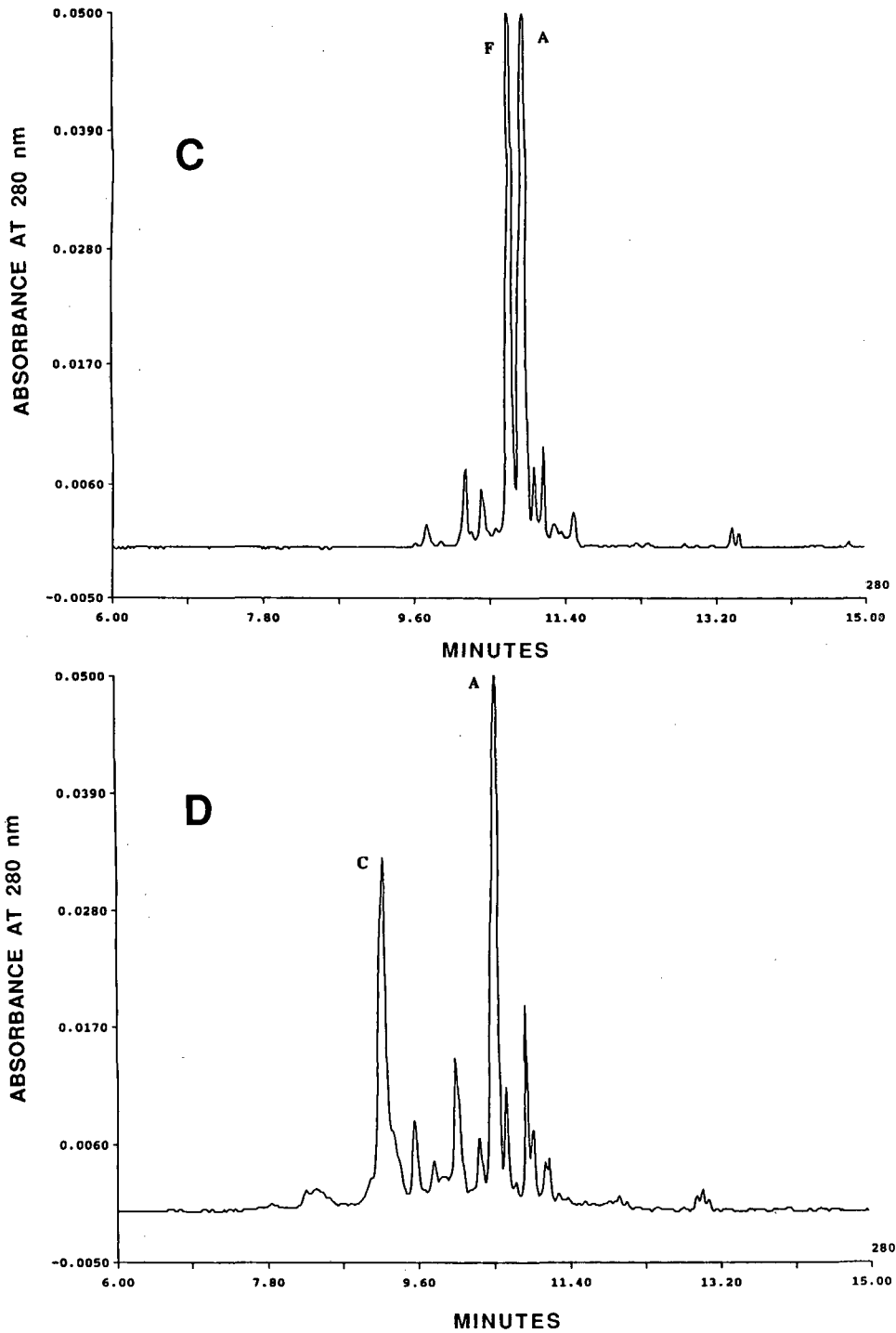


Fig. 1. Capillary isoelectric focusing of (A) hemoglobin A, (B) hemoglobins A and S, (C) hemoglobins A and F and (D) hemoglobins A and C.

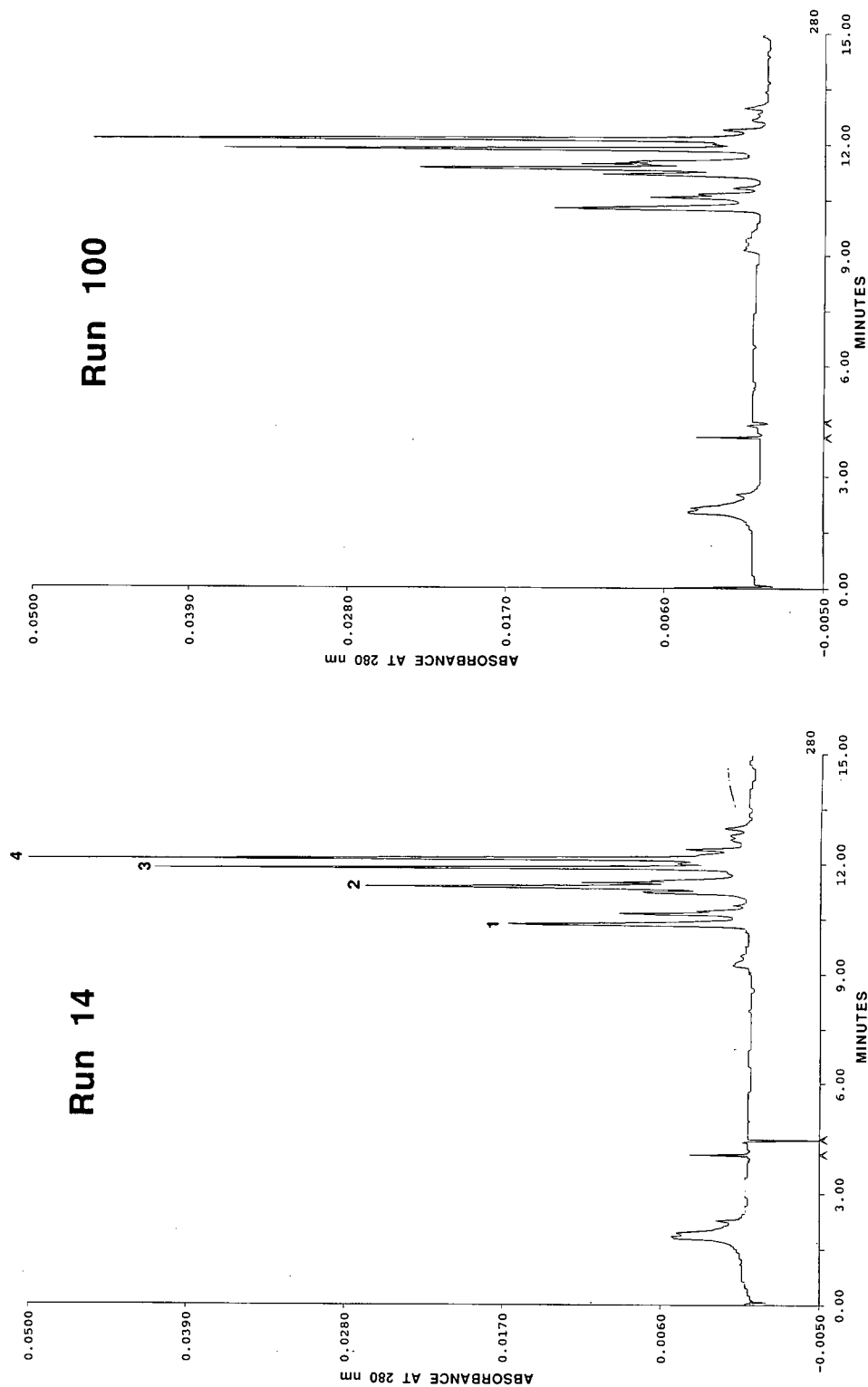


Fig. 2. Repetitive analysis of hemoglobin reference standard using a coated capillary. Peak 1 = hemoglobin C; peak 2 = hemoglobin S; peak 3 = hemoglobin F; peak 4 = hemoglobin A.

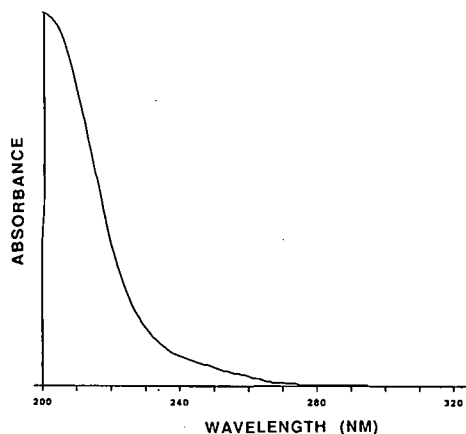


Fig. 3. Ultraviolet spectrum of Bio-Lyte pH 3–10 ampholytes.

teins differing in isoelectric points by as little as 0.02 pH units [5], and the amino acid substitutions in the major hemoglobin variants cause  $pI$  shifts of this magnitude or greater. The hemoglobin molecule is highly water soluble, and occurs within the erythrocyte at concentrations in excess of 300 mg/ml.

Therefore it should be much less susceptible than other proteins to precipitation when focused into sharp zones during the cIEF process.

Human fetal hemoglobin F has an isoelectric point of 7.15, and the  $pI$  values of the hemoglobin variants S and C are 7.25 and 7.50. These three species are easily resolved from normal human hemoglobin A ( $pI$  7.10) by cIEF using a wide-range ampholyte blend (Fig. 1). In this separation, cathodic mobilization moves focused proteins past the monitor point in order of decreasing isoelectric point. The high resolution observed in this technique is due to the use of high field strengths and the absence of electroendosmosis. High field strengths ( $> 400$  V/cm), providing strong focusing forces, are possible because the modest current levels (0.2–5  $\mu$ A) during the separation minimize the amount of Joule heat. The excellent heat dissipation qualities of the small-bore 25  $\mu$ m I.D. capillaries used in these separations further reduces any thermal zone distortion. Coating the capillaries with a hydrophilic polymer eliminates electroosmotic flow, which would otherwise disrupt the focusing process and

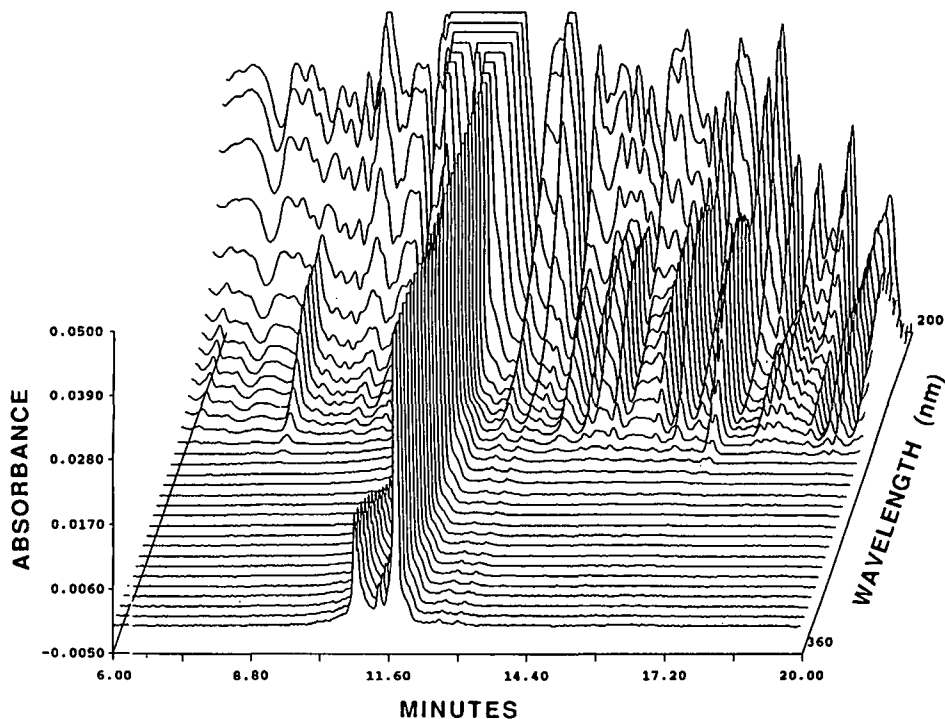


Fig. 4. Capillary isoelectric focusing separation of hemoglobin A using scanning detection in the 200–360 nm UV region. Peaks below 280 nm in the mobilization electropherogram are due to background absorbance of the ampholytes.

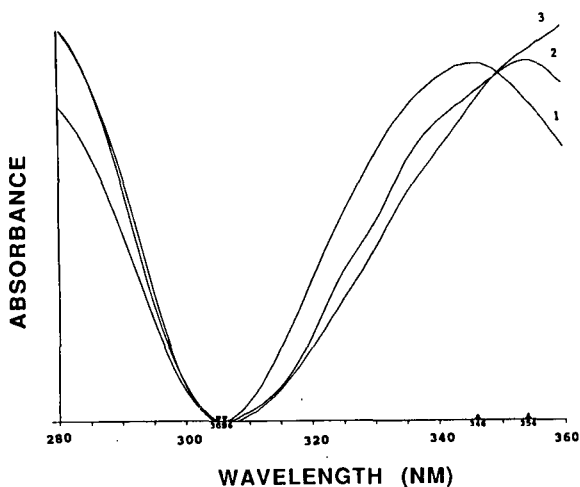


Fig. 5. UV spectra of hemoglobin A (spectrum 1) and two minor components (spectra 2,3) acquired during the cIEF separation shown in Fig. 1A. Spectrum 3 is taken from the fastest migrating minor peak, spectrum 2 is taken from the slower minor peak.

sweep proteins from the capillary before focusing was achieved. Separations are reproducible, and over one hundred repetitive runs have been achieved with no significant change in the mobilization profile (Fig. 2). Attempts to obtain good separation of native hemoglobins using free zone capillary electrophoresis were not as successful as cIEF.

The use of a high-speed scanning detector enables additional information to be obtained during the separation. The ampholytes themselves absorb in the ultraviolet region below 280 nm (Fig. 3), and when scanning detection in the 200-360 nm wavelength range is used during cIEF, a series of extra peaks is observed in the low UV region due to ampholyte absorption (Fig. 4). This pattern is reproducible and characteristic of the ampholyte blend. These peaks may be used as internal standards, and, if correlated with pI values by using external protein standards, could be used to estimate isoelectric

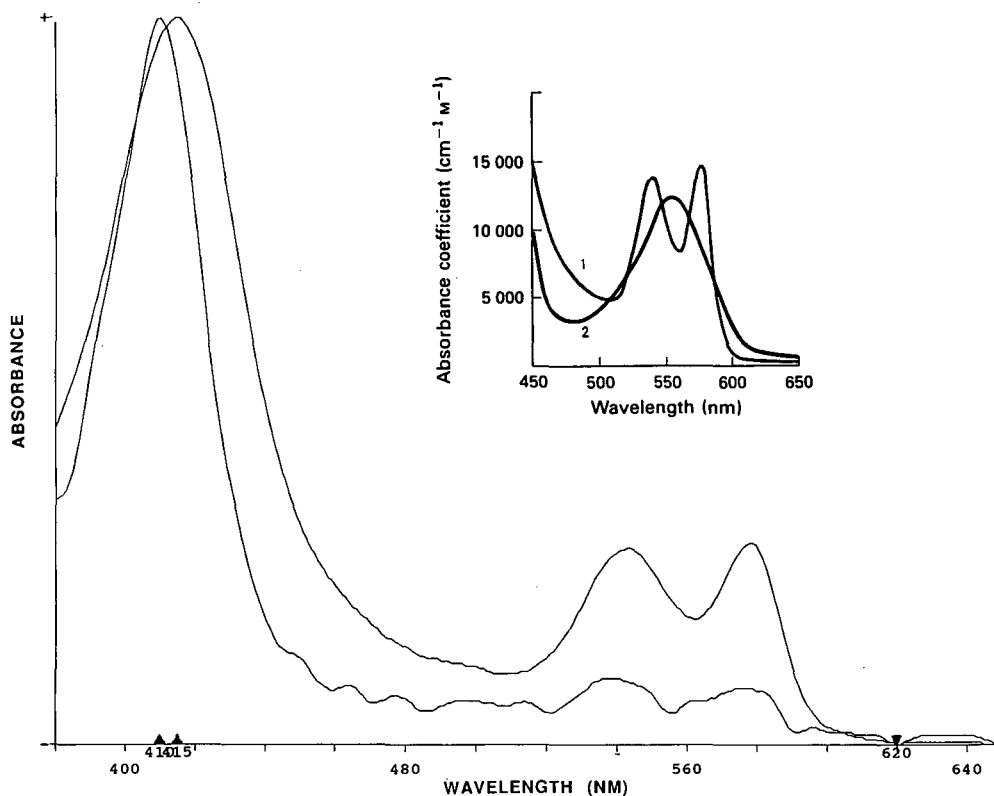


Fig. 6. Visible spectra of hemoglobin A (major peak in Fig. 1A) and minor component (first peak in Fig. 1A). Inset shows spectra of oxyhemoglobin (1) and deoxyhemoglobin (2) for reference.

points of separated proteins. Using scanning detection in the UV region above 280 nm, spectral data can be used to distinguish different components. For example, the spectra of hemoglobin A and two minor peaks exhibit different absorbance maxima

in the 300-360 nm region, suggesting structural differences for these species (Fig. 5).

The strong absorbance of the heme group in the visible region enables high-sensitivity detection of hemoglobins; the absorbance of hemoglobin A at

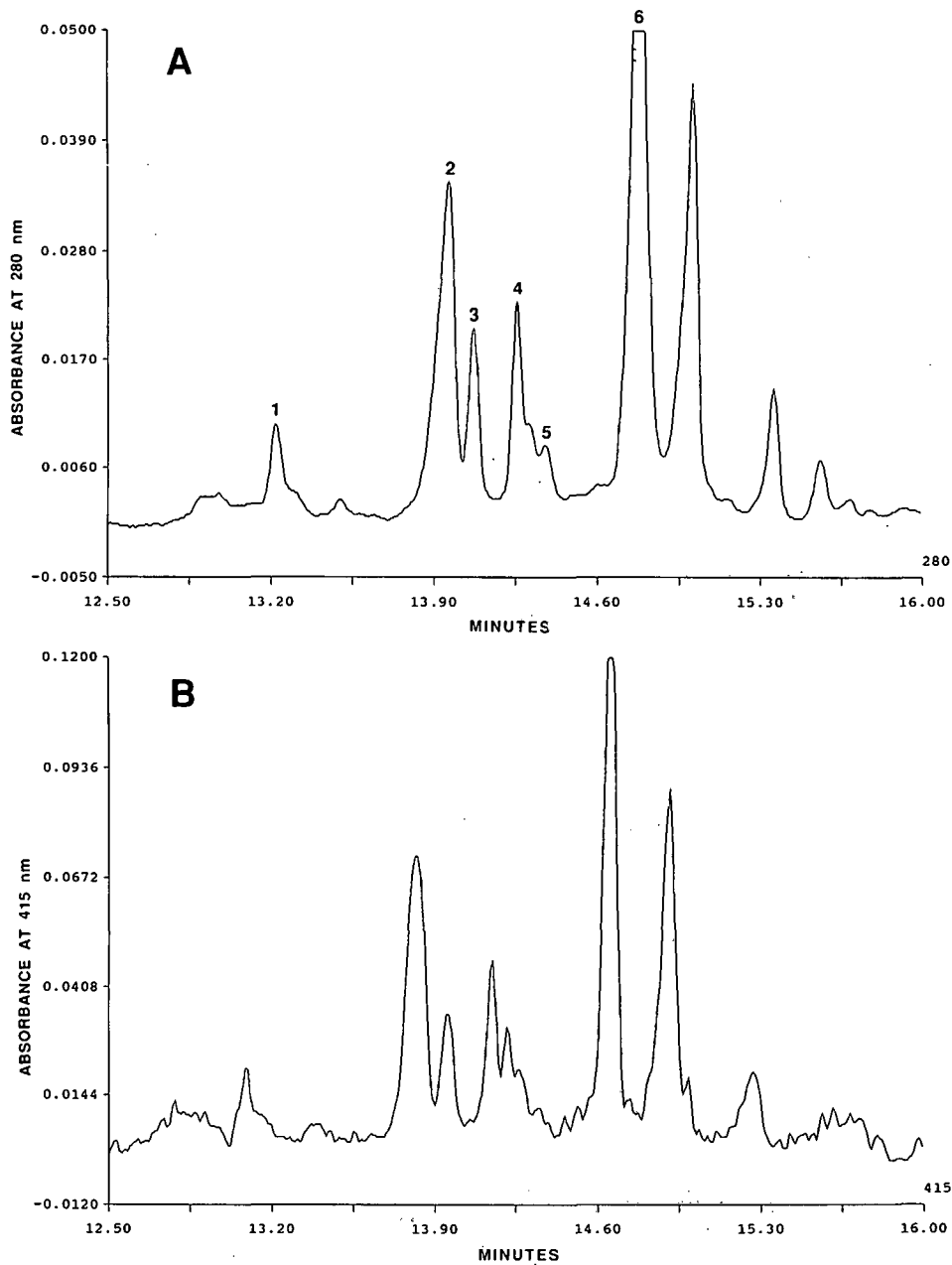


Fig. 7

415 nm is 2.7-fold greater than at 280 nm. Moreover, there is no interference from non-heme proteins at this wavelength. The shape of the hemoglobin visible spectrum depends upon the oxidation state of the heme-bound iron and the presence of

bound oxygen, and this information can be extracted from spectra acquired during the separation. For example, the spectrum of oxyhemoglobin exhibits two maxima at 542 and 578 nm, while the deoxyhemoglobin spectrum shows a single maximum at 550

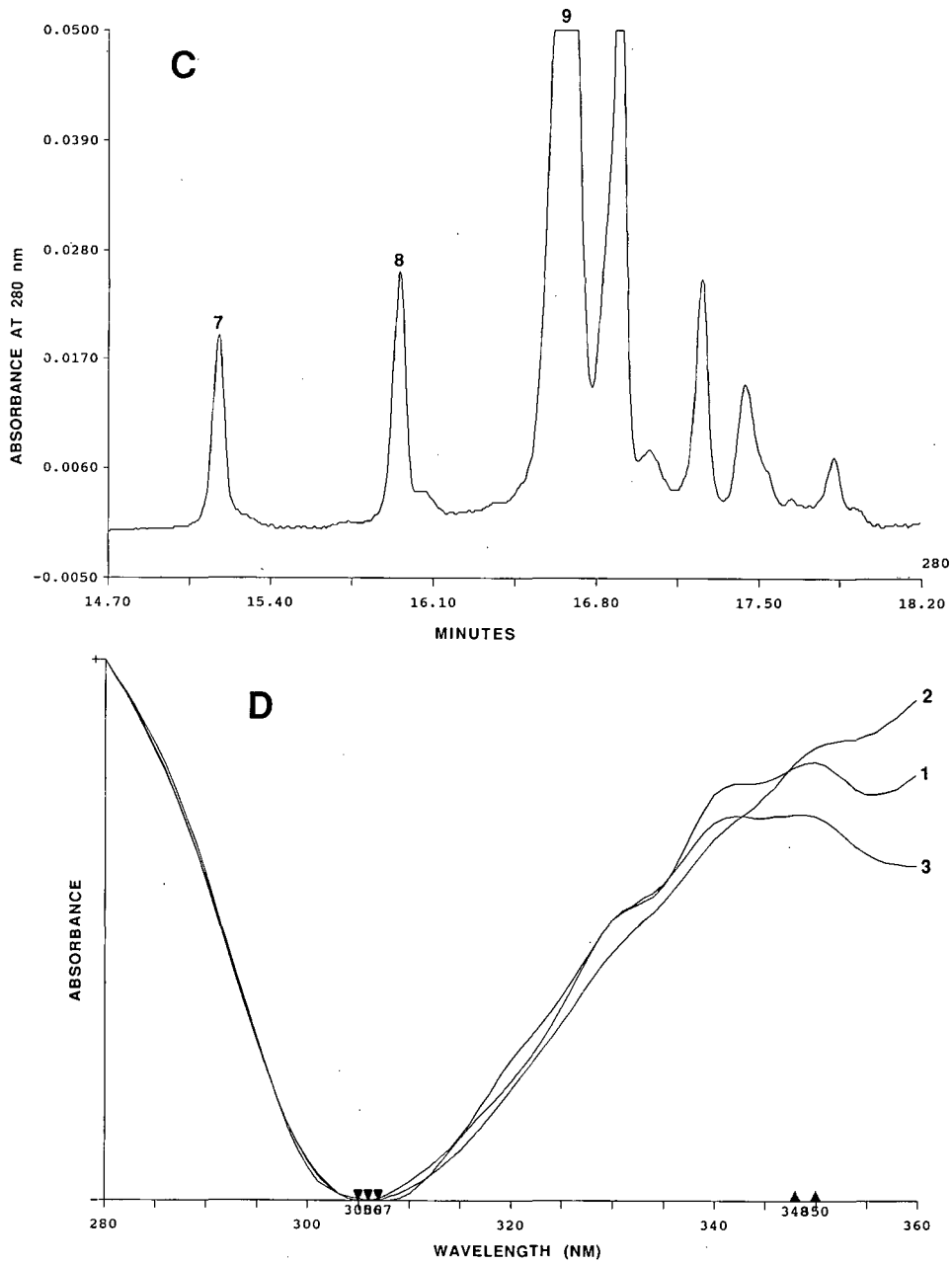


Fig. 7.

(Continued on p. 233)



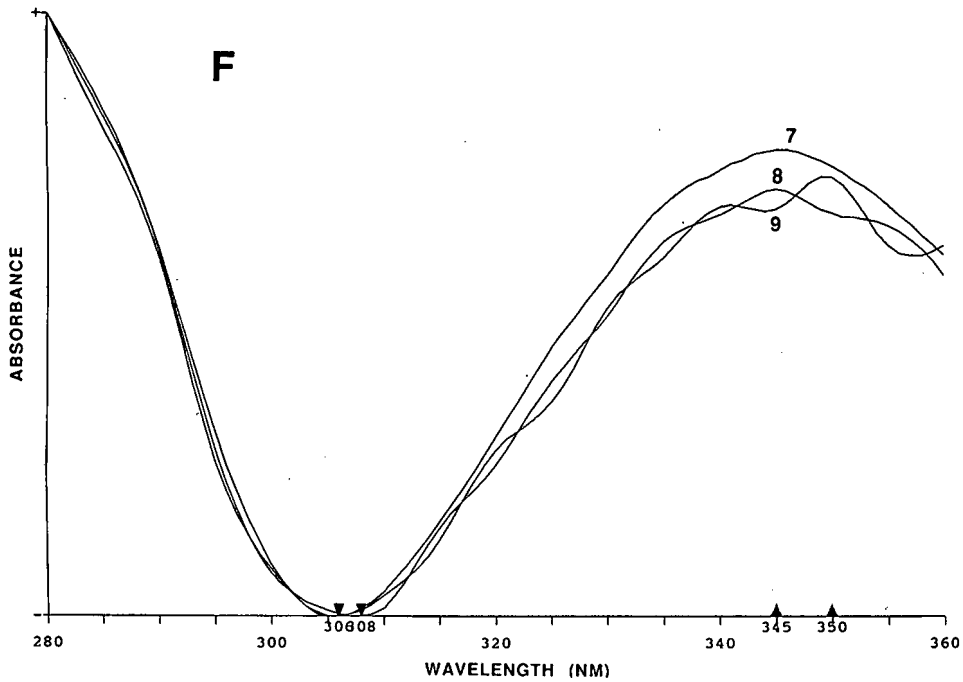
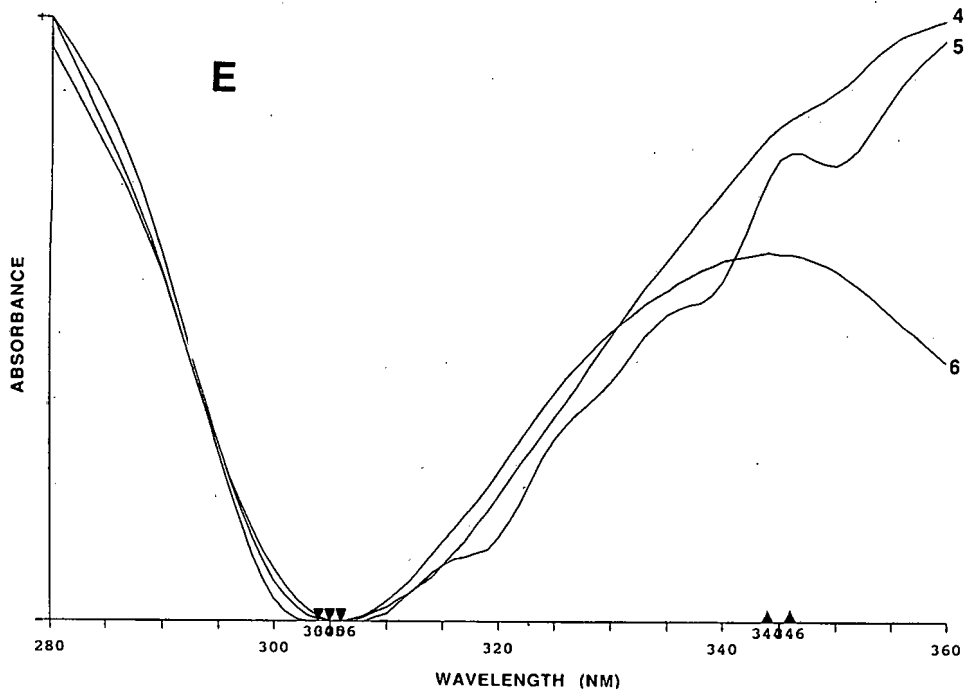


Fig. 7. Capillary isoelectric focusing of hemoglobin reference standard (containing hemoglobins C, S, F and A) using (A) detection at 280 nm, (B) detection at 415 nm, (C) detection at 280 nm following treatment of sample with 0.1% KCN. (D-F) UV spectra of peaks 1-9.

nm. Inspection of the visible spectra in Fig. 6 indicates that both the major peak and the minor peak in Fig. 1A contain primarily oxyhemoglobin.

Separation of a commercial reference standard containing hemoglobins A, F, S and C shows several minor components using detection at 280 nm (peak 1, 3 and 5 in Fig. 7A). The UV spectra of the major and minor peaks (Fig. 7D and 7E) exhibit significant differences, suggesting that they are structurally different. The electropherogram obtained with detection at 415 nm (Fig. 7B) shows the same pattern of peaks as Fig. 7A, indicating that the minor peaks are also heme-containing proteins. It is well known that hemoglobin can exist in a variety of complexed states, for example oxyhemoglobin, deoxyhemoglobin, carboxyhemoglobin, etc. Cyanide ion binds tightly to the hemoglobin molecule, and treatment with potassium cyanide converts all species to cyanohemoglobin. In the electro-

pherogram obtained after treatment of the sample with KCN (Fig. 7C) most of the minor peaks have disappeared, and the UV spectra of the separated components are similar (Fig. 7F). These results suggest that several of the minor components are different complexed states of the four major hemoglobins.

#### Free zone capillary electrophoresis of globin chains

Globin chains prepared by treatment of hemoglobins with acidic acetone could be resolved by free zone capillary electrophoresis under denaturing conditions (Fig. 8). Generally UV adsorption of proteins is greater at 200 nm than at longer wavelengths. However, the presence of urea in the electrophoresis buffer at high concentration introduces a high background absorbance below 210 nm. Therefore 210 nm was the best wavelength for detection of globin chains (Fig. 9). These separations

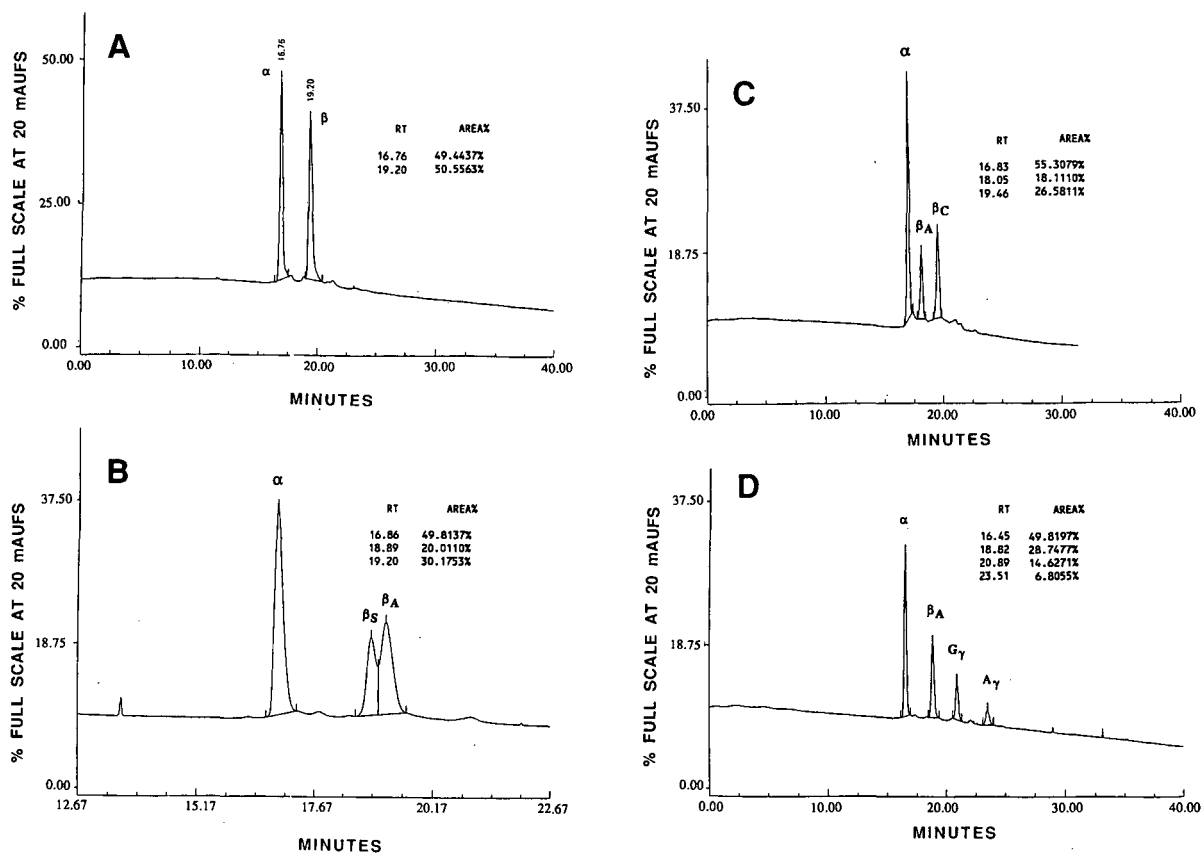


Fig. 8. Free zone electrophoresis of globin chains derived from (A) hemoglobin A, (B) hemoglobins A and S, (C) hemoglobins A and C, and (D) hemoglobins A and F. RT = Retention time in min.

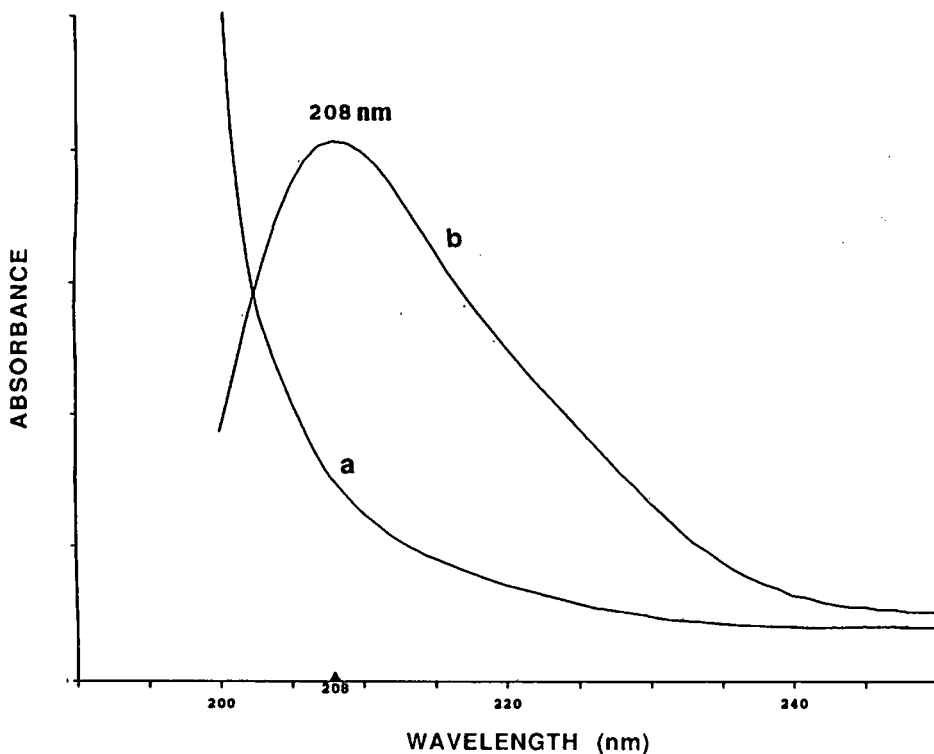


Fig. 9. UV spectra of (a) free zone electrophoresis buffer (100 mM sodium phosphate, pH 3.2, + 0.1% reduced Triton X-100 + 7 M urea), and (b)  $\alpha$ -globin in electrophoresis buffer.

were performed at pH 3.2 using positive (inlet) to negative (detector) polarity. Even though the buffer pH is well below the pK of the side-chain carboxylic acid group of glutamic acid, the substitution of valine for glutamic acid in hemoglobin S changes the mass-to-charge ratio of the  $\beta_S$  globin chain relative to  $\beta_A$  sufficiently to permit partial resolution of these globin chains (Fig. 8B). Replacement of glutamic acid by lysine in hemoglobin C results in sufficient gain in charge to allow baseline resolution of  $\beta_C$  from  $\beta_A$  (Fig. 8C).

Electrophoresis of globin chains derived from adult hemoglobin A and fetal hemoglobin F resolves the  $G\gamma$  and  $A\gamma$  globins from  $\beta_A$  and from each other (Fig. 8D). These two molecules differ by the occurrence of glycine and alanine in position 136 of the  $\gamma$  chain, respectively. A comparison of the areas of these two peaks indicates the two chains are present in a ratio of 68%  $G\gamma$ :32%  $A\gamma$ , which is close to the 75:25 ratio typical of fetal blood [1].

## CONCLUSIONS

Due to the high solubility of hemoglobins, excellent results can be obtained in the separation of hemoglobin variants using cIEF. The technique provides high resolution, reproducible separation patterns, and analysis times of less than 20 min. Absorbance detection in the visible region is highly sensitive and free of interferences from non-heme proteins. High-speed scanning detection in either the visible or UV region enables acquisition of additional information on separated hemoglobins. Following denaturation of the hemoglobin tetramer into monomers with 7 M urea, free globin chains can be analyzed by capillary zone electrophoresis.

While the methods described in this study may not be rapid enough to compete with cation-exchange HPLC for high-throughput screening for hemoglobin disorders, capillary electrophoresis offers several advantages as a secondary or confirma-

tory technique. These include high-resolution separations with selectivities complimentary to HPLC, automation and quantitative analysis.

#### ACKNOWLEDGEMENTS

The authors thank Ken Dobra, Susan P. Perrine and Yuxin Jin for many useful discussions during the course of this work.

#### REFERENCES

- 1 H. F. Bunn and B. G. Forget, *Hemoglobin: Molecular, Genetic and Clinical Aspects*, W. B. Saunders, Philadelphia, PA, 1986.
- 2 V. F. Fairbanks (Editor), *Hemoglobinopathies and Thalassemias, Laboratory Methods and Case Studies*, Brian C. Dekker, New York, 1980.
- 3 S. J. Loomis, M. Go, L. Kupeli, D. J. Bartling, and S. R. Binder, *Am. Clin. Lab.*, October (1990).
- 4 S. Hjertén, *J. Chromatogr.*, 347 (1985) 191.
- 5 M. Zhu, R. Rodriguez and T. Wehr, *J. Chromatogr.*, 559 (1991) 479.



# Attachment of a single fluorescent label to peptides for determination by capillary zone electrophoresis

Jian Ying Zhao, Karen C. Waldron, Jean Miller, Jian Zhong Zhang, Heather Harke and Norman J. Dovichi

Department of Chemistry, University of Alberta, Edmonton, Alberta T6G 2G2 (Canada)

## ABSTRACT

Complicated electropherograms are produced in the separation of fluorescently labeled peptides. Incomplete labeling of  $\epsilon$ -amino groups on lysine residues results in the production of  $2^n - 1$  reaction products, where  $n$  is the number of  $\alpha$  and  $\epsilon$  amino groups in the peptide. A single label is attached to the peptide by first taking the peptide through one cycle of the Edman degradation reaction. All  $\epsilon$ -amino groups are converted to the phenyl thiocarbamyl and the cleavage step exposes one  $\alpha$ -amino group at the N-terminus of the peptide; the fluorescent label is attached to the N-terminus.

## INTRODUCTION

Capillary zone electrophoresis is a particularly powerful technique for the separation and analysis of complex protein mixtures [1]. To avoid column overloading, only small amounts of dilute sample can be introduced onto the capillary without degrading the separation efficiency. For example, injection of 1 nl of a  $10^{-6}$  M protein solution corresponds to the introduction of 1 fmol of protein. Conventional ultraviolet absorbance detection is problematic at low femtomole sample loading. Universal detection, for example based on refractive index gradient detection, is useful in the analysis of unlabeled peptides [2]. Again, detection limits are in the low femtomole range. Alternatively, postcolumn derivatization may be used to label proteins for fluorescent detection, albeit with limited sensitivity and degraded separation efficiency [3,4].

Fluorescence detection provides outstanding detection limits for capillary electrophoresis. Labeled amino acids and DNA sequencing fragments may be detected at the low to sub-zptomole level [5]. While

precolumn fluorescent labeling is useful in amino acid and DNA analysis, it is not always useful in peptide analysis. The difficulty is straightforward: protein labeling reactions inevitably rely on reagents that attack the  $n$ -terminal  $\alpha$ -amino group. Simultaneously, the  $\epsilon$ -amino group associated with lysine residues will also react. Unfortunately, most fluorescent labels are bulky and labeling does not go to completion. The labeling reaction produces a complex mixture of products, corresponding to attachment of different numbers of labels at different sites [6]. Each of the reaction products has slightly different migration rate, giving rise to a complicated and uninterpretable electropherogram.

The number of possible reaction products may be calculated from simple combinatorial analysis. If there is no lysine residue, there is only one possible reaction product, that labeled at the N-terminal amino group. If there is one lysine group, there are three possible labeled products: one labeled only at the N-terminal  $\alpha$ -amino group, one labeled only at the lysine  $\epsilon$ -amino, and one with both sites labeled. If there are  $n$  primary amino groups that can be labeled, then there are

$$\sum_{m=1}^n \frac{(n)!}{m!(n-m)!} = 2^n - 1$$

Correspondence to: Dr. N. J. Dovichi, Department of Chemistry, University of Alberta, Edmonton, Alberta T6G 2G2, Canada.

different labeled products possible. For peptides and proteins with more than a few primary amino groups, the number of reaction products becomes very large. A peptide with three primary amino groups has seven possible labeled reaction products while a protein with 10 primary amino groups has 1023 possible products. Analysis of a mixture of peptides that are incompletely labeled is not practical; instead of observing a single peak for each peptide, many tens or hundreds of peaks are observed for each peptide and protein.

To ensure that only the N-terminus amino group is labeled, the peptide may be taken through one cycle of the Edman degradation reaction before the labeling reaction. This method first treats the sample with phenyl isothiocyanate (PITC), the classic Edman degradation reagent [7]. PITC is relatively small and efficiently reacts under basic conditions with all primary and secondary amines present in the protein. Under acidic conditions, the N-terminal amino acid is cleaved, exposing an unreacted primary amine. This peptide, now truncated by one residue, may be labeled with an appropriate fluorescent (or chromophoric) reagent. We chose to use fluorescein isothiocyanate as the labeling reagent, but other isothiocyanates or sulphonyl halides could be used. The product of the reaction is the peptide with the original N-terminal amino acid removed, with all  $\epsilon$ -amino lysine groups converted to the phenyl thiocarbonyl, and with a single fluorescent label at the N-terminus of the truncated peptide.

#### EXPERIMENTAL

Peptide 8656 (Peninsula Labs., Belmont, CA, USA) has a primary structure Arg–Lys–Arg–Ala–Arg–Lys–Glu. A  $10^{-4}$  M solution was prepared in a 0.2 M pH 9.2 borate buffer. The fluorescein derivative was prepared by mixing 100  $\mu$ l of  $4.7 \cdot 10^{-4}$  M fluorescein isothiocyanate (FITC; Molecular Probes, Eugene, OR, USA) solution prepared in acetone with 100  $\mu$ l of the peptide solution. The reaction proceeded at room temperature in the dark for 8 h.

The manual Edman degradation procedure was similar to that of Edman and Henschen [8]. Approximately 2 mg of the peptide were dissolved in 1 ml buffer in a stoppered glass test tube; the buffer was 0.4 M triethylamine (Anachemica, Montreal, Canada) in 1-propanol–water (3:2, v/v), adjusted to

pH 9.6 with 1 M trifluoroacetic acid (TFA) (Sigma, St. Louis, MO, USA). A 50- $\mu$ l volume of PITC (Sigma) was added to the peptide solution, the tube was flushed with nitrogen and incubated at 55°C for 20 min in a water bath with occasional agitation. The solution was extracted with five 2-ml aliquots of benzene with centrifugation to separate the phases. The benzene layers were discarded and the aqueous layer was freeze dried. The residue was extracted three times with 0.5-ml aliquots of ethyl acetate (Caledon Labs., Georgetown, Canada). The ethyl acetate had been passed through an alumina column and filtered before use. The ethyl acetate extract was dried under a stream of nitrogen. A 100- $\mu$ l volume of anhydrous TFA (Protein Sequencing Grade, Sigma) was added and the solution was incubated at 40°C for 15 min in a water bath with occasional agitation. The residue was dried under vacuum for about 10 min. A 3-ml volume of 1,2-dichloroethane (Caledon Labs.) was added and the solution was centrifuged to separate the layers. The dichloroethane layer was discarded, and 1 ml more dichloroethane was added. The residue was macerated with a glass stirring rod. The mixture was centrifuged and the dichloroethane layer was discarded. The aqueous layer was dried under vacuum and stored in a desiccator at 4°C until further use.

The dried, truncated peptide was dissolved in 1.00 ml of a 0.2 M pH 9.2 borate buffer, with concentration *ca.*  $10^{-5}$  M. To label the truncated peptide, 10  $\mu$ l of  $4.7 \cdot 10^{-4}$  M FITC solution prepared in acetone was mixed with 100  $\mu$ l of the truncated peptide solution. The reaction proceeded for 8 h in the dark at room temperature. Solutions were diluted to  $10^{-6}$  M with 5 mM borate buffer before injection.

The capillary electrophoresis system was identical to that described before [9]. A 44 cm  $\times$  50  $\mu$ m I.D. capillary was used for the separation. The separation buffer was 5 mM pH 9.2 borate buffer. Samples were injected for 5 s at 2 kV; separation proceeded at 13 kV.

#### RESULTS AND DISCUSSION

The primary structure of this peptide is Arg–Lys–Arg–Ala–Arg–Lys–Glu. The peptide used in this example has two lysine residues in addition to the N-terminal arginine residue. When labeled with

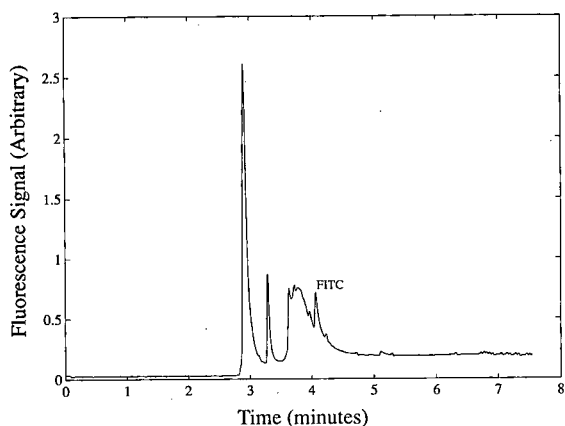


Fig. 1. Capillary zone electrophoresis separation of fluorescein thiocarbamyl derivative of peptide 8656. Peak labeled FITC is the unreacted derivatization reagent.

FITC, a total of seven fluorescent products are possible. The separation of the labeled peptide is shown in Fig. 1. In addition to the unreacted FITC peak, there are at least seven peaks present, corresponding to the different products of the labeling reaction. Comparison with the electropherogram for the single label peptide suggests that the second peak in this electropherogram contains a single label at the  $\alpha$ -amino group. The relatively close spacing of the other peaks is not surprising. Conversion of the

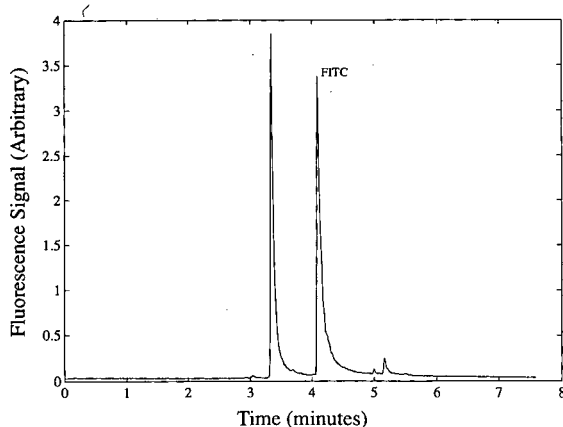


Fig. 2. Capillary zone electrophoresis separation of fluorescein thiocarbamyl derivative of treated peptide 8656. The peptide had been treated with one cycle of a manual Edman degradation; the peptide is truncated by one residue compared with Fig. 1. Peak labeled FITC is the unreacted derivatization reagent.

$\epsilon$ -amino to the phenyl thiocarbamyl derivative increases the size of the peptide slightly but should not change its charge; each positively charged thiocarbamyl replaces a positively charged  $\epsilon$ -amino group.

If the peptide is taken through one cycle of the Edman degradation reaction, the N-terminal amino acid is removed; the primary structure of the truncated peptide is Lys-Arg-Ala-Arg-Lys-Glu. In the Edman degradation step, the amino-containing side chains of the lysine residues are converted to the  $\epsilon$ -phenyl thiocarbamyl derivative. By protecting the  $\epsilon$ -amino group and cleaving the N-terminal amino acid, only one amine is available for further labeling. The reaction product shows two peaks (Fig. 2), one corresponding to the labeled peptide and the other to unreacted fluorescein isothiocyanate. The Edman treatment appears to be quite efficient; no peaks corresponding to multiple labeling are detected.

A small impurity is noted in the reaction product, with an elution time of about 5.25 min. This impurity was undetectable for the labeled native peptide because of the complex reaction mixture. However, by ensuring that only one label is attached to the peptide, the electropherogram is simplified so that the minor contaminant can be detected.

## CONCLUSION

Precolumn fluorescent labeling is convenient for high-sensitivity peptide analysis in capillary electrophoresis. When precolumn derivatization is employed, incomplete multiple labeling is problematic, producing a complicated mixture from a single analyte. A single label can be attached to the peptide by first taking the peptide through one cycle in the Edman degradation reaction; because of its small size and high reactivity, phenyl isothiocyanate quickly and efficiently labels all free amino groups in the peptide. All  $\epsilon$ -amino groups on lysine residues are converted to the  $\epsilon$ -phenyl thiocarbamyl, and cannot partake in the labeling reaction; only the N-terminal amino group is available for further labeling.

As a limitation to this technology, only unblocked peptides can be labeled. N-Terminal acetylated peptides do not have a free  $\alpha$ -amino group. While various chemical unblocking procedures, such as cyanogen bromide cleavage, can be employed, they



can produce a number of reaction products, defeating the purpose of this labeling protocol. Also, the procedure removes the N-terminal amino acid; two peptides that differ only at the N-terminal amino acid will be indistinguishable after this labeling procedure.

This reaction was performed by use of the manual Edman reaction at relatively high concentration. It would be much more efficient to use an automated protein sequencer to perform this reaction; picomoles of protein could be prepared at  $10^{-8}$  M concentration for fluorescent labeling [10]. However, the sequencer must be modified to allow facile recovery of the treated peptide; a strong solvent could be used to remove the peptide from a Polybrene treated solid-phase sequencing disk.

Last, this reaction was demonstrated with PITC as the protecting reagent and fluorescein isothiocyanate as the labeling reagent. It may prove possible to use smaller protecting reagents, such as methyl isothiocyanate, which should react more quickly than PITC. Other fluorescent reagents could be used. As always, the labeling chemistry should be chosen to provide a good match to the excitation source [11]. As an attractive reagent, the 3-(4-carboxybenzoyl)-2-quinolinecarboxaldehyde derivative absorbs strongly in the blue and appears to react quickly with primary amines [6].

#### ACKNOWLEDGEMENTS

This work was funded by the Natural Sciences and Engineering Research Council of Canada, and by unrestricted grants from Pharmacia/LKB and Millipore/Waters. J.Y.Z. and H.R.H. acknowledge predoctoral fellowships from the Alberta Heritage Foundation for Medical Research. J.M. acknowledges an undergraduate research fellowship and N.J.D. acknowledges a Steacie fellowship from the Natural Sciences and Engineering Research Council.

#### REFERENCES

- 1 J. W. Jorgenson and K. D. Lukacs, *Science (Washington, D.C.)*, 222 (1983) 266.
- 2 T. McDonnell and J. Pawliszyn, *J. Chromatogr.*, 559 (1991) 489.
- 3 D. J. Rose and J. W. Jorgenson, *J. Chromatogr.*, 447 (1988) 117.
- 4 S. L. Pentony, X. Huang, D. S. Burgi and R. N. Zare, *Anal. Chem.*, 60 (1988) 2625.
- 5 Y. F. Cheng and N. J. Dovichi, *Science (Washington, D.C.)*, 242 (1988) 562.
- 6 J. Liu, Y. Z. Hsieh, D. Wiesler and M. Novotny, *Anal. Chem.*, 63 (1991) 408.
- 7 P. Edman, *Arch. Biochem. Biophys.*, 22 (1949) 475.
- 8 P. Edman and A. Henschen, in S. B. Needleman (Editor), *Protein Sequence Determination*, Springer, Berlin, 2nd ed., 1975, pp. 232–279.
- 9 S. Wu and N. J. Dovichi, *J. Chromatogr.*, 480 (1989) 141.
- 10 P. Tempst and L. Riviere, *Anal. Biochem.*, 183 (1989) 290.
- 11 J. Gluckman, D. Shelly and M. Novotny, *J. Chromatogr.*, 317 (1984) 443.

# Analysis of antiepileptic drugs in human plasma using micellar electrokinetic capillary chromatography

Kong-Joo Lee and Gwi Suk Heo

Organic Analytical Laboratory, Korea Research Institute of Standards and Science, P.O. Box 3, Daejosi, Daeduk Science Town 305-606 (South Korea)

Nam Jung Kim and Dong Cheul Moon

College of Pharmacy, Chungbuk National University, Cheongju 306-763 (South Korea)

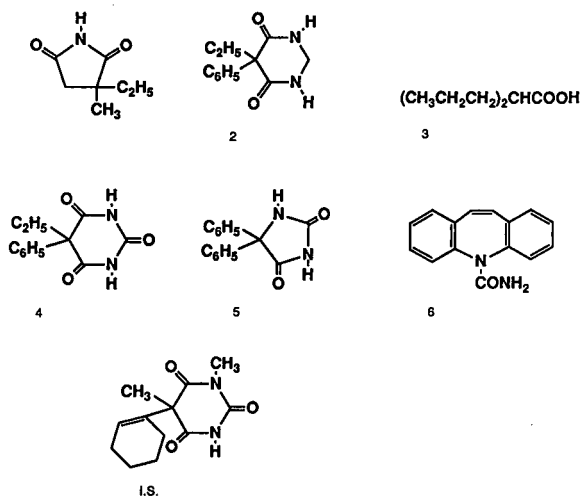
## ABSTRACT

We describe a method for the simultaneous determination of antiepileptic drugs (ethosuccimide, phenytoin, primidone, phenobarbital, carbamazepine and valproic acid) by micellar electrokinetic capillary chromatography using sodium dodecyl sulphate as the micellar phase. Factors affecting the micellar electrokinetic separation were studied for the quantitative determination of these drugs in human plasma. The confirmation of the peaks and the specificity of the method were investigated by combining multiwavelength detection with micellar electrokinetic capillary chromatography.

## INTRODUCTION

Measurements of many drugs in body fluids are important for therapeutic drug monitoring. For nearly 15 years the antiepileptics (Fig. 1) have been monitored in the plasma of patients, since a good correlation between their blood concentrations and clinical responses has been demonstrated and life-long multiple-drug therapy is necessary. Monitoring their concentrations in the body fluid, especially in plasma, is therefore essential for the optimization of pharmacotherapy. Analytical methods for the quantitation of antiepileptic drugs developed considerably in the late 1970s and early 1980s [1-3]. Recently immunological methods have become attractive for routine clinical monitoring during chronic therapy because of their ease of performance, speed of analysis and sensitivity. However,

immunoassays analyse only one drug at a time, have a limited sensitivity for quantitation of drugs



Correspondence to: Dr. K.-J. Lee, Organic Analytical Laboratory, Korea Institute of Standards and Science, P.O. Box 3, Daejosi, Daeduk Science Town 305-606, South Korea.

Fig. 1. Chemical structure of antiepileptic drugs. 1 = Ethosuccimide; 2 = primidone; 3 = valproic acid; 4 = phenobarbital; 5 = phenytoin; 6 = carbamazepine; I.S. = hexobarbital.

following a single dose, do not measure metabolites, and in some cases are subject to problems with cross-reactive interferences. Chromatographic methods are still utilized as the standard reference methods for the antiepileptic drugs. High-performance liquid chromatographic (HPLC) methods have been applied for the determination of all antiepileptic drugs. However, they still require a relatively high level of analytical skill and are relatively high-cost procedures.

As newly developed analytical methods, capillary electrophoresis and micellar electrokinetic capillary chromatography (MECC) are perceived to be attractive tools for the analysis of pharmaceuticals because of their high separation efficiency, easy operation and low running cost [4–10]. MECC, first developed by Terabe *et al.* [11], utilized the same instrumental set-up as capillary electrophoresis except that it employs the micellar solution as the electrophoretic medium. Selective partitioning of the analytes into the micellar phase as a pseudo stationary phase causes them to migrate at rates different from their electrophoretic mobility. The analytes in MECC can be separated on the basis of either the hydrophobicity or the ionic character of solutes. Separation depending on the hydrophobicity of the solutes in MECC can be performed by varying the micellar concentration, which has similar effects to changing in the surface structure in HPLC (*e.g.* changing from C<sub>8</sub> to C<sub>18</sub>). Early work by Otsuka *et al.* [12] demonstrated the use of MECC for the analysis of neutral aromatic compounds. Applications of MECC have rapidly expanded to include neutral and charged molecules combining electrophoresis and chromatography.

In spite of the high resolution of capillary electrophoresis, the problem of identifying peaks in the electropherogram remains to be solved. Capillary electrophoresis–mass spectrometry (CE–MS) is developing in many laboratories [13–15] for this purpose. Because of the technical difficulties and high cost of MS, the alternative method using multiwavelength detection with a photodiode-array detector is a suitable technique for monitoring in HPLC [16] and has recently been applied to capillary electrophoresis [10,17–20]. It allows the collection of absorption spectra of each peak in the electropherogram, and permits peak confirmation and determination of peak purity by comparison with

standard absorption spectra. The purpose of this report is to describe the factors affecting separation of antiepileptic drugs with MECC, quantification with this method and identification of patient samples using a multiwavelength UV detector.

## EXPERIMENTAL

### Chemicals

The antiepileptic drugs phenytoin (PHT), phenobarbital (PB), primidone (PRM), carbamazepine (CBZ), ethosuccinimide (ESM) and valproic acid (VPA) and sodium dodecyl sulphate (SDS) were purchased from Sigma (St. Louis, MO, USA). Sodium phosphate dibasic and sodium phosphate monobasic were from DukSan (Kyungkido, South Korea). Ethyl acetate was HPLC grade from Junsei (Japan). Human sera were obtained as lyophilized form SRM 909 from the National Institute of Science and Technology (NIST, Gaithersburg, MD, USA).

### Capillary electrophoresis apparatus

Both commercial and laboratory-made capillary electrophoresis systems were used. The commercial instrument was a Model 270A capillary electrophoresis system (Applied Biosystems, Foster City, CA, USA). For the experiments, a fused-silica capillary (Polymicro Technologies, Phoenix, AZ, USA), 72 cm (50 cm to detector) × 50 μm I.D., was used as a separation column. On-column UV detection was measured at 210 nm, and the temperature of the column chamber was kept constant at 30°C unless specified otherwise. A D-502A integrator (Young-In Scientific, Seoul, South Korea) was used for recording the electropherograms and for quantification by peak area measurements. Prior to each run, the capillary was rinsed with 0.1 M sodium hydroxide and running buffer by the built-in vacuum system at 508 mmHg for 3–5 min. The capillary was filled with running buffer, mainly 50 mM SDS in 25 mM phosphate buffer (pH 8.0). The samples were introduced by the same vacuum system for 2.0 s.

The laboratory-made capillary electrophoresis system was constructed in a similar way to that described previously [21]. A high-voltage power supply (0–40 kV, Glassman, Whitehouse Station, NJ, USA; Model PS/EH 40R 2.5 CTZR) was used to drive the electrophoretic process across the capil-

lary. The platinum wires connected to the anode and the cathode of the power supply were immersed in 3-ml buffer chambers. This system was isolated in a Plexiglas box for operator safety. A longer capillary with the same I.D. as the commercial instrument was used as a separation tube. Detection was performed by on-column measurement of UV absorption by a Linear Model 206HR variable-wavelength detector (Reno, NV, USA) which is controlled with the 206 SOFT software. Throughout the work the Model 206 detector was employed in the high-speed polychrome mode by scanning from 195 to 320 nm at 5-nm intervals.

#### Sample preparation

Standard stock solutions of each antiepileptic drug (1 mg/ml) were prepared in methanol, and a standard model mixture composed of six drugs (ESM, PRM, PB, VPA, PHT and CBZ) was prepared by diluting the standard stock solution with doubly distilled water to a certain concentration (7–100  $\mu\text{g/ml}$ ). Drug concentrations in human serum (NIST SRM 909) spiked with six antiepileptics and hexobarbital as an internal standard and in the plasma of patients treated with one of the antiepileptics were determined. Sample extractions were performed using ethyl acetate as described previously [22]. A 100- $\mu\text{l}$  aliquot of standard solution, spiked serum or patient plasma was added to 900  $\mu\text{l}$  of ethyl acetate in a glass tube. A known concentration of hexobarbital (15  $\mu\text{g/ml}$ ) was used as an internal standard. After vigorous vortex-mixing and centrifugation at 2060  $g$  for 2 min, 500  $\mu\text{l}$  of the organic layer were transferred to a conical glass tube, evaporated to dryness under a gentle stream of nitrogen gas and reconstituted with 50  $\mu\text{l}$  of 5% methanol in distilled water. This reconstituted sample was injected for capillary electrophoresis.

## RESULTS AND DISCUSSION

#### Optimization of MECC separation

Since antiepileptic drugs have wide spectrum of physical properties (solubility and  $pK_a$  values) [23], factors affecting the separation were investigated to determine the optimum separation conditions. The pH and micellar concentration of the running buffer mainly affect the resolution of solutes. When the pH was varied from 6.0 to 8.0 with 25 mM phos-

phate buffer containing 50 mM SDS, the migration times of six solutes stayed constant above pH 6.4. The migration time of the solutes increased with increasing SDS concentration, the degree of increase depending on the hydrophobicity of the molecules. The hydrophobic molecules CBZ and PHT show a dramatic increase in migration time depending on SDS concentration, and are followed by PB, PRM, ESM and VPA. This trend is consistent with previous findings by Terabe *et al.* [11]. The capacity factor,  $k'$ , defined and described previously [11], was calculated from the retention times of methanol as a neutral marker and Sudan III as a micelle marker depending on SDS concentration (Fig. 2). The capacity factors of all solutes except VPA increased linearly with increasing SDS concentration up to 80 mM SDS, which indicates that hydrophobic interaction between solute and micelle is the main interaction in the separation. However, negatively charged VPA, which is constant over the various SDS concentrations, is separated based on its

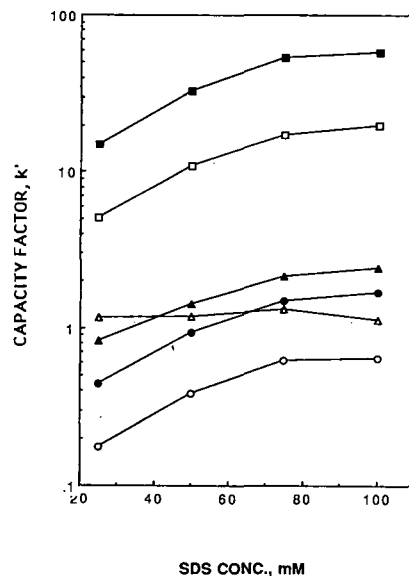


Fig. 2. Effect of SDS concentration of  $k'$  using a standard mixture of antiepileptics. Conditions: an Applied Biosystem capillary electrophoresis system was used with running buffer (25 mM phosphate buffer containing various concentration of SDS at pH 7.0). Detection at 210 nm, run at 30 kV at 30°C in a 50  $\mu\text{m}$  I.D. capillary. Symbols: ○ = ethosuccinimide; ● = primidone; △ = valproic acid; ▲ = phenobarbital; □ = phenytoin; ■ = carbamazepine.

electrophoretic mobility and does not interact with the micelle.

For the quantitative analysis of solutes by MECC, the reproducibility of the migration and peak area is important. Temperature is a crucial factor in the reproducibility. In this experiment, ambient temperature was kept constant.

With the optimization of the resolution and the separation time, the running conditions chosen were 25 mM phosphate buffer containing 50 mM SDS at 30°C with 30 kV applied voltage. Under these conditions, the antiepileptic drugs with capacity factors ranging from 0.2 (ESM) to 40 (CBZ) were well resolved in less than 13 min. With electrophoresis, antiepileptics and the internal standard all exhibited symmetrical peaks (Fig. 3). Fig. 3A shows

a typical chromatogram for the drug standard without extraction [VPA and ESM (125 µg/ml each), PHT, PRM and hexobarbital (15 µg/ml each), PB (10 µg/ml) and CBZ (7 µg/ml)]. No interfering peak was observed when the blank human serum spiked with internal standard hexobarbital was extracted with ethyl acetate and analysed (Fig. 3B). When the same standard drug mixture as in Fig. 3A was spiked in human serum and extracted with ethyl acetate as described in the Experimental section, the peak of volatile VPA completely disappeared and the ESM peak was remarkably reduced (Fig. 3C). This indicates that the extraction procedure is not appropriate for the quantitative analysis of VPA and ESM. Fig. 3D–F shows electropherograms of the plasma of a patient taking PB, PHT and CBZ as

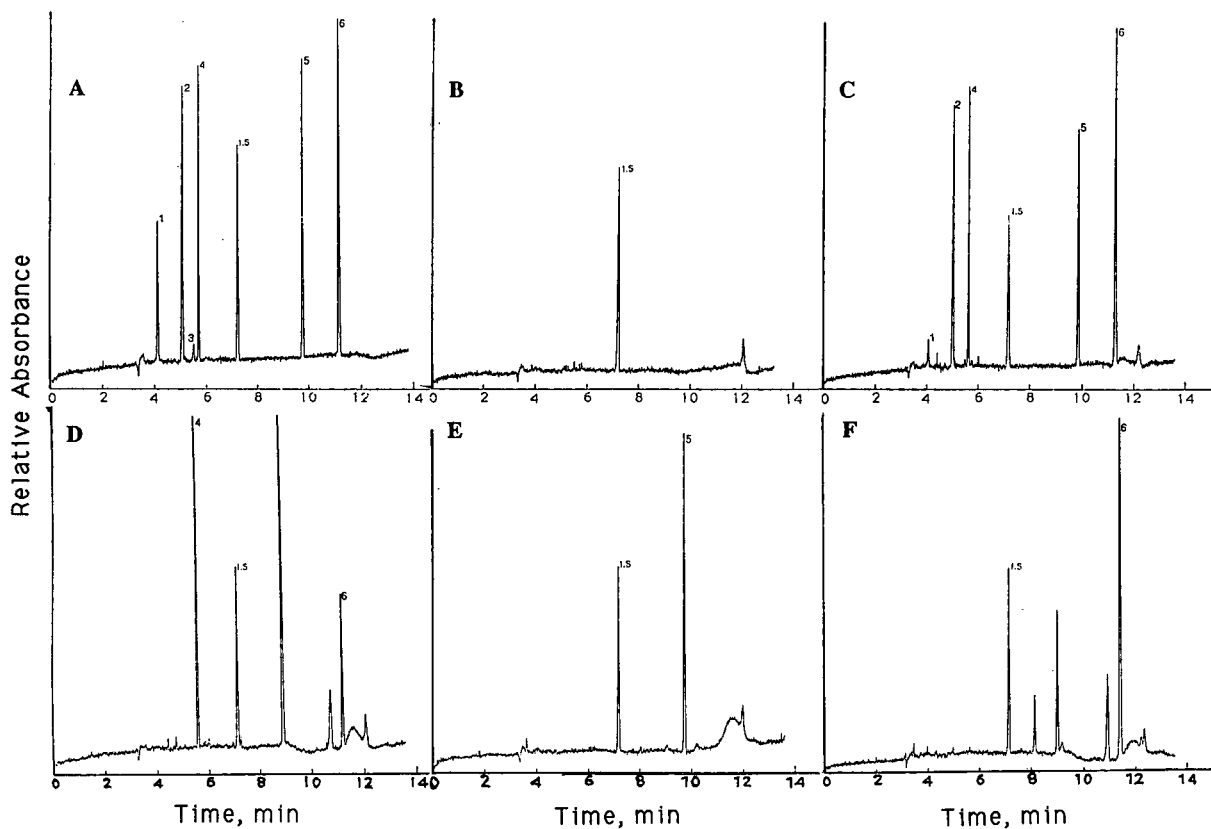


Fig. 3. Electropherograms obtained from (A) a standard mixture of ethosuccimide (1), primidone (2), valproic acid (3), phenobarbital (4), hexobarbital (internal standard, I.S.), phenytoin (5) and carbamazepine (6) without extraction; (B) extracted blank human serum spiked with internal standard; (C) extracted human serum spiked with antiepileptics and internal standard; (D–F) extracted plasma from an epileptic patient taking phenobarbital (D), phenytoin (E) or carbamazepine (F). Conditions were the same as in Fig. 2 except the SDS concentration was 50 mM.

confirmed by immunoassay. Fig. 3D, from a patient taking PB, shows the extra peaks which were not detected in the other patient taking PB. This indicates that the extra peaks might be the other medications. Human plasma from a patient taking PHT shows clear peaks of PHT and hexobarbital (Fig. 3E). However, electropherograms from two patients taking CBZ show the same pattern (Fig. 3F). The extra peaks besides CBZ and hexobarbital in Fig. 3F are presumed to be the metabolites of CBZ, *i.e.* carbamazepine-10, 11-diol and carbamazepine-10,11-epoxide. Further studies should be performed to identify metabolites.

To confirm the peak and check the peak purity, a Linear Model 206HR variable-wavelength detector, which permits automatic recording of the spectra of the peaks during analysis, was used. The three-dimensional electropherograms depicted in Fig. 3 represent the absorbance *vs.* retention time

*vs.* wavelength relationships for human serum spiked with antiepileptics (Fig. 4C) and the plasma of a patient taking PB (Fig. 4D), PHT (Fig. 4E) or CBZ (Fig. 4F). The retention times in Fig. 4 are higher than those in Fig. 3 because in this case the laboratory-made capillary system with a longer capillary than that used in Fig. 3 was used with a multiwavelength UV detector. The absorption spectrum of each peak can be extracted from the gathered data points as a so-called time slice using detector software. The absorption spectra between 195 and 320 nm of the peak, which are assumed to be PB (Fig. 5D), PHT (Fig. 5E) or CBZ (Fig. 5F) as in Fig. 4D–F are compared with those of standard drug (Fig. 5d–f). The excellent agreement between standard and sample indicates that MECC separation of these drugs in human plasma is not subjected to interference by other components in plasma, and multiwavelength scanning of peak permits a quick and reliable confirmation of the drugs.

TABLE I  
REPRODUCIBILITY OF RETENTION TIME AND PEAK AREA OF ANTIEPILEPTICS

Values are mean  $\pm$  S.D. ( $n = 5$ ); values in parentheses are coefficients of variation (%).

Compound	Concentration ( $\mu\text{g/ml}$ )	Retention time (min)	Relative peak area
Ethosuccimide	25	4.45 $\pm$ 0.01 (0.10)	0.25 $\pm$ 0.01 (4.71)
	75	4.41 $\pm$ 0.14 (0.33)	0.58 $\pm$ 0.04 (8.27)
	100	4.44 $\pm$ 0.01 (0.32)	1.03 $\pm$ 0.06 (6.30)
	200	4.41 $\pm$ 0.01 (0.08)	1.84 $\pm$ 0.08 (2.54)
Primidone	5	5.47 $\pm$ 0.01 (0.16)	0.53 $\pm$ 0.03 (5.81)
	20	5.39 $\pm$ 0.01 (0.10)	1.46 $\pm$ 0.03 (2.41)
	30	5.45 $\pm$ 0.02 (0.38)	2.21 $\pm$ 0.03 (1.59)
	40	5.42 $\pm$ 0.01 (0.35)	2.80 $\pm$ 0.03 (1.31)
Phenobarbital	5	6.03 $\pm$ 0.01 (0.20)	0.54 $\pm$ 0.01 (2.57)
	20	5.87 $\pm$ 0.01 (0.16)	1.79 $\pm$ 0.03 (1.93)
	40	5.82 $\pm$ 0.01 (0.29)	3.57 $\pm$ 0.10 (2.94)
	60	5.98 $\pm$ 0.03 (0.52)	5.15 $\pm$ 0.09 (1.86)
Phenytoin	5	10.58 $\pm$ 0.03 (0.28)	1.04 $\pm$ 0.01 (1.52)
	20	10.40 $\pm$ 0.01 (0.16)	3.51 $\pm$ 0.14 (4.12)
	30	10.39 $\pm$ 0.05 (0.50)	3.13 $\pm$ 0.07 (2.46)
	40	10.55 $\pm$ 0.05 (0.55)	2.96 $\pm$ 0.06 (2.11)
Carbamazepine	5	12.09 $\pm$ 0.03 (0.32)	1.77 $\pm$ 0.01 (0.39)
	20	11.88 $\pm$ 0.02 (0.19)	6.13 $\pm$ 0.23 (3.82)
	30	11.81 $\pm$ 0.06 (0.53)	9.90 $\pm$ 0.39 (4.01)
	40	12.10 $\pm$ 0.06 (0.53)	13.23 $\pm$ 0.32 (1.32)

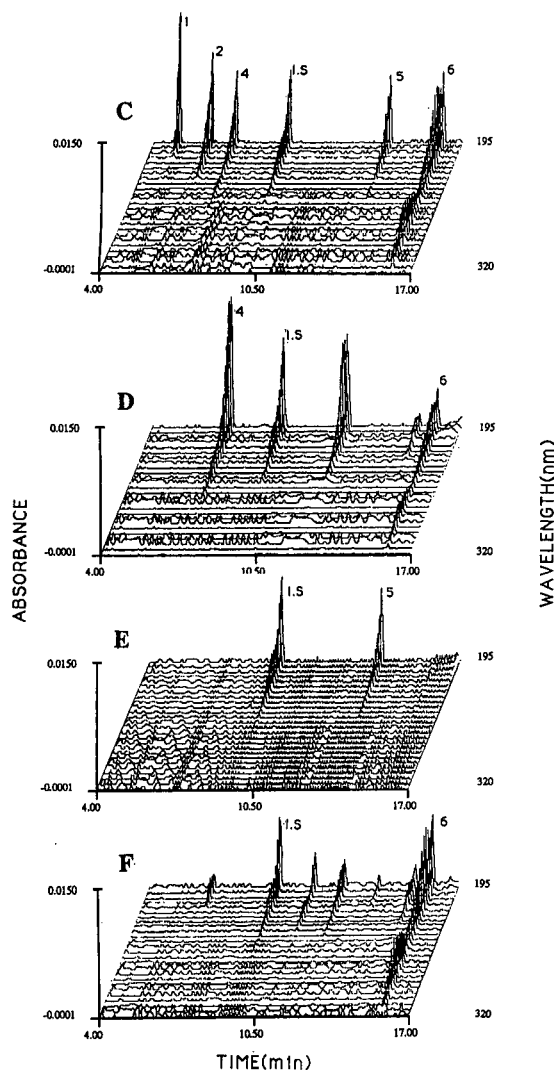


Fig. 4. Three-dimensional electropherograms of the same samples as in Fig. 3C–F. Conditions are the same as in Fig. 3 except that a laboratory-made capillary electrophoresis system with a variable-wavelength detector and a longer capillary column that that used in Fig. 3 was utilized.

#### Analytical variables

**Precision.** We assessed the precision of the method by repeated analyses of plasma specimens containing known concentrations of the drugs being investigated. As shown in Table I, the coefficients of variation (C.V.s) for within-day precision of retention time are less than 0.5% and those of peak area

are less than 4%, except for ESM, whose C.V.s vary from 2.5 to 8.27%.

**Recovery.** The absolute analytical recovery from plasma of the five drugs was measured by adding a known concentration of drugs and internal standard to drug-free plasma, as shows in Table II. This plasma was then analysed by our method. Absolute recoveries were calculated from the drug to internal standard peak-area ratio. The recoveries of PRM, PB, PHT and CBZ were 93–106% and those of ESM 77–92%, while the recovery of VPA was impossible to measure because of its volatility.

**Linearity and sensitivity.** Concentration and peak area ratio correlated linearly with each other for the

TABLE II  
RECOVERY OF ANTIEPILEPTICS DURING THE ANALYTICAL PROCEDURE

Values are mean  $\pm$  S.D. ( $n = 5$ ); values in parentheses are coefficients of variation (%)

Compound	Concentration ( $\mu\text{g/ml}$ )	Recovery (%)
Ethosuccimide	25	77.09 $\pm$ 7.98 (10.35)
	50	89.64 $\pm$ 9.85 (10.99)
	75	85.76 $\pm$ 7.05 (8.22)
	100	90.38 $\pm$ 6.99 (7.73)
	200	92.91 $\pm$ 7.64 (8.22)
Primidone	5	98.62 $\pm$ 8.11 (8.22)
	10	107.03 $\pm$ 5.69 (5.31)
	20	91.05 $\pm$ 2.85 (3.13)
	30	106.52 $\pm$ 5.64 (5.30)
	40	93.19 $\pm$ 1.71 (1.84)
Phenobarbital	5	94.21 $\pm$ 2.87 (3.05)
	10	105.72 $\pm$ 4.25 (4.02)
	20	94.01 $\pm$ 5.81 (6.20)
	40	106.65 $\pm$ 4.92 (4.61)
	60	97.82 $\pm$ 3.96 (4.05)
Phenytoin	5	97.28 $\pm$ 3.73 (3.83)
	10	98.70 $\pm$ 4.89 (4.95)
	20	93.05 $\pm$ 7.14 (7.67)
	30	81.01 $\pm$ 6.88 (8.49)
	40	68.17 $\pm$ 8.27 (12.14)
Carbamazepine	5	93.49 $\pm$ 3.21 (3.44)
	10	98.58 $\pm$ 4.65 (4.72)
	20	93.90 $\pm$ 4.33 (4.61)
	30	102.63 $\pm$ 3.84 (3.75)
	40	93.39 $\pm$ 2.75 (2.95)

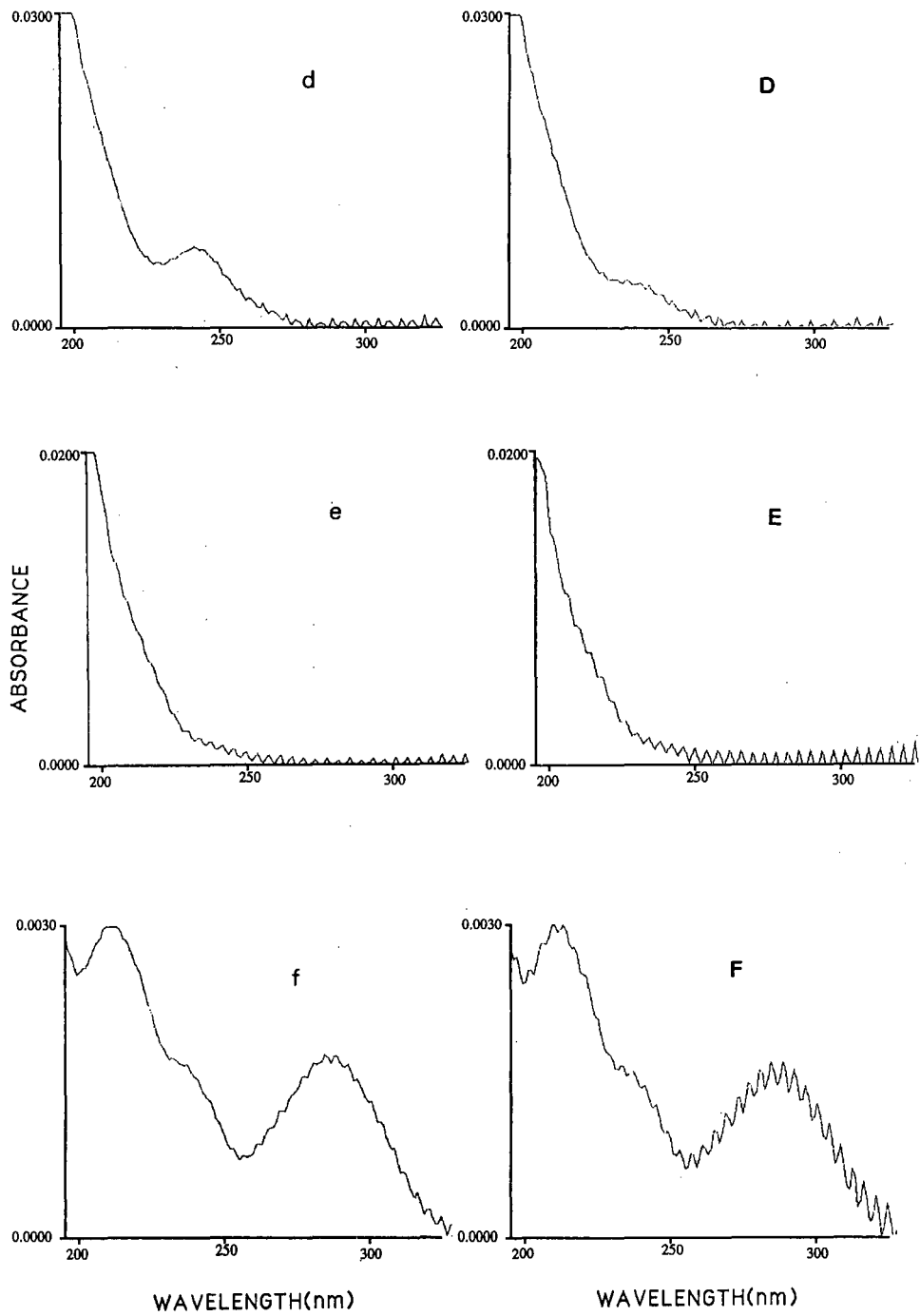


Fig. 5. Normalized time slices of (D) phenobarbital, (E) phenytoin and (F) carbamazepine of the data in Fig. 4 are compared with standard phenobarbital (d), phenytoin (e) and carbamazepine (f).



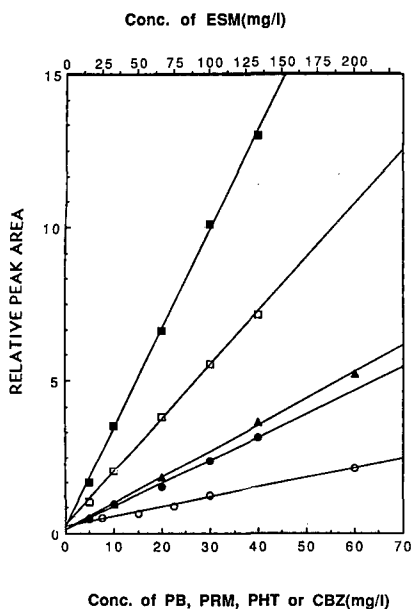


Fig. 6. Calibration curves for ethosuccimide (○), primidone (●), phenobarbital (▲), phenytoin (□) and carbamazepine (■) in a standard mixture.

drugs examined in Fig. 6. Detection ranges are reasonable for the monitoring of the therapeutic concentration.

**Interference.** To determine the potential clinical usefulness of the method, we examined the absorption spectra of the peak and compared then with the standard sample in Fig. 5. None of components in plasma showed potential interference with the method.

In conclusion, the monitoring of antiepileptic drugs in human plasma with MECC is demonstrated. Identification of solutes was performed by characterizing the sample peak in terms of the retention time and absorption spectra. Capillary electrophoresis with multiwavelength detection is a new and powerful technique for confirmation of the analysis. The detection methodology and the quantitative analysis data prove the feasibility of the method for the monitoring of the drugs in body fluids.

#### ACKNOWLEDGEMENTS

The authors acknowledge the valuable contribution of Dr. J. W. Park, Chungnam National University Hospital, for the generous gifts of patient samples. This work was sponsored by the fund from Korea Ministry of Science and Technology.

#### REFERENCES

- 1 J. T. Burke and J. P. Thenot, *J. Chromatogr.*, 340 (1985) 199.
- 2 I. M. Kapetanovic, *J. Chromatogr.*, 531 (1990) 421.
- 3 A. Fazio, E. Perucca and F. Pisani, *J. Liq. Chromatogr.*, 13 (1990) 3711.
- 4 M. C. Roach, P. Gozel and R. N. Zare, *J. Chromatogr.*, 426 (1988) 129.
- 5 D. Swaik, D. Burton, A. Balchunas and M. Sepaniak, *J. Chromatogr. Sci.*, 26 (1988) 406.
- 6 T. Nakagawa, Y. Oda, A. Shibukawa and H. Tanaka, *Chem. Pharm. Bull.*, 36 (1988) 1622.
- 7 T. Nakagawa, Y. Oda, A. Shibukawa, H. Fukuda and H. Tanaka, *Chem. Pharm. Bull.*, 37 (1989) 707.
- 8 H. Nishi, T. Fukuyama, M. Matsuo and S. Terabe, *J. Chromatogr.*, 513 (1990) 279.
- 9 H. Nishi, T. Fukuyama and M. Matsuo, *J. Chromatogr.*, 515 (1990) 245.
- 10 W. Thormann, P. Meier, C. Marcolli and F. Binder, *J. Chromatogr.*, 545 (1991) 445.
- 11 S. Terabe, K. Otsuka and T. Ando, *Anal. Chem.*, 56 (1984) 111.
- 12 K. Otsuka, S. Terabe and T. Ando, *J. Chromatogr.*, 348 (1985) 39.
- 13 E. D. Lee, W. Mueck, J. D. Henion and T. R. Covey, *J. Chromatogr.*, 545 (1991) 445.
- 14 C. G. Edmonds, J. A. Loo, C. J. Barinaga, H. R. Udseth and R. D. Smith, *J. Chromatogr.*, 474 (1989) 21.
- 15 R. D. Smith, H. R. Udseth, C. J. Barinaga and C. G. Edmonds, *J. Chromatogr.*, 559 (1991) 197.
- 16 M. Hayashida, M. Nihira, T. Watanabe and K. Jinno, *J. Chromatogr.*, 506 (1990) 133.
- 17 S. Kobayashi, T. Ueda and M. Kikumoto, *J. Chromatogr.*, 480 (1989) 179.
- 18 J. Vindevogel, P. Sanda and L. C. Verhagen, *J. High. Resolut. Chromatogr.*, 13 (1990) 295.
- 19 P. Wernly and W. Thormann, *Anal. Chem.*, 63 (1991) 2878.
- 20 K.-J. Lee, G. S. Heo and H. J. Doh, *Clin. Chem.*, (1992) in press.
- 21 J. W. Jorgenson and K. D. Lukacs, *Science*, 222 (1983) 266.
- 22 U. Juergens, *J. Liq. Chromatogr.*, 10 (1987) 507.
- 23 A. C. Moffat (Editor), *Clarkes Isolation and Identification of Drugs*, Pharmaceutical Press, London, 1986.

# Confirmation testing of 11-nor- $\Delta^9$ -tetrahydrocannabinol-9-carboxylic acid in urine with micellar electrokinetic capillary chromatography

Paul Wernly and Wolfgang Thormann

Department of Clinical Pharmacology, University of Berne, Murtenstrasse 35, CH-3010 Berne (Switzerland)

---

## ABSTRACT

The major urinary metabolite of the most commonly abused psychotropic drug,  $\Delta^9$ -tetrahydrocannabinol, is 11-nor- $\Delta^9$ -tetrahydrocannabinol-9-carboxylic acid (THC-COOH). With basic hydrolysis, extraction and concentration, this compound can easily be determined using micellar electrokinetic capillary chromatography with on-column multi-wavelength detection. After solid-phase extraction of 5 ml of urine, drug concentrations down to about 10 ng/ml can be unambiguously monitored. Peak assignment is achieved through comparison of the retention time and absorption spectrum of the eluting THC-COOH peak with those of computer-stored model runs. The effectiveness of the approach is demonstrated with data obtained from urine samples from different patients which tested positively for cannabinoids using a fluorescence polarization immunoassay.

---

## INTRODUCTION

The major psychoactive compound in *Cannabis sativa* (marijuana),  $\Delta^9$ -tetrahydrocannabinol (THC), is highly lipophilic and is therefore accumulated in tissues rich in lipids. Its release from the tissues is slow and its concentration in urine is low. The major metabolite, 11-nor- $\Delta^9$ -tetrahydrocannabinol-9-carboxylic acid (THC-COOH), is excreted in urine predominantly in its glucuronated form and can be detected up to about 10 weeks after smoking or oral ingestion of cannabis products [1]. THC-COOH is the target substance employed in screening methods for cannabinoids, such as the enzyme multiplied immunoassay technique (EMIT), fluorescence polarization immunoassay (FPIA) and radioimmunoassays (RIA). Owing to the lack of specificity of these techniques, positive results should be confirmed in order to eliminate any false-

positive answer that may have resulted from the initial screening process. For that purpose specimens are typically first hydrolysed under basic conditions and free THC-COOH is then extracted employing bonded-phase technology prior to analysis with a highly specific method, including thin-layer chromatography (TLC) [2,3], high-performance liquid chromatography (HPLC) [4,5] or gas chromatography-mass spectrometry (GC-MS) [6].

Recently, micellar electrokinetic capillary chromatography (MECC), an interface between electrophoresis and chromatography, was found to be an attractive approach for the analysis of urinary barbiturates [7], drugs of abuse and/or their metabolites, including opioids, benzoylecgonine (metabolite of cocaine), amphetamines and methaqualone in human urine [8], and illicit substances, including those in illicit seizure samples [9]. The objectives of the work described in this paper were to investigate different bonded-phase adsorption clean-up procedures for subsequent determination of THC-COOH using MECC with on-column, fast-scanning polychrome UV absorption detection and to

---

Correspondence to: Dr. W. Thormann, Department of Clinical Pharmacology, University of Berne, Murtenstrasse 35, CH-3010 Berne, Switzerland.

use this MECC method to confirm the presence of THC-COOH in urine samples which tested FPIA positive for cannabinoids.

## EXPERIMENTAL

### *Chemicals, origin of samples and drug screening*

All chemicals were of analytical-reagent or research grade. Deuterated THC-COOH {[5'-<sup>2</sup>H<sub>3</sub>]-9-carboxy-11-nor- $\Delta^9$ -tetrahydrocannabinol dissolved in ethanol (100  $\mu$ g/ml); Research Triangle Institute, Research Triangle Park, NC, USA} served as a standard compound. Urine samples were collected in our routine drug assay laboratory where they were received for drug screening. Our own urine was employed as a blank matrix. The samples were screened for the presence of cannabinoids using FPIA on a TDx analyser (Abbott Laboratories, North Chicago, IL, USA) and stored at 4°C until further analysis. The FPIA test contains THC-COOH for calibration in the range 0–135 ng/ml (six points). Samples which gave a response equal to or higher than 20 ng/ml were interpreted as positive. The detection limit of the immunoassay is 10 ng/ml.

### *Electrophoretic instrumentation and running conditions*

The instrument with multi-wavelength detection employed was described previously [7,8]. Briefly it featured a ca. 90 cm  $\times$  75  $\mu$ l I.D. fused-silica capillary (Product TSP/075/375, Polymicro Technologies, Phoenix, AZ, USA) together with a Model UVIS 206 PHD fast-scanning multi-wavelength detector with a No. 9550-0155 on-column capillary detector cell (both from Linear Instruments, Reno, NV, USA) towards the capillary end. The effective separation distance was 70 cm. A constant voltage of 20 kV was applied using an HCN 14-20000 power supply (FUG Elektronik, Rosenheim, Germany). The cathode was on the detector side.

Samples were applied manually via gravity by lifting the anodic capillary end, dipped into the sample vial ca. 34 cm for a specified time interval (typically 5 s). Multi-wavelength data were read, evaluated and stored employing a Mandax AT 286 computer system and running the 206 detector software package version 2.0 (Linear Instruments) with windows 286 version 2.1 (Microsoft, Redmont, WA, USA). Conditioning for each experiment was

done by rinsing the capillary with 0.1 M NaOH for 3 min and with buffer for 5 min. Throughout this work the Model 206 detector was employed in the high-speed polychrome mode by scanning from 195 to 320 nm at 5-nm intervals (26 wavelengths). A buffer composed of 75 mM sodium dodecyl sulphate (SDS), 6 mM Na<sub>2</sub>B<sub>4</sub>O<sub>7</sub> and 10 mM Na<sub>2</sub>HPO<sub>4</sub> (pH ca. 9.1) was employed.

### *Sample pretreatment*

Standard solutions of THC-COOH were prepared by evaporation of the ethanol and reconstitution in methanol or running buffer at a concentration of 100  $\mu$ g/ml. Blank urine was spiked by addition of known aliquots of these solutions to the urine. Glucuronated THC-COOH in samples from patients was hydrolysed under basic conditions (see below) and free THC-COOH was extracted from urine using disposable Bond Elut THC (1211-3044; sorbent amount 500 mg, reservoir volume 10 ml), Bond Elut Certify (1211-3050, 130 mg, 10 ml) and Bond Elut Certify II (1211-3051, 200 mg, 10 ml) solid-phase cartridges from Analytichem International (Harbor City, CA, USA) and also Clean Screen THC (CSTHC101, 100 mg, 1 ml) from Worldwide Monitoring (Horsham, PA, USA). For all types of columns a Vac Elut set-up (Analytichem International) served as a cartridge holder and vacuum manifold for sample extraction. No extended drying periods of the sorbents were applied and no derivatization of eluted THC-COOH was undertaken.

*Bond Elut THC.* These columns were applied according to the procedures reported by Bourquin and Brenneisen [4], Willson *et al.* [2] and Duc [3]. In all three instances the eluate was evaporated to dryness under a gentle stream of nitrogen at room temperature and the residue was dissolved in 100  $\mu$ l of running buffer.

*Bond Elut Certify.* The procedure employed is a modification of the manufacturer's recommendation. For hydrolysis 0.3 ml of 10 M KOH was added to 5 ml of urine, vortex-mixed for about 10 s, heated at 50–60°C for 20 min (with constant mixing) and cooled to room temperature. Thereafter 3 ml of 50 mM phosphoric acid were added and the pH was adjusted to 3 with concentrated HCl. The Bond Elut Certify cartridges were conditioned immediately prior to use by passing sequentially 2 ml

of methanol and an equal volume of 50 mM phosphoric acid through the columns. The vacuum was turned off as soon as the acid solution reached the sorbent bed to prevent column drying. The hydrolysed and vortex-mixed specimen was then applied and drawn slowly (1–2 ml/min) through the cartridge. The column was sequentially rinsed with 9 ml of 50 mM phosphoric acid and 3 ml of 50 mM phosphoric acid–methanol (80:20). The vacuum (about 10 mmHg for 15–20 s) was turned off as soon as the last drop of the aqueous solution had fully penetrated the column. A rinse with 1 ml of hexane followed (about 5 mmHg for 10–15 s and no complete drying of the sorbent bed) prior to a slow elution (*ca.* 1 ml/min) with 1 ml of hexane–ethyl acetate (80:20) into a test-tube. The eluate was evaporated to dryness under a gentle stream of nitrogen at room temperature and the residue was dissolved in 100  $\mu$ l running buffer.

**Bond Elut Certify II.** Very low recoveries were obtained using the manufacturer's instructions, so the procedure was modified. For hydrolysis 0.3–0.5 ml of 10 M KOH was added to 5 ml of urine, vortex-mixed and heated at 50–60°C for 15 min with stirring. A 2-ml volume of 0.1 M sodium acetate buffer (pH 7) containing 5% methanol was added and the pH was adjusted to 6.5 with concentrated HCl. The Bond Elut Certify II cartridges were conditioned immediately prior to use by passing sequentially 2 ml of methanol and an equal volume of 0.1 M sodium acetate buffer (pH 7) containing 5% methanol. The vacuum was turned off in time to prevent column drying. The hydrolysed and vortex-mixed specimen was then applied and drawn slowly (1–2 ml/min) through the cartridge. The column was rinsed with 10 ml of methanol–water (1:1). The vacuum (about 10 mmHg for 15–20 s) was turned off as soon as the last drop of the aqueous solution had fully penetrated the column. A rinse with 2 ml of ethyl acetate followed by an applied vacuum of about 5 mmHg for 15–20 s (no drying under full vacuum). Elution was effected slowly (1–2 ml/min) with 2 ml of hexane–ethyl acetate (75:25) containing 1% acetic acid into a test-tube. The eluate was then evaporated to dryness under a gentle stream of nitrogen at room temperature and the residue was dissolved in 100  $\mu$ l of running buffer.

**Clean Screen THC.** Hydrolysis and extraction were executed in a slightly modified way as recom-

mended by the manufacturer of the cartridges. For hydrolysis 0.1 ml of 10 M KOH was added to 5 ml of urine, vortex-mixed and heated at 50–60°C for 20 min with constant mixing. Thereafter the pH was adjusted to 3 with concentrated HCl. The cartridges were conditioned immediately prior to use by passing sequentially 3 ml of methanol and an equal volume of water through the columns. The vacuum was turned off as soon as the fluid reached the sorbent bed to prevent column drying. The hydrolysed and vortex-mixed specimen was then applied and drawn slowly (1–2 ml/min) through the cartridge. The column was sequentially rinsed with 2 ml of water and 2 ml of 0.1 M HCl–acetonitrile (70:30). The vacuum (about 10 mmHg for about 15 s) was turned off as soon as the last drop of the aqueous solution had fully penetrated the column. A rinse with 0.2 ml of hexane followed, prior to a slow elution (*ca.* 1 ml/min) with 2 ml of hexane–ethyl acetate (50:50) into a test-tube. The eluate was then evaporated to dryness under a gentle stream of nitrogen at room temperature and the residue was dissolved in 100  $\mu$ l of running buffer.

#### Recovery

The recovery after sample pretreatment was determined by comparing the MECC peak heights after extraction with those obtained by direct injection of equal amounts of THC-COOH dissolved in methanol.

#### RESULTS AND DISCUSSION

With the experimental conditions used in this work THC-COOH was found to elute after  $23.1 \pm 0.4$  min. Fig. 1 depicts (A) the three-dimensional electropherogram and (B) the absorption spectrum extracted as a normalized spectrum from the gathered data and referred to as the so-called time slice for THC-COOH. For MECC with on-column UV absorption detection, sample concentrations have to be at least on the  $\mu$ g/ml ( $\mu$ M) concentration level [7], which is uncommon for THC-COOH in human urine [1–6]. For direct urine injection, this sensitivity limit is not as good as that of the commonly used immunological screening methods. Therefore, extraction and concentration of THC-COOH are crucial for its confirmation by MECC.

The use of four different disposable solid-phase

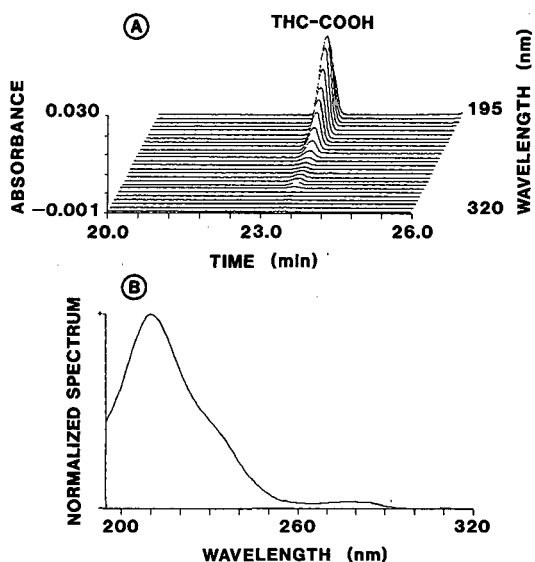


Fig. 1. (A) Three-dimensional MECC electropherogram of THC-COOH and (B) extracted, normalized absorption spectrum at 23.4 min. The sample was 100  $\mu\text{g/ml}$  of THC-COOH dissolved in running buffer. The applied voltage was a constant 20 kV and the current was *ca.* 80  $\mu\text{A}$ .

extraction columns was investigated. First Bond Elut THC cartridges containing a bonded-phase silica gel were employed according to three proce-

dures reported in the literature [2–4]. The MECC analysis of the extracts obtained with blank urine spiked with 200 ng/ml of THC-COOH provided very simple and clean electropherograms (Fig. 2A). The compound of interest was recovered, but the extraction efficiencies were found to be of the order of only 10%. No work was undertaken to try to optimize the use of this column type because the recovery was much improved with the Clean Screen THC columns which contain a proprietary bonded silica sorbent with mixed-mode properties, a hydrophobic and ion-exchange copolymer [10]. With this approach (5 ml of urine and final reconstitution in 100  $\mu\text{l}$  of SDS buffer) the extraction efficiency was always at the  $80 \pm 10\%$  level, allowing the determination of THC-COOH concentrations in urine as low as 30 ng/ml. Although the electropherograms were found to be more complex than with Bond Elut THC (Fig. 2A and B) THC-COOH eluted free from interferences. Fig. 2C and D depict single-wavelength data obtained after Bond Elut Certify and Bond Elut Certify II extraction, respectively, of blank urine spiked with 400 ng/ml of THC-COOH. With the Bond Elut Certify column, which also contains a hydrophobic and ion-exchange copolymer, THC-COOH was found to be extracted at the same level as with the Clean Screen THC

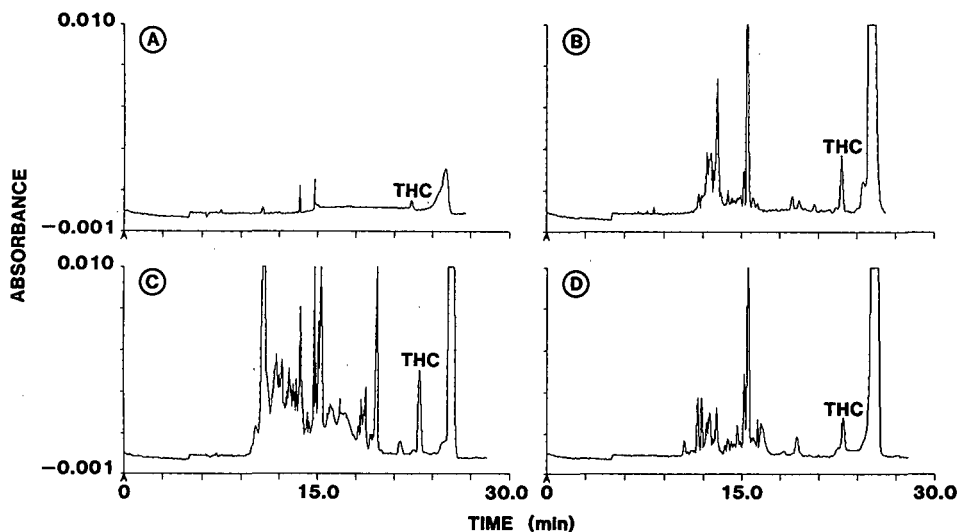


Fig. 2. Single-wavelength electropherograms (210 nm) of the MECC of THC-COOH extracted from spiked blank urine using (A) Bond Elut THC with 200 ng/ml THC-COOH, (B) Clean Screen THC (200 ng/ml), (C) Bond Elut Certify (400 ng/ml) and (D) Bond Elut Certify II (400 ng/ml). THC indicates the THC-COOH peaks. Other conditions as in Fig. 1.

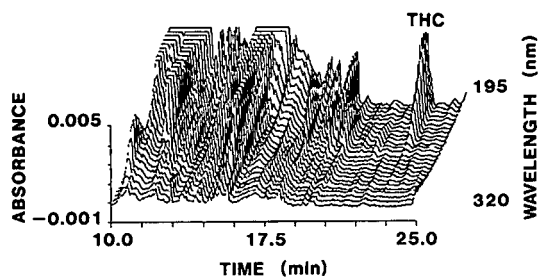


Fig. 3. Analysis of a cannabinoid-positive urine sample from a patient after extraction with Bond Elut Certify. Other conditions as in Figs. 1 and 2.

cartridge, but providing a more complex electropherogram (Fig. 2B and C). The urine matrix becomes more simplified with Bond Elut Certify II (Fig. 2D) than with Bond Elut Certify, presumably

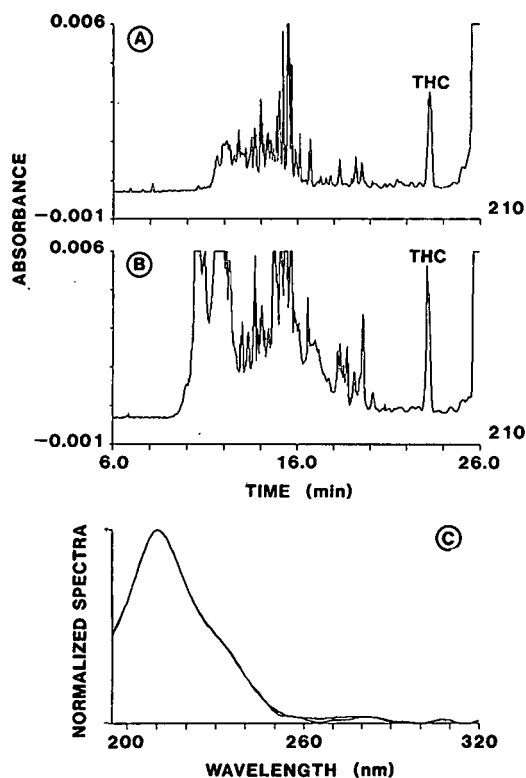


Fig. 4. (A and B) Single-wavelength electropherograms (210 nm) and (C) normalized absorption spectra of a markedly cannabinoid-positive urine sample from a patient employing (A and C) the Clean Screen THC and (B) the Bond Elut Certify extraction procedures. Other conditions as in Figs. 1 and 2.

because the former modified silica gel material exhibits three types of interactions, hydrophobic, polar and ion exchange [5,6]. The recovery, however, was not as good (about 25%), in contrast to the results reported by Dixit and Dixit [6]. With acidification of the urine specimens to pH 4.8 or 3.0 the yields with the Certify II columns became even lower than 25%.

Based on our investigations discussed above, both the Clean Screen THC and Bond Elut Certify procedures were used for confirmation of urine samples from patients which tested FPIA positive. MECC data for a urine specimen which was found to be markedly positive for cannabinoids ( $> 135$  ng/ml), and also positive for cocaine ( $> 300$  ng/ml) and negative for methadone and opiates ( $< 300$  ng/ml each) employing EMIT assays, are depicted in Figs. 3 and 4. These data clearly illustrate that with the Clean Screen THC method a much cleaner extract is obtained than with the Bond Elut Certify approach, and that with both extraction techniques well established THC-COOH peaks were monitored (Fig. 4A and B). Further, having data between 195 and 320 nm, in addition to reference spectra, permitted a rapid and reliable confirmation of the presence of THC-COOH in this urine. The excellent agreement between the time slices with those of computer-stored standards is shown by the graphs in Fig. 4C. With simple calibration graphs based on peak heights, the THC-COOH concentration was calculated to be *ca.* 300 ng/ml. It is interesting that benzoylecgonine could not be assigned to one of the peaks detected, particularly those with a retention time of about 12 min [8].

The second example presented concerned a urine sample tested FPIA positive for cannabinoids (67 ng/ml) and EMIT negative for cocaine and opiates ( $< 300$  ng/ml each). This urine sample was also treated with the Bond Elut Certify and Clean Screen THC procedures. MECC data are shown in Fig. 5. In both instances, small THC-COOH peaks were obtained which could be unambiguously assigned by comparison of spectra (Fig. 5C). The concentration of this compound in the urine was determined to be about 40 ng/ml, which compares favorably with the 67 ng/ml obtained with FPIA, a method which responds to different THC metabolites simultaneously. In the experiments performed THC-COOH was extracted from 5 ml of urine and

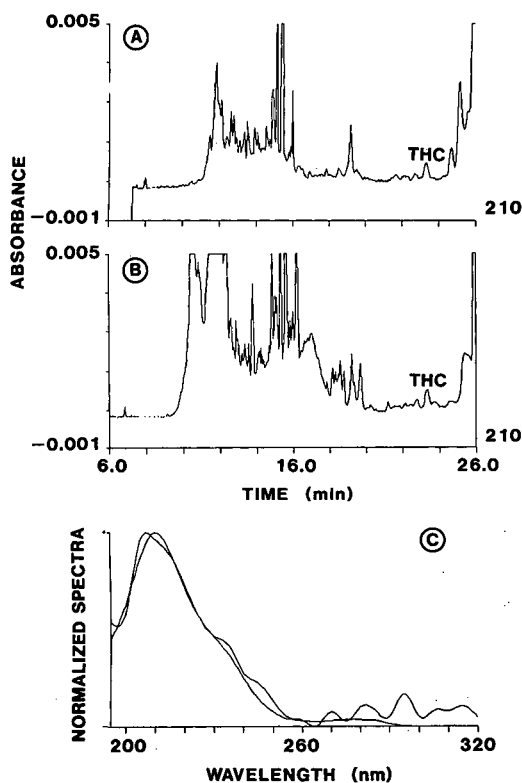


Fig. 5. Similar data to Fig. 4, but for a urine specimen with a much lower THC-COOH content, depicting the limit of the MECC approach with multi-wavelength detection.

reconstituted into 100  $\mu$ l of SDS buffer, providing THC-COOH peaks which are close to a detection limit of about 30 ng/ml. Detection limits of 10 ng/ml or lower can be attained by employing a larger urine volume and/or final reconstitution in less than 100  $\mu$ l of SDS buffer.

It is interesting that after investigating urine samples from more than fifteen patients no false-positive specimen was found. The presence of THC-COOH was confirmed in all seven positively tested specimens. Further, THC-COOH could not be found in six urines which gave no clear result with FPIA, cases in which the FPIA instrument provided a warning because of much too high background signal, a possible consequence of sample adulteration [1].

In conclusion, solid-phase extraction of THC-COOH using copolymeric sorbents has been shown to provide extracts that are sufficiently clean and concentrated for the MECC determination of THC-COOH with on-column multi-wavelength UV absorption detection and, without complete optimization, providing a detection limit of about 10 ng/ml. Thus MECC represents an attractive confirmation method for urine specimens that tested positive for cannabinoids by an immunological screening method and therefore represents an interesting alternative to existing chromatographic methods.

#### ACKNOWLEDGEMENTS

The authors acknowledge helpful discussions with Drs. R. Brenneisen and D. Bourquin and for providing the THC-COOH standard. Assistance from the technicians of the departmental drug assay laboratory and the generous loan of the Model UVIS 206 detector by its manufacturer, Linear Instruments; are gratefully acknowledged. Some of the extraction cartridges were a kind gift from ICT, Basle, Switzerland. This work was partly sponsored by the Swiss National Science Foundation.

#### REFERENCES

- 1 R. DeCresce, A. Mazura, M. Lifshitz and J. Tilson, *Drug Testing in the Workplace*, ASCP Press, Chicago, IL, 1989.
- 2 N. J. Willson, M. J. Kogan, D. J. Pierson and E. Newman, *J. Toxicol. Clin. Toxicol.*, 20 (1983) 465.
- 3 T. Vu Duc, in H. Brandenberger and R. Brandenberger (Editors), *Reports on Forensic Toxicology, Proceedings of the 2nd International Meeting of the International Association of Forensic Toxicologists*, distributed by Branson Research, Maennedorf, 1987, p. 229.
- 4 D. Bourquin and R. Brenneisen, *Anal. Chim. Acta*, 198 (1987) 183.
- 5 V. Dixit and V. M. Dixit, *J. Liq. Chromatogr.*, 13 (1990) 3313.
- 6 V. Dixit and V. M. Dixit, *J. Chromatogr.*, 567 (1991) 81.
- 7 W. Thormann, P. Meier, C. Marcolli and F. Binder, *J. Chromatogr.*, 545 (1991) 445.
- 8 P. Wernly and W. Thormann, *Anal. Chem.*, 63 (1991) 2878.
- 9 R. Weinberger and I. S. Lurie, *Anal. Chem.*, 63 (1991) 823.
- 10 B. C. Thompson, J. M. Kuzmack, D. W. Law and J. J. Winslow, *LC-GC Int.*, 3 (1990) 55.

# Study of protein–drug binding using capillary zone electrophoresis

Johan C. Kraak, Sandra Busch and Hans Poppe

*Laboratory for Analytical Chemistry, University of Amsterdam, Nieuwe Achtergracht 166, 1018 WV Amsterdam (Netherlands)*

---

## ABSTRACT

Capillary zone electrophoresis was tested for its suitability for studying protein–drug binding. Three methods were investigated, *viz.*, the Hummel–Dreyer method, the vacancy peak method and frontal analysis. Frontal analysis appeared to be the preferred method.

---

## INTRODUCTION

It is well known that drugs bind reversibly to plasma proteins, particularly albumin and  $\alpha$ -acid glycoproteins [1]. As the unbound drug determines the pharmacological activity of the drug, it is necessary to know the ratio of the bound to unbound drug in order to adjust the optimum therapeutic dose of a drug in man. Moreover, for toxic drugs with strong protein binding, additional information about the displacement of the bound drug from the plasma proteins by simultaneously administered exogenous compounds is required. The binding studies involve the determination of the binding parameters, *i.e.*, the binding constants, the maximum number of drug molecules bound to the protein and the classes of binding sites on the protein.

Methods for studying binding phenomena are concerned mainly with the measurement of either the unbound (free) or the bound drug without disturbing the equilibrium. The techniques that meet these requirements are dialysis [2,3], ultrafiltration [4] and size-exclusion chromatography (SEC) [5]. The last technique has nowadays become the method of choice and several variants have been devel-

oped, *i.e.*, the Hummel–Dreyer method [5,6], the vacancy peak method [7] and frontal analysis [8,9].

In principle, methods analogous to the SEC methods can be applied in capillary zone electrophoresis (CZE), but so far only flat gel electrophoresis has been used to study protein–drug binding [10]. CZE for studying protein–drug binding looks attractive because it is a simple system with a relatively low surface-to-volume ratio, an extremely large separation power, reasonable speed and good automation prospects. From the point of view of systematic errors and wide applicability, the CZE system appears more promising than other techniques, because of the absence of large surface areas, while the aqueous medium is similar to physiological conditions.

The aim of this investigation was to determine whether CZE can be used to study protein–drug binding and provide an attractive alternative to the aforementioned laborious methods. The study involved a comparison of the Hummel–Dreyer method, the vacancy peak method and frontal analysis using warfarin and bovine serum albumin (BSA) as test compounds.

## PRINCIPLE OF CZE METHODS FOR DRUG-BINDING STUDIES

SEC methods exploit the difference in the exclusion of the drug and the protein–drug complex from

---

*Correspondence to:* Dr. J. C. Kraak, Laboratory for Analytical Chemistry, University of Amsterdam, Nieuwe Achtergracht 166, 1018 WV Amsterdam, Netherlands.



the pores of the packing for the separation of the free drug and the bound drug [11]. In CZE, the drug and the protein–drug complex can be separated by the difference in their electrophoretic mobilities, which depend on the charge and size of the compounds. It is reasonable to assume that the size and charge on the protein are not significantly altered by the presence of adsorbed drug molecules. This means that the protein and protein–drug complex will have the same electrophoretic mobility. Hence, in principle, the same methods for studying protein–drug binding as developed for SEC (*i.e.*, the Hummel–Dreyer method, the vacancy peak method and frontal analysis) can be adapted to CZE, provided that the electrophoretic mobilities of the drug and protein differs. In this study, the electrophoretic mobility of the protein (BSA) is larger than that of the drug (warfarin).

In the Hummel–Dreyer method, the capillary is filled with the buffer containing the drug, which causes a large background detector response. Then a small sample, containing the buffer + drug + protein, is injected into the capillary. The migration of the injection plug after switching on the voltage is illustrated schematically in Fig. 1. The total concentration of the drug in the sample plug is equal to the drug concentration in the buffer, but part of the drug is bound to the protein. As the mobilities of the protein and protein–drug complex are larger than

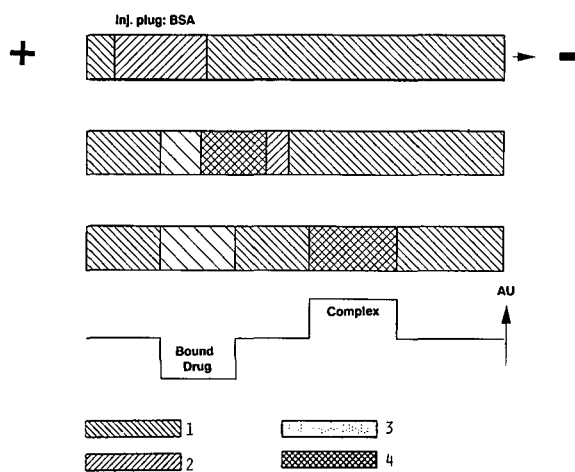


Fig. 1. Schematic representation of the Hummel–Dreyer CZE method. 1 = Drug; 2 = BSA; 3 = buffer; 4 = BSA–drug complex.

that of the drug, the protein–drug complex migrates from the injection plug, leaving a local deficiency in drug concentration. This deficiency causes a negative peak which moves with the mobility of the drug. The area of the negative peak is a measure of the amount of bound drug. During the migration, the protein–drug complex is always in equilibrium with the free drug in the buffer. Therefore, the protein–drug complex will give a positive peak. When the free protein shows no absorbance at the selected wavelength and the molar absorptivities of the drug and the protein–drug complex are the same, then in principle the areas of the negative and positive peaks must be equal. However, in practice these circumstances are almost never met. It can be seen that in Figs. 1–3 the peaks are represented as ideal blocks but it will be obvious that in practice, owing to the dispersion, the blocks appear as more or less Gaussian peaks.

In the vacancy peak method, the capillary is filled with buffer containing drug + protein, which causes a large background detector response. Then a small plug of buffer is injected into the capillary and the power supply switched on. The effect of the injected buffer plug on the migration is illustrated schematically in Fig. 2, again assuming that the mobilities of the protein and protein–drug complex are larger than that of the drug. At the front edge of the buffer plug the drug is migrating more slowly than the protein and hence stays behind. At the rear edge of the plug the protein migrates faster than the drug. This continues until the two fronts reach other. In this middle region the protein again

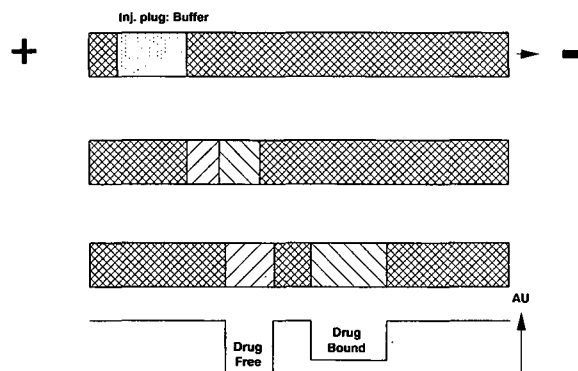


Fig. 2. Schematic representation of the vacancy peak CZE method.

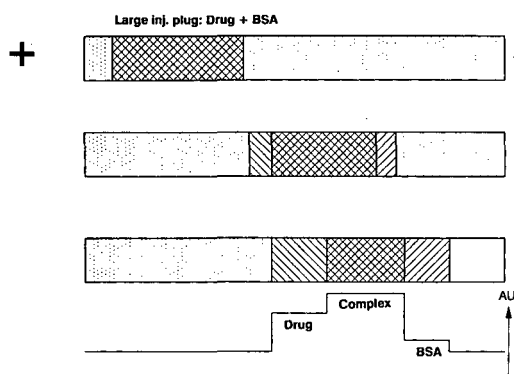


Fig. 3. Schematic representation of the frontal analysis CZE method.

adsorbs drug molecules until an equilibrium is attained, reconcentrating the drug to the original concentration. From that point on a steady state is reached, resulting in two negative bands (peaks) in the electropherogram. The first peak reflects the bound drug and the second peak the free drug concentration. The evidence that the negative peaks reflect the bound and free drug is given in ref. 7.

In frontal analysis, the capillary is filled with the buffer, then a very large sample plug, containing buffer + protein + drug, is injected into the capillary. As the mobilities of the protein and drug differ, the free drug leaks out of the plug at the rear edge (as occurs in the vacancy method) and a plateau is formed, as represented schematically in Fig. 3. Finally, the elution profile consists of three parts: at the front edge a plateau related to the free protein, in the middle region a plateau related to the protein–drug complex + free drug and at the rear edge a plateau due to the unbound (free) drug. Depending on the selected wavelength, the first plateau (the free protein) is often not detected. The height of the drug plateau reflects the free drug concentration.

## EXPERIMENTAL

### Apparatus

The CZE system was constructed from separate parts and consisted of a UV detector (Model 757, Kratos, Ramsey, NJ, USA) with a modified cell arrangement for on-column detection, a 0–35 kV d.c. high-power supply (HCN 35-35000; FUG, Rosenheim, Germany) and platinum electrodes used for connection of the supply with the buffer

reservoirs at both ends of the capillary. The detection was carried out at the cathodic side. The whole set-up (except the power supply) was placed in a Plexiglas box. For safety, an automatic shut-off switch was mounted in the door. The temperature in the box was kept at 25°C.

In one experiment, a commercial CZE system [Model 270 A-HT; Applied Biosystems Inc. (ABI), CA, USA] was used. The fused-silica capillaries (Polymicro Technologies, Phoenix, AZ, USA) were 50–60 cm × 50 μm I.D. The distance between the injection and detectors was about 35 cm. Before starting the measurements, the capillary was flushed daily for 5 min each with 1 M KOH, ethanol and buffer. The voltage was usually set to 200 V/cm. Sample injection was done by means of electromigration (2.5–60 s at 10 kV). The wavelength of detector was adjusted to 315 nm. At very high warfarin concentrations the wavelength was sometimes set at 340 nm.

### Chemicals

The 0.067 M phosphate buffer (pH 7.4) was prepared by mixing of 0.53 g of  $\text{KH}_2\text{PO}_4$  and 2.94 g of  $\text{K}_2\text{HPO}_4 \cdot 3\text{H}_2\text{O}$  (Merck, Darmstadt, Germany) in 250 ml of doubly distilled water. The buffer solution was prepared daily and filtered through a Millipore filter (Type HV, 0.45 μm) before use. Bovine serum albumin (BSA) was obtained from Merck and warfarin from Sigma (St. Louis, MO, USA). The sample solutions were daily prepared from stock solutions stored at –20°C.

### Procedures

In order to calculate properly the binding parameters of warfarin, 15–20 points of the warfarin–BSA isotherm are desired. In all studies the BSA concentration was kept constant at  $4 \cdot 10^{-5}$  M and the warfarin concentration varied according to the following scheme: 3, 6, 9, 12, 15, 18, 30, 60, 90, 120, 200, 300, 400, 600 and  $900 \cdot 10^{-6}$  M. For the Hummel–Dreyer and vacancy peak methods a small sample plug was injected (2.5 at 10 kV) and for frontal analysis a large sample plug (60 s at 10 kV). The experimental data were fitted according to a bi-Langmuir isotherm using a non-linear least-squares curve fitting program [12]. The experimental data were also visualized in a Scatchard plot [13] to show the spread of the data points.

For the calculation of the bound fraction with the Hummel–Dreyer method, the simplified method as given by Pinkerton and Koeplinger [14] was applied. The procedure involves two injections at a given warfarin concentration: the sample (consisting of buffer + protein) and the blank buffer. From the peak areas the bound drug concentration,  $[D]_b$ , can be calculated according to

$$[D]_b = \left( \frac{A_p - A_e}{A_e} \right) C_D \quad (1)$$

where  $A_p$  is the area of the sample peak,  $A_e$  is the area of the buffer peak and  $C_D$  the drug concentration in the buffer.

In the vacancy peak method, the free drug concentration was determined by internal calibration. For this purpose the buffer was mixed with increasing amounts of warfarin and then injected. By plotting the added warfarin *versus* the peak area, the free concentration can be determined by interpolating to zero absorbance (the concentration needed to fill up the vacancy peak).

In frontal analysis, the free drug concentration,  $[D]_f$ , can be calculated from the height of the sample plateau and the height of the plateau obtained on injecting a plug of buffer + the same warfarin concentration,  $C_D$ , as used in the sample according to

$$[D]_f = \left( \frac{\text{sample height}}{\text{warfarin height}} \right) C_D \quad (2)$$

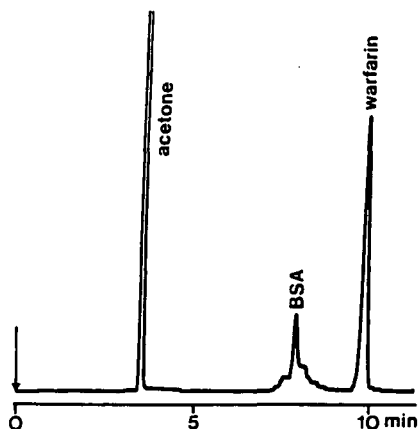


Fig. 4. Electropherogram of the test solutes. Electrophoretic mobilities ( $m^2/V \cdot s$ ): acetone (neutral compound),  $\mu_0 = +3.70 \cdot 10^{-8}$ ;  $\mu_{BSA} = -1.67 \cdot 10^{-8}$ ;  $\mu_{warfarin} = -2.00 \cdot 10^{-8}$ .

The electropherogram of the test solutes in 0.067 M phosphate buffer is shown in Fig. 4. It can be seen that the BSA is not completely homogeneous.

## RESULTS AND DISCUSSION

During the explorative experiments to adapt the liquid chromatographic drug-binding techniques to our laboratory-made CZE system, we were faced with unexpected experimental difficulties, such as blockage of the capillary, noisy detector signals and large variations in the electropherograms, particularly in the Hummel–Dreyer and vacancy peak methods. By systematically investigating these problems, it became clear that acceptable data could be produced provided that flushing of the capillary, the preparation of the solutions and the measurements were performed according to a stringent protocol. For instance, a daily pretreatment of the capillary, freshly prepared buffer and sample solutions and the analysis of a series of samples in a standardized time scheme were found to be of paramount importance for obtaining reliable isotherms. Fig. 5 shows typical electropherograms obtained with (A) the Hummel–Dreyer method, (B) the vacancy peak method and (C) frontal analysis.

### Effect of protein concentration

The reversible binding of a drug to a protein is governed by the multiple equilibria theory [15,16], expressed by the following equation:

$$r = \frac{[D]_b}{[P]} = \sum_{i=1}^m \frac{n_i K_i [D]_f}{1 + K_i [D]_f} \quad (3)$$

where  $r$  is the mean number of drug molecules adsorbed per protein molecule,  $m$  is the number of classes of independent adsorption sites,  $n_i$  is the number of sites in a class  $i$  with an association constant of  $K_i$  and  $[D]_f$  is the concentration of the unbound (free) drug;  $r$  is equal to the ratio of the concentration of bound drug,  $[D]_b$ , and the total protein concentration,  $[P]$ . For the BSA–warfarin combination two binding constants and two classes of binding sites are assumed. According to eqn. 3,  $r$ , the number of drug molecules adsorbed to a protein molecule, is independent of the protein concentration. However, it has been found that the equilibria

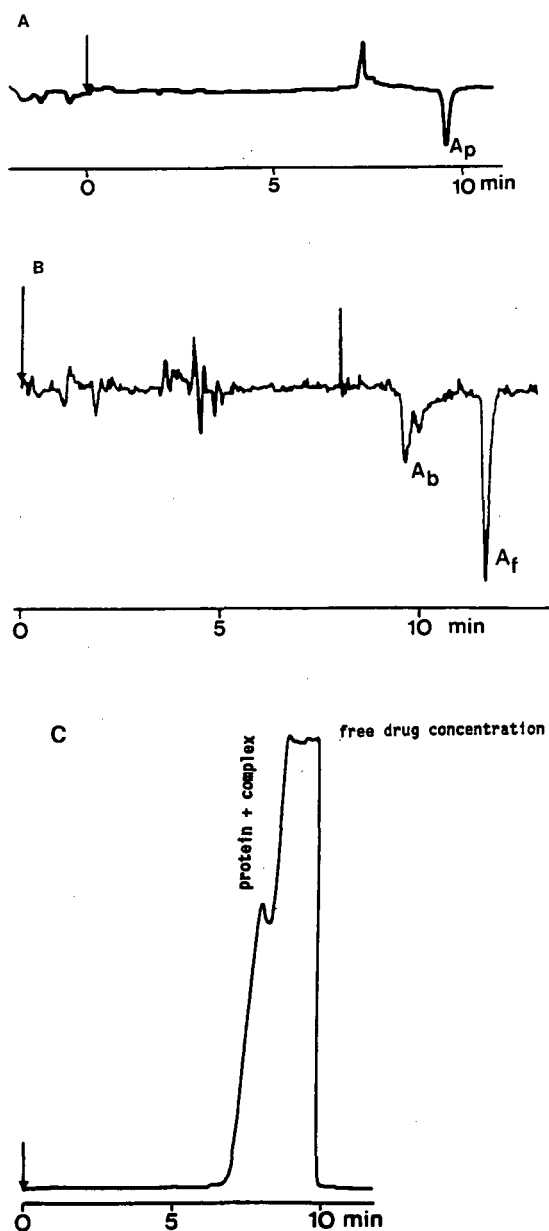


Fig. 5. Typical electropherograms obtained with (A) the Hummel–Dreyer method, (B) the vacancy peak method and (C) frontal analysis.

are disturbed at higher protein concentrations [17] and this can affect  $r$ . In order to determine the protein concentration where  $r$  is constant, different BSA concentrations were injected at a constant

warfarin concentration and the  $r$  values were calculated. The results are given in Table I. As can be seen, the  $r$  value tends to become constant with decreasing BSA concentration. In all subsequent measurements, the BSA concentration was kept below  $50 \mu\text{M}$ .

#### Hummel–Dreyer method

Fig. 6 shows a typical adsorption isotherm and the corresponding Scatchard plot as measured with the Hummel–Dreyer method. The data points are the means of duplicate measurements. As can be seen, the isotherm looks reasonable but the points in the Scatchard plot are scattered significantly at lower  $r$  values. The scattering at low warfarin concentration is due to the imprecision in the determination of the small peak heights at the highest sensitivity setting of the detector. The peak heights of duplicates vary by about 10% and this has a large effect on the calculation of  $r$ . At medium and higher warfarin concentrations the spread of duplicate measurements is smaller (5% and 2.5% respectively). Owing to the relatively large spread at lower warfarin concentrations, meaningful data points for the fitting can be obtained provided that averages of replicate experiments are used. The relatively large spreading can be partly attributed to the manual operation on our laboratory-made CZE system and better results can be expected with an automated CZE system.

The binding parameters of warfarin with BSA, by fitting the data points as reflected in Fig. 6, are given in Table II, including parameters given in the literature. The values of  $k_1$  and  $n_1$  are smaller than published values obtained using SEC. As the dilution of the bands in CZE is significantly smaller than in HPLC, the difference might be attributed to the

TABLE I

EFFECT OF THE BSA CONCENTRATION ON THE  $r$  VALUE WITH  $5 \cdot 10^{-5} \text{ M}$  WARFARIN

BSA ( $10^{-4} \text{ M}$ )	$r$
1.52	1.16
1.25	1.40
1.01	1.59
0.75	1.68
0.48	1.73

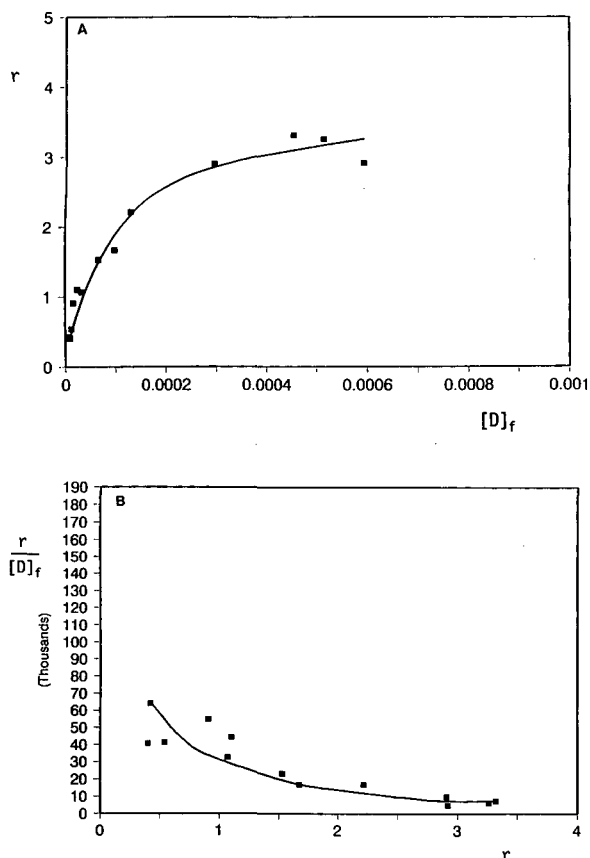


Fig. 6. (A) BSA-warfarin isotherm and (B) Scatchard plot measured with the simplified Hummel-Dreyer method.

effect of the actual protein concentration on  $r$ . This aspect is being investigated in more detail.

#### Vacancy peak method

Fig. 7 shows the isotherm and Scatchard plot obtained with the vacancy peak method. Both curves look better than those obtained with the Hummel-Dreyer method. However, also with the vacancy peak method the scatter of the data points in the Scatchard plot at smaller  $r$  values is large. The binding parameters deviate from those in the literature, probably because of the mentioned effect of the protein concentration on  $r$ . The vacancy peak method can be easily applied but requires a large number of measurements owing to the calibration procedure.

#### Frontal analysis

The BSA-warfarin isotherm and Scatchard plot obtained with the frontal analysis method are shown in Fig. 8. In contrast to the aforementioned methods, with this method smooth curves are obtained over the whole warfarin concentration range investigated. The curves are very reproducible and the binding constants fit well with those reported in the literature, as can be seen from Table II. Owing to the simple internal calibration, a complete curve can be recorded within 8 h.

Frontal analysis was tested with an automated CZE apparatus (ABI) made available for demon-

TABLE II

COMPARISON OF PROTEIN BINDING PARAMETERS FOR BSA-WARFARIN IN 0.067 M PHOSPHATE BUFFER (pH 7.4)

Method	Apparatus	$K_1$ ( $\times 10^5$ )	$n_1$	$K_2$ ( $\times 10^3$ )	$n_2$
CZE, Hummel-Dreyer	Laboratory-made	1.00	0.67	6.7	3.24
CZE, vacancy	Laboratory-made	0.70	1.98	1.4	2.74
CZE, frontal	Laboratory-made I	1.30	1.33	2.1	2.67
	Laboratory-made II	1.53	1.16	2.9	3.17
	Laboratory-made III	1.58	1.22	4.3	2.70
	ABI, hydrodynamic injection	1.51	1.31	6.9	1.63
	ABI, Electromigration injection	1.61	1.24	9.2	1.41
Ref. 18		2.41	1.46	5.6	2.42
Ref. 19		2.31	0.95	5.9	3.69
Ref. 20		2.03	1.38	2.2	3.73
Ref. 6		2.10	1.16	—	—
Ref. 6		2.18	1.31	4.2	3.75

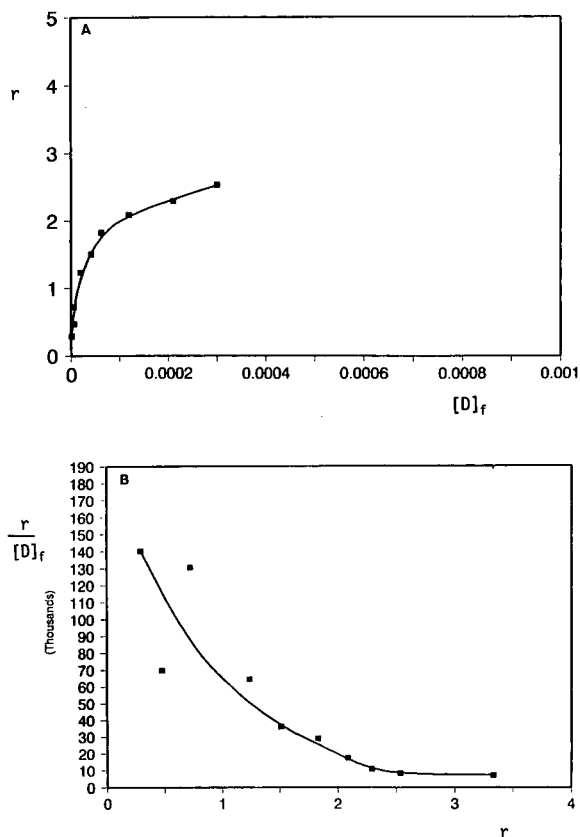


Fig. 7. (A) BSA-warfarin isotherm and (B) Scatchard plot measured with the vacancy peak method.

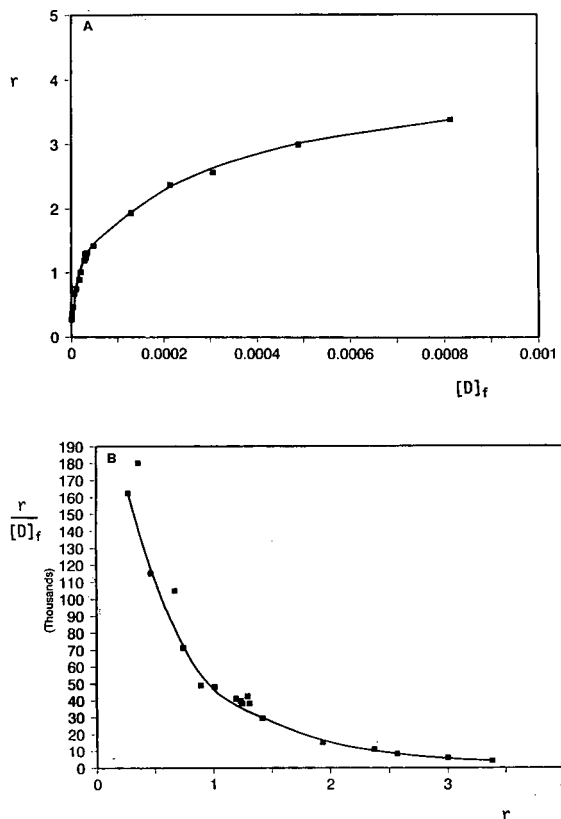


Fig. 8. (A) BSA-warfarin isotherm and (B) Scatchard plot measured with frontal analysis.

strations by the supplier. Two injection modes were applied: electromigration and hydrodynamic. The system was programmed in such a way that after each analysis a washing step (1 M KOH) was applied. The isotherm obtained is given in Fig. 9 and shows that Frontal analysis can be well automated.

From Table II, it can be seen that the number of binding sites at high warfarin concentration ( $n_2$ ) appears smaller with the ABI system than with our laboratory-made CZE system, in which the KOH flushing between each analysis was omitted. The reasons for this difference are not yet clear but is might be attributed to reversible adsorption of BSA on the surface of the capillary or to an effect of the length and type of the applied capillaries, which differed in the two systems. These aspects are under investigation.

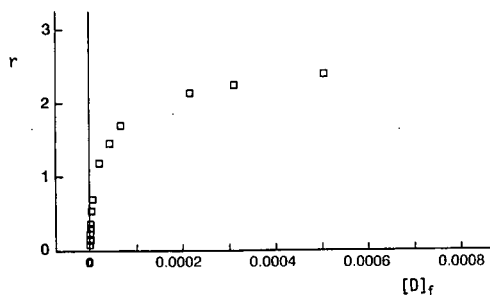


Fig. 9. (A) BSA-warfarin isotherm and (B) Scatchard plot measured with frontal analysis on an ABI CZE system. Injection mode: electromigration.

## CONCLUSIONS

The results obtained so far have shown that CZE is a suitable technique for studying protein–drug binding, provided that an automated CZE system is used. Of the methods investigated, frontal analysis appears to be the most attractive.

## ACKNOWLEDGEMENTS

The authors thank J. J. Luijt and M. Tiller for their valuable contributions and Astra Hässle, Sweden, for financial support.

## REFERENCES

- 1 W. J. Jusko and M. Gretch, *Drug Metab. Rev.*, 5 (1976) 43.
- 2 I. M. Klotz, *J. Am. Chem. Soc.*, 68 (1946) 2299.
- 3 R. Zini, D. Morin, P. Jouenne and J. P. Tillement, *Life Sci.*, 43 (1988) 2103.
- 4 W. F. Bowers, S. Fulton and J. Thompson, *Clin. Pharmacokin.*, 9 (1984) 49.
- 5 J. P. Hummel and W. J. Dreyer, *Biochim. Biophys. Acta*, 63 (1962) 530.
- 6 B. Seville, N. Thuaud and J. P. Tillement, *J. Chromatogr.*, 167 (1978) 159.
- 7 B. Seville, N. Thuaud and J. P. Tillement, *J. Chromatogr.*, 180 (1979) 103.
- 8 P. F. Cooper and G. C. Wood, *J. Pharm. Pharmacol.*, 20 (1968) 1503.
- 9 L. Soltes, B. Seville, J. P. Tillement and D. Berek, *J. Clin. Chem. Clin. Biochem.*, 27 (1989) 935.
- 10 H. Bennhold and H. Ott, in E. Bucher, E. Letterer and F. Roulet (Editors), *Handbuch der Allgemeine Pathologie*, Springer, Berlin, 1961, Band V, Teil 1, pp. 166–275.
- 11 B. Seville, R. Zini, C. V. Madjar, N. Thuaud and J. P. Tillement, *J. Chromatogr.*, 531 (1990) 51.
- 12 H. F. M. Boelens and H. C. Smit, in preparation.
- 13 G. Scatchard, *Ann. N.Y. Acad. Sci.*, 51 (1949) 660.
- 14 T. C. Pinkerton and K. A. Koeplinger, *Anal. Chem.*, 62 (1990) 2114.
- 15 I. M. Klotz and D. L. Hunston, *Biochemistry*, 16 (1971) 3065.
- 16 H. A. Feldman, *Anal. Biochem.*, 48 (1972) 317.
- 17 C. J. Bowner and W. E. Lindup, *Biochim. Biophys. Acta*, 624 (1980) 260.
- 18 R. F. Mais, S. Keresztes-Nagy, J. F. Zaroslinski and Y. T. Oester, *J. Pharm. Sci.*, 63 (1974) 1423.
- 19 J. P. Tillement, R. Zini, P. d'Athis and G. Vassent, *Eur. J. Clin. Pharmacol.*, 7 (1974) 307.
- 20 Y. T. Oester, S. Keresztes-Nagy, R. F. Mais, J. Becktel and J. F. Karolinski, *J. Pharm. Sci.*, 65 (1976) 1673.

# Chiral separations of basic drugs and quantitation of bupivacaine enantiomers in serum by capillary electrophoresis with modified cyclodextrin buffers

Helena Soini

*Department of Chemistry, Indiana University, Bloomington, IN 47405 (USA)*

Marja-Liisa Riekkola

*Department of Analytical Chemistry, Helsinki University, Vuorikatu 20, SF-00100 Helsinki (Finland)*

Milos V. Novotny

*Department of Chemistry, Indiana University, Bloomington, IN 47405 (USA)*

---

## ABSTRACT

Modified cyclodextrin derivatives were evaluated as the buffer additives in capillary electrophoresis of several racemic pharmaceutical bases. Uncoated and polyacrylamide-modified silica capillaries were compared for their effectiveness in the enantiomeric resolution and migration reproducibility of model solutes. Using cationic detergents in the mixed-micellar mode, optimized separations of the racemic drug bupivacaine are demonstrated in a spiked serum sample at the therapeutic level. Precision, linearity and sensitivity of the method appear adequate for reliable quantitation required in pharmacokinetic and clinical studies.

---

## INTRODUCTION

In pharmaceutical research and quality control, separation of optical isomers is important throughout the development and manufacturing of numerous therapeutics. In the course of checking the composition of bulk drug substances as well as in the more involved pharmacokinetic and clinical studies, the ability to measure separately quantities of optical isomers has become essential. Many pharmaceutical preparations are now administered as a 1:1 racemic mixture of (*R*)- and (*S*)-enantiomers. In the body, various enantiomers behave as two different entities; stereoselectively controlled processes

such as drug absorption, distribution, metabolism and elimination may differ substantially between the enantiomers [1]. The pharmacokinetic studies in body fluids impose challenging demands for the separation systems in use. These include, in addition to the enantioselective separations, the need for resolution between a number of endogenous biological molecules and relatively small pharmaceutical molecules present in the same sample. In addition, the performance of the analytical system must remain constant during the long analysis periods despite the presence of interfering matrix compounds.

The separation principle of capillary electrophoresis (CE) offers considerably greater separation efficiency, within a short analysis time, than that of high-performance liquid chromatography or gas chromatography [2,3]. The possibility of varying the selectivity of separation through the use of dif-

---

*Correspondence to:* Dr. M. V. Novotny, Department of Chemistry, Indiana University, Bloomington, IN 47405, USA.



ferent modifiers in buffer solutions is yet another valuable property of the general method. For example, micellar electrokinetic chromatography [4] has shown an excellent capability to solubilize disturbing proteins and other endogeneous materials during the analysis of pharmaceuticals after a direct injection of blood serum [5–7]. Short of sample pre-concentration, however, this approach is adequate only at high concentrations of pharmaceuticals.

Recently, cyclodextrins (CDs) and their derivatives have been employed in CE of various optical and geometrical isomers as well as for other small molecules of pharmaceutical interest [8–11]. The uses of CDs in CE have been reviewed by Snopek *et al.* [12]. At this date, analyses of biological materials following this approach remain unexplored.

In the recent applications of CD-modified electrokinetic chromatography, a combination of anionic surfactants and CDs has been utilized in the buffer systems to aid resolution of hydrophobic polyaromatic compounds [13] and closely related corticosteroids [14]. Structurally similar peptides, both in their native forms and as fluorescent derivatives, were successfully separated using both anionic and cationic detergents above their critical micelle concentration, together with CDs [15]. Under such conditions, the analytes are believed to incorporate themselves either into the micelles or the CD cavity [13], thus enhancing the selectivity potential of the separation system. Interactions of CD molecules with cationic and anionic surfactants under the micellar conditions have been studied by careful conductometric measurements [16,17]. According to these measurements, CDs induce an increase in the apparent critical micellar concentration of a surfactant, since the available monomers are partly associated in a complex with CDs. Furthermore, interactions of surfactants with the outer hydrophilic shells of CDs were suggested [16].

In the present study, we have investigated the properties of  $\beta$ -CD solutions modified by certain cationic surfactants in the separations of optical isomers of basic pharmaceuticals. Uncoated fused-silica and polyacrylamide-coated silica capillaries were used in the study. Effective separations of optical isomers for model pharmaceuticals—verapamil, fluoxetine, bupivacaine, mepivacaine, carvedilol and pindolol—are described. Chemical structures of these compounds are shown in Fig. 1. A

variety of additives in the CD–buffer systems were tested for both enhancing resolution between the enantiomeric pairs and improving analytical reproducibility. The effect of the cationic detergents hexadecyltrimethylammonium bromide and cetylpyridinium chloride, in combination with the  $\beta$ -CD trimethyl derivative, on the resolution of the enantiomeric pairs was investigated for fluoxetine and verapamil. Finally, an optimized separation system with the  $\beta$ -CD dimethyl derivative was demonstrated for the quantitation of bupivacaine enantiomers in spiked serum samples at therapeutic levels.

## EXPERIMENTAL

### Materials

Verapamil hydrochloride, or  $\alpha$ -[3-[[2-(3,4-dimethoxyphenyl)ethyl]-methylamino]propyl]-3,4-dimethoxy- $\alpha$ -(1-methylethyl)benzene-acetonitrile hydrochloride; pindolol, or 1-(1H-indol-4-yloxy)-3-[(1-methyl-ethyl)amino]-2-propanol; carvedilol, or 1-(9H-carbazol-4-yloxy)-3-[[2-(2-methoxyphenoxy)ethyl]amino]-2-propanol; and bupivacaine hydrochloride, or 1-butyl-N-(2,6-dimethylphenyl)-2-piperidinecarboxamide hydrochloride, were a gift from Orion Pharmaceutica, Espoo, Finland. Pure (*R*)- and (*S*)-bupivacaine hydrochloride were provided by Astra (Södertälje, Sweden). Mepivacaine, or N-(2,6-dimethylphenyl)-1-methyl-2-piperidinecarboxamide, was a USP reference standard (Twinbrook Parkway, Rockville, MD, USA). Fluoxetine hydrochloride, or ( $\pm$ )-N-methyl-3-phenyl-[( $\alpha,\alpha,\alpha$ -trifluoro-*p*-tolyl)-oxyl]-propylamine hydrochloride was a gift from Lilly Research Laboratories (Indianapolis, IN, USA). Heptakis(2,3,6-tri-O-methyl)- $\beta$ -cyclodextrin (TM- $\beta$ -CD); heptakis(2,6,di-O-methyl)- $\beta$ -cyclodextrin (DM- $\beta$ -CD); hexadecyltrimethylammonium bromide (HTAB); cetylpyridinium chloride (CTPC); 1-heptanesulfonic acid; and finally, Trizma base (Tris), were obtained from Sigma (St. Louis, MO, USA). Methylhydroxyethylcellulose 1000 and 4000 (MHEC) were purchased from Serva (Heidelberg, Germany). Ethylene glycol, hexane (HPLC grade), sodium hydroxide (1 *M* solution) and phosphoric acid (HPLC grade, 85%) were from Fisher Scientific (Fair Lawn, NJ, USA). Diethyl ether and ethylacetate (ChromAR) were purchased from Mallinckrodt (Paris, KY, USA).

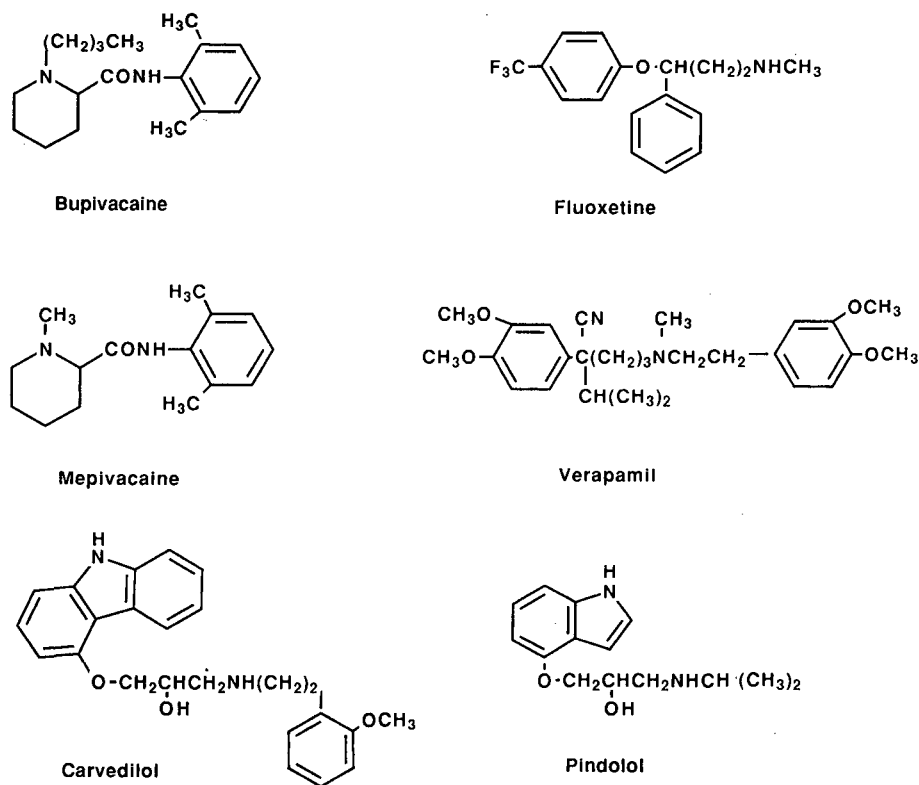


Fig. 1. Chemical structures of the basic racemic pharmaceuticals used in this study.

Polyacrylamide coating of the capillary was carried out according to the procedure described by Hjertén [18]. All buffers were filtered with 0.2- $\mu\text{m}$  Nylaflo filters (Gelman Sciences, Ann Arbor, MI, USA). Water was distilled before use.

#### Equipment

A laboratory-made CE apparatus and Beckman (Palo Alto, CA, USA) P/ACE System 2100 were used in all measurements. Capillaries (50 cm  $\times$  150  $\mu\text{m}$  O.D., 30  $\mu\text{m}$  I.D. and 64 cm  $\times$  185  $\mu\text{m}$  O.D., 50  $\mu\text{m}$  I.D.) used in the laboratory-made instrument were from Polymicro Technologies (Phoenix, AZ, USA). A high-voltage power supply (0–60 kV) was a product of Spellman High Voltage Electronics (Plainview, NY, USA). Voltages 18–20 kV were used (negative ground). The detector was a Jasco (Tokyo, Japan) UVIDEC-100-IV adjusted to 220 nm (0.01 AUFS), where all model compounds exhibited relatively strong UV absorption. The polyimide coating of the capillary was removed in a

small area (16 cm from the capillary end) to form an on-column flow-cell for UV-absorbance detection. The Beckman instrument used a capillary of 57 cm (50 cm effective length)  $\times$  367  $\mu\text{m}$  O.D., 75  $\mu\text{m}$  I.D. Buffers contained tri- and dimethylcyclodextrin derivatives (10 mM TM- $\beta$ -CD or DM- $\beta$ -CD), Tris (18 mM, pH adjusted to 2.8–3.0 with phosphoric acid) and methylhydroxyethylcellulose 1000 or 4000 (0.1%, w/w). Modifiers were added in the described buffer systems. Under the above conditions, the analytes possessed positive charge and migrated towards the negative electrode (detector end).

#### Sample preparation

Stock solutions of racemic drugs were prepared in methanol. Further dilutions were made in the same solvent. In the ethylacetate extraction of verapamil from serum, 0.25 ml of serum spiked with about 10  $\mu\text{g}$  of verapamil was alkalinized with 30  $\mu\text{l}$  of 1 M sodium hydroxide and shaken vigorously for

2 min with 0.5 ml ethylacetate. After the organic layer (0.4 ml) was evaporated to dryness under the stream of nitrogen, the residue was dissolved in 10  $\mu$ l methanol.

For the spiked bupivacaine samples, blank serum (1.0 ml) was transferred to a 5-ml test tube and the racemic bupivacaine (0.19–3.8  $\mu$ g in 15–50  $\mu$ l methanol) and mepivacaine (160  $\mu$ g/30  $\mu$ l methanol) were added. After thorough mixing, the samples were alkalized with 200  $\mu$ l of 1 M sodium hydroxide by mixing for 20 s. The samples were extracted with 1.5 ml hexane–diethyl ether (1:1) by shaking the test tube gently for 5 min in the horizontal position to avoid emulsion formation. After standing in a refrigerator 5 min to cool, the 1.3 ml organic layer was evaporated to dryness in a polyethylene conical tube by a stream of nitrogen. The residue was re-dissolved into 15  $\mu$ l of methanol. Sample introduction was carried out hydrodynamically by lifting the sample 13 cm above the buffer level and dipping the capillary end into the sample for 15-s time intervals.

## RESULTS

In a previous qualitative study [11] we used heptakis(2,6-di-O-methyl)- $\beta$ - and  $\gamma$ -cyclodextrins in a buffer (pH between 2 and 3), with methylhydroxyethylcellulose addition. The buffer system showed a promising ability to separate the optical isomers of basic pharmaceuticals using uncoated capillaries. In this present study, buffers with hydroxycellulose derivative (pH 2.7–3.0) and heptakis(2,3,6-tri-O-methyl)- $\beta$ -cyclodextrin or heptakis(2,6-di-O-methyl)- $\beta$ -cyclodextrin were modified. The aim of these experiments was to achieve separation conditions adequate for quantitative analysis of pharmaceuticals in serum samples containing a biological matrix.

### Uncoated capillaries

A dramatic effect of HTAB (0.05 mM) in suppressing the slow-migrating serum proteins from about 40 min to 20 min, in a spiked serum extract sample (levels of verapamil around 40  $\mu$ g/ml), is shown in Fig. 2. Apparently, the HTAB molecules cover the negatively charged silica wall of a capillary, forming a positive net charge. Consequently, adsorption of proteins on the wall is minimized, while the positively charged analytes are repelled.

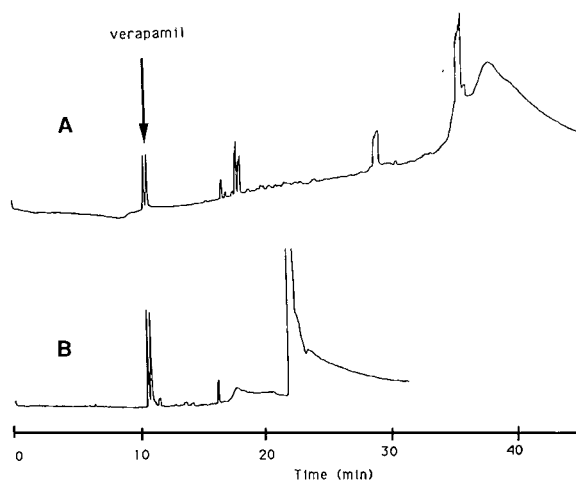


Fig. 2. Ethyl acetate extract of an alkalized serum sample containing verapamil. (A) Buffer: 10 mM TM- $\beta$ -CD–20 mM Tris, pH 2.7–0.1% MHEC 1000, capillary 64 cm  $\times$  50  $\mu$ m, uncoated silica; 20 kV voltage; 215 nm UV-absorbance detection, 0.01 AUFS. (B) Buffer as in (A), but with 0.05 mM HTAB added (pH 3.0).

Under the above acidic conditions (in the presence of cyclodextrins and cellulose), the electromigration of positively charged species towards the negative electrode was the main force in effect. Electroosmosis became negligible. Therefore, the reversed electroosmosis which had been observed in the cationic detergent buffer systems earlier under neutral and basic conditions [19,20] did not have a significant effect in our buffer system.

To enhance the enantiomer resolution and sampling precision for quantitation purposes, we explored the addition of methanol, ethylene glycol, and 1-heptanesulfonic acid to the original buffer-plus-additive system (TM- $\beta$ -CD–0.1% MHEC–0.05 mM HTAB). The addition of methanol and 1-heptanesulfonic acid improved the peak shapes of fluoxetine enantiomers, while their effect on verapamil separation appeared negative. With methanol, the verapamil enantiomers co-migrated, and broad and tailing peaks were experienced due to the use of 1-heptanesulfonic acid. The effects of selected additives are demonstrated in Fig. 3.

The merits of using cationic detergents, HTAB and CTAPC, in conjunction with the modified CDs and untreated silica capillary, were examined. The literature values [21] of the critical micelle concentration are 0.028 mM and 0.9 mM for HTAB and

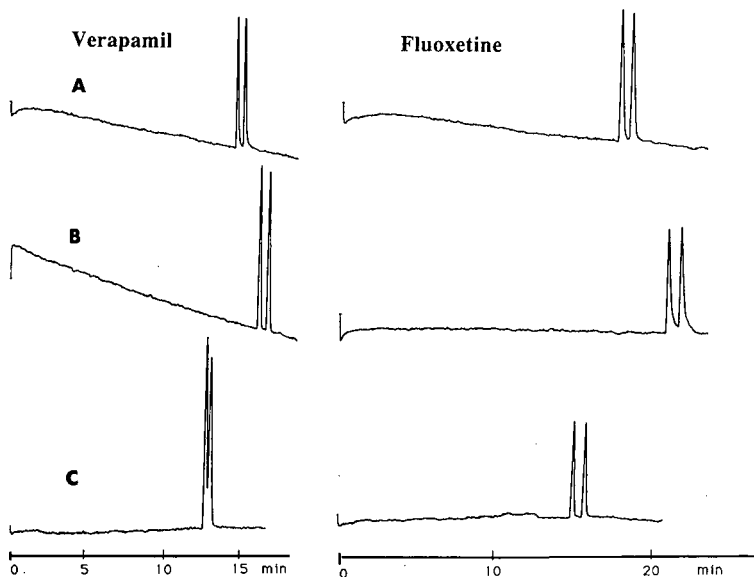


Fig. 3. Comparison of the effects of buffer modifiers on verapamil and fluoxetine enantiomer separation. Capillary: 50 cm  $\times$  30  $\mu$ m, uncoated silica, detection at 220 nm, 0.01 AUFS, 25 kV voltage. (A) Buffer: 12 mM TM- $\beta$ -CD–20 mM TRIS, pH 2.7–0.1% MHEC 1000–0.05 mM HTAB. (B) Buffer: ethylene glycol–buffer (A) (2:98). (C) Buffer: 10 mM 1-heptanesulfonic acid–buffer (A) (47:53) (6.4 mM TM- $\beta$ -CD–4.7 mM 1-heptanesulfonic acid–0.05% MHEC 1000–0.027 mM HTAB).

CTPC, respectively. Hansen *et al.* [22] reported that HTAB adsorptivity on porous silica is much stronger than the values for shorter-chain cationic detergents. It is thus expected that small changes in HTAB concentration may be effective in regulating the analytical conditions of our experiments. In addition, its minor addition to the buffer media does not significantly alter the current conditions in comparative experiments.

The enantiomeric resolution and migration reproducibility for verapamil and fluoxetine were measured here as a function of detergent concentration. Resolution ( $R_s$ ) was determined according to the usual formula,  $R_s = 2(t_2 - t_1)/(w_1 + w_2)$ , where  $t_1$  and  $t_2$  are the respective migration times and  $(w_1 + w_2)/2$  is the average peak width at the peak base. Appropriate amounts of HTAB or CTPC were added to the buffer of standard composition [10 mM TM- $\beta$ -CD–18 mM Tris-phosphate (pH = 2.9)–0.1% MHEC 1000]. The resolution vs. detergent concentration plots are shown in Figs. 4 and 5, while Tables I and II demonstrate migration reproducibility for the first isomer of fluoxetine and verapamil at different detergent concentrations.

The results indicate that there are optimum val-

ues for both migration reproducibility and the resolution of enantiomers. For HTAB, this optimum concentration is equal to or slightly higher than the critical micelle concentration (cmc); it is somewhat lower for CTPC. The optimized separations are shown in Fig. 6 A–C.

The optical isomers of mepivacaine, bupivacaine, pindolol and carvedilol were subsequently separated using dimethyl- $\beta$ -cyclodextrin buffer with the es-

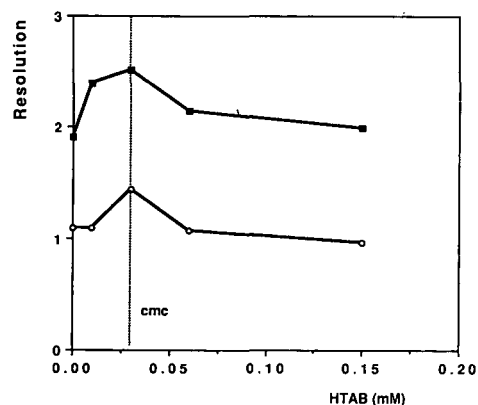


Fig. 4. Resolution of the enantiomeric pairs of verapamil (○) and fluoxetine (■) vs. HTAB concentration.

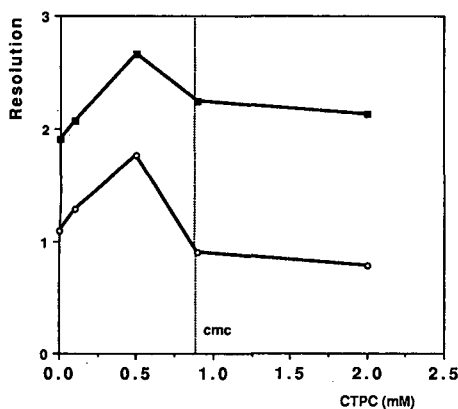


Fig. 5. Resolution of the enantiomeric pairs of verapamil (○) and fluoxetine (■) vs. CTPC concentration.

established optimum concentration of HTAB. Buffer composition was DM- $\beta$ -CD (10 mM)–Tris (18 mM, pH 2.9 with phosphoric acid)–0.1% MHEC 4000–0.03 mM HTAB.

Separations of additional analytes are seen in Figs. 7A and B and 8. For pindolol, only partial separation was achieved. The migration order of bupivacaine enantiomers was verified with pure (*R*)- and (*S*)-isomers. (*R*)-Bupivacaine eluted before (*S*)-bupivacaine, as seen in Fig. 9, where an excess of (*R*)-isomer was added to the racemic mixture.

#### Bupivacaine in serum

Bupivacaine hydrochloride is an amide-type local, long-lasting anaesthetic agent. Following the epidural analgesia with administration of 150 mg of

TABLE I

MIGRATION TIME VARIATION OF VERAPAMIL AND FLUOXETINE (RELATIVE STANDARD DEVIATION, R.S.D.,  $n = 4$ ) AS FUNCTION OF HTAB CONCENTRATION

HTAB (mM)	R.S.D. (%)	
	Verapamil	Fluoxetine
0.00	2.8	6.1
0.01	0.4	0.9
0.03	0.7	0.4
0.06	0.6	0.5
0.15	3.5	3.7

TABLE II

MIGRATION TIME VARIATION OF VERAPAMIL AND FLUOXETINE (R.S.D.,  $n = 4$ ) AS FUNCTION OF CTPC CONCENTRATION

CTPC (mM)	R.S.D. (%)	
	Verapamil	Fluoxetine
0.0	2.8	6.1
0.1	1.4	1.7
0.5	1.7	1.0
0.9	2.4	2.8
2.0	2.8	2.9

the drug before orthopaedic surgery, therapeutic levels of bupivacaine were reported to remain in serum typically at the level of 1.0–1.2  $\mu\text{g}/\text{ml}$  up to 3 h after treatment [23]. Therapeutic levels of the race-

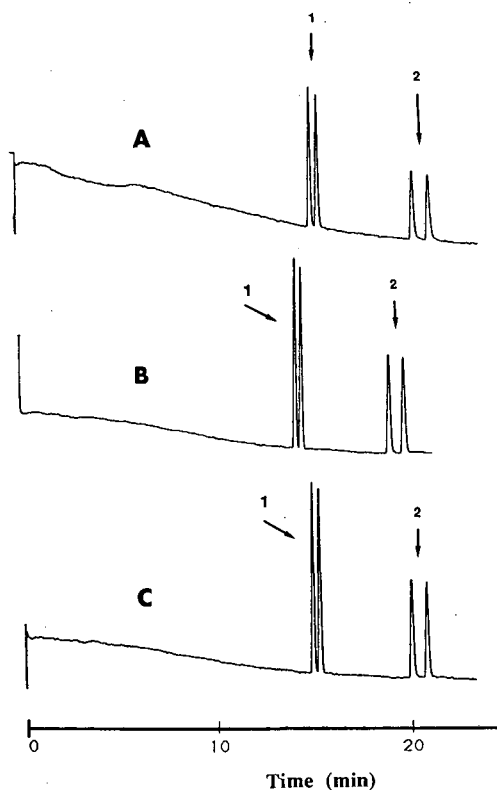


Fig. 6. Electropherograms of the enantiomers of verapamil (1) and fluoxetine (2). (A) Buffer: 10 mM TM- $\beta$ -CD–30 mM Tris, pH 2.8–0.1% MHEC 1000. (B) Buffer as in (A) with 0.03 mM HTAB. (C) Buffer as in (A) with 0.15 mM HTAB. Capillary: 64 cm  $\times$  50  $\mu\text{m}$  uncoated silica; voltage 20 kV; detection at 220 nm, 0.01 AUFS.

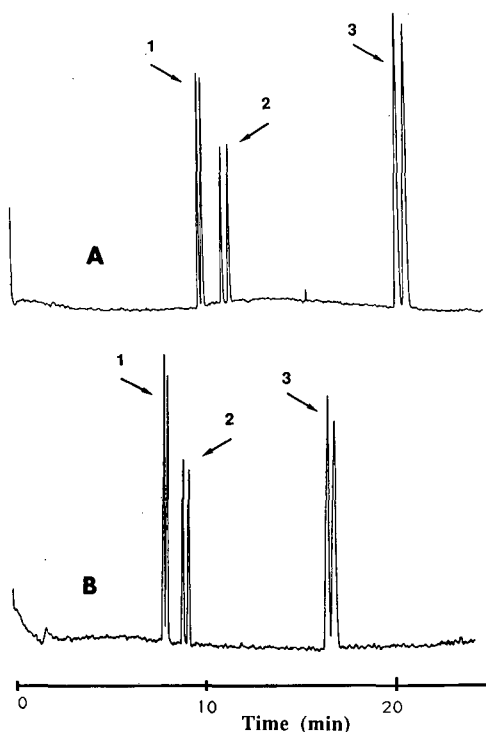


Fig. 7. Separations of the enantiomers of mepivacaine (1), bupivacaine (2) and carvedilol (3). Dimethyl- $\beta$ -cyclodextrin buffer composition is described in the text (Uncoated capillaries). Detection at 220 nm, 0.01 AUFS. (A) Uncoated 64 cm  $\times$  50  $\mu$ m capillary; 24 kV voltage. (B) Coated 64 cm  $\times$  50  $\mu$ m capillary; no HTAB added to the buffer; 24 kV voltage.

mic bupivacaine after administration of 187.5–250 mg doses can be as high as 1.5–3.5  $\mu$ g/ml using different regional anaesthesia techniques [24].

Using the DM- $\beta$ -CD buffer, as described above, calibration was performed when the serum samples

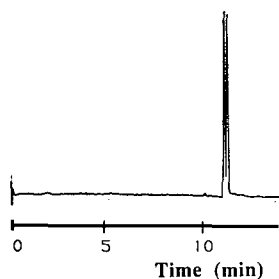


Fig. 8. Electropherogram of pindolol enantiomers (*R*, 0.89) with 10 mM DM- $\beta$ -CD–18 mM Tris, pH 3.0–0.1% MHEC 4000–0.03 mM HTAB buffer. Capillary: 64 cm  $\times$  50  $\mu$ m uncoated silica; voltage 24 kV; detection at 220 nm, 0.01 AUFS.

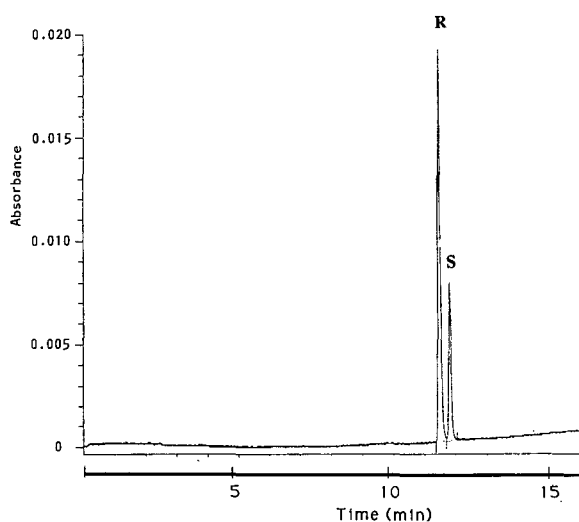


Fig. 9. Migration order of bupivacaine enantiomers: (*R*)-bupivacaine (99.9  $\mu$ g/ml; water-methanol), (*S*)-bupivacaine (35.7  $\mu$ g/ml; water-methanol). Detection at 200 nm, 0.02 AUFS; capillary: 50 cm  $\times$  75  $\mu$ m I.D. uncoated silica; other conditions as described in the text.

were spiked with the racemic bupivacaine in the concentration range of 0.19–3.8  $\mu$ g/ml. Mepivacaine was used as an internal standard. (*R*)- and (*S*)-enantiomers were quantitated separately by constructing linear regression calibration curves from the peak heights of the two bupivacaine enantiomers, which were compared with those of the mepivacaine enantiomers. Our previous experience has demonstrated that using a close analog of the substance analyzed, which migrates just before the analyte of interest, will yield excellent precision of peak-height ratio measurements [25]. The peak height ratios of (*R*)- and (*S*)-bupivacaine (RB and SB) and mepivacaine (1M and 2M) were measured for the sake of calibration and precision of sampling. Each peak height is considered here to represent 50% of the total amount of the racemic drug. For comparison, the first appearing enantiomer of mepivacaine (1M) was used as an internal standard for both enantiomers of bupivacaine.

Because a non-polar solvent at an alkaline pH was used to extract the bupivacaine, the serum background did not interfere with the CE measurements (Fig. 10). Specificity of determination was further explored by injecting the drugs cimetidine, warfarin, and diltiazem, which all migrated before

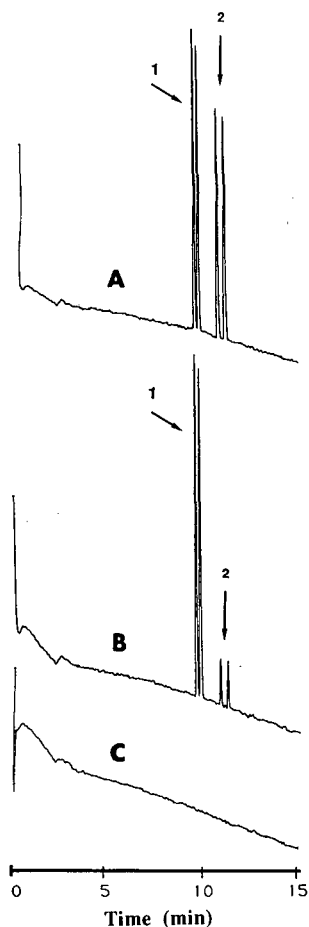


Fig. 10. Electropherograms of the racemic bupivacaine samples extracted from serum. Internal standard as: 1 = mepivacaine; 2 = bupivacaine. (A) 3.8  $\mu\text{g}/\text{ml}$ ; (B) 0.57  $\mu\text{g}/\text{ml}$ ; (C) serum blank. Run conditions: buffer, 10 mM DM- $\beta$ -CD–18 mM Tris, pH 2.9–0.1% MHEC 4000–0.03 mM HTAB; voltage 24 kV; capillary: 64 cm  $\times$  50  $\mu\text{m}$  uncoated silica, detection at 220 nm, 0.01 AUFS.

mepivacaine and bupivacaine. The acidic drugs indomethacin and ibuprofen were not detected under the analytical conditions employed. In general, acidic drugs are unlikely to interfere under the conditions we employed.

Table III demonstrates the linear regression measurements ( $y = a + bx$ ) for different methods of peak-height comparison. The calibration curves were measured for the (*R*)- and (*S*)-bupivacaine enantiomers in the concentration range of 0.095–1.9  $\mu\text{g}/\text{ml}$ . During repeated injections of serum sample with 1.15  $\mu\text{g}/\text{ml}$  (for racemic bupivacaine), the in-

TABLE III

LINEAR REGRESSION CALIBRATION DATA FOR (*R*)- AND (*S*)-BUPIVACAINE (RB AND SB)

Mepivacaine enantiomers 1M and 2M were used as internal standards

Peak height ratio	<i>r</i>	<i>a</i>	<i>b</i>	<i>n</i>
RB/1M	0.9995	0.002	0.205	5
SB/2M	0.9990	0.008	0.210	5
SB/1M	0.9992	0.005	0.201	5

jection precision (R.S.D.) was 1–2% for both bupivacaine enantiomers ( $n = 5$ ) using peak-height comparisons with the first eluted isomer of mepivacaine (1M).

#### Polyacrylamide-coated capillaries

Resolutions for mepivacaine, bupivacaine, and carvedilol were slightly decreased as shown in Fig. 7B on a coated capillary. Using a DM- $\beta$ -CD-HTAB buffer medium similar to the one described above for uncoated capillaries, the performance of coated capillaries was also evaluated. The remainder from the bupivacaine serum samples was injected in the multiple doses into the coated capillary and the peak-height ratios were measured.

We used the coated capillaries primarily to explore whether the presence of HTAB in the buffer would make any difference to the cyclodextrins' effectiveness (given that in a coated capillary there would be no free silanol moieties to cover). Our results suggest that the benefit of a cationic detergent is mainly due to the interaction of the detergent with the silanol groups in uncoated capillaries. Measurement precision for the coated capillaries (containing no silanol moieties) actually improved when the buffer did not contain HTAB. Table IV lists the precision (R.S.D.) of the measured ratios of the racemic bupivacaine sample (1.15  $\mu\text{g}/\text{ml}$  serum). The interaction of HTAB with CDs, then, is evidently not as powerful as that of the detergent with silanol moieties.

#### DISCUSSION

Interest in the use of high-performance electromigration techniques for resolution of optical iso-

TABLE IV

PEAK HEIGHT RATIOS OF (R)- AND (S)-BUPIVACAINE (RB AND SB) TO MEPIVACAINE ENANTIOMERS (1M AND 2M)

	R.S.D. (%) ( $n = 5$ )	
	With HTAB	Without HTAB
RB/1M	4.4	1.3
SB/2M	5.7	3.8
SB/1M	3.8	1.9

mers has been on a rapid rise in spite of a short induction period. Cyclodextrin derivatives [8–11] have been particularly singled out as attractive buffer additives in such separations. In general, chiral separations following this approach appear much easier to develop and optimize than the methodologies based on gas chromatography or high-performance liquid chromatography.

While the number of successful demonstrations of capillary electrokinetic chromatography in pharmaceutical applications increases, most (if not all) reports have been confined to the use of standard substances. Determination of chiral substances in biological matrices represents a set of special problems. One of the purposes of this study has been to evaluate detergents for overcoming the interference from endogenous substances in serum. Cationic micellar systems have proven effective in this regard. In addition, HTAB used at levels around its critical micelle concentration stabilized the migration times and peak shapes of various basic enantiomers with uncoated capillaries, suggesting it has a role in compensating for the negative surface charge and in decreasing the amount of irreversible adsorption.

The micellar agents can also be used to modify the selectivity of cyclodextrins towards various enantiomers, as shown with several chiral therapeutics investigated in this work. This may lessen the need to develop additional chemically modified cyclodextrins for the analysis of chiral drugs and other isomer separations.

The surface chemistry of the capillary wall is yet another variable in optimizing separations in capillary electrokinetic chromatography. In the work reported here, the use of HTAB with surface-coated capillaries was found counterproductive. Yet a sur-

face modification proved beneficial in resolving ketotifen derivatives and chloramphenicol in a different study [26]. Optimization strategies in chiral separations may need to take into account the effects of subtle changes in the buffer systems.

When biological interferences from serum samples are suppressed, it will be feasible to quantify certain chiral drugs at their therapeutic levels by CE and UV detection with adequate precision. This has been indicated by the example of bupivacaine in this study. However, reaching lower levels of detection will necessitate methodologies based on a more sensitive detection principle.

#### ACKNOWLEDGEMENTS

This research was supported by a grant GM 24349 from the National Institute of General Medical Science, US Department of Health and Human Services, and one from Beckman Instruments, Inc. We also appreciate additional funds from the Finnish Chemical Society, Jenny and Antti Wihuri Foundation, and a fellowship conferred by the Finnish Academy of Sciences to one of us (H.S.). Special thanks are due to Mr. Jan Sudor for his helpful discussions of this material and to Dr. Lars-Erik Edholm of Draco/Astra, Lund, Sweden, for donating the pure enantiomers of bupivacaine.

#### REFERENCES

- 1 E. J. Ariens, E. W. Wuis and E. J. Veringa, *Biochem. Pharmacol.*, 37 (1988) 9–18.
- 2 F. E. P. Mikkers, F. M. Everaerts and Th. P. E. M. Verheggen, *J. Chromatogr.*, 169 (1979) 11–20.
- 3 J. W. Jorgenson and K. D. Lukacs, *Anal. Chem.*, 53 (1981) 1298–1302.
- 4 S. Terabe, K. Otsuka, K. Ichikawa, A. Tsuchiya and T. Ando, *Anal. Chem.*, 56 (1984) 111–113.
- 5 T. Nakagawa, Y. Oda, A. Shibukawa and H. Tanaka, *Chem. Pharm. Bull.*, 36 (1988) 1622–1625.
- 6 T. Nakagawa, Y. Oda, A. Shibukawa, H. Fukuda and H. Tanaka, *Chem. Pharm. Bull.*, 37 (1989) 707–711.
- 7 H. Nishi, T. Fukuyama and M. Matsuo, *J. Chromatogr.*, 515 (1990) 245–255.
- 8 A. Guttman, A. Paulus, A. S. Cohen, N. Grinberg and B. L. Karger, *J. Chromatogr.*, 448 (1988) 41–53.
- 9 S. Fanali, *J. Chromatogr.*, 474 (1989) 441–446.
- 10 S. Fanali, *J. Chromatogr.*, 545 (1991) 437–444.
- 11 J. Snopek, H. Soini, M. Novotny, E. Smolkova-Keulemansova and I. Jelinek, *J. Chromatogr.*, 559 (1991) 215–222.
- 12 J. Snopek, I. Jelinek and E. Smolkova-Keulemansova, *J. Chromatogr.*, 452 (1988) 571–590.



- 13 S. Terabe, Y. Miyashita, O. Shibata, E. R. Barnhart, L. R. Alexander, D. G. Patterson, B. L. Karger, K. Hosoya and N. Tanaka, *J. Chromatogr.*, 516 (1990) 23–31.
- 14 H. Nishi and M. Matsuo, *J. Liq. Chromatogr.*, 14 (1991) 973–986.
- 15 J. Liu, K. A. Cobb and M. V. Novotny, *J. Chromatogr.*, 519 (1990) 189–197.
- 16 T. Okubo, H. Kitano and N. Ise, *J. Phys. Chem.*, 80 (1976) 2661–2664.
- 17 I. Satake, T. Ikenoue, T. Takeshita, K. Hayakawa and T. Maeda, *Bull. Chem. Soc. Jpn.*, 58 (1985) 2746–2750.
- 18 S. Hjertén, *J. Chromatogr.*, 347 (1987) 191–198.
- 19 J. Liu, J. F. Banks, Jr. and M. Novotny, *J. Microcol. Sep.*, 1 (1989) 136–141.
- 20 T. Kaneta, S. Tanaka and H. Yoshida, *J. Chromatogr.*, 538 (1991) 385–391.
- 21 P. Mukerjee, K. J. Mysels, *Critical Micelle Concentrations of Aqueous Surfactant Systems*, *Natl. Std. Ref. Data Ser.*, National Bureau of Standards, Washington, DC 1971.
- 22 S. H. Hansen, P. Helboe and U. Lund, *J. Chromatogr.*, 240 (1982) 319–327.
- 23 R. L. P. Lindberg and K. K. Pihlajamäki, *J. Chromatogr.*, 309 (1984) 369–374.
- 24 U.-W. Wiegand, R. C. Chou, E. Lanz and E. Jänchen, *J. Chromatogr.*, 311 (1984) 218–222.
- 25 H. Soini, M. L. Riekkola and M. V. Novotny, presented at the *International Symposium on Sample Preparation for Biomedical and Environmental Analysis, Guildford, July 23–25, 1991*.
- 26 J. Snopek and M. Novotny (1992), submitted for publication.

# Chiral separation by capillary electrophoresis with oligosaccharides

A. D'Hulst and N. Verbeke

Clinical Pharmacy, Catholic University of Leuven, Gasthuisberg, Herestraat 49, B-3000 Leuven (Belgium)

---

## ABSTRACT

Maltodextrins, *i.e.*, mixtures of linear  $\alpha$ -(1-4)-linked D-glucose polymers, were found to be effective as chiral electrolyte modifiers to perform direct, rapid separations by capillary electrophoresis of racemic mixtures of 2-arylpropionic acid non-steroidal anti-inflammatory compounds and coumarinic anticoagulant drugs, and also diastereomeric cefalosporin antibiotics. Enantioselectivity seemed to be dependent on an as yet unidentified combination of variables.

---

## INTRODUCTION

The importance of enantiomeric differences in biological processes has been well recognized. Numerous chiral drugs have been shown to display stereoselectivity in their pharmacokinetic behaviour and/or pharmacological action [1,2]. In environmental sciences also enantioselectivity has been demonstrated, *e.g.*, in the enantiospecific activity of chiral pesticides [3]. Knowledge of these differences has influenced decision making and in some instances this has led to a re-thinking of drug development, where the use of pure enantiomeric drugs was shown to be an advantage or even a necessity. In view of these recent considerations and the ensuing regulatory requirements, the availability of easily accessible chiral separation techniques has become increasingly important.

Chiral separations for analytical purposes have been achieved using either gas chromatography (GC) or high-performance liquid chromatography (HPLC), both generally requiring derivatization with a chiral reagent in order to form diastereoisomers which can subsequently be separated by

conventional chromatographic methods. Direct chiral GC and HPLC separations have been performed using chiral stationary phases. Apart from optical asymmetry generated by chemical synthesis (*e.g.*, L-valine-*tert.*-butylamine coupled to polysiloxane for chiral GC, helical polymethacrylates adsorbed on silanized silica for chiral HPLC), various natural products have been used, in either modified or native form, to obtain chirality for HPLC: polysaccharides (*e.g.*, cellulose or amylose) or proteins (*e.g.*, albumin,  $\alpha$ -1 acid glycoprotein). In addition, direct separation of enantiomers by HPLC has also been demonstrated using chiral mobile phase additives, *e.g.*, chiral counter ions in ion-pair chromatography. All these methods require either a cumbersome sample preparation or a long column equilibration time and a long analysis time. None of them, except for recent advances based on the development of microbore HPLC [4], are convenient enough to allow high sample throughputs. Therefore, improving the available analytical methodology has grown into a major issue for the development of chiral substances.

Capillary electrophoresis (CE) with its various modes of operation (capillary zone electrophoresis, micellar electrokinetic chromatography, isotachopheresis, etc.) has proved to be a powerful and versatile separation technique. High plate numbers

---

Correspondence to: Professor N. Verbeke, Clinical Pharmacy, Catholic University of Leuven, Gasthuisberg, Herestraat 49, B-3000 Leuven, Belgium.

and speed of analysis in comparison with HPLC are easily achieved. Expanding the resolving power of CE towards stereoselective separations is possible by adding chiral modifiers to the background electrolyte, thus introducing a so-called chiral pseudo-stationary phase. Baseline resolution of chiral compounds has been demonstrated in the micellar electrokinetic chromatography mode, which consists of performing CE separations in electrolytes containing micelles. When using micelles composed of either achiral surfactants functionalized with chiral compounds [5] or chiral surfactants [6], an enantioselectivity factor is introduced and enantiomeric separation can be achieved. Alternatively, stereoselective complexing agents, *e.g.*, cyclodextrins, which have already been demonstrated to be most effective in chiral HPLC separations, have proved to be equally valuable in performing enantiomeric resolution by CE [7].

This paper gives an overview of the properties of linear oligosaccharides as potential chiral discriminators in CE. Oligosaccharides form a vast family of polymers, among which the following com-

pounds were screened in order to obtain chiral separations of racemic 2-arylpropionic acid (2-APA) non-steroidal anti-inflammatory drugs (NSAIDs): maltodextrin mixtures and corn syrups, pure maltooligosaccharides, linear non- $\alpha$ -(1-4)-linked glucose polymers and low-molecular-mass galactose-glucose-fructose copolymers and cyclodextrins.

Maltodextrins are defined by the US Food and Drug Administration as saccharide polymers consisting of D-glucose units linked primarily by  $\alpha$ -(1-4) bonds and having a dextrose equivalent (*DE*, defined as percent reducing sugars calculated as glucose on a dry-substance basis) of <20. Corn syrups are maltooligosaccharide mixtures with *DE*  $\geq$ 20. These mixtures are prepared by partial acid and/or enzymatic hydrolysis of corn starch. Maltodextrins and corn syrups are available under different brand names as complex mixtures of maltooligosaccharides, obtained by various manufacturing procedures. During hydrolysis of starch, high-molecular-mass glucose polymers are converted into oligosaccharides of a lower degree of polymerization (*DP*, defined as the number of saccharide

TABLE I

DEXTROSE EQUIVALENT (*DE*) AND MALTOOLIGOSACCHARIDE COMPOSITION (RELATIVE AMOUNTS IN %, w/w, WITHIN THE LOWER *DP* RANGE) OF MALTODEXTRINS AND CORN SYRUPS USED

*DP* 1, *DP* 2 and *DP* 3 correspond to glucose, maltose and maltotriose, respectively.

Maltodextrin/corn syrup	<i>DE</i>	<i>DP</i> 1	<i>DP</i> 2	<i>DP</i> 3	<i>DP</i> > 3	<i>DP</i> > 2
Maltrin 200	20	2.3	7.9	9.6	80.2	
Maltrin 150	15	0.7	4.5	6.6	88.2	
Maltrin 100	10	0.5	2.7	4.3	92.5	
Maltrin 040	5	0.2	0.3	0.6	98.9	
Maldex 30	30	3	13	16	68	
Maldex 20	20	2.8	9.0	18.0	70.2	
Maldex 15	15	2.6	7.2	10.0	80.2	
Mylose HDE	60	38	37	7	18	
Mylose STD	38	14	12	11	63	
Mylose HM	44	7	50	14	29	
Glucidex 21	21	3	7			90
Glucidex 19	19	2	7			91
Glucidex 17	17	2	5			93
Glucidex*12	12	1	2			97
Glucidex 9	9	0.5	1.5			98
Glucidex 6	6	0.5	1			98.5
Glucidex 2	2	0.5	0.5			99
Lycasin 80/85	0	7	52.5			40

monomers within the oligo- or polysaccharide chain) and consequently the *DE* value rises. Therefore, maltodextrins and corn syrups of high *DE* are characterized by a lower average *DP*. The percentage of different oligosaccharides present in the maltodextrin mixtures and corn syrups depends on the hydrolysis procedure followed. As a consequence, the various brands of maltodextrins and corn syrups available display a wide range of compositions, as summarized in Table I.

Subfractionation of maltodextrins or corn syrups may be performed by either preparative gel permeation chromatography (GPC) or ultrafiltration. Some maltooligosaccharides may be purchased as pure compounds, *i.e.*, maltooligosaccharides up to maltoheptaose (*DP*7), the state of the art limit of preparative GPC.

Post-hydrolysis modifications may produce major changes in the properties of maltodextrins or corn syrups, as is the case with Lycasin corn syrup. Lycasin differs from conventional corn syrups in its extremely low *DE* value, which is obtained by subjecting corn syrup to hydrogenation, leaving a product devoid of reducing sugars.

Other oligo- and polysaccharides different from the linear  $\alpha$ -(1–4)-linked glucose polymers are also available, such as linear raffinose, stachyose and dextrans, in addition to cyclodextrins, which are circular  $\alpha$ -(1–4)-linked glucose oligomers.

In a first series of experiments, the enantiomeric resolving power of complex maltooligosaccharide mixtures was evaluated by their ability to obtain separate peaks for three racemic 2-arylpropionic acid non-steroidal anti-inflammatory drugs, flurbiprofen, ibuprofen and ketoprofen. Second, an attempt was made towards the identification of the chiral discriminating fraction using either corn syrup subfractions obtained through ultrafiltration or pure maltooligosaccharides. Moreover, a comparison was also made with various other oligosaccharides, different from the  $\alpha$ -(1–4)-linked glucose polymers. Finally, the method was applied to racemic coumarinic anticoagulant drugs and to diastereoisomeric pairs of cephalosporin antibiotics.

## EXPERIMENTAL

### Chemicals

Maltodextrins and corn syrups of different origin

were used. The Maltrin, Maldex and Glucidex maltodextrin series were kind gifts from Grain Processing Corp. (Muscatine, IA, USA), Amylum (Aalst, Belgium) and Roquette (Lestrem, France) respectively; the Mylose and Lycasin corn syrups were gifts from Amylum and Roquette, respectively. D-(+)-Maltose, stachyose, dextran 1500 and dextran 6000 were purchased from Fluka (Buchs, Switzerland); raffinose, separate maltooligosaccharides (from maltotriose to maltoheptaose) and maltooligosaccharide mixture were obtained from Merck (Darmstadt, Germany).  $\beta$ -, Dimethyl- $\beta$ - and hydroxypropyl- $\beta$ -cyclodextrin were obtained from Sigma (Deisenhofen, Germany), Avebe (Veendam, Netherlands) and Janssen Drug Delivery Systems (Beerse, Belgium), respectively. 3-[(3-Cholamidopropyl)-dimethylammonio]-1-propanesulphonate (CHAPS), N,N-dimethyl-N-myristyl-3-ammonio-1-propanesulphonate (DMAP) and *n*-dodecyl- $\beta$ -D-maltoside (DDM) surfactants were purchased from Fluka.

Pharmaceutical compounds included racemic flurbiprofen and ibuprofen (gifts from Boots, Nottingham, UK) and ketoprofen (gift from Rhône-Poulenc, Paris, France), the (*S*)-(+)-enantiomers of ibuprofen (gift from Profarma, Beerse, Belgium) and naproxen (gift from UCB, Brussels, Belgium), warfarin and 3-( $\alpha$ -acetyl-*p*-chlorobenzyl)-4-hydroxycoumarin (Sigma), phenprocoumon and *p*-chlorophenprocoumon (gift from Roche, Basle, Switzerland), acenocoumarol (gifts from Ciba-Geigy, Basle, Switzerland) and the diastereoisomers of cefalexin and cefadroxy (courtesy of Professor J. Hoogmartens, Laboratory of Pharmaceutical Chemistry, K.U. Leuven, Belgium).

Sodium dihydrogenphosphate and sodium hydroxide were obtained from Merck.

### Capillary electrophoresis

Experiments were performed with a Waters Quanta 4000 CE system, with detection using a fixed-wavelength UV detector equipped with a zinc lamp and a 214-nm filter. The system was operated at a constant voltage (30 kV). Fused-silica capillaries of 50 and 75  $\mu$ m I.D. were used with a capillary length ranging from 50 to 90 cm. Capillaries were stored overnight filled with water. Each day operation was started by purging with 0.5 M sodium hydroxide solution followed by water. When

changing electrolytes, the capillary was subjected to an electroosmotic purge following a vacuum purge with the new electrolyte. All runs were preceded by a 3-min purge with the electrolyte used. Samples were introduced by gravity-induced siphoning ( $\Delta\text{Height} \cdot \text{time} = 100 \text{ cm s}$ ). Data were collected through Waters Maxima Software.

All sample solutions were prepared with water obtained from a Milli-Q water purification system (Millipore, Bedford, MA, USA) or HPLC-grade acetonitrile (Carlo Erba, Milan, Italy). All CE running buffers were freshly prepared in Milli-Q-purified water, filtered and degassed immediately prior to use. The background electrolyte consisted of 10 mM sodium phosphate buffer (pH 7.0) unless stated otherwise.

#### Ultrafiltration

A 20% Mylose STD solution in water was subjected to three subsequent ultrafiltrations through membranes with decreasing molecular mass cut-offs (3000, 1000 and 500) using an Amicon Model 8050 ultrafiltration cell. After each step samples of the filtrate and retentate were taken and kept refrigerated until further use (within 1 day). To all samples sodium phosphate was added to give a final concentration of 10 mM and the pH was adjusted to 7. Ultrafiltration subfractions were either reconstituted with respect to the Mylose starting solution (filtrate fractions) or adjusted to obtain a multiple of the original corn syrup concentration (retentate fractions).

#### Calculations

As in chiral separations the peaks corresponding to the separate enantiomers are always geminate, the usual terms of resolution or efficiency often do not describe accurately the actual separation of the optical antipodes. Instead, a relative chiral separation (*RCS*) factor was introduced in order to compare the oligosaccharide-modified electrolytes with respect to their enantiomeric resolving power:

$$RCS = \frac{\Delta T - 2\bar{w}}{\overline{MT}} \cdot 100$$

where  $\Delta T$  is the time between the start and end of the first and second enantiomeric peaks, respectively,  $\bar{w}$  is the mean peak width and  $\overline{MT}$  is the mean migration time. Baseline separation of the antipo-

des thus results in positive values of the *RCS* factor, whereas negative values are obtained for poorly resolved enantiomers. In addition, the *RCS* factor indicates the efficiency of the separation conditions studied: increasing *RCS* values represent an increase in efficiency, owing to a shorter analysis time and/or better peak separation. However, for partially resolved enantiomers with comparable peak overlap a decrease in migration time, which in fact represents a more efficient separation, is reflected by a more negative *RCS*.

## RESULTS

### *Complex maltooligosaccharide mixtures as electrolyte additives for chiral separations*

*Influence of experimental conditions on chiral separation with a homogeneous series of maltooligosaccharide-modified electrolytes.* Four maltodextrin mixtures of the Maltrin series having different *DE* values were compared with respect to their resolving power towards three racemic 2-APA NSAIDs (flurbiprofen, ibuprofen and ketoprofen) in three different capillaries (two 75  $\mu\text{m}$  I.D. capillaries of length 50 and 90 cm, respectively, and a 50  $\mu\text{m}$  I.D.  $\times$  60 cm length capillary. The results are reported in Table II.

Baseline resolution of ibuprofen enantiomers was achieved under almost all conditions (as indicated by the positive values of the *RCS* factor). The separation of the optical antipodes of flurbiprofen was more difficult to achieve, and ketoprofen enantiomers co-migrated under all conditions tested.

Increasing the maltodextrin contents of the electrolyte increased the migration times, as expected from the rise in viscosity, and improved the resolution. Modifying the electrolyte with maltodextrins of lower *DE* value also allowed an improved separation.

Addition of acetonitrile to the electrolyte, generally known to decrease migration times and improve resolution [8], had the opposite effect, *i.e.*, an increased migration time without improved resolution. As it has been reported elsewhere that combining surfactants with circular oligosaccharides was beneficial to chiral separation [9], we added various surfactants to Maltrin-modified electrolytes. It was found that the resolution of flurbiprofen and ibu-

TABLE II

CAPILLARY ELECTROPHORETIC CHIRAL SEPARATION OF THE 2-APA NSAID COMPOUNDS FLURBIPROFEN (F), IBUPROFEN (I) AND KETOPROFEN (K) WITH MALTRIN-MODIFIED ELECTROLYTES

Migration time (*MT*) in minutes. Relative chiral separation (*RCS*) in arbitrary units.

Capillary	Maltrin		F		I		K <sup>a</sup>	
	<i>DE</i>	Concentration (%)	<i>MT</i>	<i>RCS</i>	<i>MT</i>	<i>RCS</i>	<i>MT</i>	
(a) 50 cm × 75 μm I.D.	15	10	9.61-9.96	-1.022	12.17-12.99	3.498	15.69	
		7.5	7.68-7.90	-1.284	9.30-9.68	0.316	10.96	
		5	6.93-7.11	-2.137	8.17-8.45	0.241	9.13	
	10	5	6.84-7.04	-2.306	8.08-8.36	-1.095	9.22	
		5	2.5	8.67-9.03	-1.695	10.66-11.27	2.462	12.43
(b) 90 cm × 75 μm I.D.	15	2.5	14.05-14.26	-0.212	15.35-15.60	0.582	15.77	
		5	15.02-15.29	-0.367	16.81-17.22	1.117	17.85	
		7.5	16.61-16.89	-0.359	18.81-19.32	1.259	20.40	
		10	19.64-20.01	1.160	22.49-23.21	1.838	25.00	
	10	5	12.75-12.94	-0.078	14.04-14.32	1.120	14.87	
		7.5	16.34-16.63	0.485	18.37-18.93	1.877	>20	
		10		17.86-18.16	0.333	20.02-20.67	2.162	22.46
(c) 60 cm × 50 μm I.D.	20	5			14.25-14.80	1.308		
		6.25			14.50-15.07	1.285		
		7.5			18.57-19.56	2.255		
	15	3.75			10.75-11.12	-0.823		
		5			12.04-12.56	1.301		
		6.25			14.06-14.79	2.288		
		7.5			17.65-18.84	4.166		
	10	2.5			9.13-9.36	-1.190		
		3.75			10.60-11.00	0.926		
		5			11.89-12.41	1.070		
		6.25			12.44-13.04	1.570		
	5	2.5			8.20-8.51	-0.477		
		3.75			9.45-9.82	0.415		
5				10.00-10.52	2.047			

<sup>a</sup> No separation of enantiomers.

profen enantiomers disappeared completely on addition of the non-ionic surfactant DDM at a concentration well above the critical micellar concentration (cmc), the cmc of DDM in water being 0.16 mM. Increasing the maltodextrin concentration while decreasing the surfactant concentration restored the chiral separation with migration times slightly longer. Addition of increasing amounts of the amphoteric surfactants DMAP (cmc = 0.33 mM) initially resulted in an increased migration time and eventually in complete loss of enantioselectivity. Adding CHAPS (cmc = 8 mM), another

amphoteric surfactant, had an even more pronounced deleterious effect on chiral resolution.

With a higher field strength the migration velocity increased [Table II, compare (a) and (b)]. Although higher plate numbers are expected to be achieved by increasing the field strength, this may cause a rise in temperature. Where heat dissipation is less efficient, as with shorter capillaries, separation is negatively affected. Consequently, decreasing the capillary diameter results in a higher efficiency as the increased surface to volume ratio favours convection. In a 50 μm I.D. × 60 cm capil-

lary chiral separation of ibuprofen was more easily obtained, *i.e.*, at lower Maltrin concentrations and with shorter migration times, as demonstrated by the results shown in Table II, part (c).

*Influence of the composition of maltodextrin mixtures on chiral separation.* Fig. 1. compares the chiral separation of the 2-APA NSAIDs in electrolytes modified with maltodextrins of the Maltrin (Fig. 1A), Maldex (Fig. 1B) and Glucidex (Fig. 1C) se-

ries, which display DP spectra slightly different from each other, and with Mylose corn syrups (Fig. 1D). Complete resolution of ibuprofen enantiomers was demonstrated for all Maldex and Mylose maltooligosaccharide mixtures studied and for the lower *DE* range of Glucidex, as indicated by the positive values of the *RCS* factor. The chiral separation of flurbiprofen was more limited whereas ketoprofen enantiomers did not separate at all.

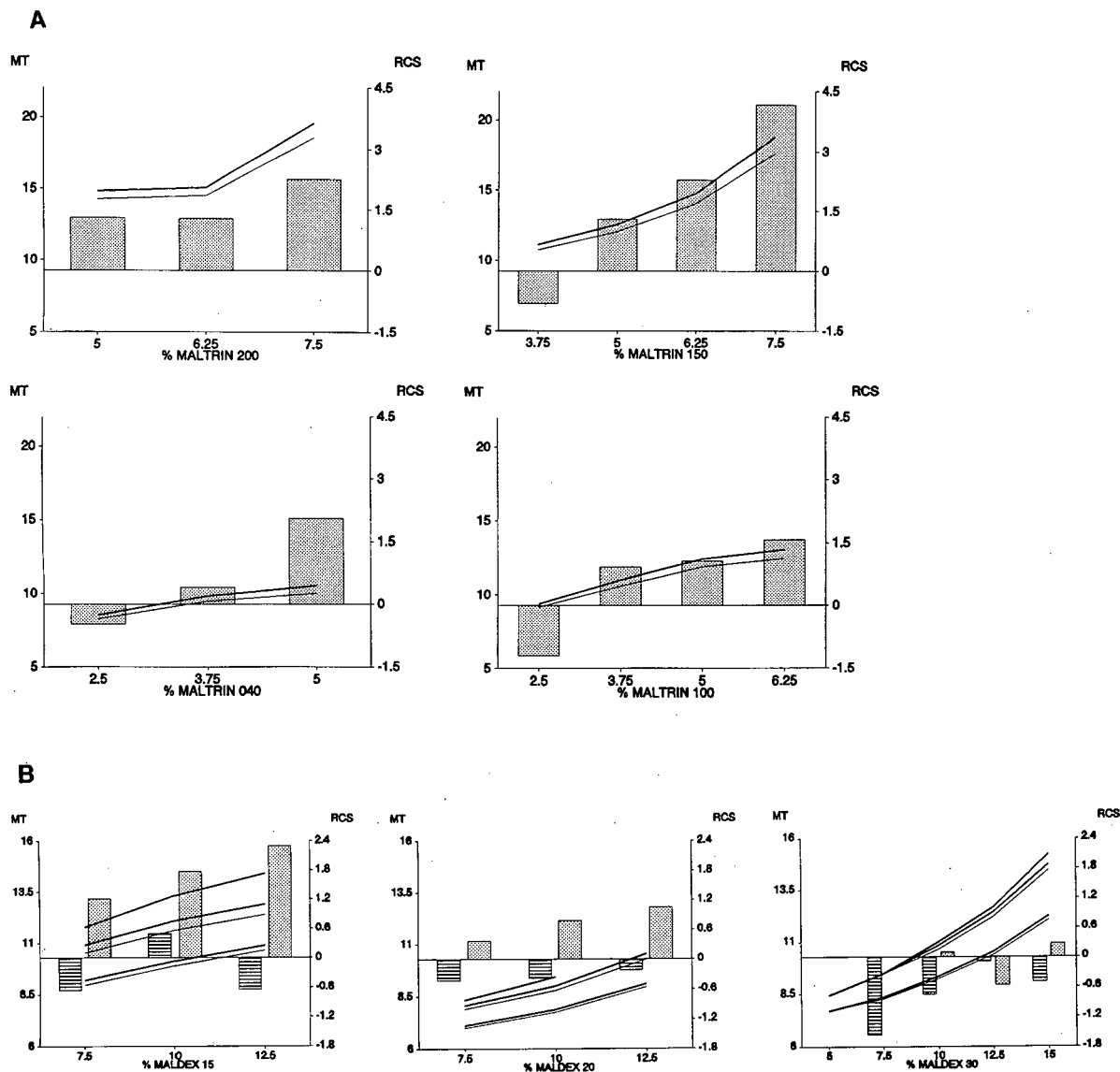


Fig. 1.

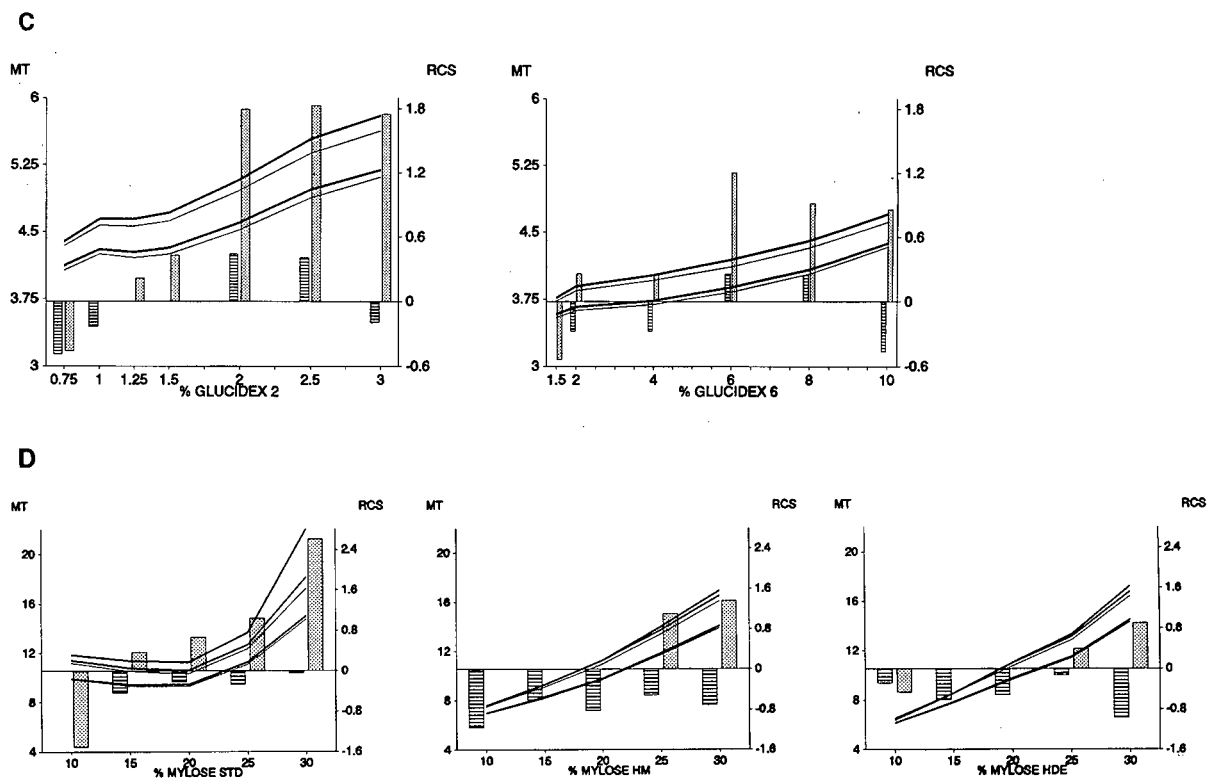


Fig. 1. Chiral separation of 2-APA NSAIDs: (*R/S*)-flurbiprofen (F), (*R/S*)-ketoprofen (K). Migration times of enantiomers (MT) in minutes (line graphs) and relative chiral separation (RCS) in arbitrary units (bar graphs) as a function of concentration in % of chiral modifier in background electrolyte. Dot-patterned bars, ibuprofen; stripe-patterned bars, flurbiprofen. Separation of ketoprofen enantiomers was not demonstrated in these experiments. (A) Modifiers, Maltrin series; sample, I. (B) Modifiers, Maldex series; sample, K (top line), I (middle pair of lines) and F (lower pair of lines). (C) Modifiers, Glucidex series; sample, I (upper pair of lines) and F (lower pair of lines). (D) Modifiers, Mylose series; sample, K (top line), I (middle pair of lines) and F (lower pair of lines).

As shown already for the Maltrin series, the chiral separation of ibuprofen enantiomers also improved for Maldex and Glucidex maltodextrins with increasing concentrations or decreasing *DE* value. Resolution was achieved in a shorter time with maltodextrins of the Maldex series as compared with Maltrin, even at higher concentrations. The analysis times with electrolytes containing low-*DE* Glucidex (*DE* 2 and 6) were found to be even lower. Glucidex 2 and 6 also allowed baseline separation of flurbiprofen enantiomers, which was not possible with the Maldex products. The longer analysis times in the presence of Maltrin as compared with Maldex of identical *DE* value and at the same concentration could possibly be ascribed to the higher contents of high-molecular-mass malto-oligosaccharides producing a higher viscosity. Ap-

parently the presence of oligosaccharides with a higher *DP* value favours chiral separation.

From the *RCS versus* concentration course of the experiments with Glucidex 2 and 6 (Fig. 1C), an optimum in the maltodextrin concentration for chiral separation was observed. This phenomenon was not observed with the Maltrin- or Maldex-modified electrolytes. Indeed, owing to their lower transparency as compared with the electrolytes containing high concentrations of Glucidex 2 or 6, the concentrations of Maltrin and Maldex maltodextrins could not be increased so as to determine a possible decline in chiral resolution and/or efficiency in the presence of higher percentages of electrolyte modifier.

As shown in Table III, Glucidex maltodextrins in the higher *DE* range were not as efficient as electro-



TABLE III

CAPILLARY ELECTROPHORETIC CHIRAL SEPARATION OF THE 2-APA NSAID COMPOUNDS FLURBIPROFEN (F) AND IBUPROFEN (I) WITH GLUCIDEX-MODIFIED ELECTROLYTES

Capillary 60 cm × 50 μm I.D. Migration time (MT) in minutes. Relative chiral separation (RCS) in arbitrary units.

Glucidex		F		I	
DE	Concentration (%)	MT	RCS	MT	RCS
2	2	4.52-4.60	0.439	4.96-5.08	1.793
6	4	3.69-3.73	-0.270	3.96-4.02	0.251
9	5			10.48-10.96	
12	5			5.78-5.90	
17	5			8.61-8.87	
19	5			5.82	
21	5			5.37	

lyte modifiers; prolonged analysis times and loss of enantioselectivity were demonstrated as the *DE* value was increased from 2 to 21.

Notwithstanding their high *DE* values, reflecting comparatively large amounts of low-*DP* oligosaccharides, Mylose corn syrups also allowed chiral separation of ibuprofen and, to a variable extent, of flurbiprofen (Fig. 1D). As expected from the *DP* values (Table I) and the observations relating to the maltodextrins described above, Mylose STD performed best. The enantiomeric resolution of flur-

biprofen improved on increasing the Mylose concentration but no baseline separation could be obtained. Chiral separation of ibuprofen was achieved in most instances. With Lycasin 80/85 hydrogenated corn syrup-based electrolytes a complete absence of enantiomeric separation for all three 2-APAs was demonstrated.

Typical electropherograms of the simultaneous chiral separation of ibuprofen and flurbiprofen using maltodextrin- or corn syrup-modified electrolytes are shown in Fig. 2A and B.

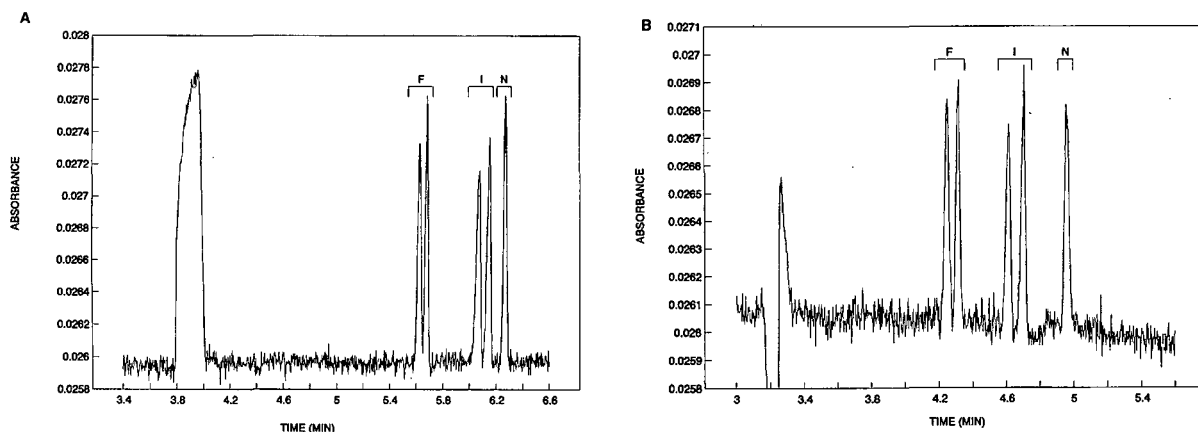


Fig. 2. Electropherograms representing chiral separation of 2-APA NSAIDs: (*R/S*)-flurbiprofen (F), (*R/S*)- and *S*-(+)-ibuprofen (I), (*S*-(+)-naproxen (N). (A) Electrolyte: 10% Mylose STD-10 mM sodium phosphate (pH 7.07). Migration times (min): (*R/S*)-F, 5.63-5.68; (*R/S*)-I, 6.08 (*S*)-6.15 (*R*); (*S*-(+)-N, 6.27. (B) Electrolyte: 1.5% Glucidex 2-10 mM sodium phosphate (pH 7.05). Migration times (min): (*R/S*)-F, 4.25-4.32; (*R/S*)-I, 4.62 (*S*)-4.71 (*R*); (*S*-(+)-N, 4.96.

TABLE IV

CAPILLARY ELECTROPHORETIC CHIRAL SEPARATION OF THE 2-APA NSAID COMPOUNDS FLURBIPROFEN (F), IBUPROFEN (I) AND KETOPROFEN (K) IN ELECTROLYTES MODIFIED WITH PURE MALTOOLIGOSACCHARIDES

DP 2 is maltose, DP 3 is maltotriose, DP 4 is maltotetraose, etc. Capillary 60 cm × 50 μm I.D. Migration time (MT) in minutes. Relative chiral separation (RCS) in arbitrary units.

Maltooligosaccharide		F		I		K	
DP	Concentration (%)	MT	RCS	MT	RCS	MT	RCS
2	10	4.76		4.80		4.68	
3	5	5.30		5.38		5.31	
4	5	4.88-4.91	-1.839	5.01-5.10	0.396	5.59-5.62	-1.070
5	5	5.71-5.74	-0.699	5.68-5.76	-2.448	6.33	
6	5	5.76-5.82	-1.036	5.49-5.62	0.360	6.82-6.87	-0.730
7	6.25			5.52-5.60	-0.899		

*Separate maltooligosaccharides as chiral electrolyte modifiers*

Separate maltooligosaccharides of DP 2-7 were screened as electrolyte additives for chiral separa-

tion. The results, summarized in Table IV, were obtained after simultaneous injection of all three racemic 2-APAs unless co-migration was observed, in which event separate runs were performed. None of

TABLE V

CAPILLARY ELECTROPHORETIC CHIRAL SEPARATION OF THE 2-APA NSAID COMPOUNDS FLURBIPROFEN (F) AND IBUPROFEN (I) WITH ELECTROLYTES MODIFIED WITH MYLOSE ULTRAFILTRATION SUBFRACTIONS

Mylose and subfractions are referred to as S (Mylose starting solution), R (retentate) and F (filtrate), and characterized by the molecular mass cut-off of the filter (MCO) and the concentration relative to the starting solution (conc. ratio). Capillary 60 cm × 50 μm I.D. Migration time (MT) in minutes. Relative chiral separation (RCS) in arbitrary units.

Material	Mylose		F		I	
	MCO	Conc. ratio	MT	RCS	MT	RCS
S		1.00	8.43-8.53	0.236	9.30-9.48	0.745
		0.67	6.81-6.89	0.146	7.45-7.57	0.399
		0.50	5.63-5.68	-0.177	6.08-6.15	-0.164
R	3000	4.00	9.54-9.64	0.104	10.39-10.63	1.332
		2.00	5.55-5.61	0	6.04-6.15	0.656
		1.00	4.42-4.47	-0.225	4.76-4.82	0
		0.67	4.12-4.16	-0.242	4.38-4.42	-0.455
		0.50	3.97-4.00	-0.753	4.18-4.21	-0.715
F	3000	1.00	7.08-7.14	-0.422	7.67-7.76	0
		0.67	5.78-5.82	-0.517	6.14-6.19	-0.811
		0.50	5.21-5.24	-0.766	5.47-5.50	-0.729
R	1000	2.00	6.32-6.38	-0.157	6.80-6.90	0.438
		1.00	4.79-4.82	-0.624	5.07-5.11	-0.589
		0.67	4.46-4.48	-1.119	4.66-4.69	0
F	1000	1.00	5.80		5.95	
R	500	4.00	6.46		6.70	
F	500	1.00	4.97		5.03	

the maltooligosaccharides used was able to resolve completely and simultaneously ibuprofen, flurbiprofen and ketoprofen into their enantiomers. In the presence of maltose or maltotriose, no enantiomeric separation was observed and ketoprofen and flurbiprofen co-migrated. Maltotetraose and -hexaose allowed the complete resolution of ibuprofen, whereas maltopentaose and -heptaose did not. In addition, a partial separation of ketoprofen enantiomers was observed with maltotetraose and -hexaose.

#### *Maltodextrin ultrafiltration subfractions*

In order to analyse further the influence of the composition of maltodextrin mixtures on chiral resolution, a 20% Mylose solution was submitted to differential ultrafiltration, yielding subfractions composed of maltooligosaccharides with decreasing *DP*. The retentate and filtrate from each fractionation step were tested at various concentrations to obtain the chiral separation of simultaneously injected racemic flurbiprofen and ibuprofen. The results are given in Table V. The retentate of the first ultrafiltration step, *i.e.*, a Mylose solution from which oligosaccharides of molecular mass  $\leq 3000$  had been removed and of a comparable concentration with respect to the higher *DP* fractions, showed a slight decrease in stereoselectivity and a substantial decrease in migration times. The corresponding filtrate, composed of maltooligosaccharides of molecular mass  $\leq 3000$ , *i.e.*, with *DP* < 19, again showed a moderate decrease in both stereoselectivity and migration times. The ultrafiltrate subfraction with molecular mass cut-offs between 1000 and 3000, corresponding to a maltooligosaccharide mixture with *DP* values ranging from 6 to 18, performed slightly less than the preceding fraction. Fractions consisting of maltooligosaccharides of molecular mass  $\leq 1000$  completely lost enantioselectivity. The latter result was confirmed by using a commercially available *DP* 2–6 standard maltooligosaccharide mixture; this modifier was unable to resolve the ibuprofen enantiomers within the concentration range tested, *i.e.*, 2.5–12.5%.

#### *Maltooligosaccharide-enriched maltodextrins*

The importance of the quantitative composition of maltooligosaccharide mixtures with respect to enantioselectivity was also briefly investigated by

selective enrichment of a maltodextrin mixture with separate maltooligosaccharides. Samples containing racemic flurbiprofen, ibuprofen and ketoprofen were run with electrolytes modified with 5% of Maltrin 150 and 2.5% of a pure maltooligosaccharide, either maltotriose, -tetraose, -pentaose or -hexaose. No influence on the chiral separation of any of the three 2-APAs was observed on addition of maltotriose (both migration times and *RCS* values were comparable), whereas the addition of *DP* 4–6 maltooligosaccharides to a maltodextrin-based electrolyte completely abolished chiral separation.

#### *Oligosaccharides different from linear $\alpha$ -(1–4)-D-glucose polymers*

Several other linear non- $\alpha$ -(1–4)-linked glucose polymers and low-molecular-mass galactose–glucose–fructose copolymers were also studied. The electrolytes contained either stachyose (7.7%), raffinose (10%), dextran 1500 (8.2%) or dextran 600 (10%). At the concentrations used none of these oligosaccharides showed any chiral discrimination towards flurbiprofen, ibuprofen or ketoprofen.

The circular  $\alpha$ -(1–4)-linked glucose oligomeric cyclodextrins which have been reported to be effective electrolyte additives for chiral CE were also included.  $\beta$ -Cyclodextrin, dimethyl- $\beta$ -cyclodextrin or hydroxypropyl- $\beta$ -cyclodextrin were added to the background electrolyte within the concentration ranges 1.35–1.85%, 7.5–20% and 25–50%, respectively. None of the three 2-APAs tested was resolved using either of the cyclodextrin-modified electrolytes. Also, addition of 5–30% acetonitrile to the cyclodextrin-based electrolyte did not lead to chiral separation.

#### *Applications*

In order to assess the applicability of maltodextrins as chiral discriminators towards various other racemic compounds using comparable conditions with respect to pH, maltodextrin concentration and migration of the compounds tested relative to the electroosmotic flow, three coumarinic anticoagulant drugs were used. Two racemic analogues commonly used as their internal standards in HPLC were also included. Chiral separation was demonstrated for warfarin and phenprocoumon and for their HPLC internal standards, but not for acenocoumarol (Fig. 3A–D). Diastereoisomers could also

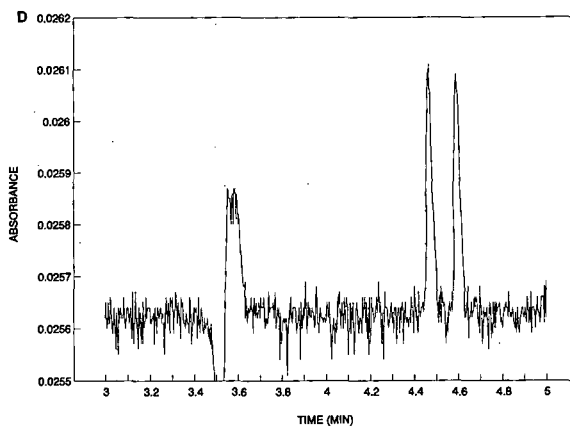
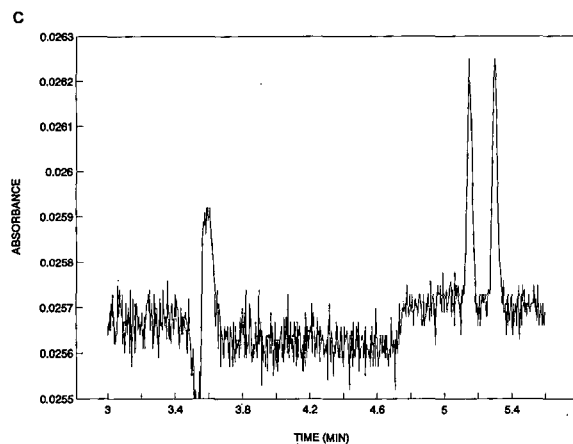
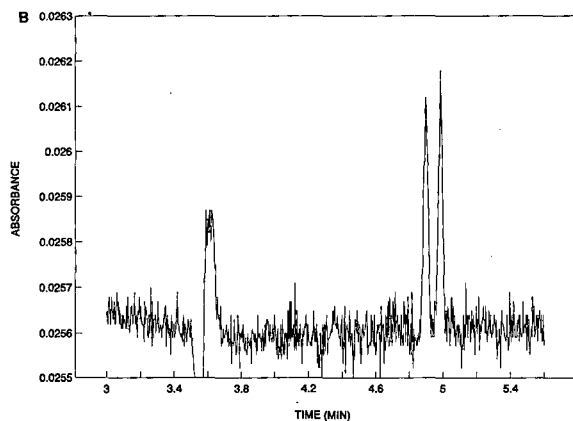
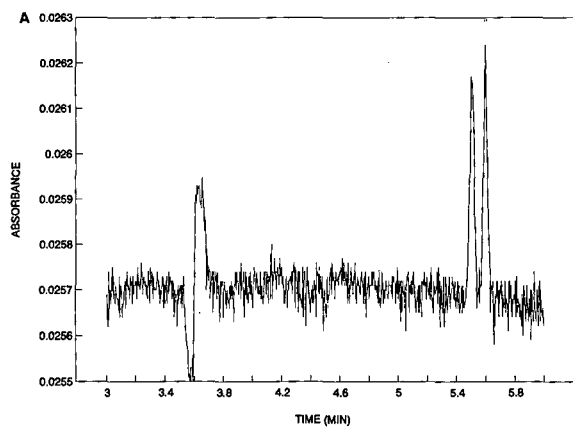


Fig. 3. Electropherograms representing chiral separation of coumarinic anticoagulants. Electrolyte: 2.5% Glucidex 2-10 mM sodium phosphate (pH 7.1). (A) (*R/S*)-Warfarin. Migration times: 5.50-5.59 min. (*R/S*)-3-( $\alpha$ -Acetyl-*p*-chlorobenzyl)-4-hydroxycoumarin. Migration times: 4.90-4.99 min. (C) (*R/S*)-Phenprocoumon. Migration times: 5.15-5.30 min. (D) (*R/S*)-*p*-Chlorophenprocoumon. Migration times: 4.47-4.60 min.

be separated, as demonstrated with two cephalosporin antibiotics, cefalexin and cefadroxy (Fig. 4A and B).

#### DISCUSSION

Using 2-APA NSAIDs as test compounds, direct chiral separation by CE was demonstrated with electrolytes modified by complex maltooligosaccharide mixtures. Although the performance of the maltodextrins and corn syrups tested displayed large variations, the chiral separations generally improved on increasing the concentration or decreasing the *DE* value, demonstrating the importance of both the qualitative and quantitative composition of the maltooligosaccharide mixtures.

In an attempt to identify the maltodextrin fractions necessary and/or sufficient for chiral separation to occur, separate maltooligosaccharides of *DP* 3-7 were studied. Maltotetraose and-hexaose showed chiral separations of all three 2-APAs tested, although to variable extents. Odd-numbered oligosaccharides performed less well under the same conditions. Additional information from experiments with maltooligosaccharides of higher *DP* is clearly needed, but so far pure separate maltooligosaccharides have been produced by preparative gel

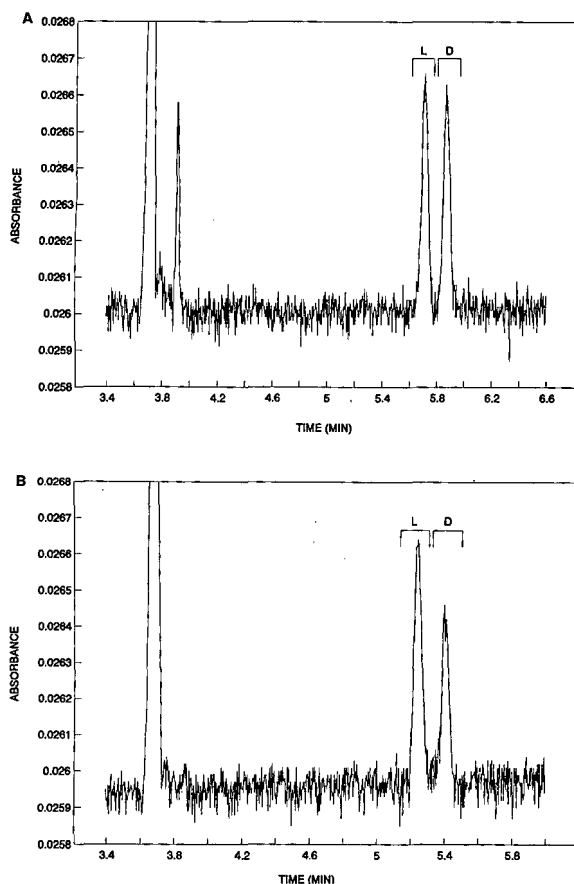


Fig. 4. Electropherograms representing the separation of the diastereoisomers of cephalosporin antibiotics. Electrolyte: 1% Glucidex 2–10 mM sodium phosphate (pH 7.5). (A) D/L-Cephalexin. Migration times: 5.72(L)–5.88(D) min. (B) D/L-Cephadroxy. Migration times: 5.25(L)–5.41(D) min.

permeation chromatography, the upper limit of which is set at  $DP$  7. Also, in order to link the chiral resolving capacity to a specific component or subfraction, a knowledge of the entire  $DP$  spectrum of the given maltooligosaccharide mixtures would be required. However, the analytical methodology available to date is limited to the identification and determination of the lower  $DP$  range, *i.e.*, up to  $DP$  43 [10].

The importance of the qualitative composition of the maltooligosaccharide mixtures was revealed by comparing the various maltodextrins used, *i.e.*, maltodextrin mixtures and corn syrups of different origins and  $DE$  values. Circumstantial evidence was

also provided by the experiments with separate maltooligosaccharides. Further conformation was obtained by the differential ultrafiltration experiments. As the maltodextrins and corn syrups are complex systems, one could speculate whether a single component might be responsible for the observed chiral separation. As pure oligosaccharides with  $DP > 7$  are not available, a different approach elucidating this question was attempted by using several corn syrup ultrafiltration subfractions. It was found that maltooligosaccharide mixtures in the lower  $DP$  range were ineffective in separating 2-APA enantiomers, whereas high- $DP$  corn syrup subfractions allowed chiral separation, although higher concentrations were needed as compared with the original solution. Apparently, the presence of high- $DP$  subfractions was not the only factor determining chiral separation. From the results described above one may conclude that particular high-molecular-mass components were necessary but not sufficient for enantioselective separations to occur. The matrix seemed to be equally, if not more, important, as was illustrated most clearly by the chiral separation of ketoprofen. The enantiomers of this racemate were separated, although not to the baseline, with either maltotetraose or -hexaose, whereas none of the maltooligosaccharide mixtures used proved to be capable of resolving ketoprofen enantiomers.

The importance of the quantitative composition, on the other hand, could be demonstrated by selective enrichment of a maltodextrin mixture with separate maltooligosaccharides of low  $DP$ . Paradoxically, this resulted in a negative effect on enantiomeric separation.

Various other oligo- and polysaccharides did not show any enantioselectivity towards 2-APAs, including circular  $\alpha$ -(1–4)- and linear  $\beta$ -(1–6)-linked D-glucose oligomers and polymers and saccharide copolymers, suggesting the key role of chains of D-glucose units linked through  $\alpha$ -(1–4) bonds. It may be speculated that in analogy with amylose some  $\alpha$ -(1–4)-linked glucose oligomers and polymers display a balanced hydrophilic–hydrophobic surface, resulting from the helical conformation, and confer the steric environment necessary for chiral interactions to occur.

Using comparable running conditions, other enantiomeric (coumarinic anticoagulant drugs) and

diastereoisomeric (cefalosporin antibiotics) pairs of compounds were easily resolved. Hence the applicability of maltooligosaccharides to perform chiral separations is not restricted to the 2-APA compounds. So far and under the given experimental conditions, only acidic racemates were found to be effectively separated. However, no premature conclusions should be drawn about the nature of racemic compounds that could be resolved through this approach.

In conclusion, linear  $\alpha$ -(1–4)-glucose polymers were demonstrated to be effective chiral discriminators in capillary electrophoresis. It was shown that an as yet undefined combination of variables relating to the maltodextrins is involved in their performance in the stereoselective separation by CE. The qualitative and quantitative composition of the maltodextrin mixtures, the importance of the vis-

cosity of the electrolyte and the physico-chemical interactions involved in chiral separations using oligosaccharides need further examination.

#### REFERENCES

- 1 D. B. Campbell, *Eur. J. Drug Metab. Pharmacokinet.*, 15 (1990) 109.
- 2 K. Williams and E. Lee, *Drugs*, 30 (1985) 333.
- 3 M. D. Müller and H.-P. Bosschardt, *J. Assoc. Off. Anal. Chem.*, 71 (1988) 614.
- 4 M. Novotny, *Anal. Chem.*, 60 (1988) 500A.
- 5 K. Otsuka and S. Terabe, *J. Chromatogr.*, 515 (1989) 221.
- 6 A. Dobashi, T. Ono, S. Hara and J. Yamaguchi, *J. Chromatogr.*, 480 (1989) 413.
- 7 S. Fanali, *J. Chromatogr.*, 474 (1989) 441.
- 8 S. Fujiwara and S. Honda, *Anal. Chem.*, 59 (1987) 487.
- 9 H. Nishi, T. Fukuyama and S. Terabe, *J. Chromatogr.*, 553 (1991) 503.
- 10 S. Churms, *J. Chromatogr.*, 500 (1990) 555.



# High-performance capillary electrophoresis of unsaturated oligosaccharides derived from glycosaminoglycans by digestion with chondroitinase ABC as 1-phenyl-3-methyl-5-pyrazolone derivatives

Susumu Honda

Faculty of Pharmaceutical Sciences and Pharmaceutical Research and Technology Institute, Kinki University, 3-4-1 Kowakae, Higashi-Osaka (Japan)

Tetsuji Ueno and Kazuaki Kakehi

Faculty of Pharmaceutical Sciences, Kinki University, 3-4-1 Kowakae, Higashi-Osaka (Japan)

---

## ABSTRACT

This paper proposes a new method for simultaneous analysis of unsaturated disaccharides derived from glycosaminoglycans by enzymatic digestion with chondroitinase ABC, based on high-performance capillary electrophoresis (HPCE) of their 1-phenyl-3-methyl-5-pyrazolone derivatives. The O-sulphate group is stable in this derivatization, and this method allows reproducible microdetermination of glycosaminoglycans. This paper also demonstrates the applicability of this method to estimation of urinary chondroitin sulphates. Urinary creatinine as an inherent internal standard could also be estimated by HPCE, though in another mode of separation, *i.e.* ion-exchange electrokinetic chromatography.

---

## INTRODUCTION

Glycosaminoglycans (GAGs) are widely distributed in animal tissues and have a variety of important physiological functions. They are basically composed of hexosamine and uronic acid residues linked alternately. The amino group in the hexosamine residue is either acetylated or sulphated, and the hydroxyl group is partially sulphated. GAGs usually occur together, hence direct analysis requires prior separation. However, there is no ideal method for separation.

However, there are various lyases that cleave the hexosaminide linkages to give oligosaccharides with

the unsaturated uronic acid residue at the non-reducing termini. Chondroitinase ABC from *Proteus vulgaris* is a typical example; it cleaves the hexosaminide bonds in chondroitin sulphates A, B, C, D and E, giving 2-acetamido-2-deoxy-3-O-( $\beta$ -D-glucopyranosyluronic acid)-4-O-sulpho-D-galactose ( $\Delta$ Di-4S), 2-acetamido-2-deoxy-3-O-( $\beta$ -D-glucopyranosyluronic acid)-6-O-sulpho-D-galactose ( $\Delta$ Di-6S), acetamido-2-deoxy-3-O-(2-O-sulpho- $\beta$ -D-glucopyranosyluronic acid)-6-O-sulpho-D-galactose ( $\Delta$ Di-di<sub>D</sub>) and 2-acetamido-2-deoxy-3-O-( $\beta$ -D-glucopyranosyluronic acid)-4,6-bis-O-sulpho-D-galactose ( $\Delta$ Di-di<sub>E</sub>). This lyase also cleaves chondroitin and hyaluronic acid to give 2-acetamido-2-deoxy-3-O-( $\beta$ -D-glucopyranosyluronic acid)-D-galactose ( $\Delta$ Di-0S) and 2-acetamido-2-deoxy-3-O-( $\beta$ -D-glucopyranosyluronic acid)-D-glucose ( $\Delta$ Di-HA), respectively. Since

---

Correspondence to: Dr. S. Honda, Faculty of Pharmaceutical Sciences, Kinki University, 3-4-1 Kowakae, Higashi-Osaka, Japan.



analysis of these unsaturated disaccharides allows characterization and determination of GAGs, various methods have been developed for this purpose. Lee *et al.* [1] devised a method based on high-performance liquid chromatography (HPLC) with UV detection, though the sensitivity was not high. Kodama *et al.* [2] improved this method by pre-column conversion of the disaccharides to reductively pyridylaminated derivatives, which are strongly fluorescent. There is another improvement by Toyoda *et al.* [3] based on post-column derivatization with 2-cyanoacetamide. We have also developed a method based on HPLC of 1-phenyl-3-methyl-5-pyrazolone (PMP) derivatives. The details will appear elsewhere.

High-performance capillary electrophoresis (HPCE) is a recently developed method for separation which allows high-resolution separation and reproducible microquantification by on-column detection. We have applied this method to carbohydrate analysis and demonstrated its high capabilities [5–8]. Al-Hakim and Linhardt [9] have also reported its application to unsaturated disaccharides derived from a few species of GAGs, but sensitivity was not high because the disaccharides were directly analysed. We present herein an improved HPCE method based on pre-column derivatization with PMP.

## EXPERIMENTAL

### Chemicals

Authentic specimens of chondroitin sulphate A (whale cartilage), chondroitin sulphate C (shark cartilage), chondroitin sulphate D (shark cartilage), chondroitin sulphate E (squid cartilage) chondroitin (derived from chondroitin sulphate A), hyaluronic acid (pig skin) and unsaturated, sulphated disaccharides ( $\Delta$ Di-4S and  $\Delta$ Di-6S) were purchased from Seikagaku Kogyo (Tokyo, Japan) and used as obtained. The authentic samples of  $\Delta$ Di-diS<sub>D</sub>,  $\Delta$ Di-diS<sub>E</sub>,  $\Delta$ Di-0S and  $\Delta$ Di-HA were prepared by digestion of chondroitin sulphate D, chondroitin sulphate E, chondroitin and hyaluronic acid, respectively, with chondroitinase ABC. Chondroitinases AC and ABC from *Arthrobacter aurescens* and *Proteus vulgaris*, respectively, were also from Seikagaku Kogyo. PMP was obtained from Kishida Chemicals (Osaka, Japan) and used after recrystallization

from methanol. The authentic sample of creatinine was from Wako Pure Chemicals (Osaka, Japan). All other chemicals and solvents were of the highest grade commercially available. Water as solvent was double distilled and filtered through a membrane filter before use.

### Apparatus

HPCE was performed by using a Beckman P/ACE 2000 capillary electrophoresis system, composed of a high-voltage power supply, a pressure-controlled injector, a UV detector equipped with 200-, 214-, 254- and 280-nm cut-off filters and a data processor. A capillary tube (51 cm  $\times$  75  $\mu$ m I.D.  $\times$  375  $\mu$ m O.D.) of fused silica was mounted on a plastic cassette, which was maintained at 30°C. Operation by this system was fully automated.

### Enzymatic reactions

The method of Saito *et al.* [10] was slightly modified. To an aqueous solution (20  $\mu$ l) of an authentic specimen of a GAG (10  $\mu$ g), a mixture of authentic specimens of GAGs (0.5–10  $\mu$ g each) or a cetylpyridinium chloride (CPC)-precipitated GAG fraction of a urine sample (5.0 ml) was added an aqueous solution (20  $\mu$ l) of chondroitinase AC or ABC (20 mU), together with 250 mM Tris–130 mM hydrochloric acid buffer (pH 8.0, 10  $\mu$ l) containing sodium acetate (2.4%, w/w), sodium chloride (1.5%, w/w) and bovine serum albumin (0.05% w/w), and the mixture was incubated for 15 h at 37°C. The reaction solution was evaporated to dryness *in vacuo*, the residue dissolved in an appropriate volume (50–100  $\mu$ l) of water, and the solution analysed by HPCE. When necessary, the residue was derivatized with PMP as described below, and the product was subjected to analysis by HPCE.

### Derivatization with PMP

The procedure of derivatization was essentially the same as that described in our previous paper [11], but slightly modified. Briefly, an authentic specimen of an unsaturated disaccharide (10  $\mu$ g), a mixture of authentic unsaturated disaccharides (10  $\mu$ g each) or a product of enzymatic reaction mentioned above was dissolved in 0.5 M sodium hydroxide (30  $\mu$ l) and a methanolic 0.5 M solution of PMP (30  $\mu$ l) was added. The mixture was allowed to stand at 70°C with the stopper tightly closed, then

neutralized with 0.3 M hydrochloric acid (30  $\mu$ l). Water (200  $\mu$ l) and ethyl acetate (200  $\mu$ l) were added to the neutralized mixture, and the whole shaken vigorously. The organic layer was removed and the aqueous layer extracted with the same volume of ethyl acetate. After three more extractions the final aqueous layer was lyophilized, the residue dissolved in water (50  $\mu$ l), and the solution analysed by HPCE.

#### Analysis of unsaturated oligosaccharides

HPCE was performed in zone electrophoresis mode. A mixture of authentic specimens of unsaturated disaccharides or a digestion mixture of authentic or urinary GAGs, either directly or derivatized with PMP, was introduced from the anodic end of the capillary tube containing a borate buffer (pH 9.0) prepared by mixing 100 mM boric acid and 25 mM sodium tetraborate. Analysis was carried out by applying a voltage of 25 kV with UV monitoring at 214 nm.

#### Collection of urinary GAGs

This was done by the CPC precipitation method described by Di Ferrante and Rice [12]. Briefly, a 5-ml aliquot of a 24-h composite sample of urine was centrifuged at 3000 rpm (1100 g) in a 10-ml centrifuge tube, and an aqueous 2.5% solution (100  $\mu$ l) of CPC was added to the supernatant. After standing overnight at 4°C, the precipitates were collected by centrifugation in a similar manner. The pellet was well vortexed with a saturated solution of sodium chloride in a 95:5 (v/v) ethanol–water mixture (30  $\mu$ l), and the mixture centrifuged. After repeating this precipitation procedure twice more, the final pellet was subjected to digestion with chondroitinase AC or ABC.

#### Assay of urinary creatinine

A urine sample was directly introduced to the cathodic end of the capillary tube filled with 100 mM borate buffer (pH 9.0) containing polybrene to a concentration of 0.1% (w/v). A voltage of 25 kV was applied, and creatinine and sodium benzoate (internal standard) separated were monitored at 254 nm.

## RESULTS AND DISCUSSION

The enzymatic reactions of GAGs with chondroitinase ABC were studied in detail by Saito *et al.* [10]. Under the optimized conditions using Tris–hydrochloric acid buffer (pH 8.0) at 37°C the yields of these disaccharides from chondroitin sulphates A and C reached plateaux in 15 h. On the other hand, a convenient method for derivatization of reducing sugars was established in our laboratory [11]. This method allows quantitative conversion of reducing mono- and oligosaccharides to derivatives which have two PMP groups in a molecule and absorb the UV light strongly.

HPCE in the zone electrophoresis mode in 100 mM borate buffer as carrier gave rather good separation of  $\Delta$ Di-4S and  $\Delta$ Di-6S. The order of migra-

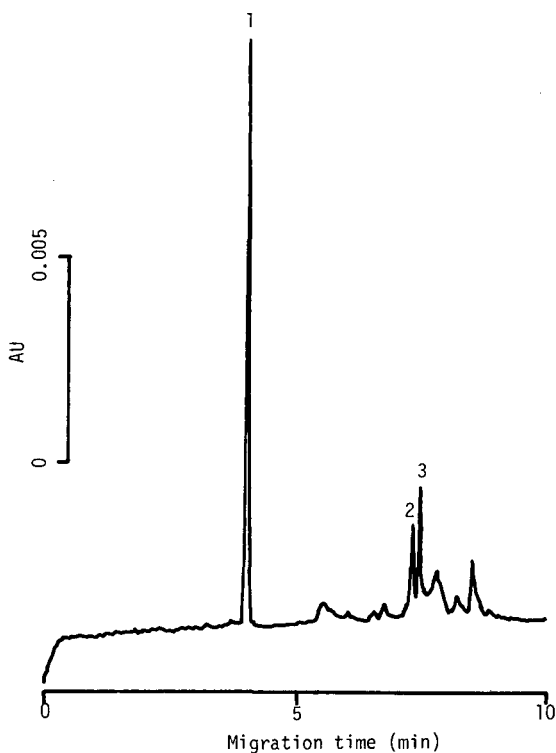


Fig. 1. Direct analysis of a chondroitinase ABC-digested mixture of chondroitin sulphates A and C by zone electrophoresis. Capillary, fused silica (51 cm  $\times$  50  $\mu$ m I.D.); carrier, 100 mM borate buffer (pH 9.0); applied voltage, 25 kV; detection, UV absorption at 214 nm. The sample was injected from the anodic end of the tube. Peaks: 1 came from the buffer for enzymatic digestion; 2 =  $\Delta$ Di-6S; 3 =  $\Delta$ Di-4S.

tion was  $\Delta$ Di-6S followed by  $\Delta$ Di-4S, presumably because of easier complexation of the latter with the borate ion. Although the authentic specimens of these unsaturated disaccharides were well separated, analysis of these disaccharides in a digestion mixture of chondroitin sulphates A and C was interfered with by non-carbohydrate materials, as shown in Fig. 1. In Fig. 1 peaks 2 and 3 correspond to  $\Delta$ Di-6S and  $\Delta$ Di-4S, respectively, and the large peak at ca. 4 min (peak 1) came from the buffer used for the enzymatic reaction. The product from a mixture of 1.5 g each of the GAG samples was dissolved in water and the solution analysed by HPCE. The unsaturated disaccharides were detected at 214 nm.

Separation and sensitivity were much improved by conversion of these unsaturated disaccharides to the PMP derivatives, as shown in Fig. 2. Fig. 2 also shows separation of the derivatives of other unsaturated disaccharides ( $\Delta$ Di-diS<sub>D</sub>,  $\Delta$ Di-diS<sub>E</sub>,  $\Delta$ Di-0S and  $\Delta$ Di-HA) obtained from the corresponding

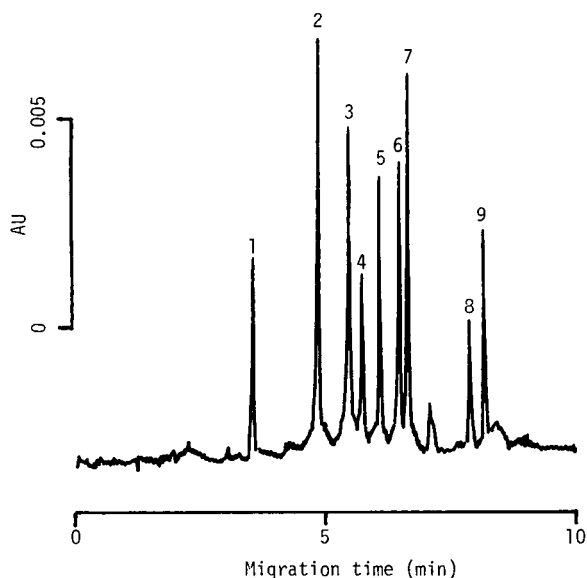


Fig. 2. Analysis of a chondroitinase ABC-digested mixture of chondroitin sulphates A–E, chondroitin and hyaluronic acid by zone electrophoresis after derivatization with PMP. The analytical conditions were as in Fig. 1. Peaks: 1 came from the buffer for enzymatic digestion; 2 = PMP (excess reagent); 3 = PMP derivative of  $\Delta$ Di-0S; 4 = PMP derivative of  $\Delta$ Di-HA; 5 = sodium benzoate (internal standard); 6 = PMP derivative of  $\Delta$ Di-4S; 7 = PMP derivative of  $\Delta$ Di-6S; 8 = PMP derivative of  $\Delta$ Di-diS<sub>D</sub>; 9 = PMP derivative of  $\Delta$ Di-diS<sub>E</sub>.

GAGs. The migration order of  $\Delta$ Di-4S (peak 6) and  $\Delta$ Di-6S (peak 7) was reversed compared with that of the intact disaccharides (Fig. 1), presumably owing to change of separation mode. Since the reducing ends were blocked by the PMP groups, complexation was hampered, and as a result these disaccharides were moved by plain zone electrophoresis mode. The limit of detection at 214 nm was at the 10-fmol level as injected amount. The absorption spectra of the PMP derivatives of these disaccharides indicated that the absorbance at this wavelength was approximately one fifth of that at the maximum (245 nm). The peak at ca. 6.6 min (peak 4) is that of sodium benzoate as an internal standard, and peaks 3 and 4 are attributable to the PMP derivatives of  $\Delta$ Di-0S and  $\Delta$ Di-HA, respectively. The separation of these non-sulphated isomers is obviously the result of the difference of the ease of complexation of the hexosamine residues with the borate ion. Peaks 8 and 9 were assigned to  $\Delta$ Di-diS<sub>D</sub> and  $\Delta$ Di-diS<sub>E</sub>, respectively. Thus, all these disaccharides were well separated from each other by zone electrophoresis as borate complexes.

It is noteworthy that the derivatized products of  $\Delta$ Di-4S and  $\Delta$ Di-6S gave no detectable peak as did the PMP derivative of  $\Delta$ Di-0S. These experimental results indicate that the O-sulphate group was stable in this operation.

The calibration curves of chondroitin sulphates A and C, as observed from the relative responses of  $\Delta$ Di-4S and  $\Delta$ Di-6S to sodium benzoate, showed excellent linearity at least for sample amounts in the range 0.5–10  $\mu$ g. This range corresponds to the 10–400 pg range of injected amount. It is noted that the rate of production of  $\Delta$ Di-4S from chondroitin sulphate A was considerably lower than that of  $\Delta$ Di-6S from chondroitin sulphate C. The relative standard deviations ( $n = 10$ ) of the relative response at the 5- $\mu$ g level were 3.0% and 2.8%, respectively. The authentic specimen of chondroitin sulphate A gave a small amount of the derivative of  $\Delta$ Di-6S together with that of  $\Delta$ Di-4S ( $\Delta$ Di-4S/ $\Delta$ Di-6S = 60.5:33.7, in molar proportion based on the assumption that both disaccharides have the same molar absorptivity). Similarly the authentic specimen of chondroitin sulphate C gave the derivative of  $\Delta$ Di-4S together with that of  $\Delta$ Di-6S as a minor product ( $\Delta$ Di-4S/ $\Delta$ Di-6S = 16.6:82.1). Therefore, the determination of chondroitin sul-

phates A and C in their mixture was corrected by using these proportions.

On the basis of these observations, the GAG fraction of a human urine sample was digested with chondroitinase ABC, the product derivatized with PMP, and the derivative analysed by HPCE. Fig. 3 shows an example of the electropherograms.

The peaks of the PMP derivatives of both  $\Delta$ Di-4S (peak 6) and  $\Delta$ Di-6S (peak 7) are distinctly detected, and the amounts of chondroitin sulphates A and C can be determined from the relative responses of these disaccharides to sodium benzoate (peak 5). The minor peak at *ca.* 6 min (peak 3) is attributable to the PMP derivative of  $\Delta$ Di-0S. Peaks 1 and 2 arose from the buffer used for the enzymatic reaction and the excess reagent, respectively. In parallel with this analysis the GAG fraction of the same urine sample was digested with chondroitinase AC from *Arthrobacter aurescens*, and the digestion mixture was derivatized with PMP. Analysis of the final product gave essentially the same electropherogram (not shown) as that in Fig. 3, and the responses of the  $\Delta$ Di-4S and  $\Delta$ Di-6S peaks relative to that of sodium benzoate were almost identical to those obtained with chondroitinase ABC. Chondroitinase

ABC cleaves the hexosaminide linkage in chondroitin sulphate B along with those in chondroitin sulphates A and C, whereas chondroitinase AC cleaves the hexosaminide linkages only in chondroitin sulphates A and C. Since chondroitin sulphate B has the sulphate group attached to the 4-position of the galactosamine residue, like chondroitin sulphate A, the yield of  $\Delta$ Di-4S obtained with chondroitinase ABC should be larger than that obtained with chondroitinase AC, if the GAG fraction contained chondroitin sulphate B. The result obtained from selected urine samples indicates that they did not contain detectable amounts of chondroitin sulphate B.

Since the concentrations of urinary substances vary greatly depending on physical and dietary conditions, they are usually expressed as a ratio relative to an appropriate inherent standard. Creatinine is the substance most widely used for this purpose. Although this compound is usually assayed by a colorimetric method using the reaction with picric acid [13], it can also be easily assayed by HPCE. Fig. 4 shows separation of creatinine from other inherent substances in urine using borate buffer (pH 9.0) containing polybrene, as carrier, as detected at

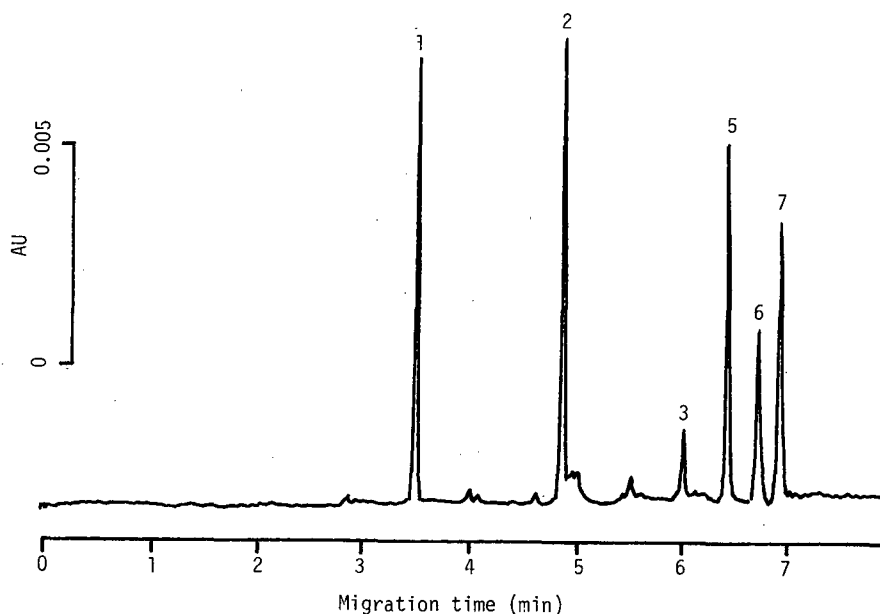


Fig. 3. Analysis of the PMP derivatives of unsaturated disaccharides derived from the GAG fraction of a urine sample digestion with chondroitinase ABC by zone electrophoresis. The analytical conditions were as in Fig. 1. Peak assignment is the same as that in Fig. 2.

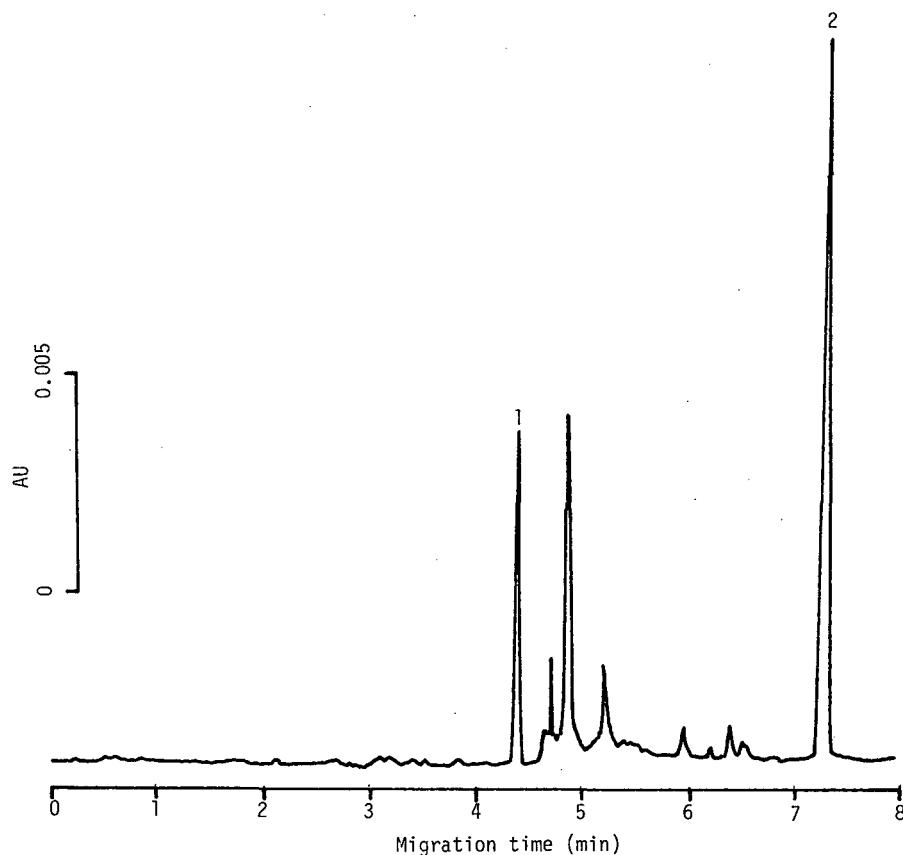


Fig. 4. Direct analysis of urinary creatinine by ion-exchange electrokinetic chromatography. Capillary, fused silica (51 cm  $\times$  50  $\mu$ m I.D.); carrier, 100 mM borate buffer (pH 9.0) containing polybrene (0.1%, w/w); applied voltage, 15 kV; detection, UV absorption at 254 nm. Intact urine was injected from the cathodic end of the capillary tube. Peaks: 1 = sodium benzoate (internal standard); 2 = creatinine.

254 nm. In this system electro-osmotic flow was toward the anode, and separation based on the difference of the magnitude of interaction with the moving molecules of polybrene (ion-exchange electrokinetic chromatography mode) was realized. Under these conditions the relative response of creatinine to sodium benzoate (internal standard) was almost linear, at least in the range 0.1–5 mg/ml of creatinine (figure not shown), and urinary creatinine could be readily estimated by using this calibration curve without any prior clean-up procedures.

We could obtain the concentrations of urinary chondroitin sulphates A and C, together with that of creatinine, by HPCE as mentioned above. The following are a few examples of the ratios of chondroitin sulphates A and C to creatinine ( $\mu$ g/mg of

creatinine). Sample 1 (male, 23 years old): A, 1.27; C, 0.59. Sample 2 (male, 23 years old): A, 0.84; C, 0.34. Sample 3 (male, 54 years old): A, 1.09; C, 0.50. Such values are consistent with the reported values [14]. The presence of  $\Delta$ Di-OS in the digest of urinary GAGs in a normal subject has been noted in the literature [15], possibly arising from chondroitin or low-sulphate-content chondroitin sulphate, but the concentration was not reported. In the above cases the production of  $\Delta$ Di-OS from samples 1, 2 and 3 was 8.9%, 13.8% and 9.3%, respectively, of total unsaturated disaccharides. Although  $\Delta$ Di-HA was not detected in the present samples, some metabolic disorders such as Hurler's disease and Morquio's disease will give high values of  $\Delta$ Di-HA, as suggested by Kodama *et al.* [2]. In such cases the present

method will be useful, since separation of  $\Delta$ Di-HA from  $\Delta$ Di-OS is good by the present method.

We are accumulating data on clinical samples. Discussion in relation to pathological conditions will be published elsewhere.

#### REFERENCES

- 1 G. J. Lee, J. E. Evans and H. Tieckelmann, *J. Chromatogr.*, 146 (1978) 439.
- 2 C. Kodama, N. Ototani, M. Isemura and Z. Yoshizawa, *J. Biochem. (Tokyo)*, 96 (1984) 1283.
- 3 H. Toyoda, K. Shinomiya, S. Yamanashi, I. Koshiishi and T. Imanari, *Anal. Sci.*, 4 (1988) 381.
- 4 S. Fujiwara, S. Iwase and S. Honda, *J. Chromatogr.*, 447 (1988) 133.
- 5 S. Honda, S. Iwase, A. Makino and S. Fujiwara, *Anal. Biochem.*, 176 (1989) 72.
- 6 S. Honda, S. Suzuki, A. Nose, K. Yamamoto and K. Kakehi, *Carbohydr. Res.*, 215 (1991) 193.
- 7 S. Honda, K. Yamamoto, S. Suzuki, M. Ueda and K. Kakehi, *J. Chromatogr.*, 588 (1991) 327.
- 8 S. Honda, A. Makino, S. Suzuki and K. Kakehi, *Anal. Biochem.*, 191 (1990) 228.
- 9 A. Al-Hakim and R. J. Linhardt, *Anal. Biochem.*, 195 (1991) 68.
- 10 H. Saito, T. Yamagata and S. Suzuki, *J. Biol. Chem.*, 243 (1968) 1536.
- 11 S. Honda, E. Akao, S. Suzuki, M. Okuda, K. Kakehi and J. Nakamura, *Anal. Biochem.*, 180 (1989) 351.
- 12 N. Di Ferrante and C. Rice, *J. Lab. Clin. Med.*, 48 (1956) 491.
- 13 R. W. Bonsnes and H. H. Taussky, *J. Biol. Chem.*, 158 (1945) 581.
- 14 G. J. Lee and H. Tieckelmann, *J. Chromatogr.*, 222 (1981) 23.
- 15 M. E. Zebrower, F. J. Kieras and W. T. Brown, *Anal. Biochem.*, 157 (1986) 93.



# Separation of natural and synthetic heparin fragments by high-performance capillary electrophoresis

Jan B. L. Damm, George T. Overkluft and Barry W. M. Vermeulen

*Department of Analytical Chemistry, Organon International B.V., Akzo Pharma Group, P.O. Box 20, NL-5340 BH Oss (Netherlands)*

Cees F. Fluitsma and Gijs W. K. van Dedem

*Biochemical R&D Laboratories, Diosynth B.V., Akzo Pharma Group, P.O. Box 20, NL-5340 BH Oss (Netherlands)*

---

## ABSTRACT

The application of capillary electrophoresis (CE) for the analysis of natural and synthetic low-molecular-mass heparin fragments at low pH is described. It is demonstrated that under the applied conditions the separation is based on charge, charge distribution and molecular mass of the heparin molecules, yielding a high resolution. It is shown that the presence of sodium chloride in the sample solution has hardly any effect on the CE performance. However, the pH of the electrophoresis buffer is a critical parameter. The resolutions obtained with CE and high-performance anion-exchange chromatography (HPAEC) are compared for various heparin fragments and it is concluded that, at least for this type of molecule, CE forms an attractive alternative to HPAEC.

---

## INTRODUCTION

Heparin occurs as a proteoglycan consisting of a small protein core to which multiple large glycosaminoglycan side-chains are attached. The glycosaminoglycan chains vary in length and consist of repeating uronic acid glucosamine disaccharide sequences in which the uronic acid may be either D-glucuronic acid or L-iduronic acid and the glucosamine residue may be either N-acetylated or N-sulphated [1]. Moreover, the disaccharide units are O-sulphated to varying extents at C-6 and/or C-3 of the various glucosamine residues and at C-2 of the uronic acid residues [1]. Thus very heterogeneous polymers, both in molecular mass and structure, are formed. A final cause of heterogeneity is the occurrence of a unique D-glucosamine-N,6-disulphate-

( $\alpha$ 1-4)-L-iduronic acid-2-sulphate-( $\beta$ 1-4)-D-glucosamine-N,3,6-trisulphate-( $\alpha$ 1-4)-D-glucuronic acid-( $\beta$ 1-4)-D-glucosamine-N,6-disulphate pentasaccharide sequence [2]. This pentasaccharide occurs in approximately one third of the heparin molecules and is responsible for the well documented anticoagulant activity of heparin through a high-affinity binding to antithrombin III, resulting in a highly increased inhibition of factor II<sub>a</sub>, X<sub>a</sub> and XII<sub>a</sub> activity [3–7].

For over 50 years the anti-blood-clotting activity of heparin, which is commercially prepared from porcine intestinal mucosa and bovine lung, has been exploited in the treatment of venous thrombosis. Until two decades ago the application was limited to therapeutic treatment of established thrombi. However, a second major use of heparin has evolved, namely the prevention of postsurgical thrombosis. After major surgery there is a greatly increased risk of thrombosis, especially for middle-aged and elderly patients [8]. A significant advantage of the prophylactic use of heparin is that lower

---

*Correspondence to:* Dr. J. B. L. Damm, Department of Analytical Chemistry, Organon International B.V., Akzo Pharma Group, P.O. Box 20, NL-5340 BH Oss, Netherlands.



dosages can be applied which prevents the persistent hypocoagulation associated with therapeutic use [9,10].

However, the vast structural heterogeneity of heparin renders the biological activity, in both qualitative and quantitative respects, undefined and presents a serious limitation of its value as a pharmaceutical drug. This concern is even greater as it is becoming increasingly clear that unfractionated heparin displays a wide variety of biological effects not related to anticoagulant or antithrombotic activity [11–18].

Therefore, during the past decade attempts have been made to produce better defined heparin preparations. This has been achieved in part by the generation of low-molecular-mass heparin fragments of more or less uniform mass by either fractional precipitation and gel filtration [19] or chemical [20] or enzymatic depolymerization [21]. It has been demonstrated that low-molecular-mass heparin fragments of relative molecular mass 4000–5000 can be effectively applied as prophylactic drugs after surgery [22]. As heparin preparations of  $M_r < 5000$  retain a high anti-factor  $X_a$  activity (for which the pentasaccharide sequence is responsible) but have a reduced or no anti-factor  $II_a$  (thrombin) activity, it has been suggested that these preparations may have a better benefit/risk ratio in terms of antithrombotic activity and risk of bleeding. Although the mechanism of action is still a matter of debate, data are accumulating that after subcutaneous injection, low-molecular-mass heparins cause less hypocoagulation, give rise to a longer lasting inhibition of factor  $X_a$  activity and are indeed less haemorrhagic than native heparin [22,23]. Moreover, it has been shown [23] that these preparations have a twofold prolonged half-life in circulation (which, in contrast to heparin, is not dose-dependent) and have a four- to ninefold higher bioavailability on subcutaneous injection. Finally, there are indications that the incidence of adverse side-effects (lipolysis, thrombocytopenia) associated with the administration of heparin is lower with low-molecular-weight heparins [23].

However, the low-molecular-mass preparations still show a considerable structural heterogeneity, thereby impeding predictions about bioactivity and

pharmacokinetics. Moreover, fractional precipitation and chemical depolymerization result in a relative enrichment of material without the unique pentasaccharide sequence and hence proportional loss of anticoagulant activity. Alternatively, enzymatic depolymerization leads to the formation of fragments with modified reducing end-groups which may raise concerns with respect to the potential immunogenic effects.

A more attractive way to produce a well defined heparin fragment with a high specific anticoagulant activity was found in the chemical synthesis of the unique pentasaccharide sequence [24–27]. These preparations have shown to be safe and effective anticoagulant drugs in *in vivo* studies [2,28] and at present clinical studies are in progress. Following the synthesis of the natural pentasaccharide, various derivatives have been synthesized [6,27,29–32], some of them displaying an increased AT-III affinity [29].

An important aspect of the production of natural and synthetic heparin fragments for pharmaceutical use is the availability of analytical procedures for the characterization of intermediates and final products. As the heparin fragments have an inherent high potential for microheterogeneity, the analytical procedures must meet stringent criteria. Described methods for the separation of mixtures of heparin fragments rely on high-performance size-exclusion [33], anion-exchange [34] and reversed-phase ion-pair chromatography [20,35] and polyacrylamide gel electrophoresis [36].

Recently, high-performance capillary electrophoresis (CE) was reported as a sensitive and high-resolution method for the determination of the disaccharide composition of several proteoglycans [37,38]. In these studies the disaccharides were fractionated as borate complexes at relatively high pH. Here we report the separation of complex mixtures of heparin fragments, having relative molecular masses up to 3500 and containing well over ten (negatively) charged groups, without the addition of borate, and we compare the performance of high-performance anion-exchange chromatography (HPAEC) with CE. It is demonstrated that CE is potentially a good method for the quality control of natural and synthetic heparin fragments.

## EXPERIMENTAL

*Materials*

Colominic acid oligomers were prepared by partial hydrolysis of colominic acid (Sigma, St. Louis, MO, USA). Heparin disaccharide reference compounds were obtained from Grampian Enzymes (Aberdeen, UK). Natural heparin-derived fragments were obtained from Diosynth (Oss, Netherlands) and were prepared by treating mucosal porcine heparin with heparinase. Synthetic pentasaccharides were made at Organon International (Oss, Netherlands) in cooperation with Sanofi (Toulouse, France) and the structures were verified by  $^1\text{H}$  and  $^{13}\text{C}$  NMR spectroscopy [30–32] and fast atom bombardment mass spectrometry [39].

*Preparation of colominic acid standards*

A mixture of polyanionic oligosaccharides was prepared by controlled depolymerization of colominic acid [poly ( $\alpha$ 2–8)-N-acetylneuraminic acid, (NeuAc) $_n$ , from *E. coli*; Sigma] as follows. A 10-mg amount of colominic acid was dissolved in 1 ml 0.1 M HCl (J. T. Baker, Deventer, Netherlands) and incubated in an air-tight reaction vial at 80°C for 45 min. The reaction products were desalted on a Bio-Gel P-2 (200–400 mesh) column (18 × 0.8 cm I.D.) (Bio-Rad, Veenendaal, Netherlands), lyophilized and stored at –20°C until used.

*Preparation of heparin fragments*

Mucosal heparin was dissolved in 0.25 M ammonium acetate solution to a concentration of 20 mg/ml and 5 U/ml of heparinase (from *Flavobacterium heparinum*, E.C. 4.2.2.7; Sigma) were added. The mixture was incubated for 60 h at 35°C. The degraded heparin was batch adsorbed on an anion exchanger and desorbed stepwise by elution with NaCl (Merck, Darmstadt, Germany) solutions of increasing molarity. The material eluting between 5 and 10% (w/v) NaCl was applied to a gel permeation chromatographic system, consisting of two columns in tandem, namely a TSK Fractogel HW 40 S column (70 × 2.6 cm I.D.) (Merck) and a Bio-Gel P-2 (400 mesh) column (100 × 2.5 cm I.D.) (Bio-Rad). Elution was carried out with 0.5 M ammonium acetate (Sigma), pH 5.0 at a flow-rate of 0.7 ml/min and the chromatogram was recorded with a refractive index detector (ERC 7510 Erma). Frac-

tions of increasing molecular mass were combined into six pools, which on the basis of elution volume correspond to di-, tetra-, hexa-, octa-, deca- and dodecasaccharides. The pools containing the di- and dodecasaccharides were not used for further studies. The remaining pools were desalted on Bio-Gel P-2, lyophilized and stored at –20°C until used.

*High-performance anion-exchange chromatography*

The colominic acid hydrolysate, the disaccharide reference compounds, the heparin fragments obtained by heparinase treatment and gel permeation chromatography and the synthetic pentasaccharides were each dissolved in water purified with a Milli-Q-system (Millipore, Milford, MA, USA) to a concentration of 0.1–5 mg/ml and separated by anion-exchange chromatography on a Hewlett-Packard (Palo Alto, CA, USA) Model 1050 HPLC system equipped with an HR 55 Mono Q column (Pharmacia, Uppsala, Sweden). The injection volume was 25–200  $\mu\text{l}$  and the column was eluted at a flow-rate of 1 ml/min using linear concentration gradients of 0–1, 0–2 or 0.88–1.60 M NaCl in Milli-Q-purified water. The elution profiles were recorded at 214 or 215 nm.

*High-performance capillary electrophoresis*

The colominic acid hydrolysate, the disaccharide reference compounds, the heparin fragments obtained by heparinase treatment and gel permeation chromatography and the synthetic pentasaccharides were each dissolved in Milli-Q-purified water to a concentration of 0.1–5 mg/ml and separated by high-performance capillary electrophoresis using a Beckman (Palo Alto, CA, USA) P/ACE 2100 CE system equipped with a UV absorbance detector and a fused-silica capillary tube (57 cm × 75  $\mu\text{m}$  I.D., detector at 50 cm). System operation and data handling were fully controlled and integrated via the System Gold software (version 6, Beckman) running on an IBM 55 SX personal computer. The apparatus was operated in the reversed polarity mode, *i.e.*, the sample was introduced at the cathodic side of the capillary. Samples were loaded by applying pressurized nitrogen for 10 s, resulting in the injection of 25 nl of sample solution. Before introduction of the first sample, the capillary was rinsed for 15 min each with 0.1 M  $\text{H}_3\text{PO}_4$ , 0.5 M NaOH, 0.1 M NaOH (all from J. T. Baker), Milli-

Q-purified water and running buffer. Between runs only the last three wash steps were applied. Separations were carried out using 200 mM  $\text{NaH}_2\text{PO}_4$  (J. T. Baker), adjusted to pH 2, 3 or 4 with concentrated  $\text{H}_3\text{PO}_4$ , as running buffer at a potential of 7.5 kV (131.5 V/cm) and 40°C. On-capillary detection was performed by UV absorbance measurement at 214 nm.

## RESULTS AND DISCUSSION

The optimum conditions for the separation of sulphated glycosaminoglycans by CE were determined using colominic acid oligomers and heparin disaccharide reference compounds. It was established that at low pH the oligosaccharides can be effectively separated without complexation with borate. The apparatus is operated in the reversed polarity mode and hence the migration time is, in principle, inversely correlated with the negative charge of the oligosaccharide. Operation at low pH ensures that the electroosmotic flow is nearly eliminated and is smaller than the electrophoretic flow, affording migration of the solutes towards the detector. Colominic acid was partially hydrolysed to afford a mixture of mono- and di- to  $n$ -mers, having the general formula  $(\text{NeuAc})_n$ , where  $n$  represents the degree of polymerization and the number of (charged) carboxyl groups. The oligomers were subjected to CE and HPAEC to compare the effect of (negative) charge on the migration and elution time, respectively. At pH 4, where the ionization of the carboxyl groups of the N-acetylneuraminic acid residues is nearly complete, CE resulted in baseline separation of the mono- to nonamers (Fig. 1A).

The identity of the peaks, as indicated in Fig. 1A, was established by injection of oligomers having a known degree of polymerization. The peaks migrating at 31.79 and *ca.* 31 min (inset in Fig. 1A) probably represent larger colominic acid polymers that remained after partial hydrolysis. As expected, the migration time increases as the degree of polymerization and hence the number of carboxyl groups decrease. The pH of the electrophoresis buffer appears to be very critical for a high resolution as neither at pH 3 nor at pH 5 was a satisfactory result obtained (results not shown). Probably at pH 3 the carboxyl groups of the colominic acid oligomers are not sufficiently ionized ( $\text{pK}$  2.9) and at pH 5 the

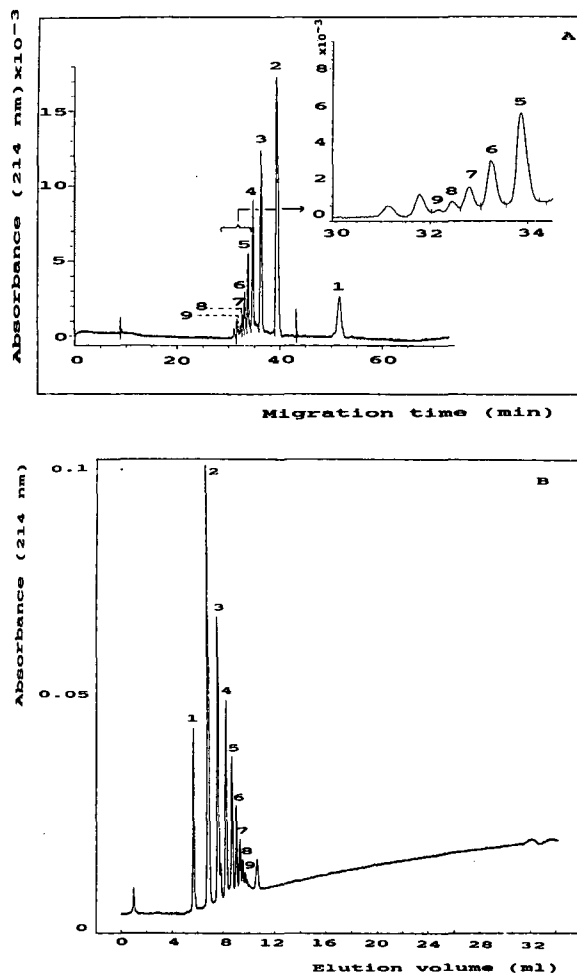


Fig. 1. (A) CE and (B) HPAEC of a partial hydrolysate of colominic acid. Prior to CE and HPAEC the hydrolysate was desalted by gel permeation chromatography on a Bio-Gel P-2 column. CE was carried out in 200 mM phosphate buffer (pH 4) at 40°C and 7.5 kV in the reversed polarity mode. Column: 57 cm (50 cm effective length)  $\times$  75  $\mu\text{m}$  I.D. On-capillary detection was at 214 nm. Injection by pressurized nitrogen: 25 nl from a solution containing 5 mg/ml of the hydrolysate. The number of (negatively charged) N-acetylneuraminic acid residues of the oligomers is indicated. HPAEC was carried out on a Mono Q HR 5/5 column using a linear concentration gradient of 0–2 M NaCl in 30 ml of Milli-Q-purified water at a flow-rate of 1 ml/min. Detection at 214 nm. Injection volume, 25  $\mu\text{l}$  from a sample solution containing 5 mg/ml of the hydrolysate.

electroosmotic flow, which is in the direction of the injection site, is too high.

In Fig. 1B, the chromatogram obtained for the same sample with HPAEC on Mono Q is depicted.

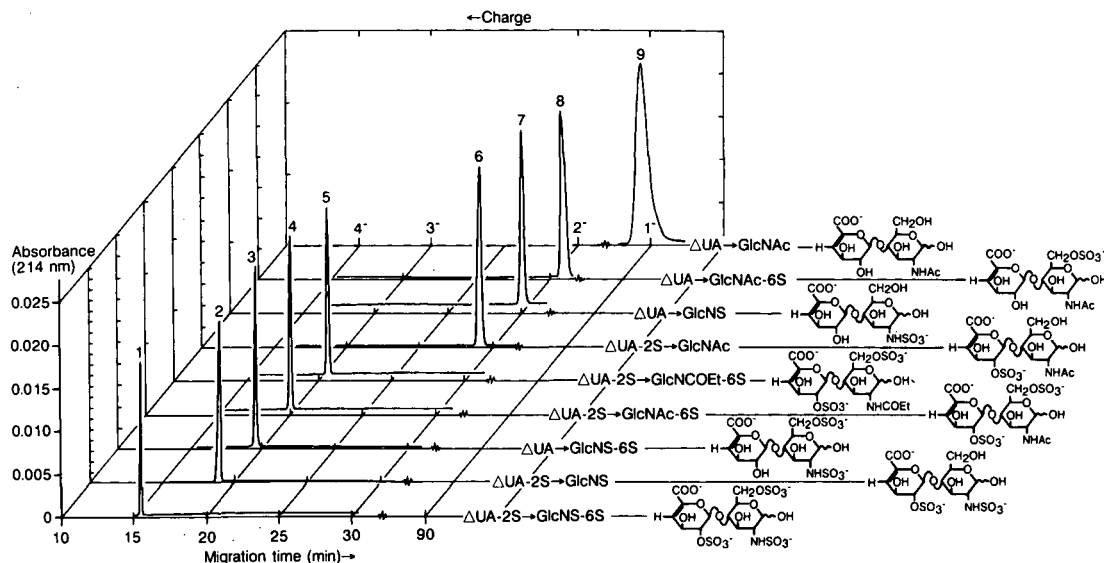


Fig. 2. CE of nine heparin disaccharides. The electropherograms are compiled in a three-dimensional plot. Electrophoresis was carried out as in Fig. 1A, except that the electrophoresis buffer was pH 3. Injection volume, 25 nl from a solution containing ca. 0.1 mg/ml of each disaccharide. The structures of disaccharides 1–9 are indicated. One part of the absorbance scale corresponds to 0.005 a.u.f.s.

Again, nine peaks, belonging to the mono- to non-amers, are visible with an additional peak at ca. 10.5 min which can be attributed to remaining polymeric material. As expected, the order of elution is reversed compared with CE. It should be noted that with HPAEC the separation is accomplished in a shorter time. However, much more material (125  $\mu$ g vs. 125 ng) is needed for the analysis.

In Fig. 2, the capillary electropherograms obtained at pH 3 for nine heparin disaccharides (denoted 1–9) are shown.  $\Delta^{4,5}$ -Uronic acid-2-sulphate-( $\beta$ 1–4)-glucosamine-N,6-disulphate (1,  $\Delta$ UA-2S $\rightarrow$ GlcNS-6S), having four negative charges (three sulphate groups and one carboxyl group), migrates at 15.5 min.

$\Delta^{4,5}$ -Uronic acid-2-sulphate-( $\beta$ 1–4)-glucosamine-N-sulphate (2,  $\Delta$ UA-2S $\rightarrow$ GlcNS),  $\Delta^{4,5}$ -uronic acid-( $\beta$ 1–4)-glucosamine-N,6-disulphate (3,  $\Delta$ UA $\rightarrow$ GlcNS-6S),  $\Delta^{4,5}$ -uronic acid-2-sulphate-( $\beta$ 1–4)-N-acetylglucosamine-6-sulphate (4,  $\Delta$ UA-2S $\rightarrow$ GlcNAc-6S) and  $\Delta^{4,5}$ -uronic acid-2-sulphate-( $\beta$ 1–4)-glucosamine-N-carboxyethyl-6-sulphate (5,  $\Delta$ UA-2S $\rightarrow$ GlcNOEt-6S), all having three negative charges (two sulphate and one carboxyl group), migrate at 19.1, 19.8, 20.2 and 20.8 min, respectively.

$\Delta^{4,5}$ -Uronic acid-2-sulphate-( $\beta$ 1–4)-N-acetylglu-

cosamine (6,  $\Delta$ UA-2S $\rightarrow$ GlcNAc),  $\Delta^{4,5}$ -uronic acid-( $\beta$ 1–4)-glucosamine-N-sulphate (7,  $\Delta$ UA $\rightarrow$ GlcNS) and  $\Delta^{4,5}$ -uronic acid-( $\beta$ 1–4)-N-acetylglucosamine-6-sulphate (8,  $\Delta$ UA $\rightarrow$ GlcNAc-6S), each having two negative charges (one sulphate and one carboxyl group), migrate at 29.7, 29.9 and 30.8 min, respectively. Finally,  $\Delta^{4,5}$ -uronic acid-( $\beta$ 1–4)-N-acetylglucosamine (9,  $\Delta$ UA $\rightarrow$ GlcNAc) with one negative charge migrates at 89.0 min. From this it is clear that the separation is based on (negative) charge, as already shown for the colominic acid oligomers, but also on structure (*i.e.*, charge distribution). Simultaneous injection of the nine disaccharides has no effect on the migration times, indicating that the migration properties do not influence each other (Fig. 3A). In this case  $\Delta$ UA-2S $\rightarrow$ GlcNAc (6) and  $\Delta$ UA $\rightarrow$ GlcNS (7), migrating at 29.7 and 29.9 min, respectively, show a large overlap.

For comparison, the nine disaccharide reference compounds were also analysed by HPAEC on Mono Q (Fig. 3B). As with CE, eight baseline-separated peaks are obtained. Compounds 4 ( $\Delta$ UA-2S $\rightarrow$ GlcNAc-6S) and 5 ( $\Delta$ UA-2S $\rightarrow$ GlcNOEt-6S), which were completely resolved by CE, give rise to overlapping peaks. On the other hand compounds 6

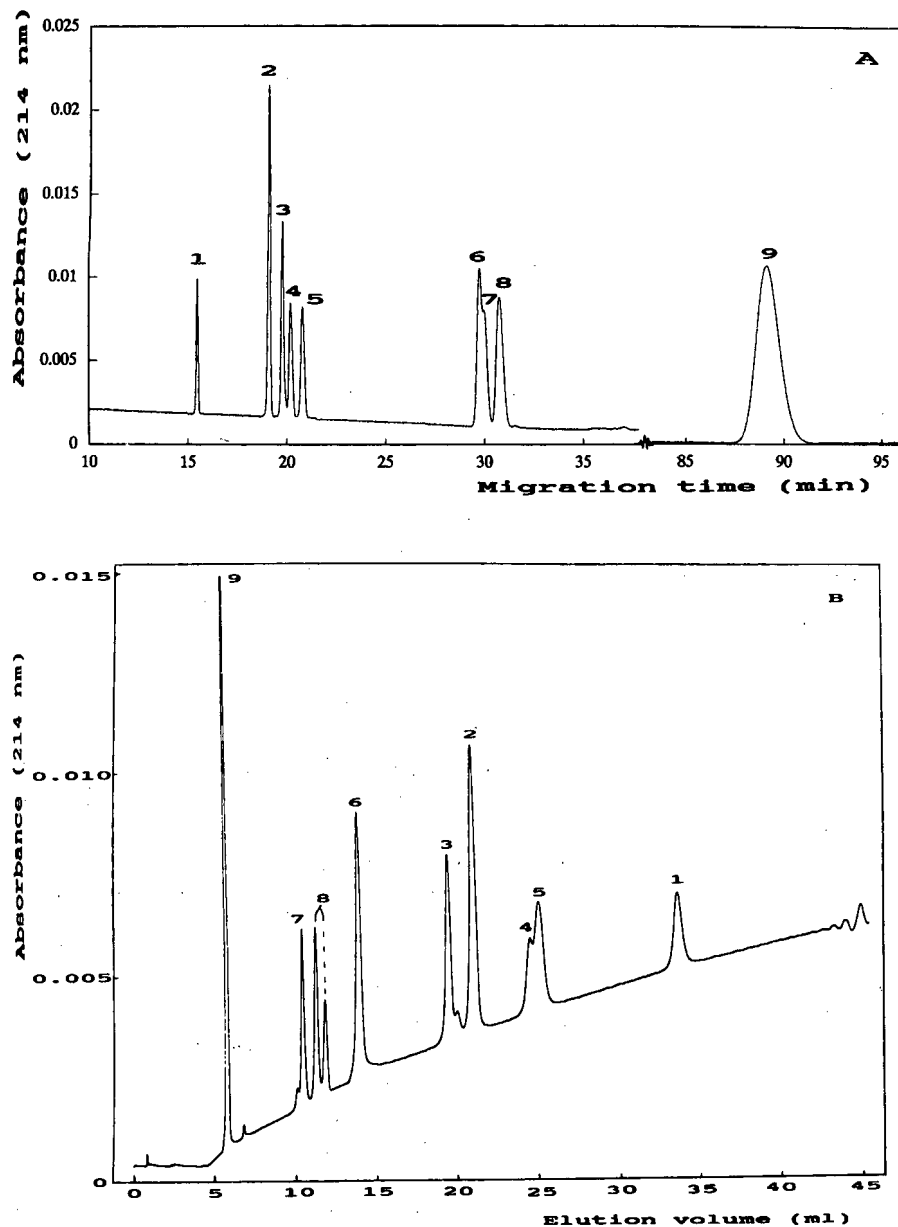


Fig. 3. (A) CE and (B) HPAEC of a mixture of nine heparin disaccharides. Conditions for CE and HPAEC as in Fig. 2 and 1B, respectively, except that for HPAEC a linear concentration gradient of 0–1 *M* NaCl in 45 ml of Milli-Q-purified water was used. Injection volume, 25 nl (CE) or 25  $\mu$ l (HPAEC) from a sample solution containing *ca.* 0.1 mg/ml of each disaccharide (for the structures of disaccharides 1–9, see Fig. 2).

( $\Delta$ UA-2S $\rightarrow$ GlcNAc) and 7 ( $\Delta$ UA $\rightarrow$ GlcNS), only partly resolved by CE, are baseline separated.  $\Delta$ UA $\rightarrow$ GlcNAc-6S (8) yields two peaks. Probably the major peak represents the disaccharide, while

the minor peak stems from a negatively charged non-carbohydrate (because it is not visible in CE) contaminant. The identity of the peaks as disaccharides 1–9 was established by injection of the individ-

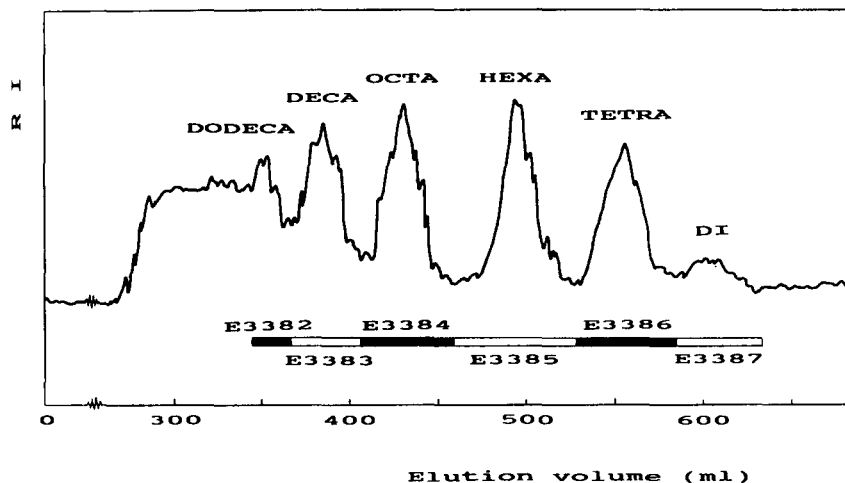


Fig. 4. Fractionation of heparinase-treated heparin by gel permeation chromatography. Heparin was partially degraded by heparinase and batch-adsorbed on an anion-exchanger. The material that desorbed from the anion-exchange column between 5 and 10% (w/v) NaCl was fractionated by a gel permeation chromatographic system, consisting of two columns in tandem, namely a TSK Fractogel HW 40 S column (70 × 2.6 cm I.D.) and a Bio-Gel P-2 (400 mesh) column (100 × 2.5 cm I.D.). The elution pattern was recorded by refractive index (RI) detection. Six fractions of increasing molecular mass were collected as indicated.

ual compounds (results not shown). The order of elution of the differently charged molecules is reversed as compared with CE, as was already shown for the colominic acid oligomers. However, the reversal of the migration/elution order is not maintained within a series of identically (negatively) charged compounds. This is demonstrated, for instance, for the disaccharides containing three negative charges, having an elution order 2→3→4→5 in CE vs. 3→2→4→5 in HPAEC. This indicates that while charge exerts an opposite effect on the migration and elution time in CE and HPAEC, respectively, the influence of charge distribution is unpredictable in this respect.

On the basis of the CE conditions established for the reference compounds, more complicated mixtures of heparin fragments were analysed by CE. Also in this instance the CE performance was compared with the performance of HPAEC. Heparin was treated with heparinase and batch-absorbed on an anion exchanger. The pool of heparin fragments that desorbed from the anion-exchange column between 5 and 10% NaCl was fractionated by gel permeation chromatography. The fractions were collected as indicated in Fig. 4 and the relative molecular mass of each pooled fraction, which still contains many carbohydrate structures, was calculated

on basis of elution position to be 4200 (E3382), 3500 (E3383), 3100 (E3384), 2500 (E3385), 1600 (E3386) and 600 (E3387). According to their apparent molecular masses, the fractions should represent mixtures of dodeca-, deca-, octa-, hexa-, tetra- and dimers, respectively; however, no attempts were made to resolve the structures. The deca- to tetramer mixtures were each subfractionated by either CE or HPAEC.

In Fig. 5A, the patterns obtained by CE are collected. The separation was carried out at pH 2 which nearly eliminates the electroosmotic flow and results in relatively short retention times. It should be noted that in this instance an optimum separation is achieved at pH 2, which is lower than that for the separation of heparin disaccharides (having a smaller molecular mass and fewer sulphate groups) and colominic acid oligomers (having carboxyl instead of sulphate groups as charged constituents). It is clear that with increasing molecular mass the structural heterogeneity of the heparin fragments increases and the resolution obtained decreases. Interestingly, the migration times of all heparin preparations are virtually in the same range (16–24 min). With increasing molecular mass the negative charge increases accordingly, which means that the separation is based not only on charge and charge distri-

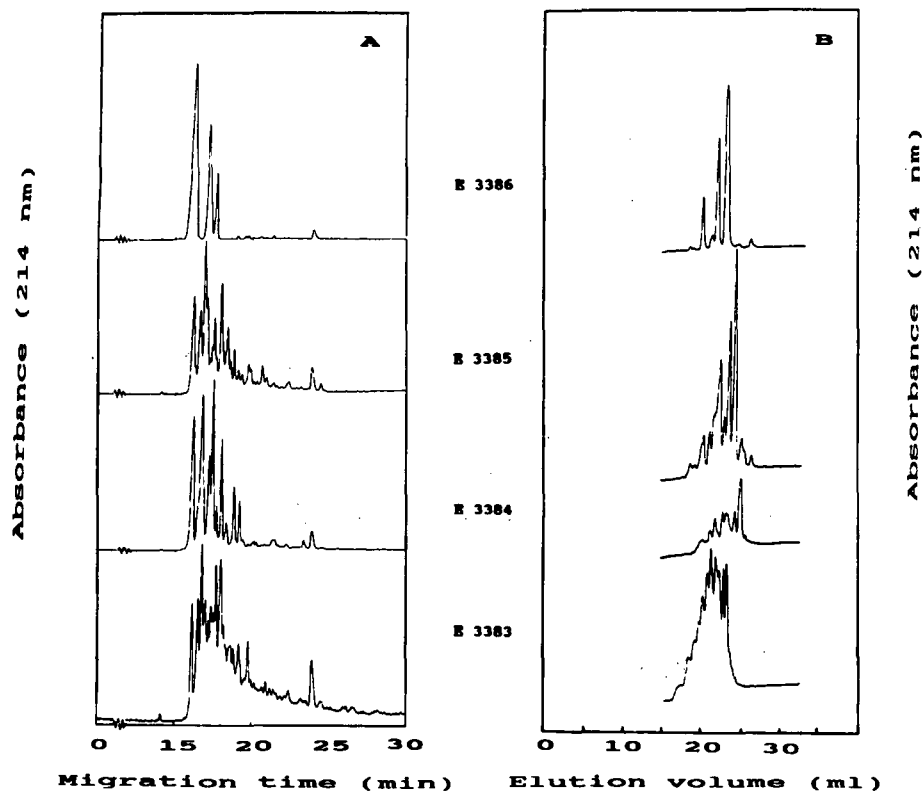


Fig. 5. (A) CE and (B) HPAEC of four heparin oligosaccharide pools. The oligosaccharide pools were obtained by anion-exchange chromatography and gel permeation chromatography of heparinase-treated heparin (Fig. 4). Each oligosaccharide pool was fractionated by CE and HPAEC using the conditions described in Fig. 1A and B, respectively, except that the total concentration of the oligosaccharides in the sample solutions was 4 mg/ml and the phosphate buffer for CE was of pH 2.

bution, as already discussed, but also on molecular mass, which apparently exerts an opposite effect on the migration time. This result is in agreement with the Debye-Hückel-Henry theory on electrophoretic mobility. According to this theory, the electrophoretic mobility is, to a good approximation, proportional to the charge-to-mass (radius) ratio of the analyte [40]. The opposing effect of the molecular mass might also explain why colominic acid oligomers, differing in negative charge and molecular mass from each other, migrate relatively close together (Fig. 1A) while heparin disaccharides, differing only in negative charge, migrate far apart (Fig. 2).

Fig. 5B shows the corresponding patterns obtained with HPAEC on Mono Q. Also with HPAEC the elution times of all heparin fragments are in the same range. When the capillary electro-

pherograms are compared with the HPAEC traces it is evident that the general pattern remains although, as expected, the order of elution is reversed, as is especially clear for fraction E3386. The resolution obtained for sample E3386 with CE and HPAEC is comparable but for the more complex samples E3385, E3384 and E3383 CE appears to be superior. It should be noted that for analysis by CE only small amounts of sample are needed. In this instance 25 nl of sample solution, corresponding to 0.1  $\mu$ g of carbohydrate material, was injected (vs. 0.1 mg for HPAEC). Concentration of the sample solution, allowing reduction of the sample volume, should yield an even better resolution.

Based on these results, the applicability of CE for assessment of the quality of synthetic heparin pentasaccharide preparations was investigated. The

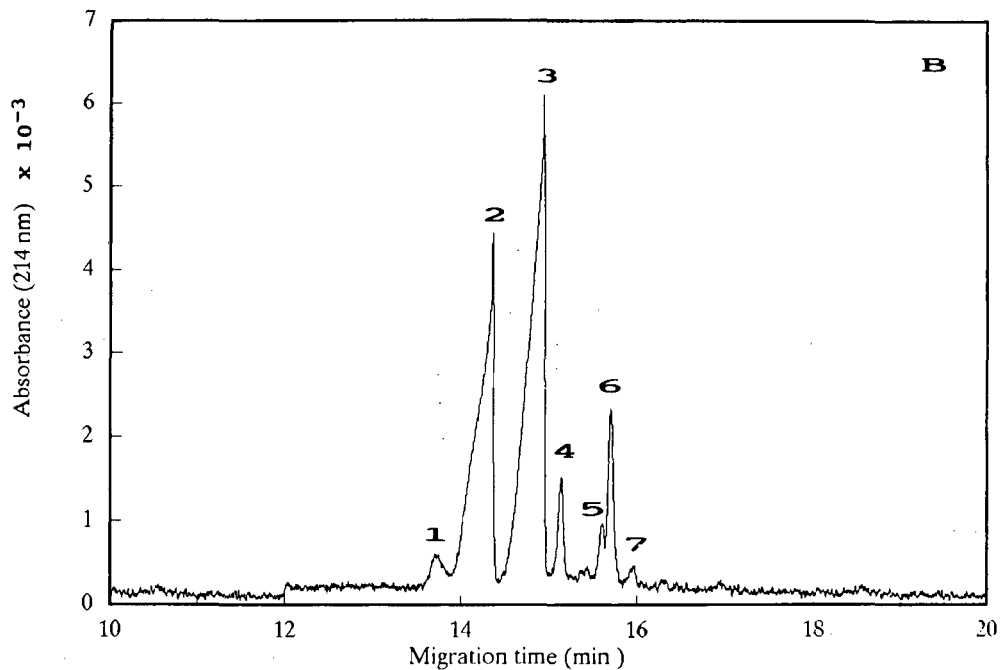
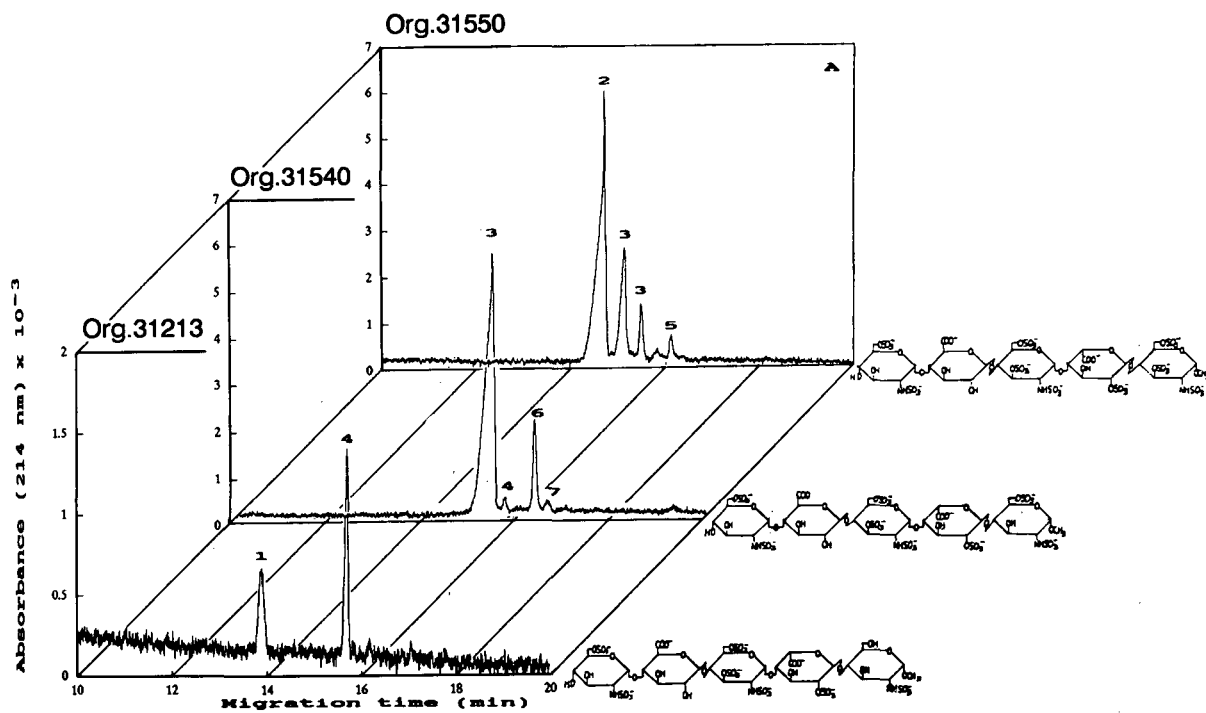


Fig. 6. CE of Org 31213, Org 31540 and Org 31550, injected (A) separately or (B) as a mixture. Conditions as in Fig. 1A, except that the pH of the electrophoresis buffer was 3 and the concentration of the Org compounds was 0.2-1 mg/ml.



pentasaccharides are identical with, or are derivatives of, the unique sequence responsible for the anticoagulant activity of heparin and were synthesized by Organon in collaboration with Sanofi via a multi-step procedure. In Fig. 6A the capillary electro-

pherograms obtained for three synthetic pentasaccharides, denoted Org 31213, Org 31540 and Org 31550, are compiled. The three compounds have an identical pentasaccharide backbone (structures in Fig. 6A) and differ from each other only with re-

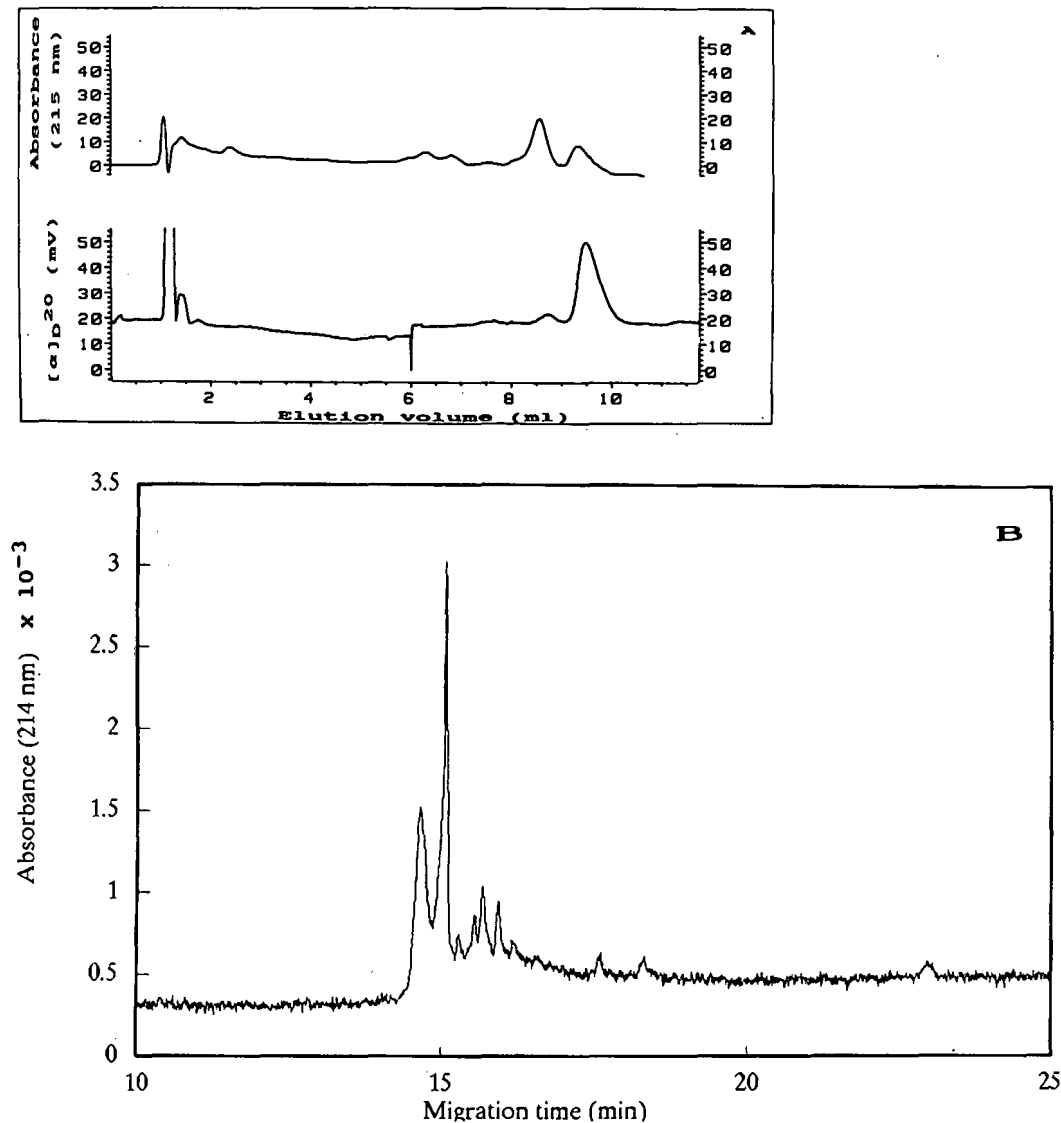


Fig. 7. (A) HPAEC and (B) CE of a batch of raw material of Org 31550 (1 mg/ml). HPAEC was carried out on a Mono Q HR 5/5 column at a flow-rate of 1 ml/min. The column was eluted with a mixture of eluents A and B, starting with 45% (v/v) A-55% (v/v) B, followed by a linear increase of B to 100% in 11 min, where eluent A is Milli-Q-purified water containing 0.1% (v/v) of dimethyl sulphoxide and eluent B is 1.6 M NaCl. Injection volume, 0.2 ml. Detection was based on UV absorbance at 215 nm (upper part) or on measurement of optical activity by a polarized laser [41] (Chiramonitor) (lower part). In both instances the detector signal is expressed in arbitrary units. CE conditions as in Fig. 1, except that the pH of the electrophoresis buffer was 3 and the concentration of Org 31550 in the sample solution was *ca.* 1 mg/ml.

spect to the number of sulphate substituents, which can be seven (Org 31213), eight (Org 31540) or nine (Org 31550). The purity of the preparations has been determined previously by 360- and 500-MHz  $^1\text{H}$  NMR spectroscopy and is at least 99% (mol/mol) [30–32]. Using the CE conditions established for the heparin disaccharides, the Org 31213 sample gives rise to two peaks at 13.9 (numbered 1 in Fig. 6A and B) and 15.7 min (4), respectively. Based on its migration time the main peak at 15.7 min is assigned to Org 31213. Similarly, CE of the Org 31540 preparation yields two peaks at 15.3 (3) and 16.2 min (6), respectively. According to its migration time, the main peak at 15.3 min is assigned to Org 31540. In addition, two minor peaks at 15.7 (4) and 16.5 min (7) are visible. Although the minor peak at 15.7 min has the same migration time as Org 31213, it is unlikely (on basis of the synthesis route) that the Org 31540 preparation could contain Org 31213. The Org 31550 sample yields four peaks, namely a main peak at 14.7 min (2), which is assigned to Org 31550, and three smaller peaks at 15.2 (3), 15.5 (3) and 16.1 min (5). Apparently, the various pentasaccharide structures can be separated efficiently from each other by CE. This is confirmed by co-injection of the three pentasaccharide samples (Fig. 6B). In this instance, however, the compounds migrating at 15.2, 15.3 and 15.5 min, which are separately visible in Fig. 6A, give rise to a multi-component peak (3). The contaminants in the pentasaccharide preparations most likely represent synthetic precursors, although at present their identity is not known. It should be realized that, in general, detection based on UV absorption is much more sensitive for the synthetic precursors, containing strong UV absorbing substituents, than for the end products, which leads to a major overestimation of the amount of contaminants. This is confirmed by the NMR data on the purity of these preparations.

The value of CE as a qualitative assay for the purity of pentasaccharide preparations is also demonstrated by the analysis of sample HH2174 by CE and HPAEC. HH2174 represents a batch of raw material of Org 31550 that was deliberately kept from further purification. NMR spectroscopic analysis had previously shown that HH2174 consists of *ca.* 85% (mol/mol) or Org 3155. HPAEC of HH2174 and detection at 215 nm give rise to two broad peaks eluting at 8.5 and 9.3 ml (Fig. 7A).

Additionally, two minor, partly overlapping peaks are discernible at 6.3 and 6.8 ml. From the injection of pure Org 31550 it is known that the peak at 9.3 ml represents Org 31550. Again, it is clear that detection of contaminants is far more sensitive than detection of the main product. A better estimate of the molar ratio of the compounds present in HH2174 is obtained when the detection is carried out with a Chiramonitor (Applied Chromatography Systems, Macclesfield, UK), where detection is based on optical activity [41]. In this instance the two minor peaks are no longer visible and the areas of the two main peaks are in accordance with the expected values. When HH2174 is subjected to CE at least nine peaks are visible in the electropherogram (Fig. 7B), demonstrating the high resolution achieved with CE. Based on the migration time (compare Fig. 6A) and relative peak area (compare Fig. 7A), the peak at 14.7 min can be attributed to Org 31550. Most likely the peak at 15.1 min represents the major contaminant that in HPAEC elutes at 8.5 min (Fig. 7A). At least six additional peaks belonging to minor contaminants are discernible. It should be noted that the order of migration of the various peaks is, as expected, reversed compared with HPAEC.

Bearing in mind, the potential suitability of CE as a quality control for heparin fragments, it was important to obtain a better insight into the ruggedness of the method. In this respect the effects of the presence of salts in the sample solution or a change of pH of the electrophoresis buffer are relevant. As a first approach, samples of E3384 were dissolved in Milli-Q-purified water, 0.5 M NaCl and 1 M NaCl, and subjected to CE (Fig. 8A). Obviously, the NaCl concentrations tested have virtually no effect on the CE performance. The slight increase in migration times that is noted is probably caused by the increased conductivity and concomitantly decreased electrical field in the sample zone. Because injection volumes are in general very small (typically 25 nl), the disturbance of the electrical field is marginal. However, the pH of the electrophoresis buffer has a major influence on the CE performance. This is exemplified in Fig. 8B where CE of E3384 at pH 3 and 2 are compared. Evidently, lowering the pH of the operating buffer, leading to a decrease in the electroosmotic flow and net charge of the heparin fragments, gives rise to an enhancement of the resolu-

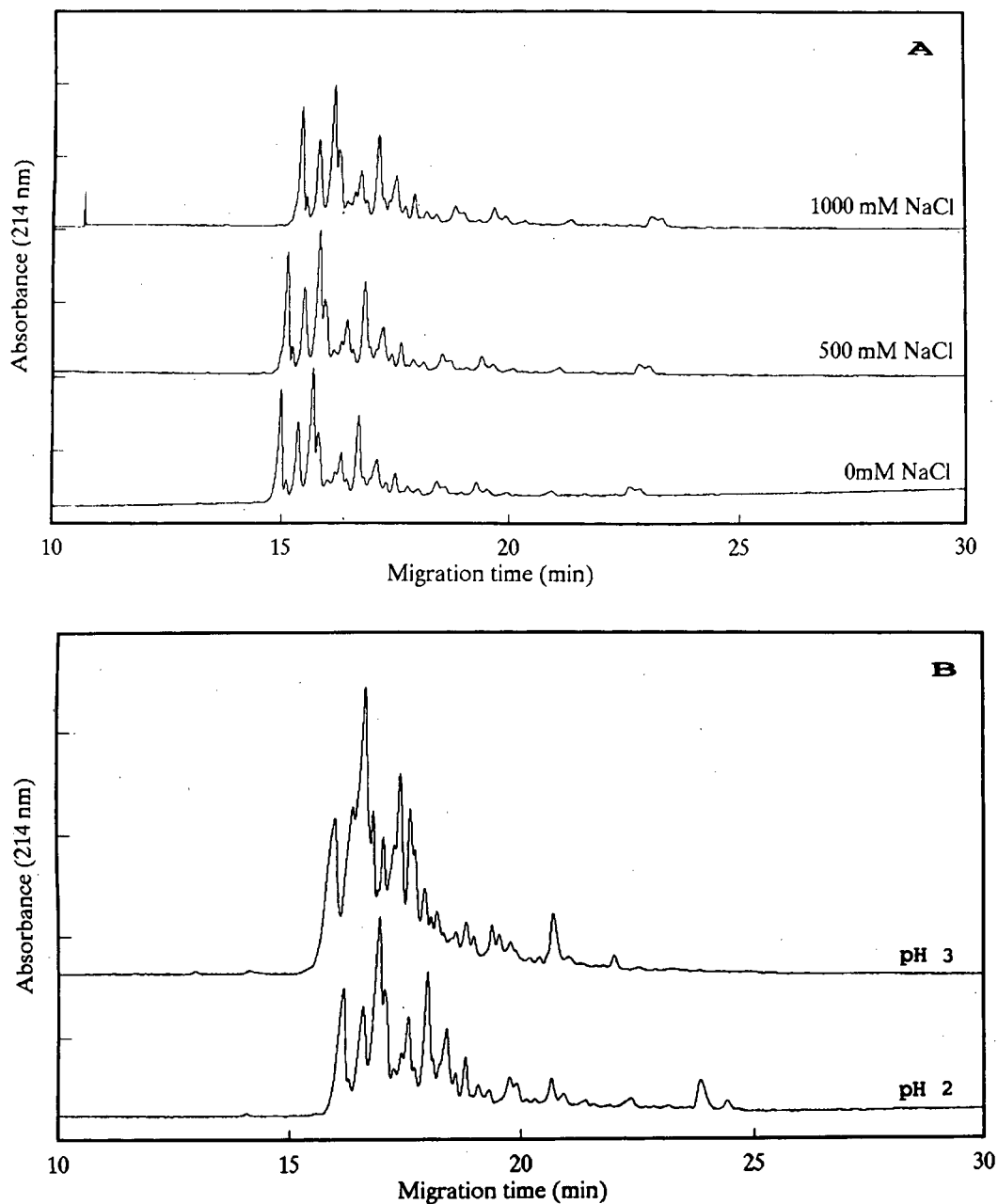


Fig. 8. Effect of (A) NaCl concentration in the sample solution and (B) pH of the electrophoresis buffer on CE of heparin oligosaccharide pool E3384. The oligosaccharide pool, denoted E3384, was obtained as described in Fig. 4. Desalted and lyophilized E3384 was dissolved in Milli-Q-purified water to a concentration of 5 mg/ml. Subsequently the effect of the presence of NaCl (0, 0.5 and 1 M) in the sample solution, using a 200 mM phosphate electrophoresis buffer (pH 2), or the influence of the pH of the electrophoresis buffer (pH 3 and 2) was examined. Injection volume, 25 nl. The absorbance at 214 nm is expressed in arbitrary units. For further details, see Fig. 1.

tion. This was also the case for the other heparinase-derived heparin fragments.

In summary, we conclude that CE may open the way to a new, sensitive and easy to use analytical procedure for the assessment of the purity of low-molecular-mass heparin preparations.

#### ACKNOWLEDGEMENTS

The authors thank P. S. L. Janssen and M. H. J. M. Langenhuizen for their advice and technical assistance in the CE experiments and C. A. A. van Boeckel and J. N. Vos for supplying the synthetic pentasaccharides.

#### REFERENCES

- 1 B. Casu, in D. A. Lane and U. Lindahl (Editors), *Heparin: Chemical and Biological Properties, Clinical Applications*, Edward Arnold, London, 1989, p. 25.
- 2 L. Thunberg, G. Bäckström and U. Lindahl, *Carbohydr. Res.*, 100 (1982) 393.
- 3 D. P. Thomas and R. E. Merton, *Thromb. Res.*, 28 (1982) 343.
- 4 U. Lindahl, G. Bäckström, M. Höök, L. Thunberg, L. A. Fransson and A. Linker, *Proc. Natl. Acad. Sci. U.S.A.*, 76 (1979) 3198.
- 5 J. Choay, M. Petitou, J. C. Lormeau, P. Sinay, B. Casu and G. Gatti, *Biochem. Biophys. Res. Commun.*, 116 (1983) 492.
- 6 J. Choay, J. C. Lormeau, M. Petitou, P. Sinay and J. Fareed, *Ann. N.Y. Acad. Sci.*, 370 (1981) 644.
- 7 P. D. J. Grootenhuys and C. A. A. van Boeckel, *J. Am. Chem. Soc.*, 113 (1991) 2743.
- 8 T. M. Hyers, R. D. Hull and J. G. Weg, *Arch. Intern. Med.*, 146 (1986) 467.
- 9 A. S. Gallus and J. Hirsch, *Semin. Thromb. Hemostasis*, 2 (1976) 291.
- 10 A. Gorsky, M. Wasik, M. Nowaczyk and G. Korczak-Kowalska, *FASEB J.*, 5 (1991) 2287.
- 11 J. Folkman and D. E. Ingber, in D. A. Lane and U. Lindahl (Editors), *Heparin: Chemical and Biological Properties, Clinical Applications*, Edward Arnold, London, 1989, p. 317.
- 12 E. Ruoslathi, *J. Biol. Chem.*, 264 (1989) 13369.
- 13 P. Bashkin, S. Doctrow, M. Klagsbrun, C. M. Svahn, J. Folkman and I. Vlodavsky, *Biochemistry*, 28 (1989) 1737.
- 14 O. Lider, Y. A. Mekori, T. Miller, R. Bar-Tana, I. Vlodavsky, E. Baharav, I. R. Cohen and Y. Naparstek, *Eur. J. Immunol.*, 20 (1990) 493.
- 15 M. Nakajima, T. Irimura and G. L. Nicolson, *J. Cell. Biochem.*, 36 (1988) 157.
- 16 E. Ruoslathi and Y. Yamaguchi, *Cell*, 64 (1991) 867.
- 17 A. Yayon, M. Klagsbrun, J. D. Esko, P. Leder and D. M. Ornitz, *Cell*, 64 (1991) 841.
- 18 T. C. Wright, Jr., J. J. Castellot, M. Petitou, J.-C. Lormeau, J. Choay and M. J. Karnovsky, *J. Biol. Chem.*, 264 (1989) 1534.
- 19 J. Pangrazzi, M. Abbadini, M. Zametta, A. Naggi, G. Torri, B. Casu and M. B. Donati, *Biochem. Pharmacol.*, 34 (1985) 3305.
- 20 Y. C. Guo and H. E. Conrad, *Anal. Biochem.*, 168 (1988) 54.
- 21 R. J. Linhardt, K. G. Rice, Z. M. Zohar, K. S. Yeong and D. L. Lohse, *J. Biol. Chem.*, 261 (1986) 14448.
- 22 J. Albada, H. K. Nieuwenhuis and J. J. Sixma, in D. A. Lane and U. Lindahl (Editors) *Heparin: Chemical and Biological Properties, Clinical Applications*, Edward Arnold, London, 1989, p. 417, and references cited therein.
- 23 E. Holmer, in D. A. Lane and U. Lindahl (Editors), *Heparin: Chemical and Biological Properties, Clinical Applications*, Edward Arnold, London, 1989, p. 575, and references cited therein.
- 24 P. Sinay, J.-C. Jacquinet, M. Petitou, P. Duchasoy, I. Lederman, J. Choay and G. Torri, *Carbohydr. Res.*, 132 (1984) C5.
- 25 C. A. A. van Boeckel, T. Beetz, J. N. Vos, A. J. M. de Jong, S. F. van Aelst, R. H. van den Bosch, J. M. R. Mertens and F. A. van der Vlugt, *J. Carbohydr. Chem.*, 4 (1985) 293.
- 26 C. A. A. van Boeckel, H. Lucas, S. F. van Aelst, M. W. P. van den Nieuwenhof, G. N. Wagenaars and J.-R. Mellema, *Recl. Trav. Chim. Pays-Bas*, 106 (1987) 581.
- 27 M. Petitou, J. C. Lormeau and J. Choay, *Eur. J. Biochem.*, 176 (1988) 637.
- 28 J. M. Walenga, J. Fareed, M. Petitou, M. Samana, J. C. Lormeau and J. Choay, *Thromb. Res.*, 43 (1986) 243.
- 29 C. A. A. van Boeckel, S. F. van Aelst, T. Beetz, D. G. Meuleman, Th. G. van Dinther and H. C. T. Moelker, *Ann. N. Y. Acad. Sci.*, 556 (1989) 489.
- 30 T. Beetz and C. A. A. van Boeckel, *Tetrahedron Lett.*, 27 (1986) 5889.
- 31 M. Petitou, P. Duchaussoy, I. Lederman and J. Choay, *Carbohydr. Res.*, 167 (1987) 67.
- 32 C. A. A. van Boeckel, T. Beetz and S. F. van Aelst, *Tetrahedron Lett.*, 29 (1988) 803.
- 33 J. X. de Vries, *J. Chromatogr.*, 465 (1989) 297.
- 34 D. A. Blake and N. V. McLean, *Anal. Biochem.*, 190 (1990) 158.
- 35 R. J. Linhardt, K. N. Gu, D. Loganathan and S. R. Carter, *Anal. Biochem.*, 181 (1989) 288.
- 36 J. E. Turnbull and J. T. Gallagher, *Biochem. J.*, 251 (1988) 597.
- 37 S. L. Carney and D. J. Osborne, *Anal. Biochem.*, 195 (1991) 132.
- 38 A. Al-Hakim and R. J. Linhardt, *Anal. Biochem.*, 195 (1991) 68.
- 39 P. L. Jacobs, G. J. H. Schmeits, M. P. de Vries, A. P. Bruins and P. S. L. Janssen, paper presented at the 12th International Mass Spectrometry Conference, Amsterdam, 1991.
- 40 R. A. Mosher, D. Dewey, W. Thormann, D. A. Saville and M. Bier, *Anal. Chem.*, 61 (1989) 362.
- 41 J. N. Vos, M. W. P. van den Nieuwenhof, J. E. M. Basten and C. A. A. van Boeckel, *J. Carbohydr. Chem.*, 9 (1990) 501.



# Identification of vitamin B<sub>12</sub> and analogues by high-performance capillary electrophoresis and comparison with high-performance liquid chromatography

D. Lambert, C. Adjalla, F. Felden, S. Benhayoun, J. P. Nicolas and J. L. Guéant

*INSERM U308, Mechanisms of Regulation of Alimentary Behaviour, Group of Biochemistry, Faculty of Medicine, Avenue Forêt de Haye, B.P. 184, 54505 Vandoeuvre Cedex (France)*

---

## ABSTRACT

High-performance capillary electrophoresis (HPCE) was compared for the identification and determination of corrinoids (hydroxy-, cyano-, 5'-deoxyadenosyl- and methyl-cobalamin and cyano-cobinamide) with high-performance liquid chromatography (HPLC). The within-run reproducibility of the retention times in HPCE and HPLC were similar (2.4 and 2.2%, respectively). The detection limit in HPCE was 20 µg/ml. HPLC can be used, in combination with radioisotope dilution assay, when very low concentrations (100 pg/ml) have to be determined in biological material. HPCE is more efficient than HPLC for the identification of corrinoids after conversion into the CN-cobalamin and CN-cobinamide forms.

---

## INTRODUCTION

Human biological fluids contain different forms of vitamin B<sub>12</sub>: hydroxo-cobalamin (OH-cbl), cyano-cobalamin (CN-cbl) and the two coenzymatic forms 5'-deoxyadenosyl-cobalamin (Ado-cbl) and methyl-cobalamin (CH<sub>3</sub>-cbl). Cobalamins can be distinguished from potentially harmful analogues of vitamin B<sub>12</sub>, devoid of enzymatic activity [1]. These analogs can be divided in two groups: cobamides that lack the nucleotide moiety (5,6-dimethylbenzimidazole) and cobamides that contain a modified nucleotide. Only analogues with a nucleotide close to that of cbl bind intrinsic factor (IF). Haptocorrin (Hc) binds both cobinamides and cobamides [2].

Human [2–4] and animal [5] tissues contain corrinoids analogues that do not have any activity, and

that sometimes inhibit growth and development and cause severe demyelination of nerve fibres [6].

The β aquo ligand (Ado or CH<sub>3</sub>) can be replaced by an aquo group after exposure to light. The β ligand is replaced by a CN group after incubation with KCN. The consecutive treatment of a mixture of cobalamins and cobinamides by exposure to light and addition of KCN produces therefore the two forms CN-cbl and CN-cobinamide.

The determination of cobalamins has been used in order to diagnose cobalamin deficiencies in humans [7,8]. In recent years, both thin-layer chromatography and high-performance liquid chromatography (HPLC) have been developed for the determination of the different forms of cobalamin present in plasma and other biological samples [9,10]. Methods combining chromatography and isotope dilution assay can be used to separate and to identify the different forms of corrinoids [11–14].

In this study, two methods for the separation of corrinoids were compared: high-performance capillary electrophoresis (HPCE) and HPLC. The application of HPCE was tested on multi-vitamin prep-

---

Correspondence to: Dr. D. Lambert, INSERM U308, Mechanisms of Regulation of Alimentary Behaviour, Group of Biochemistry, Faculty of Medicine, Avenue Forêt de Haye, B.P. 184, 54505 Vandoeuvre Cedex, France.

arations for parenteral nutrition, the corrinoids stability of which can be altered by physical conditions and interactions with other components [15,16].

## EXPERIMENTAL

### Chemicals

Crystalline OH-cbl, CN-cbl, Ado-cbl, CH<sub>3</sub>-cbl and CN-cobinamide were obtained from Sigma (St. Louis, MO, USA) and used as standards for both HPLC and HPCE. Standards were dissolved in distilled water (concentrations were chosen to obtain a good detector response), and filtered through a 0.45- $\mu$ m filter (Millipore).

NaH<sub>2</sub>PO<sub>4</sub> and orthophosphoric acid respectively were obtained from BDH (AnalaR grade) and Pro-labo, respectively. For both HPCE and HPLC, buffers were filtered (0.45  $\mu$ m) and degassed under vacuum. A multi-vitamin mineral preparation (Soluvit) was obtained from Kabi-Pharmacia.

C<sub>18</sub> cartridges (5- $\mu$ m silica, 250 mm  $\times$  5 mm I.D.) and Sep-pak C<sub>18</sub> cartridges were purchased from Waters.

### High-performance capillary electrophoresis

Capillary electrophoresis was performed using a Waters Quanta 4000 apparatus. The system was equipped with a fused-silica capillary tube (100 cm  $\times$  75  $\mu$ m I.D.) with an effective length of 93 cm. The applied voltage was 30 kV. Sample injection was maintained for 15 s and the column temperature was maintained at 26°C. The anode and cathode buffer was 20 mM NaH<sub>2</sub>PO<sub>4</sub>, adjusted to pH 2.5 with 20 mM orthophosphoric acid solution. Absorbance was measured at 214 nm.

### Reversed-phase high-performance liquid chromatography

HPLC was performed at room temperature using a two-pump gradient system (Waters). The detection wavelength was 254 nm (Lambda-max 480 spectrophotometer, Waters).

HPLC separation of corrinoids was carried out in 40 min, on a C<sub>18</sub> column, using a 10–50% linear gradient of acetonitrile in 0.085 M phosphoric acid as mobile phase. The pH was adjusted to 3.0 with triethanolamine. The flow-rate was 0.5 ml/min.

### Exposure to light and KCN treatment

Standard corrinoids were first exposed to light (45-min exposure to a 60-W tungsten lamp at a distance of 50 cm) and then subjected to KCN treatment (incubation with one volume of  $0.2 \cdot 10^{-2}$  M KCN for 2 h) in order to convert corrinoids into the CN forms.

## RESULTS

A mixture of the five standards, OH-, CN-, Ado- and CH<sub>3</sub>-cbl and CN-cobinamide, was resolved in five well separated peaks in HPCE (Fig. 1A). The retention times of the corrinoids are given in Table I. Identification was achieved by injecting either the corrinoid mixture or a sample of each corrinoid form. A better separation of CN-cobinamide, OH-cbl and Ado-cbl was obtained with a lower voltage (15 kV), the retention times of CH<sub>3</sub>-cbl and CN-cbl then being longer than 16 and 25 min, respectively (not shown).

The peaks of OH-cbl, Ado-cbl and CH<sub>3</sub>-cbl disappeared after exposure to light and treatment with KCN. Only two peaks, whose retention times corresponded to CN-cobinamide and CN-cbl, were present (Fig. 1B). The detection limit of CN-cbl was 20  $\mu$ g/ml.

The multi-vitamin mineral preparation (Soluvit) was passed through a Sep-pak C<sub>18</sub> cartridge to obtain water-soluble components [9]. The eluent was 20% 2-butanol. The identification by HPCE allowed four main peaks to be obtained. One of these had a retention time corresponding to that of CN-cobalamin (not shown). The three other peaks had retention times below those of corrinoids (2.2, 3.0 and 3.9 min). There was no similar peaks between Soluvit and corrinoid standards.

The five different forms of cobalamin were also identified by HPLC (Fig. 2A). The differences in retention times (Table I) were not as marked as with HPCE. Moreover, at pH 3, CN-cobinamide injected alone appeared to be present as two peaks corresponding to CN $\alpha$ - and CN $\beta$ -cobinamide [12,17]. The retention time of CN-cbl was intermediate between those of CN $\alpha$ - and CN $\beta$ -cobinamide.

After exposure to light and treatment with KCN, only three peaks, whose retention times corresponded to CN-cobinamide and CN $\alpha$ - and CN $\beta$ -cbl, were present on the HPLC trace (Fig. 2B).

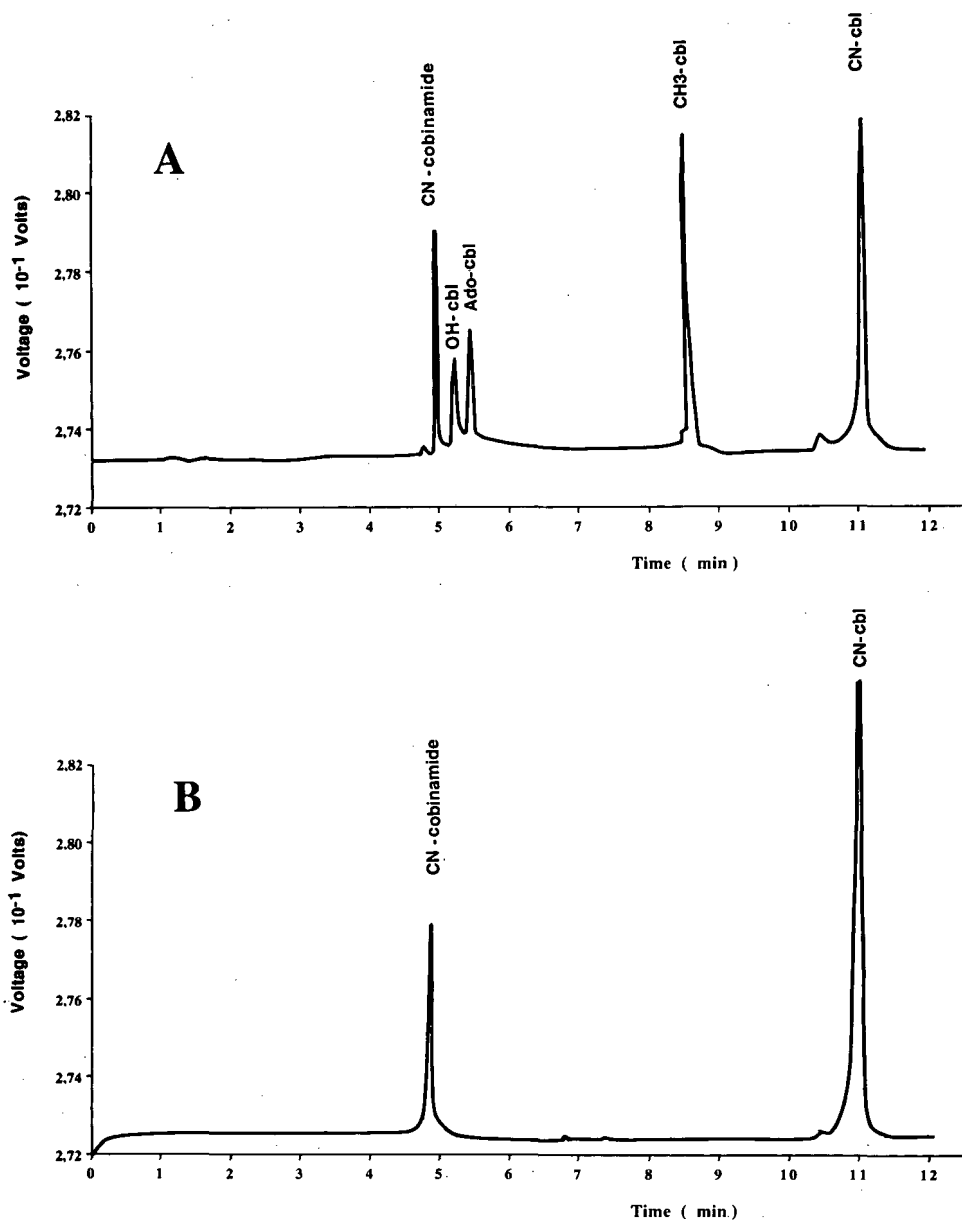


Fig. 1. HPCE of standard corrinoid samples. (A) Untreated samples; (B) samples after exposure to light (45 min, 60-W tungsten lamp; distance 50 cm) and then KCN treatment (incubation with one volume of  $0.2 \cdot 10^{-2} M$  KCN for 2 h). Electrophoretic conditions as in Table I.

The within-run reproducibilities of the retention times in HPCE and HPLC were similar, with coefficients of variation of 2.4 and 2.2%, respectively.

DISCUSSION

In HPCE, the retention times of CN-cbl and CN-



TABLE I

## RETENTION TIMES OF CORRINOIDS SEPARATED BY HPCE AND HPLC

HPCE: capillary size, 100 cm  $\times$  75  $\mu$ m I.D.; applied voltage, 30 kV; sample injection, 15 s; temperature, 26°C; anode and cathode buffer, 20 mM NaH<sub>2</sub>PO<sub>4</sub> (pH 2.5, adjusted with 20 mM orthophosphoric acid); detection wavelength, 214 nm. HPLC: C<sub>18</sub> column with a 10–50% linear gradient of acetonitrile in 0.085 M phosphoric acid as mobile phase (pH 3.0, adjusted with triethanolamine); run time, 40 min at room temperature; flow-rate, 0.5 ml/min; detection wavelength, 254 nm.

Corrinoid	Retention time (min) $\pm$ S.D. ( $n = 6$ )	
	HPLC	HPCE
OH-cobalamin	14.08 $\pm$ 0.50	5.24 $\pm$ 0.10
CN $\alpha$ -cobinamide	15.82 $\pm$ 0.31	4.95 $\pm$ 0.12
CN-cobalamin	17.21 $\pm$ 0.31	10.85 $\pm$ 0.25
CN $\beta$ -cobinamide	18.48 $\pm$ 0.18	4.95 $\pm$ 0.12
Ado-cobalamin	18.86 $\pm$ 0.45	5.50 $\pm$ 0.10
CH <sub>3</sub> -cobalamin	21.10 $\pm$ 0.47	8.45 $\pm$ 0.18

cobinamide differed by *ca.* 5.5 min. This result allowed errors of identification that could sometimes occur in HPLC, where the difference was only 1.2 min, to be avoided. For this reason, HPCE is more efficient than HPLC for the identification of corrinoids after conversion into the CN forms. HPCE allows a better discrimination between active and harmful corrinoids. However, only HPLC was able to distinguish CN $\alpha$ -cobinamide from CN $\beta$ -cobinamide. The elution of both CN $\alpha$ - and CN $\beta$ -cobinamide in the same peak in HPCE can be explained by the absence of a difference in the net charge of the two molecules.

HPLC allows fractions of the eluate to be collected which can be used for radioisotope analysis of corrinoids (radioisotope dilution assay, RIDA). For this reason we use HPLC, in combination with RIDA, when very low concentrations (100–1000 pg/ml) in biological material have to be determined. With this method for the quantification of corrinoids, the “true cbl” forms can be distinguished from cbl analogues, using intrinsic factor (IF) and haptocorrin (HC) as binders of the RIDA [14]. Such a combination with RIDA is not possible with HPCE; the amount of sample is of the order of nanolitres and the amount of corrinoid eluted in each peak is too small to be detected.

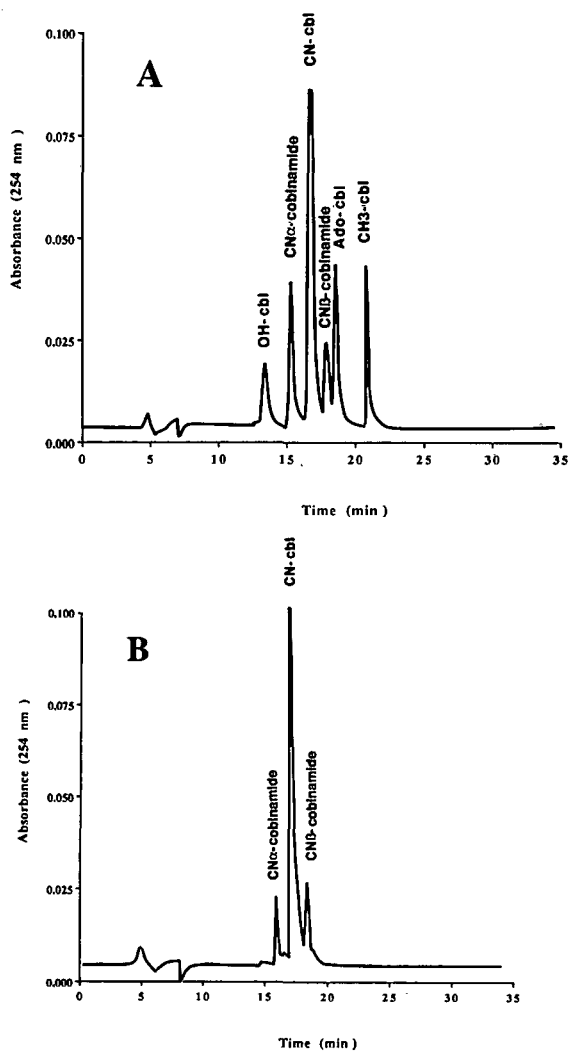


Fig. 2. HPLC of standard corrinoid samples. (A) Untreated samples; (B) samples after exposure to light (45 min, 60-W tungsten lamp; distance 50 cm) and then KCN treatment (incubation with one volume of  $0.2 \cdot 10^{-2}$  M KCN for 2 h). Chromatographic conditions as in Table I.

When concentration is not a limiting factor, HPCE is easier to perform than HPLC. For example, HPCE can be used for the analysis of multi-vitamin preparations for parenteral nutrition and to check the stability of corrinoid compounds to light exposure and temperature and the interaction of corrinoids with other vitamins and trace elements.

In conclusion, both HPCE and HPLC are effi-

cient methods for separating corrinoids. The choice between the techniques depends on the type of sample to be analysed. HPCE can be performed when the corrinoid concentration is high enough, whereas a combination of HPLC with RIDA is recommended for low-concentration samples such as biological fluids.

## REFERENCES

- 1 J. F. Kolhouse and R. H. Allen, *J. Clin. Invest.*, 60 (1977) 1381.
- 2 J. F. Kolhouse, H. Kondo, N. C. Allen, E. Podell and R. H. Allen, *N. Engl. J. Med.*, 299 (1978) 785.
- 3 J. L. Guéant, B. Monin, P. Boissel, P. Gaucher and J. P. Nicolas, *Digestion* 30 (1984) 15.
- 4 S. Kanazawa and V. Herbeth, *Am. J. Clin. Nutr.*, 37 (1983) 77.
- 5 H. Kondo, J. F. Kolhouse and R. H. Allen, *Proc. Natl. Acad. Sci. U.S.A.*, 77 (1980) 817.
- 6 R. C. Siddons, J. A. Spence and A. D. Dayan, *Adv. Neurol.*, 10 (1975) 239.
- 7 I. Chanarin, *The Megaloblastic Anemias*, Blackwell, Oxford, 1979.
- 8 E. Nexø and H. Olesen, in D. Dolphin (Editor), *B12: Biochemistry and Medicine*, Vol. 2, Wiley, New York, 1982, p. 87.
- 9 P. Gimsing and E. Nexø, in C. A. Hall (Editor), *The Cobalamins*, Churchill Livingstone, Edinburgh, 1983, p. 1.
- 10 P. Gimsing and W. S. Beck, *Scand. J. Clin. Lab. Invest.*, 194 (Suppl.) (1989) 37.
- 11 P. Gimsing, *Anal. Biochem.*, 67 (1983) 288.
- 12 P. Gimsing and W. S. Beck, *Methods Enzymol.*, 123 (1986) 3.
- 13 J. Van Kapel, L. M. J. Spijkers, J. Lindemans and J. Abels, *Clin. Chim. Acta*, 131 (1983) 211.
- 14 M. Djalali, J. L. Guéant, S. El Kholty, D. Lambert, M. Saurier and J. P. Nicolas, *J. Chromatogr.*, 529 (1990) 81.
- 15 V. Herbeth, G. Drivas, R. Foscaldi, C. Manusselis, N. Colman, S. Kanazawa, K. Das, M. Gelernt, B. Herzlich and J. Jennings, *N. Engl. J. Med.*, 307 (1982) 255.
- 16 H. Kondo, M. J. Binder, J. F. Kolhouse, W. R. Smythe, E. R. Podell and R. H. Allen, *J. Clin. Invest.*, 70 (1982) 889.
- 17 D. F. W. Jacobson, R. Green, E. V. Quadros and Y. D. Montejano, *Anal. Biochem.*, 120 (1982) 394.



# Effect of the buffer solution on the elution order and separation of bis(amidinohydrazones) by micellar electrokinetic capillary chromatography

P. Lukkari, J. Jumppanen, T. Holma and H. Sirén

*Analytical Chemistry Division, Department of Chemistry, University of Helsinki, Vuorikatu 20, SF-00100 Helsinki (Finland)*

K. Jinno

*Materials Science, Toyohashi University of Technology, Tompaku-chi, Toyohashi 440 (Japan)*

H. Elo

*Chemistry Division, Department of Pharmacy, University of Helsinki, Fabianinkatu 35, SF-00170 Helsinki (Finland)*

M.-L. Riekkola

*Analytical Chemistry Division, Department of Chemistry, University of Helsinki, Vuorikatu 20, SF-00100 Helsinki (Finland)*

---

## ABSTRACT

The effect of five different buffer solutions on the elution order and separation of bis(amidinohydrazones) by micellar electrokinetic capillary chromatography was studied at pH 7.0. The buffers were sodium phosphate, tris(hydroxymethyl)aminomethane, N-(2-hydroxyethyl)piperazine-N'-(2-ethanesulphonic acid), N,N-dimethylmethylenediamine and N,N-diethylethylenediamine. The factors affecting the elution order of the solutes were: (1) ion-pair formation between the solute and the buffer ion, (2) the cationic nature and structure of the solute, (3) reactions between ion-pair complexes and micelles and (4) the nature of the buffer solution. Sodium phosphate (0.05 M) with 1 mM N-cetyl-N,N,N-trimethylammonium bromide was the only buffer solution to fully separate eight aliphatic congeners of bis(amidinohydrazone).

---

## INTRODUCTION

Micellar electrokinetic capillary chromatography (MECC), which is an adaptation of capillary zone electrophoresis (CZE), extends the enormous power of CZE to the separation of uncharged molecules [1,2]. In MECC the addition of an ionic surfactant to the electrolyte in an amount greater than its critical

micelle concentration (CMC) makes possible the separation of neutral particles. Because the micelles provide ionic and hydrophobic sites of interaction simultaneously, MECC is also preferable to CZE for the separation of mixtures of charged and uncharged solutes. Yet another application of MECC is the separation of ionic compounds, such as the bis(amidinohydrazones) studied here, whose electrophoretic mobilities are too similar to be separated by CZE [3,4]. In MECC, the migration time of an ionic substance is a function of three factors: (1) the electrophoretic mobility of the solute, (2) the distri-

---

*Correspondence to:* Dr. M.-L. Riekkola, Analytical Chemistry Division, Department of Chemistry, University of Helsinki, Vuorikatu 20, SF-00100 Helsinki, Finland.

bution ratio of the solute between the micellar phase and the aqueous phase and (3) the chemical reactions between the solute molecules and the micelles.

The synthesis of glyoxal bis(amidinohydrazone) (GBG) was reported by Thiele and Dralle [5] toward the end of the nineteenth century. Sixty years later Freedlander and French [6] synthesized its methylglyoxal analogue (MGBG), which they showed to have strong antileukaemic activity against L1210 leukaemia in mice. These compounds are of great interest because many of them inhibit adenosylmethionine decarboxylase, a key enzyme of polyamine biosynthesis. GBG and MGBG are both potent antileukaemic agents [7,8].

In earlier work we developed a quantitative MECC method for the determination of bis(amidinohydrazones) [9]. At that time we found the elution order of these solutes to differ in inorganic and organic buffer solutions. The quality of the separation was affected by the nature of the buffer solution.

In this work, the suitability of buffer solutions of different strength, with pH adjusted to 7.0, was tested for the separation of eight bis(amidinohydrazones). The buffers were sodium phosphate, tris(hydroxymethyl)aminomethane (Tris), N-(2-hydroxyethyl)piperazine-N'-(2-ethanesulphonic acid) (HEPES), N,N-dimethylmethylenediamine (DMAEA) and N,N-diethylethylenediamine (DEAEA). N-Cetyl-N,N,N-trimethylammonium bromide (CTAB) was used for coating the inner column and for micelle and ion-pair formation. The separated solutes were detected by UV–VIS method at wavelength 280 nm.

## EXPERIMENTAL

### Apparatus

MECC was performed in a 680 mm × 0.075 mm I.D. fused-silica capillary tube (SGE, Milton Keynes, UK) where 600 mm was the effective length for separation. A Waters Quanta 4000 capillary electrophoresis system (Millipore, Waters Chromatography Division, Milford, MA, USA) was employed. Detection was at wavelength 280 nm with UV–VIS detection. All experiments were carried out at ambient temperature (ca. 24–27°C). Injections were made in hydrostatic mode for 10 or 12 s and the running negative voltage was between 20 and

25 kV. The data were collected with an HP 3392A integrator (Hewlett-Packard, Avondale, USA).

### Materials

The synthesis of the free bases of GBG, MGBG and their analogues was carried out as described previously [10]. Sodium dihydrogenphosphate monohydrate, disodium hydrogenphosphate dihydrate, Tris and CTAB were purchased from Merck (Darmstadt, Germany), HEPES was purchased from Sigma (Dorset, UK) and DMAEA and DEAEA were purchased from Fluka (Buchs, Switzerland). All compounds were used as received. Other reagents used in the development of the method were of analytical grade and were used without further purification. Distilled water was purified through a Water-I system from Gelman Sciences (Ann Arbor, MI, USA). All the micellar buffer solutions were filtered using 0.45- $\mu$ m membrane filters (Millipore, Molsheim, France) and degassed before use. Samples and other solutions were filtered through Millex filters of 0.5- $\mu$ m pore size from Millipore (Nikon Millipore, Kogyo, Yonezawa, Japan). With Tris, HEPES, DMAEA and DEAEA, the pH was adjusted to 7.0 with 0.1 M hydrochloric acid solution.

### MECC procedure

To obtain good separation, the capillary was cleaned according to the following procedure each time the buffer solution was changed: the capillary was purged for 15 min with 0.5 M potassium hydroxide and then for 2 min with the new buffer solution. In addition, the capillary was purged for 2 min with the working buffer before each injection.

## RESULTS AND DISCUSSION

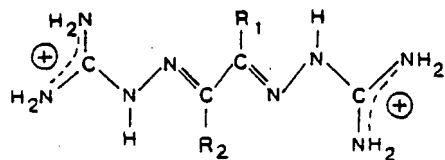
Earlier studies on the protonation equilibria and species distribution of bis(amidinohydrazones) [10] suggested to us that a good separation of these congeners would be achieved by CZE. The species distribution of GBG and MGBG (at pH 7.4 and 37°C) is distinctly different from that of the dialkylglyoxal congeners. Moreover, considerable portions of GBG (ca. 10%) and MGBG (ca. 4%) exist in the free base form, whereas the dialkylglyoxal analogues exist almost exclusively in the mono- and dicationic forms and the proportion of the free base is only

ca. 0.5% or less. The bis(amidinohydrazones) we wished to separate are listed in Table I.

To study the effect of the buffer solution on the elution order and separation, we carried out MECC experiments with five different buffers (sodium phosphate, Tris, HEPES, DMAEA and DEAEA) at pH 7.0. The concentration of the buffers was 0.05, 0.1, 1.2, 0.02 and 0.03 M, respectively, and CTAB concentration was 0.001 M (CMC [11]). The structures of the buffer solutions are shown in Table II. Sodium phosphate buffer at concentration 0.05 M gave the best separation with the lowest currents (Fig. 1). It was also the only buffer in which all eight bis(amidinohydrazone) congeners were fully separated. Accordingly, the operating conditions for this system were optimized to provide good resolution within a reasonable time. Under the optimized conditions (0.05 M sodium phosphate buffer with 1 mM CTAB, voltage -22 kV and hydrodynamic injection 12 s), the method gave good repeatability and linearity between 2.5 and 100 µg per ml of solute [9].

TABLE I  
STRUCTURE OF THE BIS(AMIDINOHYDRAZONES) STUDIED

The *Chemical Abstracts'* systematic name for MGBG is 2,2'-(1-methyl-1,2-ethanediyldine)bis(hydrazinecarboximidamide), and other congeners are named analogously.



Compound	R <sub>1</sub>	R <sub>2</sub>	M	Cationic form <sup>a</sup>
GBG	H	H	170	MC
MGBG	CH <sub>3</sub>	H	184	MC
DMGBG	CH <sub>3</sub>	CH <sub>3</sub>	198	DC
EMGBG	CH <sub>2</sub> CH <sub>3</sub>	CH <sub>3</sub>	212	DC
DEGBG	CH <sub>2</sub> CH <sub>3</sub>	CH <sub>2</sub> CH <sub>3</sub>	226	DC
MPGBG	CH <sub>3</sub>	(CH <sub>2</sub> ) <sub>2</sub> CH <sub>3</sub>	226	DC
MBGBG	CH <sub>3</sub>	(CH <sub>2</sub> ) <sub>3</sub> CH <sub>3</sub>	240	DC
DPGBG	(CH <sub>2</sub> ) <sub>2</sub> CH <sub>3</sub>	(CH <sub>2</sub> ) <sub>2</sub> CH <sub>3</sub>	254	DC

<sup>a</sup> The main cationic form of the compound at pH 7.0: MC = monocationic; DC = dicationic.

The elution order of the bis(amidinohydrazone) congeners varied with the buffer. In inorganic buffer solution (sodium phosphate), monocationic solutes eluted first and then the dicationic solutes. Evidently, the symmetric molecules interacted more strongly with the micelles and eluted more slowly than the asymmetric molecules. By contrast, in the organic buffer solutions (Tris, HEPES, DMAEA and DEAEA) the bis(amidinohydrazone) congeners eluted in decreasing size order, except for the monocationic molecules (GBG and MGBG), which behave irregularly. The concentration of the buffer and of CTAB did not affect the elution order of the solutes, only the resolution. The elution orders and relative retention times are listed in Table III.

In phosphate buffer the elution order was determined by the cationic nature and structure of the compounds (Fig. 1, Table III). Because GBG and MGBG are more monocationic than the other congeners, they eluted first. The dicationic molecules with an alkyl chain even one carbon atom shorter eluted more slowly than the molecules with longer alkyl chains, because of their stronger electrophoretic mobility and more intense interaction with the micelles. In addition, the symmetric molecules apparently reacted more strongly with the micelles and eluted more slowly than the asymmetric molecules.

The elution order in Tris differed from that in phosphate buffer solution (Fig. 2A, Table III). The Tris molecule is hydrophilic and at pH 7.0 the structure contains three free polar hydroxyl groups and one NH<sub>3</sub><sup>+</sup> group. The dicationic molecules with long alkyl chains eluted more quickly than the molecules with short alkyl chains, because they undergo stronger interactions with the slowly eluting micelles. The two monocationic compounds eluted according to their molecular weight in separation conditions (hydrophilic eluent), because the methyl substituent is more hydrophobic than hydrogen (Table I).

The elution order of bis(amidinohydrazones) was different in HEPES solution (Fig. 2B, Table III). The compounds of high molecular weight eluted before those of low molecular weight. HEPES and bis(amidinohydrazone) molecules can form ion pairs because a HEPES molecule contains one negatively charged group (Table II). There are also hydrogen bonds between these buffer molecules and

TABLE II  
STRUCTURES OF THE TESTED BUFFER IONS AT pH 7.0 WITH THEIR pK<sub>a</sub> VALUES

Buffer ion	Structure
Sodium phosphate (pK <sub>a2</sub> , 7.21) [12]	$\begin{array}{c} \text{O}^- \\   \\ \text{HO} - \text{P} = \text{O} \\   \\ \text{O}^- \end{array}$
Tris (pK <sub>a1</sub> , 8.09) [13]	$\begin{array}{c} \text{HOCH}_2 \\   \\ \text{HOCH}_2 - \text{C} - \text{NH}_3^+ \\   \\ \text{HOCH}_2 \end{array}$
HEPES (pK <sub>a1</sub> , 7.57) [13]	$\text{HOCH}_2 - \text{CH}_2 - \text{N} \begin{array}{c} \diagup \\ \diagdown \end{array} \text{N} \begin{array}{c} \diagdown \\ \diagup \end{array} - \text{CH}_2 - \text{CH}_2 - \text{SO}_3^-$
DMAEA (pK <sub>a2</sub> , 6.49) [13]	$\begin{array}{c} \text{H}_3\text{C} \\ \diagdown \\ \text{N} - \text{CH}_2 - \text{CH}_2 - \text{NH}_3^+ \\ \diagup \\ \text{H}_3\text{C} \end{array}$
DEAEA (pK <sub>a2</sub> , 7.25) [13]	$\begin{array}{c} \text{CH}_3\text{CH}_2 \\ \diagdown \\ \text{N} - \text{CH}_2 - \text{CH}_2 - \text{NH}_3^+ \\ \diagup \\ \text{H} \\ \text{CH}_3\text{CH}_2 \end{array}$

solutes. The complex is more stable and elutes more slowly the shorter the alkyl chains of the solute, owing to interaction with slowly eluting micelles.

There is only one positively charged group in the

DMAEA molecule at pH 7.0 under the separation conditions tested (Table II). Non-polar interactions should occur between DMAEA molecules and bis-(amidinohydrazones) in polar media. Under these

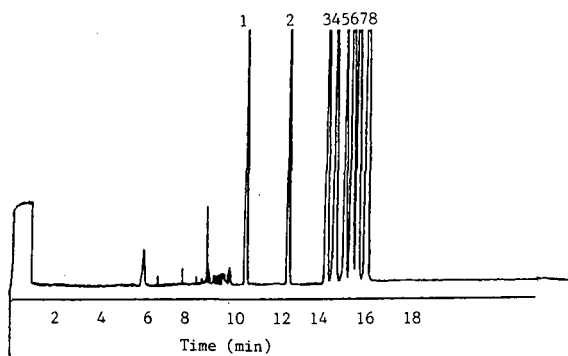


Fig. 1. Electropherogram of eight bis(amidinohydrazones) (25  $\mu$ g per ml of solute) in 0.05 *M* sodium phosphate buffer with 1 *mM* CTAB. Capillary: 68 cm  $\times$  75  $\mu$ m I.D.; pH 7.0; hydrodynamic injection mode: 12 s at 10 cm height; detector: UV at 280 nm; applied voltage: -22 kV; temperature: ambient. Peaks: 1 = GBG; 2 = MGBG; 3 = MBGBG; 4 = DPGBG; 5 = MPGBG; 6 = DEGBG; 7 = EMGBG; 8 = DMGBG [9].

forces, solutes, buffer ions and micelle molecules form large positively charged complexes. In the case of bis(amidinohydrazones) the charge of the complex is more positive when alkyl chains are long. In polar solutions a complex with large radius elutes before one with a shorter radius. Because monocations have shorter alkyl chains the complexes

formed with the monocationic solutes GBG and MGBG are smaller and less stable than those formed with the dicationic solutes, and they eluted late (Fig. 3A, Table III). The dicationic compounds eluted in order of decreasing molecular weight. The monocationic compounds eluted between EMGBG and DMGBG, but in order of increasing molecular weight because in the electro-osmotic flow large particles elute more quickly than small ones.

The DEAEA molecule has two positively charged groups at pH 7.0 under the separation conditions tested (Table II). The non-polar interactions occur in the same way in DEAEA as in DMAEA and the elution order of the bis(amidinohydrazones) is the same (Fig. 3B). In the case of GBG, the micelle and DEAEA molecules are competing for the same bonding place (two carbon atoms and the bond between them in the middle of the GBG molecule, see Table I), and the complex is positively charged. MGBG has room for one more positively charged molecule than GBG, and so the MGBG complex is more positively charged than the GBG complex. DMGBG forms an even more positively charged complex, and the elution order is GBG and then MGBG and DMGBG (Fig. 3B, Table III).

TABLE III

ELUTION ORDER OF BIS(AMIDINOHYDRAZONES) WITH RELATIVE RETENTION TIMES RELATIVE TO DPGBG IN THE DIFFERENT BUFFER SOLUTIONS AT pH 7.0 AND WITH 1 *mM* CONCENTRATION OF CTAB

Elution order	Tested buffer solutions with relative retention times				
	Sodium phosphate (0.05 <i>M</i> )	Tris (0.1 <i>M</i> )	HEPES (1.2 <i>M</i> )	DMAEA (0.02 <i>M</i> )	DEAEA (0.03 <i>M</i> )
I	GBG, 0.72	DPGBG, 1.00	DPGBG, 1.00	DPGBG, 1.00	DPGBG, 1.00
II	MGBG, 0.85	MBGBG, 1.03	MBGBG, 1.05	MBGBG, 1.05	MBGBG, 1.03
III	MBGBG, 0.97	DEGBG MPGBG, 1.08	DEGBG MPGBG, 1.12	DEGBG MPGBG, 1.13	DEGBG MPGBG, 1.08
IV	DPGBG, 1.00	GBG, 1.14	EMGBG, 1.21	EMGBG, 1.24	EMGBG, 1.12
V	MPGBG, 1.03	EMGBG, 1.16	DMGBG, 1.34	GBG, 1.28	GBG, 1.15
VI	DEGBG, 1.05	MGBG, 1.20	MGBG, 1.38	MGBG, 1.37	MGBG DMGBG, 1.20
VII	EMGBG, 1.07	DMGBG, 1.24	GBG, 1.43	DMGBG, 1.40	
VIII	DMGBG, 1.10				



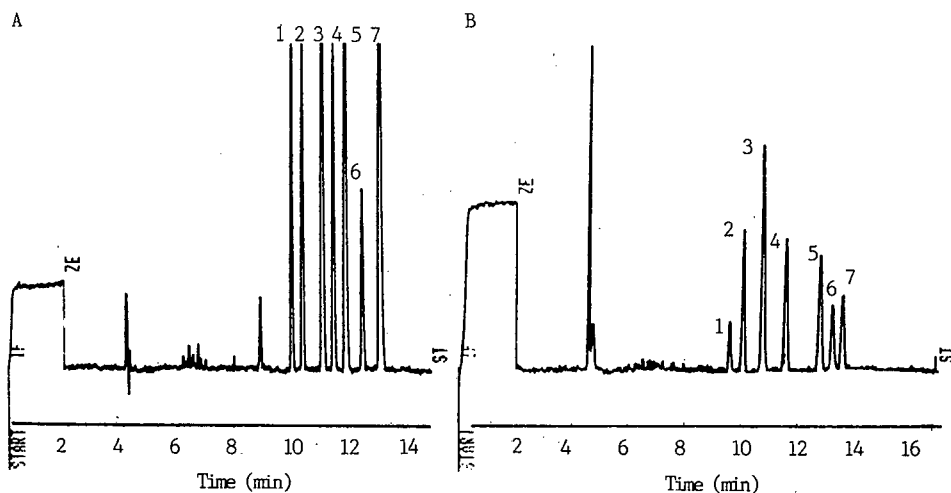


Fig. 2. (A) Electropherogram of eight bis(amidino)hydrazones ( $25 \mu\text{g}$  per ml of solute) in  $0.1 \text{ M}$  Tris buffer with  $1 \text{ mM}$  CTAB. Experimental conditions as in Fig. 1. Peaks: 1 = DPGBG; 2 = MBGBG; 3 = DEGBG and MPGBG; 4 = GBG; 5 = EMGBG; 6 = MGBG; 7 = DMGBG. (B) Electropherogram of eight bis(amidino)hydrazones ( $25 \mu\text{g}$  per ml of solute) in  $1.2 \text{ M}$  HEPES buffer with  $1 \text{ mM}$  CTAB. Experimental conditions as in Fig. 1. Peaks: 1 = DPGBG; 2 = MBGBG; 3 = DEGBG and MPGBG; 4 = EMGBG; 5 = DMGBG; 6 = MGBG; 7 = GBG.

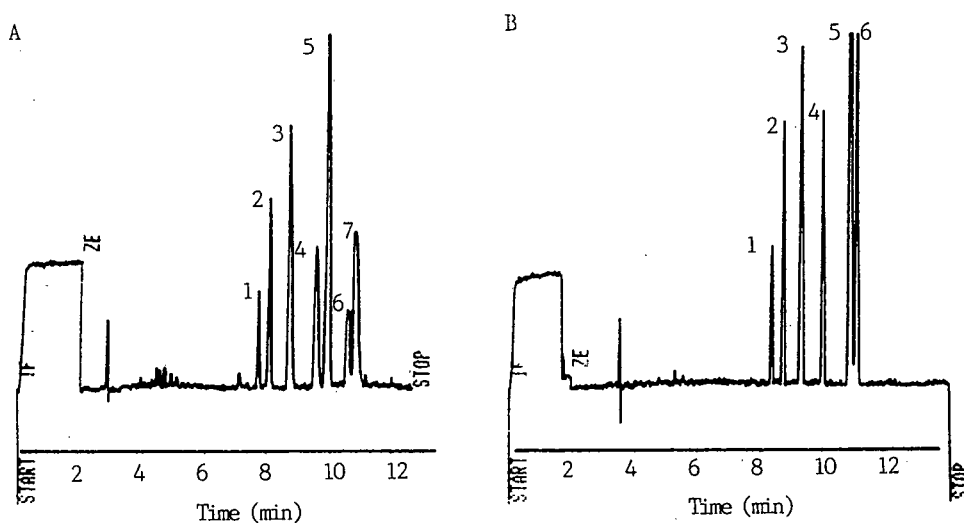


Fig. 3. (A) Electropherogram of eight bis(amidino)hydrazones ( $25 \mu\text{g}$  per ml of solute) in  $0.02 \text{ M}$  DMAEA buffer in  $1 \text{ mM}$  CTAB. Experimental conditions as in Fig. 1 except the applied voltage was  $-25 \text{ kV}$ . Peaks: 1 = DPGBG; 2 = MBGBG; 3 = DEGBG and MPGBG; 4 = EMGBG; 5 = GBG; 6 = MGBG; 7 = DMGBG. (B) Electropherogram of eight bis(amidino)hydrazones ( $25 \mu\text{g}$  per ml of solute) in  $0.03 \text{ M}$  DEAEA buffer with  $1 \text{ mM}$  CTAB. Experimental conditions as in Fig. 1 except the applied voltage was  $-20 \text{ kV}$ . Peaks: 1 = DPGBG; 2 = MBGBG; 3 = DEGBG and MPGBG; 4 = EMGBG; 5 = GBG; 6 = MGBG and DMGBG.

## CONCLUSIONS

MECC is an effective method for the separation of bis(amidinohydrazones). In phosphate buffer solution eight aliphatic congeners were fully separated. Under the other buffer conditions, MPGBG and DEGBG eluted with the same retention time. The elution order of bis(amidinohydrazones) is determined by the cationic nature and structure of the compounds. In inorganic buffer solution adjusted to pH 7.0, monocationic solutes elute first and then the dicationic. The monocationic nature of GBG and MGBG has less effect on the elution order of bis(amidinohydrazones) in organic than in inorganic buffer solutions. Ion-pair formation between solutes and buffer ions has a strong effect on the elution order.

Factors affecting the elution order of bis(amidinohydrazones) in MECC are: (1) ion-pair formation between solute and buffer ion; (2) the cationic nature and structure of the solute; (3) reactions between ion-pair complexes and micelles; and (4) the nature of the buffer solution.

## REFERENCES

- 1 S. Terabe, K. Otsuka, K. Ichikawa, A. Tsuchiya and T. Ando, *Anal. Chem.*, 56 (1984) 111.
- 2 S. Terabe, K. Otsuka and T. Ando, *Anal. Chem.*, 57 (1985) 834.
- 3 A. S. Cohen, S. Terabe, J. A. Smith and B. L. Karger, *Anal. Chem.*, 59 (1987) 1021.
- 4 H. Nishi, N. Tsumagari, T. Kakimoto and S. Terabe, *J. Chromatogr.*, 465 (1989) 331.
- 5 J. Thiele and E. Dralle, *Liebig's Ann. Chem.*, 302 (1898) 275.
- 6 B. L. Freedlander and F. A. French, *Cancer Res.*, 18 (1958) 360.
- 7 H. G. Williams-Ashman and A. Schenone, *Biochem. Biophys. Res. Commun.*, 46 (1972) 288.
- 8 L. Alhonen-Hongisto, P. Seppänen, P. Nikula, H. Elo and J. Jänne, *Recent Prog. Polyamine Res.*, (1985) 261.
- 9 P. Lukkari, J. Jumppanen, K. Jinno, H. Elo and M.-L. Riekkola, *J. Pharm. Biomed. Anal.*, in press.
- 10 H. Elo, *Ph. D. Thesis*, Helsinki, 1989, and references therein.
- 11 J. Neugebauer, *A Guide to the Properties and Uses of Detergents in Biology and Biochemistry*, Calbiochem, San Diego, CA, 1988, p. 26.
- 12 M. Windholz (Editor), *The Merck Index*, Merck & Co., Inc., Rahway, NJ, 1983.
- 13 A. E. Martell and R. M. Smith, *Critical Stability Constants*, Plenum Press, New York, 1982.



# Determination of quaternary ammonium compounds by capillary electrophoresis using direct and indirect UV detection

C. S. Weiss, J. S. Hazlett, M. H. Datta<sup>\*</sup> and M. H. Danzer

*S.C. Johnson & Son, Inc., Racine, WI 53403 (USA)*

---

## ABSTRACT

The determination of alkyl and alkylbenzyl quaternary ammonium compounds can be difficult owing to the polarity of the compounds, the formation of micelles by longer chain compounds and the lack of a chromophoric substituent for detection by standard separation techniques. The development of a free zone capillary electrophoresis method necessitated the use of organic modifiers in order to disrupt the formation of micelles by the longer chain ( $>C_{12}$ ) surfactants. The selectivity obtained by using various levels of tetrahydrofuran as an organic modifier allowed the separation of a mixture of alkylbenzyl and alkylethylbenzyl quaternary compounds. The separation of alkyltrimethyl and dialkyldimethylammonium compounds was accomplished by the addition of a chromophoric cationic compound to the buffer system in order to allow the detection of the compounds with a standard UV absorbance detector. By varying the electrophoretic mobility of the indirect detection reagent, a variety of alkyl quaternary compounds, ranging from tetramethylammonium chloride to stearyltrimethylammonium chloride, can be detected with good peak shapes. The use of these methods for the determination of quaternary ammonium compounds will also be discussed. The use of internal standard methods and the linearity and linear range of the technique are considered.

---

## INTRODUCTION

Capillary electrophoresis (CE) has been used to separate a variety of compounds, including proteins and peptides, DNA fragments, pharmaceuticals, inorganic ions and other organic compounds, and has been reviewed in several recent papers [1–3]. The technique provides high resolution and minimum solvent or buffer consumption and is appropriate to samples that are difficult to separate by gas or liquid chromatography. The successful application of CE requires that the compound of interest migrates freely through the column, with minimum adsorption or localized field effects, and that there be a suitable spectroscopic characteristic to detect the compound during the migration process.

The ability to find a suitable detection scheme for microcolumn separations, including CE, has been a major obstacle for many applications [4]. The UV absorbance detector is the most frequently used but limitations in terms of sensitivity and dependence on the absorptivity characteristic of the analyte can be limiting in the development of CE methods. Attempts to develop conductivity detectors have met with limited success [5,6] owing to the difficulty of measuring small changes in conductivity in the background electrolyte as a compound migrates through the column in the presence of the voltage which is driving the migration. The successful application of fluorescence and mass spectral detectors has been reported [7–11]. However, the universal application of these detectors is limited owing to their complexity and/or cost. Derivatization methods, both pre- and postcolumn, have been reported but require sample treatment and may have limitations based on the sample of interest [7,8,12,13]. Electrochemical detection methods have been re-

---

*Correspondence to:* Dr. C. S. Weiss, S. C. Johnson & Son, Inc., Racine, WI 53403, USA.

<sup>\*</sup> Present address: O.I. Analytical, College Station, TX 77841-2980, USA.

ported, and essentially involve the very careful preparation of a micro electrochemical cell at the outlet of the CE column [14,15]. The construction of the end column cell, using a porous joint or a micromanipulator, makes the technique difficult to perform and still has limitations based on the electrochemical characteristics of the analyte of interest.

The application of indirect methods of detection for CE have been reviewed [16]. The technique was originally developed by Small and Miller [17] for ion chromatography using indirect UV detection. The measurement is based on having a concentration of UV-absorbing ion in the mobile phase, or in the buffer for CE, which provides a constant background. As the analyte moves through the column, the concentration of the background absorbing ion must be depleted in order to maintain electroneutrality. This depletion will cause a localized decrease in the concentration of the background absorbing ion and a subsequent decrease in the UV absorbance as the analyte band passes through the detector. The application of the method does not require any modifications to a basic CE instrument. The application of this technique of the CE analysis of inorganic ions has been reported by Jandik and Jones [18], of organic anions by Foret *et al.* [19] and of aliphatic alcohols by micellar electrokinetic chromatography by Szucs *et al.* [20]. Laser-induced fluorimetry offers a very favorable dynamic reserve for indirect detection and has been reported by Kuhr and Yeung [21]. The application of indirect amperometric detection has been demonstrated by Olefirowicz and Ewing [22]. The relationship between effective mobilities and peak areas, when using conductivity or indirect UV detection, has been defined by Ackermans *et al.* [23].

Alkyl and benzalkyl quaternary ammonium compounds are frequently used as surfactants and disinfectants in a variety of industrial and consumer applications. The analysis of these compounds is difficult owing to their polarity, ability to form micelles at low concentrations, thermal instability and the lack of a chromophoric substituent in the case of the non-benzyl types. The total concentrations are typically determined by the reaction with a compound which forms an ion pair with the quaternary compound [24]. Methods which use this process include two-phase titrations using chloroform, titra-

tions using surfactant electrodes for end-point detection and liquid–liquid extractions with UV detection. Gas chromatographic methods can be used to determine the alkyl chain distributions via an injection port pyrolysis reaction to the corresponding amine. These techniques provide useful information, but for the development of experimental compounds and the evaluation of the stability of these compounds in complex matrices, methods are required that can separate the mixtures of these compounds directly without modification. High-performance liquid chromatographic methods have been developed for benzalkyl quaternary compounds, but the analysis of the alkyl varieties is more problematic, requiring conductivity [25], refractive index [26] or indirect photometric detection [27]. The development of CE methods for the analysis of these compounds has provided a complementary technique which provides improved resolution, the ability to develop indirect UV detection for non-UV-absorbing analytes, minimum solvent consumption and inexpensive column replacement.

#### EXPERIMENTAL

The capillary electrophoresis system was constructed from various components. The power supply was a Model RHR30PN30/EI/OV/SS obtained from Spellman High Voltage Electronics (Plainview, NY, USA). The UV absorbance detector was a Model CV4 obtained from ISCO (Lincoln, NE, USA) and was operated at 210 nm. The electropherograms were acquired on either a Model 4270 integrator obtained from Spectra-Physics (San Jose, CA, USA) or a Model 941 interface using Access\*Chrom software from PE Nelson (Cupertino, CA, USA; on a VAX computer obtained from Digital Equipment (Maynard, MA, USA).

Phosphoric acid was of Baker Analyzed Reagent Grade. Sodium phosphate, monobasic, was obtained from Mallinckrodt. The following compounds were obtained from Aldrich (Milwaukee, WI, USA): benzyltrimethylammonium chloride (BTMACL), benzyldimethyldodecylammonium bromide ( $C_{12}$  Benzyl), benzyldimethyltetradecylammonium chloride ( $C_{14}$  Benzyl), benzylcetyldimethylammonium chloride ( $C_{16}$  Benzyl), benzyldimethylstearyl ammonium chloride ( $C_{18}$  Benzyl), dodecyltrimethylammonium bromide ( $C_{12}$  Trimethyl).

myristyltrimethylammonium bromide (C<sub>14</sub> Trimethyl), cetyltrimethylammonium bromide (C<sub>16</sub> Trimethyl), octadecyltrimethylammonium bromide (C<sub>18</sub> Trimethyl) and sodium dodecyl sulfate (SDS). Tetramethylammonium chloride (TMACl) was obtained from Eastman Kodak. Other quaternary compounds were obtained from various suppliers. Tetrahydrofuran (THF) was obtained from EM Science.

THF-containing buffers were prepared by first mixing appropriate volumes of THF and water. The mixture was heated on a steam-bath and then vacuum filtered in order to degas. The appropriate volumes of solutions of sodium dihydrogenphosphate, phosphoric acid and, in the case of indirect detection, the alkylbenzyltrimethylammonium bromide, were then added. The buffered THF-water solutions were also heated and vacuum filtered. The concentrations of THF-water reported reflect the volume percentages of the original amounts of THF and water that were actually mixed; loss of THF during filtration was noted.

The capillary tubing was uncoated fused silica of 50  $\mu\text{m}$  I.D. and 360  $\mu\text{m}$  O.D., obtained from Polymicro Technologies (Phoenix, AZ, USA). The capillary tubes were conditioned by treating them with a sequence of washes using air pressure applied to the ground-side reservoir. This procedure was performed on new columns and only when a problem in performance was suspected. A typical sequence would include 10 min water, 20 min 1.0 M NaOH, 10 min water, 20 min 1.0 M phosphoric acid, 10 min water and at least a 20-min rinse with the buffer to be used. The capillary columns were rinsed with buffer by applying pressure to the ground-side reservoir before each run.

Introduction of the sample on to the column was achieved by hydrostatic pressure, either by elevating the high-voltage end of the capillary tube, in contact with the sample solution, about 10 cm above the ground reservoir or by lowering the ground end of the capillary tubing about 16 cm, while the high-voltage end was immersed in the sample solution.

## RESULTS AND DISCUSSION

The initial attempts to separate alkylbenzyltrimethylammonium bromides of chain lengths C<sub>12</sub>–C<sub>18</sub>

were performed using a 0.05 M phosphate buffer. Separation was achieved in under 20 min, but the peaks tailed and the tailing worsened with increasing chain length. The signal obtained for the C<sub>18</sub> quaternary compound was barely distinguishable from the baseline. We speculated that this may be due to the formation of micelles. The critical micelle concentrations (CMCs) for these compounds are given in Table I. It should be noted that the concentrations of the solutions introduced on to the CE column were of the order of 1 mM, which would indicate that the C<sub>12</sub> quaternary compound was being introduced at around its CMC. The C<sub>18</sub> quaternary compound was being introduced at a level several orders of magnitude above its CMC and would be present as a micelle. The behavior of a micelle as it passes through the column would continuously yield free quaternary molecules and could provide severe tailing. A common way to disrupt micelle formation is to add organic solvents. The addition of methanol and acetonitrile did not improve the peak shape. The addition of tetrahydrofuran provided a sufficient alteration to the buffer to improve the peak shapes. A typical electropherogram obtained for a mixture of C<sub>12</sub>, C<sub>14</sub>, C<sub>16</sub> and C<sub>18</sub> alkylbenzyltrimethyl ammonium bromides is presented in Fig. 1. The peak shapes are considerably improved, providing adequate separations of a number of quaternary compounds.

The theoretical plate number was calculated to be over 150 000 plates/m based on C<sub>12</sub> Benzyl. The precision of the technique is summarized in Table II. The relative standard deviation of the measured area is *ca.* 5%, even with manual sample introduction. Calibration of the system showed a linear response from 10 to 80 ppm. The correlation coeffi-

TABLE I  
CRITICAL MICELLE CONCENTRATIONS OF ALKYL-BENZYLDIMETHYLAMMONIUM CHLORIDE QUATERNARY COMPOUNDS [28]

Alkyl chain length	Critical micelle concentration (M)
C <sub>12</sub>	$3 \cdot 10^{-3}$
C <sub>14</sub>	$3.7 \cdot 10^{-4}$
C <sub>16</sub>	$2 \cdot 10^{-4}, 4 \cdot 10^{-5}$
C <sub>18</sub>	$8 \cdot 10^{-6}$

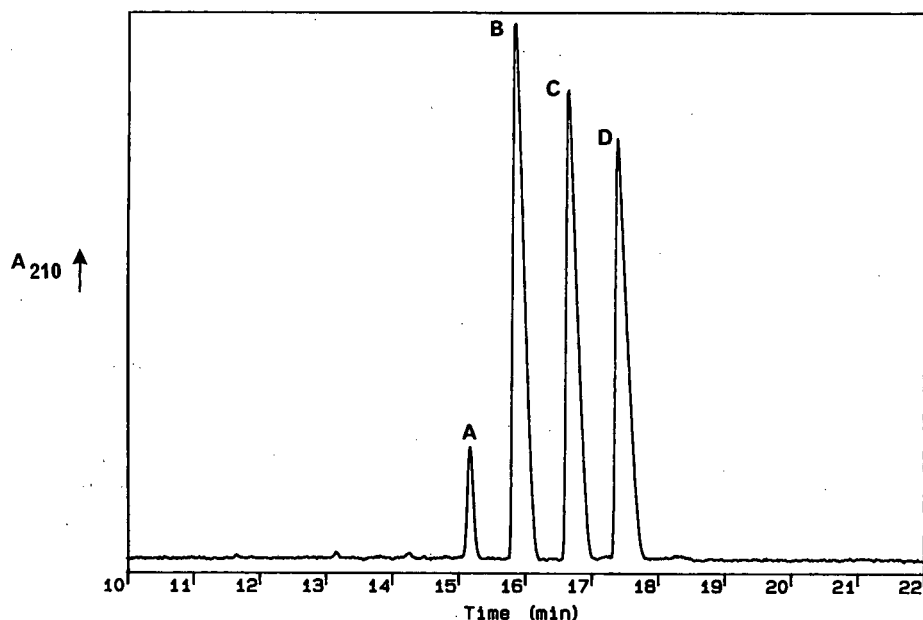


Fig. 1. Electropherogram obtained from the direct detection of (A)  $C_{12}$ , (B)  $C_{14}$ , (C)  $C_{16}$  and (D)  $C_{18}$  alkylbenzyltrimethylammonium quaternary compounds using THF-Water (57.5:42.5) containing 44 mM phosphate at 25 kV/m on a 24 cm  $\times$  50  $\mu$ m I.D. column.

cient was 0.999 for  $C_{14}$  Benzyl. The detection limit has been estimated to be less than 1 ppm. The application of this technique to the separation of a commercially available mixture of benzalkyl quaternary compounds revealed the ability not only to separate ethylbenzylalkyl from benzalkyl quaternary compounds but also to separate the *ortho* and *para* iso-

mers of the ethylbenzylalkyl quaternary compounds.

The initial attempt to develop an indirect detection mode involved the use of 0.01 M benzyltrimethylammonium chloride in THF-water (57.5:42.5). The separation of TMACL and  $C_{14}$  Trimethyl was attempted. The sensitivity of the sys-

TABLE II  
PRECISION OF AREA AND RETENTION TIME FOR DIRECT DETECTION

	$C_{14}$		$C_{16}$		$C_{18}$	
	Area (counts)	Elution time (min)	Area (Counts)	Elution time (min)	Area (counts)	Elution time (min)
	79 053	15.828	68 552	16.624	67 999	17.365
	83 797	15.663	73 964	16.448	73 169	17.178
	81 390	15.565	71 065	16.352	69 553	17.082
	79 438	15.565	68 942	16.342	67 305	17.073
	91 405	15.497	78 226	16.273	75 452	17
	91 821	15.412	80 768	16.182	81 212	16.899
	82 826	15.446	72 607	16.208	72 686	16.928
	86 099	15.386	72 545	16.157	69 327	16.878
Mean	84 479	15.55	73 334	16.32	72 088	17.05
S.D.	4958	0.15	4277	0.16	4625	0.16
R.S.D. (%)	5.87	0.94	5.83	0.96	6.42	0.96

tem for TMACL was greater than that for  $C_{14}$  Trimethyl and the peak was more symmetric. The skewing of peaks in indirect CE has been attributed to the differences in electrophoretic mobility of the analyte relative to the electrophoretic mobility of the UV-absorbing background electrolyte [18]. Subsequent method modifications were made, and the final buffer consisted of THF-water (57.5:42.5), 3 mM  $C_{12}$  Benzyl, 3 mM SLS and 8 mM sodium phosphate, monobasic.

The electropherogram obtained for the mixture of alkyltrimethylammonium quaternary compounds is presented in Fig. 2. The resolution of the  $C_{12}$ ,  $C_{14}$ ,  $C_{16}$  and  $C_{18}$  compounds is easily obtained, although the asymmetry of the peaks increases with increase in chain length, as the difference in electrophoretic mobility of the analyte and  $C_{12}$  Benzyl increases. The calibration of the system is linear from 4 to 80 ppm and the correlation coefficients for each of  $C_{12}$ ,  $C_{14}$ ,  $C_{16}$  and  $C_{18}$  trimethylammonium quaternary compounds were greater than 0.99. The detection limit was estimated to be less than 1 ppm. The precision of the indirect detection mode is summarized in Table III. It is comparable to the precision obtained in the direct mode.

The ability to analyze real samples was the objective of this work. Fig. 3 displays the electropherogram of a quaternary in an experimental disinfectant product. The  $C_{14}$  Trimethyl has been added as an internal standard. Table IV summarizes the precision of the technique. The precision based on the area of the analyte of interest is 3.5% R.S.D., but when an internal standard ratio is used the precision is improved to about 2.5% (R.S.D.).

The ability to detect UV-absorbing components using the indirect detection mode had been observed earlier in the method development. Fig. 4 displays the signal obtained for a mixture of benzyldimethylalkyl quaternary compounds using the indirect mode. The sensitivity is reduced compared with the signal obtained in the direct mode for these components, and is lower than the sensitivity obtained for the alkyltrimethyl quaternary compounds in the indirect mode. These findings are reasonable considering the mechanism of the indirect mode.

#### CONCLUSIONS

The separation of long-chain cationic surfactants

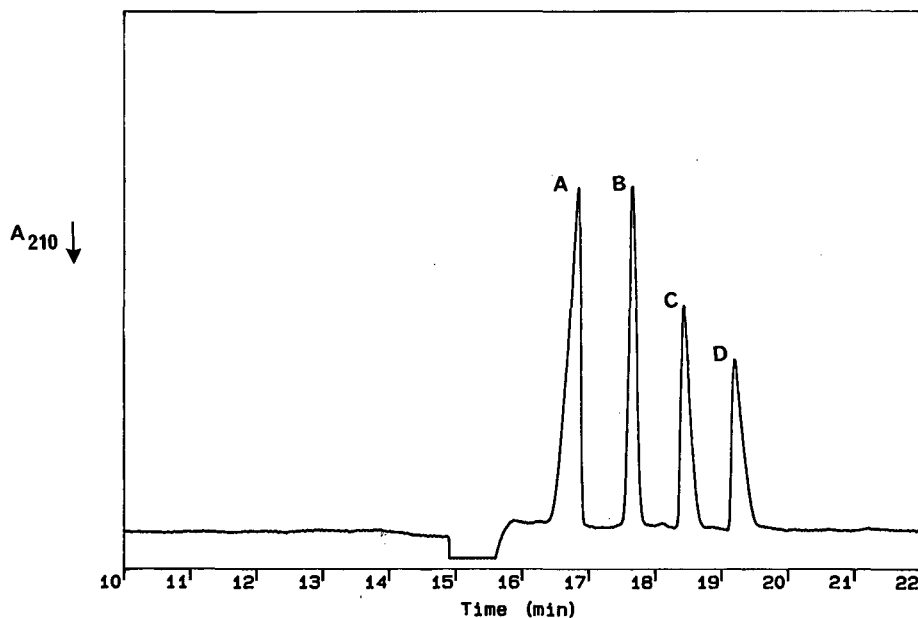


Fig. 2. Electropherogram obtained from the indirect detection of (A)  $C_{12}$ , (B)  $C_{14}$ , (C)  $C_{16}$  and (D)  $C_{18}$  alkyltrimethylammonium quaternary compounds at 18 kV/m; buffer as described in text.



TABLE III  
PRECISION OBTAINED DURING CALIBRATION FOR INDIRECT DETECTION

	Area (counts)				Elution time (min)
	4 ppm	20 ppm	40 ppm	80 ppm	
	9787	37 592	76 626	150 050	
	8189	38 647	76 830	155 305	
	8610	38 661	77 060	159 274	
	8826		77 371		
	8410		77 505		
			79 206		
Mean	8764	38 300	77 433	154 876	16.897
S.D.	618	613	928	4626	0.112
R.S.D. (%)	7.05	1.6	1.2	2.99	0.66

has been accomplished using capillary electrophoresis. The addition of THF to the buffer system has overcome the difficulty associated with micelle formation of these analytes during the the course of the analysis. The method is robust enough to develop indirect UV detection methods, which provide sufficient linear response and precision to determine

these compounds in real samples. Capillary electrophoresis serves as a complimentary technique to other methods that have been reported and provides minimization of solvent consumption and an increased number of theoretical plates. The ability to separate these compounds in a bare silica capillary column provides a robust separation compart-

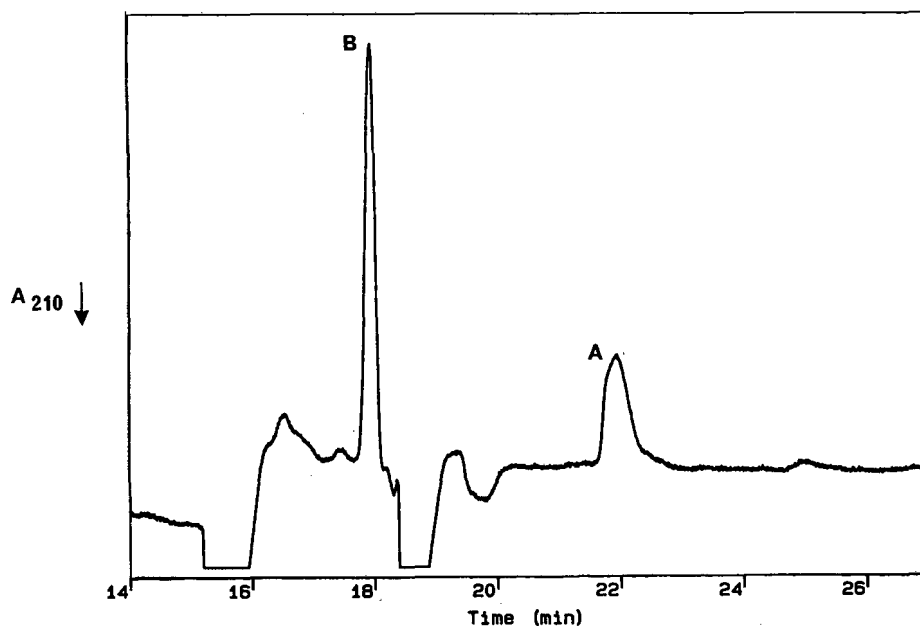


Fig. 3. Electropherogram obtained from the indirect detection of a quaternary compound (A) in an experimental disinfectant product with a  $C_{14}$  trimethylammonium quaternary (B) included as an internal standard.

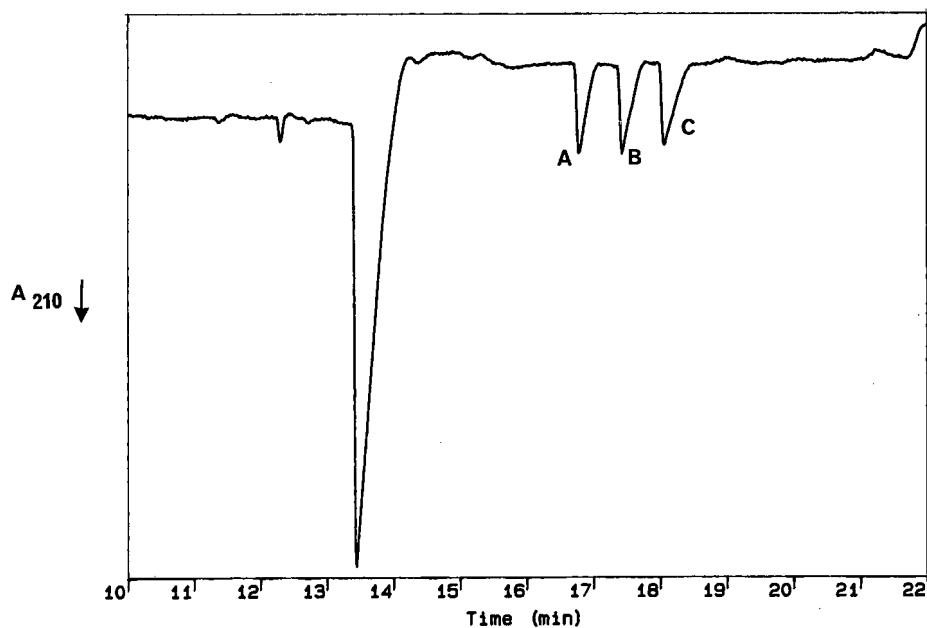


Fig. 4. Electropherogram obtained from the indirect detection of a mixture of (A)  $C_{14}$ , (B)  $C_{16}$  and (C)  $C_{18}$  alkylbenzyltrimethylammonium quaternary compounds. Conditions as in Fig. 2.

TABLE IV

PRECISION OF DATA OBTAINED FROM APPLICATION OF INTERNAL STANDARD METHOD

	$C_{14}$ Internal standard		Analyte		Area ratio
	Area (counts)	Elution time (min)	Area (counts)	Elution time (min)	
	52 951	17.948	35 312	21.3	0.67
	54 486	17.823	38 356	21.157	0.7
	55 362	17.834	39 464	21.214	0.71
	55 907	17.854	38 167	21.226	0.68
	56 052	17.773	38 123	21.116	0.68
	55 742	17.656	38 271	20.983	0.69
	56 621	17.658	38 350	20.982	0.68
	56 105	17.495	37 244	20.758	0.66
	56 911	17.318	39 269	20.558	0.69
	58 128	17.246	41 086	20.466	0.71
Mean	55 826.5	17.6605	38 364.2	20.976	0.69
S.D.	1395.53	0.24	1494.93	0.29	0.02
R.S.D. (%)	2.5	1.34	3.9	1.38	2.41

ment which can easily be cleaned and or inexpensively replaced, allowing for the development of methods for and analyses of difficult matrices with little concern for permanent damage to the column.

## REFERENCES

- 1 A. G. Ewing, R. A. Wallingford and T. M. Olefirowicz, *Anal. Chem.*, 61 (1989) 292A.
- 2 H. J. Goldner, *R&D Mag.*, June (1991) 28.
- 3 D. M. Goodall, D. K. Lloyd and S. J. Williams, *LC-GC*, 8 (1990) 788.
- 4 B. Josefsson, *J. Microcol. Sep.*, 1 (1989) 116.
- 5 X. Huang, T.-K. J. Pang, M. J. Gordon and R. N. Zare, *Anal. Chem.*, 59 (1987) 2747.
- 6 X. Huang, J. A. Luckey, M. J. Gordon and R. N. Zare, *Anal. Chem.*, 61 (1989) 766.
- 7 Y.-F. Cheng and N. J. Dovichi, *Science (Washington, D.C.)*, 242 (1988) 242.
- 8 B. Nickerson and J. W. Jorgenson, *J. High Resolut. Chromatogr. Chromatogr. Commun.*, 11 (1988) 878.
- 9 P. L. Christensen and E. S. Yeung, *Anal. Chem.*, 61 (1989) 1344.
- 10 R. D. Smith, C. J. Barinaga and H. R. Udseth, *Anal. Chem.*, 60 (1988) 1948.
- 11 E. D. Lee, W. Muck, J. D. Henion and T. R. Covey, *J. Chromatogr.*, 458 (1988) 313.
- 12 B. Nickerson and J. W. Jorgenson, *J. Chromatogr.*, 480 (1989) 157.
- 13 S. L. Pentoney, X. Huang, D. S. Burgi and R. N. Zare, *Anal. Chem.*, 60 (1988) 2625.
- 14 R. A. Wallingford and A. G. Ewing, *Anal. Chem.*, 60 (1988) 1973.
- 15 X. Huang, R. N. Zare, S. Sloss and A. G. Ewing, *Anal. Chem.*, 63 (1991) 189.
- 16 E. S. Yeung and W. G. Kuhr, *Anal. Chem.*, 63 (1991) 275A.
- 17 H. Small and T. E. Miller, *Anal. Chem.*, 54 (1982) 462.
- 18 P. Jandik and W. R. Jones, *J. Chromatogr.*, 546 (1991) 431.
- 19 F. Foret, S. Fanali, L. Ossicini and P. Bocek, *J. Chromatogr.*, 470 (1989) 299.
- 20 R. Szucs, J. Vindevogel and P. Sandra, *J. High Resolut. Chromatogr.*, 14 (1991) 692.
- 21 W. G. Kuhr and E. S. Yeung, *Anal. Chem.*, 60 (1988) 1832.
- 22 T. M. Olefirowicz and A. G. Ewing, *J. Chromatogr.*, 499 (1990) 713.
- 23 M. T. Ackermans, F. M. Everaerts and J. L. Beckers, *J. Chromatogr.*, 549 (1991) 345.
- 24 R. A. Llenado and T. A. Neubecker, *Anal. Chem.*, 55 (1983) 93.
- 25 V. T. Wee and J. M. Kennedy, *Anal. Chem.*, 54 (1982) 1631.
- 26 T. Surotti and H. Sirvio, *J. Chromatogr.*, 507 (1990) 421.
- 27 J. R. Larson and C. D. Pfeiffer, *Anal. Chem.*, 55 (1983) 393.
- 28 P. Mukerjee and K. J. Mysels, *Critical Micelle Concentrations of Aqueous Surfactants NSRDS NBS 36*, National Bureau of Standards, Washington, DC.

# Investigation of the properties of novel acrylamido monomers by capillary zone electrophoresis

Cecilia Gelfi, Patrizia de Besi, Angela Alloni and Pier Giorgio Righetti

*Chair of Biochemistry and Department of Biomedical Sciences and Technologies, University of Milan, Via Celoria 2, Milan 20133 (Italy)*

---

## ABSTRACT

A series of mono- and disubstituted acrylamide monomers [monomethylacrylamide, dimethylacrylamide, trisacryl (Tris-A), dideoxy-trisacryl and acryloylmorpholine] were investigated as potential candidates of a novel class of polyacrylamide matrices, exhibiting high hydrophilicity, high resistance to hydrolysis and larger pore size than conventional polyacrylamide gels. However, the most promising monomer (Tris-A) exhibited first-order degradation kinetics in 0.1 M NaOH, suggesting that such a structure is electronically unstable. On the other hand, the fact that, once incorporated into a polymer chain, such a monomer exhibited a strong resistance to alkaline hydrolysis suggests that, perhaps, a poly(trisacryl) matrix could be stereoregular, perhaps via helix formation. Another unique finding is the inverse relationship between the partition coefficient of such monomers and the incorporation efficiency: the more hydrophobic members of the family exhibit a very poor conversion from monomer into polymer. The efficiency, however, can be dramatically increased by increasing the polymerization temperature from 25 to 60°C.

---

## INTRODUCTION

Polyacrylamide, first reported by Raymond and Weintraub in 1959 [1] as a supporting medium for zone electrophoresis, has enjoyed enormous popularity in biochemical separations. While the chemistry of acrylamide monomers has been extensively developed (see refs. 2 and 3 for reviews), not much work has been done on the structure and properties of the polymer. Following earlier studies on the properties of some cross-linkers [4], Gelfi and co-workers [5–7] started a decade ago an extensive investigation on polymerization conditions as a function of different types and amounts of cross-linkers, temperature and amount and type of catalysts. Some general rules were derived: (a) the order of reactivity for copolymerization with acrylamide

decreases for cross-linkers in the following order: N,N'-methylenebisacrylamide (Bis)  $\approx$  N,N'-(1,2-dihydroxyethylene)bisacrylamide (DHEBA) > ethylene diacrylate  $\approx$  N,N'-bisacrylylcystamine (BAC)  $\gg$  N,N'-diallyltartardiamide (DATD) [5]; (b) high temperatures (ideally 50°C) greatly favour polymerization [6]; and (c) photopolymerization produces in general poor gels with poor conversion of the monomers into the polymer [7]. In particular, DATD was found to be an inhibitor of gel polymerization and its use was discouraged.

A decade later, having synthesized a novel series of monomers (mostly mono- and disubstituted acrylamide), we decided to investigate some physico-chemical properties of such monomers and of the matrix thus obtained by using capillary zone electrophoresis (CZE). CZE is a suitable technique for separating and determining small molecules, for which gel electrophoresis does not have much to offer. In particular, we have studied the following parameters: (a) resistance to hydrolysis of the different monomers in free solution; (b) resistance to

---

*Correspondence to:* Prof. P. G. Righetti, Chair of Biochemistry and Department of Biomedical Sciences and Technologies, University of Milan, Via Celoria 2, Milan 20133, Italy.

hydrolysis of the monomers in the polymeric phase; (c) relative hydrophobicity of the different monomers; and (d) extent of incorporation of the various monomers into the polymer. For all these aspects, CZE was instrumental in producing quantitative and highly reliable data, except for point (b); in this last instance, we had to resort to frontal analysis, which gave a precise determination of the extent of production of acrylic acid in the polymer on hydrolysis of amido bonds. These investigations were prompted by a series of studies performed by our group in the last few years on the acrylamido weak acids and bases copolymerized into polyacrylamide gels for performing isoelectric focusing in immobilized pH gradients [8-11].

As we understand more of the physico-chemical properties of such monomers, we hope to arrive at novel gel formulations.

## EXPERIMENTAL

### Materials

The following six monomers were analysed: acrylamide (Acr), N-methylacrylamide (MMA), N,N-dimethylacrylamide (DMA), N-acryloyltris(hydroxymethyl)aminomethane (trisacryl, Tris-A), N-

acryloyldimethylhydroxymethylaminomethane (di-deoxytrisacryl, DD-Tris) and N-acryloylmorpholine (ACM). Their formulae are listed in Table I and their syntheses have been described elsewhere [3,12]. All gels were prepared by cross-linking with Bis. Acrylamide, Bis, TEMED and ammonium peroxydisulphate were obtained from Bio-Rad Labs. (Richmond, CA, USA). Mandelic acid and pK 9.3 Immobiline, used as internal standards in CZE runs, were purchased from Aldrich (Steinheim, Germany) and Pharmacia-LKB (Uppsala, Sweden), respectively.

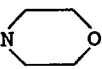
### Alkaline hydrolysis

All monomers were dissolved (20 mM each) in 0.1 M NaOH and incubated at 70°C for up to 6 h. At given time intervals (see the relevant figures) aliquots were collected and diluted in 0.1 M sodium borate buffer (pH 9.0) to 2.5 mM. After adding mandelic acid (2.50 mM) as an internal standard, the samples were analysed by CZE.

### Incorporation efficiency

In order to check for the extent of conversion of the various monomers into the polymer, 5 ml of gel (made with the different monomers in Table I) were

TABLE I  
MONOFUNCTIONAL ACRYLAMIDO DERIVATIVES

Formula	Name	$M_r$
$\text{CH}_2 = \text{CHCONH}_2$	Acrylamide (Acr)	71
$\text{CH}_2 = \text{CHCONHCH}_3$	N-Methylacrylamide (MMA)	85
$\text{CH}_2 = \text{CHCONCH}_3$   $\text{CH}_3$	N,N-Dimethylacrylamide (DMA)	99
$\text{CH}_2 = \text{CHCO-N}$ 	N-Acryloylmorpholine (ACM)	141
$\text{CH}_2 = \text{CHCONHCCH}_2\text{OH}$   $\text{CH}_3$   $\text{CH}_2\text{OH}$	N-Acryloyldimethylhydroxymethylaminomethane (DD-Tris)	143
$\text{CH}_2 = \text{CHCONHCCH}_2\text{OH}$   $\text{CH}_2\text{OH}$	N-Acryloyltris(hydroxymethyl)aminomethane (Tris-A)	175

polymerized in a test-tube under anaerobic conditions (protected by a thin film of water-saturated *n*-butanol). After polymerization (1 h, temperatures ranging from 25 to 60°C), the gel was extruded and homogenized and an equal amount of water was added (extraction was also performed in methanol). After stirring for 30 min, the gel phase was filtered through a Buchner funnel, the supernatant was diluted, internal standard (2.5 mM pK 9.3 Immobiline) was added and the mixture was filtered through an Ultrafree-MC Millipore filter (0.22 µm porosity) and analysed by CZE.

#### Capillary zone electrophoresis

CZE was performed in a Beckman (Palo Alto, CA, USA) P/ACE System 2000 instrument equipped with a 50 cm × 75 µm I.D. capillary. Runs were performed at 25°C in a thermostated environment in 0.1 M borate buffer (pH 9.0). In all instances the migration direction was toward the negative electrode, which means that the acidic species (mandelic acid) are transported there by electroosmosis as they migrate electrophoretically toward the positive electrode. The samples were injected into the capillary by pressure (55 kPa), usually for 10 s. The calibration graph for each acrylamido derivative analysed was constructed with the Beckman integration system Gold, with concentration points of 0.25, 0.50, 1.00, 1.25, 200, 250 and 3.50 mM. In each run the pK 9.3 Immobiline (2.50 mM) was used as an internal standard (except for the hydrolysis experiments, where mandelic acid was utilized). Runs were usually performed at 15 kV and 50 µA with the detector set at 254 nm.

#### Partition coefficient

In order to establish a hydrophobicity scale, the various acrylamido monomers were subjected to partitioning in water–1-octanol as described by Purcell *et al.* [13]. The partition coefficient *P* is defined as the ratio between the molarity of a given compound in the organic phase and that in the aqueous phase. Partitioning was performed as follows: each monomer was dissolved (2 mM) in water saturated with 1-octanol; 3.5 ml of this solution and 3.5 ml of 1-octanol were transferred to a separating funnel and shaken for 2 min. After decanting for 1 h, the aqueous phase was collected and centrifuged for 75 min at 1800 g. All operations were performed at

25°C. The clarified solution was diluted, internal standard (2.5 mM pK 9.3 Immobiline) was added and the mixture was analysed by CZE as described above.

#### Titration of acrylate groups in polyacrylamides by frontal analysis

In order to assess the amount of protolytic groups (acrylic acid) produced on extensive hydrolysis of the different types of polyacrylamides, the gels were cast not as continuous layers but as beads (with a concentration of 10%T and 8%C)<sup>a</sup> by emulsion polymerization [14]. The beads were extensively washed, dehydrated in methanol and dried *in vacuo*. A known amount of dry beads (from 0.25 to 1 g) was then reswollen in water and subjected to hydrolysis in 0.1 M NaOH at 70°C for up to 6 h. After extensive washing in water (to negligible conductivity), the beads were loaded on a 1.6-cm diameter column to a bed height of *ca.* 10 cm. Titration was performed with 0.1 M HCl and the eluate was pumped at constant speed (1.5 ml/min, LKB peristaltic pump) through a micro-conductimetric cell (4-µl volume, Orion conductimeter, 10 mΩ<sup>-1</sup> full-scale). The signal was registered on a Kipp and Zonen recorder (20 mV full-scale, 10 mm/min chart speed). Once the conductivity curve had reached a plateau (corresponding to the conductivity of the titrant, diluted by the dead volume of the resin) the titration was stopped and a solution, with half the molarity of the titrant, was injected directly into the conductimeter cell; this was necessary in order to measure the inflection point of the curve. For calculating the total amount of protolytic groups (acrylic acid) generated on the resin by alkaline hydrolysis (*C*<sub>tot</sub>), the following equation applies:

$$C_{\text{tot}} = [V/L(L_1 - L_0) - G_v]M_{\text{tit}}$$

where *V* is the volume of titrant utilized (in ml, as measured with a burette), *L* is the total length of the recorder tracing (in cm) for this *V* value, *L*<sub>0</sub> is the length of the recorder tracing (in cm) corresponding to the dead volume of all connecting tubings, *L*<sub>1</sub> is the length of the recorder tracing (in cm) up to the inflection point (as measured when pumping in the

<sup>a</sup> %C = g Bis/%T; T = g acrylamide + g Bis per 100 ml of solution.

titrant at half the molarity),  $G_v$  is the total gel volume (in ml) and  $M_{tit}$  is the molarity of the titrant. In our case, the value of  $C_{tot}$  obtained was divided by the resin dry weight so that our data were expressed in  $\mu\text{equiv./g}$  of dry beads. These data were finally converted into percentage hydrolysis with time (see Fig. 4).

## RESULTS

It is well known that mono- and disubstituted amides are substantially more resistant to alkaline hydrolysis than unsubstituted species. As most zone electrophoretic runs in polyacrylamides are performed at alkaline pH values, it seemed worthwhile to explore new types of matrices formed with N-substituted monomers. At first glance, Fig. 1 seems to confirm this hypothesis: when a regular polyacrylamide matrix (5%T, 4%C) is briefly exposed to 0.1 M NaOH at 70°C, washed, dried and then reswollen in carrier ampholytes, during the focusing step a strong electrosmotic flow ensues, resulting in a marked acidification of the pH gradient, which suggests the formation of polyacrylate [15]. Conversely, when a similar matrix, but made with N,N-dimethylacrylamide, is subjected to the same protocol, the pH gradient generated is just as

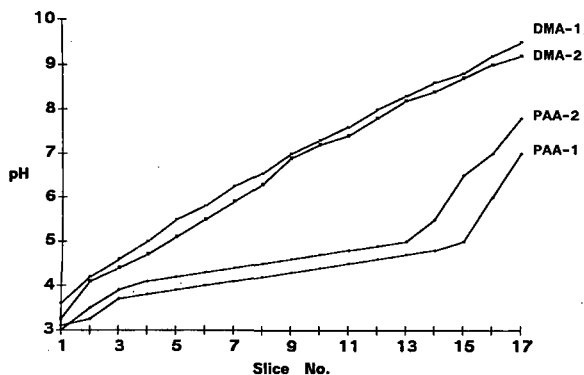


Fig. 1. Check for hydrolysis of polyacrylamide matrices. A polyacrylamide (PAA) and a polydimethylacrylamide (DMA) gel were cast on to a glass coated with Bind-Silane and then subjected to hydrolysis in 0.1 M NaOH for 20 min at 70°C. After extensive washing and drying, the gels were reswollen in 2% pH 3-10 carrier ampholytes and subjected to isoelectric focusing (2 h at 1500 V, 4°C). The gels were sliced along the electrode distance and the pH measured after equilibration in 300  $\mu\text{l}$  of 10 mM NaCl. Note the flattening and marked acidification of the pH gradient in the PAA gels.

good as in a control, non-hydrolysed matrix, suggesting a strong resistance to hydrolysis of such a polymer.

Given these findings, we decided to screen the series of monomers listed in Table I in order to check their resistance to alkaline hydrolysis. Fig. 2 shows a representative CZE run of DMA before and after hydrolysis; mandelic acid is always added as internal standard for quantitation purposes. A summary of

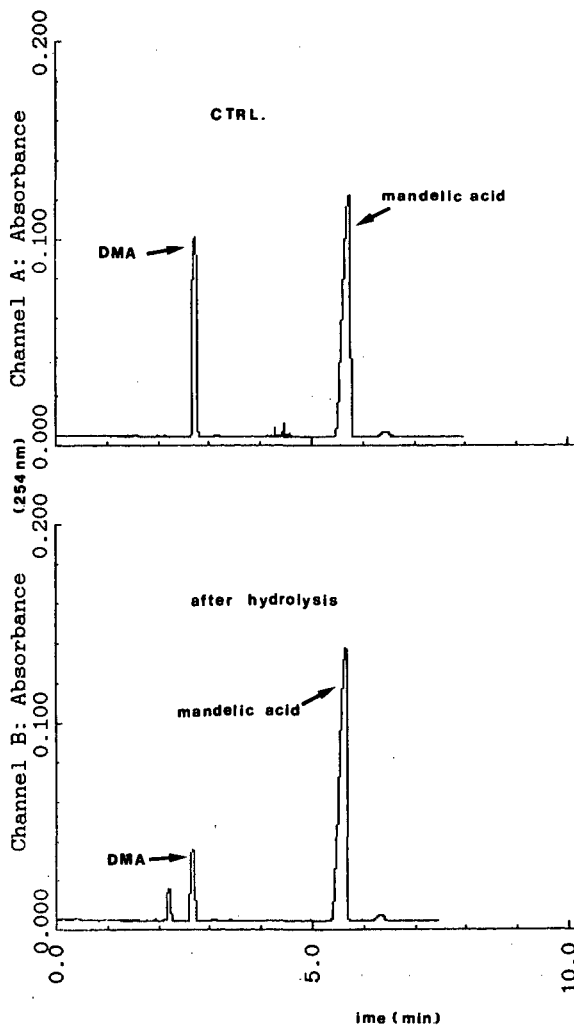


Fig. 2. Representative CZE runs for monitoring alkaline hydrolysis of acrylamido monomers. Conditions: 100 mM borate-NaOH buffer (pH 9.0), 15 kV, 86  $\mu\text{A}$  at 25°C. Uncoated fused-silica capillary (50 cm  $\times$  75  $\mu\text{m}$  I.D.). Beckman P/ACE 2000 instrument, monitoring at 254 nm. DMA = N,N-dimethylacrylamide; CTRL = control, before hydrolysis. In this and all subsequent runs the migration is towards the cathode.

all the hydrolysis data is shown in Fig. 3; surprisingly, not all substituted acrylamides exhibit a stronger resistance to alkaline hydrolysis than control acrylamide. In addition, whereas almost all acrylamido derivatives exhibit first-order degradation kinetics, one of them (trisacryl) shows zero-order kinetics, suggesting that such a monomer is intrinsically unstable. Based on the data obtained by CZE, Table II summarizes the relevant parameters of such hydrolytic processes, *viz.*, the half-lives ( $t_{1/2}$ ) and the first-order rate coefficients.

The findings in Fig. 3 were disturbing, as we had hoped to locate new monomers which would be not only more resistant to hydrolysis, but also bulkier than acrylamide, so that they would form a more porous gel, having a larger fibre diameter. However, a completely different picture emerges if one looks at the relative resistance to hydrolysis not of the free monomers, but of the monomers after incorporation into the polymer chain. In order to measure such kinetics, the gels had to be polymerized into beads, subjected to hydrolysis and then titrated by frontal analysis. The data are summarized in Fig. 4; it can now be seen that all substituted acrylamides, independent of their degradation kinetics as free

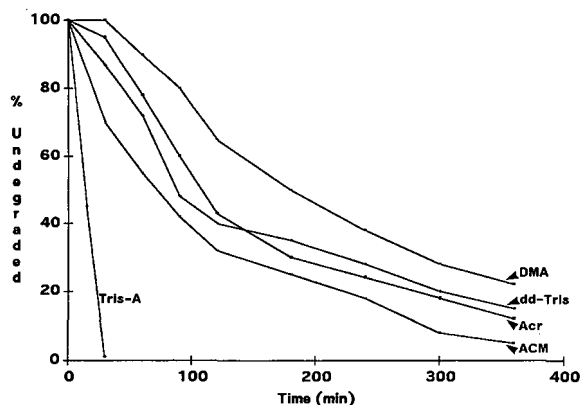


Fig. 3. Kinetics of hydrolysis of different acrylamide monomers. Hydrolysis was performed in 0.1 M NaOH at 70°C for the times indicated. The amounts were assessed by collecting in triplicate at each point, neutralizing and injecting into the CZE instrument (Beckman P/ACE 2000). Conditions: 100 mM borate–NaOH buffer (pH 9.0), 15 kV, 86  $\mu$ A at 25°C. Uncoated fused-silica capillary (50 cm  $\times$  75  $\mu$ m I.D.). Peak integration with the Beckman system Gold (mandelic acid was used as an internal standard). Abbreviations as in Table I. Note that whereas all the other monomers exhibit first-order kinetics, Tris-A follows zero-order degradation kinetics.

TABLE II

HALF-LIVES ( $t_{1/2}$ )<sup>a</sup> AND FIRST-ORDER RATE COEFFICIENTS ( $K$ )<sup>b</sup> FOR DEGRADATION OF ACRYLAMIDES IN 0.1 M NaOH, 70°C

Monomer	$t_{1/2}$ (min)	$10^3 K$ (min <sup>-1</sup> )
N,N-Dimethylacrylamide	185	3.7
Dideoxytrisacryl	130	5.3
Acrylamide	111	6.2
Acryloylmorpholine	80	8.6
Trisacryl	15	—

<sup>a</sup> The half-life of the process was calculated from the equation  $t_{1/2} = 0.693/K$ .

<sup>b</sup> The first-order rate coefficient ( $K$ ) was calculated from the slope of the line obtained when the logarithm of the residual molarity (undegraded monomers) was plotted against time.

monomers, exhibit a much higher stability in the polymer matrix as compared with control acrylamide. Most striking is the behaviour of trisacryl, which, from zero-order degradation kinetics as the free monomer, exhibits a very slow degradation process in the polymer. Such findings could provide unique information about the three-dimensional structure of polyacrylamides, still believed to be a random network of fibres (see Discussion).

We next measured the relative hydrophobicities of

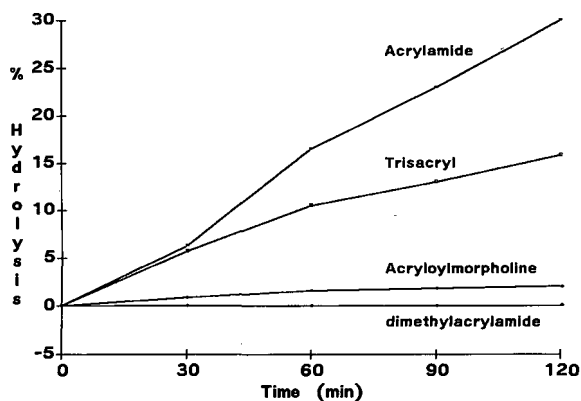


Fig. 4. Degradation kinetics of the monomers into the polymeric gel. The different monomers were polymerized (by emulsion polymerization) into beads, subjected to hydrolysis in 0.1 M NaOH at 70°C for the times indicated and then analysed for hydrolytic products. Hydrolysis was assessed in the beads by titrating free acrylic acid residues, produced by hydrolysis of the amide bond, by frontal analysis. Note the much increased stability of trisacryl in the polymer as compared to its behaviour as free monomer (Fig. 3).



the six monomers in Table I by partitioning in water–1-octanol phases. It is well known that, for protein separation by electrokinetic processes, the supporting matrix should be highly hydrophilic so as to avoid any hydrophobic interaction. The quantitative data after the partitioning process, as measured by CZE (see Fig. 5 as a representative CZE run), are summarized in Fig. 6. It is seen that, in

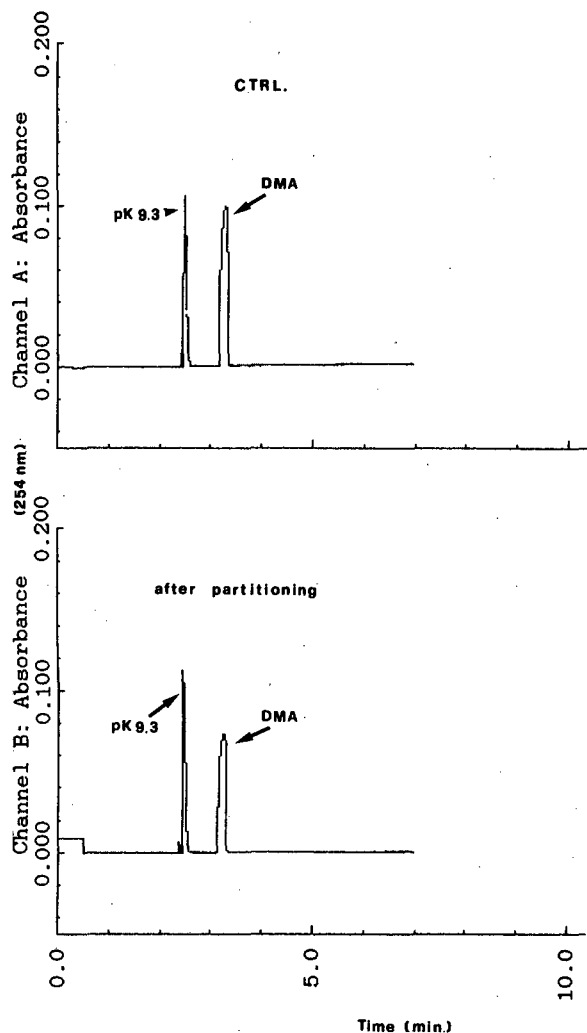


Fig. 5. Representative CZE runs for measuring partition coefficients (in the aqueous phase) of acrylamido monomers. Conditions: 100 mM borate–NaOH buffer (pH 9.0), 15 kV, 86  $\mu$ A at 25°C. Uncoated fused-silica capillary (50 cm  $\times$  75  $\mu$ m I.D.). Beckman P/ACE 2000 instrument, monitoring at 254 nm. DMA = N,N-dimethylacrylamide; pK 9.3 = Immobiline of pK 9.3 used as internal standard for peak integration.

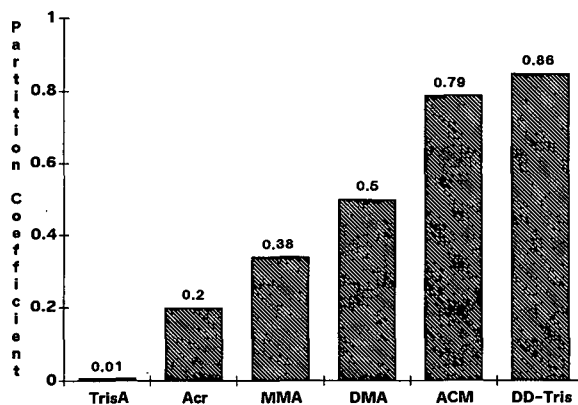


Fig. 6. Hydrophobicity scale for six acrylamide monomers. It was obtained by partitioning in water–1-octanol at room temperature and determining the concentrations in the two phases by CZE. Conditions: 100 mM borate–NaOH buffer (pH 9.0), 15 kV, 86  $\mu$ A at 25°C. Fused-silica capillary (50 cm  $\times$  75  $\mu$ m I.D.). Peak integration with the Beckman system Gold (pK 9.3 Immobiline was used as an internal standard). Abbreviations as in Table I.

general, trisacryl (as expected from its formula) is the most hydrophilic monomer: its  $P$  value is almost two orders of magnitude lower than that of DD-Tris. Acrylamide also exhibits good hydrophilicity whereas all other substituted acrylamides show progressively increasing hydrophobicity. It might be asked if there is a limiting value above which, owing to cooperative hydrophobic increments into the polymer, the gel matrix might be unable to re-swell in water. Empirically, we find this value to be located around  $P = 0.8$  (the partition coefficient of dideoxytrisacryl), as poly(DD-Tris) becomes a white plastic, which collapses in the gravitation field and exudes all the water solvent.

There seems to be another undesirable feature associated with increasing hydrophobicity of the monomers: as the  $P$  value increases, the efficiency of incorporation into the growing polymer chain diminishes. This unique finding, previously unreported, is illustrated in Fig. 7; it is seen that in fact there is an inverse correlation between  $P$  and the extent of monomer incorporation. Under exactly the same polymerization conditions, ACM ( $P = 0.79$ ) exhibits only 55% incorporation, while Tris-A ( $P = 0.01$ ) is 95% incorporated. Fig. 7 also shows another unique finding: even the poorly reacting, more hydrophobic monomers can be incorporated as efficiently as Tris-A by increasing the polymerization temperature from 25 to 60°C. The three curves

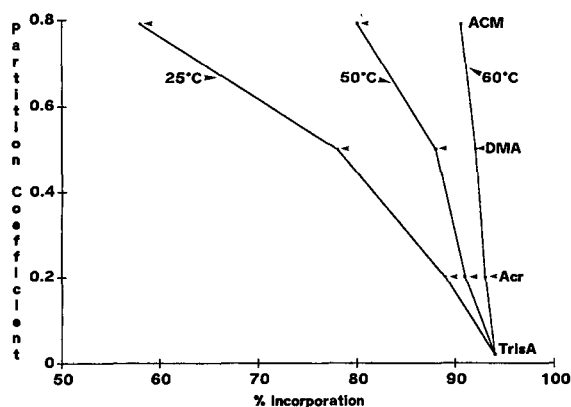


Fig. 7. Incorporation efficiency of different monomers vs. partition coefficient ( $P$ ). There seems to be a unique inverse correlation between  $P$  and incorporation efficiency. The latter was assessed by polymerizing the gel into beads, extracting ungrafted monomers by extensive washing and determining them by CZE. Conditions: 100 mM borate–NaOH buffer (pH 9.0), 15 kV, 86  $\mu$ A at 25°C. Fused-silica capillary (50 cm  $\times$  75  $\mu$ m I.D.). Peak integration with the Beckman system Gold (pK 9.3 Immobiline as internal standard). Abbreviations: as in Table I. Note how, even for hydrophobic monomers, much better incorporation efficiencies can be obtained simply by increasing the polymerization temperature from 25 to 60°C.

seem to have as a pivotal point the Tris-A incorporation efficiency, the upper, slower reacting members rotating from a diagonal curve to a vertical position above the Tris-A point. These findings seem to be paradoxical, as the acrylamide polymerization reac-

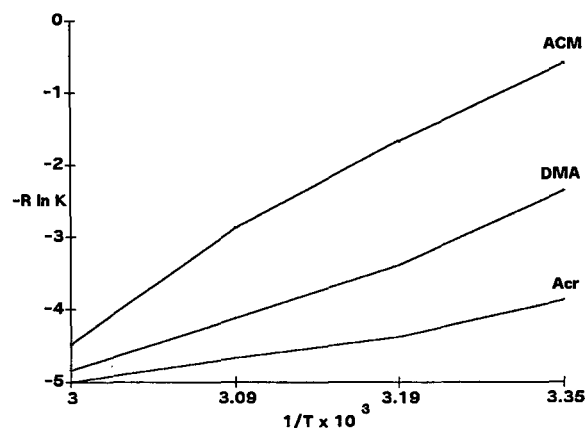


Fig. 8. Van 't Hoff plot of the data in Fig. 7. The equilibrium constant ( $K$ ) represents the molar ratio between the incorporated and free monomer at the different temperatures. The slope of the different curves represents  $\Delta H^\circ$ . Note that  $\Delta H^\circ$  is essentially constant for Tris-A and acrylamide, whereas it increases progressively with increasing monomer hydrophobicity.

tion is known to be strongly exothermic. By using the Van 't Hoff equation, and plotting  $-R \ln K$  vs.  $1/T$  (Fig. 8), it is possible to calculate  $\Delta H^\circ$  for such reactions. It is seen that  $\Delta H^\circ$  for Tris-A and acrylamide conversion is essentially constant, whereas for the more hydrophobic members of the series it increases progressively with increasing temperature.

## DISCUSSION

Our aim is to arrive at novel polyacrylamide gel formulations that satisfy the following requirements: high hydrophilicity, high resistance to alkaline hydrolysis and higher porosity. The reason is that in modern separation science there exist a dichotomy between the two most popular gel matrices: agaroses have been confined mostly to DNA separations [16], whereas polyacrylamides are utilized only for protein analysis [2,3]. However, as recently demonstrated with the Hydrolink matrices [17], there is a need for modified polyacrylamides that could properly sieve nucleic acids starting from oligonucleotides up to a few thousand base pairs (BP). This is a sort of "dark" region, where regular polyacrylamides sieve too much (in the Ogston model) [18] and agaroses are too porous. As demonstrated by Smith *et al.* [19], in a plot of  $\log(\text{BP})$  vs. %T, Hydrolink matrices are able to link diagonally the behaviour of polyacrylamides and agaroses, whose plots run parallel to each other at a distance of *ca.* three orders of magnitude (in sieving ability; see Fig. 1 in ref. 19). Hence novel monomers able to fulfil the above requirements would be welcome in electrokinetic separations. One such monomer appeared to be trisacryl; this molecule has been described by Boschetti's group [3] and represents the backbone of a number of highly hydrophilic ion exchangers for chromatography [20]. The amino-2-hydroxymethyl-2-propanediol residues create a micro-environment that favours the approach of hydrophilic solutes (proteins) to the polymer surface. As a result of grafting the "tris" moiety on to the acrylamido residue, the polyethylene backbone remains buried underneath a layer of hydroxymethyl groups. Such a matrix therefore has a pronounced advantage over polyacrylamide- or hydroxymethyl methacrylate-based supports, which have a hydrophobic character. Our data on such substituted acrylamides bring a unique insight into

the chemistry of polyacrylamides, which we shall discuss below.

#### *Structure–stability relationship for N-substituted acrylamides*

This is an argument that we have elucidated in the case of the Immobiline chemicals, which are mono-N-substituted acrylamides bearing a weak protolytic group. Although we agreed with the general knowledge on the greater stability of such compounds, as compared with unsubstituted amides, it was clear from our results [8–10] that there were other, more subtle mechanisms governing such stability. On the basis of our data, and of the known structures of these acrylamido derivatives, we derived the following rules:

(a) to afford protection of the amido bond, the most important parameter is not the degree of substitution in the nitrogen engaged in the amido plane (mono- or disubstituted) but the type of substituent;

(b) in particular, rigid ring structures are inefficient in protecting the adjacent amido bond, as their rigidity prevents them from oscillating in the surrounding space and thus shielding the amido plane;

(c) flexible chains bound to the nitrogen of the amido bond are capable of protecting the amido plane, as they can fluctuate in the nearby space and shroud the amido group;

(d) if rigid structures are present in the nitrogen substituents, they should be some distance from the plane of the amido bond;

(e) if a simple, flexible chain is present as a substituent on the nitrogen of the amido bond, greater protection of the latter is afforded by a longer chain.

None of these general rules applies to the inborn instability of the trisacryl monomer; this is due to the fact that the 2-hydroxymethyl group neighbouring the amido bond can form a hydrogen-bonded ring with the latter and, for electronic reasons, favour the hydrolytic attack (by a mechanism of N,O-acyl transfer) [21]. Thus, paradoxically, such a mono-substituted acrylamide degrades with a zero-order kinetics. However, more surprising, once this monomer is inserted into a polymer chain, the poly(trisacryl) becomes much more resistant to hydrolytic attack than a regular polyacrylamide. This novel finding could have interesting implications with

regard to the three-dimensional structure of such a polymer. The added stability in the polymer could be due now to steric factors: it could be possible that the polymer matrix is stereoregular, perhaps due to helix formation of the poly(trisacryl) coil. We are currently trying to decode such a structure (if any) by small-angle soft neutron scattering. If we could demonstrate such spatial organization, it could be an interesting advance in decoding the structure of polyacrylamide matrices, still believed to be “a random meshwork of fibres”.

#### *Polymerization efficiency*

Because the monomers are neurotoxins, one should always try to drive the reaction to completion, an almost impossible task, in fact, with radical polymerization. However, over the years, we have described conditions that ensure incorporation of the monomers into the growing chain to the extent of >95% [4–6]. An efficient removal of ungrafted monomers is also necessary in zone electrophoresis of proteins, as at alkaline pH values the double bond of unreacted acrylamide could easily add to free SH groups, forming a cysteine adduct [22]. An alternative to this could be the use of “washed” matrices, a technique we have introduced since 1980 when developing immobilized pH gradients (IPG). It is a routine, in IPGs, to wash the matrix extensively, dry it and re-swell it in any desired additive [11].

An unexpected finding was the strong dependence of the efficiency of conversion of the more hydrophobic monomers on the polymerization temperature. We had always advocated polymerizing standard polyacrylamide gels at 50°C (1 h reaction time), but the increase in conversion was from *ca.* 88% to 95% on going from 25 to 60°C (see Fig. 7). Considering that the heat of polymerization from aqueous monomer to aqueous polymer solutions is *ca.* 82.8 kJ/mol (a large amount of heat indeed), and that the overall activation energy for polymerizing in water–peroxodisulphate initiator is 70.7 kJ/mol, it is surprising that one could drive the reaction to even better yields by increasing the temperature, as we routinely do. Even more surprising is the great temperature dependence of the more hydrophobic monomers in the series; as shown in Fig. 7, for ACM, increasing the polymerization temperature from 25 to 60°C increases the efficiency from barely 55% to 94%. There might be several possible

explanations for this phenomenon: (a) the decrease in viscosity with higher temperature (nascent polymer chains would greatly augment the viscosity of bulk solution); (b) the possibility that the more hydrophobic elements of the series are not fully dissolved in water, but secluded into aggregates [6]; (c) the possibility that, as the hydrophobicity of the series increases, this is paralleled by an increase in overall activation energy (as also indicated by the increment in  $\Delta H^\circ$ , see Fig. 8). The present findings, hopefully, should terminate a 20-year-long disagreement among two main groups of polyacrylamide users: those who regularly polymerize at high temperatures and those who have been pestering us by suggesting polymerization in a thermostated ice-bath!

#### ACKNOWLEDGEMENTS

This work was supported in part by grants from the Agenzia Spaziale Italiana (ASI) and the European Space Agency (ESA) for gel polymerization in microgravity and by the Consiglio Nazionale delle Ricerche, Progetti Finalizzati Chimica Fine II and Biotecnologie e Biostrumentazione.

#### REFERENCES

- 1 S. Raymond and L. Weintraub, *Science (Washington, D.C.)*, 130 (1959) 711–712.
- 2 P. G. Righetti, *J. Biochem. Biophys. Methods*, 19 (1989) 1–20.
- 3 E. Boschetti, *J. Biochem. Biophys. Methods*, 19 (1989) 21–30.
- 4 A. Bianchi-Bosisio, D. Loherlein, R. Snyder and P. G. Righetti, *J. Chromatogr.*, 189 (1980) 317–330.
- 5 C. Gelfi and P. G. Righetti, *Electrophoresis*, 2 (1981) 213–219.
- 6 C. Gelfi and P. G. Righetti, *Electrophoresis*, 2 (1981) 220–228.
- 7 P. G. Righetti, C. Gelfi and A. Bianchi-Bosisio, *Electrophoresis*, 2 (1981) 291–295.
- 8 P. G. Righetti, C. Etori and M. Chiari, *Electrophoresis*, 12 (1991) 55–58.
- 9 M. Chiari, C. Etori, A. Manzocchi and P. G. Righetti, *J. Chromatogr.*, 548 (1991) 381–392.
- 10 M. Chiari, M. Giacomini, C. Micheletti and P. G. Righetti, *J. Chromatogr.*, 558 (1991) 285–295.
- 11 P. G. Righetti, *Immobilized pH Gradients: Theory and Methodology*, Elsevier, Amsterdam, 1990.
- 12 G. Artoni, E. Gianazza, M. Zanoni, C. Gelfi, M. C. Tanzi, C. Barozzi, P. Ferruti and P. G. Righetti, *Anal. Biochem.*, 137 (1984) 420–428.
- 13 W. P. Purcell, G. E. Bass and J. M. Clayton (Editors), *Strategy of Drug Design: a Guide to Biological Activity*, Wiley-Interscience, New York, 1973, pp. 126–143.
- 14 M. Chiari, L. Pagani and P. G. Righetti, *J. Biochem. Biophys. Methods*, 23 (1991) 115–130.
- 15 P. G. Righetti, *Isoelectric Focusing: Theory, Methodology and Applications*, Elsevier, Amsterdam, 1983.
- 16 P. G. Righetti, *J. Chromatogr.*, 516 (1990) 3–22.
- 17 P. G. Righetti, M. Chiari, E. Casale, C. Chiesa, T. Jain and R. G. L. Shorr, *J. Biochem. Biophys. Methods*, 19 (1989) 37–49.
- 18 A. G. Ogston, *Trans. Faraday Soc.*, 54 (1958) 1754–1756.
- 19 C. L. Smith, C. M. Ewing, M. T. Mellon, S. E. Kane, T. Jain and R. G. L. Shorr, *J. Biochem. Biophys. Methods*, 19 (1989) 51–64.
- 20 E. Boschetti, in P. D. G. Dean, W. S. Johnson and F. A. Middle (Editors), *Affinity Chromatography*, IRL Press, Oxford, 1985, pp. 11–15.
- 21 A. P. Phillips and R. Baltzly, *J. Am. Chem. Soc.*, 69 (1947) 200–205.
- 22 M. Chiari, A. Manzocchi and P. G. Righetti, *J. Chromatogr.*, 500 (1990) 697–704.



# Investigation of the properties of acrylamide bifunctional monomers (cross-linkers) by capillary zone electrophoresis

Cecilia Gelfi, Angela Alloni, Patrizia de Besi and Pier Giorgio Righetti

Chair of Biochemistry and Department of Biomedical Sciences and Technologies, University of Milan, Via Celoria 2, Milan 20133 (Italy)

---

## ABSTRACT

A series of cross-linkers [N,N'-methylenebisacrylamide (Bis), N,N'-(1,2-dihydroxyethylene)bisacrylamide (DHEBA), N,N'-diallyltartardiamide (DATD) and N,N'-bisacrylylcystamine (BAC)] were investigated as potential candidates of a novel class of polyacrylamide matrices, exhibiting high hydrophilicity, high resistance to hydrolysis and larger pore sizes than conventional polyacrylamide gels. The most hydrophilic cross-linker (DATD) exhibited first-order degradation kinetics in 0.1 M NaOH, suggesting that such a structure is electronically unstable, whereas the other cross-linkers displayed first-order kinetics. In addition, when used in highly cross-linked gels (for increasing pore size), DATD acts as an inhibitor of gel polymerization. Another interesting finding is an inverse relationship between the partition coefficient of such cross-linkers and the incorporation efficiency; the more hydrophobic members of the family exhibit a reduced conversion from monomer into polymer, which is more pronounced in highly cross-linked gels. When measuring the partition coefficient, DATD and DHEBA appear to be highly hydrophilic whereas BAC, owing to the two sulphur atoms in the molecule, appears to be extremely hydrophobic. The use of BAC in gels for protein separations should therefore be avoided.

---

## INTRODUCTION

In the accompanying paper [1], we reported the investigation of a series of monofunctional acrylamide monomers (in general mono- and disubstituted acrylamides), aimed at arriving at novel gel formulations. To this end, we utilized capillary zone electrophoresis (CZE) for studying such parameters as incorporation efficiency, hydrophilicity and resistance to hydrolysis. In this work, we investigated the same parameters for a series of cross-linkers, *i.e.*, the bi-functional agents used for producing the gel network. In addition to the standard molecule [N,N'-methylenebisacrylamide (Bis)], a host of them have been described over the years, and there are really no guidelines to suggest any strategy for their use. In 1976 O'Connell and Brady [2] reported the

use of N,N'-(1,2-dihydroxyethylene)bisacrylamide (DHEBA) for casting reversible gels, as the 1,2-diol structure of DHEBA renders them susceptible to cleavage by oxidation with periodic acid. The same principle should also apply to N,N'-diallyltartardiamide (DATD) gels, as described by Anker [3]. Alternatively, ethylene diacrylate gels could be used, as this cross-linker contains ester bonds which undergo base-catalysed hydrolytic cleavage [4]. Another series of poly(ethylene glycol) diacrylate cross-linkers, as reported by Righetti *et al.* [5], also belong to the same category of ester derivatives. One of the latest addition to the series, N,N'-bisacrylylcystamine (BAC), contains a disulphide bridge cleavable by thiols and as such offers gel matrices which can be liquefied under mild and almost physiological conditions [6]. BAC-cross-linked gels were first proposed for the fractionation of RNA and they can be liquefied in an excess of  $\beta$ -mercaptoethanol or with dithiothreitol. As a novel class of cross-linkers, bisacrylylpiperazine has been reported [7] as a moiety able to copolymerize with good efficiency

---

Correspondence to: Prof. P. G. Righetti, Chair of Biochemistry and Department of Biomedical Sciences and Technologies, University of Milan, Via Celoria 2, Milan 20133, Italy.

with a modified monomer, N-acryloylmorpholine. Such a cross-linker was later reported to impart unique properties to gels to be silver stained, as it produced a perfectly clear background [8].

In this work, we selected the four most common cross-linkers (Bis, DHEBA, DATD and BAC) and studied their properties by CZE.

## EXPERIMENTAL

### Materials

The formulae of the four cross-linkers studied are given in Table I. Gels were prepared by using acrylamide as a monofunctional monomer and each of the four cross-linkers. Acrylamide, N,N,N',N'-tetramethylethylenediamine (TEMED), the four cross-linkers and ammonium peroxydisulphate were obtained from Bio-Rad Labs. (Richmond, CA, USA). Mandelic acid and pK 9.3 Immobiline, used as internal standards in CZE runs, were purchased from Aldrich (Steinheim, Germany) and Pharmacia-LKB (Uppsala, Sweden), respectively.

### Alkaline hydrolysis

All cross-linkers were dissolved (20 mM each) in 0.1 M NaOH and incubated at 70°C for up to 6 h. At 30-min intervals aliquots were collected and diluted in 0.1 M sodium borate buffer (pH 9.0) to 2.5 mM. After adding mandelic acid (2.50 mM) as an internal standard, the samples were analysed by CZE.

### Incorporation efficiency

In order to check for the extent of conversion of the various monomers into the polymer, 5 ml of gel

(made with the different cross-linkers in Table I) were polymerized in a test-tube under anaerobic conditions (protected by a thin film of water-saturated *n*-butanol). After polymerization (1 h, 50°C), the gel was extruded and homogenized and an equal amount of water was added (extraction was also performed in methanol). After stirring for 30 min, the gel phase was filtered through a Buchner funnel, the supernatant was diluted, internal standard (2.5 mM pK 9.3 Immobiline) was added and the mixture was filtered through an Ultrafree-MC Millipore filter (0.22 μm porosity) and analysed by CZE. No attempts were made to separate acrylamide from the cross-linkers, so that the incorporation efficiency refers to the sum of the two monomers.

### Capillary zone electrophoresis

CZE was performed in a Beckman (Palo Alto, CA, USA) P/ACE System 2000 instrument equipped with a 50 cm × 75 μm I.D. capillary. Runs were performed at 25°C in a thermostated environment in 0.1 M borate buffer (pH 9.0). In all instances the migration direction was toward the negative electrode, which means that the acidic species (mandelic acid) are transported there by electroosmosis as they migrate electrophoretically toward the positive electrode. The samples were injected into the capillary by pressure (55 kPa), usually for 10 s. The calibration graph for each acrylamido derivative analysed was constructed with the Beckman integration system Gold, with concentration points of 0.25, 0.50, 1.00, 1.25, 2.00, 2.50 and 3.50 mM. In each run either mandelic acid or the pK 9.3 Immobiline (2.50 mM) was used as an internal standard. Runs were usually

TABLE I  
BIFUNCTIONAL ACRYLAMIDO DERIVATIVES

Formula	Name	$M_r$
$\text{CH}_2 = \text{CHCONHCH}_2\text{NHCOCH} = \text{CH}_2$	N,N'-Methylenebisacrylamide (Bis)	154
$\text{CH}_2 = \text{CHCONHCH}(\text{CH}_2\text{OH})_2\text{NHCOCH} = \text{CH}_2$	N,N'-(1,2-Dihydroxyethylene)bisacrylamide (DHEBA)	200
$\text{CH}_2 = \text{CHCH}_2\text{NHCOCH}(\text{CH}_2\text{OH})_2\text{CHCONHCH}_2\text{CH} = \text{CH}_2$	N,N'-Diallyltartardiamide (DATD)	228
$(\text{CH}_2 = \text{CHCONHCH}_2\text{CH}_2\text{S}-)_2$	N,N'-Bisacrylylcystamine (BAC)	260

performed at 15 kV and 50  $\mu$ A with the detector set at 254 nm.

#### Partition coefficient

In order to establish a hydrophobicity scale, the various cross-linkers were subjected to partitioning in water–1-octanol as described by Purcell *et al.* [9]. The partition coefficient  $P$  is defined as the ratio between the molarity of a given compound in the organic phase and that in the aqueous phase. Partitioning was performed as follows: each monomer was dissolved (2 mM) in water saturated with 1-octanol; 3.5 ml of this solution and 3.5 ml of 1-octanol were transferred into a separating funnel and shaken for 2 min. After decanting for 1 h, the aqueous phase was collected and centrifuged for 75 min at 1800 g. All operations were performed at 25°C. The clarified solution was diluted, internal standard (2.5 mM pK 9.3 Immobiline) was added and the mixture was analysed by CZE as described above.

#### RESULTS

In order to check the stability of the four cross-linkers, they were subjected to hydrolysis in 0.1 M NaOH at 70°C for various lengths of time and then analysed by CZE for separation and precise determination of the degradation products. Fig. 1 shows a representative run of the CZE analysis of DHEBA, before and after hydrolysis (mandelic acid was added as an internal standard in all runs). A summary of all the hydrolysis data is given in Fig. 2. It can be seen that, whereas all the cross-linkers exhibit first-order degradation kinetics, as expected, one of them, DATD, displays a zero-order degradation process, suggesting that this structure is intrinsically unstable. This is noteworthy, as this cross-linker has recently been proposed in highly cross-linked gels for DNA analysis [10].

Table II summarizes the data obtained on the incorporation efficiency (of the two monomers) in a polyacrylamide gel subjected to standard polymerization conditions (1 h, 50°C) as routinely adopted in the field of electrophoresis [11]. Two phenomena are apparent: (a) in general, as the amount of cross-linker increases from 4 to 10% (or 30% in some instances), the incorporation efficiency diminishes; this is true for all the cross-linkers; (b) two

of the cross-linkers (Bis and DHEBA) show very high incorporation efficiencies (>90%) whereas the other two show progressively lower incorporation rates. A case in point is DATD, which, at progressively higher percentages of cross-linker, shows dramatic decreases in incorporation efficiencies, down to as low as 50%.

Fig. 3 shows the hydrophobicity scale of the four cross-linkers, as obtained by partitioning in water–1-octanol phases. It is seen that DATD and DHEBA are highly hydrophilic, as expected given their vicinal diol structures, whereas BAC appears to be extremely hydrophobic, owing to the presence of an –S–S– bridge. These findings have important implications on the use of such gels for protein analysis, as discussed below.

#### DISCUSSION

The present findings suggest a strategy for the use of such cross-linkers, as outlined below.

#### Copolymerization efficiency

It appears that two main factors affect the copolymerization of cross-linkers with the standard monofunctional monomer (acrylamide): (a) the total percentage of cross-linker in the mixture (expressed as %C) and (b) the relative hydrophobicity of such compounds. Independently from the type of cross-linker, at progressively higher %C the incorporation efficiency diminishes (for both, the mono- and bifunctional monomers). This can be interpreted by assuming that, as %C progressively increases, the gel becomes more “knotty”, *i.e.*, the chains become shorter and thicker. Given this gradual structural change, the monomers would have difficulty in diffusing in contact with the fibres and in finding the propagation point for the chain growth [12,13]. We have also seen in the accompanying paper [1] that, as monomers become more hydrophobic, their incorporation efficiency progressively diminishes. In fact, a unique inverse correlation has been found between the partition coefficient and rate of transfer into the growing polymer (see Fig. 7 in ref. 1). Thus, it is not surprising that BAC should lower the incorporation efficiency from >90% to only 77%. It might be asked then why DATD, being so strongly hydrophilic, exhibits even poorer chain transfer. This is in fact due to complete-



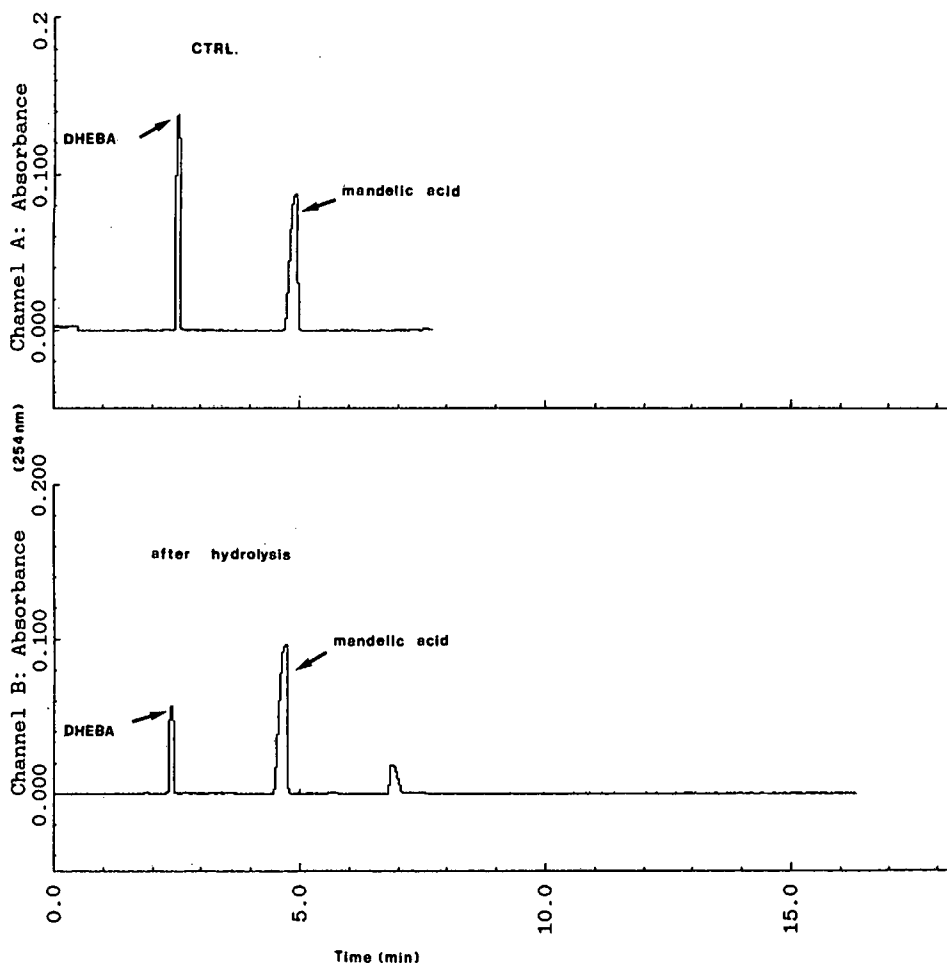


Fig. 1. Representative CZE runs for monitoring alkaline hydrolysis of cross-linkers. Conditions: 100 mM borate–NaOH buffer (pH 9.0), 15 kV, 86  $\mu$ A at 25°C. Uncoated fused-silica capillary (50 cm  $\times$  75  $\mu$ m I.D.). Beckman P/ACE 2000 instrument, monitoring at 254 nm. DHEBA = N,N'-(1,2-dihydroxyethylene)bisacrylamide; CTRL = control, before hydrolysis. In this and all subsequent runs the migration is towards the cathode.

ly different reasons: allyl derivatives are in general poorly reacting species. It has been reported that the  $C_m$  value (transfer constant to monomer) for most allyl compounds is usually 1000 times higher than for acrylamide [14]. Moreover, the  $r_1$  value (monomer reactivity ratio), which expresses the extent to which a monomer either propagates a chain by reacting with itself or by reacting with another, different monomer present in the mixture, is, for allyl derivatives, usually 100 times smaller than for acrylamide and, in some instances, is actually zero [15]. Thus, for all practical purposes, DATD, when

copolymerized with acrylic double bonds, acts like an inhibitor of gel polymerization.

#### *Use of different cross-linkers*

It is now apparent why the “old pair” acrylamide–Bis has survived unscathed all these years: as a general rule, if we follow the old adage “similar dissolves similar”, we can extrapolate it to copolymerization chemistry: “similar reacts with similar”. The rule for selecting the appropriate copolymerizing pair is that they should be very similar molecules, like acrylamide and Bis. Thus, in 1984,

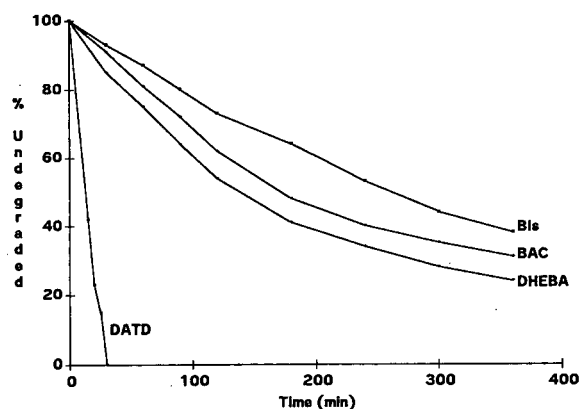


Fig. 2. Kinetics of hydrolysis of different cross-linkers. Hydrolysis was performed in 0.1 M NaOH at 70°C for the times indicated. The amounts were assessed by collecting in triplicate at each point, neutralizing and injecting into the CZE instrument (Beckman P/ACE 2000). Conditions: 100 mM borate–NaOH buffer (pH 9.0), 15 kV, 86  $\mu$ A at 25°C. Uncoated fused-silica capillary (50 cm  $\times$  75  $\mu$ m I.D.). Peak integration with the Beckman system Gold (mandelic acid was used as an internal standard). Abbreviations as in Table I. Note that whereas all the other cross-linkers exhibit first-order kinetics, DATD follows zero-order degradation kinetics.

when we reported the novel monomer N-acryloylmorpholine [7], we synthesized as a co-reacting species bisacrylylpiperazine; this pair produced ex-

TABLE II

## INCORPORATION EFFICIENCY AS A FUNCTION OF PERCENTAGE OF CROSS-LINKER (%C)

All experiments refer to standard polymerization conditions: 1 h at 50°C.

Monomer <sup>a</sup>	%C	Incorporation (%) <sup>b</sup>
BAC	4	77
	10	72
Bis	4	95
	10	90
DHEBA	4	90
	10	85
DATD	4	65
	10	58
	30	48

<sup>a</sup> %C = g Bis/%T; T = g acrylamide + g Bis per 100 ml of solution; all gels had variable %C at constant %T (total monomers, 6%T).

<sup>b</sup> The incorporation efficiency refers to the sum of the two monomers (acrylamide + cross-linker).

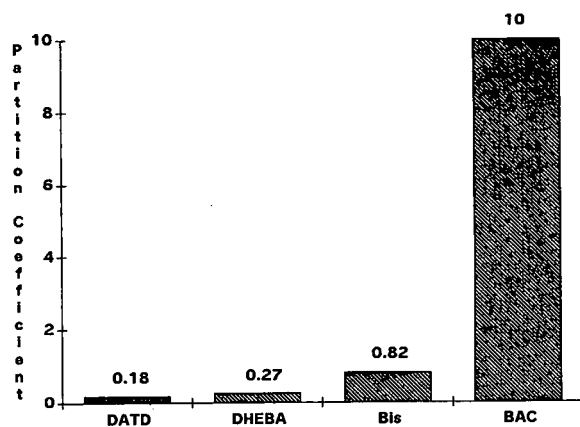


Fig. 3. Hydrophobicity scale for the four cross-linkers. It was obtained by partitioning in water–1-octanol at room temperature and determining the concentrations in the two phases by CZE. Conditions: 100 mM borate–NaOH buffer (pH 9.0), 15 kV, 86  $\mu$ A at 25°C. Fused-silica capillary (50 cm  $\times$  75  $\mu$ m I.D.). Peak integration with the Beckman system Gold (mandelic acid was used as an internal standard). Abbreviations as in Table I.

cellent gels for electrophoresis. It does not seem a promising proposition to try to copolymerize allylic with acrylic moieties, as suggested recently [10]; in all practical effects, the former acts like a radical sink, inhibiting the gel formation. The notion of using an “inhibitor” for polymerizing a gel does not seem to be based on sound polymer chemistry. In addition, DATD is electronically unstable, as it displays zero-order degradation kinetics (probably by the same N,O-acyl transfer mechanism reported for trisacryl) [16]. Given such severe drawbacks, the use of DATD as a cross-linker should in general be avoided. A word of caution should also be expressed about the use of BAC: its relative hydrophobicity seems to inhibit to some extent the conversion of monomers into the polymer. Moreover, if used for protein separations, as suggested elsewhere [17], there could be another major risk: because, for the purpose of liquefying the gel for sample recovery, highly cross-linked gels should be used, this would greatly increase the matrix hydrophobicity, with a concomitant risk of hydrophobic interaction of the protein sample with the matrix. This would not, of course, discourage the use of BAC-cross-linked gels for nucleic acid analysis, as such polymers are not prone to hydrophobic interaction with the matrix.

## ACKNOWLEDGEMENTS

This work was supported in part by grants from the Agenzia Spaziale Italiana (ASI) and the European Space Agency (ESA) for gel polymerization in microgravity and by the Consiglio Nazionale delle Ricerche, Progetti Finalizzati Chimica Fine II and Biotecnologie e Biostrumentazione.

## REFERENCES

- 1 C. Gelfi, P. de Besi, A. Alloni and P. G. Righetti, *J. Chromatogr.*, 608 (1992) 333.
- 2 P. B. H. O'Connell and C. J. Brady, *Anal. Biochem.*, 76 (1976) 63–76.
- 3 H. S. Anker, *FEBS Lett.*, 7 (1970) 293–296.
- 4 P. N. Paus, *Anal. Biochem.*, 42 (1971) 327–376.
- 5 P. G. Righetti, B. C. W. Brost and R. S. Snyder, *J. Biochem. Biophys. Methods*, 4 (1981) 347–363.
- 6 J. N. Hansen, B. H. Pfeiffer and J. A. Boehnert, *Anal. Biochem.*, 105 (1980) 192–201.
- 7 G. Artoni, E. Gianazza, M. Zanoni, C. Gelfi, M. C. Tanzi, C. Barozzi, P. Ferruti and P. G. Righetti, *Anal. Biochem.*, 137 (1984) 420–428.
- 8 D. Hochstrasser and C. R. Merrill, *Appl. Theor. Electron.*, 1 (1988) 35–40.
- 9 W. P. Purcell, G. E. Bass and J. M. Clayton (Editors), *Strategy of Drug Design: a Guide to Biological Activity*, Wiley-Interscience, New York, 1973, pp. 126–143.
- 10 L. Orbán and A. Chrambach, *Electrophoresis*, 12 (1991) 241–246.
- 11 B. Bjellqvist, K. Ek, P. G. Righetti, E. Gianazza, A. Görg, R. Westermeier and W. Postel, *J. Biochem. Biophys. Methods*, 6 (1982) 317–339.
- 12 A. Bianchi-Bosisio, C. Locherlein, R. S. Snyder and P. G. Righetti, *J. Chromatogr.*, 189 (1980) 317–330.
- 13 P. G. Righetti, in R. C. Allen and P. Arnaud (Editors), *Electrophoresis '81*, Walter de Gruyter, Berlin, 1981, pp. 3–16.
- 14 L. J. Young, G. Brandrup and J. Brandrup, in J. Brandrup and E. H. Immergut (Editor), *Polymer Handbook*, Interscience, New York, 1966, pp. II-77–II-79.
- 15 H. Mark, B. Immergut and E. H. Immergut, in J. Brandrup and E. H. Immergut (Editors), *Polymer Handbook*, Interscience, New York, 1966, pp. II-141–II-175.
- 16 A. P. Phillips and R. Baltzly, *J. Am. Chem. Soc.*, 69 (1947) 200–205.
- 17 R. Bartels and L. Bock, in C. Schafer-Nielsen (Editor), *Electrophoresis '88*, VCH, Weinheim, 1988, pp. 289–294.

# Sodium dodecyl sulfate–capillary gel electrophoresis of proteins using non-cross-linked polyacrylamide

Dan Wu and Fred E. Regnier

*Department of Chemistry, Purdue University, West Lafayette, IN 47907 (USA)*

---

## ABSTRACT

Proteins with relative molecular masses of 14 000 to 205 000 were separated by sodium dodecyl sulfate–capillary gel electrophoresis (SDS-CGE) using non-cross-linked linear polyacrylamide gels on both coated and uncoated fused-silica capillaries. It was determined that viscosity of the acrylamide solution was a major factor affecting column stability with linear acrylamide gels. When the viscosity of the acrylamide solution reaches 100 cP, electro-osmotically driven displacement of the gels is insignificant. Uncoated capillaries provided better resolution, stability, and reproducibility than surface coated capillaries when the concentration of linear polyacrylamide was greater than 4%. At lower gel concentrations, non-cross-linked polyacrylamide is easily displaced from the columns. A calibration plot of log molecular mass *vs.* mobility with non-linear polyacrylamide was linear, which indicated that resolution was equivalent to that obtained with cross-linked acrylamide. Separations with model proteins indicated that baseline resolution between protein species that vary 10% in molecular mass can be achieved.

---

## INTRODUCTION

Sodium dodecyl sulfate–polyacrylamide gel electrophoresis (SDS-PAGE) in the slab gel format has been used for over 25 years to separate proteins by molecular mass [1]. Using this method, proteins are separated on cross-linked polyacrylamide gels with low applied electric fields (10–30 V/cm) and typically detected by staining. Although SDS-PAGE is one of the most commonly used methods for determining molecular masses of proteins, it has some limitations. First, the process is slow. Gel preparation, separation and staining can require hours. Second, quantification is difficult. Stains are non-linear and present problems with amino acids, such as proline. In an effort to overcome some of these problems, Cohen *et al.* [2] examined the separation of proteins in capillaries by SDS-PAGE. SDS–capillary gel electrophoresis (CGE) was much more rapid and of higher resolution than SDS-PAGE in

the slab gel format. Separations by SDS-CGE are typically achieved in less than 20 min with on-column absorbance detection [3]. It is even possible to automate SDS-CGE. Furthermore, the CGE column may be used in multiple separations.

Both cross-linked and non-cross-linked polyacrylamide have now been used in SDS-CGE [4–8]. Traditional cross-linked gels create a sieving medium based on a rigid matrix of pores. The pore size is controlled by varying the concentration of acrylamide at a fixed concentration of crosslinking agent. Cross-linked gels were used because they provided a matrix of small pore, were reproducible, and were of sufficient mechanical strength that they could be removed from the system and stained [9]. Unfortunately, cross-linked gels are not very satisfactory in capillary columns. Voids form in the capillary as a result of gel shrinkage during polymerization. The void problem has been addressed both by polymerization under pressure [10] and by adsorbing a layer of linear polymer onto the capillary surface [11]. These techniques reduce, but do not eliminate this problem.

---

*Correspondence to:* Dr. F. E. Regnier, Department of Chemistry, Purdue University, West Lafayette, IN 47907, USA.

Attempts to circumvent the problems of cross-linked polyacrylamide in SDS-CGE have led to the examination of non-cross-linked acrylamide. It was apparently anticipated in previous studies that electro-osmosis would be a problem in the use non-linear polyacrylamide. If this were true, electro-osmosis could be effectively eliminated by applying a viscous coating at the capillary wall. This technique was first reported by Hjertén [12] for controlling electro-osmosis in capillary isoelectric focusing. Columns were prepared by coating the capillary with the bifunctional reagent 3-methacryloxypropyltrimethoxysilane (MAPS). Subsequent to silylating capillary walls with MAPS, the capillary was filled with acrylamide and polymerization initiated. Acrylamide polymer was grafted to the capillary wall through MAPS groups. Hjertén suggested the electro-osmosis flow in this capillary will be inversely proportional to the viscosity of the polymer layer attached to the surface.

Previous reports on SDS-CGE have been with surface-modified fused-silica capillaries to reduce electro-osmosis [12,13]. The surface modification most widely used has been to apply a layer of polyacrylamide. Although separations with these capillaries were outstanding, separations on uncoated capillaries were not provided as a control. Thus, it is not possible to assess the contribution of surface coatings in SDS-CGE.

This paper focuses on the importance of surface modification in SDS-CGE with linear polyacrylamide gel filled capillaries. It will be shown that (i) electro-osmosis in CGE is a smaller problem than previously anticipated and (ii) linear polyacrylamide can be used in uncoated capillaries without appreciable gel displacement when the total concentration of acrylamide in the column exceeds 4%. Polypeptides ranging in relative molecular mass ( $M_r$ ) from 2000 to 200 000 could be accommodated using a set of 4, 6 and 8% linear polyacrylamide gel-filled capillaries.

## EXPERIMENTAL

### Chemicals

All proteins were purchased from Sigma (St. Louis, MO, USA). Acrylamide, ammonium persulfate (APS), SDS, N,N,N',N'-tetramethylethylenediamine (TEMED), and Tris base were purchased

from Bio-Rad (Richmond, CA, USA). MAPS was purchased from Polyscience (Warrington, PA, USA). All of the buffer solutions were prepared by using double distilled water that was passed through 0.45- $\mu$ m nylon filters. All of the samples were stored at 0°C between analysis.

### Instrumentation

The CGE system was based on an in-house design available in our laboratory. All high-voltage components of the system were contained in a Lucite cabinet fitted with a safety interlock that would interrupt the power supply when the cabinet door was opened. A Glassman PS/EL30P01.5 (Glassman High Voltage, Whitehouse Station, NJ, USA) power supply was used to apply the electric field across the capillary. The power supply was connected to 4-ml buffer reservoirs. On-column detection was performed with an Isco CV<sup>4</sup> (Lincoln, NE, USA) variable-wavelength UV-absorbance detector.

### Preparation of acrylamide gel-filled capillaries

**Bonded acrylamide capillaries.** Fused-silica capillaries of 375  $\mu$ m O.D.  $\times$  75  $\mu$ m I.D. and 45 cm length with a detector window at 25 cm were obtained from Polymicro Technologies (Phoenix, AZ, USA) and used for all separations. The capillary was first treated with 0.01 M NaOH for 30 min followed by 15 min of washing with deionized water. The columns were coupled to a nitrogen gas supply and dried in a gas chromatography oven at 100°C for 1 h. MAPS-methanol (9:1) solution was forced through the capillaries at 50°C for 1.5 h. After the reaction was complete, the solution was purged with nitrogen and the column sequentially washed with methanol for 15 min and with water for another 15 min.

Gel-filled capillaries were prepared by a modified procedure described by Yin *et al.* [14]. A 5-ml volume of 4% acrylamide solution was degassed by aspiration for 30 min. Then 100  $\mu$ l APS (10%), 20  $\mu$ l TEMED (10%) and 50  $\mu$ l SDS (10%) were added. After stirring, the solution was pushed into the capillary under pressure. An hour later the column was ready to use.

**Uncoated capillaries.** To prepare a gel-filled column with uncoated capillaries, the initial wash procedure was followed. After washing the column, the polymerizing gel solution prepared as above, was

introduced into the capillary.

**Protein sample preparation.** SDS-Protein samples were prepared in 0.1 M Tris–0.25 M borate buffer (pH 8.1). The mass ratio of SDS to protein is 2.5:1, which ensures complete absorption of SDS to proteins. SDS–protein samples were electrophoretically injected into the gel column by setting the negative end of the column into the sample vial and applying an electrical field for 10 s at constant voltage.

**Viscosity measurements.** A dropping ball viscosimeter (Gilmont 2302) was used to measure the viscosity of the polyacrylamide solutions. Different acrylamide solutions were prepared by the procedure described above and the density of each solution was measured. The viscosimeter was filled with gel solution and the time of a ball falling freely through the gel solution was measured over a constant distance. Two different types of balls, glass and steel, were used at different concentration ranges. Viscosity ( $\eta$ ) was calculated from the equation:

$$\eta = K (d_{\text{ball}} - d_{\text{soln}})t$$

in which,  $K$  is a constant,  $d_{\text{ball}}$  and  $d_{\text{soln}}$  are the densities of the ball and the solutions and  $t$  is the time in minutes.

## RESULTS AND DISCUSSION

### *Comparison of coated and uncoated capillaries*

A comparison study was carried out using capillaries with a polymeric surface layer as previously described [14] and uncoated capillaries in which linear polyacrylamide was formed in the capillary. Capillaries with the polymeric surface layer will be referred to henceforth as coated capillaries whereas native fused-silica capillaries will be designated as uncoated capillaries. Polymer concentrations of 3, 4 and 6% were used in both types of capillaries.

A comparison of coated and uncoated capillaries in the separation of protein molecular mass standards is shown in Fig. 1. These standards ranged in from  $M_r$  from 14 400 to 78 000 in increments of approximately 10 000. Identification of the protein was accomplished by enrichment with individual standard proteins. The 4% and 6% columns are seen to be comparable in resolution and peak shape, although migration times were longer on the uncoated columns. Resolution is even slightly higher

with high-molecular-mass species on the uncoated capillary. Organic surface coating appears to make no contribution to resolution with 4% and 6% linear polyacrylamide filled capillaries.

In contrast, the 3% columns are very different. Resolution is inferior and the migration time shorter with the uncoated capillary. This is attributed to electro-osmotically driven migration of gel in the capillary. After approximately three sample runs, *i.e.* 1 h of operation, much of the acrylamide had eluted from the capillary. Polymer concentration is seen to be an important variable. Even small differences in concentration can have a large impact. This is attributed to a reduction in electro-osmotically driven transport at high polymer concentrations.

### *Viscosity of linear acrylamide gels*

A concentration-dependent reduction of electro-osmosis could be due to one of several phenomena. One could be that electro-osmotically driven flow is controlled by increases in viscosity at high polymer concentration. A second could be that  $\zeta$  potential and electro-osmosis are decreased by adsorption of polyacrylamide onto the capillary wall at high concentrations of polymer.

It can be seen in Fig. 2 that the viscosity of linear polyacrylamide increases exponentially with concentration. Viscosity changes from 40 cP for a 3% gel solution to 103 cP for a 4% solution. There is good correlation between viscosity and the observed difference in longevity of 3 and 4% uncoated capillaries. This does not eliminate the possibility that adsorption also plays some role at higher polymer concentration. Adhesion of polymer to the capillary wall favors both stability and heat transfer from the gel to the capillary wall [15].

### *Column stability*

Properties of a gel, such as viscosity, maybe influenced by the buffer and preparation procedure. To insure consistent polymerization the procedure for gel synthesis was strictly followed. Monomer solutions were always degassed for the same periods of time, and reaction time and temperature were identical for all cases. These procedures insure the reproducibility of capillaries as will be discussed below.

Column stability was studied with coated and uncoated capillaries filled with 4% linear polyacryl-

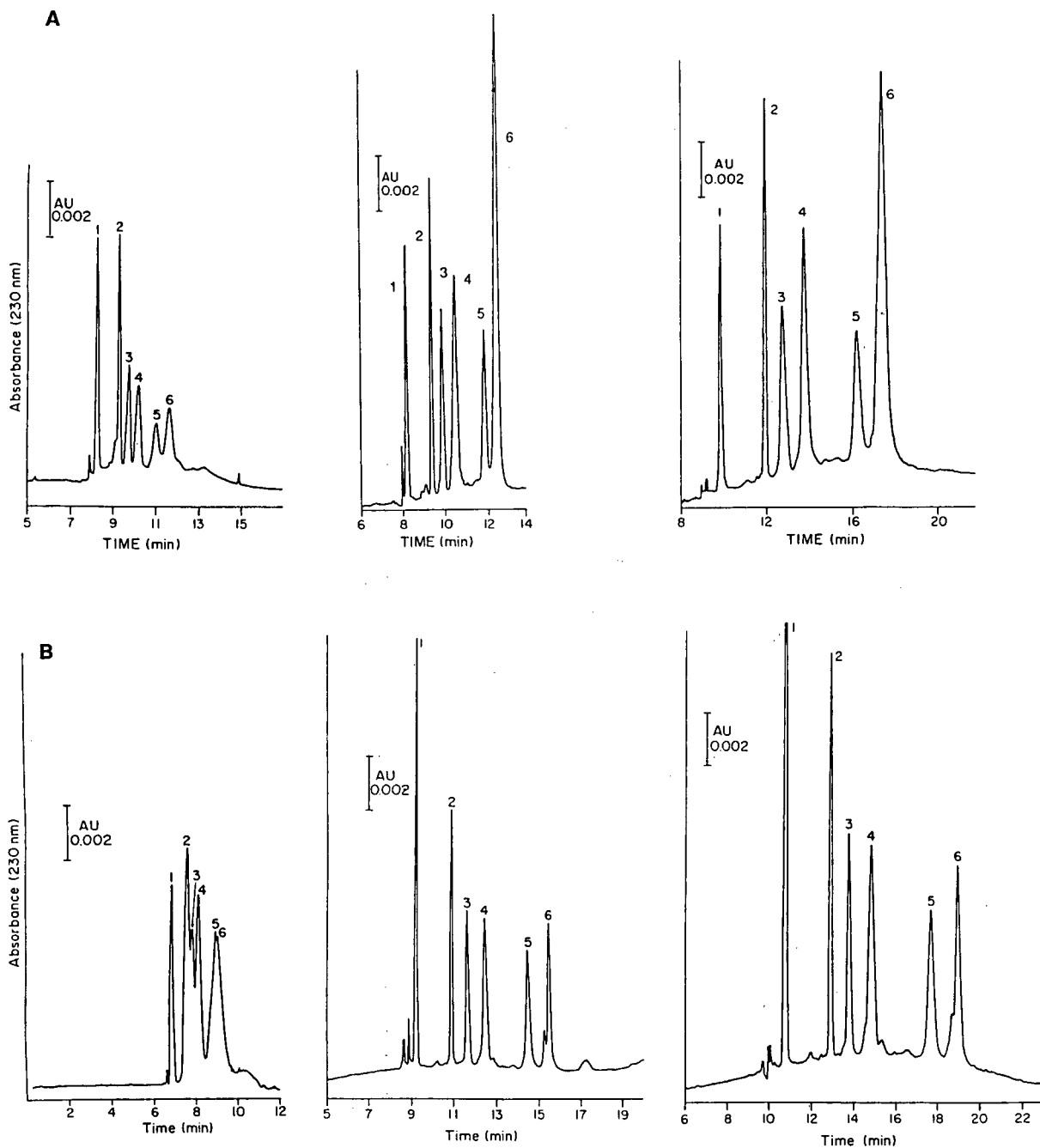


Fig. 1. Capillary gel electrophoretic separation of protein molecular mass standards on coated (A) and uncoated capillaries (B) with 3% (left), 4% (middle) and 6% (right) acrylamide concentration. Conditions: capillary length 45 cm; separation length 25 cm; 75  $\mu$ m I.D.; separation potential, 12 kV, 267 V/cm, 0.1% SDS. Peaks: 1 =  $\alpha$ -lactalbumin (bovine milk) ( $M_r$  14 400); 2 = carbonic anhydrase ( $M_r$  29 000); 3 = glyceraldehyde-3-phosphatedehydrogenase ( $M_r$  36 000); 4 = albumin (chicken egg) ( $M_r$  45 000); 5 = albumin (bovine) ( $M_r$  66 000); 6 = conalbumin ( $M_r$  78 000).

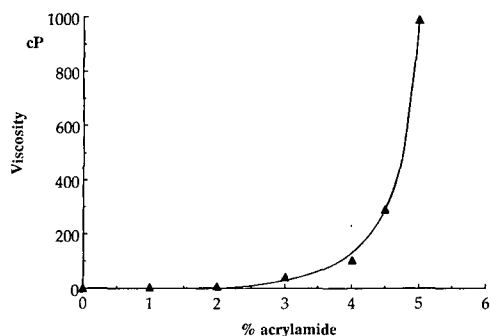


Fig. 2. Plot of the viscosity ( $\eta$ ) of the gel vs. acrylamide concentration.

amide. Coated capillaries had run-to-run and column-to-column reproducibility of 4% relative standard deviation (R.S.D.) ( $n = 14$ ) and 2% R.S.D. ( $n = 21$ ), respectively. These columns could be used for up to 6 h without significant baseline drift. Uncoated capillaries gave a run-to-run reproducibility of 2% R.S.D. ( $n = 21$ ) and could be used no more than 7 h. This generally allowed 20 samples to be run before baseline fluctuation began. Air bubble formation during use was not observed in either column type.

Baseline fluctuation was noted at 230 nm, but not at 280 nm. This phenomenon is explained in the following way. Free radical polymer polymerization of acrylamide in aqueous 0.1% SDS produces

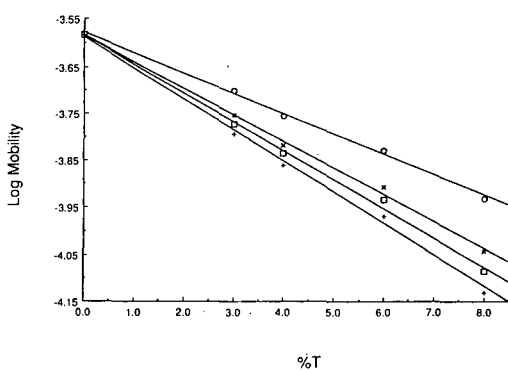


Fig. 3. Ferguson plot for linear acrylamide on uncoated capillary.  $\circ$  =  $\alpha$ -Lactalbumin (bovine milk) ( $M_r$  14 400);  $\times$  = carbonic anhydrase ( $M_r$  29 000);  $\square$  = glyceraldehyde-3-phosphate dehydrogenase ( $M_r$  36 000);  $+$  = albumin (chicken egg) ( $M_r$  45 000). Separation conditions as in Fig. 1.

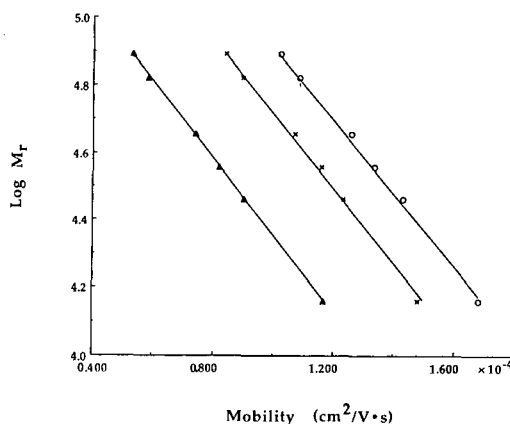


Fig. 4. Plot of log molecular mass of proteins as a function of mobility in gel columns with 4% ( $\circ$ ), 6% ( $\times$ ) and 8% ( $\blacktriangle$ ) acrylamide in uncoated columns. Separation conditions as in Fig. 1.

polymers of broad molecular mass distribution. At this concentration of SDS there will also be a weak association of the alkyl portion of SDS with the hydrocarbon backbone of polyacrylamide. Under high voltage, these SDS-polyacrylamide complexes will be induced to migrate toward the anode. Low-molecular-mass complexes will migrate more rapidly than those of high-molecular mass. After several hours of operation, an axially asymmetric molecular mass distribution of polyacrylamide should be

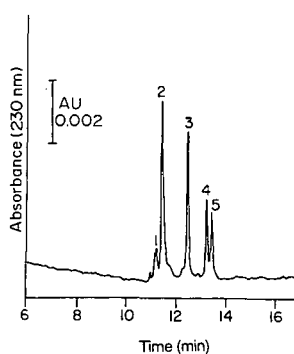


Fig. 5. Separation of myoglobin fragments on 8% acrylamide capillary. Peaks: 1 = myoglobin fragment III ( $M_r$  2510); 2 = myoglobin fragment II ( $M_r$  6210); 3 = myoglobin fragment I ( $M_r$  8160); 4 = myoglobin fragment I + II ( $M_r$  14 400); 5 = myoglobin fragment polypeptide backbone ( $M_r$  16 950). Separation conditions as in Fig. 1.



gin to occur. When the wavelength is set at 230 nm, amide absorbance is sufficiently high that these complexes are observed as they migrate past the detector. Column longevity is better at 280 nm [16].

#### Separations on uncoated capillaries

The separation of SDS denatured proteins requires a size sieving medium. A Ferguson plot [17], *i.e.* log mobility of proteins *versus* percent acrylamide (%T), exhibits a linear relationship for each protein. Fig. 3 illustrates a Ferguson plot for four proteins on uncoated capillaries containing between 3 and 8% acrylamide. The linear fits of the data were obtained by linear regression. As expected, the slopes increased with  $M_r$ , and all proteins had identical mobilities at 0% acrylamide. The relationship between electrophoretic mobility and molecular mass with linear polyacrylamide gels is seen in Fig. 4. It is interesting that in these typical plots of log

molecular mass *vs.* mobility that there is no statistically significant difference in the slopes. This is similar to cross-linked polyacrylamide gels in the slab gel format. However, higher gel concentrations are better for the separation of low-molecular-mass peptides. This is evident in the separation of myoglobin fragments of  $M_r$  2500 to 17 000 in an 8% linear polyacrylamide capillary (Fig. 5). These peptides coeluted on a 4% linear polyacrylamide gel column. Fig. 6 shows the resolution of polypeptides ranging in  $M_r$  from 6500 to 78 000 with a 6% gel while Fig. 7 shows the separation of polypeptides ranging in  $M_r$  from 29 000 to 205 000 with a 4% gel.

SDS-CGE was applied to several protein separations problems. Immunoglobulin G (IgG) purified from bovine serum by ion-exchange and reversed-phase chromatography was examined to determine purity. Following partial reduction the sample was run on a coated column with 2% polyacrylamide.

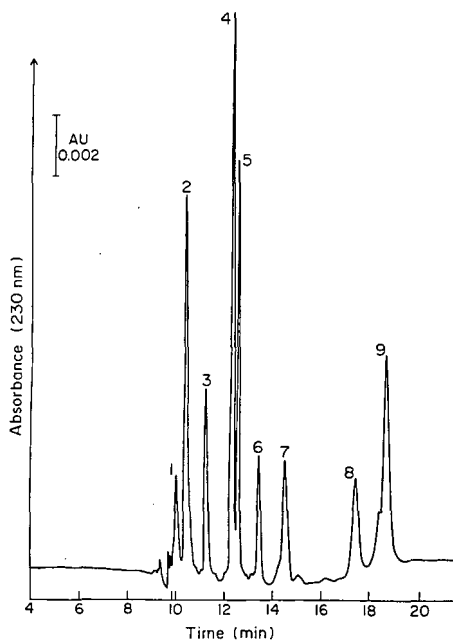


Fig. 6. Separation of protein mixture on uncoated capillary with 6% acrylamide. Peaks: 1 = aprotinin (bovine lung) ( $M_r$  6500); 2 = cytochrome *c* (horse heart) ( $M_r$  12 400); 3 = trypsin inhibitor (soybean) ( $M_r$  20 100); 4 = trypsinogen, phenylmethylsulfonyl fluoride (PMSF) treated ( $M_r$  24 000); 5 = carbonic anhydrase ( $M_r$  29 000); 6 = glyceraldehyde-3-phosphatedehydrogenase ( $M_r$  36 000); 7 = albumin (chicken egg) ( $M_r$  45 000); 8 = albumin (bovine) ( $M_r$  66 000); 9 = conalbumin ( $M_r$  78 000). Separation conditions are given in Fig. 1.

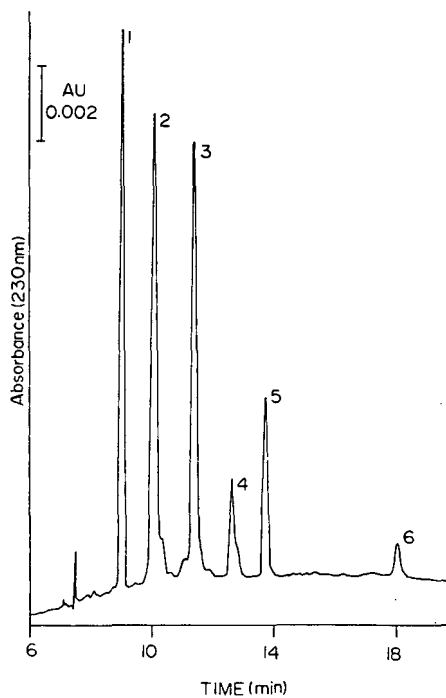


Fig. 7. Separation of protein mixture with wider molecular mass range on 4% acrylamide capillary. Peaks: 1 = carbonic anhydrase ( $M_r$  29 000); 2 = albumin (chicken egg) ( $M_r$  45 000); 3 = albumin (bovine) ( $M_r$  66 000); 4 = phosphorylase B (rabbit muscle) ( $M_r$  97 400); 5 =  $\beta$ -galactosidase (*Escherichia coli*) ( $M_r$  116 000); 6 = myosin (rabbit muscle) ( $M_r$  205 000). Separation conditions as in Fig. 1.

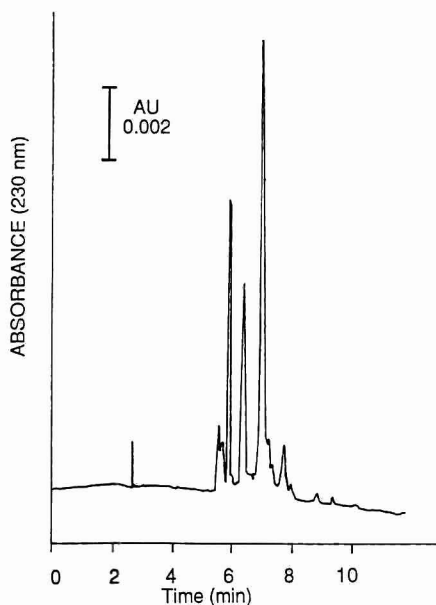


Fig. 8. Analysis of bovine IgG by capillary gel electrophoresis on coated capillary of 2% acrylamide. Separation conditions as in Fig. 1.

The three major peaks in the electropherogram (Fig. 8) represent the heavy chain of IgG ( $M_r \approx 53\,000$ ), the light chain ( $M_r \approx 22\,000$ ) and the combination of heavy and light chain ( $M_r \approx 75\,000$ ). Impurities with  $M_r$  greater than 75 000 and less than 22 000 are also clearly seen, indicating that the IgG sample still is not pure.

Human salivary proteins ranging in  $M_r$  from 14 000 to 94 000 have been separated by SDS-slab gel electrophoresis and used in clinical programs designed to monitor oral health [18]. The fact that the electrophoretic separation (Fig. 9B) and staining took over 7 h is a limitation in a clinical assay. The very high proline content of many salivary proteins is yet another complication. Proline-rich proteins are difficult to detect by conventional staining procedures. The separation and detection of human salivary proteins on a 4% linear polyacrylamide SDS-CGE system in 15 min is illustrated in Fig. 9A.

#### CONCLUSIONS

The importance of surface modification and electro-osmosis in SDS-CGE has been over-estimated

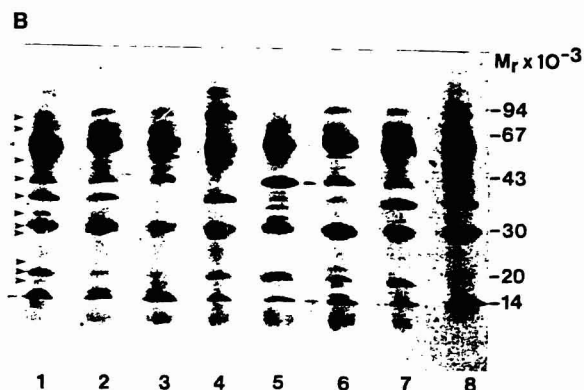
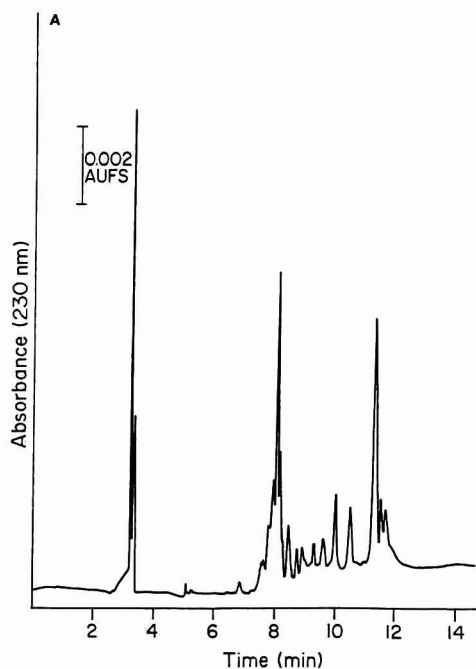


Fig. 9. (A) Separation of human salivary proteins by capillary gel electrophoresis on uncoated surface of 4% acrylamide. Separation conditions as in Fig. 1. (B) SDS-PAGE of human parotid saliva on a 12.5% slab gel. From Beeley [18].

in previous studies. When viscosity of a linear polyacrylamide solution reaches 100 cP, electro-osmosis plays no significant role in either determining separation efficiency or pumping gels from the capillary. This allows uncoated fused-silica capillaries to be used with linear polyacrylamide gels for the preparation of capillaries that may be used 20 times

without deterioration of either resolution or detection sensitivity.

#### ACKNOWLEDGEMENT

The authors thank Tim Nadler for supplying the bovine IgG sample and performing a slab SDS-PAGE separation. Funds for this research were provided by a research grant from the National Institute of Health (GM54321) and Genentech.

#### REFERENCES

- 1 K. Weber and M. Osborn, *J. Biol. Chem.*, 244 (1969) 4406.
- 2 A. S. Cohen, A. Paulus and B. L. Karger, *Chromatographia*, 24 (1987) 15.
- 3 A. S. Cohen and B. L. Karger, *J. Chromatogr.*, 397 (1987) 409.
- 4 A. Guttman, A. S. Cohen, K. N. Heiger and B. L. Karger, *Anal. Chem.*, 62 (1990) 137.
- 5 D. N. Heiger, A. S. Cohen and B. L. Karger, *J. Chromatogr.*, 516 (1990) 33.
- 6 K. Tsuji, *J. Chromatogr.*, 550 (1991) 823.
- 7 A. Guttman and N. Cooke, *Anal. Chem.*, 63 (1991) 2038.
- 8 K. Ganzler, A. S. Cohen and B. L. Karger, presented at the 3rd International Symposium on High Performance Capillary Electrophoresis, San Diego, CA, February 3–6, 1991, paper PT31.
- 9 A. S. Cohen and B. L. Karger, *J. Chromatogr.*, 397 (1987) 409.
- 10 P. F. Bente and J. Myerson, Hewlett-Packard Company, *Eur. Pat. Appl.*, EP 272 925 A2 (June 29, 1988), *US Pat.*, US 4 810 456 (Dec. 24, 1986).
- 11 A. S. Cohen, D. N. Heiger and B. L. Karger, *Eur. Pat. Appl.*, EP 417 925 A2 (March 20, 1991).
- 12 S. Hjertén, *J. Chromatogr.*, 347 (1985) 1991.
- 13 A. S. Cohen, D. R. Najarian and B. L. Karger, *J. Chromatogr.*, 516 (1990) 49.
- 14 H. F. Yin, J. A. Lux and G. Schomburg, *J. High Resolut. Chromatogr.*, 13 (1990) 624.
- 15 L. A. Osterman, *Methods of Protein and Nucleic Acid Research*, Springer, New York, 1984, p. 11.
- 16 H. Dorssman, J. A. Luckey, A. J. Kostichka, J. D'Cunha and L. M. Smith, *Anal. Chem.*, 62 (1990) 900.
- 17 K. A. Ferguson, *Metabolism*, 13 (1964) 1985.
- 18 J. A. Beeley, *J. Chromatogr.*, 509 (1991) 261.

# Assessment of the capabilities of capillary zone electrophoresis for the determination of hippuric and orotic acid in whey

P. A. Tienstra, J. A. M. van Riel, M. D. Mingorance<sup>\*</sup> and C. Olieman

Department of Analytical Chemistry, Netherlands Institute for Dairy Research (NIZO), P.O. Box 20, 6710 BA Ede (Netherlands)

## ABSTRACT

A rapid method was developed for the simultaneous determination of hippuric and orotic acid in rennet whey by capillary zone electrophoresis using an uncoated capillary utilizing a 0.04 M amino-2-methyl-1,3-propanediol (AMPD)–N,N-bis(2-hydroxyethyl)glycine (BICINE) buffer (pH 8.8) with UV detection at 254 and 280 nm. Whey proteins were removed by ultrafiltration. The method was evaluated for external, internal and standard addition procedures for both peak areas and peak heights. The use of an internal standard (sorbic acid) eliminated injection errors and gave, when applied to peak areas, the same levels for hippuric and orotic acid in those obtained with high-performance liquid chromatography. Relative standard deviations were 1–2%. Peak heights gave erratic results owing to sample matrix effects on peak widths.

## INTRODUCTION

Milk and milk products contain small amounts of hippuric and orotic acid, and milk is the main source of these components in the human diet. In addition to their possible physiological properties [1], these components are especially of interest in the processing of liquid whey to give several products where the presence of these components may or may not be desirable at low concentrations. For instance, the production of pharmaceutical-grade lactose requires that the UV absorbance at 280 nm of the final product should meet a specific criterion as described in the Dutch Pharmacopoeia [2]. Orotic acid has an absorption maximum near 280 nm and its presence in lactose could, therefore, among other

components be significant for the suitability of lactose to be classified as pharmaceutical grade. The determination of orotic acid in milk bread permits the calculation of non-fat milk solids [3]. Current methods for the determination of the title compounds are based on reversed-phase high-performance liquid chromatography (HPLC) [3–6].

Capillary zone electrophoresis (CZE) in principle offers a high separation power, which can result in short analysis times. Recently, Goodall *et al.* [7] reviewed the quantitative aspects of CZE. In order to assess the possibilities of this technique in the field of dairy research, we have developed a CZE method to determine hippuric and orotic acid in whey.

## EXPERIMENTAL

### Reagents and chemicals

Buffer A, used for CZE, consisted of a 0.04 M solution of 2-amino-2-methyl-1,3-propanediol (AMPD) (Fluka, Buchs, Switzerland) titrated to pH 8.8 with 1 M N,N-bis(2-hydroxyethyl)glycine (BICINE) (Fluka). For sample preparation 0.02 M

Correspondence to: Dr. C. Olieman, Department of Analytical Chemistry, Netherlands Institute for Dairy Research (NIZO), P.O. Box 20, 6710 BA Ede, Netherlands.

<sup>\*</sup> On leave from Estación Experimental del Zaidín (CSIC), Dept. Química Analítica Aplicada, Prof. Albareda 1, 18008 Granada, Spain.

AMPD–BICINE (pH 8.8) was prepared (buffer B).

The calibration sample for CZE was prepared by weighing about 10 mg of orotic acid (BDH, Poole, UK) and 6 mg of hippuric acid (Sigma, St. Louis, MO, USA) and dissolving them together in 200 ml of buffer B. A 10-ml volume of this solution was diluted to 25 ml with buffer B after the addition of 50  $\mu$ l of the internal standard solution of sorbic acid (50 mg/ml in buffer B) (Merck, Darmstadt, Germany) for detection at 254 nm and 625  $\mu$ l for detection at 280 nm. Appropriate dilutions were prepared in order to obtain the calibration graph.

The calibration solution used with HPLC consisted of weighed amounts of about 22 mg of orotic acid and 8 mg of hippuric acid in 100 ml of the HPLC eluent and was diluted tenfold with the HPLC eluent.

#### Capillary zone electrophoresis

Electromigration was carried out with a Beckman P/ACE System 2000 controlled with a Laser 386/2 computer with Beckman P/ACE v. 1.50 software in combination with an uncoated fused-silica capillary (50 cm  $\times$  75  $\mu$ m I.D.) fitted in a cartridge. Migrations were run at 25°C and the voltage across the capillary was maintained at 25 kV, with ground at the detector side. Injections were carried out by pressure (10 s). After each separation the capillary was flushed with 0.1 M sodium hydroxide solution for 18 s, followed by water (1 min) and buffer A (2 min). Detection was performed at 254 or 280 nm.

Peak areas and peak heights were obtained from the same raw data after processing with Caesar for Windows software (v. 1.0, B\*Wise, Geleen, Netherlands). The capillary was blown dry with nitrogen on storage.

#### Liquid chromatography

Separations were carried out with a Model 6000A pump (Millipore–Waters, Milford, MA, USA), set at 0.6 ml/min, in combination with a Model ISS-100 automatic sample injector (25- $\mu$ l injection) (Perkin Elmer, Überlingen, Germany). The column (HPX-87H; BioRad Labs., Richmond, CA, USA) was maintained at 30°C in an oven (CTO-2A; Shimadzu, Kyoto, Japan). The eluent was 0.005 M sulphuric acid, which was filtered prior to use. The solutes were detected with a Lambda Max Model 481 UV detector (Millipore–Waters) operated at 254 or 280 nm. The chromatograms were integrated with a Model SP4200 integrator (Spectra-Physics) and quantification was based on peak heights.

#### Sample treatment

For CZE analysis, 100  $\mu$ l (detection at 254 nm) or 1250  $\mu$ l (detection at 280 nm) of internal standard solution were added to a weighed amount of rennet whey (*ca.* 25 g) and the volume was made up to 50 ml with buffer A. This solution (10 ml) was diluted to 25 ml with buffer B. For standard addition 3, 5 and 10 ml of standard solution were added before the addition of buffer B. About 2 ml of the solution

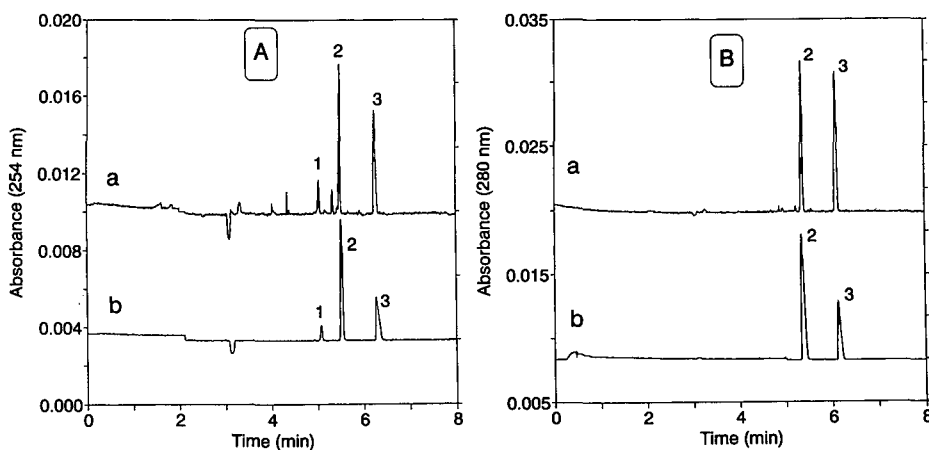


Fig. 1. Electropherogram of (1) hippuric, (2) sorbic and (3) orotic acid (a) in ultrafiltered rennet whey and (b) in a standard solution with detection at (A) 254 and (B) 280 nm. Buffer, AMPD–BICINE (pH 8.8)–0.04 M AMPD; voltage, 25 kV; detector side grounded.

obtained were ultrafiltered (LGC, modified cellulose, MW cut-off 10 000; Millipore). The first few drops were discarded and about 1 ml was collected for CZE analysis. About 30 µl of this solution were placed in a micro-insert vial.

For HPLC analysis, about 12.5 g of a weighed amount of rennet whey was diluted to 25 ml with 1 M perchloric acid and after standing for 1 h, 4 ml of this solution were filtered (MillexSLGV, Millipore, Molsheim, France) and the filtrate was used for analysis.

RESULTS AND DISCUSSION

Several buffers were investigated for the separation of hippuric and orotic acid in whey. In general we considered only so-called "super buffers", with good anion and cation buffering capacity and low conductivity. With detection at 214 nm there were in many instances interferences between matrix components and the peaks of the acids to be determined. In general, with most buffers satisfactory results were obtained when use was made of detection at 254 or 280 nm. An AMPD-BICINE (0.04 M, pH 8.8) buffer was chosen for further experiments on quantification. Sorbic acid proved to be a suitable internal standard, taking into account its migration position and its UV absorption at 254 and 280 nm

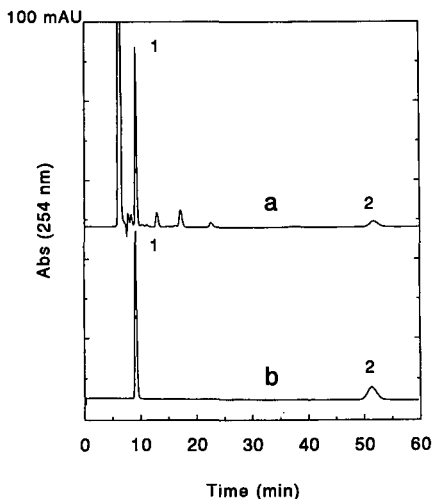


Fig. 2. Chromatogram of (1) hippuric and (2) orotic acid (a) in rennet whey and (b) in a standard solution. Column, HPX-87H at 30°C; eluent, 0.005 M sulphuric acid; flow-rate, 0.6 ml/min; detection at 254 nm.

TABLE I

RELATIVE STANDARD DEVIATIONS OF THE RESPONSE FACTORS, BASED ON PEAK AREAS, OBTAINED AFTER FIVE CALIBRATIONS OF HIPPURIC ACID AND OROTIC ACID AT DETECTION WAVELENGTHS OF 254 nm AND 280 nm, CALCULATED WITH AND WITHOUT THE INTERNAL STANDARD

Detection wavelength (nm)	Internal/external standard <sup>a</sup>	Relative standard deviation (n = 5) (%)	
		Hippuric acid	Orotic acid
254	I.S.	0.51	0.21
254	E.S.	6.8	6.8
280	I.S.	—	0.39
280	E.S.	—	1.9

<sup>a</sup> I.S. = calculated with internal standard (sorbic acid); E.S. = calculated without internal standard.

(Fig. 1). The HPLC separation is shown in Fig. 2 for the standards and whey.

The relative standard deviation (R.S.D.) of the response factors obtained with the calibration sample is given in Table I. At 280 nm the UV absorption of hippuric acid is negligible, so no response factors were obtained. A comparison of the results obtained for the external standard method with those for the internal standard method reveals that the precision of injection is sometimes poor. Errors

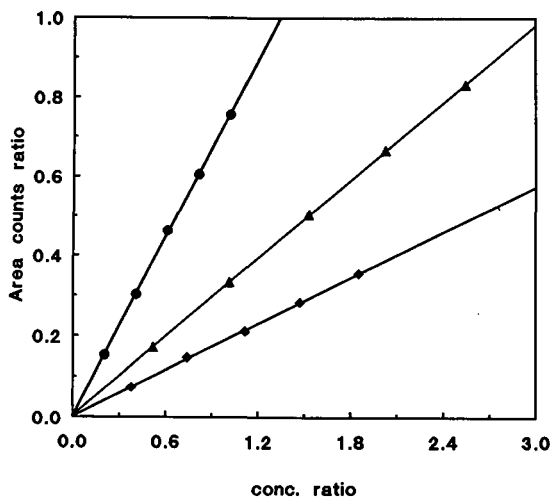


Fig. 3. Calibration graphs obtained with sorbic acid as the internal standard and detection at 254 nm for (◆) hippuric and (●) orotic acid and detection at 280 nm for (▲) orotic acid.

TABLE II

95% CONFIDENCE LIMITS FOR PREDICTED ANALYTE CONTENTS AT MEAN AREA COUNTS CORRESPONDING TO THE LOWER, MIDDLE AND UPPER PARTS OF THE CONCENTRATION RANGE USED FOR CALIBRATION

Ranges: hippuric acid, 2.85-28.5 µg/ml; orotic acid, 4.94-49.4 µg/ml.

Analyte	Detection wavelength (nm)	95% Concentration limit <sup>a</sup>					
		L (µg/ml)	M (µg/ml)	H (µg/ml)	L (%)	M (%)	H (%)
Hippuric acid	254	0.53	0.38	0.60	19	3.3	2.1
Orotic acid	254	0.96	0.67	1.13	17	3.4	2.3
Orotic acid	280	1.20	0.82	1.37	23	4.3	2.8

<sup>a</sup> L, M and H denote lower, middle and upper part of the calibration range, respectively. Calculations were performed with the Program RRGRAPH (version 4.52, Stichting Reactor Research, Delft University Press, 1990).

due to evaporation of solvent were expected to be small, because large volumes (4 ml) were used in the sample vials.

Fig. 3 shows the calibration graphs obtained at 254 and 280 nm. For both acids good linearity was

observed. The offset, obtained after linear regression, was in general significantly different from zero but small. Calculations of the accuracy of the analytical results by using the regression equation are given in Table II. For the middle and higher parts of

TABLE III

AVERAGE RESULTS AND RELATIVE STANDARD DEVIATIONS FOR THE DETERMINATION OF HIPPURIC AND OROTIC ACID IN RENNET WHEY ( $n = 5$ ) OBTAINED BY CZE IN COMBINATION WITH EXTERNAL, INTERNAL AND STANDARD ADDITION QUANTIFICATION AND WITH HPLC AS A REFERENCE METHOD

Solute	Quantification <sup>a</sup>	Concentration (mg/kg)		R.S.D. (%)	
		Peak area	Peak height	Peak area	Peak height
Hippuric acid <sup>b</sup>	E.S.	23.1	38.3	11	11
	I.S.	22.6	19.8	1.7	3.9
	S.A.i.	22.4	25.1	3.8	15
	S.A.m.	22.4	25.4	1.8	4.4
	HPLC	-	22.0	-	1.7
Orotic acid <sup>b</sup>	E.S.	75.5	111.6	10	5.8
	I.S.	74.0	58.0	0.9	3.0
	S.A.i.	74.3	172.3	2.4	23
	S.A.m.	74.5	177.0	1.0	3.3
	HPLC	-	74.9	-	0.3
Orotic acid <sup>c</sup>	E.S.	79.5	184.3	8.0	7.1
	I.S.	74.0	91.8	2.0	2.7
	S.A.i.	75.6	169.1	4.0	9.2
	S.A.m.	75.6	168.9	1.9	2.9
	HPLC	-	74.6	-	0.3

<sup>a</sup> E.S. = external standard; I.S. = internal standard; S.A.i. = standard addition, calibrated by linear regression of the three concentration levels for each sample; S.A.m. = standard addition, calibrated by linear regression of the average of three concentration levels of the five samples analysed; HPLC, average result obtained after five determinations with an HPX-87H column.

<sup>b</sup> Detection at 254 nm for CZE and HPLC.

<sup>c</sup> Detection at 280 nm for CZE and HPLC.

the calibration line acceptable results were obtained. On the basis of these observations, in practice one can obtain higher accuracy by using an average calibration (e.g.,  $n = 5$ ) at a single concentration level, comparable to that expected for the samples. This approach was used in addition to standard addition to determine the little components in rennet whey.

The results obtained for rennet whey are given in Table III. Measurement of peak areas, irrespective of the method of quantification, in all instances gave values that did not differ statistically significantly (99% confidence) from those obtained with HPLC. This means that both CZE and HPLC are devoid of systematic errors in the determination of hippuric and orotic acid in whey, because both techniques are based on entirely different principles. Moreover, for orotic acid the results were obtained at two different wavelengths, 254 and 280 nm. The repeatabilities, expressed as relative standard deviations (R.S.D.), ranged from 0.9% to 2.0% for the internal standard (I.S.) and the standard addition method with averaged response factors (S.A.m.), respectively. The external standard (E.S.) method yielded a higher R.S.D. similar to that obtained with the standards. For standard addition with calibration at three levels (S.A.i.), higher R.S.D. values were obtained. In this instance the response factor was calculated after three determinations, whereas for the I.S. methods the average of five and for the S.A.m. method the averages of five determinations at three concentration levels were used.

Peak-height measurements gave erroneous results, caused by sample matrix effects on the peak width. These effects were different for each of the acids, including sorbic acid (Fig. 1). An example is the result obtained for orotic acid with the I.S. method: at 254 nm 58 mg/kg and at 280 nm 92 mg/kg were obtained. The only difference in the sample matrix is the concentration of the internal standard sorbic acid, which is 12.5 times higher if detection at 280 nm is used, compared with detection at 254 nm. In general, one can conclude that stacking of components occurs to a different extent for each analyte and that it is highly dependent on the sample matrix. Consequently, peak height is not a good parameter for quantification, unless one can rigorously control the sample matrix.

Migration of the electrophoretic zones occurs with different speeds, and consequently the peak widths increase with increasing migration times. Peaks areas can be normalized by division by their migration times [8]. Differences between the migration times of analytes in standards and in actual samples are sometimes observed. A constant difference for the migration times of the analytes in the standard and in the sample indicates a deviation of the electroosmotic flow during a short time (probably due to sample matrix effects), after which it regains its original value. In this instance normalization of peak areas is not allowed. If there is a constant relative difference, however, then the electroosmotic flow during the whole separation is different from its original value. Normalization of peak areas is then allowed and might improve the analytical precision.

We obtained R.S.D. values for the migration times of the acids in the range 0.9–1.4%, which was caused mainly by a gradual decrease in the migration times. The differences between the migration times of the analytes in the standard and in the sample were smaller than 0.1 min. Application of normalized areas resulted in almost the same average values and R.S.D.s for hippuric and orotic acid.

## CONCLUSION

The determination of hippuric and orotic acid in whey by CZE is almost ten times faster than with HPLC. The repeatabilities are slightly lower (R.S.D. 0.9–2%) than those with HPLC (R.S.D. 0.3–1.7%), provided that use is made of an internal standard (sorbic acid). The levels found do not differ significantly from those obtained by HPLC.

## REFERENCES

- 1 J. L. Robinson, *J. Dairy Sci.*, 63 (1980) 865.
- 2 *Ned. Farmacopee*, Vol. III, SDU Uitgeverij, The Hague, 1989, p. 86.
- 3 L. V. Bui, *J. Assoc. Off. Anal. Chem.*, 72 (1989) 627.
- 4 G. H. M. Counotte, *J. Chromatogr.*, 276 (1983) 423.
- 5 W. Tiemeyer, *Dtsch. Milchwirtsch.*, 36 (1985) 807.
- 6 M. C. Gennaro and C. Abrigo, *Fresenius' J. Anal. Chem.*, 340 (1991) 422.
- 7 D. M. Goodall, S. J. Williams and D. K. Lloyd, *Trends Anal. Chem.*, 10 (1991) 272.
- 8 X. Huang, W. F. Coleman and R. N. Zare, *J. Chromatogr.*, 480 (1989) 95.





# Factors influencing the separation and quantitation of intact glucosinolates and desulphoglucosinolates by micellar electrokinetic capillary chromatography

Søren Michaelsen, Peter Møller and Hilmer Sørensen

*Chemistry Department, Royal Veterinary and Agricultural University, 40 Thorvaldsensvej, DK-1871 Frederiksberg C (Denmark)*

---

## ABSTRACT

Micellar electrokinetic capillary chromatography methods using cetyltrimethylammonium bromide as a surfactant have been developed for the qualitative and quantitative determination of intact glucosinolates and desulphoglucosinolates. The influence of changes in separation conditions has been investigated. A great number of different intact glucosinolates and desulphoglucosinolates have been used for the development of efficient separation conditions for the closely related, but structurally different, compounds. Repeatability and linearity of the quantitative analyses have been evaluated, and critical parameters have been determined. Rapid and efficient separations are possible for glucosinolates in crude extracts and for mixtures of glucosinolates isolated from seeds and the vegetative parts of plants.

---

## INTRODUCTION

Glucosinolates are plant products with well defined structures, and more than 100 glucosinolates are known [1]. Glucosinolates and degradation products of glucosinolates are of great importance for the quality of food and feed based on glucosinolate-containing plants (*e.g.* oilseed rape, cabbage and kale). High concentrations of these compounds in food and feed results in antinutritive, toxic and off-flavour effects [1,2]. This limits the possible use of economically important crops such as oilseed rape. To determine the glucosinolate content in feed, food and the various plant species containing glucosinolates, there is a need for reliable, fast and inexpensive methods of analyses for individual glucosinolates.

Available methods for the determination of individual glucosinolates include gas chromatography (GC) and high-performance liquid chromatogra-

phy (HPLC), where HPLC has several advantages over GC [1,3]. However, HPLC methods suffer from some disadvantages. Columns are expensive and sensitive to sample impurities, the chemicals are relatively expensive, the time of each analysis is typically 50–60 min, and the peak capacity and resolution obtainable are relatively low compared with that of capillary electrophoresis. An inexpensive, fast, simple and low detection limit method is therefore required.

Since the introduction of micellar electrokinetic capillary chromatography (MECC) by Terabe *et al.* in 1984 [4], this technique has been developed into very powerful and advantageous methods for the separation of various charged and uncharged compounds [5–10]. Over 700 000 theoretical plates per metre of capillary have been obtained [8]. With the experience gained from the use of ion-paired reversed-phase HPLC for the determination of glucosinolates [1,11] it was decided to investigate the use of MECC for the separation of glucosinolates.

The MECC method using cetyltrimethylammonium bromide (CTAB) has been introduced for the separation of glucosinolates [12]. It allows efficient

---

*Correspondence to:* Dr. H. Sørensen, Chemistry Department, Royal Veterinary and Agricultural University, 40 Thorvaldsensvej, DK-1871 Frederiksberg C, Denmark.

separation of various intact glucosinolates in samples obtained after a fast and simple purification and concentration step or even in the crude extracts of plants [12,13]. Furthermore, uncharged desulphoglucosinolates and various phenolic compounds can also be analysed by this technique [13,14].

This paper describes the aspects of qualitative and quantitative determinations of intact glucosinolates and desulphoglucosinolates. This includes the evaluation of the method by studying the influences of different separation conditions on migration times, peak areas, resolution, and the number of theoretical plates obtained with a wide variety of closely related but structurally different glucosinolates. The migration order of various glucosinolates is presented and discussed. Critical parameters for the repeatability and linearity of the qualitative and quantitative analyses have been determined. Furthermore, detection limits and sample solvent effects, from crude extracts or isolated samples from seeds and vegetative parts of plants, are described.

## EXPERIMENTAL

### *Apparatus*

Three different capillary electrophoresis instruments were used. The ABI Model 270A capillary electrophoresis system (Applied Biosystems, Foster City, CA, USA) was used with a 720 mm × 50 μm I.D. fused-silica capillary and detection at 500 mm from the injection end of the capillary. Data processing was performed on a Shimadzu Chromatopac C-R3A instrument (Kyoto, Japan). The Dionex capillary electrophoresis system I (Dionex, Sunnyvale, CA, USA) was used with a 650 mm × 50 μm I.D. fused-silica capillary. The detection window was 600 mm from injection end of the capillary, and data were processed by manufacturer-supplied software on an IBM PS/2 computer. The Spectra PHORESIS 1000 System (Spectra-Physics, San Jose, CA, USA) had a 690 mm × 50 μm I.D. fused-silica capillary. The detection was at 620 mm from the injection end of the capillary. Data were processed with manufacturer-supplied software on an IBM PS/2 computer.

### *Materials and reagents*

Glucosinolates (potassium salts) from the collection in this laboratory were used [1]. The com-

pounds have been extracted from various plants and isolated as intact glucosinolates or desulphoglucosinolates [1]. Determination of glucosinolate purity and identification have been based on paper chromatography, high-voltage electrophoresis, UV and NMR spectroscopy, and HPLC [1,15]. The rapeseed used was Danish-grown single and double low spring rape of different varieties (Gulliver, Ceres, Global and Line). Isolation and purification of intact glucosinolates were performed according to Bjerg and Sørensen [16] and Sørensen [1].

Sodium tetraborate and sodium phosphate were from Sigma (St. Louis, MO, USA). CTAB was from BDH (Poole, UK). All chemicals were of analytical-reagent grade.

### *Procedure*

Buffer preparation for the CTAB system consisted of stock solutions of (1) sodium tetraborate (100 mM), (2) sodium phosphate (150 mM) and (3) CTAB (100 mM). The run buffers were mixed from these stock solutions, water was added to the desired concentration, adjusted to pH 7.0, and filtered through a 0.45-μm membrane filter before use.

Buffers were changed manually on the ABI instrument after various numbers of analyses. On the Spectra-Physics instrument, buffers were changed at the detection end of the capillary between each analysis and after various numbers of analyses at the injection end. On the Dionex instrument, buffers were changed at both ends of the capillary between each analysis. Samples were introduced from the cathodic end of the capillary. Sample injections were carried out either by vacuum for 1 s (ABI) or for 6 s (Spectra-Physics), or by a hydrodynamic process at 150 mm for 25 s (Dionex). Separations were performed at 20 kV with negative polarity at the injection end unless stated otherwise. The temperatures were 30°C (ABI and Spectra-Physics) and room temperature (Dionex) unless stated otherwise. On-column UV detection was at 235 nm unless other wavelengths are stated.

The columns were washed with buffer between each analysis for 4–7 min. After various numbers of analyses, the capillary was washed for 2–4 min with 1.0 and 0.1 M NaOH.

### Calculations

Migration times were calculated relative to a reference glucosinolate in the mixture:

$$\text{RMT} = \text{MT}_1/\text{MT}_2 \quad (1)$$

where RMT is the relative migration time,  $\text{MT}_1$  is the migration time of the actual glucosinolate, and  $\text{MT}_2$  is the migration time of the reference glucosinolate for which RMT has a value of 1.

Peak areas were calculated relative to a reference glucosinolate in the sample:

$$\text{RA} = A_1/A_2 \quad (2)$$

where RA is the relative peak area,  $A_1$  is the measured peak area of the actual glucosinolate and  $A_2$  is the measured peak area of the reference glucosinolate for which RA has a value of 1.

Correct quantitation of compounds by capillary electrophoresis also involves correction of the obtained peak areas by multiplying by peak velocity [17,18]:

$$\text{VA} = A/l/\text{MT} \quad (3)$$

where VA is the velocity-corrected peak area,  $A$  is the measured peak area,  $l$  is the length of the capillary to detector, and MT is the migration time of the glucosinolate. If the capillaries have identical lengths between analyses, then the multiplication by  $l$  in eqn. 3 can be omitted [18] to obtain eqn. 4 for normalized peak area, NA:

$$\text{NA} = A/\text{MT} \quad (4)$$

The number of theoretical plates ( $N$ ) [19] was calculated as:

$$N = 16(\text{MT}/w)^2 = 5.54 (\text{MT}/w^{1/2})^2 \quad (5)$$

where  $N$  is the number of theoretical plates,  $w^{1/2}$  is the peak width at half-height, and  $w$  is the peak width at baseline.

Resolution ( $R_s$ ) [20] was calculated as:

$$R_s = 2 (\text{MT}_2 - \text{MT}_1)/1.699 (w_1^{1/2} + w_2^{1/2}) \quad (6)$$

where  $\text{MT}_1$  and  $\text{MT}_2$  are the migration times of compounds 1 and 2,  $w_1^{1/2}$  and  $w_2^{1/2}$  are their corresponding peak widths at half-height, and  $w = 1.699 \cdot w^{1/2}$ .

Repeatabilities were estimated from the means and relative standard deviations (R.S.D.). The linearity of the method was determined from linear regression analyses based on least-squares estimates.

### RESULTS AND DISCUSSION

The names and structures of the glucosinolates used in this study are presented in Fig. 1, together with numbers used in the other figures and tables. Differences between glucosinolates are due to the various types and sizes of R-groups as well as to the numerous substituents on the R-groups and the glucose moiety. More than 100 naturally occurring glucosinolates exist, but most often only a few are quantitatively dominate in the single plant species of the various glucosinolate-containing plants [1].

Preliminary high-performance capillary electrophoresis experiments were performed with buffers containing various concentrations of phosphate and borate as well as sodium dodecylsulphate. The separations obtained with the glucosinolates investigated were not acceptable, and changes of temperature and voltage did not improve the separations sufficiently in relation to expectations. The technique based on CTAB was attractive because of the possibility of both hydrophobic and ion-pairing interactions with glucosinolates [1,3,11].

The MECC separation using CTAB is based on the hydrophobic and ion-pairing interaction of the negatively charged glucosinolates and the positively charged CTAB micelles and the CTAB-coated capillary wall. This results in differential partitioning of glucosinolates in the CTAB phase in a similar way to that described for the reversed-phase HPLC method [1,3]. The electrophoretic mobility of the negatively charged glucosinolates pulls them towards the anode with electro-osmotic flow increasing their speed and CTAB retarding them, because the positively charged micelles move towards the cathode. Separations of glucosinolates can, apart from changes in voltage and temperature [12,13], also be altered by changing the composition of the running buffer (detergent, electrolyte and pH) and various other parameters.

#### Separation conditions

A systematic investigation of the influence of parameter changes on MT, RMT, NA,  $R_s$  and efficiency expressed as  $N$  have been carried out. The initial parameters used on the ABI instrument were a running buffer consisting of 18 mM borate, 30 mM phosphate and 50 mM CTAB adjusted to pH 7.0, a temperature of 30°C and the voltage set at 20

General structure:

$R_6$  and/or  $R_2$  = cinnamoyl derivatives

No.	Structure of R-groups	Trivial name	No.	Structure of R-groups	Trivial name
1	$CH_2=CH-CH_2-$	Sinigrin	23	Indole-3-ylmethylglucosinolate: $R_1=R_4=H$	Glucobrassicin
2	$CH_2=CH-CH_2-CH_2-$	Gluconapin	24		Neoglucobrassicin
3	$CH_2=CH-CH_2-CH_2-CH_2-$	Glucobrassicinapin	26	$R_1=H$ ; $R_4=OH$	4-Hydroxyglucobrassicin
4	$CH_2=CH-C(OH)(H)-CH_2-$	Proglotrin	27	$R_1=H$ ; $R_4=OCH_3$	4-Methoxyglucobrassicin
5	$CH_2=CH-C(OH)(H)-CH_2-$	Epiproglotrin	28	$CH_3-$	Methylglucosinolate
6	$CH_2=CH-C(OH)(H)-CH_2-$	Napoleiferin	29		2-Hydroxy-2-methyl-propylglucosinolate
10	$CH_3-SO-CH_2-CH_2-CH_2-$	Glucolberin	30		Epiglucobarbarin = Glucosibarbin
11	$CH_3-SO-CH_2-CH_2-CH_2-CH_2-$	Glucoraphanin	31		2-Hydroxybenzylglucosinolate
12	$CH_3-SO-CH_2-CH_2-CH_2-CH_2-CH_2-$	Glucoalyssin	32		2-Rhamnopyranosyl-oxylucosinolate
13	$CH_3-SO-CH=CH-CH_2-CH_2-$	Glucoraphenin			
14	$CH_3-SO_2-CH_2-CH_2-CH_2-$	Glucosinapin			
16		Glucotropaeolin	33	$CH_3-SO-CH=CH-CH_2-CH_2-$ $R_6$ and/or $R_2$ :	6'-Sinapoylglucoraphenin ( $R_2=H$ and $R_6=Sinapoyl$ )
17		Gluconasturtin			
18		Glucobarbarin	35		6'-Isoferuloyl-glucosibarbin ( $R_2=H$ and $R_6=Isoferuloyl$ )
20		Sinalbin			
21		Glucollmannthin			
22		Glucobrassicin			

Fig. 1. Names and structures of the glucosinolates used in MECC analyses. Numbers are used in all figures and tables, and are the same as those used by Sørensen [1].

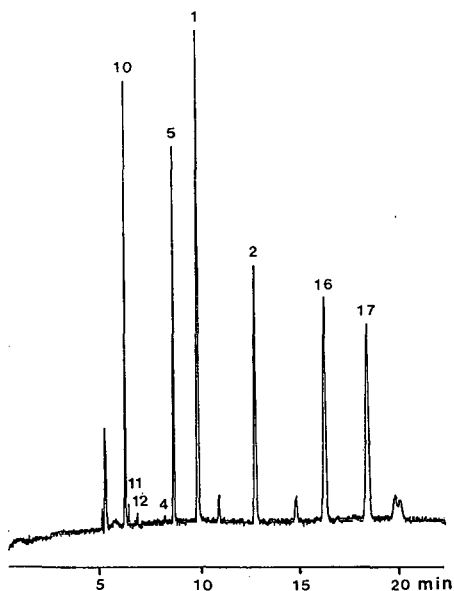


Fig. 2. Electropherogram of the mixture of glucosinolates used in the optimization studies. Numbers as in Fig. 1. Conditions: buffer of 18 mM borate, 30 mM phosphate and 50 mM CTAB adjusted to pH 7.0; temperature 30°C; voltage 20 kV; total length of capillary 720 mm and length from injection end to detector 500 mm; detection wavelength 235 nm. Vacuum injection for 1 s.

kV. The total length of the capillary was 720 mm and the length from the injection end to the detector was 500 mm. The electropherogram in Fig. 2 shows the glucosinolates used for these experiments together with their migration order.

Values of MT generally increased with CTAB concentrations from 10 to 40 mM, whereas small reductions in MT values were seen when moving from 40 to 50 mM (Fig. 3). RMT values with glucosinolate 1 as the reference compound decreased only for glucosinolates 10, 16 and 17. NA values for glucosinolates 10, 5, 1 and 2 were almost unaffected, whereas a reduction in NA values was observed for glucosinolates 16 and 17 when moving from 20 to 40 mM CTAB. NA values for these glucosinolates increased again from 40 to 50 mM CTAB (Fig. 4).  $R_s$  and  $N$  values were highest when the buffer contained 50 mM CTAB, therefore this concentration was chosen for further study.

An increase in MT values of the more hydrophobic glucosinolates with increasing CTAB concentration is anticipated due to increasing the phase ratio, *i.e.*, the ratio of the volume of the micellar phase to

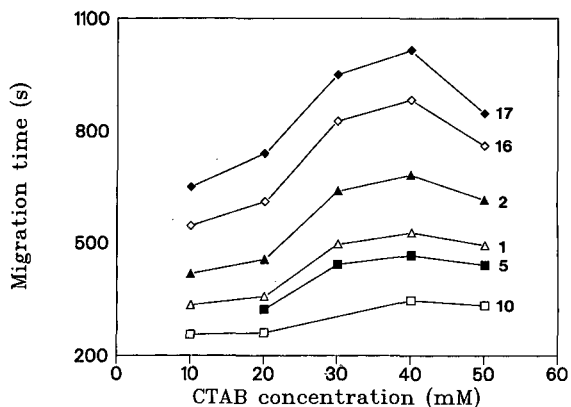


Fig. 3. Influence of CTAB concentration on migration times of glucosinolates. Numbers as in Fig. 1. Other separation conditions as in Fig. 2.

that of the aqueous phase, and may be due to changes in the magnitude of the electro-osmotic flow. The decreases in the MT values of especially the more hydrophobic glucosinolates when increasing the CTAB concentration from 40 to 50 mM may indicate an increase in the temperature of the electrolyte in the capillary [21,22] or perhaps less interaction between the CTAB micelles and glucosinolates, which is probably caused by types of CTAB aggregates other than spherical micelles [23]. In all parameters investigated here, the most profound changes were seen when increasing the CTAB concentration from 40 to 50 mM, showing

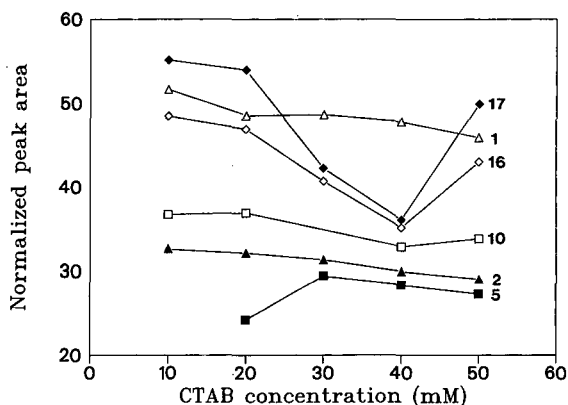


Fig. 4. Influence of CTAB concentration on normalized peak areas of glucosinolates. Numbers as in Fig. 1. Other separation conditions as in Fig. 2.

the absence of a linear response to the higher number of micelles in the buffer. The influence on NA values also indicates altered separation conditions for the hydrophobic glucosinolates. Based on these findings, it is important to note that a quantitative determination of especially the more hydrophobic glucosinolates obtained with one CTAB concentration cannot be compared with results obtained with another CTAB concentration.

Increasing the electrolyte concentration from 16 to 48 mM borate plus phosphate (in a ratio of 3:5) did not affect the MT and RMT values of the more hydrophilic glucosinolates **1**, **5** and **10**, whereas the values increased for the more hydrophobic glucosinolates **2**, **16** and **17** (Fig. 5). Only NA values of glucosinolates **16** and **17** were affected and decreased considerably when moving from 32 to 40 mM of the electrolytes (Fig. 6).  $R_s$  values were high and constant at all electrolyte concentrations for the two fastest migrating glucosinolates **10** and **5**, whereas for the other glucosinolates the  $R_s$  values increased considerably with increasing electrolyte concentration. With increasing electrolyte concentration,  $N$  values decreased for glucosinolate **10**, increased for **5**, **1** and **2**, and were unaffected for **16** and **17**.

It has been reported that electro-osmotic flow decreases with increasing electrolyte concentration [24]. This phenomena is further discussed by Bjerregaard *et al.* [14]. However, this cannot explain the observed migration times of the more hydrophilic

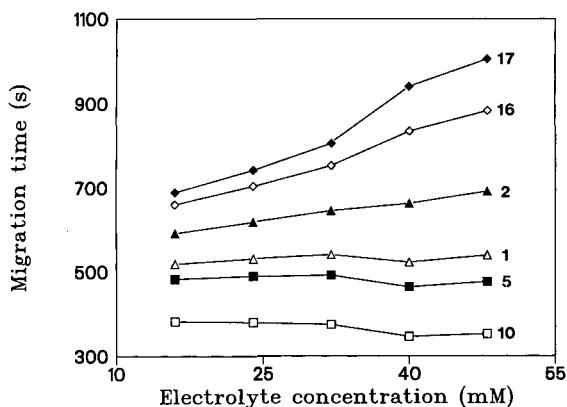


Fig. 5. Influence of electrolyte concentration (borate/phosphate in a ratio of 3:5) on migration times of glucosinolates. Numbers as in Fig. 1. Other separation conditions as in Fig. 2.

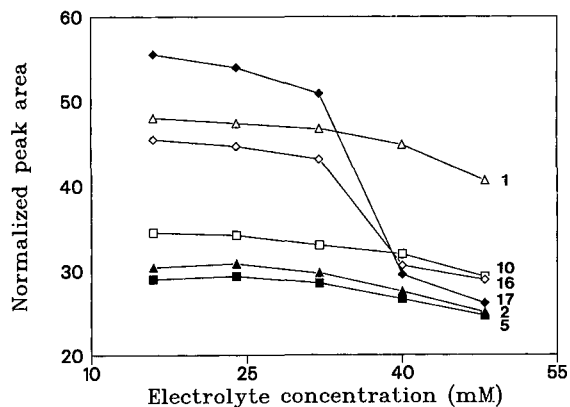


Fig. 6. Influence of electrolyte concentration (borate/phosphate in a ratio of 3:5) on normalized peak areas of glucosinolates. Numbers as in Fig. 1. Other separation conditions as in Fig. 2.

glucosinolates (Fig. 5). Increased current, due to higher electrolyte concentrations, will increase the temperature in the capillary and thereby reduce the migration times due to the lower viscosity of the buffer. This was not seen for the more hydrophobic glucosinolates. Finally, increased electrolyte concentrations in buffers containing anionic or cationic detergents may lead to an increase in the aggregation number of micelles and a decrease in the critical micelle concentration [23,25]. The same effects seem to be obtained by increasing the CTAB concentration as seen in Fig. 3. The observed behaviour of the glucosinolates is most probably a result of a combination of these effects. From the electropherograms it was seen that the large reductions in NA values for glucosinolates **16** and **17** were a result of reductions in peak height, rather than peak width. A possible explanation could be decreasing response factors (peak area/glucosinolate concentration) at high electrolyte concentrations for these aromatic glucosinolates. Response factors of glucosinolates vary in HPLC according to the glucosinolate and separation conditions [3,26], and the molar extinction coefficients vary from glucosinolate to glucosinolate [1]. Changes in response factors could also explain the variations seen in NA values when increasing the detergent concentration.

Altogether, no single effect can explain the changes observed; however, with the highest electrolyte concentration high  $R_s$  and  $N$  values were found, therefore a concentration of 48 mM was

chosen. A high electrolyte concentration in the buffer also improves the stacking conditions of sample molecules.

Changing the pH from 6.0 to 8.0 in the separation buffer had relatively little effect on the separation parameters except for NA values. MT values increased slightly, and RMT values decreased slightly, probably because of decreasing electro-osmotic flow with increasing pH [27]. Changes in NA values with pH (Fig. 7) were a result of larger peak heights and not wider peaks, indicating that band-broadening effects are not involved. The fact that the observed NA values increased for the same amount of glucosinolate at different pH values again suggests that the actual MECC response factors also change with pH. A pH of 7.0 was chosen because of slightly higher values of  $R_s$  and  $N$  at this pH value.

Increasing the voltage from 15 to 26 kV reduced the migration times and had no effect on RMT and  $R_s$  values. Only the  $N$  values determined for the two fastest migrating glucosinolates were affected. NA values for the more hydrophobic glucosinolates decreased markedly at voltages above 20 kV (Fig. 8). The reductions were a result of both lower peak heights and narrower peaks. According to Jorgenson and Lukacs [19],  $N$  would be expected to increase with increasing voltage, whereas the increase in temperature in the capillary will decrease  $N$  due to additional band broadening [28]. No clear effect on  $N$  was observed here, probably because both ef-

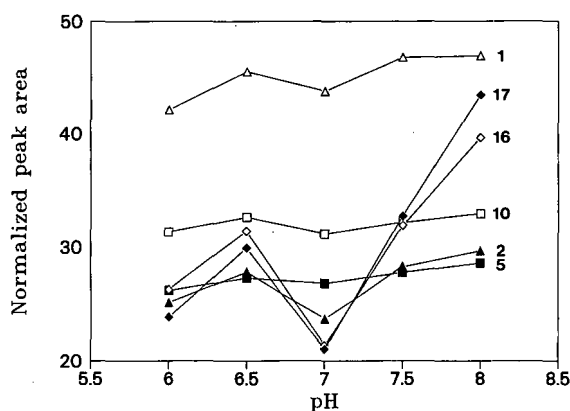


Fig. 7. Influence of buffer pH on normalized peak areas of glucosinolates. Numbers as in Fig. 1. Other separation conditions as in Fig. 2.

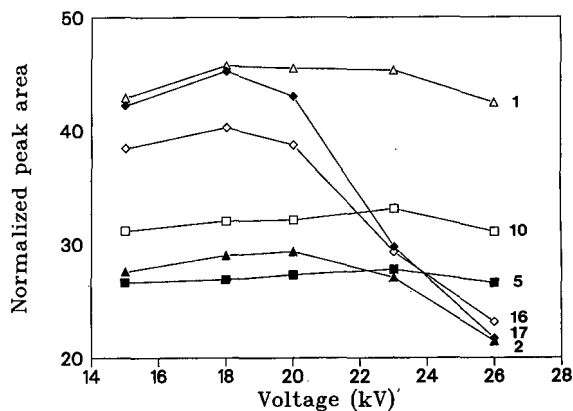


Fig. 8. Influence of applied voltage on normalized peak areas of glucosinolates. Numbers as in Fig. 1. Other separation conditions as in Fig. 2.

fects were taking place. An acceptable set of separation parameters was obtained using a voltage of 20 kV.

As mentioned in the previous discussion of changes in normalized peak areas, a general temperature increase in the capillary due to increased heat produced as a result of higher CTAB concentrations, electrolyte concentrations or voltage applied could explain the similar changes seen in NA values for the hydrophobic glucosinolates. The increase in temperature can be very significant [29], and it might result in other forms of micelles or changes in the interactions between glucosinolates and micelles.

Increasing the temperature from 25 to 45°C gave reduced migration times and had no effect on the RMT,  $R_s$  or  $N$  values. NA values increased, which again suggests changes in the response factors of glucosinolates and higher injection volume under the applied MECC conditions. These changes in NA values indicate that temperature changes within the capillary are smaller here than the changes obtained by increasing the electrolyte or CTAB concentrations or voltage. A temperature of 30°C was chosen for the separation of glucosinolates as it resulted in an acceptable total analysis time.

$N$  values determined with the chosen separation conditions for the glucosinolates 10, 5, 1, 2, 16 and 17 were 566 000, 506 000, 296 000, 350 000, 328 000 and 240 000, respectively, of theoretical plates per metre of capillary.  $R_s$  values for the glucosinolates



10–5, 5–1, 1–2, 2–16 and 16–17 were 35.8, 12.1, 22.1, 21.6 and 10.1, respectively, under the chosen separation conditions.

Separation conditions have large influences on MT, RMT, NA,  $R_s$  and  $N$  values as seen from the previously described results. The mixture of glucosinolates tested represents a wide variation of structurally different glucosinolates, and the recommendations shown for separation conditions are based on these glucosinolates. However, no single set of separation conditions can be used to separate all known glucosinolates, but changes in separation conditions can alter the absolute and relative migration times of glucosinolates. This gives the possibility of separating the actual glucosinolates found in various plant species. Once the conditions are selected, response factors of the different glucosino-

lates have to be determined for that set of conditions to use the method quantitatively. This is being undertaken now in this laboratory.

#### Repeatability

Determination of the repeatabilities of MT, RMT, NA and relative normalized peak area (RNA) values included experiments with all three capillary electrophoresis instruments. Selected results are shown in Table I and Fig. 9. The Dionex and Spectra-Physics instruments performed very well with respect to repeatabilities, whereas the ABI instrument yielded less reproducible results in the first test. When the buffer and sample were changed between each analysis, the repeatabilities improved considerably on the ABI instrument, as it is seen in test 2 (Table I). The unsatisfactory repeatabilities in

TABLE I

RELATIVE STANDARD DEVIATIONS (R.S.D.) OF MIGRATION TIMES (MT), RELATIVE MIGRATION TIMES (RMT), NORMALIZED PEAK AREAS (NA) AND RELATIVE NORMALIZED PEAK AREAS (RNA) FOR GLUCOSINOLATES

Conditions: ABI, vacuum injection for 1 s; Dionex, hydrodynamic injection for 25 s; Spectra-Physics, vacuum injection for 6 s. Other separation conditions as in Fig. 2. Numbers in bold are glucosinolate numbers (see Fig. 1).

Instrument	Relative standard deviation							
	<b>10</b>	<b>5</b>	<b>1</b>	<b>2</b>	<b>16</b>	<b>17</b>		
<i>Dionex (n = 5)</i>								
MT	0.44	0.52	0.56	0.55	0.50	0.57		
RMT <sup>a</sup>	0.22	0.16	0.09	–	0.10	0.14		
	<b>10</b>	<b>5</b>	<b>1</b>	<b>2</b>	<b>18</b>	<b>16</b>	<b>17</b>	
<i>Spectra-Physics (n = 14)</i>								
MT	1.14	1.34	1.38	1.41	1.40	1.43	1.51	
RMT <sup>a</sup>	0.51	0.37	0.26	–	0.32	0.41	0.67	
NA	0.97	0.82	0.90	1.22	1.21	1.93	2.43	
	<b>10</b>	<b>11</b>	<b>12</b>	<b>14</b>	<b>5</b>	<b>2</b>	<b>30</b>	<b>18</b>
<i>ABI test 1 (n = 16)</i>								
NA	3.25	8.46	7.64	1.99	1.71	8.57	8.63	9.01
	<b>10</b>	<b>5</b>	<b>1</b>	<b>2</b>	<b>18</b>	<b>16</b>	<b>17</b>	
<i>ABI test 2 (n = 9)</i>								
MT	2.38	2.51	2.50	2.51	2.54	2.50	2.46	
RMT <sup>a</sup>	0.28	0.18	0.10	–	0.08	0.11	0.19	
NA	2.11	1.60	1.91	2.61	1.76	1.82	1.51	
RNA <sup>a</sup>	2.23	1.58	1.45	–	1.33	1.48	1.55	

<sup>a</sup> Relative to gluconapin (2).

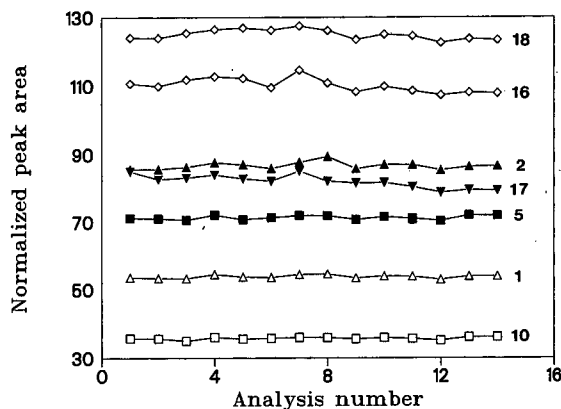


Fig. 9. Repeatability of normalized peak areas determined from fourteen analyses performed on the Spectra-Physics instrument. Vacuum injection for 6 s, other separation conditions as in Fig. 2. Numbers as in Fig. 1.

test 1 were caused by a combination of buffer depletion, running many analyses with the same buffer, and evaporation from sample vials during the test.

No anti-evaporation septa were used on the sample vials in any of the instruments, but the design of the instruments probably resulted in larger problems with evaporation from sample vials on the ABI 270A instrument due to the placement of the autosampler just under the chamber for temperature control of the capillary and fan. Evaporation from sample vials was determined in two tests at a temperature of 30°C and using four vials containing glucosinolates in a volume of 250  $\mu$ l at the beginning. The evaporation from the eight samples was determined to be 1.10–1.16% per hour. The values were obtained from the weight loss in the vials and quantitative UV measurements of glucosinolates in vials after 13 h. The introduction of the new ABI Model 270-A-MT with several buffer vials and septa for sample vials has probably reduced problems with buffer depletion and evaporation from samples when analysing many samples in a series.

R.S.D. values of similar size to the values obtained here have been reported for the peak areas of cinnamic acid and cinnamic acid analogues [27], and for migration times of various phenols [30]. As seen in Table I, the repeatability expressed as R.S.D. values was reduced considerably when RMT, NA and RNA [calculated relative to glucosinolate (2)] values were used compared with MT-val-

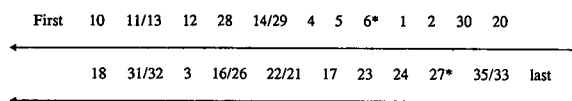


Fig. 10. Migration order of glucosinolates under standard separation conditions (see Fig. 2). Numbers as in Fig. 1. The asterisk refers to samples of *Brassica napus* seed.

ues and peak areas. R.S.D. values for RNA of between 0.8 and 2.2% were generally obtained using internal standards, showing that repeatabilities can be very high.

#### Migration order

The migration order of 28 glucosinolates was determined from MECC analyses of single glucosinolates and various glucosinolate mixtures (Fig. 10). An example of an effective separation of glucosinolates within 15 min from a mixture containing eleven different glucosinolates is seen in Fig. 11. It appears that the relatively small differences in the structure of these glucosinolates is sufficient to obtain complete separation. Desulphoglucosinolates (no charge) migrated with a higher velocity than intact glucosinolates (Fig. 12). This indicates that ion-pairing with CTAB is of greater importance than the electrophoretic mobility of the negatively charged intact glucosinolates and the hydrophobic

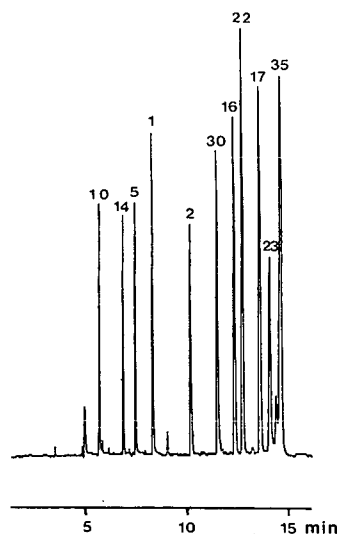


Fig. 11. Separation of eleven glucosinolates in one sample. Separation conditions as in Fig. 2. Numbers as in Fig. 1.

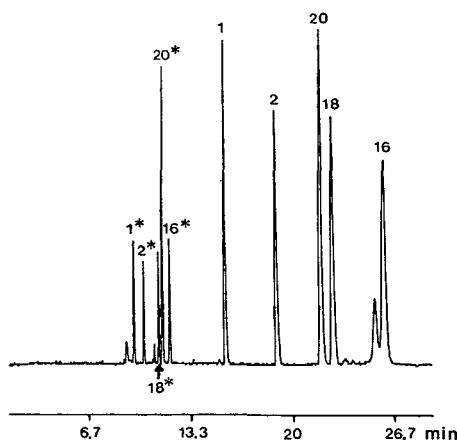


Fig. 12. Electropherogram of intact glucosinolates and desulphoglucosinolates analysed on the ABI instrument. Conditions: voltage, 16 kV; temperature, 25°C; detection wavelength, 230 nm. Other separation conditions as in Fig. 2. Numbers as in Fig. 1. The numbers with the asterisk refer to the desulphoglucosinolates.

interaction of R-groups in desulphoglucosinolates with CTAB. Furthermore, the desulphoglucosinolates of **18** and **20** changed migration order compared with that of the intact glucosinolates.

The selective retention of solutes in MECC arises from differences in the partitioning of solutes between the micellar and aqueous phases. Partitioning requires solubilization by the micelles through surface interactions or through penetration of the solute into the micelle core [31]. Solubilization of charged solutes in the micelles seems to require net-neutral ion-pairs [1,11], and solubilization may take place simultaneously or after ion-pair formation. Many complex equilibria can occur and this makes the elucidation of the solubilization mechanism difficult [31].

The behaviour of intact glucosinolates and desulphoglucosinolates was in agreement with the importance of ion-pair formation. Furthermore, the hydrophobicity of the R-group as well as steric hindrance because of the size of the R-group will influence the solubilization by micelles. The epimers **4** and **5** as well as **18** and **30** separated well, which is probably caused by differences in the steric hindrance of solubilization inside micelles. The migration order of glucosinolates in homologous series such as **10–11–12**, **5–6**, **1–2** and **16–17** showed higher hydrophobicity with longer side-chains of the

glucosinolates and no steric hindrance of solubilization. The differences in migration order of **17** compared with **18** and **30** were probably caused by the higher hydrophobicity of the glucosinolate without the hydroxygroup. Sinapoyl- (**33**) and isoferoyl- (**35**) derivatives had very high solubilities in micelles as found for reversed-phase HPLC [16]. The importance of ion-pairing for the separation of charged molecules by MECC has also been demonstrated by Nishi *et al.* [8] in the separation of water-soluble vitamins.

MT and RMT values were found to change as a result of buffer depletion and the state of the capillary. Identification of glucosinolates from RMT values should therefore be carried out with care, and identification should only be performed using standards containing one or more of the glucosinolates present in the actual samples and analysed in the same series of analyses as the samples in question. Furthermore, knowledge of the types of glucosinolates found in the actual plant material and plant species is required. As a result of differences in the number of chromophores and consequently the UV spectra of the various glucosinolates [1], it will be advantageous to use fast-scanning absorption detection for the identification of glucosinolates. Wernly and Thormann [32] demonstrated the advantages in identifying various drugs and their metabolites using fast-scanning absorption detection.

#### Linearity

The linearity of the method was determined from several tests as the correlation between increasing concentrations of different glucosinolates and the corresponding NA values. The results from one test made on the ABI instrument and one made on the Dionex instrument are shown in Table II. Correlation coefficients for the different glucosinolates were between 0.9723 and 0.9960 with only small differences between the results obtained from the two instruments. The tests were made without an internal standard, which probably would have increased the correlation coefficients [30]. However, the obtained correlation coefficients show that this MECC method gives linear increases in NA values with increasing concentrations of glucosinolates in the samples. The method can therefore be used to quantitate glucosinolates using internal standards once the correct response factors have been determined.

TABLE II

## LINEARITY TESTS USING ABI AND DIONEX INSTRUMENTS

Correlation coefficients ( $r^2$ ) from linear regression analyses by the least-squares method of normalized areas (NA) for various concentrations of glucosinolates. Conditions as in Table I and Fig. 2.

Glucosinolate	ABI ( $n = 7$ )		Dionex ( $n = 5$ )	
	Concentration range (mM)	$r^2$	Concentration range (mM)	$r^2$
10	0.146–0.488	0.9960	0.052–0.260	0.9776
5	0.119–0.396	0.9941	0.042–0.211	0.9972
1	0.169–0.566	0.9935	0.060–0.302	0.9784
2	0.160–0.533	0.9864	0.057–0.285	0.9819
16	0.198–0.660	0.9746	0.070–0.352	0.9897
17	0.337–1.123	0.9723	0.107–0.533	0.9882

*Detection limits*

Approximate detection limits have been determined from a signal-to-noise ratio of 2:1 using various dilutions of glucosinolate samples containing glucosinolate **1**, **2**, **4**, **13**, **22** and **23**. The detection limits found here correspond to the conditions applied, which were a 1-s sample injection into a 720-mm-long capillary with an internal diameter of 50  $\mu\text{m}$ . Detection limits were between 3 and 8  $\mu\text{M}$  of each glucosinolate in the sample. According to Harbaugh *et al.* [33] and Vinther [34], the injected volume should be 4.6 nl assuming a viscosity in the electrolyte and sample identical to water and with a capillary temperature of 30°C. This results in detection limits between 15 and 40 fmol for each of the glucosinolates or approximately 10 pg of glucosinolate, depending on the molecular weight.

*Sample solvent effects*

The isolation and purification of glucosinolates before HPLC analyses involve crude extracts of plant material containing up to 70% methanol [3]. Group separation of compounds in crude extracts on QMA columns described elsewhere [1] results in QMA eluates containing 50% acetonitrile, 50 mM hydrogencarbonate and 50 mM chloride [1,3]. Direct MECC analyses of QMA eluates gave very poor separations of glucosinolates. However, diluting 1:3 with water, or evaporating the solvent and redissolving in water to the same concentration,

solved the problems, showing that the high concentrations of acetonitrile in QMA eluates interfered with the CTAB micelles in spite of the low volume injected. The solvent in crude extracts also interfered with the CTAB micelles, and a dilution of 1:3 with water solved the problem. Evaporating solvent from QMA eluates and redissolving in water to the same concentration did not solve separation problems completely, whereas a further dilution of 1:1 with water did. This showed that both the solvent and high concentrations of compounds in crude extracts caused the problems seen in MECC analyses. From these results it appears that samples containing concentrations of up to 12.5% acetonitrile or up to 12–17% methanol in QMA eluates and crude extracts of glucosinolates, respectively, will not affect the separation of glucosinolates.

Many interfering compounds are seen in the electropherograms of crude extracts. However, crude extracts can, with caution, be used to identify glucosinolates present in samples. For screening purposes in plant breeding, this may in some instances be sufficient, and certainly more informative, than using total determinations of glucosinolates. Increasing the voltage or temperature will decrease migration times and make faster analyses possible.

After the group separation of plant extracts, both glucosinolates and aromatic carboxylic acids can be present in the same fractions [12]. It is possible by the method presented here to separate glucosinolates and aromatic carboxylic acids present in the same sample [12,13].

## CONCLUSIONS

In conclusion, the described MECC method gives fast and reliable determinations of glucosinolates. It is easy and fast to change the separation conditions to separate actual glucosinolates in samples from various plants. MECC analyses are inexpensive compared with HPLC analyses because of the reagents and small amounts used. The capillary is much less sensitive to impurities in samples than HPLC columns, and the capillaries are inexpensive compared with HPLC columns. Crude extracts of glucosinolates can be analysed directly. If relative migration times and normalized peak areas are used, then the repeatability and linearity of the method are good. This gives the possibility of quan-

titative determinations of glucosinolates from MECC analyses when the response factors have been determined. Critical parameters to repeatability and linearity are evaporation from samples, depletion of buffers and the state of the capillary. Precautions must be taken to avoid evaporation from the samples, and the buffers must be changed often, preferably between each analysis. The capillary must be washed with sodium hydroxide solution when migration times change too much between consecutive analyses, or as a daily routine. The peak capacity of the method is very high and can exceed 600 000 plates/m of capillary compared with typically no more than 50 000 plates/m of column in HPLC analyses of glucosinolates.

#### ACKNOWLEDGEMENTS

The authors gratefully acknowledge support from the Danish Agricultural and Veterinary Research Council and from the Danish representatives of Applied Biosystems, Dionex Corporation and Spectra-Physics with respect to use of the instruments.

#### REFERENCES

- H. Sørensen, in F. Shahidi (Editor), *Rapeseed/Canola: Production, Chemistry, Nutrition and Processing Technology*, Van Nostrand Reinhold, New York, 1990, Ch. 9, p. 149.
- B. Bjerg, B. O. Eggum, J. Jacobsen, J. Otte and H. Sørensen, *Z. Tierphysiol. Tierernähr. Futtermittelkd.*, 61 (1989) 227.
- B. Bjerg and H. Sørensen, in J.-P. Wathelet (Editor), *World Crops: Production, Utilization, Description, Glucosinolates in Rapeseeds: Analytical Aspects*, Vol. 13, Martinus Nijhoff, Dordrecht, 1987, p. 125.
- S. Terabe, K. Otsuka, K. Ichikawa, A. Tsuchiya and T. Ando, *Anal. Chem.*, 56 (1984) 111.
- A. S. Cohen, S. Terabe, J. A. Smith and B. L. Karger, *Anal. Chem.*, 59 (1987) 1021.
- M. J. Sepaniak and R. O. Cole, *Anal. Chem.*, 59 (1987) 472.
- H. Nishi and T. Tsumagari, *Anal. Chem.*, 61 (1989) 2434.
- H. Nishi, N. Tsumagari, T. Kakimoto and S. Terabe, *J. Chromatogr.*, 465 (1989) 331.
- K. Otsuka and S. Terabe, *J. Chromatogr.*, 515 (1990) 221.
- S. R. Weinberger and I. S. Lurie, *Anal. Chem.*, 63 (1991) 823.
- P. Helboe, O. Olsen and H. Sørensen, *J. Chromatogr.*, 197 (1980) 199.
- S. Michaelsen, P. Møller and H. Sørensen, *Bull. GCIRC*, 7 (1991) 97.
- C. Bjerregaard, S. Michaelsen, P. Møller and H. Sørensen, in D. I. McGregor (Editor), *Proceedings of the Eighth International Rapeseed Congress, Saskatoon, July 9–11, 1991*, Vol. 3, GCIRC, Canola Council of Canada, p. 822.
- C. Bjerregaard, S. Michaelsen and H. Sørensen, *J. Chromatogr.*, 608 (1992) 403.
- O. Olsen and H. Sørensen, *J. Am. Oil Chem. Soc.*, 58 (1981) 857.
- B. Bjerg and H. Sørensen, in J.-P. Wathelet (Editor), *World Crops: Production, Utilization, Description: Glucosinolates in Rapeseeds: Analytical Aspects*, Vol. 13, Martinus Nijhoff, Dordrecht, 1987, p. 59.
- R. G. Nielsen, G. S. Sittampalam and E. C. Rickard, *Anal. Biochem.*, 177 (1989) 20.
- R. S. Rush and B. L. Karger, *Beckman Technical Information Bulletin, TIBC-104*, Beckman, Palo Alto, 1990, 2 pp.
- J. W. Jorgenson and K. D. Lukacs, *Anal. Chem.*, 53 (1981) 1298.
- P. Gozel, E. Gassmann, H. Michelsen and R. N. Zare, *Anal. Chem.*, 59 (1987) 44.
- S. Terabe, K. Otsuka and T. Ando, *Anal. Chem.*, 57 (1985) 834.
- K. H. Row, W. H. Griest and M. P. Maskarinec, *J. Chromatogr.*, 409 (1987) 193.
- M. J. Rosen, *Surfactants and Interfacial Phenomena*, Wiley, New York, 1978, Ch. 3, p. 83.
- T. Tsuda, K. Nomura and G. Nakagawa, *J. Chromatogr.*, 248 (1982) 241.
- J. Snopek, I. Jelinek and E. Smolková-Keulemansová, *J. Chromatogr.*, 452 (1988) 571.
- R. Buchner, in J.-P. Wathelet (Editor), *World Crops: Production, Utilization, Description: Glucosinolates in Rapeseeds: Analytical Aspects*, Vol. 13, Martinus Nijhoff, Dordrecht, 1987, p. 50.
- S. Fujiwara and S. Honda, *Anal. Chem.*, 58 (1986) 1811.
- B. L. Karger, A. S. Cohen and A. Guttman, *J. Chromatogr.*, 492 (1989) 585.
- R. J. Nelson, A. Paulus, A. S. Cohen, A. Guttman and B. L. Karger, *J. Chromatogr.*, 480 (1989) 111.
- K. Otsuka, S. Terabe and T. Ando, *J. Chromatogr.*, 396 (1987) 350.
- R. A. Wallingford and A. G. Ewing, *J. Chromatogr.*, 441 (1988) 299.
- P. Wernly and W. Thormann, *Anal. Chem.*, 63 (1991) 2878.
- J. Harbaugh, M. Collette and H. E. Schwartz, *Beckman Technical Information Bulletin, TIBC-103*, Beckman, Palo Alto, 1990, 2 pp.
- A. Vinther, *Ph.D. Thesis*, Novo Nordisk and Technical University of Denmark, Copenhagen, 1991, Ch. 5, p. 5.28.

# Analysis of alkylaromatic sulphonates by high-performance capillary electrophoresis

P. L. Desbène

*UA 455, Université de Rouen, LASOC, Institut Universitaire de Technologie, 43 Rue Saint Germain, 27000 Evreux (France)*

C. Rony

*UA 455, Université P. et M. Curie, Laboratoire de Chimie Organique Structurale, 4 Place Jussieu, 75005 Paris (France)*

B. Desmazières and J. C. Jacquier

*UA 455, Institut Européen des Peptides, 76000 Rouen (France)*

---

## ABSTRACT

The potential of high-performance capillary electrophoresis for the resolution of alkylaromatic sulphonates was investigated. The operating conditions in capillary zone electrophoresis and in micellar electrokinetic chromatography were optimized on a mixture of model molecules synthesized in the laboratory. The two methods appear to be complementary. Capillary zone electrophoresis allows not only an efficient sorting out according to the number of the sulphonic groups, but also allows, using an organic solvent (acetonitrile), a better resolution in unit time of the structural homologues of the alkylbenzene sulphonates than micellar electrokinetic chromatography. On the other hand, the latter method permits the separation of alkylbenzene sulphonate isomers.

---

## INTRODUCTION

In chemical enhanced oil recovery methods such as surfactant flooding and steam foam soaks or drives, surfactants are used to achieve low interfacial tension or to make a viscous foam, respectively. The design of these processes requires a detailed study of the selection and performance of the surfactants. The surfactants usually used for these purposes are sodium alkyl aryl sulphonates made by sulphonation of a refinery stream [1]. These products consist of a mixture of homologueous series, each homologue containing isomers. Moreover, a careful design of the surfactant system is required to

tailor its composition to the characteristics of the reservoir in which it is to be applied. Hence a detailed analysis of these complex matrices appears to be essential. Linear alkylbenzene sulphonates (LAS) are anionic surfactants widely used in detergent formulations. Commercial LAS materials are mixtures of various alkyl homologues (which may vary from C<sub>9</sub> to C<sub>24</sub>) and of phenyl positional isomers [2]. Analytical methods for alkylbenzene sulphonates have therefore received considerable attention. The determination of the alkyl chain distribution of LAS was first carried out by gas chromatography (GC). This method, however, requires the conversion of the LAS into their volatile derivatives before analysis. Desulphonation with acids [3–6], alkali fusion [7], sulphochlorination [8], methylation [9], reduction [10], pyrolysis–GC [11] and acid pyrolysis–GC [12,13] are well known derivati-

---

*Correspondence to:* Dr. P. L. Desbène, UA 455, Université de Rouen, LASOC, Institut Universitaire de Technologie, 43 Rue Saint Germain, 27000 Evreux, France.

zation methods prior to GC. However, high-performance liquid chromatography (HPLC) is currently the most suitable method for the determination of the alkyl chain distribution of LAS, because it does not require the conversion of the LAS into volatile derivatives. LAS have been analysed using reversed-phase chromatography on stationary phases such as C<sub>18</sub> [14,15], C<sub>8</sub> [15] and C<sub>1</sub> [16], with mobile phases consisting of an aqueous solution of sodium perchlorate, the organic cosolvent being methanol [14], tetrahydrofuran [16] or acetonitrile [14,15]. Mixtures of LAS have also been studied using either ionic suppression [17] [on poly(styrene-divinylbenzene)phases] or ion-pair chromatography (with stationary phases of the C<sub>8</sub> [18] or C<sub>18</sub> [1,19] type and using the cetrimide or the tetrabutylammonium cation as derivatization reagent).

Some of these techniques, *e.g.* reversed-phase chromatography (with a C<sub>18</sub> stationary phase and a sodium perchlorate mobile phase) coupled with fluorimetric detection in particular, have allowed in recent years the study of the LAS in aqueous environmental samples [20] and in waste waters [21]. However, the application of these techniques to mixtures of alkylbenzene sulphonates resulting from the sulphonation of petroleum streams, such as WITCO TRS 10–80, appears to be disappointing [19]. Also, ion-exchange chromatography does not allow the resolution of complex industrial mixtures, only into mono-, di- and trisulphonates. No resolution, even partial, is possible with such broad categories of products [22]. In this context, we decided to evaluate the potential of high-performance capillary electrophoresis for the resolution of such mixtures. Taking into account the structures of the products to be analysed, we proceeded with the optimization of the operating conditions on model molecules using either capillary zone electrophoresis (CZE) or micellar electrokinetic chromatography (MEKC).

## EXPERIMENTAL

### Reagents

Butanol, which was used for the desalting of WITCO TRS 10–80 (WITCO, St. Pierre lès Elbeuf, France), chloroform and methanol, used for its de-waxing, and nitrobenzene and chlorosulphonic acid, used for the sulphonation reaction, were of

analytical-reagent grade from Merck (Darmstadt, Germany). *n*-C<sub>2</sub>–C<sub>12</sub>-alkylbenzenes and *n*-, *iso*-, *sec*- and *tert*-butylbenzene were of analytical-reagent grade from Aldrich (Strasbourg, France). For analyses by ion-exchange chromatography or high-performance capillary electrophoresis, the methanol and acetonitrile solvents were of RS HPLC grade from Fisons (Rueil-Malmaison, France). The water used for the preparation of the different buffers was systematically purified by reversed osmosis and filtration using a Milli-Ro + Milli-Q system (Millipore, Molsheim, France). The reagents needed for the buffers, *i.e.* sodium tetraborate, boric acid, phosphoric acid and monobasic sodium phosphate were of analytical reagent grade from Prolabo (Paris, France). Sodium dodecyl sulphate (SDS), used in micellar electrokinetic chromatography, was of 99% purity from Sigma (La Verpillière, France).

### Apparatus

<sup>1</sup>H and <sup>13</sup>C NMR spectra were recorded on an AC 200 system (Bruker, Wissembourg, France).

Ion-exchange chromatography was carried out on a PU 4003 chromatograph (Philips, Cambridge, UK) with a 20- $\mu$ l loop (Rheodyne, Cotati, CA, USA), a PU 4020 detector (Philips) and a Partisol SAX column (Whatman, Clifton, NJ, USA). The signal from the detector was displayed on a Kipp & Zonen (Delft, Netherlands) recorder.

High-performance capillary electrophoresis was performed on a P/ACE 2100 system (Beckman, Fullerton, CA, USA), monitored by a PS/2 computer (IBM, Greenock, UK) using GOLD software (Beckman). Data collection was performed with the same software. The UV detector was set at 214 nm. Injections were performed in the hydrodynamic mode and the injection times were set at 1 or 2 s depending on the sample. The fused-silica capillaries used were of length of 57 cm and I.D. 50 or 75  $\mu$ m.

The pH values of the buffers were systematically verified before the analyses using a Beckman Model  $\Phi$  pH meter.

### Sulphonation of alkylaromatic compounds

The alkylaromatic compounds were sulphonated using chlorosulphonic acid. The sulphonates were then precipitated as potassium salts following a

protocol adapted from Janczewski and Szczeklik [23] in order to fit the synthesis of small amounts of raw materials and to avoid the problems due to the very variable solubility of the sulphonated compounds depending on the alkyl chain length. In all instances, stoichiometric amounts of chlorosulphonic acid were added. The alkylaromatic compound was dissolved in nitrobenzene (10% solution if the solubility allowed it). The solution was cooled to 5°C and the chlorosulphonic acid was then added dropwise over 30 min, keeping the temperature at 5°C. In cases of small amounts, it was better to dilute the chlorosulphonic acid fivefold with nitrobenzene in order to allow a more regular addition.

The reaction medium was then kept at room temperature for 3 h. With relatively short substituents (chain length < C<sub>12</sub>) a volume of water equal to that of nitrobenzene was added. The solution was then allowed to settle or, if an emulsion was formed, was centrifuged. The organic phase was washed again with the same volume of water. The two aqueous phases were collected, washed with benzene and then neutralized with a 10% potassium carbonate solution. Potassium chloride solution (10%) was then added until the precipitation of the potassium sulphonate was completed. The precipitate was then filtered and dried. The raw product was used without further purification (yield 75–85%).

With long alkyl chain compounds, the sulphonic acid appeared to be insoluble in the water used for its extraction. It was then necessary to neutralize the organic phase directly with 10% potassium carbonate solution with vigorous shaking, adding 10% potassium chloride solution if necessary.

#### Purification of WITCO TRS 10–80

Mineral salts of the raw sample were precipitated using butanol. The desalted sample was then filtered and the butanol evaporated. At this stage of the purification, it was necessary to remove the non-sulphonated fractions from this complex mixture, almost all of which were alkanes. To do so, we used adsorption liquid chromatography [200 ml of Li-Chrosorb silica (Merck) for 4 g of WITCO TRS 10–80]. The sample was dissolved in *ca.* 10 ml of chloroform. This first fraction was eluted with chloroform and dried, allowing the collection of 0.46 g of waxes. The sulphonated fraction was then eluted

from the column with methanol. When the coloured strip corresponding to the polyaromatic compounds had been totally eluted, the methanol solution was vacuum concentrated, allowing the collection of 3.48 g of sulphonated compounds.

## RESULTS AND DISCUSSION

As the ion-exchange chromatography of the purified WITCO TRS 10–80 indicated that this mixture was constituted almost entirely of monosulphonated compounds (Fig. 1), we then used monosulphonated alkylbenzenes (synthesized in our laboratory) as model compounds. The model compounds were linear alkylbenzene sulphonates with alkyl chain lengths from C<sub>2</sub> to C<sub>12</sub>, as the <sup>1</sup>H and <sup>13</sup>C NMR spectra did not show evidence of very long linear chains, and all the butylbenzene sulphonate isomers, *i.e.*, *n*-, *iso*-, *sec*- and *tert*-butylbenzene sulphonates.

Taking into account the structure of the products and the very high performance of capillary electrophoresis, we first undertook the study of the behaviour of these model mixtures using CZE.

#### Capillary zone electrophoresis of linear alkylbenzene sulphonates

We used a borate–boric acid buffer at a fixed pH of 9 and studied the influence of the variation of the ionic strength on the resolution of such a mixture.

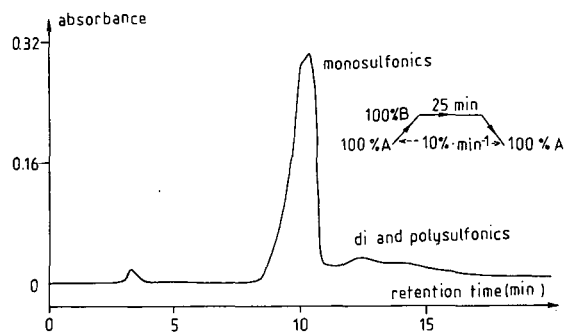


Fig. 1. Analysis of dewaxed WITCO TRS 10–80 by ion-exchange liquid chromatography. Partisil SAX column (25 × 0.46 cm I.D.), *d<sub>p</sub>* = 10 μm; UV detection at 254 nm; flow-rate 0.8 ml/min; injection, 20 μl of a 1% solution of WITCO TRS 10–80 in acetonitrile. Elution gradient: solvent A, water–methanol–acetonitrile (1:1:1); solvent B, aqueous solution of dibasic sodium phosphate–methanol–acetonitrile (1:1:1).



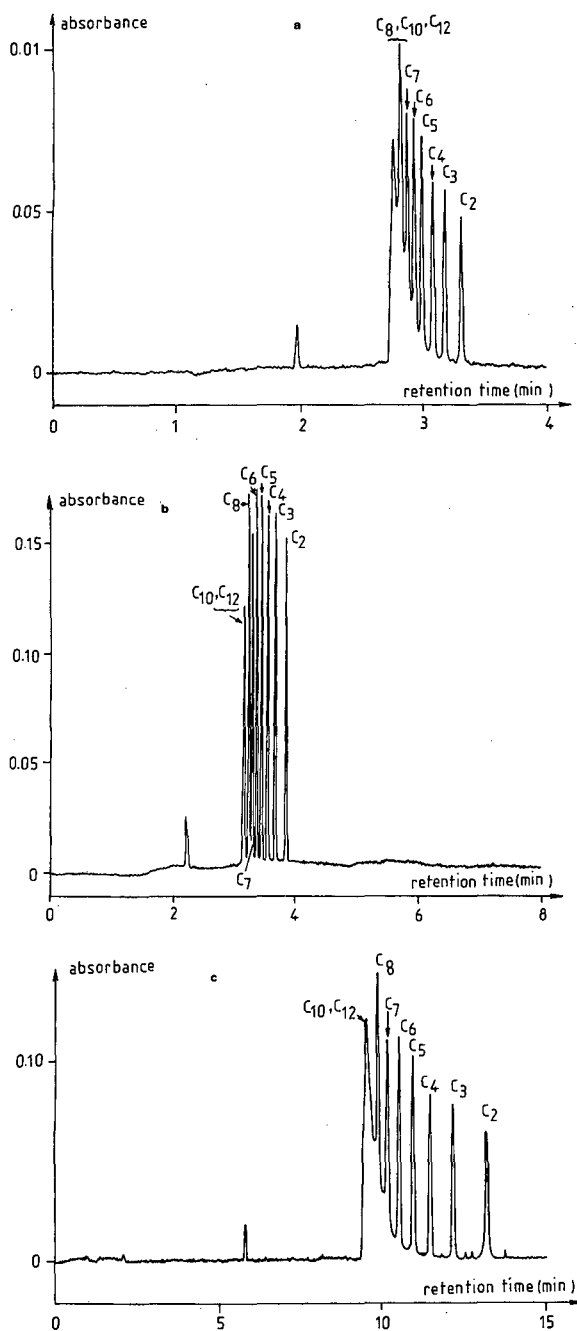


Fig. 2. Electropherograms of LAS mixture obtained by CZE. Fused-silica capillary (57 cm  $\times$  75  $\mu$ m I.D.); temperature, 30°C; hydrodynamic injection, 1 s; detection, 214 nm; borate-boric acid buffer (pH 9). (a) Buffer concentration  $6.25 \cdot 10^{-3}$  M, applied voltage 30 kV; (b) buffer concentration  $12.5 \cdot 10^{-3}$  M, applied voltage 30 kV; (c) buffer concentration  $25 \cdot 10^{-3}$  M, applied voltage 15 kV.

The capillary used was 57 cm  $\times$  75  $\mu$ m I.D., allowing us to work using voltages from 15 to 30 kV, depending on the buffer concentration. Three buffer concentrations were studied,  $6.25 \cdot 10^{-3}$ ,  $12.5 \cdot 10^{-3}$  and  $25 \cdot 10^{-3}$  M. The electropherograms corresponding to the analyses of this mixture of model compounds under each of these operating conditions are shown in Fig. 2.

It appears that the optimum buffer concentration, giving the best resolution in unit time, is  $12.5 \cdot 10^{-3}$  M. At this concentration, all the alkylbenzene sulphonates are fully separated except for the *n*-decyl- and *n*-dodecylbenzene sulphonate pair. This result is explained by the fact that this concentration still allows us to work with a high applied voltage (30 kV) while the electroosmotic flow is already low compared with that when the buffer concentration is lower ( $6.25 \cdot 10^{-3}$  M). On the other hand, with a higher buffer concentration ( $25 \cdot 10^{-3}$  M), even if the electroosmotic flow is then lower, the resolution of the mixture is worse because, taking into account the increased conductivity of the liquid medium, the applied voltage must be lowered from 30 to 15 kV, which means that the elution times will be much longer and the peaks much broader owing to the thermal agitation.

In order to resolve completely this mixture of model alkylbenzene sulphonates and so to separate the *n*-decyl- and *n*-dodecylbenzene sulphonates, we studied the influence of the addition of an organic solvent, acetonitrile in particular, on the electrophoretic behaviour of the compounds. Adding an organic solvent makes the liquid medium more hydrophobic, and one can hope to modify the conformations of the compounds and thus to modify their relative electrophoretic mobilities. Acetonitrile was chosen as the organic solvent because of its well adapted characteristics: high dielectric constant, lyophilicity and good transmittance at low wavelengths in the UV region. We therefore added acetonitrile in 5% steps, keeping the buffer pH at 9 and its concentration at  $12.5 \cdot 10^{-3}$  M, corresponding to the optimum ionic strength.

As the electroosmotic flow is systematically lowered with the addition of acetonitrile, the evolution of the elution times of the different LAS cannot be directly translated into the evolution of their electrophoretic mobility. In order to visualize such an evolution, we calculated the pseudo-capacity fac-

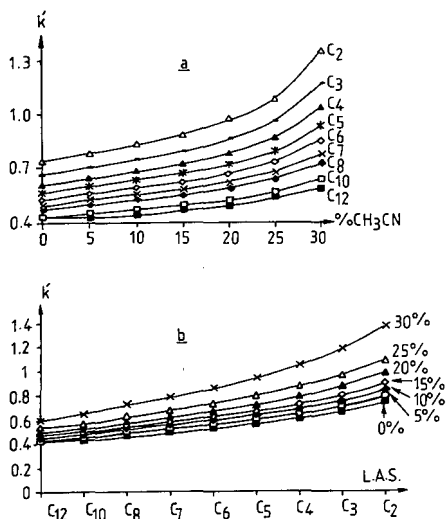


Fig. 3. Influence of acetonitrile content in the liquid medium on the electrophoretic mobility of the LAS constituting the model mixture. Borate–boric acid buffer,  $12.5 \cdot 10^{-3} M$  (pH 9); fused-silica capillary (57 cm  $\times$  50  $\mu m$  I.D.), voltage, 30 kV; detection, 214 nm; hydrodynamic injection, 2 s. (a) Evolution of the pseudo-capacity factors with the acetonitrile content for the nine studied LAS; (b) evolution of the pseudo-capacity factors with the nature of the considered LAS at different acetonitrile concentrations.

tors of the different compounds analysed. The evolution of the pseudo-capacity factors of the nine LAS studied as a function of the acetonitrile content is shown in Fig. 3a.

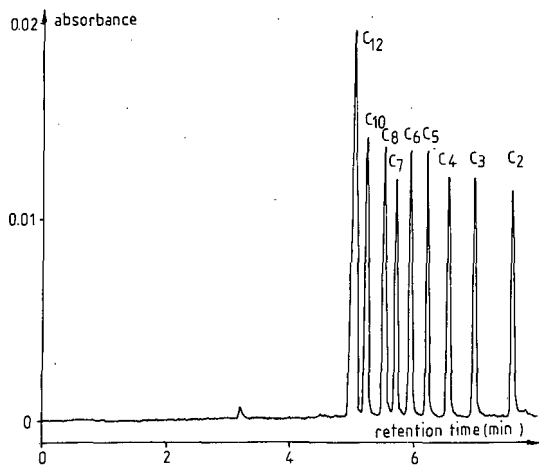


Fig. 4. Electropherogram of the LAS mixture using CZE with an acetonitrile content of 30%. Other conditions as in Fig. 3.

It appears that the electrophoretic mobility of the LAS is lowered on addition of acetonitrile, for each compound. Nevertheless, the extent of this decrease depends on the alkylbenzene sulphonate, as shown in Fig. 3b. Moreover, the selectivity of the electrophoretic system appears to be much more significant when the liquid medium contains 30% of acetonitrile when it contains none.

With the addition of 30% of acetonitrile to the liquid medium, the resolution of the nine alkylbenzene sulphonates is complete as shown on the electropherogram in Fig. 4.

#### Capillary zone electrophoresis of butylbenzene sulphonate isomers

The industrial mixture WITCO TRS 10–80 should also contain isomers of the linear alkylbenzene sulphonates, and we studied the separation of the four butylbenzene sulphonate isomers as a model.

As with the linear alkylbenzene sulphonates, we first studied the effect of ionic strength on the resolution of this mixture. The concentration used were  $6.25 \cdot 10^{-3}$ ,  $12.5 \cdot 10^{-3}$  and  $25 \cdot 10^{-3} M$ , the pH being kept at 9. As no separation occurs under these conditions, we studied for each buffer concentration the effect of the addition of acetonitrile on the resolution. Again, we obtained very poor results, with only a slight separation with 5% of acetonitrile in a  $25 \cdot 10^{-3} M$  buffer.

Hence CZE appears to be useless for the separation of such alkylbenzene sulphonate isomers. As MEKC should be more suitable for the resolution of such a mixture, its use was investigated.

#### Micellar electrokinetic chromatography of linear alkylbenzene sulphonates

We first studied the influence of the ionic strength, and therefore the influence of the buffer concentration, on the resolution of the model mixture of nine LAS. The SDS concentration was set at  $5 \cdot 10^{-2} M$ , the pH of the liquid medium at 9 using borate–boric acid buffer and the applied voltage at 25 kV. Three different buffer concentrations giving three different ionic strengths were tested:  $6.25 \cdot 10^{-3}$ ,  $12.5 \cdot 10^{-3}$  and  $25 \cdot 10^{-3} M$ . The electropherograms obtained are shown in Fig. 5.

The results indicated that the ionic strength corresponding to a buffer concentration of  $6.25 \cdot 10^{-3}$

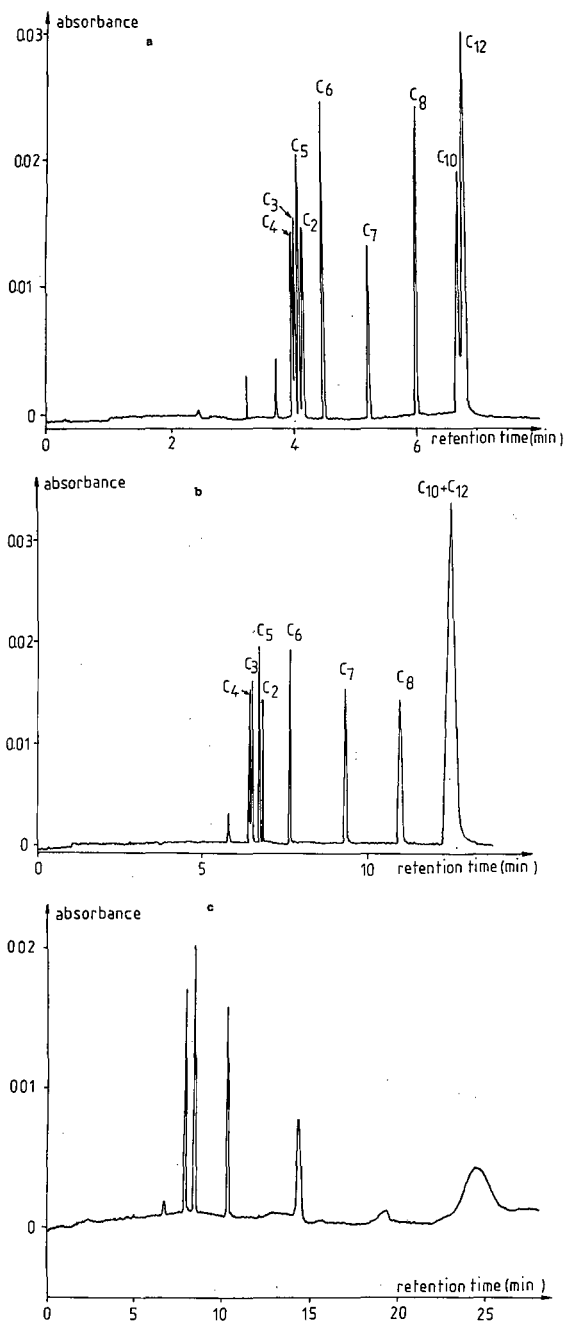


Fig. 5. Study of the influence of ionic strength on the resolution of the LAS mixture using MEKC. Fused-silica capillary (57 cm  $\times$  50  $\mu$ m I.D.); temperature, 30°C; hydrodynamic injection, 2 s; detection, 214 nm; SDS concentration,  $5 \cdot 10^{-2}$  M; borate-boric acid buffer (pH 9). (a) Borate concentration  $6.25 \cdot 10^{-3}$  M, applied voltage 25 kV; (b) borate concentration  $12.5 \cdot 10^{-3}$  M, applied voltage 20 kV; (c) borate concentration  $25 \cdot 10^{-3}$  M, applied voltage 20 kV.

$M$  is the optimum, allowing virtually a baseline separation for all the compounds except the pairs *n*-butyl- and *n*-propylbenzene sulphonates and *n*-decyl- and *n*-dodecylbenzene sulphonates. We attempted to improve the quality of the separation by studying, at this optimum concentration, the effect of the addition of an organic solvent (acetonitrile) on the resolution.

As shown by the electropherogram in Fig. 6, the addition of acetonitrile improves the resolution of the most hydrophobic LAS. However, this improvement in the resolution of *n*-decyl- and *n*-dodecylbenzene sulphonates is achieved at the expense of a decrease in the quality of separation of the less hydrophobic LAS. In fact, the resolution was poorer than that with no acetonitrile present for both the *n*-butyl and *n*-propylbenzene sulphonates and the *n*-pentyl and *n*-ethylbenzene sulphonates pairs (compare Figs. 5a and 6). Hence MEKC appears to be inferior to CZE for LAS.

#### Micellar electrokinetic chromatography of butylbenzene sulphonate isomers

We investigated the optimization of the ionic strength in separation of the model mixture of four butylbenzene sulphonates isomers. All the other parameters, *i.e.*, the applied voltage, pH and SDS concentration, were identical with those for the optimization of the resolution of the LAS model mixture using MEKC. As shown in Fig. 7a, a slight separation is obtained with buffer concentration of

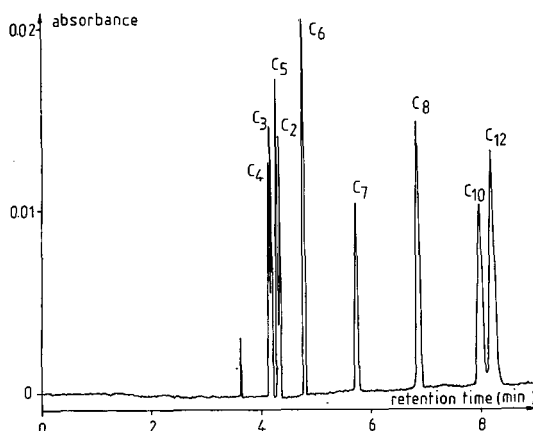


Fig. 6. Influence of acetonitrile content in the liquid medium on the MEKC behaviour of the LAS constituting the model mixture. Acetonitrile content, 5%; other conditions as in Fig. 5a.

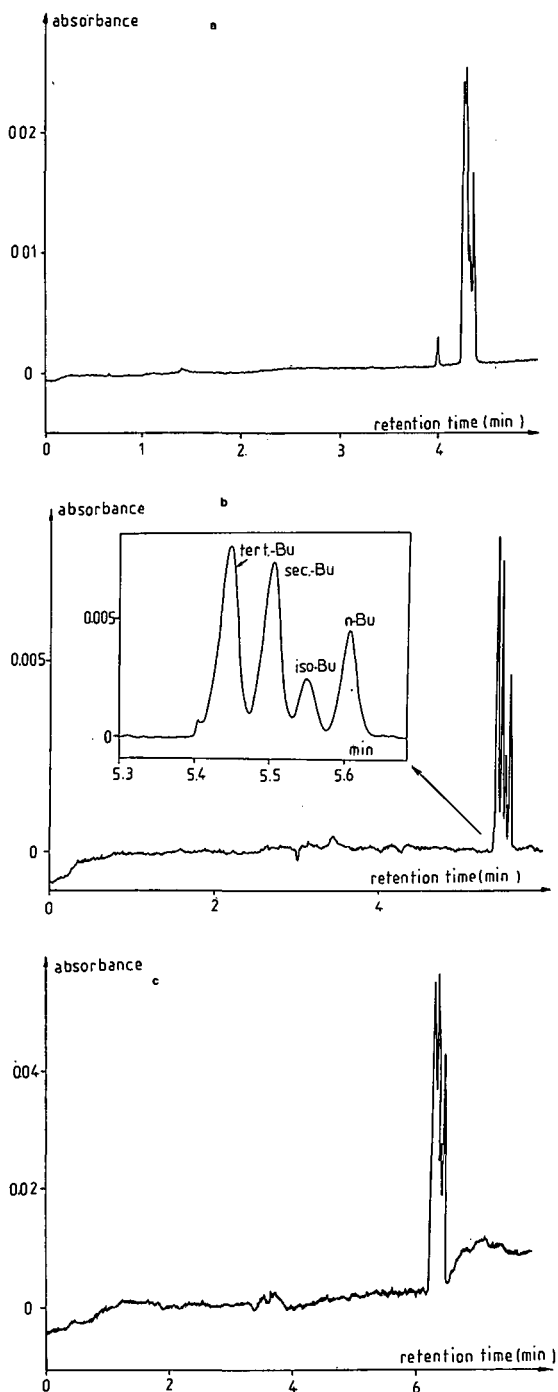


Fig. 7. Separation of the butylbenzene sulphonate isomers using MEKC. Study of the influence of the addition of an organic solvent (acetonitrile) on the separation. Acetonitrile content: (a) 0%, (b) 10% and (c) 10%. Other conditions as in Fig. 5a. Bu = butyl.

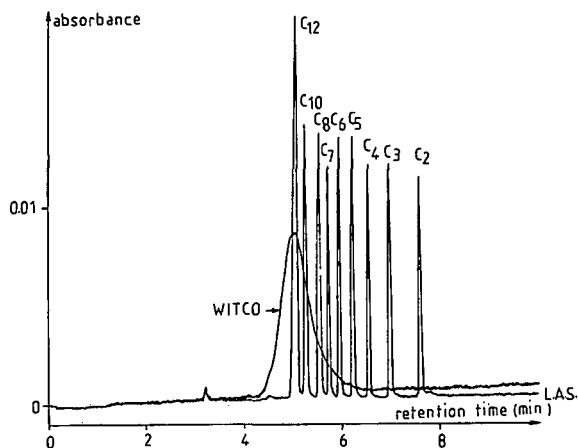


Fig. 8. Comparison of the electrophoretic behaviours of WITCO TRS 10–80 and the model LAS using CZE with the optimized operating conditions for the separation of the LAS mixture (for operating conditions, see Fig. 4).

$6.25 \cdot 10^{-3} M$ . For higher buffer concentrations, all the butyl isomers co-eluted.

As we could not achieve a satisfactory separation by varying only the ionic strength of the liquid phase, we studied the influence of the addition of acetonitrile on the resolution. The electropherograms obtained with additions of 10 and 15% of acetonitrile are shown in Fig. 7b and c, respectively. The results showed that the optimum concentration of acetonitrile in the liquid medium is 10%. Fig. 7b shows that the four isomers are almost completely separated. Therefore, MEKC appears to be a much more selective technique than CZE for the separation of alkylbenzene sulphonate isomers.

#### *Electrophoretic behaviour of WITCO TRS 10–80*

We first investigated this industrial product, which is a complex mixture of alkylaromatic sulphonates, using CZE with the previously optimized conditions for the analysis of LAS. The electropherogram obtained is shown in Fig. 8.

In order to allow a good comparison, Fig. 8 also shows the analysis of the LAS under the same conditions. It appears that WITCO TRS 10–80 gives a broad peak in the elution zone of alkylbenzene sulphonates with alkyl chain lengths between  $C_6$ – $C_7$  and  $C_{12}$ . Unfortunately, no fine resolution is obtained with WITCO TRS 10–80. Such a situation is not really surprising, as our study indicated an inability of CZE to resolve isomeric mixtures. As

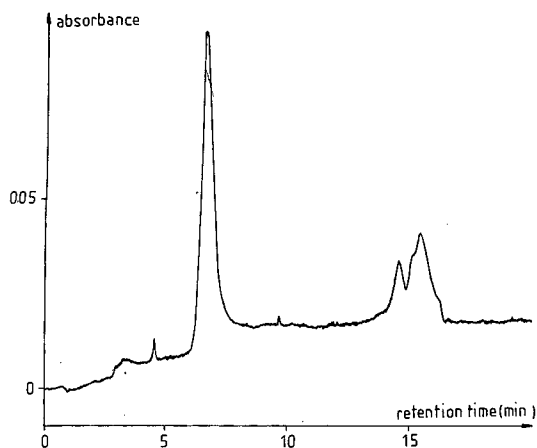


Fig. 9. Electropherogram of WITCO TRS 10–80 using CZE. Fused-silica capillary (57 cm  $\times$  50  $\mu$ m I.D.); temperature, 30°C; hydrodynamic injection, 2 s; borate–boric acid buffer,  $25 \cdot 10^{-3}$  M (pH 9); acetonitrile content, 10%; detection, 214 nm; voltage, 20 kV.

WITCO TRS 10–80 is obtained by the sulphonation of a petroleum stream, the mixture must contain a large number of isomers for each linear homologue. Despite the high performance of capillary electrophoresis, a satisfactory analysis of this complex mixture was not obtained.

Starting from these operating conditions, we tried to improve the resolution of WITCO TRS 10–

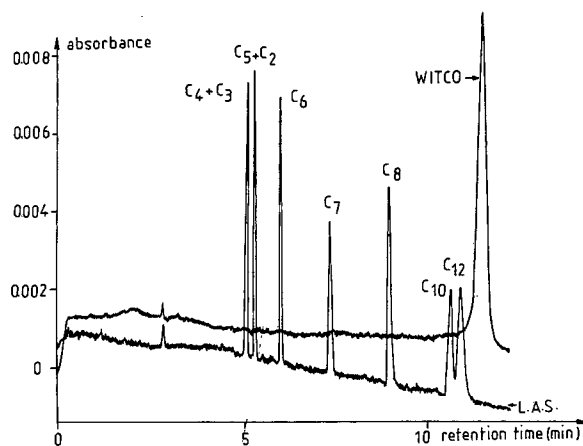


Fig. 10. Comparison of the electrophoretic behaviours of WITCO TRS 10–80 and the model LAS using MEKC. Fused-silica capillary (57 cm  $\times$  50  $\mu$ m I.D.); temperature, 30°C; hydrodynamic injection, 2 s; borate–boric acid buffer,  $6.25 \cdot 10^{-3}$  M (pH 9); acetonitrile content, 5%; SDS concentration,  $5 \cdot 10^{-2}$  M; detection 214 nm; voltage, 25 kV.

80, modifying the ionic strength and therefore the sodium tetraborate concentration and also the acetonitrile content. The electropherogram obtained is shown in Fig. 9.

Compared with the first analysis, WITCO TRS 10–80 now appeared to be a much more complex mixture. In addition to the peak previously found, this electropherogram reveals the presence of four more peaks more or less resolved. Obviously, the products corresponding to these peaks have electrophoretic mobilities clearly higher than those of the alkylbenzene monosulphonates.

Finally, we analysed WITCO TRS 10–80 using MEKC as this technique should allow the resolution not only of the homologous mixture but also of the isomers. The electropherogram for the separation of WITCO TRS 10–80 under the the previously optimized conditions for the separation of the linear alkylbenzene sulphonates is shown in Fig. 10. For comparison, the electropherogram obtained for the separation of the LAS is also shown.

This MEKC analysis confirms the results obtained by CZE, *i.e.* WITCO TRS 10–80 contains alkylaromatic sulphonates with relatively long chains. Nevertheless, because of the presence of numerous isomers, a fine resolution cannot be obtained, as the compounds constituting WITCO TRS 10–80 have elution times close to the micelle one. Effectively, the elution time of the micelle under these operating conditions was measured using Sudan III as 13 min. Under such conditions, the interactions of the analysed products with the hydrophobic micellar core are too strong and do not allow a satisfactory selectivity to reveal more or less individually the constituents.

## CONCLUSION

It appears that CZE is more selective than MEKC for the separation of linear alkylbenzene sulphonates. On adding an organic solvent (acetonitrile) to the liquid medium, a baseline separation is obtained in less than 4 min for all the studied LAS (alkyl chain lengths between C<sub>2</sub> and C<sub>12</sub>). Therefore, the analysis time is at least three times shorter compared with HPLC.

Even if MEKC appears to be less efficient than CZE for the separation of the homologous LAS mixture, it has an advantage over the latter as it

allows the resolution of alkylbenzene sulphonates isomers.

CZE and MEKC appear to be complementary techniques in the present context. Their application to the resolution of an industrial formulation (WITCO TRS 10–80) allowed us to confirm several characteristics of this complex matrix (sulphonated petroleum cut). The studies performed using either technique demonstrated that this mixture is essentially constituted of monosulphonated alkylbenzenes with relatively long alkyl chains and with a narrow distribution. Nevertheless, the presence in this mixture of numerous isomers did not allow us to obtain a good resolution and identification. The coupling of capillary electrophoresis with mass spectrometry should allow us to improve the characterization and the identification of this complex surfactant mixture.

#### REFERENCES

- 1 P. D. Pols and W. G. M. Afterof, in, *Proceedings of the 1985 SPE International Symposium on Oilfield and Geothermal Chemistry*, Society of Petroleum Engineers of AIME, Richardson, TX, 1985, Paper SPE 13571, p. 231.
- 2 A. Marcomini and W. Giger, *Anal. Chem.*, 59 (1987) 1709.
- 3 J. D. Knight and R. House, *J. Am. Oil Chem. Soc.*, 36 (1959) 195.
- 4 E. A. Sitzkorn and A. B. Carel, *J. Am. Oil Chem. Soc.*, 40 (1963) 57.
- 5 S. Lee and N. A. Puttman, *J. Am. Oil Chem. Soc.*, 44 (1967) 158.
- 6 H. Y. Lew, *J. Am. Oil Chem. Soc.*, 14 (1972) 665.
- 7 S. Nishi, *Bunseki Kagaku*, 14 (1965) 917.
- 8 S. Watanabe, M. Nukiyama, F. Takagi, K. Iida, T. Kaise and Y. Wada, *Shokuhin Eiseigaku Zasshi*, 16 (1975) 212.
- 9 M. Imaida, T. Suminoto, M. Yada, M. Yoshida, K. Koyama and N. Kunita, *Shokuhin Eiseigaku Zasshi*, 16 (1975) 218.
- 10 S. Matsutani, T. Shige and T. Nayai, *Yukagaku*, 28 (1979) 847.
- 11 T. H. Lidicoet and L. H. Smithson, *J. Am. Oil Chem. Soc.*, 42 (1965) 1097.
- 12 H. Y. Lew, *J. Am. Oil Chem. Soc.*, 44 (1967) 359.
- 13 R. Denig, *Tenside Deterg.*, 10 (1973) 59.
- 14 A. Nakae, K. Tsuji and M. Yamanaka, *Anal. Chem.*, 52 (1980) 2275.
- 15 A. Marcomini and W. Giger, *Anal. Chem.*, 59 (1987) 1709.
- 16 M. A. Castles, B. L. Moore and S. R. Ward, *Anal. Chem.*, 61 (1989) 2534.
- 17 A. Nakae and K. Kunihiro, *J. Chromatogr.*, 152 (1978) 137.
- 18 D. Thomas and J. L. Rocca, *Anal. Chem.*, 7 (1979) 386.
- 19 L. A. Verkruyse, R. V. Lewis, K. O. Meyers and S. J. Salter, in, *Proceedings of the 1983 SPE International Symposium on Oilfield and Geothermal Chemistry*, Society of Petroleum Engineers of AIME, Richardson, TX, 1983, Paper SPE 11781, p. 105.
- 20 A. Di Corcia, M. Marchetti, R. Samperi and A. Marcomini, *Anal. Chem.*, 63 (1991) 1179.
- 21 A. Marcomini, S. Capri and W. Giger, *J. Chromatogr.*, 403 (1987) 243.
- 22 F. E. Suffridge and D. L. Taggart, in, *Proceedings of the 1977 SPE International Symposium on Oilfield and Geothermal Chemistry*, Society of Petroleum Engineers of AIME, Richardson, TX, 1977, Paper SPE 6596, p. 75.
- 23 M. Janczewski and H. Szczeklik, *Rocz. Chem.*, 35 (1961) 369.



# Various approaches to analysis of difficult sample matrices of anions using capillary ion electrophoresis

William R. Jones and Petr Jandik

*Applied Technology Group, Waters Chromatography Division of Millipore, 34 Maple Street, Milford, MA 01757 (USA)*

---

## ABSTRACT

Capillary ion electrophoresis is a capillary electrophoretic technique optimized for the analysis of low-molecular-mass inorganic and organic ions. Sensitive detection is based predominantly on indirect UV since the majority of the ions lack specific chromophores. Rapid separations with efficiencies approaching 1 000 000 theoretical plates are a result of directing the electroosmotic flow towards the detector in combination with an appropriately mobile background electrolyte co-ion. Selectivity of separations can easily be predicted with the aid of readily available ionic equivalent conductances.

Described in this paper are the optimized separations of several types of samples considered until recently to be beyond the capabilities of capillary electrophoresis. These include samples of disparate concentration levels, reactive anions and trace ion analysis with detection limits in the low parts per trillion ( $10^{12}$ ) concentration range.

---

## INTRODUCTION

Capillary ion electrophoresis (CIE) (Waters' trade name: Capillary Ion Analysis, CIA) is an emerging separation technique which is rapidly expanding to encompass the various classes of ions that were once the domain of ion chromatography (IC) [1,2]. The ions characterized in our laboratory and reported in the literature include inorganic and organic anions, small chain anionic surfactants, group I and II metals, the majority of fourth period metals, Cd, Hg and the lanthanides [3–11]. Table I lists the 129 ionic species found analyzable by CIE to date. The original list reported in mid-1990 contained only 53 anions [3]. All ions were separated in fused-silica capillaries and detected at either 185, 214 or 254 nm wavelengths. The open tubular capillary provides a versatile user definable separation media which is solely dependent upon the electrolyte chemistry and polarity of the power supply. This combination controls the selectivity and mode of separation. In

contrast, IC separation selectivities are determined by type of columns which are generally specific for either anionic or cationic species. Selectivity for IC is based predominantly on the composition of the column's stationary phase and the ion-exchange moieties either covalently bound or dynamically coated to the surface, with selectivity refinements provided by the eluent [12]. IC requires more than one detection mode to visualize the ions listed in the Table I. Conductivity detection, the universal IC detection is suitable for the majority of them. Unfortunately, the less efficient separations by ion exchange (ranging from 1000 to 10 000 plates) frequently require more specific detection schemes, such as photometry with post column reaction for transition metals and amperometric detection for electroactive species such as cyanide and sulfide.

CIE achieves a very high peak capacity [13–15] for both anions and cations with rapid analysis times. Control of the electroosmotic flow (EOF) which originates from polarity and magnitude of the zeta potential [16,17] is accomplished controlling the electrolyte pH for cations and with special electroosmotic flow modifiers which dynamically coat the inner wall of the fused-silica capillary for anions.

---

*Correspondence to:* Mr. W. R. Jones, Applied Technology Group, Waters Chromatography Division of Millipore, 34 Maple Street, Milford, MA 01757, USA.



TABLE I

## ANIONS AND CATIONS THAT HAVE BEEN CHARACTERIZED BY CIE WITH UV DETECTION

The anions are divided into two categories, inorganic and organic, and are listed alphabetically. The cations are listed according to their class and in order of increasing atomic number.

<i>Inorganic anions</i>	<i>Organic anions</i>	<i>Organic anions (continued)</i>	<i>Alkali metals</i>
Arsenate	Acetate	Isocitrate	Lithium
Arsenite	<i>trans</i> -Aconitate	$\alpha$ -Ketoglutarate	Sodium
Azide	Ascorbate	Lactate	Potassium
Borate	<i>dl</i> -Aspartate	Maleate	Rubidium
Bromate	Benzoate	Malonate	Cesium
Bromide	Butanesulfonate	Methanesulfonate	<i>Alkaline earths</i>
Carbonate	Butyrate	Nonanesulfonate	Beryllium
Chlorate	4-Carboxybenzaldehyde	Octanesulfonate	Magnesium
Chloride	Chloroacetate	Orotate	Calcium
Chlorite	Citrate	Oxalacetate	Strontium
Chromate	Crotonate	Oxalate	Barium
Cyanide	Decanesulfonate	Pentanesulfonate	<i>Transition metals</i>
Fluoroborate	Dodecanesulfonate	<i>o</i> -Phthalate	Manganese
Fluoride	Dichloroacetate	Propanesulfonate	Iron
Hypochlorite	Ethanesulfonate	Propionate	Cobalt
Iodide	Formate	Pyridinedicarboxylate	Nickel
Metasilicate	Fumarate	Pyruvate	Copper
Metavanadate	Galactarate	Quinate	Zinc
Molybdate	<i>d</i> -Galacturonate	Salicylate	Cadmium
Monofluorophosphate	<i>d</i> -Gluconate	Shikimate	Mercury
Nitrate	Glucuronate	Sorbate	Lead
Nitrite	<i>l</i> -Glutamate	Succinate	<i>Lanthanides</i>
Orthovanadate	Glutarate	Tartarate	Lanthanum
Perchlorate	Glycerate	Terephthalate	Cerium
Persulfate	Glycolate	Trichloroacetate	Praseodymium
Phosphate	Glyphosate	Trifluoroacetate	Neodymium
Phosphite	Heptanesulfonate	Trimesate	Samarium
Selenate	Hexanesulfonate	<i>p</i> -Toluate	Europium
Selenite	$\alpha$ -Hydroxybutyrate	Valerate	Gadolinium
Sulfate	Hydroxymethylbenzoate		Terbium
Sulfide	2-Hydroxyvalerate		Dysprosium
Sulfite			Holmium
Thiocyanate			Erbium
Thiosulfate			Thulium
Tungstate			Ytterbium
			Lutetium
			<i>Non-metal cation</i>
			Ammonium

The EOF is made to flow towards the detector in the majority of the CIE applications. The polarity of the power supply is selected to direct electromigration of anions towards the detector as well [3]. Two important examples of EOF and analyte mobility being directed toward the detector are the simultaneous separation of alkali, alkaline earths and lanthanide

cations on one hand and the separation of 30 inorganic and organic anions on the other hand. The total run times are 1.8 and 3.1 min, respectively [4,10]. Further improvements in peak capacity are illustrated in the 36-anions electropherogram Fig. 1. The concentration range of the anions in this standard mixture is 0.3 ppb<sup>a</sup> to 3.3 ppm. The

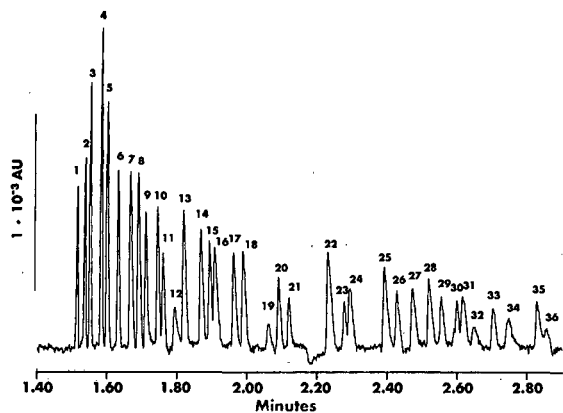


Fig. 1. Electropherogram (83-s section) of 36 anions. Peak concentrations [ppm]: 1 = thiosulfate [1.3]; 2 = bromide [1.3]; 3 = chloride [0.7]; 4 = sulfate [1.3]; 5 = nitrite [1.3]; 6 = nitrate [1.3]; 7 = molybdate [3.3]; 8 = azide [1.3]; 9 = tungstate [3.3]; 10 = monofluorophosphate [1.3]; 11 = chlorate [1.3]; 12 = citrate [0.7]; 13 = fluoride [0.3]; 14 = formate [0.7]; 15 = phosphate [1.3]; 16 = phosphite [1.3]; 17 = chlorite [1.3]; 18 = glutarate [1.7]; 19 = *o*-phthalate [0.7]; 20 = galactarate [1.3]; 21 = carbonate [1.3]; 22 = acetate [1.3]; 23 = chloroacetate [0.7]; 24 = ethanesulfonate [1.3]; 25 = propionate [1.3]; 26 = propanesulfonate [1.3]; 27 = *dl*-aspartate [1.3]; 28 = crotonate [1.3]; 29 = butyrate [1.3]; 30 = butanesulfonate [1.3]; 31 = valerate [1.3]; 32 = benzoate [1.3]; 33 = *l*-glutamate [1.3]; 34 = pentanesulfonate [1.7]; 35 = *d*-gluconate [1.7]; 36 = *d*-galacturonate [1.7]. The electrolyte is 5 mM chromate and 0.4 mM OFM Anion-BT adjusted to pH 8.0. Applied potential is 30 kV (negative polarity). Capillary dimensions are 60 cm (52 cm to detector) × 50 μm I.D. fused silica. Indirect UV detection. Injection by electromigration at 1 kV for 15 s.

standard was introduced into the capillary by electromigration. Comparing the peak capacity of a conventional anion-exchange separation, we observe only three anions, fluoride, carbonate and chloride being resolved during the same time interval Fig. 2. Using the migration time data from the 36-anion electropherogram of Fig. 2, reciprocal migration times are plotted against adjusted values of ionic equivalent conductances [18,19] adjusted to reflect the charge of the respective analyte anion found at the pH of the electrolyte [4] (Fig. 3). A good linear correlation is found with a correlation coefficient of 0.987. This is consistent with eqn. 1, where

<sup>a</sup> Throughout this article, the American billion (10<sup>9</sup>) and trillion (10<sup>12</sup>) are meant.

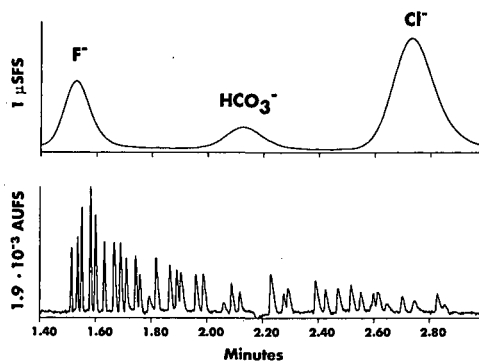


Fig. 2. Comparison of an IC separation and a CIE separation. The top plot (anion-exchange chromatogram) shows only three anions (fluoride, carbonate and chloride) using a Waters IC-Pak A, borate-gluconate eluent at 1.2 ml/min and Waters 431 conductivity detection. This separation is fully described in refs. 28 and 29. The bottom separation (CIE electropherogram) shows the 36-anion separation under conditions given in Fig. 1.

the apparent mobility,  $\mu_{app}$ , of the analyte is equal to the sum of the electrophoretic mobility,  $\mu_{ep}$ , and the electroosmotic mobility,  $\mu_{eof}$  and with  $\mu = \lambda F$ , where  $\lambda$  is the ionic equivalent conductance and  $F$  is the Faraday constant. The apparent mobility is also

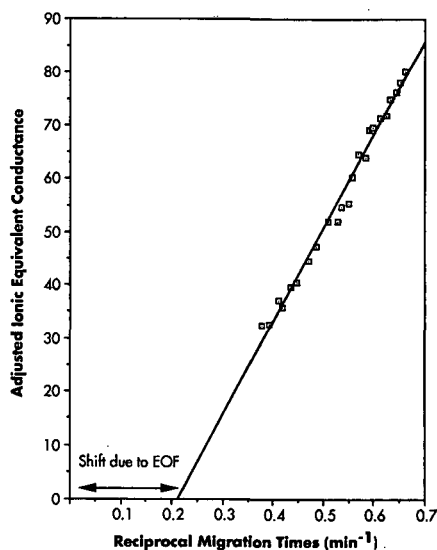


Fig. 3. Reciprocal migration times of some anions from Fig. 2 plotted against their respective values of ionic equivalent conductance for the prevalent ionic form at pH 8.0. The ionic equivalent conductances were also adjusted (□) according to valence state as described in ref. 4.  $y = -36.817 + 174.90x$ ;  $R^2 = 0.987$ .

equal to the analyte velocity,  $(L_d/t_m)$  divided by the field strength  $(V/L_t)$  (eqn. 2, where  $L_d$  is the length of the capillary to the detector,  $t_m$  is the migration time,  $V$  is the applied potential and  $L_t$  is the total length of the capillary.

$$\mu_{app} = \mu_{ep} + \mu_{eof} \quad (1)$$

$$\mu_{app} = (L_d/t_m)/(V/L_t) \quad (2)$$

From Fig. 3 the apparent electroosmotic mobility,  $\mu_{eof}$ , can be obtained from the  $x$ -intercept value and the electrophoretic mobility,  $\mu_{ep}$ , can be calculated from eqn. 1. This approach is more accurate for determining this parameter than using the water component of the sample as the neutral marker of the separation. The water peak is very broad and is measured in fractions of a minute as compared to analytes being measured in fractions of a second. Also, its apex is irregularly shaped and dependent on the sample matrix. For practical purposes, the analysis is over when the last analyte of interest has passed through the detector window, whereupon the capillary is usually purged with fresh electrolyte to remove the neutral components including the water peak and prepare for loading of the next sample.

## EXPERIMENTAL

### Instrumentation

The capillary electrophoresis (CE) system employed was the Quanta 4000 (Waters Chromatography Division of Millipore, Milford, MA, USA). Both positive and negative power supplies were employed. A Hg lamp was used for 185 and 254 nm detection and Zn lamp was used for 214 nm. Waters AccuSep polyimide-coated fused-silica capillaries are used throughout this work. The capillary dimensions ranged from 40 to 60 cm total length with the detection window placed 8 cm from the receiving electrolyte end to the detector cell. Both 50 and 75  $\mu\text{m}$  I.D. capillaries were employed. Data acquisition was carried out with a Waters 860 data station with SAT/IN and LAC/E modules connecting the CE system to the data station. Detector time constant was set at 0.1 s and data acquisition rate was 20 Hz. Collection of electropherographic data was initiated by a signal cable connection between the Quanta 4000 and the SAT/IN module.

### Preparation of electrolytes

The electrolytes were prepared from various salts. For indirect UV detection  $\text{Na}_2\text{CrO}_4 \cdot 4 \text{H}_2\text{O}$  99 + % (Aldrich, Milwaukee, WI, USA) was used exclusively. Direct UV detection electrolytes used sodium chloride (Sigma, St. Louis, MO, USA) or hexanesulfonic acid, sodium salt 98% (Aldrich). Adjustment of electrolyte pH was done with various acids and bases depending on the application. In the first step the acid and base solutions were prepared in concentrations of 100 mM from lithium hydroxide monohydrate,  $\text{H}_2\text{SO}_4$  (Ultrex grade), glacial acetic acid. (J. T. Baker, Phillipsburg, NJ, USA). Waters CIA-Pak OFM Anion-BT<sup>a</sup> a 20 mM EOF modifier concentrate was added to some electrolytes in the 0.4–0.5 mM concentration range in order to reverse the direction of EOF when using negative power supply. The OFM modifier was converted to the chloride form for low-UV work at 214 nm and the hydroxide form for certain disparate concentration level samples. In both cases conversion of the OFM modifier was accomplished through replacement of the OFM anion with anion-exchange resin in the chloride (AG1-X8, 200–400 mesh) and hydroxide form (AG1-X8), respectively. (Bio-Rad Labs., Richmond, CA, USA). All resins were precleaned by soaking resin in 18 M $\Omega$  water for 24 h prior to use. A 5-ml volume of cleaned resin bed was packed into in a Pharmaseal Stylex 10-ml Luer tip syringe (American Pharmaseal Labs., Glendale, CA, USA) with a Millex-HV 0.45- $\mu\text{m}$  filter unit (Millipore, Bedford, MA, USA) to contain the resin. The resin was rinsed once with 5 ml of 18 M $\Omega$  water prior to placing the OFM concentrate through for conversion. Milli-Q reagent-grade water (Millipore) was used for rinsing and dilution. Sodium octanesulfonate used as an additive to samples prior to preconcentration was purified by recrystallization in 18 M $\Omega$  water (Kodak, Rochester, NY, USA).

### Standard analyte solutions

All standard solutions were prepared by a dilution of 1000 ppm stock solutions containing a single anion. The stock solutions were prepared fresh every six months and were stored in 200-ml polycarbonate tissue culture flasks (Corning Glass Works, Corning, NY, USA). All mixed anion standards were

<sup>a</sup> Patents pending.

prepared freshly for each of the experiments. Milli-Q water and polymethylpentene containers (Nalgene, Rochester, NY, USA) were used throughout. For electromigrative injections, low-ppb samples were prepared by adding ppm concentrations of sodium octanesulfonate according to the procedure described elsewhere [5].

#### System operation

The CE system incorporates two modes of sample entry into the capillary—hydrostatic and by electro-migration. Two sample carousel configurations were employed. For hydrostatic mode of injection a 20-sample carousel was used with 600- $\mu$ l polypropylene centrifuge tubes (Waters) for sample vials. Electromigration injections utilized a 6-sample carousel with 2-ml polypropylene VersaVial (Sun Brokers, Wilmington, NC, USA) vials for trace analysis samples.

### RESULTS AND DISCUSSION

#### Actual samples and standards

Of the various types of samples, Kraft Black liquor from pulp and paper production is one of the more difficult samples for IC. Its high-pH matrix containing reactive sulfur species and polyphenolic compounds poisons IC columns [6]. However, open tubular capillaries are not prone to fouling as is the case with IC columns, since it does not contain any packing material that could be affected. A thousandfold dilution in water prior to injection into the CE system is the only sample preparation required [10,20].

Certain types of samples, however, do interact with CE capillaries. A sample that was found to modify the wall of a capillary was brewed coffee. Increased migration times were observed after every injection of the sample. This migration time shift could be eliminated with an automated three-stage rinse cycle of 100 mM lithium hydroxide for 2 min, 18 M $\Omega$  water (Milli-Q water) for 1 min and running electrolyte for 2 min, performed between sample injections. Fig. 4A shows four consecutive injections of a coffee sample with only a 2-min purge of electrolyte before each sample loading. Fig. 4B shows four consecutive injections of a coffee sample with the three-stage rinse cycle performed before each sample loading as described above.

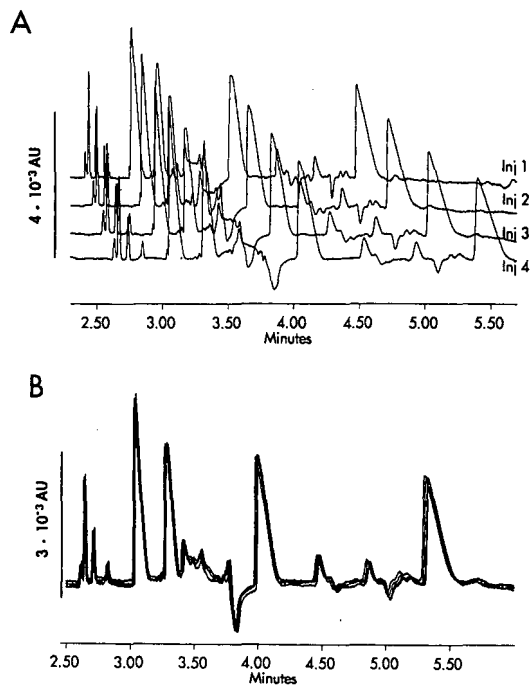


Fig. 4. (A) Four consecutive injections overlaid of a brewed coffee sample using only a 2-min purge electrolyte purge before each sample loading. (B) Four consecutive injections overlaid of a brewed coffee sample using a three-stage rinse cycle consisting of 100 mM lithium hydroxide for 2 min, 18 M $\Omega$  water (Milli-Q water) for 1 min and running electrolyte for 2 min, performed between sample injections. The electrolyte is 5 mM chromate and 0.5 mM OFM Anion-BT, pH 8. Applied potential is 20 kV (negative polarity). Capillary dimensions are 60 cm ( $L_t$ ), 52 cm ( $L_d$ ) and 50  $\mu$ m I.D. Injection is hydrostatic (10 cm for 30 s).

The monitoring of anionic disinfection byproducts in drinking water can be accomplished by the separation shown in Fig. 5. Eight common inorganic anions with inorganic oxyhalides and halogenated organic acids can be analyzed in about 4.2 min. This is another example of how selectivity inherent to CIE permits separations that are traditionally difficult by IC. Three difficult problems encountered in IC are solved by this CIE method: (1) resolution of chlorate from nitrate, (2) separation of fluoride from acetate and other monovalent organic acids and (3) determination of perchlorate which is a very highly retained anion on resin-based IC columns. A 5 mM chromate with 0.3 mM OFM Anion-BT electrolyte at pH 8.0 was used for the separation. The reduced concentration of OFM, 0.3 mM rather than 0.5 mM,

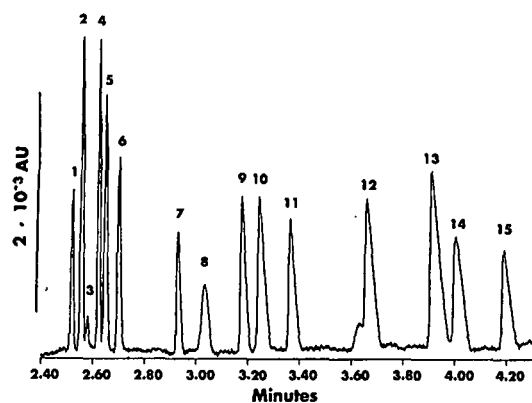


Fig. 5. Separation of fifteen inorganic and organic halides. Peaks and concentrations [ppm]: 1 = bromide [4]; 2 = chloride [2]; 3 = iodide [4]; 4 = sulfate [4]; 5 = nitrite [4]; 6 = nitrate [4]; 7 = chlorate [4]; 8 = perchlorate [4]; 9 = fluoride [1]; 10 = phosphate [4]; 11 = chlorite [4]; 12 = carbonate [4]; 13 = acetate [5]; 14 = monochloroacetate [5]; 15 = dichloroacetate [5]. The electrolyte is 5 mM chromate and 0.3 mM OFM Anion-BT adjusted to pH 8.0. Applied potential is 20 kV (negative polarity). Capillary dimensions are 60 cm ( $L_t$ ), 52 cm ( $L_d$ ) and 75  $\mu\text{m}$  I.D. Injection is hydrostatic (10 cm for 30 s).

used in most applications placed the hydrophobic perchlorate anion before fluoride. At 0.5 mM OFM the perchlorate has a reduced mobility and comigrates with carbonate. This is assumed to be a result of ion-pairing of perchlorate and OFM.

#### Disparate concentrations (analysis of fine chemicals)

Samples that contain an excess of one ion with respect to another ion often make it difficult to resolve the excess concentration from the trace constituent. Dilution of the sample solves the problem of the excess ion at the expense of lowering the concentration of the trace constituent below its detection limits. In IC, considerations must be given not only to the selectivity of the analytes, but also to total ion-exchange capacity of the column [21]. Moderate ion-exchange capacity columns reduce the risk of sample overloading at the sacrifice of short analysis times. The reequilibration time alone can exceed 1 h after a column overloading. Shown in Fig. 6A is an electropherogram of 1500 ppm citrate solution prepared from its trisodium salt. The sample was spiked with 1 ppm of chloride and sulfate. Detection limits, defined as  $2 \times$  the baseline

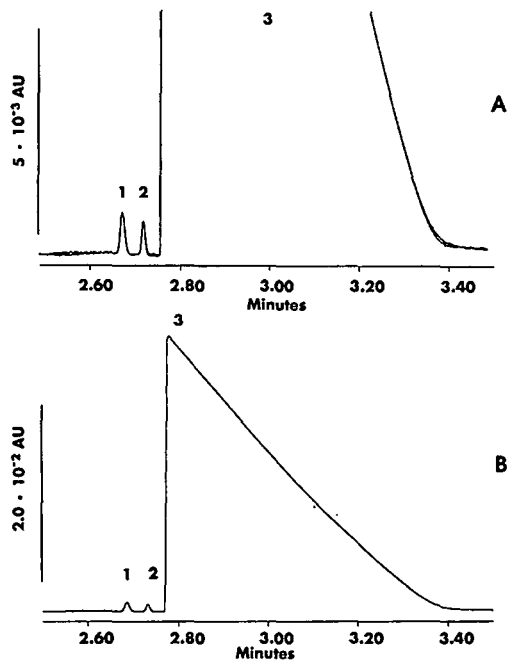


Fig. 6. (A) An expanded view of citrate sample for chloride and sulfate. Peaks and concentrations [ppm] injected: 1 = chloride [1]; 2 = sulfate [1]; 3 = citrate [1500]. (B) The same separation as in the top plot, but at a different sensitivity to show fully the citrate peak. The electrolyte is 5 mM chromate, 0.5 mM OFM Anion-BT (converted to hydroxide form), pH adjusted to 8.0 with acetic acid. Applied potential 20 kV negative polarity, detection at 254 nm, 60 cm  $\times$  75  $\mu\text{m}$  fused-silica capillary with 10 cm for 30-s hydrostatic injection.

noise, for chloride and sulfate are 48 ppm and 25.7 ppm respectively in the trisodium citrate dihydrate solid. Reproducibility is also illustrated in Fig. 6A by the overlay of four consecutive injections of the sample. Using a chromatic background electrolyte with OFM Anion-BT for electroosmotic flow control the analysis time is under 3.5 min, including the citrate. The 0.5 mM OFM Anion-BT EOF modifier was converted to the hydroxide form via hydroxide form anion-exchange resin and electrolyte pH adjusted with acetic acid.

By comparison this analysis would require a 1 h runtime using isocratic elution in IC since citrate is a highly retained trivalent anion on IC columns. Viewing the citrate peak in its entirety (Fig. 6B) reveals that it rapidly reaches its apex and then tails. For analytes that migrate after the major peak, the separation may suffer with peaks rising off the

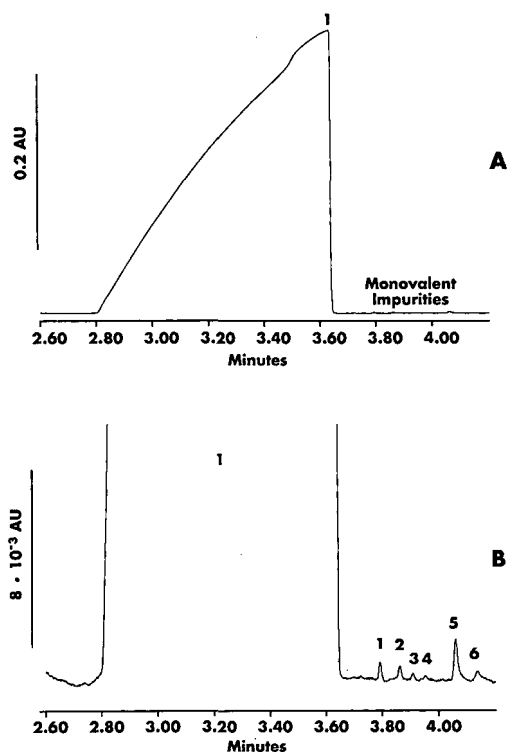


Fig. 7. Top plot is an electropherogram of a 99.9% pure terephthalic acid sample, the separation is scaled to show the complete terephthalate peak. Bottom plot is the same separation as in the top plot but at a different sensitivity to show the trace impurities. Peaks and concentrations [ppm] injected: 1 = terephthalate [5000]; 2 = unknown; 3 = benzoate [not quantitated]; 4 = unknown; 5 = toluate [0.56]; 6 = unknown. The electrolyte is a 25 mM hexanesulfonate, 0.5 mM OFM Anion-BT (converted to chloride form), pH adjusted to 10 with lithium hydroxide. Applied potential 25 kV (negative polarity), detection at 185 nm, 60 cm ( $L_i$ ), 52 cm ( $L_d$ ) and 75  $\mu$ m I.D. fused-silica capillary with 10 cm for 30-s hydrostatic injection.

downward sloping baseline created by the major constituent. Peak asymmetry is a result of electrodiffusional processes described in the literature and can be easily manipulated [22,23]. The asymmetry of a peak, created by the differences in the mobility of the electrolyte co-ion and the analyte, can be easily controlled through the proper selection of various mobility of co-ions in electrolytes. Fig. 7A shows traces of UV absorbing anions following a massive 5000 ppm terephthalate peak. In Fig. 7B the terephthalate peak is again shown completely and we can see that it is fronting with a dramatic vertical drop

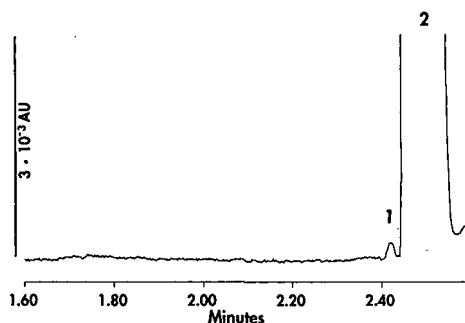


Fig. 8. Separation of chloride in the presence of excess sulfate. Peaks and concentration [ppm] injected: 1 = chloride [1]; 2 = sulfate [1000]. The electrolyte is 5 mM chromate, 1.5 mM OFM Anion-BT. Applied potential 20 kV (negative polarity), detection at 254 nm, 60 cm ( $L_i$ ), 52 cm ( $L_d$ ) and 75  $\mu$ m I.D. fused-silica capillary with 10 cm for 15-s hydrostatic injection.

immediately after it reaches its apex. Here a less mobile electrolyte co-ion, hexanesulfonate, is utilized to optimize the peak symmetry of the analytes of interest. The impurities are those usually found in a 99.9% pure solid terephthalic acid. Sample preparation consists of adding 1 g of lithium hydroxide monohydrate together with 0.5 g of the acid into a 100-ml volumetric flask. Additional sensitivity is achieved through utilization of direct UV detection at 185 nm.

When disparate levels of ion concentrations include ions having a small difference in selectivity, such as chloride and sulfate, the approach is to maximize the resolution between the two peaks. Sulfate exhibits decreased mobility with respect to chloride as the OFM Anion-BT concentration of the electrolyte increases [4]. Fig. 8 shows a separation of 1 ppm chloride in the presence of 1000 ppm sulfate with an analysis time under 2.8 min.

#### Reactive anions

Analyzing reactive anions such as hypochlorite and persulfate by IC have long been a problem especially if quantitative results were the objective. Strong oxidating agents frequently react with the stationary phase of anion-exchange columns, resulting in both a decrease in column life and poor recoveries. A literature search of IC methodologies reveals that from 1975 until today only one method is found for persulfate [24] and one method for hypochlorite [25]. The IC method for hypochlorite uses amperometric detection before the anion-ex-

change column making it actually a flow injection analysis (FIA) technique. Since no separation has taken place prior to detection, the method works only if there are no other electroactive species augmenting the hypochlorite signal. The IC method for persulfate requires excessive run times (37 min), especially if weakly retained species such as chloride have to be separated in its presence.

In the development of a CIE method, the major consideration is selecting the appropriate electrolyte that prevents degradation of the reactive analytes. From the literature, persulfate with the highest ionic equivalent conductance value with respect to the

36-anions separation, would be predicted to migrate before thiosulfate and bromide. No peak for persulfate was found in the predicted region of the electropherogram running under the same conditions as in Fig. 1. A badly shaped peak observed very late in the separation occurred only when more than 500 ppm of persulfate were injected. It was suspected that a reaction was occurring between the persulfate and the OFM Anion-BT. Removal of the OFM from the electrolyte required reversing the polarity of injection and elevating the 5 mM chromate electrolyte to pH 11.0 with lithium hydroxide. The high pH of the electrolyte generates a  $\mu_{\text{eof}}$  greater than that of the  $\mu_{\text{ep}}$  of the analytes of interest. Hence the analytes are drawn towards the detector rather than being pushed as in the former case. The result is a reversed selectivity of anions in comparison to the earlier figures, the lower-mobility anions reach the detector first followed by higher-conductivity anions. Fig. 9A shows the persulfate migrating last and after the bromide anion as expected from its ionic equivalent conductance. The same electrolyte used for persulfate is applicable also for the hypochlorite anion Fig. 9B. Chlorite, carbonate, chlorate, perchlorate and chloride all migrate after the hypochlorite peak.

Decomposition of hypochlorite occurs rapidly with a 10% reduction in area from a 31 ppm solution

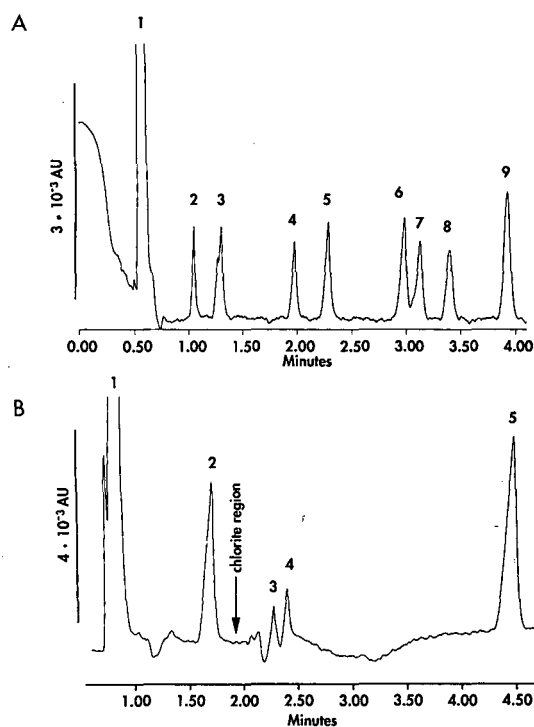


Fig. 9. (A) A separation of a reactive ion persulfate. Peaks and concentration [ppm] injected: 1 = water [not quantitated]; 2 = fluoride [1]; 3 = carbonate [not quantitated]; 4 = nitrate [4]; 5 = nitrate [4]; 6 = sulfate [4]; 7 = chloride [2]; 8 = bromide [4]; 9 = persulfate [10]. (B) Separation of hypochlorite. Peaks and concentration [ppm] injected: 1 = water [not quantitated]; 2 = hypochlorite [31]; 3 = carbonate [not quantitated]; 4 = chlorate [not quantitated]; 5 = chloride [not quantitated]. The electrolyte for both plots is 5 mM chromate with pH adjusted to 11.0 using lithium hydroxide. Applied potential (A) 30 kV and (B) 25 kV (positive polarity), detection at 254 nm, 40 cm ( $L_t$ ), 32 cm ( $L_d$ ) and 75  $\mu\text{m}$  I.D. fused-silica capillary with a 10 cm at 30-s hydrostatic injection.

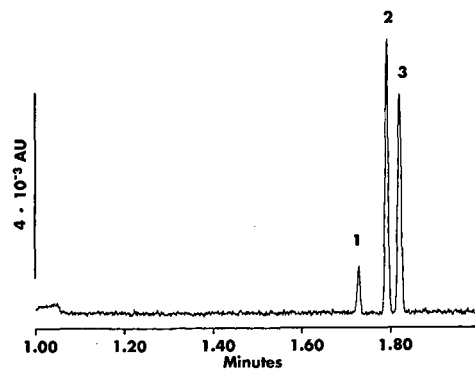


Fig. 10. Low-ppb anions using direct UV detection. Peaks and concentration [ppb] injected: 1 = bromide [4]; 2 = nitrite [4]; 3 = nitrate [4]. The electrolyte is for 25 mM chloride, 0.5 mM OFM Anion-BT (converted to chloride form), pH 8.0. Applied potential 20 kV (negative polarity), detection at 214 nm, 40 cm ( $L_t$ ), 32 cm ( $L_d$ ) and 75  $\mu\text{m}$  I.D. fused-silica capillary with a 5 kV for 45 s electromigration injection. Sample was prepared by spiking 40  $\mu\text{M}$  sodium octanesulfonate standard prior to injection.

after 10 min. A linearity study was performed on hypochlorite from 31 to 77.5 ppm where the standards were prepared immediately prior to injection from a freshly prepared hypochlorite concentrate. The correlation coefficient of the linearity plot was 0.997.

#### Trace anions

In previous work the authors [5] achieved sub-ppb detection limits for several common anions,  $\text{Br}^-$ ,  $\text{Cl}^-$ ,  $\text{SO}_4^{2-}$ ,  $\text{NO}_2^-$ ,  $\text{NO}_3^-$ ,  $\text{F}^-$  and  $\text{HPO}_4^{2-}$  using electromigration to introduce the sample and indirect UV detection. Prior to injection the sample is spiked with 40  $\mu\text{M}$  sodium octanesulfonate. The sample is enriched under the conditions of an isotachophoretic steady state as defined by the Kohlrausch regulation function [26].

Recent work with low-UV absorbing anions  $\text{Br}^-$ ,  $\text{NO}_2^-$ , and  $\text{NO}_3^-$  achieves low-ppt detection limits in Fig. 10 by using direct UV detection. The electrolyte contains 25 mM sodium chloride with 0.5 mM OFM Anion-BT converted to the chloride form using chloride form of an anion-exchange resin. After subtracting the contribution of ionic contamination found in a water blank treated with the octanesulfonate additive, the detection limits for nitrite and nitrate at  $2 \times$  baseline noise are at 125 ppt. To determine the contribution of the impurities found in the water used to make the ppb standard, the concentrate used for sample treatment (5000 ppm octanesulfonate) can be analyzed by the method described in Fig. 6. Impurities found in the sodium octanesulfonate were bromide, sulfate and iodide, with concentrations in the low-ppt range when the additive is at 40  $\mu\text{M}$  (7.73 ppm octanesulfonate) [27]. The ratio of the trace anions to the anionic sample treatment is 618:1 with respect to mass.

#### CONCLUSIONS

CIE provides a rapid and highly efficient analysis approach in comparison with IC. The simplicity of the method using only fused-silica capillaries and UV detection makes it an attractive alternative to a wide variety of sample matrices. The ability to analyze for trace analytes in fine chemicals with concentration ratios of up to 1 to 50 000, achieving

ppt detection limits in high-purity water samples and difficult industrial samples was demonstrated.

#### REFERENCES

- 1 H. Small, T. Stevens and W. Bauman, *Anal. Chem.*, 47 (1975) 1801.
- 2 D. T. Gjerde and J. S. Fritz, *J. Chromatogr.*, 176 (1979) 199.
- 3 W. R. Jones and P. Jandik, *Am. Lab.*, 22, No. 9 (1990) 51.
- 4 W. R. Jones and P. Jandik, *J. Chromatogr.*, 546 (1991) 445.
- 5 P. Jandik and W. R. Jones, *J. Chromatogr.*, 546 (1991) 431.
- 6 J. Romano, P. Jandik, W. R. Jones and P. Jackson, *J. Chromatogr.*, 546 (1991) 411.
- 7 B. J. Wildman, P. Jackson, W. R. Jones and P. G. Alden, *J. Chromatogr.*, 546 (1991) 459.
- 8 W. R. Jones, P. Jandik and R. Pfeifer, *Am. Lab.*, 23, No. 8 (1991) 40.
- 9 P. Jandik, W. R. Jones, A. Weston and P. R. Brown, *LC GC*, 9 (1991) 634.
- 10 B. F. Kenney, *J. Chromatogr.*, 546 (1991) 423.
- 11 P. E. Jackson, P. Jandik, W. R. Jones and J. Romano, presented at the 3rd International Symposium on High-Performance Capillary Electrophoresis, San Diego, CA, February 3-6, 1991, poster PT-58.
- 12 P. R. Haddad and P. E. Jackson, *Ion Chromatography—Principles and Applications (Journal of Chromatography Library, vol. 46)*, Elsevier, Amsterdam, 1990, pp. 22-25.
- 13 J. C. Giddings, *Anal. Chem.*, 56 (1984) 1259A.
- 14 J. C. Giddings, *J. High Resolut. Chromatogr. Chromatogr. Commun.*, 10 (1987) 319.
- 15 J. C. Giddings, in H. J. Cortes (Editor), *Multidimensional Chromatography: Techniques and Applications*, Marcel Dekker, New York, 1990, p. 12.
- 16 D. W. Fuerstenau, *J. Phys. Chem.*, 60 (1956) 981.
- 17 P. Somasundaran, T. W. Wealy and D. W. Fuerstenau, *J. Phys. Chem.*, 68 (1964) 3562.
- 18 R. C. Weast (Editor), *Handbook of Chemistry and Physics*, CRC Press, Boca Raton, FL, 66th ed., 1985, p. D-167.
- 19 J. A. Dean (Editor), *Lange's Handbook of Chemistry*, McGraw-Hill, New York, 13th ed., 1985, Section 6, pp. 30-31.
- 20 D. R. Salomon and J. P. Romano, *J. Chromatogr.*, 602 (1992) 219.
- 21 D. T. Gjerde, D. J. Cox, P. Jandik and J. B. Li, *J. Chromatogr.*, 546 (1991) 151.
- 22 F. E. P. Mikkers, F. M. Everaerts and Th. P. E. M. Verheggen, *J. Chromatogr.*, 169 (1979) 1.
- 23 S. Hjertén, *Electrophoresis*, 11 (1990) 665.
- 24 M. Weidernauer, P. Hoffmann and K. H. Lieser, *Fresenius' Z. Anal. Chem.*, 331 (1988) 372.
- 25 G. O. Franklin and A. W. Fitchett, *Pulp. Pap. Can.*, 83 (1982) 40.
- 26 F. Kohlrausch, *Ann. Phys. Chem.*, 62 (1897) 209.
- 27 W. R. Jones, unpublished results.
- 28 W. R. Jones, P. Jandik and M. T. Swartz, *J. Chromatogr.*, 473 (1989) 171.
- 29 W. R. Jones, P. Jandik and A. L. Heckenberg, *Anal. Chem.*, 60 (1988) 1977.





# Optimization of detection sensitivity in the analysis of inorganic cations by capillary ion electrophoresis using indirect photometric detection

Andrea Weston<sup>☆</sup> and Phyllis R. Brown

*Department of Chemistry, University of Rhode Island, Kingston, RI 02881 (USA)*

Petr Jandik, Allan L. Heckenberg and William R. Jones

*Ion Analysis Department, Waters Chromatography Division of Millipore, 34 Maple Street, Milford, MA 01757 (USA)*

---

## ABSTRACT

Capillary ion electrophoresis (Waters' trade name Capillary Ion Analysis, or CIA) is the subdivision of capillary zone electrophoresis in which the conditions for the separation are optimized for the analysis of inorganic or low-molecular-mass ions. The first reported separation of alkali, alkaline earth and transition metals by capillary ion electrophoresis, published in 1991 [LC · GC, 9 (1991) 634], showed the separation of these cations in under 10 min with mid-ppb detection limits and separation efficiencies of more than 100 000 theoretical plates. Detection sensitivity has since been improved by altering both hardware and electrolyte components. These alterations have resulted in a decrease in detection limits of more than an order of magnitude, making trace level analyses practical for many applications. The good reproducibility and linearity of this technique are also discussed.

---

## INTRODUCTION

Capillary zone electrophoresis (CZE) has developed into one of the more powerful separation techniques for the analysis of a wide variety of sample matrices. However, one of the major drawbacks in CZE is the lack of a sensitive and universal detection system. A number of variables may be manipulated to address these problems.

Indirect modes of detection provide a simple solution to the problem of universal detection, eliminating the need for pre- or post-column derivatization to convert the analyte of interest into a species

that gives a response at the detector. Because the analytes are not chemically altered, fraction collection and further studies are facilitated. Several indirect modes have been described in the literature, including indirect UV absorbance [1–5], indirect fluorescence [6–8] and indirect amperometric detection [9]. Foret *et al.* [10] employed indirect photometric detection to analyze a group of low-molecular-mass anions. They found that the best sensitivities were obtained for sample ions having an effective mobility close to the mobility of the UV background-providing co-ion. Therefore, by choosing an electrolyte with the required mobility, sensitivity enhancements can be achieved.

Owing to its universal nature and its ease of use, UV detection (indirect or direct) is still the most popular method. Separations typically take place in capillaries of  $\leq 100 \mu\text{m}$  I.D., to provide efficient heat dissipation. As the capillary dimensions are in-

---

*Correspondence to:* Dr. P. R. Brown, Department of Chemistry, University of Rhode Island, Kingston, RI 02881, USA.

<sup>☆</sup> Present address: Ion Analysis Department, Waters Chromatography Division of Millipore, 34 Maple Street, Milford, MA 01757, USA.

creased beyond 100  $\mu\text{m}$  I.D., a dramatic decrease in separation efficiency is observed [1], due to Joule heating resulting from the ionic current carried between the electrodes. However, with capillaries of  $\leq 100$   $\mu\text{m}$  I.D. considerable loss in sensitivity is encountered, consistent with the Lambert–Beer law, due to the shorter path lengths of the capillaries. Recently, several attempts have been made to extend the path length for UV detection in capillary electrophoresis (CE). Tsuda *et al.* [11] described the use of transparent, rectangular capillaries with dimensions ranging from 16  $\mu\text{m} \times 195$   $\mu\text{m}$  to 50  $\mu\text{m} \times 1000$   $\mu\text{m}$ . According to Tsuda *et al.* [11], rectangular capillaries are extremely efficient at dissipating heat compared with conventional circular capillaries. Thus, larger-volume rectangular capillaries can be used, resulting in more than an order of magnitude increase in concentration sensitivity. The authors noted that with the larger capillaries, however, normal hydrostatic or electromigration injection modes failed to give reproducible, high-efficiency separations and a split injection method had to be employed. Peak widths were wider than those normally obtained for CE separations employing circular cross-section capillaries.

Grant and Steuer [12] extended the path length of their capillary up to 3 mm, by axial illumination of the capillary using laser-induced fluorescence with indirect UV detection. Due to the presence of high background noise, however, the advantage of an increased path length by this method could not be fully exploited. Gordon [13] extended the path length of the capillary by employing an egg-shaped cell [13] “fabricated directly into the separations capillary, that increases both the flux and the path length of the ultraviolet light employed in an absorption measurement” [13]. Chervet and co-workers [14,15] constructed a Z-shaped flow cell in order to extend the path length of the capillary up to 3 mm for UV detection in CE. The loss in resolution caused by the extended path length was less pronounced than expected, while enhancements in signal-to-noise ratio of up to 6 times were observed.

In addition to optimizing the mobility of the electrolyte co-ion and increasing the capillary path length, the mode of sample introduction also plays a role in sensitivity. The high-efficiency capabilities of CE can be realized only when the injection system employed does not introduce significant zone

broadening. CE systems are easily overloaded by large sample volumes, and hence it is important that the injection system employed is capable of delivering small volumes efficiently and reproducibly [16]. Sample introduction in CE may be accomplished in a number of ways. A rotary-type injector [17] has been employed, as have various sample splitters [18]. These injectors have been designed for capillaries with an internal diameter of 200–300  $\mu\text{m}$ . For smaller capillaries with an internal diameter of 25–75  $\mu\text{m}$ , low-dead-volume coupling of injectors to the separation capillary is difficult to achieve [19]. Therefore, sample introduction into smaller capillaries is accomplished by using electromigration or hydrostatic injection. It has been stated by Huang *et al.* [20] that the use of electromigration injection introduces biases and therefore care should be taken when comparing results from different sample solutions. The biases result both from the different mobilities of the ions migrating into the capillary, and from the differences in electrical resistance of the medium in which the species are dissolved. By performing the instrument calibration and the sample analyses from solutions of similar resistance, bias due to preferential migration of analyte ions should not be a problem. Dual calibration, however, such as constant conductivity with varying concentrations and constant concentration with varying conductivity, provides a more complete solution to the problem of preferential migration.

In this paper the effects on the detection limits of inorganic metal cations, of changing the detection wavelength, the mobility of the electrolyte co-ion, the length of the detection cell and the mode of injection are investigated.

## EXPERIMENTAL

A Waters (Milford, MA, USA) Quanta 4000 CE system, equipped with a positive power supply, was used throughout this study. Indirect UV detection was achieved at 214 nm using a zinc lamp with a 214-nm optical filter, and at 185 nm using a mercury lamp with a 185-nm optical filter. Normal fused-silica capillaries, 60 cm in total length, 75  $\mu\text{m}$  I.D. and 52 cm from the point of sample introduction to the detector window, were obtained from Waters (AccuSep capillaries). Capillaries with extended path lengths (60 cm  $\times$  75  $\mu\text{m}$  I.D. with path lengths of

300  $\mu\text{m}$ ) were obtained from Waters. The samples were introduced into the capillary either by using a 30-s hydrostatic injection from a height of 10 cm, or by electromigration (10 kV) for 10 s. The separation voltage was set at 20 kV.

Standard 2-ml polyethylene sample vials (Sun Brokers, Wilmington, NC, USA) were used as containers for the carrier electrolyte and all the standards and samples. A Waters 860 data station and Waters SIM interface were used to record and evaluate the electropherograms at a sample rate of 20 points per s. The subsequent statistical processing was performed using CricketGraph (Cricket Software, Malvern, PA, USA) with a Macintosh SE personal computer (Apple Computers, Cupertino, CA, USA).

All solutions, electrolytes and standards were prepared using 18-M $\Omega$  water generated by Milli-Q laboratory water-purification system (Millipore, Bedford, MA, USA). The transition metal standards were prepared by dilution of atomic absorption standards obtained from Sigma (St. Louis, MO, USA), while the alkali and alkaline earth metal standards were prepared from salts obtained from Aldrich (Milwaukee, WI, USA). The UV background providing electrolytes, UVCat-1 and UVCat-2, were obtained from Waters. The analytical-grade complexing agents,  $\alpha$ -hydroxyisobutyric acid (HIBA) and tropolone, were both obtained from Aldrich.

## RESULTS AND DISCUSSION

The separation of alkali and alkaline earth metals in the presence of transition metals has been reported previously [4]. The electrolyte consisted of 5 mM UVCat-1 to provide the UV-absorbing background and 6.5 mM HIBA to selectively complex the metals for a better separation. Indirect UV detection at 214 nm was employed. Fig. 1a shows a separation of 11 metals under these previously reported conditions. Detection limits for the alkali and alkaline earth metals range from low- to mid-ppb levels. Fig. 1b shows the separation of the same group of metals under the same conditions as Fig. 1a, except the detection wavelength was changed from 214 to 185 nm. Although the baseline noise at 185 nm increased, the peak height is significantly larger. Thus, despite the increase in baseline noise, the de-

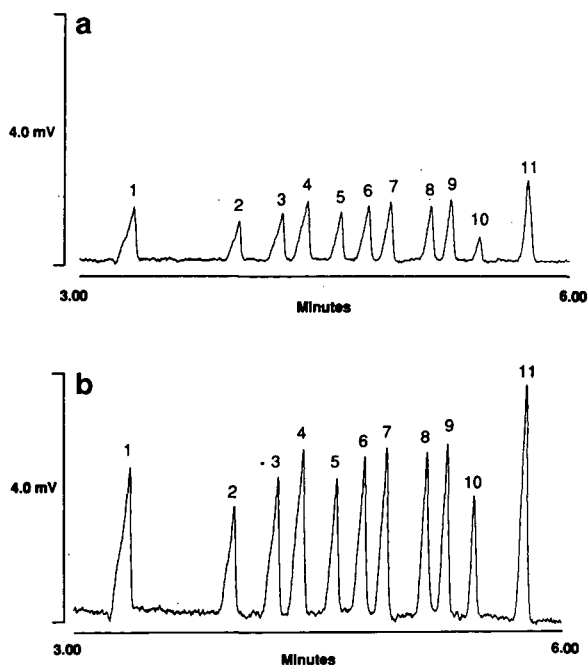


Fig. 1. (a) Capillary ion electrophoretic analysis of a standard solution of alkali and alkaline earth metals in the presence of transition metals. Carrier electrolyte: 5 mM UVCat-1, 6.5 mM HIBA, pH 4.4. Capillary: 60 cm  $\times$  75  $\mu\text{m}$  I.D. fused silica. Applied voltage: 20 kV (positive). Hydrostatic injection: 10 cm for 30 s. Indirect UV detection at 214 nm. Sample: standards. Peaks: 1 = potassium (1.6 ppm); 2 = barium (2.0 ppm); 3 = strontium (1.6 ppm); 4 = calcium (0.8 ppm); 5 = sodium (0.6 ppm); 6 = magnesium (0.4 ppm); 7 = manganese (0.4 ppm); 8 = iron(II) (0.8 ppm); 9 = cobalt (0.8 ppm); 10 = lead (2.0 ppm); 11 = lithium (0.2 ppm). (b) Capillary ion electrophoretic analysis of a standard solution of alkali and alkaline earth metals in the presence of transition metals. Experimental conditions as in (a), except indirect UV detection at 185 nm. Peaks as in (a).

tection limits improve. Table I compares the detection limits obtained using indirect UV detection at 214 nm *versus* indirect UV detection at 185 nm.

Incorporating indirect UV detection at 185 nm into the separation protocol, the effect of altering the mobility of the UV background providing component of the electrolyte on the detection limits of the alkali and alkaline earth metals was investigated. Since the mobility of UVCat-1 is less than the mobilities of the alkali and alkaline earth metals, all the metal ion peaks show some degree of fronting. As explained by Foret *et al.* [10], in addition to the dispersion resulting from diffusion, initial sample width and Joule heat, dispersion due to sorption

TABLE I

COMPARISON OF THE DETECTION LIMITS OBTAINED WITH A 185-nm LAMP AND A 214-nm LAMP

Experimental conditions as described in Fig. 1a and b.

Cation	Detection limits (hydrostatic) (ppb) <sup>a</sup>	Detection limits (electromigration) (ppb)	Difference factor
Potassium	222	142	1.56
Barium	381	237	1.60
Strontium	258	145	1.78
Calcium	102	61	1.67
Sodium	96	57	1.68
Magnesium	55	33	1.66
Lithium	18	11	1.64

<sup>a</sup> Throughout the article the American billion (10<sup>9</sup>) is meant.

phenomena and electromigration dispersion [21,22] can be expected to contribute to the dispersion of migrating zones. Electromigration dispersion always occurs during the migration of sample ions which possess effective mobilities different from that of the background electrolyte co-ion [10]. The higher the concentration of the sample component in its zone, the more pronounced the electromigration dispersion. Hence, one way of suppressing electromigration dispersion is by keeping the concentration of the analyte ions in their zones sufficiently below the concentration of the background electrolyte [10]. By keeping the concentration of the analyte ions low, however, greater detection sensitivity is required.

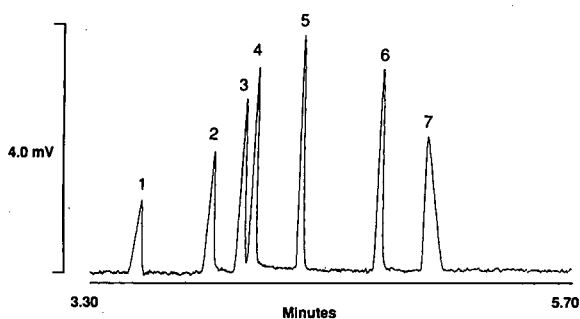


Fig. 2. Capillary ion electrophoretic analysis of a standard solution of alkali and alkaline earth metals. Experimental conditions as in Fig. 1b except using UVCat-2 and tropolone as the electrolyte system instead of UVCat-1 and HIBA. Peaks: 1 = potassium (1.0 ppm); 2 = barium (2.0 ppm); 3 = strontium (1.5 ppm); 4 = calcium (0.7 ppm); 5 = sodium (0.6 ppm); 6 = magnesium (0.4 ppm); 7 = lithium (0.2 ppm).

A more practical way of suppressing electromigration dispersion is to match the mobilities of the background electrolyte more closely with those of the analyte ions. UVCat-1 was therefore replaced by the more mobile UVCat-2. The natural pH of the UVCat-2–HIBA electrolyte was about pH 2. Since the complexing agents employed showed more significant complexation around pH 4, the pH of the electrolyte had to be raised. By raising the pH of the electrolyte, the possibility of an increased number of peaks was introduced, so HIBA was replaced by tropolone. The natural pH of the UVCat-2–tropolone electrolyte was pH 4. Fig. 2 shows the separation of the alkali and alkaline earth metals using UVCat-2 as the electrolyte. The mobility of UVCat-2 is similar to that of sodium, resulting in an almost symmetrical peak shape for sodium. The metals migrating faster than sodium all show a small degree of fronting, while the metals migrating slower than sodium show a little tailing. Under these conditions of more closely matched mobilities, the concentration of the analytes may even approach the concentration of the background electrolyte without electromigration dispersion producing a significant effect.

In Table II, the detection limits obtained using UVCat-2 and tropolone, in place of UVCat-1 and HIBA are compared, all other conditions being the same. While the sensitivity for all the metals has improved, the greatest improvement is seen for the peaks whose mobilities most closely match the mobility of UVCat-2, and less improvement is seen either side. Thus it can be seen that by matching the

TABLE II

COMPARISON OF THE DETECTION LIMITS OBTAINED WITH UVCat-1 AND UVCat-2 AS THE ELECTROLYTE

Experimental conditions as in Fig. 2.

Cation	Detection limits (hydrostatic) (ppb)	Detection limits (electromigration) (ppb)	Difference factor
Potassium	142	68	2.09
Barium	237	87	2.72
Strontium	145	46	3.15
Calcium	61	18	3.39
Sodium	57	13	4.38
Magnesium	33	10	3.30
Lithium	11	7	1.57

mobilities of the analyte ions with that of the background electrolyte, more efficient separations are obtained.

Incorporating UVCat-2 into the separation protocol, in addition to indirect UV detection at 185 nm, the effect on sensitivity of extending the capillary path length was investigated. A 75- $\mu\text{m}$  I.D. capillary was used, and a “bubble” was blown at the detection end, approximately 8 cm from the end of the capillary, producing an extended path length of 300  $\mu\text{m}$ . This resulted in an extended path length capillary similar to the “egg-shaped cell” described by Gordon [13]. From the Lambert–Beer law, it would be expected that by increasing the path

length, the sensitivity would increase. As can be seen from the electropherogram showing the separation of alkali and alkaline earth metals with the extended path length capillary (Fig. 3), the peak heights are significantly larger. Although detection limits have improved, the improvement is not as large as it would appear from the electropherogram, due to a concomitant increase in baseline noise. The detection limits obtained using the extended path length capillary *versus* a conventional capillary, are compared in Table III.

A significant enhancement in sensitivity for the analysis of inorganic metal cations is seen by altering the injection mode from hydrostatic to electromigration. The separation of 1–2 ppb of the alkali and alkaline earth metals using electromigration injection (10 kV) for 10 s is shown in Fig. 4. With electromigration injection, the sample introduction end of the capillary is placed into the sample vial and a voltage is briefly applied, causing a small band of sample to electromigrate into the capillary. Thus more analyte ions enter the capillary in a given volume of sample than is possible with hydrostatic injection. A comparison of the detection limits obtained using electromigration injection *versus* hydrostatic injection is shown in Table IV. Using electromigration injection, detection limits of the order of low ppt levels can be obtained.

The reproducibility of the technique for five consecutive injections, using electromigration injection with UVCat-2 as the background providing electrolyte, an extended path length capillary and indirect UV detection at 185 nm, is shown in Fig. 5. The

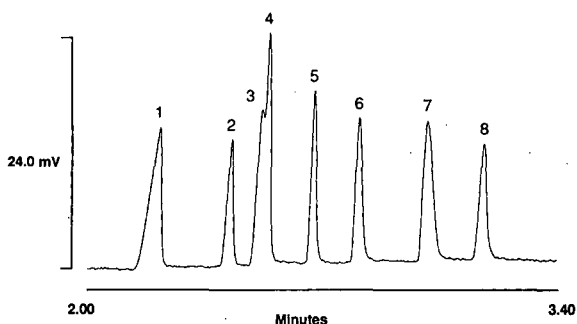


Fig. 3. Capillary ion electrophoretic analysis of a standard solution of alkali and alkaline earth metals in the presence of transition metals. Experimental conditions as in Fig. 2 except the conventional capillary was substituted for an extended path length capillary, with a path length of 300  $\mu\text{m}$ . Peaks: 1 = potassium (1.6 ppm); 2 = barium (2.0 ppm); 3 = strontium (1.6 ppm); 4 = calcium (0.8 ppm); 5 = sodium (0.6 ppm); 6 = magnesium (0.4 ppm); 7 = lithium (0.2 ppm); 8 = manganese (0.8 ppm).

TABLE III

COMPARISON OF THE DETECTION LIMITS OBTAINED WITH A CONVENTIONAL AND AN EXTENDED PATH LENGTH CAPILLARY

Experimental conditions as in Fig. 3.

Cation	Detection limits (hydrostatic) (ppb)	Detection limits (electromigration) (ppb)	Difference factor
Potassium	68	27	2.5
Barium	87	40	2.2
Strontium	46	—	—
Calcium	18	—	—
Sodium	13	10	1.3
Magnesium	10	6	1.7
Lithium	7	4	1.8

TABLE IV

COMPARISON OF THE DETECTION LIMITS OBTAINED WITH HYDROSTATIC AND ELECTROMIGRATION INJECTION

Experimental conditions as in Fig. 4.

Cation	Detection limits (hydrostatic) (ppb)	Detection limits (electromigration) (ppb)	Difference factor
Potassium	27	52	520
Barium	40	267	150
Strontium	—	210	—
Calcium	—	91	—
Sodium	10	53	190
Magnesium	6	30	200
Lithium	4	31	130

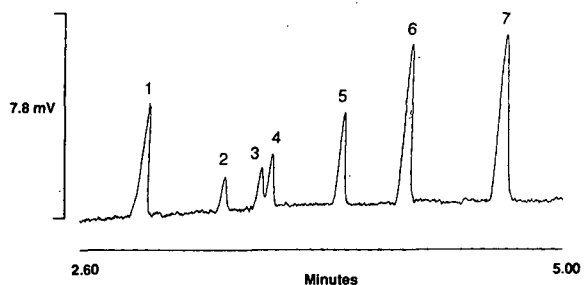


Fig. 4. Capillary ion electrophoretic analysis of a standard solution of alkali and alkaline earth metals. Experimental conditions as in Fig. 3 except using electromigration injection (10 kV for 10 s) instead of hydrostatic injection. Peaks: 1 = potassium (1.0 ppb); 2 = barium (2.0 ppb); 3 = strontium (2.0 ppb); 4 = calcium (1.0 ppb); 5 = sodium (1.0 ppb); 6 = magnesium (1.0 ppb); 7 = lithium (1.0 ppb).

sample is a 1:800 dilution of a standard solution. Despite the fact that reproducibility decreases with increasing dilution, the reproducibility in terms of peak area was between 3 and 12% relative standard deviation (R.S.D.), depending on the cation; lithium determinations showed the best reproducibility with 3% R.S.D. and barium the worst with 12%. The reproducibility in terms of migration times was less than 2% R.S.D. At higher concentrations, reproducibility was generally less than 1% R.S.D. Typical calibration curves obtained for the technique are shown in Fig. 6. Valid calibration is demonstrated over 1.5 orders of magnitude.

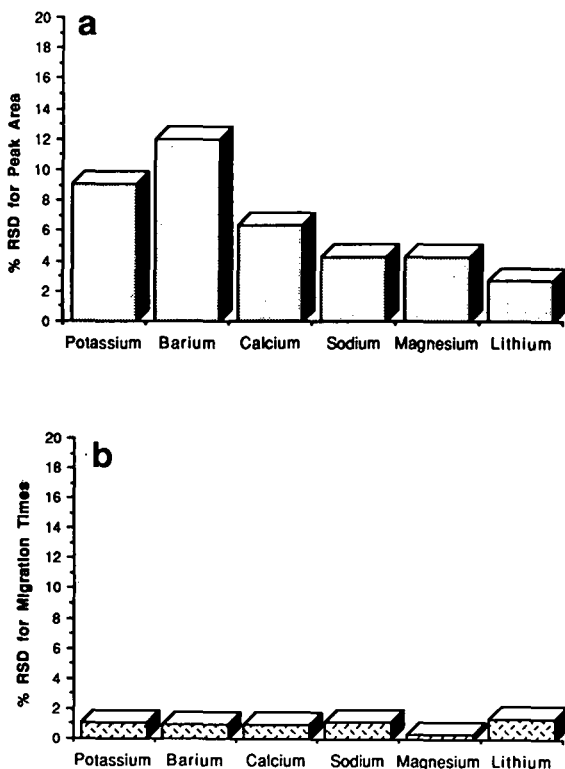


Fig. 5. (a) Graph showing the reproducibility of the technique in terms of peak area for five consecutive injections of a 1:800 dilution of the standard solution. (b) Graph showing the reproducibility of the technique in terms of migration times for 5 consecutive injections of a 1:800 dilution of the standard solution.

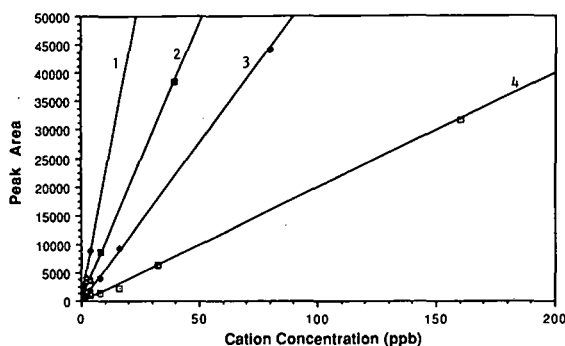


Fig. 6. Graph showing the linearity of the method over 1.5 orders of magnitude. 1 = Lithium ( $R^2 = 0.986$ ); 2 = magnesium ( $R^2 = 0.999$ ); 3 = calcium ( $R^2 = 1.000$ ); 4 = barium ( $R^2 = 0.999$ ).

## CONCLUSIONS

There are a variety of ways to improve the detection limits of inorganic metal cations by capillary ion electrophoresis (Waters' trade name Capillary Ion Analysis, or CIA), the most significant of which is electromigration injection in lieu of hydrostatic injection. Using electromigration injection, an increase in sensitivity of between 150 and 500 times is possible. The next most significant method for the enhancement of sensitivity is optimization of the mobility of the UV background providing co-ion in the electrolyte to match the mobilities of the analyte ions. With this approach, an enhancement in sensitivity of between 1.5 and 4.5 times can be achieved. In the case of the inorganic metal cations, a significant improvement in sensitivity is not obtained by extending the capillary cell path length. However, an increase in sensitivity of between 1.3 and 2.5 times could make the difference between detecting and not detecting a peak. From these results, it is also apparent that when choosing a component to provide the UV absorbing background a compromise between its mobility and its UV absorbance is often necessary.

## REFERENCES

- 1 A. Weston, P. R. Brown, P. Jandik, W. R. Jones and A. L. Heckenberg, *J. Chromatogr.*, 593 (1992) 289.
- 2 A. Weston, P. R. Brown, A. L. Heckenberg, P. Jandik and W. R. Jones, *J. Chromatogr.*, 602 (1992) 249.
- 3 P. Jandik, W. R. Jones, A. Weston and P. R. Brown, *LC-GC*, 9 (1991) 634.
- 4 W. J. Wildman, P. E. Jackson, W. R. Jones and P. G. Alden, *J. Chromatogr.*, 546 (1991) 459.
- 5 F. Foret, S. Fanali, A. Nardi and P. Boček, *Electrophoresis*, 11 (1990) 780.
- 6 W. G. Kuhr and E. S. Yeung, *Anal. Chem.*, 60 (1988) 1832.
- 7 W. G. Kuhr and E. S. Yeung, *Anal. Chem.*, 60 (1988) 2642.
- 8 L. Gross and E. S. Yeung, *J. Chromatogr.*, 480 (1989) 169.
- 9 T. M. Olefirowicz and A. G. Ewing, *J. Chromatogr.*, 499 (1990) 713.
- 10 F. Foret, S. Fanali, L. Ossicini and P. Boček, *J. Chromatogr.*, 470 (1989) 299.
- 11 T. Tsuda, J. V. Sweedler and R. N. Zare, *Anal. Chem.*, 62 (1990) 2149.
- 12 I. H. Grant and W. Steuer, *J. Microcol. Sep.*, 2 (1990) 74.
- 13 G. B. Gordon, *US Pat.*, 5 061 361 (1991).
- 14 J.-P. Chervet, *US Pat.*, 5 057 216 (1991).
- 15 J.-P. Chervet, R. E. J. van Soest and M. Ursem, *J. Chromatogr.*, 543 (1991) 439.
- 16 R. A. Wallingford and A. G. Ewing, *Adv. Chromatogr.*, 29 (1989) 1.



- 17 T. Tsuda, T. Mizuno and J. Akiyama, *Anal. Chem.*, 59 (1987) 799.
- 18 M. Deml, F. Foret and P. Boček, *J. Chromatogr.*, 320 (1985) 159.
- 19 D. J. Rose and J. W. Jorgenson, *Anal. Chem.*, 60 (1988) 642.
- 20 X. Huang, M. J. Gordon and R. N. Zare, *Anal. Chem.*, 60 (1988) 377.
- 21 F. E. P. Mikkers, F. M. Everaerts and Th. P. E. M. Verheggen, *J. Chromatogr.*, 169 (1979) 1.
- 22 F. E. P. Mikkers, F. M. Everaerts and Th. P. E. M. Verheggen, *J. Chromatogr.*, 169 (1979) 11.

# Determination of phenolic carboxylic acids by micellar electrokinetic capillary chromatography and evaluation of factors affecting the method

Charlotte Bjerregaard, Søren Michaelsen and Hilmer Sørensen

*Chemistry Department, Royal Veterinary and Agricultural University, 40 Thorvaldsensvej, DK-1871 Frederiksberg C (Denmark)*

---

## ABSTRACT

Micellar electrokinetic capillary chromatography (MECC) based on cetyltrimethylammonium bromide (CTAB) was developed for separation of individual cinnamic and benzoic acid derivatives. This method was adapted to the separation of the phenolic carboxylic acids from other anions, phenolics and glucosinolates in samples prepared from plant materials. The influence of temperature, voltage, pH, electrolyte and detergent concentrations in the buffer on migration times for the compounds considered, peak areas, resolution and number of theoretical plates were investigated. It is shown that rapid and efficient separations (> 270 000 plates/m) are possible, even for structural closely related phenolics.

---

## INTRODUCTION

Higher plants contain a large number of different cinnamic and benzoic acid derivatives, including several compounds with appreciable physiological effects [1,2]. This group of naturally occurring phenolics occur in plants, mainly as esters with various types of alcohol residues depending on the plant genera and plant parts examined [3]. Phenolic choline esters dominate in cruciferous seed material, whereas the phenolic acids are present as esters of malate and carbohydrates in vegetative plant parts [2,4]. Furthermore, recent investigations on dietary fibres (DF) isolated from peas, rapeseeds and cereals (rye and wheat) have revealed a considerable amount of phenolic acids, bound as esters or associated in other forms to the DF fraction [5].

Interest in DF has risen as a result of the large number of reports on various physiological effects connected with the intake of DF [6]. Evaluation of

the casual relationship between DF and these effects demands thorough characterization of the chemical composition, including the type and level of the associated phenolics. Current methods for determination of the free phenolic carboxylic acids comprise gas chromatography (GC) and high-performance liquid chromatography (HPLC) [2,7], both of which are relatively expensive and time-consuming techniques. However, a promising alternative has been found in free zone high-performance capillary electrophoresis (HPCE), as demonstrated for various types of phenolic carboxylic acids [8]. HPCE provides opportunities for rapid, simple and cheap analyses. Moreover, the use of detergents in the buffer system gives promise of even better results, as shown for several aliphatic low-molecular-weight carboxylic acids and other groups of compounds [9–12].

Micellar electrokinetic capillary chromatography (MECC) was introduced by Terabe *et al.* in 1984 [9] as a technique for separating neutral molecules, which otherwise migrate as a group with the electroosmotic flow. MECC can also be used to enhance the separation of charged species [13]. In this

---

*Correspondence to:* Dr. H. Sørensen, Chemistry Department, Royal Veterinary and Agricultural University, 40 Thorvaldsensvej, DK-1871 Frederiksberg C, Denmark.

paper, we present a technique for determination of individual cinnamic and benzoic acid derivatives using MECC with cetyltrimethylammonium bromide (CTAB). The method was systematically evaluated by studying the effects of various factors on the migration time, peak area, number of theoretical plates and resolution. Application of the developed conditions, including temperature, voltage, pH, electrolyte and detergent concentrations in the buffer, have been shown to provide an inexpensive and efficient method for the separation of individual phenolic carboxylic acids in solutions, including samples prepared directly from DF and other plant materials.

## EXPERIMENTAL

### Apparatus

The apparatus used was an ABI Model 270A capillary electrophoresis system (Applied Biosystems, Ramsey, NJ, USA), with a 657 mm  $\times$  0.05 mm I.D. fused-silica capillary tube. Detection was performed by on-column measurements of UV absorption at a position 445 mm from the injection end of the capillary. For data processing, a Shimadzu (Kyoto, Japan) Chromatopac C-R3A was used.

### Samples and reagents

Cinnamic and benzoic acid derivatives (Fig. 1) and flavonoids were plant products isolated and characterized by traditional methods [2,4] and/or obtained from Sigma (St. Louis, MO, USA).

Total dissolution of the compounds tested required the use of ethanol, which may alter the separation conditions in MECC. Evaporation of the ethanol prior to the final addition of water, for obtaining suitable peak heights, was therefore performed. The concentrations of the individual phenolic carboxylic acids in standard solutions ranged from  $5 \cdot 10^{-4}$  to  $1 \cdot 10^{-2}$  M.

DF samples obtained from Polish-grown double low rapeseed (cv. Bronowski), rapeseed hulls, wheat (cv. Java) and rye (cv. Danikowskie) consisted of insoluble (IDF) and soluble dietary fibres (SDF), isolated by an enzymatic gravimetric method described elsewhere [14]. Phenolic carboxylic acids were isolated either directly from DF or from DF solutions obtained by water extraction (25 ml/g, 2 h, 70°C) of DF as described [5]. The procedure con-

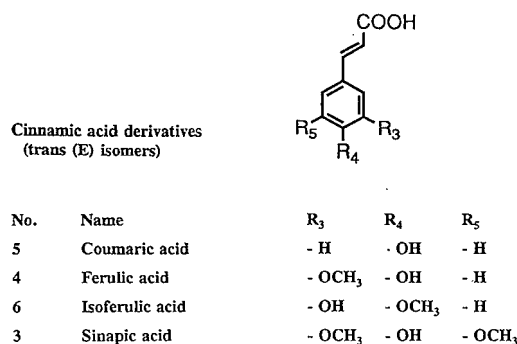
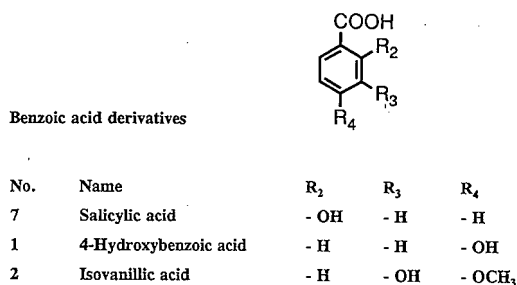


Fig. 1. Structures of cinnamic and benzoic acid derivatives used in MECC analyses. Numbers indicated are used in connection with the other figures.

sisted of hydrolysis under alkaline conditions (70 mg of DF + 5 ml of 1.0 M ammonia solution or 5 ml of water extract + 0.41 ml of 25% ammonia solution, 2 h, 100°C under reflux), centrifugation and evaporation of the supernatant to dryness, addition of 1 ml of 1.0 M HCl, extraction with chloroform (3  $\times$  2 ml) and evaporation to dryness. The residue was dissolved in 0.5 ml of 1.0 M ammonia solution, evaporated to dryness, redissolved in 4  $\times$  50  $\mu$ l of water and used for MECC after centrifugation at 3000 g for 10 min.

Sodium tetraborate and sodium phosphate were obtained from Sigma and CTAB from BDH (Poole, UK). All chemicals were of analytical-reagent grade.

### Procedure

Buffer solutions were prepared from stock solutions of sodium tetraborate (100 mM), sodium phosphate (150 mM) and CTAB (100 mM). The

different run buffers were mixed from these stock solutions, water was added to the desired concentration (borate plus phosphate, 16–48 mM; CTAB, 20–50 mM), adjusted to the required pH (6.0–8.0) and then filtered through a 0.45- $\mu$ m membrane filter prior to use. Buffers were changed manually. The samples were introduced from the negative end of the capillary by 1-s vacuum injection, resulting in injection volumes of few nanolitres. Separations were performed at 30–60°C and 17–23 kV. On-column UV detection at 280 nm was applied.

Standard conditions, while varying individual running parameters, were a temperature of 40°C, a voltage of 20 kV and electrolyte and detergent concentrations of 18 mM (borate), 30 mM (phosphate) and 50 mM (CTAB). Calculations of relative migration times (*RMT*) and normalized peak areas (*NA*) were performed according to the equations

$$RMT = MT_1/MT_2 \quad (1)$$

where  $MT_1$  is the migration time of the actual phenolic carboxylic acid and  $MT_2$  that of the phenolic carboxylic acid in the mixture given the value 1, and

$$NA = A/MT \quad (2)$$

where  $A$  is the measured peak area.

The number of theoretical plates ( $N$ ) and resolution ( $R_s$ ) were calculated as described elsewhere [15,16]. Linearity of the method was based on least-squares estimates.

Washing with buffer was performed between each analysis for a minimum of 5 min. After various numbers of analyses, the capillary was washed for 2–4 min with 1.0 M NaOH and 0.1 M NaOH solutions.

## RESULTS AND DISCUSSION

The applied MECC method is based on the electrophoretic mobility of the analytes, electroosmotic flow of the solvent and electrophoretic mobility of CTAB micelles, as described previously [17]. The pH of the applied buffer creates negatively charged silica groups on the capillary wall, giving the possibility of CTAB forming a double layer, associating one positive end to the capillary wall and the other to negative ions from the run buffer. Thereby, the direction of the electroosmotic flow is shifted towards the anode, compared with free zone capillary

electrophoresis. Micelles formed by CTAB, as the concentration in solution exceeds critical micelle concentration (CMC), move toward the cathode, opposite to the electroosmotic flow. With injection of the negatively charged analytes at the negative end of the capillary, it means, that the electroosmotic flow increases the analyte speed, whereas CTAB micelles has a retarding effect. The selective retention obtained in this MECC technique is therefore due to differential partitioning of the phenolics between the aqueous buffer and the micellar phases. A comprehensive evaluation of the migration behaviour of cationic analytes in an anionic micelle sys-

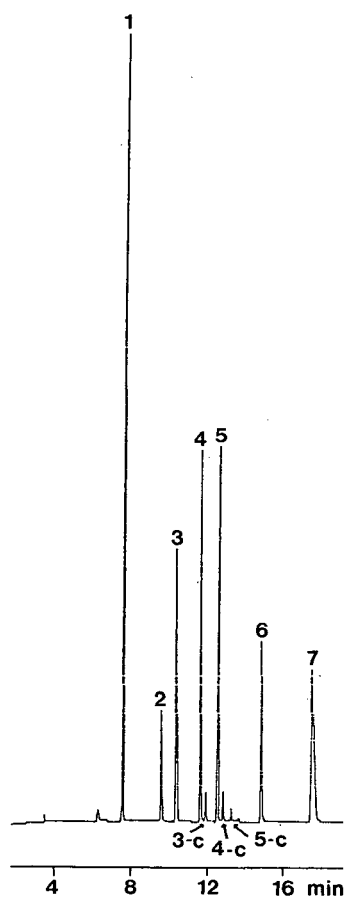


Fig. 2. Elution order of cinnamic and benzoic acid derivatives separated by the MECC technique. Numbers as in Fig. 1. Arrows show the occurrence of *cis* forms (c) of sinapic acid, ferulic acid and coumaric acid. Separation conditions: temperature, 40°C; voltage, 20 kV; buffer composition, 18 mM borate–30 mM phosphate–50 mM CTAB adjusted to pH 7.0; UV detection at 280 nm.

tem has recently been described by Strasters and Khaledi [18]. Further, the complex mechanisms of the interactions of ions and micelles have been evaluated by Wallingford and Ewing [19].

The elution order of the structurally closely related phenolic carboxylic acids investigated is presented in Fig. 2.

The ability of MECC to separate structural isomers was demonstrated by the separation of ferulic and isoferulic acid and of 4-hydroxybenzoic and salicylic acid, respectively. Moreover, the *cis* forms of the cinnamic acid derivatives sinapic, ferulic and coumaric acid, indicated by arrows in Fig. 2, were efficiently distinguished from the dominating *trans* forms.

Modifications of the MECC conditions implied changes of temperature, voltage, pH and composition of buffer, including concentrations of borate plus phosphate and detergent.

#### Temperature

Shorter migration times were seen with increasing temperatures, in agreement with the simultaneous decrease in viscosity of the solvent in the capillary. The lowering of viscosity was also reflected in an increased current intensity. *RMT* values, which in all instances were calculated relative to ferulic acid, were unchanged over the applied temperature range.

*NA* values increased with increase in temperature, the increment occurs for all phenolics, as illustrated in Fig. 3.

Corrections of peak areas (*NA*) were performed to eliminate the influences of alterations in migration time. Under the present circumstances, the changes in migration times were induced by the change in temperature, but may also be seen after series of analyses. In this case, the phenomenon may be limited by regular changes of the buffer and washing with NaOH for regeneration of the capillary. Studies of repeatability, subjected to the above and also to the problems of evaporation, showed constant normalized peak areas, even after numerous analyses [13]. However, under the present conditions, corrections for changes in migration times were insufficient to keep the *NA* values constant. As the magnitude of these changes differed markedly among the analytes tested (Fig. 3), it was assumed that evaporation could not explain the observed al-

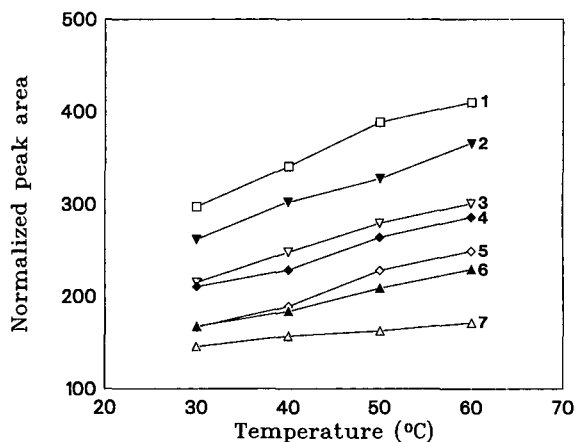


Fig. 3. Relationship between temperature and normalized peak areas of cinnamic and benzoic acid derivatives. Numbers as in Fig. 1. Other separation conditions as in Fig. 2.

terations. However, investigations on glucosinolates have shown that changes in electrolyte concentration in the run buffer, due to evaporation, had different effects on the *NA* values, depending on the migration times of the compounds involved (unpublished results). Another explanation of varying *NA* values may be the occurrence of a temperature-related alteration of solvent viscosity, injected sample volume as well as molar absorptivities with associated changes in UV absorption, as also demonstrated for different proteins [20], and related to changed interactions of phenolics with micelles (see below). Moreover, salicylic acid has the ability to form internal hydrogen bonds between the carboxy and hydroxy groups in the molecule, changing the chromophore. However, increasing voltage, electrolyte and CTAB concentrations, which may also result in higher capillary temperatures, did not confirm this hypothesis of a temperature-related effect (see below). Whatever the reason, the determination of phenolics in series of samples implies constancy of the parameters affecting the *NA* values.

The effect of temperature on separation efficiency was minor, although a tendency for decreases in *N* and *R<sub>s</sub>* values were seen for some of the compounds tested. This observation may be explained by changes in the interaction of phenolics with micelles, leading to minor reductions in peak width compared with reductions in migration time. Hence, increased temperature may change the

CMC to a higher value, affecting the micelle concentration, aggregation number and size and shape of the micelles in the solution [10,21]. The changes in  $N$  and  $R_s$  values were restricted to the cinnamic acid derivatives, indicating that the structure of the compounds may be of importance.

In MECC, in contrast to reversed-phase HPLC [2], the micellar phase (semi-stationary) will pass through the detector together with the analytes to be detected. It is then obvious that changes in the micellar interaction of phenolics may affect the molar absorptivities and thereby the  $NA$  values (see above).

### Voltage

An increase in applied voltage resulted in reductions in migration times, as illustrated in Fig. 4. The reduction was highest for compounds having long migration times, meaning that the overall time of analysis was reduced considerably at high voltage. Both  $RMT$  and  $NA$  values remained constant.

According to the HPCE theory, an increased field strength leads to improved separation efficiency, which again should be reflected in  $N$  and  $R_s$  values [15,22,23]. However, this could not be confirmed by the results obtained, as the  $N$  and  $R_s$  values were not greatly affected. Despite air-controlled temperature regulation in the apparatus, limited dissipation of the developed heat may result in band broadening and less sharp peak profiles [15,23]. This means that

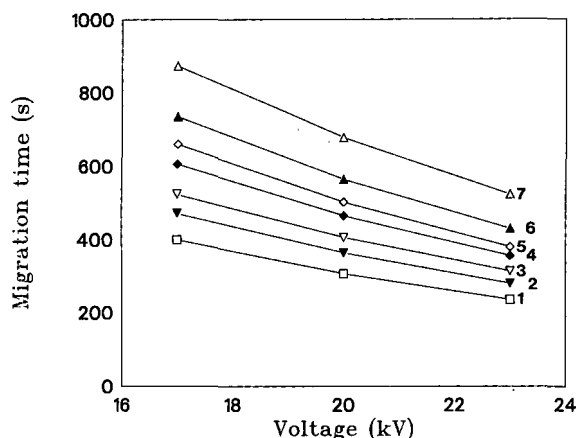


Fig. 4. Relationship between voltage and migration time of cinnamic and benzoic acid derivatives. Numbers as in Fig. 1. Other separation conditions as in Fig. 2.

the reduced separation window, owing to a shorter total time of the analysis and with a limited simultaneous reduction in peak width, will affect the  $R_s$  values in a negative direction.

### pH

Changing the pH from 6.0 to 8.0 had no marked effect on migration times, either actual or relative. The  $NA$  values were not affected, except for 4-hydroxybenzoic acid, which showed a considerable increment as demonstrated in Fig 5. Moreover, at high pH, the  $NA$  value for salicylic acid also had a tendency to increase.

Again, an effect on the molar absorptivities, here induced by the change in  $[H^+]$ , may be a suitable explanation. The observed results are probably due to ionization of the hydroxyl groups under the weakly alkaline conditions, leading to alterations in chromophore properties.

No clear effects on  $N$  and  $R_s$  values were observed with increase in pH, although a tendency for increasing separation efficiency was seen for some of the compounds tested. The reason for this is uncertain, as no change in migration time occurred and narrower peaks were not observed.

### Electrolyte concentration

Changes in the concentrations of borate and phosphate ions in the run buffer had a marked effect on the migration times of phenolics, as illustrated in Fig. 6.

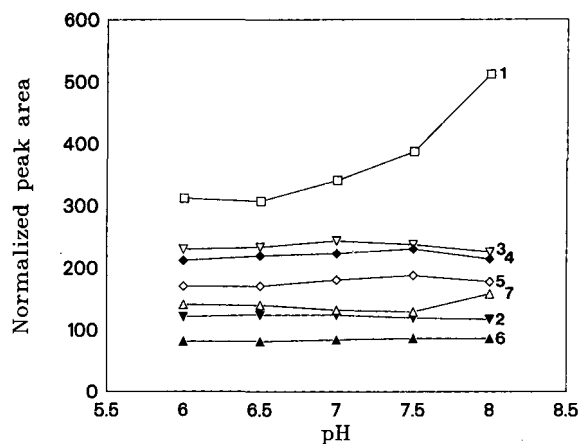


Fig. 5. Relationship between pH and normalized peak areas of cinnamic and benzoic acid derivatives. Numbers as in Fig. 1. Other separation conditions as in Fig. 2.

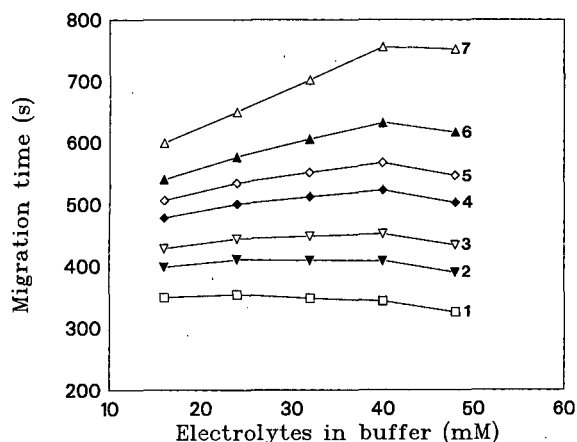


Fig. 6. Relationship between concentration of borate and phosphate ions in the buffer and migration time of cinnamic and benzoic acid derivatives. Numbers as in Fig. 1. Other separation conditions as in Fig. 2.

The increment in migration time was greatest for compounds late in the electropherogram. These compounds are associated with micelles to a greater extent than compounds with short migration times, indicating an effect on the micellar phase. In aqueous solution, the presence of electrolytes causes a decrease in CMC, owing to decreased electrical repulsions between the ionic ends of the surfactants in micelles [21]. This may result in higher micelle concentrations and thereby the observed delay in migration times, similarly to the effects found at increased concentrations of CTAB (see below). However, as the CMC of CTAB is less than 1 mM [21], the change in CMC will be small compared with the concentration of CTAB (50 mM).

A probably more important factor is the electroosmotic flow, which is considered to be changed as a result of an effect on the zeta potential. The difference in concentration of anions between the middle of the capillary and the capillary wall will decrease as the electrolyte concentration increases, leading to a reduction in electroosmotic flow [24]. Moreover, competition between CTAB and cations from the buffer may reduce the extent of the double layer on the capillary wall, leading to the same effect.

In the system described here, borate, phosphate and bromide ions are present as counter ions to CTAB micelles. An increase in borate and phosphate concentrations in the buffer may affect the

ratio of the various counter ions on the surface of micelles, and thereby change the interaction of analytes with the micellar phase. The reason for the sudden decrease in migration time, when the concentration of borate plus phosphate exceeds 40 mM is uncertain, but a possible explanation may be an increase in temperature, when the electrolyte concentration and thereby the current in the solution are increased to a certain level.

As the concentration of electrolytes in the run buffer increased, higher *RMT* values were obtained for analytes with long migration times, whereas the *RMT* values decreased for the first eluted phenolics. This is also in accordance with the changes in migration time discussed above. Changes in *RMT* values confirm that identification of peaks should be performed with a knowledge of *RMT* values under the actual running parameters. However, the *RMT* values may vary even under standardized conditions, as demonstrated by Michaelsen *et al.* [13].

The *NA* values remained relatively constant. The *N* values were affected in a non-systematic way, whereas the *R<sub>s</sub>* values, especially for the most hydrophobic compounds, increased markedly as the electrolyte concentration increased. This may be explained by the changes in CMC, as described above.

#### CTAB concentration

A positive linear relationship was found between migration time and increasing concentration of CTAB in the run buffer. This is in accordance with the theory, as a higher micellar concentration leads to changes in the partitioning of compounds in the direction of the micellar phase. Moreover, alterations in the electroosmotic flow may contribute to the effect observed. Only minor changes in *RMT* values were seen.

*NA* values were affected in a non-systematic way, the explanation for this being uncertain. However, changes in the interaction of analytes with micelles as the micelle concentration increased could be expected to influence the chromophoric systems, as previously mentioned for temperature-*NA* value interactions.

There was a tendency for improved *N* and *R<sub>s</sub>* values as the CTAB concentration in the buffer increased. Several factors may contribute to the observed effect, including changes in the shape, size and aggregation number of micelles.

The conflict existing between the demand for rapid analysis and high separation efficiency is reflected in the standard conditions chosen. Hence the short migration times obtained with application of high temperatures are obtained partly at the expense of  $N$  and  $R_s$  values. As a compromise, 40°C was chosen. Voltages exceeding 20 kV were avoided owing to the risk of considerable heat development. An electrolyte concentration at 48 mM was adapted in order to take advantage of the positive effect on  $R_s$  values together with the improvements in migration times at concentrations higher than 40 mM. The buffer pH was kept neutral, as the  $NA$  values seemed to remain relatively constant until this point. Finally, 50 mM CTAB provided the maximum separation efficiency.

### Applications

The method described was applied to the identification of cinnamic and benzoic acid derivatives associated with DF. Fig. 7 shows electropherograms

of phenolics in IDF isolated from whole rapeseed and rye.

The phenolic carboxylic acids, occurring as esters in IDF from rye, were quantitatively dominated by *trans*-ferulic acid, minor amounts of the *cis* isomer and with only trace amounts of sinapic and coumaric acid. IDF from oilseed rape had a much more complicated composition of ester-bound phenolic carboxylic acids, dominated by *trans*-sinapic acid, minor amounts of *cis*-sinapic acid, 4-hydroxybenzoic acid, vanillic acid, coumaric acid, ferulic acid and some additional unidentified compounds [3], appearing in the area of the electropherogram corresponding to flavonoids.

Flavonoids are easy to separate with the MECC technique; details will be presented elsewhere. These compounds appear mainly in areas of the electropherograms corresponding to higher migration times than the phenolic carboxylic acids, but changes in the electrophoretic conditions lead to reduced migration times, as shown in Fig. 8.

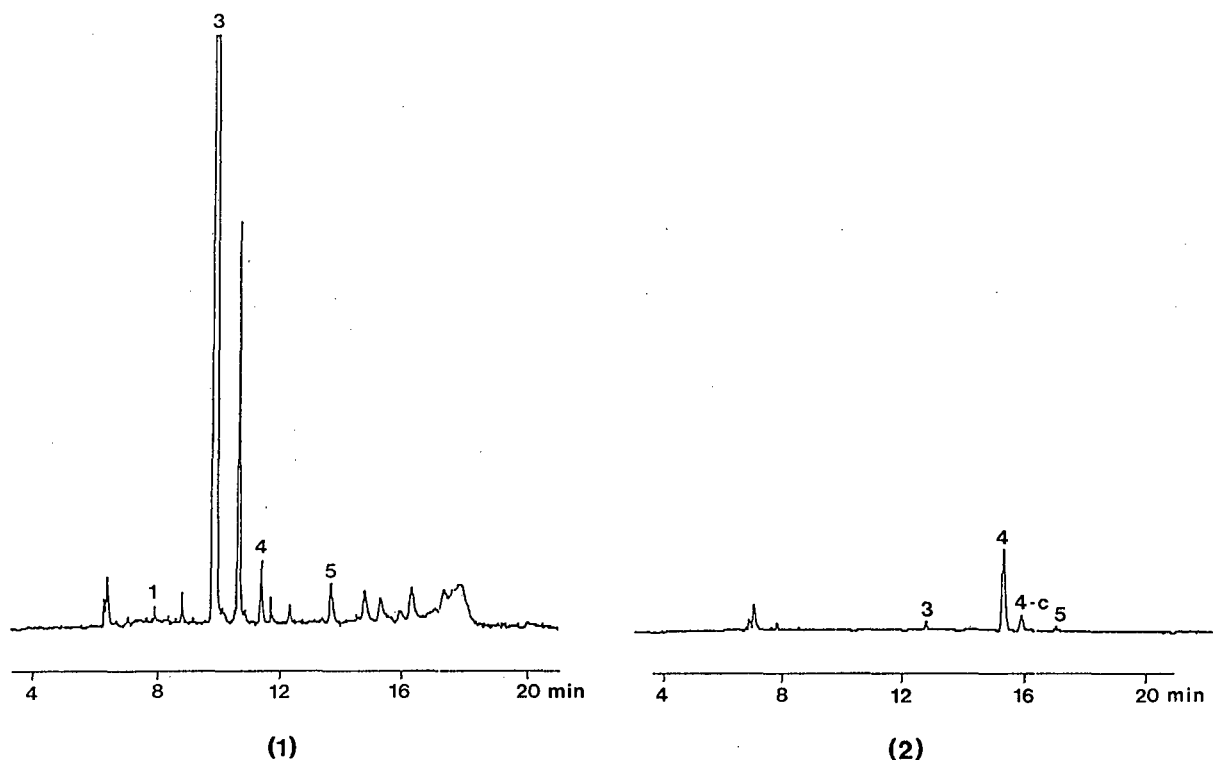


Fig. 7. Electropherograms of cinnamic and benzoic acid derivatives in IDF from (1) whole rapeseed and (2) rye (water extract). Numbers as in Fig. 1. Separation conditions as in Fig. 2.



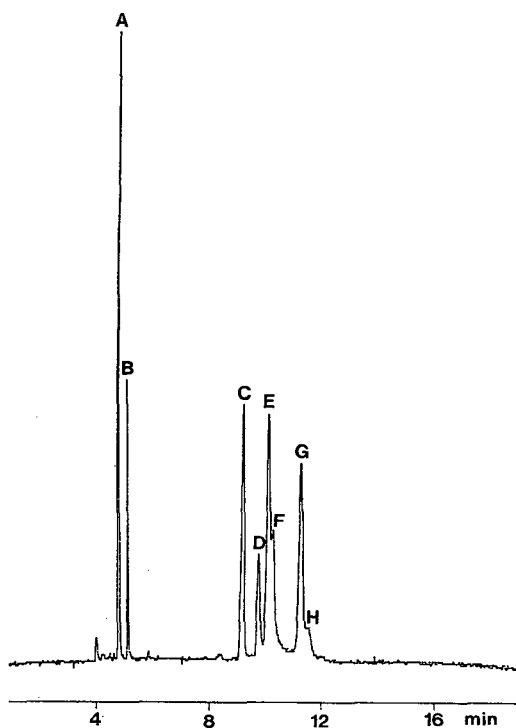


Fig. 8. Electropherogram of flavonoids. A = kaempferol-3-sophoroside-7-glucoside; B = kaempferol-3-sinapoylsophoroside-7-glucoside; C = rutoside; D = rutin; E = kaempferol-3-glucoside; F = quercetin-3-glucoside; G = kaempferol-3-(6''-carboxyglucoside); H = quercetin-3-(6''-carboxyglucoside). Separation conditions: temperature, 50°C; voltage, 26 kV; buffer composition, 12 mM borate-20 mM phosphate-60 mM CTAB adjusted to pH 7.0, 4% 1-propanol added; UV detection at 350 nm.

Phenolic carboxylic acids such as sinapic acid, isoferulic acid and benzoic acid derivatives occur in some plants as esters bound to glucosinolates [25]. These types of compounds appear in other areas of the electropherograms [13] (higher migration times than the free phenolic carboxylic acids), as for phenolic carboxylic acids bound as malate esters [2].

Identification of the compounds mentioned was based on traditional techniques described previously [2,13], including UV and NMR spectroscopy and with use of detection at various wavelengths in MECC.

Investigations on the changes in *NA* values with increasing concentrations of phenolics in standard mixtures showed good coherence. Correlation coefficients ( $r^2$ ) ranged from 0.9946 to 0.9998, indicat-

ing a strong linear relationship. This means that the method described may be employed for quantitative analyses of phenolics, taking the different factors influencing *NA* values into account.

## CONCLUSIONS

The MECC method described is highly effective, in comparison with HPLC and GC methods, for separating cinnamic and benzoic acid derivatives in standard solutions and in samples prepared from plant materials. The work has shown that migration times for free phenolic carboxylic acid derivatives are different from those of various types of other anions, glucosinolates, malate esters and flavonoids. This means that the separation of these compounds from the free acids is easy and possible with the MECC method. It is a rapid and inexpensive method compared with HPLC, and the separation capacity may be high, exceeding 270 000 plates/m. Evaluation of the method showed a considerable susceptibility towards different factors, making it relatively simple to choose the conditions that will separate just the compounds of interest. However, reliable identification requires a knowledge of the *RMT* values under the actual running parameters. Moreover, in order to obtain quantitative determinations, the variation in the molar absorptivities under different conditions is an interesting problem which has to be evaluated.

## ACKNOWLEDGEMENTS

The authors gratefully acknowledge support from the Danish Agricultural and Veterinary Research Council and from the Danish representatives of Applied Biosystems with respect to the use of the instrument.

## REFERENCES

- 1 G. G. Gross, in P. K. Stumpf and E. E. Conn (Editors), *Biochemistry in Plants*, Academic Press, New York, 1981, p. 301.
- 2 J. K. Nielsen, O. Olsen, L. H. Pedersen and H. Sørensen, *Phytochemistry*, 23 (1984) 1741.
- 3 J. B. Harborne, in E. A. Bell and B. V. Chartwood (Editors), *Secondary Plant Products*, Springer, Berlin, Heidelberg, New York, 1980, p. 329.
- 4 S. Clausen, O. Olsen and H. Sørensen, *J. Chromatogr.*, 260 (1983) 193.

- 5 C. Bjerregaard and H. Sørensen, paper to be presented at the *1st European Conference on Grain Legumes, Angers, France, June 1-3, 1992*.
- 6 I. Fulda and C. J. Brine (Editors), *New Developments in Dietary Fiber —Physiological, Physicochemical and Analytical Aspects*, Plenum Press, New York, London, 1990.
- 7 H. Kozłowska, M. Naczek, F. Shahidi and R. Zadernowski, in F. Shahidi (Editor), *Canola and Rapeseed Production, Chemistry, Nutrition and Processing Technology*, Van Nostrand Reinhold, New York, 1990, Ch. 11, p. 193.
- 8 S. Fujiwara and S. Honda, *Anal. Chem.*, 58 (1986) 1811.
- 9 S. Terabe, K. Otsuka, K. Ichikawa, A. Tsuchiya and T. Ando, *Anal. Chem.*, 56 (1984) 113.
- 10 M. J. Sepaniak and P. O. Cole, *Anal. Chem.*, 59 (1987) 472.
- 11 H. Nishi, N. Tsumagari and T. Kakimoto, *J. Chromatogr.*, 465 (1989) 311.
- 12 X. Huang, J. A. Luckey, M. J. Gordon, R. N. Zare, *Anal. Chem.*, 61 (1989) 766.
- 13 S. Michaelsen, P. Møller and H. Sørensen, *J. Chromatogr.*, 608 (1992) 363.
- 14 C. Bjerregaard, B. O. Eggum, S. K. Jensen and H. Sørensen, *J. Anim. Physiol. Anim. Nutr.*, 61 (1991) 69.
- 15 J. W. Jorgenson and K. D. Lukacs, *Anal. Chem.*, 53 (1981) 1298.
- 16 P. Gozel, E. Gassmann, H. Michelsen and R. N. Zare, *Anal. Chem.*, 59 (1987) 44.
- 17 C. Bjerregaard, S. Michaelsen, P. Møller and H. Sørensen, in *Proceedings of the Eighth International Rapeseed Congress, Saskatoon, Saskatchewan, Canada, July 9 to 11, 1991*, III, p. 822.
- 18 J. K. Strasters and M. G. Khaledi, *Anal. Chem.*, 63 (1991) 2503.
- 19 R. A. Wallingford and A. G. Ewing, *J. Chromatogr.*, 441 (1988) 299.
- 20 R. S. Rush and B. L. Karger, *Beckman Tech. Inf. Bull.*, TIBC-104 (1990).
- 21 M. J. Rosen, *Surfactants and Interfacial Phenomena*, Wiley, New York, 1978, Ch. 3, p. 83.
- 22 J. W. Jorgenson, in J. W. Jorgenson and M. Phillips (Editors), *New Directions in Electrophoretic Methods*, American Chemical Society, Washington, DC, 1987, Ch. 13, p. 182.
- 23 B. L. Karger, A. S. Cohen and A. Guttman, *J. Chromatogr.*, 492 (1989) 585.
- 24 T. Tsuda, K. Nomura and G. Nakagawa, *J. Chromatogr.*, 248 (1982) 241.
- 25 H. Sørensen, in F. Shahidi (Editor), *Canola and Rapeseed Production, Chemistry, Nutrition and Processing Technology*, Van Nostrand Reinhold, New York, 1990, Ch. 9, p. 149.



# Separation of inositol phosphates by capillary electrophoresis

A. Henshall, M. P. Harrold and J. M. Y. Tso

*Dionex Corporation, 1228 Titan Way, Sunnyvale, CA 94088 (USA)*

---

## ABSTRACT

The feasibility of determining inositol phosphates by capillary electrophoresis at levels present in physiological samples was investigated. Methods previously reported for the determination of inositol phosphates are limited, either in their ability to separate structural isomers, the need for pre- or post-column derivatization, or by analysis time. Using capillary electrophoresis with indirect photometric detection, separation of a standard mixture containing mono-, bis-, tris-, and hexakisinositol phosphates was achieved in less than 10 min. The potential for separation of inositol phosphate isomers using capillary electrophoresis was demonstrated by the separation of 1- and 2-inositol monophosphate. Under the conditions used, the minimum detection limit for inositol 2-phosphate in an electrolyte containing phthalate was in the vicinity of 200 ng/ml.

---

## INTRODUCTION

The mechanism by which cells respond to extracellular signals is a topic of considerable research activity [1]. In particular, the role of second messenger molecules in regulating cellular processes is receiving a great deal of attention [2–5]. Inositol-1,4,5-trisphosphate [Ins(1,4,5)P<sub>3</sub>], is of particular importance since it releases Ca<sup>2+</sup> from intracellular stores which in turn triggers a wide variety of cellular processes. Other inositol phosphates are implicated in secondary messenger functions but in most cases, their exact role is not clearly understood. In order to study these cellular processes, a rapid, sensitive method is needed for the determination of inositol phosphates at levels present in physiological samples. A variety of approaches have been used. These usually involve derivatization and radiolabelling detection techniques coupled with various separation techniques including open column anion-exchange chromatography [6], gas-liquid chromatography [7], ion pair chromatogra-

phy [8], and high-voltage electrophoresis [9]. Most recently, high-performance anion-exchange chromatography with chemically suppressed conductivity detection was applied to the separation of inositol mono- through pentakisphosphates, and inositol phosphate isomers [10]. Each of these approaches has limitations, either in the need for pre- or post-column derivatization, their inability to separate structural isomers, or in analysis time.

Capillary electrophoresis (CE) [11–16] is attractive for the determination of inositol phosphates for the following reasons: (1) only a few nanoliters of sample are used in each analysis; (2) there is the potential for concurrent separation of mono- through hexakisphosphate species in the same analysis; and (3) run times are usually short due to the intrinsically high efficiency of the technique.

Recently, capillary electrophoresis has been applied to the determination of high-mobility inorganic ions and low-molecular-mass organic acids [17–22]. A similar approach was selected for inositol phosphates since they are also non-chromophoric anions. For anion applications, a cationic surfactant or amine is incorporated into the electrolyte to cause the necessary reversal of the normal electroosmotic flow [22]. Indirect photometric detection

---

*Correspondence to:* Dr. A. Henshall, Dionex Corporation, 1228 Titan Way, Sunnyvale, CA 94088, USA.

[23,24] is often used to allow detection of non-chromophoric ions. In applying this technique to detect ions [19–21], a background absorbance is created by incorporating a highly absorbing ionic species in the buffer or electrolyte. The detection principle is based on the fact that the non-chromophoric analyte ions displace chromophoric ions as they pass through the detector causing a reduction in absorbance. This can be recorded as a negative peak, or as a positive peak if the detector output polarity is reversed. In order to use indirect photometric detection with CE, the chromophoric ion must also have a similar electrophoretic mobility of the analytes in order to prevent peak distortion [25].

Based on the ionization characteristics of phytic acid (InsP<sub>6</sub>) [26] and calculated charge to mass ratios for various degrees of ionization, electrolytes which had previously been used for CE of phosphate were selected as a starting point for CE of inositol phosphates. Two electrolyte systems were used in this initial investigation. They each contain a chromophoric ion (chromate and phthalate, respectively), with similar electrophoretic mobility to phosphate. They also offer different selectivity since the pH range from 5.8 to 7.3 is in the region of the pK<sub>a</sub> values for removal of second protons from the phosphate groups on the inositol phosphates [27].

## EXPERIMENTAL

### Reagents and standards

All reagents were of analytical-reagent or ACS grade. Potassium hydrogenphthalate and tetradecyltrimethyl ammonium bromide (TTAB) were obtained from Aldrich (Milwaukee, WI, USA). Sodium tetraborate, boric acid, and sodium chromate were obtained from Fisher Scientific (Pittsburgh, PA, USA).

Inositol phosphates used in this study were obtained from Sigma (St. Louis, MO, USA). These were of varying purity, as follows:

DL-*myo*-Inositol-1-monophosphate, Ins(1)P, as the cyclohexylammonium salt (Purity ca. 75%. Balance primarily 2-monophosphate isomer).

DL-*myo*-Inositol-2-monophosphate, Ins(2)P, as the di(cyclohexylammonium) salt (purity ca. 95%).

DL-*myo*-Inositol-1,4-bisphosphate, Ins(1,4)P<sub>2</sub>, as the potassium salt (purity ca. 98% by thin-layer chromatography).

DL-*myo*-Inositol-1,4,5-trisphosphate, Ins(1,4,5)P<sub>3</sub>, as the potassium salt, (86% 1,4,5-isomer and 14% 2,4,5-isomer).

Phytic acid (*myo*-inositol hexakisphosphate), InsP<sub>6</sub>, as the dodecasodium salt.

With the exception of phytic acid, inositol phosphates were stored in the dark at –20°C immediately on receipt.

### Preparation of inositol phosphate standards

Stock solutions of phytic acid and Ins(2)P were prepared in the conventional manner by weighing and volumetric dilution. Stock solutions of Ins(1)P, Ins(1,4)P<sub>2</sub>, Ins(1,4,5)P<sub>3</sub> were prepared directly in the sample vials (each containing approximately 0.1 mg) using 18-M $\Omega$  deionized water, then refrozen. Immediately prior to capillary electrophoresis runs, these stock solutions were allowed to warm to room temperature in a closed box (to minimize photodecomposition), and aliquots removed for dilution immediately prior to analysis by CE.

### Electrolyte preparation

Electrolytes used in this study were as follows: (1) 2.5 mM K<sub>2</sub>CrO<sub>4</sub>, 0.5 mM tetradecyltrimethyl ammonium bromide (TTAB), 5.0 mM H<sub>3</sub>BO<sub>3</sub>, pH 7.3; and (2) 5.0 mM potassium hydrogenphthalate, 0.5 mM TTAB, 2.0 mM Na<sub>2</sub>B<sub>4</sub>O<sub>7</sub>, pH 5.9. All electrolytes were filtered through a 0.45- $\mu$ m filter and vacuum degassed for 5 min prior to use.

### Equipment

CE was performed on a Dionex CES I system with the negative polarity power supply. Untreated silica capillaries (55 cm  $\times$  50  $\mu$ m I.D.  $\times$  375  $\mu$ m O.D.) from Polymicro Technologies (Phoenix AZ, USA) were used throughout in this work. Prior to use, they were flushed successively with 0.1 M phosphoric acid, deionized water, 0.5 M NaOH, deionized water, and finally with the operating electrolyte. A Dionex AI-450 chromatography workstation was used for data acquisition and processing. The variable-wavelength UV detector in the CES I was used for indirect photometric detection of the inositol phosphates with the signal switch polarity reversed to give positive peaks. Wavelength settings were 270 nm for the chromate electrolyte and 254 nm for the phthalate electrolyte. Output range was 0.005 AUFS.

## RESULTS AND DISCUSSION

Standard runs with individual inositol phosphates in both the chromate and phthalate electrolyte confirmed that it is possible to separate these compounds concurrently in less than 10 min. This is illustrated by the separation of a mixture of inositol phosphates with widely different numbers of phosphate groups using the chromate electrolyte at pH 7.3 (Fig. 1). As shown in Fig. 2, the selectivity is quite different with the phthalate electrolyte at pH 5.9. Separation of all the inositol phosphates was not achieved in this case since the Ins(1,4,5)P<sub>3</sub> and InsP<sub>6</sub> are poorly resolved and exhibit fronting.

Although separation of all species was obtained at pH 7.3 with the chromate electrolyte, the development of a routine method for the concurrent separation of Ins(1)P through InsP<sub>6</sub> using this particular electrolyte is questionable. The entire separation of the inositol phosphates of interest takes

place within 0.7 min, hence, small shifts in migration time could conceivably lead to misidentification. Repeatability of migration times usually were found to agree within  $\pm 0.01$  min for consecutive runs, however, significant shifts in migration times occurred from day-to-day and with different capillaries. Buffering of the electrolyte should alleviate this problem, and will very likely be necessary when analyzing physiological samples. The pH 7.3 chromate electrolyte does have potential utility for the analysis of individual inositol phosphate pairs such as mono- from bi- and tri- phosphate species since they are well resolved. For example, Ins(1)P and Ins(1,4)P<sub>2</sub> are separated by almost 1 min. The pH 5.9 phthalate electrolyte does not appear to be useful for concurrent separation of all the inositol phosphates, however, it exhibits excellent selectivity for the mono- and diphosphate species. Ins(1)P<sub>1</sub> and Ins(1,4)P<sub>2</sub> are separated by 1.38 min. In addition, the two monophosphate position isomers, Ins-

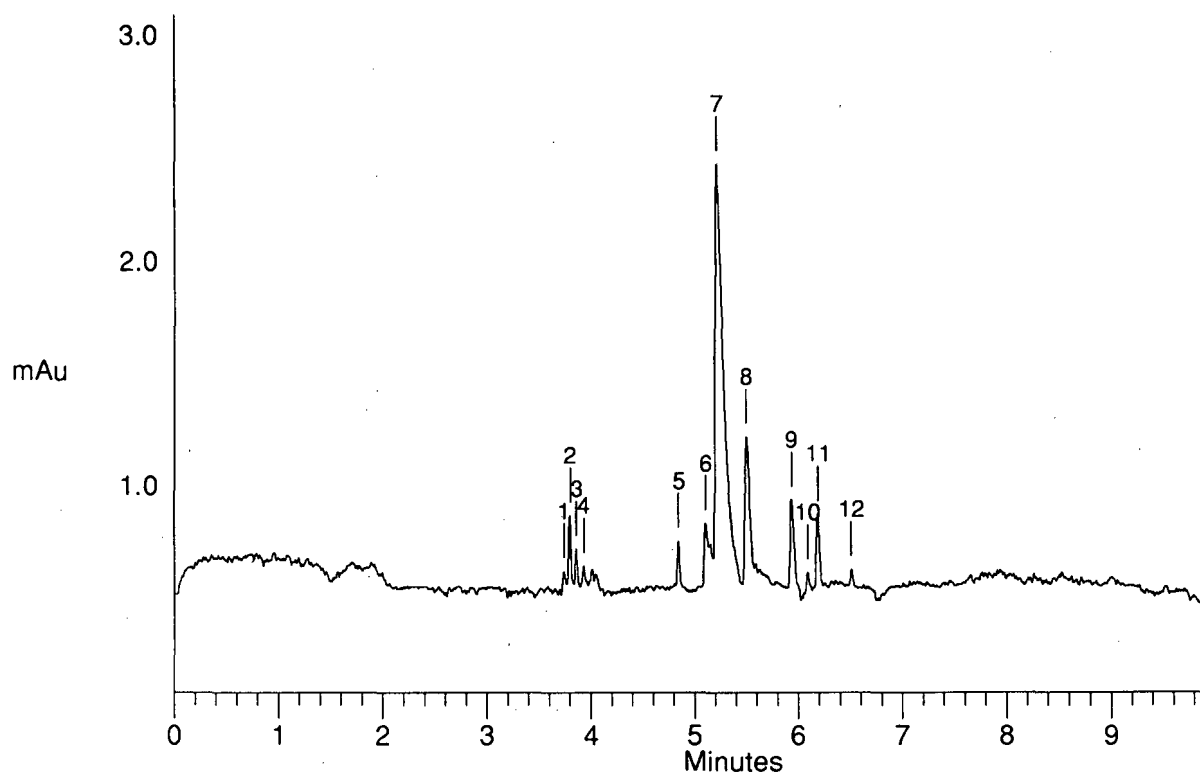


Fig. 1. Separation of inositol phosphate mixture by capillary electrophoresis. Electrolyte: 2.5 mM K<sub>2</sub>CrO<sub>4</sub>, 0.5 mM tetradecyltrimethyl ammonium bromide, 5.0 mM H<sub>3</sub>BO<sub>3</sub>, pH 7.3; operating voltage: 15 kV; electroinjection: 5 kV for 2 s; indirect photometric detection at 270 nm. Peaks: 1-4 = inorganic ions; 5 = Ins(1,4)P<sub>2</sub>; 6 = InsP<sub>6</sub>; 7 = Ins(1,4,5)P<sub>3</sub>; 8 = Ins(1)P; 9-12 = unknowns.

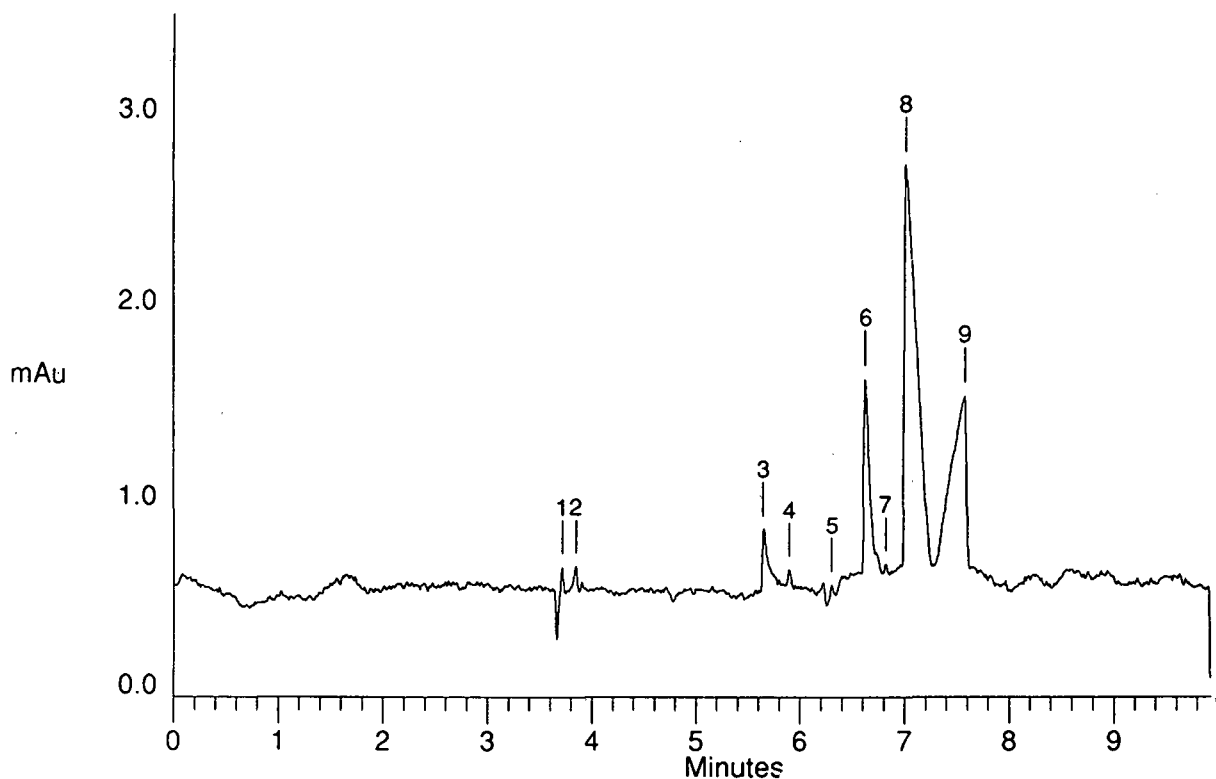


Fig. 2. Separation of inositol phosphates mixture by capillary electrophoresis. Electrolyte: 5.0 mM potassium hydrogenphthalate, 0.5 mM tetradecyltrimethyl ammonium bromide, 2.0 mM  $\text{Na}_2\text{B}_4\text{O}_7$ , pH 5.9; operating voltage: 15 kV; electroinjection: 5 kV for 2 s; indirect photometric detection at 254 nm. Peaks: 1, 2 = inorganic ions; 3 =  $\text{Ins}(1,4)\text{P}_2$ ; 4,5 = unknowns; 6 =  $\text{Ins}(1)\text{P}$ ; 7 = unknown; 8 =  $\text{Ins}(1)\text{P}$ ; 9 =  $\text{Ins}(1,4,5)\text{P}_3 + \text{InsP}_6$ .

(1)P and  $\text{Ins}(2)\text{P}$ , are also well separated. The assignment of the major impurity peak in the  $\text{Ins}(1)\text{P}$  electropherogram to  $\text{Ins}(2)\text{P}$  is supported by the good agreement in migration times for the impurity peak and  $\text{Ins}(2)\text{P}$ , as shown in Fig. 3a and b, and by spiking with  $\text{Ins}(2)\text{P}$  as shown in Fig. 3c. These runs were carried out at a later date with a different capillary and batch of electrolyte than the runs shown in Figs. 1 and 2, hence migration times between the two sets of runs are not directly comparable. Good correlation between peak areas for the amount of the spike was obtained. A further indication that this peak is due to the  $\text{Ins}(2)\text{P}$  impurity known to be present in this sample of  $\text{Ins}(1)\text{P}$ , is that the area ( $7.35 \cdot 10^5$  area units) is approximately 25% of the main peak ( $28.43 \cdot 10^5$  area units). This is in agreement with the Sigma estimate of approximately 25%  $\text{Ins}(2)\text{P}$  impurity by thin-layer chromatographic analysis. Although electromigration injec-

tion was used in these runs, concentration bias problems reported by others [28] would be expected to be minimal in this case, since the electrophoretic mobilities of the two ions in question [ $\text{Ins}(1)\text{P}$  and  $\text{Ins}(2)\text{P}$ ] are similar.

#### Detection limits

The results of a brief study to assess the linearity of response, and detection limits for inositol phosphates using indirect photometric detection with the phthalate electrolyte, are shown in Fig. 4. Six dilutions of an accurately weighed  $\text{Ins}(2)\text{P}$  standard in the range from 0.5 to 25  $\mu\text{g}/\text{ml}$  (as the free acid) were electro-injected (7.5 kV for 5 s) and yielded a close to linear calibration plot (correlation coefficient = 0.9946) at concentrations in the range from 0 to 17  $\mu\text{g}/\text{ml}$ . Detection limits under these conditions appear to be in the vicinity of 200 ng/ml for a signal-to-noise ratio of 3:1.

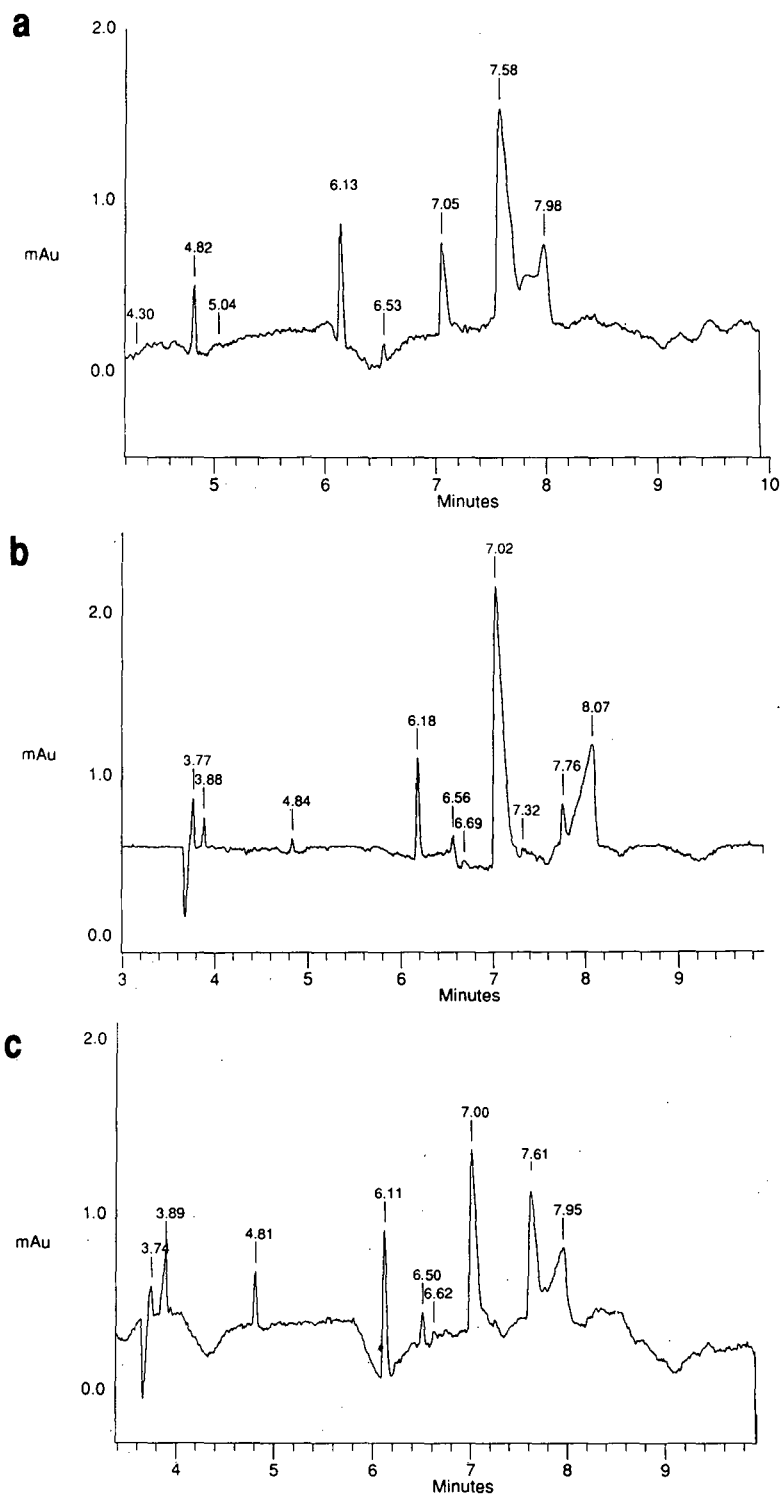


Fig. 3. Comparison of electropherograms for (a) DL-*myo*-inositol-1-monophosphate, (b) DL-*myo*-inositol-2-monophosphate, (c) a mixture of the 1- and 2-isomers. Conditions as for Fig. 2. Peak labels are migration times in minutes.



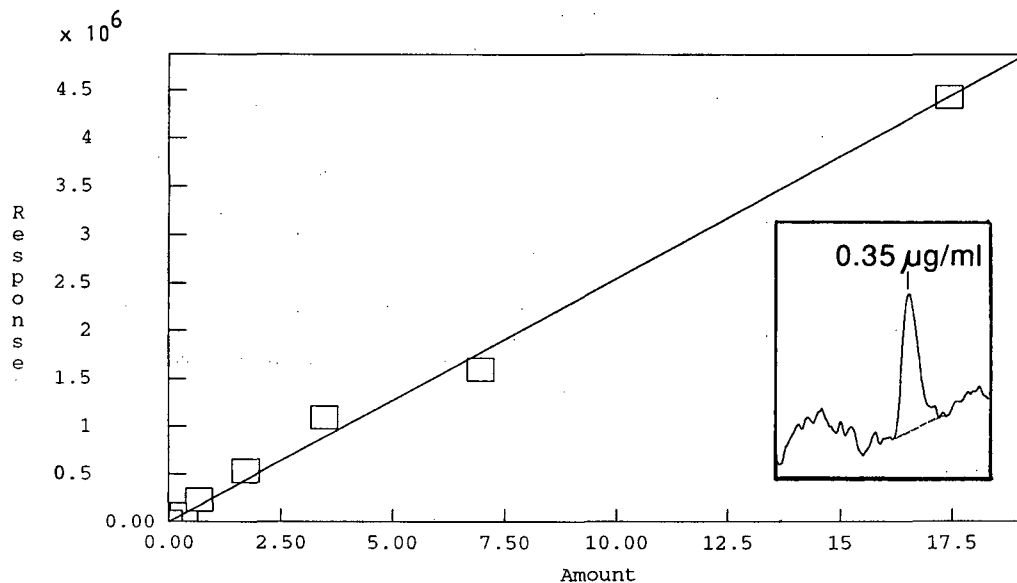


Fig. 4. Calibration plot for Ins(2)P in phthalate electrolyte. Conditions as for Fig. 2 except that the electroinjection was 7.5 kV for 2 s. Inset indicates signal to noise for 0.35  $\mu\text{g/ml}$  level.  $r^2 = 0.994602$ . x-axis: amount in  $\mu\text{g/ml}$ .

Typical levels of inositol phosphates in rat brain ranging from 0.005  $\mu\text{mol/g}$  for Ins(1,4,5)P<sub>3</sub> to 0.040  $\mu\text{mol/g}$  for Ins(4)P have been reported [29,30]. These levels translate to *ca.* 2  $\mu\text{g/g}$  wet mass of tissue for Ins(1,4,5)P<sub>3</sub> and 10.4  $\mu\text{g/g}$  wet mass for Ins(4)P. In studies of this type, therefore, it appears that indirect photometric detection may provide adequate detection sensitivity.

#### CONCLUSIONS

On the basis of this study, CE shows great promise for the concurrent analysis of inositol phosphates with 1 to 6 phosphate groups, at levels encountered in physiological samples. Separations can be achieved in less than 10 min, and only a few nanoliters of sample are required for each analysis. Selectivity of the inositol phosphates separation can be controlled by varying the electrolyte pH in the vicinity of the  $pK_a$  values for ionization of the second proton from the phosphate groups (pH 5–10.5) [26]. The position isomers Ins(1)P and Ins(2)P are easily separated in the phthalate electrolyte system demonstrating the potential for separating other inositol phosphate isomers.

Optimization of the pH for the separation may allow a mapping procedure to be developed for in-

ositol phosphates. With this objective, a more extensive study is now underway to investigate the separation of inositol phosphates in several buffered electrolyte systems over a wider range of pH. The results of this study will be reported at a later date.

#### REFERENCES

- 1 M. J. Berridge and R. F. Irvine, *Nature (London)*, 312 (1984) 315.
- 2 A. A. Abdel-Latif, *Pharmacol. Rev.*, 38 (1986) 227.
- 3 P. W. Majerus, T. M. Connolly, H. Deckmyr, T. S. Ross, T. E. Bross, H. Ishii, V. Bansal and D. B. Wilson, *Science (Washington, D.C.)*, 234 (1986) 1519.
- 4 Y. Nishizuka, *Science (Washington, D.C.)*, 225 (1984) 1365.
- 5 L. F. Fleischman, S. B. Chahwala and L. Cantly, *Science (Washington, D.C.)*, 231 (1986) 407.
- 6 R. F. Irvine, E. E. Anggard, A. J. Letcher and C. P. Downes, *Biochem. J.*, 229 (1985) 505.
- 7 A. L. Leavitt and W. R. Sherman, *Methods Enzymol.*, 89 (1982) 9.
- 8 J. A. Shayman and D. M. Bement, *Biochem. Biophys. Res. Commun.*, 98 (1988) 114.
- 9 U. B. Seiffert and B. W. Agrnoff, *Biochim. Biophys. Acta*, 98 (1965) 573.
- 10 *Applications Note No. 65*, Dionex Corporation, Sunnyvale, CA, 1990.
- 11 J. W. Jorgensen and K. D. Lukacs, *Science (Washington, D.C.)*, 222 (1983) 266.
- 12 W. G. Kuhr, *Anal. Chem.*, 62 (1990) 403R–412R.

- 13 A. G. Ewing, R. A. Wallingford, *Adv. Chromatogr.*, 29 (1989) 1.
- 14 S. Hjertén, *Electrophoresis*, 11 (1990) 665.
- 15 K. Kleparnik and P. Boček, *J. Chromatogr.*, 569 (1991) 3.
- 16 Z. Deyl and R. Struzinsky, *J. Chromatogr.*, 569 (1991) 63.
- 17 W. Kuhr and E. Yeung, *Anal. Chem.*, 60 (1988) 2642.
- 18 L. Gross, E. Yeung, *J. Chromatogr.*, 480 (1989) 169.
- 19 F. Foret, S. Fanali, L. Ossicini and P. Boček, *J. Chromatogr.*, 470 (1989) 299.
- 20 F. Foret, S. Fanali, A. Nardi and P. Boček, *Electrophoresis*, 11 (1990) 780.
- 21 W. R. Jones and P. Jandik, *J. Chromatogr.*, 546 (1990) 545.
- 22 X. Huang, J.A. Luckey, M. J. Gordon, and R. N. Zaro, *Anal. Chem.*, 61 (1988) 766.
- 23 H. Small, *Ion Chromatography*, Plenum Press, New York, 1989, pp. 195–205.
- 24 E. S. Yeung, *Acc. Chem. Res.*, 22 (1989) 125.
- 25 F. E. P. Mikkers, F. M. Everaerts and Th. P. E. M. Verheggen, *J. Chromatogr.*, 169 (1979) 10.
- 26 C. J. Martin and W. J. Evans, *J. Inorg. Biochem.*, 27 (1986) 26.
- 27 R. E. Smith, S. Howell, D. Yourtee, N. Premkumar, T. Pond, G. Y. Sun and R. A. MacQuarrie, *J. Chromatogr.*, 439 (1988) 83.
- 28 X. Huang, T. K. J. Pang, M. J. Gordon and R. N. Zare, *Anal. Chem.*, 60 (1987) 2747.
- 29 Teng-Nan Lin, G. Y. Sun, N. Premkumar, R. A. MacQuarrie and S. R. Carter, *Biochem. Biophys. Res. Commun.*, 167 (1990) 1294.
- 30 X. Huang, M. J. Gordon and R. N. Zare, *Anal. Chem.*, 60 (1988) 375.



# Chiral separations by capillary electrophoresis using cyclodextrin-containing gels

Ingrid D. Cruzado and Gyula Vigh

Chemistry Department, Texas A&M University, College Station, TX 77843-3255 (USA)

---

## ABSTRACT

Allyl carbamoylated  $\beta$ -cyclodextrin derivatives were synthesized to be used as chiral resolving agents when copolymerized with acrylamide to form gels suitable for enantiomer separations in capillary electrophoresis. Both solid and liquid gels have been produced by adjusting the concentrations of acrylamide, bis-acrylamide and the allyl cyclodextrin derivative. The liquid gels were free of the problems associated with solid gels: bubble formation, short lifetime and poor reproducibility. The chiral selectivity of the liquid cyclodextrin gels in the separation of dansylated amino acid enantiomers depended on the cyclodextrin concentration of the gel. The liquid gels were successfully used to separate the enantiomers of several chiral molecules.

---

## INTRODUCTION

Capillary electrophoresis (CE) has become a powerful analytical technique during the past decade and spun several variants of the original method ranging from free solution CE through micellar techniques to capillary gel electrophoresis [1–3]. Though capillary gel electrophoresis is mostly used to separate biopolymers based on their size differences [4], Guttman *et al.* [5] used the polyacrylamide gel matrix to support selective complexing agents, such as native cyclodextrins, to alter the separation selectivity of the CE system.

$\beta$ -Cyclodextrin ( $\beta$ -CD) is a toroidally shaped oligosaccharide composed of seven glucose units which are connected through  $\alpha$ -(1,4)-linkages. The inner surface of the hollow truncated cone is relatively hydrophobic, whereas the external surfaces are hydrophilic due to the presence of the secondary hydroxyl groups at the larger opening and the primary hydroxyl groups at the smaller opening of the cavity [6]. CDs have been successfully used for chiral separations in high-performance liquid chroma-

tography [7], capillary gas chromatography [8,9], isotachopheresis [10–13], free-solution CE [14–17], micellar electrokinetic chromatography [18,19] and capillary gel electrophoresis [5]. To the best of our knowledge, no report has been published yet on the CE use of allyl carbamoylated  $\beta$ -CD-acrylamide copolymer gels as described here.

## EXPERIMENTAL

Allyl carbamoylated  $\beta$ -cyclodextrin derivatives (ac- $\beta$ -CD) were synthesized according to the general method described in ref. 20, with some modifications as follows. A 10 mmol portion of  $\beta$ -CD (American Maize-Products, Hammond, IN, USA) was dried overnight *in vacuo* at 60°C, and then dissolved in 150 ml of dry pyridine. 25 mmol of allyl isocyanate (Aldrich, Milwaukee, WI, USA) were added and the reaction mixture was stirred for three days at room temperature. Thin-layer chromatographic separations revealed the presence of mono-, di-, tri- and tetra-substituted ac- $\beta$ -CD derivatives. No unreacted  $\beta$ -CD was detected at the end of the third day. The raw product was purified by repeated crystallization from acetone.

The ac- $\beta$ -CD-acrylamide copolymer gels were

---

Correspondence to: Dr. Gy. Vigh, Chemistry Department, Texas A&M University, College Station, TX 77843-3255, USA.

prepared by dissolving known quantities of the  $\beta$ -CD derivative, acrylamide (Aldrich) and/or bisacrylamide (Aldrich) in a known volume of pH 8.3 0.1 M Tris–0.25 M boric acid buffer. The solutions were filtered through a FHLP04700 membrane (Millipore, Bedford, MA, USA) and degassed before polymerization. Polymerization was carried out by adding, N,N,N',N'-tetramethylethylenediamine (TEMED) as catalyst, and ammonium persulfate as radical initiator [4], and the reaction mixture was left to stand overnight. When bisacrylamide was present, the result was a solid gel; when it was absent, the product was a liquid gel.

A CE system assembled from a Spectroflow 783 UV detector (ABI, San Jose, CA, USA) a Type PS/EH30R03.0 high-voltage power supply (Glassman, Whitehouse Station, NJ, USA) and a plexiglass safety box [2] was used for the measurements. A Chrom-1/AT analog/digital converter board (Keithley Metrabyte, Tauton, MA, USA), installed in a Vectra-30 IBM-compatible personal computer and controlled by a data acquisition program developed in our laboratory [21], was used to collect and analyze data. Separations were carried out in 100  $\mu$ m I.D. fused-silica capillaries (Polymicro Technologies, Phoenix, AZ, USA). The dansylated amino acid and drug standards were obtained from Sigma (St. Louis, MO, USA). Their solutions were prepared with the same buffer used in the preparation of the gels. The concentrations of the sample solutions were: 1.2 mM dansyl-D,L-aspartic acid (Asp), 1.5 mM dansyl-D,L- $\alpha$ -amino-*n*-butyric acid (But), 1.5 mM dansyl-D,L-glutamic acid (Glu), 1.2 mM dansyl-D,L-leucine (Leu), 1.2 mM dansyl-D,L-methionine (Met), 1.2 mM dansyl-D,L-norleucine (Norleu), 1.6 mM dansyl-D,L-norvaline (Norval), 1.4 mM dansyl-D,L-phenylalanine (Phe), 1.6 mM dansyl-D,L-serine (Ser), 1.4 mM dansyl-D,L-threonine (Thr), 1.0 mM dansyl-D,L-tryptophan (Trp), 1.1 mM dansyl-D,L-valine (Val), 6.2 mM homatropine and 5.9 mM atropine.

## RESULTS AND DISCUSSION

Several gel filled capillaries were prepared by keeping the concentration of acrylamide and bisacrylamide (%T and %C) constant and varying the concentration of ac- $\beta$ -CD. The observed chiral selectivity for the separation of the enantiomers of

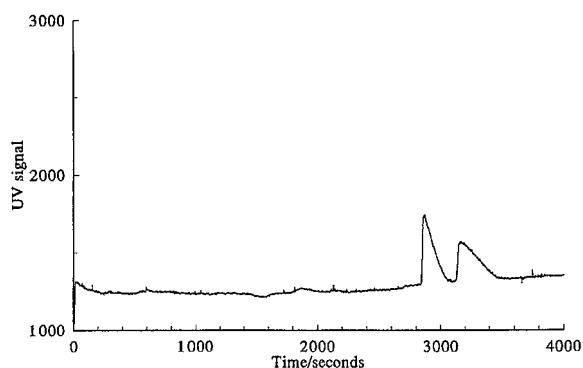


Fig. 1. Separation of the enantiomers of 1.1 mM dansyl-D,L-phenylalanine in a solid-gel filled capillary. Gel constituents: 5%T, 3.3%C and 40 mM ac- $\beta$ -CD derivative in pH 8.3 0.1 M Tris–0.25 M boric acid buffer. Field strength: 95 V/cm. Electrokinetic injection at 16 V/cm for 5 s. Capillary dimensions: total length: 19 cm, injector to detector length: 12 cm, I.D.: 100  $\mu$ m, O.D.: 170  $\mu$ m. Detection wavelength: 255 nm.

dansyl-D,L-phenylalanine increased from 1.04 to 1.21 as the concentration of ac- $\beta$ -CD was increased from 20 to 40 mM. Fig. 1 shows a typical electropherogram for the separation of the enantiomers of dansyl-D,L-phenylalanine, obtained on a 5%T, 3.3%C and 40 mM ac- $\beta$ -CD solid-gel filled capillary. Though chiral selectivity is high, separation efficiency is much lower than customary in CE. In addition, practical problems such as short lifetime due to bubble formation and gel extrusion at higher field strengths could not be eliminated easily and reliably [22]. Therefore, solid gels were abandoned in favor of the liquid gels, which were free of these problems.

Stable and reproducible liquid gels were obtained when the reaction mixture contained 1 to 2% (140 to 280 mM) acrylamide, 0 to 30 mM ac- $\beta$ -CD, 4 to 10  $\mu$ l/ml (26 to 66 mM) TEMED and 4 to 10  $\mu$ l/ml of 10% (w/w) (1.8 to 4.4 mM) ammonium persulfate in the pH 8.3 Tris–boric acid buffer. To achieve complete copolymerization, the liquid gels were allowed to stand in the reaction vessel for at least 12 h before being transferred into the separation capillaries. Though viscous, the liquid gels could be transferred from the reaction vessels with microsyringes. Figs. 2 and 3 show typical electropherograms for the enantiomers of a few dansylated amino acids. Though the chiral selectivities are slightly lower than those obtained with the solid-gel filled capillaries, the separation efficiencies are much bet-

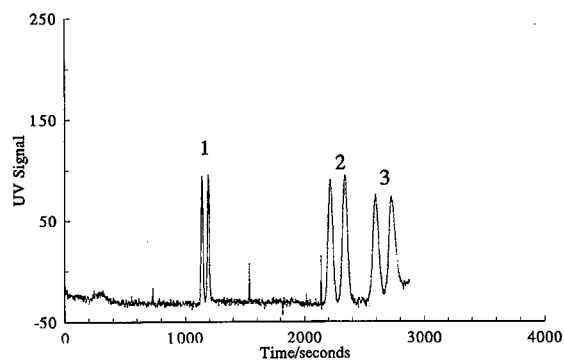


Fig. 2. Separation of the enantiomers of dansyl-D,L-aspartic acid, threonine and methionine in a liquid-gel filled capillary. Peaks: 1 = dansyl-D,L-aspartic acid; 2 = dansyl-D,L-threonine; 3 = dansyl-D,L-methionine. Gel constituents: 2% acylamide, 20 mM ac- $\beta$ -CD derivative in pH 8.3 0.1 M Tris-0.25 M boric acid buffer. Field strength 89 V/cm. Electrokinetic injection at 15 V/cm for 1 s. Capillary dimensions: total length: 20 cm, injector to detector length: 13 cm, I.D. 100  $\mu$ m, O.D. 170  $\mu$ m. Detection wavelength: 255 nm.

ter. Table I contains the selectivity and resolution data for the enantiomers of 12 dansylated amino acids. The separations were achieved with a 2% acrylamide and 20 mM ac- $\beta$ -CD liquid gel, at a field strength of 89 V/cm. The enantiomers of three amino acids: tryptophan, norvaline and  $\alpha$ -amino-*n*-butyric acid were not resolved.

Chiral selectivity and efficiency ( $N$ ) were found to depend on the concentration of ac- $\beta$ -CD in the copolymer: chiral selectivity increased, while  $N$  decreased with increasing concentration of ac- $\beta$ -CD

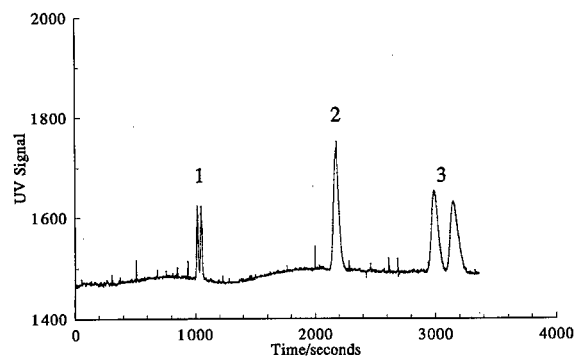


Fig. 3. Separation of the enantiomers of dansyl-D,L-glutamic acid, norvaline and phenylalanine in a liquid-gel filled capillary. Peaks: 1 = dansyl-D,L-glutamic acid; 2 = dansyl-D,L-norvaline; 3 = dansyl-D,L-phenylalanine. Conditions as in Fig. 2.

TABLE I

SELECTIVITY AND PEAK RESOLUTION FOR THE SEPARATION OF THE ENANTIOMERS OF DANSYL-D,L-AMINO ACIDS

Conditions as in Fig. 2.

Amino acid	Selectivity	Resolution
Asp	1.046	1.5
But	1	0
Glu	1.031	1.0
Leu	1.127	2.5
Met	1.050	1.1
Norleu	1.095	2.1
Norval	1	0
Phe	1.052	1.1
Ser	1.033	0.8
Thr	1.055	1.3
Trp	1	0
Val	1.027	0.6

(Figs. 4 and 5). Presumably, both phenomena are brought about by the increased number of interactions between the solutes and the cyclodextrin moieties and the slow complexation kinetics, respectively. The opposing trends lead to resolution maxima at intermediate ac- $\beta$ -CD concentrations, in agreement with the behavior observed in free solution systems [15].

The 2% acrylamide and 20 mM ac- $\beta$ -CD liquid gels were successfully used for separation of the enantiomers of chiral drugs. However, the same gel

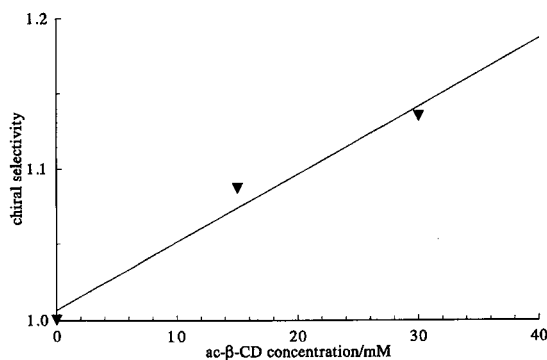


Fig. 4. Selectivity for the separation of the enantiomers of dansyl-D,L-leucine as a function of the ac- $\beta$ -CD concentration of the liquid gel. Conditions as in Fig. 2, except field strength is 74 V/cm.

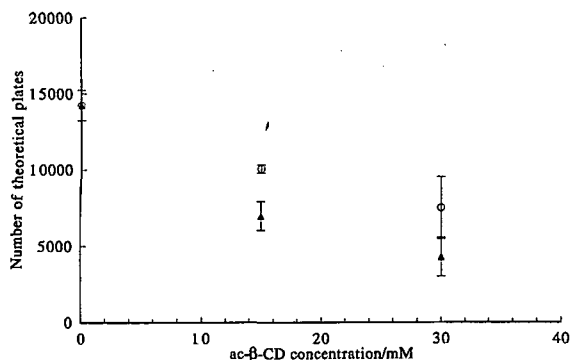


Fig. 5. Efficiencies (number of theoretical plates,  $N$ ) calculated from the electropherograms of the enantiomers of dansyl-D,L-leucine as a function of the ac- $\beta$ -CD concentration of the liquid gel. Conditions as in Fig. 4. ○ = More mobile enantiomer; ▲ = less mobile enantiomer.

does not always resolve the enantiomers of closely related chiral compounds. For example, baseline-to-baseline enantiomer separation could be obtained for homatropine (Fig. 6a), but no separation was seen for atropine (Fig. 6b). This indicates that the chiral resolving ability of CD must be tailored to match the structure of the solutes via modification of the secondary OH groups of the ac- $\beta$ -CD molecule. Further work is in progress in our laboratory in this direction.

#### ACKNOWLEDGEMENTS

Partial financial support for this project was obtained from the National Minority Merit Scholarship Fund, the National Science Foundation (CHE-8919151) and Genetech (South San Francisco, CA, USA). American Maize-Products Corporation is acknowledged for donating the  $\beta$ -cyclodextrin used in the synthesis of the gel monomers.

#### REFERENCES

- J. W. Jorgenson, *Trends Anal. Chem.*, 3 (1984) 51.
- J. W. Jorgenson and K. D. Lukacs, *Anal. Chem.*, 53 (1981) 1298.
- M. J. Gordon, X. Huang, S. J. Pentoney and R. N. Zare, *Science (Washington, D.C.)*, 242 (1988) 224.
- A. S. Cohen, A. Paulus and B. L. Karger, *Chromatographia*, 24 (1987) 15.
- A. Guttman, A. Paulus, A. S. Cohen, N. Grinberg and B. L. Karger, *J. Chromatogr.*, 488 (1988) 41.

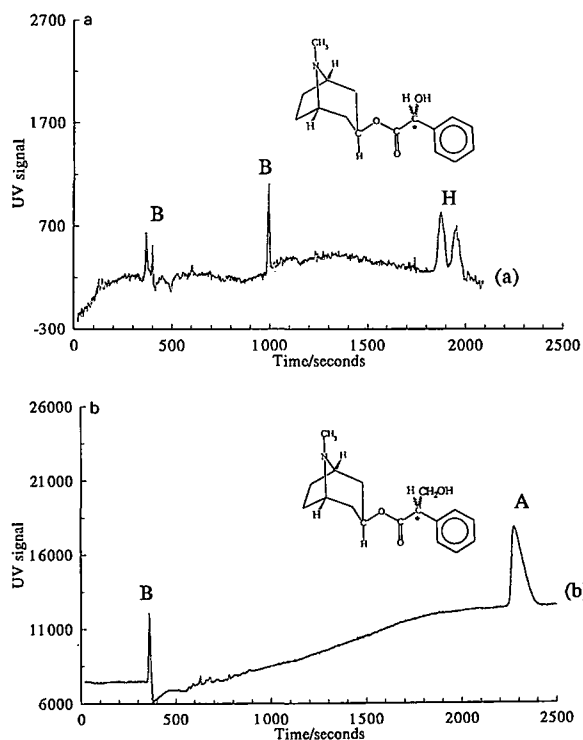


Fig. 6. Separation of the enantiomers of (a) homatropine and (b) atropine in a liquid-gel filled capillary. Peaks: B = unknown; H = homatropine; A = atropine. Conditions as in Fig. 2, except that field strength is 99 V/cm and detection wavelength is 210 nm.

- M. L. Bender and M. Komiyama, *Cyclodextrin Chemistry*, Springer, New York, 1st ed., 1978.
- D. Armstrong, *Anal. Chem.*, 59 (1987) 84A.
- E. Smolková-Keulemansová, *J. Chromatogr.*, 251 (1982) 17.
- V. Schurig and H. P. Nowotny, *J. Chromatogr.*, 441 (1988) 155.
- I. Jelinek, J. Snopek and E. Smolková-Keulemansová, *J. Chromatogr.*, 438 (1988) 211.
- I. Jelinek, J. Snopek and E. Smolková-Keulemansová, *J. Chromatogr.*, 439 (1988) 386.
- S. Fanali and M. Sinibaldi, *J. Chromatogr.*, 442 (1988) 371.
- I. Jelinek, J. Dohnal, J. Snopek and E. Smolková-Keulemansová, *J. Chromatogr.*, 464 (1989) 139.
- S. Terabe, *Trends Anal. Chem.*, 8 (1989) 129.
- A. Fanali, *J. Chromatogr.*, 474 (1989) 441.
- J. Snopek, H. Soini, M. Novotny, E. Smolková-Keulemansová and I. Jelinek, *J. Chromatogr.*, 559 (1991) 215.
- M. Tanaka, S. Asano, M. Yoshinaga, Y. Kawaguchi, T. Tetsumi, T. Shono, *Fresenius Z. Anal. Chem.*, 339 (1991) 63.
- S. Terabe, H. Ozaki, K. Otsuka and T. Ando, *J. Chromatogr.*, 332 (1985) 211.
- H. Nishi and M. Matsuo, *J. Liq. Chromatogr.*, 14 (1991) 973.

- 20 K. Fujimura, S. Suzuki, K. Hayashi and S. Masada, *Anal. Chem.*, 62 (1990) 2198.
- 21 Gy. Vigh, G. Quintero and Gy. Farkas, in Cs. Horváth and J. G. Nikelly (Editors), *Analytical Biotechnology*, American Chemical Society, Washington DC, 1990, p. 181.
- 22 I. D. Cruzado and Gy. Vigh, in A. Hedges (Editor), *Proceedings of the 6th International Symposium on Cyclodextrins*, Editions de Sante, Paris, 1992, in press.





# Author Index

- Abdel-Baky, S. and Giese, R. W.  
Capillary electrophoresis washing technique  
608(1992)159
- Adjalla, C., see Lambert, D. 608(1992)311
- Alloni, A., see Gelfi, C. 608(1992)333
- Alloni, A., see Gelfi, C. 608(1992)343
- Andrews, D., see Cheng, Y.-F. 608(1992)109
- Arai, A., see Guttman, A. 608(1992)175
- Bammel, B. P., see O'Shea, T. J. 608(1992)189
- Bao, J. and Regnier, F. E.  
Ultramicro enzyme assays in a capillary electrophoretic system 608(1992)217
- Bay, S., see Harke, H. R. 608(1992)143
- Benhayoun, S., see Lambert, D. 608(1992)311
- Bjergegaard, C., Michaelsen, S. and Sørensen, H.  
Determination of phenolic carboxylic acids by micellar electrokinetic capillary chromatography and evaluation of factors affecting the method 608(1992)403
- Boček, P., see Gebauer, P. 608(1992)47
- Brinkman, U. A. T., see Debets, A. J. J. 608(1992)151
- Brown, P. R., see Weston, A. 608(1992)395
- Bruin, G. J. M., Van Asten, A. C., Xu, X. and Poppe, H.  
Theoretical and experimental aspects of indirect detection in capillary electrophoresis 608(1992)97
- Buchberger, W. and Haddad, P. R.  
Effects of carrier electrolyte composition on separation selectivity in capillary zone electrophoresis of low-molecular-mass anions 608(1992)59
- Busch, S., see Kraak, J. C. 608(1992)257
- Cai, J. and El Rassi, Z.  
Micellar electrokinetic capillary chromatography of neutral solutes with micelles of adjustable surface charge density 608(1992)31
- Carson, W., see Cheng, Y.-F. 608(1992)109
- Chang, H.-T. and Yeung, E. S.  
Optimization of selectivity in capillary zone electrophoresis via dynamic pH gradient and dynamic flow gradient 608(1992)65
- Chen, D.-Y., see Zhao, J.-Y. 608(1992)117
- Cheng, Y.-F., Fuchs, M., Andrews, D. and Carson, W.  
Membrane fraction collection for capillary electrophoresis 608(1992)109
- Cooper, C. L., see Ma, Y. 608(1992)93
- Cruzado, I. D. and Vigh, G.  
Chiral separations by capillary electrophoresis using cyclodextrin-containing gels 608(1992)421
- Damm, J. B. L., Overkluft, G. T., Vermeulen, B. W. M., Fluitsma, C. F. and Van Dedem, G. W. K.  
Separation of natural and synthetic heparin fragments by high-performance capillary electrophoresis 608(1992)297
- Danzer, M. H., see Weiss, C. S. 608(1992)325
- Datta, M. H., see Weiss, C. S. 608(1992)325
- De Besi, P., see Gelfi, C. 608(1992)333
- De Besi, P., see Gelfi, C. 608(1992)343
- Debets, A. J. J., Mazereeuw, M., Voogt, W. H., Van Iperen, D. J., Lingeman, H., Hupe, K.-P. and Brinkman, U. A. T.  
Switching valve with internal micro precolumn for on-line sample enrichment in capillary zone electrophoresis 608(1992)151
- Denoroy, L., see Soucheleau, J. 608(1992)181
- Desbène, P. L., Rony, C., Desmazières, B. and Jacquier, J. C.  
Analysis of alkylaromatic sulphonates by high-performance capillary electrophoresis 608(1992)375
- Desmazières, B., see Desbène, P. L. 608(1992)375
- D'Hulst, A. and Verbeke, N.  
Chiral separation by capillary electrophoresis with oligosaccharides 608(1992)275
- Dirschlmayer, A., see Lindner, H. 608(1992)211
- Dovichi, N. J., see Harke, H. R. 608(1992)143
- Dovichi, N. J., see Zhao, J.-Y. 608(1992)117
- Dovichi, N. J., see Zhao, J. Y. 608(1992)239
- Elo, H., see Lukkari, P. 608(1992)317
- El Rassi, Z., see Cai, J. 608(1992)31
- Felden, F., see Lambert, D. 608(1992)311
- Fluitsma, C. F., see Damm, J. B. L. 608(1992)297
- Foret, F., Szoko, E. and Karger, B. L.  
On-column transient and coupled column isotachophoretic preconcentration of protein samples in capillary zone electrophoresis 608(1992)3
- Friedl, W., see Kenndler, E. 608(1992)161
- Fuchs, M., see Cheng, Y.-F. 608(1992)109
- Gaboriaud, R., see Tribet, C. 608(1992)131
- Gareil, P., see Tribet, C. 608(1992)131
- Gebauer, P., Thormann, W. and Boček, P.  
Sample self-stacking in zone electrophoresis. Theoretical description of the zone electrophoretic separation of minor compounds in the presence of bulk amounts of a sample component with high mobility and like charge 608(1992)47
- Gelfi, C., Alloni, A., De Besi, P. and Righetti, P. G.  
Investigation of the properties of acrylamide bifunctional monomers (cross-linkers) by capillary zone electrophoresis 608(1992)343
- Gelfi, C., De Besi, P., Alloni, A. and Righetti, P. G.  
Investigation of the properties of novel acrylamido monomers by capillary zone electrophoresis 608(1992)333
- Giese, R. W., see Abdel-Baky, S. 608(1992)159
- Giese, R. W., see Li, W. 608(1992)171
- Giese, R. W., see Yeung, E. S. 608(1992)73
- Grossman, P. D., Hino, T. and Soane, D. S.  
Dynamic light-scattering studies of hydroxyethyl cellulose solutions used as sieving media for electrophoretic separations 608(1992)79
- Guéant, J. L., see Lambert, D. 608(1992)311
- Guttman, A., Arai, A. and Magyar, K.  
Influence of pH on the migration properties of oligonucleotides in capillary gel electrophoresis 608(1992)175

- Guzman, N. A., Moschera, J., Iqbal, K. and Malick, A. W.  
Effect of buffer constituents on the determination of therapeutic proteins by capillary electrophoresis 608(1992)197
- Haddad, P. R., see Buchberger, W. 608(1992)59
- Harke, H., see Zhao, J. Y. 608(1992)239
- Harke, H. R., Bay, S., Zhang, J. Z., Rocheleau, M. J. and Dovichi, N. J.  
Effect of total percent polyacrylamide in capillary gel electrophoresis for DNA sequencing of short fragments. A phenomenological model 608(1992)143
- Harrold, M. P., see Henshall, A. 608(1992)413
- Hazlett, J. S., see Weiss, C. S. 608(1992)325
- Heckenberg, A. L., see Weston, A. 608(1992)395
- Helliger, W., see Lindner, H. 608(1992)211
- Henshall, A., Harrold, M. P. and Tso, J. M. Y.  
Separation of inositol phosphates by capillary electrophoresis 608(1992)413
- Heo, G. S., see Lee, K.-J. 608(1992)243
- Hino, T., see Grossman, P. D. 608(1992)79
- Holma, T., see Lukkari, P. 608(1992)317
- Honda, S., Ueno, T. and Kakehi, K.  
High-performance capillary electrophoresis of unsaturated oligosaccharides derived from glycosaminoglycans by digestion with chondroitinase ABC as 1-phenyl-3-methyl-5-pyrazolonone derivatives 608(1992)289
- Hupe, K.-P., see Debets, A. J. J. 608(1992)151
- Iqbal, K., see Guzman, N. A. 608(1992)197
- Ishihama, Y., see Terabe, S. 608(1992)23
- Jacquier, J. C., see Desbène, P. L. 608(1992)375
- Jandik, P., see Jones, W. R. 608(1992)385
- Jandik, P., see Weston, A. 608(1992)395
- Jaquemar, M., see Lindner, H. 608(1992)211
- Jinno, K., see Lukkari, P. 608(1992)317
- Jones, W. R. and Jandik, P.  
Various approaches to analysis of difficult sample matrices of anions using capillary ion electrophoresis 608(1992)385
- Jones, W. R., see Weston, A. 608(1992)395
- Jumppanen, J., see Lukkari, P. 608(1992)317
- Kakehi, K., see Honda, S. 608(1992)289
- Karger, B. L., see Foret, F. 608(1992)3
- Kašička, V., Prusík, Z. and Pospíšek, J.  
Conversion of capillary zone electrophoresis to free-flow zone electrophoresis using a simple model of their correlation. Application to synthetic enkephalin-type peptide analysis and preparation 608(1992)13
- Kennedler, E. and Friedl, W.  
Adjustment of resolution and analysis time in capillary zone electrophoresis by varying the pH of the buffer 608(1992)161
- Kim, N. J., see Lee, K.-J. 608(1992)243
- Kraak, J. C., Busch, S. and Poppe, H.  
Study of protein-drug binding using capillary zone electrophoresis 608(1992)257
- Lambert, D., Adjalla, C., Felden, F., Benhayoun, S., Nicolas, J. P. and Guéant, J. L.  
Identification of vitamin B<sub>12</sub> and analogues by high-performance capillary electrophoresis and comparison with high-performance liquid chromatography 608(1992)311
- Lee, K.-J., Heo, G. S., Kim, N. J. and Moon, D. C.  
Analysis of antiepileptic drugs in human plasma using micellar electrokinetic capillary chromatography 608(1992)243
- Li, W., Moussa, A. and Giese, R. W.  
Capillary electrophoresis of fluorescein-ethylenediamine-5'-deoxynucleotides 608(1992)171
- Li, W., see Yeung, E. S. 608(1992)73
- Lindner, H., Helliger, W., Dirschlmaier, A., Talasz, H., Wurm, M., Sarg, B., Jaquemar, M. and Puschendorf, B.  
Separation of phosphorylated histone H1 variants by high-performance capillary electrophoresis 608(1992)211
- Lingeman, H., see Debets, A. J. J. 608(1992)151
- Lukkari, P., Jumppanen, J., Holma, T., Sirén, H., Jinno, K., Elo, H. and Riekkola, M.-L.  
Effect of the buffer solution on the elution order and separation of bis(amidinohydrazones) by micellar electrokinetic capillary chromatography 608(1992)317
- Lunte, C. E., see O'Shea, T. J. 608(1992)189
- Lunte, S. M., see O'Shea, T. J. 608(1992)189
- Ma, Y., Zhang, R. and Cooper, C. L.  
Indirect photometric detection of polyamines in biological samples separated by high-performance capillary electrophoresis 608(1992)93
- Magyar, K., see Guttman, A. 608(1992)175
- Malick, A. W., see Guzman, N. A. 608(1992)197
- Matsubara, N., see Terabe, S. 608(1992)23
- Mazereeuw, M., see Debets, A. J. J. 608(1992)151
- Michaelsen, S., see Bjerregaard, C. 608(1992)403
- Michaelsen, S., Møller, P. and Sørensen, H.  
Factors influencing the separation and quantitation of intact glucosinolates and desulphoglucosinolates by micellar electrokinetic capillary chromatography 608(1992)363
- Miller, J., see Zhao, J. Y. 608(1992)239
- Mingorance, M. D., see Tienstra, P. A. 608(1992)357
- Møller, P., see Michaelsen, S. 608(1992)363
- Moon, D. C., see Lee, K.-J. 608(1992)243
- Moschera, J., see Guzman, N. A. 608(1992)197
- Moussa, A., see Li, W. 608(1992)171
- Nicolas, J. P., see Lambert, D. 608(1992)311
- Nielen, M. W. F.  
Indirect time-resolved luminescence detection in capillary zone electrophoresis 608(1992)85
- Novotny, M. V., see Soini, H. 608(1992)265
- Okada, Y., see Terabe, S. 608(1992)23
- Olieman, C., see Tienstra, P. A. 608(1992)357
- O'Shea, T. J., Weber, P. L., Bammel, B. P., Lunte, C. E., Lunte, S. M. and Smyth, M. R.  
Monitoring excitatory amino acid release *in vivo* by microdialysis with capillary electrophoresis-electrochemistry 608(1992)189
- Overkluft, G. T., see Damm, J. B. L. 608(1992)297

- Pawliszyn, J., see Wu, J. 608(1992)121
- Petersen, J., see Vinther, A. 608(1992)205
- Poppe, H., see Bruin, G. J. M. 608(1992)97
- Poppe, H., see Kraak, J. C. 608(1992)257
- Pospišek, J., see Kašička, V. 608(1992)13
- Prusík, Z., see Kašička, V. 608(1992)13
- Puschendorf, B., see Lindner, H. 608(1992)211
- Regnier, F. E., see Bao, J. 608(1992)217
- Regnier, F. E., see Wu, D. 608(1992)349
- Riekkola, M.-L., see Lukkari, P. 608(1992)317
- Riekkola, M.-L., see Soini, H. 608(1992)265
- Righetti, P. G., see Gelfi, C. 608(1992)333
- Righetti, P. G., see Gelfi, C. 608(1992)343
- Rocheleau, M. J., see Harke, H. R. 608(1992)143
- Rodriguez, R., see Zhu, M. 608(1992)225
- Rony, C., see Desbène, P. L. 608(1992)375
- Sarg, B., see Lindner, H. 608(1992)211
- Siebert, C., see Zhu, M. 608(1992)225
- Sirén, H., see Lukkari, P. 608(1992)317
- Smyth, M. R., see O'Shea, T. J. 608(1992)189
- Soane, D. S., see Grossman, P. D. 608(1992)79
- Søeberg, H., see Vinther, A. 608(1992)205
- Soini, H., Riekkola, M.-L. and Novotny, M. V.  
Chiral separations of basic drugs and quantitation of bupivacaine enantiomers in serum by capillary electrophoresis with modified cyclodextrin buffers 608(1992)265
- Sørensen, H., see Bjerregaard, C. 608(1992)403
- Sørensen, H., see Michaelsen, S. 608(1992)363
- Soucheleau, J. and Denoroy, L.  
Determination of vasoactive intestinal peptide in rat brain by high-performance capillary electrophoresis 608(1992)181
- Szoko, E., see Foret, F. 608(1992)3
- Talasz, H., see Lindner, H. 608(1992)211
- Terabe, S., Matsubara, N., Ishihama, Y. and Okada, Y.  
Microemulsion electrokinetic chromatography: comparison with micellar electrokinetic chromatography 608(1992)23
- Thormann, W., see Gebauer, P. 608(1992)47
- Thormann, W., see Wernly, P. 608(1992)251
- Tienstra, P. A., Van Riel, J. A. M., Mingorance, M. D. and Olieman, C.  
Assessment of the capabilities of capillary zone electrophoresis for the determination of hippuric and orotic acid in whey 608(1992)357
- Tribet, C., Gaboriaud, R. and Gareil, P.  
Analogy between micelles and polymers of ionic surfactants. A capillary isotachophoretic study of small ionic aggregates in water-organic solutions 608(1992)131
- Tso, J. M. Y., see Henshall, A. 608(1992)413
- Ueno, T., see Honda, S. 608(1992)289
- Van Asten, A. C., see Bruin, G. J. M. 608(1992)97
- Van Dedem, G. W. K., see Damm, J. B. L. 608(1992)297
- Van Iperen, D. J., see Debets, A. J. J. 608(1992)151
- Van Riel, J. A. M., see Tienstra, P. A. 608(1992)357
- Verbeke, N., see D'Hulst, A. 608(1992)275
- Verheggen, T. P. E. M.  
Foreword 608(1992)1
- Vermeulen, B.W.M., see Damm, J.B.L. 608(1992)297
- Vigh, G., see Cruzado, I. D. 608(1992)421
- Vinther, A., Petersen, J. and Søeberg, H.  
Capillary electrophoretic determination of the protease Savinase in cultivation broth 608(1992)205
- Voogt, W. H., see Debets, A. J. J. 608(1992)151
- Waldron, K. C., see Zhao, J. Y. 608(1992)239
- Wang, P., see Yeung, E. S. 608(1992)73
- Weber, P. L., see O'Shea, T. J. 608(1992)189
- Wehr, T., see Zhu, M. 608(1992)225
- Weiss, C. S., Hazlett, J. S., Datta, M. H. and Danzer, M. H.  
Determination of quaternary ammonium compounds by capillary electrophoresis using direct and indirect UV detection 608(1992)325
- Wernly, P. and Thormann, W.  
Confirmation testing of 11-nor- $\Delta^9$ -tetrahydrocannabinol-9-carboxylic acid in urine with micellar electrokinetic capillary chromatography 608(1992)251
- Weston, A., Brown, P. R., Jandik, P., Heckenberg, A. L. and Jones, W. R.  
Optimization of detection sensitivity in the analysis of inorganic cations by capillary ion electrophoresis using indirect photometric detection 608(1992)395
- Wu, D. and Regnier, F. E.  
Sodium dodecyl sulfate-capillary gel electrophoresis of proteins using non-cross-linked polyacrylamide 608(1992)349
- Wu, J. and Pawliszyn, J.  
Application of capillary isoelectric focusing with universal concentration gradient detector to the analysis of protein samples 608(1992)121
- Wurm, M., see Lindner, H. 608(1992)211
- Xu, X., see Bruin, G. J. M. 608(1992)97
- Yeung, E. S., see Chang, H.-T. 608(1992)65
- Yeung, E. S., Wang, P., Li, W. and Giese, R. W.  
Laser fluorescence detector for capillary electrophoresis 608(1992)73
- Zhang, J. Z., see Harke, H. R. 608(1992)143
- Zhang, J. Z., see Zhao, J. Y. 608(1992)239
- Zhang, R., see Ma, Y. 608(1992)93
- Zhao, J.-Y., Chen, D.-Y. and Dovichi, N. J.  
Low-cost laser-induced fluorescence detector for micellar capillary zone electrophoresis. Detection at the zeptomol level of tetramethylrhodamine thiocarbonyl amino acid derivatives 608(1992)117
- Zhao, J. Y., Waldron, K. C., Miller, J., Zhang, J. Z., Harke, H. and Dovichi, N. J.  
Attachment of a single fluorescent label to peptides for determination by capillary zone electrophoresis 608(1992)239
- Zhu, M., Rodriguez, R., Wehr, T. and Siebert, C.  
Capillary electrophoresis of hemoglobins and globin chains 608(1992)225



# Journal of Chromatography

## NEWS SECTION

### SHORT CONFERENCE REPORT

4th INTERNATIONAL SYMPOSIUM ON HIGH PERFORMANCE CAPILLARY ELECTROPHORESIS, AMSTERDAM, NETHERLANDS, FEBRUARY 9-13, 1992

Herewith we present a few pictures that might be considered an extension of what has been called the Journal of Chromatography Family Album [see *J. Chromatogr.*, 500 (1990) 2-92]. Glimpses at the faces of regular participants of this meeting may complete the impression. Here are just a few pictures of the many people who have made HPCE '92 such a success. Inclusion of such pictures in the proceedings volumes seems to be becoming a tradition in the Journal. For regular participants of HPCE meetings this may be a commemoration of the event; newcomers may be interested in linking the faces to the names of some of the contributors to this volume.



Fig. 1. A glimpse into the lecture hall, from right hand side: Professor Macek, Dr. Prusík, Dr. Kasicka, Professor Janák and Professor Regnier.



Fig. 2. During the speakers' dinner a tour was organized through the Van Loon house. Professor Regnier, Professor Macek and Shirley Schlessinger listening to the guide's explanation.



Fig. 3. Touring the Van Loon house (left Professor Jorgenson).



Fig. 4. A friendly chat: Dr. Laeven and Professor Terabe.



Fig. 5. Exchanging jokes here are Dr. Bocek, Professor Macek and Professor Westerlund.





Fig. 6. Professor Karger addressing the participants of the festive dinner.



Fig. 7. Waiting to be served, from left: Professors Yeung, Jorgens and Hancock.

## PUBLICATION SCHEDULE FOR 1992

*Journal of Chromatography and Journal of Chromatography, Biomedical Applications*

MONTH	O 1991–M 1992	J	J	A	S	O	N	D
Journal of Chromatography	Vols. 585–600	602/1+2 603/1+2 604/1	604/2 605/1 605/2 606/1	606/2 607/1 607/2	608/1+2 609/1+2			
Cumulative Indexes, Vols. 551–600		*						
Bibliography Section	610/1	610/2			611/1			611/2
Biomedical Applications	Vols. 573–577/1	577/2	578/1 578/2	579/1	579/2 580/1+2	<sup>b</sup>		

<sup>a</sup> Cumulative Indexes will be Vol. 601, to appear early 1993.

<sup>b</sup> The publication schedule for further issues will be published later.

### INFORMATION FOR AUTHORS

(Detailed *Instructions to Authors* were published in Vol. 558, pp. 469–472. A free reprint can be obtained by application to the publisher, Elsevier Science Publishers B.V., P.O. Box 330, 1000 AH Amsterdam, The Netherlands.)

**Types of Contributions.** The following types of papers are published in the *Journal of Chromatography* and the section on *Biomedical Applications*: Regular research papers (Full-length papers), Review articles and Short Communications. Short Communications are usually descriptions of short investigations, or they can report minor technical improvements of previously published procedures; they reflect the same quality of research as Full-length papers, but should preferably not exceed five printed pages. For Review articles, see inside front cover under Submission of Papers.

**Submission.** Every paper must be accompanied by a letter from the senior author, stating that he/she is submitting the paper for publication in the *Journal of Chromatography*.

**Manuscripts.** Manuscripts should be typed in double spacing on consecutively numbered pages of uniform size. The manuscript should be preceded by a sheet of manuscript paper carrying the title of the paper and the name and full postal address of the person to whom the proofs are to be sent. As a rule, papers should be divided into sections, headed by a caption (*e.g.*, Abstract, Introduction, Experimental, Results, Discussion, etc.). All illustrations, photographs, tables, etc., should be on separate sheets.

**Introduction.** Every paper must have a concise introduction mentioning what has been done before on the topic described, and stating clearly what is new in the paper now submitted.

**Abstract.** All articles should have an abstract of 50–100 words which clearly and briefly indicates what is new, different and significant.

**Illustrations.** The figures should be submitted in a form suitable for reproduction, drawn in Indian ink on drawing or tracing paper. Each illustration should have a legend, all the legends being typed (with double spacing) together on a separate sheet. If structures are given in the text, the original drawings should be supplied. Coloured illustrations are reproduced at the author's expense, the cost being determined by the number of pages and by the number of colours needed. The written permission of the author and publisher must be obtained for the use of any figure already published. Its source must be indicated in the legend.

**References.** References should be numbered in the order in which they are cited in the text, and listed in numerical sequence on a separate sheet at the end of the article. Please check a recent issue for the layout of the reference list. Abbreviations for the titles of journals should follow the system used by *Chemical Abstracts*. Articles not yet published should be given as "in press" (journal should be specified), "submitted for publication" (journal should be specified), "in preparation" or "personal communication".

**Dispatch.** Before sending the manuscript to the Editor please check that the envelope contains four copies of the paper complete with references, legends and figures. One of the sets of figures must be the originals suitable for direct reproduction. Please also ensure that permission to publish has been obtained from your institute.

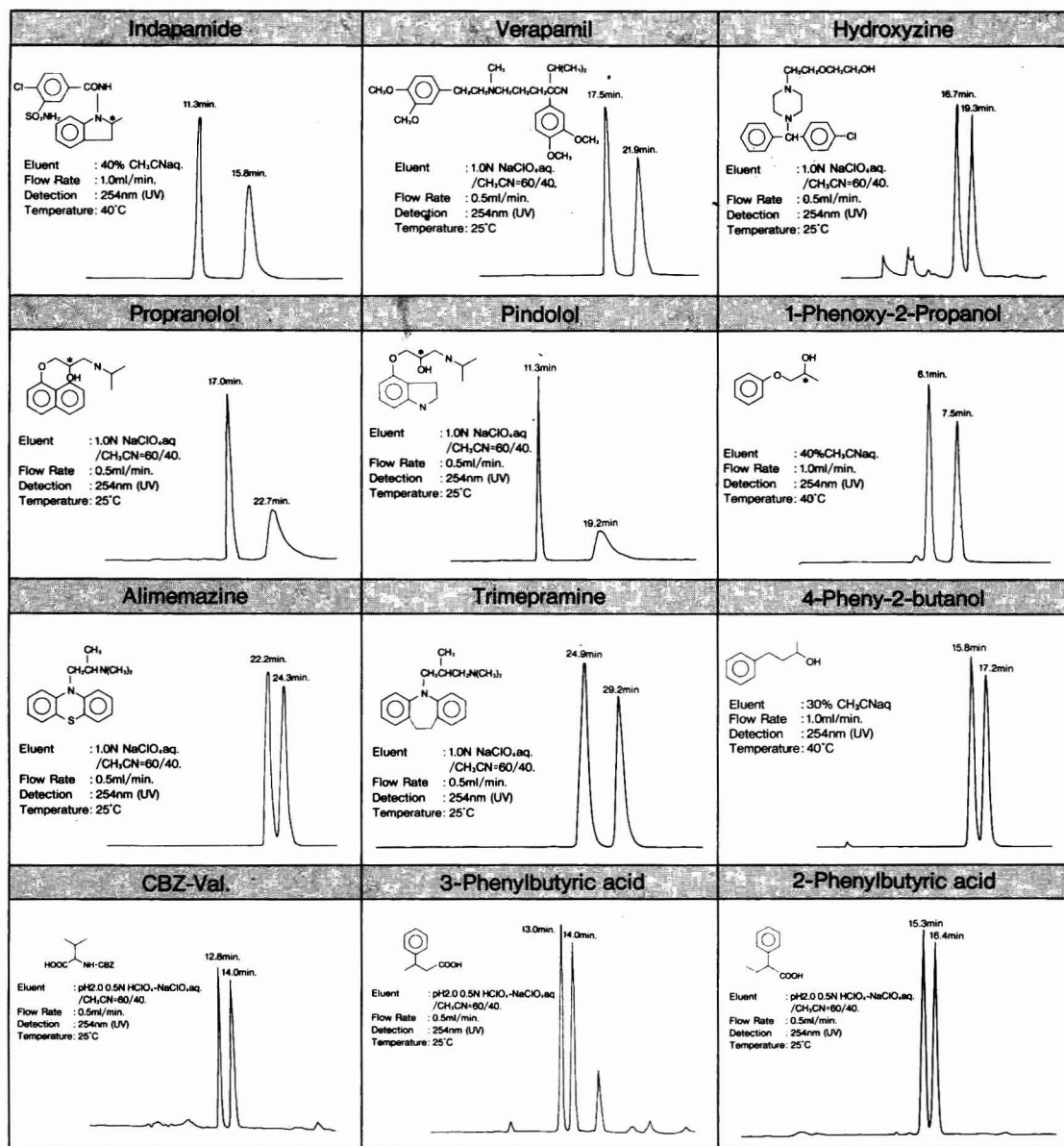
**Proofs.** One set of proofs will be sent to the author to be carefully checked for printer's errors. Corrections must be restricted to instances in which the proof is at variance with the manuscript. "Extra corrections" will be inserted at the author's expense.

**Reprints.** Fifty reprints of Full-length papers and Short Communications will be supplied free of charge. Additional reprints can be ordered by the authors. An order form containing price quotations will be sent to the authors together with the proofs of their article.

**Advertisements.** The Editors of the journal accept no responsibility for the contents of the advertisements. Advertisement rates are available on request. Advertising orders and enquiries can be sent to the Advertising Manager, Elsevier Science Publishers B.V., Advertising Department, P.O. Box 211, 1000 AE Amsterdam, Netherlands; courier shipments to: Van de Sande Bakhuizenstraat 4, 1061 AG Amsterdam, Netherlands; Tel. (+31-20) 515 3220/515 3222, Telefax (+31-20) 6833 041, Telex 16479 els vi nl. UK: T. G. Scott & Son Ltd., Tim Blake, Portland House, 21 Narborough Road, Cosby, Leics. LE9 5TA, UK; Tel. (+44-533) 753 333, Telefax (+44-533) 750 522. USA and Canada: Weston Media Associates, Daniel S. Lipner, P.O. Box 1110, Greens Farms, CT 06436-1110, USA; Tel. (+1-203) 261 2500, Telefax (+1-203) 261 0101.

# Reversed Phase CHIRAL HPLC Column

## NEW CHIRALCEL<sup>®</sup> OD-R



For more information about CHIRALCEL OD-R column, please give us a call.



**DAICEL CHEMICAL INDUSTRIES, LTD.**

CHIRAL CHEMICALS DIVISION 8-1, Kasumigaseki 3-chome, Chiyoda-ku, Tokyo 100, JAPAN  
Phone: +81-3-3507-3151 Facsimile: +81-3-3507-3193

**AMERICA**  
CHIRAL TECHNOLOGIES, INC.  
730 SPRINGDALE DRIVE  
DRAWER I EXTON, PA 19341  
Phone: 215-594-2100  
Facsimile: 215-594-2325

**EUROPE**  
DAICEL (EUROPA) GmbH  
Ost Street 22  
4000 Düsseldorf 1, Germany  
Phone: +49-211-369848  
Facsimile: +49-211-364429

**ASIA/OCEANIA**  
DAICEL CHEMICAL (ASIA) PTE. LTD.  
65 Chulia Street #40-07  
OCBC Centre, Singapore 0104.  
Phone: +65-5332511  
Facsimile: +65-5326454